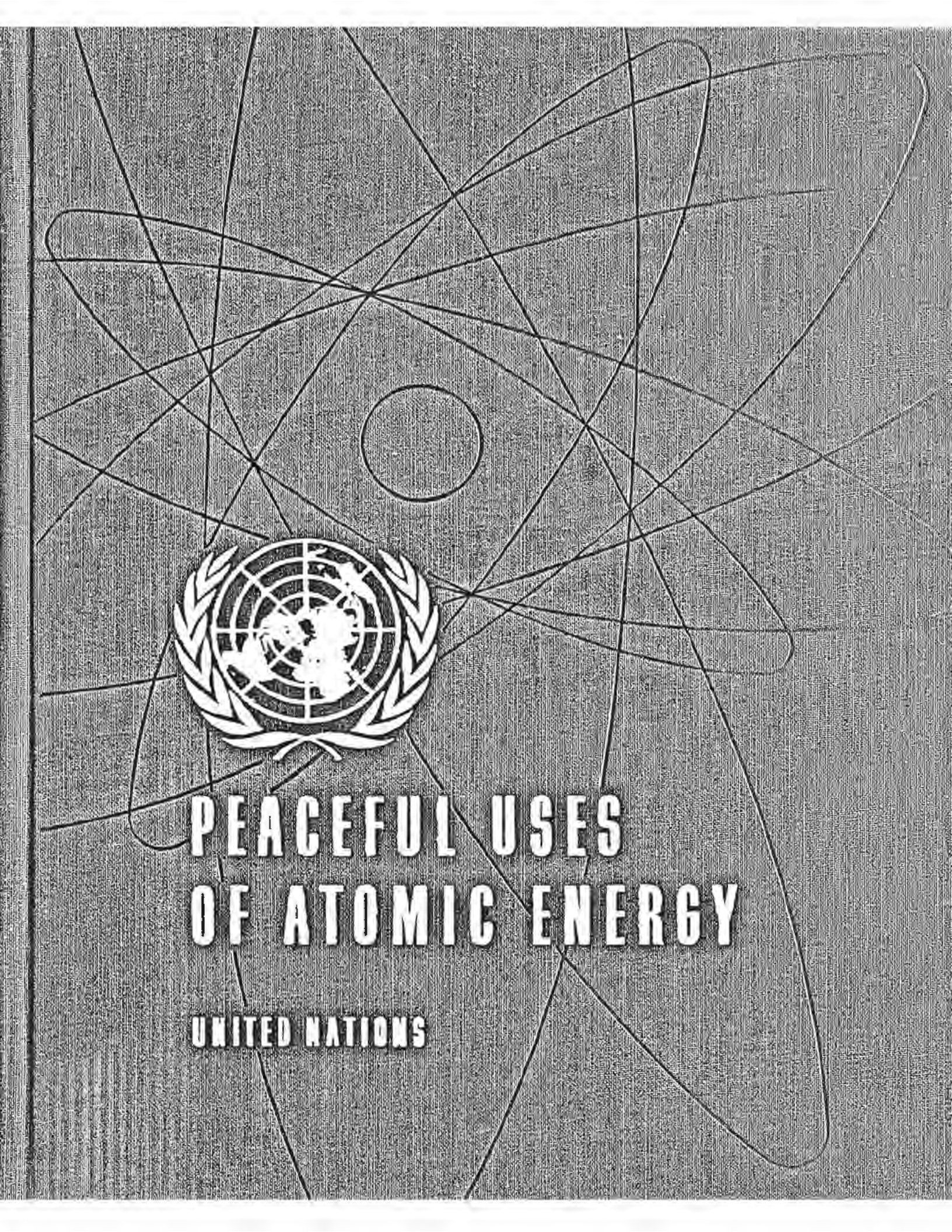
PEACEFUL USES
OF ATOMIC ENERGY
UNITED NATIONS

PROCEEDINGS
OF THE
INTERNATIONAL CONFERENCE ON THE
PEACEFUL USES OF ATOMIC ENERGY

Volume 7

NUCLEAR CHEMISTRY AND
EFFECTS OF IRRADIATION

Proceedings of the International Conference

on the

Peaceful Uses of Atomic Energy

Held in Geneva

8 August-20 August 1955

Volume 7

Nuclear Chemistry and Effects of Irradiation

UNITED NATIONS

New York

1956

UNITED NATIONS PUBLICATION

Sales No. 1956.IX.1.Vol. 7

A/CONF.8/7

Price: U.S.$10.00; 70/- stg.; 43.00 Sw. frs.
(or equivalent in other currencies)

PREFACE

The Proceedings of the International Conference on the Peaceful Uses of Atomic Energy are published in a series of 16 volumes, as follows:

Volume Number	Title	Sessions Included
1	The World's Requirements for Energy; The Role of Nuclear Power	2, 3.2, 4.1, 4.2, 5, 24.2.
2	Physics; Research Reactors	6A, 7A, 8A, 9A, 10A.1.
3	Power Reactors	10A.2, 3.1, 11A, 12A, 13A, 14A.
4	Cross Sections Important to Reactor Design	15A, 16A, 17A, 18A.
5	Physics of Reactor Design	19A, 20A, 21A, 22A, 23A.
6	Geology of Uranium and Thorium	6B, 7B.
7	Nuclear Chemistry and the Effects of Irradiation	8B, 9B, 10B, 11B, 12B, 13B.
8	Production Technology of the Materials Used for Nuclear Energy	14B, 15B, 16B, 17B.
9	Reactor Technology and Chemical Processing	7.3, 18B, 19B, 20B, 21B, 22B, 23B.
10	Radioactive Isotopes and Nuclear Radiations in Medicine	7.2 (Med.), 8C, 9C, 10C.
11	Biological Effects of Radiation	6.1, 11C, 12C, 13C.1.
12	Radioactive Isotopes and Ionizing Radiations in Agriculture, Physiology and Biochemistry	7.2 (Agric.), 13C.2, 14C, 15C, 16C.
13	Legal, Administrative, Health and Safety Aspects of Large-Scale Use of Nuclear Energy	4.3, 6.2, 17C, 18C.
14	General Aspects of the Use of Radioactive Isotopes; Dosimetry	7.1, 19C, 20C.
15	Applications of Radioactive Isotopes and Fission Products in Research and Industry	21C, 22C, 23C.
16	Record of the Conference	1, 24.1, 24.3.

These volumes include all the papers submitted to the Geneva Conference, as edited by the Scientific Secretaries. The efforts of the Scientific Secretaries have been directed primarily towards scientific accuracy. Editing for style has been minimal in the interests of early publication. This may be noted especially in the English translations of certain papers submitted in French, Russian and Spanish. In a few instances, the titles of papers have been edited to reflect more accurately the content of those papers.

The editors principally responsible for the preparation of these volumes were: Robert A. Charpie, Donald J. Dewar, André Finkelstein, John Gaunt, Jacob A. Goedkoop, Elwyn O. Hughes, Leonard F. Lamerton, Aleksandar Milojević, Clifford Mosbacher, César A. Sastre, and Brian E. Urquhart.

The verbatim records of the Conference are included in the pertinent volumes. These verbatim records contain the author's corrections and, where necessary for scientific accuracy, the editing changes of the Scientific Secretaries, who have also been responsible for inserting slides, diagrams and sketches at appropriate points. In the record of each session, slides are numbered in numerical order through all presentations. Where the slide duplicates an illustration in the submitted paper, appropriate reference is made and the illustration does not appear in the record of the session.

Volume 16, "The Record of the Conference," includes the complete programme of the Conference, a numerical index of papers and an author's index, the list of delegates, the records of the opening and closing sessions and the complete texts of the evening lectures.

TABLE OF CONTENTS

Session 11B: Effects of Radiation on Reactor Materials

Session 12B: Effects of Radiation on Liquids

Session 13B: Effects of Radiation on Solids

Session 8B.1

THE FISSION PROCESS

LIST OF PAPERS

Survey of Radiochemical Studies of the Fission Process

By E. P. Steinberg and L. E. Glendenin,* USA

Radiochemical techniques led to the discovery of nuclear fission[1] and have since played an important role in the detailed characterization of this phenomenon. Through the measurement of fission yields (probabilities of formation for the various fission products), radiochemical research has resulted in a much more accurate picture of the distribution of mass and nuclear charge in fission than could be obtained by purely physical methods. In addition to the variety of theoretical problems to which these data are relevant, the yields of fission products are of practical importance to many problems in the design and operation of nuclear reactors and processing plants. In particular, the abundance of nuclides emitting delayed neutrons or having high neutron capture cross sections (reactor "poisons") are of prime concern in reactor operation, and a knowledge of the distribution of radioactivities is important for such problems as shielding requirements, decontamination, waste disposal, etc.

Although many fission products were chemically identified and some fission decay chain relationships established during the early investigations of uranium fission, yields were measured in only a few cases. Hahn and Strassmann[2] observed that the fission yield of radioactive bromine is only about one-tenth that of radioactive iodine. Moussa and Goldstein[3] found fission yields of 0.8% for a 40-minute bromine activity and 0.5% for a 2.3-hour bromine activity. Anderson, Fermi, and Grosse[4] determined the yields of ten decay chains and observed values varying from about 0.1 to 10%. In general, these early results are in reasonable agreement with later studies. Extensive investigations of fission yields in low-energy neutron-induced fission of U^{233}, U^{235}, U^{238}, and Pu^{239} were made during the period 1942–1948 by many workers on the United States atomic energy project.[5] Similar studies of U^{233} and U^{235} were made by Grummitt and Wilkinson[6] on the Canadian project. Since 1948 yield-mass curves have also been reported for Th^{232} fission[7] and U^{238} fission.[8] In the last few years fission yield studies (utilizing mass spectrometric and improved radiometric techniques) have been directed toward refinements in the measurements to establish absolute fission yields and to examine more detailed features of the mass distribution (yield-mass curves).

*Argonne National Laboratory.

A general survey of the field of nuclear fission has been given by Whitehouse[9] covering the literature through 1951. Useful bibliographies[10] have been issued by the Information Office of the British Atomic Energy Research Establishment covering the period from January 1946 to September 1952. A survey of spontaneous and slow neutron fission properties of heavy nuclei has been given by Huizenga, Manning, and Seaborg[11] covering slow neutron fission thresholds, correlation of slow neutron fissionability with fission thresholds and neutron binding energies, and systematics of spontaneous fission half-lives as a function of atomic and mass number. Radiochemical investigations of the high energy and low-energy fission processes have been reviewed by Spence and Ford[12] and by Glendenin and Steinberg[13] respectively.

The present survey is limited to radiochemical investigations of the low-energy, neutron-induced fission process (reactor fission). The best fission yield data presently available for Th^{232}, U^{233}, U^{235}, U^{238}, and Pu^{239} are reviewed. Since U^{233}, U^{235}, and Pu^{239} are fissionable with thermal neutrons, the fission of these nuclides in a nuclear reactor is generally referred to as slow neutron-induced. Fission of U^{238} and Th^{232}, on the other hand, requires neutrons of at least 1-Mev energy and is therefore usually described as fast neutron-induced. The features of the mass distributions, including fine-structure (i.e., perturbations in fission yields presumably resulting from closed shell effects) and the distribution of nuclear charge in fission, are examined and correlated.

MASS DISTRIBUTION

A summary of fission yield data for Th^{232}, U^{238}, Pu^{239}, and U^{233} is given with references in Table I. The data for Th^{232}, U^{238}, and Pu^{239} were determined using radiometric techniques (measurement of radioactivity) and have an estimated accuracy of 10–20%. In the case of U^{233}, relative isotopic abundances of some fission-produced elements were determined mass spectrometrically and are normalized to the radiometric yields. The accuracy of relative isotopic abundances for a given element is of the order of 2%. Expressed as absolute fission yields, however, these data are of no greater accuracy than the radiometric values. Where more than one value is listed for a nuclide, the preferred one is given first.

The fission yield values of Table 1 were used to

Table I. Summary of Fission Yields

Fission product	Mass number	Fission yield (%)				
					U^{233}	
		Th^{232}	U^{238}	Pu^{239}	Radiometric	Mass spectrometric
49.0-hr Zn	72	3.3×10^{-4}[a]		1.1×10^{-4}[c]		
5.0-hr Ga	73	4.5×10^{-4}[a]				
12-hr Ge	77	9×10^{-6}[a]			0.010[d]	
38-hr As	77	0.020[a]	3.6×10^{-3}[b] 4.3×10^{-3}[c]		0.019[d]	
2.4-hr Br	83	1.9[a]		0.080[c]	0.79[d]	
Stable Kr	83					1.14[e]
Stable Kr	84					1.90[e]
10.27-yr Kr	85					0.56_2[e]
Stable Kr	86					3.1_8[e]
53-d Sr	89	6.7[a]	2.7[b] 3.3[c]	1.8[c]	6.5[d]	
28-yr Sr	90	6.1[a]				
9.7-yr Sr	91	6.4[a]		2.3[c]		
61-d Y	91			2.8[c]		
Stable Zr	91					6.5_8[f]
Stable Zr	92					6.7_0[f]
1.1×10^6-yr Zr	93					7.1_0[f]
Stable Zr	94					6.8_2[f]
63-d Zr	95		4.7[b] 7.3[c]	5.6[c]	5.9[d]	
Stable Mo	95					6.1_0[f]
Stable Zr	96					5.6_0[f]
17.0-hr Zr	97	5.4[a]		5.3[c]		
Stable Mo	97					5.3_2[f]
Stable Mo	98					5.1_8[f]
67-hr Mo	99	2.9[a]	6.4[b] 5.9[c]	6.1[c]	5.1[d]	
Stable Mo	100					4.4_0[f]
Stable Ru	101					3.0_0[f]
Stable Ru	102					2.3_7[f]
39.8-d Ru	103	0.20[a]	6.3[b] 7.4[c]	5.5[c]	1.6[d]	
Stable Ru	104					0.96[f]
36.5-hr Rh	105	0.07[a]		3.7[c]		
1.0-yr Ru	106	0.058[a]	2.9[b] 2.7[c]	4.7[c]	0.28[d]	
13.6-hr Pd	109	0.053[a]		1.0[c]	0.040[d]	
7.6-d Ag	111	0.052[a]	0.064[b] 0.072[c]	0.27[c]	0.025[d]	
21-hr Pd	112	0.065[a]		0.10[c]	0.016[d]	
43-d Cd	115^m	3×10^{-3}[a]	2.5×10^{-3}[b] 6×10^{-3}[c]	3×10^{-3}[c]	1×10^{-3}[d]	
53-hr Cd	115	0.072[a]	0.032[b] 0.057[c]	0.045[c]	0.19[d]	
Total Chain	115	0.075[a]	0.035[b] 0.063[c]	0.048[c]	0.020[d]	
27.5-hr Sn	121			0.041[c]	0.018[d]	
9.4-d Sn	125			0.068[c]	0.050[d]	
93-hr Sb	127		0.13[b] 0.12[c]	0.37[c]		
8.1-d I	131	1.2[a]		3.6[c]	2.7[d]	
Stable Xe	131					3.4_0[e]
77.7-hr Te	132	2.4[a]	4.7[b]	4.0[c]		
Stable Xe	132					4.6_4[e]
20.8-hr I	133			5.0[c]		
Stable Cs	133					5.6_8[e]
Stable Xe	134					5.9_2[e]
6.68-hr I	135			5.5[c]	5.1[d]	
3.0×10^6-yr Cs	135					$>4.4_9$[e]
86-sec I	136			1.9[g]	1.7[g]	
Stable Xe	136					$<8.0_0$[e]
33-yr Cs	137	6.6[a]	7.1[b]	5.8[h]		6.5_1[e]

Table I. Summary of Fission Yields (continued)

Fission product	Mass number	Fission yield (%) Th^{232}	U^{238}	Pu^{239}	U^{235} Radiometric	U^{235} Mass spectrometric
85-min Ba	139			5.4[c]		
12.8-d Ba	140	6.2[a]	5.7[b] 6.1[c]	5.3[c]	6.0[c]	
33.1-d Ce	141	9.0[a]		4.0[c]		
33-hr Ce	143			5.1[c]		
282-d Ce	144	7.1[a]	4.9[b]	3.7[c]	4.1[d]	
47-hr Sm	153			0.39[c]	0.095[d]	
15.4-d Eu	156		0.073[b] 0.063[c]	0.12[c]		

[a] Turkevich, A. and Niday, J. B., *Radiochemical Studies of the Fission of Th^{232} with Pile Neutrons*, Phys. Rev. 84: 52 (1951).

[b] Keller, R. N., Steinberg, E. P. and Glendenin, L. E., *Yields of Fission Products from U^{238} Irradiated with Fission Spectrum Neutrons*, Phys. Rev. 94: 969 (1954).

[c] Coryell, C. D. and Sugarman, N., Eds., *Radiochemical Studies: The Fission Products*, National Nuclear Energy Series, Div. IV, Vol. 9, McGraw-Hill Book Co., New York, (1951); Appendix B.

[d] Steinberg, E. P., Seiler, J. A., Goldstein, A., Dudley, A., *Fission Yields in Uranium-233*, MDDC-1632 (1948); yields revised by Steinberg in 1954.

[e] Fleming, W., Tomlinson, R. H. and Thode, H. G., *The Fission Yields of the Stable and Long-Lived Isotopes of Xenon, Cesium, and Krypton in Neutron Fission of U^{233}*, Can. J. Phys. 32: 522 (1954); relative yield normalized to radiometric data of reference(d).

[f] Steinberg, E. P., Glendenin, L. E., Inghram, M. G. and Hayden, R. J., *Fine Structure in U^{235} Fission*. Phys. Rev. 95: 867 (1954); relative yield normalized to radiometric data of reference (d).

[g] Stanley, C. W. and Katcoff, S., *The Properties of 86-second I^{136}*, J. Chem. Phys. 17: 653 (1949).

[h] Glendenin, L. E., *Further Study of the 13 d Cs Activity*, paper 155, in Coryell, C. D. and Sugarman, N., *Radiochemical Studies: The Fission Products*, National Nuclear Energy Series, Div. IV, Vol. 9, McGraw Hill Book Co., New York (1951).

construct the corresponding yield-mass curves of Figs. 1–4. These curves are essentially symmetrical about a mid-point which represents fission into two equal fragments and the emission of about two neutrons. The yield value given by the curves at any mass number represents the total chain yield, and the summation of yields is approximately 200%, as theoretically expected for binary fission.

Fission yields for U^{235} have been investigated in greater detail than have those for other fissile nuclides. These data with appropriate references are compiled in Table II. Radiometrically determined yields are listed in column 3, and those mass spectrometrically determined are given in column 4. In the mass spectrometric investigation of reference (g) of Table II, the isotope dilution technique was utilized to obtain the number of atoms of fission-produced isotopes of strontium, zirconium, molybdenum, cesium, barium, cerium, and neodymium present in a solution of neutron-irradiated U^{235}. For ruthenium, the number of atoms of 1.0-yr Ru^{106} was determined by absolute beta counting since a suitable isotopic tracer was not available for isotope dilution. The isotopic abundances of Ru^{101}, Ru^{102}, and Ru^{104} were determined relative to Ru^{106} by mass spectrometry. Relative isotopic abundances of fission produced krypton, xenon, and cesium (references (d), (e), and (r) of Table II) were normalized to the data of reference (g). These mass abundances were converted to fission yields by imposing the criterion that the sum of all yields be 200%. Radiometric data for mass numbers not determined mass spectrometrically were used as an aid in the summation. In general, the U^{235} fission yields of Table II based on radioactivity measurement are considered reliable to 10–20% although the uncertainty in a few cases may be smaller. The values based on mass spectrometry are believed to be somewhat more accurate and are considered reliable to about 5%. Recommended values for total chain yields are given in column 5 of Table II and plotted as a yield-mass curve in Fig. 5.

Fine structure is clearly indicated by the mass spectrometric data in the regions around mass 100 and mass 134 in the fission of U^{233} and U^{235} (Figs. 4 and 5). This effect is ascribed to the influence of closed neutron shells in fission and is discussed below. Certain characteristics of the mass distributions for the various fissile nuclides are apparent from Figs. 1–5 and are summarized in Table III. It is seen that low-energy fission is predominantly asymmetric, i.e., the mass distribution has two maxima (light and heavy group peaks) and a deep central minimum (trough) showing the low frequency of modes near symmetrical fission. With increasing mass of the fissioning nucleus the mass distribution becomes wider, and the light group peak shifts toward higher mass while the position of the heavy group peak remains relatively fixed. The mass shift of the light group is thus a useful indicator of the mass of the fissioning nucleus. For example, the yield of Ru^{105}

Table II. Summary of U^{235} Fission Yields

Fission product	Mass number	Fission yield (%) Radiometric	Mass spectrometric	Recommended total chain yield
49.0-hr Zn	72	1.5×10^{-5}[a]		1.5×10^{-5}
5.0-hr Ga	73	1.0×10^{-6}[a]		1.0×10^{-6}
12-hr Ge	77	3.7×10^{-3}[a]		
		2.3×10^{-3}[d]		
38-hr As	77	9.1×10^{-2}[a]		7.9×10^{-2}
		6.7×10^{-2}[b]		
86-min Ge	78	0.018[b]		
		0.020[d]		
91-min As	78	0.020[b]		0.020
		0.020[d]		
56.5-min Se	81m	8.0×10^{-2}[a]		
17-min Se	81	0.133[a]		0.133
25-min Se	83	0.21[a]		
2.4-hr Br	83	0.48[c]		
		0.40[e]		
Stable Kr	83		0.60$_2$[d]	0.60
30-min Br	84	0.65[a]		
Stable Kr	84		1.12[d]	1.1
4.36-hr Kr	85m		1.2[e]	
10.27-yr Kr	85	0.24[a]	0.32$_8$[d]	1.5
Stable Kr	86		2.1.[d]	2.1
55.6 sec Br	87	3.1[f]		
78-min Kr	87		2.5[e]	2.7
Stable Sr	88		3.6$_1$[g]	3.6
53-d Sr	89	4.7$_8$[b]		4.8
		4.6 [a]		
28-yr Sr	90		5.8$_6$[g]	5.8
9.7-hr Sr	91	5.1[b]		
		5.0[a]		
61-d Y	91	5.9[a]		
Stable Zr	91		5.8$_4$[g]	5.8
2.7-hr Sr	92	5.0[a]		
Stable Zr	92		6.0$_6$[g]	6.0
1.1×10^6-yr Zr	93		6.4$_6$[g]	6.4
Stable Zr	94		6.4$_6$[g]	6.4
63-d Zr	95	6.0[d]		
Stable Mo	95		6.2$_1$[g]	6.3
Stable Zr	96		6.3$_2$[g]	6.3
17.0-hr Zr	97	6.1[d]		
		5.5[h]		
Stable Mo	97		6.0$_8$[g]	6.1
Stable Mo	98		5.7$_4$[g]	5.8
67-hr Mo	99	6.1$_4$[c]		6.1
		5.9$_8$[b]		
		6.2 [a]		
Stable Mo	100		6.3$_4$[g]	6.3
14.6-min Mo	101	5.4[h]		
Stable Ru	101		5.0[g]	5.0
12-min Mo	102	4.1[h]		
Stable Ru	102		4.1[g]	4.1
39.8d-Ru	103	2.8$_8$[i]		2.9
		3.7[a]		
Stable Ru	104		1.8[g]	1.8
4.5-hr Ru	105	0.83[h]		0.85
		0.9[a]		
1.0-yr Ru	106	0.38[j]		0.38
		0.38[g]	0.38[g]	
		0.52[a]		
13.6-hr Pd	109	0.028[a]		0.028
7.6-d Ag	111	0.018[a]		0.018
21-hr Pd	112	0.011[a]		0.011
43-d Cd	115m	7.1×10^{-4}[m]		
		8.0×10^{-4}[a]		
53-hr Cd	115	9.8×10^{-3}[m]		0.011
		0.011[a]		
3.0-hr Cd	117	0.010[a]		0.010
27.5-hr Sn	121	0.014[a]		0.014
136-d Sn	123	1.2×10^{-3}[a]		

[a] Coryell, C. D. and Sugarman, N., Eds., *Radiochemical Studies: The Fission Products*, National Nuclear Energy Series, Div. IV., Vol. 9, McGraw-Hill Book Co., New York (1951); Appendix B.

[b] Sugarman, N., *Genetics of the Ge^{83}–As^{78} Fission Chain*, Phys. Rev. *89*: 570 (1953).

[c] Arnold, J. R. and Sugarman, N., *Short-Lived Isomeric States of Se^{83} and Ge^{77}*, J. Chem. Phys. *15*: 703 (1947).

[d] Thode, H. G., *Mass Spectrometry and Nuclear Chemistry*, Nucleonics, (No. 3), *3*: 14 (1948); relative yield normalized to mass spectrometric yields of reference g.

[e] Koch, J., Kofoed-Hansen, O., Kristensen, P. and Drost-Hansen, W., *Measurements on Radioactive Krypton Isotopes from Fission after Mass-Spectrographic Separation*, Phys. Rev. *76*: 279 (1949); relative yield normalized to mass spectrometric yields of reference g.

[f] Stehney, A. F. and Sugarman, N., *Characteristics of Br^{87}, a Delayed Neutron Activity*, Phys. Rev. *89*: 194 (1953).

[g] Glendenin, L. E., Steinberg, E. P., Flynn, K. F., Hayden, R. J. and Inghram, M. G., to be published.

[h] Reed, G. W. and Turkevich, A., *Uranium-235 Thermal Neutron Fission Yields*, Phys. Rev. *92*: 1473 (1953).

[i] Coryell, C. D., Sakakura, A. Y., and Ross, A. M., *Fission Yields of 65-day Zr^{93} and 17-hr Zr^{97}; Search for Other Zr and Nb Fission Chains*, Phys. Rev. *77*: 755 (1950).

[j] Terrell, J., Scott, W. E., Gilmore, J. S. and Minkkinen, *C.O., Yield of Mo^{99} from Fission of U^{235} and U^{238}*, Phys. Rev. *92*: 1091 (1953).

[k] Wiles, D. R. and Coryell, C. D., *Fission Yield Fine Structure in the Mass Region 99 - 106*, Phys. Rev. *96*: 696 (1954).

[l] Hardwick, W. H., *The Fission Yields of Ru^{103} and Ru^{106}*, Phys. Rev. *92*: 1072 (1953).

[m] Wahl, A. C. and Bonner, N. A., *Genetic Relationships and Fission Yields of Members of the Mass-115 Decay Chain*, Phys. Rev. *85*: 570 (1952).

relative to that of Ba^{140} is approximately ten-fold higher in the fission of U^{238} and Pu^{239} than in the fission of U^{235}. This marked difference may be used to determine the relative number of fissions due to U^{235} and U^{238} or Pu^{239} in fission mixtures such as normal uranium in fast-neutron reactors.

Some evidence has also been obtained in comparing thermal neutron with fast reactor neutron-induced fission of Pu^{239} for an increase in frequency of symmetric fission modes (trough yields) and very asymmetric modes (wing yields) as the excitation energy of the fissioning nucleus is increased.[5] Subsequent investigations showing the marked increase of trough yields and, to a lesser extent, wing yields with increasing excitation energy, have been reviewed by Spence and Ford.[12] The variations in peak-to-trough ratios observed for different fissile nuclides (column 5, Table III) are probably indicative of dif-

Table II. Summary of U^{235} Fission Yields (continued)

Fission product	Mass number	Fission yield (%) Radiometric	Mass spectrometric	Recommended total chain yield
39.5-min Sn	123			0.014
9.4-d Sn	125	0.012[a]		
2.7-yr Sb	125	0.023[a]		0.023
50-min Sn	126	0.1[a]		0.1
93-hr Sb	127	0.25[a]		0.25
		0.094[a]		
90-d Te	127[m]	0.056[o]		
		0.033[a]		
33-d Te	129[m]	0.34[n]		1.0
		0.19[a]		
30-hr Te	131[m]	0.42[n]		
		0.44[a]		
8.1-d I	131	3.0_8[n]		
		3.2 [p,q]		
		2.8[a]		
Stable Xe	131		2.8_5[r]	2.9
77.7-hr Te	132	4.4_9[n]		
		3.4 [a]		
Stable Xe	132		4.2_9[r]	4.3
63-min Te	133	4.6_8[n]		
20.8-hr I	133	6.6_2[n]		
		4.6 [a]		
5.27-d Xe	133	6.6_2[n]	6.4_8[r]	
Stable Cs	133		6.4_9[r]	6.5
44-min Te	134	7.0_8[n]		
		6.4_8[t]		
52.5-min I	134	~5.7[a]		
Stable Xe	134		7.5_4[r]	7.5
6.68-hr I	135	6.3_7[n]		
		5.6 [a]		
9.2-hr Xe	135	5.9 [a]		
3.0×10^6-yr Cs	135		6.2_8[r]	6.3
86-sec I	136	3.1[u]		
Stable Xe	136		6.1_8[r]	6.2
33-yr Cs	137		5.9_4[g]	5.9
Stable Ba	138		5.7_4[g]	5.7
85-min Ba	139	6.4[h]		6.2
		5.7_9[n]		
		6.1 [v]		
		6.3 [a]		
12.8-d Ba	140	6.3_2[q]		
		6.3[o]		
		6.1_7[a]		
Stable Ce	140		6.5_6[g]	6.4
33.1-d Ce	141	5.7[a]		5.7
Stable Ce	142		5.8_6[g]	5.9
33-hr Ce	143	5.4[a]		
Stable Nd	143		6.1_8[g]	6.2
282-d Ce	144	5.8_4[g]	6.2_2[g]	
		5.3 [a]		
Stable Nd	144		5.9_6[g]	6.0
Stable Nd	145		4.0_4[g]	4.0
Stable Nd	146		3.2_2[g]	3.2
2.6-yr Pm	147	2.6[a]		2.6
Stable Nd	148		1.7_1[g]	1.8
54-hr Pm	149	1.3[a]		1.3
Stable Nd	150		0.70_8[g]	0.71
47-hr Sm	153	0.13[w]		0.14
		0.15[a]		
23.5-min Sm	155	0.031[a]		0.031
15.4-d Eu	156	0.012[w]		0.013
		0.013[a]		
15.4-hr Eu	157	7.4×10^{-3}[a]		7.4×10^{-3}
60-min Eu	158	2×10^{-3}[a]		2×10^{-3}
18.0-hr Gd	159	$1.1_6 \times 10^{-1}$[x]		1.1×10^{-3}
		$1.0_5 \times 10^{-3}$[w]		
7.0-d Tb	161	8.3×10^{-6}[x]		7.8×10^{-6}
		$7.2_3 \times 10^{-5}$[w]		

[a] Pappas, A. C., *A Radiochemical Study of Fission Yields in the Region of Shell Perturbations and the Effect of Closed Shells in Fission*, Laboratory for Nuclear Science, Massachusetts Institute of Technology Technical Report No. 63 (September, 1953).

[n] Value from reference a corrected according to reference n.

[o] Bartholomew, R. M., Brown, F., Hawkings, R. C., Merritt, W. F. and Yaffe, L., *The Fission Yield of I^{131} in the Thermal Neutron Fission of U^{235}*, Can. J. Chem. *31*: 120 (1953).

[q] Yaffe, L., Thode, H. G., Merritt, W. F., Hawkings, R. C., Brown, F. and Bartholomew, R. M., *Determination of the Absolute Fission Yield of Ba^{140} in Thermal Neutron Fission of U^{235}*, Can. J. Chem. *32*: 1017 (1954).

[r] Wiles, D. R., Smith, B. W., Horsley, R. and Thode, H. G., *Fission Yields of the Stable and Long-Lived Isotopes of Cesium, Rubidium, and Strontium and Nuclear Shell Structure*, Can. J. Phys. *31*: 419 (1953); relative yield normalized to mass spectrometric yields of reference g.

[g] Katcoff, S. and Rubinson, W., *Yield of Xe^{131} in the Thermal Neutron Fission of U^{235}*, Phys. Rev. *91*: 1458 (1953).

[t] Yaffe, L., Day, A. E. and Greer, B. A., *The Fission Yield of Te^{134}*, Can. J. Chem. *31*: 48 (1953).

[u] Stanley, C. W. and Katcoff, S., *The Properties of 86-Second I^{136}*, J. Chem. Phys. *17*: 653 (1949).

[v] Grummitt, W. E., Gueron, J., Wilkinson, G. and Yaffe, L., *The Fission Yields of Ba^{139} and Ba^{140} in Neutron Fission of U^{233} and U^{235}*, Can. J. Research, *25B*: 364 (1947).

[w] Petrow, H. G. and Rocco, G., *Fission Yield of Gd^{159} and Tb^{161}*, Phys. Rev. *96*: 1614 (1954).

[x] Freiling, E. C., Bunney, L. R. and Ballou, N. E., *Identification of Gadolinium and Terbium Radioisotopes as Fission Products of U^{235}*, Phys. Rev. *96*: 102 (1954).

ferences in the excitation energies of the fissioning nuclei.

The high precision attainable in the determination of relative isotopic abundances by mass spectrometry may be utilized in studying large neutron-capture cross sections among fission products. Such determinations were made, for example, by Inghram, *et al.*,[14] and large cross sections were indicated for Sm^{149}, Sm^{151}, and Gd^{157}. The variation of the Xe^{136} abundance in fission-produced xenon as a function of neutron flux was correlated with the 3.5×10^6 barn cross section of Xe^{135} in the work of Thode and coworkers.[15] A comparison of their ratio of Cs^{133} to Cs^{137} at low flux with our results at higher flux (unpublished) also indicates a probable cross section of about 3000 barns for Xe^{133}. This is as yet unverified by direct measurement on Xe^{133}.

Radiochemical studies have resulted in the identi-

Table III. Comparison of Mass Distributions

Fissile nuclide	Average mass number at half-height		Mass width at half-height	Ratio of peak-to-trough yields
	Light group	Heavy group		
Th^{232}	92	139	14	115
U^{233}	94	138	14	390
U^{235}	95	139	15	650
U^{238}	98	139	16	200
Pu^{239}	99	138	16	150

fication of radioactive isotopes of 36 elements (zinc to terbium) covering the mass range 72 to 161 as products of binary fission. In addition, the possibility of fission into more than two fragments has been investigated[16] by searching for lighter products of uranium fission in the mass range 35 to 60. Positive identification of fission products in this mass range was not made, but upper limits of the order of 10^{-4}% fission yield were established. Fission into two heavy fragments and one light fragment in the mass region 4 to 13 based on studies with cloud chambers, photographic plates, and counters have been reported to occur with a frequency of about one per cent of binary fissions (reviewed by Whitehouse).[9] A review of the data on such ternary fission was also given by de Laboulaye, *et al.*,[17] who investigated the short-range particles (ternary products?) in a cloud chamber and interpreted them as probably knock-on atoms. The frequency of occurrence was estimated as only 1 ± 3 per 1000 binary fissions. Only a few nuclides in this mass range are suitable for radiochemical investigations. A radiochemical search for Be^7 was made by Cook[18] who set an upper limit of 10^{-5}% for the yield in uranium fission. Bendt and Scott[19] have recently reported a delayed neutron period with a half-life of 0.15 second and a fission yield of 0.05% for delayed neutron emission in U^{235} fission. They postulate the assignment of the period to 0.17-sec Li^9 formed as a light fragment in ternary fission. If this is so, the fission yield of 0.05% must be considered as a lower limit since the branching ratio for neutron emission in the decay of Li^9 is unknown. We have investigated[20] the possibility of the formation of 2.5×10^6 yr Be^{10} in ternary fission by radiochemical isolation of beryllium from an intense source of U^{235} fission products. An upper limit of 4×10^{-4}% for the fission yield was established. The radiochemical investigations indicate that ternary fission giving rise to fragments of mass greater than that of the alpha particle is extremely rare if it occurs at all. It should be noted that the upper limit for the fission yield of Be^{10} is inconsistent with the assignment of the 0.15-second delayed neutron period to Li^9. It appears more likely that this previously unresolved decay period should be ascribed to a normal product of binary fission.

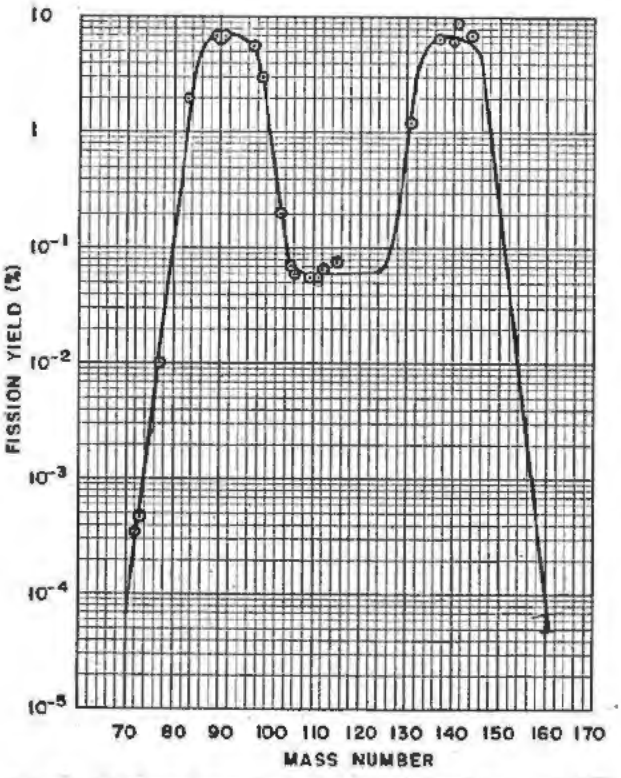

Figure 1. Yield-mass curve for fast neutron-induced fission of Th^{232}

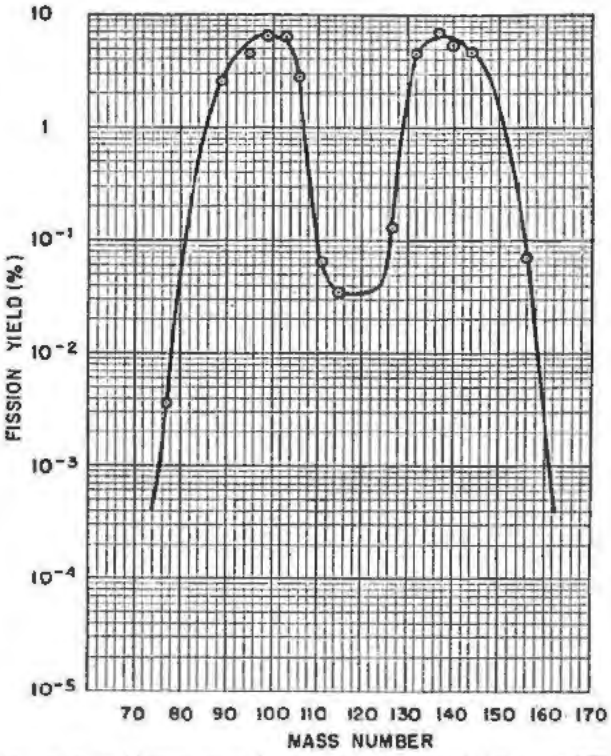

Figure 2. Yield-mass curve for fast neutron-induced fission of U^{238}

CHARGE DISTRIBUTION

The problem of nuclear charge distribution in low-energy fission may be considered to have two aspects: (1) the determination of the most probable mode of charge division for a given mass split, and (2) the distribution function for primary formation (independent yield) about the most probable nuclear

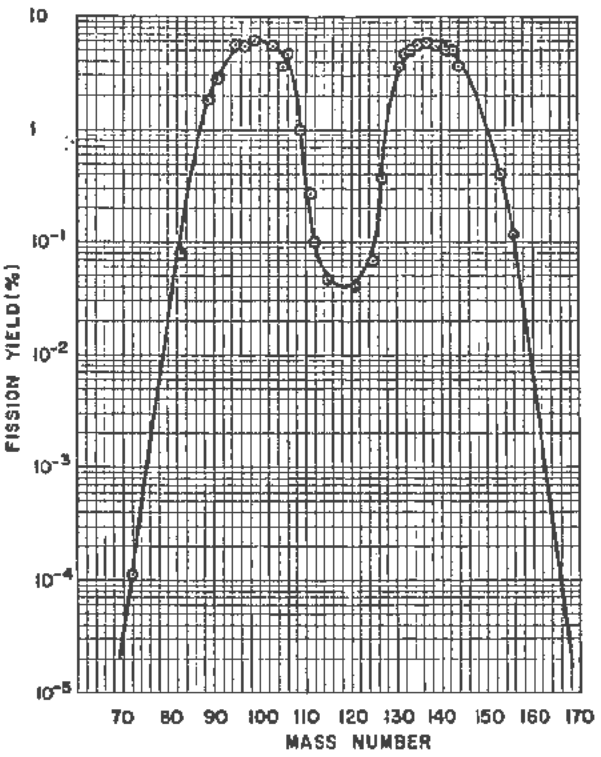

Figure 3. Yield-mass curve for slow neutron-induced fission of Pu^{239}

charge (atomic number) among fission products of the same mass number. The data of quantitative value in this problem are independent fission yields along chains and fission yields of shielded nuclides. The latter data are particularly useful since shielded nuclides are preceded by a stable nuclide in the fission chain and should therefore occur in fission only by direct formation as a primary fission product. Experimentally it is difficult to obtain accurate independent yield data for members of a decay chain. Problems of rapid and complete chemical separation of the nuclide of interest to prevent formation by beta decay of ancestors can introduce large uncertainties in some cases.

It was shown by Glendenin *et al.*[21,22] that of the various suggestions for the most probable division of charge in fission, the available fission yield data were most consistent with an empirical hypothesis that the most probable mode is that which gives rise to equal charge displacements from stability (effective chain lengths) for complementary fission product chains. It was postulated that the distribution about the most probable charge is a symmetrical function applicable to all mass splits and all fissile nuclides.

From the equal charge displacement hypothesis,

$$Z_A - Z_P = Z_A^* - Z_P^* \qquad (1)$$

where Z_A and Z_A^* are the most stable charges for the mass numbers A and A^* of the complementary fission product chains, and Z_P and Z_P^* are the most probable charges of the primary fission products of mass numbers A and A^*. The sum of the primary

Table IV. Values of Z_A

Shell group	A	Z_A	$\delta Z_A/\delta_A$
$Z < 50,\ N < 50$	70	31.2	0.38
	90	38.9	
$Z < 50,\ N > 50$	87	38.6	0.39
	120	51.7	
$Z > 50,\ N < 82$	116	49.0	0.35
	140	57.4	
$Z < 64,\ N > 82$	137	57.8	0.35
	158	65.3	
$Z > 64,\ N > 82$	155	63.6	0.37
	165	67.3	

charges Z_P and Z_P^* must equal the charge of the fissioning nucleus, Z_F. The complementary fission product masses A and A^* are related by

$$A + A^* = A_F - \bar{\nu} \qquad (2)$$

where A_F is the mass number of the fissioning nucleus and ν is the average number of neutrons emitted per fission. The equation for the most probable charge of a fission product of mass A is then

$$Z_P = Z_A - (1/2)\ (Z_A + Z_A^* - Z_F) \qquad (3)$$

Pappas[23] presented a modification of the equal charge displacement hypothesis which attempts to account for the discontinuities in Z_A at shell closures. In this treatment values of Z_A given by Coryell[24] were used. These values for the mass region of interest in fission are tabulated in Table IV with values of $\partial Z_A/\partial A$ for convenience in interpolation. For mass numbers in the vicinity of shell closures there is an uncertainty in the Z_A value to be used in Eq. (3). This is indicated in column 2 of Table IV by the occurrence of

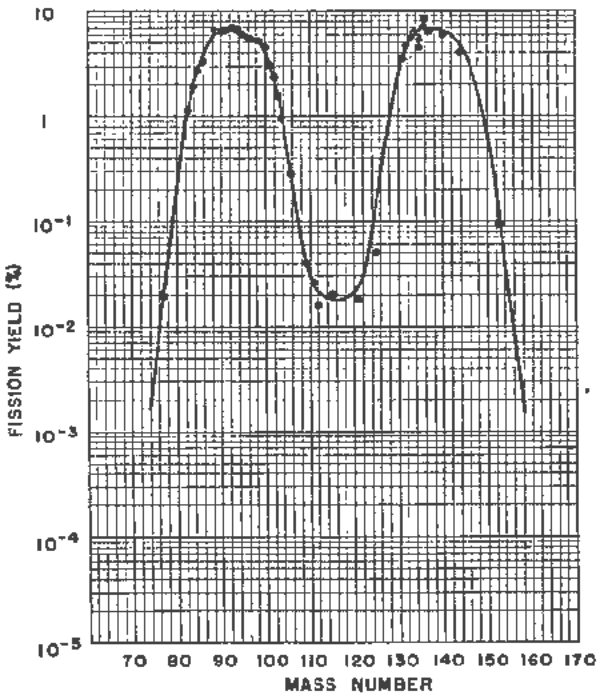

Figure 4. Yield-mass curve for slow neutron-induced fission of U^{233}

mass numbers 87–90, 116–120, 137–140, and 155–158 in two shell groups. In these mass regions we use the average of the Z_A values from the two groups. For these calculations $\bar{\nu}$ was taken as 2.5 for Th^{232}, U^{233}, and U^{235}; 2.9 for Pu^{239}; and 3.0 for Cm^{242}.

A summary of the experimental data on independent fission yields is given in column 3 of Table V. It has been suggested that certain nuclides may be preferentially formed in fission giving rise to regions of fine structure in the yield-mass curve (see below). For the purposes of an analysis of charge distribution, the "excess" yields of such nuclides are considered anomalous, and a "normal" chain yield (column 4 of Table V) is used to calculate the fraction of chain yield (column 5) represented by the observed independent fission yield. These "normal" chain yields represent the yields which would have occurred without the extra contribution of a specific preferred member of the chain. The "normal" distributions in the regions of fine structure for U^{235}, U^{233}, and Cm^{242} fission are indicated by dotted lines in Figs. 7, 8, and 9. The uncertainties in the Z-Z_P values indicated in column 6 reflect the corresponding uncertainties in Z_A values near shell closures. The data of Table V were used to construct the charge distribution curve of Fig. 6.

It has been shown[25] that the charge distribution curve for 14-Mev neutron-induced fission of U^{235} is parallel to that for low-energy fission of U^{235} with the most probable charge for a given mass split shifted

Table V. Summary of Independent Fission Yields

Fission product	*Fissile nuclide*	*Independent fission yield (%)*	*"Normal" chain yield (%)*	*Fraction of chain yield*	*Position in chain ($Z - Z_P$)*
91-min As^{78}	U^{235}	1.8×10^{-5}[a]	0.020	0.09	1.9 ± 0.1
36-hr Br^{88}	U^{235}	3.5×10^{-3}[b] 4.1×10^{-3}[c]	0.25	1.5×10^{-4}	2.6
19.5-d Rb^{86}	U^{235}	3.1×10^{-6}[d] 2.5×10^{-5}[e]	2.1	1.3×10^{-5}	3.0
	Pu^{239}	1.1×10^{-4}[e]	0.7	1.6×10^{-4}	2.7
65-hr Y^{90}	U^{235}	$<2.8 \times 10^{-8}$[e]	5.8	$<4.8 \times 10^{-4}$	3.4 ± 0.2
23-hr Nb^{95}	U^{235}	5.7×10^{-4}[e]	6.3	9.0×10^{-5}	2.5 ± 0.4
210-d Rh^{102}	U^{235}	$<5 \times 10^{-7}$[e]	2.9	$<1.7 \times 10^{-7}$	4.0
52.5-min I^{134}	U^{233}	1.0[d]	4.8	0.21	1.2
9.2-hr Xe^{135}	U^{235}	0.31[f] 0.16[g]	5.3	0.044	1.8
13.7-d Cs^{136}	U^{235}	6.2×10^{-3}[d] 5.7×10^{-3}[e]	5.7	1.0×10^{-3}	2.4
	Pu^{239}	8.9×10^{-2}[d] 1.8×10^{-2}[e]	5.9	0.015 3.1×10^{-3}	2.1
	U^{233}	0.12[h]	5.9	0.020	2.0
	Th^{232}	$<1.7 \times 10^{-3}$[i]	6.0	$<2.8 \times 10^{-4}$	2.8
	Cm^{242}	0.80[j]	7.0	0.11	1.5
40-hr La^{140}	U^{235}	<0.2[k]	6.4	<0.03	2.5 ± 0.4
3.7-hr La^{141}	U^{235}	..	..	0.02[l]	1.8
5.3-d Pm^{148}	U^{235}	$<2 \times 10^{-4}$[e]	1.8	$<1.1 \times 10^{-4}$	2.8

[a] Sugarman, N., *Genetics of the Ge^{78} - As^{78} Fission Chain*, Phys. Rev. *89*: 570 (1953).

[b] Feldman, M. H., Glendenin, L. E. and Edwards, R. R., *Identification and Yield of 34-hr Br^{89} in Fission*, paper 62 in C. D. Coryell and N. Sugarman, *Radiochemical Studies: The Fission Products*, National Nuclear Energy Series, Div. IV, Vol. 9, McGraw-Hill Book Co., New York (1951).

[c] Cook, G. B., personal communication.

[d] Glendenin, L. E., *The Distribution of Nuclear Charge in Fission*, Laboratory for Nuclear Science, Massachusetts Institute of Technology, Technical Report No. 35 (December, 1949).

[e] Swartout, J. A. and Sullivan, W. H., *Absence of Long-Lived Rhodium in Fission. II. Upper Limit to the Fission Yield of 210-d Rh^{102}*, paper 118 in C. D. Coryell and N. Sugarman, *Radiochemical Studies: The Fission Products*, National Nuclear Energy Series, Div. IV, Vol. 9, McGraw-Hill Book Co., New York (1951).

[f] Hoagland, E. J. and Sugarman, N., *Independent Fission Yield of 9.2-hr Xe^{135}*, ibid, paper 147.

[g] Brown, F. and Yaffe, L., *The Independent Yield of Xe^{135} Produced in the Fission of Natural Uranium by Pile Neutrons*, Can. J. Chem. *31*: 242 (1953).

[h] Glendenin, L. E., unpublished work.

[i] Turkevich, A. and Niday, J. B., *Radiochemical Studies of the Fission of Th^{232} with Pile Neutrons*, Phys. Rev. *84*: 52 (1951).

[j] Steinberg, E. P. and Glendenin, L. E., *Mass Distribution in the Spontaneous Fission of Cm^{242}*, Phys. Rev. *95*: 431 (1954).

[k] Sugarman, N., *Independent Fission Yield of La^{140}*, paper 170 in C. D. Coryell and N. Sugarman, *Radiochemical Studies: The Fission Products*, National Nuclear Energy Series, Div. IV, Vol. 9, McGraw-Hill Book Co., New York (1951).

[l] Ford, G. P. and Stanley, C. W., *The Fraction of the Mass 141 Chain Formed Independently as La^{141} in the Thermal Neutron Fission of U^{235}*, AECD-3551 (August 20, 1953).

toward stability, i.e., a smaller neutron-to-proton ratio for the primary fragments. Thus, it appears that for all fissile nuclides thus far investigated a single charge distribution curve is applicable over a considerable range of excitation energy (0 to 14 Mev). (In very high-energy fission, e.g., 190-Mev deuteron fission of bismuth,[26] the division of nuclear charge is apparently different, the most probable charge of the primary fragments being that which maintains the neutron-to-proton ratio of the fissioning nucleus. This may indicate that at very high energies the fission process takes place too rapidly to permit a rearrangement of charge.)

It is interesting to note that in a few cases apparent independent yields were observed which were too high to be in accord with the charge distribution curve. In these cases it was suggested[21,22] that isomerism was responsible for the discrepancies. Subsequent identification of short-lived isomers in Ge^{77} and Se^{83} by Arnold and Sugarman[27] and in Te^{133} by Pappas[23] corroborated these predictions.

CLOSED SHELL EFFECTS

The early radiochemical investigations[5,6] of slow neutron-induced fission indicated that the yield-mass curves were rather smooth. In fact, when particular determinations did not fit the smooth curve, errors arising from a failure to achieve interchange in the radiochemical analysis, the presence of an isomeric state, or difficulties in the measurement of the disintegration rate were suspected and generally found. The concept of a smooth relationship between fission yield and mass number proved extremely useful in establishing mass assignments and half-lives of long-lived fission products. Some perturbations in the yield-mass curve are, of course, expected as a result of known delayed neutron emission, but these are of the order of 0.5% in fission yield or less.[5] Marked deviations from a smooth curve were definitely established, however, by Thode and co-workers[28] in mass spectrometric determinations of the relative abundances of krypton and xenon isotopes produced in U^{235} fission and by Stanley and Katcoff[29] in radiometric determinations of the yield of I^{136} in the fission of U^{233}, U^{235}, and Pu^{239}.

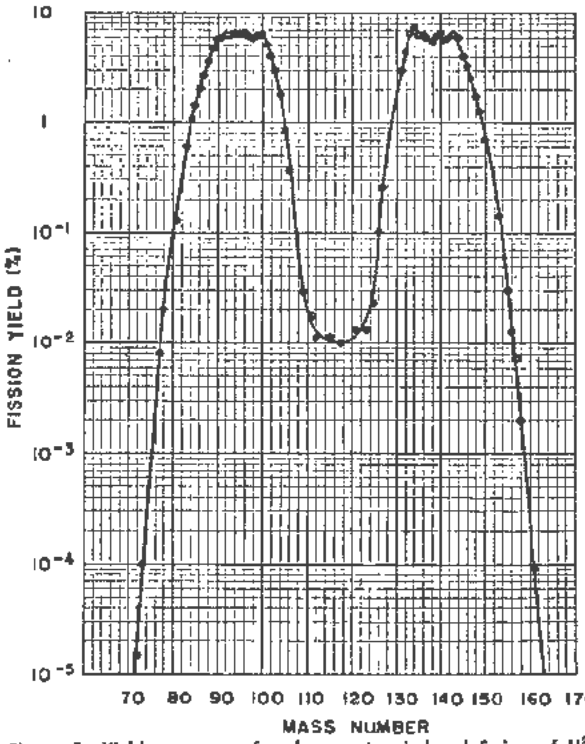

Figure 5. Yield-mass curve for slow neutron-induced fission of U^{235}

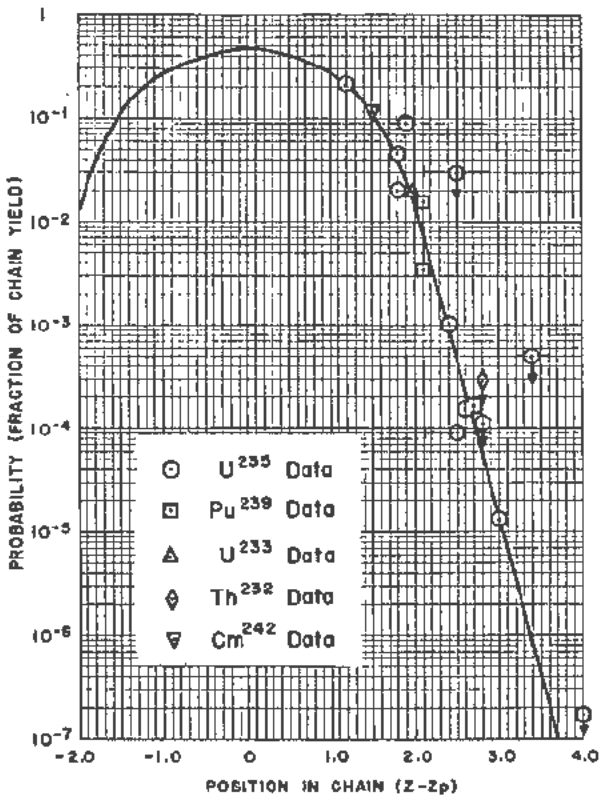

Figure 6. Charge distribution curve

A proposal to explain this fine structure in the mass distribution was made by Glendenin[22] on the basis of the stability of nuclear closed shells of 50 and 82 neutrons. Nuclei which contain 51 or 83 neutrons, i.e., one neutron more than the closed shell, have abnormally low binding energies for the odd neutron. It was postulated that a primary fission product (which has already emitted the usual number of prompt neutrons) containing one neutron in excess of a closed shell may emit this neutron in preference to a beta particle or gamma ray. This process of additional prompt neutron emission would result in perturbations in fission yields near closed shells, since the loss in yield from a given chain would not always be exactly compensated by the gain in yield from the chain of one higher mass number. Calculations based on this mechanism and utilizing the primary yields along fission chains as given by the charge distribu-

tion function indicated a fine structure pattern for the krypton and xenon isotopes and an abnormally low yield for I^{130} in qualitative agreement with the experimental observations.

In an attempt to account more quantitatively for the fine structure observed in mass spectrometric investigations, Wiles[30,15] suggested that fragments containing 82 neutrons are favored (i.e., occur in abnormally high yield) in the fission process, in addition to the postfission effect described above. If such a preference exists in fission in the 82-neutron shell region (around mass 134), a reflection must appear in the complementary region around mass 100. This possibility was investigated by Glendenin, *et al.*[31] in mass spectrometric studies of the yields of isotopes of zirconium and molybdenum in the fission of U^{235}. It was indeed observed that the fission yield of Mo^{100} is abnormally high. A further preference for a 50-proton configuration has been proposed by Wiles and Coryell[32] on the basis of radiometric studies of 15-Mev deuteron-induced fission of U^{235} and U^{238}, but this is not apparent in low-energy neutron-induced fission.

It was shown by Pappas[23] on the basis of neutron binding energy systematics that the concept of additional prompt neutron emission should be extended to include the third, fifth, and perhaps seventh neutrons outside closed shells. The perturbations in fission yield resulting from this effect in U^{235} fission were estimated and combined with known delayed neutron yields to give the fine structure pattern expected for the mass region 130–150. These calculated yields were in reasonably good agreement with available yield data except in the mass region 134–136. The discrepancy in this region was ascribed to the 82-neutron preference effect, and thus a plausible interpretation of the fine structure in the heavy group was evolved in terms of various closed shell effects.

In order to investigate fine structure in fission in greater detail, mass spectrometric determinations of fission yields for U^{235}, U^{233}, and Pu^{239} have been undertaken. Preliminary results for U^{235} and U^{233} have been published,[31,33] and the recently completed results for U^{235} are described above and given in Table II (reference *g*). The data of Table II, column 4, are presented in Fig. 7 with a few radiometric yields for mass numbers not determined mass spectrometrically. Corrections for the effects of delayed neutron emission (see below) are indicated by arrows. Since there are no important shell closures which might give rise to yield perturbations in the region of the light group peak, the high yield at Mo^{100} is ascribed to preferential formation in fission. (Although the neutron-capture cross section of Mo^{99} is unknown, it is extremely unlikely that it is large enough to account for the high yield at Mo^{100}.) It is significant that mass 100 is formed in U^{235} fission as the complement of 82-neutron containing fragments in the mass region 133–134. Mass spectrometric studies[32] of slow neutron-induced fission of U^{233} (Fig. 8) and radiometric studies[34,35] of the spontaneous fission of Cm^{242} (Fig. 9) and Cf^{252} also indicate fine structure around mass numbers 99, 105, and 114, respectively, complementary in each case to the mass region of the 82-neutron shell. These results strongly suggest a nuclear structure preference effect in fission. The approximate magnitude of this effect is indicated in Figs. 7, 8, and 9 by a solid line through the points designated by diamonds. The latter are obtained by subtraction of a hypothetical "normal" curve (dotted line) from the observed data. Corroborative evidence for this preference effect in fission, based on fission fragment velocity distributions, was recently reported by Leachman and Schmitt.[36]

Other regions of fine structure are also apparent in Fig. 7, particularly in the heavy group. The pronounced effect in the region of the 82-neutron shell (masses 133–135) and the pattern of yields at higher masses (136–144) are consistent with expectations from nuclear structure preference and additional prompt neutron emission as discussed previously. Similar effects in the region of the 50-neutron shell may be responsible for fine structure[37] in the mass region 83–86 and the dip in the light group curve at masses 91 and 92. Further mass spectrometric studies of U^{233} and Pu^{239} fission yields are now in progress to provide additional data on closed shell effects in fission.

An interpretation of delayed neutron emission among the fission products as a closed shell effect was given by Mayer[38] in terms of the abnormally low binding energy of the first neutron outside the 50- and 82-neutron shells. This was extended by Pappas[23] to include the third and fifth neutrons beyond closed shells. This interpretation is consistent with the known assignments[5] of the 22-sec I^{137} and 55-sec Br^{87} and the probable assignment of the 4.5-sec Br^{89}. It is also the basis for postulating assignments of the 1.5-sec and 0.4-sec emitters to Sb^{135} and As^{85}, respectively. Corrections for the effects of these delayed neutron emitters are shown in Fig. 7. The argu-

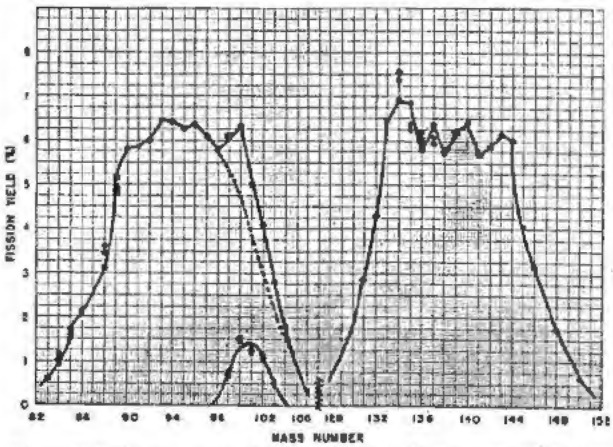

Figure 7. Yield-mass curve showing closed shell effects in U^{235} fission. Mass spectrometric data are indicated by circles, radiometric data by squares

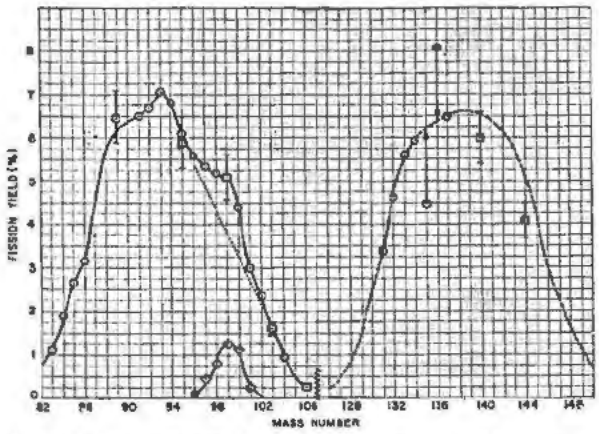

Figure 8. Yield-mass curve showing nuclear structure preference effect in U^{233} fission. Mass spectrometric data are indicated by circles, radiometric data by squares. Arrows indicate approximate correction for neutron capture in Xe^{132}

ments by Pappas based on neutron binding energy systematics near closed shells indicate that there should be more delayed neutron emitters (fission products containing closed shell plus 2, 4, and 6 neutrons) than the six periods which have been resolved from decay curves. Fission products that fall in this category are as follows: Ga^{83}, As^{87}, Br^{91}, Rd^{93}, In^{133}, Sb^{137}, 2.6-sec I^{139}, I^{141}, Cs^{141}, and Cs^{143}. Estimations of fission yields and branching ratios for neutron emission indicate that most of these short-lived nuclides are contributing to some extent to the observed delayed neutron emission in U^{235} fission. The effect of the longer average decay chain lengths in

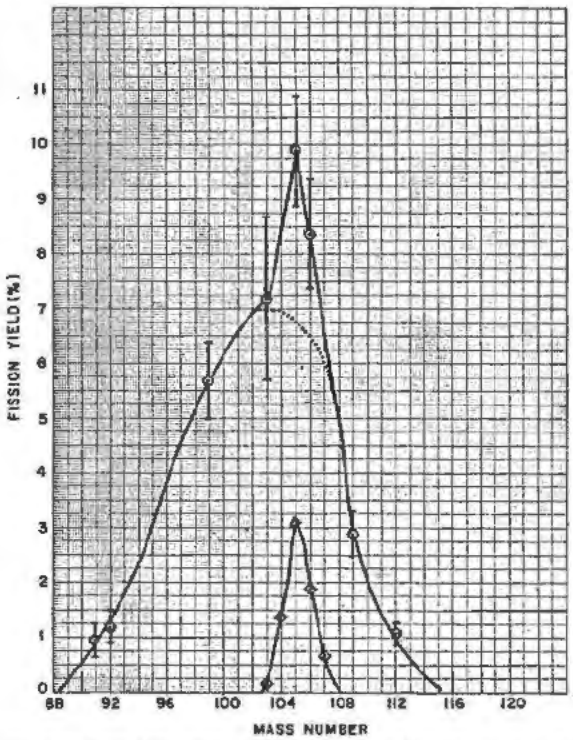

Figure 9. Mass distribution in the light group showing nuclear structure preference effect in spontaneous fission of Cm^{242}

U^{235} and Th^{232} fission is to increase the yields of many of these nuclides, resulting in an estimated total delayed neutron emission 50 to 100% greater than in U^{235} fission. Recent experimental data[30] indicate a ratio of 2.9 for delayed neutron emission in U^{238} relative to U^{235}.

SUMMARY

A considerable body of empirical data has been accumulated on the low-energy fission process, and theoretical treatments of the problem have not yet been successful in interpreting the detailed features of the mass and charge distributions observed. However, a plausible phenomenological picture may be given in terms of "normal" asymmetric splitting into two main groups of products on which is superimposed the preferential formation of fragments containing closed shells of 50 and 82 neutrons. Further perturbations in the mass distribution of the products result from the emission of additional prompt and delayed neutrons from particular products near closed shells. The most probable nuclear charges for complementary fission fragments are apparently those which result in an equal displacement of the products from the most stable charges for the mass numbers involved. An empirical curve for the distribution of charge around the most probable one appears generally applicable for all fissile nuclides over a considerable range of excitation energies.

REFERENCES

1. Hahn, O. and Strassmann, F., *Uber den Nachweis und das Verhalten der bei der Bestrahlung des Urans mittels Neutronen entstehenden Erdalkalimetalle,* Naturwiss., *27*: 11 (1939).
2. Hahn, O. and Strassmann, F., *Weitere Spaltprodukte aus der Bestrahlung des Urans mit Neutronen,* ibid., *27*: 529 (1939).
3. Moussa, A. and Goldstein, L., *Physique Nucleaire. – Sur les Isotopes Radioactif du Brome Formes dans la Rupture Nucleaire de l'Uranium,* Compt. rend., *212*: 986 (1941).
4. Anderson, H. L., Fermi, E. and Grosse, A. V., *Branching Ratios in the Fission of Uranium (235),* Phys. Rev., *59*: 52 (1941).
5. Coryell, C. D. and Sugarman, N., Eds., *Radiochemical Studies: The Fission Products,* National Nuclear Energy Series, Division IV, Vol. 9, Appendix B, McGraw-Hill Book Co., Inc., New York (1951).
6. Grummitt, W. E. and Wilkinson, G., *Fission Products of U^{233},* Nature, *161*: 520 (1948).
7. Turkevich, A. and Niday, J. B., *Radiochemical Studies of the Fission of Th^{232} with Pile Neutrons,* Phys. Rev. *84*: 52 (1951).
8. Keller, R. N., Steinberg, E. P. and Glendenin, L. E., *Yields of Fission Products from U^{238} Irradiated with Fission Spectrum Neutrons,* Phys. Rev., *94*:969 (1954).
9. Whitehouse, W. J., *Nuclear Fission,* in *Progress in Nuclear Physics,* Vol. 2, p. 120, Pergamon Press, Ltd., London (1952).
10. *Bibliography on Fission,* Atomic Energy Research Establishment, Harwell, Berks., England, Inf./Bib./76, July, 1951; Inf./Bib. 76, Suppl. 1, Oct. 1952.
11. Huizenga, J. R., Manning, W. M. and Seaborg, G. T., *The Actinide Elements,* National Nuclear Energy Series,

Division IV, Vol. 14A, Chap. 20, p. 839, McGraw-Hill Book Co., Inc., New York (1954).

12. Spence, R. W. and Ford, G. P., *High Energy Fission*, Ann. Rev. Nuclear Sci., Vol. 2, p. 399, Annual Reviews, Inc., Stanford, Calif. (1953).
13. Glendenin, L. E. and Steinberg, E. P., *Fission Radiochemistry (Low Energy Fission)*, Ann. Rev. Nuclear Sci., Vol. 4, p 69, Annual Reviews, Inc., Stanford, Calif. (1954).
14. Inghram, M. G, Hayden, R. J. and Hess, D. C., *U^{235} Fission Yields in the Rare Earth Region*, Phys. Rev., *79*: 271 (1950).
15. Wiles, D. R., Smith, B. W., Horsley, R. and Thode, H. G., *Fission Yields of the Stable and Long-Lived Isotopes of Cesium, Rubidium, and Strontium and Nuclear Shell Structure*, Can. J. Phys., *31*: 419 (1953).
16. Metcalf, R. P., Seiler, J. A., Steinberg, E. P. and Winsberg, L., *Search for Triple Fission*, Papers 47-51 in C. D. Coryell and N. Sugarman, *Radiochemical Studies: The Fission Products*, National Nuclear Energy Series, Division IV, Vol. 9, McGraw-Hill Book Co., Inc., New York (1951).
17. de Laboulaye, H., Tzara, C. and Olkowsky, J., *Sur le phenomene de tri-partition a troisieme fragment de court parcours*, Compt. rend., *237*: 155 (1953); *Quelques etudes sur la fission de l'uranium a l'aide d'une chambre de Wilson autocommande*, J. de phys. radium, *15*: 470 (1954).
18. Cook, G. B., *Search for Be^7 in Uranium Fission*, Nature *169*: 622 (1952).
19. Bendt, P. J. and Scott, F. R., *Short-Period Delayed Neutrons from Fission*, Phys. Rev., *97*: 744 (1955).
20. Flynn, K. F., Glendenin, L. E. and Steinberg, E. P., to be published.
21. Glendenin, L. E., Coryell, C. D. and Edwards, R. R., *Distribution of Nuclear Charge in Fission*, Paper 52 in C. D. Coryell and N. Sugarman, *Radiochemical Studies: The Fission Products*, National Nuclear Energy Series, Division IV, Vol. 9, McGraw-Hill Book Co., Inc., New York (1951).
22. Glendenin, L. E., *The Distribution of Nuclear Charge in Fission*, Laboratory for Nuclear Science, Massachusetts Institute of Technology, Technical Report No. 35 (December, 1949).
23. Pappas, A. C., *A Radiochemical Study of Fission Yields in the Region of Shell Perturbations and the Effect of Closed Shells in Fission*, Laboratory for Nuclear Science, Massachusetts Institute of Technology, Technical Report No. 63 (September, 1953).
24. Coryell, C. D., *Beta Decay Energetics*, Annual Review of Nuclear Science, Vol. 2, p. 305, Annual Reviews, Inc., Stanford, Calif. (1953).
25. Ford, G. P., *Nuclear Charge Distribution in U^{235} 14-Mev Neutron Fission*, AECD-3597 (1953).
26. Goeckerman, R. H. and Perlman, I., *High Energy Induced Fission of Bismuth and Lead*, Phys. Rev., *76*: 628 (1949).
27. Arnold, J. R. and Sugarman, N., *Short-Lived Isomeric States of Se^{83} and Ge^{77}*, J. Chem. Phys., *15*: 703 (1947).
28. Thode, H. G. and Graham, R. L., *A Mass Spectrometric Investigation of the Isotopes of Xenon and Krypton Resulting from the Fission of U^{235} by Thermal Neutrons*, Can. J. Research, *25A*: 1 (1947); Macnamara, J., Collins, C. B. and Thode, H. G., *The Fission Yield of Xe^{135} and Fine Structure in the Mass Yield Curve*, Phys. Rev., *78*: 129 (1950).
29. Stanley, C. W. and Katcoff, S., *The Properties of 86-Second I^{135}*, J. Chem. Phys., *17*: 653 (1949).
30. Wiles, D. R., *Fission Yields of Cesium, Rubidium, and Strontium Isotopes and their Relation to Fine Structure in Fission*, M.Sc. Thesis, McMaster University, Hamilton, Ontario (September, 1950).
31. Glendenin, L. E., Steinberg, E. P., Inghram, M. G. and Hess, D. C., *Nuclear Structure in Fission*, Phys. Rev. *84*: 860 (1951).
32. Wiles, D. R. and Coryell, C. D., *Fission Yield Fine Structure in the Mass Region 99–106*, Phys. Rev., *96*: 696 (1954).
33. Steinberg, E. P., Glendenin, L. E., Inghram, M. G. and Hayden, R. J., *Fine Structure in U^{238} Fission*, Phys. Rev. *95*: 867 (1954).
34. Steinberg, E. P., and Glendenin, L. E., *Radiochemical Investigation of the Spontaneous Fission of Cm^{242}*, Phys. Rev., *95*: 431 (1954).
35. Glendenin, L. E. and Steinberg, E. P., *Fission Yields in Spontaneous Fission of Cf^{252}*, Journal of Inorganic and Nuclear Chemistry, *1*: 45 (1955).
36. Leachman, R. B. and Schmitt, H. W., *Fine Structure in the Velocity Distributions of Slowed Fission Fragments*, Phys. Rev., *96*: 1366 (1954).
37. Fleming, W., Tomlinson, R. H. and Thode, H. G., *The Fission Yields of the Stable and Long-Lived Isotopes of Xenon, Cesium, and Krypton in Neutron Fission of U^{235}*, Can. J. Physics, *32*: 522 (1954).
38. Mayer, M. G., *On Closed Shells in Nuclei*, Phys. Rev., *74*: 235 (1948).
39. Keepin, G. R., *et al.*, P/831, *Delayed Neutrons*, Volume 4, Session 16A-3, these Proceedings.

Spontaneous Fission Correlations

By A. Ghiorso,* USA

Spontaneous fission was first observed by Flerov and Petrzhak[1] in 1940 following a suggestion by Bohr and Wheeler.[2] By dint of great effort these pioneering experimenters were able to show that U^{238} fissioned spontaneously with a half-life of the order of 10^{16} years, about a factor of 10^6 times faster than predicted. In the next ten years the half-lives of other nuclides for this process were determined by various groups but not enough information was accumulated to indicate any specific type of correlation as being correct.

Measurements of spontaneous fission half-lives in the transuranium region have in the last few years increased in number so markedly that several sorts of systematization have become possible. Seaborg[3] and Whitehouse and Galbraith[4] made the initial steps in this direction when they pointed out that in the case of even-even nuclides the half-life for spontaneous fission seemed to decrease with an exponential dependence on the value of Z^2/A while nuclides with an odd number of nucleons decayed by this process at a much slower rate. With the limited amount of data available at this time a plot of the logarithm of the partial spontaneous fission half-life against Z^2/A resulted in a fairly straight line. It was also noted[3] that this line when extrapolated to the region of instantaneous rate (that is, half-life of the order of 10^{-20} sec) gives a value of about 47 for Z^2/A, which corresponds with the predicted limiting value of Z^2/A. In a later paper Ghiorso *et al.*[5] pointed out that certain even-even nuclides (U^{234}, U^{232}, and possibly Th^{230}) exhibited substantial deviations in the direction of rates slower than predicted by the Z^2/A line.

Following these communications Kramish[6] published a correlation of the ratio of spontaneous fission to alpha half-lives versus Z^2/A. This plot was based on the thesis that spontaneous fission and alpha decay could be regarded as closely related but competitive decay processes for heavy nuclei. The nature of this competition was demonstrated by connecting consecutive alpha decay products familywise and it was thus shown that the spontaneous fission mode of decay becames more prominent as Z^2/A increases.

As more data were accumulated on the spontaneous fission rates of other heavy nuclides it became evident that, although the parameter Z^2/A accounted broadly in this manner for the variation in half-life over the range of Z values, for a given value of Z this parameter did not account for the variation of half-life with A. In 1954 Huizenga[7] pointed out that for a given value of Z the half-life goes through a maximum as A varies and on the basis of the data for isotopes of uranium it was postulated that the maximum in the spontaneous fission half-lives of even-even nuclides was analogous to the corresponding variation in beta stability. It was further suggested that the shorter spontaneous fission half-lives beyond the maximum are possibly a result of the greater deformation of the larger A nuclides; an ellipsoidal deformation presumably might increase the decay rate due to the improvement in penetration through the thinner barrier.[8] Later in the same year Studier and Huizenga[9] revived the Kramish plot of the ratio of the half-lives for spontaneous fission and alpha decay versus Z^2/A except that instead of connecting consecutive alpha decay products they were able to show a more consistent relationship by correlating nuclides differing by two Z units and six A units.

It is the purpose of this paper to call attention to a new parameter which possibly has a very pronounced influence on the variation of spontaneous fission half-lives with change in A. The effect observed is that the spontaneous fission half-lives for those even-neutron isotopes of elements 98 and 100 which have more than 152 neutrons are found to progressively decrease at a rate much faster than observed before. It has been shown that there is very good evidence from alpha decay data for a subshell at 152 neutrons.[10] At the time this paper was written the evidence for such a subshell was based entirely on the variation of alpha energies for the even-neutron isotopes of californium. Recently the nuclides Fm^{250} (fermium, element 100) and Fm^{252} have been produced in this laboratory[11] and their alpha energies when compared with that for Fm^{254} show similar variations. The basis for a subshell at 152 neutrons is thus seen to be rather firm. This possible correlation of the abrupt change in spontaneous fission half-lives with this subshell shows promise as an empirical method of predicting the spontaneous fission properties of unknown isotopes.

The principal new data that lead one to postulate this type of correlation consist of the recent measurement of the spontaneous fission half-lives of Cf^{254} and Fm^{256}. The isotope Cf^{254} has been isolated[12] by means of the electron-capture branching of the 1.5-day beta emitter, E^{254m} (einsteinium, element 99). A

*Radiation Laboratory, University of California, Berkeley, California.

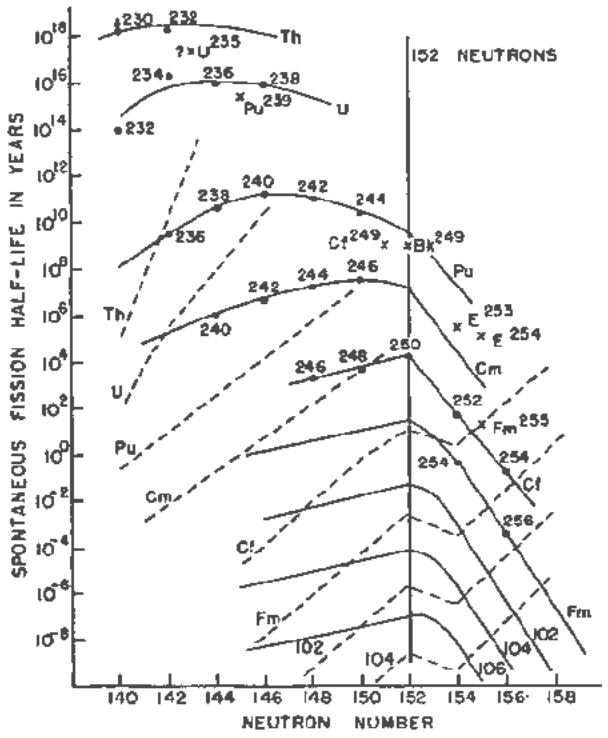

Figure 1. Spontaneous fission half-life versus neutron number. Dotted lines indicate the experimentally observed alpha half-life variation except in the cases for elements 102 and 104

californium isotope was detected which decayed by spontaneous fission with a half-life of 85 ± 15 days; no alpha particle branching was observed, but this is not surprising since one would expect an alpha half-life for this nuclide of 10^2 years. The isotope Fm^{250} has been manufactured in two ways: (1) as the electron-capture daughter of Mv^{250} (mendelevium, element 101)[13] and (2) from neutron bombardments[14] of E^{255} via a short-lived E^{256} beta emitter. In both types of experiments a 3 to 4 hour spontaneous fission emitter was isolated as an isotope of element 100. Again no alpha branching was observed since the predicted alpha half-life of Fm^{256} is about 10 days.

Other very recent measurements tend to support the postulation of a subshell influence on the spontaneous fission rates. The half-life for spontaneous fission of Pu^{244} has been found to be $2.5 \pm 0.7 \times 10^{10}$ years,[15] a value which is only three times shorter than that for Pu^{242}. Thus over the entire region of beta stability the half-lives for spontaneous fission of the plutonium isotope vary by a factor of a few hundred; the variation for californium isotopes on the other hand is about 10^5 without including the value for the unknown heaviest beta stable member, Cf^{256}. Cm^{246} has been shown[16] to have a spontaneous fission half-life of 3×10^7 years, a value consistent with the above observations.

Clearly we have not yet proved our hypothesis of the 152 neutron correlation. Much more proof will be at hand, however, if the spontaneous fission rates for Fm^{252} and Fm^{250} can be measured and shown to have the predicted values. It does seem obvious that some more powerful effect is influencing the spontaneous fission half-lives than has been proposed so far. Figure 1 is a plot of the spontaneous fission half-lives versus neutron number and contains in a simple form all the data known at this time. The predicted lines for the unknown heavier even-Z elements are, of course, drawn with the 152 neutron prejudice clearly delineated. Included on this plot will be found the spontaneous fission half-lives for six odd nucleon nuclides. The value for U^{235} is very questionable but the others, Pu^{239}, Bk^{249}, Cf^{249}, E^{253}, E^{254}, and Fm^{255} are felt to be reasonably accurate. The "hindrance factors" for these nuclides when compared to their maximum rates as determined by the even-even lines and their hypothetical odd-Z intermediates vary between 10^3 and 10^6. The most highly hindered isotope is the recently discovered long-lived isomer of E^{254} which has both an odd number of protons and an odd number of neutrons.[12] We have not yet observed any clear systematic variation in the degree of hindrance which can be correlated with 152 neutrons, but this might well be due to insufficient data.

On Fig. 1 we have also indicated the manner in which the alpha half-lives vary in this region. Examination of the trends indicates that spontaneous fission will probably not become competitive with alpha decay even at a few atomic number units above 100 except for those isotopes beyond the subshell at 152 neutrons. This is the case because the alpha decay rates increase as fast as the spontaneous fission rates at the higher Z values. However, beyond 152 neutrons spontaneous fission seems to increase so markedly that at 156 neutrons it becomes the chief mode of decay. This has been observed to date in californium and fermium.

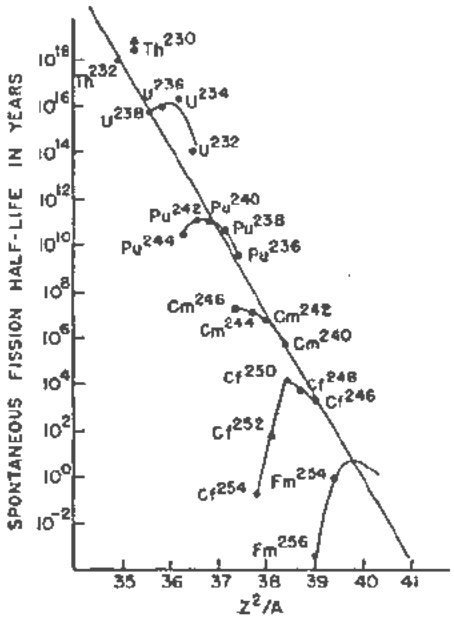

Figure 2. Spontaneous fission half-life versus Z^2/A

Table I. Spontaneous Fission Half-Lives

Isotope	$T_{1/2}(SF)(yr)$	*Ref.*	*Isotope*	$T_{1/2}(SF)(yr)$	*Ref.*
Th^{230}	$\geq 1.5 \times 10^{7}$	18	Cm^{244}	2.1×10^{7}	5
Th^{232}	1.4×10^{18}	18	Cm^{246}	7×10^{3}	16
U^{232}	$8 \pm \frac{5.5}{3} \times 10^{13}$	32	Bk^{249}	1.5×10^{3}	31
U^{234}	1.6×10^{17}	5	Cf^{249}	1.5×10^{4}	24
U^{235}	1.8×10^{17}(?)	18	Cf^{248}	66	25
U^{236}	2×10^{16}	19	Cf^{249}	0.2	31
U^{238}	8.0×10^{15}	18	Cf^{254}	3×10^{2}	28, 29, 30
Pu^{236}	3.5×10^{9}	5	Cf^{252}	1.5×10^{2}	28, 29
Pu^{238}	4.9×10^{10}	20	Cf^{254}	0.5	16, 12
Pu^{239}	5.5×10^{15}	18	E^{253}	20	26, 31
Pu^{240}	1.2×10^{11}	21	E^{254}	3×10^{-4}	31
Pu^{242}	$7.25 \pm 0.3 \times 10^{10}$	16, 17	Fm^{254}		26, 27
Pu^{244}	$2.5 \pm 0.7 \times 10^{10}$	15	Fm^{255}	6×10^{2}	31
Cm^{240}	1.9×10^{6}	5	Fm^{256}	1.4×10^{2}	13, 14
Cm^{242}	7.2×10^{6}	22, 23		3×10^{2}	

For the sake of completeness we have included the two other well-known plots. Figure 2, spontaneous fission half-life versus Z^2/A, demonstrates very well that one line cannot encompass all the data adequately. On the other hand, if one connects nuclides differing by two Z units and six A units, there is apparent a closer correlation with the notable exceptions of Th^{232}, Cf^{254}, and Fm^{256}. Figure 3 is the Kramish-Studier, Huizenga-type of plot. Here, again, one sees notable exceptions (Th^{232}, Cf^{248}, Cf^{254}, and Fm^{256}) whose spontaneous fission half-lives do not correspond with the "jump of six" lines. Perhaps the limited success of this type of correlation is merely reflecting the fact that one is dividing the slope of one straight line by that of another (see Fig. 1, dotted lines showing approximate alpha half-life variation) and that where it fails it does so because the spontaneous fission half-life probably changes for a reason that has little to do with a change in alpha half-life.

Table I includes the data and references on spontaneous fission half-lives. Those isotopes which have so far been measured only as a rather low limit are not included.

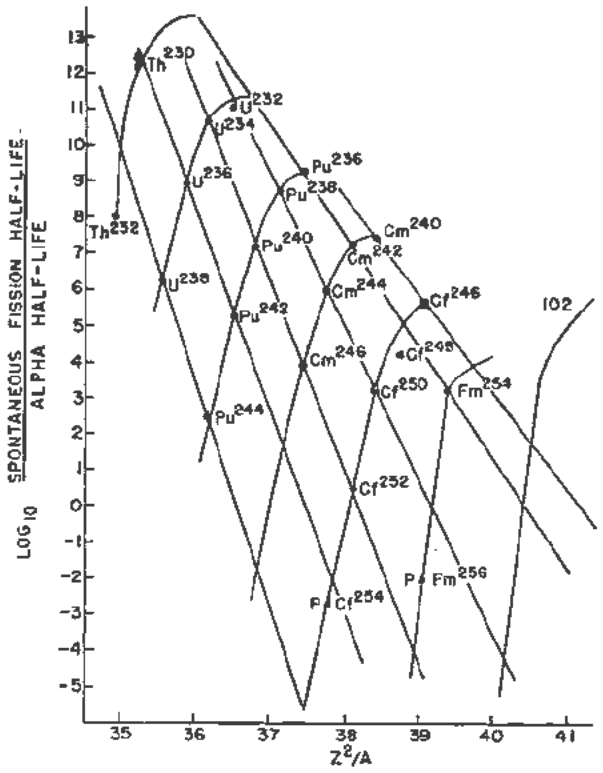

Figure 3. The ratio of spontaneous fission half-life to alpha half-life versus Z^2/A

REFERENCES

1. Flerov, G. N. and Petrzhak, *Spontaneous Fission of Uranium*, J. Phys. USRR *3*: 275 (1940); Phys. Rev., *58*: 89 (1940). See also J. Phys. USSR *4*: 283 (1941).
2. Bohr, N. and Wheeler, J. A., *The Mechanisms of Nuclear Fission*, Phys. Rev. *56*: 426 (1939).
3. Seaborg, G. T., *Some Comments on the Mechanism of Fission*, Phys. Rev. *85*: 157 (1952).
4. Whitehouse, W. J. and Galbraith, W., *Spontaneous Fission Rates*, Nature *169*: 494 (1952).
5. Ghiorso, A., Higgins, G. H., Larsh, A. E., Seaborg, G. T. and Thompson, S. G., *Spontaneous Fission of U^{234}, Pu^{236}, Cm^{240}, and Cm^{244}*, Phys. Rev. *87*: 163 (1952).
6. Kramish, A., *Spontaneous Fission Versus Alpha Decay*, Phys. Rev. *88*: 1201 (1952).
7. Huizenga, J. R., *Spontaneous Fission Systematics*, Phys. Rev. *94*: 158 (1954).
8. Hill, D. and Wheeler, J. A., *Nuclear Constitution and the Interpretation of Fission Phenomena*, Phys. Rev. *89*: 1102 (1953).
9. Studier, M. H. and Huizenga, J. R., *Correlation of Spontaneous Fission Half-Lives*, Phys. Rev. *96*: 545 (1954).
10. Ghiorso, A., Thompson, S. G., Higgins, G. H., Harvey B. G. and Seaborg, G. T., *Evidence for Subshell at $N = 152$*, Phys. Rev. *95*: 293 (1954).
11. Radiation Laboratory, to be published.
12. Harvey, B. G., Thompson, S. G., Choppin, G. R. and Ghiorso, A., *The Nuclide 99^{254}*, Phys. Rev. (July 1, 1955).
13. Ghiorso, A., Harvey, B. G., Choppin, G. R., Thompson, S. G. and Seaborg, G. T., *The New Element Mendelevium, Atomic Number 101*, Phys. Rev., in press.

14. Choppin, G. R., Harvey, B. G., Thompson, S. G. and Ghiorso, A., *Nuclear Properties of 100*^{250}, Phys. Rev. (June 1, 1955).

15. Fields, P. R., Friedman, A. M., Gridier, J. E. and Harkness, A. L., to be published.

16. Work at Argonne National Laboratory and University of California Radiation Laboratory, to be published

17. Diamond, H., Barnes, R. F., Studier, M. H., Hirsch, A., Fields, P. R. and Henderson, D., to be published.

18. Segré, E., *Spontaneous Fission*, Phys. Rev. *86*: 21 (1952).

19. Jaffey, A. H. and Hirsch, A., unpublished data (1949).

20. Jaffey, A. H. and Hirsch, A., unpublished data (1947).

21. Chamberlain, O., Farwell, G. W. and Segré, E., *Pu*^{240} *and Its Spontaneous Fission*, Los Alamos Scientific Laboratory Declassified Report LAMS-131 (September 8, 1944).

22. Ghiorso, A. and Robinson, H. P., unpublished data (1947).

23. Hanna, G. C., Harvey, B. G., Moss, N. and Tunnicliffe, P. R., *Spontaneous Fission in Cm*^{242}, Phys. Rev. *81*: 466 (1951).

24. Hulet, E. K., Thompson, S. G. and Ghiorso, A., *Spontaneous Fission Rate of Cf*^{246}, J. Phys. Rev. *89*: 878 (1953).

25. Hulet, E. K., *An Investigation of the Isotopes of Berkelium and Californium*, Ph.D. Thesis, University of California Unclassified Report UCRL-2283 (August, 1953).

26. Fields, P. R., Studier, M. H., Mech, J. F., Diamond, H., Friedman, A. M., Magnusson, L. B. and Huizenga, J. R., *Additional Properties of Isotopes of Elements 99 and 100*, Phys. Rev. *94*: 209 (1954).

27. Choppin, G. R., Thompson, S. G., Ghiorso, A. and Harvey, B. G., *Nuclear Properties of Some Isotopes of Californium, Elements 99 and 100*, Phys. Rev. *94*: 1080 (1954).

28. Ghiorso, A., Thompson, S. G., Choppin, G. R. and Harvey, B. G., *New Isotopes of Americium, Berkelium, and Californium*, Phys. Rev. 94: 1081 (1954).

29. Diamond, H., Magnusson, L. B., Mech, J. F., Stevens, C. M., Friedman, A. M., Studier, M. H., Fields, P. R. and Huizenga, J. R., *Identification of Californium Isotopes 249, 250, 251, and 252 from Pile-Irradiated Plutonium*, Phys. Rev. *94*: 1083 (1954).

30. Fields, P. R., Studier, M. H., Magnusson, L. B. and Huizenga, J. R., *Spontaneous Fission Properties of Elements 97, 98, 99, and 100*, Nature *174*: 265 (1954).

31. Ghiorso, A., Harvey, B. G., Thompson, S. G. and Choppin, G. R., to be published.

32. Jaffey, A. H. and Hirsch, A., unpublished work (1951).

The Distribution of Nuclear Charge in Low Energy Fission*

By Alexis C. Pappas,† Norway

ABSTRACT

The nature of the problem of the distribution of primary nuclear charge in fission is formulated and the associated experimental difficulties discussed. Of the previous suggested postulates and theories, only the postulate of Glendenin, Coryell, and Edwards and the theory by Present had any experimental support, but new data have now raised doubts about their validity.

It is shown that both of these theories are acceptable, but only after considerable modification. A modified postulate is proposed which takes into account closed shell effects in the nuclear stability curve, the fact that the neutrons are emitted from the fission fragments, and recent developments in our knowledge of the properties and structure of nuclear matter and of the fission process. The new postulate is in full agreement with all available experimental data. It is shown that the theory by Present, after modifications, can only be expected to give the general trend and therefore smoothes out all details.

INTRODUCTION

When a nucleus undergoes fission both its mass and its charge can be divided in a number of ways provided the following two requirements are fulfilled: (1) the sum of the masses (before neutron emission) of complementary fragments is equal to the mass of the fissioning nuclide, and (2) the sum of the charges of complementary fragments is equal to the charge of the fissioning nuclide. Thus for a given mass division there are many possibilities of charge division and vice versa. All the primary fission fragments with a given mass will (after the emission of the prompt neutrons) form a fission product β-decay chain ending in the stable end-product of that mass.‡ The fission yield of this end product represents the total chain yield and is accordingly equal to the sum of all the independent yields of the primary fragments with the same mass. The variation of the total chain yield with mass gives the well known mass distribution curves. These have been studied by a number of nuclear chemists and reference is given to the original papers for further information[1,2].

The variation of yields of primary fission fragments along a fission product decay chain (with given mass) gives the charge distribution in fission and a study of this is the aim of the present paper.

The problem has two aspects:

1. The determination of the most probable mode of charge division, i.e., (Z_p) the most probable primary charge as a function of (A) the mass number.

2. The fission probability with different modes of charge division, i.e. the variation of independent fission yields (Yi) along a fission product decay chain (Z-Z_p) for a given mass A. This gives the charge distribution curve around Z_p.

If we assume that the distribution of charge fundamentally follows simple probability laws, then we would expect the highest independent yield in a fission product decay chain to be found at about the middle of the chain and the independent yields to decrease on either side according to some smooth symmetrical probability curve. The point of the highest independent yield would represent the most probable primary charge, Z_p (non-integral) for the given mass.

From an experimental point of view the study of the charge distribution is a difficult problem. The primary fission fragments are not completely stripped of electrons and possess an ionic charge of about $20e$ and $22e$ respectively for the light and heavy fragments.[3] These charges decrease rapidly as the velocity of the fragments is reduced by their passage through matter. Thus no physical methods, such as those depending on the curvature in a magnetic field, are available, which give results directly related to the atomic number of the fragment, making possible a determination of the nuclear charge.

Therefore, the charge distribution can only be studied by using a chemical approach. This is difficult because it involves the determination of a large number of independent yields or a study of the variation in yield from one member to the next in as many different fission product decay chains as possible.

In thermal and low energy fission this object is impossible to achieve by radiochemical methods as the first members of a chain have very short half-lives. The only way to tackle the problem in these cases is

* Part of this work was carried out at the Laboratory for Nuclear Science, Massachusetts Institute of Technology, Cambridge. The work has been supported by United States Atomic Energy Commission and The Royal Norwegian Council for Scientific and Industrial Research.

† University of Oslo, Blindern, Norway and The Theoretical Study Division of the European Organization for Nuclear Research, CERN.

‡ Except for the very small effects caused by delayed neutron emission.

to accumulate as many independent yields as possible for various masses, and evaluate semi-empirically the charge distribution curve on the usual assumption that it is a smooth symmetrical probability curve and essentially the same for the whole mass region. This assumption has its support in the theoretical work by Fong[4] who showed that the charge distribution curve is roughly independent of mass, and in the observed close parallelism[5] in the yields of isotopes of krypton (89–97) and xenon (139–145) found in gas sweeping experiments.

The primary fragments in high energy fission are frequently formed on both sides of stability. This should make independent yield determinations somewhat easier if it was not for the many unknown decay schemes of neutron deficient nuclides and the high primary yield of stable fragments.

POSTULATES FOR THE DIVISION OF NUCLEAR CHARGE

From an experimental point of view the study of the charge distribution for fission induced by capture of thermal neutrons was first undertaken by Glendenin, Coryell, and Edwards[5] and further investigated by Glendenin[6] and by Pappas.[7] The following postulates and theories have previously been proposed and may be compared with the experimental results.§

1. From an energetic point of view one expects that prior to fission the charges rearrange themselves in the distorted nucleus in such a way as to make the potential energy a minimum. This assumption was put forward by Wigner and Way[8] and it can be shown by a mathematical treatment that this postulate predicts smaller charge displacement (chain length) in the light than in the heavy region.

2. From a kinetic point of view the charge division should depend on the distribution of protons and neutrons in the fissioning nucleus. Sugarman and Turkevich[9] postulated that the protons and neutrons are uniformly distributed in the fissioning nucleus and that the nuclear charge should therefore divide in the same ratio as the masses. This postulate gives greater charge displacement in the light than in the heavy region because nuclides with the high neutron to proton ratio corresponding to the fissioning nucleus are further away from stability in the light than in the heavy mass region. Both the above postulates were shown by Glendenin, Coryell, and Edwards[5] to be inconsistent with observed fission yields.

3. From the best available experimental data Glendenin, Coryell, and Edwards[5] put forward the postulate of equal charge displacement. This postulate gives charge displacements intermediate between those predicted from the two earlier postulates and the effective chain lengths (Z_A-Z_p) are assumed to be the same for both fragments.

4. Approximately the same results for the most probable mode of fission are given by the theory of Present.[10] Present uses a general nuclear model in which proton and neutron densities are not uniform. According to this theory the most probable mass division should result in equal charge displacements (chain lengths) while a very asymmetric division would give shorter chain lengths in the light than in the heavy fragment. Because of lack of data Glendenin was not able to make a final choice between Present's theory and the postulate of equal charge displacement as they were both consistent with experimental data available at that time. The charge distribution curve given by Present's theory is somewhat narrower than the one based on the hypothesis of equal charge displacement.

5. Fong[4] in a statistical theory of the fission process has theoretically computed mass distribution curves that are in good agreement with the experimental ones. He finds the shapes of the charge distribution curves to be approximately independent of the mass of the chain, but a comparison of Fong's predicted charge distribution curves with the observed independent yields immediately discloses severe disagreement in both their width, and first of all, in their positiun i.e., in the Z_p values. Fong ascribes these deviations to the formation of high-spin isomers in high yield decaying only by β-decay to other isomers and thus by-passing stable nuclides through highlying states. This, however, seems unlikely from our present knowledge of fission product decay chains. It has furthermore been shown by Sharp[11] that high-spin states may not easily be formed in fission.

6. Brunton[12] made a very interesting attempt to interpret the spread in kinetic energy of the fission fragments of a given mass raito as arising mainly from variations in charge distribution. These calculations imply that one of the fragments leads to a long decay chain, the other fragment being either stable or only nne unit from stability, in disagreement with the observed facts.

The charge distributions proposed by Fong and Brunton will not be considered further in light of their poor agreement with the experimental data.

With more data on independent fission yields large deviations have been found both from Glendenin's and Present's charge distribution curves thus casting doubt on the validity of these theories.[13] The whole problem of the distribution of primary nuclear charge in fission was therefnre reinvestigated by the present author,[14] who showed that all previous theories and postulates should be rejected on experimental grounds except that of equal charge displacement and the latter accepted only with considerable modification. Furthermore it will be suggested in this paper that the theoretical treatment of Present might be more successful if it were changed to take into account recent developments in our knowledge of the properties and structure of nuclear matter.

§ In the following the most probable primary charge will be designated by Z_p, and the most stable charge for mass A by Z_A.

A MODIFIED POSTULATE OF EQUAL CHARGE DISPLACEMENT

Recent studies of the effects of closed nuclear shells¶ on neutron and proton binding energies[15-17] have revealed discontinuities of about 2 Mev on crossing a nuclear shell edge resulting in an increased stability for nuclei with these preferred configurations. These will of course also influence the nuclear energy surface and the location of the valley of maximum stability. From studies of the influence of shells on β-decay energetics an improved stability curve—the Z_A function—has been developed by Brightsen, Coryell, and Pappas.[18 20] The function is linear with A but shows marked discontinuities at shell edges. The lines are tangent to the old empirical stability curve[21] but displaced upwards on the completion of a neutron shell and downwards on the completion of a proton shell as shown in Fig. 1.

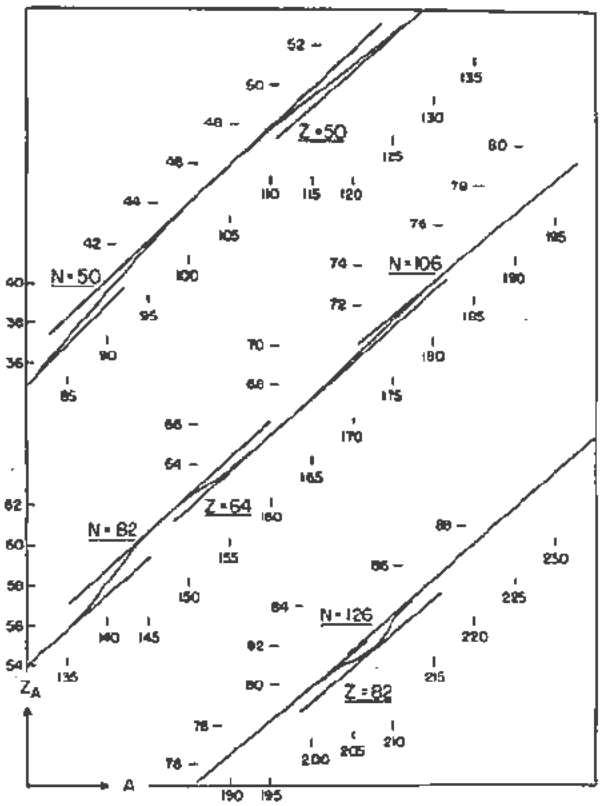

Figure 1. The effect of closed shells on the nuclear stability curve

In connection with our present problem it should be realized that these discontinuities are reflections of the discontinuities in nuclear binding energies. Therefore one might well expect shell effects to influence the Z_p function for thermal fission when any postulate with a nuclear model is used.

A systematic study of the deviations from Glendenin's charge distribution curve discloses that these are probably due to secondary effects of closed shells.

¶ The most prominent of these occur at neutron or proton numbers 20, 28, 50, 82, and 126 with subshells in between.

It was therefore thought fruitful to keep this in mind and in a semi-empirical way again approach the charge distribution problem.[7]

Let us first re-formulate the postulate of equal charge displacement in accordance with the recent developments in nuclear structure and our knowledge of the fission process.

Because the charge division is decided at the moment of fission we must consider the primary fission fragments just after their separation and *not* after the emission of the prompt neutrons as has been done in the earlier work of this type. Only then is a comparison with a purely theoretical treatment such as Present's possible.

The emission of all the prompt neutrons takes place from the excited primary fission fragments[22] but are not evenly distributed.[23] Afterwards the fission fragments decay by β- and γ-emission. The total number of β-decays that will take place depends only on the difference $(Z_A\text{-}Z)$ between the charge (Z) of the initial primary fragment (Z, A), and the Z_A-value that will be reached, and is independent of shell crossings during the decay down to stability.

In accordance with this we will generally define $(Z_A\text{-}Z)$ as the real effective chain length for the primary fission fragment (Z, A).

Retaining the basic ideas of the postulate of Glendenin, Coryell, and Edwards[5] but beginning with the fission fragments before prompt neutron emission and including the effects of nuclear shells on final stability values, the following one is now proposed.

The most probable charge division leads to equal charge displacements for the initial fission fragments from the final stability characteristic for their mass number.

In other words

$$(Z_A\text{-}Z_p)_{light} = (Z_A\text{-}Z_p)_{heavy}$$

where $A_{light} + A_{heavy}$ is the mass of the fissioning nuclide.

The most probable primary charge for a given mass A (before neutron emission) in fission of U^{235} with thermal neutrons is computed from the formula

$$Z_p = Z_A - \frac{Z_A + Z_{(236-A)} - 92}{2}$$

where Z_A and $Z_{(236-A)}$ in this equation is taken from the lines of maximum stability given by Brightsen, Coryell, and Pappas (see [20]). These Z_A values are considered to mark the theoretical end point of the fission product decay chain. The shell discontinuities in the Z_A function occur at mass numbers where lines representing the closed shells of neutrons and protons intersect the Z_A versus A function (Fig. 2 upper curve). Thus the value of Z_p is uniquely defined for each mass.

It has been shown in the author's study of the distribution of fission neutrons[23] that the average number emitted from the fragments, after subtracting

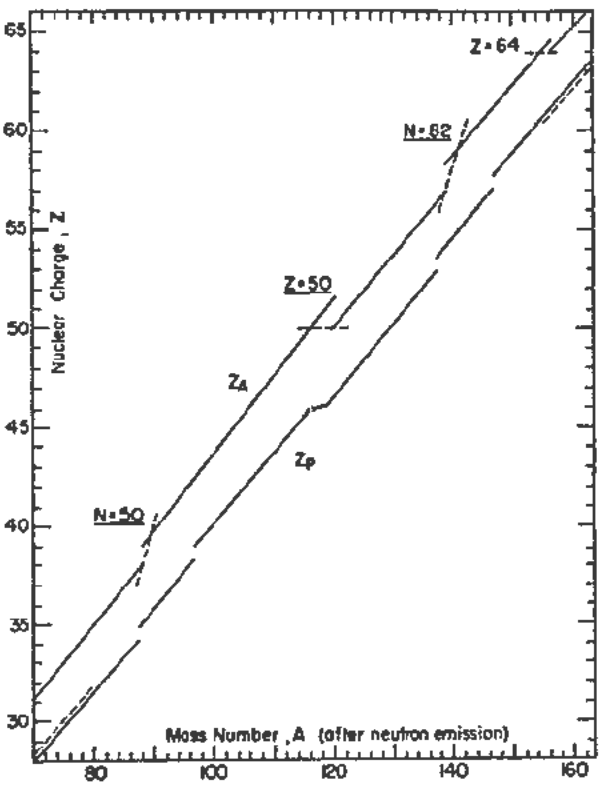

Figure 2. Most probable primary charge Z_p of fission fragments of U^{235}

those neutrons emitted in closed shell regions and thus causing fine structure in the mass distribution[16], is for thermal fission of U^{235} 2.0, Pu^{239} 2.5, and U^{233} about 2. These numbers must be used in charge distribution studies. These neutrons can be assumed to be evenly distributed among the fission fragments within the uncertainty of the results of the postulate.

The computed values of Z_p for U^{235} thermal neutron fission is given in appendix I for the *observed* mass numbers, i.e. after the emission of on the average one neutron from each fragment. The values given for Z_p are probably good to $\pm$ 0.1 charge units outside shell regions. The uncertainty at the shell crossings of Z_A is probably $\pm$ 0.2 mass units and is reflected in the corresponding values of Z_p which are probably good to 0.5–0.6 charge units either up or down (one half of the discontinuity in the Z_A function). Fine variation due to subshell effects has not been accounted for in this treatment, mainly because of the uncertainty to their exact location and their magnitude, the latter, however, being rather small (about 0.3 charge units, the effect on $Z_p \sim 0.1$).

The new function for the most probable primary charge versus fission fragment mass number (after neutron emission) is given in Fig. 2 (lower curve) for fission of U^{235} with thermal neutrons.

The most probable theoretical chain lengths are from 3.2 to 4.1 charge units depending on the fission asymmetry. The observed chain lengths will be somewhat shorter due to the occurrence of stable even A nuclides below the β-stability line.

The new Z_p function follows roughly the Z_A function but shows both shell and mirror shell effects** in accordance with the fundamentals of this hypothesis of equal charge displacement. The Z_p function given by Glendenin, Coryell, and Edwards[5] was a smooth function fluctuating between the lines of the new Z_p-function. One also finds experimental deviations from Glendenin's charge distribution curve not only in regions affected by nuclear shells but also at masses complementary to shells (mirror shell effects).

Before proceeding to the second part of the problem, the comparison with experimental data and the evaluation of the charge distribution curve, it is of interest to point out that in the recent qualitative treatment of the fission process by Hill and Wheeler,[24] using a collective nuclear model, it appears that the expected fluctuations in the length of a given fission product decay chain is in accordance with a postulate of equal charge displacement.

In Tables I and II are given all radiochemically measured independent fission yields in per cent, taken from the author's earlier compilation[14] extended with recent data. The yields are also given as fractional yields, i.e. independent yield divided by total chain yield for the mass in question. For a discussion and review of the measured values reference is given to [14].

If the most probable mode of charge division is governed as proposed in the present postulate then one would expect that a plot of logarithm of the experimentally determined fractional chain yield versus distance $(Z\text{-}Z_p)$ from the most probable primary charge as computed above should give a reasonably smooth charge distribution curve. In Fig. 3 are presented the results expected from earlier postulates and theories where the experimental points show a large scattering.††

It is therefore encouraging that all points in Fig. 4 are on a smooth curve, within the experimental errors in the measured yields and the uncertainties in Z_p. In this connection it is of interest to point out that the effect of closed shells in the Z_p function is very clear in the cases of As^{78} and Nb^{99}. These two and also some other nuclides will, if shell effects are not considered, be found far away from the charge distribution curve. As^{78} is moved on the curve due to the reflected influence of the 64 proton subshell, while the position of Nb^{99} is governed by the 82 neutron mirror shell, and so on.

The charge distribution is drawn through the points to give a total probability of unity. The shape of the resulting curve is essentially identical with that of Glendenin,[6] but the location of the maximum and

** Mirror shell: neutron (proton) number complementary to shell.

†† It has to be remembered that the charge distribution curve has to be drawn to give a total probability of unity. The deviations between the measured and the theoretical values are given by the *vertical* distance. The horizontal distance gives the deviation in the $(Z\text{-}Z_p)$ values.

Table I. Independent Fission Yields in U^{235}

Nuclide	Independent yield %	Chain yield %	Fraction of chain yield	Measured by
$_{33}As^{78}$	1.8×10^{-3}	0.02	9×10^{-2}	Sugarman, 1952
$_{35}Br^{85}$	$(3.5 \pm 1) \times 10^{-5}$ 4.1×10^{-5}	0.25	$(1.4 \pm 0.4) \times 10^{-4}$ 1.6×10^{-4}	Glendenin, 1949 Cook, 1951
$_{37}Rb^{90}$	3.1×10^{-5} 2.05×10^{-5}	1.90	1.6×10^{-5} 1.3×10^{-5}	Glendenin, 1949 Cook, 1951
$_{39}Y^{90}$	$<2.8 \times 10^{-3}$	5.35	$<5 \times 10^{-4}$	Cook, 1951
$_{41}Nb^{96}$	5.7×10^{-4}	6.40	8.9×10^{-5}	Cook, 1951
$_{52}Te^{131}$	0.46 ± 0.2	3.00	0.15 ± 0.07	Pappas, 1953
$_{52}Te^{132}$	1.5 ± 0.8	4.20	0.36 ± 0.17	Pappas, 1953
$_{53}I^{134}$	0.94 ± 0.13	5.80	0.18 ± 0.02	Pappas, 1953
$_{54}Xe^{133}$	5×10^{-3}	5.2	1×10^{-3}	Katcoff and Rubinson, 1953
$_{54}Xe^{135}$	0.31 ± 0.04 0.17 ± 0.06	6.12	$(5.1 \pm 0.7) \times 10^{-2}$ $(2.8 \pm 1.0) \times 10^{-2}$	Pappas, 1953 Brown and Yaffe, 1953
$_{55}Cs^{136}$	$(6.2 \pm 0.8) \times 10^{-3}$ 5.7×10^{-3}	6.30	$(9.8 \pm 1.3) \times 10^{-4}$ 9.0×10^{-4}	Glendenin, 1949 Cook, 1951
$_{57}La^{140}$	<0.2	6.34	$<3 \times 10^{-2}$	Sugarman, 1951
$_{57}La^{141}$	~ 0.12	6.28	$\sim 2 \times 10^{-2}$	Ford and Stanley, 1953
$_{61}Pm^{148}$	$<1.3 \times 10^{-4}$	1.90	$<6.8 \times 10^{-3}$	Cook, 1951

plotted experimental points has changed due to the modified postulate and method of computation.

Furthermore, the new charge distribution curve is also consistent with the few available data for slow neutron induced fission of Pu^{239} and U^{233}.

The charge distribution curve given in Fig. 4 has a half-width of about two charge units and in the region $|Z-Z_p| \leqslant 1.9$ is a probability curve with the Gaussian approximation:

$$P(Z) = \frac{1}{\sqrt{c\pi}} e^{-\frac{(Z-Z_p)^2}{c}}$$

where c is an empirical constant ~ 1.5. For $|Z-Z_p| > 1.9$ the deviation from the Gaussian distribution increases with increasing $Z-Z_p$, the charge distribution being steeper than the Gaussian.‡‡ In closing this part of the investigation we can conclude that the available experimental evidence supports the postulate of equal charge displacement in its new form. This postulate requires the necessity of a small redistribution of nuclear charge in the deformed nucleus undergoing fission.

Ample time is available for a rearrangement of the proton density in thermal and low energy fission as these processes are very slow ($\sim 10^{-14}$ sec) compared to the time necessary for a redistribution of charge ($\sim 10^{-20}$ sec).

In high energy fission, however, this postulate does not hold, probably in view of the much faster division of the fissioning nuclide.

PRESENT'S THEORY OF CHARGE DIVISION

Of the purely theoretical work on the charge division in fission only that of Present[10] seems to have experimental support.§§ In its present form the Present theory predicts about a 30 per cent narrower charge distribution than does the postulate of equal charge displacement considered here, and the deviations of the experimental points from the curve are quite large.[14] According to earlier interpretations this theory predicted shorter chain lengths in the light than in the heavy region.

In the development of his theory Present uses a general nuclear model, the Wigner model, and assumes a non-uniform proton density throughout the nucleus, and a uniform total particle density, i.e. incompressibility of nuclear matter. He performs the calculations on the deformed nucleus just before fission, as approximated by two spheres in contact.

‡‡ In Appendix II the fractional yield values as read off from the curve in Fig. 4 are given for values of $(Z-Z_p)$ differing by 0.1.

§§ Hill and Wheeler's treatment 24 is only a qualitative one and does not allow a further comparison with experimental results.

Table II. Independent Fission Yields in Pu^{239} and U^{233}

Nuclide	Independent yield %	Chain yield %	Fraction of chain yield	Measured by
		Pu^{239}		
$_{37}Rb^{90}$	1.2×10^{-4}	0.72	1.6×10^{-4}	Cook, 1951
$_{55}Cs^{136}$	1.9×10^{-2}	0.61	3.1×10^{-2}	Cook, 1951
		U^{233}		(preliminary values)
$_{41}Nb^{96}$	$(1.2\text{–}4.5) \times 10^{-2}$	5.7	$(2\text{–}8) \times 10^{-3}$	Glendenin, 1952
$_{55}Cs^{136}$	8.5×10^{-2}	5.7	1.5×10^{-2}	Glendenin, 1952

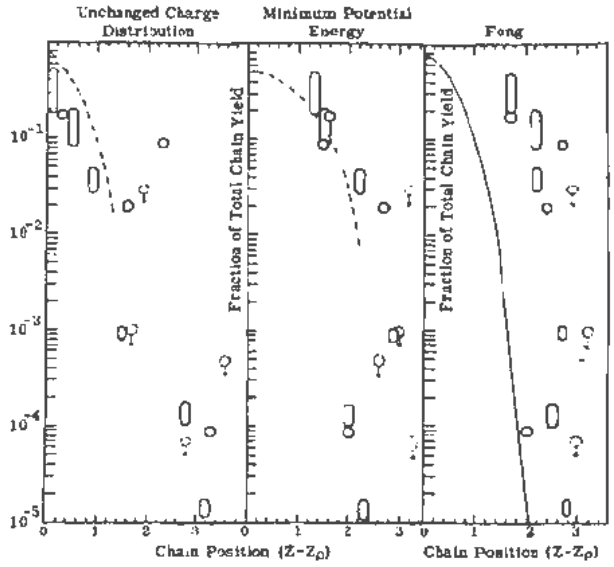

Figure 3a

On these cases he computes the quantity (usual notation)

$$\gamma = \frac{Z_1}{Z_1 + Z_2} \Big/ \frac{A_1}{A_1 + A_2}$$

Here A_1 and A_2 are the masses before neutron emission, γ can be taken as a measure for the charge redistribution in the fissioning nucleus. According to Present's calculations γ exceeds one, in other words there is a tendency for the protons to concentrate in the smaller fragment. This is reasonable from an electrostatic viewpoint alone. The computed $(\gamma - 1)$ values are 0.0158, 0.0290, and 0.0493 respectively for 2:3, 1:2, and 1:3 mass division and have been used in the previous interpretations and comparisons with experimental data. We know, however, that these values must be upper limits because of (1) Swiatecki[25] has indicated that nuclear compressibility plays an important role in fission, which would lower the value given by Present: and (2) the Wigner mass formula, containing both quadratic and linear forms in $(N\text{-}Z)$, gives essentially a theoretical justification of the semi-empirical mass formulas without attempting any detailed predictions of individual nuclei. This formula ought therefore to be replaced by the Weizsäcker formula, containing only a quadratic term in $(N\text{-}Z)$, as the formula has been shown to be valid in detail outside of closed shell regions.[10,20] Correction terms for closed shells can be applied.[26] Cancelling or even diminishing the influence of the $(N\text{-}Z)$ linear term will also reduce the $(\gamma\text{-}1)$ values given by Present.

A conservative estimate of these effects should result in about a 30% reduction in $(\gamma\text{-}1)$,¶¶ giving the new values 0.010(2:3), 0.020(1:2) and 0.034(1:3).

¶¶ According to Present his values may be too large by as much as 50%. The rough estimate of the effect of compressibility only gives 15 to 30%.

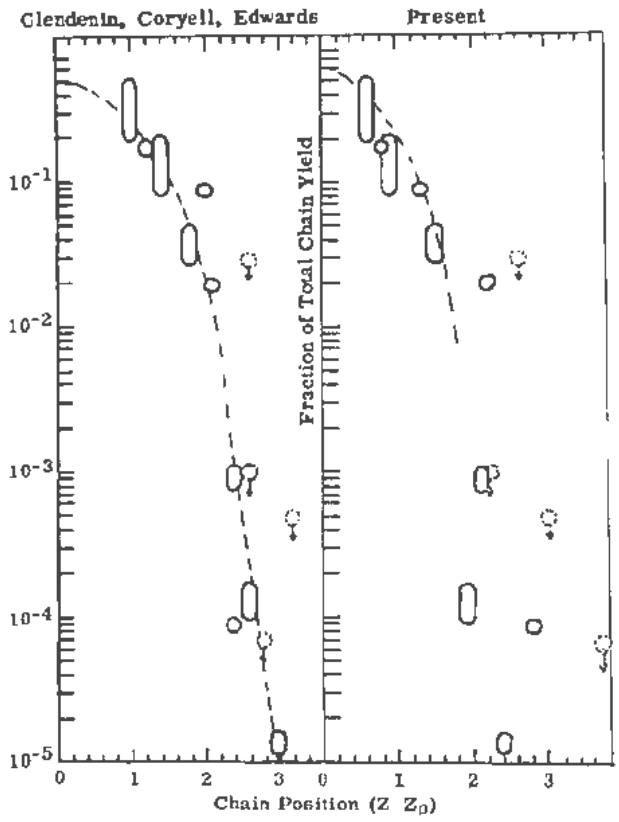

Figure 3b

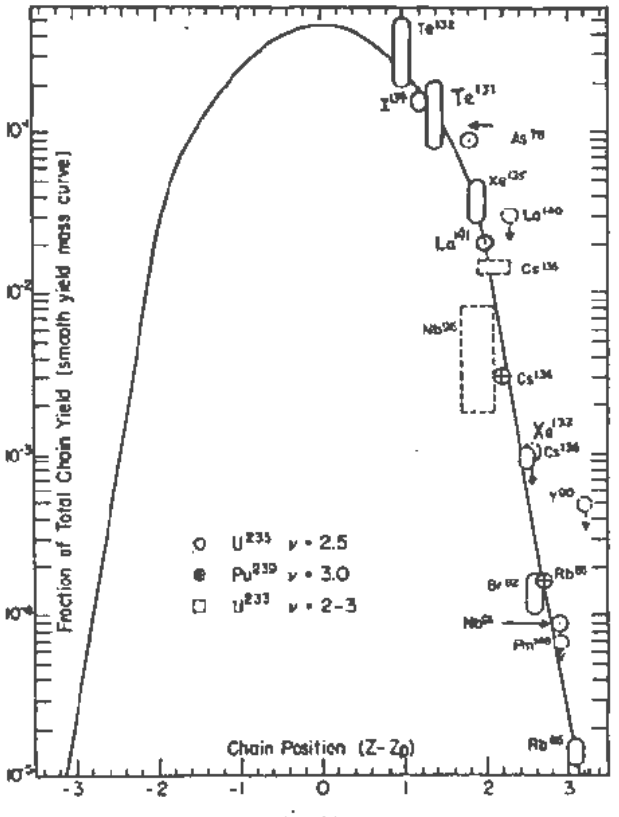

Figure 4. Variation of yield with nuclear charge

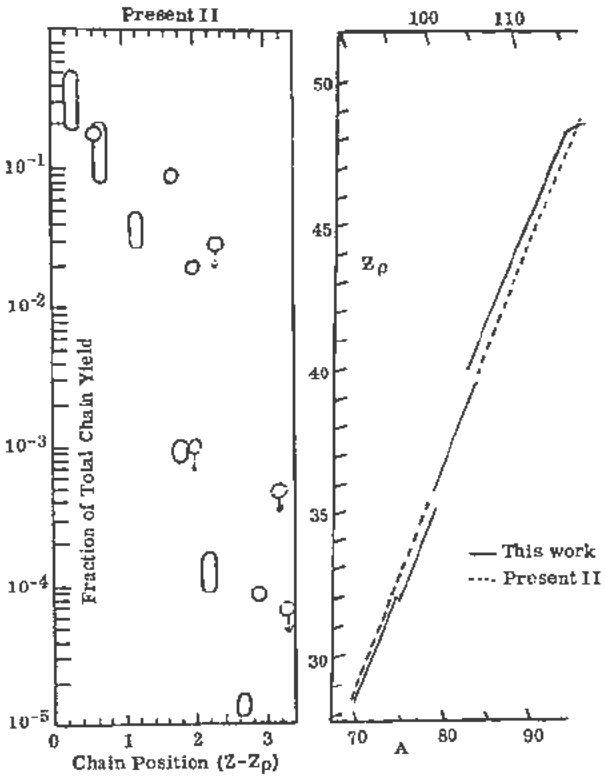

Figure 5

Figure 6

Furthermore it ought to be kept in mind that periodicities and discontinuities in nuclear binding energies are not reflected in the γ-calculations. Present's Z_p function can therefore only give the general trend of the results.

The measured independent yields from Table I have been replotted in Fig. 5 using the Z_p values computed from the new γ-values. The results are good in that the points lie on a reasonably smooth curve. The scattering is rather large, but no systematic deviations are found. The width of the Present charge distribution curve will be increased when lower $(\gamma\text{-}1)$ values are used. It will thus be in accordance with observed results. Another improvement is that the difference in chain lengths between the heavy and light fragment expected in accordance with the lower $(\gamma\text{-}1)$ values is less than one half of the previous values for very asymmetric fission when the difference is most pronounced.

Furthermore it is of interest to point out that in a plot of Z_p versus A for both the new postulate of equal charge displacement and for Present's modified theory, the Present Z_p line gives good agreement with the curve developed in this paper with the exception that displacements due to shell effects do not appear (Fig. 6).

These facts and the apparent success of the new postulate of equal charge displacement indicate that it may be fruitful to introduce compressibility, an improved mass formula, and shell effects into future theoretical treatments of charge distribution in fission, and that the postulate itself, although based on purely empirical evidence, may have real theoretical significance.

APPENDIX I. Z_p Values for U^{235} Thermal Neutron Fission

Final mass A	*Most probable charge Z_p*	*Final mass A*	*Most probable charge Z_p*
69	27.8	119	46.2
79	31.5 (31.3)	137	52.9
80	31.6	138	53.9
87	34.2 (34.7)	146	56.9
88	35.1	147	57.8 (57.3)
96	38.1.	154	60.4
97	39.1	155	60.5 (60.7)
115	45.8	165	64.2
116	45.9		
118	46.1		

In each group the Z_p function is linear. The discontinuity from one line to another takes place at the numbers marked. In cases where shell crossing influences the Z_p value both possible values are given for Z_p.

APPENDIX II. Fractional Yield Values of Charge Distribution Curve for Thermal Fission

Distance from most probable charge $(Z\text{-}Z_p)$	*Fraction of total chain yield f*	*Distance from most probable charge $(Z\text{-}Z_p)$*	*Fraction of total chain yield f*
0	4.65×10^{-1}	1.6	8.3×10^{-2}
0.1	4.62	1.7	6.7
0.2	4.59	1.8	5.1
0.3	4.40	1.9	4.1
0.4	4.25	2.0	2.9
0.5	4.00	2.1	1.9
0.6	3.70	2.2	5.0×10^{-3}
0.7	3.35	2.3	2.6
0.8	3.05	2.4	1.2
0.9	2.70	2.5	6.0×10^{-4}
1.0	2.40	2.6	3.0
1.1	2.05	2.7	1.6
1.2	1.75	2.8	8.0×10^{-5}
1.3	1.50	2.9	4.0
1.4	1.23	3.0	2.2
1.5	1.03	3.1	1.3

ACKNOWLEDGEMENT

The author wishes to thank Professor C. D. Coryell for many enlightening discussions.

REFERENCES

1. *Radiochemical Studies: The Fission Products*, Coryell, C. D., and Sugarman, N., editors, National Nuclear Energy Series, Div. IV, 9, McGraw-Hill Co., Inc., New York (1951).
2. Whitehouse, W. J., *Nuclear Fission*, Progr. Nucl. Phys., 2: 120-173 (1952).
3. Lassen, N. O., *Hp-Distribution of Fission Fragments*, Phys. Rev., 68: 142-143 (1945).
4. Fong, P., *A Theory of Nuclear Fission*, Ph.D. Thesis in Physics. University of Chicago (1953).
5. Glendenin, L. E., Coryell, C. D. and Edwards, R. R., *Distribution of Nuclear Charge in Fission*, paper 52 in reference (1).

6. Glendenin, L. E., *The Distribution of Nuclear Charge in Fission*, Technical Report 35, Laboratory for Nuclear Science, Massachusetts Institute of Technology, Cambridge (1949).
7. Pappas, A. C., *A Radiochemical Study of Fission Yields and the Effect of Closed Shells in Fission*, Technical Report 63, Laboratory for Nuclear Science, Massachusetts Institute of Technology, Cambridge (1953) and American Report AECU-2806 (1953).
8. Way, K. and Wigner, E. P., *Rate of Decay of Fission Products*, paper 43 in reference (1).
9. Sugarman, N. and Turkevich, A., a personal communication of 1946 in reference (5).
10. Present, R. D., *On the Division of Nuclear Charge in Fission*, Phys. Rev., *72*: 1-9 (1947).
11. Sharp, R. A., personal communication, May 1955.
12. Brunton, D. C., *The Division of Nuclear Charge in Fission*, Phys. Rev., *76*: 1798-1802 (1949).
13. Independent personal communications from Cook, G. B., Coryell, C. D., Glendenin, L. E., Pappas, A. C., Spence, R. W. and Sugarman, N., during the year 1951.
14. Pappas, A. C., reference (7), 122-131.
15. Harvey, J. A., *Neutron Binding Energies from (d,p) Reactions and Nuclear Shell Structure*, Phys. Rev., *81*: 353-364 (1951).
16. Pappas, A. C., *Nuclear Closed Shells and Fission Yield Fine-Structure*, Z. Elektrochemie, *58*: 620-623 (1954). See also reference (7), 132-147 (Binding Energies), 159-164 (Fine-Structure).
17. Feather, N., *A Survey of Neutron and Proton Binding Energies*, Adv. in Physics, *2*: 141 (1953).
18. Brightsen, R. A., *The Liquid Drop Model and Nuclear Shell Structure*, M.S. Thesis in Chemistry, Massachusetts Institute of Technology (1950).
19. Pappas, A. C., Brightsen, R. A. and Coryell, C. D., *The Effect of Closed Shells on the Nuclear Stability Curve*, Laboratory for Nuclear Science Progress Report, May 1951, 71-75.
20. Coryell, C. D., Brightsen, R. A. and Pappas, A. C. See Coryell, C. D., *β-Decay Energetics*, Ann. Rev. Nuclear Sci., *2*: 305-334 (1953).
21. Kohman, T. P., *The Limits of Beta-Stability*, Phys. Rev., *73*: 16-21 (1948).
22. Wilson, R. R., *Directional Properties of Fission Neutrons*, Phys. Rev., *72*: 189-192 (1947).
23. Pappas, A. C., reference (7) 151-153.
24. Hill, D. L. and Wheeler, J. A., *Nuclear Constitution and the Interpretation of Fission Phenomena*, Phys. Rev., *89*: 1102-1145 (1953).
25. Swiatecki, W. J., *Nuclear Compressibility and Fission*, Phys. Rev., *83*: 178-179 (1951).
26. Wapstra, A. H., *A Preferred-Number Correction to the Bethe-Weizsäcker Formula for the Nuclear Binding Energies*, *18*: 83-90 (1952).

Determination of Pile Constants by Chemical Methods

By C. E. Crouthamel* and E. Turk,† USA

The identification and quantitative evaluation of the events occurring in a functioning reactor is a very complex problem. In the Experimental Breeder Reactor (EBR), chemical analysis of the enriched uranium fuel and the natural uranium blanket after the reactor achieved a reasonable burnup of fuel, have proved extremely useful in supplementing and checking the physical methods of evaluation of breeding gain. The emphasis of this paper has been placed on the selection of methods, calibration, monitoring, and application of precise analytical techniques in various parts of the program of evaluating the EBR. The actual analyses have been performed by a rather large group of skilled technicians, and the results have been very gratifying. It is not the purpose of this report to give detailed procedures for chemical analysis and calculation. For the most part, the individual analyses are relatively standard.

GENERAL CONSIDERATIONS AND SCOPE OF THE PROGRAM

A considerable effort was devoted to selecting the various procedures applicable to this program. The criteria used in the selection of certain procedures and some of the reactor characteristics and working definitions employed are summarized below.

One of the major problems was the determination of the ratio of plutonium-239 production (total production minus fission) to uranium-235 consumption (fission plus capture) in the reactor as a whole after a given period of operation. This ratio will be referred to as the conversion ratio. Its determination required extensive sampling of the enriched uranium core and the natural uranium blankets around the core. Horizontal sections through the reactor were symmetrical, while vertical sections were not. The plutonium-239 production patterns in the blankets and core were plotted against the two variable dimensioas and integrated over the whole to obtain the total plutonium produced. The fuel consumed by fission and capture was determined and treated in a similar manner to obtain the total fuel consumed in the reactor. Fuel was considered as consumed by neutron capture when the nuclide formed was not fissionable.

In the enriched uranium core, a loss of fissionable fuel occurs when uranium-235 captures a neutron to form uranium-236. In the blanket material the capture of a neutron by uranium-238 to form plutonium-239 breeds new fissionable fuel. Also, fission of uranium-238 in the fast flux in the blanket will produce more neutrons, which may then be captured by uranium-238 to produce plutonium-239.

The chemical analysis of the reactor required a considerable effort from a large group. The determination of the fissinn patterns was a substantial problem. The burnup at the time of sampling was too small to be detected by direct uranium analysis. Therefore, fission product analysis had to be utilized. A calibration experiment was performed to relate the amount of cesium-137 activity produced with the number of fissions in enriched uranium. In the enriched core essentially all fission was due to uranium-235 and it was so attributed.

In the natural uranium blankets, between 50 and 80% of the total fissions originated with a uranium-238 nuclide. The ratio uranium-238 tn uranium-235 fissions was determined by a double fission product analysis. The fission yield curve is sensitive to the mass of the fissioning nuclide, large changes occurring in the light element peak and in the valley. Ruthenium-106 was selected as an isotope whose yield was very mass-sensitive. Highly enriched uranium-235 and depleted uranium-238 foils were irradiated in a fast neutron flux, and the ratios of ruthenium-106 to cesium-137 activities were determined for the two nuclides. Since the yield of cesium is essentially constant, the magnitude of the ratio of ruthenium-106 to cesium-137 is a measure of the fraction of uranium fissions due to uranium-235.

The plutonium production and quality was also an essential part of the program. The information desired from this part of the program was (1) a knowledge of the total amount of plutonium produced for breeding gain calculations, (2) a knowledge of the distribution pattern of the plutonium formed by capture in the blanket material to aid in establishing the best geometry for the blanket, and (3) a knowledge of the plutonium quality (ratio plutonium 238/240/239) to determine the blanket cycle time. This required samples from all parts of the reactor for plutonium assays. At the time of analysis, the plutonium content of the reactor was too low to be isolated and determined accurately by direct chemical assay. Therefore, the plutonium content was determined entirely by an alpha assay.

* Argonne National Laboratory.
† Phillips Petroleum Company.

ANALYTICAL PROCEDURES

Determination of Total Fissions

Many of the fission products are not acceptable for calibrating in the determination of total fission events. A comparison of the yield-mass curves[1] for uranium-235, uranium-238, and plutonium-239 shows marked variations in yield for elements in the trough and along the heavy slope of the light group. This effect has been utilized in the calibration of the ratio ruthenium-106/cesium-137 to give relative fissions due to uranium 238 and uranium-235.

For the determination of total fissions, however, it is desirable to utilize a fission product whose calibration factor is essentially independent of the fissioning nuclide and independent of small changes in the neutron spectrum. The elements at the peaks of the yield-mass curve approach these requirements. Additional considerations in moderately long and unsteady reactor operation were the decay rate of the fission product and the possibility of counting only the nuclide of interest. Cesium-137 with a 33-year half-life meets all the necessary requirements. However, cesium-136 with a 13-day half-life must be allowed to decay out. A minimum of 60 days was allowed.

The cesium-137 activity has been connected directly to the total fissions occurring by the techniques employed in absolute fission yield experiments.[3] The total fissions from a thin sample of the fissionable material were counted in a pulse ionization chamber, and the analysis for cesium-137 made from a heavy sample of the same fissionable material irradiated simultaneously in the same neutron flux to give a proportionate number of fissions. In the absolute-fission yield experiment, it would also be necessary to determine the number of cesium-137 atoms formed. This, however, was not necessary for the purpose of the determination of the total number fission events occurring. The observed counting rate of the isolated cesium-137 in a standard detector was corrected by a yield determination to the equivalent rate for 100% yield. This counting rate was associated with the total fission events in the heavy sample, as calculated from the observed fission in the light sample and the weight ratio.

The calibration factor obtained for a halogen-filled Geiger counter was 93.3 ± 1.8 counts per minute of cesium 137 per 10^{12} fissions. The mass of a typical heavy sample was 3.7893 grams; total fissions in the heavy sample were 22.15×10^{12}, and counts per minute cesium-137 observed at 100% yield of cesium were 2078.

The two most important characteristics of the cesium-137 detector were high reproducibility and long life. Reproducibility desired was ± 0.2%. This was achieved by careful monitoring with radium D, E, and F standards and cesium-137 standards. Also, considerable care was taken with the stability and reproducibility of the high voltage circuit. The high voltage was reset and checked with a portable potentiometer and standard resistor in the high voltage circuit. Proportional counters and long-lived, halogen-filled Geiger tubes are suitable for detectors for cesium-137. Several halogen-filled Geiger tubes have been in use over four years and have maintained their counting efficiency. The gas flow proportional counters are also highly reproducible and maintain counting efficiency indefinitely, and might be used if the work were repeated. They require more skill, however, both in operation and in maintenance.

The isolation of the cesium-137 activity was made by the procedure of Glendenin and Nelson.[4] The cesium-137 was weighed as the perchlorate on a glass fiber filter mat. The area and uniformity of the sample spread was controlled by slurrying the cesium perchlorate in a glass chimney placed over the filter mat. The glass fiber filter disc was placed over a medium porosity sintered glass disc sealed into a round glass base. The surfaces of the glass chimney and sintered glass disc were ground flat and the glass fiber mat centered between the two flats and spring-loaded to make a liquid tight seal. The base of the assembly was placed into a suction flask for filtering. The accuracy of the yield determination and reproducibility of the sample mount are relatively important. The glass fiber mat was far superior to paper filter discs in drying and weighing the cesium perchlorate. The cesium samples were counted over a period of time sufficient to check for the presence of short-lived activities. Also, a scintillation spectrometer has been useful in examining the samples for the presence of foreign radiochemical nuclides.

Another method for the determination of total fissions for short irradiations not used in this program is the isolation and counting of 67-hour molybdenum-99. Neptunium-239 is used to determine the ratio of fission to capture events.[2]

Plutonium Assay

In an evaluation of a reactor such as the EBR, it is necessary to analyze accurately for plutonium over an extremely wide concentration range. Some irradiation levels are so low that the plutonium-239 activity of the samples is not sufficient to make an accurate alpha assay. When this occurs, it has been found possible[2] to isolate and count the beta radiation associated with the short-lived neptunium-239 parent of plutonium-239.

At intermediate irradiation levels, however, it is more convenient to isolate the plutonium and determine the absolute alpha disintegration rate. The intermediate levels may be defined arbitrarily as 0.05 to 500 micrograms of plutonium per gram of uranium. In this region, the low concentrations of plutonium have been quantitatively isolated from uranium(VI) by extraction of plutonium(IV) from one molar nitric acid solution with thenoyltrifluoroacetone (TTA). Hyde[5] has recently summarized many of the applications of TTA extraction to the actinide ele-

ments. Also, in the intermediate region with plutonium concentrations of 20 micrograms or more per gram of uranium, a direct mount technique has been employed successfully. The uranyl nitrate solution containing the plutonium and fission products was mounted directly on a mirror-finished stainless steel plate. A very uniform spread of the sample must be obtained over a defined circular area. By means of a fine air jet, an aqueous nitrate sample was mixed into glycerine which had been placed previously on the plate, and the glycerine was slowly fumed away. With carefully calibrated and monitored counters, assays were made to an accuracy of approximately $\pm$ 1%.

For the alpha assay, low, intermediate, and 50% geometry alpha proportional counters have been particularly useful at the various plutonium concentrations. The calibration of the 50% geometry counter was the most difficult and exacting. The difficulty of this calibration was caused by the radiation at low angles to the sample plate which includes the backscattered particles and those most sensitive to self-absorption effects. A compensating factor with the 50% geometry counter was the larger sample areas which could be counted with only small corrections to the equivalent point source. Jaffey[6] has recently given a detailed discussion of the techniques of alpha measurements.

The plutonium assay requires the determination of absolute disintegration rates, a knowledge of the isotopic content of the plutonium for the calculation of specific activity, and either separation from or correction for other alpha-emitting isotopes.

Three general methods have been found particularly useful in the isotopic determinations. They are spontaneous fission counting, alpha pulse analysis, and mass spectrographic analysis. Other reports will give a more detailed discussion of these methods.

Uranium Analysis

The plutonium production and the number of fission events must be determined relative to a unit mass of uranium fuel or blanket material. This required the analysis of the uranium content of solutions to the same accuracy as the other analyses. There are many procedures in the literature which will be applicable and which will meet the requirements of the accuracy of 1%, or better.

In order to maintain a good check on the uranium analysis, the solutions were analyzed by two independent methods, each capable of an accuracy of better than 1%. One method chosen was a standard potentiometric titration of uranium(IV) with a standard iron(III) solution.[7] The second method[8] was a differential spectrophotometric procedure applied to the uranium(VI) thiocyanate complex. The results of the two procedures varied by less than 1%, and an average value was used in the calculations.

Determination of Fission to Capture Ratios and the Ratio of Uranium-235/Uranium-238 Fissions

The determination of the total fissions in a given material has been discussed above. It is now possible to determine the fission to capture ratios on such material by an isotopic analysis for the nuclide formed by the capture process. An example of this determination in the Experimental Breeder Reactor has been the determination of fission to capture ratios (uranium-235 fissions/uranium-236) at various points in the enriched uranium core. The uranium-236 was determined by mass spectrographic analysis. Also it was possible to calculate the ratio uranium-238/plutonium-239 fissions in the blanket surrounding the core. The blanket material was the natural isotopic mixture of fissionable uranium-238 and uranium-235. Therefore, the total number of fission events found had only to be corrected to uranium-238 fission. This correction was possible by chemical analysis. However, a more direct fission-to-capture ratio may be obtained by using very highly depleted uranium-238 or highly enriched uranium-235.

The basis for the determination of the ratio uranium-235 fission/uranium-238 fission has been discussed previously.

The ruthenium-106 yield varies by a factor of almost six for uranium-235 and uranium-238 fission and is higher for the uranium-238 fission. The cesium-137 yield is essentially constant for both nuclides. The method must be calibrated using uranium-235 and uranium-238 foils in a neutron flux of approximately the same energy as the irradiated samples. The cesium analysis was obtained by the method previously described. The ruthenium analysis was done by a distillation method.[9] The ruthenium samples contain two fission nuclides, ruthenium-106 with a one-year half-life, and ruthenium-103 with a 40-day half-life. To get a count representative of only the ruthenium-106 content of the sample, counts were taken with a halogen-filled Geiger tube through 164 mg/cm^2 and 2050 mg/cm^2 aluminum absorbers. The difference between these two counting rates was proportional to the ruthenium-106 content of the sample. The observed variation in the ruthenium-106/cesium-137 ratio for uranium-235 was 1.6 for a thermal flux to 2.4 for a fast flux. The same ratio obtained with uranium-238 in a fast flux was 9.0. This emphasizes the need for fair reproducibility in the neutron energy spectrum.

SUMMARY

The radiochemical analysis of the Experimental Breeder Reactor indicated that 1.00 $\pm$ 0.04 atom of plutonium was produced for each atom of uranium-235 consumed. For each 100 atoms of uranium-235 consumed in the core (fission plus capture), 110 net atoms of plutonium (total produced minus amount fissioned) were produced. However, in the same period, 10 atoms of uranium-235 were consumed in

the natural uranium blanket for a net conversion ratio of 1.00. The conversion ratio determined by physical measurements on the same experiment was calculated to be between 0.99 and 1.02.

ACKNOWLEDGEMENTS

D. Engelkemeir and T. Novey assisted in the experiments necessary to calibrate the fission product method. A. H. Jaffey performed the alpha pulse analysis used to determine plutonium-238/239 ratios. M. G. Inghram and D. Hess did the mass spectrometric work. D. Krause, R. Milham, and H. Hubbard assisted in developing the assay procedures for uranium and plutonium. Also, M. Levenson correlated the chemical data and calculated the over-all conversion ratio of the reactor.

REFERENCES

1. Steinberg, E. P. and Freedman, M. S., in Coryell, C. D. and Sugarman, N., *Radiochemical Studies: The Fission Products*, National Nuclear Energy Series, Division IV, Vol. 9, Paper 219, McGraw-Hill Book Co., New York (1951).
2. Spence, R. W. and Smith, L., Los Alamos Scientific Laboratory, Private Communication.
3. Freedman, M. S. and Steinberg, E. P., in Coryell, C. D. and Sugarman, N., *Radiochemical Studies: The Fission Products*, National Nuclear Energy Series, Division IV, Vol. 9, Paper 200, McGraw-Hill Book Co., New York (1951).
4. Glendenin, L. E. and Nelson, C. M., in Coryell, C. D. and Sugarman, N., *Radiochemical Studies: The Fission Products*, National Nuclear Energy Series, Division IV, Vol. 9, Paper 283, McGraw-Hill Book Co., New York (1951).
5. Hyde, E. K., in Seaborg, G. T., Katz, J. J. and Manning, W. M., *The Actinide Elements*, National Nuclear Energy Series, Division IV, Vol. 14-B, Ch. 15, McGraw-Hill Book Co., New York (1954).
6. Jaffey, A. H., in Seaborg, G. T., Katz, J. J. and Manning, W. M., *The Actinide Elements*, National Nuclear Energy Series, Division IV, Vol. 14-B, Ch. 16, McGraw-Hill Book Co., New York (1954).
7. Rodden, C. J., *Analytical Chemistry of the Manhattan Project*, National Nuclear Energy Series, Division VIII, Vol. 1, p. 62, McGraw-Hill Book Co., New York (1950).
8. Crouthamel, C. E. and Johnson, C. E., *Spectrophotometric Determination of Uranium by Thiocyanate Method in Acetone Medium*, Anal. Chem., *24*: 1780 (1952).
9. Glendenin, L. E., in Coryell, C. D. and Sugarman, N., *Radiochemical Studies: The Fission Products*, National Nuclear Energy Series, Division IV, Vol. 9, Paper 260, McGraw-Hill Book Co., New York (1951).

Record of Proceedings of Session 8B.1

THURSDAY AFTERNOON, 11 AUGUST 1955

Chairman: Mr. O. Hahn (Germany)

Vice-Chairman: Mr. G. B. Cook (UK)

Scientific Secretaries: Messrs. J. Gaunt and A. Finkelstein

PROGRAMME

P/614 Survey of radiochemical studies of the fission process ..... L. E. Glendenin and E. P. Steinberg

P/718 Spontaneous fission correlation..... A. Ghiorso

DISCUSSION

P/881 The distribution of nuclear charge in low energy fission..... A. C. Pappas

DISCUSSION

The CHAIRMAN: Ladies and gentlemen, before our discussion today on fission processes I would like to say how extraordinarily pleased and honoured I am to be able to act as Chairman here, although I have not worked on radioactivity or on fission for the last ten years. It is, therefore, a most exciting and interesting adventure to hear these lectures on what has happened since 1939—or rather December 1938—when Dr. Strassman, whom I have the pleasure to see here with us, discovered the presence of barium in neutron-bombarded uranium. We, of course, were not so fortunate as present-day workers in having strong sources, but we were quite content because we could easily work with our preparations of 1 or 1½ grammes of radium mixed with beryllium, and therefore there was no danger at all in carrying out separations and no need for the protection now required by those working on hot chemistry. We had the advantage of investigating these processes and I remember that Dr. Strassman and myself made our preparation with iodine and had it in the counter about 1.8 minutes after it had been irradiated and separated from the other materials. Now we can see what has become of all these things begun ten or fifteen years ago, and I am very happy to have the opportunity, and the honour, of being your Chairman this afternoon.

Mr. E. P. STEINBERG (USA) then presented paper P/614 as follows:

The complexity of the phenomenon of nuclear fission is illustrated by the fact that some 300 nuclear species of thirty-six different elements are formed in the reaction. Radiochemical studies of this process consist mainly in the determinations of the probabilities of formation or fission yields of these species. The radiochemical technique is particularly well suited to the determination of these yields, which may vary over a factor of 10^6. In such studies, as was briefly indicated by Mr. Hahn, an element produced in fission is chemically isolated and the number of atoms of one or more of its isotopes is determined by counting the radioactivity or by mass spectrometry. From this number and a knowledge of the irradiation conditions, the number of atoms actually formed during irradiation can be calculated. The ratio, then, of the number of atoms formed to the number of fissions which took place gives the fission yield of the particular nuclide. Such data are of importance to practical problems of reactor design and operation and to an understanding of the nature of the fission process itself. For convenience, we will discuss the results of these measurements under three main topics: first, the distribution of mass in fission; second, the division of nuclear charge in fission; and third, information regarding nuclear closed shell effects in fission—that is, the influence of the so-called "magic number" structures. The work to be covered is the result of the efforts of many individuals and groups and although in the interests of time, no specific references to the original workers will be made in this talk, the source material is fully referenced in the copy of the paper to be published in the Proceedings of this Conference.

The mass distributions in low-energy neutron-induced fission all exhibit the familiar twin-peaked curve representing asymmetric fission. The first five slides will illustrate the extent of our present knowledge of these fission yields in various fissile nuclides.

Slide 1 (Fig. 1 of P/614) shows the fission yield-mass distribution curve for Th^{232} with so-called fast neutrons, since thorium is not fissionable with thermal neutrons but has a threshold at about 1 Mev, and this fission is referred to as fast neutron induced fission.

Slide 2 (Fig. 2 of P/614) shows a similar curve for the fast neutron induced fission of U^{238}.

Slide 3 (Fig. 3 of P/614) shows the slow neutron or thermal neutron induced fission of Pu^{239}. The scale is semi-logarithmic so that the extent of the data on fission yield can be put easily on one slide.

Slide 4 (Fig. 4 of P/614) shows the mass distribution in U^{233}.

Slide 5 (Fig. 5 of P/614) shows the vast amount of work that has gone into the determination of fission yields in U^{235}.

It is obvious that all these curves appear quite similar, but there are some significant differences which are readily apparent on closer examination.

In Slide 6 (Table III of P/614) some of the generalizations that can be drawn from a comparison of these mass distributions are illustrated. It will be noted from the second column that a shift in the position of the light group that is indicated with increasing mass of fissile nuclide, while the position of the heavy group remains relatively fixed. In the second place a slight tendency towards a broadening of the fission yield-mass distribution with increase in mass of fissile nuclide is observed. Thirdly, variations are noted in the ratio of the peak, or the maximum fission yield, to the central minimum representing symmetric fission. It should be pointed out here that this is probably associated with differences in the excitation energy of fission in these various nuclides, and it is interesting to note that evidence has been obtained for an increase in the probability of symmetrical fission with increasing energy of excitation. In fact, at very high energies a single-hump curve is obtained with the highest probability for symmetrical fission.

In addition to the distribution in mass in the fission process, a distribution in nuclear charge for a given mass split is observed. There is a most probable charge division for each mass split and a distribution about this most probable charge. Data of quantitative value in the study of the problem of charge division and distribution in fission are fission yields along the decay chains and the yields of shielded nuclides. The latter are of particular significance since they are preceded by stable nuclides in the decay chain and should, therefore, occur in fission only as a result of direct formation as a primary fission product.

The available fission yield data are most consistent with the hypothesis that the most probable mode of charge division is that which gives rise to equal displacement of charge from stability, that is, to equal effective chain lengths for the complementary masses. Furthermore, the distribution about the most probable charge appears to be a symmetrical function which is applicable to all mass splits and to all fissile nuclides.

The fundamental equations of the equal charge displacement hypothesis are:

$$Z_A - Z_p = Z_A^* - Z_p^* \quad (1)$$

$$Z_p + Z_p^* = Z_F \quad (2)$$

$$A + A^* = A_F - \nu \quad (3)$$

$$Z_p = Z_A - \tfrac{1}{2}(Z_A + Z_A^* - Z_F) \quad (4)$$

where Z_A and Z_A^* are the most stable charges for the complementary mass A and A^*. Z_p and Z_p^* are the corresponding most probable charges. Of course, the sum of the two most probable charges must equal the charge of the fissioning nucleus Z_F. The relation between the complementary masses A and A^* is given in Equations 3. From Equations 1, 2 and 3, the equation for Z_p may be derived, and it is given as Equation 4.

The available data on primary yields are summarized in Slide 7 (Fig. 6 of P/614) with Z_p calculated on the basis of the equal charge displacement hypothesis.

The data are seen to fit well on a smooth charge distribution curve with very few exceptions. The points with arrows represent upper limit values. In these cases only upper limits were established and the actual independent yield was not positively established. In addition there are some horizontal bars on a few of the experimental data which are indicative of the uncertainty in the Z_A value to be used in calculating Z_p when one crosses one of the closed shells. In the cases here the point represents the average value and the bar represents the extent of the uncertainly at the closed shell crossing. It has been observed that the charge distribution curve for 14-Mev neutron induced fission of U^{235} is parallel to that of low-energy neutron induced fission with the most probable charge for a given mass split shifted toward stability. It thus appears that a single charge distribution curve is applicable over a considerable range of excitation energy in fission.

However, in very high energy fission, the division of nuclear charge is apparently different, the most probable charge being that which maintains the neutron-to-proton ratio of fissioning nucleus. This probably indicates that at very high energies, fission takes place too rapidly to permit a rearrangement of charge.

Refinements in the measurement of fission yields and, in particular, the introduction of mass spectrometric techniques, have revealed considerable fine structure in the mass distributions in low-energy fission.

The observed data for reactor neutron fission of U^{235} are presented in Slide 8. The co-ordinates here are linear. The circles represent mass spectrometric data and the squares represent radiochemically determined data. Appreciable structure is observed in the mass regions of the peaks of both light and heavy groups.

In Slide 9 the same data are presented with the heavy group reflected over the light group (heavier line), such that the sum of masses is 234. This assumes 2 neutrons emitted per fission.

An interpretation of these results may be given

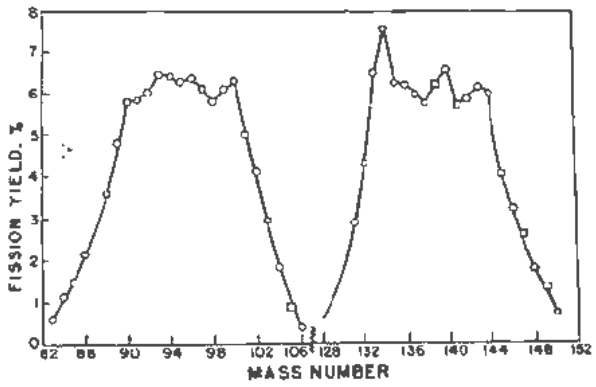

Slide 8. Yield-mass curve for slow neutron-induced fission of U^{235} (observed data)

in terms of the effects of closed shells of 50 and 82 neutrons. The large peak in the heavy group occurs at mass number 134 which is just the region of nuclides containing 82 neutrons. It is significant that a peak is also observed in the light group at mass number 100—a region in which there are no important shell closures. However, it is the region complementary to mass number 134 and may thus represent the preferential formation of the 82 neutron structure in fission. The fact that the yields in the heavy group are higher than those in the light group in the mass region 133–136 and lower in the region 136–142 is interpreted as the result of additional neutron evaporation (both prompt and delayed) from fission fragments containing 83, 85 and 87 neutrons. Such structures have abnormally low binding energies for the odd neutrons just outside the closed shell of 82. The result of such neutron evaporation would be an increase in yield for mass numbers near the closed shell at the expense of those of higher mass number, as observed. Moreover, since the loss in yield from a chain of given mass number in this region would not always be compensated by the gain from the chain of one higher mass number, a rather complex pattern of yields in this region might be expected, probably accounting for the zigzag as observed.

Similar considerations would apply to the region of the 50 neutron shell, but since this shell occurs in the region of very steeply rising yield, it is not as easily discerned.

Slide 10 (Fig. 7 of P/614), illustrates the interpretation of these data. An attempt has been made here to correct the observed data for delayed neutron emission as indicated by the arrows. The points from which the arrows start are the observed experimental data. These have been corrected for the yield of the delayed neutron emission in the chain as indicated. In addition, a hypothetical normal distribution has been indicated in the light group by the dotted line. A subtraction of this dotted line from the observed data gives one some indication of the preferential formation of the 82 neutron structure in fission. Although the data for U^{233} are not as extensive as for U^{235}, somewhat similar results have been obtained.

Slide 11 (Fig. 8 of P/614) illustrates the nuclear structure preference effect in U^{233}. In this case, a shoulder rather than a peak is observed in the light group, with a normal distribution indicated by the dotted line and the 82 neutron structure preference effect obtained by subtraction. The presence of a shoulder rather than a peak may be accounted for by the known shift of the light group towards lower mass numbers which has the tendency of sliding the peak down the side of the curve. It should be noted that there is a sparsity of data in the heavy group in U^{233}, and at this point it might be indicated that some very recent work in Canada and some work reported at the recent July Moscow conference contain information on mass spectrometric yields in U^{233} for the rare earths. In general these are in fair agreement with such a curve in relative value. However, the recent USSR data appear to be somewhat lower.

Fine structure has also been observed in the spontaneous fission of Cm^{242}, and is indicated in Slide 12 (Fig. 9 of P/614). These data are radiochemically determined data and do not have the accuracy of the mass spectrometric data indicated previously. The errors are given by the bars on each experimental point. Again a hypothetical normal distribution is indicated by a dotted line with a nuclear structure preference effect at the 82 neutron structure, or in this case the reflection of the 82 neutron structure in the light group indicated by the diamonds.

For the spontaneous fission of Cf^{252} shown in Slide

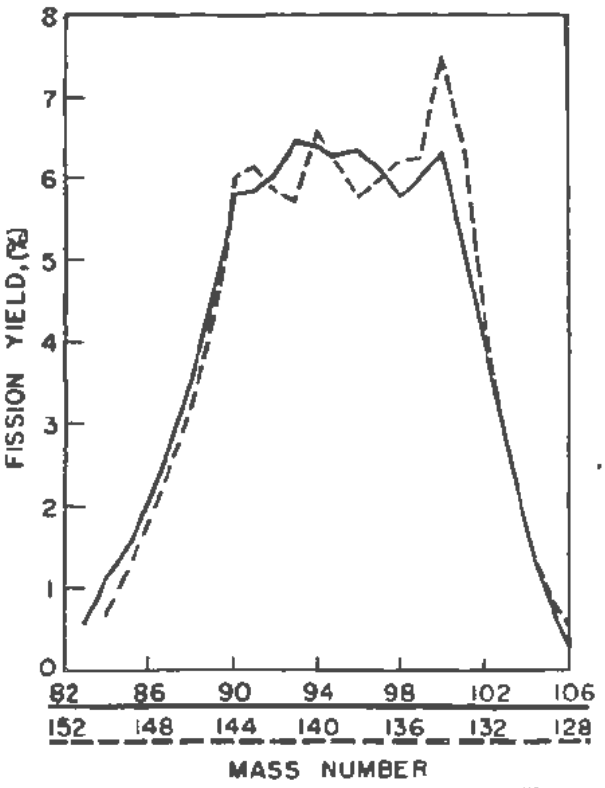

Slide 9. Comparison of light and heavy group yields in U^{235} fission

13, the data are still rather preliminary. This work was done on a very small amount of Cf^{252}. Again, there is an indication of a shoulder in the region where fine structure might be expected at the 82 neutron shell.

Table I. Positions of Fine Structure Peaks

Fissile nuclide	$\bar{\nu}$	*Mass number of 82 neutron complement*	*Mass number of observed light group fine structure*
U^{233}	2.5	98	99
U^{235}	2.5	100	101
Cm^{242}	3.0	104	105
Cf^{252}	4.0	114	114

Table I on this page summarizes the mass positions of the fine structure peaks observed in the light group mass distributions and illustrates the consistency of the observations with the expected positions of the 82 neutron complements, in each case within one mass number. Further confirmation of the existence of a nuclear structure preference effect in fission has been obtained in fission fragment velocity studies at Los Alamos.

In conclusion, then, it may be said that as a result of these radiochemical investigations of nuclear fission, a plausible interpretation of the process has developed in terms of a "normal" asymmetric splitting into two main groups of products; a superposition on this distribution of the preferential formation of fragments containing 50 and 82 neutrons; and finally, perturbations in the fission yields resulting from additional prompt and delayed neutron emission from particular products near closed shells. More detailed investigations of U^{233} and Pu^{239} fission are now in progress to provide additional information on these closed shell effects.

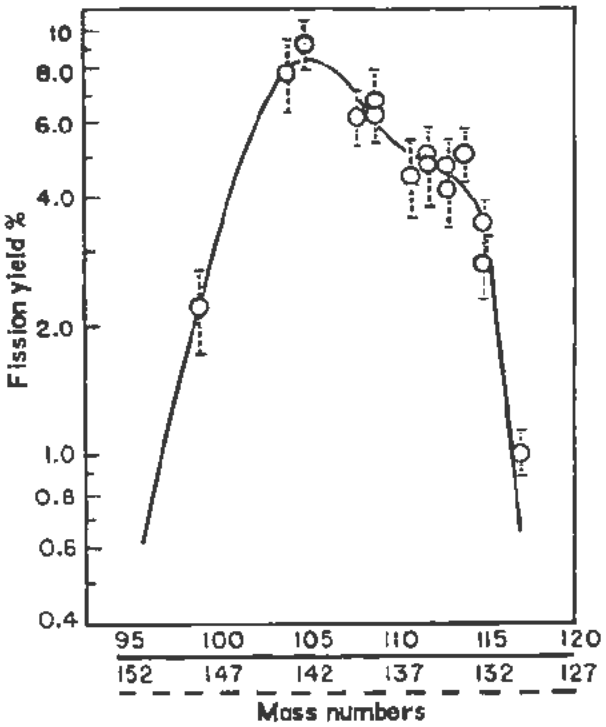

Slide 13. Yield-mass curve for spontaneous fission of Cf^{252}

Mr. GHIORSO (USA) then introduced paper P/718 as follows:

Since the field of the heaviest elements has been limited until recently to a relatively few laboratories in the world it might be helpful to those not familiar with this region of the periodic system if they had in view an isotope chart with the more significant data presented (Slide 14).

This is a conventional Seaborg Chart of the nuclides with the Z values increasing vertically and

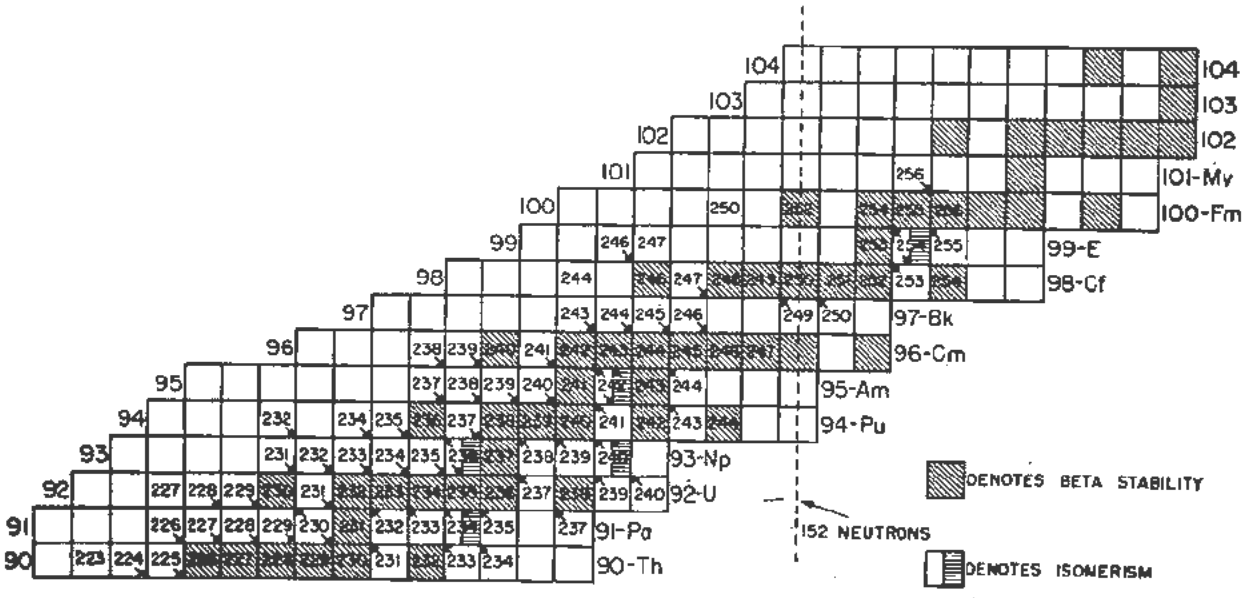

Slide 14. The heavy elements

isobars plotted diagonally. The shaded squares indicate known or predicted beta-stable isotopes. Mass numbers are shown for those nuclides which have been identified to date.

On the right are shown the chemical symbols along with the atomic numbers, and it will be noted that there are two new symbols that will now join the family of elements along with the recently discovered element 101, mendelevium, named in honor of the great Russian chemist, Mendeleev.

The discovery work involving elements 99 and 100 is appearing in the 1 August issue of Physical Review. The finding of these elements in the atomic debris from the large-scale thermonuclear explosion conducted by the United States in 1952 is described in a letter to the editor authored jointly by groups in our laboratory at Berkeley, the Argonne National Laboratory, and the Los Alamos Scientific Laboratory. As indicated in this publication, as many as 17 neutrons were captured by uranium to form the fleeting super-heavy isotope U^{255} and thus subsequently isotopes of elements 99 and 100 by successive beta-decays. Since this first experiment however, the more prosaic methods of manufacture of the heavy elements have prevailed and it has been found by Berkeley and the Argonne National Laboratory that relatively large quantities can be made by long intense slow neutron irradiations of plutonium. We have suggested as names for elements 99 and 100 einsteinium (symbol E) and fermium (symbol Fm), respectively.

With this preface Mr. Ghiorso went on to the presentation of this paper as it appears in the Proceedings of this Conference.

DISCUSSION OF PAPERS P/614 AND P/718

The CHAIRMAN: Mr. A. P. Vinogradov (USSR) wishes to ask Mr. Steinberg: What is the shortest half-life of a radioisotope which can be detected by mass spectrometry?

Mr. STEINBERG (USA): The question of the detectability of isotopes by mass spectrometry will depend considerably on the element involved since elements differ greatly in the efficiency of ion-emission from the sources. In general, one should probably phrase the question in terms of the number of atoms present, and the number of atoms that would be present, of course, is related to the half-life in terms of activity. In general, our own work has been limited to half-lives in the range of approximately a year. However, the technique has been applied to rare-gas isotopes with half-lives as short as a few hours and in special cases could probably be extended to even shorter half-lives.

The CHAIRMAN: Mr. Adyassevich wishes to make a few remarks on the measurement of the life-time of the spontaneous fission of thorium-232 made in the USSR.

Mr. B. P. ADYASSEVICH (USSR): The results of measurements of the period of the spontaneous fission of thorium obtained by Segrè which gave $T_1 = 1.4 \times 10^8$ years have not been confirmed in the USSR. According to measurements which were carried out in the USSR under conditions excluding cosmic ray effects $T = 10^{20}$ years.

The question is whether Segrè has revised the results previously obtained by him?

Mr. GHIORSO (USA): As I understand the remarks, this value is considerably longer than 10^8 years. If it is, this is not unreasonable. On the other hand, one must reconcile it with the fact that, supposedly, the spontaneous fission half-life of thorium-232 has also been measured by determining the number of neutrons given off by a source. This value gives a half-life which corresponds with the Segrè value if one assumes something like two neutrons per fission. Therefore, if the half-life in reality is longer than this value, the number of neutrons per fission would go up accordingly to something like 10 or more neutrons per fission—which is a point which is both surprising and interesting and one worth pursuing.

Mr. A. C. PAPPAS (Norway) then presented paper P/881 on which there was no discussion.

Session 8B.2

FACILITIES FOR HANDLING HIGHLY RADIOACTIVE MATERIALS

LIST OF PAPERS

An Atomic Energy Radiochemical Laboratory— Design and Operating Experience

By R. Spence,* UK

The radiochemical laboratory at Harwell was designed at a time when there was very little experience, amongst British chemists, of the handling of radioactive materials. In order to fulfil the production programme, as conceived in 1946, it was nevertheless essential to create facilities for a large number of scientists to carry out researches of a more or less unspecified nature on irradiated uranium, fission products, plutonium and all the other radioactive materials likely to be of interest. A Ministry of Works design team was sent out to Canada early in 1946 to draw up a design on the basis of a general specification which had been prepared by chemists of the U.K. Group then working in Chalk River. Rapid progress was made and the team was able to return to England after less than six weeks in Canada. Site work began at once and we were able to move into the laboratory in June 1949.

The building was probably the first large atomic energy radiochemical laboratory of permanent construction to be built in the world, as at that time most of the great United States laboratories were still housed in temporary quarters.

The basic principle of design was to achieve as much isolation of different laboratories as possible whilst retaining ease of accessibility and good communications. Each laboratory with its associated office and vestibule was designed as a self-contained suite (Fig. 1). The vestibule serves as a buffer area between laboratory and the main building corridor. It contains an emergency shower, ventilation control which allows the laboratory to be sealed off from the main ventilation system in case of accident, fire and radioactivity alarm buttons, hand washing equipment and personal monitoring equipment. It has been found useful to have an air hood and respirator receptacle in the vestibule and also to provide a box for rubber gloves and french chalk. Air flow is from the corridor, through the vestibule and into the laboratory.

The laboratories themselves are fitted with eight fume hoods and a ventilated cupboard. The main input air enters through a diffuser in the ceiling and is augmented by the flow from the corridor. The fume cupboards are of stainless steel painted with strippable lacquer and the windows and movable partitions are of armoured glass. Shielding between office and laboratory consists of a total of 14½ inches of brick, a 2 ft 6 in. service space behind the fume cupboards, and 1 inch of lead at the back of the fume cupboards. Laboratory floors are designed to take a loading of 2 tons per square foot and reinforced concrete bases permit the use of plenty of lead shielding in the fume cupboards. Practically all services are provided from the service floor above.

The laboratory suites are arranged in two wings, one for α work and one for β and γ work, together with counting rooms, balance rooms and so on. The wings are joined at one end (Fig. 2) by an administrative block containing some offices, library, conference room, stores, workshop, changing rooms, and laboratories for health physics, electronics maintenance and glassblowing services. At the opposite ends of the wings are special purpose laboratories. Those on the $\beta\gamma$ side are of concrete with facilities for small plants handling material containing high fission product activities etc.

At the end of the α-wing, there is a special laboratory for work with large amounts of plutonium and other α-emitters such as U^{233}. This consists of a double row of sealed boxes, each about 11 ft high, 15 ft long and 5 ft deep, with a service corridor between. The boxes have perspex fronts pierced with ports for rubber gloves and removable panels facing on to the service corridor at the back. When the boxes are clean, the perspex panels can be removed and access for the erection of apparatus is from the front. Once the equipment has become contaminated, the boxes can be entered only from the service corridor by men wearing pressurised suits which are supplied with fresh air through a hose line (Fig. 3). Each box is connected to the air extraction system via a separate

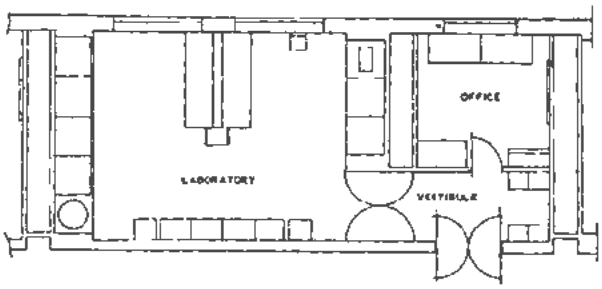

Figure 1. Self-contained standard suit comprising vestibule, office and laboratory

* Atomic Energy Research Establishment, Harwell, Didcot, Berks.

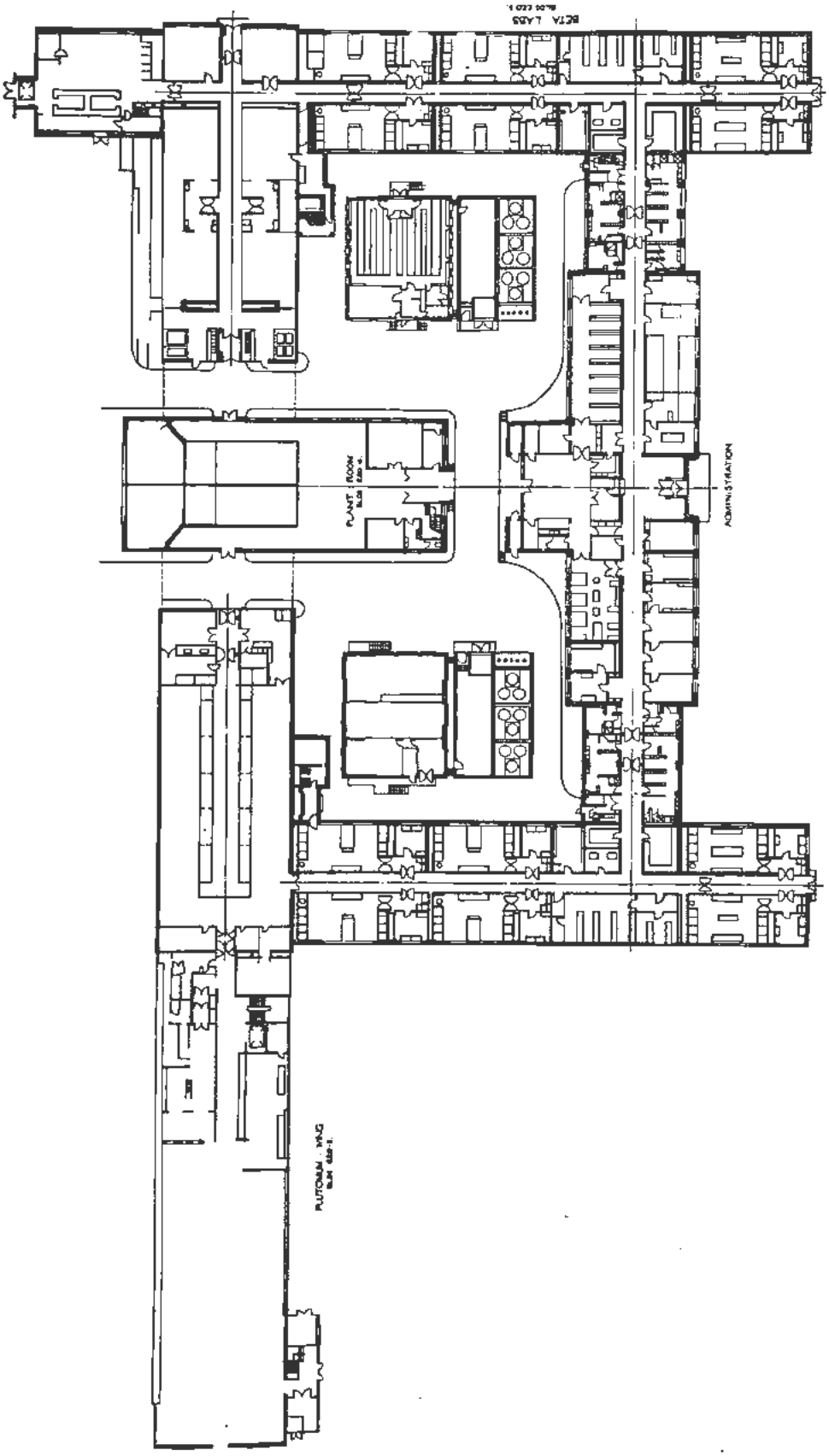

Figure 2. Plan of the radiochemical laboratory

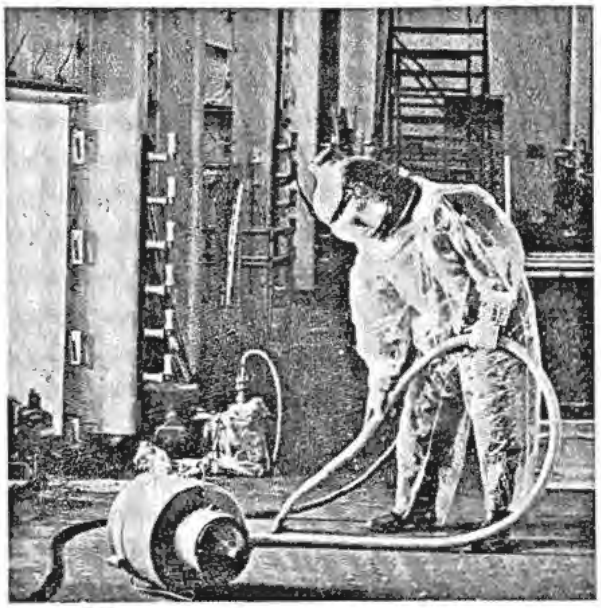

Figure 3. Pressurized suit worn in the active corridor between two rows of large glove boxes. The suit is protected by a disposable plastic overall

filter and the pressure inside is always less than that in the operating area.

Recently, a new wing has been added which is intended for work with α-active materials using equipment of more permanent nature. More than half of it is occupied by the Metallurgy Division and the remainder by Chemistry Division. The decontamination area, which is operated by men in pressurised suits, is at one end of a large open hall and movable glove boxes are connected to services in the ceiling (Fig. 4). These boxes are accessible from all sides, which is a considerable advantage. Each is fitted with an individual filter and a reduced air pressure is maintained in the box by means of a simple locally designed compressed air ejector unit. These units have been so successful that practically all the free standing glove boxes in the building have been fitted with them in place of the usual electric motor and fan. The exhaust from the box is, of course, connected by hose line to the exhaust trunking in the service floor above. When apparatus in a box is to be dismantled or modified, it is bolted to a panel on the wall of the decontamination room and the perspex side is removed so that the interior is accessible to the decontamination staff without being exposed to the main laboratory (Fig. 5).

All these precautions seem to be rather elaborate but when it is remembered that the permitted lifetime body burden of plutonium is less than one microgram, they are brought into better perspective. Moreover, as there are at least as many industrial workers employed as scientific staff, industrial conditions of operation have frequently to be introduced. The air in the laboratory working areas is continuously sampled and tested for α-activity and urine analyses are carried out regularly on the staff working in α-active areas.

Even if it were possible to carry out all operations involving radioactive materials in totally enclosed boxes a substantial ventilation system would be required merely to provide the standard of ventilation normally found in an ordinary chemical laboratory. The highly toxic nature of most radioactive materials necessitates that they be handled in fume cupboards or in glove boxes. The laboratory was designed before the use of glove boxes had become as general as it is now and it was afterwards thought that the application of glove box techniques might lead to a large reduction in the ventilation requirement. This has not been found to be so in practice. Fume cupboards are still used for the less hazardous operations because of the saving in time. On the other hand, special laboratories intended for glove box work only, such as the new wing which has been described, require very much less ventilation than the other laboratories.

The building is supplied with air through two main input systems and there are four separate exhaust systems. Both intake and exhaust air is passed through precipitrons. The total capacity of the system is about 360,000 cubic feet per minute. Owing to the large size of the ducting there is very little noise and once adjusted it works extremely well. It is somewhat inflexible, however, since adjustments to the air flow in one laboratory cause changes in several others. The large ducts can be entered for decontamination and cleaning purposes but little trouble has been experienced from activity build up. The ducting was originally protected by bituminous paint but chlorinated rubber paint has been found to be much better as regards both protection and decontamination.

Health Physics Division has set the following limits on radioactivity in the discharge from the exhaust stack:

α-activity, 75 microcuries/24 hours
β-activity, 75 millicuries/24 hours

Normally the amounts detected correspond to much less than one-tenth of these quantities, but on one or two occasions they have been exceeded by a factor of two or three, usually on account of some identifiable operation.

All drainage from sinks is passed into stainless steel tanks in the courtyards of the building; samples are taken and the effluent is pumped to the effluent farm only if the level of activity is acceptable. If it is too high, a special tanker removes that particular batch separately. Effluent which should normally be uncontaminated and which is produced in large amounts, e.g., cooling water, is collected in 20,000 gallon tanks and this is also tested before pumping to the main effluent farm.

Total active effluent from the building is about 5000 gal per day and process water (inactive) amounts to about 21,500 gal per day. The usage of water per man has decreased from about 400 gal/man/day two years ago to about 115 gal/man at present. This is probably due to the abolition of straight-through process water in the new wing and the substitution of

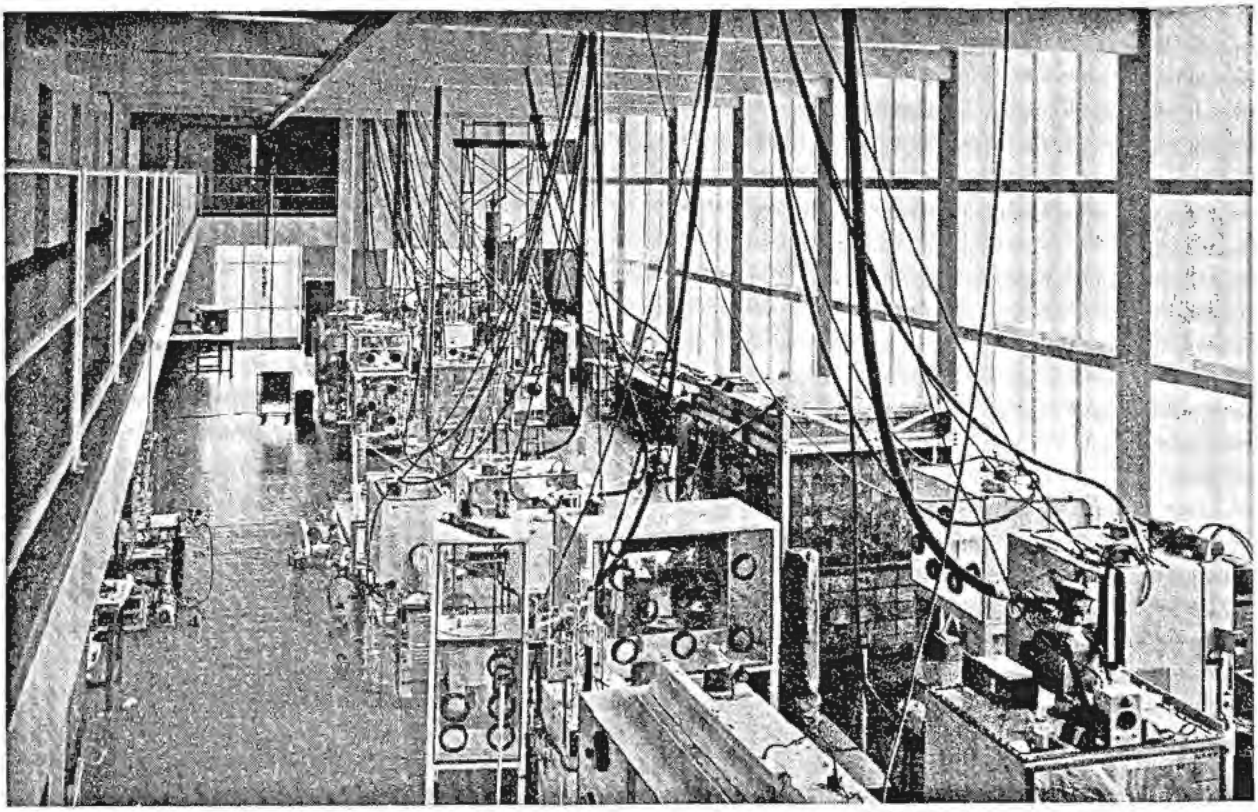

Figure 4. View of the new plutonium wing. The decontamination room is behind the camera

portable water circulating units incorporating a fan operated cooler. Solid waste arising in the laboratories is divided into "low level-undefined" and "high level" and placed in separate containers to which a certificate is attached by the scientist.

Engineering operation and maintenance of the building is under the control of the building engineer who is on the staff of the Establishment Engineering Services Division. He is in charge of workshop staff, maintenance staff and decontamination and general engineering services staff. His responsibilities include decontamination after radioactive spills, decontamination of laboratories and dry boxes including pressurised suit operations and provision of assistance in emergencies of all kinds.

One of the most serious questions in a laboratory of this type is that of fire. A general conflagration involving quantities of plutonium of the order of 1000 gm or more might dangerously contaminate the rest of the site. Special care has been taken, therefore, to prevent the spread of fire, especially in the plutonium laboratories. Fires have actually originated in dry boxes containing plutonium on a few occasions but in each case they were dealt with before much damage could be done. A special stock of non-inflammable perspex is held for use in boxes where large amounts of plutonium are being handled and where there is the possibility of a fire risk. Installations for flooding laboratories or dry boxes with inert gas (CO_2, N_2 or argon) are also employed. Steel bench and office furniture has been introduced in the plutonium laboratories and the whole building is of course regularly patrolled at night.

There is only one general alarm for the whole building and when this is sounded, either for an incident inside the building or for a site incident, staff vacate the laboratories and collect in the administrative area. There is also a local alarm in the two large plutonium laboratories which is sounded when there has been a serious spill or an outbreak of fire. Incidents throughout the building are signalled on boards in the offices of the health physics officer, control engineer, watchkeeper and Division Head.

Good ventilation and a high standard of maintenance have prevented any spread of contamination. Backgrounds recorded in the counting rooms are still indistinguishable from those recorded elsewhere. For health physics control purposes, the laboratory has been divided into three areas, namely white (inactive area), blue (buffer area) and red (active area). Laboratory shoes and clothing must be worn by those working in the red areas but these must not be taken into white areas. Visitors to red areas are provided with laboratory coats and "shoe bags" of cotton or cotton with canvas sole and elastic tops. These, which are all big enough to cover the largest size of shoe, have been found to be infinitely more convenient for visitors than shoes or overshoes. Wherever there is a special risk of contamination, as for instance in a polonium laboratory, a local barrier is set up in the vestibule where shoe bags or shoes can be changed on leaving the laboratory. This system has worked ex-

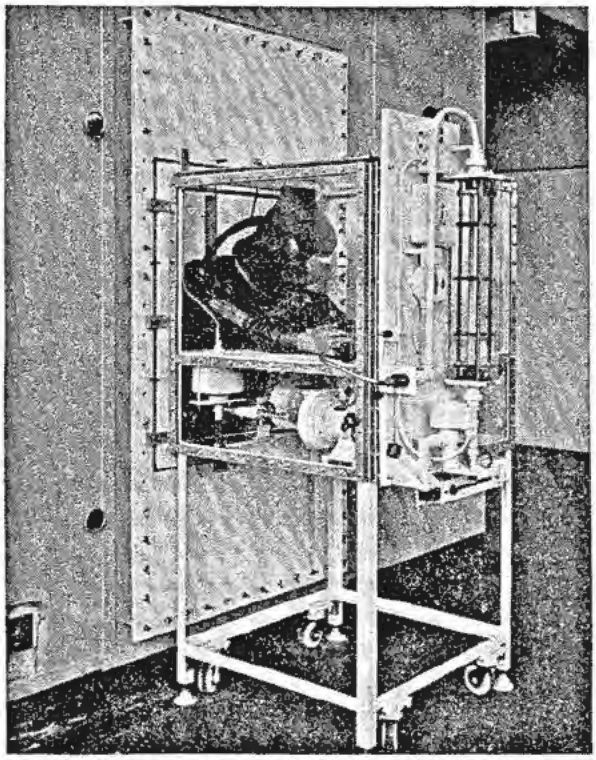

Figure 5. Glove box attached to one of the panels of the decontamination room showing worker in pressurized suit

tremely well; there have been several instances of very heavy contamination in the laboratory, necessitating the use of air hoods, without there being any spread of contamination into the main corridor. Smoking is allowed in buffer areas, which now include corridors and offices attached to laboratory suites, but dining is restricted to the administrative area.

The return of equipment which has been used in the laboratories, to the main stores or workshop in the administrative wing, is prohibited. Local stores and workshops for dealing with contaminated or possibly contaminated apparatus and equipment are located in the active laboratory wings. In this way a reliable supply of uncontaminated apparatus is always available.

There have been few accidents of any kind and none involving radiation damage to an individual. The main incidents have been four minor fires, chiefly in plutonium glove boxes, three spills due to breakage of X-ray capillaries, a few cases of bursting of containers due to decomposition by internal radiation and several "fume offs" occurring in active residue storage vessels such as the standard active waste carboy, into which solutions containing nitric acid and organic solvents had been introduced. All such vessels are now maintained neutral by addition of alkali and have given no further trouble. Safety measures throughout the laboratory are discussed by a Safety Committee. Representatives of Medical, Health Physics and Engineering Services Divisions sit on this Committee together with members of the scientific staff. The latter serve for periods of six months so as to give as many as possible a personal interest in safety procedures. The chairman is a senior scientist who serves for a number of years.

General operating experience of the laboratories has been satisfactory. The system of partially isolated suites has worked well and it is doubtful whether a less permanent, more flexible structure would have any advantage. As it is, they are exceptionally well insulated from outside noise and are easy to decontaminate. The plutonium laboratory facilities have also been most useful. Trouble was experienced in the pressurised suit area of the original plutonium wing when air tolerances were exceeded due to spread of contamination during showering, and removal of the suit. These difficulties were overcome by providing better arrangements and higher grade supervision.

The concrete shielded area of the $\beta\gamma$ wing has proved to be the least satisfactory. It was very useful for pilot plant work but this has now been removed to the Chemical Engineering building and the current requirement is for easily operated cells with good vision. It would probably be best to do away with the internal walls and to have a large open laboratory for this work. Temporary or semi-permanent shielding and cells could then be erected as required without the space restrictions imposed by internal walls.

On the whole, linoleum flooring has proved to be satisfactory and cheaper than other alternatives which have been tried. Regular wax polishing and de-waxing removes surface contamination quite well but creates a slight risk due to slipperiness. The floors themselves have borne extremely heavy loads but covered floor ducts have sometimes failed. It is important therefore to make these strong.

Strippable paint was used originally on rather a generous scale but experience has shown that a good hard gloss enamel is quite adequate for laboratory walls, etc., and that strippable coatings need only be used in the immediate vicinity of activity, e.g., fume cupboards and dry boxes. Recent practice has been to lay down a strippable coating first and then to cover this with a coating of a chlorinated rubber paint which has better decontamination properties.

The ventilation plant is, of course, expensive to operate but has been most valuable from the users point of view. Local filtration of exhaust air is becoming more general and it may be that the main exhaust precipitron could ultimately be eliminated. In order to economise on operating costs, the input air temperature is reduced by 10°F and the air flow is also reduced after normal working hours.

In conclusion, it can be said that whilst many designs are possible for a large radiochemical laboratory, the experience of this particular design has been reasonably satisfactory and provides a useful basis for discussion of future developments.

ACKNOWLEDGEMENTS

The author wishes to thank Mr. W. E. Harris, Mr. G. N. Walton and Mr. E. J. Bennellick for their assistance in providing information.

Hot Laboratory Facilities for a Wide Variety of Radiochemical Problems

By P. R. Fields and C. H. Youngquist,* USA

Many different types of chemical problems varying from intense irradiations of plutonium to produce the heavier elements such as 99 and 100[1] to the processing of different cyclotron target materials have been successfully handled in the shielded caves at Argonne National Laboratory. The caves are divided into three categories: (*a*) the large caves capable of shielding 10,000 curies of gamma activity; (*b*) the intermediate caves which can shield up to 100 curies of gamma activity; and (*c*) the junior caves which can shield about 1 curie of gamma activity.

Figure 1 shows a large cave used primarily for metallurgical studies. The cave is designed to handle safely 10,000 curies of a 1-Mev gamma emitter.[2] The inside of the cave is 10 ft wide, 6 ft deep, and 12.5 ft high. Observation of operations inside the cave is made through two 36 by 30 in. zinc bromide solution windows at the front and 30 by 20 in. windows at either side. Access to the interior is provided in the rear of the cave, through two 14-in. thick steel overhung doors. The cave is equipped with a pair of large master-slave manipulators.[3]

Figure 2 illustrates one of the several types of intermediate level caves. These facilities are new and have not been used as yet for radio-chemical studies. The cave is divided into three cells. The walls consist of two feet of high density concrete designed to shield 100 curies of 1-Mev gamma radiation. The interior of each cell is 7 ft wide, 6 ft deep, and 12.5 ft high. The upper portion of the 8-in. thick steel partitions between cells are movable to allow passage of manipulators from cell to cell. Each cell has a zinc bromide solution front window, 50 by 30 in., and each end cell has a side window, 34 by 24 in. Access to the cells is through rear doors similar to the large caves. Master-slave manipulators are used in these caves.

Another type of intermediate level cave used exclusively for chemical problems is illustrated in Figs. 3 and 4. The walls consist of 6 inches of steel designed to contain sources up to 100 curies of 1-Mev gamma radiation.[4] The interior of the cell is 18.5 ft long, 3 ft wide, and 7.5 ft high. There are four 23 by 35-in. laminated plate glass windows. Access doors are at each end of the cave, and four more are located in the back of the cave. Inside, running the full length of the cave is a rectilinear manipulator operated electrically from a control box connected to the face of the cave.

Figures 5, 6 and 7 show several different types of junior caves. In general, these caves have three-inch thick steel walls.[5] The interior is about 5 ft wide, 3 ft deep, and about 4 ft high. The windows are high density lead glass. In general, the face of the cave is movable and provides access to the interior, as shown in Figs. 5 and 7. Some of the caves have master-slave manipulators which enter through the top, and some

* Argonne National Laboratory.

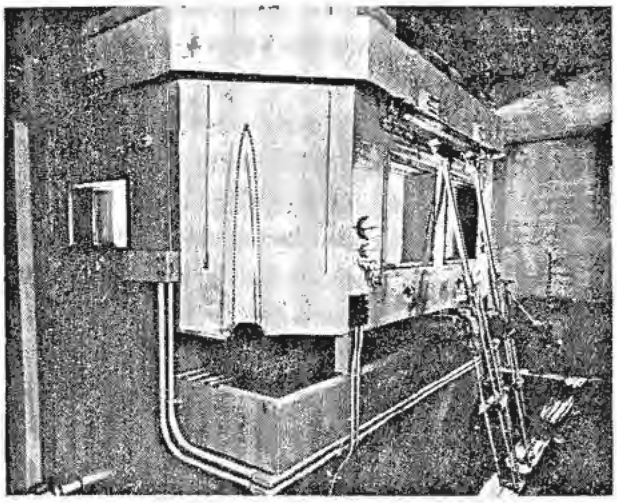

Figure 1. High level metallurgy cave for 10,000 curies

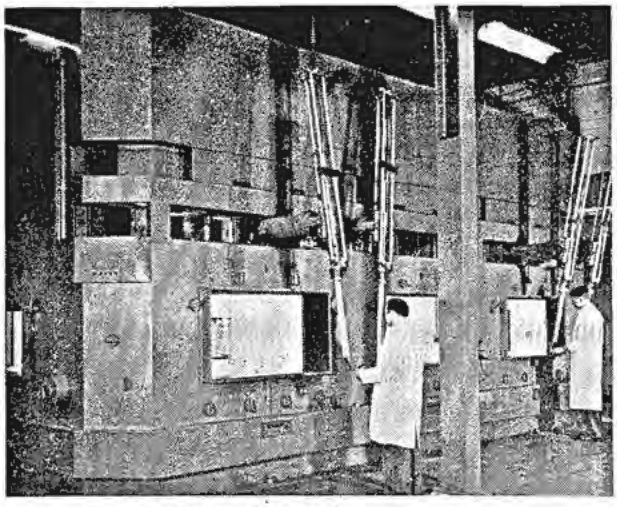

Figure 2. Three cell intermediate level metallurgy cave for 100 curies

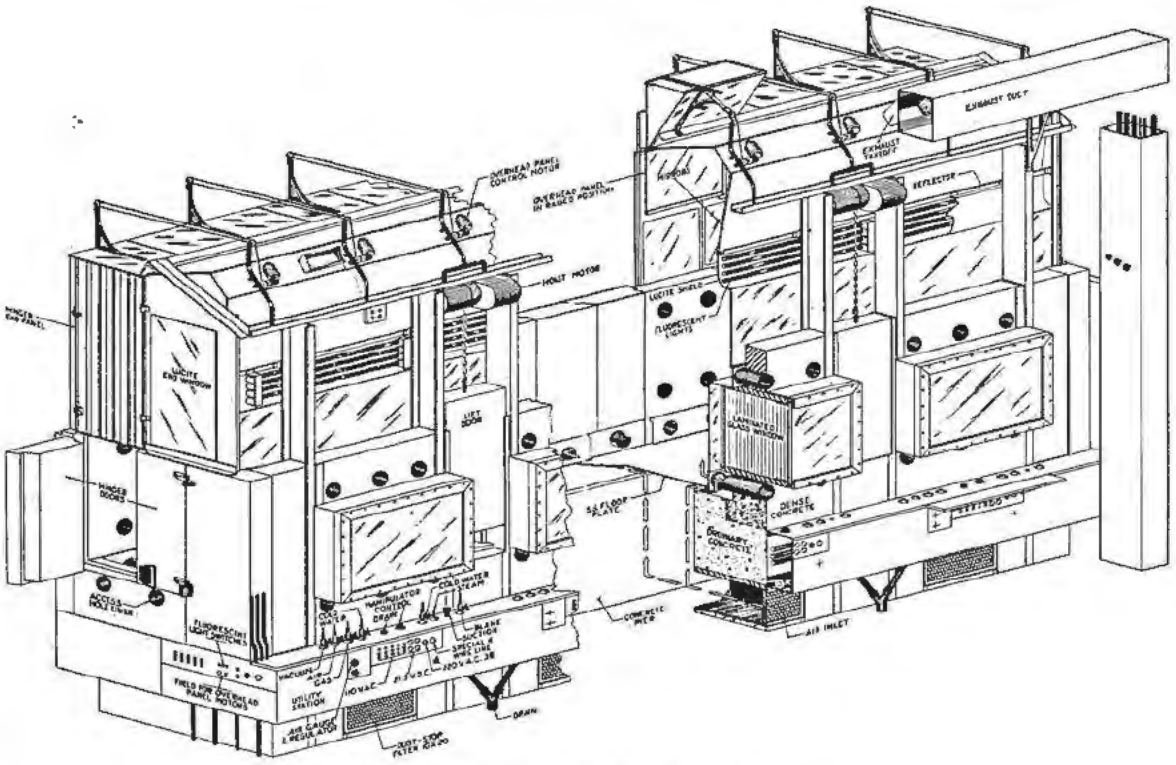

Figure 3. Diagram of intermediate level chemistry cave

have tong manipulators mounted in the face of the cave in ball joints (Fig. 7). The latter type has proven to be less convenient and versatile than the slaves, but is much more economical to construct and maintain.

The caves are all ventilated by a steady stream of air that enters at all cracks and joints as well as the regular air intakes. This air is passed through a prefilter in or adjacent to the cave before being drawn through high efficiency filters and finally discharged to atmosphere. Where chemical operations normally take place, air is drawn into the cave so that the velocity at an access door is about 135 feet per minute.

For work with high level alpha activity, glove boxes of the type shown in Fig. 8 are used. From 15 to 25 cubic feet per minute of air enters each of these boxes, through the ends, and is exhausted in the center through the prefilter chamber above the glove box. These chambers are constructed so that a contaminated prefilter can be covered before being pulled out into the room. Also, during this process, the air flow is into the chamber, thereby minimizing the scattering of active particulate matter.

Active material is brought into the box through the end transfer chamber and removed, when necessary, in closed paper cartons through the same chamber. When the outer transfer chamber door is opened, air flow is into the box at a higher than normal velocity. The glove boxes frequently have equipment built into them such as centrifuges and devices for preparing samples of radioactive solutions.

The following examples illustrate the types of problems encountered in working with high levels of radioactivity.

The Chemistry Division at Argonne National Laboratory has recently been engaged in a series of plutonium irradiations in the Materials Testing Reactor to produce the heavier transplutonium elements. The chemical processing of the samples was carried out in the intermediate level chemistry cave.

When the samples were returned to Argonne from the Materials Testing Reactor, they contained about one curie of alpha activity and about 3×10^5 r/hr (roentgens per hour) of beta and gamma activities.

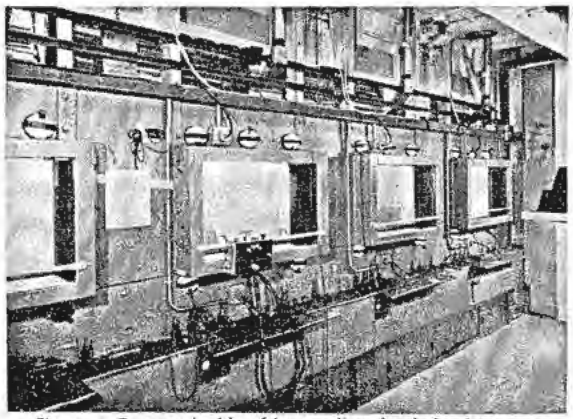

Figure 4. Operator's side of intermediate level chemistry cave

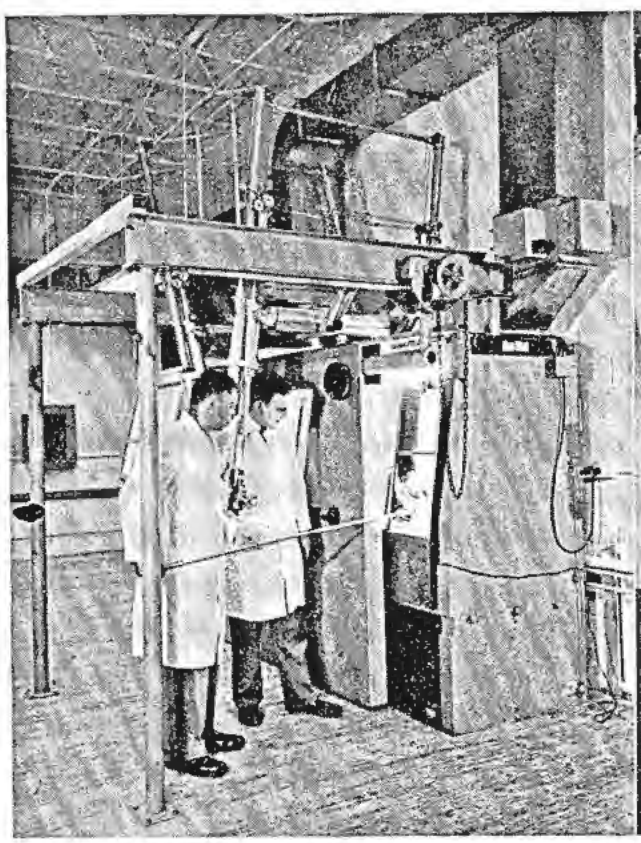

Figure 5. Loading sample in one curie junior cave

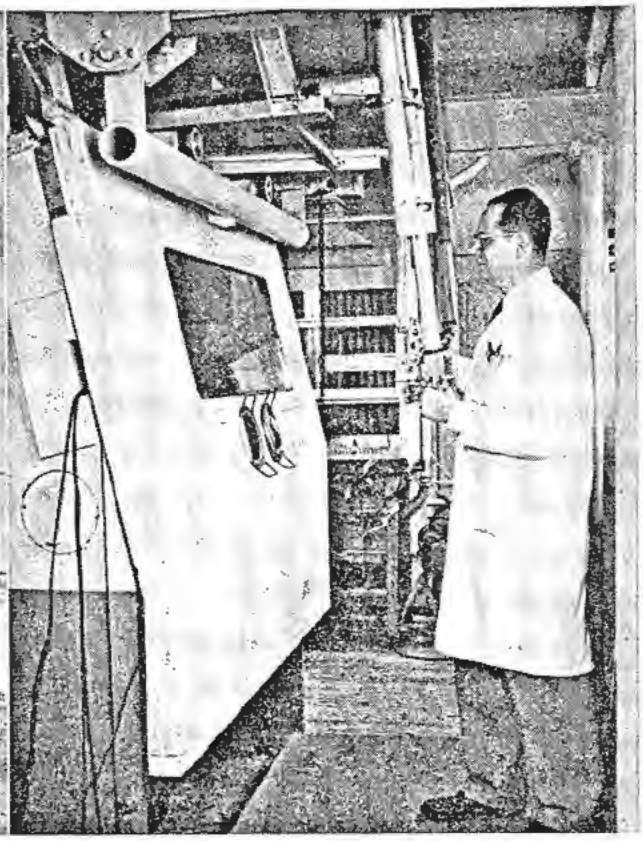

Figure 6. Operating manipulators of a junior cave

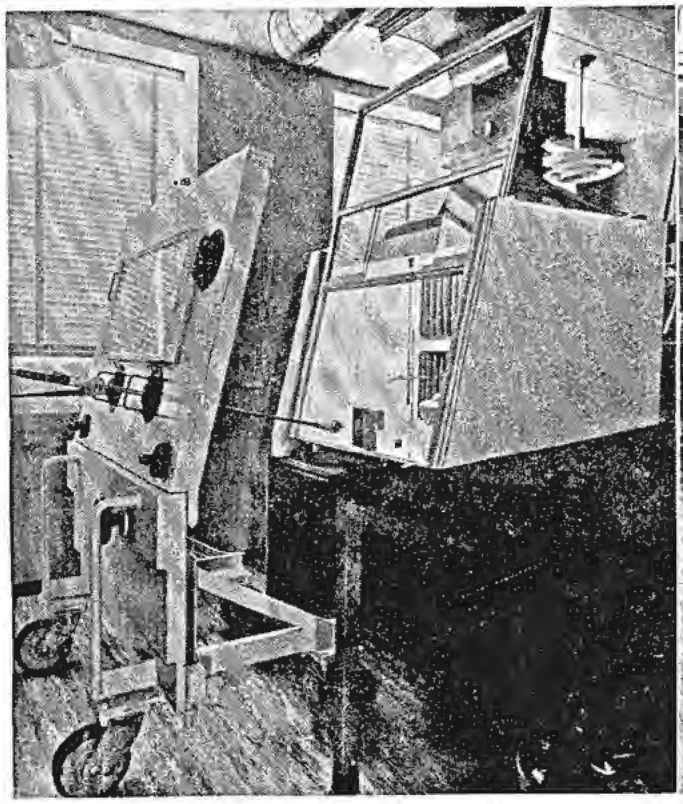

Figure 7. Shielded hood with ball joint manipulators

Figure 8. Glove box for work with alpha activity

The samples were inspected for physical changes by the metallurgists in their large caves and then transferred to the intermediate cave, where they were introduced through a port hole from a horizontal cask which was rolled up against the opening so there was no hazard to personnel during the transfer.

For heat transfer purposes, the plutonium was actually irradiated as a plutonium-aluminum alloy. In order to remove the aluminum from the plutonium, the samples were dissolved in concentrated sodium hydroxide solution, and the insoluble fission products and heavy elements were concentrated by centrifugation. The centrifuged material was dissolved in concentrated hydrochloric acid and passed through an anion column. The decomposition of the hydrochloric acid by the intense radioactivity, was fairly rapid. In order to reduce the complications due to the gas bubble formation in the resin column, wide columns having a diameter of two inches were used. The plutonium was adsorbed on the anion resin and was thus separated from the effluent, which contained most of the fission products and the transplutonium elements. The effluent was evaporated, dissolved in dilute hydrochloric acid and adsorbed on a cation resin column. The transplutonium fraction was separated from almost all the fission product activities by eluting the resin with concentrated hydrochloric acid. Again, the best procedure was to use a fairly wide column, a coarse resin, and rapid flow rate to defeat the decomposition of the aqueous solution. As a result of the two column separations, the fission product activity in the transplutonium fraction was reduced from the initial 300,000 r/hr to approximately 1 r/hr.

All the operations were carried out by the rectilinear manipulator, which was controlled from a small portable box outside of the cave (see Figs. 4 and 10). The manipulator is versatile and easy to use with a minimum of previous experience.

All the fractions from the column separations were analyzed outside the large cave. This was accomplished by passing a small, self-filling pipet, fitted with a cork collar, into the radiation lock at one end of the cave. The manipulator then picked up the pipet by gripping around the collar, removed a sample from a fraction, and then returned the pipet to its holder in the radiation lock. The pipet was then removed from the lock and the sample was analyzed in another hood designed for work with alpha activity.

When additional separation from fission products was necessary, the chemical operations were generally carried out in a "junior" cave. The junior caves are much more convenient to use and are equipped with master-slave manipulators.

After the transplutonium fraction was concentrated, the gas evolution from aqueous solutions became even more intense. In cases where the transcurium elements were being sought, it was found best to carry out additional ion exchange separations using ammonium glycolate or similar complexing solutions as the eluting agent.

When doing ion exchange separations with high

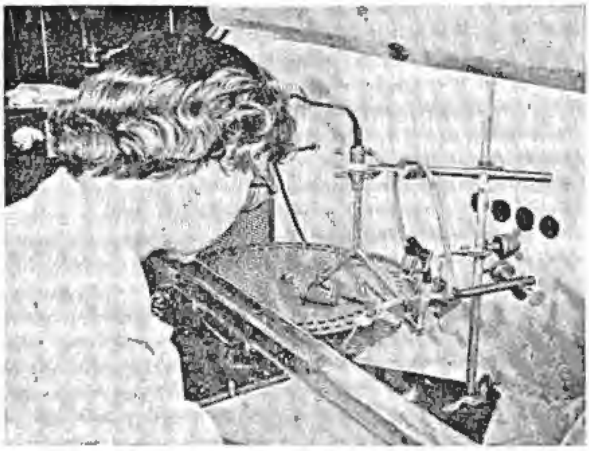

Figure 9. Placing counting plate under horizontal resin column in glove box

levels of alpha activity, it was found best to use horizontal columns. The gas bubbles generated during the separations rose to the top along the length of the column and did not disturb the adsorption bands (see Fig. 9).

Another example of a hot laboratory operation was the isolation of milligram amounts of actinium from 30 grams of irradiated radium. The initial process was designed to separate the radium from the actinium using a cation resin column. However, the intense alpha and gamma activity from the radium, actinium, and daughter activities decomposed the resin (sulfonated hydrocarbon) and caused the formation of sulfate ions, which in turn caused the precipitation of radium sulfate on the resin bed. The procedure had to be abandoned and a chelate extraction method substituted.

A very serious hazard associated with the actinium work was the radon gas evolution. To solve this problem, most of the operations were confined in Lucite boxes and air was swept through the boxes. The radon was removed from the air by adsorption on cold, activated charcoal, where it was held until it

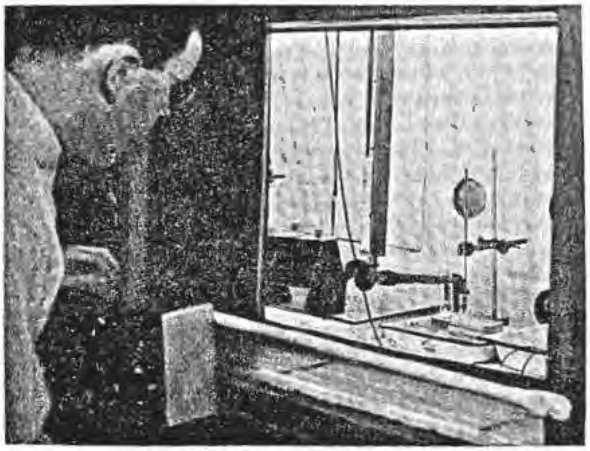

Figure 10. Operating electric manipulator in chemistry cave from control box

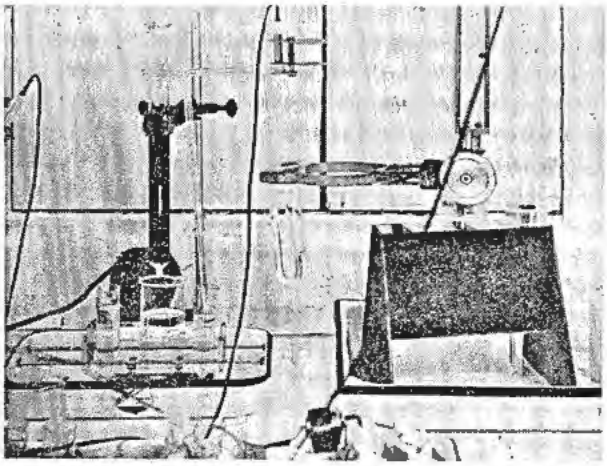

Figure 11. Transferring solution by means of a transfer pipet in chemistry cave

decayed sufficiently. The air was expelled into a 100-foot tall exit stack to effect dilution in case of accidental release of activity. Air dilution was sufficient to prevent any serious amount of activity from settling out. Additional precautions were taken by performing certain operations when wind direction and velocity were satisfactory.

The bulk of the work with radioactive material, such as cyclotron bombardments and the usual reactor irradiations, falls in the range nf 1 to 2 curies or less. This type of work is most conveniently carried out in the junior caves. It is a relatively simple matter to carry out almost any chemical operation in these facilities because of the versatility of the master-slave manipulators.

In planning a hot laboratory operation, the movements, size and weight of the equipment are frequently determined by the limits of the manipulator. What is equally important, but more often overlooked, is that the clean-up operations after the chemical processing should also be within the capabilities of the manipulator. With these facts in mind, resin columns are clamped in a manner that permits ready dismantling for disposal with the manipulator. Transfer pipets of the type shown in Fig. 11 are used for the safe transfer of solutions. When shielding material is to be handled remotely, miniature lead bricks weighing a little over three pounds are used.

With both high levels and intermediate levels of activity, the possibilities of accidents are anticipated and provisions made for containing the active material in the event of a spill, and thereby permitting recovery if necessary. Hence, much of the work is done in or over small enamel trays which would contain spilled liquids.

The insides of the caves used for chemical operations are covered with vinyl paints and wide industrial tape, which is again painted with the vinyl coating. By doing this, the contaminated spots which do not clean up by wiping can be removed by peeling off the contaminated section of the tape. Much of the contaminated equipment removed from the cave is sprayed with a plastic coating or covered with molten wax or a quick drying paint to fix the contaminant before removing the equipment.

In spite of such hazardous operations as dissolution of active metals, centrifugation, evaporation and frequent sampling, as well as the ever present problem of radiation-induced water decomposition, only trivial amounts of contamination have occurred and there has been no hazard to laboratory personnel.

REFERENCES

1. Bentley, W. C., Diamond, H., Fields, P. R., Friedman, A. M., Gindler, J. E., Hess, D. C., Huizenga, J. R., Inghram, M. G., Jaffey, A. H., Magnusson, L. B., Manning, W. M., Mech, J. F., Pyle, G. L., Sjoblom, R., Stevens, C. M., and Studier, M. H., P/809 *The Formation of Higher Isotopes and Higher Elements by Reactor Irradiation of Pu*[239]*; Some Nuclear Properties of the Heavier Isotopes,* volume 87, session 10B.1, these Proceedings.
2. Rylander, E. W., and Blomgren, R. A., *Operating Procedures of a Hot Lab for Solid State Tests,* Nucleonics *12*: 98-100 (1954).
3. Goertz, R. C., *Fundamentals of General Purpose Manipulators,* Nucleonics *10*: 36-42 (1952).
4. Blomgren, R. A. and Hagemann, F. T., *Improved Chemistry Cave,* ANL-4426 (March, 1950).
5. Blomgren, R. A., *Shielded Hood, Model 1,* ANL-4964 (January, 1953).

Metal-Research "Hot Laboratory"

By N. F. Pravdjuk, USSR

Changes in the structure and in the physical and mechanical properties of various structural and fissionable materials irradiated in reactors are studied in the metal-research "hot laboratory."

Highly-radioactive substances are investigated in several "hot" cells separated from the observer by a sufficiently thick shielding layer of cast iron and concrete. The cells are in a chain formation and are connected with a transporter that conveys the objects under investigation from the distribution cell, which is linked up with the storage cell, into the research cells. The layout of the cells of the metal-research "hot laboratory" is given in Fig. 1.

The chain begins with the "hot machine shop" where there is a special remote-controlled metal-cutting machine used to produce samples for various metallographic, physical and mechanical tests.

Figure 2 gives an inside view of the "hot machine shop" cell. The bed of a special milling-machine (1) and a moving table (2) are mounted on a-frame rigidly bolted to a concrete foundation on the cave floor. The milling-machine support (3), which moves at an angle of 45 degrees to the bed, is fixed on the bed carriage. A cutting head with a cutter is attached to the support. Remote-replacing of the cutter is envisaged.

The spindle of the cutting head is revolved by a rigid shaft (4) connected by a universal joint with the transmission of a 1.2 kilowatt electric motor. The electric transmission circuit (Leonardo system) is geared to achieve a smooth change from 0 to 300 rpm.

Transverse and longitudinal displacement is automatically controlled by means of the universal joint transmission and a gearbox from the operator's room.

The machine does both transverse and longitudinal cutting of irradiated material. The support is encased in a Plexiglas jacket (5) to protect the milling-machine mechanism from radioactive dust. Cutting of an active sample is performed in distilled water or some other liquid, which is then forced into a special drainage system through the receiving tank. The plug (6) of the cutting bath has been withdrawn and may be seen on the moving table in the background of the picture. The moving table carries a trolley with a tool manipulator and auxiliary equipment, and also serves for keeping the plug in a closed position when the receiving tank is pressurised to force the liquid into the drainage system. The level gauge in the operator's room indicates the level of the liquid in the tank.

The walls and floor of the "hot machine shop" are lined with polished stainless steel. The cell and the machine are washed by means of a stream of water, nitric acid or other chemicals at a pressure of 1.5-2 atm from a manipulator-controlled hose.

A special mirror-system (7), located in a niche of the front wall of the cell, has been designed in order to observe the cell from the operator's room. The mechanical master slave manipulators (8) are inserted through sleeves in the front wall of the cell.

There is a double-system of lighting in the cell consisting of seven 300-watt lamps behind the glass ceiling, and two with three 500-watt lamps on each of two soffits. The back wall of the cell (not seen in the photograph) has an exhaust ventilation filter which can be replaced by remote-control.

The vertically moving gate on the right-hand wall closes off the direct channel from the distribution cell. Transportation of material to and from the distribution and cutting cells is performed by means of a trolley on rails which may be seen at the upper part of the gate.

The automatic container conveying the radioactive materials to the "hot" laboratory can also be unloaded in the "hot machine shop." The container is operated from the control desk in the operator's room.

A massive door on roller bearings which opens by an electric motor leads into the cell.

There is a sloping channel into the cell wall for introducing small tools into the cell. The channel can be closed from the operator's room by means of a cast iron shutter.

A dosimeter, fixed to the side wall of the cell, and a portable counter are used to ascertain the degree of contamination in the cell. The readings from these counters are transmitted to the operator's room.

Figure 3 gives a general view of the operator's room of the "hot machine shop" and the mechanisms and devices used for the remote control of all the operations in the cell.

The cell of the "hot machine shop" is connected with the distribution cell. The distribution cell is intended for the storage of radioactive materials and their supply to the different technological cells. The cell of the "hot machine shop" and the distribution cell are designed for use with materials having an activity of up to 50,000 curies.

The distribution cell is connected to the other cells by a trolley transporter which is controlled from the

Original language: Russian.

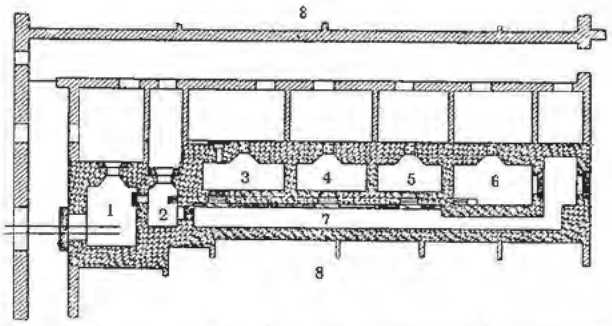

Figure 1. Layout of cells of metal-research "hot laboratory"; (I) cell of "hot" machine shop, (II) distribution cell and storage, (III) metallographic cell, (IV)-(V) physical measurements cell, (VI) mechanical tests cell, (VII) transportation corridor, (VIII) "semi-hot" laboratories

operator's room of the distribution cell; light signals show the exact position of the trolley carrying the active material in front of the research cell.

All the research cells of the metal-research "hot laboratory" are intended for use with activities up to 20,000 curies. Each cell has manipulators and viewing windows of lead-glass.

METALLOGRAPHIC EXAMINATION CELL

Specimens and replicas for electron microscopy examination are produced in the metallographic cell; the examination of specimens and their photographing by means of a remote-controlled metallographic microscope are also performed in the same cell.

The cell contains the following equipment: (1) a device for pouring the active sample with the fusible material into a casing for subsequent preparation of a specimen; (2) a grinding-machine with six grinding and polishing wheels; (3) a device for electrolytic etching and electropolishing; and (4) a metallographic microscope.

The microscope in the cell is protected from the grinding-machine by a wall of lead bricks.

The photographic camera and remote-control desk operating the microscope (replacement of lenses, light filters and so on) are shown in Fig. 4. The microstructure of the active metal is clearly visible on the frosted glass of the microscope.

Figure 5 gives an inside view of the metallographic cell from the viewing window. The grinding-machine with its six grinding and polishing wheels (1) is seen in the foreground. The support holding the casing with a specimen perpendicular to the grinding wheel plane (2) is seen in front of the machine. The abrasive paper of the grinding wheels can be changed by a remote-control device (3) attached to a movable lead plate on the left (4).

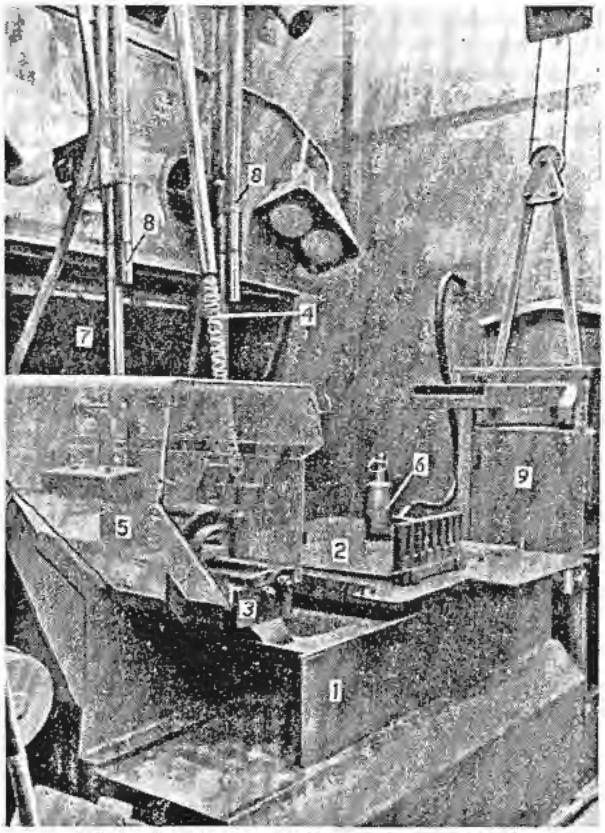

Figure 2. Inside view of "hot machine shop" cell

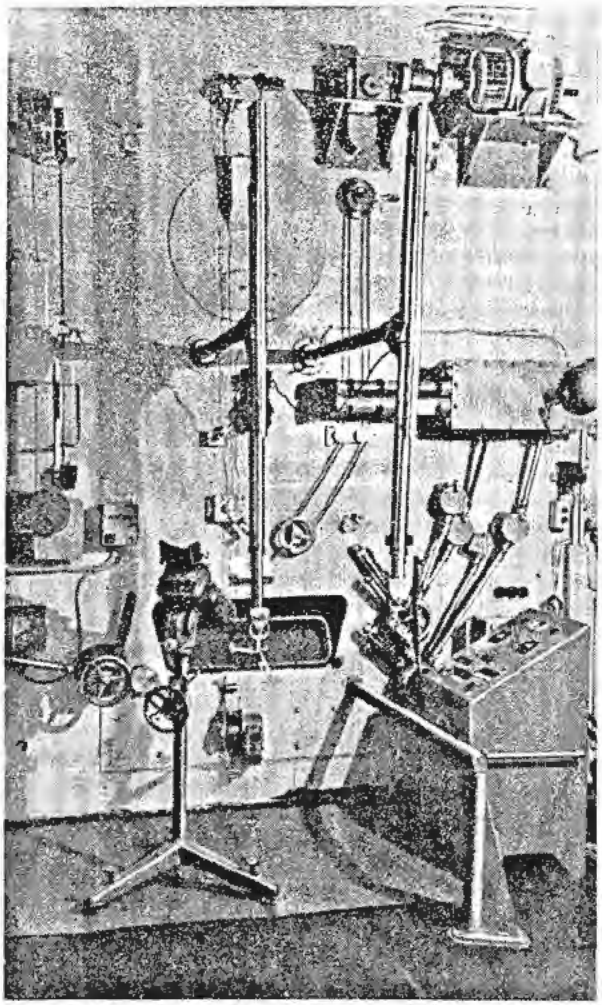

Figure 3. General view of operator's room of "hot machine shop"

When personnel need to work in the cell, the grinding machine is first lowered and then closed off by means of a movable plate to reduce the hazard of irradiation. The rod with the trolley for the manipulator tools (5) is seen in the background.

PHYSICAL MEASUREMENTS CELLS

Physical measurements cells are used for the study of physical properties of irradiated materials. When needed, devices for physical measurements (electrical and thermal conductivity, thermoelectric force, thermal analysis, dilatometric measurements, etc.) are introduced into the cell and fixed in special places. There are two balances installed in the cell (remote controlled from the operator's room) for measuring the specific weight of powders, wires, etc.

Figure 6 shows a photograph of the cell taken through the viewing window from the operator's room. The manipulators (1) and the trolley with the changeable tools (2) for the manipulators may be seen in the foreground. A remote controlled microanalytical balance (3) for the measurement of the specific weight of small specimens is located behind the trolley. The door (4) through which the technological cell is supplied with the active material, is seen on the right in the background.

Figure 7 shows part of the operator's room with the potentiometer unit (1) for measuring the electrical conductivity, thermoelectric force, etc. The instruments (2) for recording the radioactive level in the cell and in the operator's room are seen on the wall above the potentiometer unit.

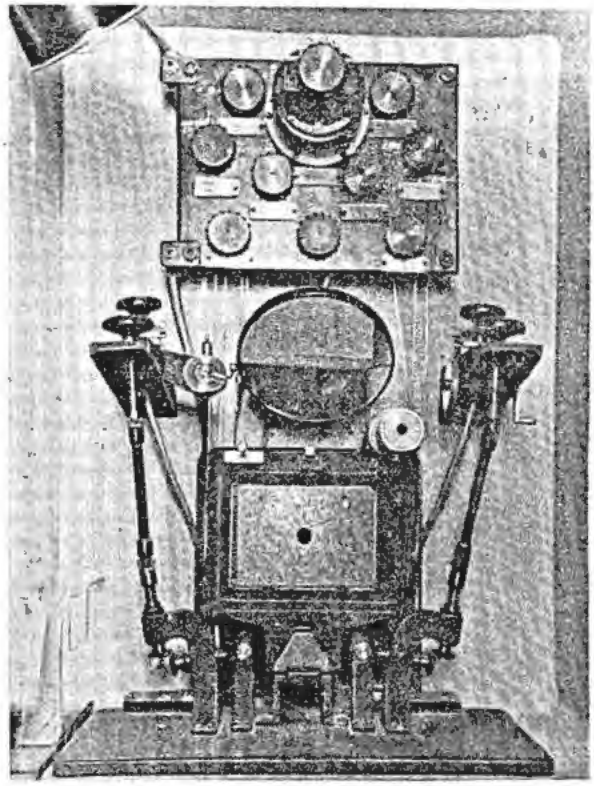

Figure 4. Photocamera and desk for remote control of the metallographic microscope

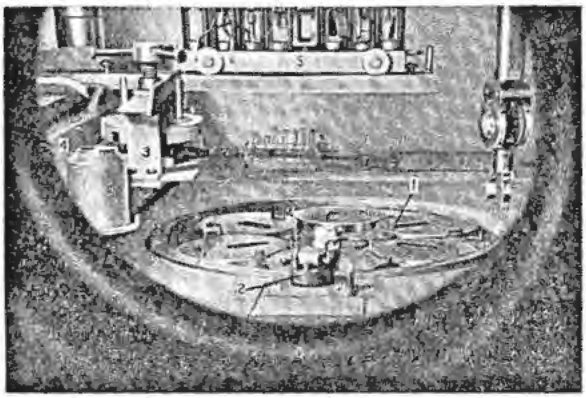

Figure 5. Inside view of metallographic cell. Grinding machine in foreground

A vacuum electric furnace for remote heat treatment of active materials is located in another physical measurements cell. So, too, is the equipment for the vibration-method of determination of the modulus of elasticity and internal friction and also an X-ray installation. An automatic storage designed for specimens with an activity up to 100 curies is attached to the back wall of the cell.

The cell is equipped with a viewing window and rectilinear manipulators (Item 1, Fig. 8), controlled from the operator's room. A television transmitter with changeable lenses (2) for more detailed observation and photographing of various active specimens is attached to a side wall. The television receiver and its control desk are located in the operator's room.

MECHANICAL TEST CELL

The mechanical test cell is intended for the study of the mechanical properties of irradiated materials; "mould-casts" from active samples are made in the same cell. The cell is equipped with a viewing window and master-slave manipulators. A cast iron door (2.4 × 1.4 m) in the left wall of the cell provides an entrance for mounting equipment.

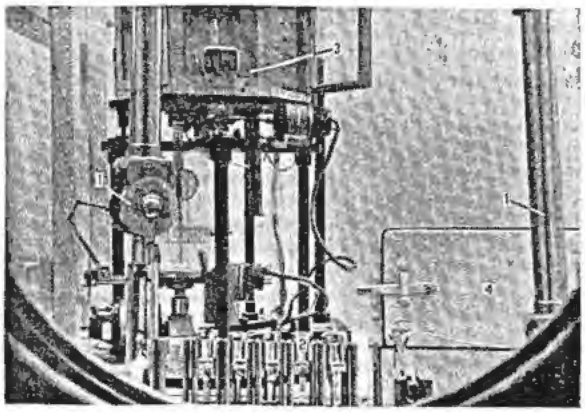

Figure 6. General view of physical measurements cell

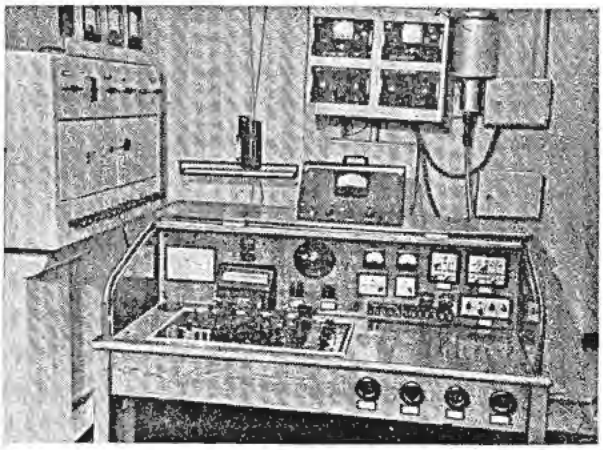

Figure 7. Operator's room of physical measurements division

The active materials are conveyed to the cell by means of the trolley-transporter, which runs directly into the cell.

The test machines and instruments are located on a revolving stand and on the two movable trolleys in the cell.

Figure 9 gives a general view of the mechanical test cell from the entry door.

All the operator's rooms of the metal-research "hot laboratory" are connected with the corresponding "semi-hot" laboratories used for work with low-activity samples, preparation work and for the development and testing of new methods and devices.

DESCRIPTION OF CERTAIN APPLICABLE RESEARCH METHODS

A. X-ray Study of Radioactive Materials

To understand the nature of the changes in the properties of irradiated materials a study of the structural changes resulting from irradiation is essential. The methods of X-ray study of highly radioactive materials are outlined below.

The existing methods of X-ray study of materials, which are based on photographic or ionization measurements of the diffraction maxima, are of little use for the investigation of radioactive materials having intensive β and γ radiation, due to the interference of the strong radioactive "background." As the penetrating power of this radiation is, as a rule, higher than that used for X-ray study, the use of filters does not give positive results.

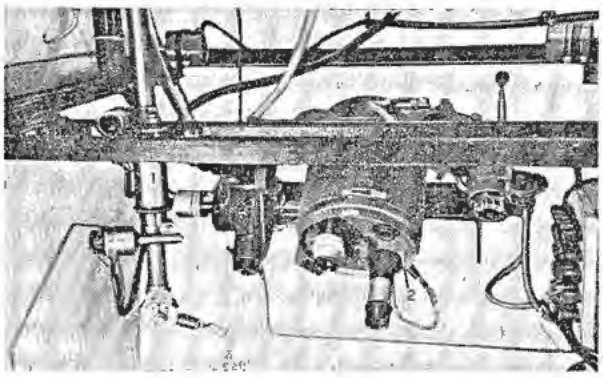

Figure 8. Rectilinear manipulator (1) and television transmitter (2)

A method for the X-ray study of materials having a considerable radioactivity was developed. The design is based in the "Norelco" type γ-ray spectrometer.

The method consists of measuring the diffraction maxima of a specimen after "reflection" in a crystal-monochromator. This makes it possible to place the detector (e.g., the end-window counter) out of the path of the diffracted ray and to protect it from the radiation from the sample by placing a shield between them.

Figure 10 is a diagram of an operating installation. The diverging X-ray beam from the focal spot of a roentgen tube (A) is incident on a flat specimen (B); the radiation scattered by the specimen is focused onto the entrance slit (C), is "reflected" by the curved crystal monochromator (K) and is registered by the counter (D). A kinematic device enables the diffraction pattern to be automatically recorded on potentiometer paper within range 15-45 degrees Wulf-Bragg, or the diffraction lines counted by a mechanical counter. The lead screens (3_1, 3_2, 3_3) protect the counter from

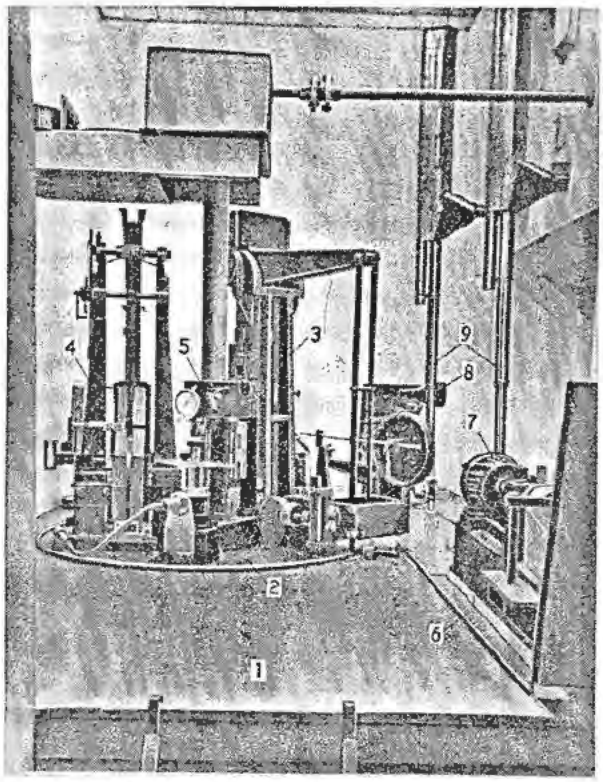

Figure 9. General view of mechanical test cell: (1) stainless steel working platform; (2) revolving stand with equipment on it; (3) combined testing machine (up to 5 tons); (4) 10 kg pendulum impact testing machine; (5) "Rockwell" hardness-tester; (6-7) one of the lateral trolleys with a fatigue machine; (8) trolley with the remote microhardness tester; (9) manipulators

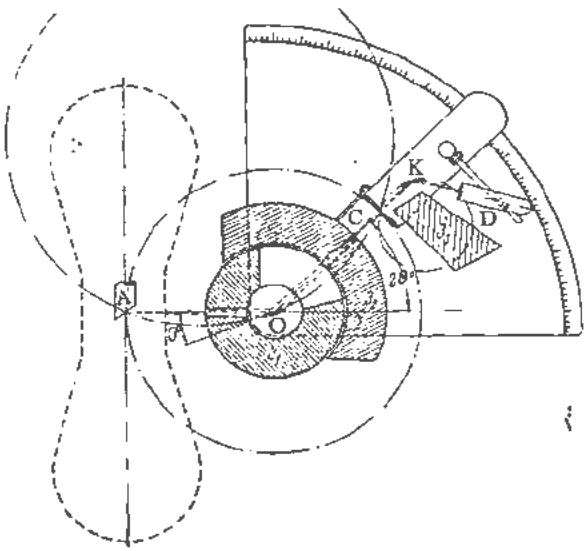

Figure 10. Drawing of instrument for X-ray analysis

direct radiation from the specimen, but do not interfere with the transmission of the X-ray beam to be registered. One of the screens (3_1) is fixed while the other two (3_2, 3_3), the entrance slit, the monochromator and the counter are rigidly connected together and during the process of the recording rotate around point O at an angular velocity double that of the specimen.

The wall thickness of the three shielding lead screens (3_1, 3_2, 3_3) is: 25 mm, 35 mm, and 30 mm respectively. Thus, when in operation, a 65 mm thickness of lead separates the specimen from the counter. The geometry of the instrument enables the thickness of this shielding layer to be increased by 130%, when necessary.

By means of the instrument described above, patterns were obtained from flat specimens (10 × 7.5 × 0.1 mm) of cold-rolled uranium after irradiation and having a residual activity of 10 mc. In this case, the intensity of the strong lines constituted 50–100% of the "background" intensity. If we take into account the fact that lines whose intensity is 10% of the "background" intensity are sufficiently reliably registered by the ionization method, it may be assumed that similar specimens with an activity of up to 50–100 mc may be examined with the aid of this equipment.

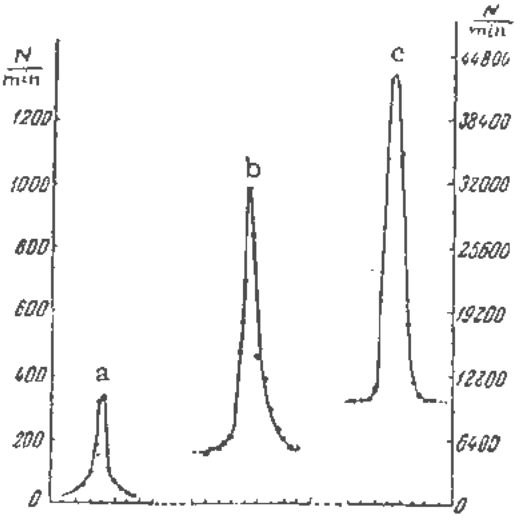

Figure 11. Roentgenogram of line (III) aluminium

A plastically curved (according to Johann) crystal of sodium chloride was used as the monochromator for obtaining a high intensity. The radius of curvature of the crystal was 28 mm, the crystal itself being 20 × 15 × 1.5 mm.

The monochromator was set for copper radiation using the second order reflection because in this case the counter was more effectively screened from interfering radiation and the ratio of the intensity of the diffraction lines to that of the background substantially increased, though the general intensity of the instrument decreased.

Figure 11 shows the aluminium line (III) plotted in the following three ways: (*a*) with the monochromator in the second order; (*b*) with the monochromator in the first-order; and (*c*) without the monochromator.

The number of counts per minute above the cosmic background of the counter is given on the vertical axis (the right-hand scale gives the recording without the monochromator).

When the monochromator is adjusted for the first order of reflection, it enables lines of average intensity to be automatically recorded on the potentiometer paper: in the second order, a reliable automatic recording is obtained only for strong diffraction lines.

B. Method of Metallographic Examination of Irradiated Materials

In metallographic examination of irradiated metals all operations for the preparation of a specimen are remote-controlled by special devices and manipulators.

Sulphur or Rosée alloy is poured into a mould with the prepared sample of the active metal. The specimen is prepared on a grinding-machine installed in the "hot" cell. The design of the grinding-machine makes it possible to change the grinding materials and to obtain high-quality specimens. Electrolytic or chemical etching is used to reveal the microstructure. The etching process is performed in equipment which permits the use of various etching substances and for changes in the etching period.

To examine and photograph the microstructure of irradiated metals, a remote controlled metallographic microscope is used, by means of which one may observe the image of the specimen on ground glass under ordinary and polarized light with various magnifications and using changeable light filters. The microscope is installed in the "hot" cell while the control devices and camera are in the operator's room (Fig. 4).

C. Method of Electron Microscope Examination of Irradiated Uranium

An active sample is poured by remote control with Rosée alloy into the mould in the metallographic cell; it is mechanically ground and polished on a machine-tool. Then, the specimen is electrolytically polished in a dilute alcoholic solution of orthophosphoric acid (2 parts of concentrated acid + 4 of water + 1 of ethyl alcohol) at 6 v and 50°C for two minutes. The electrolytic etching of the specimen is performed in the same electrolyte at 2 v and 50°C for 30 seconds, as a result of which the prominent uranium structure is revealed under ordinary light in the metallographic microscope.

The prepared specimen is coated with a 2% solution of nitrocellulose in amylacetate. After drying, a hollow plastic former is stuck to the plastic film in order to strip it from the specimen. This process is facilitated by immersing in water. The film is then easily stripped from the specimen and removed from the cell with the aid of manipulators. If the replica is contaminated, the active substances can be washed off by means of a 10% solution of hydrochloric acid, and the replica then rinsed in distilled water and dried. All the succeeding operations on the replica are performed without shielding under ordinary conditions. A thin layer of aluminium is evaporated onto the surface of the plastic replica in a vacuum of 10^{-4} mm and then the aluminium replica is shadowed with gold under 20–30 degree angle. This reproduces clearly the surface structure of the irradiated uranium and may be subjected to metallographic examination instead of the active specimen. Figure 12 shows the irradiated uranium microstructure as obtained from an aluminised plastic replica.

The aluminised plastic replica is then cut into squares (2 × 2 mm) for examination by electron-microscopy, each square being dipped into amylacetate to dissolve away the nitrocellulose layer. The washed aluminium replicas are then scooped out onto the object grids where they are dried and examined with the aid of an electron microscope.

D. Remote-Controlled Microhardness Tester for Radioactive Specimens

The remote-controlled microhardness tester is intended for hardness tests of materials by impression with 2–200 gm loads; a diamond pyramid with a square base and a peak interfacial angle of 136 degrees is used.

The microhardness test is similar to the hardness test performed by the Vickers tester; as a result of the test, the diagonal size is measured and the hardness value is calculated as the quotient obtained from the division of the applied load by the surface of the received imprint; the hardness value is expressed in kg/mm².

The instrument is designed for remote control (by selsyns and motors) of all operations connected with microhardness determination, e.g.: (*a*) Selection of the imprint position and observation of microstructure, rough and precise pointing of the microscope, lateral and traverse movement and rotation around the vertical axis of the table, locating under the diamond pyramid and microscope objective; (*b*) Impressing of the diamond pyramid into the material under test; and (*c*) Measuring of the diagonals of the imprint seen on the screen.

Figure 12. Microstructure of irradiated uranium obtained from aluminized plastic replica by metallographic microscope under inactive conditions; X240

The remote microhardness tester consists of three units: (1) microscope, (2) control desk, and (3) starting rheostat with ammeter.

The main tube of the microscope has an electric drive and is operated by a transmission system, the transmissions being run by a selsyn for rough and precise focussing. The shift of the rough and precise focussing gears is performed by an electromagnet actuated from the control desk.

The micrometer has a 0.3 micron pointer which is operated by an electric motor.

The picture of the microstructure is thrown onto a ground glass screen 138 mm in diameter, which is attached to the micrometer.

A focussing spotlight using a mercury lamp is mounted on the main tube for illumination purposes.

The load mechanism operated by a Warren motor communicates a reciprocating motion by a flexible shaft to the diamond tip.

The lateral, traverse and rotation displacements are alternated by a clutch on the driving gears.

Figure 9 shows the remote-controlled microhardness meter in the chamber, in the working position.

E. Equipment for Measuring Internal Friction and Modulus of Elasticity of Irradiated and Non-Irradiated Materials

This instrument makes possible the determination of the modulus of elasticity of irradiated and non-irradiated materials by measurement of the frequency of transverse vibrations of specimens and also the internal friction by the additional determination of the amplitude of the resonance curve. Young's modu-

Table I

Metal under investigation	Before irradiation			After irradiation			Change value in %	
	Internal friction	Critical shear stress gm/mm²	Modulus of elasticity kg/mm²	Internal friction	Critical shear stress gm/mm²	Modulus of elasticity kg/mm²	Internal friction	Modulus of elasticity
Aluminium	1.20×10^{-3}	30	0.714×10^4	1.04×10^{-3}	1200	0.691×10^4	−15	−3.2

lus is determined from the vibration frequency of the specimen, its geometry and its density.

The effect of neutron irradiation on the internal friction and Young's modulus is studied by means of a comparative method; the same specimens are measured before and after irradiation.

A special form of specimen was developed in order to ensure the reproducibility of measurements which is essential for the comparative method, as well as to carry out remote measurements on irradiated materials.

The specimen was made in the form of a plate or cylindrical rod with a lugged head to enable the specimen to be fixed in the clamping device.

Transverse vibrations in the specimen are forced and detected by an electromagnetic method.

The equipment for measuring the modulus of elasticity and internal friction consists of a driver and detector device, amplifier, electronic oscillator, oscillo graph, cathode voltmeter and counting device.

Indicators of 0.01 mm precision are used for measuring the amplitude of vibration of the specimen from the gap between the poles of the driving and detecting coils and the specimen. A microscope with a micrometer was used for measuring very small vibration amplitudes.

A counting device attached to the output end of an amplifier enables an exact count to be made of the number of vibrations per second made by the specimen, using a mechanical counter and stopwatch.

In the case of non-ferromagnetic specimens, ferromagnetic riders "1" and "2" are attached (Fig. 13).

The rider "1" which serves for forcing the vibration is close to the point of fixation of the sample and does not substantially affect the vibration frequency, while rider "2" does affect the vibration frequency.

To measure the absolute value of the modulus, rider "2" is removed and the maximum value of the vibration amplitude of the specimen under resonance is measured.

An example of the effect of irradiation on the internal friction and modulus of elasticity of aluminium is given below. The aluminium was irradiated in a neutron flux of about 1.5×10^{19} nvt at 20°C. The precision of the determination of the modulus of elasticity is 0.6% and for the internal friction, 4%. The results are given in Table I.

The data in the table were obtained from a study of the curves of the dependence of the internal friction on the tension caused by the amplitude of vibration, shown in Fig. 14 for aluminium, with curve 1 for non-irradiated metal, and curve 2 for irradiated metal.

The value of the internal friction given in Table I is determined from the tension caused by the amplitude of vibration in the area where this friction is independent of the amplitude. The shear stress value was calculated from the vibration amplitude, modulus of elasticity and geometry of the specimen.

The critical shear stress value (designated with K) is the stress above which the internal friction becomes dependent on the tension caused by the amplitude of vibration.

F. Method for Obtaining "Mould-Casts" from Radioactive Specimens

The method for obtaining a precise copy of the shape and dimensions of a specimen under investigation in a manipulator operated area consists of the preparation of a "mould" form in the cell with the subsequent filling of this mould with fusible alloy in an inactive area.

A divided pouring box is made from Plexiglas. The dimensions of this box must be chosen so that the solidified layer of gypsum is not thinner than 1 cm. Two prismatic supports are placed on the bottom of the box so that the diametric plane of the specimen on these supports coincides with the plane of splitting of the box. A quantity of solution is prepared after the specimen is placed on the supports, the solution being composed of 4 parts of gypsum and 3 parts of

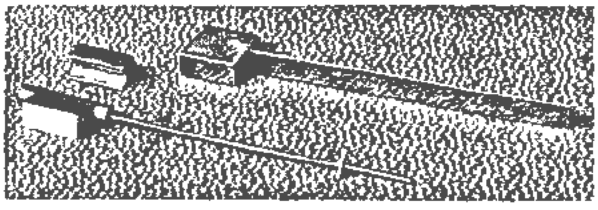

Figure 13. Specimens for determination of internal friction and modulus of elasticity

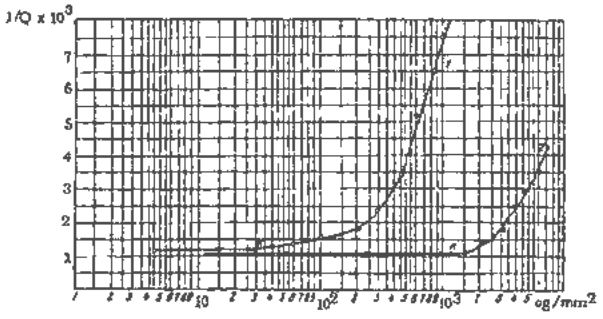

Figure 14. Curve of internal friction versus tension caused by amplitude of vibration before (1) and after (2) irradiation

water. The solution is thoroughly mixed for 30–40 seconds and then quickly poured into a funnel, with a rubber hose attached, through a sloping channel into the cell. Since the solution hardens very quickly, the pouring should be finished within 1.5–2 minutes. After 25–30 minutes, when the lower part of the mould is hard enough, the upper part is filled with gypsum in the same manner. Half an hour later, the divided box is taken apart, and the active specimen is carefully extracted. The gypsum form in the box is conveyed along a sloping channel to the operator's room for subsequent casting with the fusible alloy. To make the gypsum form harder it should be dried in a drying hood at 90–95°C for 5 hours or in the open air for several days.

Wood's metal is poured into the form. This alloy fills the form well and if necessary can be poured into a wet form. The split plane of the gypsum form must be carefully lined up before casting.

After casting, the cast is extracted from the form, the riser is removed and the seam is cleaned.

This method enables casts to be obtained whose dimensions differ from the original by not more than 0.1–0.2 mm

A Hot Analytical Laboratory

By G. N. Yakovlev, E. P. Dergunov, I. A. Reformatsky and V. B. Dedov, USSR

The hot analytical laboratory is designed for studying the chemical properties and technology of separation of the transuranium elements. Investigations are carried out both with tracer and weighable amounts of radioactive materials; this defines the character of the laboratory which consists of several sections.

The principal rooms of the laboratory contain hot cells for handling high-activity samples obtained by irradiation in a pile. Besides hot cells there are divisions for work with millicurie- and curie-level samples, and a counting room. The chemical laboratory where investigations with radioactive tracers are made is located in a separate building.

The section for work with multicurie-level samples (up to 10,000 curies) consists of independent subsections with facilities for various chemical and technological processes (Fig. 1). Each sub-section consists of two hot technological cells (1), with operating area (2), preparation room (3), and semi-hot room (4), with shielded glove-boxes installed (5).

Cells, preparation-room and glove-boxes of the semi-hot room are connected with an automatically controlled conveyor (7). The necessary additional equipment, chemical vessels, reagents, etc. are transferred to the conveyor through a lock (6) located in the preparation-room.

The hot cells are arranged so that the access doors open into the cave (8) (see also Fig. 2) isolated from the working area. Thus wastes cannot get into the other areas.

Each hot cell is 2 × 3 × 3.5 m, lined inside with polished stainless steel. A lead-glass window in the middle of the wall separates the operating area from the hot cell. On both sides, the window is covered with Plexiglas plates to protect the glass from mechanical damage. When no work is being performed in the cell, the glass is covered on the inside with a lead plate.

A pair of master-slave manipulators is inserted into channels which penetrate the front wall. The manipulators are provided with a set of instruments — different tongs, pincers, scissors, etc. (Fig. 4). At one side of the window there is a slightly inclined channel with a thick cast-iron door. A special iron drawer fixed on a rope, passing inside the channel, is used to deliver the necessary small equipment into the cell. Four emergency channels in the wall are closed by lead plugs. On the side section of the operating area are mounted electrical inlets with panels, radiation monitors for indicating the presence of activity in the cell and in the operating area, valves to control compressed air, cold water and hot water supplies into the cell, and a valve at the vacuum line. The most frequently used solutions of acids and alkalis are transferred into the cell by gravity via stainless-steel tubes from storage tanks, fixed on shelves in the operating area.

For protection purposes the ventilating system is connected with the illumination of the cell so that the light cannot be turned on if the ventilation is not operating. The ducts of the input-exhaust ventilation are in the side walls of the cell and are supplied with prefilters which can be changed by remote control. A manometer fixed on the face wall shows the pressure difference between the operating area and the cell; the ventilating system produces 15 changes of air per hour.

The interior of the hot cell is shown in Fig. 5. Under the steel coating of the back wall there are inlet tubes for water, compressed air and vacuum. Two doors lead into the cell — the big one can serve, if necessary, for the entrance of personnel and the delivery of equipment; and the small one closes the channel leading to the cave and connects the cell with the conveyor. A dosimeter is located at the side of the big access door to record the radiation being received by the personnel in the operating area.

The floor of the cell is slightly inclined so that liquid accidentally spilled on the floor flows down into a collection bottle; later this liquid can be exhausted by the vacuum system. A plugged drain for wastes and other radioactive liquids is located in a corner of the cell.

The drain is connected to the water-purifying section. A conveyor, moving on rails near the back section

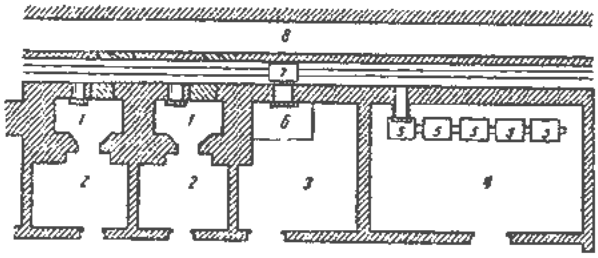

Figure 1. Plan of multicurie-level section of the hot analytical laboratory: (1) hot cells; (2) operating area; (3) preparation room; (4) semi-hot room with shielded glove-boxes; (5) shielded glove-boxes; (6) lock for transferring additional equipment and reagents; (7) conveyor; (8) cave (transportation corridor)

Original language: Russian.

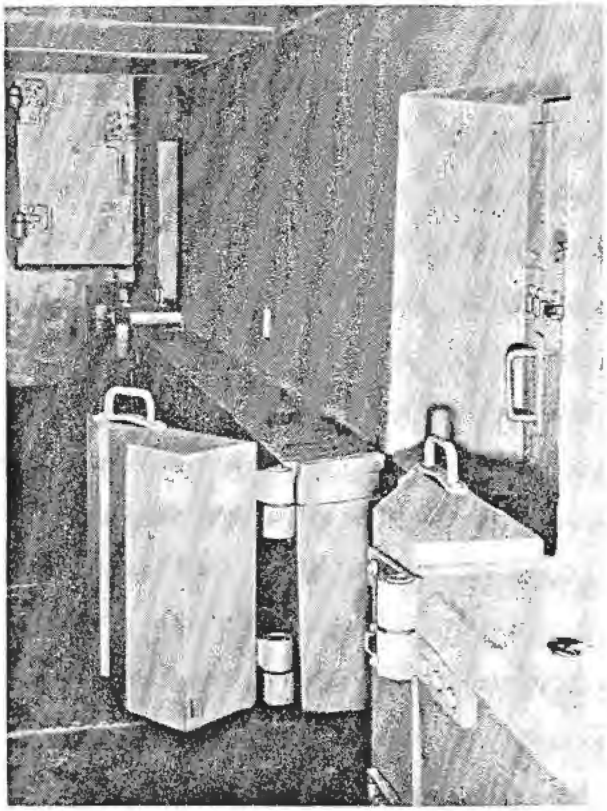

Figure 2. Cave with access doors to cells

of the cell, along the cave, transfers reagents, vessels and instruments out of the preparation-room into the cells, and samples out of the cells into the semi-hot boxes. The conveyor is controlled from a control panel installed in the preparation room. The control panel is equipped with light and sound signal systems to indicate the position of the conveyor. In addition, the preparation-room is connected with the cells by selector-communication.

The different chemical and technological operations in handling highly radioactive irradiated uranium, thorium and other samples (in the form of metal slugs and chemical compounds) are performed in the hot cells. In some cases the slugs are first cut in a cutting-cell, equipped with a remote controlled milling machine (Figs. 6, 7).

The primary operations carried out in the cells are the dissolution of the irradiated samples; separation of the transuranium and other radioactive elements, their regeneration, etc.

Dissolution and precipitation are usually carried out in graduated, high-quality glass vessels (reactors), supplied with traps for condensed vapour and sprays (Fig. 8). The reactors are placed in transparent plexiglas vessels to permit the experimentor to control the process visually and to shield the reactors from accidental damage.

The transfer of liquids from one vessel to another is performed by means of transfer-vessels joined to the air-vacuum system (Fig. 9).

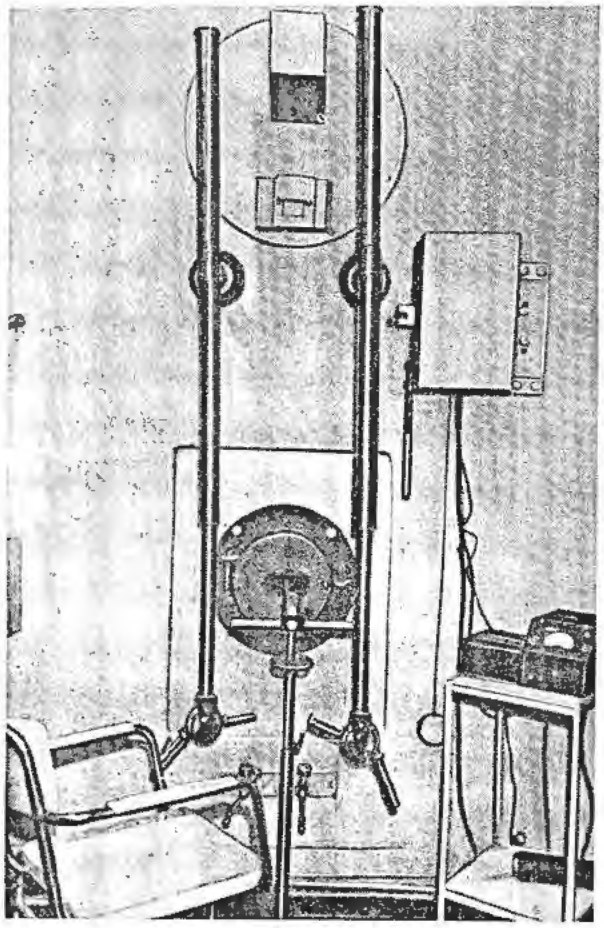

Figure 3. Operating area of hot cell

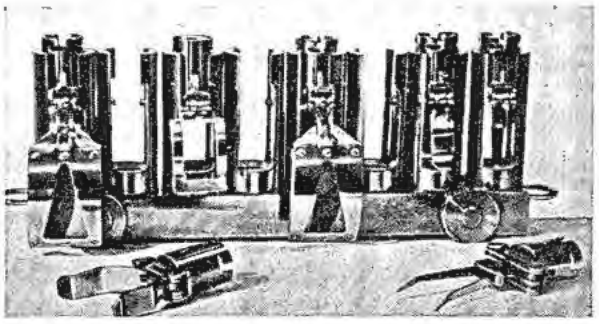

Figure 4. Instruments for manipulator

The air-vacuum system, remotely controlled from the operating area, is joined to the central air- and vacuum-line of the building. In addition, in each cell there is a reserve water pump designed to pump and exhaust the air; the water pump is operated if the central line gets damaged. It is convenient to have two parallel lines available. The remote control of the air-vacuum system is shown in Fig. 10.

Solutions are agitated in the cells by bubbling of air. Many chemical processes are accomplished by extractions performed in countercurrent extraction columns connected to the air-vacuum system. One of the extractors is shown in Fig. 11.

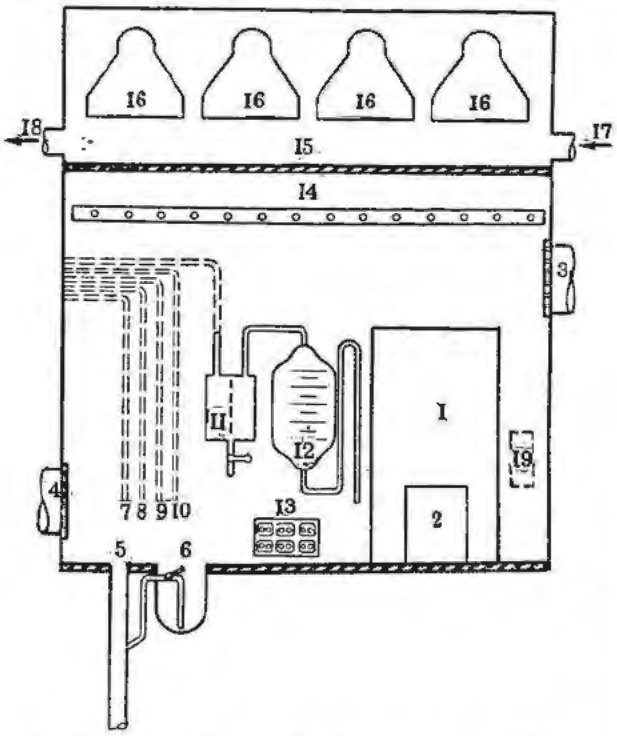

Figure 5. Equipment of a hot cell: (1) access door for entrance of personnel and delivery of equipment into the cell; (2) small door which closes the channel, connecting the cell with conveyor; (3) indraft ventilation duct with prefilter; (4) exhaust ventilation duct with prefilter; (5) drain; (6) collection bottle; (7) hot water; (8) cold water; (9) portable shower; (10) duplicate line of the air-vacuum system; (11) trap, filled with alkali solution; (12) intermediate buffer vessel; (13) electrical inlet; (14) wall shower; (15) glass, separating the illuminating lamps from the cell; (16) illuminating lamps; (17) indraft ventilation duct for cooling the illuminating lamps; (18) exhaust ventilation duct for cooling the illuminating lamps; (19) dosimeter

Remote controlled couplings joined to line ends and operated by master-slave manipulators are used to connect different lines with reactors, transfer vessels and with the other chemical equipment of the cell.

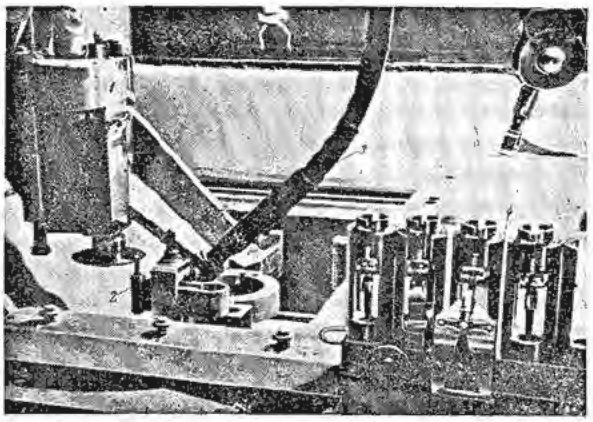

Figure 7. Cutting cell interior with milling machine: (1) head of the machine and mill; (2) cut-off rest of the machine with sample; (3) flexible shaft to the mechanism for clamping the samples; (4) instruments for manipulator

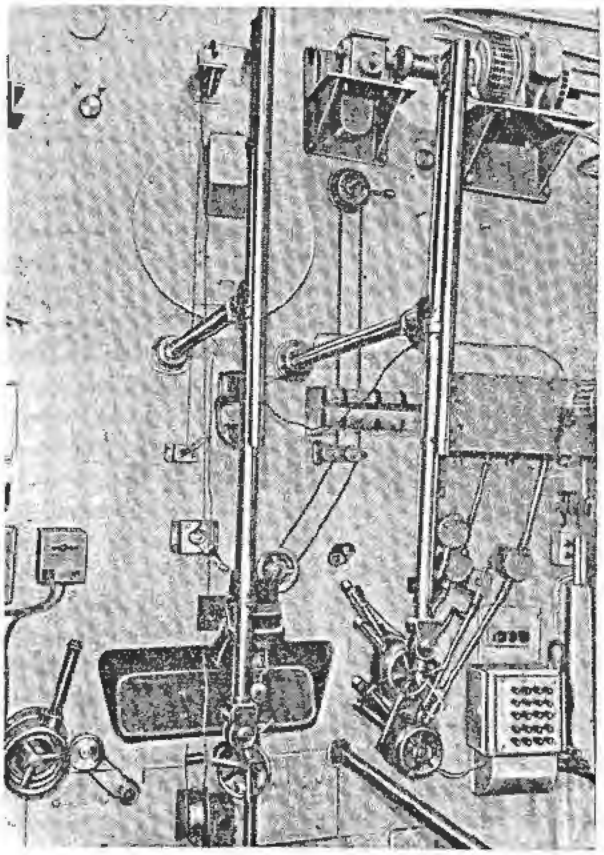

Figure 6. Operating area of cutting cell

Both electric heating stoves, and heaters (coils enclosed in quartz tubes and immersed in the liquid) are used to perform a number of processes in the cell. The heaters, lamps and other necessary electrical devices are connected to the panel located in the cell. The switching of instruments is accomplished from the operating area.

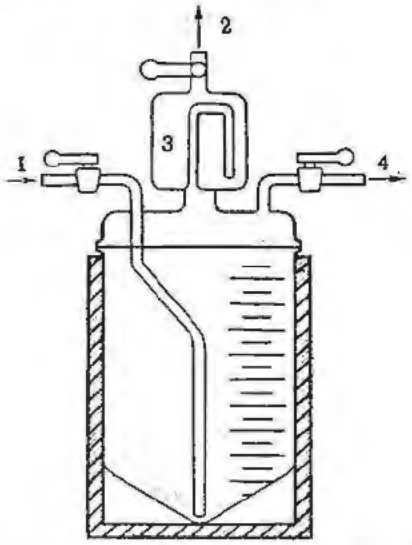

Figure 8. Diagram of dissolver: (1) inlet and outlet of solutions; (2) to ventilation; (3) trap; (4) to air-vacuum system

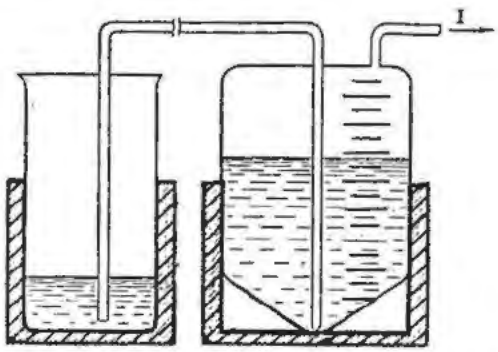

Figure 9. Transfer of solutions by the air-vacuum system: (1) to air-vacuum system

After each operation the cells are decontaminated by remote controlled wall and portable showers. Rotary brushes with hydraulic drive attached on the master-slave manipulators are used to decontaminate the surfaces of the floor and walls of the cell.

The separation of transuranium elements from the irradiated fuel as well as of fractions containing weighable quantities of rare-earth fission products, can serve as an example of work in a hot cell.

A uranium sample, containing 5 per cent of U^{233} (its activity was 1000 curies and its weight 1 kg) was transferred by the conveyor from the storage cell into the left-hand cell of the hot area (Fig. 1) and was placed in the dissolver by means of a manipulator.

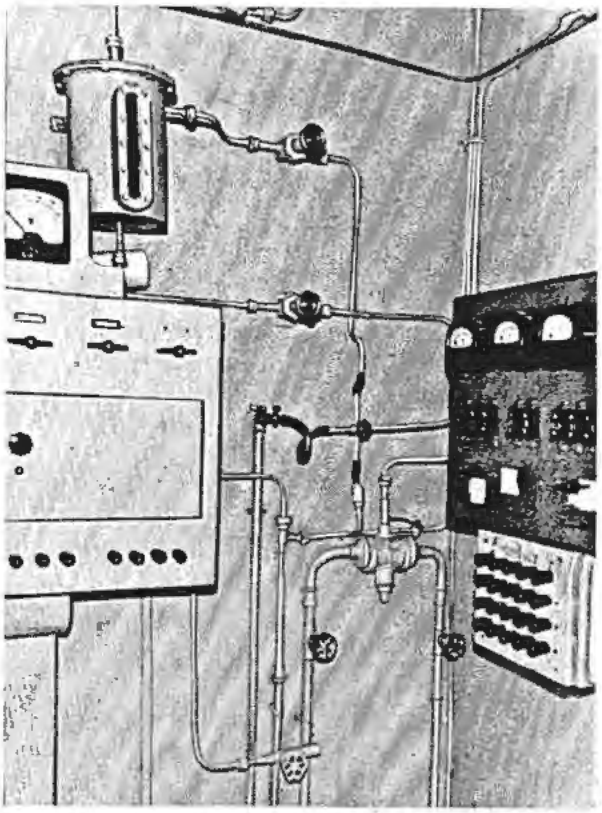

Figure 10. Remote control of air-vacuum system and electrical panel in the operating area

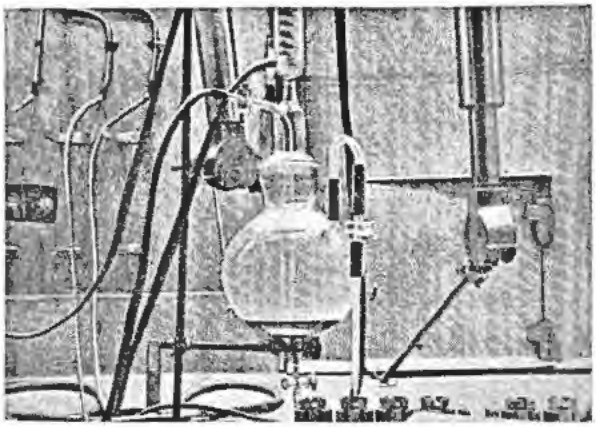

Figure 11. Extractor in the hot cell

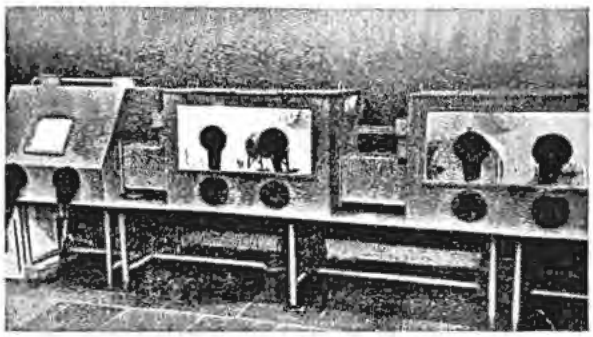

Figure 12. Shielded glove-boxes

Uranium, neptunium and plutonium were extracted from the nitric acid solution and transferred for testing into the glove-boxes in the semi-hot room.

The highly active solution, containing americium, curium and rare-earth elements was transferred into the second cell, intended for handling smaller volumes of solutions.

Here the americium was oxidised in carbonate solution according to the method described in the paper by Yakovlev and Gorbenko-Germanov, "Coprecipitation of americium-V with double carbonates of uranium-VI or plutonium-VI and potassium" (Paper P/677, Vol. 7, Session 10B.2, these Proceedings), and was thus separated from rare-earths and curium.

Five grams of isolated rare-earth elements and curium mixture were used for further separation and investigation of their chemical and nuclear properties.

Different physical and chemical investigations with transuranium elements are carried out in the millicurie- and curie-level section (up to 1.0 curie of γ-radiation). In these sections various compounds including complex compounds are received, their solubility isotherms are examined, and electrochemical, spectrophotometric and other investigations are performed.

According to the problems and methods of investigation, the above sections are provided with many facilities and devices necessary to carry out experiments. Ordinary metallic and plexiglas glove-boxes (Fig. 12) and thick cast-iron plate shielding boxes (Fig. 13) equipped with ball-joint tongs, table and

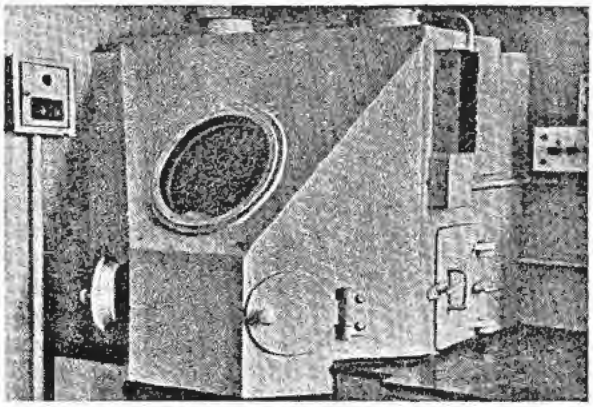

Figure 13. Special shielded box

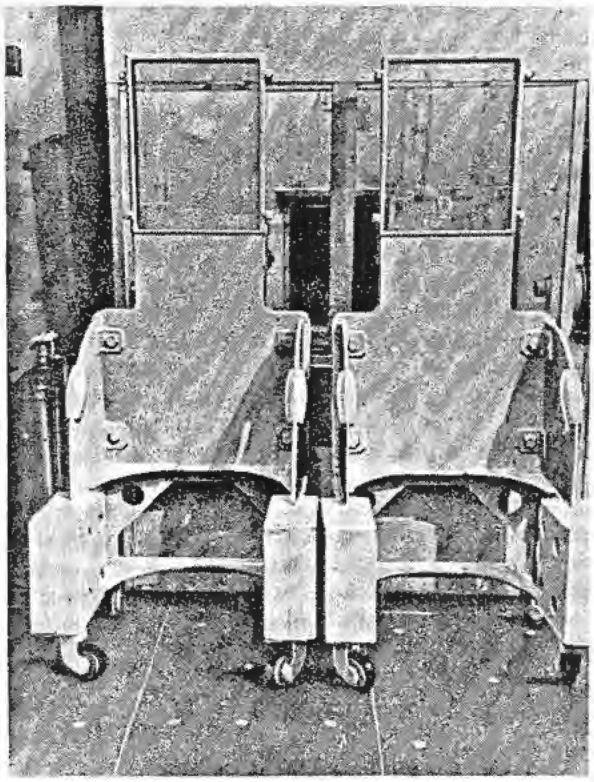

Figure 14. Mobile shields

mobile shields are installed for protecting personnel from radioactive hazards (Fig. 14).

Special glove-boxes required for investigation of chemical properties of transuranium elements and their compounds in milligram quantities serve for experiments with high-activity α-emitters.

The investigations with specimens of 1 curie activity are carried out in a shielded cast iron box 1000 × 900 × 950 mm. This is connected to the ventilation system producing a pressure drop that prevents the escape of the contaminated air from the box into the room. A round lead-glass window with a diameter of 400 mm and two lead plugged openings are mounted on the slightly tilted front face of the box; there, if necessary, ball-joint tongs or gloves can be inserted. The tightly closed side door is used for the introduction of containers with radioactive specimens, reagents, vessels, etc.

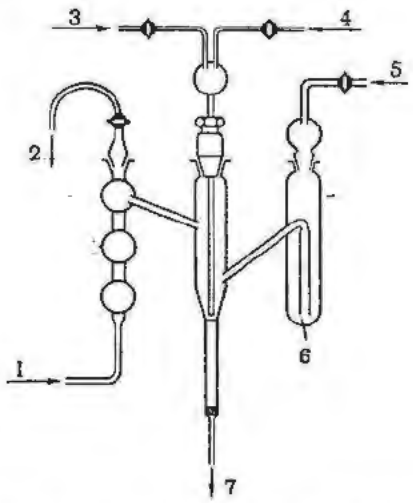

Figure 15. Diagram of ion-exchange resin-column: (1) eluant; (2) air; (3) active solution; (4) pressure, vacuum; (5) pressure; (6) resin

A sample irradiated in the pile is transferred into the box in a container. Then the sample is withdrawn from the container with tongs and put into the dissolver. All procedures connected with separation of α-activity from β-γ-emitters are carried out with tongs. The final purification is performed by hand with gloves on.

An automatically controlled ion-exchange resin column in the curie-level section is used for the chromatographic separation of high-activity elements (Fig. 15). The remote separation of rare-earths and actinides isolated from irradiated samples is carried out in this column.

Chemical investigations carried out in the hot analytical laboratory of the Academy of Sciences of the USSR have made it possible to measure the cross sections of a number of uranium, neptunium, americium and curium isotopes, as well as of some fission products for monochromatic and thermal neutrons.

Several investigations on the chemistry of transuranium elements performed in the laboratory described above are presented in reports in these Proceedings.

Laboratory Handling of Radioactive Material

By N. B. Garden,* USA

There is little question now but that nuclear disintegration is going to play a very important part directly or indirectly in influencing practically all aspects of human activity throughout future time — at least on this planet. In the several years we have had this new tool at our disposal, a few practical applications have been achieved, stimulating our imaginations to soar and picture fantastic roles for this newly found power to play in our existence. As these visions are worked out and become realities in the laboratories, passing from the imaginative realm to the accomplished fact, the transition is usually reported by dwelling on highlights of technicological aspects only — the kinds and quantities produced, the characteristics and qualities, the means of detection and measurement, the results of tests on usage, with conclusions and prognostications. Relatively little attention is given to describing the special equipment and necessary precautions that are so important in carrying out work in this new field successfully. Knowledge of many little details are not only of interest but may be necessary for the planning of similar work.

Since we have given a special name designation of *radioisotope* to chemical elements undergoing nuclear disintegration, we thus have set them apart from chemical elements outside this category. This has been done because they have unique characteristics, and these unique characteristics make the radioisotopes useful, but at the same time very special treatment and consideration are required to employ this usefulness.

It is proposed to describe the special treatment aspects of handling radioisotopes in the chemistry laboratories as developed by the relatively few who have intimately worked with radioactivity in the United States.

If one is contemplating work with radioactivity, the sooner the special factors are taken into consideration, the better one will achieve the desired results. Whether new buildings are constructed, present structures remodeled, or attempts of any sort made to use existing facilities, the very early stages of designing or planning should be based on requirements which will provide three obvious necessities:

1. Radioactive work must be carried out with minimum of hazard to personnel or damage to material.

2. Radioactive work must produce results that are accurate and reliable.

3. The above requirements 1 and 2 must be accomplished by compromise in the interest of economy.

It must be assumed that the alpha, beta, gamma and neutrons of radioactive material are understood, as there is not time here to summarize what radioactivity is and why it is useful. Also it must be assumed that the reasons for requiring special precautions are understood and agreed upon. These precautions are based on recommendations of the International Commission on Radiological Protection, which has reported on the biological aspects and has published values of quantities for isotopes that may be considered hazardous. Thus quantities of radioactive material that introduce the possibilities of exceeding the values listed by the committee require planning so that they be handled in compliance with requirement No. 1 above.

Where small amounts of radioactivity are employed, there is usually the desire to carry out fine, accurate tracer-detecting work, and here extraneous radioactivity or cross contamination can interfere and, in many cases, make the results worthless. This type of contamination is referred to as "technical contamination" and is the important basis for design in complying with requirement No. 2.

The individual opinions under No. 3 as to where a compromise is to be drawn will vary from situation to situation, with many factors influencing the considerations. The choice of geographical location has been considered an important factor in the initial planning and this has been used to great advantage in the early developments in the United States by locating the work in remote sections of the country. This method of simplifying some of the problems cannot be extended indefinitely nor to all areas where radioactive work is desired. To analyze the problem of laboratory handling of radioactive materials, with the three requirements as guides, one should consider the following factors:

1. Liability: workers, community, local property, sewer systems, rivers, etc.

2. Technical aspects: work room, air ventilation, proper equipment, decontamination plan, disposal system, and storage.

3. Economics: original cost of building, laboratories, equipment; operating costs of waste disposal, laundry, decontamination, special clothing, blower systems, heating systems, continuous inspection, sampling and analysis.

* Radiation Laboratory, University of California.

All these items are so interlocked that all should be analyzed before drawing final conclusions. After an evaluation has been made it is possible to choose wisely the equipment and procedures for a chemistry laboratory.

Before we examine the kind of precautions necessary and the systems employed to achieve these precautions, let us take a brief review of the evolution of radioactive laboratory equipment and procedures. When radioactivity was first produced, little knowledge of its characteristics and behavior was available. Work of necessity had to be carried out in the equipment on hand and precautions were based on simple expedients to protect the worker. Hoods were used with increased flow of air to make sure contaminated particles were carried away from the chemist. Through the use of tongs distance was employed to furnish protection; some remote handling systems were hastily put together. Special clothes proved to be necessary, with shoe covers and masks in some cases. After the work was completed, not only the work area was contaminated but also the ducts and sewers; these items, plus roofs and environs, were monitored with such portable instruments as could be made, for none was available commercially. It proved necessary to learn about decontamination and put such knowledge to extensive use. Then the first improvised tools were improved and developed into manipulators and master-slaves; efficient caves were designed and built, and special materials were employed to facilitate decontamination. Air filters were developed to limit the amount of activity that could escape to the atmosphere, and many improvements were made in remote controlled devices. It soon became necessary to have a special laundry for the "hot" clothes. Certain limits had to be established, denoting the area in which radioactivity was to be confined: a portion of the community over which control and monitoring were to be carried out, including the sewer system, might be designated as the "laboratory." The selected "hot" region might be a whole building, or only one laboratory, but in any event a clearly defined locale was established in each case. This manner of proceeding and thinking has been the approach taken in solving the problem at many of the sites in the United States, where excellent work has been done almost without incident of injury from radioactivity.

If the present laboratories were called on to describe their policies and equipment for handling radioactivity problems, there would seem to be no general agreement; however, an analysis of such reports would indicate that all could be classified under digressions from or variations of two fundamental philosophies. The extremes of these two systems have been referred to as the Concentrate and Confine, or CC, system, where total control is accomplished by total enclosure, and the Dilute, Disperse and Decontaminate, or DD, system, which provides for working in contaminated areas with the control achieved through employing dilution, dispersion and decontamination of radioactivity as indicated in the title.

Ventilation is one of the most important factors that enter into the design and use of chemistry facilities for radioactive work. Inescapably tied to the ventilation considerations are the air cleaning aspects. Basically, the building which houses the radioactive work should be pressurized, and the flow of supplied air in the building should pass from halls to offices to laboratories. The ideal arrangements of exhaust ducts provide for each laboratory room to discharge its air to the outside, employing exhausters to insure the correct rate. This system avoids the possibility of dispersing contaminated air from one laboratory to another, a situation which might arise where intercommunicating systems are in use. The ducts themselves should be made of material both resistant to corrosion and least likely to adsorb radioactivity. Plastic pipe or plastic coatings on ordinary piping material have proven most satisfactory. New and improved plastics are constantly being submitted for test and it seems certain that ducting will ultimately be some form of plastic. In most cases the building intake air should be cleaned, and experience has shown that the cost of this will more than pay for itself in many ways. The proper planning of air handling facilities, when used in conjunction with thoughtfully designed and employed equipment to confine radioisotopes, should eliminate the necessity of the average laboratory being confronted with vast volumes of contaminated air requiring huge filter banks and high stacks. Then, too, a hood containing a truly efficient filter requires much power for maintenance of a reasonable air flow. Furthermore, if filters are necessary, it is presupposed that radioactivity will be discharged, and this act will obviously result in the contamination of the hoods and filters, with periodic difficulties.

A hood requires an air flow of from 600 to 2200 cubic feet per minute (cfm), depending on its size. Where the Concentrate and Confine system has been employed, using boxes as the basic enclosing unit, adequate air flow for practically any laboratory chemical operation is a 5–12 cfm stream. This air can be cleaned rigorously and economically right at the box, and the relationship of this air to that of the building supply, heating system, etc., is simplified, as is the ducting. In special cases the supply to the box may be a noble gas or other special requirement. There are possibilities of economies in recirculation of air, and in some cases involving box systems, the recirculation has been combined with scrubbers, condensers and filters to achieve the desired results. Electrostatic precipitators have appeared to offer an attractive means of cleaning particulate matter out of the discharge, but there have been difficulties in actual operation, and this system has not been widely employed in the United States.

There is a trend towards making filters for exhaust air almost entirely of glass fibers of various combinations of sizes to meet the individual problem. Particulate filters for chemical processes may require special material such as sintered nickel or membrane plastics.

There is frequently a desire or a demand to monitor room air or exhaust for radioactivity. Although an installation may be designed for safe operation, a verbal assurance is not sufficient and it becomes necessary to demonstrate with instruments that there is a negative reading. There is no easy, reliable system available for determining promptly low levels of air contamination. The presence of chemical fumes and natural radon and thoron presents extra complications to a difficult problem. Several approaches to the solution have been employed with varying success. Parallel electronic units, assaying simultaneously the air to be tested and air known to be free of laboratory contamination, have been satisfactory in some installations. Large ionization chambers will serve for short periods, but they build up internal contamination that is not readily removed. The practice in practically all laboratories in the United States where air sampling is carried out is to draw known volumes of air through special filter papers and to allow a decay period of two days or more before counting.

In every laboratory, the arrival of actual radioactive material presents the problem of whether it is to be stored in the individual laboratories or placed in a central storage vault, if available. Although it was originally thought that small users could treat this problem casually, it has been proved that in most cases, central storage facilities are justified for a number of reasons. In considering this along with the other points, it might be well to make a rough classification of the quantities of radioactivity that one might expect to find in laboratories according to the following listing:

Location	*Use*	*Size*
AEC sites	Manufacturing and processing	Large
Factories	Industrial applications	Medium
Universities	Research and production	Medium
Hospitals	Medical application	Medium
Small laboratories	Investigations	Small
Individual physicians	Individual treatment	Small

The large and medium sized users save laboratory space and find it more economical to provide one central facility rather than a number of small storage locations. At the same time this plan prevents the accumulation of radioactivity in the individual laboratories with the increased possibility of contamination. Also, where I^{131}, Co^{60}, Na^{24}, Ra^{226} and other such gamma emitters are used, the background for counting can be influenced and cause trouble if not properly cared for. Even many of the small users have found it desirable to provide special storage facilities.

Some large users have installed complex systems, such as lead turn-tables and remote controls to select and remove the desired material. Most storage facilities consist of horizontal chambers or drawers in heavy shielding material, or vertical tubes into a shielding pit where containers can be lowered, either manually or with a crane.

The containers themselves are made up in a large number of styles to meet the individual requirements. Standardization of these containers is becoming more and more possible, which is desirable, as it offers many advantages. One such container that is used extensively is shown in Fig. 1; it is available with one or two inches of lead shielding. Where short-lived isotopes must be transported long distances, requiring air travel, containers of uranium are employed, since they are economically justified due to the saving of weight by the sixty per cent superior shielding of uranium compared to lead.

All areas where radioactivity is worked must be capable of undertaking proper monitoring, for this is not only an important part of laboratory procedure but is compulsory, since no one can be licensed to obtain radioisotopes unless specified conditions are met. The details of monitoring routines have been thoroughly covered over the years and the latest developments will be presented in other papers at this conference. In general, the laboratory policies in the United States consider that for the medium and small users of radioactivity, portable instruments and film badges provide adequate detection. For the large users, these are augmented by pocket dosimeters and hand-and-foot counters wherever advisable. In those cases where radioactivity may be discharged up stacks or into sewers, these items are monitored to make sure that hazardous levels do not develop. These routines are quite standard.

The disposal of radioactive waste is receiving much attention. Usually consideration begins after the waste has left the production channels or laboratory. Proper planning of the process and of laboratory procedure can greatly simplify the problem. Regardless of whether the waste is to be stored for a decay period or packaged for burial in the land or at sea, the volume of the waste is the important factor. Since all radioactivity must surely be a small physical unit in the beginning, the ultimate volume of waste is dependent upon the care taken in planning for a minimum increase in volume. An example of this will be given in a specific case discussed later.

The decontamination problems vary with the different laboratories, depending on their philosophy and

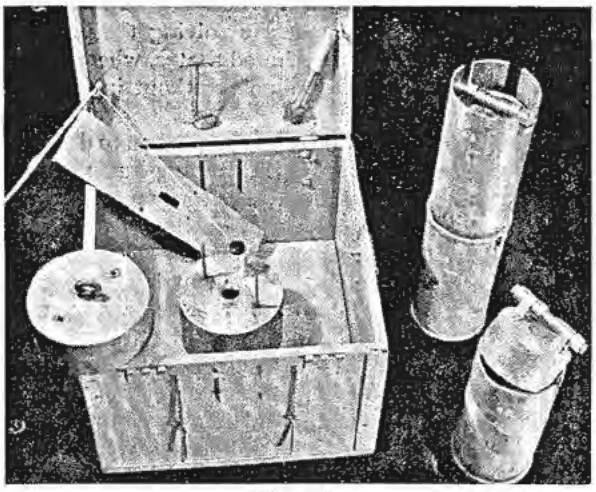

Figure 1

the possible presence of a health hazard, a technical requirement, or interest in the economical recovery of equipment for reuse. All laboratories have made a great effort not to use—in active areas—any materials that would be hard to decontaminate. Covering of some kind is being used more and more, whether on equipment or on personnel. Several years ago it was believed that strippable coatings could be sprayed onto surfaces to furnish an easy means of decontamination, but this method is not widely used. Where the "Dilute, Disperse and Decontaminate" philosophy is practised, shoe covers and clothing are furnished and are decontaminated in a special laundry. Decontamination procedures vary with the isotope and chemical form involved; washing with solvents, acids, bases and complexing agents meets most requirements. Installations of ultrasonic decontamination show great promise.

Although house vacuum systems are provided in most laboratories, there is a policy to employ individual vacuum pumps where radioactivity is concerned. This prevents the accumulation of radioactive contamination in vacuum pipe lines throughout the building; the discharge from the individual vacuum pump is filtered.

So far there have been listed most of the general factors that receive consideration in planning for chemistry with radioactive materials. Most sites have met all of the requirements successfully with the Dilute, Disperse and Decontaminate approach. Their installations are described in the many publications available for reference. It seems appropriate at this point to illustrate with a specific example how the various problems are solved by the Concentrate and Confine philosophy, as practised at the University of California Radiation Laboratory.

Assume that a chemical problem is to be carried out involving material such as fission products, with 1000 curies of beta-gamma activity, and 100 curies of alpha-emitting substance. The confined space would be provided by a metal box maintained at a negative pressure of approximately one-quarter inch of water. The air to the box would be recirculated, passing through scrubbers, condensers and filters. Leakage, outgassing and process fumes can be expected such that approximately 0.03 cfm will have to be discharged to the atmosphere to maintain the negative pressure. Any radioactivity carried by this excess air, after its scrubbing, condensing and first filtering, is removed in a second and third filter, leaving essentially no particulate radioactivity to be discharged to the atmosphere.

Noble gases will not be removed in this cleaning, but the quantities present can be calculated or estimated by monitoring, and if the presence of their insignificant percentage of the discharge should introduce possibilities of trouble, the exhaust air is trapped in an evacuated tank.

The boxes are made of sheet metal and provide a work space of about a forty-inch cube. The inside is finished with a chemically resistant paint, covered with a polyethylene lining to facilitate decontamination. The heat from lighting and processes is not removed by the air circulation, so a portion of the side walls is jacketed for external water cooling. Lighting is supplied through a top window and a front window of one-quarter inch safety glass, which gives a good view of the work area. The front also has two plastic accordion-pleated sections (usually 0.040 inch vinyl) to allow for the free movement of the ball-and-socket or castle manipulator. The plastic fronts are attached to plastic pleated sleeves, which cover tong shafts, introduced from the front through the ball-and-socket or castle manipulator. The tongs can be connected to a desired tong head from a stock of same within the box. Equipment to be used in the particular chemical process is selected and installed in the box, and the box is rolled into place behind the cave wall.

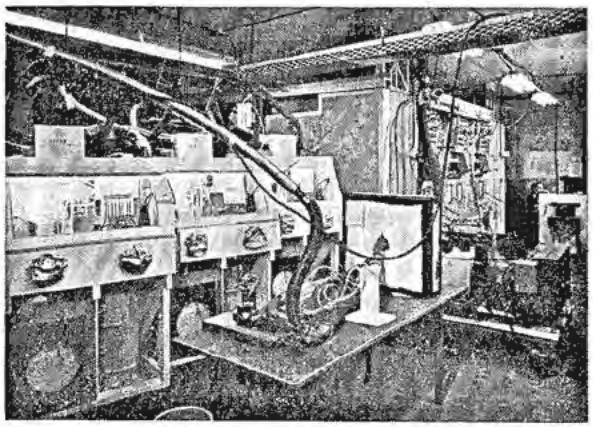

Figure 2

Where the process may require space in excess of one box, two or three will be set up and interconnected behind the cave so that items can be passed from one to the other. Figure 2 shows an installation of the type described. The six inch lead front of the cave provides three working faces, each with manipulators and a shielding window of twelve inch thickness, made of high density (6.2) lead glass. The sides of the cave consist of thirty inches of concrete, and a concrete slab on the top can be controlled to eliminate shine. Since the air circulating system for the work boxes can accumulate considerable radioactivity, a ventilation box is provided for each work box. The three boxes shown hold the ventilation control equipment for the work boxes that are installed in the cave.

Through the bottom of the boxes a six-in.-diameter plastic connection leads to a plastic waste container that may be imbedded in concrete. As the work progresses, waste is discharged into this container, and at the conclusion of the operation the plastic sleeve can be heat-sealed without opening. With the sealed sleeve pushed down the addition of a small amount of concrete will make the waste well prepared for any disposal. Thus we see that the air discharge and the waste are handled without release of radioactivity.

The processes set up within the box can be any standard chemical operation—dissolving, evaporation, extraction, distillation with jackets, centrifugation,

etc. Also, mechanical operations such as milling or hydraulic pressing have been carried out in boxes.

The cave and all the related equipment are designed to be mobile so that the entire unit can be disassembled and put together in a new location or to meet special circumstances.

The same principles described for these higher radioactive levels can be applied easily to work requiring two inches of lead shielding and even more simply to work where protection is provided by rubber gloves. For the lower levels the closed work space may be a slightly smaller box so that the area may be reached by a man working in 27-in. rubber gloves. The equipment inside is standardized; hot or cold baths, rotating reagent racks, small glass hoods for immediate local activity capture, stirring devices, centrifuge equipment can all be taken from stock and assembled in a reasonable time. Heating is accomplished either by induction, hot plates, resistance furnace or heat lamp. Although work employing a flame has been done in a box, this act is to be discouraged. Metal parts are usually made of aluminum, brass or stainless steel with a phenolic resin spray coat baked on. Simple pieces such as racks that will not justify decontamination are made of plywood and painted with a chemically resistant paint.

Items to be taken from the box are passed out through a plastic sock which is heat-sealed by high-frequency current. Here again, no radioactivity is released.

Many who examine this Concentrate and Confine approach to the handling of radioactivity form a hasty conclusion that the special equipment and exacting installations will result in a more expensive operation. To make a fair appraisal it is essential to see how this philosophy meets the original requirements set down earlier. Except for accidental spills the liabilities mentioned are almost eliminated. The technical contamination is controlled to any degree desired. The original cost of the buildings and laboratories is much lower by actual experience, and through the elimination of laundry and clothing, change rooms and loss of workers' time, economy in heating and ventilating and greater use of laboratory space, the system has more than paid for itself. An advantageous by-product develops with an increase in the efficiency of the workers, since there is no restricted area where smoking or eating is forbidden.

It is a popular pastime to make predictions as to the levels of radioactivity that can be expected on the surface of the earth in future periods. In every case many assumptions must be made to arrive at any approximation, but one exact point from which to start is that for every megawatt of energy produced by fission, an equilibrium state of fission products of 10^{30} radioactive molecules will be approached. If one assumes that there will be 10^6 megawatts operating by the year 2000 and that our over-all confining efficiency for these fission products is 99.99%, it can be seen that an even distribution over all the land areas of the earth will give a fairly active deposition per square yard. Further assumptions that an average half-life of 100 years can be used for the deposition and that nearly 10 per cent of the deposition is strontium-90, the uptake of activity for man directly and indirectly through concentration in food at levels existing fifty years hence will quickly exceed the amount now considered hazardous as a body burden.

One group today takes the attitude that we can afford to be careless now, as there is no immediate prospect of dangerous levels and that when the background does present a hazard, controls will be introduced promptly. It seems much more likely that it will require the fifty years for us to develop the ability to confine and concentrate this radioactivity to better than the 99.99 per cent, regardless of what techniques are developed or what useful applications it may be put to. With the many thousands of workers actively engaged with radioactivity, even a small additional daily contamination of long- or short-lived isotopes on top of an ever-increasing background may be sufficient at some time to throw the values into a hazardous category.

It does not matter what assumptions one chooses to make if we cannot arrive at almost perfect confinement; the results are the same and only the date when trouble will occur will change.

With the strong desire and need for nuclear power throughout the world being stressed at this time, it is quite natural that this control of radioactivity receive the attention that it requires. Many who are familiar with the various problems recognize that the ability to confine radioactivity may be the deciding factor in how successful the broad use of nuclear power may be. Certainly international agreements will be necessary if nuclear power and the use of isotopes are to assume safely the important role in human existence now contemplated.

Hot Laboratory Facilities and Techniques For Handling Radioactive Materials

By S. E. Dismuke, M. J. Feldman, G. W. Parker and Frank Ring, Jr.,* USA

This paper will discuss some of the hot laboratory facilities and techniques for handling radioactive materials. The configurations of the laboratory building and shielding structure, the remote operating contrivances and some of the more interesting operations will be explained.

In a broad sense, the term "hot laboratory" would include a suitable building with shielded working facilities for safely carrying on basic research, development work, and in some cases fabrication, disposal facilities for radioactive wastes, and the necessary remotely operated tools and handling devices. The "hot laboratory" is called upon to handle remotely and with the same degree of precision the development, testing, and experimental work usually done in the normal development laboratory. To list several kinds of hot laboratory in-cell work we have:[1] pilot plant chemical processes; metallurgical tests, such as profile, hardness, impact, tensile and the preparation of metallographic specimens; process and sample analysis relative to specific gravity, viscosity, acidity and composition; and general machine shop operations (lathe work, drilling, milling, cutting and grinding).

CELL WORKING ENCLOSURES

Structure

In general, the designs of hot laboratory facilities are based on protection against gamma radiation and the hazards of contamination from airborne particles, vapors and liquid penetration. Hence, the laboratory work is done inside protective walled enclosures called cells or caves. Since mass with high density provides shielding against gamma radiation, the cell walls are constructed of lead, steel or concrete.[2] For a temporary enclosure, lead bricks are stacked up. The concrete enclosure may consist of stacked solid block or poured concrete. Barytes or some other heavy aggregates may be used in the concrete mixture to increase the density of the concrete structure and thus provide greater shielding value for a wall of the same thickness. It is very important that a shielding wall be uniform in thickness, have no voids and be homogeneous in composition so that the protective barrier has no weak places from the standpoint of radiation leakage.

In present day cell structure, lead and steel wall thicknesses vary from 3 inches to 12 inches. Concrete walls vary from 2 feet to 6 feet with the most common wall thickness now being 3 feet.

Where chemical development, with the probability of corrosive and radioactive spills and vapors, is carried on, stainless linings are frequently used in the interior of the cells. All welds on these linings must be sound and ground smooth. Where only dry type work is done in the cells, a stainless steel floor with stainless steel cove base is used. The concrete walls are painted and sometimes coated with a strippable plastic to facilitate removal of deposited contamination.

Services

Services should be readily available at the cell face and the controls should be arranged to be within the reach of the operator. Depending on the work to be done, services such as air, steam, gas, power in several voltages, water, vacuum, etc., should be installed.

Cell Wall Penetrations

The handling of radioactive materials and the setting up and operation of remotely controlled laboratory devices requires that the barrier walls and roof structures of totally enclosed cells be penetrated with access tubes with stepped diameters, manipulator holes, spiral pipe and wire holes, large rectangular and circular window framings, stepped access doors, roof plugs and transfer devices.

Where lower levels of radiation intensity permit, the cells may consist of barrier walls with open tops. With this arrangement "over-the-wall" access eliminates the need for most or all of the above mentioned penetrations.

Ventilation

Totally enclosed cells should always be ventilated to the extent that the pressure within the cell is lower than *all* adjoining areas. This insures that air leakage will be into the cell aad eliminates the possibility of personnel being exposed to airborne contamination. The number of cell air changes per given time is contingent upon the amount of contaminated fumes generated within the cell and the type of cell enclosure.

For open top cells and hoods, ventilation must be arranged to insure a draft of air into the enclosure and away from the operator.

* Oak Ridge National Laboratory.

All ventilation and off-gas should be filtered before being exhausted to the atmosphere in order to remove all contaminated particles.

Viewing

To date, four methods of viewing the hot area beyond the barrier wall have been devised and all are in active use.

The simplest, the mirror, is used extensively for viewing over the barrier wall. Where applicable, it has the advantage of low cost and the disadvantage of reversed images at apparently greater distances.

Periscopes are in use in both open top cells and totally enclosed cells. For open top cells (over the wall viewing) the periscope is generally in the form of a large inverted "U." When used for viewing the interior of a totally enclosed cell, the periscope is usually pointed at the corner of the cell interior and a hinged mirror controlled from the outside of the cell is used to scan the cell horizontally. Rotation of the periscope tube enables some vertical scanning. Some periscopes are equipped with special optical devices such as adjustable eyepieces and auxiliary lenses to increase the effectiveness of the instrument (see Fig. 1).

Window viewing is considered the best type for viewing operations within hot cells. This type affords direct viewing. These direct viewing windows may vary in configuration from cylindrical ports to large tanks. The viewing media may be regular or high density glasses or heavy transparent liquids. Cerium bearing, non-browning glass having a specific gravity of 2.4 or 80% solution of $ZnBr_2$ with a specific gravity of 2.4 is compatible with regular concrete cell wall construction. Lead bearing glass with a specific gravity of 3.3 is compatible with barytes aggregate concrete cell construction. Lead bearing glass with a specific gravity of 6.2 is employed in connection with steel wall construction.

Both liquid and glass type viewing media are usually built into a steel enclosure tank which is cast or grouted into the barrier wall. The cover plates, that is the glass surfaces at the hot and cold sides, are made of plate glass. Usually two sheets of one inch thick glass laminated with plastic is used. The plate glass at the hot side is the non-browning type, while that at cold side is regular plate glass.

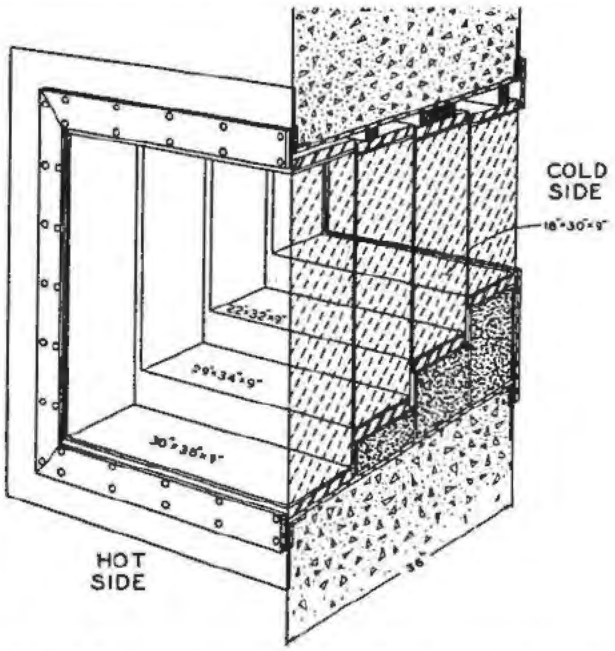

Figure 2. Section through glass radiation window showing four slabs of 3.2 density glass, the stepped tank casting and the packing around the window

The glass radiation protection windows are usually made up of one or more 4 inch to 9 inch thick slabs with a liquid such as mineral oil or zinc bromide introduced between the surfaces of the slabs to reduce interfacial reflections, thereby increasing overall viewing efficiency (see Fig. 2).

Attenuation of the light through liquid or glass type viewing windows is quite high. Glass windows of 3 foot thickness have a transmission efficiency of 25 to 40 per cent. These relatively low transmission efficiencies are somewhat compensated for by very high lighting intensity within the cell.

The liquid window, compared to the equivalent glass window, has many advantages and several disadvantages. The liquid zinc bromide solution window costs about one-half as much as an equivalent glass window. For close work the optical homogeneity of the liquid window is advantageous. The window tanks must be leak tight; and the all metallic surfaces exposed to the solution must be protected against the

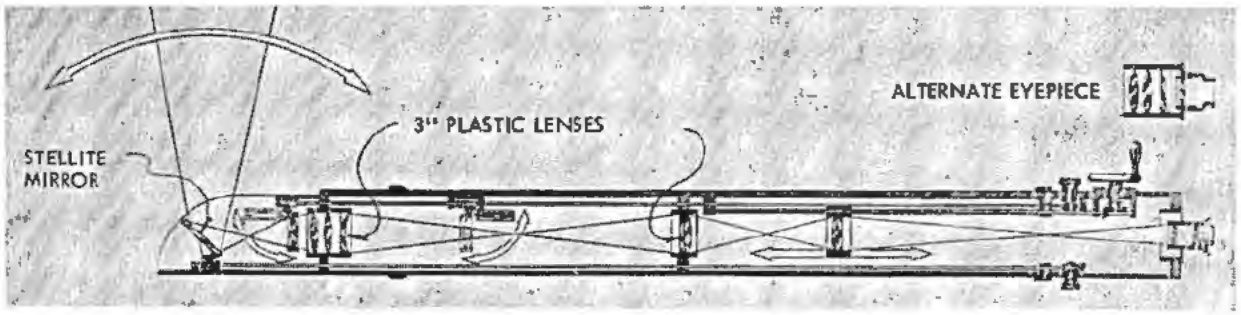

Figure 1. Through-wall periscope showing arrangements of mirror control, lens interchange and light path

zinc bromide corrosive action which might cause leaks or develop discoloration. Of prime importance in the choice between liquid or glass filled windows is the fact that an accidental break in a solution filled window would immediately reduce the shielding between a source and an operator. An equal occurrence with a glass filled window would reduce its usefulness as a window but maintain its shielding value.

The liquid and glass window materials referred to above have a high index of refraction. This enables the observer to look into the window diagonally from the side and see objects that are out of the normal line of sight in the cell at the side of the window. However, with large angles (over about 50 degrees from normal) there is some distortion.

Wired television has been used to a limited extent for cell viewing. Binocular viewing is used to give some depth perception. To date, television has been used mainly for monitoring at considerable distances.

Cell Lighting

In open top cells, the lighting used is usually incandescent with reflectors to give to the order of 50 foot candles of lighting intensity at the working surfaces. Spot illumination is used to light individual pieces of equipment when necessary.

Totally enclosed cells are usually equipped with sodium vapor or mercury fluorescent units. Due to the high attenuation of the viewing windows, it is good practice to illuminate to a level of about 400 to 500 foot candles.

The sodium vapor light is especially suited to in-cell lighting since it does not cause spectral dispersion which is prevalent with incandescent type of lighting when viewing through thick liquid or glass radiation windows.

Manipulators

The manipulator may be defined as a tool or device for extending the operator's movements to some distance. These devices can multiply motions and forces. The simplest manipulator is probably a plain pair of tongs providing distance protection of from one to several feet.

The more complex manipulators are of three types; namely, mechanical, electric and hydraulic, or any combinations of these three.

The ball socket or cylinder disk type manipulator is one of the more widely used types (see Figs. 3 and 11). This type consists of a set of tongs on one end of a 3-foot to 5-foot tube with a trigger or squeeze hand actuator on the other end. This tube is inserted through a ball mounted in the shielding wall. Motions along polar coordinates can be obtained by swinging the tube in any direction and by sliding the tong tube in and out of the wall unit. Tong rotation can be obtained by twisting the master end of the tube.

Several types of pantograph manipulators have been widely used. One type, known as the ANL Model 4 is used in cells which are not totally enclosed. In this type, the manipulator enters the cell through an opening in the roof. See Fig. 3. Another variation of this manipulator, the ANL Model 8, enters the totally enclosed cell through a hole which is located high in the front cell wall. These pantograph types faithfully reproduce the operator's shoulder to finger motions. They also provide a good feedback of feel to the operator. Their rated capacity is 5 to 10 pounds.

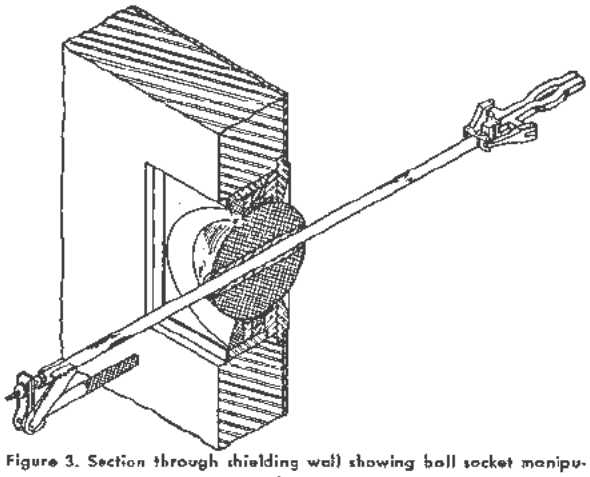

Figure 3. Section through shielding wall showing ball socket manipulator

Electrically actuated manipulators are also used. Some of the larger, higher capacity types are controlled by elaborate consoles. The electric types are generally classed as rectilinear, since their slave motions are confined to the X, Y and Z coordinates. Their design is somewhat like a bridge crane (see Fig. 4). The track is mounted on the front and rear walls of the cell. Most types provide, in addition to the X, Y and Z motions, tong gripping, wrist rotation, elbow swing and shoulder rotation. Their capacity may be as high as 750 pounds vertical lift. Tong squeeze is frequently electrically indicated to the operator by sound, lights or ammeter dial pointer position.

An electric servo actuated manipulator has been developed in which master and slave motions are proportional. Some work has been done on hydraulic actuated servo manipulators.

In the following several sections, hot laboratory facilities for carrying on radiochemical and hot metallurgical work will be discussed.

THE RADIOCHEMICAL LABORATORY

Since hot laboratory work has become common to all types of research work, it is natural that a certain degree of specialization should become identified with each general field.

Many design features become associated with the scale and production demands of a hot laboratory facility.[3] Thus, we find radiochemistry performed on as many as five or more distinct levels at a single laboratory site. For example, these may be listed as the bench laboratory, the hot analytical laboratory, the radioisotope research and development laboratory, the radioisotope production laboratory and the chemical engineering research and development pilot plant.

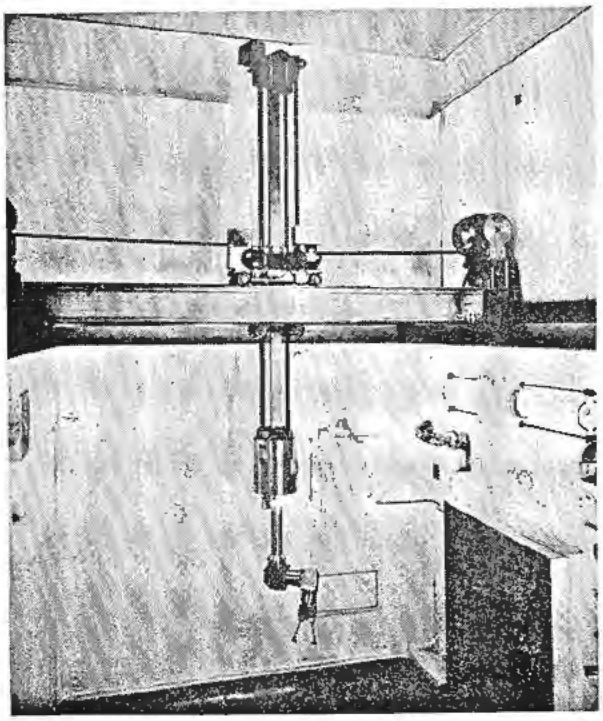

Figure 4. The interior of a hot cell which is used at Oak Ridge National Laboratory for solid state and metallurgical work is shown with an electric rectilinear manipulator which travels on the wall mounted rails. At the right side of the photograph are shown the sodium vapor lights, the interior of the liquid radiation window and the spot lights

Beyond this, there are innumerable specialized fields; however, a few features characterize to some extent all hot radiochemistry in contrast to physics or metallurgy. Important among these is the extensive design for containment of liquids, the general use of fluid transfer as in piping, tubing, etc. with its associated hazards, the constant danger of corrosion from varied chemicals, and the biological hazard of volatile radioactive fumes.

In order to attain the most nearly satisfactory balance of design features, the hot laboratory should conform within the scale of intended operation to an optimum in such criteria as: freedom in choice of chemical methods, maximum biological shielding and adequate contamination control.

The provision for many varied chemical systems in the hot laboratory is required to make the greatest possible use of the facility.

It is assumed that design should afford protection of personnel from penetrating radiation on the basis that any exposure which can be avoided is too much. The problem of contamination in invalidating technical data goes closely with the safeguard against ingestion and inhalation of radioactive materials.

Building Design for Performing a Wide Range of Radiochemical Operations

The accompanying sketches, Figs. 5 and 6, serve to illustrate the methods of radiation level zoning and controlled air flow planning.[4] In Fig. 5, a floor plan, the isolation of the Hot Area is provided by separating it from the cold area by one or more low or intermediate level zones. The cold areas, which are at a higher air pressure, thus help to confine airborne dust or fumes to the hot areas. When limited air conditioning is involved, it often becomes necessary to interconnect the supplementary air systems so that the desired controlled air flow is obtained.

In Fig. 6, the section in elevation illustrates the principle of down-draft ventilation used in hot cells and hoods, providing at the same time for shielding of contaminated ducts and ease in hosing for decontamination. Figure 7 illustrates some details of the hot cell design, such as the high degree of access, the elaborate design for contamination control such as the opening in-to-the-cell glass doors between the heavy outer lead doors, the plastic coated stainless steel interior liner and the extensive viewing equipment. Since the cells may extend into both the basement and second floor crane-bay area, unusual cell heights may be obtained. By using 3 feet of a barytes base concrete of specific gravity 3.2, it was possible to gain the shielding value of four and one half feet of ordinary concrete. This effects a considerable advantage in shortening the distance through the wall and hence the cost of the inward sloping sleeves and control devices. Another feature of the building design includes a versatile system of plastic tube transfer lines for the exchange of radioactive liquids between underground tank storage and the cells.

The special provision for extensive ion exchange work is indicated by the multiple unit bottle storage and sampling service, or vault-cave storage unit, and the associated shielded transport truck (see Fig. 8).

In the hot laboratory rooms, which are individually isolated by the use of 24 inch concrete walls, intermediate scale work is performed in special-designed hoods (Fig. 9). Particularly useful for routine washing of contaminated glassware and small parts, as well as for disposal of hot waste is the hotsink in Fig. 10.

Heavy handling in the building is by means of bridge cranes, a system of monorails, and heavy-duty electric lift trucks.

TYPICAL RADIOCHEMICAL OPERATIONS

Hoods and Glove Boxes

The scale of radiochemical operations has become the dominant factor in the radioisotope research facility. In a few cases, the scale is suitable for use of the isolation-box principle,[5] a contamination control device, which requires that all operations be performed inside a disposable plastic case. In general, however, this scale is far surpassed; although a typical laboratory hood is often used in a similar way. Of special importance in hood use for radioactive materials is an increased air flow. This poses some problem in connection with air conditioning; however, a minimum recommended discharge rate is about 2000 cfm for an eight-foot hood or in excess of 100 linear feet per minute face velocity.

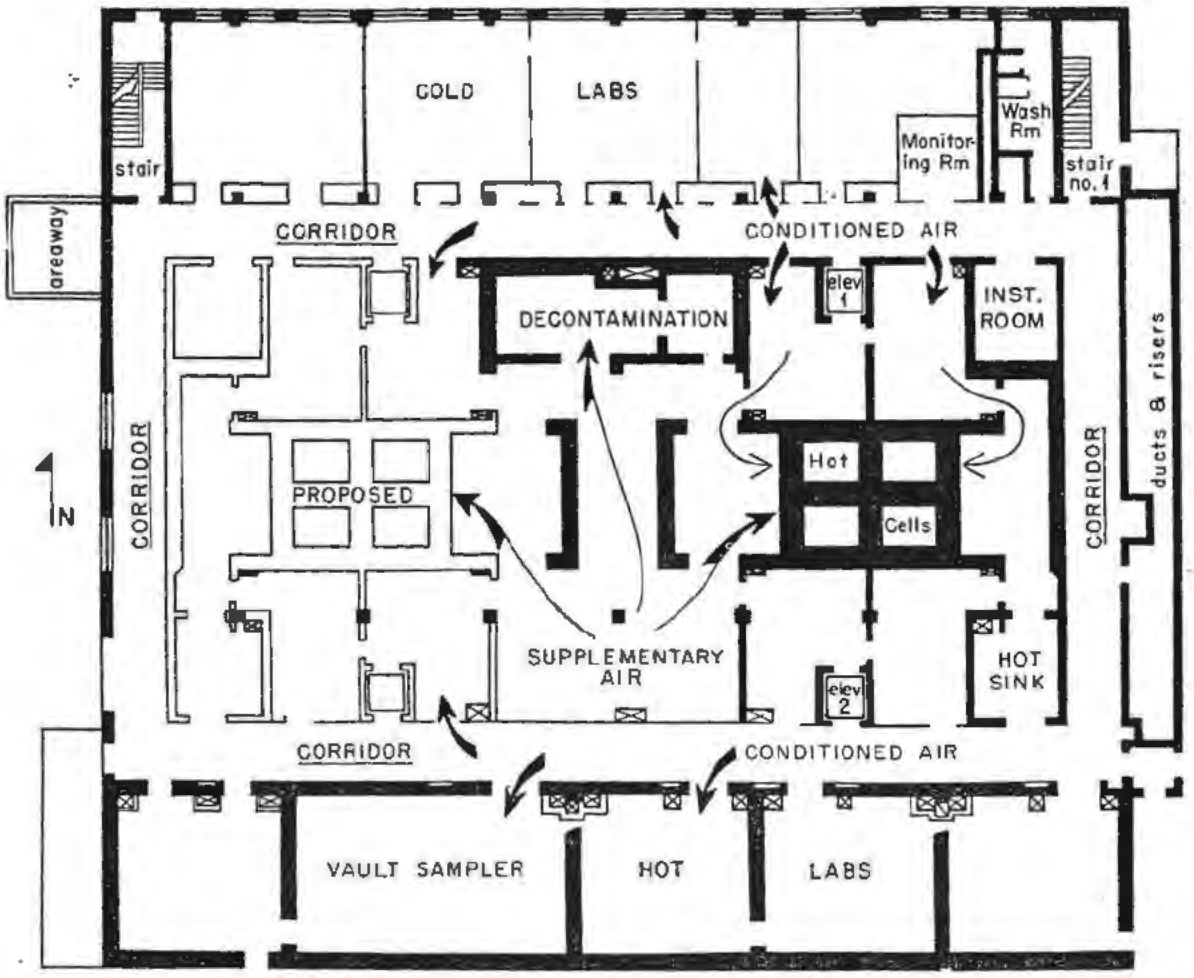

Figure 5. Floor plan of a radiochemical laboratory building with radiation zoning and air flow planning

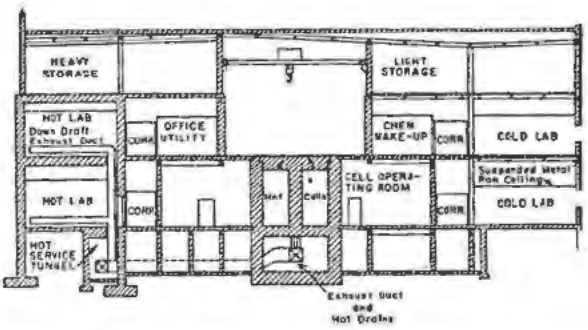

Figure 6. Isotope research building: section in elevation of a radiochemical laboratory building with hot down-draft exhaust in a basement service tunnel

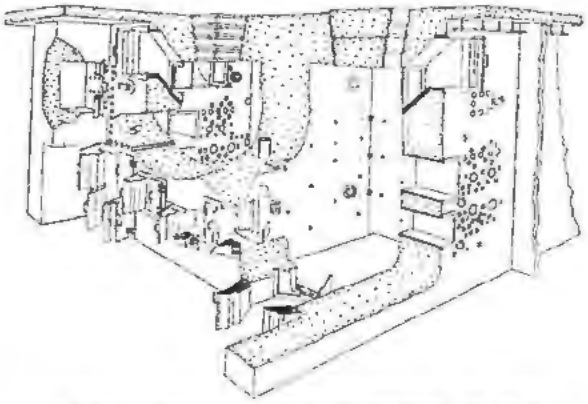

Figure 7. Perspective of typical radiochemical hot cells

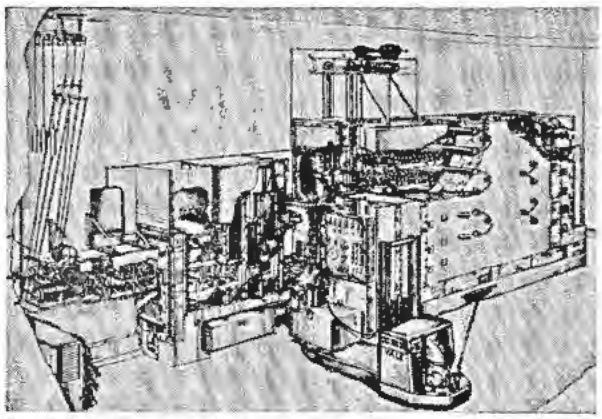

Figure 8. Large-scale hot storage and multiple sampling facility for chromatographic ion-exchange processes

The glove box principle for alpha contamination has been adapted to gamma emitters in varying degrees of complexity.[6] One variation is shown in Fig. 11. In this type atmosphere box, radioactive solids which are easily airborne may be handled with some security even if they must be shielded from atmospheric moisture.

Hot Cell Operations

In some cases, hot cells have been equipped with standard laboratory glassware arranged for a specific chemical sequence. Of such a nature is the process shown in Fig. 12 for chemical dissolution of irradiated metal and further processing through standard operations such as solvent extraction, metathesis, precipitation, etc. A particular necessity in this type of sequence is some dexterity by the operator as well as various safety control devices to prevent hazardous spills. Usually ion-chamber monitoring is required to check the location of radioactivity in the cell and a more sensitive device is always placed near the operator.

Chemical steps which produce volatile radioactive fumes such as the halogens, ruthenium, or airborne sprays require an extra ventilation provision for the cells. It has become the rule in this case to designate a minimum negative pressure of 1 to 2 inches of

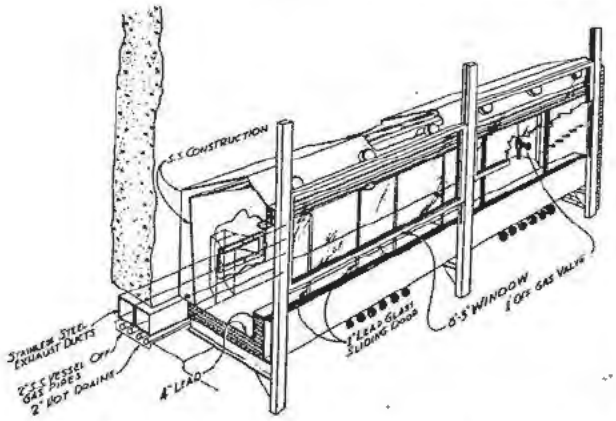

Figure 9. Adaptation of a fume hood for radiochemical use

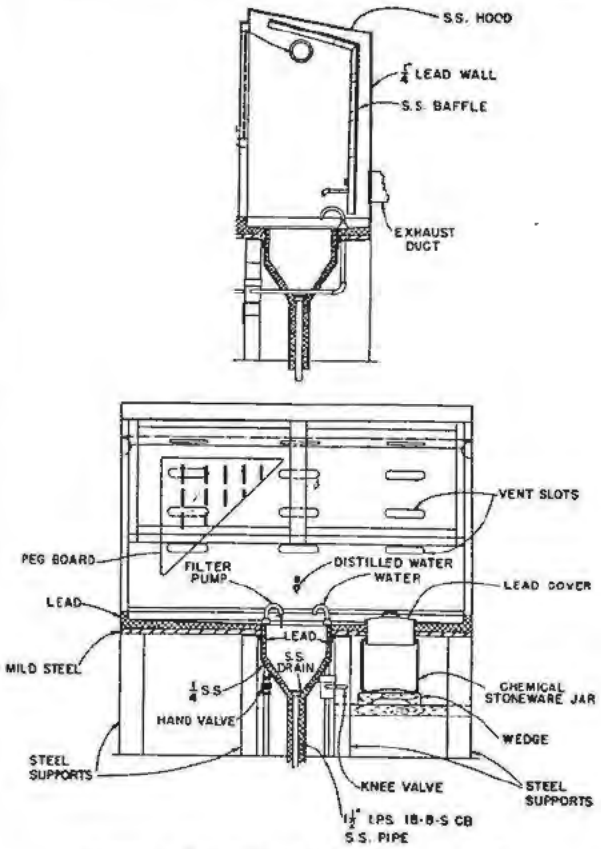

Figure 10. Hot waste and decontamination sink

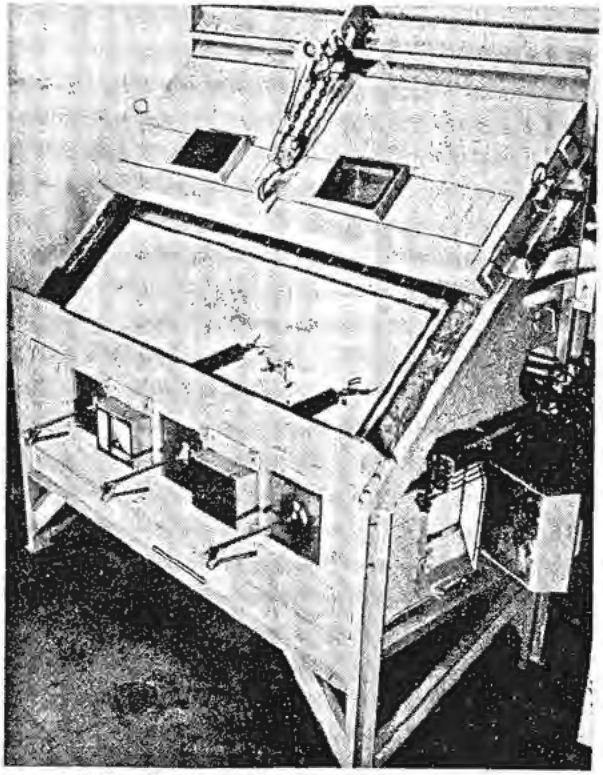

Figure 11. Atmosphere box for gamma radiation

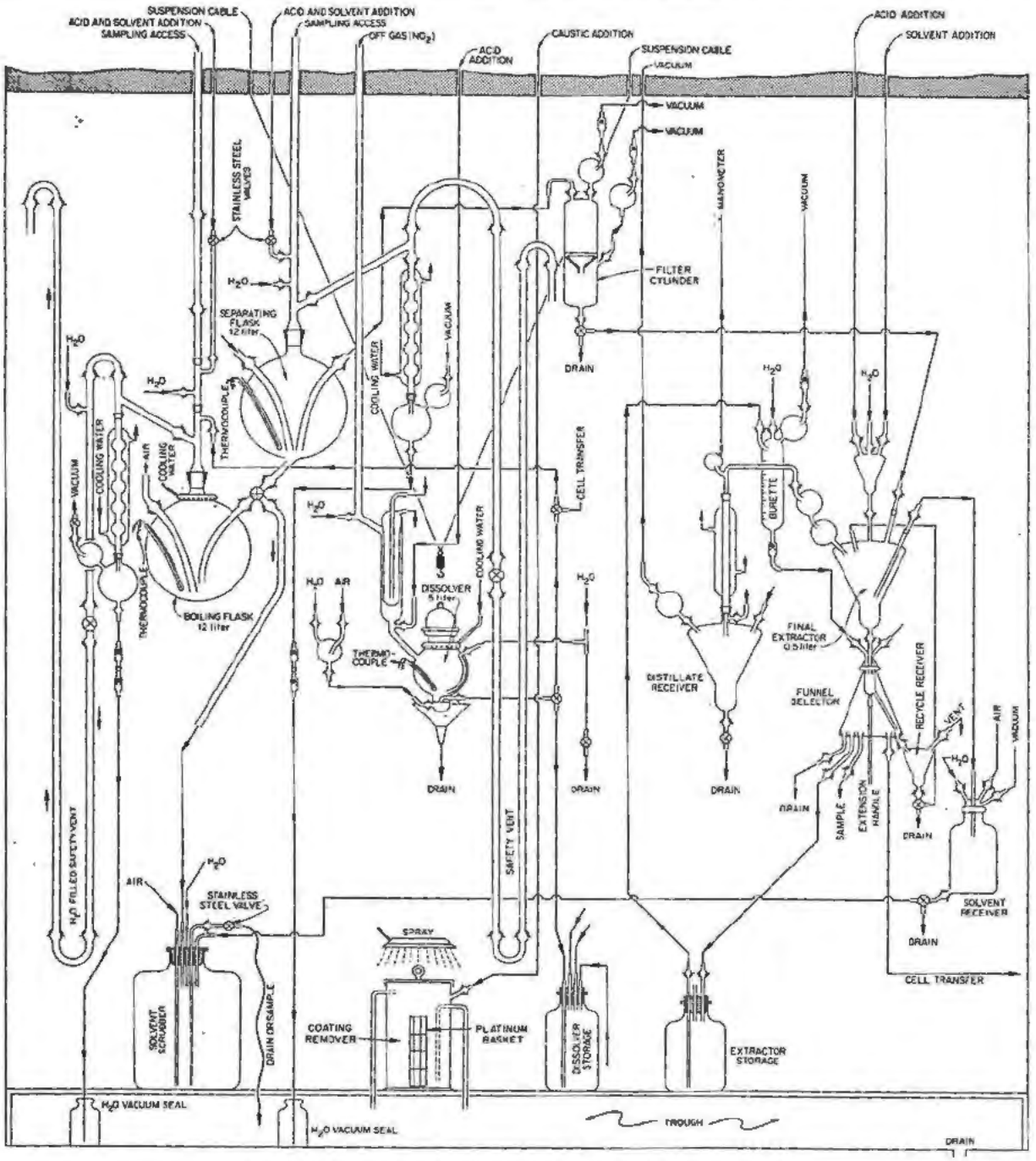

Figure 12. Laboratory-scale solvent extraction equipment for remote operation

water for an essentially closed cell in addition to a minimum face velocity of 200 feet per minute for necessary openings such as access doors. Primary confinement of active fumes is provided by a negative pressure off-gas system of 30 inches of water.

A typical cell arrangement for small scale ion-exchange separation is illustrated in Fig. 13. In this cell, no special bottle handling facility has been provided, therefore, the individual bottles must be removed from the bottle changer device by means of long tongs. Later designs utilize a tray system for twelve bottles which are handled by automatic devices.[7]

An approach to pilot-plant scale equipment is shown in Fig. 14. In this case equipment and piping conform to nearly standard practice while valving and control instrumentation are adapted for remote operation by means of long extension handles through the cell walls.

In all cell work, contamination-control and provision for decontamination are of vital importance. Stainless steel is considered the standard material of choice; however, more economical materials such as resin coatings on steel or concrete, porcelain enamel, weldable plastics, etc. are widely used. Decontamination studies[8] assist in making this selection.

Special significance is attached in all radiochemical operations to a prior shake-down program to indicate operability of equipment, to afford opportunity for leak correction, and to prove chemical yield before moderate radiation levels are introduced. This is a final safeguard against unforeseen difficulties.

THE SOLID STATE HOT LABORATORY

Solid state physical and metallurgical investigations concerned with the effect of nuclear radiations on the properties of solids require hot cells considerably different from those used for handling radiochemical operations.

The hot cell designer must keep in mind not only that the cells must be a little more than adequate, but also that costs should be kept as low as possible considering both the initial installation and the long range operation. To provide adequate cells, the following items must be kept in mind.

Type of Material Handled

The materials handled are solid for the most part, though etchant and cleaning solutions are used. There is a great variety of small test specimens such as tensile, notched impact, electrical conductivity, etc. There are also larger devices such as complete test assemblies that have been in a reactor, and parts of reactors themselves such as fuel elements.

Type of Cell Equipment Used

The type of equipment used should be commercially available, as far as possible, since the testing and examination equipment are about the same as that found in a physical and metallurgical laboratory where metallographic, tensile, impact, electrical and thermal conductivity, X-ray diffraction, heat treating and other tests are made.

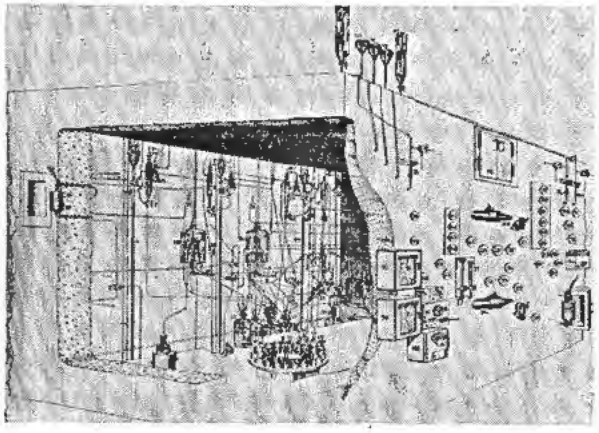

Figure 13. Hot cell for ion-exchange processes

There is also a need for machine tools such as lathes, millers, saws, grinders, impact wrenches, etc. Most test specimens must be removed from the sealed containers in which they are irradiated. Irradiated test apparatus and reactor components are frequently disassembled for inspection and parts selected for further tests. Tensile, impact and other types of samples may need to be made from selected radioactive material.

The Biological Shield

Shielding for gamma rays must be able to attenuate radiations from the most active sample handled in a given cell to about 8 milliroentgens per hour or less. The facility described here was designed to handle a fuel element, from a particular reactor, after about one week decay.

Viewing Facilities

Because of the wide variety of equipment to be used and the fairly involved manipulations that are necessary, large windows for direct viewing are considered best.

Manipulators to Handle the Radioactive Material

Sample handling devices or manipulators must be versatile enough to remove the sample from a cask, rotate and translate it into any position in the cell for viewing or inserting into examination or test equipment. At times the manipulator should be able to lift the lids off casks which weigh several hundred pounds and handle samples weighing up to fifty pounds. Since there can be several manipulators per cell or different cells for different types of manipulation, not all of them need to handle the large loads.

Control of the Testing and Examination Equipment

Direct remote control of testing and examination equipment ranges from simple extension rods to complicated servo-systems. The development of sensitive master-slave type manipulators has, to a large extent, eliminated the problem of remoting all equipment that is put in a cell. Since remoting is frequently a costly and time consuming task, it must be considered carefully. If a specific piece of equipment is used approximately fifty per cent of the time or more, and direct remote controls will speed the operation, remoting is justified. At times commercially available equipment does not meet the specific requirements that hot cells place on it and so must be adapted for use in a hot cell; an example of this is the polishing wheel for remote metallography mentioned later.

Facilities for the Introduction, Storage and Removal of Radioactive Material

Heavy lead-filled casks are used to transport radioactive samples, so means of handling them must be provided; this is generally done with overhead cranes or lift trucks.

The introduction of samples into a cell is accomplished usually in one of three ways. First, by placing

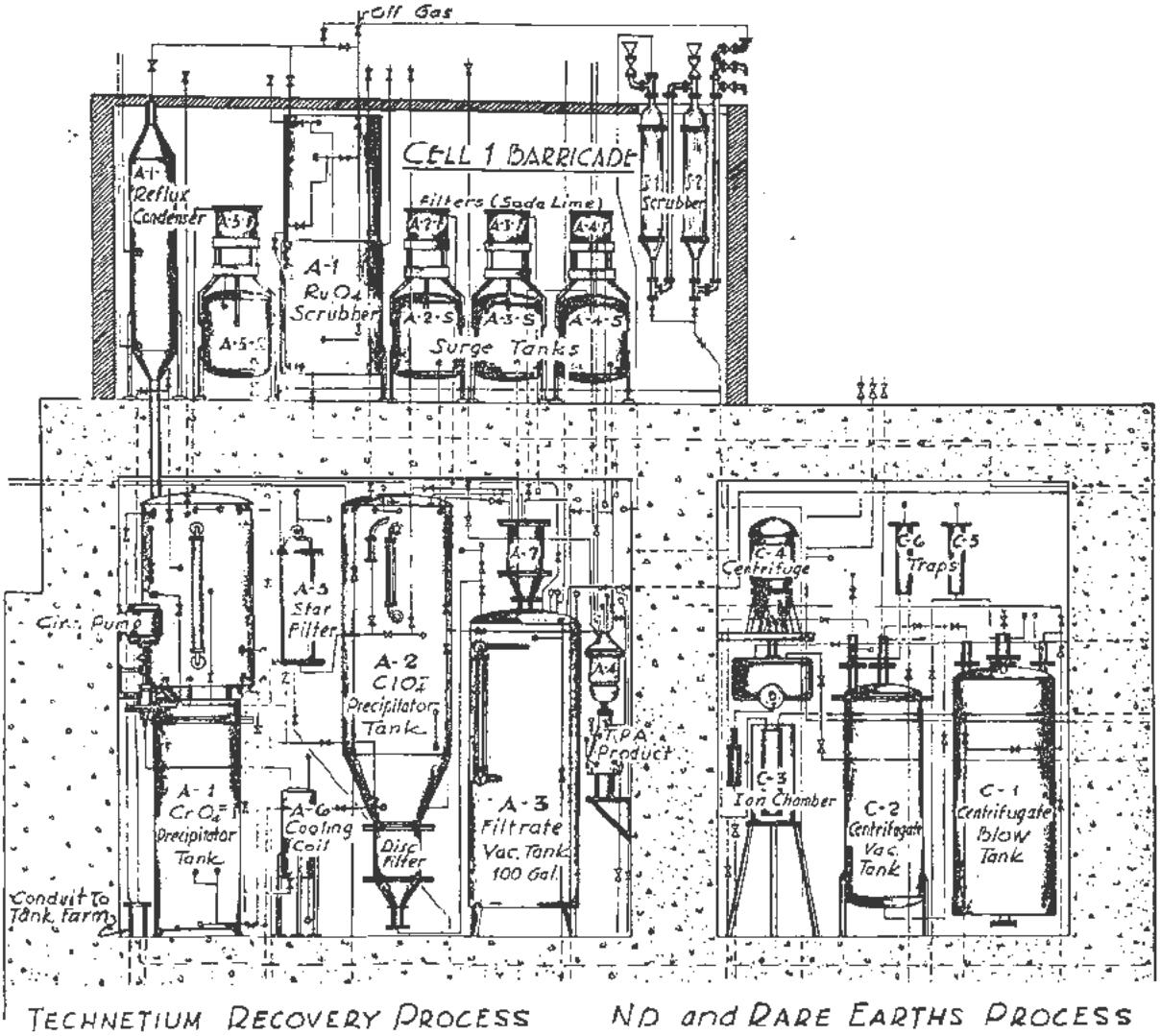

Figure 14. Typical radiochemical pilot plant scale equipment

the sample carrier on the floor of the cell and removing the sample with a manipulator; secondly, by placing the cask under the floor of the cell and drawing the sample up into the cell; and third by holding the cask horizontally against the cell wall and pushing the sample into the cell through an access hole. Samples can be removed in the same cask they came in.

Sample storage outside the cells may be in either a water pit or a dry storage facility. The dry facility consists of pipes placed vertically in the ground with appropriate plugs for shielding. Storage in the cell is in casks or special enclosures mounted in the cell walls.

Contamination Control and Waste Removal

Contamination generally starts inside the hot cells from grinding dust, machine cuttings or from material rubbed or knocked off the active material handled. After a hot operation the manipulator is used, to store the samples in an appropriate container, to put the bulky waste material in another appropriate container, (generally a garbage can), and to collect the chips and dust by using a vacuum cleaner. Liquids are drained to an underground storage tank and disposed of later. The sample container, garbage can, and dust bag from the vacuum cleaner are removed from the cell before someone dressed in protective clothing enters to finish the job. In removing samples and scrap from the cells uncollected dust may be carried out of the cell to where it can spread. By wearing special protective clothing in the cell and removing these when leaving; and by using clean plastic bags to contain all contaminated equipment that is removed, the spread of dust is controlled. Frequent checking and cleaning of the areas around the cell entrances minimizes the possibility of contamination of the working areas. Equipment and containers are removed to special cleaning stations for further decontamination.

There have been many approaches toward achieving the aforementioned criteria; the one stressed here has been highly successful.

Building and Hot Cell Design

The floor plan and section of the building and hot cells are shown in Figs. 15 and 16. A three ton bridge crane covers the entire area north of the work area. There is a storage area above the small rest room and north of the work area. The water tank is used to store hot materials for future use and to transfer samples from one cask to another.

The hot cells are of two types. The first type has an inside floor area of 6 ft × 11 ft and a 12-ft ceiling with the cell floor 2 ft above the main floor level. The walls are made of a high density concrete. They are 3 ft thick up to a 6-ft height above the cell floor, where they are stepped back to allow for the manipulator tracks. The roof is 1 ft thick and can be removed in sections about 3 ft wide.

The entrance for personnel is a hinged 6 in.-thick 3 ton lead-filled door. The barrier between cells is steel 8 inches thick and 6 ft high. The rest of the intercell barrier is a 1-in. thick steel plate that may be lifted by a jib crane to allow the manipulators to pass from one cell to another.

Viewing is done through 3 ft thick zinc bromide filled windows. The special glass inside the cell does not darken under gamma radiation as ordinary plate glass does. It is made of two 1-in. thick plates laminated together in safety glass fashion. The glass outside the cell is built up the same way, except that it is ordinary plate glass.

The second type of cell utilizes an Argonne master-slave manipulator. The manipulator is essentially a three-dimensional pantograph working on polar coordinates with two fingers and a wrist. It is completely counterbalanced and has low inertia. The maximum load is of the order of 5 pounds.

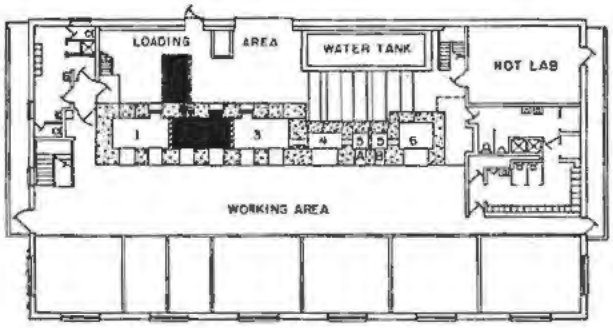

Figure 15. Main floor plan of solid state building

The cell walls are 3 ft thick and made of a barytes concrete block held together with a lime-sand mortar. Viewing is through zinc bromide filled windows. Entrance to the cell is accomplished by moving the back wall from the cell. The back wall is mounted on wheels rolling on tracks embedded in the floor. The in-cell floor is at table top level, about 42 inches above the main floor. It is a disposable ¾-in. thick plywood board mounted on brackets. The 4-in. thick steel roof is 8 feet above the outside floor and has two openings through which the master-slave arms enter the cell.

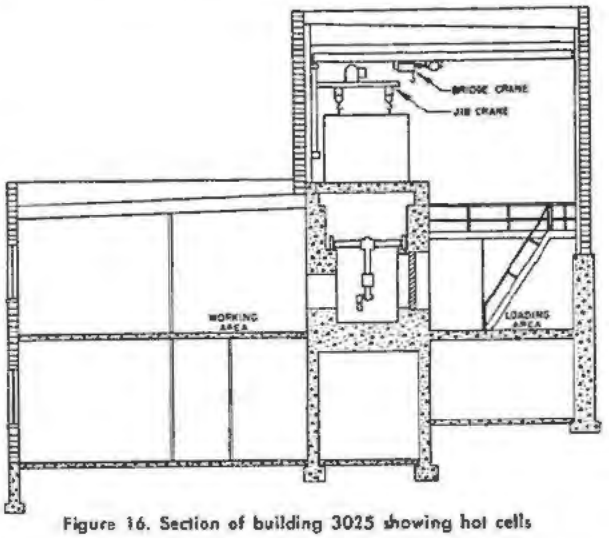

Figure 16. Section of building 3025 showing hot cells

Barrier transfer and storage units have been placed in all of the intercell barriers so that samples may be transferred from one cell to another or stored when it is necessary for workers to enter the cells.

The operating area (Figs. 17 and 18) and loading area (Fig. 19) are separated purposely so that personnel must go through a change room in moving from one area to the other. Since special clothing is always used in the loading area, and extra special clothing is worn in the cells, contamination is thereby controlled.

Some of the advantages of an in-line arrangement of cells are as follows: contamination is controlled by separation of the operating and loading areas, the elimination of some carrier use by transferring samples directly from one cell to another, a more efficient use of floor space and the ability to transfer the rectilinear manipulators into any cell when needed.

Typical Operations

Manipulator Operations

The use of an extremely flexible manipulator such as the Argonne master-slave to control apparatus is

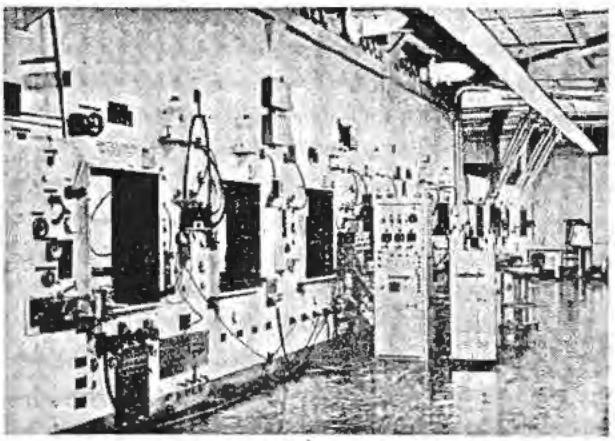

Figure 17. Cell operating area

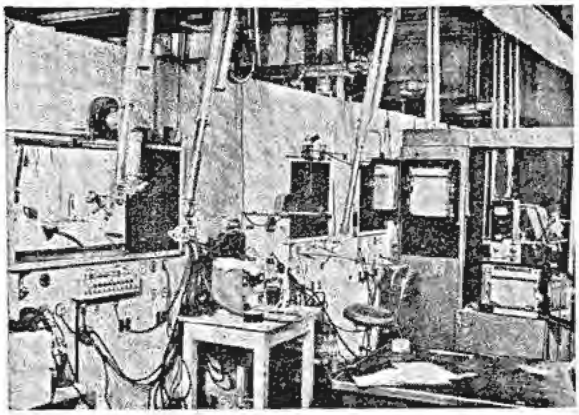

Figure 18. Master-slave cell operating area

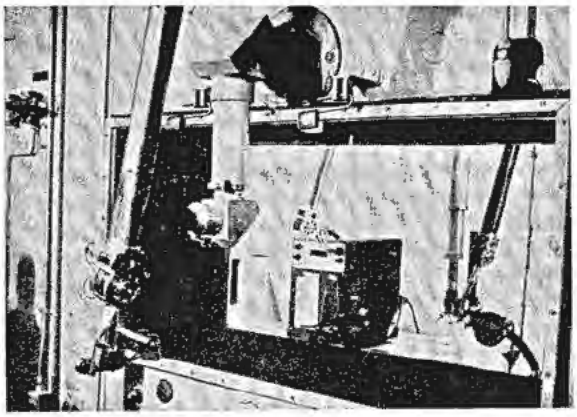

Figure 20. Master-slave operation of balance and microscope

demonstrated in the use of analytical balances (Fig. 20). Standard two-pan balances have been successfully employed, but the single-pan analytical balance is better in many ways; the case needs to be opened only to insert or remove specimens; the balance weights can be changed by turning appropriate knobs with the manipulator. Some difficulty has been encountered with balances using an optical lens since ordinary lenses darken under gamma radiation.

Another example of manipulator control is the use of a toolmakers microscope for the measurement of sample dimensions, area reduction in tensile and notched bend tests, etc. A periscope is used to look into the microscope. At times air or hydraulic specimen clamps are remotely controlled, but all the other motions (i.e., focusing and table control) are easily done with the master-slave.

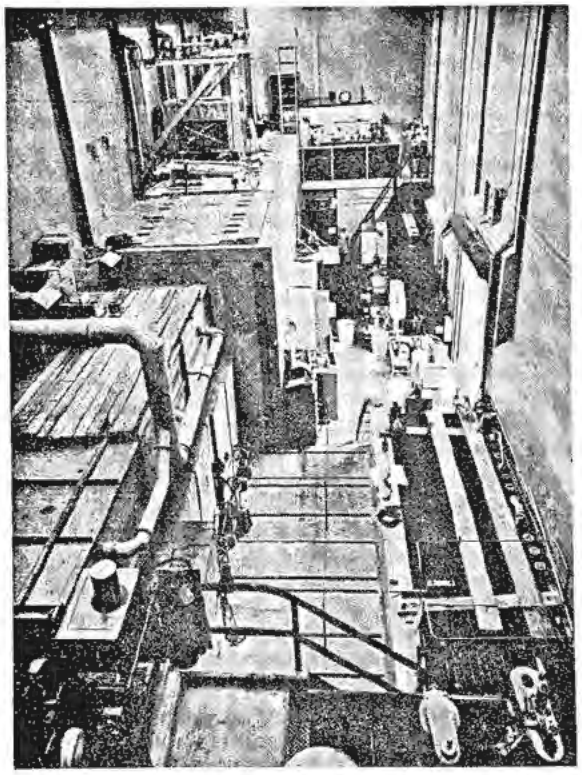

Figure 19. Cell loading area

Metallographic Processing

The preparation of metallographic specimens in the hot cell is an example of a multistaged sequence operation. Metallic components of reactors or portions of experiments irradiated in the various reactors are prepared for examination under the microscope. The metallographic process as a unit is able to handle sections that are 15 inches long and 1½ inches in diameter. Samples larger than these limiting dimensions are transferred to the machine shop cell[9] where they are reduced in size.

Initially the metallographic process from sectioning to examination and photography was operated in one cell.[10] Recently, with the addition of an annex to the metallographic cell it has been possible to eliminate the obvious disadvantages confronted in having mechanical, chemical and optical operations in one cell. The shaded area in Fig. 15 (Cells 2 and 2A) houses the metallographic equipment. Figure 21 is a schematic presentation of the facilities and equipment which comprise the process.

While the physical separation of the steps of sample preparation was motivated by a general incompatibility, additional factors were involved. With the knowledge gained in three years of operating this type of equipment the mechanical phase (cutting, mounting, lapping, cleaning and polishing) of the operation can be conducted on a production basis. That is, for a particular metal a designated process with reference to abrasives and time of operation can be scheduled with confidence that a properly prepared sample will be produced. The succeeding operations of etching, microscopy and photography require the skill of a metallographer. It was reasonable to separate the two major steps of sample preparation in order to utilize fully the potentials of both the cell operators and the metallographers. Because of the delicate nature of research photomicrographic equip-

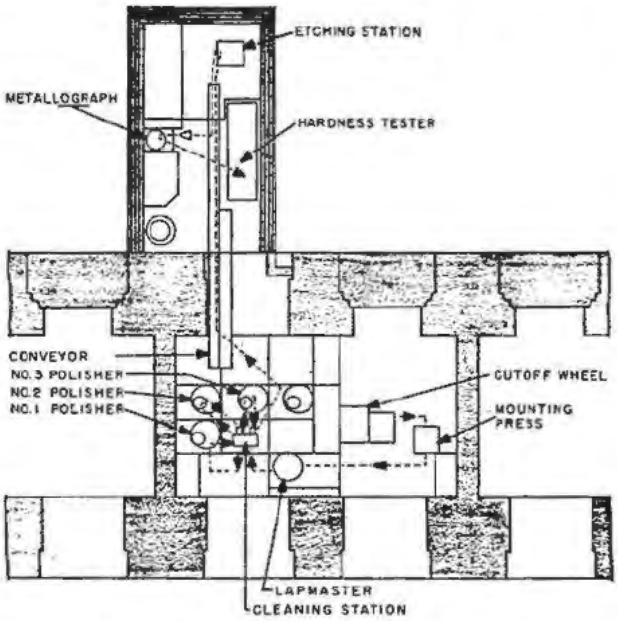

Figure 21. Schematic of metallographic processes

ment it was advisable to separate the metallographers equipment into a chemical area for etching, and an optical area for microscopy and photography.

The procedure is planned so that the radioactive metals which enter the annex are those which are contained in a standard 1¼-inch bakelite mount. This restriction in the size and amount of radioactive material allowed the use of lighter shielding than the main cell and also made feasible the use of Argonne master-slave manipulators. Both of these factors contribute to a better utilization of metallographic skills in a remote operation.

One notes that the addition of the annex to the metallographic cell violates our philosophy of cell operation. Personnel operating the annex will be working in the loading area. Because of physical and economic restrictions the only feasible location for the addition was in the loading area. Individuals using this facility do not have the freedom of movement which is offered by the working area, but the advantages gained surpass the necessary restrictions which are imposed.

If the samples are within the 15 in. × 1½ in. limits mentioned earlier, they are sectioned on the remotely operated cut-off wheel. Primarily the cut-off machine was designed to isolate specific samples of usable size from larger metallic sections. Of equal importance to the process is the surface imparted to the sample face by wet abrasive cutting. In terms of normal metallographic preparation, the wet abrasive cutting is used to replace much of the abrasive paper preparation. Figure 22 shows the cut-off machine and controls.

From the cut-off wheel the sample is transferred to the mounting press. Here it is molded into a standard 1¼-in. bakelite mount of approximately ¾-in. height. During the mounting operation a thin ferromagnetic disc, 1 inch in diameter, is placed in the top face of the bakelite cylinder. This disc has a number stamped on it so that, once mounted, the sample is permanently identified. The ferromagnetic disc is also used as a means of manipulating the sample. The diameter of the mount is a critical dimension in the metallographic process. By cooling the plastic under pressure the cylinder diameter is held within tolerances of +0.000 in. and -0.001 in. on 1.250 inches.

The next step in the preparation of a sample is a lapping operation. A commercially available laboratory machine was easily adapted for remote operation. A half-hour cycle using an 800-mesh alumina abrasive in an oil vehicle is adequate to prepare the wet abrasive cut surface for fine polishing. Where it is necessary to process samples whose surfaces are rougher, an extended lapping time can be used.

Before transfer to the next polishing step the sample is thoroughly cleaned. The thoroughness of the cleaning operation is a key to the successful remote preparation of metallographic specimens. Recently ultrasonic cleaning was introduced into the process.[11] The sample is held by a magnet and is transported in an arc through the focal lines of a pair of transducers set at right angles. The sample is also rotated about its own axis as it passes through a perchloroethylene bath. As the sample emerges from the ultrasonically agitated bath it is deluged with fresh solution to remove any adhering contaminants.

Ultrasonic cleaning was ideal for adaptation to remote operation. The only essentials in the cell are the

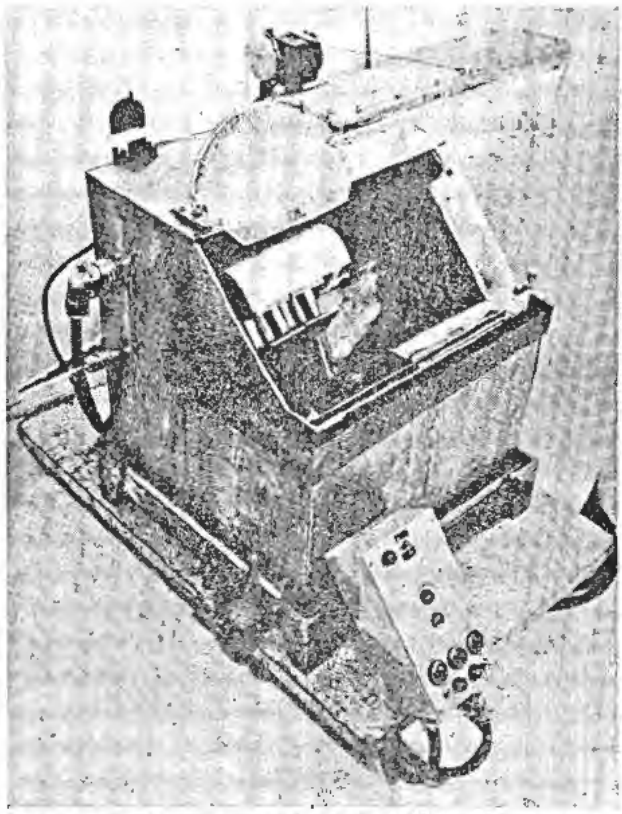

Figure 22. Remotely operated cut-off machine and its controls

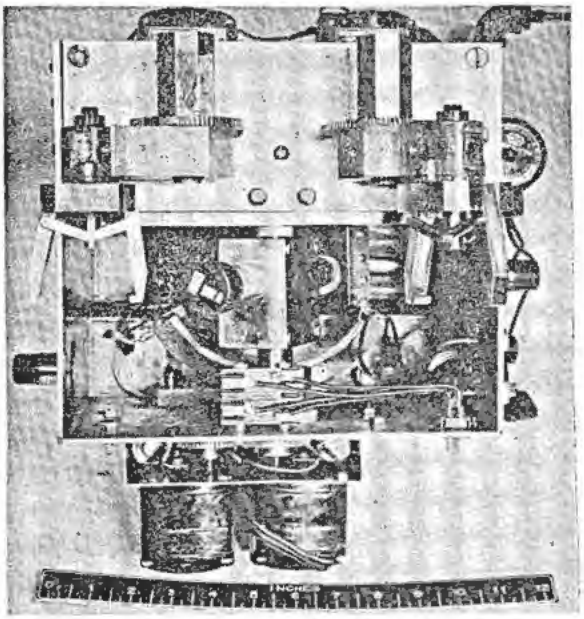

Figure 23. In-cell portion of ultrasonic specimen cleaner

transducers (barium titanate) and a simple transporting mechanism. The more complex components, the generator, the still, the reservoir and the pumping system, are all outside of the cell and easily accessible for maintenance. Figure 23 shows the in-cell portion of the ultrasonic cleaner. At the upper right and left are the fingers for placing the contaminated sample on the magnet and for removing the cleaned sample. In the center are shown the rotating magnets with samples in place. In the tank the two transducers at right angles can be seen.

The tank and transporting mechanism for the ultrasonic cleaner were designed for modular construction. That is, the unit is made up of four to five parts, each of which accomplishes a specific operation. In case of mechanical failure the inoperative portion can be quickly removed and replaced by a duplicate part. Maintenance can then be performed outside of the cell which allows for a minimum of personnel radiation exposure. The basic idea of modular construction is being utilized in all new equipment going into the metallographic process.

Following the lapping operation the samples are subjected to three stages of polishing. Diamond abrasives of 6–12 micron, 1–6 micron, and 0–1 micron are used. An adaptation of a standard cloth covered polishing wheel has been made. A rotating turret, placed eccentrically to the polishing wheel, houses four samples. The samples are positioned horizontally in the turret by reason of a 0.001 inch clearance between the turret holes and the sample diameter. The samples are free in the vertical plane and are weighted against the polishing cloth by a specimen holder. The specimen holder is fitted with a permanent magnet to facilitate the removal of the specimen. Projections are machined on the upper end of the holders to impart a quarter revolution of the sample per revolution of the turret. The turret and polishing wheel revolve counter to each other. A polishing unit mounted in a section of subflooring is shown in Fig. 24. A cleaning operation is required between each of the polishing stages.

The samples, after the final polishing operation, are ready for examination. The annex to the cell has been so designed as to encompass the stage of an in-line type metallograph. Figure 25 is a sketch of the cell annex showing schematically the installation of the metallograph. The bellows and light source are outside the cell. An extension to the monocular has been added to allow for direct viewing. Stage motions and focusing controls are brought to the outside. Critical optical adjustments and objective changes are made manually through a small door in the shield.

For macroscopic inspection and general survey work a stereo-viewing system has been installed. The unit, designed by Bausch & Lomb Optical Co. to the specifications of four cooperating laboratories, is also equipped to take stereo-photographs. The optics in the in-cell leg of the periscope are made of non-browning glass. The threshold for darkening of the non-browning optical glass is approximately 10^6 roentgens. Non-browning optics for the microscope are now under test and should be available for commercial distribution in the near future.

Since no universal etching technique is available, this operation is accomplished at the discretion and ingenuity of the metallographer. A stainless lined isolated section of the annex is equipped with a master slave manipulator and is used for the various etching operations. A section of the floor of this area serves as an elevator for the quick insertion of etching solutions.

The preparation of metallographic samples utilizes nine pieces of specially designed equipment. In sequence each machine is dependent upon the successful operation of the preceding machine. Continuous operation is dependent upon an ability to maintain the machines in peak condition with a minimum of personnel radiation exposure.

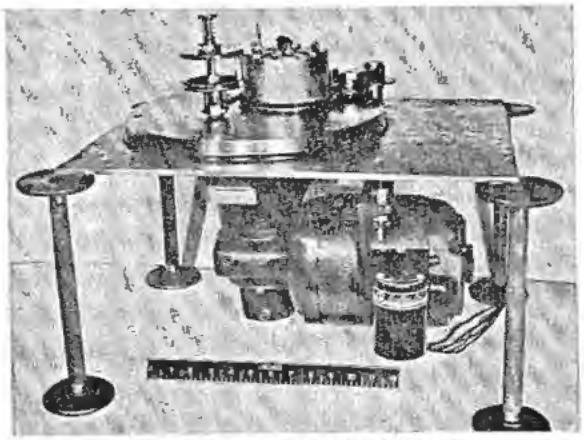

Figure 24. Remotely operated polishing wheel

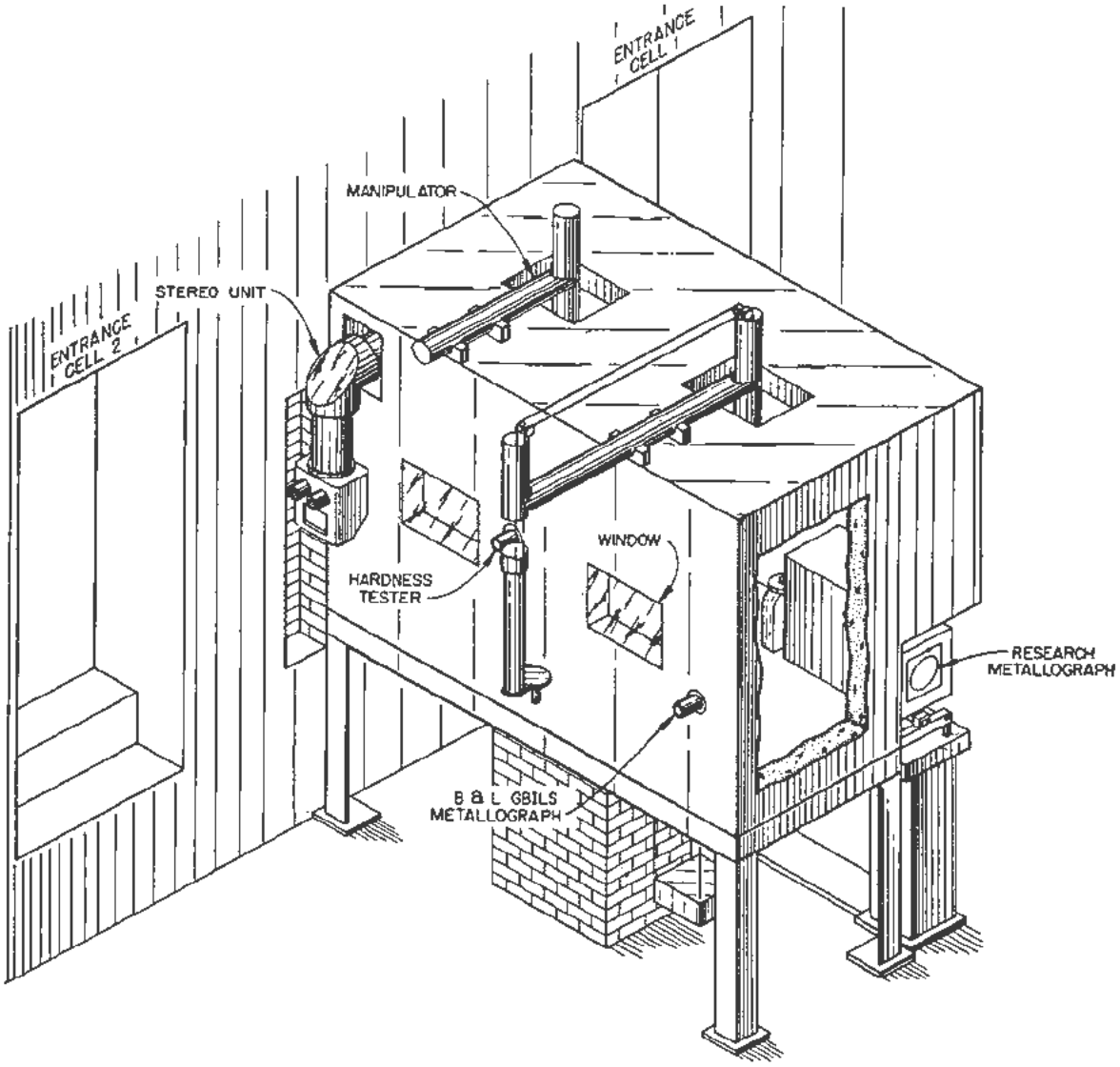

Figure 25. Schematic of cell 2A showing metallographic installation

SUMMARY

This paper has described general hot laboratory design, radiochemical laboratory design and operation, solid state hot laboratory design and operation and the specific design and operation of a metallographic hot cell. While this material represents a successful solution to the various problems, there has been no intention to represent it as the only usable approach. The basic ideas of cell design and operation presented can best serve as experience-gained guide posts in the development of the new science of the remote operation of research, development and production projects.

To date there is no "one best" approach or method to be applied to the handling of radioactive materials. Each individual operation is conceivably a multiple compromise between the optimum conditions and the economics and long range feasibility of attaining them.

REFERENCES

1. *Special Report on Hot Labs,* Nucleonics *12,* No. 11 (1954).
2. Goldstein, H. and Wilkins, J. E., Jr., *Calculations of the Penetration of Gamma Rays,* AEC Report NYO-3075, Nuclear Development Associates, Inc. (1954).
3. Tompkins, P. C. and Levy, H. A., *Impact of Radioactivity on Chemical Laboratory Techniques and Design,* Ind. and Eng. Chem. *41,* No. 2: 228 (1949).
4. Tompkins, P. C., *A Radioisotope Building,* Ind. and Eng. Chem. *41,* No. 2: 239 (1949).
5. Miller, L. F. and Kinderman, E. M., *Equipment for Remote Chemical Separations,* Nucleonics *12,* No. 11: 82 (1954). Also Ruehle, W., *Separating Trans-plutonium Isotopes from Irradiated Plutonium,* Nucleonics *12,* No. 11: 84 (1954).
6. Garden, N. B., *Control and Shielding of Isotopes in Radioactive Laboratories, Proceedings, Building Research Advisory Board,* Conf. Report No. 3, *Laboratory Design for Handling Radioactive Materials* (1951).

7. Trent, T. L. and Wallace, J. J., *Large-Scale Automatic Storage and Sampling Unit*, Nucleonics *12*, No. 11: 70 (1954).
8. Terrill, J. G., *Surfaces and Finishes for Radioactive Laboratories Proceedings, Building Research Advisory Board*, Conf. Report M-3. *Laboratory Design for Handling Radioactive Materials* (1951).
9. Dismuke, S. E., *Robot-run Tools*, American Machinists *98*, No. 8: 161 (1954).
10. Feldman, M. J., *Metallography of Highly Radioactive Metals*, Metal Progress (1953).
11. Feldman, M. J., *The Use of Ultrasonic Cleaning in the Hot Cell*, Nucleonics *12*, No. 11: 65 (1954).

Record of Proceedings of Session 8B.2

THURSDAY AFTERNOON, 11 AUGUST 1955

Chairman: Mr. O. Hahn (Germany)

Vice-Chairman: Mr. G. B. Cook (UK)

Scientific Secretaries: Messrs. J. Gaunt and A. Finkelstein

PROGRAMME

P/438 An atomic energy radiochemical laboratory—design and operating experience ..... R. Spence

P/725 Hot laboratory facilities for a wide variety of radiochemical problems ..... P. R. Fields and C. H. Youngquist

P/673 Metal research "hot" laboratory ..... N. F. Pravdjuk

DISCUSSION

Mr. R. SPENCE (UK) presented paper P/438 as follows: The radiochemical laboratory at Harwell was designed at a time when we had very little experience in the handling of large amounts of radioactivity. It is interesting now to review the operating experience over the past six years to see what lessons can be learned. As will be seen in the following slides, the building offers a variety of facilities.

Slide 1 (Fig. 2 of P/438) shows the general layout—administrative block, laboratory suites, concrete shielded area and plutonium laboratories, and a new wing which is also for plutonium and other substances.

Slide 2 (Fig. 1 of P/438) shows the layout of a single laboratory suite more clearly with the laboratory, the office and the vestibule. I do not propose to describe the facilities in any detail now as this is done in the paper; I shall concentrate more on the operating experience which we have had.

The laboratory suites were originally designed so as to give a high degree of isolation. This arrangement has been extremely satisfactory in practice, especially when an additional shoe change barrier was installed in the vestibule. I should say, of course, that one only uses this additional shoe change when it is needed. For example, there was at one stage, for a short time, more than 1000 times the maximum permissible level of alpha radiation in the atmosphere of a laboratory and the staff had to work in respirators, yet the corridor outside remained uncontaminated and the counting room, which was actually next to this particular laboratory, remained quite unaffected. This particular problem was solved mainly by the introduction of a sealed plastic bag technique for removal of active material from glove boxes in place of the older transfer chambers which we formerly used.

This plastic bag technique is quite simple. A plastic sock is attached to the box and whatever one wishes to transfer into this sock is dropped in. A high frequency sealer then seals off the end of the plastic sock, and the material can be removed without ever being exposed to the atmosphere of the laboratory. This technique is completely effective with the most troublesome materials.

Originally, the internal walls and ceilings of the laboratory were coated with strippable lacquer. This is no longer considered to be necessary as experience has shown that a good hard gloss enamel paint is quite adequate for these surfaces and that one should confine the more expensive strippable lacquers to the immediate vicinity of activity, for example, fume cupboards and glove boxes. A recent practice has been to lay down a second coat of a chlorinated rubber paint over the strippable lacquer, as this has much more favourable decontamination properties. If the contamination is really bad, then the whole thing can be stripped off.

The concrete shielded area (Fig. 1 of P/438) served its purpose very well in the early days when it was used mainly for pilot plant work, and the concrete cells were quite useful when pilot plants were located there. Now that the chemical engineering work is done in a special chemical engineering radioactive laboratory, this area is no longer used for these small plants. The chemists are much more interested in using easily operated concrete cells with good vision and good manipulation and feel that this particular kind of design is not so appropriate for their type of work. We would rather have a single open space where cells could be erected as we wished, and have plenty of room about them.

Large quantities of plutonium have been subjected to a wide variety of processes in the plutonium wing. The double row of large glove boxes are serviced from an active corridor by men wearing pressurized suits. The working area in this particular laboratory has always remained completely free from activity as far as health physics requirements are concerned, although of course there is lots of activity on occasion in this servicing corridor. We did get considerable trouble actually in the changing area of these pressurized suits, mainly due to showering and changing, but this has been eliminated by more careful operation

and particularly—most important—by having a reasonably senior supervisor to take charge of the changing operations.

Slide 3 (Fig. 3 of P/438) shows the service corridor with a man in one of the pressurized suits, and in this case it is covered also by a light plastic disposable suit. The airline also can be seen. He is in telephonic communication with the controller and with the other people who wish to speak to him. The rear of one of the large alpha boxes is visible; it has a removable hermetically sealed back.

A new wing was added to the building about two years ago, when it was decided to install another kind of facility and to use mobile glove boxes which could be bolted to a panel in the wall of a central decontamination room for active servicing.

Slide 4 (Fig. 5 of P/438) shows one of the mobile boxes, which is normally free-standing. Here, for purposes of removing contaminated equipment, it is bolted to the panel which will take any of a number of sizes of these boxes up to the full size of the panel. These can be successfully serviced from the decontamination room without any activity getting into the main laboratory.

Slide 5 (Fig. 6 of P/438) gives a general view of this particular laboratory. All sorts and sizes of boxes can be seen about here. At one end they are mainly metallurgical equipment—lathes, etc.—and at the other end contain chemical equipment of various kinds. All the services, as in the rest of the building, come from the roof; there is nothing on the floor. We find this very successful. The boxes are all mobile and by and large of course they are meant for rather more permanent equipment—not things that you are going to alter every few minutes.

On the basis of the experience we have had in the older plutonium laboratory it was felt that no special ventilation was necessary in this working area other than that normally required for a public building – that is about eight to ten air changes per hour—and this meant only a small addition to the ventilating plant of the main building. So far this has worked perfectly satisfactorily.

The ventilation system of the main laboratory, of course, is very large, elaborate and expensive to run. At one time it was thought that with the increasing use of glove boxes one might do with less ventilation but experience has been that the demand for air has remained approximately constant, because it was found that one can make great use of fume cupboards if they are there and if they are well ventilated because of the saving in time. We still find therefore that this ventilation system is fully used and is very valuable. Filtration of the air is carried out through precipitrons both for input and for exhaust air, and we do not find that these are particularly efficient. However, if you went to an alternative filtration system you would then have a disposal problem to deal with, so whilst we are not terribly satisfied with precipitrons we think that probably we might not be very much better off with other alternatives.

The Health Physics Division has set limits to the activity in the exhaust air from the building. These are 75 microcuries of alpha activity and 75 millicuries of beta activity per day from the stack. Normal emissions correspond to much less than one-tenth of this quantity but on one or two occasions at any rate these limits have been exceeded by a factor of two or three and in each instance the incident could be traced directly to a particular operation of the laboratory. Contamination of the ventilation ducting has been negligibly small, probably on account of the very large dimensions of the ducting. This is no doubt very expensive to install but it does offer a very great advantage to the staff of the laboratories in that the noise level is extremely low. Systems with a centralized exhaust such as this one are rather inflexible. When more air is required in a particular laboratory, a considerable effort is required to readjust and rebalance the ventilation system in the other laboratories. In our experience, however, such changes have been made relatively infrequently. As a measure of economy the incoming air temperature is reduced by 5.5°C and the flow velocity is also reduced outside of normal working hours. This represents quite a saving in steam.

The system of segregating liquid effluent into uncontaminated process water and contaminated effluent has worked very well. The process water is diverted actually on the working bench. There is an orifice on the bench into which the tube from the condenser can be inserted, the orifice being constructed in such a way that nothing else can be poured down it. Unacceptable contamination of this process water system has been found not more than three or four times during the six years of operation. It is quite a nuisance when it occurs because the delay tanks for the process water hold 20,000 gallons and to move this by tanker is troublesome. Although it has only happened two or three times in six years, we have nevertheless made an effort to cut down the water used in the laboratory by introducing small circulating systems which are equipped with a fan-operated cooler, and in this way the water usage in the building has been reduced from about 400 gallons per man per day some years ago to about 115 gallons per man per day now, and we hope to reduce this still further and to simplify the effluents from the building by local introduction of absorption units, evaporators and solid waste treatment. If we do this, it will be an experiment with local effluent treatment to compare with central effluent treatment which we operate on the station at the moment.

There has been a number of minor incidents in the laboratories and I thought you might like to hear what they have been. Fortunately, we have had no serious accidents. The greatest working hazard has always been the ingestion of alpha active material through the lungs. The maximum permissible levels of radioactive species in the air have been exceeded on several occasions and each of these has been very carefully monitored and controlled by the Health Physics Division. Urine analysis—and I should say

that in the ultimate urine analysis is almost the only check you have for many of these alpha activities—have revealed the presence of small amounts of plutonium and other materials in a few individuals, but this has never exceeded the tolerance level.

We had a good deal of trouble at one time through "fume-offs." This was due to organic solvents and aqueous residues containing high nitric acid concentrations which were allowed to stand in the effluent vessels at various awkward places so that you would get nasty contamination quite unexpectedly owing to the sudden "fume-off" of this liquid. It is now a rule of the laboratory that the contents of all such effluent vessels shall be adjusted to neutral, and since this rule was instituted there have been no further "fume-offs."

There have been several fires in the glove boxes and, while none of them has had serious consequences, we have investigated each one very carefully because a general conflagration in a building containing as much plutonium as this would be highly undesirable. In one particular case, a fire was started by an electric motor, and in another by a glass-blower's torch, but in neither instance was there an escape of plutonium from the box, even where there was more than 100 grammes present in the box, and when the filter had actually been blown off its housing. This was very fortunate and certainly rather remarkable, but it does point to the need for fire precautions in laboratories of this type, because a general fire might seriously contaminate — and dangerously contaminate — the neighbourhood.

The important lesson to learn here is that there must be a reliable system for checking fires in plutonium laboratories at the earliest possible moment, and that the laboratories should be of such a nature that the rapid spread of fire is difficult. The buildings at Harwell are of brick, steel and concrete construction with a plaster interior. The paints and lacquers have been tested for inflammability—this point is always worth looking into. We have also obtained a stock of non-inflammable plastic window material to use in glove boxes where it is considered that the fire risk might be very serious. As a further precaution wooden bench and office furniture in the plutonium laboratories has been replaced by steel. We also have installations for flooding the laboratories or dry boxes with inert gas such as CO_2 or argon. Another point is that one should have a good alarm system which should be clearly audible to all those working in the area involved. This, by the way, is not always the case. It is quite difficult to make sure that your alarm system is audible to everyone working in the building. We have only one general alarm for the whole building and when this is sounded, either for an incident inside the building or for a site incident, staff vacate the laboratories and collect in the administrative area.

There is also a local alarm in the two large plutonium laboratories which is sounded when there has been a serious spill or an outbreak of fire. These alarms, in our experience, should not be of such a nature that they can be easily accidentally operated. In the early days of this laboratory and others I know of, the alarm sounded accidentally quite regularly and the staff became quite immune to alarms.

Changing facilities in a building of this sort are most important and we have always tended to underestimate the need. Not only has the scientific staff expanded but the growth of the industrial staff to its present level was entirely unforeseen. New changing rooms have had to be built therefore for industrial staff in the courtyards of the building, over the effluent delay tanks.

The changing requirements for the scientific staff have been kept as flexible as possible. The minimum requirements are that laboratory shoes or shoe bags be worn in corridors and offices and that laboratory coats be worn in the laboratories. Staff working full time in the laboratories, especially with hazardous materials, usually change completely. This flexible system allows visitors to be taken into the laboratory without a great deal of fuss. But in the earlier days we used to provide visitors with rubber overshoes, and I have been to other laboratories where shoes have to be put on, and this is very inconvenient.

The poor visitors usually shuffle or limp around the building and they are quite unable to take an intelligent interest in what they see. The introduction of cotton shoe bags with canvas soles and elastic tops big enough to go over the largest shoe has entirely eliminated this trouble and should any of the present audience visit the Harwell Laboratory, I think at least they will have comfortable feet.

Mr. W. M. MANNING (USA) presented paper P/725 as follows: Many types of chemical problems have been successfully handled in the shielded caves at Argonne National Laboratory. Work undertaken in these caves has included, for example, the processing of plutonium intensely irradiated with neutrons to produce the heavier elements 95 through 100, by the series of steps outlined by Mr. Ghiorso earlier. Another example is the processing of cyclotron target materials. The caves may be divided into three categories: first, thick-walled large caves capable of shielding 10,000 curies of gamma activity, that is, with an average energy of 1 Mev. Secondly, intermediate caves which can shield up to 100 curies of 1 Mev gamma activity; and finally, the low-level caves or junior caves, as we usually refer to them, which can shield about 1 curie of activity.

Slide 6 (Fig. 1 of P/725) shows a high level metallurgy cave. This has been used, as the name suggests, almost exclusively for metallurgy operations and only slightly for chemical operations. This cave has interior dimensions of approximately 3 meters in length, a depth of 1.9 meters and a height of 3.8 meters. The walls consist of 9/10ths of a meter of dense concrete. The windows are of about the same thickness but consist essentially of a nearly saturated solution of zinc bromide with a specific gravity of about 2.5.

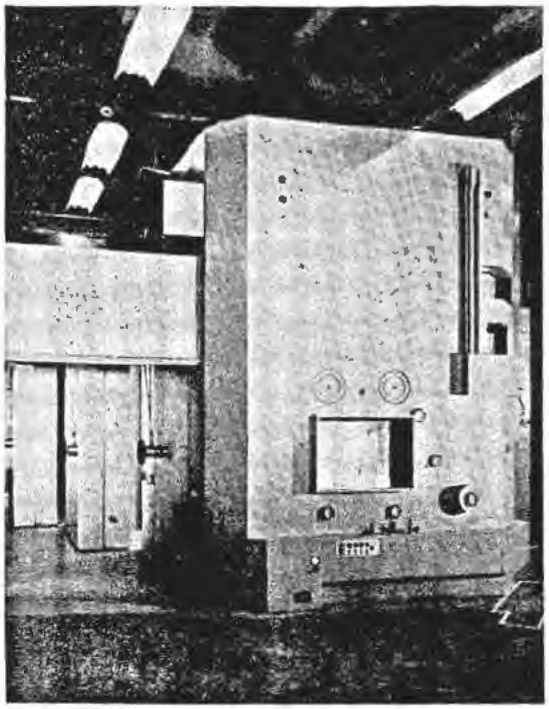

Slide 8. Access doors in 3 cell cave

There are numerous ports around the cave, in various positions, to permit the insertion of a variety of different service leads into the interior of the cave and master-slave manipulators are used for work in the cave.

Slide 7 (Fig. 2 of P/725) shows another intermediate level, metallurgy cave which is designed to permit work with up to 100 curie of activity and has three sets of master-slave manipulators. This cave has three separate cells. The exterior walls are again of dense concrete, about 6/10th of a meter thick, and the windows are of an equivalent thickness of zinc bromide.

The dimensions of each cell approximate a width of 2.2 meters, a depth of 1.9 meters and a height of 3.8 meters. The partitions between the three cells consist of about 20 centimeters of steel. These partitions are in two parts in each case, with the upper half of each partition movable so that the master-slave manipulators can be moved along through the slot from cell to cell.

Slide 8 shows simply a different view of the same cave taken from the side and rear, and one can see an end window and, at the rear, three access doors which can be drawn back to permit the assembly of equipment inside the cell prior to an operation. The loading of samples into this cave is through special ports in these rear access doors.

Slide 9 (Fig. 4 of P/725) shows another type of intermediate level cave designed for work up to approximately 100 curies of activity. This is a cave which has been used almost exclusively for chemistry operations and was built a little earlier than the other caves. Here the length of the entire cave is about 6 meters. The depth is about 1 meter and the height is about 2½ meters. The shielding is about 15 or 16 centimeters of steel. The windows in this case consist of laminated plate glass with a total thickness of 56 centimeters. The access doors do not show in this particular picture, but there is one at each end and there are four access doors in the rear of the cave, their positions roughly corresponding to the windows in front. At the right end of the cave there is a loading lock with access in the rear, which is used for loading or insertion of the hot samples and which is also used very frequently for the removal of analytical samples during operation with hot materials.

The manipulator here is not of the master-slave type but an electrically driven rectilinear manipulator. The control panel may be seen also. The operation of the manipulator is quite similar in principle to that of a fairly refined crane. The control panel is portable and can be moved to any position along the front of the cave.

At this point I would like to interrupt the description of the facilities to give two examples of chemical operations to illustrate the use of this particular cave. One example of an operation which has been carried out several times successfully in this cave is the processing of plutonium samples which had been irradiated in the Materials Testing Reactor to produce the heavier transplutonium elements.

These particular samples contained from 200–300 milligrams of plutonium-239 and generated several kilowatts of heat when placed in the reactor thermal flux of 3×10^{14} neutrons per square centimeter per second. Hence, the plutonium was dispersed in aluminum to permit adequate heat removal during the first stages of irradiation. At this high flux, the heat generation rapidly diminishes with time because most of the fissionable material is burnt up within the first couple of months. A sample like this, when returned to Argonne after an irradiation for several months and a transportation period of two or three days, may show gamma activity approximating 3×10^5 roentgens per hour. Alpha activity of the sample, due primarily to curium isotopes, may approximate one curie. The operations carried out in this cave are as follows:

First, treatment with concentrated sodium hydroxide to dissolve the aluminum with which the plutonium is alloyed. This leaves an insoluble residue of most of the fission products and all of the heavy elements. This residue is centrifuged. The centrifugate is then dissolved in concentrated hydrochloric acid and this solution then passed through a resin exchange column which serves to adsorb and remove the plutonium, still permitting most of the fission products and the heavier transplutonium elements to pass through. The eluate from the column is evaporated, dissolved in dilute hydrochloric acid and then passed through an ion-exchange column and elutes with concentrated HCl, a technique developed at Berkeley which serves to separate the remaining fission products almost completely from the plutonium elements. This

series of operations can be carried out, in a cave like the one which was shown, in a period of two to three days of almost continuous operation, when things go smoothly. The decontamination obtained by this series of operations is sufficient to bring the initial level of 3×10^5 roentgens down to a final level of 1 roentgen per hour. This is low enough so that further operations can be carried on with only minor shielding.

Another type of operation in this same cave posed a different problem. This was the processing of a sample of 30 grams of radium which had been irradiated in a reactor for several months to produce a number of milligrams of actinium-227. Here the particular problem posed was the constant and considerable evolution of radon gas from the 30 grams of radium during the entire processing operation. This problem was overcome by the use of Lucite boxes around the individual pieces of equipment in the cave. Air was pulled through each of the boxes and then passed over cold activated charcoal to freeze out the radon before this air was passed through the usual filters and up the 30 meter stack which is used in connection with this laboratory.

Slide 10 (Fig. 10 of P/725) shows a close-up of part of the same hot cave. The jaws of the rectilinear manipulator can be seen. The particular operation is the changing of collection tubes under a moderate size resin column inside the cave. It will be noted that trays are routinely placed under the equipment in this cave to catch solutions in case of spills.

Slide 11 (Fig. 6 of P/725) shows a low-level cave, which is referred to as a chemistry junior cave designed for work with about one curie of activity. This cave is a type which can be installed in a standard chemistry laboratory. Here, again, master-slave manipulators are used. This particular cave is about 1.6 meters in width, 9/10ths of a meter in depth, and 1.2 meters in height. The shielding material is 12 cm of steel or an equivalent thickness of lead glass.

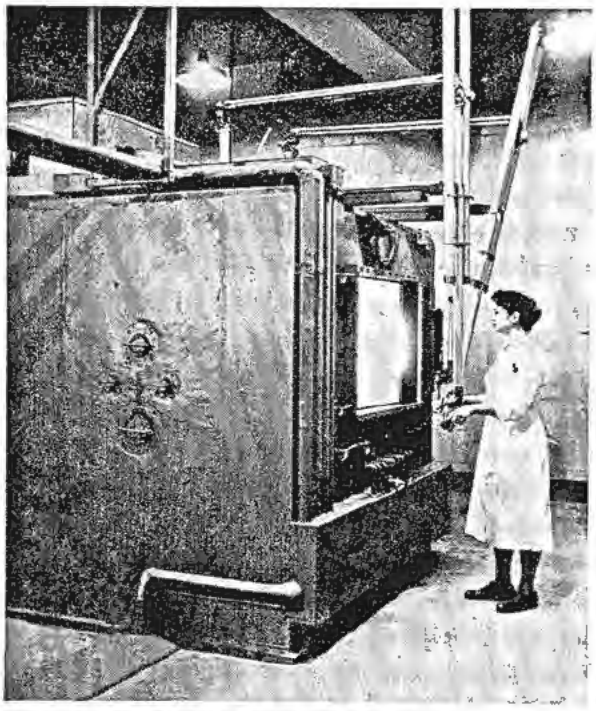

Slide 12. Junior cave made of dense concrete

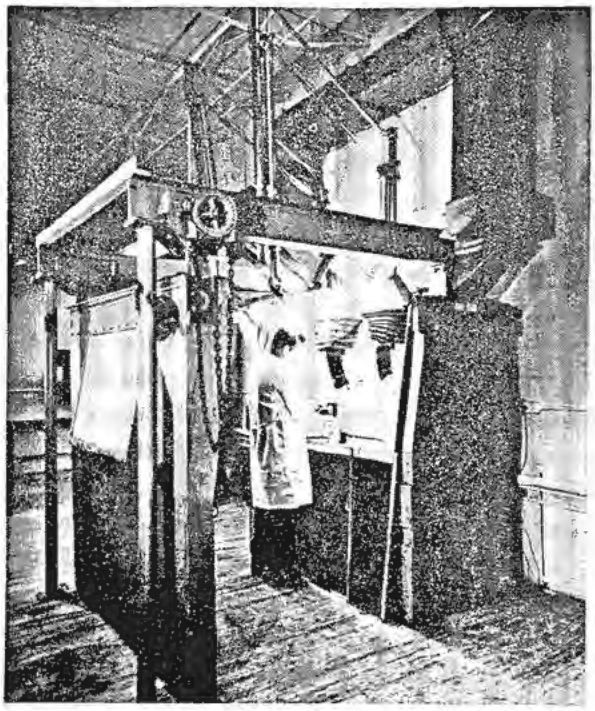

Slide 14. Erecting apparatus in junior cave

Slide 12 shows another type of junior cave made of dense concrete instead of steel shielding, resulting in a bulkier installation. It would not be very suitable for installation in a standard laboratory room.

Slide 13 (Fig. 7 of P/725) shows a standard Argonne laboratory hood, with a steel shield which can be moved in front of the hood to convert it into a kind of junior-junior cave. Shielding can also be placed at the sides of the hood. It will be noted that the manipulators, which are the ball-joint type, are much simpler than the master-slave manipulators but are less versatile.

Slide 14 shows a junior cave shown with the front shield pulled out to permit the erection of apparatus in the cave and showing the inner working arms of the master-slave manipulator.

Slide 15 (Fig. 5 of P/725) shows a junior cave with the front shield slid a little to one side to permit the insertion and unloading of a hot sample. It will be noted that the operators still have most of the shielding while carrying out this operation. This is good for working with samples of moderate activity.

Slide 16 (Fig. 8 of P/725) shows a glove box which is excellent for work with high levels of alpha activity where there are negligible levels of gamma activity. This is another type of box developed at the University of California Radiation Laboratory. Notice

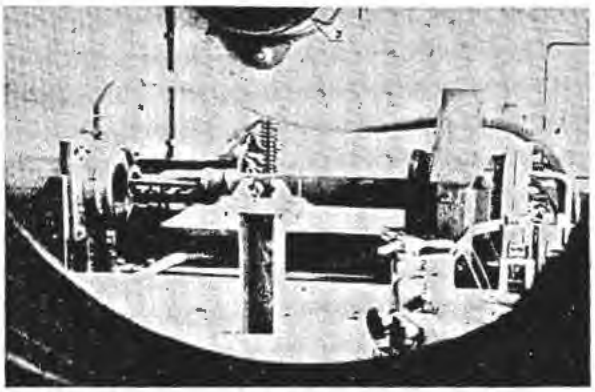

Slide 19

the loading port or air loft through which alpha samples can be put into the possibly highly contaminated interior and later taken out without any appreciable danger of introducing contamination into the laboratory atmosphere. Air is exhausted from the back of this glove box through a pre-filter at a rate of approximately 600 liters per minute and then passed into the regular laboratory and out through the standard filters of the laboratory exhaust system.

In spite of such hazardous operations as the dissolving of active materials, centrifugation and evaporation, as well as the problem of radiation-induced water decomposition, we have experienced only minor amounts of contamination outside the caves as a result of work inside the caves, and there have been no serious mishaps to personnel. The closest to a serious mishap which we have had resulted not from planned working with alpha emitters, but from the unremembered presence of contaminated forceps inside one of the regular laboratory hoods. A worker was reaching in with gloves to move a lead brick or something of that nature and brushed against the sharp point of the forceps, which penetrated the glove and the outer skin. The activity was due to a sample of thorium-227 and quite a considerable amount of activity was found in the blood stream. We were concerned at first because if the sample had not been rather well freed from the parent actinium-227, this material would have remained at a high enough level to give some concern about the health of the person over a period of years, since the long-lived actinium parent would have maintained the short-lived daughter. Fortunately, the activity had been almost pure thorium-227 and decayed rapidly to a safe level inside the worker's body.

Mr. G. B. ZHDANOV (USSR) presented paper P/673 as follows:

The metal-research "hot laboratory" is used for studying the changes which take place in the structure and in the physical and mechanical properties of various structural and fissionable materials irradiated in reactors.

Highly radioactive substances are investigated in a number of "hot" cells separated from the observer by a sufficiently thick shield of cast iron and concrete.

Slide 17 (Fig. 1 of P/673) shows the layout of the metal research "hot laboratory."

The chain of cells begins with the "hot machine shop," where there is a special metal-cutting machine used to produce samples for various metallographic, physical, and mechanical tests.

Slide 18 (Fig. 2 of P/673) shows the inside of the "hot machine shop" cell, and Slide 19 shows the milling machine in greater detail. Slide 20 (Fig. 3 of P/673) is a view of the operator's room of the "hot machine shop."

The "hot machine shop" cell is connected with the distribution cell where radioactive materials are stored and from which they are supplied to the different research cells. The "hot machine shop" cell and the distribution cell are designed for work with materials with an activity of up to 50,000 curies and are equipped with mechanical master-slave manipulators and mirror-viewing systems.

The distribution cell of the metal-research "hot laboratory" is connected with the research cells by a transporter on which active material is transferred to the cells. Slide 21 shows the transport corridor seen from inside, and the entrance to the cells.

All the research cells of the metal-research "hot laboratory" are designed for work with materials having an activity of up to 20,000 curies. Each research cell is equipped with manipulators and lead-glass viewing windows.

Specimens and replicas for examination by electron microscopy are produced in the metallographic examination cell, where the specimens are examined and photographed by means of a remote-controlled metallographic microscope.

Slide 22 (Fig. 4 of P/673) shows the photo-camera of the microscope; the microstructure of the active specimen under examination can be clearly seen.

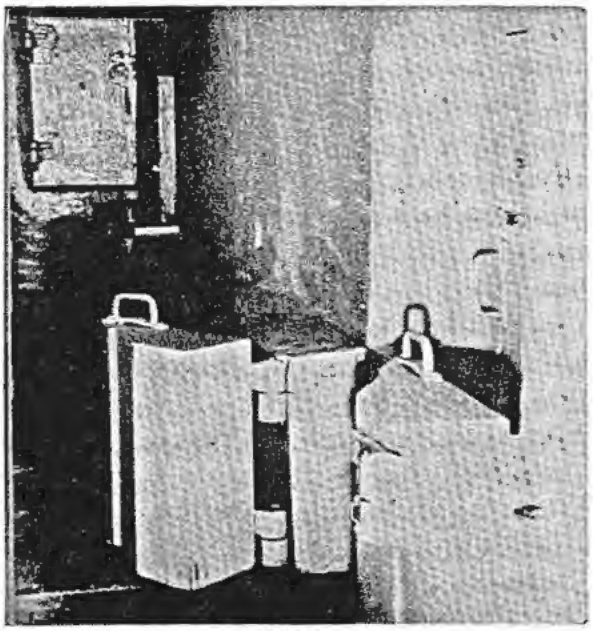

Slide 21

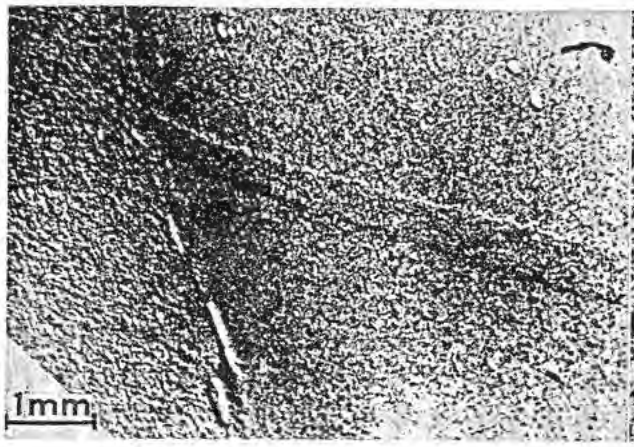

Slide 23

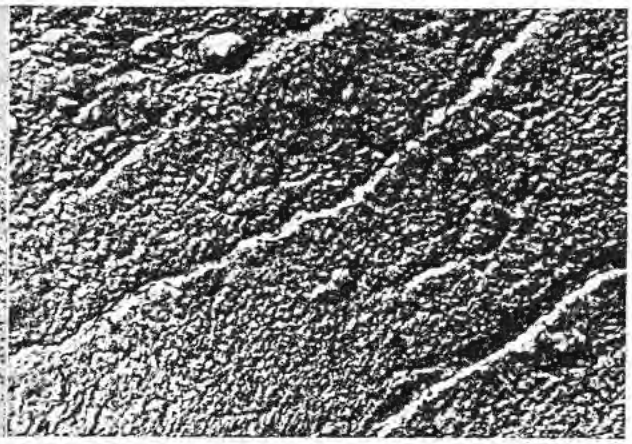

Slide 24

Plastic replicas are prepared from active samples in the "hot" cell (the method used is more fully described in the paper) and subsequent treatment of the non-active replica makes it possible to carry out the metallographic and electron-microscopic examination of the active materials by conventional methods in "semi-hot laboratories."

Slides 23 and 24 show electron-microphotographs of non-irradiated and irradiated uranium.

The two physical measurements cells contain equipment and apparatus for studying the various physical properties nf irradiated materials, including electrical and thermal conductivity, variation of emf with temperature, density and thermal expansion. Dilatometric and X-ray analysis can be undertaken and Young's modulus of elasticity and the modulus of internal friction can be measured. One of the cells (Slide 25, Fig. 8 of P/673) is equipped with a television viewing system and rectilinear manipulators.

Slide 26 shows the interior of one of the physical measurement cells and the vacuum electric furnace for the thermal treatment of active materials.

One of the cells contains X-ray equipment based on the "Norelco" X-ray spectrometer, shown diagrammatically in Slide 27 (Fig. 10 of P/673).

The X-ray beam diverging from the focal spot of an X-ray tube falls onto a flat specimen of the active material which is being studied; the radiation scattered by the specimen is focused onto the entrance slit, reflected by the curved crystal monochromator and detected by the counter. The roentgenogram is automatically recorded in the range from 15 to 45 degrees Bragg angle, or the diffraction lines counted by a mechanical counter. Lead screens protect the counter from radiation from the specimen but they do not cut off the X-ray beam which is to be detected. Materials with an activity of up to 50–100 mc can be studied with this equipment and its geometry is such that the thickness of the lead shielding screens can, if necessary, be increased by 130 per cent for work with specimens having a higher radioactivity.

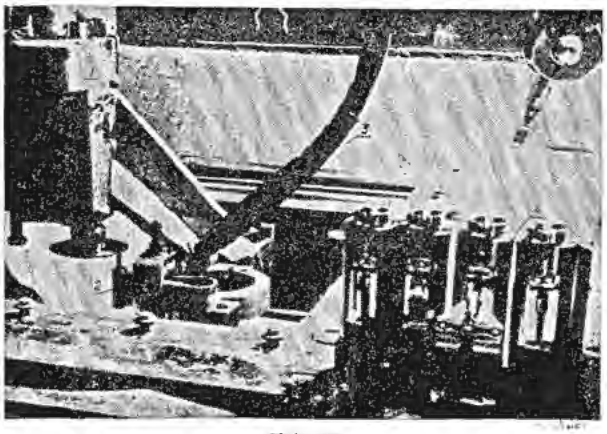

Slide 26

One of the physical measurements cells contains equipment for measuring internal friction and Young's modulus of elasticity. With this apparatus Young's modulus of elasticity can be determined for non-irradiated and irradiated materials by measuring the frequency of the forced transverse vibrations in the specimen; internal friction can be determined by measuring, in addition, the amplitude of the resonance curve.

The equipment consists of a device for starting and stopping vibrations, an amplifier, an electronic oscillator, an oscillograph, a cathode voltmeter and a counting device.

The effect of irradiation on Young's modulus of elasticity and on internal friction is studied by a process of comparison, that is to say the same specimens are measured before and after irradiation. A special form of specimen (Slide 28, Fig. 13 of P/673) has been used to ensure that the measurements can be duplicated exactly. In the case of non-ferromagnetic specimens, magnetic riders for starting and stopping the vibration are attached.

To give an example, Slide 29 (Fig. 14 of P/673) shows the results of measuring the internal friction of aluminium irradiated by a neutron flux of 1.49×10^{19} n/cm^2 at a temperature of 20°C. The logarithms of the tension caused by the amplitude of vibration (o) are plotted on the abscissa and the internal friction ($1/Q$) on the ordinate. The curves numbered "1" and "2" are,

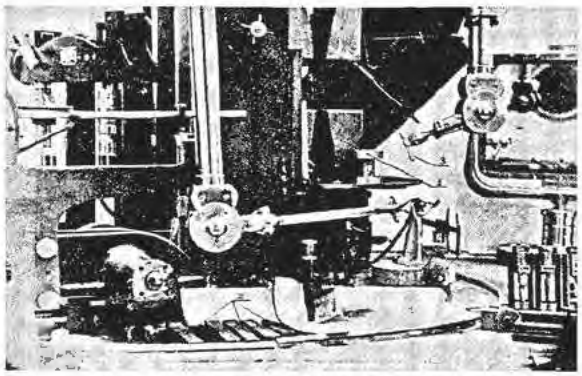

Slide 31. A five-ton combined testing machine

respectively, the curves for the substance before and after irradiation.

The results show that the critical sheer stress value (designated by the letter K on the graph) increases from 30 gm/mm² to 1200 gm/mm², i.e., by 40 times.

The mechanical properties of irradiated materials are studied in the mechanical tests cell (Slide 30, Fig. 9 of P/673). The testing machines and instruments are mounted on a revolving stand and on two movable trolleys.

The following slides show some details of the mechanical machine shop and were taken through the window in the operator's room. Slide 31 shows a five-ton combined testing machine. Slide 32 shows a 10 kg impact testing machine and a "Rockwell" hardness tester. Slide 33 shows the machine for testing irradiated specimens for fatigue. Slide 34 shows in operation the remote-controlled instrument for measuring the microhardness of radioactive specimens. The imprints of the diamond pyramid on the specimen can be clearly seen. The microhardness test performed by this instrument is similar to that performed by the Vickers tester. All the instruments for the determination of microhardness by remote control are located on the control desk in the operator's room.

All the operator's rooms in the metal-research "hot laboratory" are connected, as already stated, with corresponding "semi-hot laboratories" used for work with low-activity samples, preparatory work and the development and testing of new methods.

DISCUSSION OF PAPERS P/438, P/725 AND P/673

The CHAIRMAN: There is a question by Mr. G. Jenssen (Norway) for Mr. Spence.

Do you have a continuous inspection by health physicists in the laboratory, and what is the ratio between health physicists and other personnel in your laboratory?

Mr. SPENCE (UK): The Health Physics Division has an office and laboratory in the building and it maintains a team of about three or four people who constantly monitor the building. If one has a particularly hazardous operation, then one or two more people may be specially drafted for that particular operation. This gives a ratio of about one health physicist to about twenty-five scientists.

The CHAIRMAN: Another question for Mr. Spence comes from Mr. W. M. Manning (USA): Since you have considerable experience with your facilities, are there some design features that have given you trouble? How would you change the design if you were to build another facility?

Mr. SPENCE (UK): I think that we would like to have a more open structure in the area for high gamma activities. I believe that is rather certain. The present one is built on the ideas which were current in 1945. They tended to give a somewhat maze-like structure with substantial internal concrete walls. We would not, I think, do that to-day. We would rather build a large and very much cheaper open hall, with a very strong floor, and put in whatever equipment we required at the time. A similar type of laboratory has been built at Harwell by the Chemical Engineering Division.

The CHAIRMAN: We have a question from Mr. G. N. Walton (UK) directed to Mr. Manning: It is not easy to construct a manipulator that operates into a completely sealed shielded box or cave. Has it been necessary in your experience to operate extensively inside completely sealed-up boxes with master-slave manipulators?

Mr. MANNING (USA): I shall answer part of that question and then I might refer part of the answer to Mr. Goertz. In general we have not done work with extremely high levels of activity. We have always relied on having rather substantial ventilation pulling air into these large caves. I believe that the plan is always to have air flowing inward, even when the working doors are open, at a velocity of 60 or 70 centimeters per second.

Would Mr. Goertz care to make some comments on the way one might design these manipulators to go into a completely closed box?

Mr. R. C. GOERTZ (USA): We shall describe in another paper a manipulator which will work in a junior size cave and also one that will work in a high level cave, which may have the slave-arm completely booted with a synthetic or plastic boot. In this way the contamination can be completely controlled.

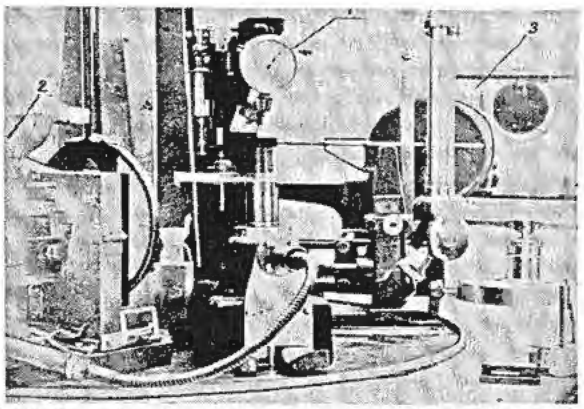

Slide 32. A 10 kg impact testing machine and a "Rockwell" hardness tester

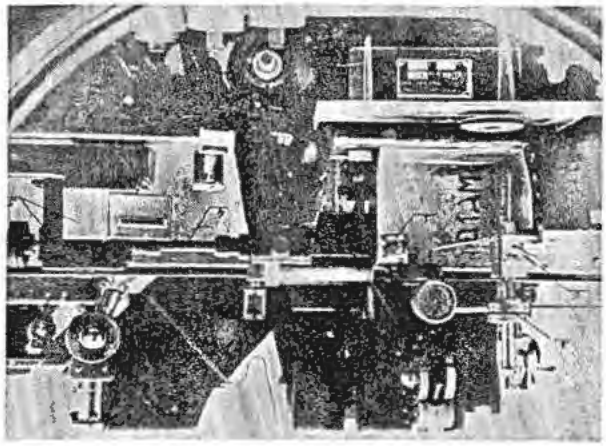

Slide 33. The machine for testing irradiated specimens for fatigue

The CHAIRMAN: There is another question for Mr. Manning submitted by Mr. Spence: Can Mr. Manning state what is the experience of the ventilation equipment in the Argonne radiochemical laboratory?

Mr. MANNING (USA): We had a somewhat complicated installation in the first place in order to conserve conditioned air, including, among other things, multiple exhaust units for each module of the building. The idea was that only one fan and blower should be going until the demand called for others to go on. At first we were troubled with suck-backs into the laboratories, especially when there were high winds outside, as a result of a lag in the motor turning on when additional airflow was required. This was overcome by having all of the motors operating continuously—the blowers operate but ordinarily just draw air from the attic, and a damper swings over when the demand is for conditioned air from inside. Aside from that, our only difficulty was with an inadequate over-all level of ventilation as a result of last minute economy cutbacks below the plenum level. These cutbacks are being rectified in changes that are taking place now. The original design level will, we are sure, be very satisfactory when the capacity is brought up to that level.

The CHAIRMAN: The next question for Mr. Manning from Mr. G. B. Cook (UK) reads: In the operation of a master-slave manipulator in the junior type cave, does not the distance away that the operator has to stand from the cell interfere with small scale chemical manipulation?

Mr. MANNING (USA): I wish that Mr. Fields, who has done a great deal of this type of work, were here to answer that question. It is my impression that one can really get up to about as close to the front of the cave as one might wish and that the manipulator arms have a flexibility. Is that correct, Mr. Goertz?

Mr. GOERTZ (USA): The manipulators that are used in the junior caves have a fixed distance between the handle and the tongs, and therefore the operator is forced to stand a certain distance from his work. This is generally not objectionable for the junior size caves, because the cave is shallow and the walls are fairly thin. Generally, lead glass is used to keep the window thin. With larger caves, I think that you have seen in a US exhibit a manipulator which has the slave arm whose distance may be changed from the master arm so that the operator may stand closer to his work to aid in viewing.

The CHAIRMAN: The next question for Mr. Manning from Mr. J. M. Lavigne (Canada) reads: What is the life of the zinc bromide solution when exposed to radiation?

Mr. MANNING (USA): I should like also to refer that question to Mr. Goertz. I shall make the preliminary remark that I believe that with hydroxylamine as a stabilizer, in the lower level caves, the lifetime is indefinite. I believe that there is a limited duration with the very high activity levels and one only needs to replace the solution occasionally.

Mr. GOERTZ (USA): I am not the best authority on this but the hydroxylamine is a reducing agent which is added to absorb the free bromine which is liberated when the solution gets irradiated. One can stand considerable amounts of radiation by adding additional hydroxylamine hydrochloride. I do not know exactly how much this would be, but I would guess the limit would be 10^{10} or more incident radiation.

Mr. V. N. KOSIAKOV (USSR): Mr. Manning, I would like to know whether other methods are used for eliminating hazardous gases which might be formed from the decomposition of water when working with high level alpha activity.

Mr. MANNING (USA): I hope that I succeed in answering this question. Ordinarily the air which comes out of these large caves is passed through a series of filters and then disposed of. This physical filter, I believe, has sufficed for trapping most activities except the radon gas which is trapped, as described, by condensation. We have not used catalysts to inhibit gas formation in resin columns. I do not know whether it would be possible to do so.

The CHAIRMAN: Now we have a question from Mr. Goertz of the United States to Mr. Zhdanov:

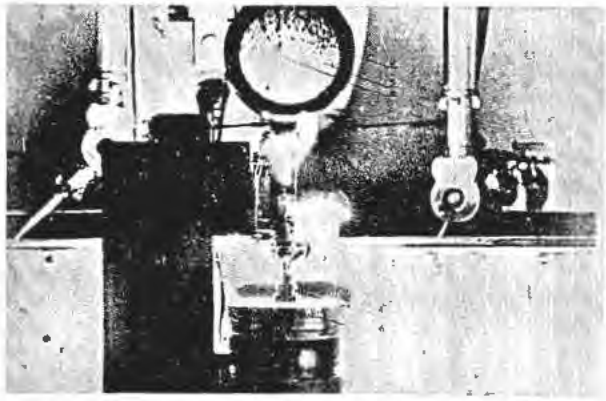

Slide 34. The remote-controlled instrument for measuring the microhardness of radioactive specimens, in operation

Is the cell designed to handle high-level alpha activity as well as gamma activity? If so, what methods are used to control alpha contamination?

Mr. ZHDANOV (USSR): All these cells are designed for work with high gamma activity.

Mr. SPENCE (UK): I would like to ask Mr. Zhdanov whether he uses glass objectives in his microscope for this high flux gamma radiation, or whether he uses plastic or a special glass?

Mr. ZHDANOV (USSR): Objectives made from ordinary glass are used.

Mr. GOERTZ (USA): My question is to Mr. Zhdanov. Can you give us approximately the physical size of your facility, and can you also tell us if the lead glass has any radiation stability material added to it?

Mr. ZHDANOV (USSR): The total area of the "hot laboratory" is about 1000 m².

The cells have the dimensions 3 m × 5 m and the equipment for mechanical measurements and other equipment is of normal size.

Ordinary lead glass is used.

Mr. J. P. BAXTER (Australia): I should like to ask the representatives of the United States whether they have had any experience in the use of stereoscopic television for controlling and observing remote-control operations inside highly active caves as an alternative to the difficulty of looking through very thick windows?

Mr. GOERTZ (USA): We have not had any experience in using these stereoscopic television systems in operating conditions. We have experimented with units to anticipate times when we might need them in emergencies. The evidence that we have derived from these experiments indicates that the windows are considerably better than the television as it exists to-day.

Session 9B.1

SOLUTION CHEMISTRY OF GROSS FISSION PRODUCTS

LIST OF PAPERS

Chemical Processing in Intense Radiation Fields

By R. Philip Hammond,* USA

INTRODUCTION

The utilization of atomic energy depends upon chemical operation at every stage—fuel preparation, reactor control, fuel reprocessing, fission product separation, waste processing and disposal. Some of these operations of necessity involve treatment of highly radioactive materials, such as the separation of certain fission products in pure form for specific uses. The operation of reactors of high specific power also requires fuel and waste processing at high radioactivity levels, since inventory charges and storage facility costs make it difficult to justify long cooling periods. Both of these incentives—demand for pure fission products and economic pressure on reactor operating costs—may be expected to increase the trend toward chemical processing at the highest possible radiation intensities.

In our present state of knowledge the chemical processing of highly radioactive materials must be regarded as hazardous and costly, requiring highly specialized facilities, expensive instrumentation, and in some cases imposing severe limitations on the chemical procedures used. The "hazard" of radioactivity is a relative term and looms large at present because of unfamiliarity. As experience is gained, processes become standardized, and hazards, in the sense of unpredicted or uncontrolled failures, are reduced. Many "ordinary" chemical operations such as ammonia or explosives manufacture are equally hazardous, but once the proper precautions are understood and adopted, these operations become among the safest in industry.

From the economic standpoint, the handling of radioactive materials may be expected to become cheaper by an order of magnitude, both from the usual lowering of costs as volume is increased, and from the effects of fuller understanding, more efficient and less "over-safe" designs, and routine operation. This cost lowering will be accentuated by two effects: (1) the logarithmic effect of shielding, so that, for example, if five feet of concrete are needed for 1000 curies, six feet is good for 10,000 and seven for 100,000; (2) the better understanding of hot chemical processing will enable higher specific activities to be used, permitting the larger quantities to be handled in smaller plants. Thus, while processing at low radiation intensities is much simpler and well understood, we find that economic considerations and in some cases technical requirements insist that processing be done at the highest possible intensity.

Within the last few years several varied types of chemical operations have been carried out in the United States at high radiation levels. It will be the purpose of this paper to summarize this experience to indicate the limiting effects of radiation intensity, if any, on various types of chemical operations.

DOSE UNITS

In order to discuss the radiation sensitivity of various processes some unit of measurement for radiation energy and energy-density must be adopted. Such units as roentgens per hour per cubic centimeter and curies per gram have been widely used. However, a convenient unit for high intensity work is the watt-hour per gram, as suggested by Bruce and Cathers and others. This unit may be related to others as follows:

1 watt-hour per gram

$= 2.25 \times 10^{22}$ electron volts per gram
$= 169$ curie-hours per gram per Mev decay energy
$= 4.34 \times 10^{5}$ roentgen (air) per gram
$= 3.74 \times 10^{-4}$ gram moles per unit G value per gram
(Unit G value is one molecule converted per 100 electron volts absorbed energy)

For beta and gamma emitters the decay energy is not all deposited in the local system, and an appropriate correction must be applied. Because of neutrino recoil energy only about 0.4 of the beta energy is available, while the gamma absorption varies with the size and geometry of the system.

GENERAL OBSERVATIONS

The most important general conclusion from the experience is that effects of radiation are surprisingly small in number and influence. Chemical reactions for the most part proceed with utter indifference to the radiation. From the recent advances in understanding of radiation chemistry the effects which are observed can be readily explained, and it should now be possible to predict what radiation effects would be likely for any proposed chemical operation.

As is well known, the result of the absorption of ionizing radiation in molecular material is the breaking of chemical bonds and the forming of free radicals, ions, excited molecules, and, in solids, lattice vacan-

* Los Alamos Scientific Laboratory.

cies or "holes." In dilute solutions most of the energy is absorbed by the solvent, and the primary products formed are characteristic of the solvent rather than of the solute. For water, these are H and OH free radicals, H_2O_2, and H_2 gas.[1] In other substances the products are of course determined by the composition. The influence of the particular type of ionizing particle on the products formed has been widely studied and found to be one of degree rather than kind.

In the following discussion the types of radiation effects encountered in chemical processing are described, and in the following section the result of these effects on limiting the radiation level is given for six common separation steps.

Oxidation Reduction

The products formed in irradiated material contain equal amounts of potential oxidizing and reducing substances. These can react with any substance present which is capable of oxidation or reduction *provided the oxidized or reduced form is stable in the existing environment*. Thus, ceric sulfate solution, ordinarily quite stable, suffers reduction to the cerous state when irradiated. Ceric ion would not be reduced, however, in the presence of persulfate ion, since it would be immediately re-oxidized, and the net result would be destruction of persulfate. Chromate solutions suffer reduction by radiation, but large scale runs on radioactive barium at high intensity have been made, precipitating the barium quantitatively as the chromate. The precipitate remains stable as long as it is mixed with the mother liquor, even though the excess chromate in the solution is being slowly reduced. But if the precipitate is filtered and washed, no excess reagent remains, and the barium is rendered soluble as the chromate is reduced without replacement.

Another example of a hypothetical nature might be a solution of europium in sulfuric acid. Under intense radiation it could be hypothesized that a portion of the europium might be reduced, and immediately precipitated as insoluble europous sulfate, since both forms are stable in the environment. If there were some means of continuously drawing such a precipitate to a region shielded from the radiation, a net reaction might be obtained. Without such removal, however, a steady state would be reached with only a minute quantity thus precipitated, since the precipitate too would occasionally be disrupted by the radiation, and the freed europium would have an overwhelming tendency to return to the oxidized state.

The conclusion to be emphasized is that while radiation provides energy and local oxidizing and reducing effects, these effects cancel unless a more stable form results in one direction than in the other, or unless the reaction is irreversible. The high susceptibility of organic compounds to radiation damage is thus understood. The bonds broken will not generally re-form, and the disruption is irreversible.

The action of radiation as a promoter of only those oxidation and reduction reactions which are compatible with the environment corresponds to that of a catalytic rather than chemical agent. But its nature is that of a consumable catalyst, since the effect cannot exceed the amount corresponding to the radiation absorbed. Thus the time of exposure and the geometry of the equipment become important factors. If a sensitive precipitate which is not itself the main source of radioactivity can be quickly formed and removed from the bulk of the solution, a large portion of the radiation attack may be avoided and a successful result obtained. A protective effect can also be obtained by addition of a more sensitive material than the one which it is desired to isolate.

Gas Evolution

In substances in which a stable gas phase can exist upon molecular disruption, gas formation will usually be a result of irradiation. In addition to the chemical changes, gas formation may influence the success of a chemical separation process by profound physical effects such as stirring the solution, disrupting precipitates, sweeping volatile reagents out of solution, plugging filters and resin beds, etc. The control of these effects is discussed in the next section under particular unit operations.

In the phenomenon of gas evolution lies one of the principal differences in the behavior of different kinds of ionizing radiation. In pure water alpha particles and fission fragments produce mostly molecular hydrogen and hydrogen peroxide, with a net formation of hydrogen and oxygen gas, while beta and gamma rays produce a preponderance of free radicals, which tend to recombine, with very little net gas formation. Thus, water-moderated reactors having solid fuel elements experience almost no radiolytic gas formation (if the water is pure), while homogeneous reactors using aqueous solutions must contend with large quantities of explosive off-gas mixed with highly radioactive fission gases. Thus, a remote-control chemical problem at high radiation intensity is created.

The homogeneous reactor work in the United States has led to three solutions to this problem, suited to different reactor types. One solution is to use a catalytic recombining apparatus containing usually platinized alumina pellets. The gas is conducted through the apparatus at high temperature and the resulting water is condensed and returned to the reactor. Such a device is in operation on the Los Alamos Water Boiler.[2]

A second method makes use of small quantities of copper ion dissolved in the reactor solution. If the solution is operated at about 300°C or above, the radiolytic gas is recombined internally. The third approach consists of operating the reactor at such a temperature that the thermal recombination rate, assisted by the catalytic effect of uranium ion, is sufficient to control the gas formation. Reactors at Los Alamos using this method are described in a separate paper in these proceedings.

Only the first method described constitutes a real processing operation, since the other methods essentially remove the problem. It can only be reported that

after several years operation there is no observable effect of the intense radiation field (0.1 watts per cubic centimeter of gas) upon the catalyst bed.

Peptization

The peptization of solid precipitates may be related in some cases to gas formation within the crystal. Process difficulties of some magnitude may result when an ordinarily well-behaved precipitate becomes a stable colloid above some radiation level, refusing to settle, passing through filters, etc. Because of the difficulties of handling solids by remote control there are not many examples of high specific activity precipitates, but in the separation of Ba^{140} and La^{140}, precipitates of nearly carrier-free LaF_3 have been formed and collected without colloid formation at levels of 2000 curies. The estimated energy dose in this case was 230 watts per gram for 2 hours, or 460 watt-hours per gram. However, a special technique was necessary in this case to prevent peptization. The radioactive lanthanum was first precipitated as oxalate, stirred long enough to allow crystal growth, and then converted to fluoride by adding HF. The intermediate compound may have been an oxalato-fluoride. Although the oxalate was itself rapidly destroyed by the radiation, it persisted long enough to form large crystals, and the resulting fluoride found itself in large pseudocrystalline masses with less water content than directly precipitated fluoride and therefore less gel-like in nature. It is believed that this agglomerate resisted dispersion and that the lowered water content decreased internal gas formation, thus accounting for the improved results. It is probably evident that an anhydrous precipitate will be less subject to disruption than one containing water of crystallization or hydrophilic gel water.

Heating Effects

The absorption of radiation energy, of course, produces heat. In special cases, such as with plastics or other organic materials, problems may be encountered but in general the quantities of heat produced in handling radioactive materials may be removed readily by standard means. Solution operations have been done at energy inputs of 0.4 watts per gram (200,000 curies per liter) without special cooling troubles, and refractory solid precipitates have been handled at 500 watts per gram (500,000 curies per cubic centimeter).

Heating effects are mentioned here, however, to point out that the self heating may be turned to advantage in the process. One example is the evaporation of La^{140} solutions, where the external heat is turned off, and the radiation heat provides boiling without bumping and greatly speeds up the process. Another is the vacuum distillation of polonium, which provides its own heat to distill from an insulated surface to a cooled surface.

Effects on Organic Materials

The discovery of the cross-linking of polyethylene[9] under irradiation seems to have resulted in an important commercial process, but similar effects have been observed in high-intensity processing operations, usually with the most disagreeable results. In the original process for isolation of radioactive barium at Oak Ridge, use was made of a precipitation step with an ethyl ether-hydrochloric acid mixture. When the step was prolonged or repeated, or when the activity level was increased, tars and resins were produced. Subsequent tests showed that this effect was produced by about 0.14 watt-hours per gram of ether-acid solution. A destructive effect was also observed with a Versene reagent, where the destructive dose was estimated at 0.04 watt-hours per gram of Versene. No deleterious effects were observed with acetates, which leads to the supposition that only gaseous products were formed by radiation damage.

Two important conclusions may be drawn from contemplation of the effect of radiation on organic materials. One is that, without careful testing, organic reagents should be excluded from high intensity processing schemes. The other is that the free radicals resulting in organic materials upon irradiation can combine in ways unattainable by conventional methods. This use of nuclear radiation to produce useful new substances will result in an important branch of a high-intensity chemical processing industry.

Hot-Atom Effects

Hot-atom effects are those in which the particular atom undergoing a nuclear event, such as neutron absorption, fission, etc., manages to characterize itself chemically so profoundly that notice may be taken of it process-wise. The classical example is the well-known Szilard-Chalmers process. It must suffice here to merely mention this type of effect as one which may lead to rapid and unusual means for isolating particular isotopes in extremely high specific activity. Each such process would be highly specialized.

A negative version of a hot-atom process is observed with dismay in homogeneous reactors whose corrosion resistance lies in a protective oxide film. If a uranium atom can penetrate the film slightly, it will sooner or later undergo fission, and literally blow off a piece of the protective film.

Unit Operations

Chemical processing of radioactive materials involves, at many points, phase separating steps, or unit operations, such as filtration, resin bed separation, distillation, etc. Although it is difficult to make general deductions from the few known high-level processes, six such operations will be discussed as to radatinn effects and means of overcoming them. Attempts to estimate energy input levels which can be successfully handled must be regarded as subject to considerable uncertainty since each case will have its own variations as to quantity, geometry, acceptable performance standard, etc.

Filtration

Filtration is one of the most fundamental chemical operations, and yet it has been avoided as much as pos-

sible in remote control processes. This has, in general, not been so much because the filtration gave trouble, but because means for setting up and cleaning the filter and handling the separated solid have been difficult to achieve by remote control. The usual industrial techniques of filter-aid precoat, belt-discharge continuous filters and the like cannot be considered in their present form because of maintenance difficulties, lack of miniaturized models, and because the filter-aid forms a bulky disposal problem.

There is no particular reason, however, why a successful filtration technique cannot be devised for use in a high radiation-intensity process. Porous metallic filter media, such as stainless steel and platinum, have been used with good success in small scale operations. The equipment must be arranged so that the filter can be cleaned or replaced with ease. A filter-stick type of apparatus is an example.

Radiation effects on the filtering operation will vary somewhat depending on whether the bulk of the radioactive material is in the solid or the liquid phase. As discussed above, gas-evolution, peptization, and oxidation-reduction effects may limit the energy density at some level. The filtration of polonium sulfate and polonium hydroxide have been accomplished at an energy density of about 100 watts per gram with no particular troubles, as has also barium nitrate at an energy density of about 4 watts per gram. The successful filtration of LaF_3 at 230 watts per gram has been mentioned above. This salt is difficult to filter even when non-radioactive. It is believed that, with favorable conditions, the limiting radiation intensity for successful filtration has not yet been reached.

Centrifugation

The centrifuge has always been an attractive alternative to filtration for liquid-solid separation, and is used for liquid-liquid separation as well. There appears to be no reason why the centrifuge cannot effect phase separation at the highest activity levels. However, the type of machine must be selected carefully. The laboratory cup-type centrifuge has been adapted to remote-control operation in small-scale work, and it must be reported that the results are unsatisfactory due to radiation effects above moderate power inputs. The centrifugation of polonium hydroxide was found to be unsatisfactory (100 watts per gram) and centrifugation of barium nitrate was acceptable only up to about 0.5 watt per gram, and completely unsatisfactory above 1 watt per gram. In all these cases, the difficulty was that after stopping the centrifuge the compacted precipitate became dislodged due to gas evolution, before the decantation could be performed.

The obvious solution is to use a centrifuge of the bowl type which allows continuous overflow or skimming of the liquid phase while spinning at full speed. The precipitate can be re-slurried and washed or removed as desired. Such a centrifuge has been designed for a moderate scale, high-intensity process at the National Reactor Testing Station in Idaho. There is no reason to indicate that this type of centrifuge separation will be limited in any way by radiation intensity.

Distillation-Evaporation-Ignition

In all of these processing operations the self-heating of the radioactive materials can be used to aid the operation. All of these processes have been accomplished by remote control at low intensity using nearly conventional equipment. Evaporation and ignition operations have been done with radioactive lanthanum materials at high specific activities (500 watts per gram). The only observations made were that smaller splattering losses were encountered (using open cups) when evaporations were done without external heat.

In the field of waste disposal the Los Alamos Laboratory has shown that with proper equipment waste air streams bearing radioactive particulate matter can be scrubbed with highly contaminated waste water, with transfer of radioactivity only from the air to the water.[4] The Oak Ridge National Laboratory has shown that liquid wastes may be readily concentrated many-fold by distillation. These observations may be utilized to advantage in high-level processing plants of the future.

Electrodeposition

The use of electrodeposition of radioactive materials will undoubtedly be limited to specialized applications. However, since it is a regularly used method for purifying polonium, it has been observed at high specific activity (130 watts per gram). The hydrogen peroxide produced in the solution by the polonium alpha particles was observed to affect the current efficiency markedly, and to limit the quantitative deposition of the metal in some cases.

Another interesting application of electrodeposition to high radiation-intensity processing is the production of fission-product barium. Upon dissolution of the uranium slugs a considerable quantity of lead salt is added. When sulfuric acid is added to precipitate barium, lead sulfate comes down also, acting as a carrier. This lead is later removed from the barium-lead solution by electrodeposition, leaving the barium to continue without carrier for the rest of the process.

Solvent Extraction

Selective extraction by contacting of aqueous solutions with immiscible organic solutions has become an important part of the atomic energy industry. However, because of the organic materials involved these methods are far from qualifying as high radiation-intensity processes. Careful studies at Oak Ridge indicate that the best organic complexing materials can be exposed to only 0.0001 watt-hours per gram.

Solvent extraction methods will continue to be used for highly radioactive materials by diluting the solutions. For large scale work this means very large shielded plants, but the simple equipment of the solvent extraction system helps this method compete. As pointed out above, there are some radioactive products which cannot be handled at high dilution, and there

are economic tendencies which at the large scale will weigh against the solvent system.

Ion Exchange

One of the most important contributions of the American atomic energy program to industrial technology has been the thorough exploitation of ion-exchange separations. Resin bed columns have enabled the large scale separation of pure rare earths, and the isolation of new transuranium elements. In the field of high radiation-intensity processing, ion-exchange techniques appear to hold a promising position.

In the separation of radio-barium an organic cation exchange resin of the sulfonated phenolic type has been used at dosages up to 0.270 watt-hours of beta energy per gram. The loss in capacity of the resin was about 4 per cent. Anion resins were shown to have less radiation stability than cation resins.

An example of use of an inorganic exchange bed is the process for production of fission product zirconium, using a silica-gel adsorption column. The column was operated successfully for sorption and elution of zirconium in a flux depositing 0.025 watts per gram. No ill effects were observed and this dose rate is believed to be far from the upper limit.

In addition to possible destruction of the exchange bed material, the most probable limitation which radiation intensity will place on ion exchange columns is the formation of gas bubbles, which tend to plug the column. Various attempts are being made to overcome this limitation by such devices as up-flow columns, pressurized columns, etc.

REFERENCES

1. Allen, A. O., "Yield of Free H and OH in Irradiation of Water," *Radiation Research 1*, 85 (1954).
2. King, L. D. P., Hammond, R. P., Leary, J. A., Bunker, M. E. and Wykoff, W. R., "Gas Recombination System for a Homogeneous Reactor," *Nucleonics 25* (1953).
3. Charlesby, A., "The Cross-Linking and Degradation of Paraffin Chains by High Energy Radiation," *Proc. Roy. Soc. (London) A222*, 60 (1954).
4. Leary, J. A., Clark, R. A. and Hammond, R. P., "Design and Performance of a Disposal Plant for Radioactive Wastes," *Nucleonics 12*, 64 (1954).

Solvent Extraction Chemistry of the Fission Products

By F. R. Bruce,* USA

A vast amount of information on the chemistry of fission products has been accumulated in the development of fertile and fissionable material separation processes, which have been described in other papers. Although these processes employ methylisobutyl ketone and tributyl phosphate as solvents, many other solvents have also been investigated for the purification of fissionable and fertile materials. These include pentaether, diisopropyl ether, tertiary alcohols, dibutyl cellosolve, thenoyl trifluoroacetone, and dibutyl carbitol. The extraction of inorganic ions by chelating solvents such as thenoyl trifluoroacetone has been adequately reported previously by Reid and Calvin. Work with dibutyl carbitol in the United States has been of limited scope compared to the studies conducted in other countries. Therefore, thenoyl trifluoroacetone and dibutyl carbitol will not be considered here.

An understanding of the application of solvent extraction to the problem of purifying fissionable material will aid in the discussion of the solvent extraction chemistry of the fission products which follows. Solvent extraction processes are usually continuous, being carried out, for example, in a column. The aqueous feed is introduced at a point near the middle of the column and flows downward, passing countercurrently to the organic phase which is introduced at the bottom and flows upward. In this portion, the extraction section, the desired products transfer to the organic phase while the contaminating fission products remain in the aqueous phase. In the top, or scrubbing section of the column, the product-bearing organic phase flows upward countercurrently to a fresh aqueous phase which is introduced at the top. In this portion of the process residual traces of contaminating fission products are removed from the product-bearing organic phase. Almost all the observed separation from fission products occurs in the first column, in which the products are transferred to the organic solvent and the organic phase is subsequently scrubbed with fresh aqueous phase.

With respect to transferable species, the organic solvent passing upward is in equilibrium with the feed flowing downward at the point of feed introduction to the column. Therefore, the degree of separation of product from contaminants which is achieved in the extraction section may be predicted accurately by a single batch equilibration of feed with solvent of a composition representative of that at the feed point. Such simple experiments are employed frequently to study the solvent-extraction behavior of fission products. When an organic and an aqueous phase are mixed, an equilibrium is established with respect to the transferable species, and the distribution ratio of transferable species is defined as the concentration in the organic phase divided by the concentration in the aqueous phase. Throughout this paper the term "distribution ratio" will be used to describe the solvent-extraction behavior of fission products.

Solvent that has been equilibrated with feed, and therefore contains contaminating fission products, may be contacted with fresh scrub solution, and the separation that is obtainable in the scrub section of a column may be determined. This experiment is also widely used in studying the solvent extraction of fission products. Most of the chemistry which is to be discussed will be based on these two simple types of experiments.

A more sophisticated method of studying solvent extraction of fission products is the countercurrent batch extraction technique. In this method a continuous countercurrent process is simulated on a laboratory scale by introducing fresh organic solvent at one end of a series of vessels; the feed solution containing the ions to be extracted is introduced near the middle; and fresh scrub solution is introduced at the end opposite the organic introduction point. The organic solvent and aqueous phases are mixed in each vessel, the phases separated, and the organic phase passed in one direction to the next stage, and the aqueous phase in the other direction. A detailed discussion of countercurrent batch extraction is given in Perry, "Chemical Engineer's Handbook". Excellent correlation is obtained between fission product behavior in plant runs and well-conceived batch countercurrent solvent-extraction experiments.

Solvent-extraction chemistry of fission product mixtures may be studied by determining gross β- or γ-activity in solutions of irradiated uranium; by assaying for individual fission products in solutions of irradiated uranium; or by total activity measurements

* Oak Ridge National Laboratory. Including work by Chemical Engineering Division, Argonne National Laboratory; Chemical Research Section, Hanford Atomic Products Operation; Separations Chemistry Unit, Knolls Atomic Power Laboratory; Chemical Technology Division, Oak Ridge National Laboratory; Chemistry Division, Oak Ridge National Laboratory; and Radiation Laboratory, University of California.

made in systems of pure radioisotopes. Gross β- and γ-measurements are difficult to interpret since the fission product spectrum depends on irradiation and decay times. Such information, however, often presents a valuable qualitative picture of fission product behavior. While experimental techniques are greatly simplified by using pure tracers, it has been well established that many radioisotopes, notably ruthenium, zirconium and niobium, exhibit marked differences between their tracer chemistry and their chemistry in solutions obtained directly from dissolution of irradiated uranium. Accordingly, fission product behavior inferred from radiochemical analysis of samples originating directly from dissolver solution is more valid than behavior deduced from experiments conducted with tracers.

Early solvent extraction research quickly disclosed the fact that some of the fission products are more difficult to separate from uranium and plutonium than others. All the Groups I and II elements show very low solubility in organic solvents. Group III elements with the exception of cerium are likewise easily separable from fissionable materials. Zirconium and niobium, in Groups IV and V, exhibit complex solvent extraction chemistry and are difficult to separate from fissionable and source materials. Group VI fission products have either very long or very short half-lives and are therefore of little importance. Iodine, in Group VII, is of some importance since it reacts with many organic solvents and is extracted. In Group VIII, ruthenium with its multiple valence states is an important contaminant in products from solvent-extraction processes. It is natural that the solvent-extraction chemistry of the fission products should center around those elements which are most difficultly separable from materials of interest. These fission products are: Ce^{141}, Ce^{144}, Zr^{95}, Nb^{95}, I^{131}, Ru^{103}, and Ru^{106}. In the absence of complicating factors, such as complexing agents, all the other fission products are easily separated from uranium, plutonium, and thorium by solvent extraction.

METHYLISOBUTYL KETONE EXTRACTION OF FISSION PRODUCTS

Methylisobutyl ketone is employed as solvent for uranium and plutonium recovery processes. In these processes the separation of the desired products from fission products is influenced by the following variables: solvent purity, salting strength, acidity, temperature, and the presence of minor components in the system. The uranium concentration and phase contact times are not significant factors.

Effect of Solvent Purity

Mesityl oxide, methylisobutyl carbinol, and an aromatic, probably mesitylene, are the most important impurities in commercial methylisobutyl ketone. For aqueous solutions containing aluminum nitrate, nitric acid, and fission products, as much as 1 vol % mesityl oxide, methylisobutyl carbinol or mesitylene, in the organic phase did not increase the extraction of cerium, zirconium, or gross β-activity. However, in the presence of sodium dichromate they increased the extraction of cerium and zirconium markedly.

Effect of Salting Agent and Acidity

Several inorganic nitrates, including those of aluminum, ammonium, calcium, magnesium, and sodium, have been investigated for increasing the nitrate ion concentration in the aqueous phase and thereby enhancing uranium and plutonium extraction. All have been found approximately equivalent as salting agents except ammonium nitrate, which yields higher separation of fissionable material from fission products than the others. It was observed in tests employing aluminum nitrate as salting agent in the extraction and scrub sections that decontamination of uranium was fivefold less than in cases where ammonium nitrate was used in the scrubbing solution. With aluminum nitrate scrubbing, the fission product activity in the recovered product was 80% ruthenium and 20% zirconium, while with ammonium nitrate scrubbing ruthenium was more effectively removed, and the contamination in the product was 20% ruthenium and 80% zirconium. The poor decontamination with aluminum nitrate may be attributable to the presence of nitrite ion which complexes ruthenium, since analyses showed several times more nitrite ion in the aluminum nitrate employed than in commercial ammonium nitrate. However, attempts to remove nitrite from the aluminum nitrate scrub stream by adding 0.05 M sulfamic acid or by precontacting it with methylisobutyl ketone, which extracts nitrite, did not improve decontamination to the level obtained with the ammonium nitrate scrub.

Within fairly wide limits a linear relationship exists between the logarithm of the γ-activity distribution ratio and the aluminum nitrate concentration. A 50% increase in the salting agent strength increases the γ-activity distribution ratio by almost a factor of 2.

Nitric acid acts as a much more effective salting agent for fission product activity than does aluminum nitrate, particularly in the region of zero free nitric acid. On increasing the acidity from 0.1 M acid deficient to the acidity of stoichiometric aluminum nitrate, the γ-activity distribution ratio increases sevenfold. Acidifying the solution of 0.1 M nitric acid results in an additional sixfold increase in the γ-activity distribution ratio. The effect of aluminum nitrate and nitric acid concentrations on fission product extraction is summarized in Table I and Fig. 1. While the distribution ratio of gross γ-activity as a function of aluminum nitrate concentration is readily expressed mathematically, no simple relation exists for the distribution coefficient as a function of nitric acid concentration at constant aluminum nitrate concentration.

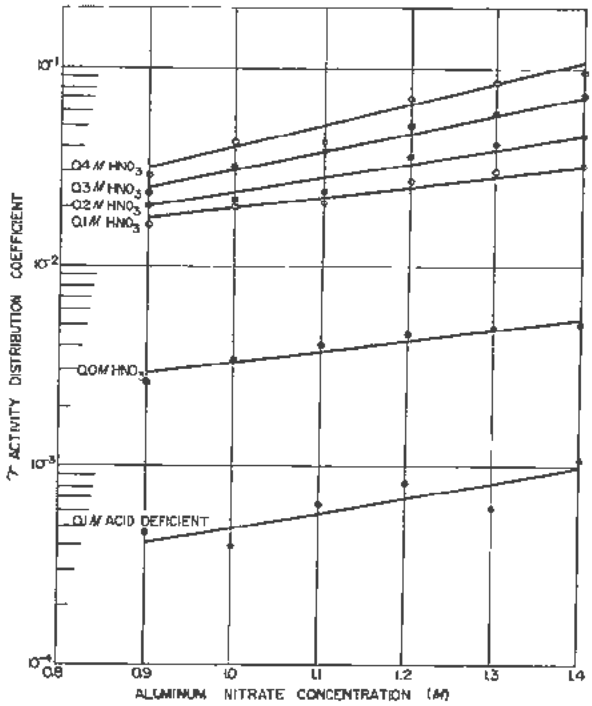

Figure 1. Effect of aluminum nitrate concentration on the γ-fission product distribution coefficient in methylisobutyl ketone extraction at various nitric acid concentrations

Effect of Temperature

The distribution ratio of gross fission product activity decreases with increasing temperature. In the system 1.25 *M* aluminum nitrate—0.45 *M* nitric acid —methylisobutyl ketone, the distribution ratio of gross γ-activity may be represented by the expression $y = 0.020(10^{-0.012t})$ where y is the gross gamma activity distribution ratio and t is the temperature in degrees Centigrade.

Table I. Expression of the Aluminum Nitrate Concentration Effect on Gross γ-Emitting Fission Product Distribution in Methylisobutyl Ketone Extraction at Various Nitric Acid Concentrations

Total HNO_3 (M)*	*Empirical equation†*
−0.10‡	$y = 8.7 \times 10^{-3}(10^{0.73x})$
0.00	$y = 8.6 \times 10^{-4}(10^{0.59x})$
0.10	$y = 4.6 \times 10^{-3}(10^{0.92x})$
0.20	$y = 2.8 \times 10^{-3}(10^{0.90x})$
0.30	$y = 4.4 \times 10^{-3}(10^{0.86x})$
0.40	$y = 2.5 \times 10^{-3}(10^{1.17x})$

* Arbitrarily, all nitric acid was considered as being in the aqueous phase. The total nitric acid is the sum of that in the aqueous and the organic phases, expressed as moles of nitric acid per liter of aqueous phase.

† y = distribution ratio of gross γ-activity (O/A) and x = aluminum nitrate molarity.

‡ This represents a solution containing 0.1 mole less nitrate ion than would be present in stoichiometric aluminum nitrate. The solution is termed "acid deficient."

Effect of Minor Components

Many organic bases which are soluble in methylisobutyl ketone increase the extraction of both uranium and fission products. Studies of this effect were made with hydrazine, tri-*n*-butylamine, 2-hexyl pyridine, and dibenzoyl methane.

An interesting effect is observed in the case of hydrazine, where digestion of the aqueous phase containing hydrazine, at 85°C, results in a lowering of the gross γ-activity distribution ratio. The presence of ferrous ion increases the rate of the reaction by which fission product extraction is depressed. Ruthenium and niobium distribution ratios are reduced tenfold, and the zirconium distribution ratio is reduced fivefold as a result of the treatment. Since zirconium and niobium exhibit only one valence state in aqueous solution, the reason for the effect of hydrazine on them is not understood.

Tri-*n*-butylamine, 2-hexyl pyridine, and dibenzoyl methane all increase the extraction of fission products. The most significant effect of these complexing agents is their ability to make the degree of separation of uranium from fission products independent of the nitric acid concentration.

The complexing of fission products by thioglycolic acid was studied as a method for increasing decontamination. Feed solution was digested with 0.1 *M* thioglycolic acid for 2 hr at 50°C. Following the digestion, an extraction-scrub study was made and the results compared with an untreated run. Improvement factors of 3.7, 2.1 and 3.9 were observed for β, γ, and ruthenium activities. However, zirconium and niobium were adversely affected by a factor of 2.

A minor component of considerable significance in the methylisobutyl ketone extraction processes is sodium dichromate. The unique effect of this on cerium extraction will be discussed later.

Behavior of Zirconium and Niobium

Zirconium and niobium are responsible for a large fraction of the γ-activity associated with uranium at the end of a solvent-extraction cycle, although ruthenium contributes the major portion of the β-activity. The forms of zirconium in process solutions are not well understood, although its behavior is generally consistent with the following picture. At low acidities, zirconium is probably hydrolyzed and present as a nonextractable colloid. On increasing the acidity of the solution, the proportion of colloidal zirconium decreases. In strongly acidic solutions it appears to be present as tetravalent zirconium ion, which is highly extractable.

Aluminum nitrate and nitric acid concentrations are the chief variables that may be exploited to minimize zirconium and niobium extraction by methylisobutyl ketone (see Figs. 2 and 3). It is clear that a low acidity should be maintained and that a low aluminum nitrate concentration should be used in scrubbing.

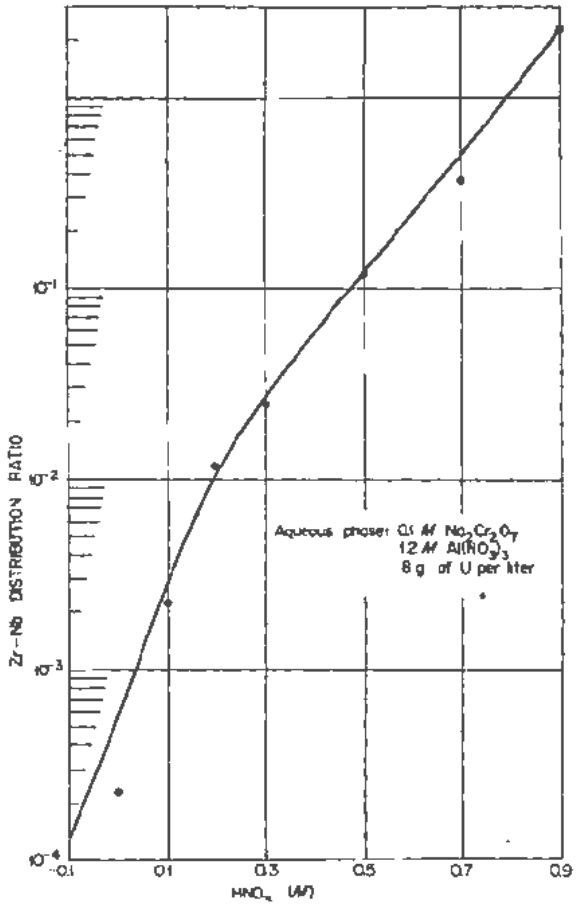

Figure 2. Effect of nitric acid concentration on distribution ratio of zirconium and niobium in methylisobutyl ketone extraction

Attempts were made to increase zirconium and niobium removal in the scrubbing step by formation of their oxalate complexes. However, oxalate addition impairs uranium extraction without significantly improving zirconium and niobium decontamination.

Behavior of Iodine

Relatively few data have been collected on the behavior of iodine in solvent-extraction processes since its short half-life makes it unimportant in processing long-decayed material. It has been observed, however, that iodine is highly soluble in methylisobutyl ketone, forming addition compounds with the solvent. These compounds are not backwashed when the products are stripped with water nor are they removed from the solvent by washing with caustic or acid. Iodine promises to be a major problem in solvent-extraction processes handling short-decayed U or Pu.

Behavior of Ruthenium

In all methylisobutyl ketone extraction processes ruthenium is by far the most difficult fission product to separate from uranium and plutonium, contributing 75–90% of the β-activity in the first cycle solvent-extraction product. In typical methylisobutyl ketone extraction processes operated under acid-deficient conditions, a form of ruthenium having a distribution ratio of about 0.003 predominates in the extraction section. However, significant quantities of ruthenium with distribution ratios greater than 1 are also present, and these, of course, are not completely removed in the scrubbing. In process systems of interest, ruthenium chemistry is extremely complicated, the element probably existing in the tri-, tetra-, and octavalent states under certain conditions. It is well established that reduced valence states of ruthenium are less extractable than the oxidized. For example, oxidation with 0.1 *M* sodium dichromate at 90°C increases the distribution ratio of ruthenium tracer about twofold. A similar effect is observed in dibutyl cellosolve extraction. The presence of ferrous sulfamate reduces the ruthenium distribution ratio by a factor of about two. Whether these effects are attributable to the oxidation-reduction behavior of ruthenium itself or to an effect produced on another component in the system, such as the nitrite ion, has not been established.

Ruthenium forms an extremely stable nitrosyl complex, $Ru(NO)(NO_3)_3$, in aqueous solutions. Since addition of nitrite ion results in a marked increase in

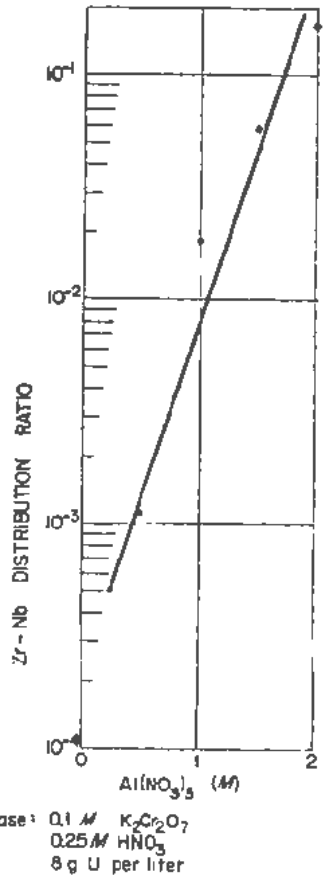

Figure 3. Effect of aluminum nitrate concentration on distribution ratio of zirconium and niobium in methylisobutyl ketone extraction

ruthenium extraction under certain conditions, it is evident that the nitroso complex plays an important part in the ruthenium extraction mechanism. The possibility of employing a methylisobutyl ketone-soluble material which reacts with nitrite, thereby destroying this complex and decreasing the organic solubility of ruthenium, was investigated. Sulfanilamide, a specific reagent for the nitroso group, was added to methylisobutyl ketone, but no significant effect was observed in subsequent extraction. It is inferred that the nitroso complex of ruthenium is extremely stable and reacts very slowly or not at all with sulfanilamide. In other experiments it was found that while macro, inactive ruthenium nitroso nitrate could be oxidized to ruthenium tetroxide and subsequently reduced to a solvent-insoluble compound, ruthenium in the solution obtained by dissolving irradiated uranium did not behave in the same fashion, and the treatment yielded ruthenium decontamination factors which were 10–20 times less than those observed with inactive ruthenium. The extreme stability of the nitroso complex has been confirmed in other experiments where it has been shown to resist treatment with strong sulfuric and perchloric acids.

It has been proposed that colloidal ruthenium is the cause for the poor decontamination observed. In attempts to confirm this, irradiated uranium dissolver solution was dialyzed through cellophane into a comparable uranium solution, containing no fission products originally. Samples from each side of the membrane were removed, oxidized with periodic acid, reduced with formic acid, and extracted with methylisobutyl ketone. When the resulting solvent phases were scrubbed with acidic aluminum nitrate, no significant difference in ruthenium behavior was observed, indicating the unimportance of colloids.

Numerous attempts have been made to develop theories for explaining the solvent extraction behavior of ruthenium. None has gained wide acceptance, nor do they enjoy consistent experimental corroboration. Callis and co-workers postulate the presence of at least three different ruthenium species in irradiated uranium dissolver solution. The predominant oxidation state is pictured as the tetravalent. The average distribution ratio for the total ruthenium in the dissolver solution under acid-deficient aluminum nitrate conditions is approximately 0.008. The three ruthenium species are postulated to have distribution ratios of 0.015, 0.004, and 0.0018.

Elliot and Miles postulate four forms of ruthenium and describe the conditions necessary for their existence. The four forms are designated A, B, C, and D. Each of the four forms acts in a characteristic manner. The distribution ratios of ruthenium A, B, C, and D in methylisobutyl ketune extraction are described as being approximately 7.4, 0.05, 0.001, and 15, respectively. Ruthenium C is obtained by allowing ruthenium tetroxide to stand in dilute nitric acid for several days. Ruthenium tetroxide decomposed in dilute nitric acid containing potassium permanganate forms Ru D. Strong oxidation of Ru C yields a material possessing the extraction properties of Ru D. Conversely, the strong reduction of Ru D yields a form that resembles Ru C. It is accordingly inferred that Ru D represents a higher oxidation state than Ru C. On either long standing in aluminum nitrate solutions containing nitric acid or on treatment with nitrous acids, Ru C is converted to Ru A or B. Ruthenium A and B in turn may be reverted to Ru C by treatment with urea. Since urea reacts with nitrous acids according to the equation $CO(NH_2)_2 + 2HNO_2 \rightarrow 2N_2 + 3H_2O + CO_2$, Elliot and Miles conclude that Ru A and D are nitroso complexes of Ru C. Ruthenium C is tentatively identified as the trivalent and Ru D as the tetravalent form. It is possible to explain much of the solvent-extraction chemistry of ruthenium by assuming it to be present in these four forms.

A feed pretreatment method for decreasing ruthenium extraction, especially under acid flowsheet conditions, has been proposed by Gresky. The recommended treatment consists of adjusting the feed to 0.3*N* nitric acid—0.05 *M* sodium nitrite and digesting for 1 hr at room temperature. One per cent by volume of acetone is then added to the solution, and the mixture is digested at 85–90°C for 4 hr. After cooling, the solution is made 0.3*N* in nitric and 0.1 *M* in sodium dichromate. The pretreatment is dependent upon acid concentration, the optimum range being 0.3–0.4 *M* nitric acid during the digestion step. The treatment usually results in a 140-fold increase in ruthenium decontamination in acidic aluminum nitrate processes, and a fourfold increase in acid-deficient processes. In many cases, however, very little or no effect is observed, testifying to the complex solvent-extraction chemistry of ruthenium. The chemistry of this process is not fully understood.

A unique approach to the ruthenium problem was taken by Miles and co-workers who proposed the use of diphenyl thiourea as a solvent additive. With ruthenium, diphenyl thiourea forms a stable complex which is soluble in the solvent phase and only very slightly soluble in the aqueous phase. Therefore, when diphenyl thiourea is present in the solvent, ruthenium is complexed and is not stripped with the desired products in the back-extraction step. At a diphenyl thiourea concentration of 10 gm/liter, complex formation occurs with a half-time of about 30 min at 25°C and with a half-time of about 1 min at 60°C. This treatment prior to stripping results in a ruthenium distribution ratio of about 50 in the stripping step, thereby yielding a very significant separation of uranium from ruthenium. An attempt was also made to suppress the extractability of ruthenium by formation of an aqueous-soluble complex with thiourea. However, with this technique reproducibility was very poor, and the small amount of ruthenium that was extracted exhibited a very high distribution ratio in favor of the organic phase in the scrubbing step. Ethylene thiourea behaved similarly.

In spite of all the study that has been devoted to the solvent-extraction chemistry of ruthenium, the most useful devices for inhibiting its extraction are the simple expedients of nitric acid and aluminum nitrate concentration control. The tremendous significance of these variables is indicated by the following results.

In an aluminum nitrate-sodium dichromate system, increasing the nitric acid concentration from 0.2 *M* acid deficient to 0.9 *M* acid increases the ruthenium distribution ratio from 1.5×10^{-3} to 660×10^{-3}. Increasing the aluminum nitrate concentration from 0.5 *M* to 2 *M* increases the ruthenium distribution ratio from 0.17 to 2.3. The effect of nitric acid concentration is shown in Fig. 4. The effect of aluminum nitrate concentration on ruthenium extraction is shown in Fig. 5. It is clear that a low acidity should prevail in extraction and scrubbing, and that the lowest permissible aluminum nitrate concentration should be maintained in scrubbing.

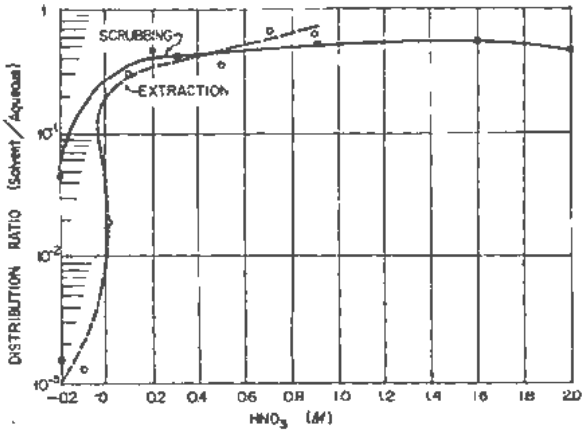

EXTRACTION
Aqueous: 0.1 *M* $Na_2Cr_2O_7$, 1.2 *M* $Al(NO_3)_3$, 8 g U per liter

SCRUBBING
Aqueous: 0.75 *M* $Al(NO_3)_3$

Figure 4. The effect of HNO_3 concentration on the distribution ratio of ruthenium in methylisobutyl ketone extraction and scrubbing

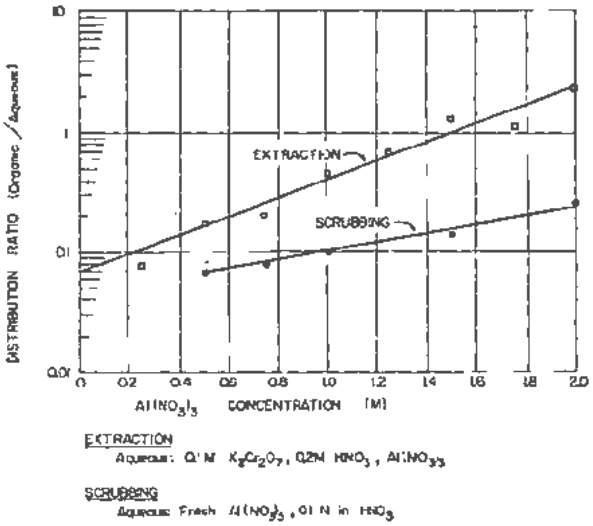

EXTRACTION
Aqueous: 0.1 *M* $K_2Cr_2O_7$, 0.2 N HNO_3, $Al(NO_3)_3$

SCRUBBING
Aqueous: Fresh $Al(NO_3)_3$, 0.1 N in HNO_3

Figure 5. The effect of $Al(NO_3)_3$ concentration on the ruthenium distribution in methylisobutyl ketone extraction and scrubbing

Behavior of Cerium

Cerium may exist in the tri- and tetravalent states in process solutions. In macro experiments with nonradioactive cerium it was found that trivalent cerium is practically unextractable in methylisobutyl ketone. Tetravalent cerium, in 1.2 *M* aluminum nitrate—0.1 *M* nitric acid—methylisobutyl ketone has a distribution ratio of 0.8 at 25°C and 1.5 at 0° C. The difference is attributed to the less rapid reduction of tetravalent cerium by methylisobutyl ketone at the lower temperature rather than to a significant difference in the equilibrium ratio. Addition of sodium dichromate decreases the distribution ratio of tetravalent cerium, indicating formation of a less readily extractable complex.

Cerium extraction exhibits the same general type of dependence on aluminum nitrate concentration and acidity that is observed with other fission products. A 50% increase in aluminum nitrate concentration results in about a fourfold increase in cerium extraction (Fig. 6). Cerium extraction is markedly affected by nitric acid concentration, the distribution ratio increasing from 0.001 for a 0.17 *M* acid-deficient solution to 0.14 for 0.25 *M* acid solution (Fig. 7).

The effect of inert cerium on the methylisobutyl ketone extraction of tracer cerium was investigated, and it was found that addition of 0.012 *M* cerium to the aqueous phase depressed the distribution ratio from 0.30 to 0.008 (Fig. 8). The presence of inert cerium at a concentration of 0.002 *M* effected a tenfold decrease in the cerium distribution ratio in the scrubbing step, while at a concentration of 0.02 *M*

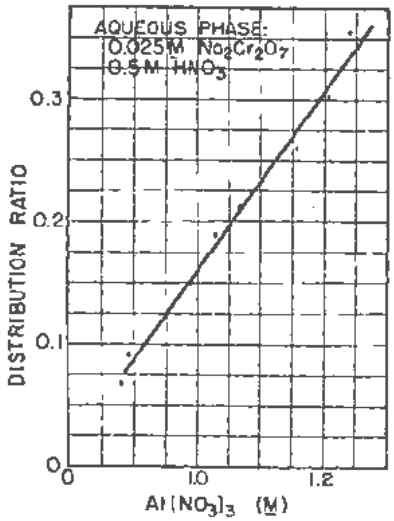

Figure 6. Effect of aluminum nitrate concentration on extraction of cerium by methylisobutyl ketone containing 0.3 *M* HNO_3

the distribution ratio was depressed almost 50-fold (Fig. 9). These results are particularly interesting since such an effect has not been observed in the case of other fission products when attempts have been made to depress fission product extraction by addition of inactive material.

During the pilot plant testing of a methylisobutyl ketone solvent-extraction process, a very peculiar effect was observed with cerium. At the conclusion of a run, the shut-down procedure consisted in discontinuing the flow of feed, which contained uranium, plutonium, fission products, and sodium dichromate, and continuing the flow of scrub solution and solvent to recover residual fissionable materials from the column. The extraction of cerium increased instead of decreasing as its concentration in the aqueous phase became more dilute, passed through a maximum, and then decreased. Pitzer studied this phenomenon and found that cerium extraction is markedly dependent on sodium dichromate concentration, with the maximum distribution ratio occurring in the range 0.001–0.002 *M* sodium dichromate (Table II). In attempting to elucidate this, permanganate and bismuthate ions were studied as alternate oxidizing agents. Despite their more negative potentials these materials do not increase the extraction of cerium; hence, it appears that the cerium extraction mechanism involves dichromate in a manner other than simple oxidation.

FISSION PRODUCT EXTRACTION BY TRIBUTYL PHOSPHATE

Tributyl phosphate (TBP) is used, in a manner similar to methylisobutyl ketone, as solvent in plutonium and uranium recovery processes. It also may be used to separate thorium from fission products. These applications have been discussed in other papers where it has been shown that the distribution ratio of TBP-extractable materials depends on the concentration of uncomplexed TBP in the organic phase. For this reason one of the most important variables in fission product extraction by TBP is the degree of solvent saturation with elements such as uranium, plutonium, or thorium, which are more strongly complexed by TBP than the fission products. Also, it is necessary to mix TBP with an inert diluent, such as kerosene, to obtain desirable physical properties and the extraction of fission products depends on the TBP concentration in the solvent and to a lesser degree on the nature of the diluent selected. Typical fission product behavior in a TBP uranium recovery process is shown in Table III.

Effect of Solvent Purity on Fission Product Extraction

Common impurities in commercial TBP are butanol, and mono- and dibutyl phosphate. The separation of uranium or plutonium from fission products is less satisfactory when commercial TBP is used as solvent than when butanol-free TBP is employed. The difference in effectiveness is primarily attribut-

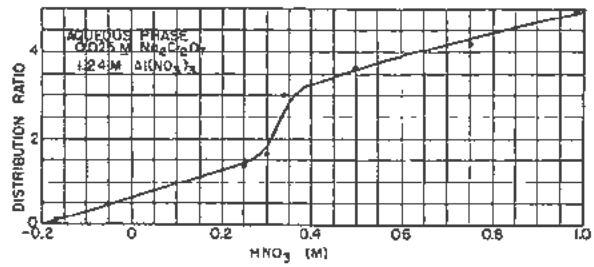

Figure 7. Effect of nitric acid concentration on the methylisobutyl ketone extraction of cerium

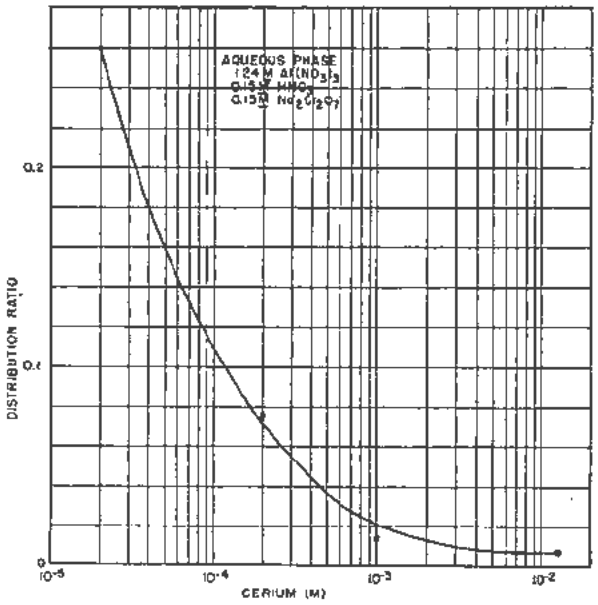

Figure 8. Effect of inert cerium on the extraction of tracer cerium with methylisobutyl ketone containing 0.5 M nitric acid

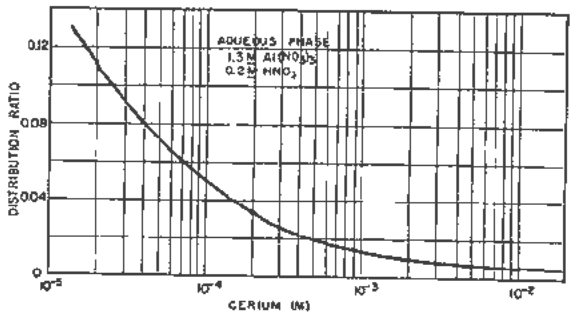

Figure 9. Effect of inert cerium on the scrubbing of tracer cerium from methylisobutyl ketone containing tracer cerium

Table II. Effect of Sodium Dichromate Concentration on Methylisobutyl Ketone Extraction of Cerium

Aqueous: 1.2 M $Al(NO_3)_3$, 0.15 M HNO_3

$Na_2Cr_2O_7$ concentration (*M*)	Distribution ratio
0.0001	0.0005
0.0005	1.21
0.001	1.48
0.0015	3.20
0.0025	3.25
0.0050	2.11
0.0075	1.37
0.05	0.34

Table III. Behavior of Fission Products in Tributyl Phosphate Countercurrent Batch Extraction

Aqueous phase: 0.5 M $UO_2(NO_3)_2$, 3 M HNO_3; 3 volumes
Organic phase: 15% TBP—85% Varsol, 0.15 M HNO_3; 10 volumes
Scrub: 3 M HNO_3; 2 volumes
7 extraction and 2 scrub stages

	Distribution ratio		*Decontamination factor*		
Activity	*Feed plate*	*2nd scrub stage*	*Extraction*	*Scrub*	*Over-all*
Gross β	0.0017	0.11	330	30	9.8×10^3
Ru	0.0045	0.22	106	5.0	530
Ce	0.00035	0.0058	1.4×10^9	380	5.3×10^8
Zr	0.0064	0.022	71	210	1.5×10^4
Nb	0.00035	...	1.5×10^5	5.6	8.3×10^5

able to increased β-activity distribution ratios in the scrub section when commercial TBP is used, indicating that butanol, or its reaction products with nitric acid, complexes fission products in the solvent phase and prevents their being removed. With commercial TBP a typical β-activity distribution ratio in the scrub section is about 5, compared to 1 for butanol-free TBP.

Mono- and dibutyl phosphates increase the extraction of fission products significantly. For example, a 12.5 vol % TBP solution in carbon tetrachloride to which 0, 0.01, 0.1, and 1.0 vol % dibutyl phosphate had been added gave over-all γ-emitting fission product distribution ratios of 0.0017, 0.011, 0.070, and 0.41, respectively, and β-emitting fission product distribution ratios of 0.00084, 0.0025, 0.014, and 0.033. The primary effect of dibutyl phosphate is increased zirconium extraction, cerium and ruthenium being unaffected by these concentrations of DBP.

Diluent composition is also an important factor in tributyl phosphate extraction. For example, a series of solvent mixtures containing 15% TBP in various diluents was used to extract a nitric acid solution containing uranium and fission products. The resulting solvent phases were scrubbed four times with nitric acid, and the distribution ratio of β-activity determined in the fourth scrub solution. The β-activity in the fourth scrub varied by a factor of almost 10 between the best and worst diluents. The adverse effect was attributable to aromatics and olefins which react with nitric acid to give nitration products that form solvent-soluble complexes with fission products.

Effect of Saturation of Solvent

As available TBP is complexed with extractable ions such as uranium or thorium, the quantity of solvent free to extract fission products becomes less, and fission product extraction decreases (see Fig. 10). Increasing the uranium saturation of the solvent from 37% to 86.8% lowered the gross β-distribution ratio 16-fold; zirconium, 3.6-fold; ruthenium, 56-fold; and total rare earths, 46-fold. It is clear that ruthenium and total rare earth extraction are markedly dependent on solvent saturation, and zirconium extraction shows a lesser dependency.

The results of a countercurrent batch extraction run in which the degree of saturation of the solvent was varied are shown in Table IV. Increasing the solvent saturation from 48% to 90% decreased the gross β-distribution ratio at the feed plate tenfold. However, it is interesting to observe the higher fission product distribution ratios in scrubbing under the high saturation conditions, suggesting that the decontamination factor for extraction plus scrubbing would be something less than tenfold greater for the high saturation case. Nevertheless, solvent saturation is the most important means of controlling fission product extraction by tributyl phosphate.

Effect of TBP Concentration

The distribution of fission products into the organic phase increases as the concentration of TBP in the diluent increases at constant uranium saturation of the solvent (Fig. 11). Increasing the TBP concentration, at 60% uranium saturation, from 0.2 M to 0.4 M increases the gross β- and γ-activity distribution ratios about 3.5- and twofold, respectively. The advantage of employing the lowest TBP concentration that is consistent with other process considerations is clear.

Effect of Nitric Acid Concentration

The distribution ratios of gross β- and γ-activities increase by factors of 5 and 21, respectively, when the nitric acid concentration of the aqueous phase is increased from 1 M to 5 M. The zirconium distribution ratio increases almost tenfold (Fig. 12) on increasing the acidity from zero to 5 M, while ruthenium extraction increases only by about 50% over the same range of acidity.

Effect of Salt Concentration

Inorganic nitrates other than nitric acid may be employed as salting agents in TBP extraction. Sodium nitrate, for example, effects a fourfold increase in zirconium extraction when its concentration is increased from zero to 3 M. It is interesting to note that sodium nitrate does not increase the extraction of trivalent cerium over this range (Fig. 13).

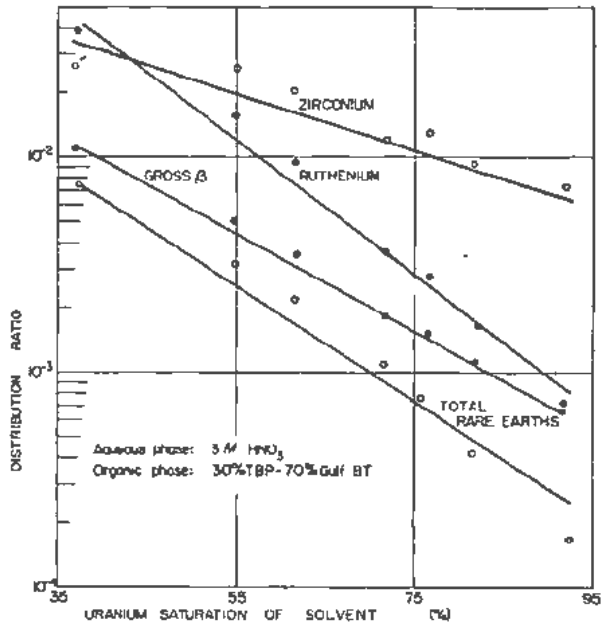

Figure 10. Effect of uranium saturation of tributyl phosphate on fission product extraction

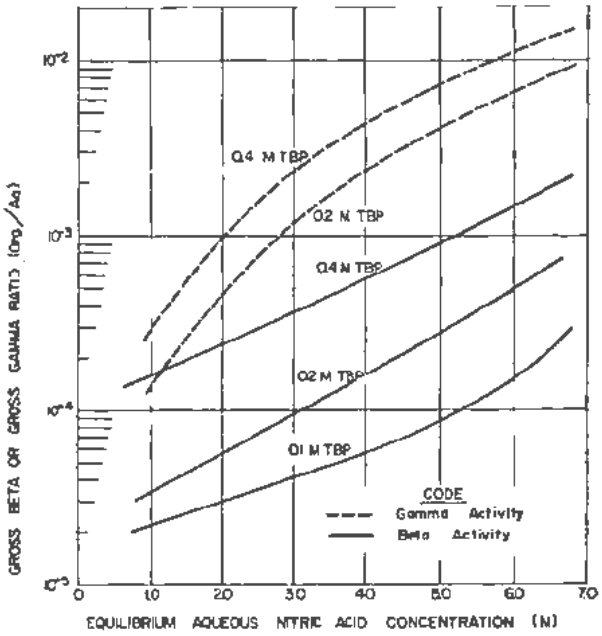

Figure 11. Distribution of fission product activity between aqueous nitric acid and diluted tributyl phosphate systems: 60% U saturation

Effect of Temperature

The effect of temperature on fission product distribution in TBP extraction differs from that in methylisobutyl ketone extraction in that the distribution ratios for gross β-activity, ruthenium, zirconium, and niobium increase with increasing temperature. Rare earth extraction shows little dependence on temperature (see Table V).

Barton and co-workers studied the effect of temperature on uranium decontamination by tributyl phosphate in a batch countercurrent extraction system consisting of ten extraction and seven scrub stages. At 70°C decontamination was improved, over room temperature values, by a factor of 13 for β-activity, 4 for γ-activity, 30 for ruthenium, and 7 for niobium; zirconium was not affected. Comparable work in simple batch extractions confirmed the previously described increase in fission product extraction with increasing temperature. Improvement in decontamination in the over-all extraction-scrub process at elevated temperatures is believed to result from increased scrubbing efficiency. A continuation of this study showed that zirconium-niobium first cycle decontamination was greatly diminished, decreasing from 3000 to 30 for zirconium and 8000 to 380 for niobium, suggesting that the nature of the effect may be complicated.

Table IV. Effect of Uranium Saturation of Tributyl Phosphate on Fission Product Extraction

Aqueous phase: 6 M HNO_3
Organic phase: 15% TBP, 85% Varsol, 0.15 M HNO_3
Volume ratio: Feed/solvent/scrub = 3/10/2
5 extraction and 4 scrub stages

Conditions at feed plate		*Distribution ratios in scrub section*	
U saturation of solvent (%)	*Gross β distribution ratio*	*2nd stage*	*4th stage*
48	0.026	0.04	0.15
77	0.016	0.025	0.27
86	0.0037	0.032	0.41
90	0.0025	0.030	0.74

Behavior of Ruthenium

It has been previously shown here that ruthenium extraction is depressed by increasing the solvent saturation with uranium, and that it is relatively independent of nitric acid concentration and temperature.

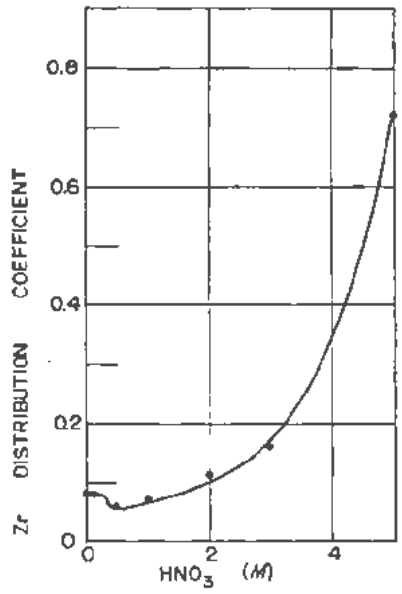

Figure 12. Effect of nitric acid concentration on extraction of zirconium by 15% tributyl phosphate in Varsol

Table V. The Effect of Temperature on the Tributyl Phosphate Extraction of Fission Products

Aqueous phase: 200 gm of uranium per liter, 3 *M* HNO_3
Organic phase: 30% TBP-70% Amsco, 80% saturated with uranium under conditions of experiment

Temperature (°C)	Distribution ratio				
	Gross β	Ru	Zr	Nb	Total rare earths
25	1.06×10^{-3}	0.96×10^{-3}	9.80×10^{-3}	0.39×10^{-3}	4.57×10^{-4}
50	2.62×10^{-3}	0.98×10^{-3}	26.8×10^{-3}	1.44×10^{-3}	5.61×10^{-4}
75	4.48×10^{-3}	1.10×10^{-3}	52.3×10^{-3}	4.57×10^{-3}	4.23×10^{-4}

Ruthenium is the most difficult fission product to separate from thorium by tributyl phosphate extraction, and the third most difficult to separate from uranium.

In the thorium recovery process, where thorium nitrate and nitric acid are employed as salting agents to extract uranium and thorium into the organic phase, and acid-deficient aluminum nitrate is employed as the scrub, ruthenium is the decontamination limiting fission product. While gross β, total rare earth, zirconium, and niobium decontamination factors are about 120, 6.8×10^5, $> 3 \times 10^4$, and $> 1.6 \times 10^4$, respectively, ruthenium decontamination is only 8.6. The low ruthenium decontamination factor results from a ruthenium species in the extraction section which is about 5–10% of the total and has a distribution ratio of greater than 1. The remaining 90–95% of the element exists as an inextractable species which has a distribution ratio of about 0.001.

Numerous methods for increasing ruthenium decontamination in the thorium recovery process have been studied. The process includes a feed-digestion step in which the solution is evaporated to approximately 4 *M* thorium nitrate. The chemical environment of the feed treatment aids in obtaining reproducible decontamination factors of 200 or more for ruthenium. Ruthenium distribution ratios in extraction of about 3×10^{-4} are observed when this step is used while they are 0.02–0.002 in its absence. The feed adjustment step is more beneficial to subsequent solvent extraction when carried out in stainless steel equipment than in glass. Ferrous ion appears to play a part in achieving the enhanced decontamination since its presence results in roughly fourfold higher ruthenium decontamination. The effect of feed adjustment at various acidities, in the absence and presence of ferrous ion, is shown in Table VI.

A different approach to increasing ruthenium decontamination in thorium purification by TBP extraction consists of alternate oxidation of the feed with periodic acid, and reduction with formic acid. This approach has the objective of converting all the ruthenium to the tetroxide and then uniformly reducing it to a lower, solvent-insoluble state. The results of various feed pretreatments are summarized in Table VII. The conclusions that can be drawn from this series of experiments are: (1) feed digestion results in an approximately eightfold increase in decontamination; (2) feed digestion in the presence of

Table VI. The Effect of Feed Pretreatment on Decontamination in Tributyl Phosphate Extraction

Aqueous phase: 1.5 *M* $Th(NO_3)_4$, 0.6 *M* $Al(NO_3)_3$; 1 volume
Organic phase: 42% TBP 58% Amsco; 5 volumes
Scrub: 0.6 *M* $Al(NO_3)_3$, 0.4 *M* acid deficient, 0.002 *M* PO_4, 0.005 *M* Fe^{++}; 1 volume
5 extraction and 8 scrub stages

HNO_3 in feed (*M*)	Decontamination factor		Remarks*
	Gross β	Ru	
0.56	127	8	No feed adjustment
0.60	96	8	
−0.14	2.8×10^3	238	Feed adjustment
−0.44	2.2×10^3	244	
−0.46	1.5×10^3	160	
−0.14	1.3×10^4	740	Feed adjusted in presence of 0.01 *M* Fe^{++}
−0.20	1.3×10^4	823	
−0.28	1.8×10^4	875	Feed adjusted in presence of 0.005 *M* Fe^{++}
−0.06	1.0×10^4	940	Feed adjusted in presence of 0.0025 *M* Fe^{++}
−0.45	1.7×10^4	1010	Feed adjusted in presence of type 309 S Nb-stainless steel

* Feed adjustment consists in evaporation of the dissalver solution to 4.5 *M* $Th(NO_3)_4$ and digestion at 150°C for 1 hr. The solution is then diluted to feed conditions.

Table VII. Effect of Feed Pretreatment on Fission Product Extraction by Tributyl Phosphate

Aqueous phase: 1.5 *M* $Th(NO_3)_4$, 0.6 *M* $Al(NO_3)_3$, 0.5 *M* HNO_3; HIO_4 added and digested at room temperature for 15 min, then HCOOH added and digested; 1 volume
Organic phase: 42% TBP in Amsco; 5 volumes
Scrub: 0.6 *M* $Al(NO_3)_3$, 0.7 *M* acid deficient, 0.002 *M* PO_4^{---}; 1 volume
5 extraction and 8 scrub stages

Feed pretreatment				*Decontamination factor*				
		Digestion						
HIO_4 (*M*)	HCOOH (*M*)	*Time (hr)*	*Temperature (°C)*	*Gross β*	*Ru*	*Nb*	*Zr*	*Total rare earths*
...	...	...	...	127	8	1.3×10^4	2.4×10^4	5.2×10^4
...	...	3*	110	852	63	2.9×10^7	6.5×10^7	8.1×10^7
...	0.005	2	90	660	37	2.3×10^6	1.3×10^6	4.5×10^6
0.0005	0.005	0.5	25	600	29	5.5×10^4	2.9×10^4	7.3×10^5
0.0005	0.005	2.0	90	1030	54	1.4×10^6	1.0×10^6	7.0×10^5
0.0005†	0.005	2.0	90	770	68	7.5×10^6	8.6×10^6	6.5×10^6
0.005	0.05	0.5	25	840	43	3.2×10^6	3.9×10^6	3.8×10^5
0.005	0.05	2.0	50	860	51	5.6×10^6	2.9×10^6	3.7×10^5
0.005*	0.05	3.0	110	7350	570	3.9×10^7	8.7×10^7	3.5×10^6

* Type 347 stainless steel turnings were added to digester. † Feed was 0.1 *M* acid deficient.

stainless steel results in an additional eightfold increase in decontamination; and (3) addition of periodic acid and formic acid has little effect.

Feed pretreatment with nitrite ion and urea has also been investigated in the tributyl phosphate system. The treatments considered include refluxing with sodium nitrite, refluxing with urea, and digestion at 85°C with either nitrite or urea. A 16-fold increase in decontamination results from digestion with 0.05 *M* sodium nitrite for 3 hr, while digestion with urea results in about a sixfold increase in decontamination (Table VIII). The addition of nitrite via nitrogen dioxide and sodium nitrite are equivalent in effectiveness. However, in employing these pretreatment steps, it is observed that the amenability of feeds to the pretreatments differs widely.

It has been observed that hydrogen peroxide accelerates the formation of nonextractable ruthenium. Watts in studying this problem made a dissolver solution 0.07 *M* in potassium permanganate, and heated it 1 hr at 70°C and 1 hr at 90–95°C in order to break the ruthenium complexes and oxidize the ruthenium to the tetroxide. Sufficient hydrogen peroxide was added to the cooled solution to completely precipitate the uranium. The solution was boiled to decompose peroxide, and one extraction and three scrubs were carried out. In a subsequent solvent extraction a ruthenium decontamination factor of 440 was obtained while a factor of 150 was observed in a similar run without pretreatment.

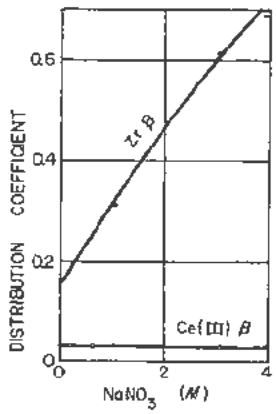

Aqueous phase: 0.1 *M* $UO_2(NO_3)_2$, 3.0 *M* HNO_3, $NaNO_3$, tracer

Figure 13. Effect of sodium nitrate concentration on extraction of cerium and zirconium by 15% tributyl phosphate in hexane

Behavior of Iodine

One of the most troublesome fission products in the tributyl phosphate extraction of short-decayed irradiated material is iodine which is extracted by the usual solvent-extraction mechanism and also forms addition compounds with unsaturated materials in the solvent. The extraction of iodine was studied by treating solvents with either tracer iodine

Table VIII. Effect of Feed Pretreatment on Fission Product Extraction by Tributyl Phosphate

Aqueous phase: 1.47 *M* $UO_2(NO_3)_2$, 2 *M* HNO_3 (product from first cycle TBP extraction); 30 volumes
Solvent phase: 30% TBP in Amsco; 100 volumes
Scrub: 3 *M* HNO_3; 20 volumes
5 extraction and 4 scrub stages

Feed pretreatment	*Decontamination factor*	
	Gross γ	*Ru*
None	160	50
Made 0.05 *M* in $NaNO_2$; digested 3 hr at 85°C	450	800
Made 0.05 *M* in $NaNO_2$; refluxed 30 min	560	500
Made 0.05 *M* in urea; digested 3 hr at 85°C	400	155
Made 0.1 *M* in urea; digested 3 hr at 85°C	430	100
Made 0.1 *M* in urea; refluxed 1 hr	435	290

Table IX. Effect of Complexing Agents on Tributyl Phosphate Extraction of Fission Products

Aqueous phase: 0.2 M $UO_2(NO_3)_2$, 3 M HNO_3, complexing agent
Organic phase: 12.5% TBP in CCl_4
Scrub: 3 M HNO_3, complexing agent
Feed/scrub/extractant volume ratio — 3/2/10 in a countercurrent batch extraction

Complexing agent	Fission product	Distribution ratio			
		Extraction	1st scrub	2nd scrub	3rd scrub
None	Gross β	8.4×10^{-4}	7.0×10^{-2}	4.3×10^{-3}	9.2×10^{-2}
	Zr	2.9×10^{-3}	1.1×10^{-3}	1.4×10^{-2}	5.6×10^{-2}
	Ru	2.8×10^{-4}	1.9×10^{-2}	8.6×10^{-2}	0.43
0.1 M H_3PO_4	Gross β	3.3×10^{-4}	2.8×10^{-2}	0.16	0.92
	Zr	3.0×10^{-5}	7.8×10^{-3}	0.31	0.09
	Ru	3.8×10^{-4}	1.6×10^{-2}	4.1×10^{-2}	0.37
0.1 M H_2SO_4	Gross β	7.1×10^{-4}	4.2×10^{-2}	7.2×10^{-2}	0.29
	Zr	5.3×10^{-4}	1.6×10^{-2}	2.7×10^{-2}	0.12
	Ru	4.0×10^{-4}	4.0×10^{-2}	0.12	0.07
0.01 M $(NH_4)_2SiF_6$	Gross β	2.5×10^{-4}	5.0×10^{-3}	0.11	0.07
	Zr	2.6×10^{-4}	5.2×10^{-3}	9.2×10^{-2}	0.52
	Ru	3.2×10^{-4}	1.3×10^{-2}	5.2×10^{-2}	0.14

or tracer hydriodic acid in 5 M nitric acid. Under these conditions, molecular iodine reacts extensively with commercial hexane, about 0.7 gm of the iodine being extracted per liter of solvent. Hexane, from which unsaturates have been removed by washing with concentrated sulfuric acid before equilibration, does not extract a significant quantity of iodine. Amsco 123-15 extracts 0.4 gm/liter; Amsco 125-90, 0.7 gm/liter; and Amsco 190-10, 0.9 gm/liter. After eight washes with concentrated sulfuric acid, Amsco 123-15 extracts 0.2 gm/liter. Under the same conditions commercial benzene extracts no iodine. Hydriodic acid does not react readily with any of the solvents but adds molecular iodine rapidly under the same conditions. These results indicate that iodine extraction may be minimized by careful diluent selection or by maintaining iodine in the reduced valence state.

Behavior of Zirconium-Niobium

Since zirconium is one of the principal fission products contaminating uranium, plutonium, or thorium recovered by TBP extraction, a number of aqueous-soluble complexing agents for reducing its extractability were investigated (Table IX).

The zirconium distribution is decreased about 100-fold by 0.1 M phosphate, tenfold by 0.01 M fluosilicate, and sixfold by 0.1 M sulfate. However, after three scrub stages the over-all decontamination factors are only slightly improved by the complexing agents. One of the more promising methods for decreasing zirconium is complexing with oxalate ion (Table X). At a concentration of 0.01 M oxalate ion the extraction of zirconium is reduced almost 60-fold.

Moore investigated the effect of prolonged digestion on zirconium-niobium decontamination in subsequent TBP extraction. A portion of dissolver solution was maintained at 90°C for a 4-week period, and extraction-scrub studies were carried out with samples of the solution, which were withdrawn at 1-, 2-, and 4-week intervals. After 4 weeks' digestion, the niobium decontamination factor decreased from an initial value of 6×10^4 to a value of 7×10^3. Although the effect was not as marked as with niobium, zirconium decontamination was adversely affected.

OTHER SOLVENTS

Limited work has been done on the separation of fissionable materials from fission products by the use of other solvents. For the most part the work is of a scouting nature and incomplete. The solvents considered include: pentaether, diisopropyl ether, dibutyl cellosolve, and many alcohols.

Pentaether

Pentaether is the dibutyl ether of tetraethyleneglycol. Poor separation of fissionable material from fission products is obtained with pentaether primarily because ruthenium is extracted very readily by it. Mixtures of pentaether and butyl alcohol also yield very poor separation from ruthenium. An additional disadvantage is their instability toward the nitric acid systems used in radiochemical processing.

Diisopropyl Ether

Diisopropyl ether has been investigated as a solvent for the recovery of U^{233} from thorium and fission products. This solvent yields separation from fission products comparable to that obtainable with TBP

Table X. Effect of Oxalate on Tributyl Phosphate Extraction of Fission Products

Aqueous phase: 0.1 M $UO_2(NO_3)_2$, 4 M HNO_3
Solvent phase: 0.3 M TBP

Oxalate concentration (M)	Distribution ratio		
	Gross β	Gross γ	Zr
0	2.6×10^4	4.5×10^{-3}	2.9×10^{-3}
0.0001	...	...	2.7×10^{-3}
0.001	...	...	4.1×10^{-3}
0.01	8.7×10^{-5}	6.0×10^{-4}	4.9×10^{-3}

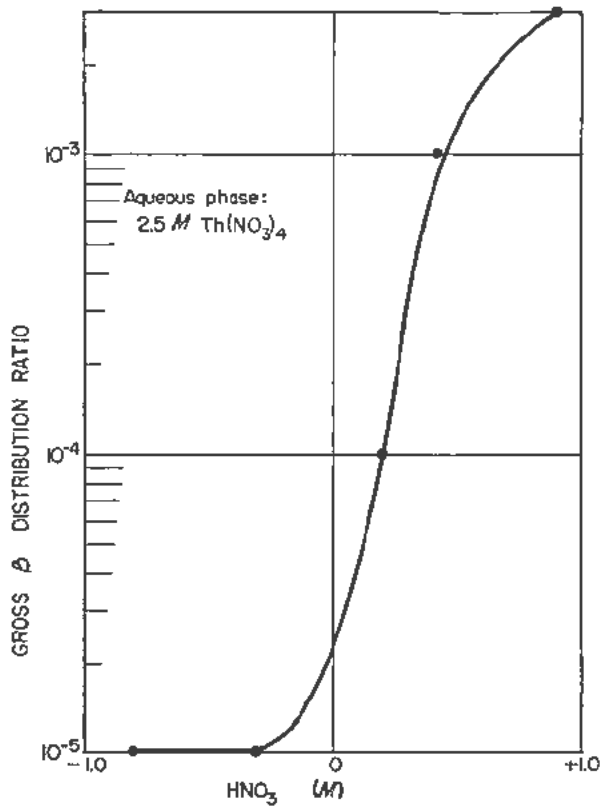

Figure 14. Effect of nitric acid concentration on diisopropyl ether extraction of fission products

and methylisobutyl ketone. However, its low flash point and relative instability toward nitric acid make it less desirable than some of the other solvents. The effect of thorium nitrate and nitric acid concentration on fission product distribution in diisopropyl ether solvent extraction was investigated. Increasing the thorium nitrate concentration from 1.9 *M* to 2.5 *M* increases the gross β distribution ratio from about 2×10^{-5} to 1×10^{-4}. Increasing the acidity in the region of zero free acid results in a marked increase in the fission product distribution ratio. A marked decrease is observed when the acidity is decreased from neutral to the acid deficient region (Fig. 14).

The fission product distribution ratio in ether extraction is practically independent of temperature.

Dibutyl Cellosolve

Dibutyl cellosolve (ethylene glycol dibutyl ether) has also been investigated for the separation of uranium from fission products and thorium. For a given set of conditions in the aqueous phase the distribution ratio of fission products in dibutyl cellosolve extraction is considerably lower than in methylisobutyl ketone extraction. However, the uranium distribution coefficient is correspondingly lower.

Increasing the nitric acid concentration in the region of 0.1 *M* acid causes the fission product distribution ratio to increase rapidly, while a corresponding effect is observed in methylisobutyl ketone when the acidity exceeds the neutral point.

The effect of salting agent concentration on the distribution of γ-emitting fission products in dibutyl cellosolve extraction is interesting since the fission product distribution ratio increases until a strength of about 1 *M* aluminum nitrate is reached and then remains constant. In the salting range between 1 and 2.75 *M*, the γ-activity distribution ratio is almost constant, suggesting the value of this solvent for extraction from highly salted solutions.

Tertiary Alcohols

The extraction of ruthenium tracer by tertiary alcohols from an equal volume of 1 *M* aluminum nitrate—0.2 *M* nitric acid was studied. For tertiary amyl alcohol, 2-methyl—2-pentanol, 2-methyl—2-hexanol, 2-methyl—2-heptanol, and methylisobutyl ketone, ruthenium distribution coefficients were 1.39, 0.55, 0.345, 0.219, 0.087, respectively. Uranium distribution ratios observed with these solvents were low, and it is evident that all are inferior to methylisobutyl ketone as extractants for fissionable material.

Anion Exchange Studies of the Fission Products

By K. A. Kraus and F. Nelson,* USA

I. INTRODUCTION

During the last decade the popularity of ion exchange as a tool in analytical, physical and inorganic chemistry has increased tremendously. The field has repeatedly been reviewed in recent years and a number of excellent books and review articles may be cited for general references.[1-9] A glance at the literature shows that the lion's share of attention has gone to cation exchange, while exploitation of anion exchange has not become prominent until a few years ago. Although large scale anion exchange installations now exist, particularly with respect to hydrometallurgy of uranium, exploitation of anion exchange still lags behind that of cation exchange. It is anticipated that, particularly as far as applications in analytical chemistry are concerned, this situation will change in the next few years. Anion exchange, especially of metal complexes, exhibits a number of unique features, and appears to be a new, powerful and versatile tool which should find soon further broad applications. At present, conditions have been found for the adsorption of essentially all metals on anion exchange resins except for the heavy alkali metals. Since the nonmetals of course are more readily handled as negative ions, this implies that anion exchange may be a more general tool than cation exchange.

Anion exchange of metal complexes shares with cation exchange the many advantages which presumably underlie the rapid expansion of this field and make it so attractive for many applications compared with conventional procedures. Ion exchange procedures in general are simple and separations can be achieved with great speed, provided the ions to be separated have sufficient differences in adsorbabilities. The large number of theoretical plates per unit length which ion exchange columns exhibit, particularly with fine mesh resins, is an additional distinct advantage. Further, with conventional ion exchange resins, diffusion rates are usually sufficiently large to permit operation at reasonably rapid flow rates.

Ion exchange separations are characterized by low cross-contamination, probably one of its most attractive features compared with precipitation techniques. Ion exchange techniques are fairly insensitive to the concentration of the materials to be separated. Concentrations ranging from a few atoms per cm^3 to essentially molar concentrations may be handled with equal ease and similar efficiency, provided column capacities are properly designed. While loading considerations affect mainly the cross-sectional areas of the columns, their length is determined by relative adsorbabilities of the ions to be separated.

The initial impetus towards detailed study of anion exchange of metal complexes came when it was recognized in our laboratory that certain commercial strong-base anion exchange resins show great, and at times startling, selectivities for certain complex ions, particularly the chloride complexes of a number of metals. It thus became possible to operate effectively at high electrolyte concentrations and even in concentrated acids where the commercial resins show remarkable stability. In contrast, cation exchange often fails in these concentrated electrolyte solutions in no small measure because in these media many metals become complexed and improper targets for cation exchange.

Anion exchange is an ideal tool for the handling of those metal ions which must be complexed to keep them in solution, e.g., to prevent hydrolytic precipitation. Many of these elements in the proper complexing medium apparently form negatively charged complexes in sufficient concentration to permit good adsorption on anion exchange resins.

The suitability of anion exchange resins for adsorption from concentrated electrolyte solutions permits exploitation for analytical purposes of the more unusual complexing properties of the elements. These complexes often are formed in sufficient concentration only at high electrolyte concentrations. Apparently the activity coefficient quotients for the complex (formation) equilibria decrease rapidly with increasing ionic strength and complexes whose formation constants are small may become prominent. In view of the high selectivity of the resins for certain complexes, good adsorption may often be achieved with a small fraction of the metal in the form of negatively charged complexes though, of course, in equilibrium with other species.

With anion exchange techniques, separations of metals can often be achieved which "normally" exhibit similar properties. Such "similar" metals, it appears, may show large differences in the stability constants of the higher complexes, even if they have similar stability constants for the lower complexes.

Since anion exchange techniques thus permit ex-

*Oak Ridge National Laboratory.

ploitation of maximum differences among elements. separations can often be achieved with columns very much shorter than customary in cation exchange work with a resultant decrease in the time required to effect a given separation. In favorable cases good separations may even be achieved in times short compared with a minute. Thus daughter radioactivities with half-lives of the order of seconds and of less than a second have been separated from long-lived parent activities.[10] The speed of separation is greatly aided by the fact that with reversible complex equilibria adsorption may, for example, be carried out at high electrolyte concentration and desorption by a simple change in electrolyte concentration or even with water without change in the overall composition of the resin.

Ion exchange techniques may be used for elucidation of the solution chemistry of the materials studied. In this application, anion exchange in dilute solutions resembles the well-established cation exchange techniques which in recent years have been exploited particularly by Schubert.[11] Since adsorbabilities of many metal complexes on anion exchange resins are very high, extension to concentrated electrolyte solutions becomes very attractive, i.e., to a field where further studies are greatly needed. Although a brief outline of the theoretical considerations leading to identification of species and equilibria will be given later, one might mention here that information gained from these ion exchange studies is essentially thermodynamic (see also reference 12). Ion exchange studies of this type can be reduced to the thermodynamics of two-phase equilibria with the resin considered a special solvent.[13] Anion exchange of metal complexes gains its added strength from the fact that the anion exchanger is intrinsically sensitive to detection and measurement of the negatively charged complexes and thus permits elucidation of complex equilibria starting with the most complexed species rather than with the uncomplexed metal ions, for which many thermodynamic methods are available.

These general remarks regarding the advantages of anion exchange are, of course, directly applicable to fission product chemistry. We may classify the use of anion exchange in fission product work: (1) research with fission products, (2) analytical problems involving fission products, and (3) large scale isolations and separations. At the present time the use of anion exchange unquestionably is most promising for research and analysis. Extensive exploitation at high radiation levels will depend on the solution of a number of serious problems, particularly problems involving the radiation stability of the resins. The resins apparently are stable enough for work in moderate radiation fields. Regarding work at very high radiation levels, where many applications are probably not realizable, one may, however, still often be able to use anion exchange effectively if the processes are designed to adsorb the minor activities and permit passage of the major activities through the columns.

II. ANION EXCHANGE TECHNIQUES

We shall confine ourselves to a brief discussion of the techniques which have been used in this laboratory. These, of course, are similar to and largely based on the cation exchange techniques in general use. Differences principally stem from our rather broad utilization of radiometric methods of analysis. Actually, of the about 65 elements studied in this laboratory, radioactive tracers have been used for approximately 55.

The convenience and speed of the tracer method has often been stressed. In recent years the advent of scintillation counters with high γ-efficiency has further increased the attractiveness of the method. Particularly useful is the re-entrant hole scintillation counter[14] which permits direct measurements of activity of a solution in a small test tube. With this instrument analyses can be completed in a few minutes. Additional advantages of the tracer method may be cited. In many cases adsorbabilities may be studied at very low loading of the resin with respect to the metal of interest. In this way results become directly comparable. In general, adsorbability decreases with increasing loading. This effect is small up to about 1% loading but may amount to a 5 to 20-fold decrease between 1 and 20% loading.

Since general access to tracers is rapidly becoming easier, the main disadvantages of the tracer methods appear to be the strict requirements for purity for many applications and the difficulties engendered when the element of interest may have more than one oxidation state under the conditions studied. We have found the anion exchange technique to be of great value in preparing tracers of very high purity. The solution of the oxidation state problem probably can be achieved by supplementing the tracer techniques with more conventional methods at macro concentrations. However, once the anion exchange behavior of the various oxidation states has been established, the technique may be used for identification of the oxidation states, even at concentrations where conventional methods fail.

It must be stressed, however, that in spite of the enormous advantages which the tracer method offers, a great deal of work in the field of ion exchange and anion exchange may be done rapidly and efficiently without tracers. In this laboratory polarography, spectrophotometry, colorimetry and flame spectrophotometry, as well as standard volumetric techniques, have been used to good advantage. For colored ions visual observation of band motion (chromatography) can of course be used as well as spot testing of the effluent. For the spot testing method it appears advantageous to operate with columns of sufficiently small cross-sectional area so that each drop represents an appreciable fraction of a column volume and can be collected and analyzed without aliquoting.

Most of the separation work which has been carried out has involved short columns (usually less than 5

cm). In general a search is made for conditions where such small columns would be effective and careful chromatographic techniques not necessary. Further, a search was made for eluting conditions where adsorption is sufficiently small to permit effective removal of the ions in a few column volumes or preferably in one column volume. To achieve these objectives it has become standard in this laboratory to measure adsorbabilities over a large range of conditions.

Adsorbabilities have been studied principally by four techniques: (1) column effluent analysis, (2) column scanning, (3) equilibration method, and (4) special methods for measurement of high distributon coefficients.

The column effluent analysis appears to be most suited for conditions where the ion of interest is not strongly adsorbed. It becomes rather cumbersome when more than ca 10 column volumes are necessary to remove the adsorption maximum. The column effluent method directly yields the elution constant, E.[15] From $1/E$, the number of (geometric) column volumes necessary to obtain the eluted ion in maximum concentration in the effluent, the volume distribution coefficient, D_v (amount per liter of bed/amount per liter of solution), may be evaluated by the relationship

$$D_v = 1/E - i \qquad (1)$$

where i is the fractional interstitial space. For more strongly adsorbed ions the scanning method may be used[15] which also yields E.

For strongly adsorbed ions the equilibration technique, however, appears to be more convenient, as pointed out particularly by Schubert.[11] Samples of resin and solution are agitated long enough to establish equilibrium which with the resins used here was usually less than 1 to 2 days. The ratio of resin weight to solution volume is preferably adjusted so that approximately 50% of the material of interest is adsorbed. From the decrease in concentration on equilibration the distribution coefficient D (amount per kg dry resin/amount per liter of solution) may be computed. The values of D may readily be correlated with anticipated column behavior since the number of column volumes necessary to elute the material in maximum concentration is given by $(D_v + i)$ and since D and D_v are related by the bed density (ca 0.45 kg dry resin per liter of bed).

For measurements of extremely high distribution coefficients (e.g., $D > 10^4$ or 10^5) it has been found advantageous first to adsorb the tracer uniformly on the resin and then to measure the concentration of solutions in equilibrium with it. Equilibrium may be achieved either by passing solutions through a bed containing the tracer loaded resin or by agitating resin and solution. Placing the tracer on the resin first permits attainment of equilibrium in each individual experiment in very much shorter times at high values of D than when adsorption is carried out with the tracer originally in the solution.

III. SURVEY OF ANION EXCHANGE STUDIES

For the last six or seven years a systematic survey of the anion exchange behavior of the metals has been carried out in this laboratory. Although the investigations have involved a number of media, the survey in HCl solutions is most nearly complete, and at present includes most of the fission products.

The original intent was to study only those metals which form relatively weak complexes and for which the complexes are in rapid equilibrium with the uncomplexed ions. If these metals show good adsorption at high concentration of complexing agent (e.g., concentrated HCl) adsorption-elution cycles would become particularly simple since negligible adsorption should occur at low concentration of complexing agent, and elution with dilute HCl or even water becomes possible. As this survey progressed, it became desirable, for comparative reasons, to include the more stable complexes, those which are not in rapid equilibrium with the uncomplexed species and those for which no adsorbable complexes were anticipated.

The adsorption data for HCl solutions are summarized in Fig. 1 as a series of graphs of log D_v vs M HCl, where D_v is the volume distribution coefficient and M the molarity. Figure 1 was compiled from previously published and unpublished results obtained at this laboratory. The only exceptions are the data for Nb(V) and Ta(V), taken from the work of Huffman and Lilly, and the data for Te(IV) where the observations of Sasaki were used. Literature references pertinent to Fig. 1 may be found italicized in Table I-A.

In a few cases quantitative information as a function of M HCl was not available, but sufficient experiments had been carried out to indicate that the elements were strongly adsorbed over most of the conditions studied (0.1 M HCl to 12 M HCl). These cases are identified in Fig. 1 by "Str. Ads." Work at this laboratory in hydrochloric acid solutions was carried out with one batch of resin (quaternary amine polystyrene divinyl benzene resin, ca 200 mesh, 10% DVB). Difficulties resulting from differences in selectivities, particularly with resins of different cross-linking, were thus avoided, and the data in Fig. 1 are essentially comparable.

From a glance at Fig. 1 it becomes apparent that the elements can be roughly classified into three groups with respect to their anion exchange behavior:

1. Many elements are not adsorbed from HCl solutions at any concentration. In this class fall the alkali metals, the alkaline earths and largely the elements of Group III-B (Y to Ac). Surprisingly Al(III) is also in this group of non-adsorbable ions, as well as Ni(II) and Th(IV).

2. Many elements show increasing absorption with increasing M HCl and usually good adsorption only

Table 1. Survey of Anion Exchange Studies of Metal Complexes

A. Hydrochloric Acid and Other Chloride Solutions

(Figure 1 based on italicized references)

Atomic no. and element		References	Atomic no. and element		References
3	Li	J-1, *K-9*, M-4	45	Rh	B-3, C-3, *K-15*, M-1
4	Be	*K-9*, K-12, M-4	46	Pd	B-3, *K-9*, N-1, M-1
11	Na	J-1, *K-9*, M-4	47	Ag	*K-15*
12	Mg	J-1, *K-9*, M-4	48	Cd	B-5, J-1, K-9, *K-15*
13	Al	B-1, J-1, *K-9*, M-4	49	In	J-1, *K-9*
19	K	J-1, *K-9*, M-4	50	Sn	J-1, *K-15*
20	Ca	J-1, *K-9*, M-4	51	Sb	*K-15*
21	Sc	*K-9*, K-12	52	Te	*S-3*
22	Ti	*K-9*	55	Cs	*K-9*, M-4
23	V	*K-9*	56	Ba	*K-9*, M-4
24	Cr	H-8, *K-15*, M-4, N-1, S-6	57-71	R.E.	*K-9*, M-4
25	Mn	B-1, H-8, J-1, *K-8*, K-12	72	Hf	H-4, H-7, *K-15*
26	Fe	B-1, H-8, J-1, *K-8*(II), K-11 K-12, *K-15*(III), M-4, R-2	73	Ta	*H-7*, K-6
			74	W	*K-13*
27	Co	B1, H-8, J-1, *K-8*, K-12, M-5	75	Re	*K-15*, M-2
28	Ni	B-1, H-8, J-1, K-8, *M-5*	76	Os	*K-15*
29	Cu	J-1, *K-8*(II), *K-15*(I)	77	Ir	C-3, B-3, *K-9*(IV), M-1, *K-15*(III)
30	Zn	B-5, J-1, *K-8*, K-12, M-3	78	Pt	B-3, *K-9*, M-1, N-1
31	Ga	*K-9*, K-12	79	Au	*K-10*, K-12, N-1, S-6
32	Ge	*N-5*, Y-1	80	Hg	*K-15*
33	As	J-1, *N-5*, Y-1	81	Tl	*K-9*
34	Se	S-3, *K-15*	82	Pb	C-1, J-1, *N-2*
37	Rb	*K-9*, M-4	83	Bi	C-1, *N-2*
38	Sr	*K-9*, M-4	84	Po	*S-3*
39	Y	*K-9*	87	Fr	*K-9*
40	Zr	H-4, H-7, *K-15*	88	Ra	*K-9*
41	Nb	*H-7*, K-5	89	Ac	*K-9*
42	Mo	*K-13*, M-2, S-6	90	Th	*K-14*
43	Tc	*K-15*	91	Pa	*K-4*, K-7, K-11
44	Ru	B-3, *K-15*	92	U	*K-13*

B. Anion Exchange Studies of Fission Products in Other Media

Solution	Element	References
Fluoride and HF-HCl Mixtures	Zr	F-2, F-3, F-4, H-6, K-2, K-5, K-7
	Nb	F-4, H-1, K-3, K-5, K-7
	Mo	F-4, H-1, K-13
	Sn	F-4
Bromide and Iodide	Zn	B-5, H-3
	Ga	H-3
	Cd	B-5, F-5, L-1
	Sb	L-2
Hydroxide	Ge	E-1
	As	E-1
	Mo	F-1, H-2, M-2
	Ru	B-3
	Rh	B-3
	Pd	B-3
	$I(IO_3^-)$	K-1
Nitrate	$Br(Br^-)$	A-1, R-1
	$I(I^-)$	A-1
Cyanide	Zn	B-4
	Ag	J-2
Thiocyanate	Tc^-	A-1, H-2
Sulphate	Cd	L-1
	In	S-5
Acetate	Ce	F-5
Oxalate	Ga	B-2
	Y	C-2
	Zr	W-1
	Nb	G-1, W-1
	Mo	M-2
	Sn	L-2, S-4
	Sb	L-2, S-4
	Te	S-4
Citrate	Sr	N-4, S-1
	Ba	N-4, S-1
	R.E.	H-5
Ethylenediaminetetraacetic acid (EDTA)	Zn	S-7
	Rb	N-3
	Cs	N-3

A-1 Atteberry, R. W. and Boyd, G. E., J. Am. Chem. Soc. *72*: 4805 (1950).

B-1 Biasius, E. and Negwer, M., Naturwissenschaften *39*: 257 (1952).

B-2 Biasius, E. and Negwer, M. Z. anal. Chem. *143*: 257 (1954).

B-3 Biasius, E. and Wachtel, U., Angew. Chem. *66*: 305 (1954).

B-4 Burstad, F. H., Kembler, N. F., Forrest, P. and Weeks, R. A., Ind. Eng. Chem. *45*: 1648 (1953).

B-5 Baggott, E. R. and Willcocks, R. G. W., Analyst *80*: 53 (1955).

C-1 Campbell, E. C. and Nelson, F., Phys. Rev. *91*: 499A (1953).
C-2 Crouthamel, C. E. and Martin, D. S. Jr., J. Am. Chem. Soc. *72*: 1382 (1950).
C-3 Cluett, M. L., Berman, S. S. and McBride, W. A. Analyst *80*: *204* (1955).
E-1 Everest, D. and Salmon, J. L., Chem. Soc. 2438 (1954).
F-1 Fisher, S. A. and Meloche, V. W., Anal. Chem. *24*: 1100 (1952).
F-2 Forsling, W., Arkiv Kemi *5*: 489 (1953).
F-3 Forsling, W., Arkiv Kemi *5*: 503 (1953).
F-4 Freund, H. and Miner, F. J., Anal. Chem. *25*: 564 (1953).
F-5 Fronaeus, S., Svensk Kem. Tidskr. *65*: 1 (1953).
G-1 Gillis, J., Eeckhaut, Z., Cornand, P. and Speecke, A., Mededel. Koninkl. Vlaam. Acad. Wetenschap. Belg. *15*: 3 (1953). See also C. A. *48*: 9862^e (1954).
H-1 Hague, J. L., Brown, E. D. and Bright, H. A., J. Research Nat. Bur. Standards *53*: 261 (1954).
H-2 Hall, N. and Johns, D., J. Am. Chem. Soc. *75*: 5787 (1953).
H-3 Herber, R. H. and Irvine, J. W., J. Am. Chem. Soc. *76*: 987 (1954).
H-4 Huffman, E. H. and Lilly, R. C., J. Am. Chem. Soc. *71*: 4147 (1949).
H-5 Huffman, E. H. and Ostwalt, R. L., J. Am. Chem. Soc. *72*: 3323 (1950).
H-6 Huffman, E. H. and Lilly, R. C., J. Am. Chem. Soc. *73*: 2902 (1951).
H-7 Huffman, E. H., Lilly, R. C. and Iddings, G. M., J. Am. Chem. Soc. *73*: 4474 (1951).
H-8 Hague, J. L., Maczkowske, E. E. and Bright, H. A., J. Research Nat. Bur. Stds. *53*: 353 (1954).
J-1 Jentzsch, D. and Frotscher, I., Z. anal. Chem. *144*: 17 (1955).
J-2 Jones, L. H. and Penneman, R. A., J. Chem. Phys. *22*: 965 (1954).
K-1 Kikindai, M., Compt. rend. *237*: 250 (1953).
K-2 Kraus, K. A. and Moore, G. E., J. Am. Chem. Soc. *71*: 3263 (1949).
K-3 Kraus, K. A. and Moore, G. E., J. Am. Chem. Soc. *71*: 3855 (1949).
K-4 Kraus, K. A. and Moore, G. E., J. Am. Chem. Soc. *72*: 4293 (1950).
K-5 Kraus, K. A. and Moore, G. E., J. Am. Chem. Soc. *73*: 9 (1951).
K-6 Kraus, K. A. and Moore, G. E., J. Am. Chem. Soc. *73*: 13 (1951).
K-7 Kraus, K. A. and Moore, G. E., J. Am. Chem. Soc. *73*: 2900 (1951).
K-8 Kraus, K. A. and Moore, G. E., J. Am. Chem. Soc. *75*: 1460 (1953).
K-9 Kraus, K. A., Nelson, F. and Smith, G. W., J. Phys. Chem. *58*: 11 (11954).
K-10 Kraus, K. A. and Nelson, F., J. Am. Chem. Soc. *76*: 984 (1954).
K-11 Kraus, K. A. and Moore, G. E., J. Am. Chem. Soc. *77*: 1383 (1955).
K-12 Kraus, K. A., Nelson, F., Clough, F. B. and Carlston, R. C., J. Am. Chem. Soc. *77*: 1391 (1955).
K-13 Kraus, K. A., Nelson, F. and Moore, G. E., J. Am. Chem. Soc. *77*: 3972 (1955).
K-14 Kraus, K. A. and Moore, G. E. (to be published).
K-15 Kraus, K. A. and Nelson, F. (previously unpublished work).
L-1 Leden, I., Svensk Kem. Tidskr. *64*: 145 (1952).
L-2 Luré, Yu. Yit. and Filippova, N. A., Zavodskaya Lab. *14*: 159 (1948).
M-1 MacNevin, W. M. and Crummet, W. B., Anal. Chem. *25*: 1628 (1953).
M-2 Meloche, V. W. and Preuss, A. F., Anal. Chem. *26*: 1911 (1954).
M-3 Miller, C. C. and Hunter, J. A., Analyst *79*: 483 (1954).
M-4 Moore, G. E. and Kraus, K. A., J. Am. Chem. Soc. *72*: 5792 (1950).
M-5 Moore, G. E. and Kraus, K. A., J. Am. Chem. Soc. *74*: 843 (1952).
N-1 Nachod, F., U.S. Patent 2,371,119 (March 6, 1945).
N-2 Nelson, F. and Kraus, K. A., J. Am. Chem. Soc. *76*: 5916 (1954).
N-3 Nelson, F., J. Am. Chem. Soc. *77*: 813 (1955).
N-4 Nelson, F. and Kraus, K. A., J. Am. Chem. Soc. *77*: 801 (1955).
N-5 Nelson, F. and Kraus, K. A., J. Am. Chem. Soc. *77*: 4508 (1955).
R-1 Rieman, W. III. and Lindenbaum, S., Anal. Chem. *24*: 1199 (1952).
R-2 Reents, A. C. and Kohler, F. H., Ind. Eng. Chem. *47*: 75 (1955).
S-1 Samuelson, O., Lunde, L. and Schramm, K., Z. Anal. Chem. *140*: 330 (1953).
S-2 Samuelson, O. and Sjoström, K., Anal. Chem. *26*: 1908 (1954).
S-3 Sasaki, Y., Bull. Chem. Soc. Japan *28*: 89 (1955).
S-4 Smith, G. W. and Reynolds, S., Anal. Chim. Acta *12*: 151 (1955).
S-5 Sunden, N., Svensk Kem. Tidskr. *66*: 173 (1954).
S-6 Sussman, S., Nachod, F. C. and Wood, W., Ind. Eng. Chem. *37*: 618 (1945).
S-7 Samuelson, O., Sjoström, K. and Forsblom, S., Z. Anal. Chem. *144*: 21 (1955).
W-1 Walker, R. E. and Baldwin, W. H., U.S. A.E.C. Report ORNL-637 (1950), Nuclear Sc. Abstr. *4*: 469 (1950), Brit. Abst. C244 (1951).
Y-1 Yoshino, Y., Bull. Chem. Soc. Japan *28*: 382 (1955).

at high *M* HCl. Some of these elements show adsorption maxima.

3. Many elements, located principally in the central part of the periodic table, show only decreasing adsorption with increasing *M* HCl, at least in the region 1 to 12 *M* HCl. In this group fall the second and third row transition elements which are generally recognized to be excellent complex formers with chloride ions.

References to similar work carried out in other laboratories are given in Table I-A. In general, agreement between various laboratories using different resins, though of the same type, has been gratifying. Table I-A is considered reasonably complete except for the large body of work on stable anions, e.g., halides, nitrates, etc., which has been a standard part of the important basic studies on the selectivities and characterization of anion exchange resins (see e.g., references 16 and 17). For more detailed information regarding the ion exchange behavior of these stable anions the many review articles and books on the field may be consulted.

In Table I-A, references to chloride solutions other than hydrochloric acid have been included. Recently (reference K-12 of Table I) a startling difference in the adsorbability of a large number of metal ions in lithium chloride solutions compared with hydrochloric acid solutions has been observed. Further exploitation of these low acidity media appears highly attractive.

A survey of the anion exchange studies of the fission products in other media is given in Table I-B.

As far as our work is concerned, relatively little attention to media other than hydrochloric acid has been given except when special reasons necessitated it. Thus, for example, certain elements particularly of the fourth and fifth groups show highly unfavorable hydrolytic properties in most HCl solutions,

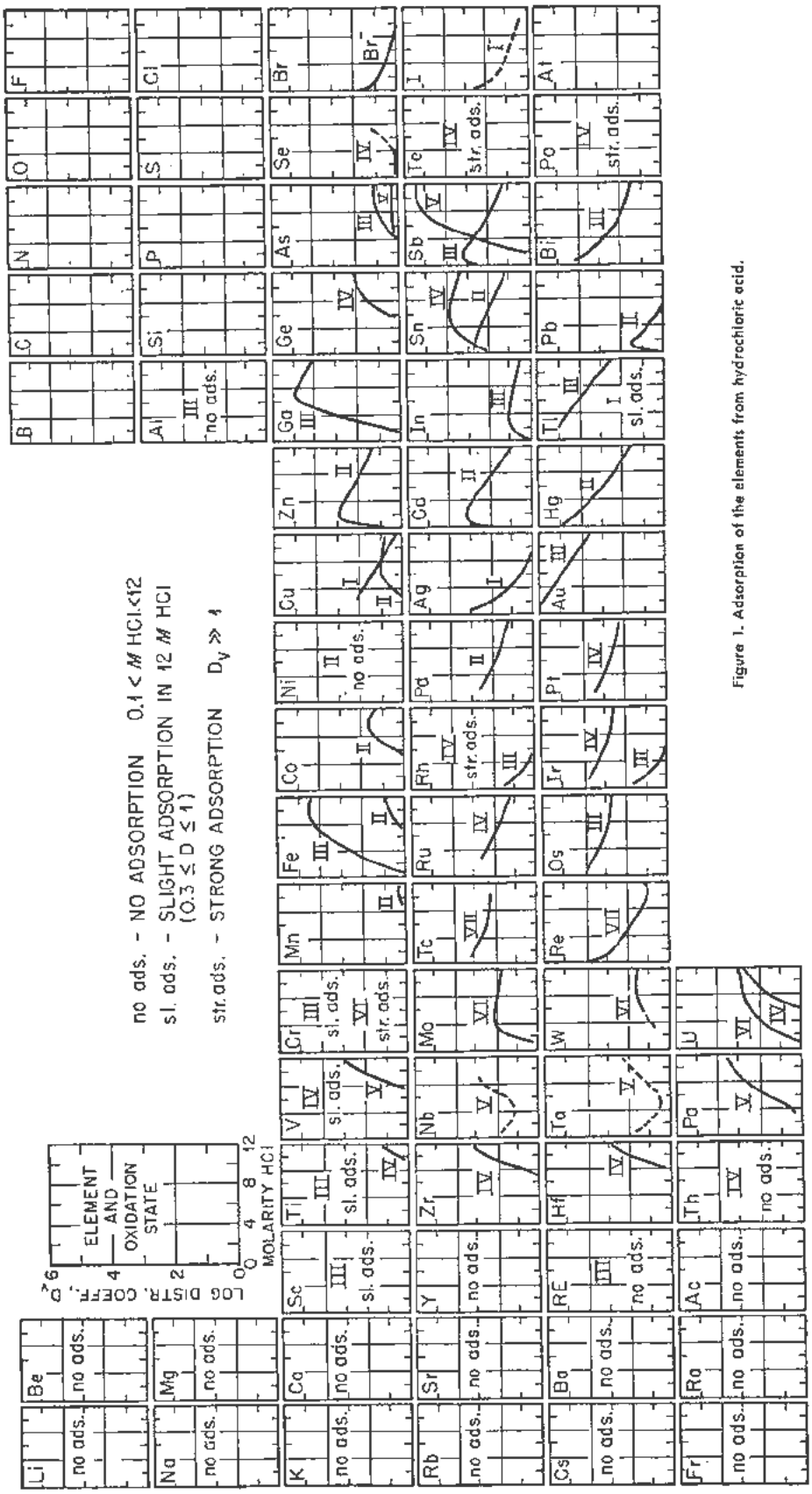

Figure 1. Adsorption of the elements from hydrochloric acid.

which might seriously interfere with separations. In an attempt to avoid these difficulties, studies were carried out in HF-HCl mixtures. Further, for the elements which show essentially negligible adsorption from HCl solutions, other complexing agents are indicated. In many cases citrates or ethylenediaminetetraacetic acid (EDTA) proved satisfactory. Our investigations with the other common mineral acids (nitric acid and sulfuric acid) have so far been limited to uranium and very few other elements. Exploitation of these media appears highly promising.

IV. ANION EXCHANGE STUDIES OF THE FISSION PRODUCTS AND URANIUM

This section will deal principally with the implications and applications of the anion exchange studies at ORNL to separations involving the fission products. A brief discussion of each fission product will be given. Since uranium occupies an obviously unusual position with respect to fission product chemistry, information regarding this element is also included in some detail.

The adsorption data described in Fig. 1 can be used directly to devise a large number of separation schemes. Actually, it may be noticed that most elements differ sufficiently from each other in their adsorbabilities that separations are at least intrinsically possible although for a few of these some reservations must be made.

Anion Exchange Studies of Uranium(VI)

Adsorption behavior of uranium(VI) has been studied in HCl solutions and HF-HCl mixtures (reference K-13, Table I), as well as in nitrate and sulfate solutions (reference K-15). Adsorption of uranium(VI) occurs from all these media although the characteristic adsorption functions ($\log D$ vs M HCl) differ widely.

The adsorbability of uranium(VI) rises steeply with increasing HCl concentration from D = ca 1 in 1 M HCl to D = ca 1800 near 9 M HCl. At higher concentrations, D decreases slightly (Fig. 2).

In nitric acid, adsorbability of uranium(VI) becomes significant near 2M HNO_3 where D = ca 1 and then rises to D = ca 20 near 8 M HNO_3 (Fig. 2). Above this concentration the equilibration experiments yielded irreproducible results, probably due to decomposition of the resin by the rather concentrated nitric acid.

Adsorption of uranium(VI) from other nitrate solutions of low acidity has also been studied. At constant nitrate concentration, adsorbability from these media is considerably larger. For example, distribution coefficients of the order of 10^3 have been found for 2.5 M $Al(NO_3)_3$—0.5 M HNO_3 solutions.

The adsorption function of uranium(VI) in sulfuric acid differs markedly from those in HCl or HNO_3 (Fig. 2). Thus, adsorption is very high at low sulfuric acid concentration (D = 35,000 in 0.01 M H_2SO_4) and decreases rapidly with increasing M H_2SO_4 to D = ca 1 in 4 M H_2SO_4. However, at 4 M H_2SO_4, quantitative elution of uranium cannot readily be achieved at room temperature with small volumes of eluent, probably because of slow rates of diffusion. By increasing the elution temperature, satisfactory removal with little tailing can be achieved, even with 1–2 M H_2SO_4.

Adsorption of uranium(VI) from $(NH_4)_2SO_4$ solutions resembles that from H_2SO_4. At low concentrations the distribution coefficients for both media are approximately the same. However, the decrease in D with concentration is considerably less rapid for ammonium sulfate than sulfuric acid. Thus D = 500 in 4 M $(NH_4)_2SO_4$.

Adsorption of uranium(VI) from HF solutions has not been studied. However, data are available on adsorbabilities from HF-HCl mixtures at constant HF concentration (1 M). It was found that presence of 1 M HF affects adsorption of U(VI) little at high M HCl, that at low M HCl adsorption from these mixtures is considerably poorer than from HCl alone, and that at still lower HCl concentration (< 1 M HCl) adsorption of U(VI) rises again rapidly with decreasing M HCl. This behavior is presumably due to formation of positively charged fluoride complexes of U(VI) at high M HCl, which decrease the fraction of U(VI) in the form of an adsorbable chloride complex, and to adsorption of negatively charged fluoride complexes at low M HCl.

The highly varied adsorption properties of uranium(VI) in the various mineral acids should make anion exchange separations of this element from es-

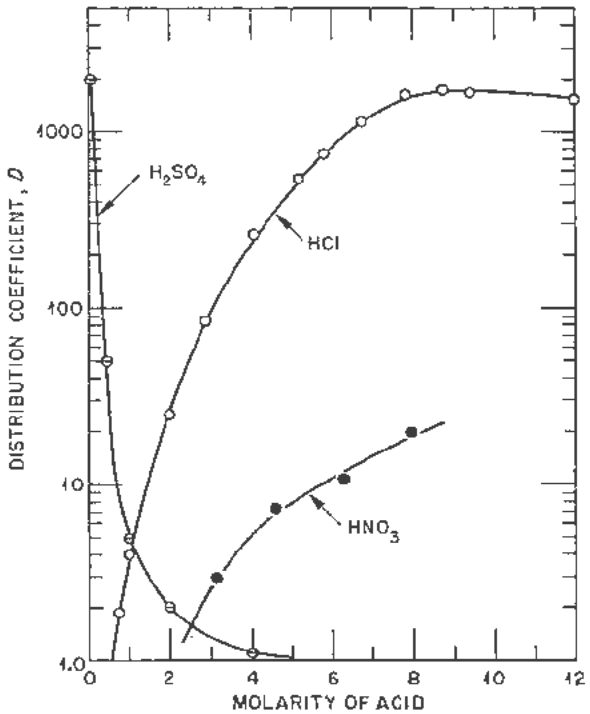

Figure 2. Adsorption of U(VI) from various mineral acids

sentially all other elements relatively simple. Actually, the unusual complexing properties of U(VI) might be expected to produce interesting anion exchange behavior for this ion in many other media.

Rb, Cs, Sr, Ba, Y, Rare Earths

These fission products [except Ce(IV)] show essentially negligible adsorption from HCl solutions and apparently also from LiCl solutions. However, separation of this group of "non-adsorbable" elements from uranium and all other fission produets cannot be achieved in a single pass of e.g., a concentrated HCl solution through an anion exchanger. Although under these conditions uranium and most of the fission products will be retained, a number of other elements (e.g., As(V), Rh(III), Ag(I), Br^-) may also appear in the effluent. Of these "interfering" ions, As(V) poses the most serious problem, although it is removable when the solution volume is small compared with the column volume. Most of the other interfering ions may readily be removed by a second pass through the exchanger at low HCl concentration (e.g., 0.5 *M*) i.e., under conditions where these interfering elements show good adsorption.

To achieve separations within this group on HCl-nonadsorbable-elements, other complexing agents are needed. Citrates and ethylenediaminetetraacetic acid (EDTA) have been used to good advantage. Thus the alkali metals show negligible adsorption from citrate solutions while Sr, Ba, Y, rare earths and, presumably, most other elements in the periodic table show good adsorption (see also reference S-1 of Table I). Thus citrate promises to become the hasis of a very simple anion exchange method for the specific isolation of the fission products Rb and Cs. Other techniques (e.g., cation exchange) will probably be necessary to separate these two elements from each other. A similar situation appears to occur with EDTA where Rb and Cs may be the only non-adsorbable fission products (see also reference S-7).

Citrate and EDTA media may also he used for more detailed separations within this group of elements. Thus, the separation of Ba from Sr has been reported for citrate solutions. Excellent separation of the rare earths from Ba (and presumably also Sr) can be achieved with either citrates or EDTA (see Fig. 3). Further, partial separation of the rare earths, Pm(III) and Eu(III), has been reported (reference H-5).

Zr and Nb

Both of these elements are strongly adsorbed from concentrated hydrochloric acid solutions. Zr(IV) may be eluted, though with extensive tailing, at low HCl concentrations. At very low metal concentration elution of Nb(V) at low *M* HCl may also be feasible. However, in view of the unfavorable hydrolytic properties of these elements, particularly Nb(V), the use of HCl media for separations does not appear attractive. Instead, operation in stronger complexing solutions is desirable. Successful separations involving Zr and Nb have been achieved in HF-HCl media and details regarding these separations have been described. The insensitivity of uranium(VI) adsorption to presence of HF at high HCl concentrations and its sensitivity at low *M* HCl permits its separation from these elements under a variety of conditions.

Separations involving Zr(IV) and Nb(V) have also been described for oxalate solutions (reference G-1, W-1).

Mo and Tc

Only the higher oxidation states, Mo(VI) and Tc(VII), have been studied. The adsorption function of Mo(VI) in hydrochloric acid is very similar to that of U(VI). This similarity precludes satisfactory separation of these elements in HCl. However, they may readily be separated from each other in HF-HCl mixtures.

Detailed studies on the adsorption behavior of Mo(VI) in oxalate, hydroxide and perchlorate solutions have also been reported (reference F-1, M-2).

Tc(VII) (TcO_4^-) shows good adsorption in the range 0.1 to 12 *M* HCl. Adsorption decreases with increasing *M* HCl in a manner which appears to be characteristic for stable negatively charged ions. Unfortunately, however, adsorption does not become low enough to permit simple removal in 12 *M* HCl. Elution of Tc(VII) from anion exchange columns has

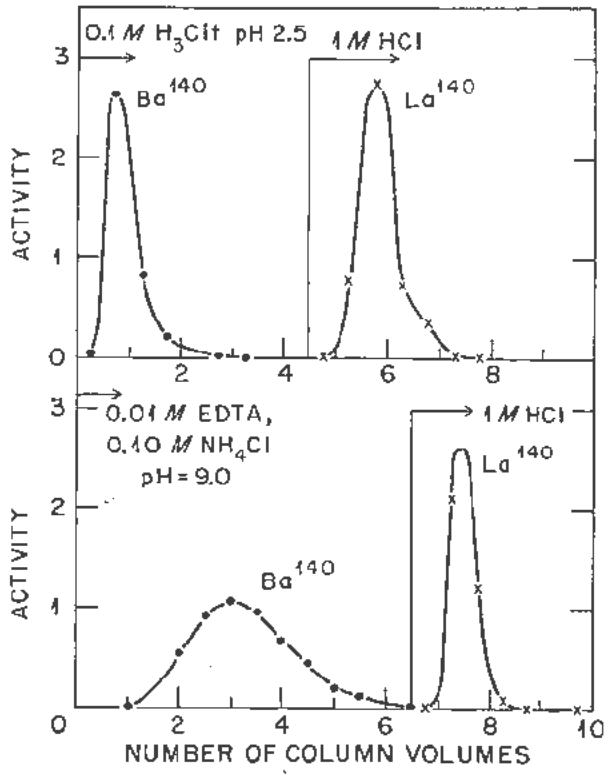

Figure 3. Separation of Ba and La by anion exchange

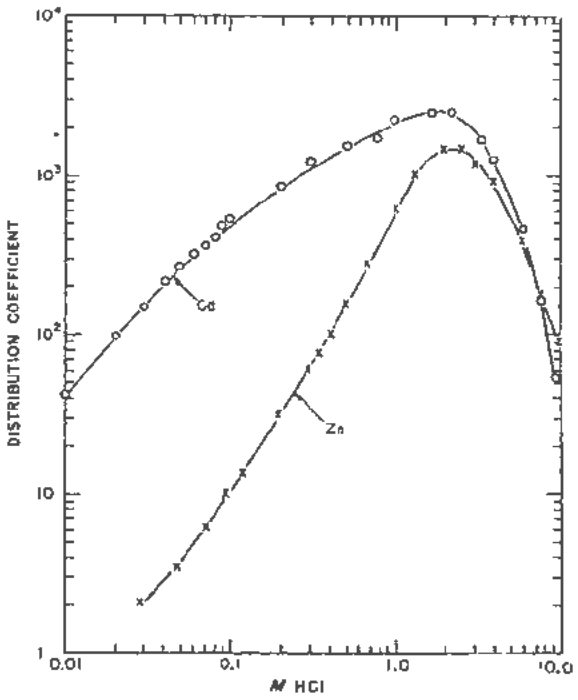

Figure 4. Anion exchange adsorption of Zn(II) and Cd(II)

been reported with SCN^- in connection with the separation of Mo and Tc (reference A-1).

Ru, Rh and Pd

These elements in the various oxidation states studied show decreasing adsorption with increasing HCl concentration of the type characteristic for stable negatively charged complexes. The chloro-complexes of Ru(IV), Rh(IV) and Pd(II) (and presumably also of Pd(IV)) are still strongly adsorbed at high hydrochloric acid concentrations and their removal from the anion exchange columns calls for special techniques. Displacement of the strongly adsorbed Pd(II) complex by other strongly adsorbed chloro-complexes (those of Zn(II) or Cd(II) has proven successful. Rh(III) ($RhCl_6^{---}$) shows only negligible adsorption above 4 *M* HCl and hence it may readily be removed from columns. Further, the low adsorbability of Rh(III) at high *M* HCl may become the basis of anion exchange separations involving this element. The chemistry of Ru has not been studied in sufficient detail to predict its behavior under most conditions apt to be encountered. Unquestionably detailed investigations involving this element in its multiplicity of oxidation states and with its large variety of species (not in equilibrium with each other) must be carried out before it can be handled with confidence.

The anion exchange behavior of the platinum metals in several media including also hydroxides and oxalates has been described (reference B-3).

Ag

This element adsorbs strongly at low *M* HCl and the distribution coefficients decrease with increasing *M* HCl. Adsorbability becomes negligible in concentrated HCl. The anion exchange behavior of Ag(I) is sufficiently unusual to permit rapid isolation of this element, for most purposes in one adsorption-elution cycle, such as adsorption at low *M* HCl and elution at high *M* HCl. The relatively low solubility of Ag in chloride solutions does not appear to present difficulties at tracer concentrations.

Zn and Cd

Adsorption of both of these elements from hydrochloric acid solutions is already high in 0.1 *M* HCl, reaches a maximum near 2 *M* HCl and then decreases with further increasing *M* HCl. Removal of these elements from anion exchange columns can readily be achieved at very low hydrochloric acid concentrations or with water. The differences in the adsorption characteristics of these two elements at low acidities are sufficient to permit their separation from each other (Fig. 4). Thus, Zn may be removed with 0.01 *M* HCl where $D_{Zn} < 1$ and where D_{Cd} is still ca 40. Elution of Cd(II) can then be carried out at *M* HCl $< 10^{-3}$ *M*.

The adsorption functions for these two elements are sufficiently unique to permit isolation of these elements usually in one adsorption-elution cycle.

Ga and In

Adsorption of Ga(III) from HCl solutions becomes appreciable near 2 *M* HCl and rises rapidly to a maximum near 8 *M* HCl. Adsorption of In(III) becomes appreciable near 0.1 *M* HCl, rises slowly to a shallow maximum near 4 *M* HCl ($D = 23$), and then decreases to $D =$ ca 7 in 12 *M* HCl. As described earlier, the separation of Ga from In may readily be achieved and the adsorption functions of these two elements are sufficiently unique to permit ready isolation from most fission products.

Ge and Sn

Adsorption of Ge(IV) becomes appreciable near 4 *M* HCl and increases rapidly with increasing *M* HCl. The adsorption function is sufficiently different from those of the other fission products to make unique isolation of this element feasible. However, the high volatility of Ge(IV) from concentrated HCl solutions and the resulting possibility of loss limits the usable hydrochloric acid concentrations to less than ca 8 *M* if no further precautions are taken.

Both Sn(II) and Sn(IV) adsorb strongly from concentrated hydrochloric acid solutions. The adsorption function of Sn(II) decreases with increasing *M* HCl, while that of Sn(IV) shows a maximum near 7 *M* HCl. Elution of Sn(II) and Sn(IV) with HCl is difficult since these ions hydrolyze at low hydrochloric acid concentrations. However, the high

stability of the fluoride complexes, particularly of Sn(IV), suggests that elution may be carried out with HF-HCl mixtures (see also reference F-4 in Table I). Actually, the use of HF-HCl mixtures should prove advantageous for these elements and the elements of group V-A, as they had earlier been shown to be advantageous for separations involving groups IV-B and V-B (see e.g., section on Zr and Nb).

Separations involving Sn(IV) have also been reported for oxalate solutions (reference L-2, S-4).

As and Sb

Adsorption of As(III) becomes appreciable above 4 *M* HCl and increases with increasing *M* HCl to $D =$ ca 25 in concentrated HCl. Adsorption of As(V), though appreciable even in 0.1 *M* HCl, never becomes very large, *D* remaining less than 4 even in concentrated HCl. The differences between the two ions are sufficient for separation of the two oxidation states, and they both differ sufficiently from the other fission products and uranium(VI) to make their isolation relatively simple.

Adsorption of Sb(III) is already high near 0.1 *M* HCl. Adsorption of Sb(V) becomes appreciable near 2 *M* HCl. For both ions adsorption first increases with increasing *M* HCl. An adsorption maximum occurs for Sb(III) near 2 *M* HCl. In concentrated HCl both oxidation states are strongly adsorbed. Separations involving antimony are difficult in HCl alone since the rate of desorption of Sb(V) in dilute HCl is slow, possibly because of slow equilibria between various Sb(V) complexes and since for Sb(III) hydrolytic difficulties appear at low *M* HCl, where desorption otherwise should be feasible.

As with Ge and Sn, study of the adsorbabilities of these elements in HF-HCl media should prove profitable for separations.

Work on separations involving Sb(V) in oxalate solutions has been reported (reference L-2, S-4).

Se, Te, Br and I

Se(IV) adsorbs only slightly in solutions of moderate HCl concentration. Distribution coefficients increase rapidly above 6 *M* HCl. Separations involving Se(IV) have been described (S-3) in which Se(IV) is adsorbed from 12 *M* HCl and eluted with 6 *M* HCl. Work in this Laboratory, however, shows (K-15) that if Se(IV) is permitted to age several hours in concentrated HCl, selenium species form (possibly $SeCl_4$ or $SeOCl_2$) which are not in rapid equilibrium with each other and which cannot easily be eluted with HCl solutions. However, rapid elution was achieved with methyl alcohol.

Tellurium has not been studied in this Laboratory. Data on the adsorbability of Te(IV) from HCl solutions (reference S-3) and oxalate solutions (reference S-4) have been reported.

Br^- and I^- adsorb strongly from dilute HCl solutions, as is well known, and adsorbability decreases rapidly with increasing *M* HCl. Since I^- (and to some extent Br^-) tends to be oxidized to the element in strong hydrochloric acid solutions and since the elementary halogens are strongly adsorbed by the resins, separations in these media, particularly at tracer concentrations, become complicated. Separation of the halides in nitrate solutions are described in the literature (reference A-1, R-1).

Separation and Identification of Different Oxidation States of the Same Elements

As one might anticipate, different oxidation states of an element usually show considerable differences in adsorption properties. In many cases these differences may be utilized for separation of the oxidation states from each other. As a corollary, they also permit identification of specific oxidation states. This latter application appears particularly attractive for studies at trace concentrations where the usual tests with more concentrated solutions cannot be used and where precipitation reactions leave a considerable margin of error because of cross-contamination (carrying). Among the elements of interest here, useful differences in adsorption properties are shown in hydrochloric acid solutions as As(III) and As(V), Rh(III) and Rh(IV), and U(IV) and U(VI).

V. SOME CONSIDERATIONS REGARDING SPECIES IN SOLUTION

Detailed discussion of the thermodynamic aspects of anion exchange cannot be undertaken here. For dilute solutions the thermodynamics has repeatedly been discussed for cation exchange and the same considerations apply here. However, since a considerable portion of anion exchange studies is carried out in concentrated electrolyte solutions where available discussions are inadequate, a brief review of the pertinent considerations seems in order. Without significant loss in generality we shall restrict ourselves to those cases where the eluting ion and the complexing ion are the same as occurs, for example, in HCl media.

The mass action expression for the equilibrium

$$aMA_n^{-\nu} + \nu(A^{-a})_r \rightleftharpoons a(MA_n^{-\nu})_r + \nu A^{-a} \quad (2)$$

may be written as

$$K = \frac{(MA_n^{-\nu})^a_r\,(A^{-a})^\nu}{(MA_n^{-\nu})^a\,(A^{-a})_r^\nu} G \quad (3)$$

where

$$G = \frac{(g_{MA_n^{-\nu}})^a_r\; g_A^{-a\nu}}{(g_{MA_n^{-\nu}})^a\;\overline{(g_A^{-a})^\nu_r}} \quad (4)$$

Parentheses indicate concentration of species and subscript *r* the resin phase. Where no subscript is given, the aqueous phase is implied. *G* is the proper activity coefficient quotient, *g* the activity coefficient of species, and *K* the ion exchange constant, which may be set equal to unity with proper assignment of standard

states. Similar equilibria may be written for any species which distribute between the two phases. As pointed out earlier,[13] these mass action expressions imply independent distribution of components, and hence apply for both equivalent and non-equivalent exchange.

The distribution coefficient D may be defined as

$$D = (m_M)_r/m_M \tag{5}$$

where $(m_M)_r$ is the stoichiometric concentration of M in the resin phase (irrespective of species) and where m_M is the concentration of M in the aqueous phase. In general, both m_M and $(m_M)_r$ represent sums of concentration of a number of species. For example, for the aqueous phase, one may write

$$m_M = (M^{+v}) + (MA^{+v-a}) + \ldots + (MA_n^{-v}) = \sum_i (MA_i^{+v-ia}) \tag{6}$$

We shall assume for simplicity that

$$(m_M)_r = (MA_n^{-v})_r \tag{7}$$

i.e., that only one species is adsorbed by the resin in significant amounts. Although this implies a considerable loss in generality, somewhat more complicated equations involving many species in the resin phase may readily be derived. For present purposes, however, most of the pertinent arguments can be made with equations derived with the restriction of Equation 7. Under these conditions

$$D = \frac{(MA_n^{-v})_r}{m_M} \tag{8}$$

Combination of Equations 3 and 8, after multiplication of the numerator and denominator of Equation 3 by m_M^a, yields

$$\frac{K}{G} = D^a \frac{m_M^a}{(MA_n^{-v})^a} \frac{(A^{-a})^v}{(A^{-a})_r^v} \tag{9}$$

Thus measurement of the distribution coefficients D permits, in principle, evalnation of $(MA_n^{-v}/m_M = F_v$, the fraction of metal in the form of the complex, through measurement of the concentrations of A^{-a} in the aqueous and resin phases and estimation of K/G.

Before discussing the implications of Equation 9 for measurements in concentrated electrnlyte solutions, a few limiting situations will be reviewed.

It has become customary tn assume that K/G is constant and independent of medium in dilute electrolyte solutions if the Debye-Hückel term vanishes. If we further restrict ourselves to stable, negatively charged ions (i.e., where $F_v = 1$) and to low loading, thus making $(A^{-a})_r$ = constant at low ionic strength, then the charge v can be evaluated since

$$\frac{d \log D}{d \log m_A^{-a}} = -v/a \tag{10}$$

Typical applications of Equation 10 are given in

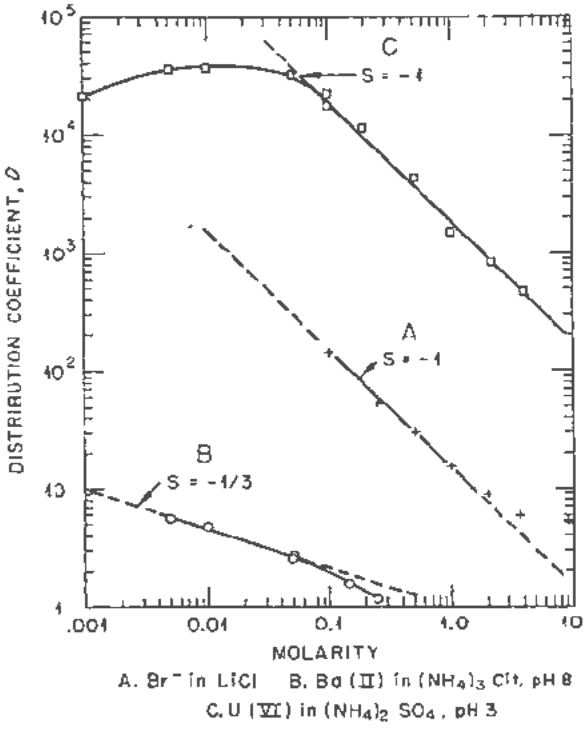

Figure 5. Determination of charge of ions by anion exchange: (A) Br^- in LiCl; (B) Ba(II) in $(NH_4)_3$ Cit. pH 8; (C) U(VI) in $(NH_4)_2SO_4$, pH 3

Fig. 5. For the "known" case of tracer bromide adsorption the slope of a plot of log D_{Br} *vs* log m_{HCl} has a slope of −1 at low m_{HCl}, as anticipated, since here $v = 1$ and $a = 1$. Deviations from this straight line, however, become serious at high m_{HCl}, presumably primarily because of non-constancy of G. Curve B (Fig. 5) gives a plot of log D_{Ba} *vs* log $m_{Cit^{---}}$. The slope is approximately −1/3 at low $m_{Cit^{---}}$. Since here $a = 3$, one may conclude that $v = 1$, as expected for the complex $BaCit^-$. From measurements of U(VI) in $(NH_4)_2SO_4$ solutions, curve C was constructed and d log $D_{U(VI)}/d$ log $m_{SO_4^{--}}$ was found to have a slope of −1 over a rather large range of sulfate concentration. Since here $a = 2$, one may conclude that $v = 2$, i.e., that the complex probably has a charge of −2, suggesting the formula $UO_2(SO_4)_2^{--}$. The same conclusion can also be obtained from a plot of log $D_{U(VI)}$ *vs* log $m_{H_2SO_4}$ from adsorption studies in sulfuric acid. In this case the slope is approximately −2 in the range 0.1 to 1 M H_2SO_4. Since here the eluting ion is probably HSO_4^-, i.e., $a = 1$, one obtains $v = 2$ in agreement with the proposed formula $UO_2(SO_4)_2^{--}$.

Most important for applications in concentrated electrolyte solutions is evaluatinn of variations of G with medium If we assume that v and a are known and that $F_v = 1$, K/G may he evaluated from Equation 9 through measurement of D, (A^-) and $(A^-)_r$.

Distribution coefficients have been measured for

tracer bromide in HCl and LiCl solutions and the concentration of Cl^- in the resin phase determined analytically (see also ref. 18). The values of D and the computed values of K/G are given in Fig. 6 for both LiCl and HCl solutions. Note that in this case $K/G = D(Cl^-)/(Cl^-)_r$. It may be noticed that K/G is not constant even for this relatively simple 1:1 exchange. Further, K/G is different for LiCl solutions and HCl solutions. For both media log K/G varies linearly with molality. The slopes $(d \log K/G)/dm = -d \log G/dm = b$ have different signs for the two media. Thus, $b_{Br^-}(LiCl) = 0.019$ and $b_{Br^-}(HCl) = -0.021$. These differences probably do not result from differences in the appropriate activity coefficient ratios in the aqueous phase, but probably principally reflect differences in the activity coefficients in the resin phase ($\gamma'_{HBr}/\gamma'_{HCl}$ and $\gamma'_{LiBr}/\gamma'_{LiCl}$). Considerably greater non-constancy of K/G had earlier been reported[13] for the adsorption of Au(III) ($AuCl_4^-$) ($b_{Au(III)} = 0.13$), though, it now appears, for very different reasons.

Recently a very large difference was found[19] for the adsorption of a number of metal complexes from HCl and LiCl solutions. Since then a more detailed study has been carried out on the adsorbability of Au(III) and log $D_{Au(III)}$ was found to increase steeply with LiCl concentration which may be compared with the rapid decrease of $D_{Au(III)}$ in HCl solutions. Further, at least in the range $1 < m_{LiCl} < 10$, log D $(Cl^-/Cl^-)_r$ varies essentially linearly with m_{LiCl}. It was suggested[19] that this large difference in adsorbabilities in LiCl and HCl solutions could be caused either by unexpected differences in the activity coefficients in the resin phase or by rather extensive formation of undissociated complex acids at high HCl concentrations. Originally the former explanation was preferred, particularly in view of the great generality of the "lithium chloride effect". The weight of more recent evidence, however, makes the assumption that undissociated complex acids are formed more probable. A study of the activity coefficients of lithium chloride in the resin phase in a manner analogous to the earlier studies[18] of the activity coefficients of HCl revealed no large differences. Further, measurements of the distribution coefficients of Au(III) as a function of acidity at constant total molality ($m = 10$) in LiCl-HCl mixtures have been carried out. The data could be fitted reasonably well by assuming the equilibrium

$$HAuCl_4 \rightleftharpoons H^+ + AuCl_4^- \qquad (11)$$

with concentration quotient $k_h^m =$ ca 0.1 at this ionic strength though this quotient showed some not unexpected drift with composition.

One may thus with reasonable confidence postulate that those chloride complexes which show a pronounced lithium chloride effect form relatively weak complex acids. According to present data this includes the chloro complexes of the fission products Zn(II), Ga(III) and Cd(II), but not Ag(I). Actually, in

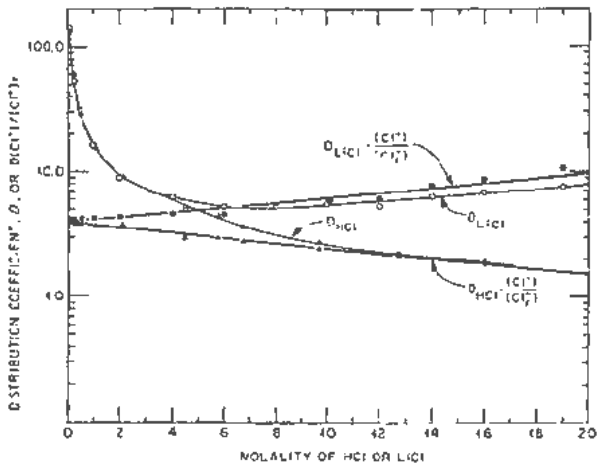

Figure 6. Adsorption of trace bromide from HCl and LiCl solutions

the case of Ag(I), adsorption from LiCl solutions is only slightly stronger than from HCl solutions, the effect being of about the same order of magnitude as for Br^- adsorption. This implies that Ag(I) does not form undissociated complex acids to any large extent even in concentrated HCl, in agreement with the known acid insensitivity of the solubility of AgCl in chloride media.[20]

Although the differences in the results in LiCl and HCl solutions throw considerable doubt on the earlier qualitative interpretations of the shapes of the adsorption functions present, more detailed work with Ga(III) gives hope that these earlier qualitative interpretations might still be applicable. It had been felt that the steeply rising portions of the distribution functions are due to the formation of the negatively charged complexes, i.e., reflect the rapid rise in F_n, that the maxima occur (at high ionic strength) at approximately those HCl concentrations where the negatively charged complexes become predominant, and that the region of decreasing D which corresponds to a decrease in D $(Cl^-)^a/(Cl^-)_r^a$ at high M HCl, coincides with the region where the negatively charged complexes or complex acids are essentially completely formed. In the case of Ga(III) this conclusion was confirmed in recent Raman work in HCl and LiCl solutions which was carried out in collaboration with Young and Krawetz (University of Chicago). A Raman line apparently characteristic for $GaCl_4^-$ (or $HGaCl_4$) was found to have essentially constant intensity above 8 M HCl, the position of the adsorption maximum. Further, a rapid decrease in intensity of the line occurred with decrease in M HCl. Thus, the qualitative interpretations suggested appear to apply. One may, therefore, apparently classify the elements according to their tendencies to form negatively charged complexes from the position of the adsorption maxima. The order of stability, on this basis, for uranium and the fission products is as follows:

1. Strong negatively charged complexes, essentially fully formed below 1 M HCl: (Tc(VII)),

Ru(IV), Rh(III), Rh(IV), Pd(II), Ag(I), Sn(II) (?).

2. Negatively charged complexes formed in the range 1 to 12 *M* HCl (in decreasing order of stability): Cd(II) ≈ Sb(III) ≈ Zn(II) > In(III) ≈ Mo(VI) > Sn(IV) > Ga(III) > As(III) ≈ Sb(V) ≈ U(VI) (?).

3. Negatively charged complexes not completely formed in 12 *M* HCl: Ge(IV), Zr(IV), U(IV).

4. No evidence for negatively charged complexes: As(V), Rb(I), Sr(II), Y(III), Cs(I), Ba(II), R.E.(III).

In several instances this order may appear surprising. Most striking is the fact that Cd(II) and Zn(II) appear to form negatively charged complexes at approximately the same HCl concentration, though unquestionably the positively charged complex MCl^+ is much more stable for Cd(II) than Zn(II) (see also Fig. 4). Thus, as had already become apparent with other anion exchange studies, e.g., of the first row transition elements (see ref. K-8, Table I), there appears to be for many cases no simple relation between stability constants within a series of complexes MCl_i.

The anion exchange results in general are of course susceptible to considerably more detailed and quantitative interpretation in terms of species formed and the corresponding equilibria, than given here. Most interesting in this respect will be interpretations of the behavior of the metals in concentrated electrolyte solutions. As pointed out, these are intimately tied to evaluation of the activity coefficient term G, whose more exact determination is the objective of present research. It is to be hoped that these more quantitative interpretations will become feasible, at least in a few cases, in the not too distant future.

REFERENCES

1. Nachod, F. C., *Ion Exchange: Theory and application*, Academic Press, Inc., New York (1949).
2. Kunin, R. and Myers, R. J., *Ion Exchange Resins*, John Wiley and Sons, Inc., New York (1950).
3. Osborn, G. H., *Applications of Ion Exchange Resins*, Analyst *78*: 220 (1952).
4. Lederer, E. and Lederer, M., *Chromatography*, Elsevier Pub. Co., Inc., Houston (1953).
5. Samuelson, O., *Ion Exchangers in Analytical Chemistry*, John Wiley and Sons, Inc., New York (1953).
6. Schubert, J., *Ion Exchange*, Ann. Rev. Phys. Chem. *5*: 413 (1954).
7. Kunin, R. and McGarvey, F. X., *Annual Review of Ion Exchange*, Anal. Chem. *26*: 104 (1954).
8. Kunin, R. and McGarvey, F. X., *Annual Review of Ion Exchange*, Ind. Eng. Chem. *47*: 565 (1955).
9. *Ion Exchange Resins in Medicine and Biological Research*. Ann. N. Y. Acad. Sci. *57*: 61 (1953).
10. Campbell, E. C. and Nelson, F., *Chemical Separation of 0.82 sec. Pb^{209m} from Bi^{209}*, Phys. Rev. *91*: 490A (1953).
11. Schubert, J., *The Use of Ion Exchangers for the Determination of Physical-Chemical Properties of Substances, Particularly Radiotracers, in Solution*. I. J. Phys. and Colloid Chem. *52*: 340 (1948).
12. Fronaeus, S., *On the Use of Anion Exchangers for the Study of Complex Systems*, Svensk Kem. Tidskr. *65*: 1 (1953).
13. Kraus, K. A. and Nelson, F., *Ion Exchange in Concentrated Electrolytes. Gold (III) in Hydrochloric Acid Solutions*, J. Am. Chem. Soc. *76*: 984 (1954).
14. Borkowski, C. J., (1949) as reported in CRNL-1160 (1951).
15. Kraus, K. A. and Moore, G. E., *Separation of Zirconium and Niobium in HCl-HF Mixtures*. J. Am. Chem. Soc *73*: 9 (1951).
16. Wheaton, R. M. and Bauman, W. C., *Properties of Strongly Basic Anion Exchange Resins*, Ind. Eng. Chem. *43*: 1088 (1951).
17. Kunin, R. and McGarvey, F. X., *Equilibrium and Column Behavior of Exchange Resins*, Ind. Eng. Chem. *41*: 1265 (1949).
18. Kraus, K. A. and Moore, G. E., *Adsorption of Hydrochlorid Acid by a Strong Base Anion Exchanger*, J. Am. Chem. Soc. *75*: 1457 (1953).
19. Kraus, K. A., Nelson, F., Clough, F. B. and Carlston, R. C., *Adsorption from Lithium Chloride Solutions*, J. Am. Chem. Soc. *77*: 1391 (1955).
20. Seifell, A., *Solubilities of Inorganic Compounds*, D. van Nostrand Co., New York (1940).

Record of Proceedings of Session 9B.1

FRIDAY MORNING, 12 AUGUST 1955

Chairman: Mr. A. P. Vinogradov (USSR)

Vice-Chairman: Mr. J. W. T. Spinks (Canada)

Scientific Secretaries: Messrs. R. Hara and J. Gaunt

PROGRAMME

P/724 Chemical processing in intense radiation fields ..... R. P. Hammond
P/719 Solvent extraction chemistry of the fission products..... F. R. Bruce
P/837 Anion exchange studies of the fission products.... K. A. Kraus and F. Nelson

DISCUSSION

The CHAIRMAN: As a result of the development of atomic energy, large numbers of radioactive isotopes have been placed in the hands of research workers. Through the use of these radioactive isotopes as labelled atoms, certain transformations in science and technology are taking place before our eyes, and, having once begun, this process will continue. Many isotopes are formed by the fission of the nuclei of uranium, thorium and other heavy elements.

The whole of this spectrum of fission fragments can be determined only after very complicated chemical work in separating and isolating the isotopes, and here the chemist's work is particularly important. By radiochemical methods it is possible to determine the half-life, the nature of the radiation, the energy of that radiation, and the daughter products of the decay of radioactive chains. Accordingly, it is possible to determine the mass number or atomic number of a given isotope. This work of the chemist, which will be discussed in this session, is of exceptional importance to an understanding of the chemical mechanism of the fission of complex nuclei and of the structure of such nuclei, and has a considerable bearing on the theory of this process.

Mr. R. P. HAMMOND (USA) presented paper P/724 as follows:

One of the principal characteristics of the nuclear power industry, as distinguished from conventional power, is that it is inherently a chemical industry. In addition to the production of electricity, each year tons of spent fuel elements must be reprocessed and tons of fission products separated, and these must be treated for disposal as waste or for sale as valuable by-products.

The magnitude of these necessary chemical operations is increased by the need for remote control operation and heavy shielding. Indeed the cost of this chemical portion of the industry may in some cases determine the economic feasibility of the entire operation. Now the most economical processing can be done if concentrated materials can be handled, since the plant required is smaller, and the investment and amount of shielding are proportionately less with a higher capacity. Also the cost of storage facilities and inventory charges are lower if we begin processing after the shortest possible cooling period.

But this combination of high concentration and short cooling times gives high radiation intensity, and radiation damage from these radiation fields may cause failure of the chemical processes themselves and thus limit the success with which we can obtain the most economical processing. It will be the purpose of this paper to summarize briefly the American experience, very limited as it is, in this field of high intensity processing and to indicate to what extent processes will be limited by radiation effects.

Table I. Energy Density of "Pure" Fission Products Based on Reactor Operating at 10,000 Watts per Gram of Fuel

Cooling time	*Approx. energy per gram*
1 day	20 watts
1 week	10
1 month	2
1 year	0.2

To compare various processes it is necessary to have some unit of dosage or deposition of radiation energy, and the watt-hour per gram has perhaps been the most widely used for this. It compares with other possible units as follows:

1 watt-hour per gram
- $= 2.25 \times 10^{22}$ electron volts per gram
- = 169 curie-hours per gram per Mev decay energy
- $= 4.34 \times 10^{8}$ roentgen (air) per gram
- $= 3.74 \times 10^{-4}$ gram moles per unit G value per gram (unit G value is one molecule converted per 100 electron volts absorbed energy)
- = 8.6 grams radium (in equilibrium) per gram

Next we must consider what level of radiation intensities will be encountered when we start processing highly concentrated fission products from a high-

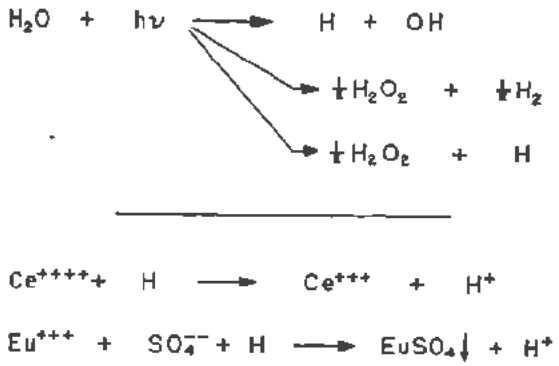

Slide 1. Oxidation-reduction

power-density pile after short cooling times, and it will be seen from Table I on this page that the cooling time of one day gives a power density of about 20 watts, in one week 10 watts, in a month 2 watts and in a year 0.2 watt. It might be deduced from this that a chemical process which will not work successfully above 1 watt per gram may in some cases influence the success of attempts to get the most economical process because it will require an uneconomically long cooling period.

There are six types of radiation effects which I should like to mention, and then I will try to give the extent to which the success or failure of these may be determined by chemical radiation damage.

The first effect (Slide 1) is oxidation and reduction. The products formed in irradiated material contain equivalent amounts of potential oxidizing and reducing agents. These can react with any substance in a solution which is capable of being oxidized or reduced, but the product formed must be stable in the existing environment if a net reaction is to be obtained.

In the case of the cerium solution, the third equation in Slide 1, the reaction can be in both directions. It will be predominantly in a forward direction until equipotential equilibrium is obtained. Thus, radiation is like an electro-chemical catalyst, but of the two it is a consumable catalyst. Its quantitative effect is strictly proportional to the amount of radiation absorbed. This points out the importance of the time of exposure in chemical processes since, by working quickly, even very sensitive materials can be processed in high radiation fields. The last equation is only a hypothetical example because the reaction would go predominantly in a reverse direction. But if the tiny amount of precipitate in the equilibrium could be swept out of the solution to a region shielded from radiation a net forward reaction might be produced. The conclusion is that radiation provides local oxidizing or reducing effects, which cancel each other unless a more stable form results, in one direction, or unless the reaction is irreversible. In general, the disruption of organic bonds is irreversible.

The second effect is gas evolution, which is one form of an irreversible process in most cases. In addition to the chemical effects of gas evolution, there may be profound physical effects on the chemical process. Because of the difference in effect of fission fragments and beta-gamma radiation on water, various reactors have different amounts of trouble from gas evolution. The solid fuel water moderated reactor has essentially no gas evolution if the water is pure, whereas a homogeneous reactor with an aqueous fuel solution experiences a severe problem.

In the United States there have been three main approaches to this problem: first, the use of external recombining apparatus; second, a dissolved catalytic ion apparatus; third, the use of a reactor temperature high enough for thermal recombination. The first method has been used at Los Alamos, in the Water Boiler, with a platinized aluminum catalyst.

After several years of operation in which the catalyst received a dose of one-tenth of a watt per gram, the observed effects were nil. There had been no apparent damage to the catalyst.

The third effect is peptization or colloid formation. It can be quite disconcerting if the precipitate to be filtered becomes a stable colloid. The peptization can be related to the formation of gas within the crystal or solid. It is observed infrequently at very high radiation density such an lanthanum fluoride at 230 watts per gram. In this particular case there was some measure of control of the effect by special techniques which reduced the water content of the solid.

Three other effects of radiation are self-heating, destruction of organic compounds and hot-atom effects, which can only be mentioned at this point.

A chemical process consists of a series of reagent additions and phase separating steps.

I should like to talk about six such unit operations or steps at this time regarding their tolerance of radiation effect. Examples given are drawn from only a few high intensity processes and, since different processes will have different requirements and conditions, the numerical values given can be only a rough guide in other processes.

Filtration is one of the most fundamental chemical operations, but it has been largely avoided up to now in remote control techniques. This is probably due to the lack of proper equipment since it is a difficult task to devise a reliable method for setting up and cleaning a filter remotely and to handle separated solids. Equipment such as the chemical engineer is used to is obviously not quite suitable, but the use of a porous metal filter made of platinum or stainless steel shows promise and this type of apparatus seems well adapted to remote control operations as it can be cleaned or replaced with ease. Radiation effects are observed in filtration steps. Gas formation, peptization and oxidation-reduction may produce effects calling for some variation in the regular technique, but such methods can get around most of the trouble. Polonium sulfate and hydroxide have been

filtered at 100 watts per gram. Lanthanum fluoride, which is a difficult material to filter even when not radioactive, has been filtered successfully at 230 watts per gram. Filtration is probably not limited by radiation effects too greatly and I think it should be utilized perhaps more than it is at present.

The cup-type laboratory centrifuge has been adapted to remote control operation, but I must report that it is severely limited by radiation effects. With about half a watt per gram, the gas formation dislodges the collected solid material as soon as the centrifuge stops, before decantation can be performed. This has been observed in both polonium hydroxide and barium nitrate. The obvious solution is the use of the more modern bowl-type centrifuge in which the liquid can be removed while the centrifuge is at speed. Such a centrifuge for a high intensity, moderate scale process has been designed at the Argonne Testing Station, and although it has not yet been tried out there is probably no reason why it should not be successful at almost any radiation intensity.

Distillation, evaporation and ignition are three steps which can be considered together since all of them are aided by the self-heating of the radiation and nearly conventional equipment can be used. Evaporation and ignition have been carried out successfully at about two hundred watts per gram and, in a few cases, at 500. For those who think in terms of curies, this is 500,000 curies per cm^3.

The observation on evaporation is that the self-heated material went, in general, more smoothly with less bumping than externally heated material.

The use of electro-deposition will probably be limited to specialized cases in the high intensity process. However, since it has been regularly used for purification of polonium, it has been observed at high radiation intensity—130 watts per gram. This is probably near the successful limit, since hydrogen peroxide formation reduced the current efficiency and affected the completeness of deposition. Another interesting application of electro deposition to high intensity processing is a method for purifying fission-product barium. To the solution of uranium slugs a considerable quantity of lead salt was added, and when sulfuric acid was used to precipitate the barium, lead sulfate came down also acting as a carrier. Then the lead was later removed from the barium lead solution by electro-deposition, leaving the barium to continue the process.

Solvent extraction by organic solvents has become an important part of the atomic energy industry. However, because of the organic materials involved, it can hardly qualify as a high intensity process. Careful studies at Oak Ridge have indicated that some of the best complexing agents can be exposed to only a ten thousandth of a watt per gram. The solvent extraction method will probably continue to be an important method of handling radiation but this will be by means of diluting the solution and allowing longer cooling times. For large scale work this means a large shielded plant, but the simplified equipment of solvent extraction methods will to some extent offset the size of the plant.

Ion-exchange techniques appear to hold a promising position in the high level processing field. In the separation of radiobarium an organic cation exchange resin has been exposed to two-tenths of a watt per gram. This was a sulfonated phenolic type resin. Anion resins are in general less stable than the cation exchange resins. An example of an inorganic extraction process is in the separation of fission-product zirconium, using a silica-gel adsorption column. This column was operated at $\frac{3}{100}$ watt per gram with no ill effects, and it is believed that this is far from the upper limit.

In addition to the destruction of bed material, the limitation of column operation by gas formation may be observed, since the gas can plug the column. Various attempts have been made to control this by the use of horizontal columns, upward-flow columns, pressurized columns, etc.

The conclusion which may be reached from our experience with high intensity radiation processing is that, except for organic materials, chemical operations can be carried out successfully with fission products which are highly concentrated and with low cooling times. Efforts in this field should be continued so that the large scale development of nuclear energy will not be handicapped by lack of economic processing techniques.

Mr. F. R. Bruce (USA) presented paper P/719 as follows:

When organic solvents such as methyl isobutyl ketone and tributyl phosphate are equilibrated with aqueous nitrate solutions containing fission products, the fission products distribute themselves in a characteristic manner between the two phases. The ratio of the concentration of the fission product in the organic phase to its concentration in the aqueous phase is defined as its distribution ratio.

Table II on this page shows typical values of fission product distribution ratios in methyl isobutyl ketone and tributyl phosphate extractions.

Table II. Extraction of Important Fission Products by Solvents

Fission product	Distribution ratio (organic/aqueous)	
	Methyl isobutyl ketone*	Tributyl phosphate†
Cesium	$<10^{-4}$	$<10^{-4}$
Total rare earths	0.01	0.0004
Gross beta emitters	0.03	0.001
Cerium	0.03	0.01
Zirconium	0.04	0.01
Ruthenium	1.0	0.001

* 1.5 *M* $Al(NO_3)_3$–0.25 *M* HNO_3.
† 3 *M* HNO_3–30% TBP (80% saturated with uranium).

Cesium is an example of a very non-extractable fission product. Others that fall in this category are barium and strontium. The total rare earths, exclusive of tetravalent cerium, exhibit distribution ratios of 0.01 and 4×10^{-4} in methyl isobutyl ketone and tributyl phosphate. The total fission product beta activity of 90-day cooled irradiated uranium exhibits distribution ratios of 0.03 in methyl isobutyl ketone and 10^{-3} in tributyl phosphate. Cerium and zirconium exhibit approximately equal extractability to the gross beta-emitting fission products in methyl isobutyl ketone and approximately 10-fold higher extractability than the gross beta-emitting fission products in tributyl phosphate. Ruthenium exhibits a methyl isobutyl ketone distribution ratio of 1 under highly acidic aluminum nitrate solutions in metal and a distribution ratio of 10^{-3} with tributyl phosphate extraction. With the exception of ruthenium, zirconium, niobium, cerium, and iodine, the fission products may be readily separated from fissionable material by solvent extraction. In this paper the chemistry of only ruthenium, zirconium, niobium, cerium, and iodine in methyl isobutyl ketone and tributyl phosphate extractions will be considered.

Methyl isobutyl ketone extraction of fission products is dependent on the concentrations of nitric acid and metal nitrates in the aqueous phase, as shown in Slide 2 (Fig. 1 of P/719).

Increasing the aluminum nitrate concentration at constant acidity results in increasing the extraction of gross gamma-emitting fission products. Fission product extraction exhibits about second power dependence on nitrate ion concentration over all of the acidities studied. At constant aluminum nitrate concentration increasing the nitric acid concentration from 0.1 *M* acid deficient to 0.1 *M* acid results in a 50-fold increase in fission product extraction. Here we define an acid deficient solution as one which contains less nitrate ion than a solution of stoichiometric salt, that is, it contains hydrolyzed species. Fission product extraction exhibits a marked dependence on acidity in the neighborhood of zero-free acidity. This is believed attributable to the fact that a fission product extraction involves species whose valences are fully satisfied with nitrate ion, and in the neighborhood of zero-free acidity the concentration of fission product nitrate is changing most rapidly with change in acidity. The pattern for individual fission product extraction is qualitatively the same as the behavior indicated for the gross gamma-emitting mixture shown here.

Zirconium and niobium extraction are also very dependent on acid concentration. They are believed to be hydrolyzed and present as non-extractable colloids in solutions of low acidity. When the acidity is increased, the proportion of zirconium or niobium nitrate increases, with a corresponding increase in metal extraction.

Ruthenium may exist in the plus 3, plus 4, and plus 8 valence states in aqueous solution, although

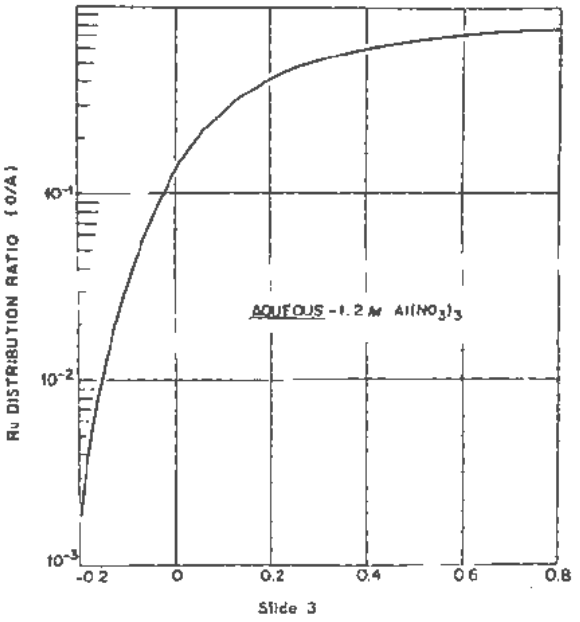

Slide 3

we believe the tetravalent state predominates. In addition, it may be present as nitrosyl complexes in solution. Its existence in multiple valence states and as complexes contributes to the complex solvent extraction chemistry of ruthenium. The lower valence states of ruthenium are less extractable than the higher. For example, ruthenium extraction by methyl isobutyl ketone is 4-fold less from a solution reduced with ferrous ion than from a solution oxidized with dichromate ion. The striking effect of acidity on ruthenium extraction by methyl isobutyl ketone is shown in Slide 3.

Increasing the acidity from 0.2 *M* acid deficient to 0.4 *M* acid results in a 265-fold increase in ruthenium extraction into the organic solvent. Formation of solvent-soluble complexes of ruthenium may be utilized to increase ruthenium separation from fissionable material. The ruthenium is converted to a highly extractable compound by the addition of a solvent-soluble complexing agent, such as dephenyl thiourea to the methyl isobutyl ketone. When this is done 98 per cent of the ruthenium, instead of following the fissionable material, remains in the methyl isobutyl ketone phase when the fissionable material is back-extracted into water. Although the solvent extraction chemistry of ruthenium has been studied extensively, it is not yet thoroughly understood. Simple control of nitric acid and aluminum nitrate concentrations are most useful for inhibiting ruthenium extraction.

Cerium may exist in the tri- and tetravalent states. However, the tetravalent state is reduced by methyl isobutyl ketone to the moderately inextractable trivalent state. The solvent extraction chemistry of cerium in the presence of dichromate ion is particularly interesting in two respects.

As Slide 4 (Fig. 8 of P/719) shows, the addition

of cerium in macro quantities to the system results in the effect shown. When the aqueous phase is 0.012 M in inactive trivalent cerium, the distribution ratio is decreased to a value of 0.008 from an original value of 0.3 in the absence of inactive cerium. An explanation of this inverse relationship between the cerium distribution ratio and cerium concentration is postulated as:

$$\tfrac{2}{3}\ H^{+} + Ce^{+3} + \tfrac{1}{6}\ Cr_2O_7^{-2} \rightleftharpoons Ce^{+4} + \tfrac{1}{3}\ Cr^{+3} + \tfrac{7}{6}\ H_2O$$

$$K' = \frac{(Ce^{+4})^{4/3}}{(Ce^{+3})} \qquad k = \frac{(Ce^{+4})_{org}}{(Ce^{+4})_{aq}}$$

$$DR = \frac{(Ce^{+4})_{org}}{(Ce^{+4})_{aq} + (Ce^{+3})_{aq}} \quad \therefore$$

$$DR' = \frac{(Ce^{+4})_{aq}}{(Ce^{+4})_{aq} + (Ce^{+3})_{aq}}$$

$$DR' = \frac{K'^{3/4}}{K'^{3/4} + (Ce^{3+})^{1/4}}$$

An equilibrium constant may be written for the Redox reaction for the oxidation of trivalent cerium to tetravalent cerium by dichromate ion. The concentration of hydrogen ion, dichromate ion and water may be considered constant under the conditions of interest, and therefore dropped from the expression. Since the concentration of reduced chromium equals one-third of the concentration of trivalent cerium, this substitution may be made to give a relationship for the Redox reaction constant in terms of cerium concentrations. The distribution coefficient, k, for tetravalent cerium agrees with the previous definition of a fission-product distribution coefficient. Since the extraction of trivalent cerium is negligible compared to that of tetravalent cerium, the observed distribution ratio of total cerium, trivalent plus tetravalent, DR', is also defined. The tetravalent cerium term may be eliminated from this expression by substituting values for it from the relationships for the Redox reaction constant, K', and the definition of the distribution ratio, k. This yields the last expression.

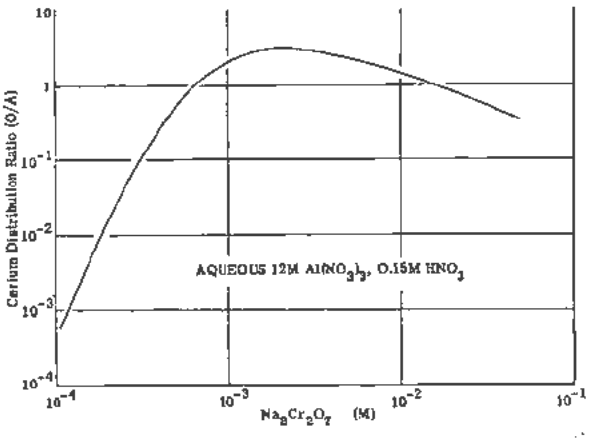

Slide 5. Effect on $Na_2Cr_2O_7$ on the distribution of cerium in methylisobutyl ketone extraction

Since the fraction of total cerium oxidized is quite small over most of the experimental conditions, the value of concentration of trivalent cerium is very nearly equal to the total cerium concentration. Therefore, the value of the observed distribution ratio is inversely related to the one-fourth power of the total cerium concentration. The cerium distribution ratio is also markedly dependent on the dichromate ion concentration, as shown in Slide 5.

The maximum distribution ratio occurs at a sodium dichromate concentration of between 0.002 and 0.003 M, where the distribution ratio is about 6000 times greater than at a dichromate ion concentration of 10^{-4} M. This effect does not involve the simple oxidation of trivaleot cerium to tetravalent cerium and extraction of the higher valence state, since it is not observed with permanganate and bismuthate ions, which are stronger oxidizing agents than dichromate. A reasonable explanation of this effect may be outlined as follows. Increasing the dichromate ion concentration from a concentration of 10^{-4} M to about 2×10^{-3} M results in enhanced oxidation of non-extractable trivalent cerium to the extractable tetravalent cerium. At concentrations above about 0.002 M, dichromate or chromate complexing of tetravalent cerium becomes more important, yielding a non-extractable specie, with a resulting decrease in the cerium distribution ratio. We believe that the complexing reaction has a higher power dependence on chromate ion concentration that the oxidation reaction.

Tributyl phosphate extraction of fission products is brought about through formation of a co-ordination compound involving the fission product ion, nitrate ions, and tributyl phosphate molecules:

$$FP_{aq}^{+a} + a(NO_3)_{aq}^{-} + b\ TBP_{org} \rightleftharpoons [FP(NO_3)_a \cdot b\ TBP]_{org}$$

$$k = \frac{[FP(NO_3)_a \cdot b\ TBP]_{org}}{(FP^{+a})_{aq}\ (NO_3^{-})_{aq}^{a}\ (TBP)_{org}^{b}}$$

$$D_{O/A} = \frac{[FP(NO_3)_a \cdot b\ TBP]_{org}}{(FP^{+a})_{aq}}$$

$$k = \frac{D_{O/A}}{(NO_3)_{aq}^{a}\ (TBP)_{org}^{b}}$$

A fission-product ion of valence $+a$ combines with a nitrate ions and b TBP molecules to form the extractable compound $FP(NO_3)^a \cdot b$ TBP. The equilibrium constant for the reaction may be written in the usual way. We have defined the distribution ratio of a fission product as the ratio of its concentration in the organic phase to that in the aqueous phase. Therefore, the reaction constant for the extraction may be written in terms of the distribution ratio and the nitrate ion concentration and the TBP concentration. This enables us to define the distribution ratio of a fission product in terms of the extraction reaction constant k, nitrate ion concentration and tributyl phosphate concentration.

Although most experimental data have been obtained in systems of high ionic strength—where it is difficult to treat the results rigorously—we find that the coefficient a is usually equal to the valence of the fission-product ion, and b is numerically equal to the difference between the co ordination number of fission product and its valence. In this expression for the distribution ratio, TBP_{uc} is the concentration of uncomplexed tributyl phosphate. As available tributyl phosphate is complexed with extractable ions such as uranium or thorium, the quantity of solvent which is free to extract fission products decreases and fission-product extraction decreases.

This effect is shown in Slide 6 (Fig. 10 of P/719) where distribution ratios are plotted as a function of uranium saturation of the solvent. The ruthenium distribution ratio, for example, is decreased about 50-fold by increasing the solvent saturation from 37 per cent to 90 per cent.

Ruthenium extraction by tributyl phosphate is markedly dependent on nitric acid concentration, as shown in Slide 7. In the region between 1 M acid deficiency and zero free-acid, ruthenium extraction increases as a result of formation of a solvent-soluble ruthenium nitrate species. At acidities above zero, a significant fraction of the available tributyl phosphate is being complexed with nitric acid and is unavailable for ruthenium complexing. This effect is observed with most fission products that do not exhibit high tributyl phosphate extractability.

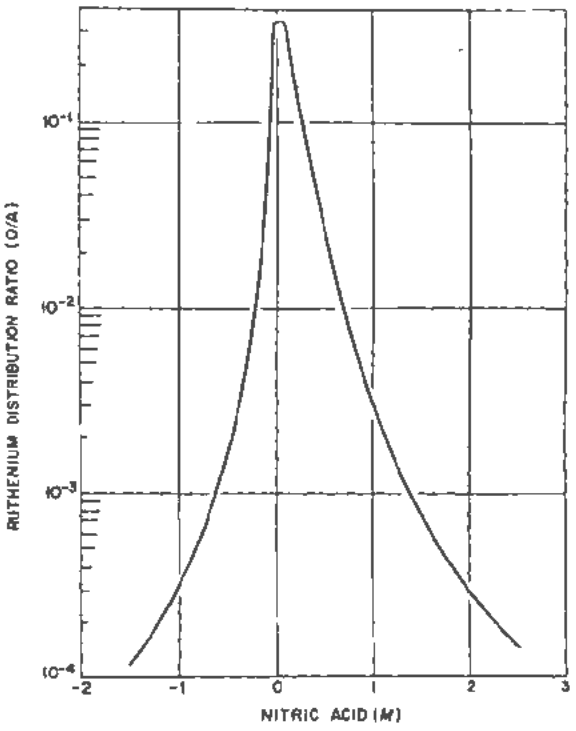

Slide 7. Effect of acid concentration on ruthenium extraction

There are two reproducible methods for reducing ruthenium extraction by tributyl phosphate: (1) digestion in nitrate solutions of very high ionic strength, and (2) reduction of ruthenium to a lower, less extractable valence state. Digestion of 4.5 M thorium nitrate at 150°C for one hour, for example, results in an 8-fold decrease in ruthenium extraction after the solution is cooled and diluted to approximately 1 M thorium nitrate. Likewise, reduction with ferrous ion of a thorium nitrate solution containing ruthenium results in an approximately 8-fold decrease in ruthenium extraction.

The tributyl phosphate extraction behavior of zirconium differs from that of ruthenium and of most of the other fission products in that no maximum is observed when the acid concentration is increased to 12 M. This may be attributed to the fact that zirconium is more extractable than nitric acid and is preferentially complexed. Zirconium extraction is also complicated by the fact that the tributyl phosphate/kerosene solvent mixture may contain contaminants which increase zirconium extraction. The most important of these contaminants are mono- and dibutyl phosphates, which are powerful extractants for zirconium. In addition, butanol, aromatics, and olefins, which react with nitric acid to give nitration products forming solvent-soluble complexes with fission products, may be present.

Relatively few data have been collected on the behavior of iodine in solvent extraction processes since its short half-life makes it unimportant in processing long-decayed material. It has been observed, however, that iodine is highly extractable into methyl isobutyl ketone and tributyl phosphate. The mechanism of extraction involves formation of addition compounds between iodine and unsaturated compounds in the solvent, as well as simple extraction. These addition compounds are not backwashed when fissionable materials are stripped with water, nor are they removed from the solvent by washing with caustic or acid. Prior treatment of the solvent with concentrated sulfuric acid for removal of unsaturates results in substantially less iodine extraction. Reduction of iodine to the iodide also reduces its extraction markedly. Iodine promises to be a major problem in solvent-extraction processes handling short-decayed uranium or plutonium.

Mr. KRAUS (USA) presented paper P/837 as follows:

During the last ten to twenty years, as synthetic organic ion exchange resins of high stability became readily available, the popularity of ion exchange as a tool in inorganic and analytical chemistry increased tremendously. Most of these ion exchange studies involve cation exchange resins, resins which can exchange positively charged ions. On the other hand,

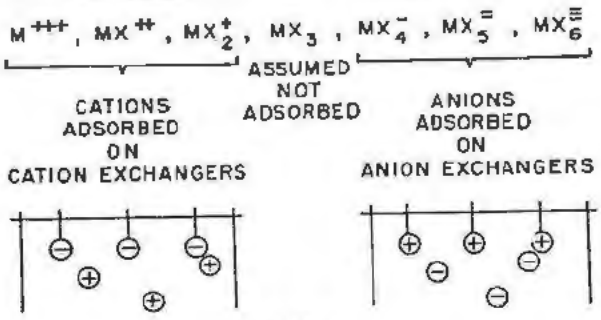

Slide 8

studies involving anion exchange resins, that is resins which exchange negative ions, have lagged greatly, although it now appears that at least in the fields of inorganic and analytical chemistry, not to speak of hydro-metallurgy, anion exchange holds at least as great, if not greater, promise than cation exchange. It is now possible, by complexing with various ligands, to convert almost any normally positively charged metal into an anionic species which then may be absorbed on anion exchange resins.

Slide 8 illustrates the conceptual difference between anion exchange and cation exchange of metals. The positively charged metal ions and their positively charged complexes, in principle, are adsorbable on cation exchange resins which have fixed negative charges, such as sulfonate ions. The negatively charged complexes, in principle, can be adsorbed on anion exchange resins with their fixed positive charges which may, as in our case, be quaternary ammonium ions or other amines. We used a commercial polystyrene divinyl benzene resin of high cross-linking with quaternary amine functional groups.

Regarding the complexes which may be adsorbed, it is convenient to consider two different types. One type would include the ferro- and ferri-cyanides and, to some extent, the chloroaurates, chloroplatinates, etc., which are very stable either because of slow rates of interconversion of species or because of high thermodynamic stability. These complexes can be adsorbed by anion exchange resins but for many purposes they are less interesting than the less stable negatively charged complexes which can rapidly be interconverted from one species to another through a simple change of medium.

A typical example of a metal forming rapidly interconvertable complexes is cobalt which, although it is not a fission product, lends itself to demonstration

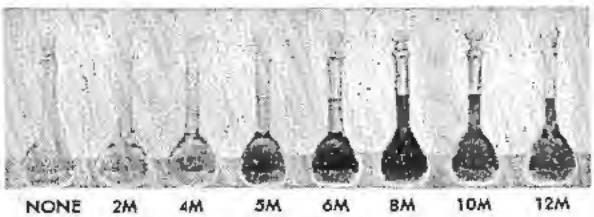

Slide 9. $CoCl_4^{=}$ in HCl

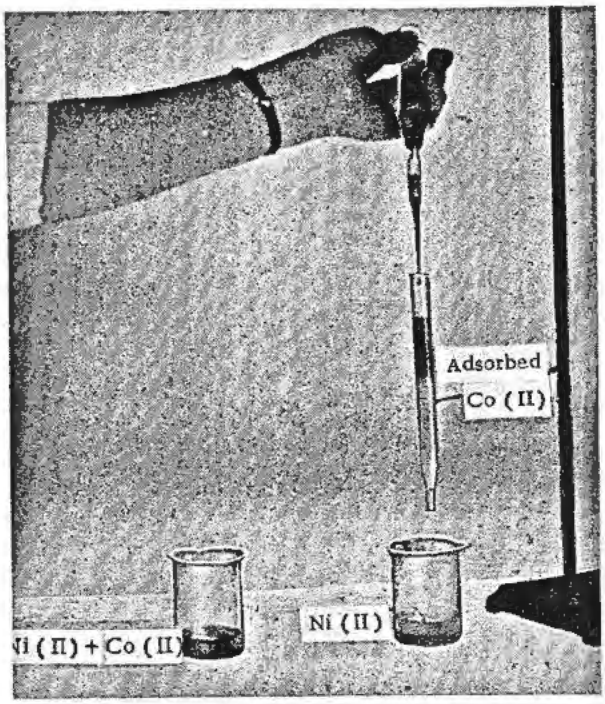

Slide 10

readily (Slide 9). At low HCl concentration, cobalt is pink. At higher HCl concentration it turns blue. The pink color is usually associated with the simple ion Co^{++}. The blue represents chloride complexes which may be formed. Dilution of a blue solution with water will immediately change the color to pink; similarly, the addition of HCl will immediately change the color to blue. When cobalt is in the blue form, it may be adsorbed strongly by anion exchange resin.

If one adds a solution of cobalt in strong HCl to an anion exchange column, which in most nf our work was of the small type illustrated in Slide 10, the cobalt will adsorb in a tight band at the top of the column, limited mainly by capacity considerations. In this particular example, we also added nickel to the solution. It was found that nickel, which is an element usually considered to be very similar to cobalt, does not absorb but immediately "drops" through the column and can be caught purified from cobalt, while the cobalt is retained by the exchanger.

In this separation, one could continue after having added all the sample, by washing out the interstitial nickel with 9 *M* HCl, and then remove the cobalt rapidly by elution with weaker HCl or water.

Slide 11 shows a beaker with purified nickel. The interstitial nickel was removed with a 9 *M* HCl wash and the final beaker contains the cobalt which had been removed, let us say with 1 *M* HCl, where the cobalt does not adsorb significantly. In favorable cases, this type of separation can be made extremely rapidly. It can often be carried out in a few minutes and has even been adapted to separation of short-lived radioactive daughters, with half-lives of the

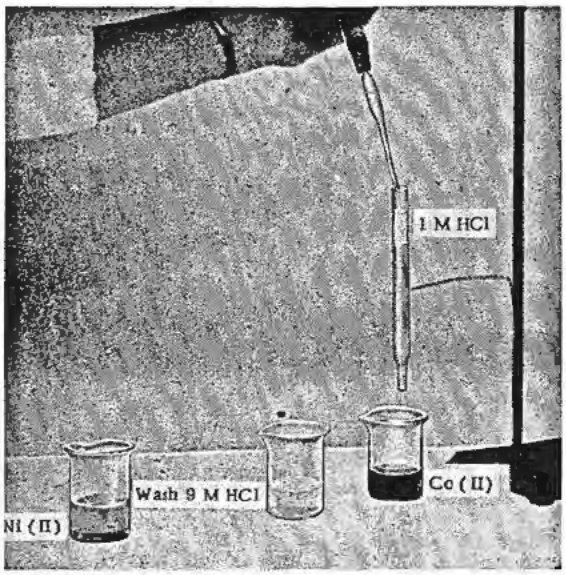

Slide 11

order of a second or less from long-lived parents.

Columns of the type illustrated here may be used not only for separations but also to obtain quantitative information regarding the adsorbability of ions. If a small amount of a metal is placed on the top of a column in a specified medium and elution carried out with the same medium, the metal will eventually appear in the effluent in a typical Gaussian distribution of concentrations (see Slide 12).

The position of the elution maximum in terms of column volumes directly gives the distribution coefficient on a volume basis, D_v, provided the fractional interstitial space i of the column is estimated. In general, i = ca 0.4, meaning that 40 per cent of the column is "void."

The same information may be obtained by so-called "shaking" or equilibration experiments which are of the same type as in any other two-phase equilibrium. One can equilibrate a small amount of resin and solution and determine the equilibrium concentration of the metal in the resin, and in the solution, and compute the distribution coefficient D, as (amount per kg resin)/(amount per liter solution). This distribution coefficient obtained in shaking experiments is readily related to the distribution coefficient obtained in column experiments. The ratio is given by an easily determined quantity, the bed density, $\rho \approx$ 0.45 (kg dry resin)/(l bed), and $D = \rho D_v$.

In general it had been our plan to study adsorbabilities of the elements over a relatively wide range of conditions and in this way to search for media in which the distribution coefficients of a given metal may be high for good adsorption, or low for good elution. Of course, the characteristic shape of the adsorption functions also forms the basis of interpretations in terms of the pertinent complex equilibria.

A typical set of such adsorption functions for U(VI) is shown on Slide 13 (Fig. 2 of P/837). The distribution coefficients are plotted on a logarithmic scale versus the molarity of the acid. If we trace through the hydrochloric acid data we may note that the adsorbability of U(VI) increases rapidly with HCl concentration. It reaches values of the order of 2000. I would like to remind you that according to an earlier slide this implies that about 1000 column volumes can be processed before 50 per cent breakthrough would occur, provided of course capacity limitations of the column resin are not exceeded. Uranium(VI) in nitric acid behaves very similarly, although the adsorption function does not rise as dramatically. In the case of sulfuric acid the situation is reversed—adsorbability decreases with increasing sulfuric acid concentration. At very low sulfuric acid concentrations of the order of 1000 column volumes might be processed and elution could be achieved with ca 2–4 M sulfuric acid, where the distribution coefficients become approximately unity.

It should be noticed that for this type of operation the resin always remains in the same form through both adsorption and elution cycles. One may of course also effect elution by a switch in medium. For example, one may adsorb U(VI) from sulfate solutions and elute with chloride or nitrate if one is prepared to consume reagents and to wait until the column is converted from the chloride form.

The striking adsorption characteristics of U(VI) may be used to effect directly a very large number of separations. They also form, as will be discussed in other papers, the basis of processes for the recovery of uranium from ores. One may, for example, separate uranium in hydrochloric acid from a large number of non-adsorbable elements by the simple device of passing the mixture in, e.g., 9 M HCl through an anion exchange column. The technique would be exactly the same as in the nickel-cobalt separation previously described.

One may readily extend such a separation scheme to other fission products.

Slide 14 (Fig. 4 of P/837) gives results (distribution coefficients) for zinc and cadmium. You may notice that best adsorption, distribution coefficients of the order of 1000 occurs around 1–2 M HCl, i.e., in that range of HCl concentrations where uranium does not adsorb. Elution can be carried out for zinc

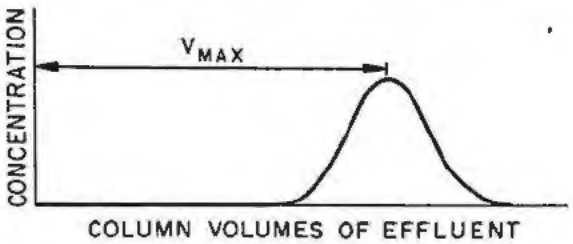

Slide 12. Column method: $V_{max} = i + D_v$ where i is fractional interstitial volume, D_v is volume distribution coefficient (amount per liter bed/amount per liter solution)

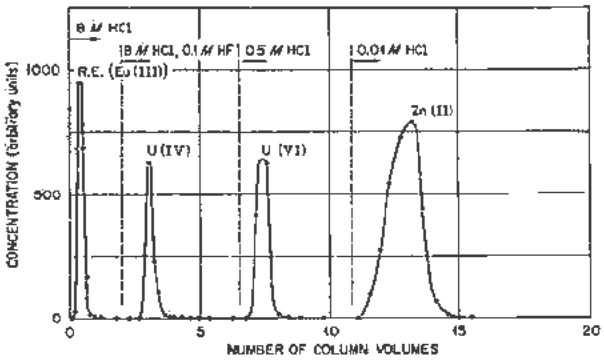

Slide 15. Separation involving U(IV) and U(VI) (0.17 cm² × 7.2 cm column)

in the vicinity of 0.01 *M* and for cadmium in the vicinity of 10^{-3} *M* HCl.

We may combine this type of information into a typical separation (Slide 15). A mixture of Eu (a typical rare earth), U, and Zn in 8 *M* HCl was passed into a small column. On elution with 8 *M* HCl the rare earth appeared immediately in the effluent in a sharp band. Uranium(VI) and zinc were retained. The U(VI) was removed with ½ *M* HCl, where it does not adsorb. Zinc is returned by the column. The zinc was removed, as I pointed out before, with 0.01 *M* HCl. Had cadmium been present in the same sample it would have stayed behind on the column but could have been removed in another band with 0.001 *M* HCl. In this particular experiment U(IV) was also added, which, like U(VI), adsorbs from strong HCl but can be removed at an intermediate HCl concentration. We have chosen, however, in this case to remove it with a mixture of HCl and HF, because I wanted to point out that a small amount of fluoride will drastically affect the adsorbability of U(IV) but not of U(VI) at high HCl concentrations.

During the last seven years or so we have tried to make a relatively complete study of the adsorption behavior of most metals, including most fission products. Most of this work has been carried out in HCl solutions.

Slide 16 (Fig. 1 of P/837) is a summary of these results.

This study looks like a rather dramatic effort with its coverage of the major part of the periodic table. However, with modern techniques, and particularly with radioisotopes and modern counting equipment, this is not anywhere near as heroic a job as might appear at first glance. The most time-consuming task normally is the analytical work involved in the determination of the distribution coefficients. This analytical problem now vanishes, since one or two minutes of counting may take the place of elaborate analyses which might otherwise be necessary.

Slide 17 is an enlarged section of Slide 16 (Fig. 1 of P/837) with distribution coefficients plotted vertically on a logarithmic scale and molarity plotted horizontally. The large difference in the adsorbability of the elements shown is typical for many other elements. Simple separation techniques are implied, although some caution is necessary with tin and antimony because these elements having rather high distribution coefficients at low HCl concentrations, may be at low HCl concentrations (Sn) or may have slow rates of interconversion of species (Sb).

Slide 18 illustrates how such data may be used for separations. The separation of arsenic(III) and arsenic(V) is given, based on the different adsorbabilities of the two oxidation states. The separation of germanium and arsenic is also illustrated.

Slide 19 is taken from the central part of the periodic table. In this part of the periodic table the chloride complexes are strong. These elements show a characteristic decrease in adsorbability with in-

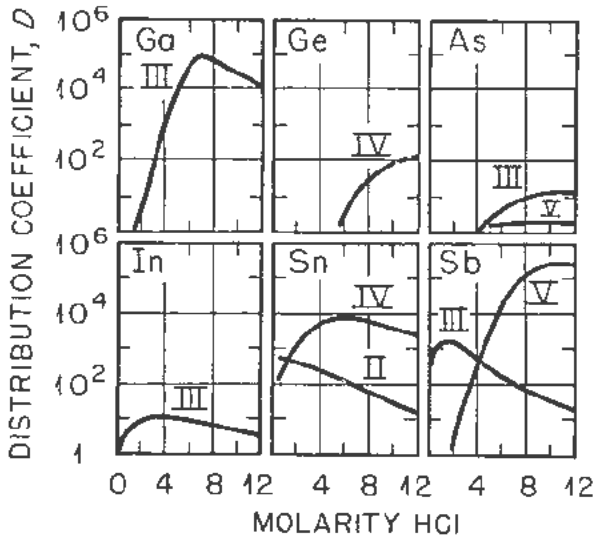

Slide 17

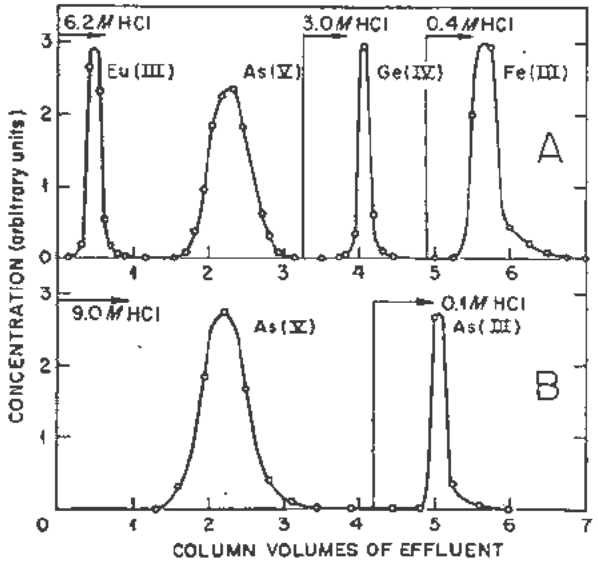

Slide 18. Separations involving Germanium and Arsenic

creased molarity of HCl. Although the adsorption functions all have the same characteristic shape, I would like to point out that certain elements have very low adsorbabilities at high HCl concentration, such as rhodium(III), iridium(III) and silver(I). This implies an extremely simple method of separation of these elements from the other platinum elements shown.

Of course, no single reagent can be hoped to be satisfactory for complete separation of all fission products. For example, molybdenum(VI) and U(VI) are very difficult to separate in HCl solutions (see Slide 20) since, at low HCl concentrations where elution is feasible, the distribution coefficients are too similar for rapid refining.

However, in the presence of HF, molybdenum and uranium differ widely (Slide 21) and separations can be achieved. For instance, uranium can be eluted with 2 *M* HCl-1 *M* HF, leaving molybdenum still on the column. Mo(VI) may then be removed with dilute HCl with absence of HF.

Separation of the HCl-non-adsorbable elements at first also appeared to be a rather difficult problem. But there are now complexing agents available such as citrates or versenates, which permit anion-exchange separation rather readily (Slide 22, Fig. 3 of P/837).

From the thermodynamic point of view, anion exchange may be considered a two-phase equilibrium and the adsorption data should thus be usable, with caution, for the elucidation of the properties of the two phases.

At low ionic strength a number of simplifying assumptions may be made and the interpretations become straightforward. However, at high ionic strength this is not the case because there the pertinent activity coefficient quotients will vary rapidly with composition. We had originally hoped, and I believe

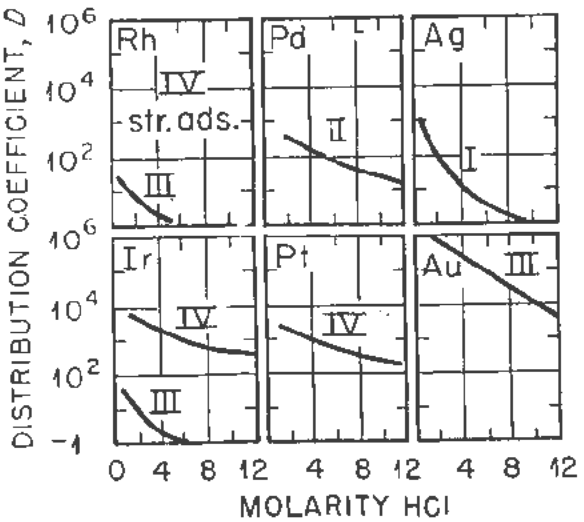

Slide 19

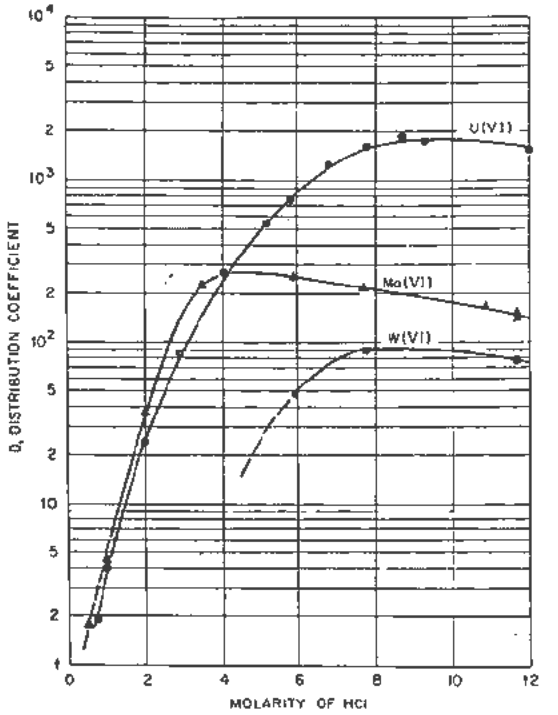

Slide 20. Adsorption of Mo(VI), W(VI), and U(VI) from HCl solutions

that it is still true to a certain extent, that as long as the distribution coefficients increase with concentration of HCl, the negatively charged species are being formed. When the distribution coefficients decrease, the negatively charged complexes are essentially completely formed. However, this qualitative picture may now have to be revised on the basis of newer data.

For example, it was found (see Slide 23) that there is an enormous difference in adsorbability from lithium chloride and hydrochloric acid solutions. Distribution coefficients are of the order of a thousandfold higher in concentrated lithium chloride than in concentrated HCl.

Similar results have been found for a large number of elements, though surprisingly not for silver. I would like to point out that in some cases the distribution coefficients are now becoming truly fantastic. For Ga(III) they are reaching towards 10^8, which also implies considerable complications in obtaining accurate measurements. Our present belief is that the large difference between the HCl and lithium chloride results are caused by the formation of undissociated complex acids in strong HCl solutions and that only in lithium chloride solutions are we really dealing with the negatively charged complexes themselves. This conclusion is not unambiguously established at the present time and work is continuing. We hope that in the not too distant future it will become possible to add more definite statements regarding equilibria in concentrated electrolyte

solutions to our present data on separations with anion exchange resins.

DISCUSSION ON PAPERS P/726, P/719, P/837

Mr. C. M. Nicholls (UK): Mr. Hammond has given some very useful guiding criteria for the radiation limitations in various types of chemical equipment. I wonder whether he could give similar limitations for the use of the fully fluorinated plastics such as Teflon, to use American terminology, or PTFE, to use British terminology. I have in mind the application of such materials in pump components and the like.

Mr. Hammond (USA): I do not have any exact numbers for the radiation stability of plastics. I believe they are available in published literature. I do know that Teflon, as you mentioned, is attacked very readily by radiation and is not the best choice. Also, when it is attacked, it gives off hydrofluoric acid which is another corrosive agent.

Mr. V. G. Timoshev (USSR): Mr. Bruce, I am interested in how the nature of the solvent influences the distribution of the fission products. Various paraffin fractions, carbon tetrachloride and other solvents may be used. To what degree does the use of one solvent rather than another affect the distribution of the fission products?

Mr. Bruce (USA): The total subject of solvent selection and the effect of solvent selection on the distribution of fission products has been studied quite extensively. There is no good generalization which can be made about the distribution of fission products in various classes of solvents. However, we have observed that as a general thing the solvent extraction of fission products increases with increasing water solubility in the solvent. We do not know what the fundamental significance of this is. As I indicated, methyl isobutyl ketone and tributyl phosphate show a very, very great difference in the extractability of fission products.

Mr. J. M. Fletcher (UK): I would like briefly

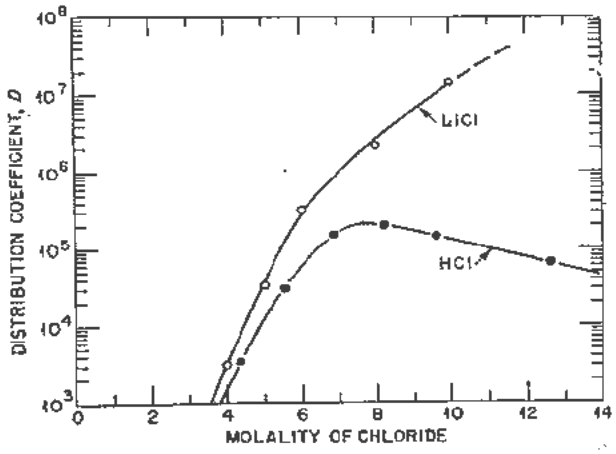

Slide 23. Adsorption of Ge(IV) from HCl and LiCl solutions

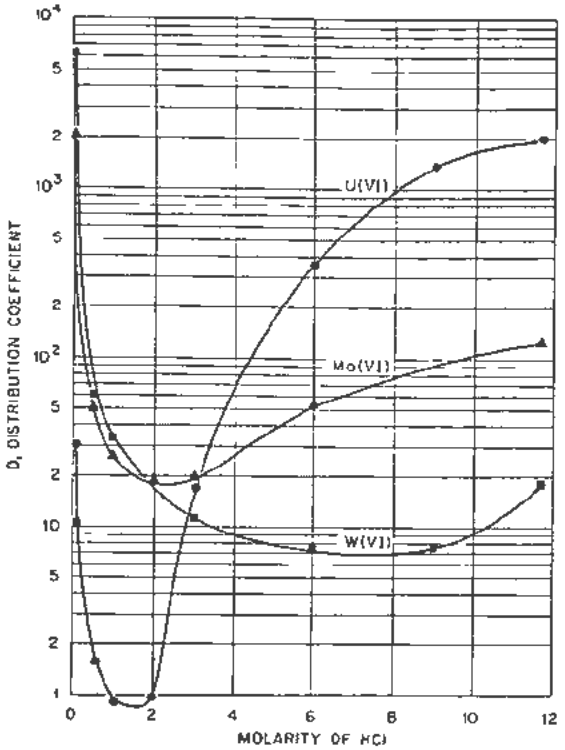

Slide 21. Adsorption of Mo(VI), W(VI), and U(VI) from HCl-HF solutions

to comment on one or two points in Mr. Bruce's paper; firstly, with regard to the influence of the valency of ruthenium on extraction by organic solvents. It may be of interest to state that our experience is that when ruthenium is in the 3, 4, or higher states in nitric acid solutions, we find no significant extraction by organic solvents. It is only when it is converted to the nitrosylruthenium form, in which ruthenium can be, strangely enough, considered divalent, that there is appreciable or considerable extraction by organic solvents. This leads to two effects with reagent such as nitrous acid, or sodium nitrite. If the ruthenium in the first place is in the 3 or 4 valent state, it is converted by the nitrous acid or sodium nitrite to the extractable nitrosylruthenium type of complex. But among the nitrosylruthenium complexes there are very many possible types, all of which give different distribution ratios with various organic solvents. There is a second effect of nitrous acid by which it converts one nitrosylruthenium complex to a nitro one. Mr. Bruce also mentioned the effect of heating with reagents such as ferrous sulphamate. We find in this case that the reduced extractability in this case is directly connected with elimination from the nitrosylruthenium group.

The second point which I would like to ask Mr. Bruce is, if in his experiments on the extractability of ruthenium he studied the influence of time. Our experience is that unlike other metals and all the other fission products, for ruthenium, the distribution ratios and the performance of extractors seem very

dependent on the hold-up time in the extractors. Therefore, it would be of interest if he could give us some idea of the time factor in the experiments that he described.

Mr. BRUCE (USA): The times which were described were about 5 minutes. In connection with Mr. Fletcher's comments on the valence state of the extractable ruthenium compound I would like to make a few observations. First, we have observed that the effect of ferrous sulfamate on the reduction of the ruthenium extraction is greater than the effect of the sulfamate ion alone. Since sulfonic acid is a specific reagent for a nitrite ion, which presumably is involved in the extraction of ruthenium, we feel that we are observing a valent state effect. To substantiate this we also note that the addition of an oxidizing agent such as sodium dichromate to the system enhances the extraction of ruthenium.

There are some interesting points which one can make about the effect of time on the extraction of ruthenium. We have observed, for example, that if one dissolves irradiated uranium in nitric acid and then divides the solution in two parts and extracts one immediately with tributyl phosphate and allows the other solution to sit for several days before extraction, the solution which has been allowed to sit for several days will show approximately 10-fold greater extraction than will the one which is freshly dissolved and extracted.

Therefore, I think that Mr. Fletcher's point is very good. The time element here is a very important point.

The CHAIRMAN: We will take three questions to Mr. Kraus together.

Mr. J. SHANKAR (India): I was wondering whether Mr. Kraus had studied the temperature coefficients. In the studies in the ionic active resonance in some of our work we find that the temperature coefficients are quite large. I wonder if he would comment on this?

Mr. GLUECKAUF (UK): I should like to ask Mr. Kraus whether he could say a few words about the application of anion exchange methods to the separation of neptunium from fission product solutions, with specific reference to nitrate solutions.

Mr. D. I. RYABCHIKOV (USSR): Hitherto, many authors have undeservedly paid less attention to anion exchangers than to cation exchangers for separation purposes, whereas in a number of cases preference might actually be given to anion exchangers.

As regards the separation of uranium from other accompanying elements, it is pertinent to note that uranium and these elements yield a variety of complex compounds with very many reagents in which the atom of these metals can, under suitable conditions, appear in the form of an anion complex. There is a wide variation of complex-forming reagents which yield with different metals complexes of different stability. This diversity is considerably increased by the influence of the medium on the stability of the complex forms. Accordingly, it can be anticipated that under certain selected conditions it should be possible in practice to solve any problem relating to the separation of any particular element from a number of other accompanying elements.

In conclusion, I should like to indicate briefly one other broad possibility in connection with anion exchangers, which has not yet been achieved in practice. What I have in mind is the possibility of their conversion into different anionic forms. By this means it is possible to form specialized anion exchangers which will exercise a selective action in relation to individual elements.

Mr. KRAUS (USA): I should like to comment first on the question regarding temperature coefficients. We have done relatively little work on temperature coefficients, but there are two problems which we shall have to keep in mind in this study. In the region where the complexes are being formed, the observed temperature coefficient will include both the temperature coefficient of the ion exchange equilibrium and the temperature coefficient of the complex equilibria. Regarding the temperature coefficient of the ion exchange equilibrium, our indication is that it is relatively small, while the temperature coefficient of the complex equilibria may be quite large. But we have relatively little data on this question. We have done some work on uranium in sulfate solutions at various temperatures, but the purpose mainly was to increase the rate of desorption, which is rather slow at room temperature.

Regarding the application of ion exchange to work on neptunium in nitrate solutions, I am sorry to report that we have done practically no work on this. We have used other systems in our studies of neptunium. We have some data on Np in fluoride and chloride solutions and, in general, find that neptunium behaves similarly to uranium.

I should like to refer Mr. Glueckauf to a paper by Hyde which, I presume, will go into more detail on available work at the Berkeley laboratory in the United States, but I understand that he also finds that neptunium and uranium are very similar provided the same oxidization states are compared.

I am not sure that I understood all the comments by the Soviet Union representative, but I do agree with him that it does look as though it should become possible to isolate almost any element by anion exchange from all other elements with relatively little effort. I know of only three exceptions, the heavy alkali metals. The light alkali metals can be complexed, e.g., with ethylene diamine tetraacetic acid. We have reported lithium, sodium and potassium in this way, but the separation of the heavy alkali metals has not to my knowledge yet been achieved by anion exchange. On the other hand, anion exchange with EDTA should permit isolation of the heavy-alkali metals in a single pass.

We ourselves have done no work on building groups into resins which can cause specific complex formation. I understand that work of this sort is going on at various places. We ourselves have had little interest in it because I, personally, am convinced that the inorganic chemistry of the elements is sufficiently different, if one only searches for these differences, to make it in most cases unnecessary to have special resins. It has been our approach to work with a simple, commercially available resin and relatively simple ligands, and in this way to by-pass the need for special resins. The special resins undoubtedly do have their place for special applications in chemical processing.

Session 9B.2

CHEMISTRY OF INDIVIDUAL FISSION PRODUCTS

LIST OF PAPERS

The Chemistry of Ruthenium

By J. M. Fletcher and F. S. Martin,* UK

The utilisation of the energy liberated in the process of fission has led to extensive chemical investigations of the actinide elements. It has also focused attention on certain fission products, e.g., elements such as promethium and technetium which do not occur naturally, and on others such as ruthenium and zirconium which present difficulties in chemical separation processes or effluent disposal systems. Although there are references in Gmelin[1] to about 500 ruthenium compounds, only three are relevant to the behaviour exhibited by fission product ruthenium when irradiated uranium is dissolved in nitric acid: of these, one, nitrosylruthenium trinitrate,[2] prior to 1950, had not been obtained in a solid form, and had only once been mentioned since its original formation in 1899 by Joly: the other two, the sodium and potassium salts of the anion $[RuNO(NO_2)_4OH]^{2-}$ have hitherto[3] been incorrectly assumed to be nitrites of Ru(III).

This gap in the knowledge of the chemistry of ruthenium has proved a considerable handicap not only in the development of primary processes, which involve nitric acid, for the separation of fission products from uranium and plutonium, but also in ancillary stages involving further purification, evaporation, ion exchange, precipitation and effluent disposal. The difficulties are accentuated by certain similarities of the ruthenium compounds to those of uranium and plutonium; yet whereas the behaviour of the latter elements has been reasonably reproducible, the behaviour of fission product ruthenium has varied due to slow changes between a wide variety of compounds, such as occurs with C in organic chemistry.

As a result of work undertaken at A.E.R.E. or sponsored by this establishment, it has become clear that the ruthenium compounds arising from the dissolution of irradiated fuel in nitric acid, are mainly trivalent nitrosylruthenium, (RuNO)(III), derivatives which display the characteristics of octahedral six coordination complexes with d^2sp^3 orbitals, associated for example with Co(III) or Pt(IV). With these particular complexes, the penultimate shell has 18 electrons. There are numerous references in the literature to amino, halogen, cyano, etc. complexes of (RuNO).

*Atomic Energy Research Establishment, Harwell, nr. Didcot, Berks.

NITROSYLRUTHENIUM COMPLEXES IN AQUEOUS NITRIC AND NITROUS ACIDS

In aqueous solutions containing only nitric and nitrous acids, i.e., with the ligands NO_3^-, NO_2^-, OH and H_2O available, it is possible to postulate a considerable number of combinations by which these four ligands occupy the five coordination positions available in a mononuclear (RuNO) compound, the sixth position being occupied by NO. Examples, with compounds so far identified are given in Table 1. The number of compounds possible is further increased, (*a*) when spatial considerations are considered, e.g., $[RuNO(NO_3)_3(H_2O)_2]$ could exist as shown in Fig. 1, and (*b*) if bi- and polynuclear species exist.

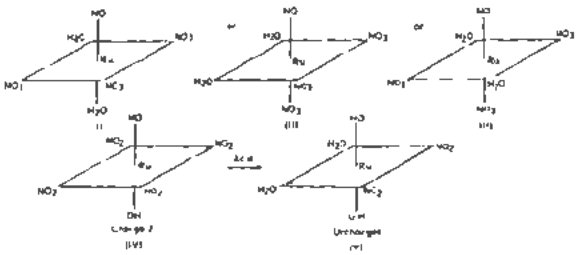

Figure 1

Polynuclear formation occurs in the later stages of hydrolysis of the nitrato complexes; thus a heminitrate, represented with a diol bridge as

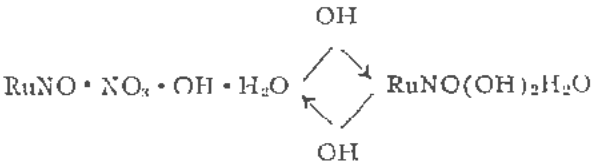

has been isolated.[3] Binuclear oxygen bridged compounds, e.g., $Ru_2N_6O_{15}$,[3] also exist as in other ruthenium compounds, e.g., $K_4[Ru_2Cl_{10}O]H_2O$.[5]

Hydroxide

The parent of these hydroxoaquo complexes of (RuNO) is nitrosylruthenium hydroxide, empirically $RuNO(OH)_3$, for which a simple method of preparation, minimising its tendency to form colloidal solution, has been found.[5] The conditions necessary for

Table 1. Examples of Possible Mononuclear Six Coordination Complexes Composed of (RuNO) and the Ligands NO_3^-, NO_2^-, OH^-, H_2O

Ligands	*Possible complex*	*Existence*
OH, H_2O	1. $RuNO(OH)_3(H_2O)_2$	As polynuclear derivatives;[3] nitrosylruthenium hydroxide, brown, amorphous solid.
NO_3	2. $[RuNO(NO_3)_5]^{2-}$	Unknown
NO_3, OH	3. $[RuNO(NO_3)_4OH]^{2-}$	Not yet isolated, but formed in organic solutions of high nitrate concentration[4]
NO_3, H_2O	4. $[RuNO(NO_3)_4H_2O]^-$	
	5. $[RuNO(NO_3)_3(H_2O)]_2$	With additional $2H_2O$ as rose-red hygroscopic solid[2, 3]
	6. $[RuNO(NO_3)_2(H_2O)_3]^+$	Formed in solution from 5: evidence from ion exchange resins, pH measurements etc.[3]
	7. $[RuNO(NO_3)(H_2O)_4]^{2+}$	
NO_3, H_2O, OH	8. $[RuNO(NO_3)_3OH \cdot H_2O]^-$	
	9. $RuNO(NO_3)_2OH(H_2O)_2$	Red to brown mixtures isolated[3]
	10. $RuNO \cdot NO_3(OH)_2(H_2O)_2$	
	11. Anionic and cationic forms of 9 and 10	—
NO_2	12. $[RuNO(NO_2)_5]^{2-}$	Unknown
NO_2, OH	13. $[RuNO(NO_2)_4OH]^{2}$	Na and K salts as orange crystalline solids[5]
NO_2, H_2O	14. $[RuNO(NO_2)_4H_2O]^-$	Unknown but may exist in solution of 13
	15. $RuNO(NO_2)_3(H_2O)_2$	Unknown
NO_2, H_2O, OH	16. $RuNO(NO_2)_2OH(H_2O)_2$	Yellow solution obtained, solid not yet isolated[3, 4]
	17. $RuNO \cdot NO_2(OH)_2(H_2O)_2$ etc.	Unknown
NO_2, NO_3	18. $[RuNO(NO_2)_2(NO_3)_3]^{2-}$ etc.	Unknown
NO_2, NO_3, OH	19. $[RuNO(NO_2)_2(NO_3)_2OH]^{2-}$ etc.	Unknown
NO_2, NO_3, H_2O	20. $RuNO \cdot NO_2(NO_3)_2(H_2O)_2$	Orange crystalline solid[4]
NO_2, NO_3, OH, H_2O	21. $RuNO \cdot NO_2 \cdot NO_3 \cdot OH(H_2O)_2$	Unknown

its formation from nitrosylruthenium complexes indicate the usual order for the stability of this type of complex, viz. ClO_4, $F < NO_3 < OH$, $Cl < NO_2$.

Nitrato Complexes

These have been prepared from ruthenium tetroxide[2,3] and from ruthenium alloys[3] by treatment with oxides of nitrogen and nitric acid. In dilute HNO_3, nitro complexes are first formed: boiling with concentrated nitric acid converts these to the nitrato complexes; the trinitrate and mixtures of lower nitrates have been isolated from these solutions by evaporation under reduced pressure. In solution in water or dilute nitric acid, the trinitrate is hydrolysed at a measurable speed at room temperature to the di- and mononitrato complexes; at pH 5–8, hydrolysis proceeds to a crude form of the hydroxide which retains a small proportion of complexed nitrate groups.[3] The reaction, trinitrate complex → dinitrate complex is first order with respect to [Ru] in nitric acid solution over the range 10^{-2} to 10^{-5} *M*.[4] Both anionic and cationic exchange resins remove ruthenium species from aqueous solutions of these complexes.[3] The trinitrato complex is readily extracted from aqueous solution by a variety of organic solvents; if these contain additional nitrates (e.g., nitric acid, quaternary ammonium nitrates), conditions exist for the formation of nitrato complexes with $[NO_3] : [RuNO] > 3$; but if the organic phase contains a high ratio of $[H_2O] : [NO_3]$, hydrolysis occurs as in a purely aqueous phase.[4]

Some or all of the nitrato groups of the nitrates are readily displaced in warm dilute acid solution by (NO_2) groups using NO-NO_2 mixtures,[4] by (SH) using hydrogen sulphide,[3] by Cl using hydrochloric acid,[3] by (SO_4) using sulphuric acid and by (C_2O_4) using oxalic acid.[3]

The spectrophotometric absorption spectrum of a solution of the trinitrate in aqueous nitric acid shows[3] a broad band between 435 and 590 mμ; this band is less prominent with the lower nitrates. Regularly spaced peaks (at about 1000 cm^{-1} intervals) which are scarcely distinguishable in aqueous solution, become more prominent with organic solutions; the intervals are attributed to the fundamental vibration frequencies of the Ru-N-O bonds (cf. the 727 cm^{-1} interval in organic solutions of uranyl nitrates[6]).

Nitro Complexes

These have been obtained either as yellow to orange crystalline solids or in aqueous solution.[3,4] Recrystallisation of salts of the tetranitro anion from water, acetone or alcohol is feasible. The dinitro complex is the stable form in warm dilute mineral acids; two further nitro groups can be introduced using sodium nitrite at pH~7, but when boiled in alkaline solution (pH>11) all the nitro groups are displaced and nitrosylruthenium hydroxide is formed. As with the ni-

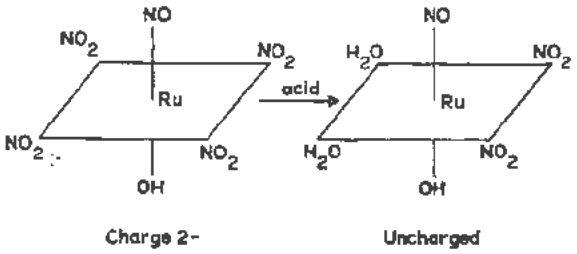

Figure 2

trato complexes, hydrogen sulphide forms an insoluble nitrosylruthenium hydrosulphide.[3]

The displacement of two of the four nitro groups from $[RuNO(NO_2)_4OH]^{2-}$ by warming with dilute nitric or perchloric acid illustrates the importance of spatial distribution on the reactivity of these complexes, by the operation of the "*trans*-effect".[7,8] These reactions lead one to suppose that the structure of the $[RuNO(NO_2)_4OH]^{2-}$ anion is that of (IV), giving, due to the high *trans*-effect of the (NO_2) group, the *cis* dinitro complex (V) (see Fig. 2).

The absorption spectrum of an aqueous solution of the tetranitro complex shows no prominent peaks in the visible region, but prominent peaks in the infrared region are found. Bands common to both this complex and to $Na_3[Co(NO_2)_6]$ are found at 1420, 1338, 1270, 841, 826, 636 and 619 cm^{-1}; a further strong band at 1907 cm^{-1} arises from the N=O stretching vibration of the nitrosyl group, and there is another weak one at 3617 cm^{-1} in agreement with the presence of a hydroxyl group.[9]

General Properties (Oxidation, Reduction, etc.)

When heated with strong oxidising agents in acid solution (e.g., periodic acid, Ce(IV), $KMnO_4$, ozone and boiling concentrated nitric acid) these nitrosylruthenium complexes are slowly oxidised to ruthenium tetroxide. When heated in a stream of hydrogen the metal is formed, and when fused with alkaline-nitrate mixtures, the nitrosyl group is eliminated; the latter reactions form the basis of analytical methods for estimating ruthenium in these complexes. Many of these compounds explode violently when evaporated from solutions in organic solvents.[3]

CHLORO COMPLEXES

These complexes are relevant to the field of nuclear energy since trace quantities of fission product ruthenium may appear in sea-water or in the digestive systems of mammals. Their stability is intermediate between the weak nitrato and strong nitro complexes. The hydrolysis of the pentachloro and trichloro complexes has received detailed study[10] and in principle resembles that of the trinitrato complex. The acid of the tetrachloro complex, $H_2[RuNOCl_4OH]$, has been isolated and found to be relatively soluble in lower alcohols and ketones.[3]

RELATION OF (RuNO) TO OTHER FORMS OF RUTHENIUM AND OTHER METALS

The general properties of the nitrosylruthenium complexes show a marked difference from those of Ru(IV). Nitrato complexing of Ru(IV) is very weak and the behaviour of solutions of Ru(IV) nitrates[11] have been interpreted in terms of proton transfer between aquohydroxo ions, e.g., $[Ru(OH)_2(H_2O)_4]^{2+} \rightarrow [Ru(OH)_3(H_2O)_3]^{+} + H^{+}$. In this respect the behaviour of Ru(IV) is related to Zr(IV), U(IV), etc., but is very different in degree on account of the small ionic radius of Ru^{4+}. In these quadrivalent metals fluoride complexing is strong,[12] whereas with (RuNO) it is very weak,[3] just as it is exceptionally rare with Co(III) and Pt(IV). In the presence of oxides of nitrogen, other forms of ruthenium are readily converted to (RuNO). The considerable stability of the nitrosyl group in these compounds can be interpreted as strengthening of the covalent bond between Ru(II) and NO^{+}, i.e., $Ru{\leftarrow}N{\equiv}O$, by π-bonding in which the metal donates two $d\pi$ electrons.[13] The *trans*-effect of the nitrosyl group is likely to be even greater than that of (NO_2), and provides the reason for particular differences observed between (RuNO) complexes on the one hand, and Co(III) and Pt(IV) complexes on the other hand: it can be related, for example, to the predominance of the $[RuNO(NH_3)_4X]$ type of complex amongst other amino complexes of (RuNO),[14] it being likely that X occupies the position *trans* to (NO), and thereby is readily substituted between monovalent ligands such as Cl^{-}, Br^{-}, NO_3^{-}, OH^{-}, etc.

IMPLICATIONS ON EFFLUENT TREATMENT

Due to the stability of the nitro group, the formation of an insoluble nitrosylruthenium hydroxide does not occur when mixed fission product solutions containing these complexes are neutralised with alkali. Although this hydroxide is formed more readily from the (NO_3) complexes than from the (NO_2) complexes, it is colloidal under many conditions. In view of these properties, it is not surprising that in experiments with mixed fission products originating from nitric acid solution, ruthenium rarely follows one and only one course. Normal methods of effluent treatment (e.g., precipitation, ion exchange, microbiological treatment) usually fail to remove fission product ruthenium completely. The ultimate fate in nature of traces of ruthenium from effluent plants has led to investigations on its behaviour in mammals, fish, plants and algae.[15]

REFERENCES

1. *Gmelin's Handbuch der Anorganischen Chemie*. System No. 63, Ruthenium (1938).
2. Martin, F. S., *Ruthenium Nitroso-Trinitrate*, Chem. Ind.: 824 (1953).
3. Fletcher, J. M., Jenkins, I. L., Lever, F. M., Martin, F. S., Powell, A. R. and Todd, R., *Nitrato and Nitro Complexes of Nitrosylruthenium*, J. Inorganic and Nuclear Chemistry, (in press).

4. Brown, P. G.M., Fletcher, J. M., Jenkins, I. L. and Wain, A. G., Unpublished results. A.E.R.E. Chemistry Division.
5. Mathieson, A. M., Mellor, D. P. and Stephenson, N P., *The Crystal Structure of* $K_4[Ru_2Cl_{10}O] \cdot H_2O$, Acta Cryst. *5*:185 (1952).
6. Kaplan, L., Hildebrandt, R. A. and Ader, M., *The Absorption Spectra of Uranyl Nitrate in Organic Solvents*, ANL 4521: (1950).
7. Chernyaev, J. J., *Nitrates of Platinum*, Ann. Inst. Platine *5*: 118 (1927).
8. Burkin, A. R., *The Stabilities of Complex Compounds*, Quarterly Review *5*:1 (1951).
9. Gaunt, J. and Meaburn, G. M., *Infra-Red Spectrophotometric Measurements*, quoted in Ref. 3.
10. Smith, A. J., *A Physico-Chemical Study of the Chemistry of Ruthenium*, Ph.D. Thesis, London (1954).
11. Anderson, J. S. and McConnell, J. D. M., *Ruthenium (IV) Nitrates*, J. Inorganic and Nuclear Chemistry, (in press).
12. Hepworth, M. A., Peacock, R. D. and Robinson, P. L., *Complex Fluorides of Quadri- and Quinquevalent Ruthenium*, J. Chem. Soc.: 1197 (1954).
13. Craig, D. P., Maccoll, A., Nyholm, R. S., Orgel, L. and Sutton, L. E., *Chemical Bonds Involving d-orbitals*. Part I, J.C.S.: 332 (1954).
14. Werner, A., *Zur Kenntnis der Rutheniumammoniakverbindungen*, Beitrag III, Zur Theorie der Hydrolyse, Ber. 40(II) : 2614 (1907).
15. Biological Investigations sponsored by M.R.C./A.R.C. Joint Committee on the Biological and Non-Medical Aspects of Radiation.

Some Chemical Properties of Technetium

By J. B. Gerlit, USSR

As early as 1877 Mendelyev predicted from the periodic law which he had previously formulated, a number of the physical and chemical properties of elements with atomic weights of approximately 100 and 187.[1] Later, Kern[2] announced the discovery of an element with an atomic weight of 100 and described some of its chemical properties. Kern's data were confirmed by Mallet,[3] but these works were undeservedly neglected. Reports by Noddak and Noddak[4,5,6] on their discovery of an element with an atomic number of 43 also have not been finally confirmed. Comparison of the chemical and physical properties of masurium and technetium reveals great similarity between their characteristics, quite obvious in their characteristic roentgenographic spectra. Thus, according to Noddak, Noddak and Berg,[4] the spectrum of masurium is characterized by lines $K_{\alpha 1} = 672$, $K_{\alpha 2} = 675$, $K_{\beta 1} = 601$, while the spectrum of technetium, according to Burkhardt and co-workers[7] is $K_{\alpha 1} = 673.5$, $K_{\alpha 2} = 677.8$, $K_{\beta 1} = 601.4$ and $K_{\beta 2} = 589.9$ X-units.

Detailed study of the properties of element 43 became possible after its isolation first radiochemically from irradiated molybdenum,[8,9,10] and then in weighable quantities from slag left after plutonium production.[11,12,13] At present 19 isotopes of this element are known with half-lives ranging from a few seconds to hundreds of thousands of years,[14] and in the interval of mass numbers 92 to 107. The most interesting among them are isotopes with atomic weights of 97, 98 and 99. The first two have not been studied at all, but appear to have long half-lives.[15] The isotope 99, having a half-life of 2.15×10^5 years, is obtained with an extremely large fission yield of uranium and plutonium (6.3 to 6.5%).[16]

Recently the presence of technetium has been established, not only in the atmospheres of the sun and young stars,[18,19] but also in the crust of the earth,[20] therefore it is very tempting to determine its origin. However, its chemical and analytical properties, of great importance for studying the geochemical behaviour of this element, are comparatively little known.

The corrosion resistance of technetium and the small cross section of isotope 99 for thermal neutrons permits the use of this element both in reactor technique[17] and in other fields of industry.

Original language: Russian.

This paper contains results of our studies on the analytical chemistry of this element.

METHODS OF EXTRACTION AND TECHNIQUE OF MEASUREMENT

A study of the chemical properties of technetium was carried out using the 6.1-hour isomer Tc^{99m} obtained by the reaction $Mo(n, \gamma, \beta)Tc^{99m}$. A test of known methods for separating technetium from molybdenum showed that the best results can be obtained by the methods of Jacobi[21] and Beinbridge and co-workers,[22] based on coprecipitation and distillation. However, after we had established the possibility of extracting technetium from alkaline and acid media, more appropriate methods were worked out by which the isolation of technetium was subsequently conducted.

Since the isomeric transition from Tc^{99m} to Tc^{99} is accompanied by the emission of soft γ-rays, the activity of preparations was determined with γ-counting apparatus. According to a number of authors,[23,24] the γ-ray spectrum of the isomeric transition is characterized by the emission of 2.0, 140.3, 142.3 and 181 kev, but according to Baranov, the transition of 181 kev was not observed.

The counting device consisted of an argon-methanol Geiger-Mueller counter with a copper cathode, a high voltage amplifier, a scaler and mechanical counter. Due to the necessity for measuring the soft γ-radiation, the lead-iron block of the counter was screened with thick black paper to avoid excitation of the counter by light quanta. For measuring, the preparations were placed in similar test tubes made of molybdenum glass and fixed rigidly in the Plexiglas holder in a manner ensuring geometrical constancy. In all the tests only the relative activity of the samples was determined by comparing with Tc^{99m} standards. The radiochemical purity of the isolated preparations was controlled by the half-lives. Approximate measurements of the contamination of the technetium samples by radioactive molybdenum were made with a lead filter of 4 gm/cm² which completely absorbed the soft γ-radiation of the isomeric transition and was determined by the formula

$$I_{Mo} = a\, I_f$$

where I_{Mo} is the approximate activity of the molybdenum, I_f is the intensity of the hard radiation of the preparation, determined in the presence of a filter,

and a is the ratio between the intensity of the γ-radiation of molybdenum after complete separation of technetium, measured without a filter, and the intensity of the radiation determined in the presence of the filter.

The a was calculated according to the decay scheme suggested by Medicus and co-workers,[23] and also determined experimentally. The maximum differences did not exceed 3.5%. Statistical errors did not exceed $\pm$ 2.5%, the activity of samples being about 5000 counts per min. Considering that the alteration of the decay constant due to the nature of the chemical compound of Tc^{99m} isomer is less than the calculated error[22]

$$\left(\frac{\lambda_{KTcO_4} - \lambda_{Tc\ metal}}{\lambda_{Tc\ metal}} \cdot 100 \approx 0.3\% \right)$$

this value was usually ignored.

For studying the behaviour of rhenium in a number of reactions, the isotopes Re^{186} and Re^{188}, obtained by (n, γ) reactions, were used. The properties of ruthenium were studied with the aid of Ru^{106}, being in equilibrium with Rh^{106} isolated from fission products. Owing to the presence of hard radiations in their γ-spectra the activities of the rhenium, ruthenium and molybdenum preparations were measured on the apparatus described above, using a lead filter of 4 gm/cm^2. The degree of purity was checked by the hardness of the β-radiation, estimated by absorption in aluminum.

STUDIES ON CERTAIN PROPERTIES OF HEPTAVALENT TECHNETIUM

Coprecipitation

For concentrating traces of technetium the most convenient methods are coprecipitation, electrolysis, extraction and ion exchange. As radiochemical investigations have shown, in a number nf cases at the first stage of separation of microcomponents, the method of coprecipitation on isotopic or nonisotopic carriers is most suitable. Among the methods of coprecipitation of technetium, its coprecipitation with rhenium, copper, bismuth and platinum sulphides[8,10,21] has been studied in detail. However, a difference exists between these processes in hydrochloric and in sulphuric acid solutions. Thus, coprecipitation does not occur in 9 N hydrochloric acid, which Jacobi[21] explains by the solubility of the technetium sulphide under these conditions. We have established that hydrochloric acid reduces heptavalent technetium to the tetravalent state; experiments were conducted in this connection to determine the valency form of the non-coprecipitated technetium during the precipitation of rhenium sulphide from 9 N hydrochloric acid. The data obtained showed that practically all the technetium was tetravalent. Investigations on the precipitation of rhenium sulphide from a hydrochloric acid solution containing known tetravalent technetium, showed that in this case no coprecipitation occurs.

Table 1. Coprecipitation of Technetium (VII) with Certain Insoluble Salts of Perrhenic and Perchloric Acids

No.	Coprecipitant	Solubility of coprecipitant at 20°, M/l	Coprecipitation of technetium, in %
1	Nitron perrhenate	0.0026	99.8
2	Cesium perrhenate	0.0040	85.7
3	Rubidium perrhenate	0.0061	81.2
4	Potassium perrhenate	0.038	23.8
5	Thallium perrhenate (1)	0.0035	91.4
6	Nitron perchlorate		99.7
7	Cesium perchlorate	0.0069	83.2
8	Rubidium perchlorate	0.0050	85.4
9	Potassium perchlorate	0.012	28.2
10	Ammonium perchlorate	—	14.6

The experiments also showed that technetium sulphide may be precipitated with rhenium as a carrier from 3 N sulphuric acid solutions by potassium thiosulphate, the coprecipitation proceeding considerably faster and more thoroughly than with the use of hydrogen sulphide. The same takes place when copper salts are used as carriers. The above method may be recommended for quick concentration of technetium traces. Usually insoluble perrhenates[8] are also recommended for the same purpose, but there is almost no literature on the quantity of coprecipitation of technetium except for precipitation with nitron perrhenate. It is also known that the structures of the ReO_4^-, MnO_4^- and ClO_4^- ions are very similar. Therefore it may be supposed that to a certain degree insoluble perchlorates must be coprecipitants for technetium. Owing to the absence in print of even preliminary data on the question, it was desirable to obtain rough semiquantitative values without detailed consideration of the mechanisms of coprecipitation processes, and to compare the behaviour of technetium during precipitation of perrhenic and perchloric acids by nitron, cesium, rubidium, potassium, and monovalent thallium. All experiments were conducted with perrhenate and perchlorate ion concentrations of 0.018 M. Precipitation of nitron perrhenate and perchlorate and thallium perrhenate was conducted from an acetate medium, and of cesium, rubidium and potassium perrhenates and chlorates from a neutral medium. Table 1 shows the results of these experiments, demonstrating that the most complete coprecipitatinn of technetium is observed in the case of less soluble perrhenates and perchlorates.

For practical purposes the use of perchlorates has the advantage that there is no need of further separating technetium from rhenium.

Extraction of Technetium Compounds

Data have been published on the extractability of tetraphenylarsonium pertechnetiate by chloroform[28,29] from neutral media and of sodium pertechnetiate by pyridine from alkaline media.[30] It seemed desirable for developing rapid methods of separating technetium from a number of elements to determine the possibility of extracting it from acid, neutral and alka-

line solutions, as well as to explore the thoroughness of its extraction by means of various reagents and to compare its behaviour with that of such elements as molybdenum and ruthenium. The experiments showed, as reported in Table II, that both rhenium and technetium are extracted from neutral media with comparatively small coefficients by a number of alcohols, ketones and amines; from alkaline media they are extracted by ketones, pyridine and piperidine; and from acid media they are extracted by certain alcohols with somewhat higher distribution coefficients. Molybdenum and ruthenium are extracted from alkaline media by amines with comparatively small distribution coefficients (from 0.01 to 5.7), and from acid media by tributylphosphate. Comparison between the behaviour of technetium and rhenium during their extraction from acid, neutral and alkaline media by alcohols shows that the distribution coefficient has a definite tendency to increase in more acid media; for ketones this is true in the case of alkaline and neutral media; and for aniline and dimethylaniline only in neutral media. Since technetium solutions in various acids are the most common, investigations were made on the effect nf concentration and the nature of the acid oo the distribution coefficient. The results are shown in Figs. 1 and 2. The most complete extraction of technetium and rheoium is achieved from sulphuric acid media (Fig. 2). The decrease of the technetium extraction coefficient (as opposed to that of rhenium) from hydrochloric acid media is explained by partial reduction which is confirmed by the presence of tetravalent technetium in the water phase.

Analysis of extractions from neutral and alkaline media yielded the results shown in Fig. 3.

It is noticeable that the distribution coefficient of technetium and rhenium in aniline and dimethylaniline decreases with increasing alkaline concentration, whereas with ketones the coefficient increases sharply.

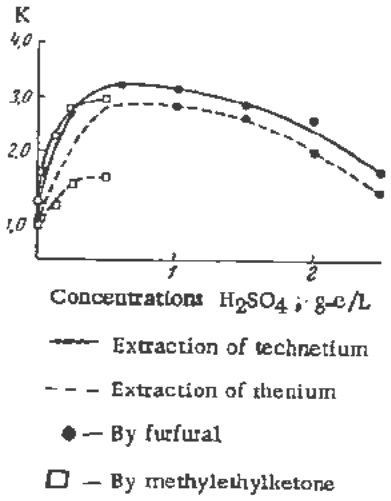

Figure 1. Effect of sulphuric acid concentration on the extraction of technetium and rhenium

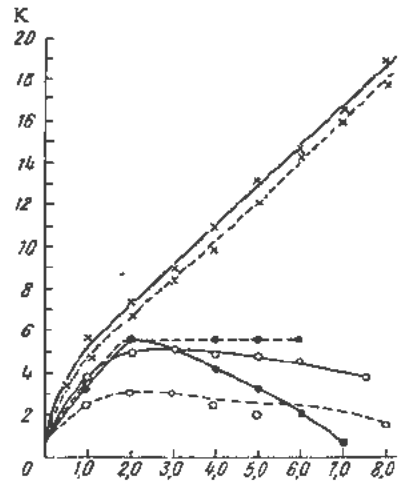

Figure 2. Effect of the concentration and nature of the acid on the extraction of technetium and rhenium by isoamyl alcohol

All this indicates a difference in the mechanisms of the process of extraction. To find out in which form rhenium, and by analogy technetium, are extracted by ketones and amines from neutral media, the ratio K:Re was worked out for the solvent phase for the extraction of an aqueous solution of potassium perrhenate. The results of the analyses showed that in the case of extraction by methylethylketone this ratio is 1 ± 0.17, while in the case of aniline, potassium was not detected in the organic solvent phase. Evidently, in the extraction by aniline, rhenium passes into the solvent phase in the form of an "ammonium" compound[31] of the type $[ReO_4]^-$ $[H_3N — C_6H_5]^+$ which is not formed in alkaline media because of the suppression of the dissociation of the "anilinium" hydrate $[C_6H_5NH_3]^+OH^-$.

In the extraction of technetium and rhenium from acid and alkaline media by oxygen-containing solvents, the respective acids or salts are evidently dissolved. This assumption is confirmed, on the one hand, by direct experiments, conducted with radioactive rhenic acid and potassium perrhenate, and on the other, by spectrophotometric data (Fig. 4) on the behaviour of the perrhenate ion in neutral, acid and alkaline media.

As will be seen from Fig. 4, the absorption spectrum does not change appreciably in the above media.

When the crystalline acid was treated with isoamyl alcohol and methylethylketone, active rhenium was found in large quantities in both solvents (up to 55%), but potassium perrhenate on treatment was found only in the methylethylketone. In addition, as Fig. 5 shows, foreign ions in the solution also influence the coefficient of extraction of technetium.

Evidently, the presence of large quantities of salts leads to the "salting out" of sodium pertechnetiate on extraction of methylethylketone, and sharply decreases the extraction by aniline due to competition in the formation of "anilinium" salts.

Table II. Extraction of Technetium(VII), Molybdenum(VI), Rhenium(VII), and Ruthenium(IV) from Alkaline, Neutral and Acid Media

Extracting agent	Coefficient of distribution											
	5N NaOH				Neutral medium				2N H_2SO_4			
	Tc	Mo	Re	Ru	Tc	Mo	Re	Ru	Tc	Mo	Re	Ru
Isoamyl alcohol	< 0.001	< 0.001	< 0.001	< 0.001	0.82	< 0.001	0.56	< 0.001	7.8	0.1	7.0	< 0.001
Isobutyl alcohol	< 0.001	< 0.001	< 0.001	< 0.001	—	—	—	—	—	—	—	—
Benzyl alcohol	< 0.001	< 0.001	< 0.001	< 0.001	0.26	< 0.001	0.17	0.01	6.6	< 0.001	5.8	≈ 0.002
Hexalin	1.7	0.02	1.5	< 0.001	4.5	< 0.001	3.2	0.022	13.5	0.2	10.2	0.05
Furfural	—	—	—	—	1.0	< 0.001	0.75	< 0.001	3.0	0.001	2.8	—
Methylethylketone	49	0.2	46	< 0.001	1.04	≈ 0.005	0.72	< 0.001	2.9*	< 0.001*	1.5*	< 0.001*
Diethylketone	41	0.05	37	< 0.001	0.93	0.001	0.67	< 0.001	5.3	0.005	3.7	< 0.001
Methylisobutylketone	17	< 0.001	8.2	< 0.001	0.28	≈ 0.003	0.008	< 0.001	6.9	0.01	3.8	—
Diethyl ether	Does not extract											
Diisopropyl ether	Does not extract											
Ethylacetate	Does not extract											
Tri-n-butylphosphate	—	—	—	—	6.4	8.5	3.7	1.2	17.5	21.6	13.2	8.5
Pyridine	39	0.88	24	5.7	Phases are not separated							
Piperidine	27.2	0.79	18.6	4.2	Phases are not separated							
Aniline	0.15	< 0.001	0.008	0.7	5.6	—	4.3	—	—	—	—	—
Dimethylaniline	< 0.001	< 0.001	< 0.001	< 0.001	0.33	—	0.25	—	—	—	—	—
N-benzylpyrrole	Does not extract											
Cyclohexane	Does not extract											
Chloroform	Does not extract											
Heptane	Does not extract											
Dichlorethane	Does not extract											

*For 0.5N H_2SO_4.

Table III. Extraction of the Thiocyanate Compound of Technetium by Ether

No.	Order of adding reagents				Acid concentration, M/l	K_{Tc}
1	TcO_4^-	+KSCN	+HCl		0.1	14.3
2	TcO_4^-	+KSCN	+$SnCl_2$	+HCl	0.1	3.0
3	TcO_4^-	+HCl	+$SnCl_2$	+KSCN	0.1	0.14
4	TcO_4^-	+KSCN	+HCl		1.0	13.9
5	TcO_4^-	+KSCN	+HCl	+$SnCl_2$	1.0	0.03
6	TcO_4^-	+HCl	+$SnCl_2$	+KSCN	1.0	0.001
7	TcO_4^-	+KSCN	+HCl		3.0	8.7
8	TcO_4^-	+HCl	+$SnCl_2$	+KSCN	3.0	0.001

Table 2 shows that neither rhenium nor technetium is extracted by non-polar solvents. The experiments also showed that mixtures of oxygen-containing and non-polar solvents do not extract these elements if they can be almost quantitatively extracted by oxygen-containing solvents alone. We took advantage of this property to reextract rhenium and technetium from the organic solvent phase into the water phase.

On the bases of the above data, methods were developed for separating technetium from molybdenum and ruthenium by extraction with ketones from 3 to 5 *N* solutions in alkali or alkaline metal carbonates, with subsequent reextraction into the water phase by chloroform, and for its separation from rhenium by

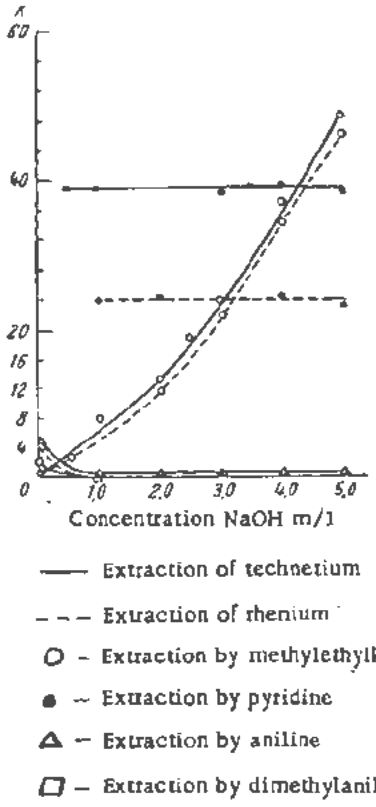

Figure 3. Effect of alkali concentration on the extraction of technetium and rhenium

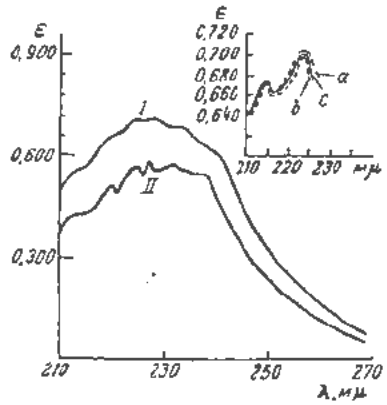

I 0.00018 M solution of $HReO_4$
II Crystalline $HReO_4$
a Spectrum of ReO_4 in 9 M of H_2SO_4
b Spectrum of neutral solution of $HReO_4$
c Spectrum of ReO_4 in 10 M NaOH

Figure 4. Absorption spectrum of rhenic acid: (I) 0.00018 M solution of $HReO_4$, (II) crystalline $HReO_4$; *(a)* spectrum of ReO_4 in 9 M of H_2SO_4, *(b)* spectrum of neutral solution of $HReO_4$, (c) spectrum of ReO_4 in 10 M NaOH

the extraction of rhenium from sulphuric acid solution by isoamyl alcohol, the technetium being previously reduced to its tetravalent state by hydrazine.

Data on the extractability of the thiocyanate compound of technetium are contradictory.[8,82] This is probably because certain authors used the method developed for separating rhenium, i.e., they conducted this reaction with large amounts of stannous chloride and hydrochloric acid present. Experiments, results of which are given in Table III, have shown that in the absence of reducing agents, extraction by diethyl ether proceeds with a rather satisfactory distribution coefficient (see Table III).

The decrease of the technetium extraction coefficient with the increase of HCl concentration and addition of $SnCl_2$ is most probably connected with the reduction of technetium to its lower valence states. The difference between the conditions for forming complex compounds was utilized for developing the method for separating rhenium from technetium.

In addition it was established that technetium may be extracted from acid media in the form of a diethyldithiocarbamate compound by chloroform and certain other solvents (see Fig. 6).

Rhenium, molybdenum and ruthenium under similar conditions are also extracted with rather good distribution coefficients. Technetic acid, like rhenic acid, may be extracted by chloroform and oxygen-containing solvents from acetate solutions in the form of a compound with nitron.

PRODUCTION AND STUDY OF THE PROPERTIES OF THE LOWEST VALENT FORMS OF TECHNETIUM

After comparison between the potentials of the systems MnO_4^{2-}/MnO_4^- and ReO_4^{2-}/ReO_4^- in alkaline media, which equal −0.567 and +0.7 volts re-

spectively,[33] it may be assumed that under similar conditions the potential of the system TcO_4^{2-}/TcO_4^- must be about +0.2 to +0.5 volts. Therefore, the sesquivalent state of technetium must be fairly stable in alkaline media, although according to Boyd and co-workers,[34] in aqueous solutions it should be disproportionate.

Experimental data have shown that with weak reducing agents like hydrazine hydrate in an alkaline medium in the cold, technetium is reduced to its lowest valency and is extracted by neither ketones nor pyridine, nor is it precipitated on ferric hydroxide, but is quantitatively coprecipitated with molybdenum oxyquinolate and silver and lead molybdates, which suggests the sesquivalency of the element.

It is of interest also that, while as a result of irradiation of salts of molybdic acid by neutrons, heptavalent technetium is formed, in the case of the irradiation of molybdenum blue, subsequently dissolved in concentrated alkalies, technetium, on the contrary, will be sesquivalent.

When an alkaline solution of sesquivalent technetium is diluted to an OH^- ion concentration of about 0.02 to 0.05 *N*, a change occurs in time in the technetium valency and it becomes septivalent and tetravalent. After equilibrium is attained the ratio of Tc(VII) to Tc(IV) is about 2:1 (from 1.74:1 to 2.3:1) and the sesquivalent technetium almost completely disappears.

Thus, the process of disproportionation evidently goes on as in the case of rhenium and manganese as follows:

$$2TcO_4^{3-} + H_2O \rightarrow TcO_4^- + TcO_3^- + 2\,OH^-$$
$$2TcO_3^= \rightarrow TcO_4^{2-} + TcO_2$$

The sesquivalent form of technetium can be extracted by chloroform and other non-polar solvents from weak alkaline media in the form of complexes with dioximes.

In addition to the method of reduction by potassium iodide in a hydrochloric medium, described elsewhere,[35] the tetravalent form of technetium may easily be obtained, as experiments have shown, both from acid and alkaline media. In a sulphuric acid

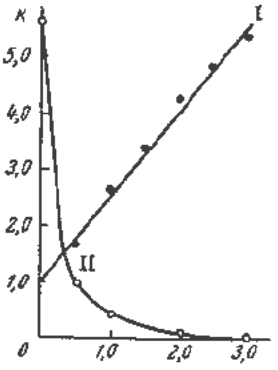

Figure 5. Effect of sodium nitrate concentration on technetium extraction: (I) by methylethylketone, (II) by aniline

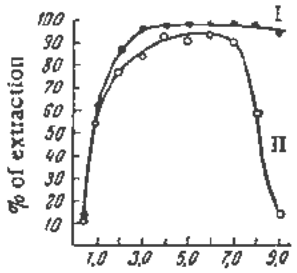

Figure 6. Effect of the concentration and nature of the acid on the extraction of the diethyldithiocarbamate compound of technetium by chloroform: (I) sulphuric acid medium, (II) hydrochloric acid medium

medium technetium may be reduced to the tetravalent form by hydrazine, hydroxylamine, ascorbic acid and $SnCl_2$. In alkaline media reduction proceeds with these reagents only with prolonged boiling. Reduction of technetium by concentrated hydrochloric acid proved to be very interesting. A study of the reaction kinetics showed that the reduction depends on the temperature and concentration of the hydrochloric acid. Thus, at 20°C in 5 *N* HCl it can be observed in three hours, while in 13 *N* acid it takes place quantitatively in one hour. At 75°C in a 4 *N* solution it can be observed in one hour, while in a 9 *N* solution it takes place quantitatively in half an hour.

In sulphuric acid media tetravalent technetium is apparently present in the form of a hydrated dioxide; in alkaline media, as a hydrate. This is confirmed by its quantitative coprecipitation with similar rhenium compounds. It seems that an anion $TcCl_6^{2-}$ is present in hydrochloric acid media, since technetium precipitates quantitatively with thallium chlorrhenites and $\alpha - \alpha'$ dipyridyl and does not coprecipitate with cupferronates, phosphates and phenylarsonates of tetravalent cations.

Tetravalent technetium is easily oxidized by nitric acid and hydrogen peroxide, and in alkaline and sulphuric acid solutions by atmospheric oxygen.

A method was developed on the basis of the above mentioned data for the rapid separation of technetium from rhenium, consisting in the reduction of the former by concentrated acid with heating for half an hour and precipitation on ferric hydroxide. After thorough washing with a solution of hydrazine sulphate, the precipitate was dissolved in a minimum volume of concentrated nitric acid, the technetium oxidized to the heptavalent form. The iron was separated by precipitation as the hydroxide by a small excess of ammonia.

Reduction in concentrated hydrochloric acid solutions by zinc resulted in a new valency state of technetium, thus behaving differently from the quantitative precipitation of rhenium in the form of $Re_2O \cdot XH_2O$. In this form technetium is not coprecipitated either from hydrochloric acid media with thallium chlorrhenite, or with oxalates of rare earth and alkaline earth elements in weak acid and neutral media,

or with copper sulphides and zinc sulphides in weak acid media, but it is quantitatively precipitated with iron, manganese and zirconium hydroxides and with the sulphide and oxyquinolate of divalent manganese.

These appear to be properties of bivalent technetium, which oxidizes easily with atmospheric oxygen, hydrogen peroxide, nitric acid and other oxidizing agents.

CONCLUSIONS

Studies conducted with labelled atoms have confirmed the assumption of a greater similarity between the properties of technetium and rhenium than between technetium and manganese. This similarity is especially characteristic for the valency states 7, 6, and 4.

The assumed similarity between the bivalent compounds of technetium and manganese is still to be investigated. A more detailed check should be made with weight quantities of the element.

It is also necessary to obtain spectrophotometric data on 6, 4, and 2 valent compounds of technetium as well as to study the kinetics of the disproportionation of the sesquivalent form and to determine the presence of 5-valent technetium in this process.

Studies on the extraction properties of technetium and rhenium in their higher oxidized states indicate the different nature of the processes taking place when using oxygen containing solvents and amines. The conditions for the extraction of thiocyanide and diethyldithiocarbamate complexes of technetium have been described. Several methods have been evolved for extracting this element and separating it from rhenium, molybdenum and ruthenium.

From the study of the conditions of the coprecipitation of technetium sulphide with rhenium sulphide in hydrochloric acid media it is evident that the possibility of reducing technetium to tetravalency is of great importance in this process. It has been found that insoluble chlorates of alkali metals may be used as carriers for concentrating traces of technetium. As in the case of insoluble perrhenates, the less soluble the respective carrier, the greater the amount of coprecipitated technetium.

REFERENCES

1. Mendelyev, D. I., Ann., *8*: 133, 205 (1877).
2. Kern, S., Chem. News, *36*: 4, 114 (1877); *37*: 33 (1878).
3. Mallet, G., Am. Chem. J., *20*: 776 (1898).
4. Noddak, W., Take, I. and Berg. O., Naturwiss., *13*: 567 (1925); S. B. Preussische Acad. Wissen., *19*: 400 (1925).
5. Noddak, W. and Take, I., Metallbörse, *15*: 1597 (1925).
6. Noddak, W., Metallbörse, *16*: 2129, 2633 (1926).
7. Burkhardt, F., Peed, W. F. and Saunders, B. G., Phys. Rev., *73*: 347 (1948).
8. Perrie, C. and Segré, E., J. Chem. Phys., *5*: 721 (1937); *7*: 155 (1939).
9. Flagg, J. F. and Bleidner, W. E., J. Chem. Phys., *13*: 269 (1945).
10. Seaborg, G. T. and Segré, E., Phys. Rev., *55*: 808 (1939).
11. Hahn, O., Helv. Chim. Acta, *36*: 617 (1953).
12. Cobble, J. W., Boyd, G. E., Smith, W. T. and Nelson, C. M., Parker, G. W., J. Am. Chem. Soc., *74*: 1852 (1952).
13. Cobble, J. W. and Boyd, G. E., J. Am. Chem. Soc., *74*: 556 (1952).
14. Nesmeyanov, An. N., Lapitsky, A. V. and Rudenko, N. P., *Production of Radioactive Isotopes*, State Chem. Publ. House, Moscow (1954).
15. Segré, E., Nuovo Cimento, *9*:1008 (1952).
16. Hunter, H. F. and Ballou, N. E., Nucleonics, *2* (1951).
17. *Science News Letter*, *67*: 117 (1955).
18. Hubenet, H., Jager, C. and Zwann, C., Ext. Mém. Soc. roy Liegé, *4*: 13, No. 3, *471* (1953).
19. Merrill, P. W., Science, *115*, 484 (1952); Astrophys. J., *116*: 21 (1952).
20. Herr, W., Z. Naturforsch., *9a*: 180, 907 (1954).
21. Jacobi, E., Helv. Chim. Acta, *31*: 2118 (1948).
22. Beinbridge, N., Goldhaber M. and Wilson, E., Phys. Rev., *90*: 430 (1953).
23. Medicus, H., Maeder, D. and Schneider, H., Helv. Phys. Acta, *24*: 72 (1950).
24. Michelich, J. W., Goldhaber, M. and Wilson, E., Phys. Rev., *82*: 972 (1951).
25. Sugarman, N. and Richter, H., Phys. Rev., *73*: 1411 (1948).
26. Geilmann, W. and Bode, H., Z. anal. Chem., *130*: 222 (1950).
27. Wolfsberg, M. and Gelmholz, L., J. Chem. Phys., *20*: 837 (1952).
28. Tribalat, S. and Beydon, H., Anal. Chim. Acta, *8*: 22 (1953).
29. Tribalat, S., Anal. Chim. Appl., *3*: 113 (1949).
30. Goishi, W. and Libby, W. F., J. Am. Chem. Soc., *74*: 6109 (1952).
31. Kuznetsov, V. I., Ach. of Chem., *23*: 654 (1954).
32. Boyd, G. E., J. Am. Chem. Soc., *72*: 4805 (1950).
33. Latimer, V., *Oxidable States of Elements and Their Potentials in Water Solutions*, Mosc., Int. Lit. (1954).
34. Cobble, J. W., Boyd, G. E. and Smith, Wm. T., J. Am. Chem. Soc., *75*: 5773 (1953).
35. Boyd, G. E., Cobble, J. W. and Smith, Wm. T., J. Am. Chem. Soc., *75*: 5777 (1953).

Determination of the Half-Life of Tc^{102}

By J. Flegenheimer and W. Seelman-Eggebert,* Argentina

In the isotope tables a value of "less than 25 seconds" is given for the half-life of technetium-102, the parent substance of which is the 11.5-minute molybdenum, which is found in fission products.[1] In order to measure such a short half-life, a chemical method was designed to make it possible to effect a very rapid separation; the measurements were made with equipment especially designed by Fraenz for measuring short half-lives.[2]

The chemical method consisted of separating pure molybdenum from the fission products by the methods already described[3,4] and then dissolving the lead molybdate in a mixture of tartaric and hydrochloric acids. The tartaric acid forms a complex with the molybdenum and inhibits its precipitation by tetraphenylarsonium chloride. Previous precipitation of the technetium was carried out by adding perrhenate ion and an excess of tetraphenylarsonium chloride, filtering on a colloidal filter from which the solution was obtained ready for the precipitation of the technetium by the addition of a few drops of perrhenate ion. The solution thus obtained was passed through a Buchner funnel (of the type which can be dismantled, using a colloidal filter mounted on a vacuum filtering tube as shown in Fig. 1. In the absence of vacuum, the filter does not pass the liquid. A GM tube, connected to the measuring circuits, was mounted over the bowl as close to it as possible. At a given point, a few milligrams of rhenium were added to the liquid in the bowl, vacuum was applied; the bowl was removed after filtration had ceased and the measurements were started. With such a procedure, only 5 to 6 seconds elapse from the time at which rhenium is added to that at which the measurements are begun. The technetium precipitate does not account for the whole of the technetium present at the time the reagent is added, and it retains some of the molybdenum, but the major part of the latter is sepa-

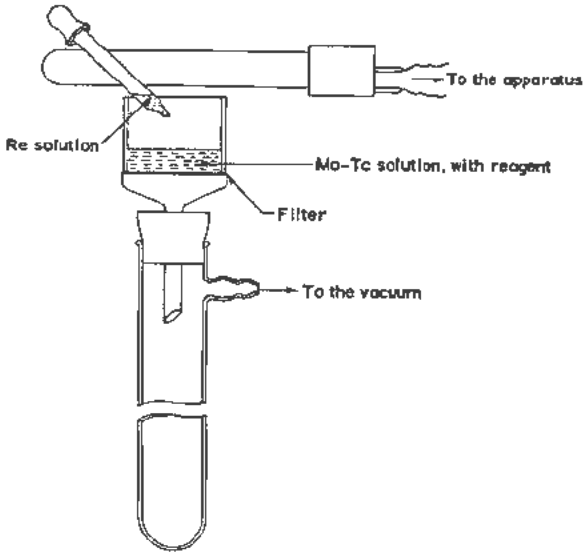

Figure 1

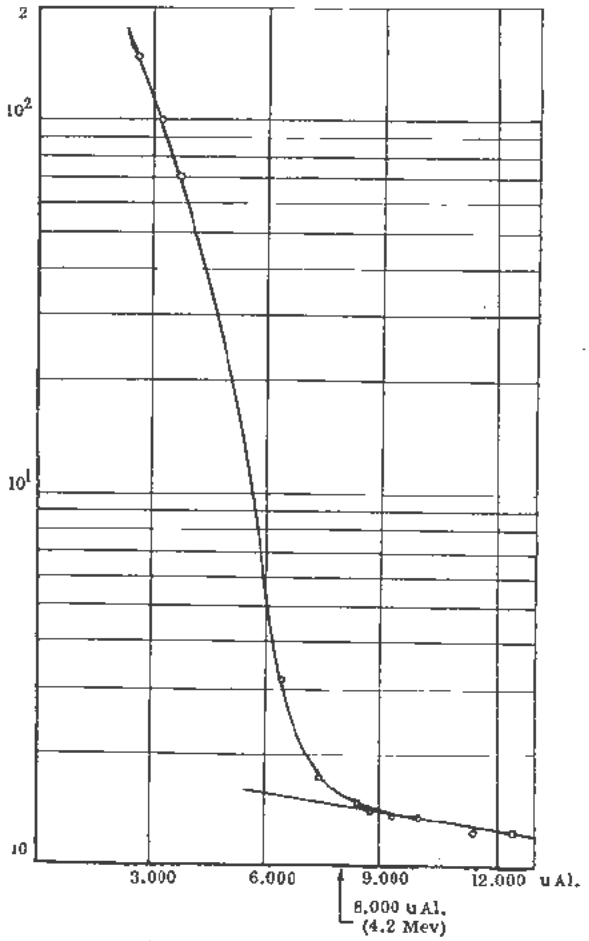

Figure 2. Absorption Mo fission: Eman. Tc^{102}

Original language: Spanish.

* Comisión Nacional de la Energía Atómica, Argentina.

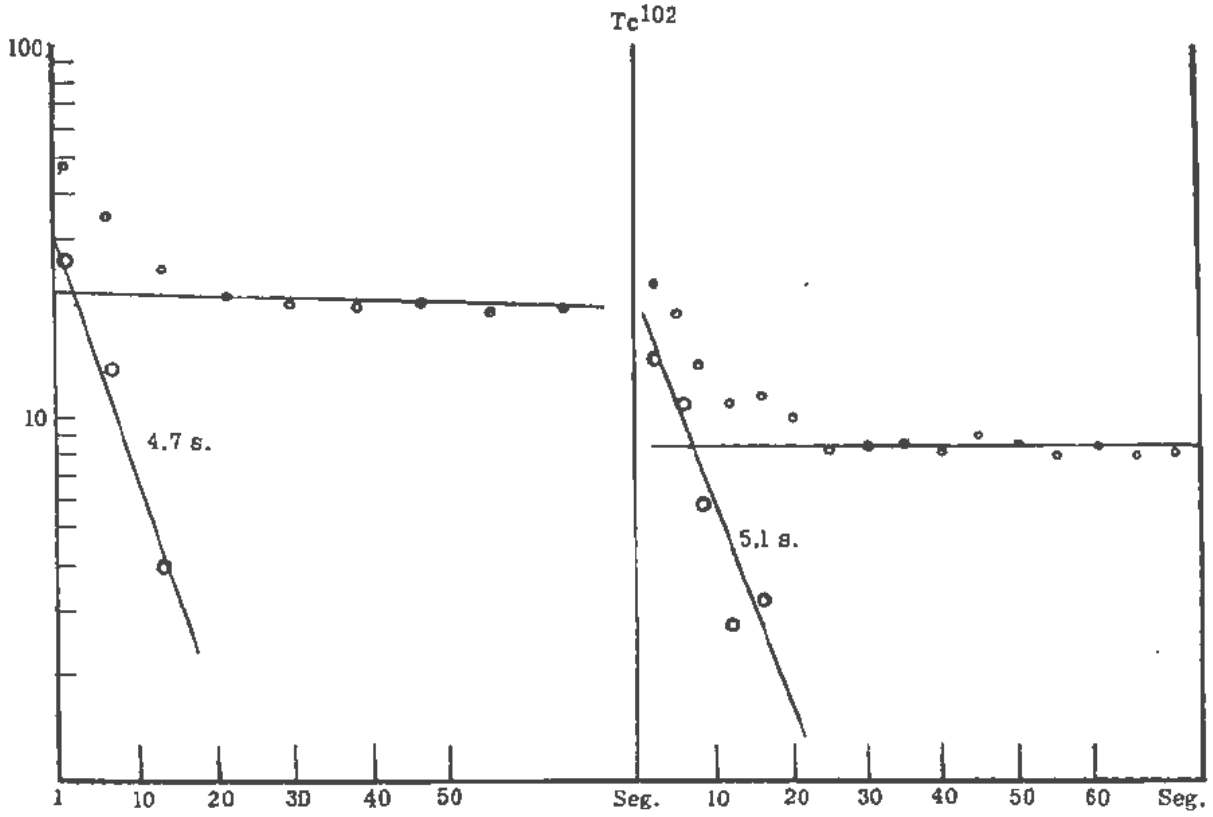

Figure 3

rated, and since it settles at the bottom of the tube, it influences the measurements very little by reason of the distance which separates it from the counter.

Figure 3 shows the decay curves of the technetium fraction. The average of the values found for the short half-life observed is 5 ± 1 seconds. The tails correspond to the absorbed technetium-101 and molybdenum-102.

For the determination of the energy of technetium-102, the molybdenum absorption curve from the fission products was drawn. The beta radiation of the molybdenum-technetium-101 series is almost completely stopped by an aluminum plate 3000 microns thick. If the gamma radiation corresponding to the series of 101 isobars also is subtracted, a half-life of approximately 11.5 minutes is then observed, corresponding to molybdenum-102. With a greater Al thickness, the hard betas due to 5-second technetium are partly absorbed as shown in Fig. 2. Total absorption of the beta particles is obtained with 8000 ± 500 microns Al, which corresponds to a maximum energy of 4.2 ± 0.3 Mev. This value is in good agreement with other figures published earlier.[5,6]

REFERENCES

1. Hollander, J. M., Perlman, I. and Seaborg, G. T., Rev. Mod. Phys. *25*: 525 (1953).
2. Fraenz, K., *Recording of radioactive substance by means of recording apparatus.* (Report presented to the Argentine Physics Society), Buenos Aires, May (1954).
3. Flegenheimer, J. and Seelman-Eggebert, W., Vol. 7, Session 9B, P/1026, these Proceedings.
4. Flegenheimer, J., *Determination of the half-life of* Tc^{101}; Thesis for Doctorate of the Faculty of Exact and Natural Sciences, University of Buenos Aires.
5. Coryell, Ch. D., *MIT Progress Report*, Feb. 28 (1953). idem Nov. 30 (1952).
6. Boyd, G. E. and Larson, Q. V., ORNL-286 and ORNL-499. See King, R. W., *Table of total beta-disintegration energies.* Rev. of Mod. Phys., *26*: 353 (1954).

Determination of the Half-Life of Tc^{105}

By J. Flegenheimer and W. Seelman-Eggebert,* Argentina

Tc^{105} can be obtained only as a fission product. Its half-life is given as "short" in the table of isotopes.[1] The value of approximately 15 minutes was published in 1947.[2]

While the other technetium isotopes found in fission processes (mass numbers 99, 101 and 102) disintegrate by the emission of electrons to give stable isotopes of ruthenium, the 105 isotope disintegrates into ruthenium-105 having a half-life of 4.5 hours which can readily be measured.

Advantage was taken of this property to measure the half-life since it is difficult to do it directly. This is due to the fact that technetium-101 which has a similar half-life and greater activity also appears in large yield in fission processes.

In order to obtain the fission products, a few grams of ammonium diuranate were exposed to the neutron beam from a 1.2 Mev cascade accelerator for 10 to 15 minutes. The diuranate was dissolved in hydrochloric acid and, after copper had been added as a carrier, copper sulfide was precipitated by means of a rapid flow of hydrogen sulfide. The copper sulfide retains the activities of the elements of the second analytical group, among which molybdenum and technetium are to be found.

The copper sulfide was redissolved in hydrochloric acid with a small amount of bromide, adding molybdate, perrhenate and ferric ions as carriers. By adding ammonia, ferric hydroxide was precipitated, and retained the activities of tin, antimony, ruthenium, selenium, tellurium and possibly rhodium and palladium. The molybdenum and technetium passed to the filtrate from which lead molybdenum was precipitated by acidifying with acetic acid and adding lead acetate. The lead molybdate can be obtained in this fashion within 5 minutes if the filtrations are carried out under a vacuum. The technetium (with a rhenium carrier) is found in the filtrate of lead molybdate.

The solution was divided into three equal parts. In each one, technetium was coprecipitated with rhenium by means of tetraphenylarsonium chloride at 10 minute intervals. In Fig. 1 on the left-hand side, the three disintegration curves of Tc^{101} can be seen. They showed that the precipitations were nearly complete. After decay of the Tc^{101}, the various preparations were measured again in order to determine the Ru^{105} content of each one of them. Plotting

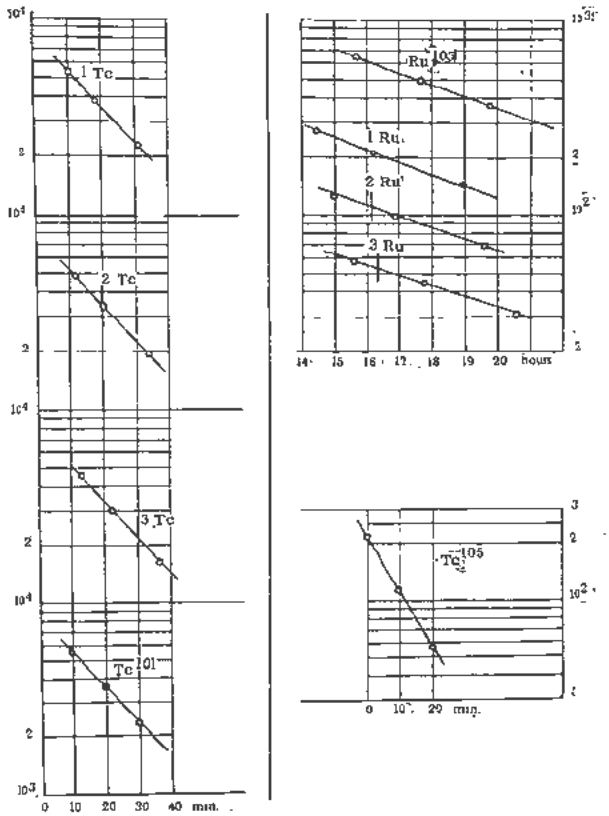

Figure 1. Determination of the half-life of Tc^{105}

the activities of Ru^{105} at appropriate intervals on semilogarithmic paper gave a half-life of 10.5 minutes for technetium-105 (Fig. 1 on the right).

This way of proceeding is correct only if there is no coprecipitation of the ruthenium with the technetium preparation. In order to confirm this, a radioactive ruthenium tracer was added (Ru^{106}) to the technetium solution before the precipitations were carried out. Two weeks after the test, the technetium preparations were measured again in order to determine their Ru^{106} content. In all cases, coprecipitation of ruthenium with technetium was less than 2 per cent.

REFERENCES

1. Hollander, J. M., Perlman, I. and Seaborg, G. T., Rev. Mod. Phys. 25: 525 (1953).
2. Seelman-Eggebert, W. and Strassmann, F., Z. Naturforsch., 2a, 83 (1947).

Original language: Spanish.

* Comisión Nacional de la Energía Atómica, Argentina.

The Condition of Fission Product Iodine in Irradiated Uranium Metal

By G. N. Walton, B. Bowles and I. F. Croall,* UK

Very few observations have been published on the chemical condition of any of the fission products in irradiated uranium metal before dissolution in acids. Before the first pile was built in 1943, F. H. Spedding and co-workers studied the diffusion of fission products from irradiated uranium metal and oxide. Reports of this work have recently become available[1] and no comparable work has since been published. This type of information, however, is still required particularly for designing fuel elements in which a high burn-up is proposed. In their experiments they observed that the major products diffusing from irradiated sintered uranium metal heated at 400°C and 1000°C in a vacuum were active isotopes of rare gases, iodine, and tellurium.

As considerable information is available on the molecular and atomic condition of iodine a study of this fission product might be expected to give clues as to the general conditions prevailing inside irradiated metal. Iodine is the most electronegative of all the longer lived fission products, and if for instance any compound formation between the different fission products took place iodine might be expected to be involved.

The direct approach was taken of treating with different solvents a large surface of highly irradiated enriched uranium metal freshly exposed by grinding, to find out into which the iodine was preferentially extracted, and to compare its behaviour under these conditions with that of other fission products.

EXPERIMENT

Grinding Irradiated Metal

The apparatus used is shown in Figs. 1 and 2. It consisted of a polythene mould in which the uranium pellet was sealed by Marco Resin "SB 28C" (Scott Bader Co. Ltd., 109 Kingsway, London W. C. 2) on to the end of a tufnel rod. The latter was then unscrewed from the mould, removed from the lead cell in which it had been mounted, pushed through the lead shielding of a second cell and screwed into the sealing bush shown in Fig. 2 so as to bear against the emery wheel. As the resin and its contained metal pellet was ground down, the rod was screwed in further until all the metal had gone. Viewing was carried out by means of a telescope and moving mirrors. The emery wheel rotated in the tube filled with solvent through which dry argon was continuously flushed so as to maintain an oxygen free atmosphere. After the grinding the metal and solvent were blown by argon pressure through the central tap on to a fine glass sinter (no. 4 porosity) through which the solvent was run. The latter was passed on through a glass spiral exposed to a GM counter and recorder, and from thence to a sampling flask containing carriers for the fission products to be measured. The metal and the whole apparatus was then washed through with further quantities of solvent until the counting rate recorded as the solvent passed through, showed that the bulk of the activity had been removed. A second solvent was then introduced and the metal again washed repeatedly until the activity passing out was low. This was continued until the final solvent of nitric acid dissolved the metal completely and cleared the apparatus of activity. Each solvent was bulked separately (normally to 250 ml), sampled and analysed for the various fission products and for uranium, according to the following scheme.

Analysis for Ru, Cs, Ba, Sr, Te, and Ce

An aliquot of the solvent was made up to contain 10 mg each of Ru and Te as chlorides, and Cs, Ba, Sr, Ce, as nitrates. The solution was evaporated to dryness in a nickel crucible and fused at 500°C for 2 hours with alkali so as to ensure isotopic exchange, particularly in the case of ruthenium. The residue was leached with water and then with acid.

From these solutions the elements were separated and purified by standard methods,[2] weighed on filter papers, mounted on aluminum trays and counted in an end window counter for β-activity.

Iodine Analysis

In carbon tetrachloride and hexane, iodine carrier was added as molecular iodine in the solvent concerned. This was allowed to stand for about one week and the iodine was then washed out into water by reducing it with SO_2. It was purified by repeatedly back extracting into carbon tetrachloride, and water, (3 cycles), and mounted, weighed and counted as silver iodide. This method only estimated those forms of iodine that exchanged with molecular iodine.

* Chemistry Division, A.E.R.E., Harwell, UK.

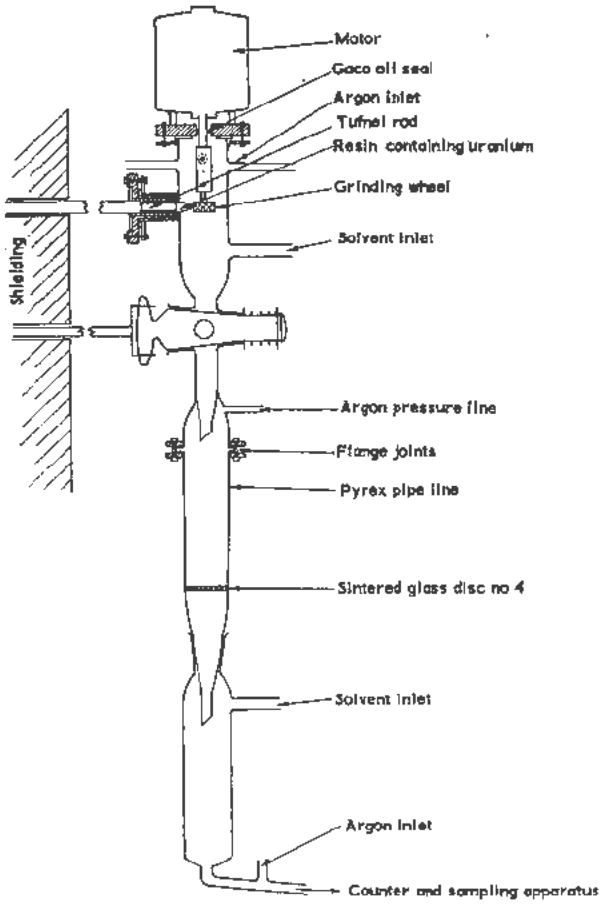

Figure 1. Grinding apparatus (half size)

In ethyl alcohol a small aliquot of the alcohol (containing molecular iodine carrier) was diluted with water and treated with potassium periodate to give 10 mg of iodine. SO_2 was blown in which reduced the periodate through its valency states down to iodide. This was then oxidised to molecular iodine with nitrous acid, extracted into carbon tetrachloride and purified as before.

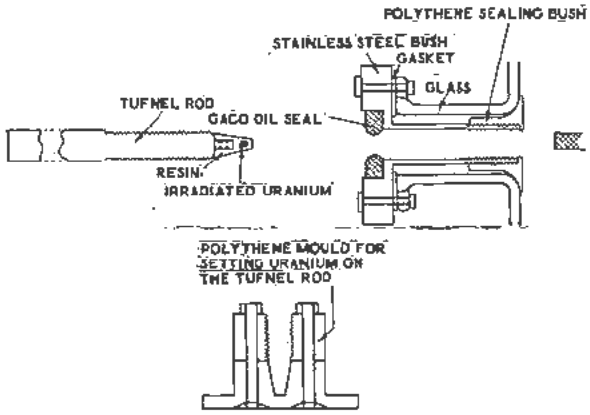

Figure 2. Details of grinding bush and mould

In water and nitric acid solntions, the periodate method was used as for alcohol.

Zirconium Analysis

A photo peak due to the γ-activity of Zr^{95} (0.73 Mev) and Nb^{95} (0.76 Mev) is clearly differentiated in a mixture of activities by a sodium iodide crystal γ-scintillation spectrometer. Aliquots of the solutions containing zirconium carrier were therefore evaporated to dryness and the areas of the photo peak compared to give the relative proportions of the zirconium activity in each. This was done four months after the chemical separation when the Nb and Zr would be approaching their radioactive equilibrium condition. Calibration curves were run to give the height of the photo peak for different ranges of the spectrometer as a function of the size of aliquot taken.

Activities of the various fractions for each fission product were counted at the same time and were therefore directly comparable for estimating the proportions present. For Ru, Cs, Sr, Te and Ce, aluminium absorption curves were plotted to ensure that the activities measured in the different samples were comparable. For I^{131} and Ba^{140}, decay curves were followed for about 3 half-lives.

Uranium Analysis

Where the uranium was present at low concentrations it was analysed by the microfluorimetric method using the standard addition technique[3]—the mean of eight observations being taken on each sample. At high concentrations it was analysed spectrophotometrically.

Results

Before each grinding experiment the apparatus was dried out by heating in a current of air. It was then assembled and dry argon run through for 24 hours. In the preliminary experiment irradiated natural uranium was ground in carbon tetrachloride. In the main experiment normal hexane was used in order that there should be no possibility of a uranium-chlorine reaction. The uranium metal was enriched to 25% with U^{235} and consisted of a cut cast pellet weighing 120 mg. It was irradiated in a pile until 0.4% of the uranium atoms had undergone fission. During irradiation it was surrounded by sodium metal at 320°C in a sealed steel capsule.

Table I shows the results that were obtained. These are expressed as the percentage extracted in each solvent relative to the total amount present. Each analysis was carried out in duplicate and the uncertainties are the differences from the mean. In most cases counting rates were of the order of 10,000 cpm and the statistical error was negligible.

Extraction of Fission Product Iodine from Uranium Metal Powder into Hexane

Natural uranium metal powder prepared by calcium reduction of uranium oxide and kept in an argon

Table I. Preferential Extraction of Fission Products in Highly Irradiated Metal

Preliminary Experiment

Isotope measured	Amount Extracted CCl_4 %	Amount Extracted $EtOH$ %	Amount Extracted H_2O %	Amount dissolved by HNO_3 %
Ru^{105}	0.67	7.34	0.36	91.6
I^{131}	1.9	2.2	0.31	95.5
Ba^{140}	0.07	0.57	8.7	90.6
Total $\beta\gamma$	0.22	8.92	7.56	83.
Uranium	0.01	2.35	3.4	94.

Main Experiment

	Hexane	EtOH	H_2O	HNO_3
Sr^{89}	0.011±.001	0.68 ±0.07	2.07 ±0.04	97.2±0.9
Zr^{95}	<0.002	0.20 ±0.01	0.03	99.8±3.0
Ru^{106}	0.020±0.001	3.68 ±0.03	0.221±0.004	96.1±0.8
Te^{132}	0.14 ±0.01	0.52 ±0.05	0.141±0.007	99.2±4.0
I^{131}	0.61 ±0.12	0.032±0.002	0.10 ±0.01	99.4±0.8
Cs^{137}	<0.001	0.070±0.001	1.73 ±0.04	98.2±0.09
Ba^{140}	0.61 ±0.004	0.46 ±0.02	9.9 ±0.3	89.6±0.8
Ce^{144}	0.003	0.30 ±0.01	0.37 ±0.005	99.4±1.0
Total $\beta\gamma$	0.003	0.77 ±0.01	0.87 ±0.01	97.5±0.5
U	0.01	0.98 ±0.03	0.28 ±0.01	98.7±2.0

atmosphere, was filled into small silica ampoules also under argon. These were evacuated, heated and sealed. They were then irradiated for one hour in a flux of about 1.6×10^{12} n/cm²/sec and kept for one week to allow all the I^{131} to grow. The ampoules were opened and the contents extracted in an enclosed Pyrex apparatus. This was first completely dried out by heating in air, assembled, and flushed with dry oxygen free argon for 24 hours. The ampoule was then crushed by shifting an iron filled glass weight inside the apparatus with a magnet. Hexane, dried with magnesium perchlorate and sparged with argon was introduced and stirred with a magnetically rotated stirrer on a sintered glass filter. The hexane was then blown through the filter into a flask containing carrier iodine in hexane, and the extraction procedure was repeated at definite time intervals. Each sample of the iodine was extracted into water, purified by three cycles of extraction into carbon tetrachloride, and eventually mounted, weighed and counted as silver iodide. The uranium powder was finally dissolved out in hydrochloric acid and analysed for I^{131} which was mounted and counted in the same way as that from the hexane.

Figure 3 shows the results obtained and the various conditions used. The ampoules were irradiated and extracted in pairs so as to compare an air filled ampoule with an evacuated ampoule, and a moist sample with a dry sample. When the rate of extraction was established dry air was allowed into the apparatus to see if there was any change in the rate.

A preliminary experiment in which an evacuated ampoule containing U_3O_8 was irradiated is also recorded in Fig. 3.

Some experiments with special "spec-pure" normal hexane showed no significant differences from those with the laboratory reagent hexane and it was concluded that hexane impurities were playing no major part in these effects.

Adsorption of Molecular Iodine from Hexane onto Uranium Metal Powder

The adsorption of molecular iodine onto uranium powder was studied by shaking mechanically flasks containing known amounts of uranium metal powder and known amounts of molecular iodine in hexane. For higher concentrations the iodine was measured by its violet colour with a "Spekker" absorptiometer (filter no. 4), and for lower concentrations the iodine was measured by counting after labelling it with active I^{131}. Samples were taken, centrifuged to remove any suspended material, measured and returned to the flask on the shaker, allowances being made for any small changes of volume that occurred during measurement.

Figure 4 shows the adsorption of iodine from hexane at different concentrations. The full lines show "Spekker" measurements and the dotted lines activity measurements. The latter did not agree with the former, and this was found to be due to the fact that the active solutions had been made up in contact with aqueous solutions, whereas the inactive solutions were dry. Moisture had a very marked effect and Fig. 5 shows some results for wet and dry conditions. Here measurements were made both by absorptiometry and by counting on the same solutions, and good agreement was obtained. A drop of water added to a flask in which the violet hexane solution had remained for many days with uranium was sufficient to decolorise it in a few minutes.

State of Molecular Iodine Adsorbed from Hexane onto Uranium Metal Powder

A solution of iodine in hexane (0.5 mg/ml) was shaken until it was completely decolorised with ura-

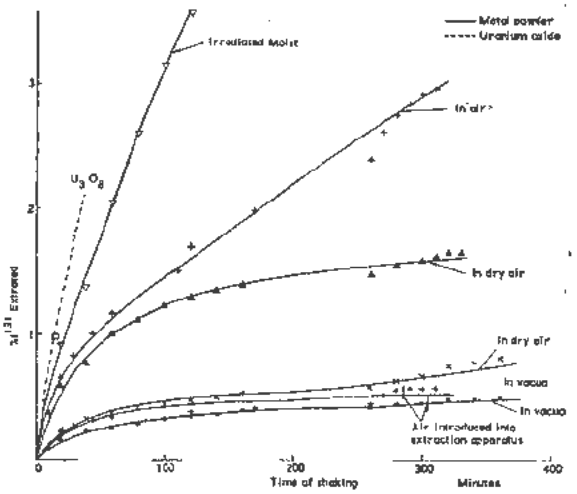

Figure 3. Extraction of I^{131} from uranium powder irradiated under various conditions

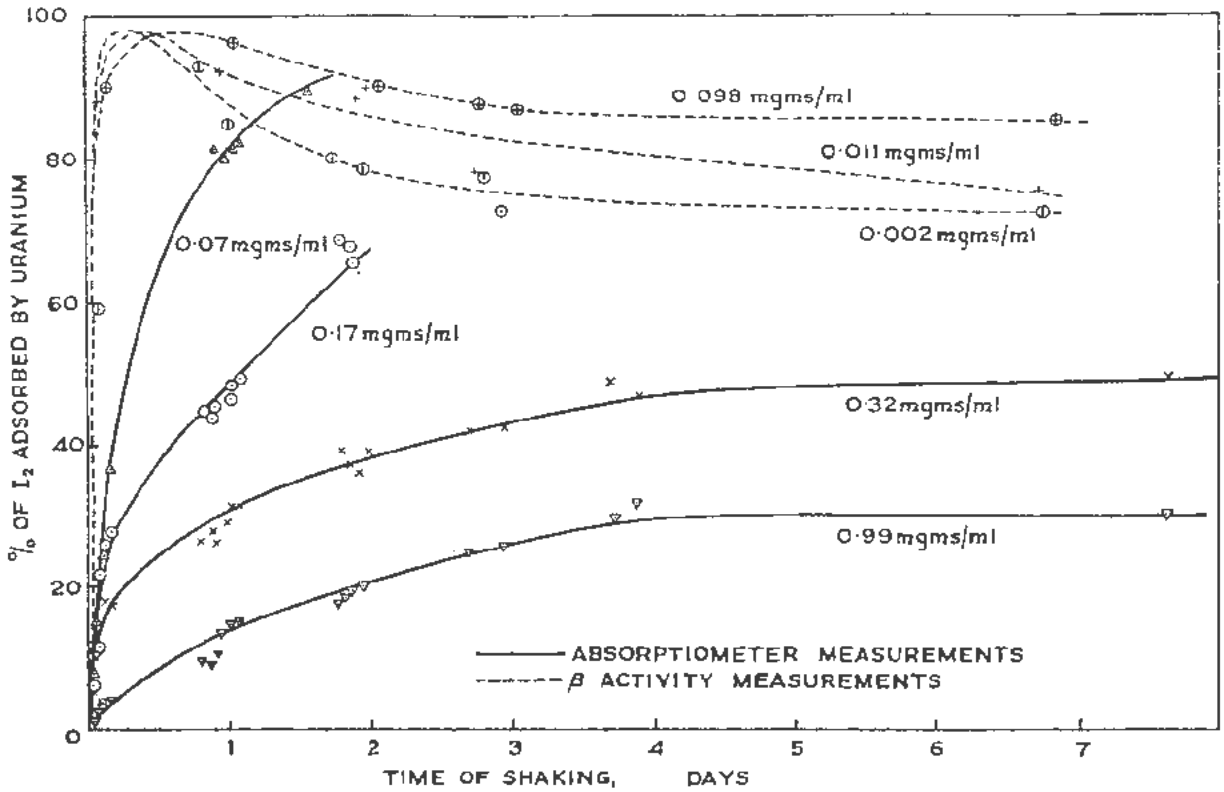

Figure 4. Adsorption of molecular iodine at different concentrations in hexane by uranium metal powder

nium metal powder. The components were then tested as follows:

(*a*) The decolorised hexane was shaken with acid silver nitrate solution, but no visible precipitate of silver iodide was formed. The violet colour could not be regenerated by shaking with nitrous acid and it was concluded that no iodine was present as iodide or as molecular iodine in the hexane.

(*b*) The uranium powder was washed with hexane, dried in air, and extracted with water. To the water nitrous acid was added. This released iodine which could be extracted into hexane and compared with the original iodine solotion. The recovery was found to be quantitative and some results are shown in Table II.

Table II. Recovery of Iodine Adsorbed on Uranium Metal Powder by Extraction into Water

I_2 before adsorption, mg/ml	*I_2 after adsorption, mg/ml*	*I_2 recovered, mg/ml*	*% recovery*
0.488	0.284	0.179	95.7
0.488	0.284	0.188	97.4
0.227	0.125	0.101	99.7

(*c*) The uranium powder with adsorbed iodine was washed with water and the water washed with carbon tetrachloride. No coloration was observed. Again no coloration was observed when the uranium metal was washed with carbon tetrachloride. Less than 1% (4μg/ml) of the iodine in the original solution would have been observed in these circumstances, and it was concluded that if any of the iodine was adsorbed in the molecular condition it was less than 1% of that present as a water soluble form.

(*d*) The aqueous extract containing the desorbed iodine was tested for uranium, and found to contain it in amounts equivalent to the iodine. Table III shows the results of analyses carried out on 4 separate aqueous extractions. The constancy of the ratio sug-

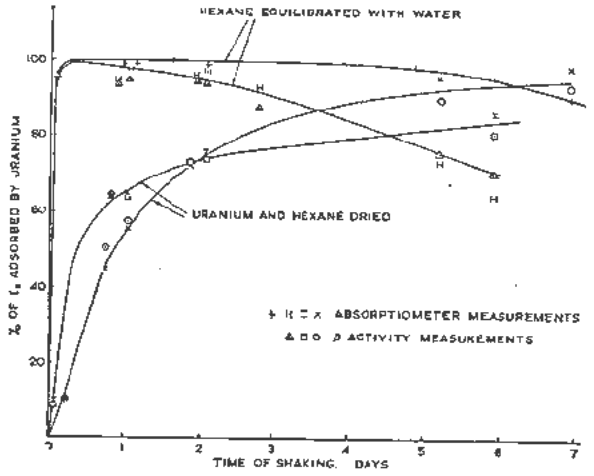

Figure 5. Effect of moisture on rate of adsorption of iodine from hexane on to uranium metal powder

Table III. Ratio of Uranium to Iodine in Aqueous Solution Containing Desorbed Iodine

Concentration of U, gram atoms/litre	*Concentration of I, gram atoms/litre*	$\frac{[I]}{[U]}$
1.83×10^{-2}	1.90×10^{-2}	1.04
1.30×10^{-3}	1.33×10^{-3}	1.02
0.744×10^{-3}	0.752×10^{-3}	1.01
0.460×10^{-3}	0.439×10^{-3}	0.95

gests that some compound of uranium and iodine is being desorbed although in the expected compounds UO_2I_2, or UI_4, the ratio is greater than unity.

DISCUSSION

Figure 6 gives the results in Table I plotted to show into which solvent the fission products prefer to go. They are seen to fall into groups. Caesium, barium, and strontium, in that order, are extracted mainly by water; ruthenium, zirconium, and uranium itself turn up mainly in the alcohol, while cerium and the total $\beta\gamma$ activity fall half way. Unlike the other elements, iodine, and to a lesser extent, tellurium, are extracted by hexane preferentially. These are the same two elements that Spedding observed to diffuse from the metal into a vacuum preferentially.

As seen in Table IV the order of extraction is the same as the order of the first ionization potential[4] of the elements, iodine being highest, and caesium lowest. The data are hardly sufficient to come to a firm conclusion; for instance as shown in Table IV again, the order may be connected with ionic size. The ionic sizes of Sr, Ba, and Cs are outside the 14% rule for solubility of metals, and Ru, Zr, Ce have ionic sizes close to those for uranium.

The manner in which iodine is separated from the alkalis suggests that no appreciable proportion of these elements had associated to form salts.

This extraction of iodine from freshly exposed metal appears to contradict the results shown in Figs. 4 and 5 where molecular iodine is seen to be adsorbed by the metal. At high concentrations Fig. 4 suggests that the surface becomes saturated and a limited amount is adsorbed, but at lower concentrations nearly all the iodine is initially taken up. Complete adsorption could not be demonstrated and this

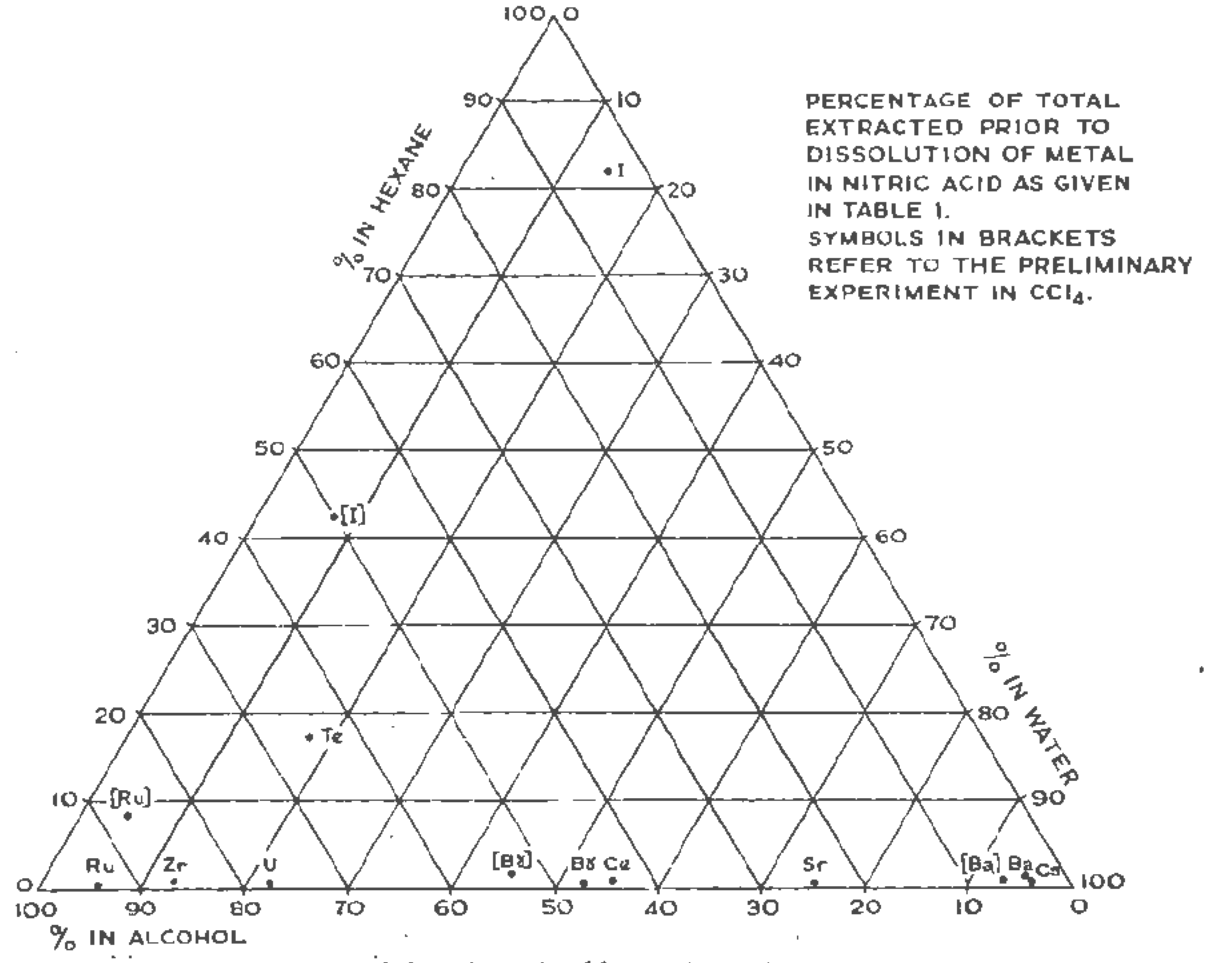

Figure 6. Preferential extraction of fission products by different solvents

Table IV. Extractability of the Fission Products

Solvent	Order of extraction	1st ionisation potential, volts	Crystal structure and ionic radii of elements[3]		
			Within 14% of uranium		Outside 14% of uranium
Hexane	Iodine	10.6	ortho	2.70	
	Tellurium	8.96	hex.	2.86	(3.40)
Alcohol	Ruthenium	7.7	o.p.h.	2.64 2.70	
	Zirconium	6.92	b.c.c.	3.12	
	(Uranium)	(5.7)	b.c.r.	2.98	
			complex	2.8 (3.3)	
	Cerium	6.54	f.c.c.		3.63
Water	Strontium	5.67	f.c.c.		4.29
	Barium	5.19	b.c.c.		4.34
	Caesium	3.87	b.c.c.		5.24

appears due to the back reactions in which air oxidises the uranium, or moisture hydrolyses it, while in the absence of moisture the forward reaction becomes exceedingly slow. Similar observations have been made by Gindin and Pavlova[6] who showed that iodine in benzene catalyses the corrosion of iron in air and moisture by a process in which FeI_2 is formed and decomposed continuously.

Table V shows the heat (ΔH) and entropy (ΔS) changes that have been reported to occur at room temperatures (298°K) in the reactions between uranium metal and different forms of molecular iodine to give the iodides UI_4 and UI_3 in their crystalline form.[7]

Table V. Data for Uranium-Iodine Reactions

Reaction	ΔH kcal/mole	ΔS cal/mole/°
$U + 2I_2 \rightarrow UI_4$ gas	−156.7	−71.6
$U + 2I_2 \rightarrow UI_4$ (CCl_4 soln)	−139	
$U + 2I_2 \rightarrow UI_4$ (solid)	−127	−2.83
$U + {}^3/_2 I_2 \rightarrow UI_3$ gas	−137.0	−50

These figures show that the equilibria for all the reactions lie completely in favour of the uranium iodides. For instance the free energy change in the formation of UI_4 is such that the theoretical partial pressure of molecular iodine above UI_4 and metallic uranium at room temperature is 10^{-36} atmospheres which is quite negligible even in comparison with the very low concentrations that are detectable by fission product counting techniques. UI_4 is the stable form at room temperature, but the negative entropy causes UI_3 to be the more stable form at higher temperatures. Iodine is released in the change over, but none would be expected to be emitted in the presence of excess metal.

Table VI gives some heat and entropy changes in reactions with oxygen or water leading to the release of iodine.[7]

Reactions of the type shown in Tables V and VI have in fact been observed.[8,9,10,11]

In the grinding experiment the iodine, including the other fission isotopes I^{127}, I^{129}, was present in the metal at a concentration of 24 parts per million by weight.[12] Oxygen impurity was of the order 50 parts per million in the argon. Moisture was carefully excluded and could not have been greater than an amount of this same order. At such dispersions of all three reactants no rapid mutual interaction would be expected which would enable iodine to be released from the metal as soon as it was exposed. The effect of the resin in which the metal was embedded was however unknown.

Figure 3 shows that when no resin is present, and under dry and air free conditions, iodine is still released from irradiated metal into hexane. The metal powder used was not entirely free of oxide, and the oxygen content of comparable samples was of the order 60 parts per million by weight. Oxide on uranium does not normally form a protective film and would not be expected to prevent the iodine reacting with the free metal. When moisture is present, which from Fig. 5 would have been expected initially to promote retention, the release of iodine is greater. This is probably due to the increased surface resulting from oxidation or hydrolysis of the metal during irradiation. No satisfactory control of this factor was achieved as indicated by the three different curves for air irradiations in Fig. 3. When air was introduced to a sample which was slowly emitting iodine, as shown in Fig. 3, the latter was not, as expected, released more rapidly, and no effect could be detected. In Table I the iodine is seen to be extracted preferentially relative to uranium and the other fission products into hexane, and it is not extracted appreciably into water, whereas the experiments described earlier show that iodine adsorbed apparently as an iodide, is not released into hexane but is rapidly dissolved by water. These observations suggest the conclusion that fission product iodine in irradiated uranium metal is not present in the same chemical form as in uranium iodide.

The thermodynamic data of Tables V and VI assume that at some stage the iodine is able to form molecules. The atoms of iodine are however formed in fission individually. The rate of recombination of iodine atoms has been measured by Marshall and Davidson and others, in the gaseous state[13] and in non-polar solution[14] and in the latter case the data suggest that there is no activation energy or steric factor for recombination, and that this occurs whenever the iodine atoms meet. The combination reaction in a liquid or solid medium may be written

$$I + I \rightarrow I_2$$

$$\text{for which } \frac{d[I]}{dt} = -2k[I]^2 \qquad (1)$$

$$\text{and} \qquad k = \pi D\sigma \qquad (2)$$

where [I] is the concentration of iodine, D is a diffusion constant and σ is an effective collision diam-

Table VI. Data for Uranium Iodide-Oxygen Reactions

Reaction	ΔH kcal/mole	ΔS cal/mole/°
$UI_4 + O_2(gas) \rightarrow 2I_2(gas) + UO_2$	−113.3	+29.2
$UI_4 + {}^5/_2 O_2\,gas \rightarrow 2I_2(gas) + UO_3$	−145	+10
$UI_4 + 2H_2O \rightarrow UO_2 + 4HI$	−59.9	+24.2

eter.[15] No measurements have been reported of D in fissile material during irradiation. Lomer[16] has made some estimates for the diffusion of ion vacancies in irradiated copper, and for the experiment recorded in Table I, the value of D at 320°C might be expected, from his figures, to be between 10^{-23} cm²/sec and 10^{-19} cm²/sec—say 10^{-21} cm²/sec. The value of σ may be calculated from Marshall and Davidson's work[14] to be 10.7×10^{-8} cm. In the case of a pile irradiation the concentration of iodine atoms (consisting mainly of stable ones) steadily increases at a constant rate, f, and Equation 1 should be written

$$\frac{d[I]}{dt} = f - 2k\,[I]^2 \qquad (3)$$

The integrated form for the condition

$$[I] = 0 \text{ when } t = 0$$

is

$$[I]_t = \sqrt{\frac{f}{2k}}\left(1 - e^{\frac{2}{2t\sqrt{2fk}}} + 1\right) \qquad (4)$$

where $[I]_t$ is the concentration of free iodine atoms after time t. The total number of iodine atoms combined and uncombined $[I]_0$ at time t is given by

$$[I]_0 = ft \qquad (5)$$

Substituting in Equation 4 from Equation 2 and using the above value for D, the proportion of uncombined iodine atoms in the uranium used for the grinding experiment may be calculated to be:

$$[I]_t/[I]_0 = 90\%$$

A comparable result would be expected for the interaction of any two major fission product elements.

In the Table I experiment and also in the short irradiation experiments, most of the iodine atoms therefore will have remained isolated. These in their formation will be expected to be initially positively charged. The theory of fission recoil[17] predicts that recoil fragments have initially about 20 positive charges and gather in electrons as they slow down. In the isomeric transition of Te^{131m}, over 60% of the γ-rays are reported to be internally converted and this process is known to lead to high positive charging which Wexler and Davies have found to be as much as 10 for $Br^{80m} \rightarrow Br^{80}$.[18] In the recoil from γ-emission without internal conversion, positive ions are also formed as has been shown by Davies.[19] In the decay of Te^{131} β-rays of 1.35 and 2.0 Mev are given off, and these would lead to a recoil of about 20 ev[20] together with a loss of electrons due to excitation following the change of charge on the nucleus. The extent of this positive charging is in doubt[21] but the emission of a β-ray in itself leaves the atom positively charged.

We have then to consider what happens to an isolated positively charged iodine ion in uranium metal. Initially the ion may be either inside the metal grains, or in the grain boundaries, but in any process of extraction which does not dissolve the metal, the extracted ions must inevitably pass through the metal surface. The electron affinities of positively charged gaseous iodine atoms, and also that of the neutral atom are shown in Table VII. The ionization potential of neutral uranium atoms, and work function for the removal of electrons from the surface of uranium metal are also shown. These figures suggest that positively charged iodine atoms are able to remove electrons from the metal surface to become neutral, but a neutral iodine atom has insufficient electron affinity to become a negative ion, i.e., the following reaction has a positive heat change:

$$U_{metal} + I_{gas} \rightarrow U^+_{metal} + I^-_{gas}\ \Delta H \text{ positive}$$

The isolated iodine atom would therefore not be expected to exert a strong coulombic force either between itself and the electrons of the metal, or between itself and the uranium ions of the metal, and would in fact be expected to behave like a rare gas atom in the lattice. The neutral atom might, however, associate readily with a non-polar solvent such as hexane and be removed from the surface of the uranium as observed.

Chackett and Chackett[26] have made observations on an analogous system, i.e., the chemical form of phosphorus P^{32} formed in aluminium metal by bombardment with $N^{14\,6+}$ ions. They also conclude from the products formed on dissolution in water that the phosphorus atoms may be present with zero charge.

CONCLUSION

Considerations of diffusion and ionization suggest that fission product iodine arises as isolated neutral atoms in irradiated uranium which exert no strong attractive forces with the metal. Although there has been no entirely unambiguous proof that air or mois-

Table VII. Electron Affinities of Iodine Atoms and Uranium

Reaction	Electron affinity, kcal/gram-atom
$e^- + I^{++} \rightarrow I_{gas}^+$	−682[7]
$e^- + I_{gas}^+ \rightarrow I_{gas}$	−242[7]
$e^- + I_{gas} \rightarrow I_{gas}^-$	−75.6[7,22]
$U_{gas} \rightarrow U_{gas}^+ + e^-$	+131 Ionisation potential[23]
$U_{metal} \rightarrow U_{metal}^+ + e^-$	+84 Photoelectric work function[24]
$U_{metal} \rightarrow U_{metal}^+ + e^-$	+83 Thermionic work function[25]
$U_{metal} \rightarrow U_{metal}^+ + e^-$	+75.2 Thermionic work function of very pure metal[25]

ture are not responsible, this is supported by the fact that fission product iodine is released from the same metal surfaces that readily adsorb macro amounts of molecular iodine. There is also no evidence to show that an appreciable fraction of the iodine combines with the other fission products under the conditions of these experiments.

ACKNOWLEDGEMENT

The assistance of members of the Metallurgy Division, A.E.R.E. in providing the highly irradiated enriched uranium is acknowledged with thanks.

REFERENCES

1. Spedding, F. H., Johns, I. B. and Newton, A. S., *The Thermal Diffusion of Fission Products from Uranium and Uranium Oxide*, Argonne National Laboratory Report Nos. CC 354 (1942), CC 390 (1942), CC 594 (1943).
2. Meinke, W. W., *Chemical Procedures Used in Bombardment Work at Berkeley*, University of California Radiation Lab. Report AECD 2738 (1949).
3. Price, G. R., Feretti, R. J. and Schwarz, S., *The Microfuorimetric Determination of Uranium*, Argonne National Laboratory, Report No. AECD 2282 (1948).
4. Taylor, H. S. and Glasstone, S., *Treatise on Physical Chemistry*, D. Van Nostrand, Inc., New York, 3rd Ed. pg. 287 (1942).
5. Smithells, C. J., *Metals Reference Book*, London, Butterworths, pg. 165 (1949).
6. Gindin, L. G. and Pavlova, M. V., *Corrosion of iron by benzene solutions of iodine*, Zhuv. Pvik. Khimii, *24*: (11) 1151 (1954).
7. National Bureau of Standards Circular No. 500. "Selected Values of Chemical Thermodynamic Properties" (1952).
8. Guichard, M., Bull. Soc. Chim. (4), 3, 11 (1908).
9. Guichard, M., Compt. Rend. (145) 921 (1907).
10. Mueller, M. E., "The Vapour Pressure of Uranium Halides", U.S.A. Atomic Energy Commission Report AECD 2029, Declassified 1948.
11. Prescott, C. H., Reynolds, F. L. and Holmes, J. A., "The Preparation of Uranium Metal by Thermal Dissociation of the Iodide", U.S.A. Atomic Energy Commission Report MDDC 437 (1948).
12. Walton, G. N., "The Specific Activity of Separated Fission Products from Reactor Fuels", Harwell Report AERE C/R 1231 (1953).
13. Marshall, R. and Davidson, N., *Photoelectric Observation of the Rate of Recombination of Iodine Atoms*, J. Chem. Phys. *21*: 659 (1953).
14. Marshall, R. and Davidson, N., *The Rate of Recombination of Iodine Atoms in Solution*, J. Chem. Phys. *21*: 2086 (1953).
15. Moelwyn Hughes, E. A., *Kinetics of Reactions in Solution*, O.U.P. Oxford, 2nd Ed. p. 245 (1947).
16. Lomer, W. M., *Diffusion Coefficients in Copper under Fast Neutron Irradiation*, Harwell Report AERE T/R 1540 (1954).
17. Bohr, N., *Velocity Range Relation for Fission Fragments*, Phys. Rev. *59*: 272 (1941).
18. Wexler, S. and Davies, T. H., *The Average Electric Charge of Daughter Atoms from β Decay and Isomeric Transitions*, Phys. Rev. *88*: 1203 (1952).
19. Davies, T. H. and Yosim, S., *Recoil Atoms from Slow Neutron Capture by Gold and Indium Surfaces*, J. Phys. Chem. *56*: 599 (1952).
20. Davies, T. H., *Symposium on the Effects of Nuclear Transformations*, J. Phys. Coll. Chem. 595 (1952).
21. Schwartz, H. M., *Atom Excitation in β Decay*, J. Chem. Phys. *21*: 45 (1953).
22. Buchdahl, R., *Negative Ion Formation in Iodine Vapour by Electron Impact*, J. Chem. Phys. *9*: 146 (1941).
23. Finkelnburg, W., *Ionisation Potentials and Electron Shielding in the Periodic Scheme*, Z. Naturforsch. *2a*: 16 (1947).
24. Rentschler, C., Henry, D. E. and Smith, K. O., Rev. Sci. Insts. *3*: 794 (1932).
25. Hole, W. L. and Wright, R. W., *Emissive and Thermionic Characteristics of Uranium*, Phys. Rev. *2*, *56*: 785 (1939).
26. Chackett, G. A. and Chackett, K. F., *Chemical Form of Phosphorus 32 Produced in Aluminium by Bombardment with Nitrogen*, Nature 174, 4422, 232 (1954).

Emission of Active Rare Gases from Fissile Material During Irradiation with Slow Neutrons

I. Experimental Technique and Identification of Gases

By F. J. Stubbs and G. N. Walton,* UK

The detection and estimation of krypton and xenon emitted from fissile material during irradiation with slow neutrons affords a direct means of studying the manner in which fission products originate. The rare gases that recoil from the surface of the metal either escape into the surrounding atmosphere or become embedded in nearby solid material. The rare gases formed within the bulk of the metal (either remaining as single atoms or coalescing with other rare gas atoms to form tiny pockets) will diffuse to the surface. The contribution of each mode of release will be expected to depend on the half-life of the species measured and on the temperature and other experimental variables. This report describes a new experimental technique for studying these effects and gives some preliminary results.

The measurement of rare gases by mass spectrometry is precise but most of those formed in fission are active, have very short half-lives, and are present in amounts too small for easy detection by mass identification. The active rare gases can, however, be readily detected in very small concentrations by counting techniques.

The active rare gases were first studied by β-counting using differential decay and chemical separation to distinguish them. Irradiated uranium metal was dissolved in nitric acid and the liberated gases were passed into a counting chamber.[1,2] In this way the half-life, β-energy and γ-energy were obtained for the longer lived gases. The method was quantitative and enabled fission yields to be calculated.[3]

The shorter lived rare gases were studied by passing them up a long tube and their decay products were collected on a central wire, negatively charged.[4] From the distribution and rates of flow the half-lives were determined. Raynor[5] has described a gas sweeping apparatus for large scale collection of fission products (from a solution of uranyl nitrate that was being irradiated) using this technique. Irradiation of aqueous solutions in an atomic pile has many disadvantages however and radio-chemical analysis of the products deposited on the wire is tedious, and gives rather indirect information about the gaseous precursors.

Overstreet and Jacobsen[6] irradiated a uranium plate with deuterons and using argon as carrier gas measured the half-lives of several fission product gases by this charged wire technique. Sugarman[7] has directly measured the gross radioactivity introduced into a circulating helium stream by fission products recoiling from uranium under neutron irradiation. In this way the total activity (gas plus solid) was registered but no analysis to find the contribution of each species was possible by this method.

Recently the γ-scintillation spectrometer has been used successfully to identify fission products by their γ-activity.[8] The present work describes how this instrument can be used to identify individual active fission product gases in the mixture immediately after formation. The fissile material in the form of a metal foil was irradiated by slow neutrons in an atomic pile. The emitted rare gases were carried away and their γ-spectrum obtained. In this way the formation of the active rare gases was followed quantitatively over a period of time long enough for their precursors to have attained equilibrium concentrations. The limiting factor has been the complexity of the γ-energy spectrum obtained when a mixture of some twenty active rare gases was examined 20 seconds after formation. The γ-energies of most of the short lived active gases have not been determined and this presents an interesting though formidable problem for the future.

By utilizing slower helium flow rates only the longer lived gases were measured and this report deals mainly with the quantitative determination of Kr^{85m}, Xe^{133} and Xe^{135}. The measured rate of formation can be correlated approximately with the rate of production by recoil calculated theoretically. This will indicate the efficiency of the technique employed and provide information on the mode of release of fission product gases from metal from the point of view of reactor fuel studies.

EXPERIMENTAL TECHNIQUE

A diagram of the apparatus used is shown in Fig. 1. The fissile material in the form of a foil (surface area 10 cm^2) was suspended in a silica cell (volume 135 cm^3) having ground flanges held together with spring clips. The silica cell was surrounded by an

* Chemistry Division, Atomic Energy Research Establishment, Harwell, Berks, UK.

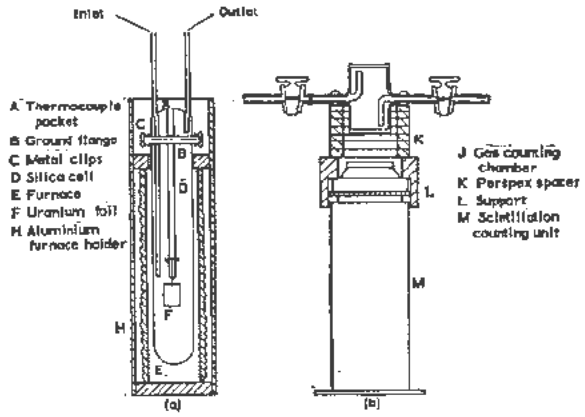

Figure 1. Diagram of apparatus

electrically heated furnace, the temperature of the foil being measured by a thermocouple inserted in the thermocouple pocket shown. This equipment (Fig. 1a) was mounted at the end of an aluminium tube (6 metres long) which was lowered into a vertical experimental hole in the atomic pile (B.E.P.O.). Helium from a cylinder was purified by passage over uranium turnings at 350°C and its rate of flow into the apparatus was accurately measured by a calibrated flowmeter. The helium was passed from the top of the pile down the silica inlet tube to the cell and carried with it any rare gases through the outlet tube and then, any condensed matter was removed by passage through a lambswool filter. The gas finally passed through the counting chamber (volume 70 cm^3) which could be mounted at various fixed distances from the γ-scintillation unit as shown in Fig. 1b. The unit was mounted within a lead castle for shielding against stray γ-radiations.

The γ-scintillation spectrometer had a sodium iodide crystal (2.5 cm thick) mounted on a photomultiplier tube which was connected to a pulse amplifier. The output pulses were analysed with a single channel kick sorter incorporating a sweep recording unit and this resulted in an automatically drawn spectrum. By switching out the sweep recorder and setting the instrument at a particular γ-energy a decay curve was automatically drawn. The output pulses could also be fed to a multichannel pulse analyser.

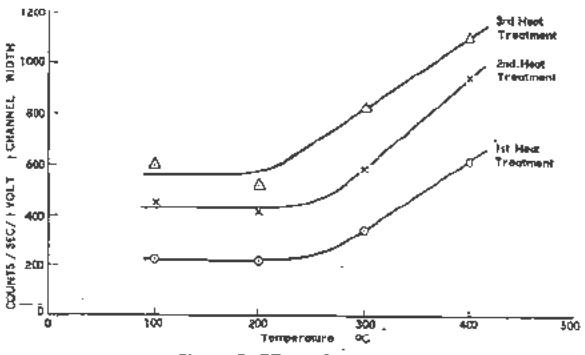

Figure 2. Effect of temperature

The γ-scintillation spectrometer was calibrated with standard sources having well established decay schemes. These were sealed in small glass ampoules and supported in holders which could be mounted in the same position as the gas counting chamber.

The silica cell was made gas tight by melting sulphur on the ground flanges and allowing it to solidify with the flanges held together. This proved most effective since it was not affected by radiation and could be taken apart easily.

EXPERIMENTAL RESULTS

Preliminary experiments were carried out using a piece of natural uranium foil (10 cm^2, 0.01 cm thick) and with a helium flow rate of 500 cm^3/minute. Little γ-activity was found in the region above 1.5 Mev but from 0.1 to 1.5 Mev there was an appreciable amount. A blank experiment using the same apparatus but without the uranium foil showed that there was no observable activation of helium or its impurities and no γ-activity was observed.

Increase in temperature of the uranium foil had little effect at first but from 200 to 400°C there was an over-all increase in activity as shown in Fig. 2. (The γ-activity was measured at 0.8 Mev but the same relative increase was observed over the whole energy range.) When the temperature was returned to 100°C the gas output was greater than before heat treatment. A second heat treatment had a similar effect and so had a third. After three successive heat treatments the activity at a particular γ-energy was increased by a factor of 3.5. In each heat treatment the foil was only maintained at the experimental temperature long enough to reach a thermal equilibrium. All subsequent measurements at 100°C gave consistent results.

The volume of the cell and connecting tubes to gas counting chamber was about 300 cm^3 and with a helium flow rate of 500 cm^3/minute any active gas produced reached the counting chamber in about 30 seconds. A typical γ-energy spectrum for a helium flow rate of 500 cm^3/minute and cell temperature of 100°C is shown in Fig. 3 together with the position of the ruthenium-106 and caesium-137 used as standards. Peaks were observed at 0.25, 0.46, 0.76, 1.0 and 1.2 Mev. By stopping the helium flow and trapping the active gas in the counting chamber the decay at various γ-energies was determined. The decay curves were of a composite nature showing components of half-lives from 30 seconds to several hours. It was advantageous therefore to identify the longer lived components first before studying the short lived activities.

By allowing the active gas to accumulate in the silica cell (in a static atmosphere of helium) and then sweeping it into the counting chamber, the longer lived components predominated. Figure 4 shows a γ-energy spectrum obtained in this way using a multichannel pulse analyser. Two peaks predominate and over a period of 20 hours these peaks gradually di-

minished and their decay curves were thus obtained. At 0.25 Mev (channel 16) the half-life ($t_{1/2}$) was 9.2 hours identifying the gas as xenon-135. At 0.15 Mev (channels 5/6) $t_{1/2}$ was 4.4 hours identifying this active gas as krypton-85*m*. At first sight it might appear that the 0.15 peak was the "Compton continuum" of the 0.25 Mev photo-peak, but at a γ-energy of 0.25 Mev the "Compton continuum" is very small.

In a similar experiment a sharp peak was obtained at 0.084 Mev. (Calibrated against thulium-170 source which also has a γ energy of 0.084 Mev.) Decay measurements over 15 days gave $t_{1/2}$ of 5.2 days identifying the gas as xenon-133 (cf. current literature values $\gamma = 0.081$ Mev, $t_{1/2}$ 5.27 days).[9]

Xe^{133} is the daughter product of I^{133} ($t_{1/2}$ 21 hr) and Xe^{135} is the daughter product of I^{135} ($t_{1/2}$ 6.7 hr). The Xe^{133} and Xe^{135} continue to be produced from their iodine precursors after irradiation of the uranium foil has ceased. Sweeping up an accumulation of active gas under these conditions gave a simple γ-energy spectrum with very distinct peaks at 0.084, 0.25 and 0.52 Mev. The decay of the 0.52 Mev peak (over a period of 45 minutes) gave a half-life of 15.2 minutes identifying the active gas as Xe^{135m}.

When the original foil was removed from the apparatus after some 1500 hours of irradiation in the atomic pile it was found to have flaked somewhat and was very brittle due probably to oxidation by a trace of oxygen in the helium. In subsequent experiments the helium was purified (by passage over uranium turnings at 350°C) and a new foil of the same dimensions was used and maintained at 100°C.

For a quantitative determination of these active gases a continuous helium flow must be used. When the flow rates are high (as in Fig. 3) the concentration of a particular active species diminishes and because the time taken to reach the counting chamber is shorter, the contribution from shorter lived active

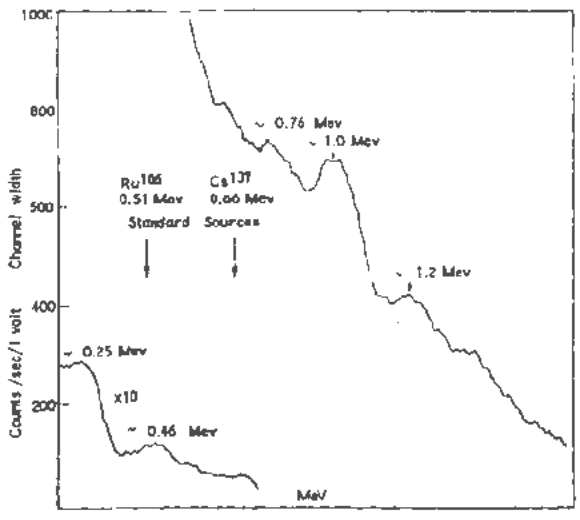

Figure 3. γ-spectrum of active rare gases in He flow of 500 cm³/minute

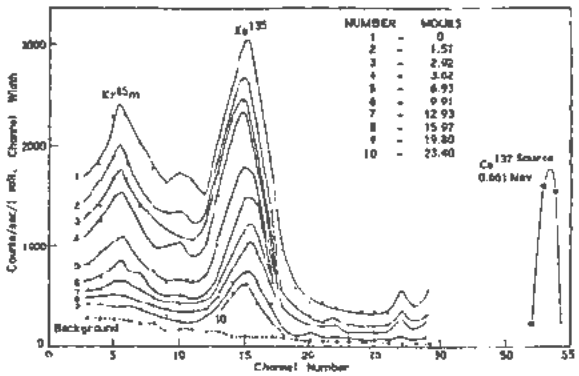

Figure 4 γ-spectrum on multi-channel pulse analyser

gases becomes greater and the mixture of active gases is composite.

With a helium flow rate of 1 cm³/minute the active gases take some 5 hours to reach the counting chamber by which time the short-lived components have decayed away. Distinct γ-energy peaks were observed at 0.084 Mev (Xe^{133}), 0.15 Mev (Kr^{85m}) and 0.25 Mev (Xe^{135}) and these were calibrated against Tm^{170} (γ 0.084), Ce^{141} (γ 0.145), Hg^{203} (γ 0.279). By trapping in the counting chamber a sample from a continuous helium flow of 1 cm³/minute it was shown that the γ-energy peak at 0.25 Mev decayed away with a half-life of 9.2 hours showing it to be entirely Xe^{135}. Similarly the contribution at 0.15 Mev was all due to Kr^{85m} and that at 0.084 was entirely due to Xe^{133}.

The γ-energy spectrum of the active gases in a continuous helium flow of 1 cm³/minute showed a distinct peak at 1.30 Mev with accompanying "Compton continuum" (Fig. 5). This was calibrated against a cobalt-60 source (1.17 and 1.33 Mev). Decay of a trapped sample showed that there were two components and subtraction of the longer lived component ($t_{1/2}$ 264 minutes, 28% of total), gave a shorter lived component of half-life 82 minutes (72% of total). The 28% component was shown to be a solid deposit because, in another experiment, sweeping out the counting chamber with pure helium removed the peak at 1.30 Mev but left behind a γ-activity 28% of the original peak height. Interposing a trap immersed in a freezing mixture at −127°C between the outlet of the apparatus and gas counting chamber caused no diminution of peak height indicating that the active

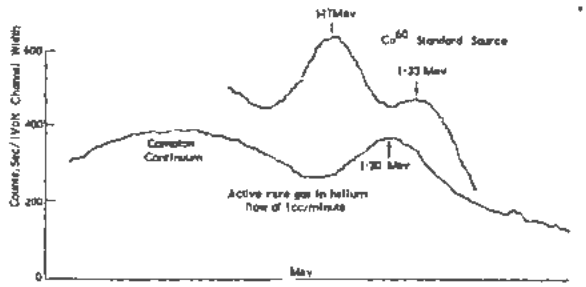

Figure 5. γ-spectrum of active rare gases in He flow of 1 cm³/min

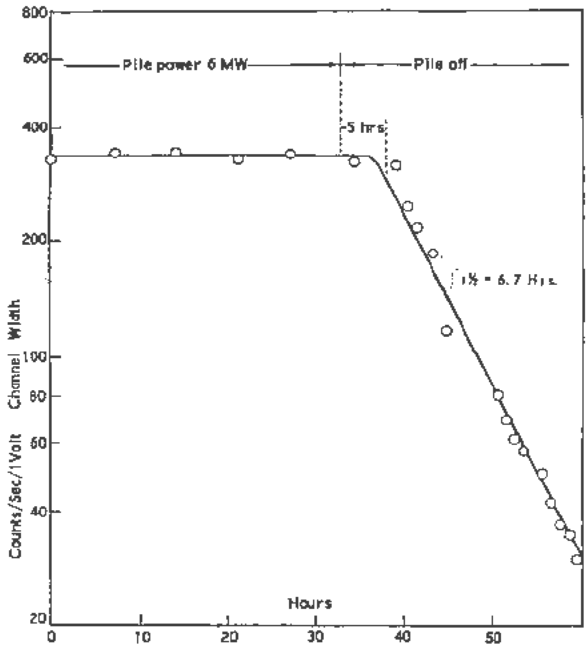

Figure 6. Xe^{135} evolved after pile shut-off (He flow lcc/min)

gas was not a xenon isotope (boiling point —107°C). In other experiments the trap was immersed in liquid oxygen (boiling point —183°C). There was an appreciable diminution in the height of the known xenon and krypton γ-energy peaks and a similar reduction at 1.30 Mev. This indicated that the new peak was a krypton isotope (boiling point —153°C) and was not due to argon-41 (boiling point —186°C). (The incomplete removal of xenon and krypton by liquid oxygen is probably due to the very minute partial pressure of these gases in the helium carrier. A γ-spectrum of the condensate showed very sharp peaks at the known γ-energies.)

Argon-41 (formed from atmospheric A^{40} by (n, γ) reaction in pile) also has a γ-energy peak at 1.30 Mev. This has been demonstrated by passing a stream of air (0.94%A) through the apparatus while in the atomic pile but without the uranium foil present. However, as described previously similar blank experiments with helium showed there was here no γ-energy peak at 1.30 Mev. Krypton-87 has a listed half-life of 78 minutes (from β counting).[10] The bromine-87 precursor ($t_{1/2}$ 56 seconds) decays away quickly when irradiation of the uranium foil has ceased and in fact no γ-energy peak at 1.30 Mev was found under these conditions. It is probable then that this γ-energy peak at 1.30 Mev is due to krypton-87.

Interesting experimental results were obtained in studying the gas evolved at the time when irradiation ceased (pile shut-off) and for a subsequent period. Figure 6 shows that when equilibrium has been attained the amount of γ-activity at 0.25 Mev (Xe^{135}) remains constant while the pile power remains at 6.0 Mw. (The helium flow in this experiment was 1 cm³/minute, the active gas taking 5 hours to reach the counting chamber.) While the pile was shut off, the activity of 0.25 Mev decayed away with the half-life of its iodine precursor (I^{135}, $t_{1/2}$ 6.7 hours). Back-extrapolating the 6.7 hours half-life to a point 5 hours after pile shut off shows that more than 90% of the Xe^{135} removed continuously comes from the iodine precursor (cf. literature value of 95%).[11]

The uncertainty of the above experiment with a helium flow of only 1 cm³/minute was the exact time taken for the active gas to reach the counting chamber. With a helium flow of 600 cm³/minute this time was 0.5 minutes and the actual response could be studied. Figure 7 shows how, when the pile was shut off, the pile power dropped away to zero to be followed just over *one minute* later by a closely parallel fall off in the γ-activity at 0.25 Mev. The γ-activity diminished almost to zero, but thereafter, it was due only to Xe^{135} and over several hours decayed with the 6.7 half-life of its iodine precursor. The rapid response when the pile was shut off was due to the short-lived rare gases which cease to be produced when irradiation ceases and also their short-lived precursors which decayed away rapidly. With a flow rate of 600 cm³/minute the Xe^{135} was diluted so much that its contribution at 0.25 Mev was only 0.1% of the total.

Other experiments with fast flows at varying pile power showed that the γ-activity at a particular energy was proportional to the pile power.

On the lambswool filter before the gas counting chamber traces of the following iodine precursors were identified.

	γ-energy	$t_{1/2}$
I^{131}	0.36, 0.28, 0.64 Mev	(8.1 day)
I^{133}	0.53 Mev	(21 hr)

A few experiments using nitrogen as carrier gas showed that under identical conditions the over-all γ-activity brought up by the nitrogen was about 50% greater than with helium. A blank experiment with nitrogen showed no γ-activity.

DISCUSSION

The results quoted above have shown how the γ-scintillation spectrometer can be used to measure

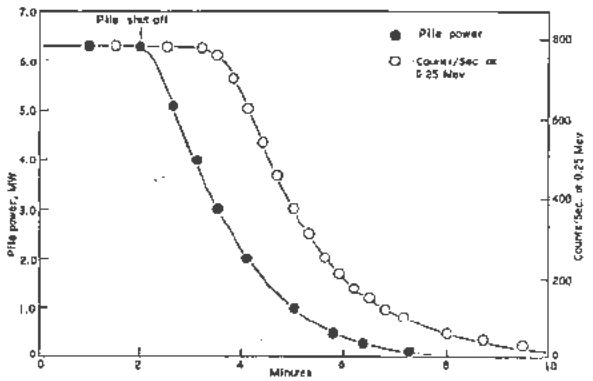

Figure 7. Active gas evolved after pile shut-off (He flow 6000 cm³/min)

active rare gases emitted from uranium foil during irradiation with slow neutrons. With rapid helium flow rates the short-lived rare gases can be detected but as their γ-energies have not been established and the mixture is complex no quantitative conclusions can be made at this stage.

No conclusions can be drawn from the observations on the effect of heat treatment, apart from observing that changes do occur. Heating will be expected to increase the diffusion of rare gases from the foil possibly making the uranium surface more porous and thus facilitating further diffusion, whereas temperature should have no primary effect on the recoil process.

More precise results were obtained with a helium flow of 1 cm³/minute Kr^{85m}, Xe^{133} and Xe^{135} were identified from their known γ-energies and half-lives. Furthermore, when irradiation ceased the amount of the xenon isotope produced fell off with the half-life of its iodine precursor. Back extrapolation of these decay curves enables, in principle, the independent yield of a particular active gas to be determined. Unfortunately, the independent yields of Xe^{133} and Xe^{135} are very small and no precise value has yet been obtained.

From the observed intensity of γ-radiation recorded the actual number of atoms of a particular active rare gas emitted from the surface of the uranium foil during irradiation was calculated as follows:

Let V = volume of cell and leads to counting chamber, cm³; f = flow rate of helium carrier gas, cm³/sec; v = volume of gas counting chamber; N_o = number of atoms of active gas produced/sec; N_t = number of atoms of active gas reaching counting chamber/sec; t = time taken by active gas to reach counting chamber, sec; λ = disintegration constant of active gas, sec^{-1}; p = efficiency of γ-scintillation spectrometer; b = correction factor for internal conversion of electrons and chain branching; and I = intensity of γ-radintion reaching counter.

$$t = \frac{V}{f}$$

$$N_t = N_o e^{-\lambda V/f}$$

Effective concentration of active gas in counting chamber is

$$\frac{v}{f} \cdot N_o e^{-\lambda V/f}$$

Actual number of disintegrations is

$$\lambda \frac{v}{f} \cdot N_o e^{-\lambda V/f}$$

Apparent number of disintegrations as measured on γ-scintillation spectrometer is

$$I = pb\lambda \cdot \frac{v}{f} \cdot N_o e^{-\lambda V/f} \qquad (1)$$

Thus

$$N_o = \frac{If}{pb\lambda v} e^{\lambda V/f} \qquad (2)$$

Differentiating Equation 1 with respect to f shows that from any one isotope a maximum of intensity is registered when $\lambda V = f$ and this has been confirmed by experiment.

The measurements were made with a helium flow of 1 cm³/minute after the foil had been irradiated for 140 hours (corresponding to 99.5% equilibrium concentration of I^{133}). The efficiency of the γ-scintillation spectrometer was determined by calibration against standard sources (calibrated by β-counting). Corrections were applied for internal conversion of electrons and branching ratios of standard sources and active rare gases.[12]† The results are recorded in Table I.

The observed rate of emission of active rare gases can be compared with the number of atoms recoiling from the surface calculated theoretically. The recoil of fission fragments is taken to occur within 5×10^{-4} cm from the surface of the foil.[13] A factor of 0.25 is introduced to account for recoils originating in this volume which fail to reach the surface.[14] The capture cross section of U^{235} is of the order 550×10^{-24}, its abundance in natural uranium is 0.7% and the pile neutron flux was 1.6×10^{12} neutrons/cm²/sec. The percentage fission yields of Kr^{85m}, Xe^{133} and Xe^{135} are taken as 1.9, 6.3 and 5.9 respectively.[15,16,11] The results are recorded in Table I.

Table I. Number of Atoms of Active Rare Gas Emitted/Second from 10 cm² Uranium Foil during Irradiation with Slow Neutrons

Active rare gas	*Calculated from fission yields*	*Determined by experiment*
Kr^{85m}	1.2×10^7	0.15×10^7
Xe^{133}	4.5×10^7	3.6×10^7
Xe^{135}	4.2×10^7	0.45×10^7

The observed rate of emission of Xe^{133} is only slightly less than that calculated theoretically whilst the Kr^{85m} and Xe^{135} occur only to about one tenth of that expected. The theoretical value of the Xe^{133}/Xe^{135} ratio is 1.05 which is much less than the apparent experimental value of 8.0. The anomaly could be due to an inaccurate decay scheme, but this seems unlikely and there are other possible explanations. Xe^{135} has a high capture cross section but calculation shows that only about 5% could be removed by neu-

† Some difficulty was experienced in determining the efficiency of the γ-scintillation spectrometer at 0.084 Mev since Tm^{170} gave an anomalous result probably due to inaccuracy in the decay scheme. An additional check with I^{131} was not conclusive since the contribution of 0.080 Mev is only 4% of total and the higher energy γ-radiation must contribute at lower energies. There was no difficulty with Ce^{141} (0.145 Mev) and Hg^{203} (0.279 Mev) and a curve between these points extrapolates to a value intermediate between that given by Tm^{170} and I^{131}.

tron capture under the experimental conditions. In the theoretical calculation it has been assumed that all recoiling atoms which escape from the surface are carried away in the helium. The recoil path length in helium at 1 atmosphere is about 8 cm[17] though for atoms recoiling part of the distance within uranium it will be less. In the silica cell the foil was about 2 cm from the wall and many recoiling fragments would be expected to be embedded in the cell wall and not measured. Thus in experiments with nitrogen as carrier gas the measured activity increased by 50% because the path length being inversely proportional to the density was then about 2 cm.[18] If a factor is introduced to account for these losses it would bring the theoretical yields of Kr^{85m} and Xe^{135} toward the observed values. The high proportion of Xe^{133} must now be accounted for.

In the theoretical calculation only those atoms recoiling from within 5×10^{-4} cm of the surface have been considered. The uranium foil is about twenty times thicker than this distance and so a considerable number of the active rare gas atoms formed in fission will be trapped in the body of the uranium. These will slowly diffuse to the surface and escape to be measured with the recoiling atoms. The Kr^{85m} ($t_{1/2}$ 4.4 hr) and Xe^{135} ($t_{1/2}$ 9.2 hr) will decay appreciably while they diffuse to the surface but not so the Xe^{133} ($t_{1/2}$ 5.2 days). For Xe^{133} there will be a much greater contribution from diffusion and its yield will therefore appear high. Further experimental work on, for instance, very thin foils where the diffusion contribution will be minimised, is necessary to make these conclusions quantitative.

A few measurements were made on the amount of Xe^{135m} formed. Several hours after irradiation had ceased and with a helium flow rate of 20 cm^3/minute the Xe^{135m} formed per second was 1.8×10^5 atoms. An observation on Xe^{135} (0.25 Mev) under the same conditions gave a value of 17×10^5 atoms/sec. Applying a correction for the Xe^{135m} which has decayed into the Xe^{135} it appears that I^{135} gives about 10% Xe^{135m} and 90% Xe^{135}. This agrees with Glendenin and Metcalf[19] but not with Peacock, Brosi and Bozard[20] who quote 30% and 70% respectively.

It is probable that the peak at 1.30 Mev is due to Kr^{87}. Thulin[21] has obtained the γ-spectrum of Kr^{87} (electromagnetically separated from other rare gas isotopes). He reports peaks at 0.40, 0.89, 1.6 and 2.1 Mev but there is no indication in the present data that an observed peak at 1.3 Mev could be compounded of energies 0.89 and 1.6 Mev.

ACKNOWLEDGEMENT

The authors wish to thank Mr. P. J. Silver for his assistance in the experimental work.

REFERENCES

1. Ayres, J. A. and Johns, I. B., *Separation of long-lived fission gases*, Radiochemical Studies: The Fission Products, McGraw-Hill Co., New York (1951) Paper 311.
2. Hoagland, E. J. and Sugarman, N., *Discovery of ~10y Kr^{85} in fission*, Radiochemical Studies: The Fission Products, McGraw-Hill Co. New York (1951) Paper 69.
3. Hoagland, E. J. and Sugarman, N., *Independent fission yield of 9.2h Xe^{135}* Radiochemical Studies: The Fission Products, McGraw-Hill Co. New York (1951) Paper 147.
4. Dillard, C. R., Adams, R. M., Finston, H. and Turkevich, A., *Determination of gas half-lives by the charged-wire technique*. II. Radiochemical Studies: The Fission Products, McGraw-Hill Co. New York (1951) Paper 68.
5. Raynor, S., *Gas-sweeping apparatus for large-scale collection of fission products on charged wire*. Radiochemical Studies: The Fission Products, McGraw-Hill Co. New York (1951) Paper 312.
6. Overstreet, R. and Jacobsen, L., *Determination of gas half-lives by the charged-wire technique*. I. Radiochemical Studies: The Fission Products, McGraw-Hill Co. New York (1951) Paper 67.
7. Sugarman, N., *Collection of fission-product recoils in a flowing gas stream*. Radiochemical Studies: The Fission Products, McGraw-Hill Co. New York (1951) Paper 315.
8. Hofstadter, R. and McIntyre, J. A., *Gamma-Ray Spectroscopy with crystals of NaI (Tl)*. Nucleonics, Vol. 7, 3, 32 (1950).
9. Elliot, N., *Characteristics of 5.3d Xe^{133}*. Radiochemical Studies: The Fission Products, McGraw-Hill Co. New York (1951) Paper 149.
10. Koch, J., Kofoed-Hansen, O., Kristensen P. and Drost-Hansen, W., *Measurements on radioactive krypton isotopes from fission after mass spectrographic separation*. Phys. Rev., *76*: 279 (1949).
11. Hoagland, E. J. and Sugarman, N., *Independent fission yield of 9.2h Xe^{135}*. Radiochemical Studies: The Fission Products, McGraw-Hill Co. New York (1951) Paper 147.
12. Hollander, J. M., Perlman, I. and Seaborg, G. T., *Table of Isotopes*. Reviews of Modern Physics 25, 469 (1953).
13. Ozeroff, J., *Atomic displacements produced by fission fragments and fission neutrons in matter*. USA Atomic Energy Commission Report A.E.C.D. 2973.
14. Wahl, A. C. and Bonner, N. A., *Radioactivity applied to chemistry*. Wiley and Sons, New York, 286 (1951).
15. Pappas, A. C., *A radiochemical study of fission yields in the region of shell perturbations and the effect of closed shells in fission*. Massachusetts Institute of Technology, Technical Report No. 63.
16. Coryell, C. D. and Sugarman, N., *Radioactivity of the fission products*. Radiochemical Studies: The Fission Products, McGraw-Hill Co. New York, 519 (1951).
17. Katcoff, S., Miskel, J. A. and Stanley, C. W., *Ranges and mass identification of plutonium fission fragments*. Phys. Rev., 74, 631 (1948).
18. Lassen, N. O., *The total charges of fission fragments in gaseous and solid stopping media*. Det Kongelige Danske Videnskabernes Selskab, Mat-fys. Medd 26, 5 (1951).
19. Glendenin, L. E. and Metcalf, R. P., *Characteristics of 6.7h I^{135}*. Radiochemical Studies: The Fission Products, McGraw-Hill Co. New York (1951) Paper 140.
20. See ref. 12.
21. Thulin, S., *The decay of Kr^{87}*, Phys. Rev., 87, 684 (1952).

The Chemistry of Ruthenium

By O. E. Zvyagintsev, USSR

Radioactive ruthenium is obtained as a result of nuclear reactions. The yield of ruthenium among the other products of uranium fission constitutes approximately 6 per cent of the total. The ruthenium isotope with atomic weight 106 belongs to the long lived group of fission products and its isolation from solutions left after treatment of uranium rods is an important problem. This, however, presents considerable difficulties; having a variable valency (from 0 to 8), ruthenium gives rise to many different compounds, the nature of which has not been completely established.

The dissolution of uranium rods in nitric acid is accompanied by intensive oxidation of ruthenium, the compound produced having the highest valency and being RuO_4. Possessing a low boiling point, ruthenium tetroxide may partly be carried away with the gaseous products of the reaction. However, the dissolution of uranium gives rise to large quantities of the oxides of nitrogen, which start reacting with RuO_4 and reduce the ruthenium to its tri- and bivalent state. Martin (1952), by reacting NO with a RuO_4 solution in nitric acid, obtained a compound to which he ascribed the following structural formula: $RuNO(NO_3)_3 \cdot 4H_2O$ and the origin of which he assumed to be trivalent ruthenium. The author, together with Starostin and Artykbaev, obtained bivalent ruthenium compounds of the following composition: $RuNO(NO_3)_2 \cdot 2H_2O$ and $RuNO(NO_3)_2 \cdot 3H_2O$.

The experiments were carried out as follows. The RuO_4 was distilled into a 10% solution of nitric acid, in the presence of a stream of NO. The coloured solution of the compound formed was evaporated to a thick syrup, which was cooled and the solidified salts treated with acetone. The pure salt was recrystallised from acetone solution. On distillation of the RuO_4, if the stream of NO was sufficiently strong, and its passage was prolonged for one hour, the resulting compound of $RuNO(NO_3)_2 \cdot 3H_2O$ was obtained in good yield. If the stream of NO was moderate and short, the result was the formation of $RuNO(NO_3)_2 \cdot 2H_2O$, the yield being generally small (not more than 25%). The residue after dissolution in acetone contained other compounds as yet unknown.

The nitroso-nitrates crystallise in dark-brown coloured crystals.

The determination of ruthenium in these compounds, as in those described below, was carried out radiometrically with the aid of radioactive ruthenium isotope Ru^{106}. The use of the radioactive isotope considerably shortened the time required for analysis, made the results of analysis considerably more precise and permitted the use of smaller samples.

Nitroso-nitrates are diamagnetic, which indicates that the ruthenium is in the bivalent form. The salts are readily soluble in water, ethyl alcohol and acetone and produce intensely coloured red-brown solutions. Caution is required in drying the salts, as they are readily inflammable, a blue spongy mass of oxidised metal remaining after combustion.

These compounds of bivalent ruthenium are interesting because it is impossible to detect ruthenium in them by the aid of chemical reagents, while precipitation with such precipitants as thionalid, 2-mercaptobenzothiazole, is impracticable. The nitroso-nitrates of ruthenium react with ammonia. A solution of $RuNO(NO_3)_2 \cdot 3H_2O$ does not produce any precipitate and does not change colour when acted on by a concentrated solution of ammonia. But its properties nevertheless change. Thiourea precipitates a dark amorphous substance from it while the solution becomes lighter coloured; 2-mercaptobenzothiazole produces a white precipitate which darkens in light. However, ruthenium is not completely precipitated from ammoniacal solutions even by 2-mercaptobenzothiazole and thionalid.

Excess acid, acting on $RuNO(NO_3)_2 \cdot 3H_2O$, may result in the nitrate-ions being substituted by other acid radicals, such as sulphate, acetate, oxalate, etc. Thus, when the $RuNO(NO_3)_2 \cdot 3H_2O$ is treated with an excess of concentrated acetic acid, a new compound ruthenium nitroso-acetate $RuNO(CH_3COO)_2$, is obtained. This compound is red-brown in colour and almost completely insoluble in water. It was subjected to chemical analysis, with the determination of its molecular magnetic susceptibility; the salt is diamagnetic which is true for even-valent ruthenium. The compound is almost insoluble in water but readily soluble in an excess of acetic acid, evidently with the formation of a nitroso-ruthenium-acetic acid. With $CH_3 \cdot COONa$ the nitroso-acetate produces a salt ($NaRuNO(CH_3COO)_3 \cdot H_2O$) readily soluble in water and alcohol but not soluble in acetone.

Like the preceding salts it is red-brown in colour and is diamagnetic. Determinatioa of its molecular

Original language: Russian.

weight shows that it is monomeric, while tests of its molecular electric conductivity show that in aqueous solution the salt ionises. Its formula should, therefore, be written as follows:

$$Na/RuNO[CH_3COO]_3/ \cdot H_2O$$

A similar substance may be obtained by the action of oxalic acid on ruthenium nitroso-nitrate or by the reaction between a solution of ruthenium tetroxide and oxalic acid. The nitroso-oxalate is light pink in colour and almost insoluble in water.

Taking into account the results of this part of our work, we may state that the compound previously mentioned which was obtained by Martin, has the formula $H[RuNO(NO_3)_3] \cdot 4H_2O$ and not $RuNO(NO_3)_3 \cdot 4H_2O$, suggesting an acid complex of bivalent ruthenium. The compound is produced according to the equation:

$$RuNO(NO_3)_2 + HNO_3 = H[RuNO(NO_3)_3]$$

This is confirmed by the existence of salts of this acid extracted by us—$Na[RuNO(NO_3)_3]$ and $(NH_4)[RuNO(NO_3)_3]$—which are intensely coloured compounds readily soluble in water.

It is noteworthy that it is impossible to precipitate ruthenium completely from nitroso-nitrate solutions with reagents which readily precipitate it from other compounds. We have carried out experiments to obtain the nitroso compounds of ruthenium just described using Ru^{106}. The action of various adsorbents and precipitants on these solutions did not result in removal of all the Ru^{106}. It is extremely difficult to distil ruthenium in the form of its tetroxide from nitroso-compound solutions using NaBr. The presence of ruthenium cannot be detected in solutions of nitroso compounds of bivalent ruthenium with the use of thiourea (light-blue colouration).

So it may confidently be stated that the reason for the difficulty in the industrial purification of ruthenium solutions lies in the formation of nitroso complexes of bivalent ruthenium. Clear understanding of this point will assist the further development of practical measures directed at overcoming difficulties encountered in separating solutions from radioruthenium.

Notes on the Half-Life of I^{131}

By F. Barreira and M. Laranjeira,* Portugal

The oxidation of the iodide ion has been a subject of preoccupation to many workers who use I^{131}, since the release of the volatile element causes contamination of instruments and further leads to a faster decay than that due to disintegration.[1,2]

The difficulty is aggravated by the fact that the apparent decay is dependent on external conditions such as humidity, pressure and temperature.

In order to obviate this drawback, use has been made, among the iodides, of silver or cuprous iodide, according to the mass thickness of sources used.[1,2,3]

In this paper we shall study the stability of I^{131} tagged cuprous iodide in sources prepared by various techniques, and stored under varying conditions. We shall consider specially the influence of humidity.

EXPERIMENTAL

Cuprous iodide was always prepared from a solution of I^{131} potassium iodide by precipitation with cupric sulfate, according to the reaction:

$$2\,CuSO_4 + 4KI \rightarrow 2\,K_2SO_4 + Cu_2I_2 + I_2$$

(*a*) Since the use of this salt is justified for sources of fairly substantial mass, for which silver iodide is not to be advised in view of its granular condition, this type was the first one studied.

A mixture is made, in a test tube, of 1 cm^3 of I^{131} potassium iodide (concentration: 1.05 m*M*/l) and 1 cm^3 of a cupric sulfate solution (0.824 m*M*/l). Thus, there is an excess of the latter.

The liquid and the precipitate are poured into a filtration tube which can be dismantled, equipped with a filter-paper disc (Whatman 542) on which the precipitate is deposited by suction.

The precipitate is washed with water until every trace of iodine is removed, and then treated with 5 cm^3 of acetone; the paper disc which carries the precipitate is mounted in an aluminum source carrier, 0.7 mm thick, and dried by infra-red lamp.

The precipitate is distributed over a 2.69 cm^2 surface, giving a 37.2 mg/cm^2 thickness.

Eleven sources were prepared and various lots were formed with them, in order to study the influence of temperature and pressure. Activity was measured each day with a Geiger tube equipped with a mica window 4 mg/cm^2 thick, in a lead vessel.

The activity curves, as a function of time, are straight lines, showing the absence of any other detected radioelement.

In Table I, the storage conditions for each lot of sources are shown, as well as the data obtained for the effective half-life.

The values obtained for the effective half life of I^{131} under those conditions are somewhat high as compared with those found by various authors.[1,4,5,7] In our estimation, they guarantee the stability of the cuprous iodide prepared and kept as described.

(*b*) Sources having a substantial mass may lead to erroneous conclusions, due to the retention of the released iodine, so that we were led to study the behavior of thin sources.

The preparation technique must be different, since we do not have the necessary amount of precipitate for the operations described above.

We endeavoured to use direct precipitation on the source carrier by reducing the iodine formed by sodium sulfite in an acid medium. Due to the reaction of the medium, we used a plastic source carrier. The sources were stored in various manners and, in all cases, we were led to finding a natural half-life of I^{131}, this being due to the existence of free iodine

Original language: French.

* Nuclear Energy Research Center (Physics Laboratory), Lisbon.

Table I

Source	*Storage conditions*	*Half-life, days*	*Observations*
1	Ordinary laboratory $T \approx 8°C$	8.1	Graphical determination
2	Ordinary laboratory $T \approx 8°C$	8.3	Graphical determination
3	Ordinary laboratory $T \approx 8°C$	8.2	Graphical determination
4	40°C incubator	8.2	Graphical determination
5	40°C incubator	8.2	Graphical determination
6	40°C incubator	8.1	Graphical determination
7	Ordinary laboratory	8.0	Graphical determination
8	Ordinary laboratory	8.13 ± 0.018	Analytical determination
9	Desiccator (3 cm Hg)	8.12 ± 0.024	Analytical determination
10	Desiccator (3 cm Hg)	8.13 ± 0.014	Analytical determination
11	Desiccator (3 cm Hg)	8.11 ± 0.018	Analytical determination

which was not reduced by the sulfite and which sublimes progressively.

An increase in the quantity of sulfite is not to be advised, since it would lead to an increase in the amount of inert material in the source.

In order to obtain a source having a small mass, it is necessary to resort to another technique, which will be described below:

The quantity of potassium iodide required to give 10 mg of cuprous iodide is placed in a centrifuging tube, and precipitation obtained by adding an excess of a saturated cupric sulfate solution. Following centrifugation, the supernatant liquid is separated. This is washed three times with water, and the liquid is separated each time by centrifuging. The precipitate is transferred to the aluminum source carrier by means of a pipette, and dried with infra-red light.

As was done before, a measurement is made each day of the activity of the sources, which are broken up into four lots, in order to determine their effective half life. In Table II, we show the data found, as well as the conditions under which the sources were stored. All half lives were found graphically.

Table II

Sources	*Storage conditions*	*Mass, mg*	*Period, days*
12	Water vapor, saturated (3 cm Hg)	1.1	7.6
13	Water vapor, saturated (3 cm Hg)	1.3	6.6
14	Desiccator (3 cm Hg)	1.0	8.1
15	Desiccator (3 cm Hg)	1.2	7.9
16	60°C incubator	1.0	8.0
17	60°C incubator	0.7	7.9
18	Ordinary laboratory	1.3	7.8
19	Ordinary laboratory	1.2	7.9

For the sources kept dry, the values found agree with those commonly found for the physical half-life of I^{131}.

The sources kept in a water vapor saturated atmosphere give values which are much lower than the above, while those which remain in the laboratory atmosphere, with average humidity, show a tendency towards lower values.

The sources of the last two groups, after 25 days, are covered with a bluish layer which is not to be found on the dry sources.

It is to be noted that the curves which represent the variation of activity of these sources as a function of time always are straight lines, as shown on Fig. 1, which proves, on the one hand, that there is no other detected isotope and, on the other hand, that the loss of active material follows an exponential law.

Taking the average value of the half-lives of sources 12 and 13 it is found that the loss of radioactive material takes place at a rate of $1.5\%d^{-1}$.

It was pointed out above that, the presence of water plays an important role in the stability of I^{131} cuprous iodide.

We assume that water does not act of itself, but rather through the products of its radiolysis.

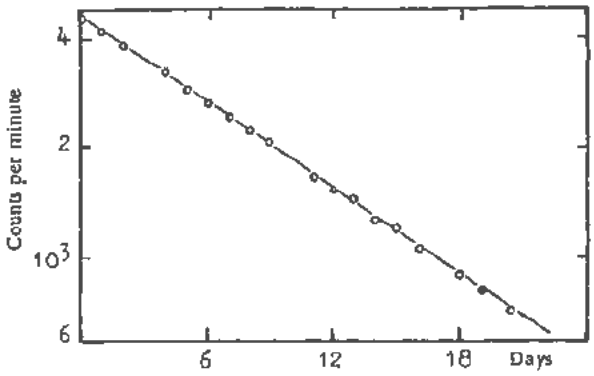

Figure 1. Decay curve of a cuprous iodide source (I^{131}) having an effective half life of 7.864 ± 0.017 days

In order to check on such a hypothesis, we prepared 8 sources having a large mass and low specific activity by the technique described in (*a*) and we subjected them to a flux of gamma rays supplied by Co^{60}, having an intensity of 0.5r/hr.

The sources were divided into four lots, as to the means used for their storage: (*A*) in a dry non-irradiated atmosphere (control); (*B*) in a dry irradiated atmosphere; (*C*) in a water vapor saturated atmosphere (control); and (*D*) in a water vapor saturated atmosphere, also irradiated.

All these lots were subjected to a pressure of 3.5 cm of mercury to facilitate the release of any iodine present.

Table III shows the values found for the effective half-life of I^{131} in each source, as well as its characteristics.

Observation of the results shows that the sources stored in a wet atmosphere suffer a decrease in their half-lives, due to a loss of active material. It is to be noted that sources having a high specific activity (in a wet medium), even in the absence of outside gamma rays, show a net loss (Source 26) in their half-lives, due to radiolysis caused by radiation from the source itself.

It is to be noted, as already stated, that the decay curve of the sources always is a straight line (Fig. 1).

When the storage medium is kept free, even in the presence of outside radiation, the value of the half-life is such that it is possible to guarantee the stability of the compound under these conditions.

DISCUSSION

The results obtained show that water plays an important role in the instability of cuprous iodide, as was pointed out for other iodides.[1]

When water is subjected to the action of ionizing radiations, it undergoes decomposition, which can be expressed by the following equations:

$$2H_2O \longrightarrow H_2 + H_2O_2$$

$$H_2O \longrightarrow H + OH$$

$$2H_2O \longrightarrow 2H + H_2O_2$$

Table III

Source	Medium	Mass	Initial specific activity μc/mg	Half-life in days	Method used for determination	Time of observation (8-day-periods)
20	Dry	19.5	0.279	8 143 ± 0.010	Analytical	3
21	Dry	5.5	0.247	8.1 ± 0.1	Graphic	2.5
22	Dry irrad.	7.4	0.292	8.149 ± 0.023	Analytical	3
23	Dry irrad.	6.1	0.139	8.0 ± 0.1	Graphic	3
24	Wet	15.9	0.295	8.05 ± 0.05	Graphic	4
25	Wet	5.4	0.720	7.95 ± 0.1	Graphic	2.5
26	Wet	1.9	0.747	7.7 ± 0.1	Graphic	3
27	Wet irrad.	7.9	0.0824	7.821 ± 0.022	Analytical	3.5
28	Wet irrad.	7.8	0.0568	7.853 ± 0.024	Analytical	3.5
29	Wet irrad.	5.8	0.137	7.846 ± 0.017	Analytical	3.5
30	Wet irrad.	2.9	0.149	7.766 ± 0.021	Analytical	2.5

The values of G for the various products of this decomposition are much influenced by the presence of foreign matter,[8,9] in particular I^- and Br^- which may react with some of the decomposition products of water, with a shift of the equilibrium toward oxidation of the ions of the free elements, as soon as concentration reaches adequate values.

It is assumed that this technique takes place at the surface of the grains of the precipitate, where a certain amount of water is absorbed, everything taking place as in a true solution, which accounts for the anomalous results found.

We can conclude that cuprous iodide is a convenient form for the sampling of I^{131}, as long as the atmosphere is dry.

REFERENCES

1. Sinclair, W. K. and Emery, E. W., *The Half-Life of I^{131} and the Anomalous Decay of Exposed Sodium Iodide Sources*, Brit. J. Radiology, XXIII, 567 (1950).
2. Hawkins, R. C., Hunter, R. F. and Mann, W. B., *The Standardization of I^{131}*, National Research Council of Canada, Atomic Energy Project, CRM 410.
3. Sinclair, W. K. and Holloway, A. F., *Half-Lives of Some Radioactive Isotopes*, Nature, *167*: 365 (1951).
4. Bartholomew, R. M., Brown, F., Hawkins, R. C., Merrit, W. F. and Yaffe, L., *The Fission Yield of I^{131} in the Thermal Neutron Fission of U^{235}*, Can. J. Chem., *31*: 120 (1953).
5. Livingood, J. J. and Seaborg, G. T., *Radioactive Isotopes of Iodine*, Phys. Rev., *54*: 775 (1938).
6. Lockett, E. E. and Thomas, R. H., *The Half-Lives of Several Radioisotopes*, Nucleonics, *11*: 3, 14 (1953).
7. Seliger, H. H. and Schewebel, A., *Standardization of Beta-Emitting Nuclides*, Nucleonics, *12*: 7, 54 (1954).
8. Sworski, T. J., *Yields of Hydrogen Peroxide in Decomposition of Water by Cobalt Radiation. I-Effect of Bromine Ion*, J. Am. Chem. Soc., *76*: 4687 (1954).
9. Schwarz, H. A., Lesce, J. P. and Allen, A., *Hydrogen Yields in the Radiolysis of Aqueous Solutions*, J. Am. Chem. Soc., *76*: 4693 (1954).

Method of Extraction of Indium Activities Produced in Tin

By N. Nussis, J. Pahissa Campá and E. Ricci,* Argentina

A method has been investigated for the extraction of the indium activities produced by the irradiation of anhydrous stannic chloride, in order to study the short-lived indium isotopes. The possibility of extracting this activity by means of concentrated sulfuric acid has been investigated.

It was observed, in the first place, that stannic chloride is extracted only to a very limited extent by sulfuric acid ($d = 1.84$). Two cm³ of anhydrous stannic chloride were stirred in a small flask together with an equal amount of concentrated sulfuric acid, centrifuged for one minute at 2000–3000 rpm, and the amount of anhydrous stannic chloride extracted in the sulfuric acid phase was determined chemically. The extraction factor obtained in this case was less than 1% (Table I).

Subsequently, pure anhydrous stannic chloride was prepared from tin irradiated two years earlier in the Harwell reactor. Under these conditions the only radioisotope of interest is Sn^{113} which, by K capture, decays to In^{113m}, the half-life of which is 104 minutes.

The extraction test with concentrated sulfuric acid was repeated using this stannic chloride; the sulfuric acid was separated, diluted to about 0.5 N and, in the presence of indium as a carrier, the tin was precipitated as the sulfide and washed in a 0.1 N hydrochloric acid solution saturated with hydrogen sulfide. The indium was precipitated from the filtrate as the sulfide in the presence of an adequate amount of ammonium acetate.

The activity of this precipitate, which contained purified In^{113m}, was measured with an automatic activity recorder consisting of an integrator, a logarithmic amplifier[1] and a recorder. In this way, curves, similar to that appearing in Fig. 1, were obtained from several experiments and show that the activity ratio of Sn/In^{113m} is of the order of 10^{-3}. Further, the purity of the separated In^{113m} activity was checked with a scintillation counter having a differential discriminator.[2,3]

The extraction coefficient of the indium activity without a carrier was determined in consecutive extractions, always using the same stannic chloride preparation as starting materials. In the latter, the In^{113m} returns to equilibrium after 20 hours from the last extraction. The results obtained (Table II) show that 98–99% of the In^{113m} activity is extracted.

Summing the results of all the runs, it may be stated that the purification factor is:

1st stage (extraction)	10^{-3}
2nd stage (chemical separation)	10^{-2}
Complete run	10^{-5}

About 10 minutes elapse for the completion of a run.

CONCLUSIONS

The proposed method facilitates the rapid extraction of high purity radioactive indium produced from stannic chloride.

Table I

Extraction	Results	Average
1	0.89%	0.81%
2	0.73%	
3	0.82%	

Table II

Extraction	1	2	3
Results	98%	99%	99%

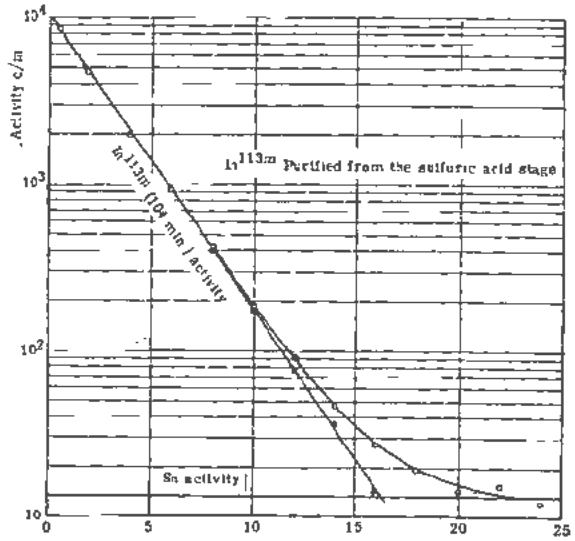

Figure 1. Indium^{113m} purified from the sulfuric acid stage

Original language: Spanish.

* Comisión Nacional de la Energía Atómica, Argentina.

It can be combined with other proposed methods of separation of indium activities without any carrier.[4,6]

REFERENCES

1. Fränz, K. and Marcó del Pont, A., *Amplificador Logarítmico,* Revista Telegráfica Electrónica *495*: 767 (1953) (Buenos Aires).
2. Cork, J. M., Stoddard, A. E., Branyan, C. E., Childs, W. J., Martin, D. W. and Le Blanc, J. M., *Additional Data on the Radioactive Isotopes of Tin and Tellurium,* Phys. Rev., *84*: 596 (1951).
3. Deschamps, Y. and Avignon, P., *Rayonnement γ de la transition ^{115}Sn ^{115}In,* Compt. Rend., *236*: 478 (1953).
4. Kenjiro Kimura and Ikeda Nagao, *Carrier-free extraction of radioactive indium from irradiated unit Sb 125,* J. Sci. Research Inst., (Tokyo) *45*: 128-132 (1951) (in English).
5. Jacobi, E., *Eine traegerlose Trennung des Radioactiven Indiums von Cadmium,* Helv. Phys. Acta, *22*: 66-68 (1949).

Notes on an Isomer of Rh^{106}

By G. B. Baró, W. Seelman-Eggebert and I. Zabala,* Argentina

A study was made of those isotopes having an excess of neutrons which are formed by the action of deuterons and neutrons on palladium, or of neutrons on silver. The formation of the unknown isotopes of mass numbers 108 and 110, and of the unknown isomers of mass numbers 102, 106, 108 and 110 was to be expected. Similarly, the formation of Rh^{109} by an (n,pn) reaction and of Rh^{108} by (n,pn) and (d,an) reactions is possible.

It can be assumed that isotopes 108, 109 and 110 would be short lived since they have high Q values which, computed on the basis of the liquid drop model, give values of about 3.8, 2.5 and 5.0 Mev.

All these nuclides may also be formed as fission products, but, due to the difficulties encountered when trying to separate rhodium quickly from the fission products, it was deemed more convenient to use the (n,p) and (n,a) reactions for their formation.

The well-known isotopes rhenium-102, 104, 105, 107 and others of lower mass numbers, are formed together with the above mentioned nuclides (d,axn), $(x:1,2,3,)$. Their over-all activity is very low.

In order to find the unknown nuclides already mentioned, the activities of rhodium with a neutron excess and half-lives of more than 15 minutes were first studied.

REACTIONS WITH NEUTRONS

Neutrons were produced by the reaction of 1.2 Mev deuterons on metallic lithium. The deuteron flux from the cascade accelerator utilized about 200 μa. The substance was irradiated in cadmium capsules 0.1 mm thick at the center of, and very close to, the target.

Later, using a synchrocyclotron capable of producing 28 Mev deuterons with an ion current of up to 25 μa, it was possible to obtain a more intense beam of fast neutrons for the (d,n) reaction, using as a target, an open copper tube to the end of which a piece of metallic beryllium had been welded.

One gram of palladium or of metallic silver was used for the irradiation with the fast neutrons. The exposure time generally was 20 minutes.

CHEMICAL SEPARATION

The irradiated substance was dissolved in a small volume of concentrated nitric acid, and 20 mg Rh^{+++}, 10 mg Ru^{++} and 10 mg Ag^{+} were added.

The silver chloride was precipitated and filtered on a colloidal filter. The filtrate was partly neutralized with sodium hydroxide and potassium nitrite was added. The product was brought up to the boiling point in order to form the potassium hexanitritorhodium salt, cooled and filtered. This precipitate was dissolved in concentrated hydrochloric acid, Ru^{++} and Pd^{++} were again added as carriers and the potassium hexanitritorhodium was reprecipitated.

The operation was repeated in order to eliminate all the palladium and ruthenium activity. The silver chloride was precipitated until an inactive precipitate was obtained. The elimination of silver activity was necessary after the separation of the rhodium and palladium, since the disintegration of palladium produces active silver.

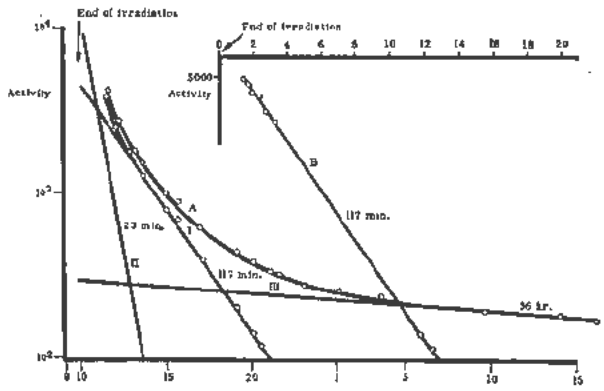

Figure 1. (A) Disintegration curve of Rh obtained from Pd by the (n,p) reaction, measured on a scaler: (I) 117-min and 23-min Rh activity curve; (II) 23-min Rh activity curve; (III) 36.5-hr Rh activity curve: (B) Disintegration curve of Rh obtained from Ag by the (n,a) reaction, measured on a scaler

Finally, the rhodium was precipitated in metallic form using a titanium trichloride solution.

To check for rhodium in the product, rhodium was extracted with pyridine, following the Ballou method.[1]

Several tests were made with indicators such as Ag^{111}, Ru^{106} and Pd^{111}, in order to check on the efficiency of the chemical method used. The chemical run described was made in the presence of high activities of these indicators, checking that no silver, palladium and ruthenium contamination higher than 0.05% of the activity of the initially added indicator remained in the rhodium.

Original language: Spanish.

* Comisión Nacional de la Energía Atómica, Argentina.

The chemical yield determined by the use of Rh^{102} as an indicator was 50 to 60%. This low yield is due to the relatively high solubility of the potassium hexanitritorhodium.

The separation of the rhodium from the irradiated silver took place as follows: the silver was dissolved in nitric acid containing 30 mg Rh^{+++} and 10 mg Pd^{++}. The silver was precipitated with potassium chloride several times until the dissolved active silver had been eliminated. The rhodium present in the filtrate was precipitated in the form of potassium hexanitritorhodium, which was then dissolved and reprecipitated in the presence of 10 mg Pd^{++}. This purification was repeated once.

The complete chemical run lasted almost one hour between the end of irradiation and the first measurement so that no half-lives under 10–15 minutes were detected.

MEASUREMENT

The preparations were measured with a bell counter having a 2 mg/cm² mica window. The activities were recorded by an instrument comprizing a fully zero stabilized integrator, a logarithmic amplifier[2] and a mechanical recorder. The values of the curve so recorded were replotted on a semilogarithmic scale. A device comprising a scintillation counter with a sodium iodide crystal, simple discriminator and scaler was used as gamma detector.

RESULTS OF IRRADIATION BY NEUTRONS

Curve *A* of Fig. 1 shows a typical decay curve; on analysis, it reveals the presence of three half-lives: 23 minutes, 117 minutes and 36.5 hours.

The activity corresponding to the 23-minute half-life is relatively low, due to the small cross section of the processes by which it is formed: Pd^{108} (n,pn) Rh^{107}, and $Pd^{110}(n,\alpha)Ru^{107}$ which in turn yields Rh^{107} by beta decay.

The activity corresponding to 36.5-hr Rh^{105} is relatively much higher since it is formed by Pd^{105} (n,p) RH^{105} and, to a lesser degree by $Pd^{108}(n,\alpha)$ Ru^{105} which yields Rh^{105} by beta decay.

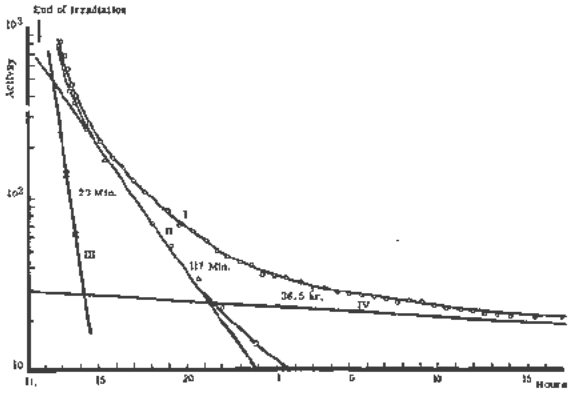

Figure 2. (I) Disintegration curve of Rh obtained from Pd by the (d,α) reaction; (II) curve obtained by subtracting curve IV from curve I; (III) 23-min Rh curve; (IV) 36.5-hr Rh curve

The main activity is due to a 117-minute half-life rhodium isotope.

Curve *B* shows the beta activity of the rhodium obtained by the Ag^{109} or $Ag^{107}(n,\alpha)Rh^{106}$ or Rh^{104} reaction.

REACTIONS WITH DEUTERONS

The 117-minute isotope is also formed during the irradiation of palladium by deuterons.

Powdered metallic palladium in an aluminum target provided with nine 1 mm diameter holes was irradiated. Deuterons having an approximate energy of 28 Mev were used. Irradiation was for 20 minutes, with a 15–20 μa ion current. The chemical separation previously described was done after the end of the irradiation.

The resulting disintegration curve (I) Fig. 2 is more complex than that obtained with neutrons, since it contains in addition to the 23-minute, 117-minute and 36.5-hour half-lives, the very weak activities of the neutron deficient rhodium isotopes (4.4 days, 4.5 hours, 30 minutes and 210 days).

FISSION PRODUCTS

Remembering the nuclear reactions leading to the 117-minute Rh and the known rhodium isotopes, the assumption that the isotope engaging our attention has a mass number higher than 105 is logical; for this reason, a search for it was made among the fission products.

Uranium oxide was directly irradiated with 28 Mev deuterons for 5 minutes; dissolved in nitric acid and neutralized with potassium hydroxide; 20 mg R^{+++} and a few mg Ru^{+++}, Pd^{++}, Cd^{++} and $MoO_4^{=}$ were added. Potassium hexanitritorhodium was then precipitated to separate the rhodium from the uranium and from most of the fission products. This precipitate was dissolved in 25% hydrochloric acid, the solution was neutralized with sodium hydroxide; sodium nitrite and 2–3 mg Fe were added, as well as sodium hydroxide, in order to make the solution weakly alkaline. This process was repeated several times in order to eliminate the impurities absorbed or coprecipitated with the ferric hydroxide. The filtrate was made weakly acid and an excess of potassium chloride was added to precipitate the potassium hexanitritorhodium; the purification of the rhodium was continued as previously described, until it was finally obtained in metallic form.

The corresponding disintegration curve may be seen on Fig. 3; analysis of it indicated a strong activity of 23-minute Rh and the corresponding activity of Rh^{105} (36.5 hours); we were unable to detect another half-life between these two.

The following experiments were also made: separation of rhodium from the strong activities Ru^{107} (4-minute) and Ru^{105} (4-minute), and from Rh^{105} (4.6-hour); also from Ru^{106} obtained from Harwell.

Neither the 117-minute half-life, nor any other unknown rhodium activity between the 12-minute

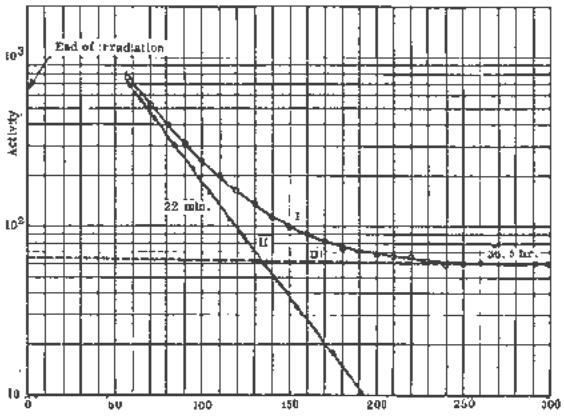

Figure 3. (I) Disintegration curve of Rh obtained by the fission of uranium; (II) Rh^{117} curve; (III) Rh^{105} curve

and several-day half-lives was found in any of these rhodium fractions.

It will be inferred from these results that the 117-minute rhodium is not a normal fission product; should it be formed during the fission, its yield is a hundred times less than would correspond to the total yield of the series of isobars of that mass number.

CHARACTERISTICS OF THE 117-MINUTE RHODIUM

Rhodium obtained by the irradiation of palladium with fast neutrons was used for the study of the 117-min Rh radiations; this preparation produced only a weak Rh^{105} activity in addition to the 117-minute activity.

Rhodium was also produced by the Ag^{109} (n,α) Rh^{106} reaction and only the 117-minute half-life activity was obtained; however, it was weaker than that of the rhodium obtained by the (n,p) reaction.

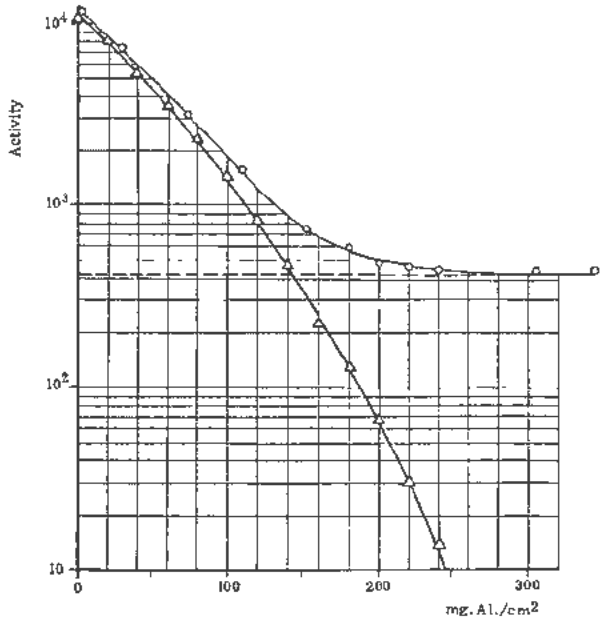

Figure 4. Absorption curve of 117-min Rh^{106m}

The absence of positrons was checked with an ordinary magnet. The maximum energy of the emitted electrons was determined from the absorption curve using aluminum plates. The maximum range was 240 mg/cm² (Fig. 4).

A maximum energy of about 0.7 Mev was found. The absorption curve also indicated the existence of a gamma radiation whose total energy would be 2.9 Mev per beta particle emitted; considering the gamma ray sensitivity of the counter used, this would give a total disintegration energy of some 3.6 Mev.

The preparation was measured with a scintillation counter (thallium activated sodium iodide crystal) in order to determine the half-life more exactly, using a simple discriminator that would permit the detection of gamma rays of energies higher than 0.6 Mev in order to rule out the detection of the Rh^{105} and Rh^{107} gamma rays.

Figure 5 shows three curves with only one 117-minute half-life. They refer to rhodium preparations produced by the (n,p), (n,α) and (d,α) reactions.

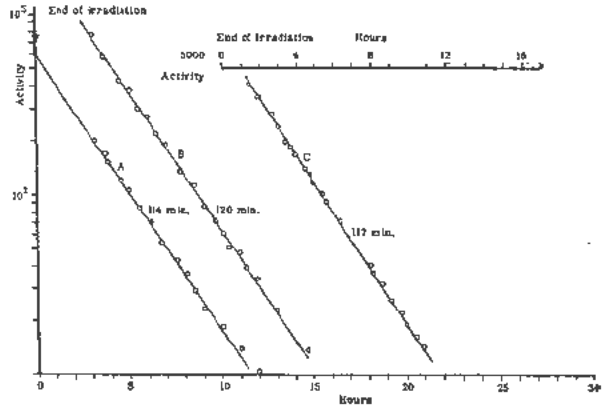

Figure 5. (A) Disintegration curve measured with a scintillation counter and integrator for 117-min Rh obtained by (n,p); (B) curve measured as above but obtained by (d,α); (C) curve also measured with scintillation counter for Rh obtained by (n,α) from Ag

DISCUSSION OF RESULTS

The following are the stable isotopes of palladium and silver, and their yields:

Pd^{102}	0.8%	Pd^{108}	26.8%
Pd^{104}	9.3%	Pd^{110}	13.5%
Pd^{105}	22.6%	Ag^{107}	51.9%
Pd^{106}	27.2%	Ag^{109}	48.1%

Each of the rhodium isotopes having mass numbers 104 and 105 presents two well-defined isotopes.

Although no Rh^{102} isomers are known at the moment of writing, it seems very doubtful that the 117-minute half-life belongs to this mass number since the activity obtained is relatively high, due to its formation from Pd^{102}, whose relative yield is 0.8; or from silver by the $(n,\alpha 2n)$ reaction. Moreover, the values for the total disintegration energy of Rh^{102} and 117-minute Rh differ by more than 2 Mev, for which reason one cannot be dealing with two isomers.

The mass number 110 may be excluded, since the 117-minute Rh is also formed by the irradiation of palladium with deuterons as well as from silver by neutron irradiation.

Mass number 107 is very improbable, due to the great difference in Q values, and because the 117 half-life was not found in the fission products. Furthermore, the formation of rhodium having a mass number of 107 by an $Ag^{109}(n,2pn)Rh^{107}$ reaction seems to be practically impossible.

Mass number 109 can also be excluded, since it was not possible to isolate the 13.4-hour Pd^{109}, which should have been formed in a strongly activated 117-minute rhodium preparation. Furthermore, its formation by the irradiation of silver with neutrons is impossible.

This leaves mass numbers 106 and 108. Mass number 108 is unlikely, since it has not been found in fission even as a daughter of the short-lived ruthenium.[3] In addition, an $Ag^{109}(n,2p)Rh^{103}$ reaction is unlikely.

This leaves for the 117-minute Rh, mass number 107. What remains to be explained is the reason for it failing to appear as a normal fission product. This may be due to the fact that Ru^{106} presents a very low Q value (0.04 Mev), so that a 30-second half-life isomer having a Q value higher than the known 0.04 Mev for Rh^{106}, could not be formed as a daughter of this ruthenium. Naturally, there also is the possibility that the beta disintegration of the Rh^{106} leading to a lower level than that of the 30-second rhodium might be so rigidly ruled out that it may not have been detected to this date. In this case, it could only be formed directly during the fission of heavy nuclei, and it would have a very low independent fission yield, since the 106 series of isobars offers maximum formation probability for technetium and molybdenum. For this reason, the yield for its independent formation during the course of the fission process would be less than 0.1% of the ruthenium produced, and this would account for the difficulty in detecting it in a mixture of the 23-minute and 36.5-hour isotopes. On the other hand, the mass number for 117-minute Rh has been sufficiently well determined by its formation from the $Ag^{109}(n,a)Rh^{106}$ reaction.

The gamma spectrum of the 117-minute rhodium was provisionally measured at the C.N.E.A. nuclear spectrography laboratories. This spectrum was similar to that of Ru^{106}, Rh^{106} and Ag^{106}, with more gamma lines in the 117-minute rhodium spectrum but to date, no comparative measurements have been made with Rh^{106} and Ag^{106}.

The conclusion may be reached from these comments, that the 117-minute half-life belongs to an isomer of the 30-second Rh^{106}, with a Q value probably higher than this; in other words, that the 117-minute Rh would be Rh^{106m}.

The gamma-ray transition probability of Rh^{106m} to Rh^{106} should be less than 1%, since no beta rays of an energy corresponding to such an emission were detected. Should the 30-second rhodium be an isomer with a higher Q, it would not be transformed into 117-minute rhodium in a yield higher than 0.1%, since no 117-minute half-life was found in the Ru^{106}.

REFERENCES

1. Ballou, N. E., "The Fission Products." Paper 263 NNES Radiochemical Studies (May 1954).
2. Franz, K. and Marcó del Pont, A., *Revista Telegráfica*, Buenos Aires, *495*: 767 (1953).
3. Baró, G. B., Rey, P. and Seelman-Eggebert, W., Zeitschrift Naturforschung, *10a*: 81-82 (1955).

A New Series of Isobars of Tin and Antimony

By I. G. de Fraenz, J. Rodriguez and H. Carminatti,* Argentina

Of all elements, tin is the one which has the greatest number of stable isotopes because its nucleus has 50 protons, and according to the theory of nuclear layers,[1] the nuclei which have 8, 20, 50, 82, etc. protons or neutrons have a greater binding energy than the others. Furthermore the radioactive isotopes of tin are particularly stable, since their disintegration energies are about 1.5 Mev below that computed[2,3] without taking the magic number of protons into account. The heaviest isotope of known disintegration energy is Sn^{125}. Other isotopes with a greater mass number, Sn^{126} and Sn^{127}, have been found, although the disintegration energies are not known. Some of the evidence available suggests the existence of isotopes with an even greater excess of neutrons having half-lives of such duration that it is possible to study them by radiochemical methods. The still unknown Sn^{132} not only has a magic number of protons but also 82 neutrons, itself again a magic number. It is well known[2] that the last neutron of a complete layer has a high binding energy and that the previous ones are also bound with greater energies than the isotopes farther removed from those having magic numbers. A low disintegration energy and a longer half-life correspond to a higher binding energy.

These considerations prompted us to look for unknown tin isotopes. A direct measurement of the said isotopes being difficult, we suggested their identification by means of the daughter substances which are antimony isotopes, thus making it necessary that the half-lives and energies of the corresponding antimony isotopes be known.

Barnes and Freedman[4] identified 50-minute Sn^{126} and 1.5-hour Sn^{127} by separation at intervals of their daughter products, 9.3-hour Sb^{126} and 93-hour Sb^{127}. The mass number 127 for the 93-hour antimony has been unequivocally established; and mass number 126 was determined on the strength of the change in yield of the relevant isotopes in the fission of U^{235} induced either by thermal neutrons or by 14 Mev neutrons, so that the said mass number, 126, may be classified as probable.

Barnes[5] also announced the identification of an antimony of about 10-minute half-life, whose parent would be a 29-minute tin to which he ascribes a mass number equal to, or greater than, 126. Pappas[6] found among the fission products of uranium, a 12-minute antimony to which he ascribes mass number 130, based on his measurements of the fission yield on the assumption that the corresponding tin has a life which is short compared with 10 minutes.

According to our measurements, which are not compatible with the data quoted, a 10.3-minute antimony is formed from a 57-minute tin during uranium fission.

EXPERIMENTAL

Fission was induced by 28 Mev deuterons from the synchrocyclotron of the National Atomic Energy Commission of Buenos Aires, Argentina. Five mg UO_2 was irradiated for 10 minutes and then dissolved in boiling concentrated nitric acid. The uranium was precipitated using ammonia in order to eliminate such nitrates as would interfere with precipitation by hydrogen sulfide, and to reduce the ammonia soluble activities such as molybdenum and barium. The precipitate was then dissolved in hot hydrochloric acid, tin [Sn(II) and Sn(IV)] was added to the solution as a carrier and was then precipitated by hydrogen sulfide. The tin sulfide was dissolved in 6*N* sodium hydroxide and diluted to 1*N* with water. A precipitate of the sulfide was obtained from alkaline medium after adding 1.5 mg of copper in order to partly eliminate the activities of zirconium, niobium, silver, zinc, etc. Tin sulfide was again precipitated from the filtrate by adding acetic acid, and treating with hydrogen sulfide. The precipitate was dissolved in hot concentrated hydrochloric acid and a tellurium [Te(IV)] carrier was added, which was then precipitated by hydrogen sulfide. The tin was complexed in a solution with hydrofluoric acid and was purified by three precipitations of antimony sulfide, after adding antimony Sb(III) and Sb(IV) as carrier. This purification was completed 15 minutes after the end of the irradiation. The antimony activities were allowed to develop for 15 minutes, after which a new antimony sulfate precipitation was made. The activity of this precipitate decreased in accord with a 10.3-minute half-life.

It is of interest to determine how the conclusion was reached that the activity of this precipitate is an antimony daughter of tin and not an arsenic daughter of germanium, since the latter behaves chemically, under such working conditions, similarly to that of the former two. Analogons with tin, germanium complexes with hydrofluoric acid and does not precipi-

Original language: Spanish.

*Comisión Nacional de la Energía Atómica, Argentina.

tate with hydrogen sulfide, while under the same conditions, antimony and arsenic are precipitated. This was checked as follows: The active antimony precipitate obtained with hydrogen sulfide, under the conditions mentioned above, was dissolved in concentrated hydrochloric acid, after which the solution was diluted to 2.5N. With arsenic as a carrier, this solution was emptied slowly into a distillation flask containing powdered zinc. The antimony was distilled in the form of stibine and was recovered in a 5% silver nitrate solution. The resulting silver antimonide precipitate was filtered and by measure of its activity, it was observed that it decayed according to a 10-minute half-life. The arsine also formed during the reduction remains soluble in the silver nitrate solution, showing that this 10.3-minute activity is that of antimony. Another test made to check that no short half-life arsenic activities interfere, gave the following results: from the hydrochloric solution obtained by the treatment of antimony sulfate with concentrated hydrochloric acid, to which arsenic had been added as a carrier, the arsenic was precipitated with hydrogen sulfide. The activity of this precipitate was low compared with that of the antimony sulfate precipitated after diluting the solution and, furthermore, it decreased in accord with long half-lives.

A particularly pure activity was necessary for the determination of the maximum energy of the particles from the 10-minute antimony. For this purpose, the tin fraction was purified about 6 hours after the end of irradiation, permitting the activities of the tin isotopes to decrease in the meantime. In an antimony precipitate obtained 10 minutes later and immediately distilled, two activities were observed: the 10-minute antimony and the 93-hour Sb^{127}. Due to the short waiting time, less than 1% of the Sb^{127} had been formed relative to the 10-minute activity which had appeared at the time of tin separation.

The active antimony was precipitated with a small amount of carrier, and part of it was lost during the distillation, so that the precipitate used for the absorption measurement had a thickness of less than 0.5 mg/cm^2. The colloidal filter containing the active compound was cemented to a lucite plate in which a hole had been drilled. On drying, the colloidal filter becomes completely flat and it is not necessary to fix the precipitate which adheres perfectly, although in small quantity, to the filter. The activity of the compound was measured by a tube with a 1.8 mg/cm^2 mica window, and using aluminum absorption plates. The values obtained were corrected for the resolution time of the tube and the corresponding Sb^{127} activities were subtracted. Taking the disintegration of the substance into account, an absorption curve for a 10.3-minute antimony was obtained (Fig. 1).

A maximum β-radiation energy of 2.9 Mev was obtained, using the method by Feather.

In the absorption curve, a gamma radiation is observed, the measured activity of which is about 1.3% that of the β-activity. It is known that the

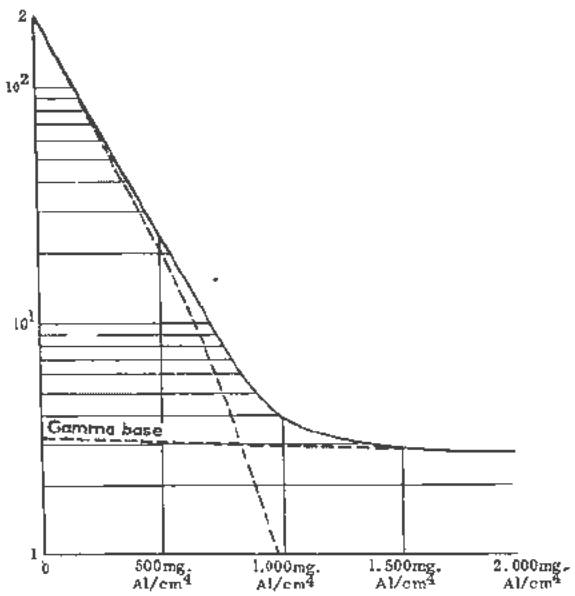

Figure 1. Absorption curve of 10.3-min Sb; maximum range 1450 mg Al/cm^2; maximum beta energy 2.9 Mev

gamma radiation is measured at about 1% per Mev relative to the β-radiation in the measuring equipment used. In this fashion, a total energy $Q \sim 4$ Mev is obtained for the disintegration of the 10.3-minute antimony.

For the determination of the half-life of the parent substance of the 10.3-minute antimony, separations of antimony sulfide were made at one hour intervals using the purified tin solution. Filtrations can be made in 30 seconds using colloidal filters under vacuum. The mean filtration time was taken to be the separation time. It was proved that the filtration is quantitative by making a new precipitation 2 minutes after the first. This precipitate gives only a measure of the activity corresponding to that expected in the time interval. It is observed that a low-energy activity with a long half-life as compared to the 10.3-minute activity remains in the antimony compounds. From the ratio of the activities, one may deduce that tin absorption is less than 0.2%.

To avoid loss of the active solution, hydrofluoric acid resistant materials made entirely of lucite were always used. Another advantage of the use of lucite is that the activities do not readily stick to its surface.

The measurements on the antimony sulfide compounds were made with a GM tube in an easily reproduced geometric position. In order to suppress the measurement of activities of lower energy, the measurements were taken through a 270 mg/cm^2 aluminum sheet. It may be seen from Fig. 2, that all the curves decreased according to a 10.3 $\pm$ 0.3-minute half-life, and that none contained foreign activities in amounts greater than 1%.

By extrapolation of these curves up to the separation times, a disintegration curve of the parent sub-

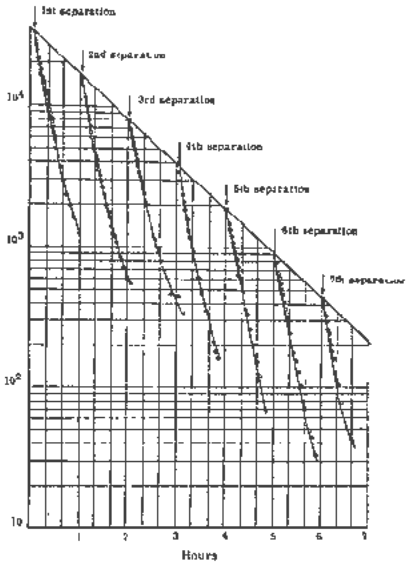

Figure 2. Separations at intervals of 10.3-min Sb from parent substance, 57-min Sn

stance is obtained, showing a half-life of 57 ± 2 minutes.

MASS NUMBER

During fission, the tin isotopes may give rise to antimony isotopes with even mass numbers higher than 124 and odd mass numbers higher than 123. It is not possible that our series of isobars have odd mass numbers since all the antimony isotopes with numbers 125, 127, 129 and 131 are known and their mass numbers well established. Furthermore, according to the layer theory, there are no odd numbered isomers for antimony isotopes. From an (n,p) reaction on tellurium, whose heaviest stable isotope is 130, antimony with a 10-minute activity was found. For this reason, it is unlikely that the mass number of our series is higher than 130. No activity that may have been formed from the 10-minute antimony was found on separating tellurium from antimony at intervals.

For these reasons, mass numbers 126, 128 and 130 remain possible ones, since these antimony isotopes disintegrate to stable tellurium isotopes. Some antimony isotopes are known which might have the same mass numbers: the 9.3-hour Sb^{126}, the 1.2-hour Sb^{128}, a 40-minute Sb^{130} and a 12-minute Sb^{130}. These nuclides are not well established and, furthermore, there may exist isomers for even numbers, up to 130.

It would be possible to assign definitive mass numbers to our isobar series by measuring the fission yield, or by (n,p) reaction on isotopes separated from tellurium.

CONCLUSIONS

Using the chemical method described and separations at intervals, it has been possible to find a 57 ± 2-minute tin isotope which disintegrates to a 10.3 ± 0.3-minute antimony isotope.

It was established that the maximum energy of the 10.3-minute beta radiation of the antimony is 2.9 Mev. It was also shown that it emits gamma radiations and that it does not form active daugbter substances, so that it should be an isobar of a stable tellurium isotope. Considering the probable mass numbers, the mass numbers 126, 128 and 130 are left for this series of isobars.

REFERENCES

1. Mayer, M. G., *Nuclear configurations in the spin-orbit coupling model,* Phys. Rev., *78*: 22 (1950).
2. Way, K. and Wood, M., *A β decay energy systematics,* Phys. Rev., *94*: 119 (1954).
3. Metropolis, N. and Reitwiesner, G., *Table of Atomic Masses,* Los Alamos Scientific Laboratory. Ballistics Research Laboratory - Aberdeen Proving Ground - NP 1980 (March 1950).
4. Barnes, J. M. and Freedman, A. J., *Some new isotopes of Antimony and Tin,* Phys. Rev., *84*: 365 (1951).
5. Barnes, J. M., Personal Communication to Coryell, D. C.
6. Pappas, A. C., *A radiochemical study of fission yields in the region of shell perturbations and the effect of closed shells in fission,* Technical Report No. 63, Massachusetts Institute of Technology, 63 (1953).

A New Iron Isotope, Fe^{61}

By E. Ricci, J. Pahissa Campá and N. Nussis,* Argentina

By irradiating nickel with fast neutrons, it is possible to obtain by the (n,α) process, radioactive isotopes of iron whose mass numbers are lower by three units than those of the corresponding stable nickel isotopes: Ni^{58} (67.76%), Ni^{62} (3.66%) and Ni^{64} (1.16%).

Following the chemical separation of the iron fraction of the irradiated target, a half-life of approximately 5 minutes was identified.

The neutrons used are produced by the (d,n) reaction on beryllium, the deuterons being supplied by the 28 Mev synchrocyclotron in which the target current is maintained at approximately 22 μa.

Together with the (n,α) reaction, the (n,p), (n,γ), $(n,2n)$, (n,pn), $n,\alpha p)$ and probably other reactions take place.

The radioisotopes of iron that may be obtained by the (n,α) reaction, are Fe^{55} (2.9 years) and Fe^{59} (45 days), which are already known,[1] and Fe^{61}, the subject of this article.

In order to be able to determine the characteristics of this new iron isotope, it is necessary to separate it from the other nuclides formed during the irradiation; these are nickel, cobalt and manganese isotopes. The Fe^{55} and Fe^{59} activities do not interfere, since, as their half-lives are relatively long, they are not formed in appreciable amounts during the short irradiation time.

The target used in most of the experiments was nickel oxide prepared by subjecting powdered nickel, supplied by Johnson Matthey & Co., to the action of nitric acid and calcining the nitrate obtained.

The irradiated sample was dissolved in concentrated hydrochloric acid containing nitric acid in the proportion of 1:20. Copper, cobalt, iron and manganese carriers were added to the hydrochloric solution, which was then diluted to 6 *N*. The iron was extracted immediately with ethyl ether,[2] saturated with 6 *N* hydrochloric acid; the ether phase was washed with the 6 *N* hydrochloric acid containing the proper carriers and, from this, the iron was again extracted with water. The iron was precipitated from this medium with ammonia; ammonium chloride and the necessary carriers having been added beforehand.

It was found possible by this method, to have separated the iron fraction about 11 minutes after the end of the irradiation. The exposure times of the sample to the neutrons were about 20 minutes. The measurements were taken with a G.M. tube of the bell type, with a mica window 3.2 mg/cm² thick.

Figure 1 shows one of the decay curves of the iron fraction. A half-life of 5.8 minutes will be seen from the curve corresponding to Fe^{61}, with another one of 94 minutes, corresponding to Co^{61}, a daughter of the first by beta disintegration as will be proven below. The proportions of both activities, extrapolated at the time of separation of the pure iron fraction, agree approximately with the theoretical values.

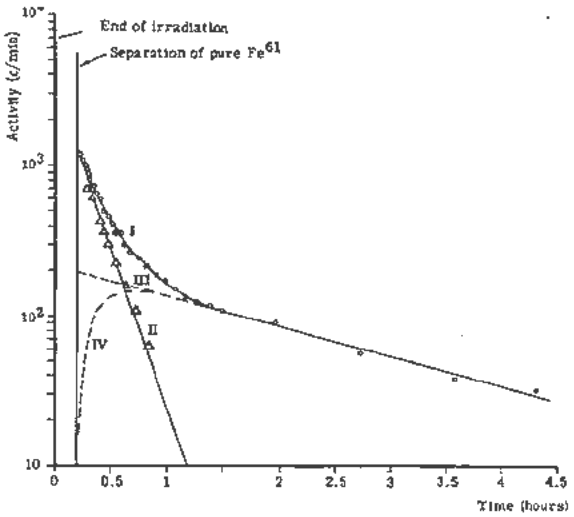

Figure 1. (I) Fe disintegration curve obtained by the (n,α) reaction on Ni; (II) Fe^{61} activity curve; (III) Co^{61} activity curve; (IV) theoretical curve of Co^{61} growth in Fe^{61}

The $(n,\alpha p)$ and $(d,\alpha p)$ processes were also studied.

Figure 2 shows the results of the $(n,\alpha p)$ reaction on a copper oxide target. The working conditions were similar to those described for the (n,α) process, the copper oxide being obtained by the calcination of crystallized copper nitrate supplied by Merck.

The $(d,\alpha p)$ reaction was produced by irradiating powdered metallic nickel supplied by Johnson Matthey & Co. with the 28 Mev deuterons of the synchrocyclotron. Since this process produces a greater proportion of foreign activities than by the neutron induced reaction, it was necessary to modify the chemical process. Figure 3 shows the data from these experiments.

Original language: Spanish.

* Comisión Nacional de la Energía Atómica, Argentina.

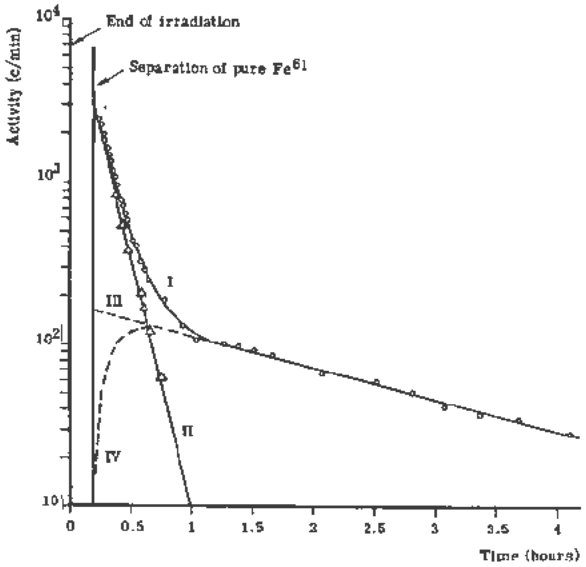

Figure 2. (I) Fe disintegration curve obtained by the $(n,\alpha p)$ reaction on Cu; (II) Fe^{61} activity curve; (III) Co^{61} activity curve; (IV) theoretical curve of Co^{61} growth in Fe

It follows from Figs. 2 and 3 that the $(n,\alpha p)$ and $(d,\alpha p)$ reactions agree with the results obtained by the (n,α) reaction, confirming the number 61 assigned to the new nuclide.

In order to determine the half-life of the Fe^{61}, its daughter (Co^{61}) was separated at 6-minute intervals. The parent iron fraction was obtained by the (n,α) reaction and purified by the method previously described. The parent fraction (precipitated ferric hydroxide) was redissolved in hydrochloric acid, reprecipitated in the presence of a cobalt carrier, and

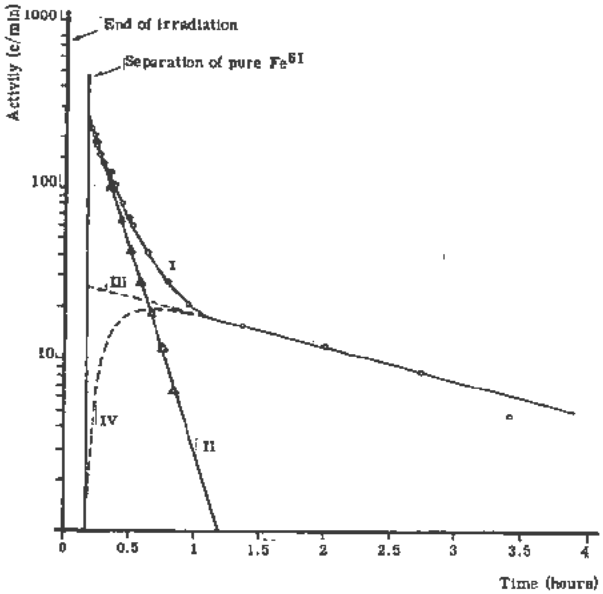

Figure 3. (I) Fe disintegration curve obtained by the $(d,\alpha p)$ reaction on Ni; (II) Fe^{61} activity curve; (III) Co^{61} activity curve; (IV) theoretical curve of Co^{61} growth in Fe^{61}

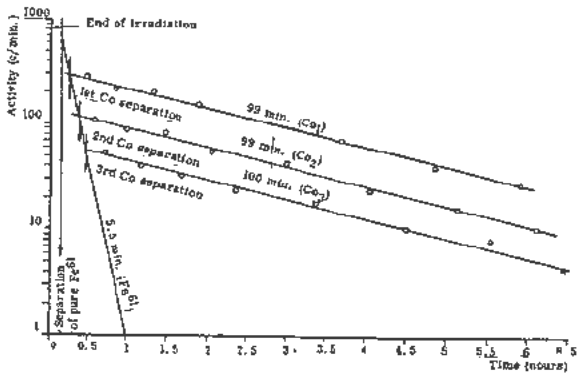

Figure 4

filtered. The Co^{61} was precipitated from the filtrate in the form of a sulfide, adding sodium acetate beforehand. Subsequent separations were carried out in a similar manner. Figure 4 contains the results of one of these experiments. The data obtained in similar tests warrant the assigning of a half-life of 5.5 ± 0.5 minutes to Fe^{61}.

It was shown that the new nuclide emits more energetic γ-radiation than Co^{61} by measurements made with a scintillation counter equipped with a differential discriminator. The measurements were made by absorbing the β-radiation with a lead sheet and eliminating that of Co^{61} with the differential discriminator. Figure 5 shows one of the disintegration curves obtained under the conditions mentioned.

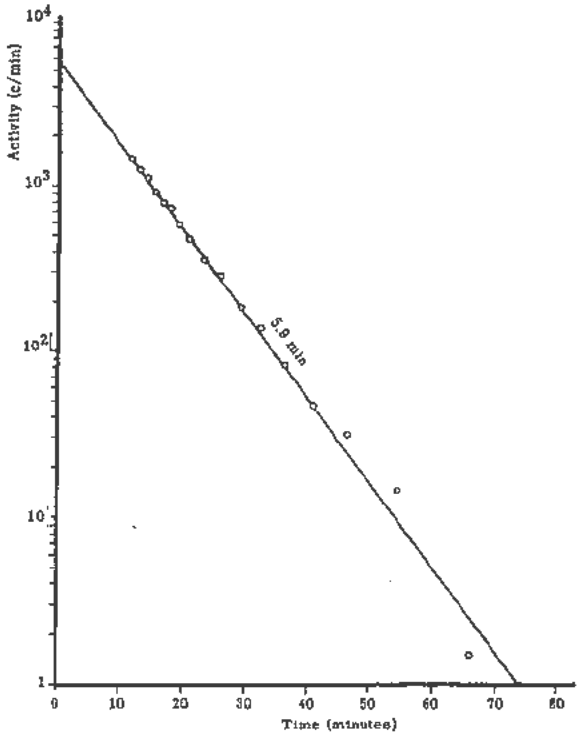

Figure 5. Disintegration curve of Fe obtained by (n,α) reaction and measured in a scintillation counter

The average of the 11 disintegration curves of the daughter substance of the new isotope, obtained by separation at intervals, corresponds to a half-life of 99 ± 2 minutes, agreeing with the data in the tables[3] assigned to Co^{61} appearing in them within class A.[1]

Bearing in mind the fact that Parmley, Moyer and Lilly irradiated Ni^{64} with fast neutrons,[4] Fe^{61} must have been formed by the (n,α) reaction during the irradiation. The possibility thus remains that the half-life of four to five minutes ascribed by the authors to Co^{64} (class F), may really correspond to Fe^{61}.

REFERENCES

1. Hollander, J. M., Perlman, I. and Seaborg, G. T., *Table of Isotopes,* Revs. Modern Phys., *25*: 494 (1953).
2. Welcher, F. J., *Organic Analytical Reagents,* Vol. I, p. 360.
3. Smith, L. A., Haslam, R. N. H. and Taylor, J. G. V., *The decay of Co^{61},* Phys. Rev., *84*: 842 (1951).
4. Parmley, Th. J., Moyer, B. J., Lilly, R. C., *The radioactivities of some high mass isotopes of cobalt,* Phys. Rev., *75*: 619 (1949).

Two New Isotopes of Ruthenium and Rhodium

By G. B. Baró P. Rey and W. Seelman-Eggebert,* Argentina

The purpose of this work was the investigation of possible ruthenium and rhodium isobars having a mass number greater than 107 since there are no theoretical reasoos ruling out their formation as fission products.

The disintegration energy was computed by means of the liquid drop model,[1] applying certain corrections for the range involved on the basis of Way's curves,[2] so that short half-lives have to be assumed for the isobars under study (Fig. 1).

EXPERIMENTAL

Uranium oxide was irradiated with fast and thermal neutrons, or directly with 28 Mev deuterons. Irradiation was carried out either with a Philips cascade generator giving 1.4 Mev at 180 microatoperes and provided with a metallic lithium target, or with the Philips synchrocyclotron which produces 28 Mev deuterons. The Be (d,n) reaction was also used in the latter case, in order to be able to irradiate with neutrons. The synchrocyclotron produces a maximum deuteron current of some 23 microamperes.

The irradiation times were 10 minutes in the cascade generator and 4 minutes in the synchrocyclotron.

The irradiated material was dissolved in a minimum of nitric acid containing 10 mg of the ruthenium ion. The solution obtained was heated in a distillation flask with a U-shaped outlet tube (adjustable by means of ground joints), together with 30–50 ml of 25% sulfuric acid and a saturated solution of potassium bromate, persulfate or bismuthate. The ruthenium tetroxide formed was distilled and condensed into concentrated hydrochloric acid. The hydrochloric acid solution of ruthenium was boiled in order to eliminate bromine which distilled together with the tetroxide.

Chlorides and bromates were added as carriers for the halogens that may have remained in the distillate and were not eliminated by heating. The solution then was diluted with boiling water to an acidity of 5–10%, and ruthenium sulphide was precipitated with hydrogen sulfide. Filtration was carried out with a two-second colloidal filter under vacuum, which was then placed, still containing the precipitate, in another vessel similar to the first one. The operation was repeated, finally yielding ruthenium sulfide free of any foreign activity (ruthenium fraction).

By this method, we were able to start the measurement of the ruthenium fraction 5 to 6 minutes after ending the irradiation.

When it was desired to measure the rhodium isotopes formed by ruthenium decay, the hydrochloric solution from the second distillation was brought down to weak acidity with a saturated solution of potassium hydroxide; 20 mg of rhodium ion were added as a carrier and potassium hexanitritorhodium was precipitated in the presence of potassium chloride with the mixture at the boiling point.

After washing with a saturated solution of potassium chloride in alcohol and water, slightly acidified with hydrochloric acid, this precipitate was dissolved in 2–3 ml of hot 25% hydrochloric acid, adding ruthenium and palladium ions as carriers; the rhodium being precipitated as before (rhodium fraction).

Analysis of the decay curve of the rhodium fraction gave 23-minute and 36.5-hour half-lives, corresponding to Rh^{107} and Rh^{105} (Fig. 2).

Comparing the values obtained by us for the half-life of Rh^{107} with those obtained by Glendenin[3] and Born and Seelman-Eggebert,[4] ours appears somewhat low. The maximum energy, obtained from absorption methods was set at 1.25 Mev (range: 540 mg/cm² aluminum), which is in agreement with that obtained by Born and Seelman-Eggebert[4] (Fig. 3). The Nuclear Spectroscopic Laboratories of the National Atomic Energy Commission are measuring the spectrum and have already found a strong line at 315 kev. More weak lines will probably be found with energies above that mentioned.

Analysis of the decay curve of the ruthenium fraction produced half-lives of 4 minutes, 23 minutes, 4.5 hours and 35.5 hours (Fig. 4).

Comparing the activities of the 4-minute ruthenium with the 23-minute rhodium extrapolated to the moment of the second distillation, a ratio of activities was found similar to that determined by Glendenin,[3] i.e., 4-min Ru/23-min Rh = 11/1, while the activity ratio extrapolated to the last moment of the separation would give, in the case of a simple parent-daughter relation, a ratio of 5/1.

In order to find an explanation for the anomalous behavior of the above-mentioned activity ratio, an attempt was made to produce the series of 107 isobars using the Pd^{110} (n,α) Ru^{107} reaction. For this purpose, one gram of powdered palladium was irradiated for 6 minutes with fast neutrons obtained from the Be (d,n) reaction in the synchrocyclotron.

Original language: Spanish.

* Comisión Nacional de la Energía Atómica, Argentina.

The palladium was dissolved in a minimum of nitric acid containing 10 mg of ruthenium ion as a carrier, and the ruthenium tetroxide was distilled as described previously, but this time with a mixture of potassium persulfate and bromate which possesses the advantage of considerably reducing the foaming on heating in the presence of palladium. The rest of the run was made as indicated under ruthenium fraction.

Analysis of the decay curve of the fraction obtained by the Pd (n,α) reaction revealed half-lives of 4 minutes, 23 minutes, 4.5 hours and 36.5 hours. The activity ratio between the 4-minute ruthenium and the 23-minute rhodium was now found to be in agreement with the calculated figure, i.e., 5/1. (Fig. 5).

This confirmed the mass number of the series of 107 isobars:

$$\mathrm{Ru} \xrightarrow{4\ \mathrm{min}} \mathrm{Rh} \xrightarrow{23\ \mathrm{min}} \mathrm{Pd} \xrightarrow{7\times10^{6}\ \mathrm{years}} \mathrm{Ag\ stable.}$$

In this reaction, Ru^{105} is formed at a higher rate than Ru^{107}. This would not be accounted for adequately by the relative abundances of Pd^{108} and Pd^{110} (26.8% and 13.5%); one must further assume that the cross sections with respect to the neutron spectrum used are different, a fact that will be explained by the great difference between the decay energies of the two series of isobars (5.5 Mev for number 105 and 2.58 Mev for number 107).

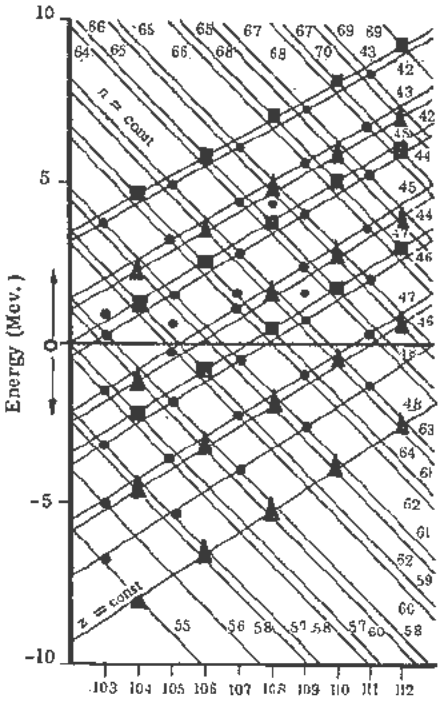

Figure 1. Decay energies calculated by the formula for the liquid drop model for the isotopes of Mo, Te, Ru, Rh, Pd, Ag and Cd, between mass numbers 103 and 112, inclusive

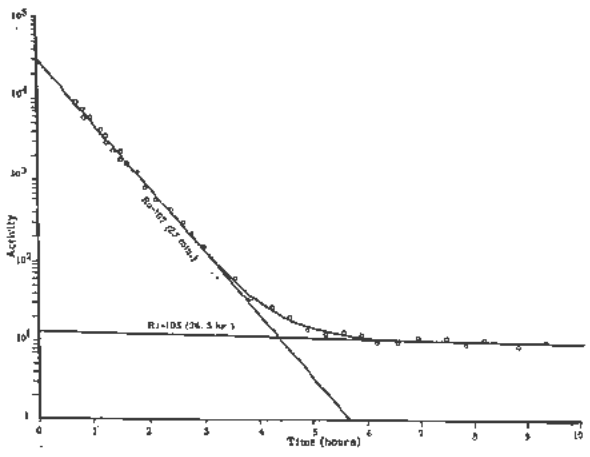

Figure 2. Rh^{107} and Rh^{105} decay curve [$U(d,f)\ {}^{B}Ru \rightarrow Rh$]: the ordinate at the origin indicates the end of the irradiation period

The maximum energy of Ru^{107} obtained by the Pd (n,α) reaction was determined by the absorption method. The computed value, based on a 950 micron half-thickness of aluminum (256.5 mg/cm^2) was about 4 Mev.

The discrepancy between the 4-minute ruthenium obtained by fission and that produced by the Pd (n,α) reaction led to the possibility of the existence of closely similar half-lives. In this case, two active daughter products would be found; one of them came to be Rh^{107}, while the other was unknown.

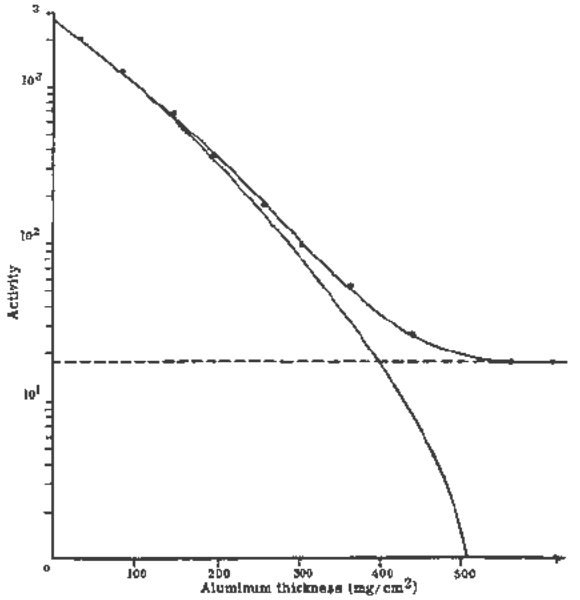

Figure 3. Rh^{107} absorption curve

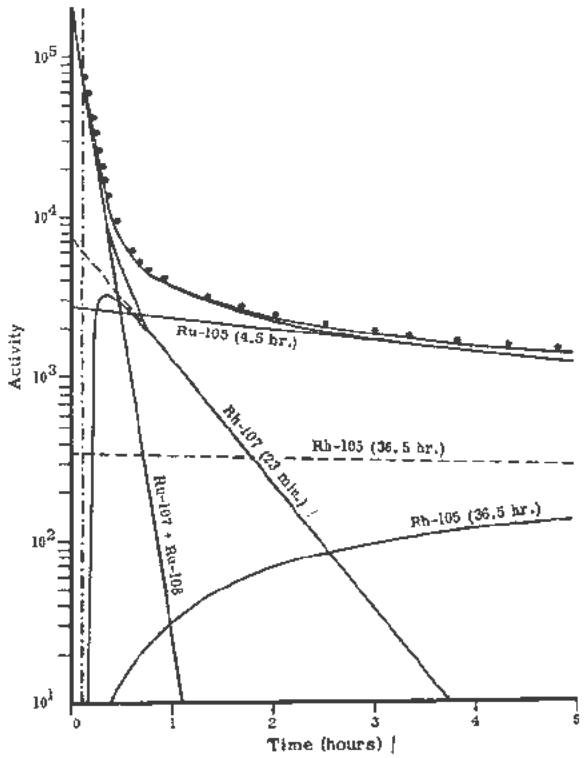

Figure 4. Ru^{107} + Ru^{108}, Rh^{107}, Ru^{105} and Rh^{105} decay curve [U(d,f) Ru→Rh] measured with a bell tube having a 2 mg/cm² window: the dotted line indicates the mean distillation time

An attempt then was made to find another rhodium isotope whose half-life would be either under a minute or very large (the latter really very unlikely for Rh^{108} or larger mass), since it would otherwise have been detected very readily.

For this purpose, potassium hexanitritorhodium was precipitated from the "short" fission ruthenium solution in the presence of 20 mg of rhodium ion and heated to the boiling point. Due to the short life of the rhodium sought it is impossible to redissolve and reprecipitate it, so it remained without purification with a 1% ruthenium activity. The mid-point between the beginning and ending of the filtration was takeu as the zero time for the separation. In this way it was possible to start measurements on the rhodium fraction some 10 seconds after its separation from the ruthenium.

Starting from the "short" ruthenium produced by fission, we found a new rhodium isotope having a half-life of 18 ± 2 seconds (Fig. 6).

The 18-second and 23-minute rhodium isotopes were separated from the ruthenium fraction hy precipitation of potassium hexanitritorrhodium at 4-minute intervals. The beta rays of the 23-minute rhodium found together with those of the 18-second isotope were stopped by an 1800 micron aluminum plate.

By joining the points corresponding to the various activities of the 18-second rhodium obtaioed by successive separations and extrapolating to the instant of separation, a decay curve of about 4.5 minutes was found due to the parent ruthenium. The 18-second rhodium was allowed to disintegrate in the precipitates separated every 4 minutes, and the remaining 23-minute rhodium was measured. Another curve was drawn with these data in a similar fashion to the previous one and corresponds to the parent of the 23-minute rhodium; it proved to have a 4-minute half-life (Fig. 7).

The relative fission yield of the two ruthenium isotopes having a half-life of about 4 minutes was computed on the basis of the activity of the daughters separated after a 4-minute interval (Fig. 7). The yield obtained was about 1 :1 ; which indicates that the ruthenium parent of the 18-second rhodium is also a direct fission product and that their mass numbers are not very different.

It was found by the absorption method that the 18-second rhodium separated from the ruthenium, emits beta rays having an energy of about 4.5 Mev. Due to the very short life of the 18-second rhodium, several preparations were made with a 2000-micron aluminum plate in order to stop the 23-minute rhodium beta rays and, at the same time, to obtain a transformation factor that would mutually relate the preparations. In addition, each preparation was meas-

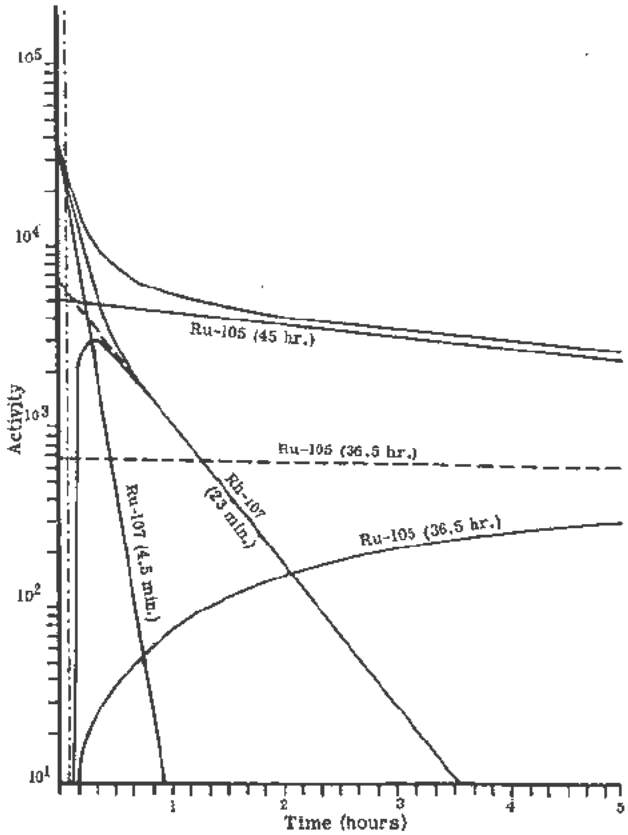

Figure 5. Ru^{107}, Rh^{107}, Ru^{105} and Rh^{105} [Pd(n,α) Ru → Rh] decay curves measured with a bell tube having a 2mg/cm² window: the dotted line indicates the mean distillation time

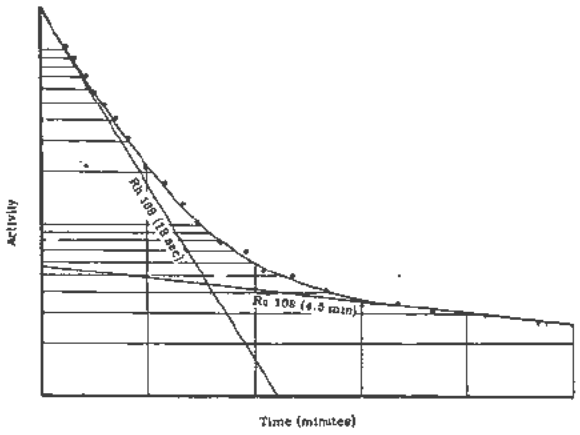

Figure 6. Rh^{106} disintegration curve: the ordinate at the origin indicates the end of the separation

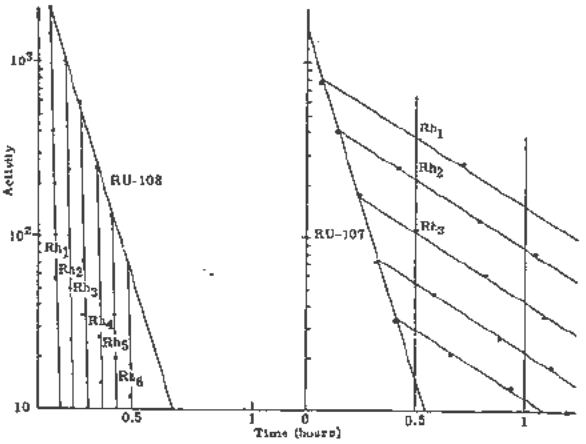

Figure 7. Ru^{108} and Ru^{107} decay curve: obtained by separating rhodium at intervals

ured with the 3000-micron plate and another one from the set (different for each preparation) with the purpose of measuring the absorption curve.

By interposing a 2000-micron aluminum plate and using a scintillation counter, several γ energies were found.

To decide whether the mass number of the new series was 109 or not, the separation of palladium from the ruthenium was necessary. For this purpose the palladium was permitted to develop during one hour in the "short" ruthenium, adding Pd as carrier. A hydrochloric solution of ruthenium was evaporated down to a small volume by heating, was diluted with water, neutralized with ammonium hydroxide, and then made weakly acid with 5% hydrochloric acid. Ruthenium and rhodium ions were added as carriers and later, 5 ml of 1% dimethylglyoxime in an alcoholic solution; heat was applied for a few minutes and the solution was then left to cool to room temperature. Filtration was carried out using a 2-second colloidal filter under vacuum, and washing was carried out with 3% hydrochloric acid. The procedure was repeated twice, in order to give a precipitate free from foreign activities.

It was proved that the new series found does not have mass number 109, since it was not possible to find the 13.4-hour Pd^{109} in the resultant activity of the mixture of 4-minute ruthenium activities, although the total ruthenium activity present was large enough to account for several hundred counts per minute of a 13.4-hour isotope if it were formed from only half of the activity of the 4-minute ruthenium mixture.

MEASUREMENTS

The preparations were measured using a bell type tube with a 2 mg/cm² mica window, or one having a 27-30 mg/cm² glass window, or again with a scintillation counter equipped with a simple discriminator.

In cases of weak activity, the preparations were measured with two tubes connected to two scalers, in order to get simultaneously a decay curve with absorption foils and another one without them.

The integrator modified by Fränz[5] was also used, in which the activity was measured directly when quick readings were necessary. Where long tails were found, the integrator was connected to a logarithmic amplifier operating with a recording device which gave tracings of the decay curves.

ASSIGNMENT OF MASS NUMBER

The mass number of the 18-second rhodium cannot be under 105, since this is a normal fission half life, and the substance emits high energy electrons. Mass numbers 105, 106 and 107 are already taken up, and it is almost impossible that one could be dealing with an Rh^{107} isomer, since it has a much higher Q value. Mass numbers 105 and 106 are also highly improbable, since they are not formed from the 4-minute ruthenium. On the other hand, the separation of the Pd^{109} from ruthenium was not possible, and, for this reason, this mass number is to be eliminated. Numbers 111 and higher are also eliminated since the 18-second rhodium does not give the relevant active nuclides by the decay process. Number 110 also is possible, although to a lesser degree, since its computed Q value according to the liquid drop model, is higher than that computed for mass number 108 and, for this reason, its half-life should be shorter. On the other hand, the value obtained for number 108 agrees quite well with an 18-second rhodium decay energy.

REFERENCES

1. Table of Atomic Masses, U.S.A.E.C., N. P. 1980 (March 1950).
2. Way, K. and Wood, M., Phys. Rev., *94*: 119 (1954).
3. Glendenin, L. E., The Fission Products Radiochemical Studies, *p115*: 848 (1951).
4. Born, H. J. and Seelman-Eggebert, Naturwiss, *31*: 420 (1943).
5. Fränz, K. and del Pont, Marcó, Revista Telegráfica, 495: 767 (1953) Buenos Aires.

Relative Ru^{105}: Ba^{104} Yield, in Fission Caused by Deuterons of Different Energies

By D. Benison and F. E. Más,* Argentina

Uranium was irradiated with deuterons of various energies produced by the 32 Mev synchrocyclotron. The fission yield: Ru^{105}/Ba^{140} was then determined.

The target was obtained by deposition of uranium oxide on aluminium by the following method.[1] An aluminium sheet was degreased with organic solvents, then immersed successively in 25% sulfuric acid and in a saturated solution of sodium zincate. Thus treated, the sheet was used as the cathode of an electrolysis bath containing a saturated solution of uranyl nitrate in ammonium oxalate, 0.2 *N*. The work was done with a current density of 40 $\mu a/cm^2$ and the time of electrolysis varied according to the deposit thickness sought.

Under these conditions, one obtains a very thin and uniform layer of uranium oxide. One side of the sheet was cleaned with nitric acid, so that the uranium remained only on the other.

After this treatment, the aluminium sheets were used as targets, and arranged in such a way that the deuteron beam passed through them before reaching the uranium. The rate of energy loss of the deuterons causing fission varied with the thickness of the film (Fig. 1).

The uranium was dissolved in nitric acid 1½ hours after irradiation in the synchrocyclotron and the Ru and Ba were separated from the fission products.

The Ru was distilled as tetroxide and the Ba was precipitated as chloride in concentrated hydrochloric acid and ether, and the yields of the runs were determined using Ru^{100} as a tracer in the case of Ru, and by weighing as sulfate in the case of Ba.

Measurements were done with identical geometry and were corrected to zero absorption thickness; Ba^{140} was measured by the growth of its daughter La^{140}.

The measured preparations contained several milligrams of carrier. No self-absorption corrections were made.

Activities were computed at the end of irradiation and, from them, the relative fission yield.

Original language: Spanish.

* Comisión Nacional de la Energía Atómica, Argentina.

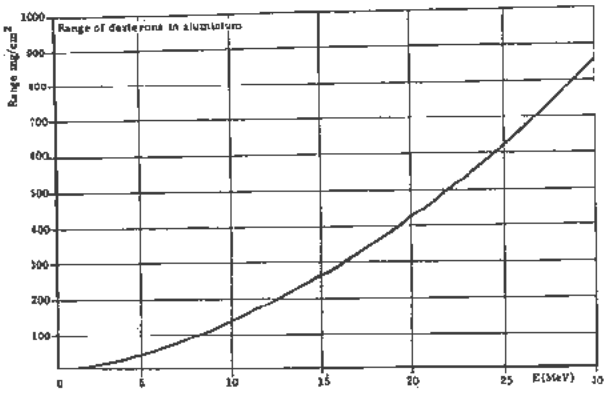

Figure 1. Range of deuterons in aluminum

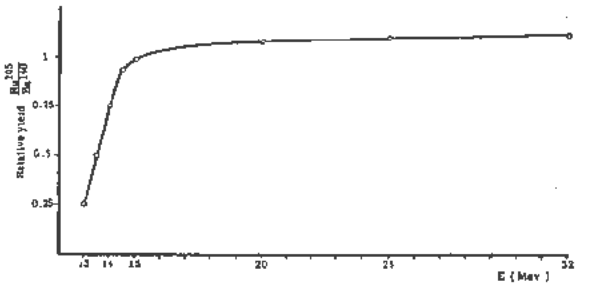

Figure 2

It was observed that, with deuteron beams of over 15 Mev, the relative yield is very close to 1; being slightly higher (1.12) for Ru^{105} at energies above 25 Mev.

The relative yield rises considerably with the energy for deuterons of under 15 Mev (Fig. 2).

The findings for 15 Mev are in satisfactory agreement with those of other authors.

REFERENCES

1. Wilson, C. and Langer, A., *Electrodeposition of uranium oxide on aluminum*, Nucleonics, *11*: 48 (1953).
2. Wiles, D. R. and Coryell, Ch. D., *Fission yield fine structure in the mass region 99-106*, Phys. Rev., *96*: 696 (1954).

A New Isotope of Technetium Produced by an (n,p) Reaction

By J. Flegenheimer,* Argentina

Technetium isotopes of the same mass number may be obtained by (n,p) reactions bombarding ruthenium with fast neutrons. Neutrons are produced by the reaction $Li(d,n)$ in a 1.4 Mev cascade accelerator; the upper limit of their spectrum is about 15 Mev. A neutron flux was obtained in the 28 Mev synchrocyclotron by the Be (d,n) reaction. Reactions of lesser intensity, of the (n, α) and (n,np) types can also be produced besides the (n,p) reaction.

The mass numbers of the technetium isotopes that may be obtained by the (n,p) reaction are 96, 98, 100, 101, 102 and 104. Of these, mass numbers 96, 99, 100 and 101 are known, although there may exist some other, as yet unknown, isomers. Isotope 102 is probably the 5-second half-life found in fission.[1] There are theoretical and experimental reasons to believe that isotope 98 is very long-lived.[2,3] There are no data on 104. The other known beta emitting nuclides of technetium obtained by this reaction are either long-lived or have a half-life of a very few seconds, except Tc^{101}, whose half-life is 14.3 minutes.

Irradiating ruthenium with neutrons yields a very complex curve[4] if the results are measured directly without separating the technetium. The ruthenium and molybdenum should be separated to determine which half-lives correspond to the technetium nuclides.

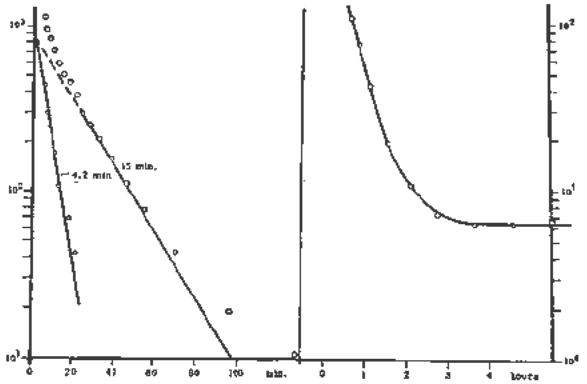

Figure 1. Tc from RuO_2: irradiation time 7 min

The following method was used to obtain these results in a few minutes: ruthenium dioxide was used as the target. The dioxide was prepared by distilling ruthenium tetraoxide from B.D.H. ruthenium trichloride, obtained in 50% sodium hydroxide. The hydrated dioxide was precipitated with hot methyl alcohol, and the product was washed several times in distilled water. The dried product is a fine black powder, insoluble in ammonia, which decomposes hydrogen peroxide catalytically like manganese dioxide, to which it is similar. It was found that, if the irradiated dioxide is used during the decomposition of hydrogen peroxide, most of the technetium formed passes into the solution. Filtration through a colloidal filter is sufficient to separate the technetium (and perhaps the molybdenum) from the dioxide, which is insoluble. The small amount of dioxide that may pass, may be eliminated by adding carriers for the molybdenum and tech-

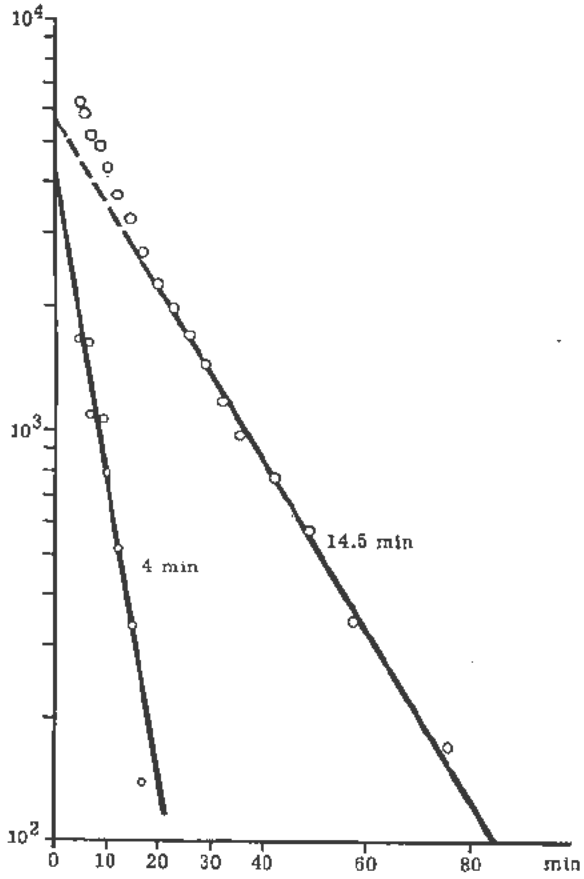

Figure 2. Tc from RuO_2; irradiation time 5 min; β-measurement with magnet

Original language: Spanish.

* Comisión Nacional de la Energía Atómica, Argentina.

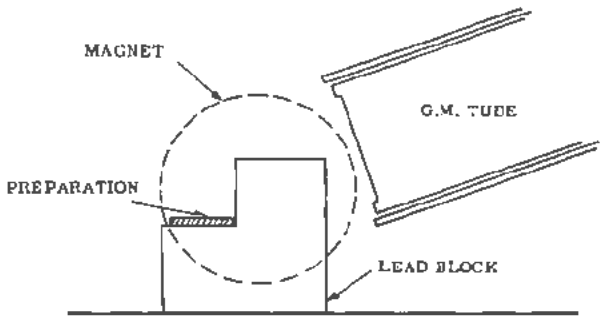

Figure 3

netium, and precipitating the ferrous hydroxide. From the clear filtrate thus obtained, technetium can be precipitated with rhenium, using a tetraphenyl-arsonium chloride solution. Molybdenum remains soluble in the ammoniated medium.

This method made it possible to separate the technetium fraction five minutes after irradiation ended. Figure 1 shows the disintegration curves of the technetium fraction. Irradiation with neutrons from the cascade accelerator lasted 7 minutes and measurement was made in a cylindrical G.M. tube 30 mg/cm² thick. Besides the 14.3 minute half-life of technetium-100, a half-life of about 4.2 minutes is observed which, averaging the results obtained, gives an overall value of 3.8 ± 0.2 minutes. Extrapolating the activities to the end of the irradiation, it will be observed that they are about equal. A small residue was observed which, in longer irradiation, was shown to be made up of half-lives of between 6.6 hours and several days.

The measurement was taken with the magnet arranged to measure only negatrons proving that short half-life is due to negatrons and not positrons (Fig. 3). Figure 2 shows the disintegration curve thus obtained after a 5-minute irradiation and measured with a bell type G.M. tube with 5.8 mg/cm² thick window.

It was possible to determine the presence of gamma radiations by measuring the technetium fraction with a scintillation counter, after absorbing the beta radiation with a lead sheet.

REFERENCES

1. Flegenheimer, J. and Seelman-Eggbert, W., *Über einige Isotope des technetiums*, Z. Naturforsch, *9a* 806 (1954).
2. Segrè, E., *The problem of the stability of Technetium*, Il nuovo Cimento, *9*, 1008 (1952).
3. Herr, W., *Über Natürliches Technetium*, Z. Naturforsch, *9a*, 907-8 (1954).
4. Sullivan, W. H., Sleight, N. R. and Gladrow, E. M., *Search for the previously reported 20 m Ru*, The Fission Products, Ed. Coryell, Ch. D. and Sugarman, N., McGraw-Hill Co., *3*, 1968 (1951).

Determination of the Maximum β-Ray Energy of Xe^{138} (17 min) And Xe^{137} (3.8 min) by Absorption

By Sonia J. Nassiff and W. Seelman-Eggebert,* Argentina

The main difficulty in measuring the maximum beta energy of Xe^{138} is that it can only be determined in the presence of its daughter nuclide, Cs^{138}, whose disintegration pattern is known and reproduced in Fig. 1, and which has a half-life of 32 minutes with a maximum energy of 2.65 Mev, as determined by absorption.

The same is not true of Xe^{137}, since its disintegration product, Cs^{137} (33 years), is not formed in detectable amounts in the time needed for readings to be made on the gas. In this case, it was sufficient to eliminate the interference due to Xe^{138} and Cs^{138} with a suitable absorption plate, or to separate it from the I^{137} previously extracted from the irradiated uranium.

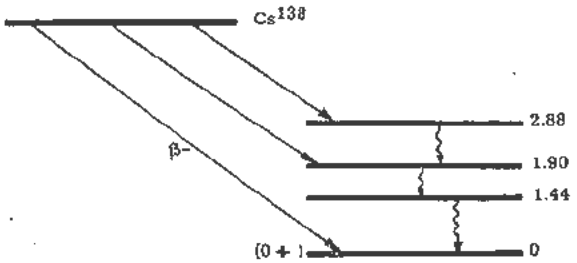

Cs^{138} Disintegration Diagram

Figure 1

EXPERIMENTAL

Xe^{138} was obtained by the fission of a uranium solution brought about by thermal neutrons produced by the $Li(d,n)Be$ reaction in the C. N. E. A. accelerator, with an irradiation time of 15 minutes; also by fission of natural uranium in the synchrocyclotron with 28 Mev deuterons for three minutes, with a current of 10 μa.

With the selected irradiation times, the proportion of long lived isotopes is kept very low. Other fission gases, mainly the Kr isotopes, are obtained together with the Xe.

A series of preliminary tests led us to the conclusion that Kr free Xe may be obtained by absorption with activated carbon at a temperature somewhere between −12° and −15°C, although the recovery is not quantitative, since some of the Xe is carried away by the Kr.

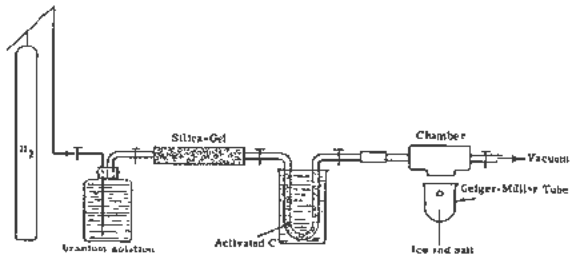

Figure 1'

Therefore, by circulating H_2 for 2 minutes in an apparatus similar to the one illustrated on Fig. 1', the Xe is absorbed in a "U" shaped tube containing activated carbon and submerged in a bath at −12° to −15°C.

In order to eliminate the gases not absorbed by the carbon and remaining in the tube, a current of H_2 is circulated. Only the Xe isotopes produced by the fission are obtained under such conditions; the very short lived ones are completely disintegrated during the treatment following irradiation. The 9.6-hour Xe^{135} and 15-minute Xe^{135m} isotopes appear in the tube in very small proportions, firstly because their direct formation is very small (Chien-shiung-Wu and Segrè[3]), and particularly if the washing with H_2 is done immediately after the radiation, there only being the small amount formed during the operation, from the 6.7-hour I^{135} produced during the fission.

On the other hand, the Xe^{137} is almost totally absorbed in the activated carbon, and it is necessary to wait for its complete disintegration.

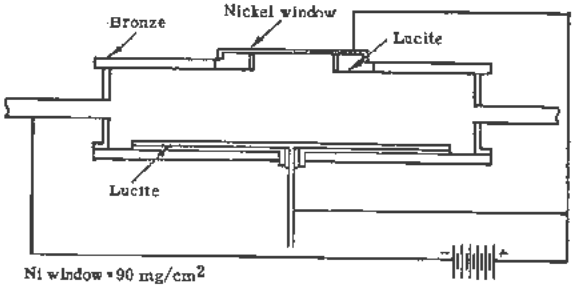

Figure 2

Original language: Spanish.

* Comisión Nacional de la Energía Atómica, Argentina.

The Xe^{138} was introduced into the gas chamber (Fig. 2) 30 minutes after the end of irradiation; the system including the U-tube and gas chamber having previously been evacuated, and the tube heated in a sulfuric acid bath.

The activity of the Xe^{138}, plus that of the Cs^{138} formed by the disintegration of the former, was measured directly as a function of time (Fig. 3).

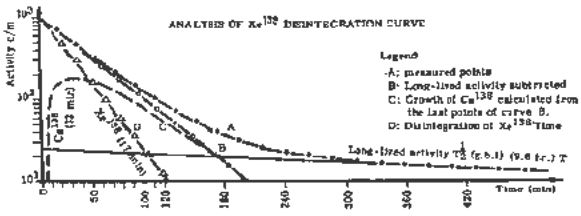

Figure 3

The long-lived activity seen in the curve corresponds to Xe^{135} (9.6 hours). In the irradiation with deuterons in the synchrocyclotron, we found at $t = 0$, 2.5% Xe^{135} activity relative to Xe^{138}; on the other hand, we found only 0.4% when irradiating in the accelerator. In a new experiment we managed to increase the Xe^{138}/Cs^{138} ratio (Fig. 4) by applying 600 volts to the terminals of a gas chamber so constructed that the Cs^{138} could be electrically deposited outside the measuring angle (Fig. 2).

This enabled us to construct an absorption curve

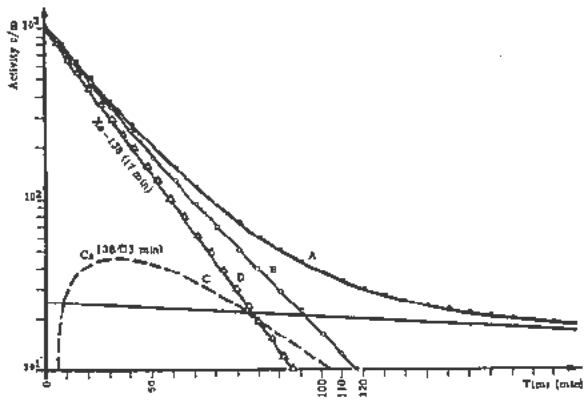

Figure 4. Analysis of the Xe^{138} disintegration curve obtained by applying 600 volts to the chamber

for Xe^{138} in which the correction for the influence of Cs is much smaller.

The construction of this curve was as follows:

Figure 5 shows the family of curves, obtained with different thicknesses of aluminum. For clarity, only a few points were marked on it, drawing only the curve corresponding to 274 mg/cm². The numbers indicate the thickness of Al used.

At the points corresponding to Cs^{138} activity (i.e., after the Xe^{138} had completely disintegrated), the activity of the Xe^{135} was subtracted, obtaining in this way the reduction in the activity of the Cs^{138} for that thickness.

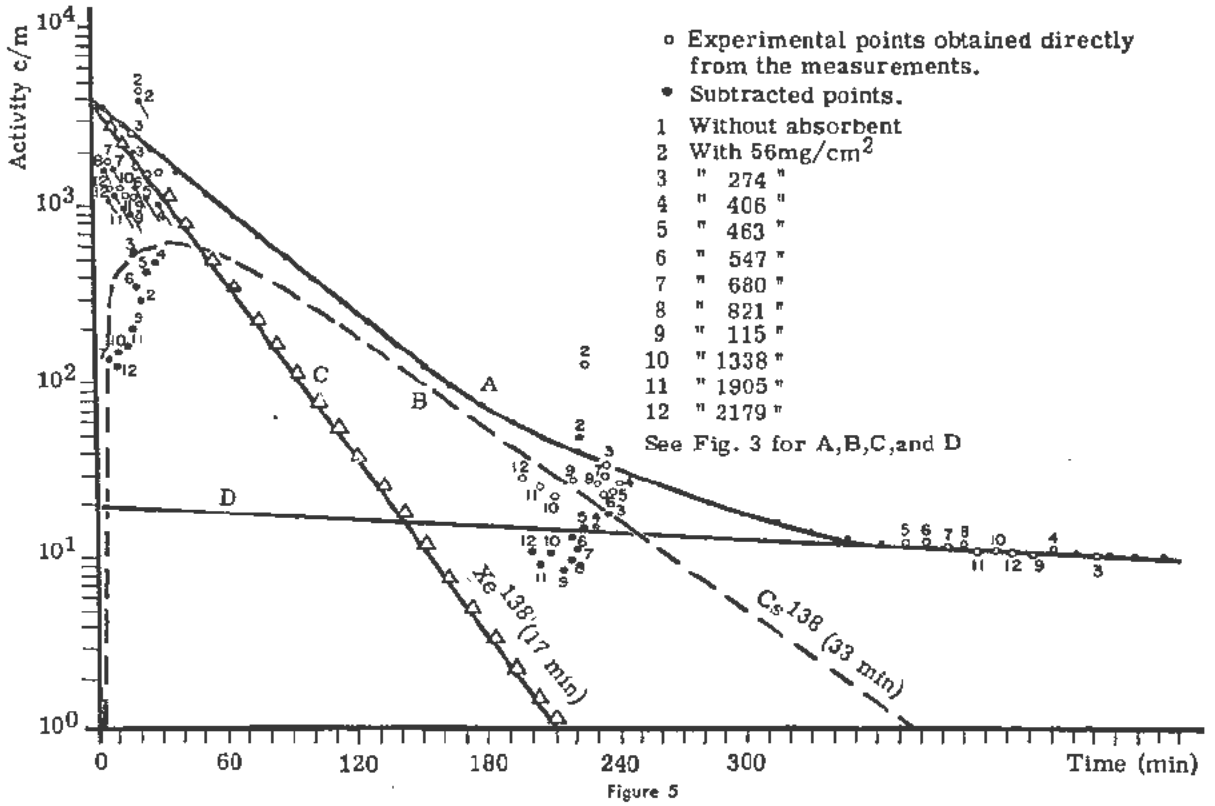

Figure 5

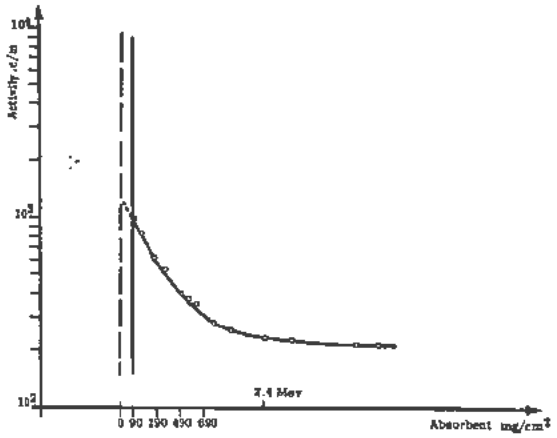

Figure 6. Xe^{138} absorption curve

From the activities obtained with the same Al thickness in the first minutes when the Xe/Cs is higher (Fig. 4), we subtracted the activity of Cs for that time. The data obtained from different irradiations were normalized to the same value for the initial activity. Figure 6 illustrates the values obtained in this way.

It shows a range of 1135 mg/cm², i.e., an E_{max} of about 2.4 Mev, if we compare it with the absorption curve for pure Cs^{138} (Fig. 7), measured with the same geometry as for the gas. If there are more penetrating β-rays, they must be found in a smaller proportion.

The daughter product was measured in another experiment as follows: after injecting the gas into the chamber, the Cs^{138} was allowed to grow until it reached a maximum, after 30 minutes; the Xe^{138} was then washed by circulating H_2 and the remaining Cs was measured using different Al thicknesses.

We also found that Xe^{138} emits γ-radiations, although we are unable, at this date, to make any statement as to its energy.

We compared our results: $Q_\beta = 2.4 + A$ with the Q_β data found in a paper by Way and Wood,[5] and we believe that our experimental value is acceptable, since a discontinuity is observed due to a magic number of neutrons (82) in Xe^{136}.

The absorption curve for Xe^{137} was measured, separating the gas as was done for Xe^{138}, but placing it in the chamber as soon as possible after irradiation. The Al plates used always exceeded the range of the Xe^{138} and Cs^{138}. A range of about 1790 mg/cm² was determined, corresponding to a maximum β energy of 3.5 Mev.

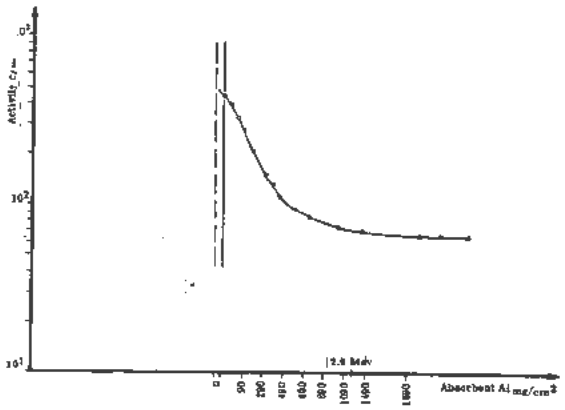

Figure 7. Cs^{138} absorption curve

We also checked, with a scintillation counter, that this Xe isotope is a γ-emitter.

CONCLUSIONS

The maximum beta energies of the isotopes of Xe having mass numbers 138 and 137 were determined by absorption in Al. The values found were as follows: for Xe^{138}: 2.4 Mev; for Xe^{137}: 3.5 Mev.

It was very useful, in the first case, to enclose the gas in a special chamber and to apply a potential difference in order to have the Cs electrically deposited outside of the angle of measurement.

γ-radiation was detected in the two Xe isotopes.

REFERENCES

1. Bleuler, E. and Zünti, W., Helv. Phys. Acta *19*, 375 (1946).
2. Langer, L. M., Duffield, R. B. and Stanley, C. W., *Radioactivity of Cesium 138*, Phys. Rev. *89*, 907 A (1953).
3. Wu, Chien-shiung and Segrè, Emilio, *Radioactive Xenons*, Phys. Rev. *67*, 142 (1945).
4. Thulin, S., *Decay Schema of Xe^{135}*, Phys. Rev. *94*, 734 (1954).
5. Way and Wood, *A Decay Energy Systematics*, Phys. Rev. *94*, — 119–28 (1954).
6. Seelman-Eggbert, W., Naturwissenschaften *31*, 491 (1943).
7. Han, O. and Strassmann, F., Naturwissenschaften *27*, 529 (1939).
8. Heyn, F. H., Aten, A. H. W., Jr., and Bakker, C. J., Nature, *143*, 516–679 (1939).
9. Glasoe, G. N. and Steigman, J., *Radioactive Products from Gases Produced in Uranium Fission*, Phys. Rev. *58*, 1 (1940).
10. Hahn, O. and Strassmann, F., Naturwissenschaften, *28*, 54 (1940).

Radiochemical Analysis of Radioactive Dusts

By Kenjiro Kimura,* Japan

Shortly after the nuclear detonation at Bikini Atoll in March, 1954, radioactive dust fell on a Japanese fishing boat, the No. 5 Fukuryu Maru, which happened to be in the vicinity of the Bikini Atoll.

Physical examination of the crew revealed that this dust, the Bikini Ashes, caused serious radiation damage to the crew.

In order to find the most effective medical treatment for the victims, it was urgent to determine the species and amounts of radioactive elements in the dust. The present authors were requested by the Hospital of Tokyo University, to perform a series of radiochemical analyses on some radioactive samples offered by the hospital. Samples of radioactive dust were collected separately from various parts of the contaminated boat at the Yaizu port, Shizuoka Prefecture. Radiochemical analyses have been carried out on these samples since 18 March, 1954. Chemical methods using carriers and ion exchange were used to separate the radioactive elements. Special efforts were made to perform the separation and determination of individual elements rapidly. The authors succeeded in detecting fifteen nuclides by 25 March. On 31 March, the number of detected nuclides was iacreased to seventeen, and the results of the quantitative analyses of the alkali earth elements were made public.

This report covers the results of radiochemical analyses which were carried out by the authors. Although some of the results obtained in the early stage of this experiment were not accurate enough, this paper could be considered as one of the most detailed and complete reports on the Bikini Ashes published so far.

CHEMICAL COMPOSITION OF THE ASHES

The appearance of the ashes was white porous graoules about 0.2 mm in diameter, and illustrated in Fig. 1. Analytical data have been tabulated in Table I. Analyses of Ca + Mg and Ca were performed by titrimetric determinations with EDTA reagent, using Eriochrome B.T. and murexide, respectively, as indicators. Conway's microdiffusion method was also employed for the determination of carbonate.†

Table I. Chemical Composition of Ashes (May 25, 1954)

CaO	55.2%
MgO	7.0
CO_2	11.8
H_2O (by difference)	26.0
	100.0%

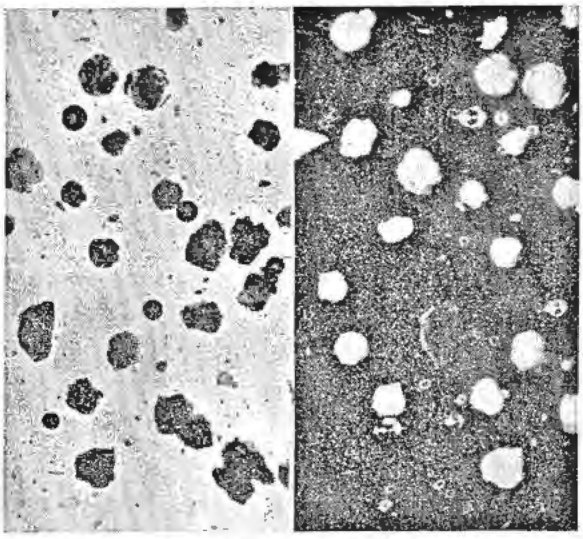

Figure 1. Microscopic detail of ashes

MEASUREMENT OF RADIOACTIVITY

In the course of the experiments, measurements of radioactivity were made with two sets of scalers. One, made by the Tracerlab, Inc., USA, is equipped with and end-window G-M tube, having a mica window of 1.5 mg/cm² thickness (hereafter called Tube No. 1). The other, made by the Scientific Research Institute, Tokyo, is used with the same type of G-M tube, having a mica window of 3.5 mg/cm² thickness (hereafter called Tube No. 2). When the sample was

* Department of Chemistry, Faculty of Science, University of Tokyo. This study was prepared jointly with 16 other members of the above Department: Eiichi Minami, Masatake Honda, Yuji Yokoyama, Nagao Ikeda, Keiichiro Fuwa, Haruo Natsume, Tatsujiro Ishimori, Yukiyoshi Sasaki, Hitoshi Sakai, Kunihiko Mizumachi, Masako Asada, Shuji Abe, Hisao Mabuchi, Yasuo Suzuki, Kazuhiro Komatsu and Kenji Nakada.

† The present authors wish to thank Miss K. Saruhashi of the Geochemical Laboratory of the Meteorological Institute in Tokyo for her help in performing the microdiffusion analysis. The figures indicating the mean chemical composition showed that the sample was a mixture of hydroxide and carbonate of calcium containing small amounts of magnesium. By spectrochemical analysis (dc arc method) Al, Fe, Si and Sr were detected, in addition to Ca and Mg.

placed 1.3 cm below the mica window of Tube No. 1, the counting yield for β-particles was approximately 10%, while the corresponding counting yield of Tube No. 2 was about 5% when the sample was placed 2 cm below the end-window. For this paper, measurements of radioactivity were mostly made under these counting conditions. When the measurements were made under different counting conditions, the values were converted to those corresponding to the above conditions. The samples were usually evaporated to dryness in glass counting dishes. In the case of some samples, the precipitates were collected on sheets of filter paper of 3 cm² area by using a removable filter tube and then mounted on either metal or glass dishes.

GROSS RADIOACTIVITY OF ASHES

The specific radioactivity of a sample was estimated by comparing it with a reference sample of Co^{60} of known absolute disintegration rate. Since the sample was composed of various nuclides as shown in the following paragraphs, accurate data should not be expected. A small amount of Co^{60} sample, 1.72×10^{-4} mc on 23 April, and 0.83 mg of ashes were taken and spread uniformly in separate counting dishes of the same size. Absorption curves of both activities were measured under the same geometrical conditions (see Fig. 2).

To obtain the values of zero absorption, the corrections were made graphically on the experimental data for the absorptions due to the mica window and the air between the sample and end-window ($1.5 + 7.1 = 8.6$ mg/cm²). The figures shown in Table II are those of net counting rates due to β-particles which were corrected for the γ-ray background using a lead absorber (585 mg/cm²).

Specific activity of sample:

$$1.72 \times 10^{-4}\ \text{mc} \times \frac{5000}{2800}/0.83\ \text{mg} = 0.37\ \text{mc/gm}$$

Since 16 March the decay curve of ashes (Fig. 3) was measured at the Radioisotopes Research Laboratory, the University of Tokyo. It was found that the gross decay of the ashes is represented by the following formula for approximately three months.[1,2]

$$I = ct^{-1.37}$$

where I, c and t stand for the counting rate, a constant and the time that elapsed since the detonation, respectively.

By using the above figures and formula, a value of 1.4 curies/gm was obtained by extrapolation as the

Table II. Measurement of Absolute Activity
(23 April 1954)

	β-ray activity under same geometrical conditions	Activity extrapolated to zero absorption
Co^{60}	1499 cpm	2800 cpm
Ashes	3748	5000

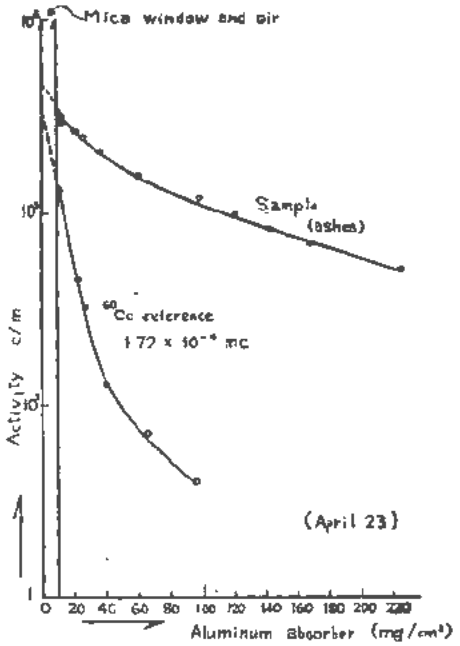

Figure 2. Aluminum absorption curves of ashes and Co^{60} reference sample

specific activity of the ashes at 7.00 am, on 1 March, the time when the ashes were supposed to have fallen on the Fukuryu Maru.

GROUP SEPARATION OF ELEMENTS

For the group separation of elements, the coprecipitation method using scavengers and carriers was used with great effectiveness.

Carrier-free separation using ion exchanger was also found to be very useful.

Radiochemical Qualitative Analyses Using Carriers

Ten mg of each of the following carriers were added to a hydrochloric acid solution containing approximately 1 mg of the ashes: Copper (as copper sulfate), iron (as ferric chloride), lanthanum (as lanthanum nitrate), zinc (as zinc chloride), calcium (as calcium chloride) and sodium (as sodium chloride).

The scheme for group separation of elements is shown in Table III. Since complete group separation cannot be assured by this process alone, repeated precipitations with either scavengers or hold-back carriers were also carried out to avoid cross contamination.

It was found that more than a half of the total activity was concentrated in the third group, while some activity was concentrated in the second and fifth groups. Since a low level of activity might be due to cross-contamination, no definite conclusion could be arrived at from this result. But it is certain that the activity in the first and fourth groups consists of only a very small fraction of the total activity in the sample of ashes.

Table III. Group Separation of the Active Elements

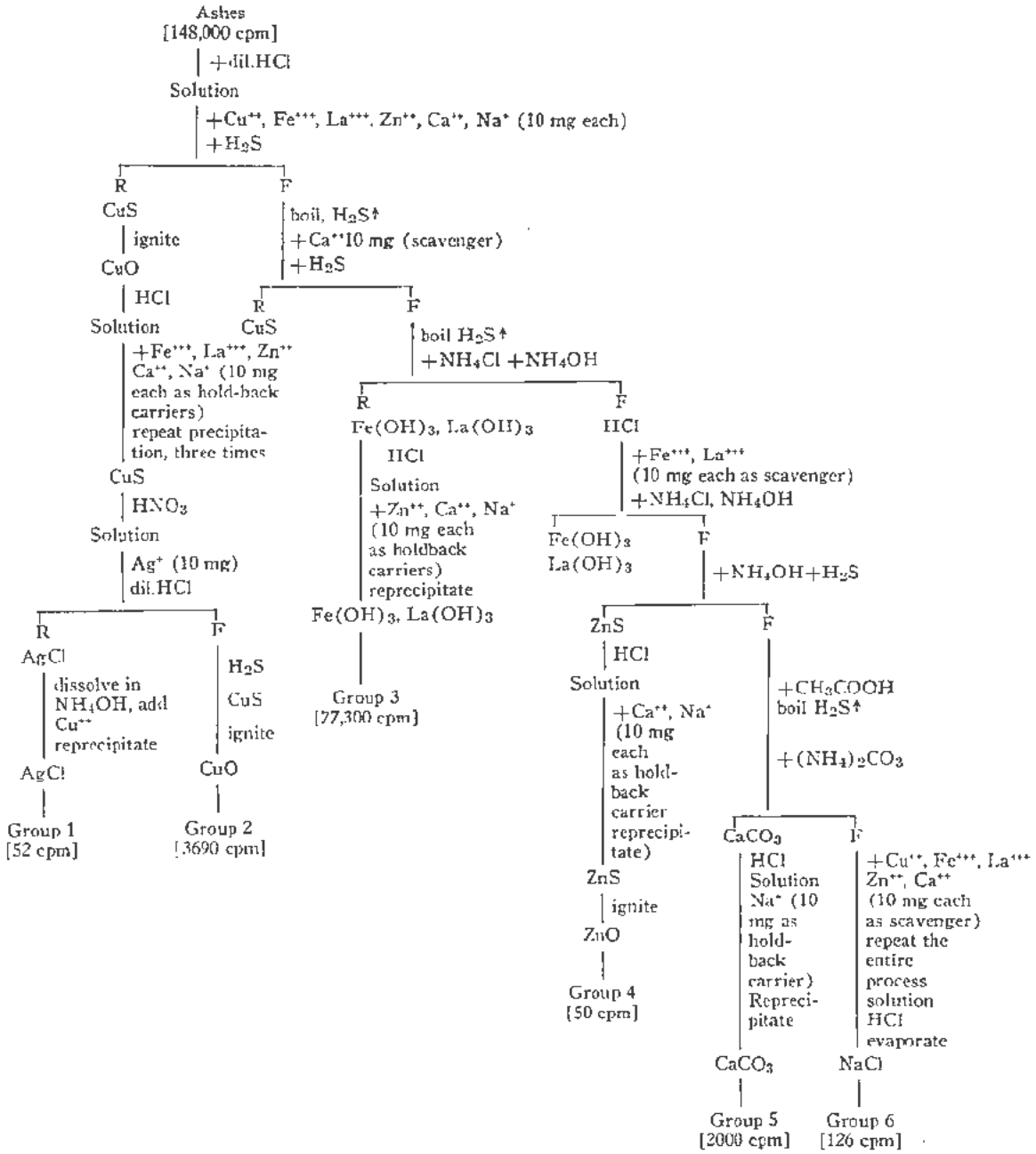

Further separation was performed on the second, third, and fifth groups, which were strongly radioactive, by adding other kinds of carriers.

Although the activity in the third group was carried down by zirconium and niobium carrier, most of the activity was fouod to be coprecipitated with rare earths. Almost all of the activity in the fifth group was concentrated in the barium and strontium precipitates, while the activity in the calcium precipitate was negligibly small.

Group Seporation with Cation Exchange Resin

Carrier-free group separations of elements have been successfully carried out by the use of cation exchange resin, Dowex 50 or Amerlite IR-120. A typical experiment, which is illustrated in Fig. 4, was carried ont under the following conditions.

About 10 ong of ashes having an activity of nearly 10^6 cpm (measured by Tube No. 2), were dissolved in dilute hydrochloric acid, evaporated and redissolved in about 5 cm³ of 0.2 *N* hydrochloric acid

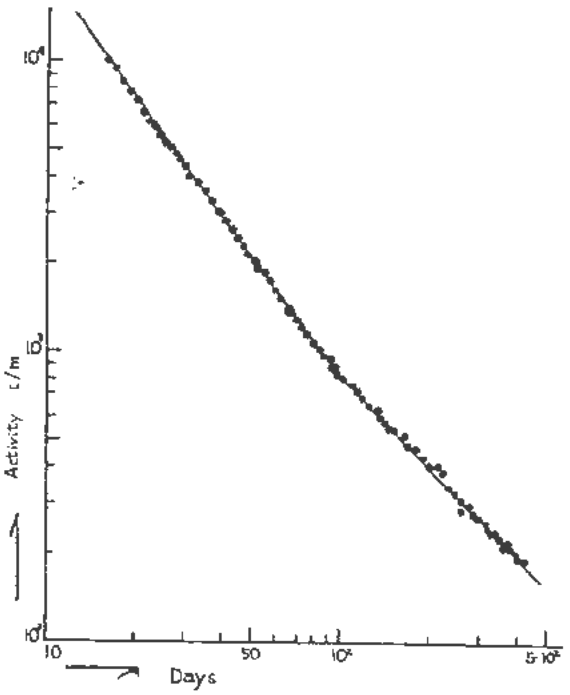

Figure 3. Decay curve of ashes

solution. The solution was allowed to flow at 0.5 cm³ per min, through a cation exchange resin bed (2.5 cm³), which was prepared with hydrogen form of Dowex 50, 8% cross-linked (80–120 mesh). At certain intervals, each drop of the effluent was collected on a small filter paper (2 cm), mounted on a glass plate and its radioactivity was measured.‡

First, the filtrate from the sample solution and the succeeding effluent from the washing solution (0.2 *N* HCl) were collected and used as the sample for the analyses of anions: I, Te, Ru and Rh. According to the method described by Tompkins *et al.*,[3, 4] 0.5% oxalic acid solution and ammonium citrate solution were employed successively as the eluting reagents for several groups of the constituents. Care was taken in the selection of the pH value of the citrate solution. In a preliminary experiment,§ 3.5 and 6.5 proved to be favorable pH values for the elution of rare earth elements and alkali earth elements, respectively.[5]

In this experiment, however, the pH value of the citrate was raised by 0.5 for each elution. As a result, alkali earth elements were separated more completely than expected, and rapid detection of Sr^{90} was not successful because of the difficulty in identifying elution positions of calcium and strontium. After treatment of the bed with the final eluent at a pH of 6.4, residual activity in the resin was about 4000 c/m (0.4%), which was measured on the ignited residue of resin

‡ In the later work, the effluent was counted continuously and directly as a liquid sample. This was performed by passing the effluent through a vinyl tube which was wound in a spiral shape and by placing the tube under the window of counter.

§ The preliminary work performed on 18 March showed that the activity of ashes might be attributed mainly to fission products.

IDENTIFICATION AND DETERMINATION OF INDIVIDUAL NUCLIDES

Tellurium

The experiment was started with a sample having an activity of the order of 10^6 cpm (measured by Tube No. 1). The sample solution was passed through an ion exchange resin bed, Amberlite IR-120 (hydrogen form). The resulting effluent was mixed with 10 mg each of iodine, tellurium, and ruthenium carriers. The acidity of the solution was adjusted to 3 *N* by adding nitric acid and then iodine was separated by distillation. The distilled iodine was received in a flask containing sodium hydroxide solution. After iodine was completely distilled off, perchloric acid was added to the residual solution. The system was again subjected to distillation. The distilled ruthenium tetroxide was received in a flask containing 3 *N* hydrochloric acid. After the distillation, the pH of the residual solution was adjusted to about 2.

The resulting solution was passed through an anion exchange resin bed, Amberlite IRA-400 (chloride form). Tellurium was not adsorbed on the resin bed under this experimental condition. Thus, the separation of tellurium from other anions was easily performed. The acidity of the effluent was adjusted to 3 *N* by the addition of hydrochloric acid. Then, the tellurate ions were reduced to metallic tellurium by hydrazine hydrochloride and sulfur dioxide. After the metallic tellurium was filtered and dried, its activity was measured. On the 26th March, the counting rates of 15,000 cpm were observed. The aluminum absorption curve of this tellurium fraction is shown

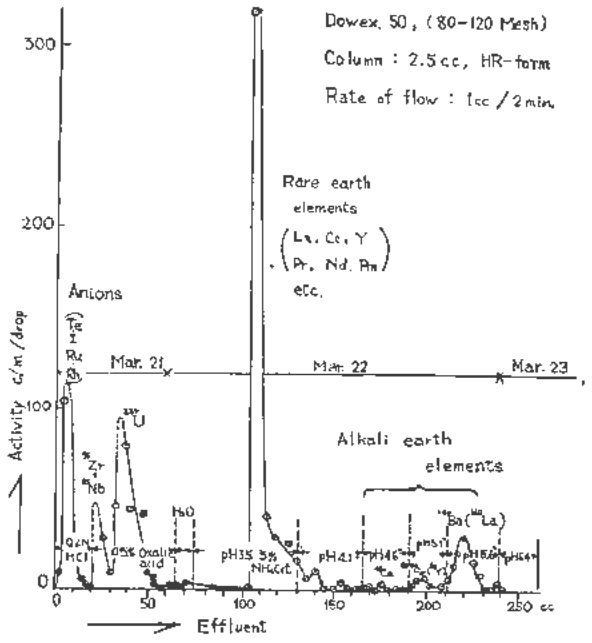

Figure 4. Elution curve of cation exchange group separation

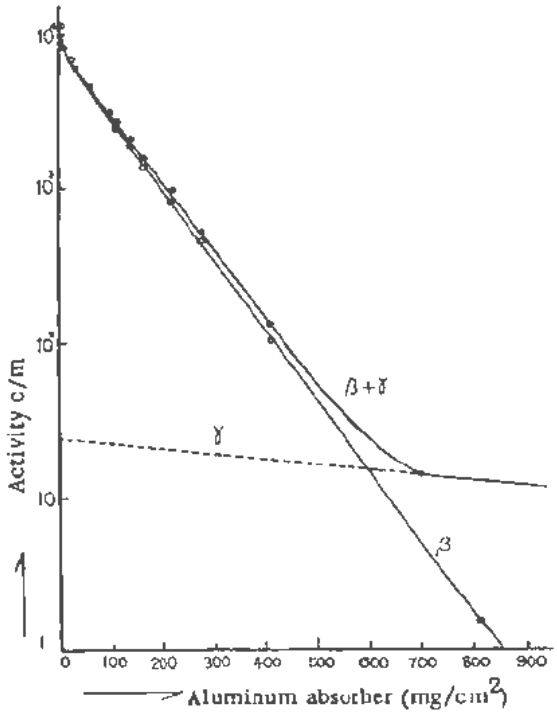

Figure 5. Aluminum absorption curve of Te fraction

in Fig. 5. The analysis of the curve revealed that two kinds of β-particles were emitted from the tellurium fraction. One had a low maximum energy of approximately 0.1 Mev, while the other had a fairly high maximum energy of around 1.8 Mev. The former is considered to be due to internally converted electrons resulting from the transition: $Te^{129m} \rightarrow Te^{129}$. The latter is attributable to particles from Te^{129}.

The half-life measurement on this fraction indicated the existence of nuclides having the half-life of a little more than 30 days. It was certain, therefore, that the fraction contained Te^{129m} (half-life: 33.5 days, and its daughter nuclide, Te^{129} (half-life: 72 min). The existence of Te^{132} in the fraction was also confirmed (cf. following subsection).

Iodine

The sample was dissolved in a small amount of nitric acid and then diluted with water until the acidity of the solution was 0.05 *N*. The resulting solution was passed through an ion exchange resin bed, Amberlite IR-120 (hydrogen form). After the separation of iodine from tellurium, ruthenium and other elements in the effluent was carried out, iodine was precipitated as silver iodide. The precipitate was dried and its activity was measured. The activity decay in the fraction is illustrated in Fig. 6A. The decay was fairly rapid during the first several hours. Then, it decayed slowly with the half-life of approximately 8 days (observed around 20th March). The initial part of the decay curve is illustrated in Fig. 6B, in which the time scale along the abscissa is expressed in hourly units. Analysis of the decay curve indicated that the nuclide with the shorter half-life was I^{132} (half-life: 2.4 hr).†

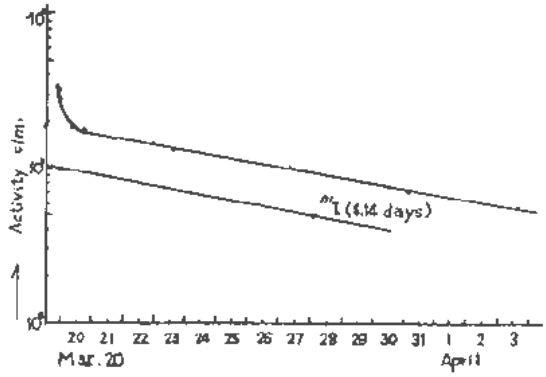

Figure 6A. Decay curve of iodine fraction

The silver iodide fraction was kept standing until the activity due to I^{132} had completely decayed. Then absorption measurements with aluminum foil were carried out on the fraction. As shown in Fig. 7, the existence of both β- and γ-emitters in the fraction were confirmed by the absorption experiment.

From the absorption curve, the maximum energy of the β-particles was estimated to be 0.6 Mev. This value is in good agreement with the reported value on the maximum energy of β-particles from I^{131} (0.595 Mev).

A sample collected from the contaminated boat was dissolved in dilute hydrochloric acid and the volume of the solution was made up to approximately 100 cm³. The activity of this solution was of the order

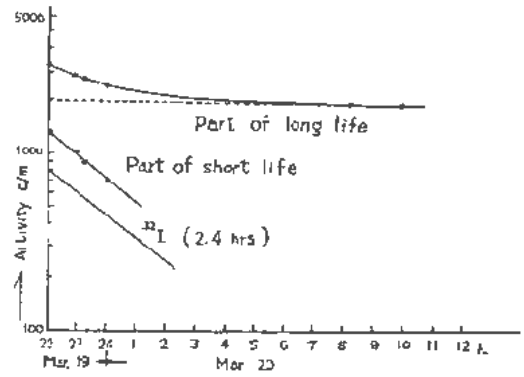

Figure 6B. Decay curve of iodine fraction

of 10^3 cpm (measured by Tube No. 2). Then cations in the solution were absorbed on an ion exchange resin bed (volume: 5 cm³), Amberlite IR-120. Potassium permanganate and concentrated sulfuric acid were added to one third of the effluent. Ruthenium tetroxide was distilled and received in a flask containing 10 cm³ of cold, dilute nitric acid and a drop of 3% hydrogen peroxide solution.

According to the study by Hume, this is a convenient method of carrier-free separation of ruthe-

† I^{132}, which was detected in this experiment, is thought to be produced by the β-decay of a fairly long-lived nuclide, Te^{132} (half-life: 77.7 hr), because of the shorter half-life of I^{132}. Accordingly, the presence of I^{132} in the ashes indicates the presence of its parent nuclide, Te^{132}.

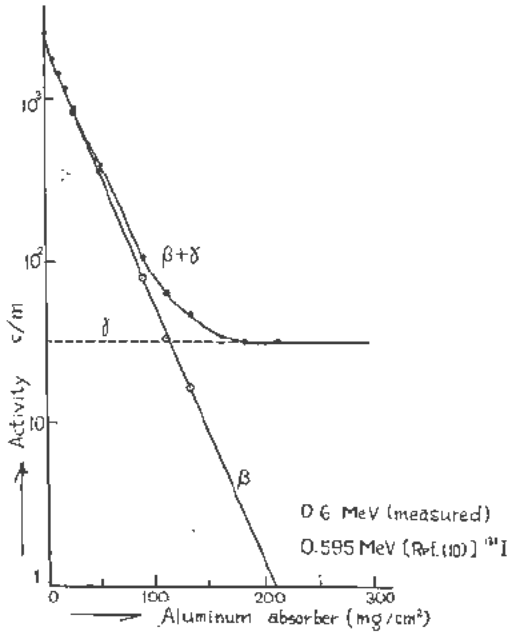

Figure 7. Absorption curve of iodine fraction

nium; therefore, no carrier was used in this experiment. In order to eliminate contamination by iodine, about 10 mg of iodine (as potassium iodide) were added to the distillate. Thereafter iodide was oxidized by hydrogen peroxide, and free iodine was extracted with carbon tetrachloride. Even though considerable activity was removed by the carbon tetrachloride, the aqueous layer still showed fairly high counting rates; as much as 10^5 cpm (counting conditions same as before). 3 to 4 mg of the previously prepared ruthenium carrier (sodium ruthenate) were added to the aqueous solution. Reduction of ruthenium to the metallic state was carried out by adding metallic magnesium.

The activity of metallic ruthenium was found to be approximately 3×10^4 cpm (measured by Tube 1). No activity remained in the mother solution. The aluminum absorption curve of this fraction is shown in Fig. 8. Analysis of the curve revealed the existence of Ru^{103} as well as Ru^{106} in the fraction.**

Zirconium and Niobium

Oxalic acid solution (0.5%) was passed through a cation exchange resin bed on which cations were absorbed in the preceding experiment. Zirconium and niobium were eluted from the resin bed first. 10 mg of zirconium and niobium carriers were added to the effluent.

After the solution was evaporated to dryness, the residue was fused with sodium bisulfate. The fused mass was treated with dilute sulfuric acid (1:20) containing 1% tannin by weight. While zirconium

Table IV. Separation of Zr and Nb

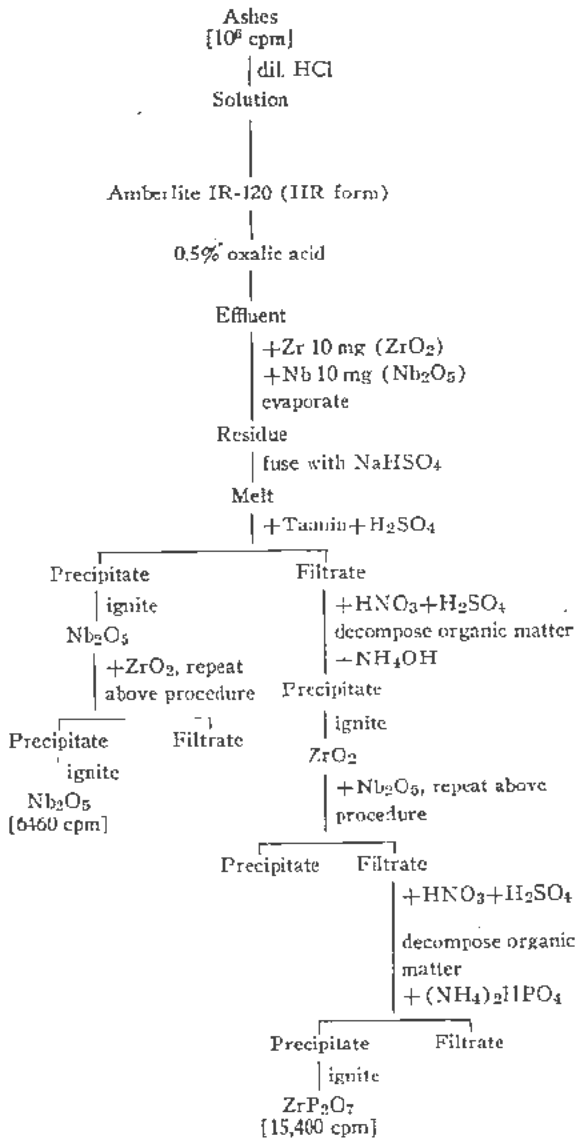

was leached out with this solution, niobium remained undissolved. To avoid cross-contamination, the precipitate was filtered and ignited to niobium pentoxide. A small amount of zirconium oxide was added to the ignited oxide. Then the fusion with sodium bisulfate as well as the treatment of the fused mass with tannin solution was repeated. Sulfuric acid and nitric acid were added to the filtrate containing zirconium. After the solution was heated to destroy organic matter, it was diluted with water. Zirconium in the solution was precipitated with ammonium hydroxide, filtered, and ignited to zirconium dioxide. The radiochemical purification of the oxide was performed by mixing it with a small amount of niobium followed by the fusion and extraction described above.

** Since the originally produced Rh^{106} should have decayed very rapidly, the detected Rh^{106} is considered to be the decay product of Ru^{106}. Although β-particles from Ru^{106} were too soft to be detected by our counters, the presence of Ru^{106} in the sample is certain.

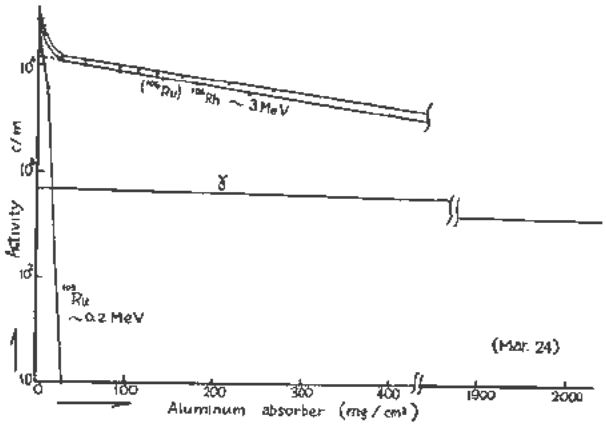

Figure 8. Absorption curve of Ru (Rh) fraction

Finally zirconium was precipitated as zirconium phosphate. The measurement of the maximum energy of β-particles from this fraction indicated the existence of Zr^{95} (half-life: 65 days) and Nb^{95} (half-life: 35 days).

Uranium

In the effluent of 0.5% oxalic acid solution, another remarkable peak was observed after the sharp elution peak of zirconium and niobium, as illustrated in Fig. 4. The half-life and maximum energy of β-particles from this portion were measured to be 7 days and 0.22 Mev, respectively. It was known that hafnium, iron, uranium, thorium, etc., in addition to zirconium and niobium,[6,7,8] could be eluted with an oxalic acid solution. A rare earth element was not expected to be eluted in this fraction. With reference to recently published tables of isotopes,[9] radioactive properties of the nuclide under consideration

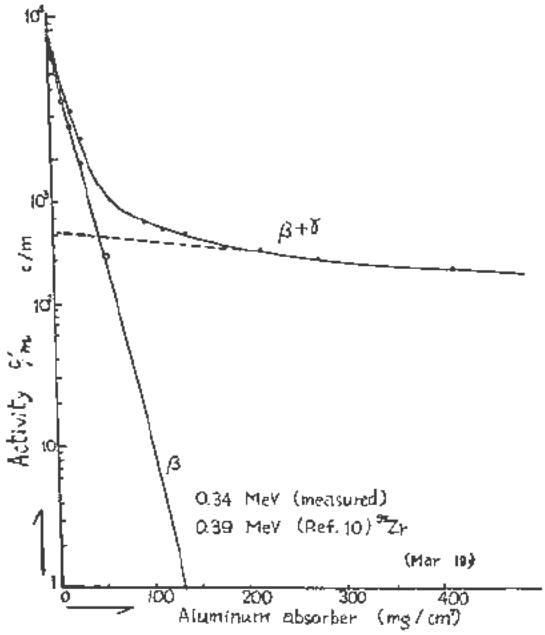

Figure 9. Absorption curve of Zr fraction

were similar to those of Mn^{52}, Xe^{133}, Tb^{161}, Eu^{169}, Ir^{196}, Au^{196}, Bi^{206} and U^{237}.

Several chemical procedures were employed to purify and identify the nuclide present in this fraction after the addition of antimony, iron, and zinc carriers. The results showed: (1) The activity was concentrated in the third group (iron group) and coprecipitated with iron hydroxide; (2) Iron was removed by ether extraction from hydrochloric acid solution, while the activity was not extracted in the ether layer; (3) Good extractability (of the activity) into the ether layer was observed when nitric acid solution was used; (4) Contamination of radioactive zirconium was removed by extraction with chloroform by the use of cupferron. Finally, repeated cation exchange adsorption and elution were carried out using oxalic acid and diluted hydrochloric acid solutions. Eluted positions using these eluents were close to those of uranyl ion. Although no further experiments could be carried out on this fraction, all of the results obtained thus far indicated the existence of U^{237}.

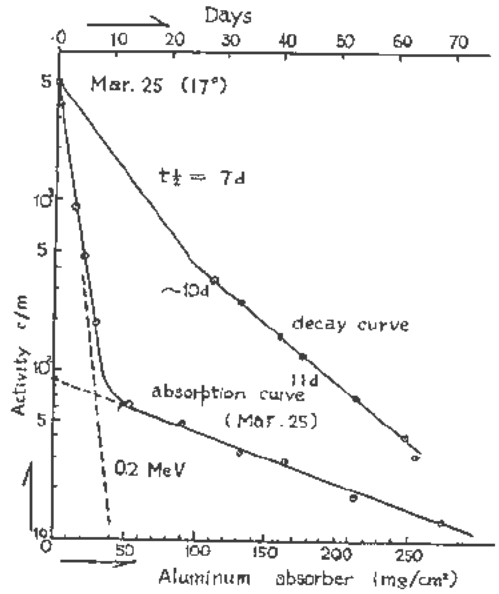

Figure 10. Decay curve and aluminum absorption curve of uranium fraction

Rare-Earth Elements

Group Separation of Rare-Earth Elements[4]

A sample of the rare earth fraction was isolated by the cation exchange group separation method previously described. That is, 5% ammonium citrate solution at a pH of 3.7 was used for the elution of the rare earth fraction, and the effluent was divided into 10 cc aliquots. Activity of rare earth elements was found at the break-through point of ammonium ion which was detected by the color change of thymol blue indicator from pink to yellow. Two aliquots of effluent containing the total rare earth activity were combined and small amounts of cation exchanger of

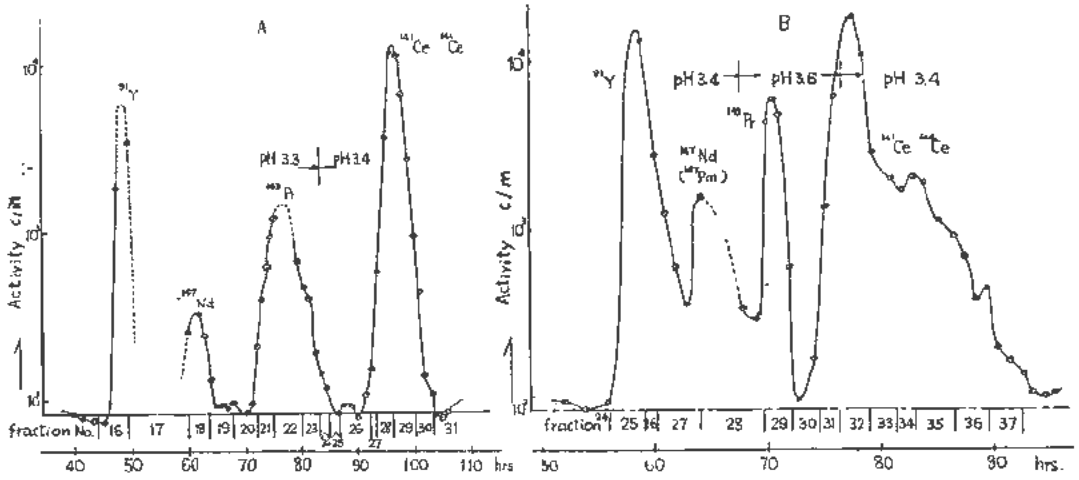

Figure 11. Elution curve of rare earths fraction

hydrogen form were added. At higher hydrogen ion concentrations the activity was completely adsorbed in the resin phase. The resin was transferred to the top of another cation exchange resin bed with the mother liquor.

Conditions for Chromatographic Separation

The separation of rare-earth elements was carried out under the following experimental conditions:

Figure 11A: ion exchanger, Dowex 50-X 8, 8mm × 20 cm, 150–270 mesh; eluent, NH_4-citrate, pH 3.3, 3.4; rate of flow, 0.3 cm/min.

Figure 11B: ion exchanger, Dowex 50W-X 8, 8 mm × 120 cm, 70–120 mesh; eluent, NH_4-citrate, pH 3.3, 3.4, 3.6; rate of flow, 0.4 cm/min.

Cation exchange resin bed prepared for the chromatographic separation of rare earths, was conditioned with ammonium citrate at a pH of 2.5 and converted to the ammonium form. After the addition to the bed of the resin which adsorbed rare earth activity, 5% ammonium citrate solution was allowed to flow down through a funnel attached to the top of the column. The movement of the adsorption band was observed with a survey meter. The pH of the eluent was successively raised from 2.8 to 2.9 to 3.1 and finally to 3.3 until a measurable movement of the band was observed. Two drops of effluent were collected on a small piece of filter paper mounted on a glass plate at intervals ranging from 30 min to 2 hr. and their activity was measured after drying. Figures 11A and 11B were obtained from the experiment. The dotted lines indicate the parts of the elution curve where the experiment was interrupted temporarily and some leaking of the eluent was observed.

Assignment of Nuclide

Four peaks were observed in both elution curves. Fractions, A16, A18, A21, A28, B25, B26, B29, B32, and B35 were selected as representative samples for the assigoment of nuclides separated. Measurements of A28, B32 and B35, the last peaks, showed the presence of rather hard β-activity attributed to Pr^{141} (maximum energy: 2.97 Mev). The presence of Ce^{144}, the parent nuclide of Pr^{144}, was also indicated. Moreover, the presence of Ce^{141} was certain, because the apparent half-life was about 90 days according to the measurements made for 20 days early in June. A16 and B25 showed the presence of activity emitting about 1.5 Mev β-particle. The half-life of the activity was 60 days. The radioactive properties of the nuclide are in good agreement with those of Y^{91} (1.54 Mev; half-life: 61 days).

A21, A23 and B29 showed 0.9 Mev β-particles and 14-day half-life. On the other hand, A18 and B28 showed two kinds of β-particles, 0.8 and 0.3–0.5 Mev, respectively, and 12–13-day half-life. Although these two species of samples were of a somewhat analogous nature, the former activity could be assigned to Pr^{143} (maximum energy of β-particles: 0.93 Mev; half-life: 13.7 days) and the latter to Nd^{147} (0.83, 0.60, 0.38 Mev; 11.3 days), because the latter contained a larger fraction of low energy β-particles. Several aluminum absorption curves are presented in Figs. 12 and 13.

Y^{91}, Ce^{141}, Ce^{144}, Pr^{143}, Pr^{144} and Nd^{147} were detected in the above-mentioned way. Besides, the existence of a small quantity of Pm^{147}, daughter nuclide of Nd^{147}, was also confirmed.

Alkali Earth Elements

Each alkali earth element was isolated by the cation exchange separation method using ammonium acetate as the eluent.[10] The samples used were both alkali earth carbonates and alkali earth nitrates obtained by chemical and ion exchange group separations. Small amounts of carriers were added to both samples.

Experiment 1

Carbonate precipitates of the fifth group shown in Table III were treated with fuming nitric acid after

Table V. Separation of Alkali Earths and α-Emitter Fractions

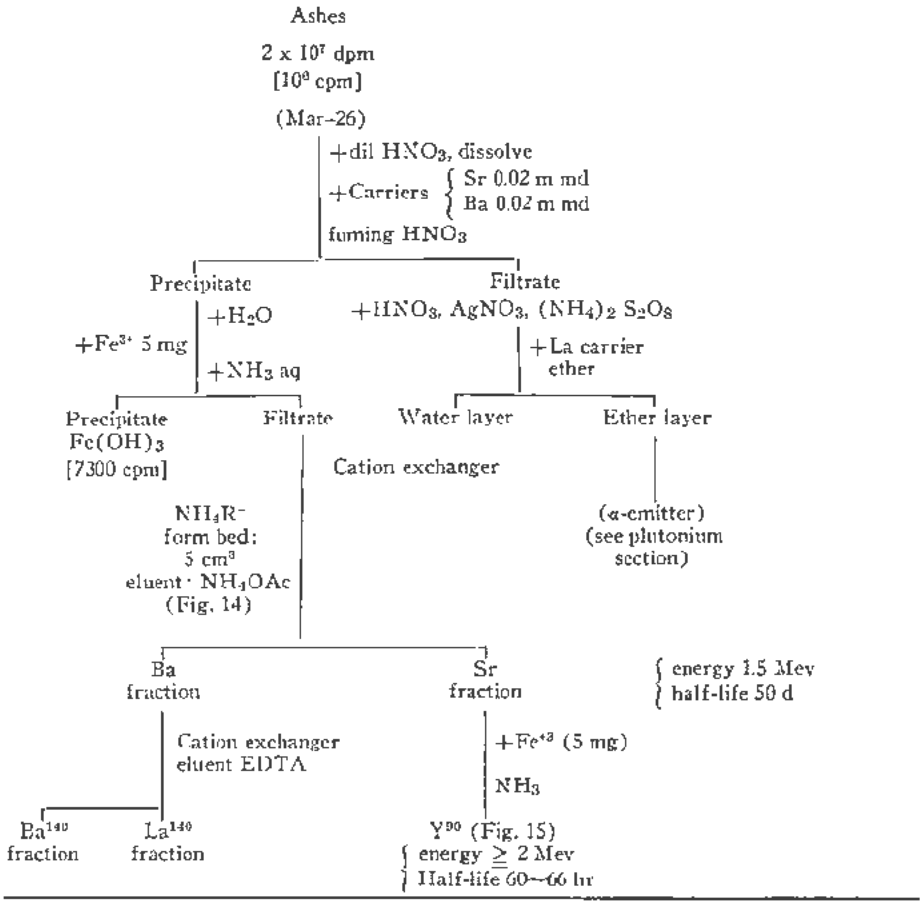

the addition of strontium and barium carriers. No measurable activity was found in the filtrate, i.e., calcium fraction. Then the precipitates were dissolved in water and separated into individual constituents by cation exchange separation as described in the following paragraph. The barium fraction obtained was treated with ether-hydrochloric acid mixture. Ba^{140} (870 cpm) was found in the precipitates, and La^{140} (940 cpm; measured half-life: 39 hr) was found in the filtrate, whereas lower activity was found in the strontium fraction (200 cpm).

Experiment 2

The original sample of ashes was dissolved in dilute nitric acid, with carriers of strontium and barium, and was treated with fuming nitric acid. Nitrates of strontium and barium were precipitated and filtered. Finally, the cation exchange method was employed for the detection and estimation of Sr^{89}, Sr^{90}, Y^{90}, Ba^{140}, and La^{140} (cf. Table V, Fig. 14).

Alkali earth metal ions were adsorbed at the top of the bed (5 cm³) of strongly acidic cation exchanger of ammonium form which was previously conditioned with ammonium acetate and EDTA solutions. The eluent was neutral 2 *N* ammonium acetate solution. The elution curve of carriers was found by titrimetric determinations using 0.01 M EDTA with Eriochrome B.T. indicator for each aliquot (5 cm³) of the effluent.[10]

After the titration, each aliquot was evaporated in a glass counting dish and its activity was measured. As shown in Fig. 14, the chief fractions of strontium, No. 5 and 6, contained 6600 cpm, and 1.38×10^{-2} millimole was recovered out of the 1.90×10^{-2} millimole of the added carrier. The activity of strontium consists of 0.9% of the total activity in the original sample, while that of Ba^{140} is 5%.

The identification of Sr^{90} in the fraction was attempted by following the activity of the daughter nuclide, Y^{90}. The strontium fraction, which was isolated according to the above procedure, was ignited, dissolved in hydrochloric acid and allowed to stand for two days. Then Y^{90} was collected with iron hydroxide (5 mg Fe) in the ordinary way. The activities which were coprecipitated with iron hydroxide were 200 cpm (sample No. 1, on 28 March, 65 hr after separation) and 80 cpm (no. 2, on 31 March, 48 hr after the precipitation of No. 1).

There was a possibility that Sr^{90} was contaminated with Ba^{140} and La^{140}. A contamination of more than 0.1% of the total Ba^{140} present in the ashes would yield some activity of La^{140}. This lanthanum activity

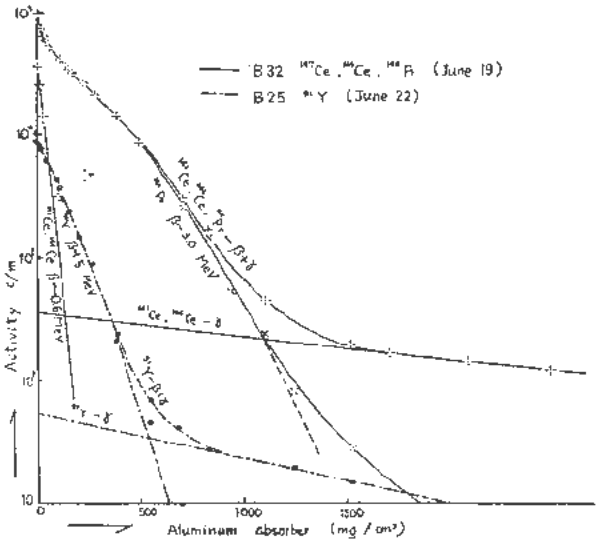

Figure 12. Aluminum absorption curves of Ce and Y fractions

might be mistaken for Y^{90}. Accordingly, the detection of activity in the iron hydroxide precipitate could not give any immediate proof of the presence of Sr^{90} (Y^{90}) in the sample. The measurements of decay of the activity in fraction No. 9 and its preceding fractions in Fig. 14, however, showed about 50 cpm of La^{140} being contaminated at the time of elution, and the contamination of Ba^{140} was not more than 10 cpm in the value on the 31 March. (Later measurements showed that contamination with Ba was negligibly small, less than a few cpm.) La^{140} actually contaminated the No. 1 sample, but was

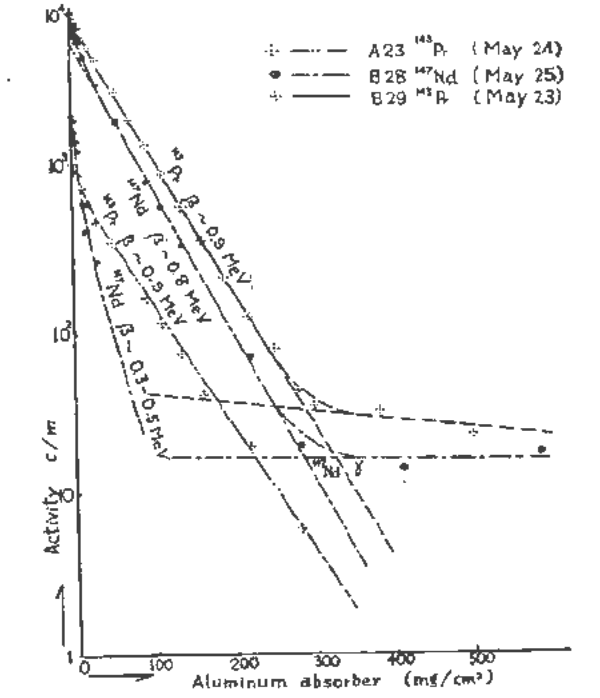

Figure 13. Aluminum absorption curves of Pr and Nd fractions

removed completely in No. 2 and the following fractions. In consideration of these results, on the 31 March, the ratio of the activity of Sr^{90} (and Y^{90}) to total activity was estimated to be 0.02%. Milking, collection and decay measurements of Y^{90} were repeated four times for more than one month, and finally the value of 0.02% (on 26 March) was arrived at.

Experiment 3

Activities of calcium, strontium and barium were also found and estimated in the fractions obtained by cation exchange group separation which was performed on 21 and 22 March (cf. Fig. 4).

The fractions at pH 4.6, 5.1 and 5.6 were evaporated, ignited, and used for cation exchange separation following on the addition of strontium and barium carriers.

Activity of Ba^{140} was found in the sample at a pH of 5.6, and radioactive strontium was found in one of 5.1. Moreover, it was also noticed that the effluent at a pH of 4.6 contained calcium activity and trace activity due to strontium, about 0.4% of its total activity (on 3 May).†† Energy (0.2 Mev) and decay (170 days) of calcium fraction are in good agreement with those of Ca^{45}.‡‡

At the same time, titrations indicated that the amount of calcium recovered from the original sample was 10 mg as $CaCO_3$.

Plutonium

Extraction and Detection of α-Emitter§§

A sample having an activity of 10^6 cpm (with tube No. 2) (same sample was used for the determination of Ba^{140}) (cf. Experiment 2 in previous section and Table V) was converted to nitrate and then evaporated to dryness. The residue was dissolved in 3 cc of concentrated nitric acid. After silver nitrate and ammonium persulfate were added, the solution was heated until the black color due to silver peroxide disappeared. Then, about 10 mg of lanthanum

†† In these experiments, each fraction of ammonium acetate was evaporated in order to decompose acetate, and the activity was measured under the condition of minimum self-absorption. Then, titration with EDTA was carried out. This process also facilitated the titration procedures.

‡‡ Because the energy of Ca^{45} is soft, the observed value of activity was corrected for the absorption ($d_{1/2} = 5$ mg/cm²) due to the mica window (1.5 mg/cm²) and the air (1.3 cm) between the sample and counter tube, as well as for self-absorption of the sample. The detection coefficient of β-particles from Ca^{45} was estimated to be 70% for a sample 4 mg/cm² thick

§§ On the assumption that the emitter is plutonium the following experiment was carried out. Using a sample which had the activity in a range of 30,000 to 40,000 counts per minute, cupferron complex was extracted with ether from a dilute sulfuric acid solution. After the ether layer was dried and ashed, the detection of α-tracks was attempted with the aid of the Sakura nuclear track plate. But the β-tracks due to zirconium, and other nuclides interfered with the detection of α-tracks. Only a few obscure tracks due to α-particles were observed. Therefore, no definite conclusion was obtained by this experiment.

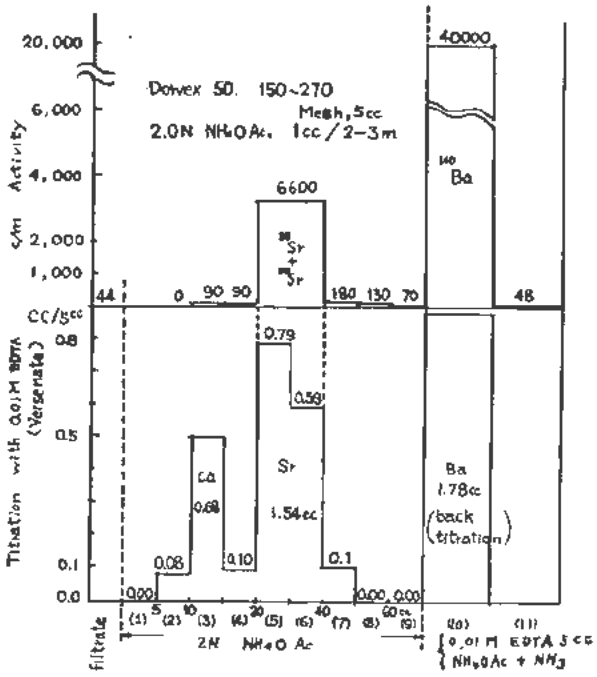

Figure 14. Ion exchange separation, identification and determination of Sr and Ba (Mar. 26)

carrier¶¶ and 3 cm³ of nitric acid (1:9) containing 70 gm of ammonium nitrate per 100 cm³ were added to the solution. The resulting solution was transferred to an automatic Soxhlet extractor and the ether extraction was made for several hours.***

The total ($\beta + \gamma$) activity of the evaporated ether layer was more than 900 cpm on the 3 May.

This sample is hereafter called sample A. In order to perform precise quantitative analyses, two more samples were prepared. These samples are called sample B and sample C.

¶¶ Special efforts were made in selecting pure reagents which did not contain radioactive impurities such as thorium. The purity of a reagent was checked by autoradiography.

*** Plutonium or neptunium is oxidized by silver peroxide to plutonyl (PuO_2^{++}), or neptunyl (NpO_2^{++}) ion which is soluble in ether. While uranyl ion (UO_2^{++}) is not reduced to lower oxidation states by sulfur dioxide, the plutonyl ions is reduced by the same reagent.

Samples A and B were used for quantitative analysis, and sample C for qualitative analysis.

Qualitative Analysis

After sample C was evaporated to dryness, the organic matter in the sample was destroyed by heating. By adding hydrochloric acid, it was converted to chloride, and sulfur dioxide was passed through the solution. The resulting solution was again evaporated to dryness. The residue was dissolved in 0.3 N hydrochloric acid and 4 mg of lanthanum carrier were added to precipitate lanthanum oxalate from the solution. After the precipitate was filtered, another 10 mg of lanthanum carrier was added to the filtrate. Precipitation and filtration of lanthanum oxalate were repeated on this filtrate. The precipitates and the residue, which was obtained by heating the last filtrate, were examined for their α-activities by nuclear emulsion technique. Only the first precipitate was found to be radioactive. At the same time it was confirmed that the α-emitter under consideration was co-precipitated with lanthanum oxalate from the solution containing reducing agents. In the oxidized state, the emitter was extractable with ether from a nitric acid solution. This chemical behavior led us to the conclusion that the emitter under study must be either neptunium or plutonium.

Quantitative Analysis

After samples A and B were converted to chloride, they were dissolved in a small amount of hydrochloric acid. Then 0.1 to 0.2 gm of EDTA was added to the solution. The solution of sample A was neutralized with sodium hydroxide, while the solution of sample B was treated in the same way with sodium carbonate. Phenolphthalein and methyl red were used as indicators during the neutralization of these solutions. The resulting solutions were transferred to volumetric flasks to adjust their volumes to 10 cm³††† theo 0.03 cm³ of the above solutions was placed on a Fuji ET-6B nuclear track plate (thickness of emulsion: 25μ) and the plate was

††† The sensitivity of emulsion for the detection of α-tracks is lowered when the impregnated solution is acidic. EDTA was added to the system to prevent the formation of precipitates or colloid.

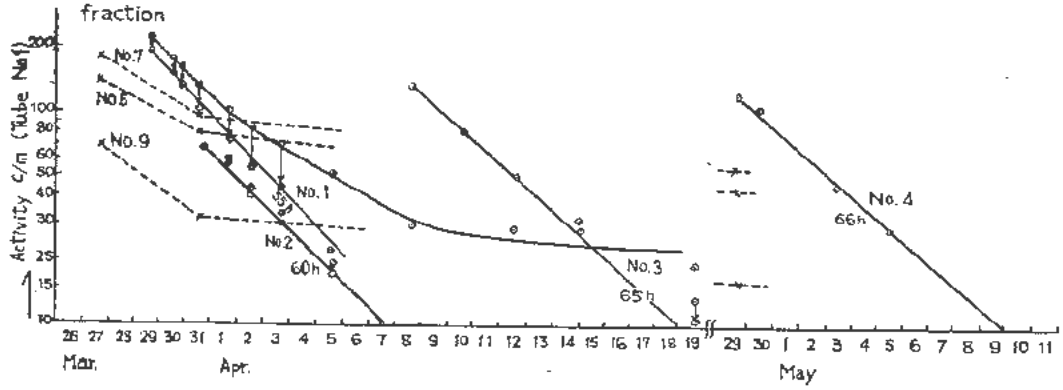

Figure 15. Decay curves of Y fraction collected with $Fe(OH)_3$ from Sr fraction

dried in a dark room. After being covered with a Fuji ET-6B stripping film (thickness of emulsion: 26μ), the whole system was exposed to radiation for 120 hours at temperature range from 7 to 16°C. In each system the number of α-tracks was counted under a microscope at a fairly high magnification ($\times$ 600). In sample *A*, fairly uniform distribution of tracks was observed in the emulsion while, in sample *B*, some aggregates of tracks were detected. These results indicate the possible formation of radiocolloids in the solution of sample *B*.

For this reason, sample *A* was selected as a sample for the quantitative analysis of α-emitter. Using the above-mentioned technique, as many as 1700 tracks were observed in 0.03 cm^3 of sample *A* solution. Therefore, α-activity of 80 dpm is present in this sample having a total activity of 2×10^7 dpm (cf. Fig. 18).

Energy of α-Particles[11]

Because of the scarcity of α-tracks in the Fuji ET-6B emulsion, precise measurement of the length of the tracks in the emulsion was very difficult. Nevertheless, semi-quantitative experiments showed that the length of α-tracks due to the unidentified emitter was longer than that of U^{234} but shorter than that of Po^{210}.

The reported values on the length of tracks of several α-particles are summarized below:

	Length of tracks	*Energy (Mev)*
U^{234}	19.4μ	4.21
α-emitter in the sample	22.5μ	5*
Po^{210}	23.7μ	5.29
Pu^{239}		5.15(69%) 5.13(20%) 5.99(11%)
Np^{237}		4.77
U^{235}		4.20 (4%)

* This value was calculated by interpolation.

Comparing the experimental value with these data, the authors came to the conclusion that the emitter must be Pu^{239}. ‡‡‡ On the basis of the present experimental results, the absolute amount of plutonium was estimated to be approximately 6×10^{-10} gm. Even though there is a possibility that natural uranium and Np^{237} are also present in the "Bikini Ashes", the detection of such nuclides seems to be almost impossible because of their long half-lives.§§§

Other Elements

The authors detected some nuclides of short half-lives in the second group. The result of an ion exchange study of this group indicated that the nuclides detected are probably Sb^{127} and/or Mo^{99}.

Another nuclide was found in the anion fraction containing sulfate (cf. Fig. 4). The nuclear property

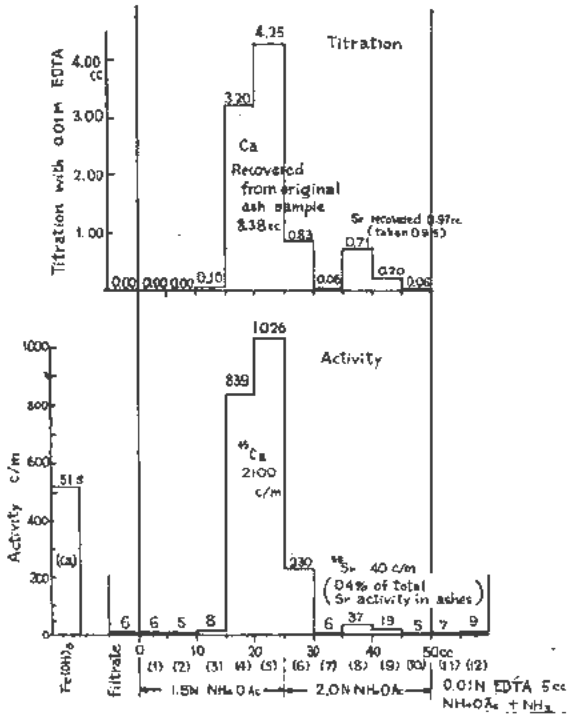

Figure 16. Elution curve of Ca fraction; separation, identification and determination of Ca and its activity in ashes sample (pH 4.6 fraction of Fig. 4)

of this nuclide was identical with that of S^{35}. Other radioactive species such as radioactive In, Sn, Co, Cs^{137}, Ba^{137m}, Ag^{111}, Xe^{133}, and radioactive Be could not be detected so far.

DISCUSSION OF THE RESULTS

The radionuclides detected in the ashes are summarized in Table VI.

In addition, the contribution of each nuclide to the total activity was calculated and tabulated in Table VI.

These estimations were made in the following way:

First, the separation of individual nuclides with or without a carrier was performed by ion exchange or chemical methods. The activity of each nuclide was measured by G-M counter. Then the correction was made, if necessary, to the observed values with respect to self-absorption of the sample as well as absorption due to the mica-window and air between the sample and window. From these corrected values, the activity of each nuclide on the 26th March (25 days after detonation) was determined by extrapolation. The above date is important because the quantitative measurements of activity were started on this date. Using the fission yield data given by Coryell and Sugarman,[12] the contribution of individual nuclides to the total activity at slow neutron fission of plutonium was estimated. The results are shown in Table VI. In some cases where the fission yield for a particular nuclide was not found in the text, the value was estimated from the fission yield

‡‡‡ The ratio of two activities, $Ru^{103}/Ru^{106}(Rh^{106}) = 4$ (cf. Fig. 8), and the value of activity of Sr^{89} indicate indirectly that Pu^{239} was used for the atomic bomb.

§§§ Considering the value on the activity of U^{237}, the possibility for the detection of Np^{237} by this technique seems to be very small.

curve. The formula used in these calculations is expressed as follows:

$$A = k \frac{f}{T} \exp\left(-\frac{0.693 \times 25}{T}\right)$$

where the symbols, A, T, f and k, stand for the contribution of a particular nuclide to total activity 25 days after fission, half-life in days, fission yield in per cent and a constant, respectively.

In the case of Nb^{95}, the total activity was assumed to be produced directly by the decay of Zr^{95}. Such assumption was also made for other nuclides such as La^{140}, Y^{90}, Pr^{144}, Pm^{147}, etc.

Comparing the experimental values with the calculated values for Pu-fission, alkali earth elements' contribution to total activity seems to be smaller than for plutonium fission. On the other hand, the corresponding contribution of rare earth elements' activity seems to be larger than for Pu-fission.

Since the ashes do not represent the total fission products produced by the atomic explosion but only consist of a mixture of activities adhering to the dust floating in the air, good agreement between these present experimental values and the values for Pu-fission should not always be expected. For instance, a fraction of the activity of alkali earth elements is produced through the decay of inert gases such as krypton and xenon. In such cases some activity might be selectively lost from the ashes. As a whole, however, most of the values obtained in this experiment seem to be in fair agreement with those for Pu-fission.

Assuming that the fission products uniformly and completely adhered to the ashes, the ratio of the number of fissioned Pu^{239} atoms to that of remaining atoms was calculated. First, on the basis of the results

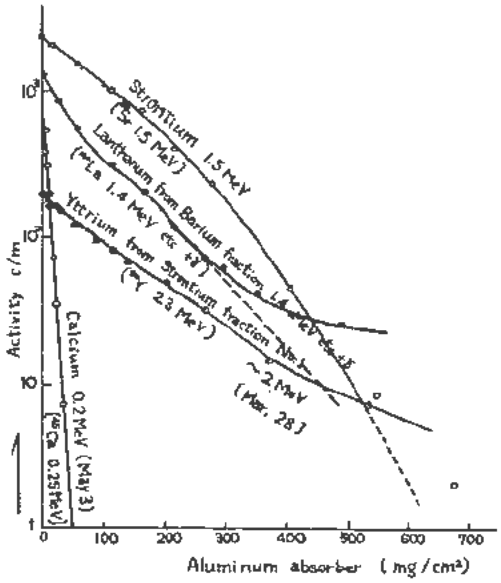

Figure 17. Aluminum absorption curves of Sr(*), La(*), Y(*) and Ca(*) fractions

obtained for the sample tabulated in Table V (2×107 dpm), the number of fissioned Pu^{239} atoms was estimated from the absolute counting rates of Ba^{140} ($0.05 \times 2 \times 10^7$ dpm). Then this value was compared with the value on the remaining Pu^{239} atoms (80 dpm). The calculation was made using the equation described below.

$$\frac{\text{Number of fissioned } Pu^{239}}{\text{Number of remaining } Pu^{239}} = \frac{(\text{activity of } Ba^{140}) \exp[\lambda_{Ba^{140}} t] \text{ (half-life of } Ba^{140})/(\text{fission yield of } Ba^{140})}{(\text{activity of } Pu^{239}) \text{ (half-life of } Pu^{239})}$$

$$= \frac{20 \times 5 \times 10^4 \times \exp(0.693 \times 25/12.8) \times 12.8}{80 \times 2.4 \times 10^4 \times 365} \frac{1}{0.054}$$

$$= 1.3$$

Based on the activity of Ba^{140}, the total amount of

Table VI. Summarized Presentation of the Analytical Data

Nuclide	*Half-life*[9]	*Determined activity of individual nuclides (on 26th March)*	*Calculated relative activity of nuclides* (25 days after fission)*	*Slow neutron fission yield*[12] *for* Pu^{239}
S^{35}†	87.1 d	–	–	–
Ca^{45}†	152 d	0.2±0.1%	–	–
Sr^{89}†	53 d	1±0.5	2.7%	1.8%
Sr^{90}†	19.9 yr	0.02±0.01	~0.03	~2
Y^{90}†	6 hr	0.02±0.01	~0.03	–
Y^{91}†	61 d	8±3	3.8	2.8
Zr^{95}†	65 d	5±2	7.4	5.6
Nb^{95m}†	90 hr	–	–	–
Nb^{95}†	35 d	3±1	3.2	–
Mo^{99}†	67 hr	–	0.5	6.1
Ru^{103}†	39.8 d	–	10.0	5.5
Ru^{106}†	1.0 yr	–	1.4	4.7
(Rh^{106})	(30 sec)			
Ag^{111}	76 d	–	0.2	0.27
Sn^{125}	99.4 d		0.1	0.068
Sb^{127}	93 hr	–	0.1	0.37
Te^{127}	9.3 hr	–	0.3	–
Te^{120m}	33.5 d	–	~1.1	~0.5
(Te^{129})†	(72 min)			
Te^{132}†	77.7 hr	–	0.7	4.9
I^{131}†	8.141 d	–	6.1	3.6
I^{132}†	2.4 hr	–	0.7	–
Xe^{133}	5.270 d	–	4.5	5.0
Cs^{137}	33 yr	–	~0.02	~5
Ba^{137m}	2.60 min	–	–	–
Ba^{140}†	12.80 d	5±1	12.1	5.36
La^{140}†	40.0 hr	6±1	13.9	5.36
Ce^{141}†	33.1 d	7±5	9.7	4.9
Ce^{144}†	282 d	2±1	1.3	3.7
Pr^{143}†	13.7 d	16±5	11.9	5.1
Pr^{144}†	17.5 min	2±1	1.3	–
Nd^{147}†	11.3 d	9±4	6.3	3
Pm^{147}†	2.6 yr	–	0.3	–
Eu^{156}	15.4 d	–	0.26	0.12
U^{237}†	6.75 d	20±10	–	–
Pu^{239}†	24,360 yr	α; (4±2)×10^{-4}	–	–

* These figures were calculated from the slow neutron fission yield for Pu^{239}.

† Nuclide detected.

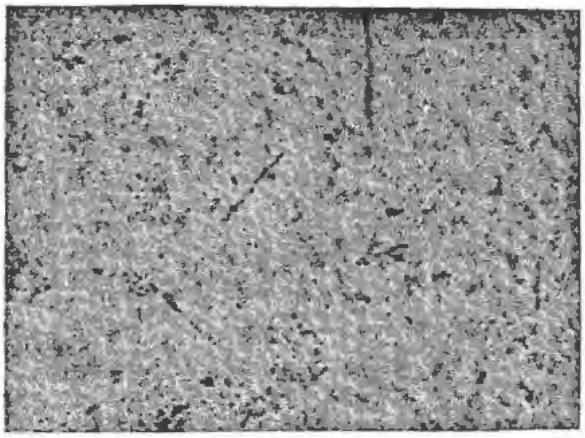

Figure 18. Microscopic detail of a nuclear plate showing Pu^{239} alpha tracks

fission products adhering to the ashes was estimated to be 8×10^{-8} gm/gm.

REFERENCES

1. Way, K. and Wigner, E. F., Phys. Rev., *73*, 1318 (1948).
2. Yamasaki, F., *J. Scientific Research Inst.* (Japan) 46, 59 (1952).
3. Cohn, W. E., Parker, G. W. and Tompkins, E. R., Nucleonics 3, No. *5*, 22 (1948).
4. Tompkins, E. R., Khym, J. X. and Cohn, W. E., J. Am. Chem. Soc., *69*, 2769 (1947).
5. Schubert, J., Nachod, F. C., (Ed.), *Ion Exchange*, p. 167 (1949) (Academic Press).
6. Dizdar, Z., *Rec. Tr. Inst. Recherches Structure Matière*, 2, 85 (1953); C. A. 47, 6816 (1953).
7. Dolar, D. and Draqaine, Z., *ibid.*, 2, 77 (1953); C. A. 47, 6816 (1953).
8. Dyrssen, D., Sv. Kem. Tid., *63*, 153 (1951).
9. Hollander, J. M., Perlman, I. and Seaborg, G. T., Rev. Mod. Phys., *25*, 469 (1953).
10. Honda, M., Japan Analyst, *3*, 132 (1954).
11. Beiser, Rev. Mod. Phys., *24*, 273 (1952).
12. Sugarman, Coryell, *Radiochemical Studies: The Fission Products* (National Nuclear Energy Series) Book 2-3 (1951).

Radiochemical Interpretation of the Radioactive Fallout

By Kenjiro Kimura, Eiiti Minami,* Nobufusa Saito,† Yukiyoshi Sasaki‡ and Nobuhide Kokubu,§ Japan

After the nucleat detonation at Nagasaki in August 1945, radioactive contamination was observed on the ground in the vicinity of the blasted area. It was confirmed by some Japanese physicists that the soil at Nishiyama, a small village 2.5 kilometers east of the explosion center, was badly contaminated by some radioactive substances. Although protected by a small hill from direct exposure to the blast, the area had rainfall shortly after the detonation. It was possible therefore that the rain carried some air-borne activity to the ground.

In order to determine the nature of this radioactive fallout, Sagane collected some samples at Nishiyama, which were sent to the present authors for radiochemical examination. One of the present authors (Kimura), in cooperation with Ohashi, Saito and Yamatera, performed radiochemical analyses on the samples. The result showed that the samples were contaminated by several fission products such as Sr^{89}, Ba^{140}, Ce^{144}, Pr^{144} and Zr^{95}.[1]

Later, in 1951, the same samples were subjected to another series of radiochemical analyses. By this time the short-lived radionuclides in the samples had decayed. But the samples still had detectable activity, as much as several hundreds cpm per gram, at approximately 10% counting yield. This fact indicated the existence of some long-lived radionuclides in the sample.

EXPERIMENTS

The Nature of the Samples

The samples were composed of soil, roots of plants and some pieces of plaster; soil was the predominant substance. The activities of the samples ranged from 100 cpm to 400 cpm per gram when they were measured by a G.M. counter having an end-window of 1.5 mg/cm² thickness. The counts were made on samples spread on the counting dishes of 4.0 cm² area. The counting yield was of the order of 10%. The distribution of radioactivity in the samples was not uniform.

Qualitative Radiochemical Analysis

The experiment was started with a sample which had an activity of approximately 300 cpm per gram under the above-mentioned counting conditions. About 7.5 gm of the sample was digested with 100 cm³ of 6 *N* hydrochloric acid for 1 hour at approximately 100°C. Then the residue was filtered off. The above treatment was repeated twice on the residue. After three successive leachings the last residue showed slight activity: as small as 15 cpm per gram.

Several carriers such as lanthanum (5 mg of

Table I. Group Separation of Elements

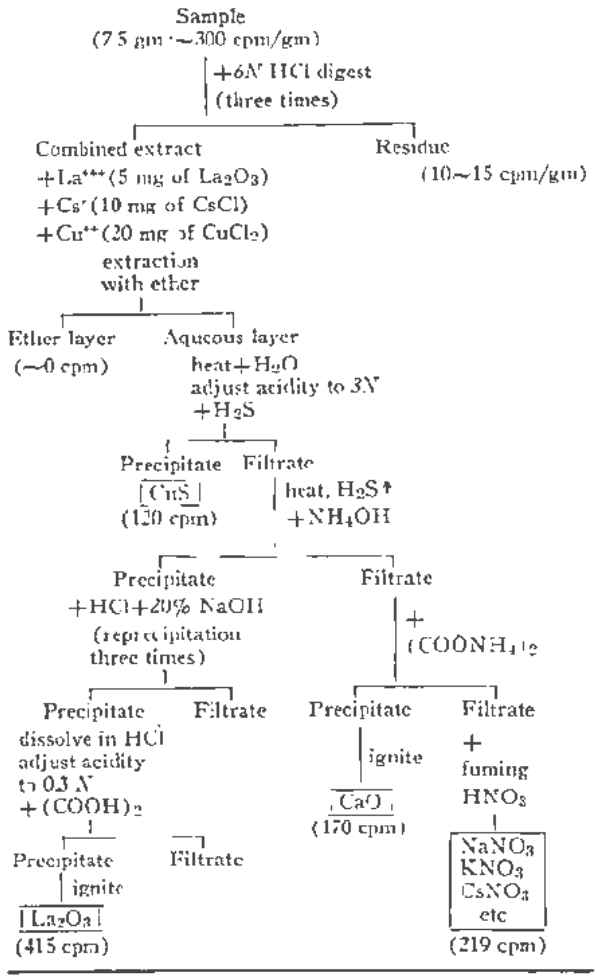

* Professor, Department of Chemistry, Faculty of Science, the University of Tokyo.

† Assistant Professor, Department of Chemistry, Faculty of Science, the University of Tokyo.

‡ Graduate student, Department of Chemistry, Faculty of Science, the University of Tokyo.

§ Assistant, Department of Chemistry, Faculty of Science, Kyushu University.

oxide dissolved in hydrochloric acid), cesium (10 mg of chloride) and copper (20 mg of chloride) were added to the combined filtrates. Since it was confirmed by preliminary experiments that no activity was concentrated in the zinc sulfide precipitate, zinc was not added to the filtrate as a carrier.

Group separation of the elements in the sample was performed on the basis of the ordinary scheme of qualitative analysis.

The results are shown in Table I, which indicates that the activity is concentrated in the second, third, fifth and sixth groups of the scheme.

Physical Measurements on Each Group

Activity in the Sixth Group (Alkali Elements)

The aluminum absorption curve was measured for the activity in the sixth group. The results showed the existence of a nuclide which emits β-particles having a maximum energy of approximately 0.5 Mev.

Since decay of the activity was extremely slow, the nuclide under consideration has a long half-life.

Now, the possible nuclides which could be concentrated in the sixth group are K^{40}, Rb^{87}, Cs^{137} and Ba^{137m}, etc. Their nuclear properties are summarized in Table II. Considering these data, it seems fairly certain that the nuclides existing in this group are Cs^{137}, and its daughter nuclide, Ba^{137m}.

Table II. Some Nuclides of Alkali Elements

Nuclides	*Decay*	*Half-life*	*Max. β (Mev)*
K^{40}	β^-, EC (γ)	1.32×10^9 yr	1.33
Rb^{87}	β^- (no γ)	6.0×10^{10} yr	0.275
Cs^{137}*	β^-	33 yr	0.523
Ba^{137m}*	IT	2.6 min	——

* Detected in our experiment.

Activity in the Fifth Group

A similar experiment on the fifth group revealed the existenee of a long-lived nuclide which emits β-particles having a maximum energy of 2.2 Mev. This maximum energy value is very close to that of Y^{90}, the daughter nuclide of Sr^{90}. To confirm the existence of Y^{90} which was thought to be in equilibrium with Sr^{90}, the addition of an iron carrier was followed by the precipitation of iron hydroxide from the hydrochloric acid solution of this fraction. A nuclide coprecipitated with iron hydroxide had a half-life of approximately 66 hr. The decay curve is shown in Fig. 1.

Rapid precipitation of calcium oxalate from the filtrate was carried out to confirm the existence of some radionuclides in the filtrate. The calcium oxide prepared from oxalate was found to carry a β-emitter of which the maximum energy was approximately 0.6 Mev. This value is in fair agreement with that of β-particles due to Sr^{90}.

In addition, an increase of radioactivity was observed on the freshly prepared calcium oxide. Successive extraction of the activity of 66-hr half-life from the old calcium oxide was also possible.

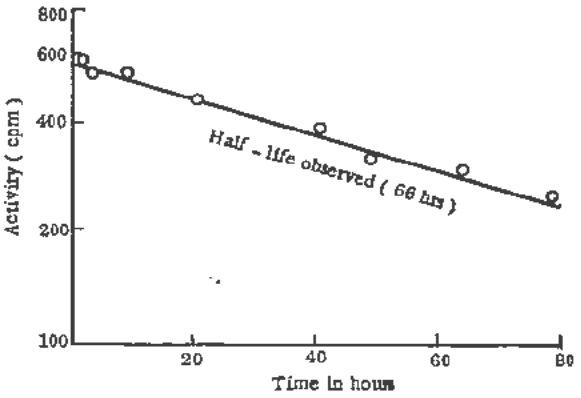

Figure 1. Decay of $Fe(OH)_3$ fraction

These facts led us to the conclusion that at least Sr^{90} and Y^{90} are present in this fraction.

Activity in the Third Group

The decay of the activity in this fraction was also very slow so that measurement of half-life in a short time was impossible. The aluminum absorption curve of this fraction had a fairly complicated shape. Two breaks in the absorption curve appeared at the thickness of 10 and 20 mg Al/cm^2. The maximum energy estimated from the absorption curve is approximately 3.1 Mev. The above-mentioned breaks correspond to the energy of approximately 0.09 and 0.15 Mev, respectively. The nuclear properties of the long-lived rare earth nuclides which are possibly concentrated in the fraction are summarized in Table III.

Table III. Some Nuclides of Rare Earth Elements

Nuclides	*Decay*	*Half-life*	*Max. β (Mev)*
Ce^{144}*	$\beta^-(\gamma)$	282 d	0.30 (70%) 0.17 (30%) 0.09 (e^-)
Pr^{144}*	$\beta^-(\gamma)$	17.5 min	2.97
Pm^{147}	β^-(no γ)	2.6 yr	0.22
Sm^{151}	$\beta^-(\gamma)$	73 yr	0.08
Eu^{155}	$\beta^-(\gamma)$	1.7 yr	0.15 (80%) 0.24 (20%)

* Detected in our experiment.

Comparison of our experimental data with previously reported values in Table III suggests the possibility of the existence of both Ce^{144} and Pr^{144} in this fraction. The existence of Pm^{147} or Eu^{155} is also probable. It seems, however, that the experimental data are too scanty to deduce definite conclusions as to the kind of nuclides present. Only one definite conclusion has been so far obtained: the fraction contains at least Ce^{144} and its daughter nuclide. The existence of these two nuclides was already confirmed by one of the present authors in his previous work.[2] The present authors also confirmed the above conclusion by detecting strong activity in cerium

iodate which was precipitated from the acid solution of lanthanum oxide in the presence of cerium carrier.

Activity in the Second Group

When copper sulfide was reprecipitated, the activity in the original precipitate disappeared. Therefore, this apparent activity in copper sulfide seems to be caused by the incompleteness of group separation. The nature of this contamination was not studied in our experiment.

Detection of α-Emitter

Autoradiography of La_2O_3 Fraction

Approximately 5 mg of lanthanum oxide was mounted on a glass slide. The slide was covered with a nuclear track plate, type Fuji ET-2E (thickness of emulsion: 15μ). The exposure to radiation was made for 35 days and the nuclear plate was developed with D-19 for 3 min. Many tracks due to α-particles were observed under a microscope ($\times$ 300).

Decay of α-Activity

α-activity of the lanthanum oxide fraction was measured by a modified Lauritsen electroscope. The decay measurement showed that the α-emitter under consideration has a very long half-life. The α-activity of the lanthanum carrier used was also measured with the electroscope. The activity was found to be negligibly small.

Chemical Properties of α-Emitter

Ether Extraction of α-Emitter

In this experiment about 20 mg of lanthanum oxide fraction was used. The original activity of this sample was 11.1 div./min when it was measured by Lauritzen electroscope under a definite geometrical condition. The sample was dissolved in a mixture of 2 cm^3 of nitric acid and 2 cm^3 of dilute nitric acid (1:9) containing 700 gm of ammonium nitrate per liter.

The resulting solution was transferred to a Soxhlet extractor and subjected to extraction with ether for 1.5 hours. The activity in the ether layer was from 5.4 to 5.7 div./min when the evaporated layer was measured under the same geometrical conditions as described above.

After this extraction, 1 mg of silver nitrate as well as 5 mg of ammonium persulfate were added to the acid layer and the second extraction was made. The activity in the ether layer in the second extraction was 1.1 div./min. A parallel experiment with Th^{+4} revealed that the transfer of Th^{+4} into ether was negligibly small.

Coprecipitation with Lanthanum Fluoride

About 3 mg of lanthanum oxide were dissolved in hydrochloric acid. After adding ammonium hydroxide, the solution was evaporated. Then hydrofluoric acid was added to the concentrated solution to precipitate lanthanum fluoride. All of the α-activity was found in this precipitate, while none was found in the filtrate (La_2O_3: 2.9 div./min; Filtrate: 0 div./min).

Extraction of Cupferron Complex

About 0.5 gm of cupferron was dissolved in 6 cm^3 of water and the insoluble matter was filtered out. To the filtrate was added 5 cm^3 of 6 *N* sulfuric acid. Then cupferron was extracted with 6 cm^3 of ether.

Lanthanum oxide was dissolved in sulfuric acid (1:19). This solution was shaken with 1 cm^3 of cupferron-ether solution five times. The combined ether layer was dried and heated to destroy organic matter. The activity of the ether layer was 4.0 div./min, while none remained in the aqueous layer.

Similar experiments were made on the solutions containing UO_2^{++} or Th^{+4}. The UO_2^{++} ion gave the same result as the above ion, while only 10% of the Th^{+4} was transferred to the ether layer.

Coprecipitation with Lanthanum Oxalate

Trace amounts of α-emitter from the ether extract were mixed with 9 mg of inactive lanthanum oxide. The mixture was then dissolved in 0.3 *N* hydrochloric acid, and lanthanum oxalate was precipitated with a saturated solution of ammonium oxalate. The precipitation was quantitative. About 85% of activity was carried down by the precipitate (precipitate: 2.4 div./min; filtrate: 0.4 div./min). A similar experiment with UO_2^{++} ion showed that only 2% of UO_2^{++} ion was carried down by the precipitate under the same conditions.

Discussion

The above results are summarized in Table IV, together with some properties described in the literature cited.

Table IV. Chemical Properties of the α-Emitter

Ion	Solubility of Compound*				Extraction of cupferron complex	Ether extraction
	OH^-	F^-	$C_2O_4^{--}$	Cl^-		
U^{+4}	(i)	(i)	(i)	(s)	(yes)	—
UO_2^{++}	i	s	s	s	no	(yes)
Th^{+4}	i	i	(i)	s	no	no
α-emitter	i	i	i	s	yes	yes
Pu^{+4}	(i)	(i)	(i)	(s)	(yes)	(no)
PuO_2^{++}	(i)	(s)	(s)	(s)	(no)	(yes)

* *Note:* s = soluble; i = insoluble; ( ) = data from literature cited.

As shown in Table IV, the chemical properties of the α-emitter are similar to those of Pu^{+4} or U^{+4}. But the behavior at the ether extraction from nitric acid is rather similar to that of PuO_2^{++} or UO_2^{++}.

If the emitter extracted by ether from nitric acid solution is UO_2^{++}, the emitter should not be coprecipitated with lanthanum oxalate, because under present circumstances UO_2^{++} is much more stable than U^{+4}.

On the other hand, if one assumes that the emitter extracted by ether is PuO_2^{++}, the coprecipitation of

α-emitter with lanthanum oxalate may be explained as follows.

Since the stability of Pu^{+4} in solution is fairly large and PuO_2^{++} can be reduced to Pu^{+4} without much difficulty, the presence of Pu^{+4} in the solution from which lanthanum oxalate was precipitated is quite possible. If so, the emitter should be carried down by oxalate precipitate as shown in the experiment.

Now, if the emitter in the lanthanum oxide fraction is plutonium, its oxidation state should be + 4, because it was coprecipitated with lanthanum oxalate. In the ether extraction experiment, the emitter was found in the ether layer. The oxidation state at this stage should be + 6. This fact indicates that the oxidation of Pu^{+4} to PuO_2^{++} occurred in the concentrated nitric acid solution within less than 2 hours.

It is not yet clear whether or not Pu^{+4} is rapidly oxidized to PuO_2^{++} in the concentrated nitric acid solution. According to the literature published so far,[2] the oxidation in the dilute nitric acid solution occurs easily, while in concentrated nitric acid only less than 15% of Pu^{+4} ions are oxidized during a period of 15 minutes at 80°C.

It is possible, however, that this oxidation proceeds easily and rapidly in concentrated nitric acid containing large amount of foreign salts. Or, prolonged heating in concentrated nitric acid might make this oxidation much easier. At the present stage of our experiment, no clear explanation can be made on this point.

The authors are of the opinion that the α-emitter in the sample is plutonium. Since this emitter has very long-life, it might be Pu^{239}.

Extraction of Fission Products from the Soil

The samples were heated on a hot plate to destroy organic matter. Then these preheated samples were subjected to leaching with water. No activity was leached out with water at 100°C.

The same samples were then treated with acid of different concentrations. About 5 gm of the sample were heated with 50 cm³ of hydrochloric acid on a water bath for 40 minutes. When the concentration of hydrochloric acid was raised up to 5 *N*, all the activity due to alkali and alkali earth elements was completely leached out. In the case of rare earth elements, however, the leaching was not complete even with 5 *N* hydrochloric acid. The relationship between the extractability and the acid concentration is shown in Table V.

Table V. Extraction of Rare Earth Elements

Concentration (N) of HCl	*Extractable fraction (%)*
0.0	0
0.1	17
1.0	34
3.0	54
5.0	70

Leaching of the original, unheated samples gave different results. In this case, 5 mg of the sample having a total activity of approximately 1000 cpm were heated with 50 cm³ of water for 1 hour on a water bath. The residue was filtered using filter paper Toyo No. 5 A. Ten cpm of Cs^{137} ($+Ba^{137m}$), 60 cpm of Sr^{90} ($+Y^{90}$) and 55 cpm of rare earth elements were leached out from the sample. This fact seems to indicate the importance of the effect of organic matter on the leaching of fission products from contaminated soil.

SUMMARY

In the soil at Nishiyama, near Nagasaki, where the atomic bomb fell in August 1945, several long-lived fission products such as Sr^{90} ($+Y^{90}$), Cs^{137} ($+Ba^{137m}$) and Ce^{144} ($+Pr^{144}$) were detected by radiochemical analysis. The long-lived α-emitter which is supposed to be Pu^{239} was also detected in the soil. The detection of Pu^{239} in the soil afforded the present authors the opportunity to study the chemical aspects of transuranium elements for the first time in Japan.

REFERENCES

1. Kimura, K., Ohashi, S., Saito, K. and Yamatera, H., *Report on the Atomic Bomb Effects*, 53 (1953).
2. Seaborg, G. T., Katz, J. J. and Manning, W. M., *The Transuranium Elements*, UNES-IV-14B, New York (1949).

Record of Proceedings of Session 9B.2

FRIDAY MORNING, 12 AUGUST 1955

Chairman: Mr. A. P. Vinogradov (USSR)

Vice-Chairman: Mr. J. W. T. Spinks (Canada)

Scientific Secretaries: Messrs. R. Hara and J. Gaunt

PROGRAMME

P/437 The chemistry of ruthenium ..... J. M. Fletcher and F. S. Martin

DISCUSSION

P/671 Some chemical properties of technetium ..... J. B. Gerlit

P/1023 Determination of half-life of Tc^{102} ..... J. Flegenheimer and W. Seelman-Eggebert

P/1026 Determination of half-life of Tc^{105} ..... J. Flegenheimer and W. Seelman-Eggebert

DISCUSSION

P/436 The condition of fission product iodine in irradiated uranium metal ..... G. N. Walton *et al.*

DISCUSSION

Mr. J. M. FLETCHER (UK) presented paper P/437 as follows:

It might well be asked why attention should be devoted in this session to the chemistry of ruthenium rather than to one of the many other fission products. There are two reasons.

Firstly, in the processing of irradiated fuels by aqueous methods after dissolution of the metal in nitric acid, ruthenium, which is relatively long lived and still present even after aging, is the fission product most difficult to separate from uranium and plutonium. In solvent extraction processes, conditions to give good decontamination from ruthenium have required prolonged and intensive experiments often largely based on methods of trial and error. At each ancillary stage, such as an evaporation or precipitation step in further purification or in effluent disposal, there has been difficulty in persuading ruthenium to follow in a quantitative manner one particular course. As Shakespeare said of fantasy, it is "more inconstaat than the wind."

The second reason is that little attention has hitherto been paid to the ruthenium compounds which happen to be formed in nitric acid solution. These include trivalent nitrosylruthenium, the study of which, in view of difficulties in their preparation and identification of some of the complexes, has been almost entirely neglected since 1890.

As with the relatively well known ammino, halogeno and cyano complexes of nitrosylruthenium, we have interpreted the new compounds prepared as octahedral six co-ordination complexes and we find a general similarity with comparable trivalent cobalt and tetravalent platinum complexes; for example, the complexes formed with the ligands perchlorate and fluoride are very weak; with nitrate, somewhat stronger; with hydroxide and chloride, relatively strong; and with nitro, very strong.

Since we have been particularly interested in nitrosylruthenium complexes present in nitric and nitrous acids, attention has been largely directed to the four ligands, nitrate, nitro, hydroxo and water, as competitors for the five positions — the sixth position being occupied by nitrosyl — grouped around a ruthenium atom. With these four ligands alone, a large number of complexes have been postulated, particularly when different spatial arrangements and polynuclear species are included. Over twenty examples are given in Table I of our paper, but the total number of possibilities far exceeds this quantity. The relative slowness with which one complex is converted to another makes this field of chemistry comparable in its variety and complexity to a branch of organic chemistry. In spite of the coloured nature of the complexes, it is unfortunate that absorption spectra, except in the infra-red, have been of little use as a means of identification or for following the course of reactions.

I should like first to refer to the nitrato complexes of nitrosylruthenium (Slide 1).

Amongst these we have studied in particular the red trinitrato complex, since it is formed in solution by boiling other nitrosylruthenium complexes with eight to fifteen molar nitric acid and can be isolated by slow evaporation at room temperature. Like the di- and trinitrato uranyl complexes, it is readily extracted from aqueous solutions by many organic solvents. In water or in dilute nitric acid, it is hydrolyzed to lower nitrato complexes, which are also soluble in a wide variety of organic solvents, but less extractable from aqueous solutions than the trinitrato complex.

Trinitrato $[RuNO(NO_3)_3(H_2O)_2]$

Dinitrato $[RuNO(NO_3)_2OH(H_2O)_2] \rightleftharpoons [RuNO(NO_3)_2(H_2O)_3]$

Mononitrato $[RuNO.NO_3(OH)_2(H_2O)_2]$ or $[RuNO.NO_3(H_2O)_4(NO_3)_2]$

Heminitrato $H_2O.OH.NO_3.RuNO \begin{matrix} OH \\ \diagup \\ \diagdown \\ OH \end{matrix} RuNO(OH)_2H_2O$

Slide 1. Nitrato complexes of nitrosylruthenium

We postulate, as you will see on Slide 1, a series of nitrato and hydroxo nitrato complexes in which the total number of groups joined to the central ruthenium atom is six. For the lower numbers, such as the mononitrato, we formulate them in two possible forms, the uncharged form and, secondly, in a form in which the ruthenium is in a cationic state and the charge is balanced by one or more nitrato groups outside the complex.

These three complexes, the tri-, di-, and mononitrato, may be related to one another, by considering that the NO_3 groups in the trinitrato complex are successively replaced, either by OH giving the uncharged forms of the lower nitrato complexes or, alternatively, by H_2O, giving the cationic forms. We also have evidence for the existence in solution of a higher complex than the trinitrato, but we do not know whether this is a tetra or pentanitrato complex. To illustrate our knowledge with these complexes, I would choose as an example the conditions which prevail at equilibrium in 7.5*M* nitric acid. We find under these conditions that there is about 50 per cent of the tri-, about 22 per cent of the di- and about 28 per cent of the mononitrato complex. As one goes to lower nitric acid concentrations, the quantities, at equilibrium, of the trinitrato are very much smaller, for example, about 10 per cent, in 3*M* nitric acid. Another aspect of some interest is that when aqueous solutions of these complexes are titrated, we find that with the trinitrato complexes two rather than one nitrato groups are readily displaced together, giving the fairly stable mononitrato complex. This gives us a clue to the likely spatial arrangements in this type of complex.

Slide 2 (Figs. 1, 2, 3 of P/437) shows the three spatial arrangements possible for the trinitrato complexes. We conclude from the stability of the mononitrato that, in it, the NO_3 group is opposite to the NO group. For the trinitrato, this eliminates possibility number 1. Our evidence of the similarity of two of the other three groups leads us to choose formula number 2 in preference to number 3.

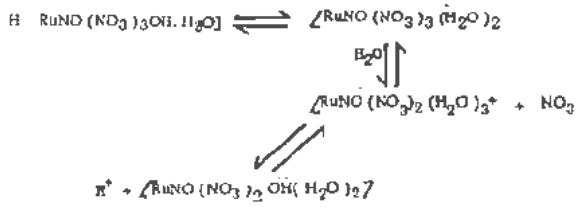

Slide 3. Nitrato complexes of nitrosylruthenium relationship of anionic and cationic forms

We find that both anion and cation exchange resins remove ruthenium species from solutions of these complexes. Slide 3 illustrates how this happens and how anionic and cationic ruthenium-containing species may be formed. From the uncharged trinitrato complex, proton transfer from one of the aquo groups leads to an acidic form with a ruthenium anion. Also, however, replacement of a nitrato group by an aquo group leads to a ruthenium-containing cation. Of course, the equilibria are shifted in one direction or another by removal of species on the ion exchange resins that are used.

Amongst other reactions of these complexes, I may briefly mention that they are converted to the insoluble nitrosylruthenium hydroxide and hydrosulphide; this test provides a means of identification for the presence of the RuNO group.

It may also be of some interest to mention the differences in their partition coefficients with various organic solvents. These differ widely between the tri-, di-, and mononitrato complexes. For example, we find with 20 per cent tributyl phosphate at 0°C, when the aqueous phase is 0.75*M* nitric acid, that the proportion coefficients are respectively well over 100 for trinitrato complex, about five for the dinitrato, whereas for the mononitrato they are only about 0.1. The differences are roughly a factor of 50 between each one.

Turning now from the nitrato to the nitro complexes, as with the well-known cobaltinitrites, the nitro complexes of nitrosylruthenium are roughly relatively stable. For over fifty years, yellow sodium and potassium compounds, first prepared by Joly, have been thought to contain a penta-nitrato complex of trivalent ruthenium. We have shown that these compounds are not of that composition, but are salts of the tetranitro complex of the trivalent nitrosylruthenium radical, that is, one of the five nitrogen atoms in the molecule is present as NO and not as NO_2. In warm dilute sulphuric or perchloric acids, this anion is converted to the uncharged dinitro complex, which is also extractable from aqueous solutions by a variety of organic solvents.

This reaction illustrates the relevance in these complexes of the *trans*-directing effect of groups such as NO and NO_2. We represent the tetranitro anionic complex by the first arrangement shown in Slide 4. In acid solution, we find two, not one, three or four, nitro groups are readily displaced and it is converted to the uncharged dinitro complex. No pentanitro nitrosylruthenium complex is known. We have, how-

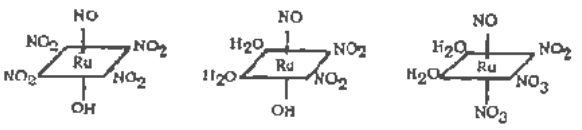

Slide 4. Nitro complexes of nitrosylruthenium

ever, prepared a mononitro dinitrato complex by the action of oxides of nitrogen on a solution of the nitrato complex in nitric acid. It is an orange crystalline solid for which we suggest the composition shown in the last formula on Slide 4.

It is of some interest, we feel, that in this complex nitrogen is present at the same time in one complex, as NO, NO_2, and NO_3.

Turning to the general relationships of ruthenium to other ions, it is clear that the presence of the nitrosyl group profoundly affects the nature of the complexes of ruthenium. With tetravalent ruthenium, nitrato complexing is very weak and nitro complexing unknown.

Allowing for the small ionic radius of Ru^{4+}, its complexing follows the pattern of other tetravalent ions. In Table I, attention is drawn to the small ionic radius of tetravalent ruthenium compared to other tetravalent ions, such as zirconium and uranium. But in principle, its complexing is similar to them, in so far as it is weaker by nitrate than by fluoride, but in the nitrosylruthenium ion the position is quite different. It has resemblances in its strong nitro and weak fluoro complexing to the platinum metals. It also resembles the uranyl ion in that complexing by fluoride is much weaker than by nitrate.

Finally, in solutions of irradiated fuels in nitric acid, nitrato complexes of uranyl, plutonyl and of tetravalent plutonium and thorium will occur. For any one of these, the rates of nitration and denitration reactions are so rapid that with organic solvents, ion exchange resins, etc., equilibrium conditions are rapidly reached. But with these nitrato and nitro complexes of nitrosylruthenium the rates of reaction are slower and equilibrium conditions may not occur for an hour or more at room temperature.

In processing by aqueous methods, substantial complications to chemical plant have been necessary to allow for the vagaries of fission product ruthenium. We envisage that an understanding of the nature and properties of ruthenium compounds involved will be of substantial advantage in the future by helping to lower the cost of processing fuels used for nuclear power production. The knowledge should also assist in the disposal of fission product waste of low activity and in an understanding of the ultimate fate of fission product ruthenium in biological surroundings, for example, in mammals, fish and plants.

Table I. Relationship of Ru^{4+} and $(RuNO)^{3+}$ to Other Ions Complexing

	Ionic radius (A)	$(NO_3)^-$	F^-
Ru^{4+}	0.67	Weak	Moderate
Zr^{4+}	0.80	Moderate	Strong
U^{4+}	0.96		
$(RuNO)^{3+}$	—	Moderate	V. weak
$(UO_2)^{2+}$	—		

DISCUSSION ON PAPER P/437

Mr. G. Fayed (Egypt): I have a question and a comment. I should first like to ask Mr. Fletcher if he would kindly give us some idea of which of the exposed compounds is the most stable and to what extent there might be no aging effect as regards this compound. My comment is that the problem of the separation of ruthenium from uranium and plutonium would perhaps be solved through the anodic oxidation of the volatile tetroxide of ruthenium.

Mr. Fletcher (UK): In answer to Mr. Fayed's question, I would say that my knowledge on this subject is still relatively elementary and I would not like to state any definite answer. But I would draw attention to the fact that I mentioned that the nitro complexes are most stable in nitric and nitric acid solutions. If one is therefore dealing with a solution in what is broadly speaking nitric acid, it is the nitro rather than the nitrato compounds which are most stable. I would go so far as to suggest that the piece of information which Dr. Bruce gave us earlier this morning about the effect of aging prior to extraction, is related to these slow changes between nitrato and nitro complexes.

The Chairman: We will take the next two questions to Mr. Fletcher together.

Mme. R. Ripan (Romania): Did Mr. Fletcher find a relationship between the size of the molecule and the phenomenon of absorption by anion exchangers, in ruthenium chemistry where he has obtained a combination of high molecular weight with two ions of ruthenium per molecule? If the molecule is large, is the absorption different for exchange phenomena, even where the molecules have the same electrical charge depending on whether it is of a mononuclear or of a binuclear ion? Does it depend on the size of the molecule?

Mr. A. M. Rollier (Italy): Has the crystal structure of that ruthenium compound which is obtainable in the solid state been investigated?

Mr. Fletcher (UK): I shall reply first to the question put by the Italian delegate. The properties in the solid state have been investigated in so far as three or four of the complexes mentioned have been isolated. For example, the infra-red spectrum of the tetranitro complex has been very clearly distinguished and has shown the presence simultaneously of the nitrosyl group and of the nitro group.

The crystal structures have not been isolated and examined, much as we would like to do so, largely because most of these materials are extremely hydroscopic. In the case of the pentachloro nitrosylruthenium complex, one of our research scientists is at the moment investigating this.

As regards the question from the Romanian delegate; in one particular case we have isolated uncharged species, by passing mixtures of the nitro complexes through a mixed bed of anion and cation exchange resins; the uncharged di-nitro complex

passed through. We have not examined the relation of the size of these complexes, for the same charge to anion exchange absorption.

Mr. J. W. T. SPINKS (Canada) then took the chair while the chairman, Mr. A. P. Vinogradov (USSR), presented paper P/671, as follows:

In recent years the physical and chemical properties of such elements as neptunium, plutonium, americium and technetium have received closer study than have the properties of some "ordinary" elements. Nevertheless, while for minute quantities of plutonium and of some other actinides, quantitative methods of extraction from minerals of highly complex chemical structure have been developed, in the case of technetium the number of methods of extraction even from the basic raw materials — waste matter from the production of plutonium and uranium-233 and molybdenum irradiated in the reactor — is extremely small. This may be illustrated by the fact that, apart from the papers by Jacobi and Glendenin, which date from as long ago as 1949, no quantitative data on methods of concentrating and separating technetium are to be found in the literature. As regards the solution of the extremely important problem of the content of technetium in uranium ores and its geochemical behaviour, the data so far available are purely qualitative and, in our view, not entirely reliable.

As is well known, the most convenient techniques for the concentration of traces of elements are co-precipitation, electrolysis, distillation, ion exchange and extraction. For the extraction of technetium from fission products and its separation from molybdenum, the method actually most widely used is the tetraphenylarsonium chlorate method, consisting in the co-precipitation of tetraphenylarsonium pertechnetiate with tetraphenylarsonium chlorate. However, according to the data given by the authors of this method, further extraction of technetium involves the extremely protracted and difficult process of breaking down this compound, in which an appreciable quantity of technetium is lost. Other known methods of co-precipitation of technetium, such as with sulphides of rhenium, copper or bismuth, with insoluble perrhenates and, as described in our paper, with insoluble chlorates, cannot be applied with entirely satisfactory results in the first stage of extraction owing to the necessity of adhering to certain conditions which are not always feasible during the extraction of traces of technetium from chemically complex waste solutions of the atomic industry and, more particularly, during extraction from minerals and ores.

Nor is the application of electrolysis methods, which are less predictable than the precipitation methods, expedient in all cases, especially in the case of ultra minute quantities, since according to the data in the literature a minimum concentration of technetium is necessary for the full extraction of this element. The chromatographic method, which has found an application in the separation of technetium from comparatively small quantities of molybdenum, cannot be used for the quantitative extraction of technetium either from atomic industry waste, owing to the presence therein of large quantities of different salts, or from large quantities of molybdenum and uranium, which is necessary for analyses of the mineral raw material. The methods of distillation and extraction are the most promising. However, as shown by Herr's data and our own experiments, the distillation of radiochemical quantities of technetium in the immediate presence of large quantities of salts does not lead to quantitative extraction. Thus, in the extraction of 10^{-15} gm of technetium from 300 gm of molybdenum the yield obtained by distillation does not exceed 70 per cent. The distillation of technetium from atomic industry wastes on the one hand, as in the case of the separation of this element from molybdenum, does not yield quantitative results, and on the other hand requires extremely complicated apparatus for the processing of large volumes of highly active products.

The extraction methods have a number of important advantages, but their application to technetium has been comparatively little studied. Also comparatively little studied are the oxidation-reduction reactions of technetium and the analytical characteristics of its lower-valency forms. Accordingly, our research studies of the chemico-analytical properties of technetium have been focused chiefly on the extraction behaviour of technetium in the presence of molybdenum, iron, manganese, rhenium, uranium and columbium, and also of such elements as thorium, zirconium, ruthenium, the rare earths, strontium, antimony and tin, which occur in atomic industry wastes. In addition, attempts have been made to study some of the chemical properties of tetravalent technetium and the possibility of making use of these properties for analytical purposes.

All the investigations were carried out either with the 6.1-hour isomer Te^{99m} or with microgramme quantities of the basic isotope Te^{99}. The study of the behaviour of the other elements (except magnesium, manganese, thorium and uranium) was carried out with the aid of the corresponding tagged atoms.

The results of the research into the behaviour of technetium and rhenium during extraction from neutral, acidic and alkaline media and the behaviour of molybdenum and ruthenium in the same process are given in the paper submitted. Accordingly, with your permission, I shall not dwell on this question, and shall merely draw attention to the summary table, from which it will be seen that a number of oxygenous and nitrogenous solvents may be used in particular cases for the extraction of technetium (Slide 5, Table II of P/671). In Table II on the next page data are given on the behaviour of a number of elements during the extraction of technetium from various media.

From these data it is evident that most elements except rhenium are not extracted together with

technetium either from alkaline or from carbonate or acidic media. The establishment of the possibility of extracting the diethyldithiocarbonate compound of technetium by means of chloroform was also turned to account for the purpose of separating small quantities of technetium from a number of elements, although this method does not permit of the quantitative separation of technetium from molybdenum, iron, columbium, manganese, antimony and tin.

In connection with the fact that non-polar solvents do not extract technetium, a method was evolved for re-extracting this element from the oxygenous-solvent phase into the aqueous phase by the addition of chloroform. A two-fold treatment with small amounts of water leads to 90 per cent re-extraction.

Table II. Value of the Distribution Ratio of Some Elements during Extraction with Methylethylketone and Isoamylalcohol

Element to be extracted \ *Medium, extraction agent*	*5 N NaOH methylethyl-ketone*	*2 N H_2SO_4 isoamyl-alcohol*	*2 N K_2CO_3 methylethyl-ketone*
Uranium(VI)	–	–	<0.001
Thorium(IV)	–	–	<0.001
Rhenium(VII)	46	7.0	7.2
Technetium(VII)	49	7.8	8.5
Manganese(VII)	Is reduced to manganese(IV)		
Molybdenum(VI)	0.2	0.1	0.013
Zirconium(IV)	–	0.2	–
Columbium(V)	<0.001	<0.001	0.015
Ruthenium(IV)	<0.001	<0.001	<0.001
Cerium(III)	–	<0.001	–
Antimony(III)	–	<0.001	–
Tin (IV)	–	<0.001	–
Magnesium	–	≈0.005	–
Strontium	<0.001	<0.001	–

A study of the oxidation-reduction properties indicated the possibility of reducing heptavalent technetium both in acidic and in alkaline media. A most detailed study was made of the process of reduction by means of concentrated solutions of hydrochloric acid, leading to the formation of the complex anion $TcCl_6^{--}$, which is readily hydrolyzed in weakly alkaline media. By utilizing the difference in the behaviour of rhenium and technetium during such reduction, a quantitative method was evolved for separating these elements by co-precipitation of the technetium with ferric hydroxide after reduction, oxidation of the technetium to the heptavalent form by dissolution in nitric or chloric acid, and subsequent separation of the iron by repeated precipitation as a hydroxide. This method was tested with a rhenium content of 5×10^{-5} gm and a technetium content of 10^{-13} gm. A single cycle of operations led to the extraction of over 98 per cent of the technetium. Experiments carried out with tagged rhenium showed that two cycles were fully sufficient for the isolation of radiochemically pure technetium.

The above-mentioned methods were verified both on molybdenum (in the form of molybdenum anhydride or ammonium molybdate) irradiated in the reactor and on several atomic industry waste solutions.

The separation of technetium from irradiated molybdenum anhydride dissolved in a 5*N* solution of caustic soda was carried out by the extraction of the technetium with methylethylketone with subsequent re-extraction into the aqueous phase. The performance of two cycles led to the extraction of practically all the technetium with a radiochemical purity which was determined by the half-life. The time necessary for the separation of the technetium was two to three minutes. Separation from a partially extracted alkali was carried out either by extraction of sodium pertechnetiate with chloroform, by distillation, or by co-precipitation with sulphides.

Though highly diverse in their chemical composition, all the waste products accumulating from the production of plutonium and uranium-238 usually contain some quantity of nitrate ions. Accordingly, the extraction of technetium from acidic and neutral solutions was effected with isoamyl alcohol. Treatment of the original solutions, to which was added sulphuric acid with three volumes of isoamyl alcohol, resulted in the complete extraction of the technetium, although it sharply increased the volume. Because of this, fivefold extraction of technetium was later performed with a volume of isoamyl alcohol equal to one-eighth of the volume of the aqueous phase. Re-extraction of the technetium into the aqueous phase was done with two volumes of concentrated ammonia solution. The subsequent concentration of the technetium was carried out by extraction of the diethyldithiocarbamate compound with chloroform after steaming and acidification of the alkaline solution with sulphuric acid. This operation was necessary owing to partial extraction of nitric acid by the isoamyl alcohol. The diethyldithiocarbamate compound of technetium, after distillation of the chloroform, was treated with sulphuric acid in the presence of a small quantity of ammonium persulphate and the technetium was separated by distillation into a solution of caustic soda. This method enabled as much as 95 per cent of the technetium to be separated out with a purification factor, according to the intensity of β-radiation, of $2\text{–}3 \times 10^6$.

In the first stage, the technetium was removed from the alkaline waste solutions by extraction with methylethylketone after making alkaline with caustic soda to a total hydroxyl-ion concentration of 5–6 *N*. After re-extraction into the aqueous phase with chloroform, further concentration and purification of the technetium was carried out either by co-precipitation with copper sulphide and subsequent distillation, or by electrolysis, likewise with subsequent distillation. The yield of technetium amounted to 93–95 per cent, with a radiochemical concentration, according to the β-radiation, of approximately 10^7.

The most suitable method of extracting technetium from molybdates would seem to be by extraction from alkaline media by methylethylketone after prelimi-

nary treatment of the mineral with nitric acid, and subsequent purification by the distillation method.

In connexion with Vinogradov's hypothesis that technetium-99 is present in uranium minerals as a product of spontaneous fission, calculations have been made which show that the content of this element in old uranium minerals must be about 10^{-7} per cent by weight of the uranium content. That being so, the uranium materials are of great interest in connexion with the study of the geochemistry of technetium. The isolation of technetium from materials of this kind entails a number of difficulties, especially during the breakdown of the minerals. As experiments with trial mixtures showed, when silicate rocks are fused with carbonate, the technetium often volatilizes in the form of a higher oxide, while part of it remains with the uranium. By interception of the technetium heptoxide and extraction of the residual technetium by means of methylethylketone after treatment of the melt with concentrated solutions of potassium carbonate or sodium carbonate it is possible to isolate the technetium more or less completely. After re-extraction into the aqueous phase, the concentration and purification of the technetium are best effected by co-precipitation of technetium sulphide with copper sulphide and subsequent distillation. The most convenient method of separating rhenium from technetium would seem to be reduction of the latter with concentrated hydrochloric acid.

The methods I have described require further testing, and this is being done at the present time on milligramme quantities of Tc.

Mr. W. SEELMAN-EGGEBERT (Argentina) presented papers P/1023 and P/1026 as follows:

In the tables of nuclides the half-life of technetium-102 is given with an indeterminate value of less than 25 seconds. It was therefore necessary to evolve a chemical method for the very rapid separation of molybdenum and technetium. Special measuring equipment had also to be used, with which half-lives of a few seconds could be measured.

Following a method proposed by Fränz, the linear growth of the condenser charge of a common integrator was recorded during intervals that were brief in relation to the time constant of the equipment. By repeatedly charging to a fixed potential and instantaneously discharging, the intervals are made inversely proportional to the activity studied.

The chemical method consisted in separating molybdenum from the other fission products by dissolving the lead molybdate in a mixture of hydrochloric acid with tartaric acid. The tartaric acid complexes the molybdenum and prevents its precipitation with tetraphenylarsonium chloride. A preliminary precipitation of technetium was carried out by adding perrhenate ion and an excess of tetraphenylarsonium chloride and then filtering through a colloidal filter; by this procedure the solution is clarified and becomes ready to precipitate technetium again on the addition of a few milligrammes of perrhenate ion. The solution so prepared was transferred to a dismountable Buchner funnel with a colloidal filter mounted on a vacuum filtering tube.

So long as no vacuum is applied, the filter prevents the passage of the liquid. The Geiger-Muller tube, which was already connected to the measuring apparatus, was arranged over the ring and as close to it as possible. At a given moment a few milligrammes of perrhenate were added to the liquid in the ring, a vacuum was applied, the ring was removed when filtering was completed, and measuring was then begun. With this method of operation only five or six seconds elapse between the addition of rhenium and the beginning of measurements.

The technetium precipitate does not constitute the whole of the technetium present at the time the reagent is added, and it retains a little molybdenum, but the greater part of the molybdenum separates and, settling at the bottom of the tube, has little effect on the measurement owing to its distance from the counter.

The Geiger Müller tube was shielded with sheet aluminum in order to reduce the measurable activity of the technetium-101 which is formed through the decay of the molybdenum-101 always found in the molybdenum fraction from fission.

Analysis of the curve recorded yields an average of 5 ± 1 sec for the short period half-life observed.

The longer lived activities correspond to technetium-101 and to molybdenum-101 and 102, absorbed by the tetraphenylarsonium perrhenate precipitate.

In order to determine the maximum energy of technetium-102, the absorption curve of molybdenum obtained by brief irradiation of uranium was plotted. The beta rays from the molybdenum-technetium-101 fission chain are almost completely stopped by an 850 mg per square centimeter of thickness aluminum sheet. If the gamma radiation corresponding to the 101 series of isobars is removed, a half-life of approximately 11.5 minutes, corresponding to molybdenum-102, is observed. With a greater thickness of aluminum the hard beta radiation due to the technetium of 5 sec half-life is reduced. Total absorption of the hard beta radiation is obtained with 2200 mg per cm^2 of aluminum, which corresponds more or less to a maximum energy of 4.2 Mev. This value agrees well with other published values. Gamma rays are also emitted by the isobars of molybdenum and technetium-102, the energy of which is now being determined.

In the fission of heavy nuclei, the isotopes of technetium having mass numbers greater than 102 must also be formed. Technetium-103 probably has a half-life of some minutes, but so far it has not been possible to determine its half-life directly in the mixture of technetium isotopes formed by fission.

Attempts have been made to determine its half-life indirectly by repeated separation of its daughter element at regular intervals.

Satisfactory results have not been obtained as yet, probably owing to the fact that the half-life of ru-

thenium-103 is long, so that a very high technetium activity will be required.

The half-life of technetium-104 is probably so short that its separation as a fission product will be extremely difficult, but it is possible to determine the half-life of technetium-105 if advantage is taken of the fact that the activity of its daughter element, ruthenium-105, is measurably increased through the decay of technetium-105.

Direct measurement is difficult. This is due to the fact that technetium-101 has a similar half-life and is more active because its yield in fission is greater. Technetium-105 is obtainable only as a fission product. Its half-life is indicated as short in the tables of isotopes.

In order to obtain fission products, a few grams of ammonium diuranate were exposed to the neutron flux of a cascade accelerator of 1.2 Mev for 10 to 15 minutes. The diuranate was dissolved in hydrochloric acid, and when copper was added as a carrier, copper sulphide was precipitated with a rapid stream of hydrogen sulphide. The copper sulphide retains the activities of the elements of the second analytical group, which includes molybdenum and technetium.

The copper sulphide was redissolved in hydrochloride acid with a little bromine; adding molybdate, perrhenate and ferric ions as carriers. On the addition of ammonia, ferric hydroxide was precipitated, which retained the activities of tin, antimony, ruthenium, tellurium and other elements. The molybdenum and the technetium pass to the filtrate, from which lead molybdate was precipitated when the filtrate was acidified with acetic acid and lead acetate added. Lead molybdate can be obtained in this manner within 5 minutes if the filtrations are carried out in a vacuum and with 2 sec colloidal filters. The technetium, with the rhenium as carrier, is found in the lead molybdate filtrate.

This solution was divided into three aliquot parts. In each part the technetium was co-precipitated with rhenium by means of tetraphenylarsonium chloride at intervals of a few minutes.

By measuring the strong activity of the technetium-101 it was ascertained that the precipitations were practically complete; at least, the same percentage of technetium was precipitated every time. After the decay of the technetium-101, the individual preparations were again measured to determine the ruthenium-105 content in each.

By plotting the activities of the ruthenium-105, with the corresponding intervals, on semilogarithmic paper, a half-life of 10.5 minutes was found for technetium-105.

This method of working is accurate only if there is no co-precipitation of ruthenium with the technetium preparations. In order to confirm this, a radioactive indicator of ruthenium, ruthenium-106, was added to the technetium solution before the precipitations were made. Two weeks after the experiment the technetium preparations were again measured to determine their ruthenium-106 content. In all of them, the co-precipitation of ruthenium with the technetium was less than 2 per cent.

The approximate half-life of molybdenum-105 was also determined in a similar manner, the indirect method of separating the daughter element at regular intervals being employed in this case also.

A figure of about 4 minutes was obtained for its half-life. Direct measurement of this half-life is now being attempted by the selection of a position on a differential discriminator suitable for a gamma radiation typical for this nuclide.

These experiments confirm the provisional values for these nuclides published in 1947. The half-lives determined are longer than had been anticipated for nuclides so remote from the line of stability, and for this reason we feel that it would be worth while for the subject to be studied at another laboratory also.

Mr. G. N. WALTON (UK) presented paper P/436 and also made reference to paper P/435.

DISCUSSION ON PAPERS P/437, P/671, P/1023, P/1026, P/436 AND P/435

Mr. STEINBERG (USA): In the quantitative separations in radiochemistry, one must always take into account the interchange of the radioactive species formed in fission with the carriers added. Iodine has been one of those which has caused some difficulty. It is interesting that Mr. Walton's remarks indicate that in fission iodine apparently is formed as neutral atoms. I would wonder if Mr. Walton would care to comment on the possibility that the difficulties encountered in radioactive exchange in the many valence states present during the radiochemical separations are the result of the action of the solvents used in the dissolution of the uranium.

Mr. WALTON (UK): I certainly think that the different valency states of iodine which appear to be present after you have dissolved up uranium metal are perhaps effects that take place after dissolution, as the result of the interaction of the iodine atoms with the medium in which the dissolution takes place. In nitric acid, these effects are most marked, whereas in hydrochloric acid the effects are less. The different valency states do not cause so much trouble in one's experience in hydrochloric acid. On the other hand, I must point out that these experiments that I described were only done on the iodine that is exposed during grinding up the metal, which is only one or two per cent of the total amount present, and we make the assumption that the rest of the iodine present is in the same sort of state as the little bit we have seen.

Mr. F. MORGAN (UK): The extraction of technetium from irradiated molybdenum by roasting in oxygen is a very convenient method. Would Mr. Vinogradov care to comment on any experiments that may have been done on the possibility of extraction of technetium from uranium oxide, as a possibility of getting larger quantities of technetium from high burn-up uranium rods?

The CHAIRMAN: We have not carried out such extraction directly from uranium rods, but have used ordinary waste solutions. The method I described can be employed in hot-laboratory conditions.

Mr. L. YAFFE (Canada): I should like to ask Mr. Walton what is probably a very elementary question. Mr. Steinberg brought up the question of exchange and I should like to carry this a little further. Is it not very difficult to draw conclusions about the different valence species one finds in irradiated material unless all factors are studied, such as possible exchange between species which may be induced by the solvent during the extraction process?

Mr. WALTON (UK): No carrier iodine was added at the time of separation and I have not been able to think of any type of exchange that could affect the conclusions drawn. We were worried about the analysis of the iodine extracted into the hexane and into the alcohol, and one of the things that we have done is to count aliquots of this solvent with a spectrometer, enabling us to see the iodine before chemical separation.

The other point also is that iodine atoms in hexane have been studied by Marshall and Davidson in the photo-chemical decomposition of molecular iodine, and they find no attack of the hexane by iodine atoms.

Mr. ROLLIER (Italy): You extracted when grinding uranium only 2 per cent of the iodine present: did you look also for iodine-129 from tellurium or not?

Mr. WALTON (UK): It is a fact that it was only some 2 per cent that was extracted by this means. What we would like to know is the size of the particles and their surface area, and so on, which would enable one to do more studies on these lines.

We did look at the other isotopes, but rather briefly and we could not show any isotopic separation. All our fractions seemed to be the same.

Session 10B.1

SURVEYS OF CHEMISTRY OF TRANSURANICS

LIST OF PAPERS

Thermodynamics of the Heavy Elements

By B. B. Cunningham,* USA

Thermodynamic data that enable the engineer or technologist to predict by calculation alone whether or not a chemical reaction can proceed under certain specified conditions of technological interest are of great practical value, and find extensive application in many phases of modern chemical industry.

The thermodynamic properties of the heavy elements are of concern, therefore, not only to scientists engaged in basic research, but also to engineers and chemists interested in practical methods for the production and utilization of nuclear power. The purpose of this paper is to summarize briefly advances in knowledge of the thermodynamic properties of the elements of atomic number 89 and higher. Although a number of these elements are of little immediate practical interest, trends in thermodynamic properties that are revealed by study of the series as a whole help in correlating the data and in estimating properties that have not been determined experimentally.

There is no attempt here to review in detail thermodynamic values that are summarized in such recent publications as the United States Bureau of Standards Circular 500 (entitled "Selected Values of Chemical Thermodynamic Properties" and issued in February, 1952) or the various volumes of the National Nuclear Energy Series (published by the McGraw-Hill Book Company, Inc.). This paper discusses only recent work that appears to be of special significance, experimental or calculated values that have not been published previously in standard journals, and correlations of properties.

The individual elements are considered first.

THERMODYNAMIC PROPERTIES OF INDIVIDUAL HEAVY ELEMENTS

Actinium

The summary publications mentioned above give no thermodynamic functions for actinium derived from experimental data. Separation of the element in the form of pure compounds was not accomplished until 1950, when milligram amounts of the twenty-year isotope Ac^{227} were produced by neutron irradiation of Ra^{226}.[1,2] The preparation of the metal and the determination of its crystal structure and approximate melting point are reported in recent publications.[3,4]

* Radiation Laboratory, University of California, Berkeley, California.

Actinium Metal

Crystal structure: face-centered cubic, with $a_0 = 5.311$ Å.[4] The metallic radius is 1.88 Å, 0.1 Å larger than that of thorium in the metallic state and 0.01 Å larger than that of lanthanum in the β or face-centered cubic form. The metallic radius is somewhat smaller than might be expected from the difference between the crystal radius of Ac^{+3} and that of La^{+3}, but the valence in the metal appears to be close to +3.

Entropy at 25°C (estimated): 14 cal mol^{-1} deg^{-1}.

Melting point: 1323 ± 50°K.[3]

Entropy of fusion (estimated): 2.0 cal mol^{-1} deg^{-1}.

Heat of fusion: approximately 2.6 cal mol^{-1}.

Heat of vaporization (from the liquid state): estimated to be 10 cal more positive than that of americium,[5] or 70 kcal mol^{-1}.

Entropy of vaporization (from the liquid state): estimated as 22 cal mol^{-1} deg^{-1} at ~1300°K.

Actinium Trifluoride

Heat of formation at 298°K: approximately —477 kcal mol^{-1} is a lower limit consistent with the formation of actinium metal by reduction of trifluoride with $Li_{(g)}$ at 1473°K, after application of estimated high-temperature heat content and entropy increments for the metal and trifluoride. A check by means of the Born-Haber cycle, based on the calculated crystal energy of AcF_3 and an estimate of ionization potentials, gives —420 kcal mol^{-1} for the heat of formation.

Actinium Trichloride

Heat of formation at 298°K: —271 kcal mol^{-1} is a lower limit consistent with the reduction of $AcCl_{3(c)}$ to metal with potassium vapor at ~800°K.

Actinium Oxyfluoride

Heat of formation at 298°K: —265 kcal mol^{-1} is a lower limit imposed by a consideration of the equilibrium at 1000°K for the reaction

$$AcF_3 + H_2O_{(g,\ p\ =\ 0.01\ atmos.)} = AcOF_{(c)} + 2HF_{(g)}$$

which evidently lies far to the left, since no oxyfluoride is detected. The reaction would be expected to proceed rapidly if $p_{HF_g} = 10^{-4}$ atmosphere. Corrections for high-temperature heat content and entropy increments give ~—265 kcal mol^{-1} as stated above.

Thorium

Although thorium has been available in substantial amounts for many years, there have been relatively few careful studies of its thermodynamic properties.

Thorium Metal

Entropy: 12.76 cal mol^{-1} deg^{-1}. This value is derived from measurements of the heat capacity of thorium metal in the range 15° to 300°K,[6] and excludes nuclear and possible electronic-spin contributions. Of particular interest is the absence of a significant anomaly such as is found with cerium in the range 130° to 180°K. It appears that there are no f electrons in the metal, consistent with the $6d^27s^2$ ground state configuration assigned to ThI from studies of the emission spectrum.[7] States based on f configurations lie at considerably higher energies than the ground state.[7]

Crystal structure: a new allotropic form of thorium, body-centered cubic, appearing above 1400 ± 25°C, has been reported.[8]

Thorium Oxide

Entropy: 15.59 cal mol^{-1} deg^{-1} at 298°K. This value is derived from low-temperature heat-capacity measurements[9] and is of special interest as a representative value for the lattice entropies of the heavy-element dioxides, permitting close estimation of entropy contributions due to the presence of unpaired electrons in the 5f subshell of heavier elements.

Heat of formation: − 293.2 kcal mol^{-1}. The value is based on recent careful measurements[10] of the heat of combustion of pure metal. The extreme stability of the dioxide is one of the fundamental sources of difficulty in thorium metallurgy, since, in general, refractory oxides are attacked by thorium metal at high temperatures.

Vapor pressure: The relation

$$\log P_{mm} = \frac{-3.71 \times 10^4}{T} + 11.53$$

derived from experimental data on the vapor pressure of ThO_2 at high temperatures,[11] has significant applications to technolngical processes involving the use of thoria as a refractory.

Thorium Halides

Heats of formation at 298°K: −206 kcal mol^{-1} is reported[12] for the tetraiodide from a study of the equilibrium

$$Th_{(c)} + 4I_{(g)} = ThI_{4(g)}$$

as a function of temperature; −156 ± 2 kcal mol^{-1} may then be derived for the heat of formation of the triiodide by a consideration of the conditions reported[13] for the disproportionation of the tetraiodide; −190 ± 2 kcal mol^{-1} is the value calculated for the heat of formation of the trichloride from analogous considerations.

Aqueous Ions

Heat of formation of $TH^{+4}_{(aq)}$: −184.4 kcal mol^{-1}. This value deserves emphasis although it was reported some years ago,[14] since it is a basic value for the calculation of standard heats of formation of other aqueous thorium species.

Protactinium

Although a number of notable advances have been made in recent years in the knowledge of the chemistry of protactinium, only a few thermodynamic properties may be estimated from available data.

Protactinium Metal

Crystal structure: body centered tetragonal.[15] The metallic radius, calculated for coordination number 12, is 1.63 A, close to that expected for a valence of +5 in the metal, which therefore probably has no f electrons.

Entropy at 298°K: 11 cal mol^{-1} deg^{-1}. This value is estimated from trends in entropies of neighboring elements.

Melting point: undetermined, but consideration of the conditions used to produce agglomerated metal[16] suggests an upper limit of 1873°K for the melting point.

Protactinium Tetrafluoride

Heat of formation at 298°K: −477 kcal mol^{-1} is deduced from a consideration of the conditions used to reduce the tetrafluoride to metal with barium vapor at 1773°K and the application of estimated high-temperature heat-content and entropy increments for the substances involved in the reaction.

$Pa(IV)_{(aq)}$ and $Pa(V)_{(aq)}$

Entropy of $Pa(V)_{(aq)}$: +5 cal mol^{-1} deg^{-1}. This value is estimated on the basis of recent studies by Welch,[17] which have been interpreted by him as indicating a PaO_2^+ structure for pentapositive protactinium in solution.

Potential of the $Pa(IV) = Pa(V) + e^-$ couple: +0.1 ± 0.3v from recent studies[18] of Pa(IV) in aqueous solution.

Uranium

Uranium Metal

Heat of vaporization: 106.7 kcal mol^{-1} for liquid uranium in the neighborhood of 1600°K.

Heat of fusion: 4.7 ± 0.2 kcal mol^{-1}. Both values are taken from the work of Rauh and Thorn,[19] who noted a pronounced effect of very slight pressures (10^{-6} to 10^{-7} mm) of residual oxygen on the vapor pressure. Their experience suggests that other data on the vapor pressures of heavy element metals may be substantially in error.

Uranium Oxides

Heats of formation of UO_2 and U_3O_8 at 298°K: −259.1 and −853.5 cal mol^{-1}, respectively.[20]

Entropy of UO_2. The magnetic entropy effects noted in UO_2 by Jones, Gordon, and Long[21] are of general significance in heavy-element thermodynamics, as the majority of the heavy-element compounds are paramagnetic, and low-temperature heat-capacity anomalies may be expected because of splitting of the degegenerate ground-state level by the crystalline field of the surrounding ions. Other effects, however, due to exchange interaction and quadrupole forces, exist also. Undoubtedly much more experimental work and theoretical development will be required before these effects can be thoroughly understood.

Uranium Halides

Entropy of UF_4: From their measurements of the heat capacity of UF_4 and the assumption that the lattice entropies of ThF_4 and UF_4 would be expected to be the same within a fraction of an entropy unit, Lohr, Osborne, and Westrum[22] conclude that earlier measurements of the heat capacity of UF_4 by Brickwedde, Hoge, and Scott[23] were not extended to sufficiently low temperatures to reveal an expected magnetic anomaly below 20°K.

Aqueous Solutions

Activity coefficients and heat of dimerization of uranyl fluoride: activity coefficients of UO_2F_2 have been determined recently,[24,25] and evidence was obtained for association of the fluoride to form a dimer. The heat of dimerization has a small positive value.

Activity coefficients of uranyl sulfate: Conductances of uranyl sulfate solutions at concentrations of 10^{-4} to 7.28 normal and at temperatures from 0° to 200°C have been measured by Brown, Bunger, Marshall, and Secoy,[26] who tabulate activity-coefficient data for these solutions.

Neptunium

Neptunium Dioxide

Entropy and enthalpy of neptunium dioxide: 19.19 ± 0.1 cal mol^{-1} deg^{-1} and 2770 ± 15 cal at 298.16°K, respectively. These values were determined by low-temperature heat-capacity measurements.[27] A pronounced hump in the heat capacity curve at 25.3°K is attributed to the incidence of antiferromagnetism.

Neptunium Pentachloride

Heat of formation: Failure to form $NpCl_5$ from Np_2O_5 and Cl_2 at 500°K, noted by Gibson, Gruen, and Katz,[28] indicates that the presently accepted value of − 246 ± 2 cal for the heat of formation of $NpCl_5$ is considerably too negative.

Neptunium Solutions

Np(V)-Np(IV) couple: The formal potential of the reaction

$$NpO_{2(aq)}^{+} + \tfrac{1}{2}H_{2(g)} + 3H^{+} = Np_{(aq)}^{+4} + 2H_2O_{(l)}$$

has been calculated by Magnussun and Huizenga[29] from their study of the reduction of $NpO_{2(aq)}^{+}$ by Fe^{+2}. The potential is given as 0.738 v at 25°C, and the partial molal heat as −35.3 kcal mol^{-1}. It is to be noted that the difference in the partial molal entropies of Np(IV) and Np(V) which they derive from their data is substantially different from that given by the values listed by Latimer.[30]

Neptunium oxalate complex: A study by Gruen and Katz[31] of the temperature dependence of the equilibrium between $NpO_{2(aq)}^{+}$ and oxalate ion at various hydrogen ion concentrations gives a value of 0.0 ± 0.3 kcal for the heat of the reaction

$$NpO_{2(aq)}^{+} + C_2O_{4(aq)}^{-} = NpO_2C_2O_{4(aq)}^{-}$$

Plutonium

Plutonium Metal

Crystal structure: Five allotropic modifications of Pu metal are reported to exist in the temperature range 136° to 480°C.[32,33] The complicated structure of the metal makes any estimate of the entropy highly uncertain. The entropy cannot be determined from third-law measurements on Pu^{239}, because of the large amount of radioactive heating. Such measurements may eventually be possible with the 500,000-year isotope, Pu^{242}.

Magnetic susceptibility: 2.52 × 10^{-6} cgs unit per gram is reported[34] for the magnetic susceptibility of metallic plutonium at 20°C. The susceptibility of two samples was nearly independent of temperature, while a third showed a rapid decrease with decreasing temperature. The magnetic data gave indications of structure transitions at 119°, 205°, and 300°C.

Plutonium Tetrafluoride

Heat of formation at 298°K: −400 kcal mol^{-1} has been calculated from a study[35] of the equilibrium

$$3PuF_{4(c)} + PuO_{2(s)} = 4PuF_{3(c)} + O_{2(g)}$$

but the extreme state of subdivision of the oxide required to achieve reversibility in the reaction may have substantially altered the heat content of this material as compared with its macrocrystalline state.

Plutonium Pentafluoride

The same investigation[35] also provided evidence for the disproportionation of PuF_4 into PuF_3 and PuF_5 at elevated temperatures, confirming earlier work, but the product PuF_5 was not definitely characterized. The thermodynamic properties of the pentafluoride remain uncertain.

Sodium Plutonyl Acetate

Electronic configuration of the PuO_2^{++} ion: paramagnetic resonance absorption studies of single crystals of sodium plutonyl acetate[36] show definitely that there are two f electrons in this salt, and thus there is no evidence for a $6d$ electron configuration in any heavy-element compound of plutonium contrary to deductions made previously from magnetic-susceptibility data. A theoretical analysis of the susceptibility

data by Elliott[37] has shown that it is compatible with 5*f* rather than 6*d* electrons.

Aqueous Solutions

Oxidation potentials of aqueous couples: Slight revisions of previously published values for the oxidation potentials of plutonium have been made by Connick and McVey[38] to correct for autoreduction of plutonium due to alpha irradiation. Current values for the formal potentials of the plutonium (III-VI) and (IV-VI) couples in 1 *M* $HClO_4$ are -1.043 ± 0.003, and -1.002 ± 0.002 v, respectively; and -1.053 ± 0.003, and -1.025 ± 0.002 v, respectively in 1 *M* HCl.

Americium

Amoricium Metal

Heat of vaporization: 60.2 kcal mol^{-1} is reported[39] for the heat of vaporization of the liquid at around 1200°K.

Americium Trifluoride

Heat and free energy of vaporization: Measurements of the vapor pressure of americium trifluoride at elevated temperatures[40] give values of $\Delta H_0^\circ = -112{,}670 \pm 20$ cal mol^{-1} and $I = -155.50 \pm 0.05$ cal mol^{-1} deg^{-1} for the constants in the equation for free energy of sublimation,

$$\Delta F_{sub}^\circ = \Delta H_0^\circ - 2.3\ (-14)\ T \log T - IT$$

Entropy of sublimation at high temperature: less positive than that for the sublimation of PuF_3 by 1.5 cal mol^{-1} deg^{-1}.

Aqueous Ions

Heats of formation of $AmO_{2(aq)}^+$ and $AmO_{2(aq)}^{+2}$: -207.8 ± 2.9 and -171.0 ± 2.7 cal mol^{-1}, respectively.[40] Feay[41] calculates that the entropies of $AmF_{3(aq)}$ and $AmF_{2(aq)}^+$ are 17.6 ± 4 and -11.9 ± 4 cal mol^{-1} deg^{-1}, respectively.

Curium

Entropies of $CmF_{3(aq)}$ and $CmF_{2(aq)}^+$: 18.9 and -12.1 cal mol^{-1} deg^{-1}, respectively.[41]

Higher Elements

No elements of atomic number higher than 96 have been isolated as yet in the form of pure compounds, and thermodynamic studies will not be possible until these higher elements are available in greater abundance.

TRENDS IN THERMODYNAMIC PROPERTIES OF THE HEAVY ELEMENTS

Thermodynamic properties that have not been measured experimentally are often estimated by extrapolation or interpolation of established values which appear to follow some regular trend as a function of atomic number. Such trends are evident in the heavy elements, as is illustrated in Fig. 1, in which the free energies of formation of the aqueous ions M^{+3}, M^{+4}, MO_2^+, MO_2^{+2} are plotted as a function of atomic number.

The nearly regular increase in stability of the tripositive state and the decreasing stability of higher states is very clearly evident.

In Fig. 2 are plotted the free energies of various oxidation-reduction couples of the heavy elements as a function of atomic number. Unlike the values plotted in the previous figure, the free energies of the couples are independent of the free energies of fusion and sublimation of the metals.

A smooth trend is evident in the free energy of the $M^{+3} = M^{+4} + e^-$ couple (where M = a heavy element) through element 95. A discontinuity appears at element 97, almost certainly owing to the decrease in the ionization potential just beyond the point of half filling of the 5*f* subshell. Before this point is reached, the increase in the fourth ionization potential appears to increase slightly more rapidly than the difference in hydration energies between the tri- and tetrapositive ions.

In contrast to the behavior of the couple $M^{+3} = M^{+4} + e^-$, the M^{+4}—MO_2^+ couple remains much more nearly constant as a function of atomic number, indicating that the stability of the oxygenated ion increases at about the same rate as the fifth ionization potential.

It is to be noted that when a couple involves oxidation to an ion with a noble-gas structure—Pa(IV) to Pa(V), for example—the free energy of that couple is abnormally small. If account is taken of this fact, the trend of the oxidation-reduction couples of the heavy elements is seen to be remarkably regular, suggesting a regular progression of ionization potentials due to the progressive filling of an inner subshell.

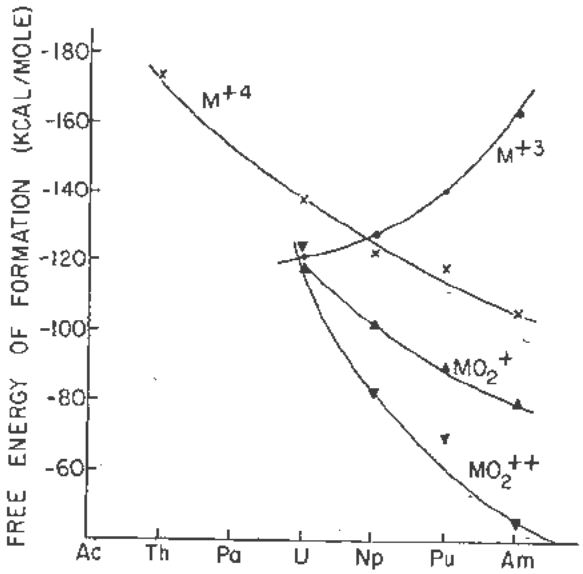

Figure 1. Free energies of formation of some aqueous ions of the heavy elements (plus 113.4 kcal mol^{-1} for the ions MO_2^+ and MO_2^{++})

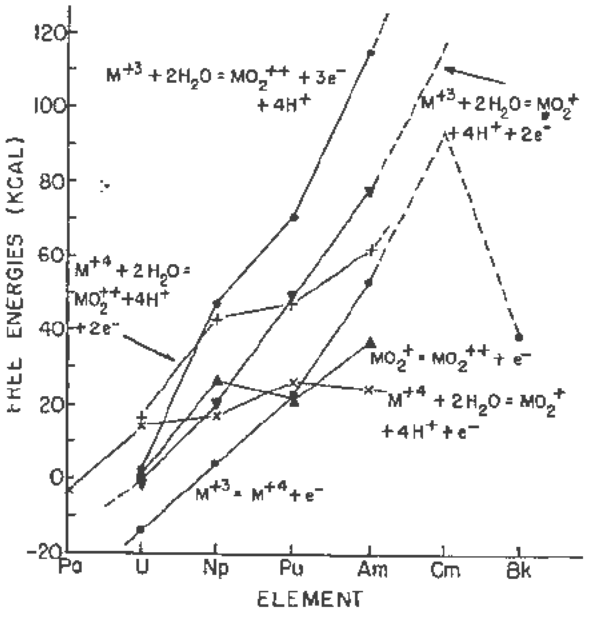

Figure 2. Free energies of various oxidation-reduction couples of the heavy elements

Some mention should be made here of the estimation of thermodynamic properties from the "constant difference" principle. For example, it has often been assumed that the difference between the heats of formation of $CmCl_3$ and CmF_3 is the same as the difference between the heats of formation of UCl_3 and UF_3 or of $PuCl_3$ and PuF_3.

A study[42] of the high-temperature hydrolysis of lanthanide and actinide trihalides has shown that this assumed relation may be in error by many kilocalories.

In conclusion, it may be remarked that there is a great practical need for further work on heavy-element thermodynamics, particularly over extended ranges of temperature and pressure in concentrated aqueous solutions, so that the results may be applied directly to chemical problems associated with the operation of certain types of nuclear reactors.

REFERENCES

1. Hagemann, F. T., *The Isolation of Actinium*, J. Am. Chem. Soc. 72: 768 (1950).
2. Fried, S., Hagemann, F. T. and Zachariasen, W. H., *The Preparation and Identification of Some Pure Actinium Compounds*, J. Am. Chem. Soc. 72: 771 (1950).
3. Stites, J. A., Jr., Salutsky, M. L. and Stone, B. D., *Preparation of Actinium Metal*, J. Am. Chem. Soc. 77: 237 (1955).
4. Farr, J. D., Giorgi, A. L., Money, R. K. and Bowman, M. G., *The Crystal Structure of Actinium Metal and Actinium Hydride*, Los Alamos Scientific Laboratory Declassified Report LA-1545 (1953).
5. Carniglia, S. C. and Cunningham, B. B., *The Vapor Pressure of Americium Metal*, J. Am. Chem. Soc. 77: 1502 (1955).
6. Griffel, M. and Skochdopole, R., *The Heat Capacity and Entropy of Thorium from 18 to 300°K*, J. Am. Chem. Soc. 75: 5250-1 (1953).
7. Stokenbrocker, G. L. and McNally, J. R., *Isotope Shifts in Thorium—Thorium*^{230} *and Thorium*^{232}, J. Optical Soc. Am. 43: 36-41 (1953).
8. Chiotti, P., *Thorium-Carbon System*, Iowa State College J. Sci., 26: 185-6 (1952).
9. Hubner, E. J., Holley, C. E., Jr. and Meierkord, E. H., *The Heats of Combustion of Thorium and Uranium*, J. Am. Chem. Soc. 74: 3406-8 (1952).
10. Osborne, D. W. and Westrum, E. F., Jr., *The Heat Capacity of Thorium Dioxide from 10 to 305°K. The Heat Capacity Anomalies in Uranium Dioxide, and Neptunium Dioxide*, J. Chem. Phys. 21: 1884-7 (1953).
11. Shapiro, E., *Vapor Pressure of Thorium Oxide from 2050 to 2250°K*, J. Am. Chem. Soc. 74: 5233-5 (1952).
12. Allen, T. L. and Yost, D. N., *Equilibria in the Formation of Molybdenum and Thorium Iodides from the Elements*, J. Chem. Phys. 22: 855 (1954).
13. Hayek, E., Rehner, T. and Frank, A., *Halides of Bivalent and Trivalent Thorium*, Monatsch. 82: 575-87 (1951).
14. Eyring, L. and Westrum, E. F., Jr., *The Heat of Formation of Thorium Tetrachloride*, J. Am. Chem. Soc. 72: 5555-5556 (1950).
15. Zachariasen, W. H., *Identification and Crystal Structure of Protactinium Metal and of Protactinium*, Acta Cryst. 5: 17-19 (1952).
16. Seaborg, G. T. and Katz, J. J., editors. *The Actinide Elements*, National Nuclear Energy Series, Plutonium Project Record, Vol. 14A, McGraw-Hill Book Co., Inc., New York (1954), Chapter 5 by Elson, R. E., "The Chemistry of Protactinium".
17. Welch, G. A., *Protactinyl Ion*, Nature 172: 458 (1953).
18. Fried, S. and Hindman, J. C., *The +4 Oxidation State of Protactinium in Aqueous Solution*, J. Am. Chem. Soc. 76: 4863 (1954).
19. Rauh, E. G. and Thorn, R. J., *Vapor Pressure of Uranium*, J. Chem. Phys. 22: 1414-20 (1954).
20. Hubner, E. J., Holley, C. E., Jr. and Meierkord, E. H., *The Heats of Combustion of Thorium and Uranium*, J. Am. Chem. Soc. 74: 3406 8 (1952).
21. Jones, W. M., Gordon, J. and Long, E. A., *The Heat Capacities of Uranium, Uranium Trioxide, and Uranium Dioxide from 15°K to 300°K*, J. Chem. Phys. 20: 695-9 (1952).
22. Lohr, H. R., Osborne, D. W. and Westrum, E. F., Jr., *Thermodynamic Properties of Thorium Tetrafluoride from 5 to 300°K and the Magnetic Entropy of Uranium Tetrafluoride*, J. Am. Chem. Soc. 76: 3837 (1954).
23. Brickwedde, F. G., Hoge, H. J. and Scott, R. B., *The Low-Temperature Heat Capacities, Enthalpies, and Entropies of UF_4 and UF_6*, J. Chem. Phys. 16: 429 (1948).
24. Johnson, J. S. and Kraus, K. A., *Activity Coefficients of Uranyl Fluoride from Freezing Point Depressions: Undissociated Species and Dimerization*, J. Am. Chem. Soc. 74: 4436-9 (1952).
25. Johnson, J. S., Kraus, K. A. and Young, Fraser T., *Determination of Activity Coefficients by Ultracentrifugation. Ultracentrifugation of Uranyl Fluoride Solutions*, J. Am. Chem. Soc. 76: 1436-43 (1954).
26. Brown, R. D., Bunger, W. B., Marshall, W. L. and Secoy, C. H., *The Electrical Conductivity of Uranyl Sulfate in Aqueous Solution*, J. Am. Chem. Soc. 76: 1532-5 (1954).

27. Westrum, E. F., Jr., Hatcher, J. B. and Osborne, D. W., *The Entropy and Low-Temperature Heat Capacity of Neptunium Dioxide*, J. Chem. Phys. 21: 419 23 (1953).

28. Gibson, G., Gruen, D. M. and Katz, J. J., *Some Observations on Neptunium (V) Compounds*, J. Am. Chem. Soc. 74: 2103-4 (1952).

29. Magnusson, L. B. and Huizenga, J. R., *Stabilities of +4 and +5 Oxidation States of the Actinide Elements: The Np(IV)—Np(V) Couple in Perchloric Acid Solution*, J. Am. Chem. Soc. 75: 2242-6 (1953).

30. Latimer, W. M., *Oxidation Potentials*, Second Edition, Prentice-Hall, Inc., New York (1952).

31. Gruen, D. M. and Katz, J. J., *Spectrophotometric Study of Np(V) Oxalate Complexes*, J. Am. Chem. Soc. 75: 3772-6 (1953).

32. Lord, W. B. H., *Some Physical Properties of Metallic Plutonium*, Nature 173: 534-5 (1954).

33. Ball, J. G., Robertson, J. A. L., Mardon, P., Lee, J. A. and Adams, E. T., *Some Physical Properties of Metallic Plutonium*, Nature 173: 535 (1954).

34. Dawson, J. K., *Magnetochemistry of the Heaviest Elements. VIII. Metallic Plutonium*, J. Chem. Soc. (1954), 3393-6.

35. Dawson, J. K., Elliott, R. M., Hurst, R. and Truswell, A. E., *The Preparation and Some Properties of Plutonium Fluorides*, J. Chem. Soc. (1954), 558-64.

36. Hutchinson, C. A., Jr. and Lewis, B. W., *Paramagnetic Resonance Absorption in Sodium Plutonyl Acetate*, Phys. Rev. 95: 1096 (1954).

37. Elliott, R. J., *A Theory of the Paramagnetism of Uranyl-like Ions*, Phys. Rev. 89: 659-60 (1953).

38. Connick, R. E. and McVey, W. H., *Disproportionation Equilibria and Rates in Perchloric and Hydrochloric Acid Solutions of Plutonium: Influence of α-Particles*, J. Am. Chem. Soc. 75: 474-9 (1953).

39. Carniglia, S. C. and Cunningham, B. B., *The Vapor Pressure of Americium Metal*, J. Am. Chem. Soc. 77: 1502 (1955).

40. Gunn, S. R., *Thermodynamics of the Aqueous Ions of Americium*, Ph.D. Thesis, University of California Radiation Laboratory Declassified Report UCRL-2541 (1954).

41. Feay, D. C., *Some Chemical Properties of Curium*, Ph.D. Thesis, University of California Radiation Laboratory Declassified Report UCRL-2547 (1954).

42. Koch, C. W. and Cunningham, B. B., *The Vapor Phase Hydrolysis of the Rare Earth Halides. III. Heat and Free Energy of the Reactions* $PrCl_3(s) + H_2O(g) = PrOCl(s) + 2HCl(g)$ *and* $NdCl_3(s) + H_2O(g) = NdOCl(s) + 2HCl(g)$. J. Am. Chem. Soc. 76: 1471 (1954).

Electronic Configuration of the Actinide Elements

By J. K. Dawson and G. R. Hall,* United Kingdom

Bohr first suggested that a series of elements might exist in which electrons would populate the 5*f* energy levels, the properties of these elements resembling those of the lanthanides.[1] Several authors later attempted to predict the exact point in the periodic table at which the new series would be expected to begin, but much of the relevant experimental information did not become available until after the discovery of the transuranium elements. Seaborg reviewed these early predictions together with the considerable amount of evidence obtained in the United States atomic energy programme and in 1949 he put forward the "actinide concept", extrapolating back from the marked similarities between the properties of, for instance, curium and gadolinium, to predict that the first 5*f* electron might appear in thorium.[2] Protoactinium might then have two, and uranium three, unpaired electrons in the 5*f* shell.

At about the same point in the periodic table, it is also expected that electrons might enter the 6*d* energy levels, giving rise to another group of elements similar to the transition series. Most of the evidence from which deductions have been made on the conflicting claims of the 5*f* and 6*d* energy levels has been derived from observation not of the elements themselves but of their ions. Thus, the main evidence which led Seaborg to put forward the proposition that the elements of atomic weight higher than actinium form a series in which electrons successively enter the 5*f* energy level was derived from X-ray diffraction data, absorption spectra, chemical properties and magnetic investigations. Ions which contain unpaired electrons possess a permanent magnetic moment which may be measured by effects produced in a magnetic field. This magnetic moment includes contributions from both the orbital and the spin motions of the electrons. If Hund's rule applies to these heavy element ions, then each additional electron in excess of the radon core will enter the most stable electron shell so as to maintain maximum multiplicity of the spin quantum number. For the 5*f* shell, therefore, the electrons should not begin pairing until seven sub-states have been filled; for the 6*d* shell, five sub-states, by analogy with the well-known lanthanide and transition groups respectively. The magnetic moments of the lanthanides are close to those which may be predicted for the ideal gaseous state because the 4*f* electrons lie predominantly below the surface of the peripheral electrons and consequently are relatively free from interaction with surrounding ions. On the other hand, the magnetic moments of the transition element ions are considerably modified by exchange forces acting on the unshielded *d*-shell electrons; the moments then consist almost entirely of the electron spin contribution, the orbital moment having been quenched out. Consequently, comparison of the magnetic properties of the heavy element ions with the differing types of behaviour known to be associated with *f*- and *d*-shell electrons should prove a useful approach to the problem of their electron configurations.

A considerable amount of magnetic data has become available since Seaborg's paper, and this was reviewed up to 1952 by Dawson.[3] At that time there appeared to be reasonable agreement between the observed magnetic properties and those predicted on the basis of 5*f* electrons for the following ions with four, five and seven unpaired electrons: Pu^{4+}, Pu^{3+} and Cm^{3+}. This agreement will be discussed briefly below, together with further information which has recently become available on some of the ions which have one and two unpaired electrons.

The magnetic susceptibility temperature behaviour of trivalent samarium is unique in the way it deviates from the Curie-Weiss law, there is a shallow susceptibility minimum in the region of 400°K. Van Vleck was able to explain this by allowing for a contribution to the magnetic moment from energy levels not greatly above the ground state.[4] A similar type of behaviour has been shown to exist for trivalent plutonium, the susceptibility minimum observed on the fluoride and the chloride being at about 520°K.[5] Since the magnetic behaviour of ions having the same number of electrons in *d*-levels is entirely different from this, it is reasonable to suppose that the magnetic electrons in the Pu^{3+} ion are in 5*f* orbitals rather than in 6*d* orbitals.

Magnetic susceptibility measurements made on the quadrivalent plutonium ion, Pu^{4+}, in dilute mixed crystals of the fluoride with isomorphous thorium tetrafluoride have shown that extrapolation to infinite dilution gives a moment close to the theoretical value for four unpaired *f*-electrons in the ideal gaseous state, but quite different from the spin-only value to be expected for the same number of *d*-electrons.[6] Finally, Crane using only 30–50 μgm of curium trifluoride found that the susceptibility of Cm^{3+} was very high and comparable with the extremely high

* Atomic Energy Research Establishment, Harwell.

value for trivalent gadolinium, but was not in good agreement with the observed properties of, for instance, the cobaltous ion which has seven electrons in the $3d$ shell.[7]

For these three heavy element ions the electron configurations deduced from the observed magnetic properties are in agreement with the known chemical properties, but in the case of the ions having only one or two unpaired electrons the situation is more complex since both the chemical and the magnetic evidence show some characteristics of both f- and d-level electrons.

A considerable number of measurements have been reported on the quadrivalent uranium and the hexavalent plutonium ions, U^{4+} and PuO_2^{2+}, both of which contain two unpaired, magnetic electrons.[8] In most compounds the magnetic susceptibility of U^{4+} is either equal to or close to the spin-only value to be expected for two unpaired d-electrons, and this is true also in very dilute solutions of the tetrafluoride and dioxide in the corresponding thorium compounds. The plutonyl ion in solution[9] and in solid sodium plutonyl acetate[10] similarly shows the spin-only value and by analogy with the transition elements this was taken in the previous review[3] to imply a $6d$ electron configuration. On this type of evidence it was postulated that the last row of elements in the periodic table could be sub-divided, so that ions having only one or two unpaired electrons accommodated them in the $6d$ shell, whereas in ions having more than three unpaired electrons the $5f$ levels were stabilised. Recently, however, detailed calculations have been made on the magnetic properties of the neptunyl and plutonyl ions by Elliott[11] and by Eisenstein and Pryce,[12] and they have shown that the spin-only susceptibility PuO_2^{2+} is consistent with a $5f^2$ electron configuration. The basis for this conclusion is given below.

Uranium has six unpaired electrons in excess of the closed radon core, and in the formation of the linear uranyl complex ion two of these are lost by ionisation and the remaining four are used to form covalent bonds with the oxygen atoms. The bonding in this complex was discussed by Eisenstein and Pryce. It involves two σ-type hybrid orbitals made up from the $5f$, $6d$ and $7s$ orbitals of the uranium, using the sub-states with $m_l = 0$. In this way two orbitals are produced which are strongly directional towards the two oxygen atoms and which bond with the latter by overlap with their sp_σ hybrid orbitals. The bonds formed are symmetrical about the O-U-O axis. The uranyl ion has no residual unpaired electrons and is only very weakly paramagnetic.

Both Elliott and Eisenstein and Pryce observed that in the uranyl-like complexes, the strong electric field associated with the O-U-O bonding should simplify considerably the calculation of magnetic and optical properties. Thus, whilst in the case of the transition elements the magnetic properties are strongly influenced by the crystal field due to surrounding ions, in these complexes the field due to the bonding electrons is the dominating factor.

The neptunyl ion, NpO_2^{2+}, is structurally similar to UO_2^{2+} but contains one unpaired electron. By assuming that this is an f electron the energy levels which could be available for it are those with $m_l = \pm 3$, ± 2, ± 1 ($m_l = 0$ having been used in bonding to the oxygen). These states will have different energies but, because of the repelling effect of the bonding electrons along the O-Np-O axis the state of lowest energy is $m_l = \pm 3$. This is due to the fact that in this state the electron distribution is the most concentrated in the equatorial plane and is also concentrated furthest away from the O-Np-O axis. On this basis, the predicted anisotropic g-values are $g_\parallel = 4$, $g_\perp = 0$, and the derived magnetic susceptibility is fairly close to that determined experimentally[13] ($\mu_{exp} = 1.85$, $\mu_{theor} = 2$ Bohr magnetons).

In the plutonyl ion, two unpaired electrons have to be accommodated. Again on the assumption that these are f-electrons, there appear to be two reasonable alternatives: (a) the electrons occupy the states $m_l = \pm 3$, ± 2, respectively, with the spins parallel i.e., giving the maximum multiplicity as expected from Hund's rule, or (b) if the repelling effect of the O-Pu-O bonding electrons is sufficiently strong the electrons may go into the states $m_l = +3$, -3, again with spins parallel. As Bleaney[14] has observed, both these alternatives give rise to a magnetic susceptibility close to the spin-only value and measurements on powder samples cannot therefore distinguish between them. However measurements on a single crystal of, for example, rubidium plutonyl nitrate ($RbPuO_2(NO_3)_3$) would. This is because only the first alternative would give a strong anisotropic susceptibility ($L = 5$), whereas in the second the anisotropy would be small ($L = 0$).

Although magnetic susceptibility measurements on suitable single crystals containing neptunium and plutonium have not been made, paramagnetic resonance measurements have been described and these have led to complete confirmation of the theory of Eisenstein and Pryce. The salt, rubidium uranyl nitrate in which small amounts of either neptunyl (NpO_2^{2+}) or plutonyl (PuO_2^{2+}) ions have isomorphously replaced uranyl (UO_2^{2+}) ions is particularly suitable for such measurements. This salt crystallises in the hexagonal system with all the uranyl ions identical and lying parallel to the c-axis. Paramagnetic resonance experiments on single crystals of this salt have been described by Bleaney, Llewellyn, Pryce and Hall.[15,16,17] The observed spectroscopic splitting factors for the plutonyl[15,16] ion were $g_\parallel = 5.32$, $g_\perp = 0$, which are in reasonable agreement with the values derived theoretically i.e., $g_\parallel = 6$, $g_\perp = 0$, on the assumption that the magnetic electrons are in $5f$ energy levels with $m_l = \pm 3$, ± 2. Paramagnetic resonance absorption measurements on a single crystal of sodium uranyl acetate containing 2% of sodium plutonyl acetate and on a crystal of the pure plutonyl salt by Hutchison and Lewis[18] have pro-

duced a similar result and their observed splitting factors are $g_{\parallel} \approx 5.9$, $g_{\perp} \approx 0$.

Similar experiments have been described by Bleaney *et al.*[17] for neptunium. Thus a crystal of rubidium uranyl nitrate containing about 1% of the isotope Np^{237} has been examined and the spectroscopic splitting factors $g_{\parallel} = 3.41$, $g_{\perp} = 0.21$ were obtained. There is not such good agreement between these and the theoretically predicted values of $g_{\parallel} = 4$ and $g_{\perp} = 0$, but Bleaney[14] has pointed out that closer agreement is possible by modifying the theory to take account of possible overlap between the wave functions of the magnetic electrons with orbitals from the oxygen atoms of the complex. This amounts to allowing for a certain amount of bonding in addition to the σ-bond earlier described. This would have the effect of reducing the orbital moment of the magnetic electrons, hence also $g_{\parallel}$ would be smaller.

Finally, paramagnetic resonance has been reported on powdered samples of uranium trifluoride and uranium tetrafluoride by Ghosh, Gordy and Hill.[18] The spectroscopic splitting factors for trivalent uranium were given as $g_{\parallel} \approx 2.8$, $g_{\perp} \approx 2.1$. Experimental results obtained on such magnetically concentrated materials are always difficult to correlate with theory, but O'Brien[20] has recently considered uranium trifluoride. Calculations were made of the effect of the crystal field on several possible electronic configurations. For a configuration $5f^3$, with ground state[4] $I_{9/2}$, values of $g_{\parallel} = 2.6$, $g_{\perp} = 1.8$, which are reasonably close to the observed results, were obtained. For the configuration $6d^3$ it would appear likely that the ground state would have $g_{\perp} \approx 0$, as is the case for most ions with $3d^n$, $4d^n$, $5d^n$ configurations; however, if spin-orbit coupling is very important and there is *jj* coupling, then the *g* values of the ground state are $g_{\parallel} = 0.8$, $g_{\perp} = 1.4$.

The considerable amount of information now available on the magnetic properties of the heavy element ions evidently gives strong support to the "actinide concept" of Seaborg (*loc. cit.*). As shown above there is substantial evidence for the following electronic configurations:

Ion	UO_2^{2+}	NpO_2^{2+}	PuO_2^{2+}	U^{3+}	Pu^{4+}	Pu^{3+}	Cm^{3+}
Unpaired $5f$ electrons	0	1	2	3	4	5	7

There, are, however, some outstanding problems which remain to be elucidated. For instance, in many investigations, the magnetic susceptibility of quadrivalent uranium in a magnetically dilute environment has been shown to have a value equal to or very close to the spin-only value for two electrons.[3] In its present form the theory of Eisenstein and Pryce applies specifically to the uranyl-like ions and has not been developed for other types of ions. Similarly there is a superficially closer resemblance of the observed magnetic susceptibility of thorium triodide to that of compounds of the transition elements rather than to compounds of cerium. Uranium metal has been investigated magnetically[21] and the temperature dependence of the susceptibility is similar to that of elements such as iridium rather than the lanthanides. The evidence on plutonium metal is conflicting, different samples having shown different types of behaviour.[22]

It will be of great interest to measure the susceptibilities of the elements beyond curium, if these should become available in weighable amounts, and to investigate the lanthanide analogy as electrons in the $5f$ shell commence to pair. There may be considerable difficulty in making such measurements, however, because of the short half lives involved. For instance, even in sodium plutonyl acetate Dawson[10] found a drop of about 1% per day in the susceptibility for several days. It would appear that this might correspond to some change in the plutonium valency or the crystalline environment caused by the plutonium alpha particle decay. Further measurements have been made recently in rubidium uranyl nitrate and on a 1% solution of rubidium americyl nitrate ($RbAmO_2(NO_3)_3$) in rubidium uranyl nitrate. For the plutonium salt the decrease in susceptibility was initially about 1% per day and then this attained a constant value in two weeks. For the americium compound the susceptibility dropped very rapidly and attained a steady value in less than a day. Unfortunately the amount of americium was so small that only a very small magnetic effect was measurable and no reliable figure was obtained for the susceptibility of the americyl ion directly after the preparation of the salt. It would appear that this greatly increased rate of change in susceptibility compared with that for plutonium is connected with the change in half-life, i.e., 24,000 years for plutonium and 470 years for americium. It is possible that the americyl ion is becoming reduced in the crystal to a lower valency, hence causing the reduction in susceptibility. Such changes occur in aqueous solution for both plutonium and americium; for the americyl ion Hall and Markin[24] found a reduction rate of about 3% per hour due to the formation of reducing products by the alpha particle bombardment of the solution.

REFERENCES

1. Bohr, N., Nature, 112: 30 (1923).
2. Seaborg, G. T., *Place in the Periodic System and Electronic Structures of the Heaviest Elements*, Nucleonics, 5, No. 5: 16 (1949).
3. Dawson, J. K., *Electronic Configurations of the Heaviest Elements*, Nucleonics, 10, No. 9: 39 (1952).
4. Van Vleck, J. H., *Electric and Magnetic Susceptibilities*, Oxford University Press, London, Chapter IX (1932).
5. Dawson, J. K., Mandleberg, C. J. and Davies, D., *Magnetochemistry of the Heaviest Elements, Part IV*, J. Chem. Soc., 2047 (1951).
6. Dawson, J. K., *Magnetochemistry of the Heaviest Elements, Part VI*, J. Chem. Soc., 1882 (1952).
7. Crane, W. W. T., *Some Physical and Chemical Properties of Curium*, University of California Radiation Laboratory Report, U.C.R.L. 1220 (1951).
8. See Dawson, J. K., reference 3.

9. Calvin, M., Kasha, M. and Sheline, G. E., *Magnetic Susceptibilities of Plutonium in its Various Oxidation States in Aqueous Solution,* The Transuranium Elements, N.N.E.S. IV-14B, McGraw-Hill Book Co., New York, 632 (1949).

10. Dawson, J. K., *Magnetochemistry of the Heaviest Elements, Part VII,* J. Chem. Soc., 2705 (1952).

11. Elliott, R. J., *A Theory of the Paramagnetism of Uranyl-like Ions,* Phys. Rev. 89: 659 (1953).

12. Eisenstein, J. C. and Pryce, M. H. L., *The Electronic Structure and Magnetic Properties of Uranyl-like Ions, Part I.* Proc. Roy. Soc. (A), 229: 20 (1955).

13. Gruen, D. M. and Hutchison, C. A., *Magnetic Susceptibilities of Np^{6+}, Np^{5+} and Np^{4+}.* J. Chem. Phys., 22: 286 (1954).

14. Bleaney, B., *Paramagnetism of the Actinide Group.* Paper given at the Faraday Society Discussion on Microwave and Radio-frequency Spectroscopy at Cambridge, April 1955.

15. Bleaney, B., Llewellyn, P. M., Pryce, M. H. L. and Hall, G. R., *Paramagnetic Resonance in Plutonyl Rubidium Nitrate, and the Spin of ^{239}Pu,* Phil. Mag., 45: 773 (1954).

16. Bleaney, B., Llewellyn, P. M., Pryce, M. H. L. and Hall, G. R., *Nuclear Spin of ^{241}Pu,* Phil. Mag., 45: 991 (1954).

17. Bleaney, B., Llewellyn, P. M., Pryce, M. H. L. and Hall, G. R., *Paramagnetic Resonance in Neptunyl Rubidium Nitrate,* Phil. Mag., 45: 992 (1954).

18. Hutchison, Jr., C. A. and Lewis, W. B., *Paramagnetic Resonance Absorption in Sodium Plutonyl Acetate,* Phys. Rev., 95: No. 4, 1096 (1954).

19. Ghosh, S. N., Gordy, W., and Hill, D. G., *Paramagnetic Resonance in Uranium Salts,* Phys. Rev., 96: No. 1, 36 (1954).

20. O'Brien, (Miss) M. C. M., *Magnetic Ground State of UF_5.* Proc. Phys. Soc., 68: 351 (1955).

21. Bates, L. F. and Mallard, J. R., *Magnetic Properties of Uranium and Uranium-Iron Alloys,* Proc. Phys. Soc., 63: 520 (1950).

22. Dawson, J. K., *Magnetochemistry of the Heaviest Elements, Part VIII,* J. Chem. Soc., 3393 (1954).

23. Dawson, J. K. and Hall, G. R., unpublished.

24. Hall, G. R. and Markin, T. L., unpublished.

The Chemistry and Crystal Chemistry of Heavy Element Compounds

By Sherman Fried* and W. H. Zachariasen,† USA

The elements from actinium, $Z = 89$, to curium, $Z = 96$, form a sequence which can best be designated as a "5*f*" series by analogy with the rare earths of 4*f* series.

The recent isolation and/or production of these heavy 5*f* elements in weighable quantities invited the systematic investigation of their chemical properties. Elements such as actinium, thorium, protactinium, and uranium were, of course, known and studied chemically in a cursory fashion for many years, while the elements neptunium, plutonium, americium and curium have been available only since the development of the chain-reacting pile.[1,2,3,4]

It is the purpose of this paper to describe the methods used in the preparation of identifiable compounds of these elements and to discuss the chemical reactions involved. In many cases comparisons can be made between the various elements and the analogies indicated.

It should be pointed out that this series of 5*f* elements constitutes a remarkably regular sequence. The regularity is not only evident in the chemical reactions of these elements but also in the crystal structures of any homologous series of their compounds. This regularity has in many cases made it possible to predict the course of chemical reactions as well as the crystal structures and lattice dimensions of the various compounds.

Many of the elements were, at first, available in only microgram quantities. This, coupled with the fact that some of them were highly radioactive, necessitated the development of techniques which would permit the preparation of compounds in such a manner as to be safe and at the same time to yield the most information. In addition, it was to be expected that many preparations would be reactive with the oxygen or water of the atmosphere, and that reactions would in many cases have to be carried out under anhydrous air-free conditions.

The techniques selected were the ultra-micro methods of Kirk and his group which were developed at the Argonne National Laboratory and were used in conjunction with the X-ray diffraction method of analysis. Using these methods it was possible to prepare compounds of the elements, determine the crystal structures and from this deduce the chemical formulae. Such determinations led, in turn, to the elucidation of the course of the chemical reactions used in the preparations as well as of the oxidation states exhibited by these elements.

In many cases it was possible to prepare these elements in the metallic form, determine some of the properties and examine their behavior with various reagents.

As the work progressed the regularities in crystal structure and chemical reactivity, alluded to above, became more apparent and subsequent work became much easier to interpret. As the backlog of information accumulated, predictions of the reaction of a given reagent or of the lattice dimensions of a compound could be made with great certainty.

In this manner more than sixty compounds of these elements have been prepared and identified. The crystal structures of these compounds and ionic radii of the various elements have been determined.

The several 5*f* elements exhibit various oxidation states. The distribution of oxidation states throughout the 5*f* series is illustrated in Table I, where a definitely identified oxidation state is indicated by a cross or by a circle. A cross is used to designate a bona fide oxidation state capable of existence in solution as well as in the solid state, and it is believed from crystal structure results that the non-bonding valence electrons in these normal oxidation states are all of the 5*f* type. A circle is used to designate what may be termed a subnormal oxidation state characterized by the presence of non-bonding 6*d* electrons. The subnormal oxidation states cannot exist in solution, and the corresponding compounds are apt to show pronounced metallic character. Typical examples[5] of subnormal valence compounds are monoxides and monosulfides, ThI_2, ThI_3 and Th_2S_3. The tripositive oxidation state of uranium and neptunium is of normal type in the trihalides, but of subnormal type in the compounds U_2S_3 and Np_2S_3.

Table I. Observed Oxidation States

	Element							
	Ac	*Th*	*Pa*	*U*	*Np*	*Pu*	*Am*	*Cm*
II		o	o	o	o	o	o	
III	x	o		ox	ox	x	x	x
IV		x	x	x	x	x	o	o
V			x	x	x	x	x	
VI				x	x	x	x	

* Argonne National Laboratory.

† University of Chicago.

The elements in the normal +III oxidation state may be said to form an "actinide"[6] series, with actinium as the prototype element analogous to the lanthanide series for the rare earth elements in the same oxidation state. In contrast to the lanthanide series, there is no unbroken actinide series, for the normal tripositive oxidation state has not been observed for either thorium or protactinium, the known trivalent compounds of thorium being analogous to corresponding compounds of titanium and zirconium rather than to those of actinium.

The tetrapositive oxidation state extends without break from thorium to curium, forming a "thoride" series in which every member is thorium-like. The "protactinide" and the "uranide" series are observed in the same manner in the +V and +VI states,[7] respectively. Every one of the elements uranium, neptunium, plutonium and americium exhibits all the oxidation states from +II to +VI, the +II state being in every instance of subnormal type.

Some isotopes of these elements are too highly radioactive to be used for the study of compound formation. In these cases the intense self-bombardment may destroy the compound or the radiation emitted is so penetrating that the X-ray film is fogged before a diffraction pattern is obtained. Thus, isotopes were chosen with the longest half-life consistent with easy procurement. The isotope Np^{237} is obtained as a by-product in the operation of a reactor[8] and the isotope Cm^{244} with a half-life of about 20 years (compared with a half-life of 162 days for Cm^{242}) by prolonged irradiation of plutonium.[9]

TECHNIQUES

It is important that all equipment used in the preparations be scrupulously clean and all reagents rigorously purified. Small fragments of dirt or other debris represent significant or even overwhelming impurities when compared with microgram quantities of the elements. Small quantities of impurities in reagents may completely alter the course of a reaction.

Preparation of Capillaries for X-ray Samples

In order to obtain satisfactory X-ray diffraction patterns of microgram quantities of a solid in a glass or quartz capillary the wall thickness must not be greater than 0.030 mm. A 20-cm length of clean Pyrex tubing 10–15 mm diameter is heated in a sharp *oxygen-gas* flame and constricted to approximately one-third of its diameter. The constricted portion of the tube is heated with a rather broad *air-gas* flame and then rapidly drawn out into a capillary. Capillaries of 0.100-mm inside diameter with a wall thickness of 0.010 mm may be readily produced with a little practice. A sharp flame may be used to seal off the ends.

Quartz capillaries are produced in much the same manner, except that a sharp *oxy-hydrogen* flame is used for the initial constriction and a more diffuse flame for the final drawing.

A capillary may be filled with solids easily if the large tubing from which it is drawn is left attached. Powders can be shaken or vibrated down its length by tapping or rubbing the tubing with a knurled edge. Care should be taken not to introduce too much material at one time or that the particles are not too big to fall to the bottom of the capillary.

After the particles have been shaken down, the capillary may be cut by scratching with a chip of unglazed porcelain or sealed off to the proper length with a flame. If the original tubing from which the capillary is drawn is made part of a standard taper, ground-glass joint, the whole capillary system and its contents may be attached to a vacuum apparatus. This permits the investigation of the reaction of various gaseous reagents with the contents of the capillary.

Capillaries are emptied by breaking after scratching with a porcelain chip. The opened capillary is fixed to a stout wire by means of wax and is inverted over a suitable container. The wire is tapped sharply causing the contents of the capillary to fall into the container.

Precipitates

The hydroxides of these elements tend to precipitate in a gelatinous form. When a solution in a micro centrifuge cone of 200 microliters capacity is treated with NH_3 gas, the hydroxide may be centrifuged as a tightly packed mass at the bottom of the cone. When the product has been washed several times to remove ammonium salts and dried at about 70°C, the packed precipitate has a tendency to shrink away from the walls of the cone. Thus it may form a loose single piece or at most a few pieces. These may be easily transferred to X-ray capillaries and further operations performed. In this work the dried hydroxide or oxalate was frequently used as the starting material for the preparation of other compounds.

COMPOUNDS

Oxides

Most compounds of these elements when heated to over 500°C in air, containing moisture, will hydrolyze or decompose to the oxide. An exception is AcF_3 which is evidently so stable towards hydrolysis that at 1000°C it merely melted. The oxide of this element was prepared by heating the oxalate to 1100°C in oxygen.[10]

The formulae of the oxides formed are Ac_2O_3 (white), ThO_2 (white), Pa_2O_5 (white),[11] U_3O_8 (black), NpO_2 (green-brown),[12] PuO_2 (brown), AmO_2 (black),[13] and Cm_2O_3 (white).[14]

It is possible to prepare other oxides of these elements. Protactinium oxide, Pa_2O_5, may be reduced to black PaO_2 by heating in hydrogen to 1500°C.[11]

Much milder conditions suffice for the reduction of U_3O_8 to UO_2. Reduction of PuO_2 to Pu_2O_3 requires the action of carbon or barium at high temperatures,[15] while Am_2O_3 may be prepared by gentle decomposition of the oxalate in vacuum. Americium sesquioxide is easily reoxidized in contact with air.[16]

Heating U_3O_8 with oxygen at 30 to 150 atm and 500°C results in the formation of UO_3.[17] Neptunium, however, cannot be made to form the +VI oxide, but treatment with N_2O_4 or ozone results in the formation of Np_3O_8.[18] Curium sesquioxide may be oxidized to a compound that is very close in composition to CmO_2 by heating gently in ozone or oxygen.[19]

Fluorides

The fluorides of all these elements may be obtained by the action of gaseous hydrogen fluoride on the oxalate, dried hydroxide, or oxide at approximately 500°C.[10,11,13,20] If a reducing agent such as hydrogen is present, the product will frequently be a fluoride of lower oxidation state if such exists, and if oxygen is present a higher fluoride may be obtained.

The apparatus consisted of a nickel tube, 2.5 cm in diameter, heated with an electric furnace. The fragments of oxide (or other compound) were placed in a small platinum boat which, in turn, was placed in the nickel tube. The nickel tube was fitted with valves in such a manner that a gas or mixture of gases could be led from tanks, over the material to be acted upon. In addition, connections to a source of vacuum were made so that the system could be evacuated if necessary. Generally the gases were passed over the oxides for one or two hours at the desired temperature, measured by means of a thermocouple. After the reaction was completed, the system was allowed to cool and was then flushed with an inert gas. The particles of the resulting fluoride were mounted in an X-ray capillary which was sealed off and analyzed by X-ray diffraction.

The reactions may be represented by the equations

$$M_2O_3 + 6HF \rightarrow 2MF_3 + 3H_2O \quad (1)$$

$$MO_2 + 4HF \rightarrow MF_4 + 2H_2O \quad (2)$$

The trifluorides and tetrafluorides of these elements are non hygroscopic, high melting solids.

The fluorides of actinium and thorium are AcF_3 and ThF_4, respectively.[10]

The action of hydrogen-hydrogen fluoride mixtures on PaO_2 yields the red PaF_4, while under the same conditions Pa_2O_5 yields a volatile compound of unknown composition.[11] This mixture, however, yields the purple fluorides NpF_3 and PuF_3 when allowed to act on NpO_2 and PuO_2, respectively.[20,21]

The fluorides UF_4 (green), NpF_4 (light green) and PuF_4 (beige) are formed by the action of hydrogen fluoride alone on the corresponding oxide at 500°C.[20,21] Americium, however, yields the pink fluoride AmF_3.[13]

To prepare the higher fluorides of these elements it is generally necessary to use a fluorinating agent such as free fluorine or cobaltic trifluoride. The compound UO_3 does not yield UF_6 by treatment with hydrogen fluoride, but rather the oxyfluoride UO_2F_2. Treatment of UF_4 and NpF_4 with fluorine results in the formation of UF_6 and NpF_6, respectively.[22] Americium trifluoride is converted to AmF_4 under these conditions.[23]

The fluorides of some of these elements undergo special, peculiar reactions with dry oxygen at elevated temperatures. The reaction of UF_4 with oxygen is given by the equation

$$2UF_4 + O_2 \xrightarrow{600°C} UO_2F_2 + UF_6 \quad (3)$$

This reaction provides a method of preparation of UF_6 without the use of elementary fluorine.[24]

Other special reactions are[25-27]

$$2UF_5 + O_2 \rightarrow UO_2F_2 + UF_4 \quad (4)$$

$$4NpF_5 + O_2 \rightarrow 3NpF_4 + NpO_2 \quad (5)$$

$$4PuF_3 + O_2 \underset{\leftarrow \text{vacuum}}{\xrightarrow{600°C}} 3PuF_4 + PuO_2 \quad (6)$$

A noteworthy point about reaction 6 is its apparent reversibility at 600°C in vacuum.

Chlorides

The oxides or oxalates of these elements react with carbon tetrachloride vapor at elevated temperatures according to one or the other of the following equations

$$MO_2 + 2CCl_4 \rightarrow MCl_4 + 2COCl_2 \quad (7)$$

$$MO_2 + 2CCl_4 \rightarrow MCl_3 + 2COCl_2 + \tfrac{1}{2}Cl_2 \quad (8)$$

$$M_2O_3 + 3CCl_4 \rightarrow 2MCl_3 + 3COCl_2 \quad (9)$$

Equation 7 represents the reaction of the dioxides ThO_2, PaO_2, UO_2 and NpO_2 to form the tetrachlorides. The colors of these compounds are white, yellow, green, and orange, respectively.[11,20]

The formation of the green trichloride from PuO_2 and the pink trichloride from AmO_2 is shown by Equation 8.[13,28] The sesquioxides Ac_2O_3, Am_2O_3, and Cm_2O_3 react according to Equation 9. The chlorides of actinium and curium are white.[10,14] The higher oxides such as Pa_2O_5, U_3O_8 and UO_3 yield higher chlorides or mixtures of chlorides under these conditions. The trichlorides sublime at 700-800°C, the tetrachlorides 400-550°C, and the higher chlorides may be volatile at 200°C.

In some cases lower chlorides may be formed by reduction with hydrogen, and higher chlorides by reaction with chlorine depending on the element in question. Equations 10 and 11 are examples of these reactions:[8]

$$NpCl_4 + \tfrac{1}{2}H_2 \rightarrow NpCl_3 + HCl \quad (10)$$

$$4UCl_4 + 3Cl_2 \rightarrow 2UCl_5 + 2UCl_6 \quad (11)$$

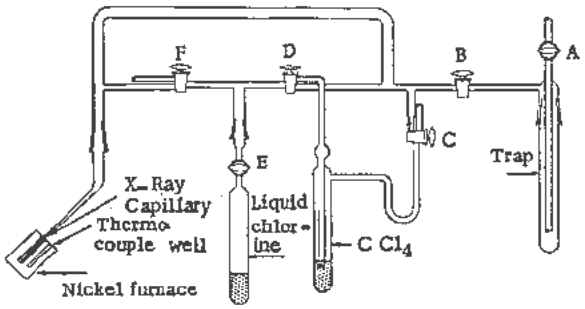

Figure 1. Apparatus for the preparation of chlorides

The chlorides, particularly the trichlorides and tetrachlorides, may be partially hydrolyzed by action of water vapor at low concentrations. Thus the compounds $UOCl_2$ and $NpOCl_2$ are formed[20] from the respective tetrachlorides, while the compounds AcOCl,[10] PuOCl,[28] and CmOcl,[14] are formed from the corresponding trichlorides.

All of the chlorides and oxychlorides are hygroscopic to varying degrees. On exposure to moist air they form various chloride hydrates which decompose to the oxides when heated.

The apparatus used in making these preparations is shown in Fig. 1. By manipulation of stopcocks *B* and *C*, it is possible to admit carbon tetrachloride vapor into the evacuated system or to pump it out along with any volatile reaction products. During the time the capillary is evacuated any heavy metal chloride formed has an opportunity to subline to the cold portion of the capillary. The temperature of the reaction is maintained by the nickel furnace, which is wound with nichrome wire.

The vapors of chlorine, bromine, or other liquid reagents are introduced through stopcock *E*, while the action of hydrogen is studied by admitting the gas through stopcock *F*.

When the reactions are completed the product is usually found condensed as a solid in a zone just outside the heated portion of the X-ray capillary. The X-ray capillary may be evacuated, sealed off above the sublimate, and submitted for X-ray diffraction analysis.

Bromides and Iodides

The oxides of the elements react with aluminum bromide or iodide to form these halides according to the reactions

$$3MO_2 + 4AlX_3 \rightarrow 3MX_4 + 2Al_2O_3 \quad (12)$$

$$3MO_2 + 4AlX_3 \rightarrow 3MX_3 + 2Al_2O_3 + \tfrac{3}{2}X_2 \quad (13)$$

$$M_2O_3 + 2AlX_3 \rightarrow 2MX_3 + Al_2O_3 \quad (14)$$

Fifty-microgram samples of the oxide are mixed with several times the quantity of aluminum powder. The mixture is placed in a quartz X-ray capillary which is attached to the apparatus shown in Fig. 1. After the system has been evacuated, bromine or iodine vapor is admitted onto the mixture of aluminum metal and oxide. The halogen vapor is allowed to act on the aluminum at 200°C. As the aluminum halide is formed, it distills into a cool portion of the tube. When all the aluminum has reacted, the system is evacuated and sealed off to a length of about 15 cm. For protection, the capillary is placed in a heavy-walled glass tube, which is sealed off. The heavy tube with the capillary inside is heated uniformly in a furnace at 500°C for eight hours. The system is cooled, the heavy tube broken open, and the capillary attached to the apparatus shown in Fig. 2. When the stopcock is turned, the capillary is broken without allowing air to come in contact with the reaction mixture.

The contents are heated by means of a furnace as shown in the figure. As the temperature is raised, unreacted aluminum halide sublimes at temperatures below 400°C. At temperatures from 400 to 500°C tetrabromides distill, and at 700 to 800°C tribromides and triiodides volatilize. The other product of the reaction, Al_2O_3, remains at the bottom of the capillary. The section of the capillary containing the condensed zone of interest is sealed off from the rest for X-ray diffraction studies.

Under the conditions described above, the elements thorium, uranium, and neptunium form tetrabromides which are white, brown and brown-red, respectively.[18] Neptunium tetrabromide may be partially decomposed to the green tribromide during the volatilization in vacuum.

The oxides of actinium, plutonium, and americium form tribromides under these conditions which are white, green and pink, respectively.[10,18,19]

The triiodides are formed under these conditions from all the oxides with the exception of thorium and uranium. The iodide UI_4 can be thermally decomposed to UI_3.

Mild hydrolytic conditions yield oxyhalides such as AcOBr, PuOBr, and PuOI.[10,23,24]

Metals

The metals are prepared by the reaction of barium vapor with the tri- or tetrafluorides at 1200 to 1400°C. The furnace in which this reaction is carried out is shown in Fig. 3. The whole furnace is en-

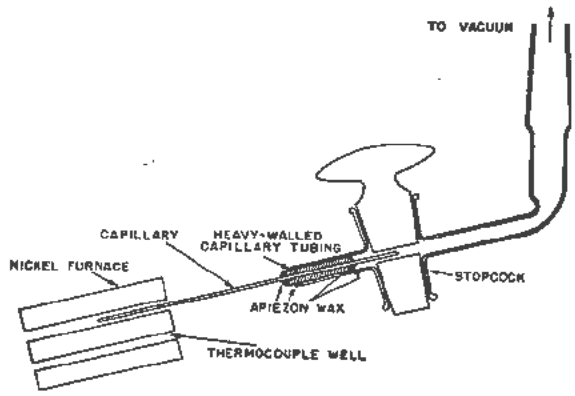

Figure 2. Apparatus for opening capillaries

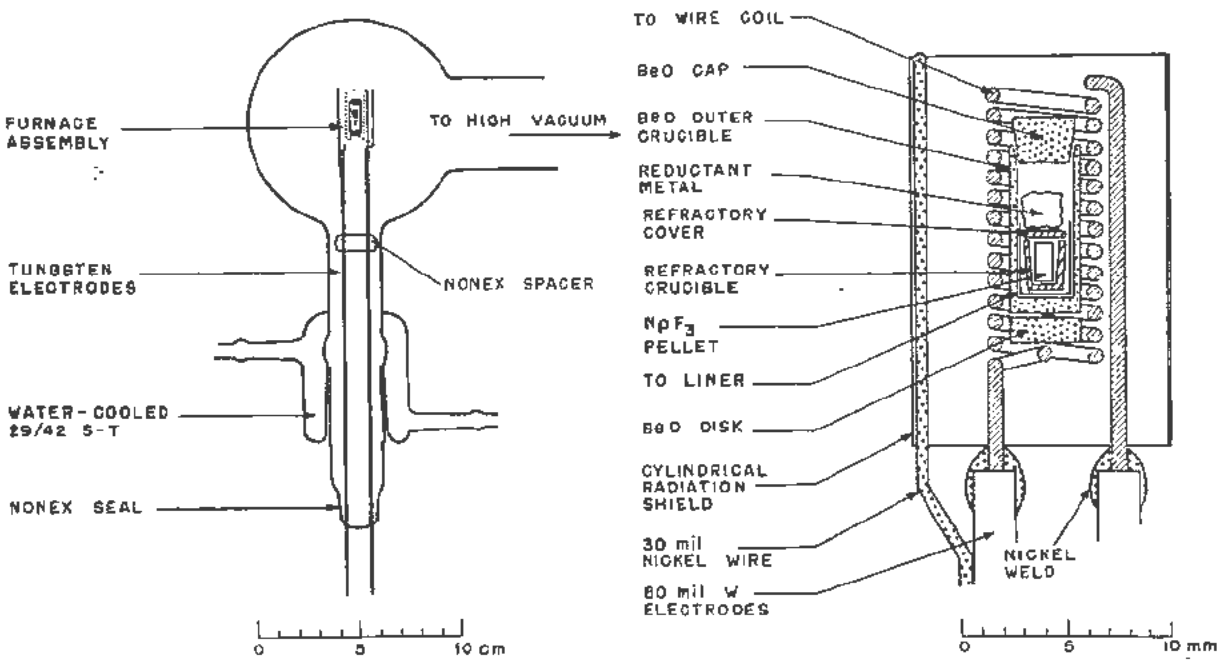

Figure 3. Furnace assembly

closed in a glass bulb of about 500-ml capacity which is attached to a high-speed vacuum line. The blank systems are outgassed before use at 1400°C until the pressure is reduced to 10^{-6} mm Hg.

When a current of 10 to 15 amperes is passed through the tantalum or tungsten coil, the temperature rapidly rises to 1200°C. After about 20 seconds the barium metal vaporizes, reacting with the fluoride; the excess barium vapor diffuses into the outer volume of the bulb, where it condenses as a mirror on the walls. After 50 seconds, the reaction is complete; the system is then cooled.

On opening the crucible system, the metal is found as shiny, round globules, adhering to the walls. The globules of metal can be pried off with a needle.

In this manner the metals protactinium, uranium, neptunium, plutonium, and americium have been prepared.[11,20,31]

The metals unite with hydrogen at slightly elevated temperatures to form hydrides. Using the apparatus shown in Fig. 4, a piece of neptunium weighing 20.88 micrograms absorbed hydrogen rapidly at 50°C and formed a black flaky powder. The volume of hydrogen absorbed corresponded to the formula $NpH_{3.6-3.8}$.[20]

Sulfides

When the oxides are heated to high temperatures in a stream of hydrogen sulfide containing carbon disulfide vapors, various sulfides and oxysulfides are formed. Actinium, uranium, neptunium, plutonium, and americium yield the sesquisulfides on treatment with this mixture at 1200 to 1400°C.[19,20,13]

Oxysulfides such as PaOS, UOS, and NpOS are obtained from the corresponding elements under milder conditions, while plutonium yields the compound Pu_2O_2S.

Miscellaneous Compounds

The oxides of these elements react with carbon at temperatures above 2500°C to form the carbides. These preparations are made by heating the oxide in a graphite crucible in a hydrogen atmosphere using a high frequency generator as a source of power. Carbides also result when metal preparations are carried out in graphite crucibles.

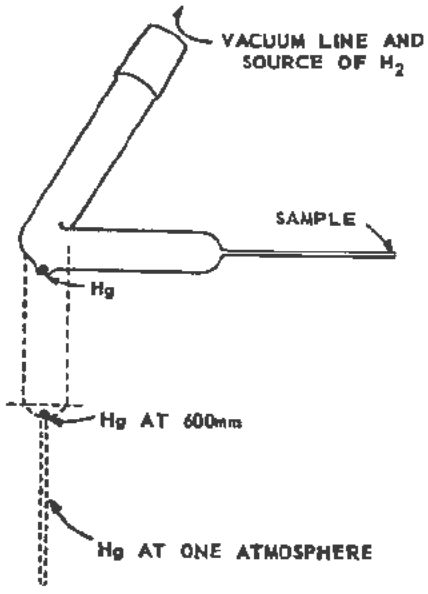

Figure 4. Hydride apparatus

Table II. Chemical Similarity between the 4f Elements and Other Elements

No. of 4f electrons	I K Rb	II Ca Sr	III Sc Y	IV Ti Zr	V V Nb	VI Cr Mo	VII Mn Tc	VIII Fe Ru	Co Rh	Ni Pd
0	Cs	Ba	La	Ce						
1			Ce	Pr						
2			Pr							
3			Nd							
4			Pm							
5			Sm							
6		Sm	Eu							
7		Eu	Gd	Tb						
8			Tb							
9			Dy							
10			Ho							
11			Er							
12			Tm							
13			Yb							
14		Yb	Lu	Hf	Ta	W	Re	Os	Ir	Pt

Thus, neptunium oxide yielded the carbide NpC_2 by reaction with graphite at 2660–2800°C, while reduction of 100 micrograms of NpF_3 with lithium metal in a graphite crucible yielded NpC and Np_2C_3.[32] The plutonium carbides are PuC and Pu_2C_3.[33]

Neptunium nitride, NpN, was prepared by the reaction of neptunium hydride with ammonia gas presumably according to the equation[32]

$$NpH_3 + NH_3 \xrightarrow{750°C} NpN + 3H_2 \qquad (15)$$

The silicides may be formed by reaction of calcium silicide or silicon metal on the oxide or fluorides of these elements. The compounds $PuSi_2$ and $NpSi_2$ have been identified.[32,34]

The compound Np_3P_4 resulted from the reaction of neptunium metal with red phosphorus at 750°C for 16 hours.[32]

From the foregoing, it is evident that certain generalizations can be made regarding the properties of these elements.

As was to be expected, the highest oxidation states are exhibited in combination with the small and difficulty polarizable anions, such as O^{--} and F^-, rather than with the more readily polarizable and oxidizable anions, Cl^-, Br^- S^{--}, and I^-. Thus UF_6 and UO_2 may be prepared but not UBr_6 or UI_4; AmF_4 and AmO_2 exist but $AmCl_4$ and $AmBr_4$ have not been made.

Comparisons of the stability of various oxidation states of the anhydrous compounds with those found in solution are probably only of limited validity. However, in aqueous solutions it is evidently easier to obtain the higher oxidation states than in the solid compounds. The stability is apparently increased by solvation and complex formation, and in this connection it is noteworthy that Pu(III) may be oxidized to Pu(IV) by chlorine or bromine, though $PuCl_4$ and $PuBr_4$ do not exist in the anhydrous state.

CRYSTAL STRUCTURES OF HEAVY ELEMENT COMPOUNDS

In discussing the chemistry and crystal chemistry of the heavy elements it is often useful to make comparisons with the elements from cerium to ytterbium, the 4f elements. It is convenient to define a 4f element as one in which the 4f subshell is partly occupied. According to this definition cerium is the first 4f element and ytterbium is the last, although in the strict sense of the definition, cerium, when it is tetravalent, and ytterbium, when it is divalent, are not 4f elements. For many purposes it is useful to include among the 4f elements the immediately preceding element in which there are no 4f electrons and the immediately following element for which the 4f subshell is completed.

Table II shows the number of electrons in the 4f shell for the various oxidation states observed for the 4f elements. It should be remarked, however, that subnormal oxidation states are not included in the table. Thus the +2 oxidation state exhibited by cerium in the compound CeS has been omitted, and this is done because the crystal structure results show that the non-bonding valence electrons are at least in part 5d rather than 4f type.

In regard to chemical and crystal chemical properties the important consequences of the filling of the 4f shell are twofold. In the first place, the 4f electrons do not participate significantly in chemical bond formation, and, as a result, atoms or ions whose electronic configurations differ only in the number of 4f electrons will show similar chemical behavior. Secondly, the filling of the 4f shell is accompanied by a slow monotonic contraction in atomic dimensions for a given oxidation state. Since the degree of chemical and crystal chemical similarity between any two atoms with analogous electronic configurations depends on relative size, the effect of the "4f contraction" is to make neighboring 4f elements show almost identical chemical properties. The 4f contraction was discovered by Goldschmidt,[35] who also called attention to a number of interesting consequences. The contraction occurs regardless of whether the binding is of ionic, covalent or metallic character and whether the oxidation state is 2, 3 or 4. Table III illustrates the magnitude of the 4f contraction as reflected in ionic crystal radii.

Analogous compounds of the heavy elements under consideration in this article are almost invariably isostructural. In all such series of isostructural compounds corresponding to the normal oxidation states of Table I there is a monotonic decrease in lattice dimensions and interatomic distances with increasing atomic number. This observation is equally true for a series such as XF_3, in which the binding is predominantly ionic, as it is for an isostructural series of compounds such as $Na(XO_2)(C_2H_3O_2)_3$, where the binding is of predominantly covalent type. The observed extremely close similarity in structure and interatomic distances cannot be accounted for unless the configuration of the bonding electrons is the same and non-bonding electrons are 5*f* rather than 6*d* electrons. While it is true that the presence of 5*f* electrons in the heavy elements was deduced on the basis of chemical and crystal chemical behavior in analogy with the 4*f* elements, additional and more direct evidence, such as magnetic properties, has confirmed the earlier conclusions. Table IV, which should be compared with the corresponding Table II for the 4*f* elements, shows the number of electrons in the 5*f* shell for the elements Ac to Cm in the oxidation states of normal type, while the magnitude of the "5*f* contraction" as exhibited in ionic crystal radii is shown in Table V.

If a 5*f* element is defined analogously to a 4*f* element, namely, as one in which the 5*f* shell is incomplete, then, as seen from Table IV, protactinium in the tetravalent oxidation state becomes the first 5*f* element. Barium, lanthanum and cerium are the prototypes for the 4*f* elements in the 2, 3 and 4 oxidation states, and one may thus speak of "baride," "lanthanide" and "ceride" series of 4*f* elements, depending upon the oxidation state with which one is concerned. In a similar manner actinium, thorium, protactinium and uranium serve as prototypes for the 5*f* elements in the oxidation states 3, 4, 5 and 6, respectively, and one may analogously speak of "actinide," "thoride," "protactinide" or "uranide" series of elements. It is particularly to be noted that thorium and protactinium have not yet been found in the normal +3 oxidation state, and hence they are not true actinide elements. Such compounds as ThI_3 and Th_2S_3 are known,[5] but the oxidation state of thorium in these

Table III. Ionic Radii of 4f Elements in Various Valence States

Element	Ionic radius, A, in indicated valence state		
	+2	+3	+4
Barium	1.29		
Lanthanum		1.04	
Cerium		1.02	0.92
Praseodymium		1.00	0.90
Neodymium		0.99	
Promethium		(0.98)	
Samarium	1.11	0.97	
Europium	1.09	0.96	
Gadolinium		0.94	
Terbium		0.92	0.84
Dysprosium		0.91	
Erbium		0.89	
Holmium		0.87	
Thulium		0.86	
Ytterbium	0.93	0.85	
Lutecium		0.84	
Hafnium			0.77

compounds must be termed a subnormal valence state, analogous to the trivalent state of titanium, for crystal structure studies show that the non-bonding electron is of 6*d* rather than 5*f* type.

One of the obvious differences between the properties of 4*f* and 5*f* elements is the greater multiplicity of oxidation states for the heavier series. Whereas any given 4*f* element exhibits at most two normal valence states, namely, 3 and 4 or 3 and 2, there are four bona fide valence states for each of the elements uranium, neptunium, plutonium and americium. This difference is due to the fact that the separation 5*f*-6*d* is considerably smaller than is the corresponding 4*f*-5*d* separation. By varying the oxidation-reduction conditions under which chemical reactions are carried out, it is thus possible to bring about demotion or promotion of several electrons in the 5*f* elements but of, at most, only one electron in the 4*f* group.

Another important difference is the generally higher oxidation state for the heavy elements as compared to the light group. Table VI illustrates this difference. Were there strict analogy between 4*f* and 5*f* elements one should expect americium to exhibit the oxidation states +2 and +3 as does europium, whereas americium actually occurs in the oxidation states +3, +4, +5 and +6.

Table IV. Crystal Chemical Similarity between the 5f Elements and Other Elements

	I	*II*	*III*	*IV*	*V*	*VI*	*VII*	*VIII*		
	K	*Ca*	*Sc*	*Ti*	*V*	*Cr*	*Mn*	*Fe*	*Co*	*Ni*
No. of 5f electrons	*Rb*	*Sr*	*Y*	*Zr*	*Nb*	*Mo*	*Tc*	*Ru*	*Rh*	*Pd*
	Cs	*Ba Eu Yb*	*La Gd Lu*	*Ce Tb Hf*	*Ta*	*W*	*Re*	*Os*	*Ir*	*Pt*
0	Fr	Ra	Ac	Th	*Pa*	*U*				
1				*Pa*	U	Np				
2				*U*	Np	Pu				
3			U	*Np*	Pu	Am				
4			Np	*Pu*	Am					
5			*Pu*	*Am*						
6			*Am*	Cm						
7			Cm							

Table V. Ionic Radii of 5f Elements in Various Valence States

Element	Ionic radius, Å, in indicated valence state +3	+4	+5	+6
Actinium	1.11			
Thorium	(1.08)	0.99		
Protactinium	(1.05)	0.96	0.90	
Uranium	1.03	0.93	0.87	0.83
Neptunium	1.01	0.92	0.88	0.82
Plutonium	1.00	0.90	0.87	0.81
Americium	0.99	0.89	0.86	0.80

The crystal chemistry of the heavy elements as regards the tripositive and tetrapositive oxidation states of normal character has been adequately discussed in an earlier survey article,[7] and the crystal chemical discussions of this paper will therefore be limited to newer results concerning the other oxidation states.

THE CRYSTAL CHEMISTRY OF THE +5 AND +6 OXIDATION STATES

It is found that the oxygenic compounds of the elements U to Am in the hexapositive state, and of the elements Np to Am in the pentapositive state, contain collinear groups $(XO_2)^{+2}$ and $(XO_2)^{+}$, respectively. These O-X-O radicals have been observed to be collinear within experimental error even in structures where the collinearity is not required by the space group symmetry. However, no satisfactory theoretical explanation has yet been given why the heavy elements in these oxidation states should form two oppositely directed strong bonds.

Owing to the small X-ray scattering effects of oxygen as compared to that of the heavy atom it is difficult to obtain precise values for the length of the X-O bond. The only reliable results for the bond length within the O-X-O group have been obtained for uranyl compounds. It is important to emphasize, however, that although radicals O-X-O involving two short bonds are found in all structures of the compounds under consideration, other bonds are nevertheless formed by the heavy atom X. Four, five and six such secondary bonds to other oxygen atoms or to fluorine atoms have been observed. Table VII shows the available data as to the length of the primary bonds within the O-X-O groups (X-O_I) and of the secondary bonds (X-O_{II} or X-F).[36]

It is seen from Table VII that the primary as well as the secondary bond lengths show large variations from one compound to the next. These variations begin to make empirical sense if one tries to divide up the normal valence of each atom between the various bonds so as to give local valence balance. In this way it becomes possible to assign a bond strength s to each bond so that the sum of the strengths of the bonds ending on an atom is equal to its accepted valence. The bond strengths so obtained are listed in the last column of Table VII, and it is noted how the bond length decreases with increasing bond strength in a very striking fashion.

Table VI. Valences of 4f and 5f Elements

5f element	Valence	4f element	Valence
Actinium	3	Lanthanum	3
Thorium	4	Cerium	3,4
Protactinium	4,5	Praseodymium	3,4
Uranium	6,4,3,5	Neodymium	3
Neptunium	4,3,6,5	Promethium	
Plutonium	4,3,6,5	Samarium	3,2
Americium	3,4,6,5	Europium	2,3
Curium	3,4	Gadolinium	3

THE SUBNORMAL VALENCE COMPOUNDS

A number of compounds corresponding to the +2 oxidation state of the heavy elements are known. Thus the monoxide of every element from thorium to americium has been observed as a coating on the metal. The monosulfides of thorium, uranium and plutonium are known, and the preparation of the diiodides has been reported.[5] The oxides and the sulfides show pronounced metallic character.

Table VII. Observed Bond Lengths

Compound	Bond	Bond length in Å	Bond strength, s
$RbUO_2(NO_3)_3$	U−2 O_I	1.58±0.10	1.93
$K_3UO_2F_5$	U−2 O_I	1.76±0.03	1.63
$CaUO_2O_2$	U−2 O_I	1.91±0.10	1.25
$MgUO_2O_2$	U−2 O_I	1.92±0.03	1.33
UO_2	U−2 O_I	2.08±0.01	1.00
$MgUO_2O_2$	U−4 O_{II}	2.18±0.02	0.83
$BaUO_2O_2$	U−4 O_{II}	2.17±0.10	0.75
UO_2	U−6 O_{II}	2.39±0.10	0.67
$CaUO_2O_2$	U−6 O_{II}	2.29±0.02	0.58
$RbUO_2(NO_3)_3$	U−6 O_{II}	2.72±0.10	0.36
$KPuO_2CO_3$	Pu−6 O_{II}	2.55±0.10	0.25
$K_3UO_2F_5$	U −5 F	2.24±0.02	0.55
UO_2F_2	U−6 F	2.50±0.10	0.33
$KAmO_2F_2$	Am−6 F	2.47±0.10	0.29

If all the non-bonding valence electrons were 5f electrons, then these elements in the +2 oxidation state should be radium-like, i.e., they should be members of a radide series. Thus, beginning with radium, there should be a slow monotonic decrease in ionic crystal radius with increasing atomic number, and it is reasonable to suppose that this 5f contraction would correspond closely in character and magnitude to the observed 4f contraction for the halide series. Since the ionic crystal radius of Ra^{+2} is known to be 1.37 Å from the RaF_2 structure, it becomes possible to make reliable predictions of the radii of the radide ions. The validity of the assumption of radium-like ions can accordingly be tested by means of a comparison of predicted and observed interatomic distances for the monoxides and the monosulfides, and this comparison is made in Table VIII.

It is seen that the observed interatomic distances in the compounds under consideration are very much smaller than the values predicted on the basis of a 5f contraction in a radide series, thus leading to the conclusion that the non-bonding valence electrons

Table VIII. Predicted and Observed Interatomic Distances for Monoxides and Monosulfides

Element	Predicted radide radius, Å	Monoxides, Å		Monosulfides, Å	
		Predicted	Observed	Predicted	Observed
Ra	1.37	2.83		3.27	
Ac	1.32	2.78		3.22	
Th	1.28	2.74	2.60	3.18	2.84
Pa	1.25	2.71	2.48	3.15	
U	1.22	2.68	2.45	3.12	2.74
Np	1.20	2.66	2.50	3.10	
Pu	1.18	2.64	2.48	3.08	2.76
Am	1.16	2.62	2.50	3.06	

cannot possibly be of the 5*f* type. On the other hand, the observed results are in agreement with expectation if one assumes the non-bonding valence electrons to be 6*d* electrons, for it is known from other regions of the periodic system that the addition of non-bonding electrons to the *d* subshell produces far greater contraction in interatomic distances than does the addition of electrons to the *f* subshell. For example, the addition of three non-bonding 3*d* electrons causes a decrease in interatomic distance from 2.40 Å at CaO to 2.04 Å at VO. The experimental results given in Table VIII suggest that, as far as monoxides and monosulfides go, the first 5*f* electron does not appear until neptunium. However, the data do not permit any reliable estimate as to how many of the non-bonding valence electrons of neptunium, plutonium and americium are of 5*f* and how many of 6*d* type.

The interatomic distances observed in the trihalides of uranium and neptunium are precisely those to be expected on the basis of a 5*f* contraction in an actinide series, and it may thus be concluded that the three non-bonding valence electrons of uranium and the four non-bonding valence electrons of neptunium in the trihalides are of 5*f* type. However, the situation is quite different for the sesquisulfides of uranium and neptunium. The crystal structure is known for the sesquisulfides of actinium, thorium, uranium, neptunium, plutonium and americium. The actinium, plutonium and americium compounds are isostructural; but the thorium, uranium and neptunium compounds have a different structure, and the latter three compounds show moreover a much more pronounced metallic character. The observed interatomic distances and those predicted on the basis of a 5*f* contraction in an actinide series are shown in Table IX.

Table IX. Predicted and Observed Interatomic Distances (Å) in Sesquisulfides

Compound	Predicted	Observed
Ac_2S_3	3.09	3.10
Pu_2S_3	2.98	2.92
Am_2S_3	2.97	2.92
Th_2S_3	3.02	2.90
U_2S_3	2.97	2.82
Np_2S_3	2.95	2.81

The good agreement between prediction and observation for the plutonium and americium compounds suggests that all the non-bonding electrons of these atoms are of 5*f* type. The lack of agreement in the cases of the thorium, uranium and neptunium, on the other hand, necessitates the conclusion that some of the non-bonding electrons of these atoms are of 6*d* type, and the numerical results suggest that there are no 5*f* electrons in Th_2S_3 and U_2S_3 and not more than about 5*f* electron in Np_2S_3. In other words, in the sesquisulfides, thorium behaves as a homologue of zirconium, and uranium as a homologue of molybdenum, whereas plutonium and americium behave as true actinides.

REFERENCES

1. McMillan, E. M. and Abelson, P. H., *Radioactive Element 93*, Phys. Rev. 57: 1185 (1940).
2. Seaborg, G. T., McMillan, E., Kennedy, J. W. and Wahl, A. C., *A New Element: Radioactive Element 94 from Deuterons on Uranium*, Paper 1.1a of *The Transuranium Elements*, National Nuclear Energy Series, Division IV, Vol. 14B, McGraw-Hill Book Co., New York (1949); Seaborg, G. T., Wahl, A. C., Kennedy, J. W., *A New Element: Radioactive Element 94 from Deuterons on Uranium*, Paper 1.1b, ibid.; Kennedy, J. W., Seaborg, G. T., Segrè, E., and Wahl, A. C., *Fissionable Isotope of a New Element: 94*^{239}, Paper 1.2, ibid.
3. Seaborg, G. T., James, R. A., and Morgan, L. O., *The New Element Americium (Atomic Number 95)*, Paper 22.1 of *The Transuranium Elements*, National Nuclear Energy Series, Division IV, Vol. 14b, McGraw-Hill Book Co., New York (1949).
4. Seaborg, G. T., Jones, R. A., and Ghiorso, A., *The New Element Curium (Atomic Number 96)*, Paper 22.2 of *The Transuranium Elements*, National Nuclear Energy Series, Division IV, Vol. 14B, McGraw-Hill Book Co., New York (1949).
5. Anderson, J. S., and D'Eye, R. W. M., *The Lower Valency States of Thorium*, J. Chem. Soc., (1949) (Suppl. Issue No. 2), 244-48.
6. Seaborg, G. T., *Correlation of Properties as Actinide Transition Series*, Chapter 17 of *The Transuranium Elements*, National Nuclear Energy Series, Division IV, Vol. 14A, McGraw-Hill Book Co., New York (1954).
7. Zachariasen, W. H., *Crystal Chemistry of the 5f Elements*, Chapter 18 of *The Transuranium Elements*, National Nuclear Energy Series, Division IV, Vol. 14A, McGraw-Hill Book Co., New York (1954).
8. Seaborg, G. T., *Chemical and Radioactive Properties of the Heavy Elements*, Chem. Eng. News, 2190 (1945); Magnusson, L. B., and LaChapelle, T. J., *The First Isolation of Element 93 in Pure Compounds and a Determination of the Half-Life of* $_{93}Np^{237}$, J. Am. Chem. Soc. 70: 3534 (1948).
9. Reynolds, F. L., Hulet, E. K., and Street, K., Jr., *Mass-Spectrographic Identification of* Cm^{243} *and* Cm^{244}, Phys. Rev. 80: 467 (1950).
10. Fried, S., Hagemann, F. T., and Zachariasen, W. H., *Preparation and Identification of Some Pure Actinium Compounds*, J. Am. Chem. Soc. 72: 771 (1950).
11. Elson, R., Fried, S., Sellers, P. A., and Zachariasen, W. H., *The Preparation of Some Protactinium Compounds and the Metal*, J. Am. Chem. Soc. 76: 5935 (1954).
12. Magnusson, L. B., and LaChapelle, T. J., *The First Isolation of Element 93 in Pure Compounds and a*

Determination of the Half-Life of $_{93}Np^{237}$, J. Am. Chem. Soc. 70: 3534 (1948).

13. Fried, S., *The Preparation of Anhydrous Americium Compounds*, J. Am. Chem. Soc. 73: 416 (1951).
14. Fried, S. and Zachariasen, W. H., unpublished work.
15. Mooney, R. C. L. and Zachariasen, W. H., *Crystal Structure Studies of Oxides of Plutonium*, Paper 20.1 of *The Transuranium Elements*, National Nuclear Energy Series, Division IV, Vol. 14B, McGraw-Hill Book Co., New York (1949).
16. Asprey, L. B. and Cunningham, B. B., reported in Chapter 14 of *The Transuranium Elements*, National Nuclear Energy Series, Division IV, Vol. 14A, McGraw-Hill Book Co., New York (1954).
17. Sheft, L., Fried, S. and Davidson, N. R., *Preparation of Uranium Trioxide*, J. Am. Chem. Soc. 72: 2172 (1950).
18. Katz, J. J. and Gruen, D. M., *Higher Oxides of the Actinide Elements. The Preparation of* Np_3O_8, J. Am. Chem. Soc. 71: 2106 (1949).
19. Asprey, L. B., Ellinger, F. H., Fried, S., and Zachariasen, W. H., *Evidence for Quadrivalent Curium: X-ray Data on Curium Oxides*, J. Am. Chem. Soc. 77: 1707 (1955).
20. Fried, S. and Davidson, N. R., *The Preparation of Solid Neptunium Compounds*, J. Am. Chem Soc. 70: 3539 (1948).
21. Florin, A. E. and Heath, R. E., reported in Chapter 10 of *The Transuranium Elements*, National Nuclear Energy Series, Division IV, Vol. 14A, McGraw-Hill Book Co., New York (1954).
22. Florin, A. E., private communication.
23. Asprey, L. B. and Penneman, R. A., reported at the 123rd meeting of the American Chemical Society, Los Angeles, California; Abstract 96, p. 40P.
24. Fried, S. and Davidson, N. R., unpublished work.
25. Fried, S., unpublished work.
26. Fried, S., unpublished work.
27. Fried, S. and Davidson, N. R., *Studies in the Dry Chemistry of Plutonium*, Paper 6.11 of *The Transuranium Elements*, National Nuclear Energy Series, Division IV, Vol. 14B, McGraw-Hill Book Co., New York (1949).
28. Abraham, B. M., Brody, B. B., Davidson, N. R., Hagemann, F., Karle, I., Katz, J. J., and Wolf, M. J., *Preparation and Properties of Plutonium Chlorides and Oxychlorides*. Paper 6.7 of *The Transuranium Elements*, National Nuclear Energy Series, Division IV, Vol. 14B, McGraw-Hill Book Co., New York (1949).
29. Davidson, N. R., Hagemann, F., Hyde, E. K., Katz, J. J., and Sheft, I., *Preparation and Properties of Plutonium Tribromide and Oxybromide*, Paper 6.8 of *The Transuranium Elements*, National Nuclear Energy Series, Division IV, Vol. 14B, McGraw-Hill Book Co., New York (1949).
30. Hagemann, F., Abraham, B. M., Davidson, N. R., Katz, J. J., and Sheft, I., *Studies of the Preparation and Properties of Plutonium Iodide and Oxyiodide*, Paper 6.170 of *The Transuranium Elements*, National Nuclear Energy Series, Division IV, Vol. 14B, McGraw-Hill Book Co., New York (1949).
31. Westrum, E. F., Jr., and Eyring, L., *The Preparation and Some Properties of Americium Metal*, J. Am. Chem. Soc. 73: 3396 (1951).
32. Sheft, I. and Fried, S., *Neptunium Compounds*, J. Am. Chem. Soc. 75: 1236 (1953).
33. Reported in Chapter 10 of *The Transuranium Elements*, National Nuclear Energy Series, Division IV, Volume 14A, McGraw-Hill Book Co., New York (1949).
34. Westrum, E. F., Jr., *Preparation and Properties of Plutonium Silicides*. Paper 6.5 of *The Transuranium Elements*, National Nuclear Energy Series, Division IV, Vol. 14B, McGraw-Hill Book Co., New York (1949).
35. Goldschmidt, V. M., Barth, T., and Lunde, G., *Geochemische Verteilungsgesetze der Elemente*, V. Skrifter Norske Videnskaps-Akad. Oslo. I. Mat.-Naturv, Klasse No. 7 (1925).
36. Zachariasen, W. H., *Crystal Chemical Studies of the 5f Series of Elements XXIII. On the Crystal Chemistry of Uranyl Compounds and of Related Compounds of Transuranic Elements*. Acta Cryst. 7: 795 (1954).

Hydrolytic Behavior of the Heavy Elements

By K. A. Kraus,* USA

The elements from actinium upwards, those elements which are commonly referred to as the actinide series, represent an unparalleled opportunity to inorganic and physical chemists who are interested in the comparative study of elements. Various aspects of the chemistry of these elements can be found in numerous reviews.[1-7] As a first approximation these elements form a very coherent group which, particularly for the higher members of the series, show a persistence of properties which is reminiscent of the rare earths. However, the actinides show greater richness in properties, resulting principally from their existence in a variety of oxidation states. For a study of aqueous solutions the actinides are further very attractive because many of their ions have absorption spectra with optical density very much higher than those of the rare earths, though of similar sharpness, because many of the elements show reversible potentials, and because many occur in high oxidation states with a resulting abundance of complexing properties.

In spite of the opportunity presented by these elements, their comparative chemistry so far has not been greatly exploited. The most detailed systematic studies relate to their crystal chemistry.[8-13] Further, one may cite work on the systematic identification of oxidation states and oxidation potentials, of absorption spectra in acidic solutions, of magnetic properties[14] and particularly of the ion-exchange behavior.[2,15,16] Fragmentary studies on the hydrolytic properties of these elements are also available and will be summarized in this paper.

From present information, it appears that the hydrolytic properties are quite sensitive to change in atomic number and oxidation state. Study of these properties is particularly attractive since experimental procedures are often simple and since, in addition, the results are basic for an understanding of the aqueous solution chemistry of the elements. For the purposes of this paper the hydrolytic properties will be defined to include identification of the species in acidic solutions under "non-complexing" conditions and identification of species and equilibria as a function of acidity. Although the solid phases formed by hydrolysis of the ions (hydroxides, basic salts, etc.) form a group of extremely interesting compounds, little is known regarding them, and detailed comparison therefore is not considered feasible at this time.

* Oak Ridge National Laboratory.

Comparison of the elements will be made for each of the major oxidation states in solution, i.e., the oxidation states 3, 4, 5 and 6.

GENERAL CONSIDERATIONS AND SYMBOLS

Equations and Formulas of Ions

The various hydrolytic equations and the formulae of the ions will be written in terms of unhydrated species, although unquestionably the ions in solution are heavily hydrated. This conventional procedure has been selected since most of the measurements are essentially thermodynamic and hence not sensitive to the degree of hydration of the ions. If one desired to assign coordination numbers, one might consider eight for the ions of the +3 and +4 oxidation[17] states [$M(H_2O)_8^{+3}$, $M(H_2O)_8^{+4}$] as well as for the +5 and +6 oxidation states, i.e., $MO_2(H_2O)_6^{+}$ and $MO_2(H_2O)_6^{++}$. These are the coordination numbers which one is likely to find in crystals, e.g., oxides or basic salts.[11,18-20] However, such assignments should not be taken too seriously, and lower coordination numbers may occur. Although six water molecules of hydration[17] are probable for the ions MO_2^{+} and MO_2^{++}, this cannot be taken completely for granted since the coordination number of the MO_2 groups tends to vary from compound to compound.[18] (M is a metallic ion.)

Symbols and Definitions

a_x = activity of x
g_x = activity coefficient of species x
G_i = proper activity coefficient quotient (or product) for reaction i
k_h = acid constant
k_h^m = concentration quotient for acid constant
K_{sp} = solubility product
K_{sp}^m = concentration product for K_{sp}
m_x = concentration (molarity or molality) of x
M = molarity (moles per liter of solution)
n = hydroxyl number, average number of hydroxide ions per metal ion
N = degree of polymerization, number of metal ions in a polymeric aggregate
pk_h = $-\log k_h$
z' = charge on polymer per monomer unit
μ = ionic strength (molarity or molality units)

The simple, monomeric, hydrolytic reaction will be assumed to be

$$M^{+z} + H_2O \rightleftharpoons MOH^{+z-1} + H^+ \qquad (1)$$

with the acid constant

$$k_h = \frac{a_{MOH}{}^{+Z} a_{H}{}^{+}}{a_{H_2O} a_{M}{}^{+Z}} = k_h{}^{m} G_h \qquad (2)$$

where

$$k_h{}^{m} = m_{MOH}{}^{+Z-1} m_{H}{}^{+} / m_{M}{}^{+Z} \qquad (3)$$

is the concentration quotient and $G_h = g_{MOH}{}^{+Z-1} g_{H}{}^{+} / a_{H_2O} g_{M}{}^{+Z}$ the proper activity coefficient quotient. In most cases only concentration quotients $k_h{}^{m}$ have been evaluated. These will be functions of the medium. In a few cases data have been expressed in terms of the solubility product

$$K_{sp} = a_{M}{}^{+Z} a_{OH}{}^{-Z} = K_{sp}{}^{m} G_{sp} \qquad (4)$$

where

$$K_{sp}{}^{m} = m_{M}{}^{+Z} m_{OH}{}^{-Z} \qquad (5)$$

and $G_{sp} = g_{M}{}^{+Z} g_{OH}{}^{-Z}$.

All the work to be discussed and all constants given refer to room temperature, usually 25°C, except where otherwise noted.

THE +3 OXIDATION STATE

Species in Acidic Solutions

The actinide elements with oxidation number three (M(III)) are generally considered to exist in acidic solutions as the species M^{+3}. There is little doubt that this assignment is correct for acidic solutions. Strongest evidence in its favor comes probably from the oxidation-reduction potentials of uranium,[21] neptunium[22] and plutonium[17] couples as a function of acidity. This assignment is further strengthened by the striking similarity of the properties of the actinides and lanthanides of oxidation number three. If one accepts the species M^{+3} for the early actinides, their similarity to the higher actinides and the essentially regular drift of properties as a function of atomic number[15,16,23-27] makes this assignment virtually certain for all the actinides M(III).

Hydrolytic Reactions

The actinides of oxidation number three form relatively insoluble hydroxides and basic salts in a manner analogous to the rare earths. There is no evidence for amphoteric character. Relatively little is known quantitatively regarding the hydrolysis of the ions M^{+3}, acid-base titrations of Pu(III) being the only ones available.[28,29]

Using the data of Moeller and Kremers[30] on the solubility of the lanthanide hydroxides, Latimer[31] computed values of K_{sp} for some of the actinide hydroxides, taking the similarity of the ionic radii of the lanthanides and actinides into consideration. In this manner he estimated $K_{sp} = 1 \times 10^{-9}$ for U(III), 2×10^{-20} for Pu(III), 2.7×10^{-20} for Am(III) and 1.9×10^{-21} for Cm(III). Latimer's value for K_{sp} (Pu(III)) compares favorably with $K_{sp}{}^{m} = 2 \times 10^{-20}$ calculated by Busey and Cowan[29] from their acid-base titrations of dilute $PuCl_3$ solutions (μ = ca 4×10^{-2}). For comparison, Busey and Cowan obtained $K_{sp}{}^{m} = 2.5 \times 10^{-9}$ for La(III) from similar acid-base titrations of dilute lanthanum chloride solutions (μ = ca 2×10^{-2}), in good agreement with $K_{sp} = 1 \times 10^{-19}$ given by Latimer. As pointed out by Latimer, these values of the solubility products only hold for the freshly precipitated hydroxides and aging effects would cause significant decrease of K_{sp} with time.

From an analysis of the acid-base titration curves of Pu(III) $pk_h{}^{m} = 7.3$ (μ = 0.24 to 0.07) was obtained.[28] This compares favorably with pH = 7.0 to 7.5 observed by Busey and Cowan at $n = 0.5$ for somewhat more concentrated Pu(III) solutions of approximately the same ionic strength. These pH values may be compared with pH ca 8.3 at $n = 0.5$ which Busey and Cowan observed for a 2×10^{-3} M $LaCl_3$ solution. This implies that $pk_h{}^{m}$ of La(III) is ca 8.3 if the initial hydrolysis follows the simple monomeric reaction (1). Similarly, an estimate of the acid constant of Pr(III), whose ionic radius is almost identical with that of Pu(III), indicates that these two elements have approximately the same acidity.[28] However, as pointed out,[28] detailed comparison of the acidity of the actinides and lanthanides of oxidation number three is not feasible since as far as the lantbanides are concerned, the data in the literature are not always consistent, possibly because polymeric hydrolysis products are formed in titrations at high concentration of metal, precluding sensible evaluation of $k_h{}^{m}$.

On the basis of simple coulombic (charge-radius) arguments, a slight increase in acidity of the actinides is expected with increasing atomic number in view of the "actinide contraction." Although such arguments do not apply to the actinides of higher oxidation number, the reasonably close agreement in the hydrolytic properties of the actinides and lanthanides suggests that they hold for the ions M^{+3}. The difference in the acidity of La(III) and Pu(III) is approximately as expected. Kasper[32] has shown that the acid constants of a large number of ions can readily be correlated by consideration of their size and charge. According to a simplified analysis, using his basic correlation,[32] it appears that the acid constant should increase at the rate of ca 0.085 pk units for each 0.01 Å decrease in the metal-oxygen distances for +3 ions of this size. Accordingly, with Pu(III) approximately 0.04 Å smaller than La(III), pk_h (La(III)) should be approximately 0.4 units larger than pk_h (Pu(III)). Although the observed difference is larger, this rather sensitive test reveals a startling similarity between these ions. However, one should mention that the agreement, however gratifying, cannot be taken as evidence for the similarity of the electronic configurations of these ions, since by Kasper's method many ions, as diverse electronically as Ca(II), Zn(II), Fe(III) and Pu(III), can reasonably well be correlated. Using this correlation, one predicts that pk_h(Ac(III)) is ca 0.9 pk units larger and pk_h of the last actinide (element 103) ca 1 pk unit smaller

than pk_h(Pu(III)). This makes the estimated acidity of Ac(III) about equal to that of La(III). Comparing the radii of these ions, however, Ac(III) should be more basic by ca 0.6 pk units, in qualitative agreement with data on vapor phase hydrolysis.[12]

THE +4 OXIDATION STATE

Species in Acidic Solutions

Until recently there was considerable doubt regarding existence of the species M^{+4} in acidic solutions. For example, it has often been proposed that in aqueous solutions these ions were oxygenated "—yl" ions of the type MO^{++}. Although doubt remains regarding the existence of the species M^{+4} for many metals in acidic solutions of moderate M(IV) concentration, these doubts have definitely been resolved for most actinides. Actually, it appears that the actinides may be unique with respect to the broad stability range of the species M^{+4} and the occurrence of this species in moderately acidic solutions.

The existence of the unhydrolyzed species M^{+4} has been unambiguously established for Th(IV) and U(IV) from measurements[34,35] of the acidity of solutions of $ThCl_4$ and UCl_4. Further confirmation comes from solvent extraction studies with acetylacetone[35a,b] and with oxine and cupferron.[35c] In studies with thenoyltrifluoroacetone (TTA)[36,37], a charge of +4 on the extractable species was established, although the studies were not carried far enough to disprove possible extraction of polymeric products, e.g., $(MO)_2^{+4}$. Proof for the species Pu^{+4} and Np^{+4}, though not quite so direct as for Th^{+4} and U^{+4}, seems nevertheless firm, not only from studies of the comparative behavior of these ions but also from the consistency of the oxidation-reduction potentials with this hypothesis.[17,22,38,39] In view of the general coherence of the properties of the actinides, one may probably safely assume that all of these in the oxidation state +4, including the recently discovered Pa (IV),[40-43] exist as the species M^{+4} in acidic solutions.

Hydrolytic Reactions

The actinides M(IV) form highly insoluble hydroxides and basic salts. Solubility product constants K_{sp} of the order of 10^{-39} (Th(IV)), 10^{-45} (U(IV)), 10^{-52} (Pu(IV)) and 10^{-56} (Am(IV)) have been estimated for the hydroxides.[12] There is no evidence for amphoteric character.

The mechanism of hydrolysis appears to be complicated and was studied recently in some detail for Th(IV),[34,44,45] U(IV)[35] and Pu(IV)[35,46] (references to earlier work may be found in the papers cited). At least three types of hydrolysis products have been recognized: (1) simple monomeric hydrolysis products, (2) low-molecular-weight hydrolytic polymers in equilibrium with each other and with M^{+4}, and (3) high-molecular-weight polymeric products (probably more than one type) not in equilibrium with the monomer. As discussed below, the mechanism of hydrolysis of Th(IV) appears to differ from that of U(IV) and Pu(IV) while that of the latter two is very similar.

In the case of Pu(IV) and U(IV) the earliest stage of hydrolysis involves the simple monomeric reaction, equation (1). At $\mu = 0.5$, $k_h^m = 2.9 \times 10^{-2}$ has been determined for U(IV) by a spectrophotometric method.[35] With essentially the same method $k_h^m = 2.5 \times 10^{-2}$ ($\mu = 0.5$) was determined for Pu(IV).[35] This value is in reasonable agreement with $k_h^m = 3.1 \times 10^{-2}$ at $\mu = 1$, which was obtained by a potentiometric method.[46] It was found possible to use a modified Debye-Hückel plot for extrapolation[35] of k_h^m to $\mu = 0$ even for equilibria involving such highly charged ions. In this way $k_h = 0.21$ can be estimated for U(IV) and $k_h = 0.18$ for Pu(IV).

In the region of acidities where hydrolysis according to Equation 1 occurs, slower hydrolytic (irreversible polymerization) as well as other reactions also take place and the constants listed[35] were obtained by extrapolation of all data to "zero time," the time of preparation of the solutions. With U(IV), polymerization (and oxidation) is sufficiently slow so that extrapolation introduces only minor correction, even up to $n = 0.8$ (10^{-3} M U(IV)). However, in the case of Pu(IV) such extrapolations are of considerable significance since at the higher acidities disproportionation reactions also occur and since near $n = 0.5$ "irreversible" polymerization becomes very rapid even in 10^{-3} to 10^{-4} M Pu(IV) solutions.

These results may be contrasted with those for Th(IV). The simple monomeric hydrolysis product $Th(OH)^{+3}$ appears to be of little significance.[34,44] If reaction (1) occurs at all, k_h^m for Th(IV) is very much smaller than for U(IV) and Pu(IV); an estimated k_h^m = ca 5×10^{-5} ($\mu = 1$, perchlorate media) was obtained.[34] At high dilution there is evidence for the formation of the monomeric hydrolysis product $Th(OH)_2^{+2}$ and the constant ${}^1k_2 = 1.5 \times 10^{-8}$ for the reaction $Th^{+4} + 2H_2O \rightleftharpoons Th(OH)_2^{++} + 2H^+$ was estimated.[34] However, even in the most dilute solutions studied (2.5×10^{-4} M Th(IV)) and for $n < 0.1$ polymeric hydrolysis products are also present. It is of interest to note that only for Th(IV) the postulated "oxygenated" species $Th(OH)_2^{++}$ (or ThO^{++}) has been confirmed in recent work. No such evidence was found with U(IV) and Pu(IV) and similarly the species has not been found for aqueous solutions of Zr(IV), Hf(IV) and Ce(IV). Even with Th(IV) the stability range of the species ThO^{++} is very narrow and the species has become of negligible importance long before $n = 2.0$ has been reached. Further, plots of n vs m_{H^+} (or log m_{H^+}) do not tend to level near $n = 2.0$, as expected for either the species MO^{++} or its polymers $(MO)_x^{+2x}$. Instead, the curves appear to level off near $n = 2.5$ for Th (IV)[44,45] and near $n = 2.3$ for Zr(IV), Hf(IV)[47] and Ce(IV),[48] although dilute metal solutions and extrapolations to zero time are necessary in these cases for clear recognition.

Regarding detailed interpretation of the hydrolytic

data of Th(IV), Kraus and Holmberg[34] postulated that besides the species $Th(OH)_2^{++}$, a dimer with probable composition $Th_2(OH)_2^{+6}$ is formed at low values of n. At higher values of n further hydrolysis and continued polymerization occurs, yielding species apparently in equilibrium with each other, at least up to $n = 2$. However, Hietanen,[44] interpreting similar acid-base data by the continuous polymerization ("core-link") method of Sillén,[49-51] concluded that Th(IV) does not form any monomeric hydrolysis products, but only a series of polymers of probable composition $Th(Th(OH)_3)_{N-1}^{+N+1}$.

Although the agreement of Hietanen's data, as well as those of Kraus and Holmberg, with the postulated continuous series of polymers, appears good at high (though not the highest) hydroxyl numbers, it is not considered satisfactory at low values of n, as can readily be demonstrated by a plot of log n vs log h rather than n vs log h, as essentially used by Hietanen. Since Hietanen used a very simple mechanism for interpretation which involves only one parameter (equilibrium constant), such disagreement is not surprising. Apparently, additional equilibria, of the type proposed by Kraus and Holmberg, must be considered in the early stages of hydrolysis.

Equilibrium ultracentrifugations of Th(IV) in perchlorate solutions at high hydroxyl numbers ($n = 1.0$, 1.5, 2.0 and 2.4) at $m_{Th} =$ ca 0.015 also revealed existence of polymeric hydrolysis products of Th(IV), apparently in equilibrium with each other.[45] The degree of polymerization N was found to change continuously with n. There was no evidence for a low molecular weight hydrolysis product of special stability. The degree of polymerization N was approximately 2.5 near $n = 1$, ca 3 near $n = 1.5$, ca 4.5 near $n = 2$, and rapidly rose to $N =$ ca 9 near $n = 2.4$.[52] These degrees of polymerization are in reasonable agreement with those calculated by Hietanen up to $n = 2.0$ but diverge near $n = 2.4$, where we compute a weight average degree of polymerization of 6.5 from Hietanen's results. This disagreement is not necessarily significant since the type of average molecular weight obtained here with the centrifuge emphasizes heavier species more than the weight average (*Z*-average[53,54]) and since at present the effect of polymer charge on the computed molecular weights cannot accurately be determined. The core-link method of intrepreting emf data thus in the case of Th(IV) yields degrees of polymerization substantially the same as the centrifuge. It will be interesting to see if this agreement continues after the additional equilibria needed to explain the early stages of hydrolysis have been incorporated in the interpretation of the emf data.

It should be mentioned that until recently a serious discrepancy existed between the core-link method of interpretation of emf data and the results of equilibrium ultracentrifugation. Thus for Bi(III) in perchlorate solutions very much smaller degrees of polymerization ($N =$ ca 5 or 6) were found by ultracentrifugation[45] than were computed by Graner and Sillén[55] from potentiometric data. Different centrifugations were carried out over a large range of conditions, including those where the core-link theory yielded a degree of polymerization $N =$ ca 40,[51,55] as well as for more basic solutions where N should be considerably larger than 40, according to Graner and Sillén. However, recently new emf measurements were carried out by Sillén and coworkers over a much larger range of conditions[55a] than before. Their interpretation by the core-link method suggests existence of a hexamer, in substantial agreement with the equilibrium ultracentrifugations.[55a]

Although the polymeric products in perchlorate solutions are usually written with the assumption that perchlorate complexing does not occur, it should be pointed out that even at relatively low degrees of polymerization such a hypothesis may probably not be tenable. These polymers are probably the inorganic analogues of the organic polyelectrolytes, and one must assume that the counter ions may associate with the polymers to decrease the effective charge to a value considerably less than the maximum theoretical possible from hydrolytic consideration. Experimental evidence that this association occurs has recently been obtained by ultracentrifugation of Hf(IV) solutions in chloride media where the maximum charge per monomer unit would be approximately $z' = 2$, while the actual charge on a trimeric (or tetrameric) polymer was found to be $z' =$ ca 1.[54] Similarly, in the case of Bi(III) in 1 *M* ClO_4 solutions the maximum charge on the hexamer (or pentamer) is $z' = 1$, while the actual charge found was $z' =$ ca 0.5.[46] Such association of counter ions with the polymers in some cases may greatly influence the polymeric products formed. Thus the degree of polymerization of Th(IV) in chloride solutions is very much greater than in perchlorate solutions of the same degree of hydrolysis, as shown by recent equilibrium ultracentrifugations[45] (e.g. at $n = 1.5$ and 0.015 *M* Th(IV), $N =$ ca 4.5 in 1 *M* ClO_4 and $N =$ ca 50 in 1 *M* Cl^-).

As has been mentioned earlier, polymeric products are also formed with U(IV) and Pu(IV). In contrast to the polymers described for Th(IV), those for U(IV) and Pu(IV) apparently are not in equilibrium with the monomer. Further, they grow rapidly to very large size, probably *via* an autocatalytic mechanism, once polymerization is initiated. Low molecular weight intermediates may exist, but have not been experimentally demonstrated. After the polymers have been permitted to age for any significant length of time, reversibility is very slow and depolymerization needs drastic conditions.[56]

A study of the hydrolytic polymer of Pu(IV) is particularly attractive since the polymer has little tendency to precipitate with time and formation of the polymer is strikingly revealed by a change in the

color of the solution. As expected from the visual color the absorption spectra of Pu^{+4} and polymeric Pu(IV) differ greatly. Most striking is the absence of the 476 mμ band of Pu^{+4} in the polymer spectrum and the very high values of extinction coefficients of the polymer (ca 180) near 400 mμ where Pu^{+4} shows an extinction coefficient of ca 30. The difference in the colors of Pu^{+4} and the polymer caused the rather early recognition of the existence of a polymeric form, the first recognition resulting from an observed color change from brown to green on heating weakly acidic (ca 0.3 M HNO_3) solutions of Pu(IV). Polymerization was later found to occur on treating Pu(IV)-hydroxide with acid. For example, as acid seeps into a packed hydroxide the color changes from olive to green and the material disperses, yielding a solution with typical polymer spectrum. Similarly, the polymer forms in ca 0.04 M H^+ (2×10^{-4} M Pu(IV) at room temperature very rapidly. The rate of polymerization decreases with decreasing Pu(IV) concentration. Minor changes in the spectrum occur with aging at room temperature or heating the polymer solutions in weakly acidic media. Unquestionably major changes in molecular weight (degree of polymerization) accompany these minor spectral changes. Although a number of attempts were made to determine the degree of polymerization, most convincing evidence for the high degree of polymerization comes from high speed centrifugations (not ultracentrifugations) with a "Misco"[37] air-driven centrifuge at ca 26,000 rpm. Small test tubes, collapsed to a capillary at the center and located at 1.2 to 4.3 cm from the center of rotation, were used. Decrease in Pu(IV) concentration in the upper portion of the test tubes was measured radiometrically. After two hours' centrifugation, this decrease amounted to 43 to 97% for heater polymers and up to 23% for unheated polymers, the exact amounts depending on the specific preparations. These measurements imply molecular weights of the order of hundreds of thousands, if not millions.

Depolymerization of the polymer at room temperature is very slow except in the presence of strong complexing agents such as fluoride or sulfate. Thus in 1 to 2 M HCl or HNO_3, depolymerization was essentially negligible after several weeks but became appreciable in 6 to 10 M HNO_3, as determined from spectral changes (growth of the 476 mμ peak of Pu^{+4}). Surprisingly, depolymerization rates are approximately first order in the concentration of polymeric Pu(IV). Half-lives of depolymerization were for unheated polymers ca 30 minutes and 95 minutes in 10 M HNO_3 and 6 M HNO_3, respectively, and ca 400 minutes and 730 minutes for the heated polymer in the same acids. At 90°C depolymerization even of heated polymers was very rapid in 6 M HNO_3.

The polymer shows very interesting precipitation properties. For example, it may be precipitated in moderately concentrated nitric acid and the precipitate redissolved with further excess nitric acid without depolymerization. Small amounts of IO_3^-, SO_4^{--}, $C_2O_4^{--}$, PO_4^{---}, and $Fe(CN)_6^{--}$ are sufficient for essentially complete precipitation. As a first approximation, ca 0.15 equivalents of negative ions were needed for precipitation irrespective of the charge type of the precipitating anion. This implies that the average positive charge (per monomer unit) of the polymer is $z' =$ ca 0.15. Analysis of polymer precipitates from chloride solutions indicated that chloride ions were not incorporated in the polymer network since no additional chloride was released after depolymerization with sulfuric acid. Thus the polymer is apparently held together by oxide or hydroxide bridges.

It is interesting to note that hydroxide precipitation in the case of Pu(IV) does not necessarily involve the polymer as an intermediate. Thus, it was found that when the hydroxide is rapidly precipitated from a solution of Pu(IV), which contained originally only monomeric Pu^{+4}, and if this precipitate is redissolved in acid, the resulting solution is largely composed of monomeric Pu^{+4}, though containing small and variable amounts of polymer. In contrast, if Pu(IV) is first polymerized, then precipitated with base, redispersion with acid yields Pu(IV) solutions of the polymer only without monomeric Pu^{+4}.

The polymer of Pu(IV) in many respects resembles the polymers (or colloids) which are formed by many highly charged ions on hydrolysis, and to some extent this polymer has the properties often ascribed to "meta acids." In particular, it may be compared with the properties of heated Zr(IV) solutions,[38] with which it shares the unusual precipitation behavior with various negative ions, although recent ultracentrifugations imply[45] that the polymer formed by heating Zr(IV) to ca 100° for an hour has relatively low molecular weights (N = ca 40), compared with the molecular weights observed for the Pu(IV) polymer. The properties of the Pu(IV) polymers seem to be paralleled by the properties of U(IV) polymers which also have a startlingly different color from U^{+4} (dark brown vs green) although the properties of the U(IV) polymer have not been studied so extensively.

To summarize, the most striking difference between the polymers of Th(IV) described above and those of the Pu(IV) polymer is the fact that the thorium polymers apparently are reversible and in equilibrium with each other, while those of Pu(IV) need drastic change in conditions for reversal (depolymerization). Further, the thorium polymers increase in molecular weight continuously with change in acidity, while those of Pu(IV) form abruptly with only a minor change in conditions and grow to large size. It is apparent that "irreversible" polymers can also be formed in the case of Th(IV) but extreme conditions, e.g., high temperature, are necessary. Presumably these latter irreversible polymers of Th(IV) are formed during the autoclaving of Th(IV)-sulfate

solutions as used in the preparation of the basic sulfate $Th(OH)_2SO_4$.[19] The polymers (colloids) prepared by Dobrey, Guinand and Mathieu-Sicaud,[59,60] though at least partially "irreversible," may occupy an intermediate position. The work of this French group is particularly interesting since it represents a concerted effort to characterize these polymers (or colloids) by methods standard in the polymer field.

Comparison of the hydrolytic data for the actinides of oxidation number +4 with Ce(IV) is tempting. As a first approximation Ce(IV) has the same size as Pu(IV),[5] and in view of the position of these elements in the periodic table one might expect that they would behave very similarly hydrolytically. Instead, Ce(IV) is considerably more acidic than Pu(IV). Recently Hardwick and Robertson[61] have shown by a spectrophotometric method that Ce(IV) is still considerably hydrolyzed in 10^{-3} *M* solutions in 2 *M* $HClO_4$. In this respect they agree with the potentiometric determinations of Shertill, King and Spooner[62] and the spectrophotometric observations of Kraus, Holmberg and Nelson.[48] However, it is not clear why Noyes and Garner[63] did not find evidence for the hydrolysis of Ce(IV) in 1 *M* HNO_3 by a potentiometric method. Unless the conclusions of Noyes and Garner are subject to revisioo these results indicate considerable and unexpected differences in the hydrolytic properties of Ce(IV) in nitrate and perchlorate media. Ia recent equilibrium ultracentrifugations[48] low-molecular-weight polymers were observed for 0.05 *M* Ce(IV) solutions in HNO_3-$NaNo_3$ solutions ($\mu = 2$). At an acidity of 0.1 *M* these low-molecular-weight polymers (possibly trimers) are unstable. During centrifugation, high-molecular-weight polymers centrifuge out rapidly without affecting the molecular weight of the residual low-molecular-weight component in the centrifuge cell. Thus, there appear to be no other reasonably stable low-molecular-weight intermediates. The observed increase in the hydroxyl numbers with time at low acidity[48] apparently parallels this growth in the size of the polymer, as does also the pronounced change in other properties which occurs on aging weakly acidic Ce(IV) solutions. Thus, for example, the rate of oxidation of I^- to I_2 shows a profound decrease with the age of weakly acidic Ce(IV) solutions.[45] Attempts to determine the molecular weight of the Ce(IV) polymer in 0.5 *M* HNO_3, 1.5 *M* $NaNo_3$ and 2 *M* HNO_3 ($\mu = 2$) by ultracentrifugation were undecisive although not inconsistent with the assumption that Ce(IV) under these conditions exists as a dimer, as suggested by Heidt,[64] Thomas and Kolp,[65] and Hardwick and Robertson.[61]

Although the details of the interpretation of the hydrolytic behavior of Ce(IV) by Hardwick and Robertson[61] appear in doubt since spectral changes of Ce(IV) solutions are still observable in concentrated $HClO_4$ solutions,[48] their estimate of $k_h^m = 5.6$ for Ce(IV) appears to he at least a lower limit. Thus in spite of the similarity in size and the similarity in position in the periodic table, Ce(IV) is very much more acidic than either Th(IV), U(IV) or Pu(IV).[66]

Of the supposedly similar actinides and lanthanides *M*(IV), Ce(IV) thus appears to stand in a class by itself. It is considerably more acidic than any of the actinides, it forms irreversihle polymers readily like Pu(IV), and appears to form low-molecular-weight specific intermediates like Zr(IV) and Hf(IV), with which elements it also shares its great tendency to form polymers, although a search for such low-molecular-weight intermediates might also prove rewarding with Pu(IV), it nppears that Ce(IV) has more similarities with Zr(IV) and Hf(IV), elements of a considerably smaller radius than Ce(IV), than with any other element in this part of the periodic table.

The acidity of Pa(IV) and its mode of hydrolysis are most difficult to predict on the basis of present knowledge because of this wide divergence in the acid-base characteristics of Ce(IV) and of the actinides so far studied. For a regular progression of properties one would of course predict that the acidity of Pa(IV) is intermediate between those of Th(IV) and U(IV). However, the unusually high acidity of Ce(IV) implies that at the beginning of a rare-earth-like series, i.e., when the *f*-electron shell drops below the *d*-electron shell, the properties may change abruptly and not necessarily monotonically. Thus, a study of the hydrolytic properties of Pa(IV) would be particularly interesting, though extremely difficult because of the unfavorable oxidation-reduction potential of the Pa(IV)/(V) couple, which has been estimated to be ca +0.1 volts[43] in 1 *M* acid and is probably considerably more positive at lower acidity.

THE +5 OXIDATION STATE

Species in Acidic Solutions

Protactinium(V) does not appear to exist in the form of ionically dispersed species in reasonably acidic solutions of even moderate Pa concentration. Instead, it tends to precipitate as a hydroxide (or basic oxide) and in more dilute Pa solutions may form hydrolytic polymers (colloids).[67-71]

In contrast, U(V) and the transuranic elements of this oxidation state do not precipitate in acidic solutions but apparently form the species MO_2^+ (UO_2^+,[72-77] NpO_2^+,[39,78-80] PuO_2^+,[81] AmO_2^+.[82] Early evidence for this formula came largely from the observed acid indepeadence of the *M*(V)/(VI) couples. The electrochemical reversibility of these couples suggested similarity in the structures of the *M*(V) and *M*(VI) ions, i.e., MO_2^+ and MO_2^{++}. More recently, convincing evidence for this structural similarity has come from studies of the infrared spectra of a number of *M*(V) and *M*(VI) ions[83] and from crystallographic work, particularly on Np and Am compounds.[13,81]

Recently, Welch[68] claimed to have established a charge of +1 for Pa by ion exchange methods at tracer concentrations in moderately acidic solutions. He concluded that Pa(V) exists as the oxygenated ion PaO_2^+, as was earlier also proposed by v. Grosse.[86] It is felt that the evidence so far presented is too scant to make this assignment convincing. Should Pa(V) have a charge of +1 under the conditions studied by Welch and be monomeric, the conclusion that Pa(V) and U(V) (as well as the transuranic elements M(V)) form ions of similar structure still does not seem warranted. The enormously greater tendency of Pa(V) to precipitate or polymerize surely implies that the structure of its ion differs greatly from that of the other actiuides M(V).[83]

Hydrolytic Reactions

There is essentially no information regarding the hydrolytic properties of Pa aside from observations regarding its solubility (see, e.g., references 69–71).

A hydrolytic study of UO_2^+ is complicated by the fact that its stability range with respect to disproportionation is quite narrow. Millimolar solutions of U(V) have been prepared near pH 3[76,77,87] and these contained the species UO_2^+. The acid constant of UO_2^+ must, therefore, be considerably smaller than 10^{-3}.

Acid-base titrations have been carried out on Np(V) and Pu(V).[33,88] While Np(V) is quite stable in basic solutions, Pu(V) tends to disproportionate. Nevertheless, buffering regions could be detected for both elements. These were concentration dependent and located in the vicinity of pH 7 to 9 for Np(V) (9×10^{-3} to 3.2×10^{-4} M Np(V)) and in the range pH 8 to 9.5 for Pu(V) (7.7×10^{-3} to 4.2×10^{-4} M). The relative acidities of Np(V) and Pu(V) were compared[88] in a plot of the observed pH values at $n = 0.4$ as a function of metal concentration, which is reproduced in Fig. 1. As seen from this figure, Np(V) is considerably more acidic than Pu(V). Further, the plot of pH ($n = 0.4$) vs log $m_{M(V)}$ is roughly linear and with slope ca −1. The data therefore can be fitted to an apparent solubility product constant, K_{sp}^m, although the hydrolytic reactions are probably more complicated than implied by the reaction $MO_2^+ + H_2O \rightleftharpoons MO_2OH(s) + H^+$. The computed apparent pK_{sp}^m values averaged ca 9.2 for Np(V) in the range $n = 0.1$ to 0.8 and ca 8.6 for Pu(V). The deviations of the computed pK_{sp}^m values from constancy were minor except for the most dilute solutions at low values of n. On the assumption that at the highest dilution hydrolysis proceeds via the monomeric reaction (1), yielding soluble MO_2OH, the apparent values for the acid constants pk_A^m = ca 8.9 for Np(V) and ca 9.7 for Pu(V) were calculated.

THE +6 OXIDATION STATE

Species in Acidic Solutions

It is now generally recognized that the elements, uranium, neptunium and plutonium, in their +6 oxidation states exist as the species MO_2^{++} in acidic solutions. A considerable amount of evidence in favor of this assignment has been accumulated and summary of these considerations is beyond the scope of this paper. Many of the arguments have been collected in the various review articles quoted. During the last few years the +6 oxidation state of americium has also been prepared and convincing evidence presented that it too forms an oxygenated species of the type MO_2^{++}.[89,90] With this discovery a series of four ions of a rather uncommon type has become available for comparative study. This series of ions as a first approximation seems to show the regular progression of properties as a function of atomic number which one might anticipate,[9,90] although as pointed out by Jones and Penneman[83] in their interesting infrared studies of these ions, unexpected though minor deviations from a simple progression of properties may occur. Thus, these authors found that the force constants for M-O stretching vibrations show a maximum at neptunium rather than a monotonic increase or decrease with atomic number.

Hydrolytic Reactions

As might be expected from the much greater availability of U(VI), its hydrolytic reactions have been studied in much greater detail than those of the other actinides. On addition of sufficient base, highly insoluble materials are formed from U(VI) solutions which often are described as uranates, diuranates, etc. Although U(VI) is unquestionably amphoteric, the products of the precipitations at present cannot be considered to have been unambiguously established (see, e.g., references 91, 92 and 92a for recent work on this subject). Thus, for the precipitated amorphous materials, formation of simple stoichiometric compounds is highly questionable, solid solutions of varying composition probably being formed. Precipitation of a simple hydroxide has not been unambiguously established.

At first glance the hydrolytic properties of Pu(VI) seem to differ greatly from those of U(VI).[88,93] Quantitative precipitations, so characteristic for U(VI), do not occur with Pu(VI) on addition of base. In moderately dilute solutions no precipitates are formed, even on addition of excess base, and at high concentrations (e.g., above 0.01 M) only partial precipitation can be achieved. The precipitation behavior of Np(VI) appears to be intermediate, partial precipitation occurring at lower concentratinns than with Pu(VI).

These gross differences in properties, however, tend to disappear on closer examination. Thus, buffering regions occur for all three elements in roughly the same pH range, though at progressively lower acidity, with increasing atomic number. Further, increasing amounts of base may be added as the U(VI) solutions are diluted before precipitation occurs. However, when precipitation of U(VI) occurs, it is often accompanied by an abrupt decrease in pH. The titration curves of all three elements give

evidence for amphoteric character at high pH. Amphoteric behavior has also been demonstrated in the case of Pu(VI) by preparation of a barium polyplutonate, with approximate composition $Ba_{0.35}PuO_2(OH)_{2.7}$.[94,95] Further, during the titration of all three elements polymeric hydrolysis products are unquestionably formed (and they are anticipated for Am(VI)). Thus the large differences in the precipitation characteristics of the elements probably mainly reflect differences in the tendencies of the polymeric products to coagulate or possible differences in the degree of aggregation of the polymers. However, since these differences are as large as indicated, one may have to be prepared to assume different structures of these polymers.

The hydrolytic reactions of UO_2^{++} have been extensively studied in recent years by a number of authors.[86,96-100] There appears to be general agreement that during this hydrolysis, polymeric products are formed. Thus, MacInnes and Longsworth[96] proposed the formation of the species $UO_2(UO_3)^{++}$. Sutton[98] proposed, in addition, formation of the species $UO_2(UO_3)_2^{++}$ and felt that higher polymers than this trimer are not formed. Further, he suggested that this trimer hydrolyzes to neutral and negatively charged polymers, e.g., $U_3O_4(OH)_4^-$. Faucherre[97] gave evidence for existence of the species $UO_2(UO_3)^{++}$. Similarly, Ahrland[99] concluded that polymers are formed during the hydrolysis of U(VI), although he also proposed formation of UO_2OH^+, the "simple" hydrolysis product, and computed the acid constant of UO_2^{++}. However, the data of Ahrland were recently re-evaluated by Ahrland, Hietanen and Sillén[101] according to the core-link hypothesis of Sillén.[79,80] These authors agree with the earlier worker that the polymers have the formula $UO_2(UO_3)_{N-1}^{++}$, although they could not reach an unambiguous conclusion regarding the maximum degree of polymerization N and state that they could not distinguish between an infinite series of polymers or a series of polymers which abruptly breaks at N = ca 4 or 5. Since special stability of a few polymers appears unlikely to them, they prefer the former interpretation. It is interesting to note that except for the first paper by Ahrland,[99] recent evidence for the existence of the simple monomeric hydrolysis product UO_2OH^+ is lacking. However, a search for such a species may still prove rewarding since most of the work quoted was not designed to detect this species should it occur only at low n and low m_U.

In acid-base titrations with Pu(VI)[93] it had been established that a buffering region exists in the range pH 5 to 6. Polymeric reactions had been proposed since on back titrations with acid a hysteresis loop occurred with pronounced drifts in pH. Actually, however, this hysteresis is relatively minor and surely less spectacular than the abrupt change in acidity found during the titrations of U(VI). The hydrolytic properties of Pu(VI) were later re-examined[85] and

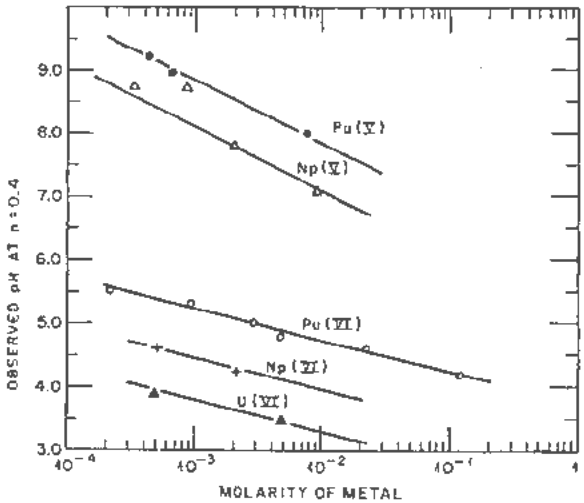

Figure 1. Relative acidities of Np(V), Pu(V), U(VI), Np(VI) and Pu(VI)

it was shown that, as anticipated, the titration curves were concentration dependent. Further, by high speed centrifugations with a Misco air-driven centrifuge[57] it could be demonstrated that relatively high-molecular-weight polymers are formed, particularly at high concentration and $n \geqslant 1$. Thus at $n = 1$ and $m_{Pu} = 2.1 \times 10^{-2}$, 40% of the Pu(VI) could be centrifuged down in 15 minutes at 18,000 rpm. Only 9% was centrifuged down under essentially the same conditions for $m_{Pu} = 1.5 \times 10^{-3}$.

In the same paper[85] a few acid-base titrations are also reported for Np(VI) and U(VI). These were carried out in an attempt to establish the relative acidities of the ions MO_2^{++}. The titration curves were similar but moved to higher acidities with decreasing atomic number. They all were concentration dependent. To demonstrate the trend in acidity of these ions the observed pH values at $n = 0.4$ were plotted as a function of logarithm of the metal concentration. The resulting curves are reproduced in Fig. 1. The data fall roughly on parallel straight lines with slope – 0.5. Apparent solubility product constants were calculated for the reaction $MO_2^{++} + 2H_2O \rightleftharpoons MO_2(OH)_2 + 2H^+$, although unquestionably the mechanism of hydrolysis is considerably more convolicated than implied by this equation. The values of $-\log K_{sp}^m$ were 23.5, 21.6 and 20.5 for U(VI), Np(VI) and Pu(VI), respectively. Thus the ions MO_2^{++} show approximately the same decrease in acidity with atomic number as the ions MO_2^+.

A number of proposals have been made to explain this drift in properties with atomic number.[88,93,102] Thus it was pointed out that if a regular actinide contraction would occur, an increase in acidity with atomic number would have been expected.[88,93] However, since the acidity of the ions is probably determined by the properties of the coordinated water molecules, it was felt possible that contraction along the O-M-O axis might be paralleled by increased

metal-water distances. Other suggestions involved assumption that *d*-electron orbitals[95] or *f*-electron orbitals[102] might become less available for bonding to the coordinated water molecules. However, all these "explanations" now must reckon with the observed non-monotonic decrease in the O-*M*-O force constants.[83] Although such reconciliation could readily be achieved on a qualitative basis, it is felt that with present restricted quantitative techniques further speculation regarding this relatively small effect (1 to 2 kcal in ΔF^0) cannot be considered satisfying.

Further, any explanation must take into consideration possible differences in the structures of the polymeric aggregates. Such differences in structure are by no means unexpected since uranates are known to crystallize in several different crystal modifications.[13,101] Thus, calcium uranate forms hexagonal orthouranate layers, the barium compound tetragonal layers and the magnesium compound chains. However, it appears likely that at high dilution all three elements form polymers of the same type (chains or sheets?) and that the abrupt formation of insoluble materials (and abrupt increase in acidity) during titrations of U(VI) is due to a change in structure of the U(VI) polymers, e.g., a transition from chains to sheets or sheets to 3-dimensional structures. Should this view be correct, the observed differences in the acidities of U(VI), Np(VI) and Pu(VI) might indeed become again legitimate targets for further explanations.

TEMPERATURE COEFFICIENT OF HYDROLYTIC REACTIONS

At the present time very little is known regarding the temperature coefficients of hydrolytic reactions in general and of the actinides in particular. In view of the large variety of possible hydrolytic reactions and products, i.e., monomers, low-molecular-weight polymers and high-molecular-weight polymers, a great deal of work will be required before this subject can be clarified.

Regarding the temperature coefficient of the hydrolytic polymerization reactions, relatively little is known, although present evidence suggests that these reactions may have positive values of ΔH^0. A slight increase in the degree of polymerization of Th^{+4} with temperature has been observed[45] by equilibrium ultracentrifugation experiments. Thus at a hydroxyl number $n = 2.4$ and $m_{Th} = 0.015$ the apparent degree of polymerization N was ca 40% larger at 30°C than at 3°C. A similar though more pronounced effect was observed for Zr(IV) and Hf(IV).[45] These observations are consistent with the more general notion that "colloid formation" in hydrolytic reactions is favored by high temperature. In contrast to this $\Delta H = -16$ kcal has been reported by Hardwick and Robertson[61] for the dimerization of Ce(IV) ($2CeOH^{+3} \rightleftharpoons Ce_2(OH)_2^{+6}$). For this reaction a negative value of ΔH is unexpected and such a large negative value is considered surprising. As pointed out below, a similarly unexpected entropy change for the simple monomeric hydrolysis reaction has also been reported by Hardwick and Robertson.

Data regarding the temperature coefficient of the simple monomeric hydrolytic reaction (1) are also very scant. Recently[103] the acid constant of U(IV) has been studied as a function of temperature. The heats and entropy of the reaction were found to be $\Delta H^0 = 11.7$ kcal and $\Delta S^0 = 36.2$ e.u. From these data $S^0_{UOH^{+3}} = -25$ e.u. was obtained. Thus the entropy of the hydrolysis product UOH^{+3} is approximately equal to that of U^{+3}, though about 5 e.u more positive ($S^0_{U^{+3}} = -30$ e.u.[140]). The same situation may pertain in the hydrolysis of Fe(III) where $S^0_{FeOH^{+2}} = -23.2$ e.u. has been reported, which is approximately equal to, though slightly more positive than, $S^0_{Fe^{+2}} = -27.1$ e.u.,[104] although recently the reliability of earlier work on Fe(III) hydrolysis has been questioned.[105] If, in spite of this, one may generalize from these few cases, one could predict the entropy of the simple hydrolytic reactions and hence ΔH^0 by combination with ΔH^0. This should not be restricted to those cases where the entropy of the ions in the appropriate oxidation states are known since the effect of change in charge on S^0 can be estimated with reasonable certainty from an estimate of the change in metal oxygen distances with charge and entropy-radius relations of the type proposed by Latimer.[105,106]

It has earlier been shown that the hydrolytic properties[33] of PuO_2^{++} and the difference in hydrolytic properties of PuO_2^{++} and PuO_2^{+} are in reasonable agreement with those predicted for ions of formal charge +4 (or +3.5) and formal charge +3 (or +2.5), respectively. This implies that electrostatic effects may also be dominant in a determination of the differences in the entropy of these ions and one might therefore estimate the entropy change for the reaction $MO_2^{++} + H_2O \rightleftharpoons MO_2OH^{+} + H^{+}$ (if it occurs at all) in the following manner. Since $S^0_{UO_2^{++}} = -17$ e.u., $S^0_{UO_2^{+}} = 12$ e.u., one expects $S^0_{NO_2OH^{+}} =$ ca 16 e.u. and $\Delta S^0 = 16$ e.u. for the simple hydrolytic reaction. This, with an estimated $\Delta F^0 = 6.5$ kcal (from Ahrland's value $k_1 = 2 \times 10^{-5}$) yields ΔH^0 for this hydrolytic reaction of 11 kcal.

It thus appears that the dimerization and polymerization reactions may have a less positive value of ΔH^0 than the hypothetical simple monomeric reaction. This poses the interesting possibility that the simple monomeric step might be more readily identifiable at high temperatures than at room temperature provided rates of polymerization to yield "irreversible" polymers do not become dominant.

HYDROLYTIC PROPERTIES AND THE ACTINIDE HYPOTHESIS

There has been a great deal of discussion in the literature regarding the exact place at which the 5*f* shell drops below the 6*d* shell, i.e., regarding the beginning of rare-earth-like behavior in the last row of the periodic table. This problem has been discussed

in numerous papers since Bohr made his original suggestion in 1923 that such a series would start in the neighborhood of uranium. A detailed discussion of this problem cannot be undertaken here. We shall confine ourselves instead to the information we might gain on this topic from the comparative study of hydrolytic properties of the heaviest elements.

The hydrolytic behavior of the heavy elements in the oxidation state +3 does not contribute significantly to the resolution of the question. As a first approximation the acidity is as expected for ions of this size and charge, irrespective of electron configuration, although Pu(III) seems to be somewhat too acidic compared with La(III).

The ions of oxidation number four show a definite break in properties between Th(IV) and U(IV). A typical rare-earth-like persistence of properties appears to occur from U(IV) upwards, as indicated by the startling similarity in the hydrolytic properties of U(IV) and Pu(IV). Studies of the hydrolytic properties of Pa(IV) would greatly assist in locating the break in properties more accurately. Unfortunately, the great complexity of the hydrolytic properties of the +4 ions may make unambiguous conclusions difficult. One may recall that U(IV) and Th(IV) are not acidic enough compared with Ce(IV). An "anomalous" acidity of the type shown by Ce(IV) may be characteristic for the beginning of a "rare-earth-like" series.

The pronounced difference in acidity of the +4 actinides and lanthanides is not reflected in the crystallographic data on the compounds of the type MO_2. Instead, as is pointed out by Katz,[107] the metal oxygen distances (lattice constants) show regular contraction with increasing atomic number for both series. Since the crystal structures do not reflect such major changes in properties one must conclude that the metal oxygen distances in the oxides are inadequate for identification of changes in the electronic structure of these elements.

The ions of oxidation number five show the most unambiguous break in properties. It had been apparent for some time that hydrolytically there is an enormous difference between Pa(V) and Pu(V) and that these elements should not be classified as part of the same series.[33] The work of Kolthoff and Harris[72] and Heal[74] suggested that the break in hydrolytic properties occurs between Pa and U. To strengthen this evidence further, a search for conditions under which U(V) could be prepared and studied in macro concentrations was hence instituted and the similarity between U(V), Np(V) and Pu(V) unambiguously established.[16] From a hydrolytic point of view, the break in hydrolytic properties thus occurs between Pa(V) and U(V), i.e., typical rare-earth persistence of properties starts with U(V), which is consistent with the hypothesis that near uranium the 5*f* shell becomes more stable than the 6*d* shell, as suggested, for example, by M. Goeppert-Mayer.[108] For recent work on this subject, see reference 109.

The ions of oxidation number six from uranium on up unquestionably show the persistence of properties expected for a rare-earth-like series, as already recognized by MacMillan and Abelson, the discoverers of element 93. The interesting decrease in acidity with increasing atomic number which occurs for the ions MO_2^{++}, as well as MO_2^{+}, might qualitatively be explained in a number of ways but will probably have to await further data, perhaps from other fields, before its significance with respect to the 5*f* shell entry can be completely understood.

One might thus conclude that the hydrolytic properties support the point of view expressed also by Paneth,[110] Coryell,[111] Haissinsky,[112] and others, that we are dealing with a series of elements for which persistence of properties starts principally with uranium, i.e., a uranide series. However, since unquestionably the properties of the elements of higher atomic number behave as if the series had started with actinium, as pointed out particularly by Seaborg, classification of these elements as an actinide series appears fully justified provided that the implied limitations are recognized.

ACKNOWLEDGEMENTS

The author is indebted to Messrs. R. W. Holmberg and J. S. Johnson for permission to cite previously unpublished work and for critical reading of the manuscript.

REFERENCES

1. Seaborg, G. T., *Electronic Structure of the Heaviest Elements,* National Nuclear Energy Series, IV, 14B, Paper No. 21.1, page 1492, McGraw-Hill Book Co., Inc., New York (1949). (Note: To be abbreviated as NNES.)
2. Seaborg, G. T., *The Actinide Series,* in Comprehensive Inorganic Chemistry, edited by Sneed, Maynard and Brastad, Vol. 1, page 161.
3. Seaborg, G. T., *Place in Periodic System and Electronic Structure of the Heaviest Elements,* Nucleonics 5: No. 5, 16 (Nov., 1949).
4. Katz, J. J. and Manning, W. M., *Chemistry of the Actinide Elements,* Ann. Rev. Nucl. Chem. 1: 245 (1952).
5. Hindman, J. C., *Ionic and Molecular Species of Plutonium in Solution,* NNES IV, 14A, Chapter 9, page 301 (1954).
6. Lister, M. W., *Chemistry of the Transuranic Elements,* Quart. Rev. 4: 20 (1950).
7. Nast, R. and Krakkay, T. V., *Chemistry and Actinide Theory of Transuranics,* Fortschr. chem. Forsch. 2: 484 (1952).
8. Zachariasen, W. H., *Crystal Chemistry of the 5f Elements,* NNES IV, 14A, Chapter 18, page 769 (1954).
9. Zachariasen, W. H., *Crystal Radii of the Heavy Elements,* Phys. Rev. 73: 1104 (1948).
10. Zachariasen, W. H., *The UCl_3 Type of Crystal Structure,* J. Chem. Phys. 16: 254 (1948).
11. Zachariasen, W. H., *Crystal Chemical Studies of the 5f Series of Elements,* Numerous papers — Acta Cryst. 1: (1948) to 8: (1955).
12. Fried, S., Hagemann, F. and Zachariasen, W. H., *Preparation and Identification of Some Pure Actinium Compounds,* J. Am. Chem. Soc. 72: 771 (1950).

13. Zachariasen, W. H., *On the Crystal Chemistry of Uranyl Compounds and of Related Compounds of Transuranic Elements*, Acta Cryst. 7: 795 (1954).

14. Dawson, J. K., *Electronic Structure of the Heaviest Elements*, Nucleonics 10: No. 9, 39 (1952).

15. Diamond, R. M., Street, K. Jr. and Seaborg, G. T., *An Ion Exchange Study of Possible Hybridized 5f Bonding in the Actinides*, J. Am. Chem. Soc. 76: 1461 (1954).

16. Street, K. Jr., Thompson, S. G. and Seaborg, G. T., *Chemical Properties of Californium*, J. Am. Chem. Soc. 72: 4832 (1950).

17. Kraus, K. A., *Oxidation Reduction Potentials of Plutonium Couples as a Function of pH*, NNES IV, 14B, Paper 3.16, page 241 (1949).

18. Lundgren, G. and Sillén, L. G., *The Crystal Structure of* $Th(OH)_2CrO_4 \cdot H_2O$, Arkiv Kemi 1: 277 (1950).

19. Lundgren, G., *The Crystal Structure of* $Th(OH)_2SO_4$, Arkiv Kemi 2: 535 (1951).

20. Lundgren, G., *The Crystal Structure of* $U(OH)_2SO_4$, Arkiv Kemi 4: 421 (1953).

21. Kritchevsky, E. S. and Hindman, J. C., *The Potentials of the Uranium (III)/(IV) and (V)/(VI) Couples in Perchloric and Hydrochloric Acids*, J. Am. Chem. Soc. 71: 2096 (1949).

22. Cunningham, B. B. and Hindman, J. C., *The Chemistry of Neptunium*, NNES IV, 14A, Chapter 12, page 456 (1954).

23. Thompson, S. G., Cunningham, B. B. and Seaborg, G. T., *Chemical Properties of Berkelium*, J. Am. Chem. Soc. 72: 2798 (1950).

24. Harvey, B. G., Thompson, S. G., Ghiorso, A. and Choppin, G. R., *Further Production of Transcurium Nuclides by Neutron Irradiation*, Phys. Rev. 93: 1129 (1954).

25. Studier, M. H., *et al., Elements 99 and 100 from Pile-Irradiated Plutonium*, Phys. Rev. 93: 1428 (1954).

26. Thompson, S. G., Harvey, B. G., Choppin, G. R. and Seaborg, G. T., *Chemical Properties of Elements 99 and 100*, J. Am. Chem. Soc. 76: 6229 (1954).

27. Ghiorso, A., Harvey, B. G., Choppin, G. R., Thompson, S. G. and Seaborg, G. T., as reported in Chem. Eng. News, 33: 1956 (1955).

28. Kraus, K. A. and Dam, J. R., *Acid-Base Titrations of Plutonium(III)*, NNES IV, 14B, Paper No. 4.14, page 466 (1949).

29. Busey, H. M. and Cowan, H. D., *Behavior of Plutonium(III) Chloride in Titrations with Base and Acid*, LAMS-1105, March (1950).

30. Moeller, T. and Kremers, H. E., *Observations on the Rare Earths LI.*, J. Phys. Chem. 48: 395 (1944).

31. Latimer, W. M., *Oxidation Potentials*, Prentice-Hall, Inc., New York (1952) (Second Edition).

32. Kasper, J., *The Ionization Constants of Hydrated-Ion Acids*, Ph.D. Dissertation, Johns Hopkins University (1941).

33. Kraus, K. A. and Dam, J. R., *Hydrolytic Behavior of Pu(V)*, NNES IV, 14B, Paper No. 4.15, page 478 (1949).

34. Kraus, K. A. and Holmberg, R. W., *Hydrolytic Behavior of Metal Ions. III. Hydrolysis of Thorium (IV)*, J. Phys. Chem. 58: 325 (1954).

35. Kraus, K. A. and Nelson, F., *The Acid Constants of Uranium(IV) and Plutonium(IV)*, J. Am. Chem. Soc. 72: 3901 (1950).

35a. Rydberg, J., *On the Complex Formation Between Thorium and Acetyl Acetone*, Acta Chem. Scand 4: 1503 (1950).

35b. Rydberg, J., *Studies on the Extraction of Metal Complexes, XII-B.*, Arkiv Kemi 8: 113 (1955).

35c. Dyrssen, D., *On the Complex Formation of Thorium with Oxine and Cupferron*, Svensk Kem. Tidskr 65: 43 (1953).

36. Betts, R. H. and Leigh, Rita M., *Ionic Species of Tetravalent Uranium in Perchloric and Sulphuric Acids*, Can. J. Research B28: 514 (1950).

37. Zebrowski, E. L., Alter, H. W. and Heumann, F. K., *Thorium Complexes with Chloride, Fluoride, Nitrate, Phosphate and Sulfate*, J. Am. Chem. Soc. 73: 5646 (1951).

38. Hindman, J. C. and Kritchevski, E. S., *The Polarographic Behavior of the Np(III)/(IV) Couples in Chloride and Perchlorate Solutions*, J. Am. Chem. Soc. 72: 953 (1950).

39. Magnusson, L. B. and Huizenga, J. R., *Stabilities of +4 and +5 Oxidation States of the Actinide Elements —The Np(IV)/Np(V) Couple in Perchloric Acid Solutions*, J. Am. Chem. Soc. 75: 2242 (1953).

40. Bouissières, G. and Haissinsky, M., *Chemical and Electrochemical Properties of Protactinium*, Proc. Inter. Congr. Pure and Appl. Chem. (London) 1: 17 (1947).

41. Haissinsky, M. and Bouissières, G., *About the Existence of a Valence State of Protactinium less than 5*, Compt. rend. 226: 573 (1948).

42. Haissinsky, M. and Bouissières, G., *Researches on the Chemistry of Pa. I. Existence and Properties of Pa (IV)*, Bull. soc. chim. France, 146: (1951).

43. Fried, S. and Hindman, J. C., *The +4 Oxidation State of Protactinium in Aqueous Solution*, J. Am. Chem. Soc. 76: 4863 (1954).

44. Hietanen, S., *The Hydrolysis of the Thorium Ion,* Th^{4}, Acta Chem. Scand. 8: 1626 (1954).

45. Kraus, K. A., Johnson, J. S. and Holmberg R. W. (to be published).

46. Rabideau, S. W. and Lemons, J. F., *The Potential of the Pu(III)/(IV) Couple and the Equilibrium Constants for Some Complex Ions of Pu(IV)*, J. Am. Chem. Soc. 73: 2895 (1951).

47. Kraus, K. A., Tyree, S. Y., Jr. and Holmberg R. W. (to be published).

48. Kraus, K. A., Holmberg, R. W. and Nelson, F., Abstracts 114th Meeting of American Chemical Society, Portland, Oregon, Sept. 13-17 (1948), Paper 6, page 4-0.

49. Sillén, L. G., *On Equilibria in Systems with Polynuclear Complex Formation, I.*, Acta Chem. Scand. 8: 299 (1954).

50. Sillén, L. G., *On Equilibria in Systems with Polynuclear Complex Formation, II.*, Acta Chem. Scand 8: 318 (1954).

51. Hietanen, S. and Sillén, L. G., *Studies on the Hydrolysis of Metal Ions, VIII.*, Acta Chem. Scand. 8: 1607 (1954).

52. In an earlier paper (ref. 34) it had been stated parenthetically that "tetramers (might) possibly be occurring for n just less than 2 and considerably larger polymers for n barely larger than 2." This statement has been interpreted by Hietanen (ref. 44) to imply special stability of a tetramer. The original statement was only intended to qualitatively describe the centrifugation results and was not intended to imply special stability for a tetramer.

53. Lansing, W. D. and Kraemer, E. O., *Molecular Weight Analysis of Mixtures by Sedimentation Equilibrium in the Svedberg Ultracentrifuge*, J. Am. Chem. Soc. 57: 1369 (1935).

54. Johnson, J. S., Kraus, K. A. and Holmberg, R. W., J. Am. Chem. Soc. (in press).

55. Granér, F. and Sillén, L. G., *On the Hydrolysis of the Bi^{+3} Ion*, Acta Chem. Scand. 1: 631 (1947).

55a. Sillén, L. G. (Private Communication).

56. Most of this information regarding the properties of polymeric Pu(IV) was obtained by the author in 1944 and early in 1945. Some of this work was partially summarized earlier, see e.g., ref. 17 and the review article by B. B. Cunningham, NNES IV, 14A, Chapter 10, page 371.

57. (Misco) Micro Chemical Specialties Corp., 1834 University Avenue, Berkeley 3, California.

58. Ruer, R., *On Metazirconic Acid, A Zirconium Hydroxide Corresponding to Metastannic Acid*, Z. anorg. allgem. Chem. 43: 282 (1905).

59. Dobrey, A., Guinand, S. and Mathieu-Sicaud, A., *On Colloidal Thorium Hydroxide*, J. chim. phys. 50: 501 (1953).

60. Dobrey, A., *Solutions of Thorium Hydroxide*, J. chim phys. 50: 507 (1953).

61. Hardwick, T. J. and Robertson, E., *Ionic Species in Ceric Perchlorate Solutions*, Can. J. Chem. 29: 818 (1951).

62. Sherrill, M. S., King, C. B. and Spooner, R. C., *The Oxidation Potential of Cerous-Ceric Perchlorates*, J Am. Chem. Soc. 65: 170 (1943).

63. Noyes, A. A. and Garner, C. S., *Oxidation Potential of Cerous-Ceric Salts*, J. Am. Chem. Soc. 58: 1265 (1936).

64. Hexdt, L. J. and Smith, M. E., *Quantum Yield of the Photochemical Reduction of Ceric Ions by Water and Evidence for the Dimerization of Ceric Ions*, J. Am. Chem. Soc. 70: 2476 (1948).

65. Kolp, D. G. and Thomas, H. C., *Rates of Water Oxidation in Ceric Perchlorate Solutions*, J Am. Chem. Soc. 71: 3047 (1949).

66. It has been stated by Hindman (ref. 5) that Ce(IV) has approximately the same acidity as Pu(IV). Hindman cited as evidence early unpublished results by the author on spectrophotometric and pH observations on Ce(IV) solutions. It had been found that in the range 0.01 *M* to 0.1 *M* H^+, pronounced spectral changes occur for Ce(IV). These, however, apparently do not involve equilibria with Ce^{+4}, as discussed in the text.

67. See, e.g., work by Grosse, A. v., Graue, G. and Käding, H., etc., as reported in Gmelin's Handbuch d. anorg. Chem., *Protactinium and Isotopes*, Syst. No. 51, Verlag Chemie, Berlin (1942) 8th Ed.

68. Kraus, K. A. and Van Winkle, Q., *Isolation and Purification of Protactinium using HF*, NNES IV, 17B, Paper 6.2, page 298.

69. Thompson, R. C., *Solubility of Protactinium in the Common Acids*, AECD-2488 (1949).

70. Bouissières, G. and Haissinsky, M., *Researches on the Chemistry of Protactinium. II*, Bull. soc. chim. (France), 18: 557 (1951).

71. Miles, G. L., *The Chemistry of Protactinium*, Rev. Pure and Appl. Chem. (Australia), 2: 163 (1952).

72. Harris, W. E. and Kolthoff, I. M., *The Polarography of Uranium. I*, J. Am. Chem. Soc. 67: 1484 (1945).

73. Harris, W. E. and Kolthoff, I. M., *The Polarography of Uranium. II*, J. Am. Chem. Soc. 68: 1175 (1946).

74. Heal, H. G., *Electrochemistry of Uranium*, Nature 157: 225 (1946).

75. Heal, H. G., *Some Observations on the Electrochemistry of Uranium*, Trans. Faraday Soc. 45: 1 (1949).

76. Kraus, K. A., Nelson F. and Johnson, G. L., *Chemistry of Aqueous U(V) Solutions. I*, J. Am. Chem. Soc. 71: 2510 (1949).

77. Kraus, K. A. and Nelson, F., *Chemistry of Aqueous Uranium(V) Solutions. II*, J. Am. Chem. Soc. 71: 2517 (1949).

78. Magnusson, L. B., Hindman, J. C. and LaChapelle, T. J., *Chemistry of Np(V). Formal Oxidation Potentials of Neptunium Couples*, NNES IV, 14B, Paper No. 15.4, page 1059 (1949).

79. Huizenga, J. R. and Magnusson, L. B., *Oxidation Reduction Reactions of Neptunium(IV) and (V)*, J. Am. Chem. Soc. 73: 3202 (1951).

80. Sjoblom, R. and Hindman, J. C., *Spectrophotometry of Neptunium in Perchloric Acid Solutions*, J. Am. Chem. Soc. 73: 1744 (1951).

81. Kraus, K. A. and Moore, G. E., *Chemistry of Pu(V)*, NNES IV, 14B, Paper No 4.19, page 550 (1949).

82. Werner, L. B. and Perlman, I., *The Pentavalent State of Americium*, J. Am. Chem. Soc. 73: 495 (1951).

83. Penneman, R. A. and Jones, L. H., *Infrared Spectra and Structure of Uranyl and Transuranium(V) and (VI) Ions in Aqueous Perchloric Acid Solution*, J. Chem. Phys 21: 542 (1953).

84. Nigon, J. P., Penneman, R. A., Staritzky, E., Keenan, T. K. and Asprey, L. B., *Alkali Carbonates of Np(V) and Am(V)*, J. Phys. Chem. 58: 403 (1954).

85. Welch, G. A., *Protactinyl Ion*, Nature 172, 458 (1953).

86. Grosse, A. v., *Element 91: Its Properties and Isolation*, Ber. 61: 233 (1928).

87. Nelson, F. and Kraus, K. A., *Chemistry of Aqueous U(V) Solutions. III*, J. Am. Chem. Soc. 73: 2157 (1951).

88. Kraus, K. A. and Nelson, F., *The Hydrolytic Behavior of Uranium and the Transuranic Elements. I. The +5 and +6 Oxidation States*, AECD-1864 (1948)

89. Asprey, L. B., Stephanou, S. E. and Penneman, R. A., *A New Valence State of Americium, Am(VI)*, J. Am. Chem. Soc. 72: 1425 (1950).

90. Asprey, L. B., Stephanou, S. E. and Penneman, R. A., *Hexavalent Americium*, J. Am. Chem. Soc. 73: 5715 (1951).

91. Tanford, C., Tichenor, R. L. and Young, H. A., *The Reaction Between Calcium Hydroxide and Uranyl Nitrate Solutions*, J. Am. Chem. Soc. 73: 4491 (1951).

92. Wamser, C. A., Belle, J., Bernsohn, E. and Williamson, B., *The Constitution of the Uranates of Sodium*, J. Am. Chem. Soc. 74: 1020 (1952).

92a. Sutton, J., *Hydrolysis of the Uranyl Ion and Formation of Sodium Uranates*, J. Inorg. and Nucl. Chem. 1: 68 (1955).

93. Kraus, K. A. and Dam, J. R., *Hydrolytic Behavior of Plutonium(VI). Acid-Base Titrations of Plutonium (VI)*, NNES IV, 14B, Paper 4.18, page 528 (1949). Fig. 1a of this reference had inadvertently been reversed. The figure should be turned by 180° so that the pronounced hysteresis loop appears at low pH and low moles OH^- per mole Pu. Further, the ordinate should read –log (H_3O^+) rather than log (H_3O^+).

94. Gevantman, L. H. and Kraus, K. A., *Hydrolytic Behavior of Plutonium(VI). A Note on the Analysis of Barium Polyplutonate*, NNES IV, 14B, Paper 4.21, page 602 (1949).

95. Connick, R. E., McVey, W. H. and Sheline, G. E., *Note on the Stability of Plutonium(VI) in Alkaline Solution*, NNES IV, 14B, Paper 2.150, page 345.

96. MacInnes, D. A. and Longsworth, L. G., *The Measurement and Interpretation of pH and Conductance Values of Aqueous Solutions of Uranyl Salts*, MDDC-911 (1942).

97. Faucherre, J., *On the Condensation of Basic Ions in the Hydrolysis of Aluminum and Uranyl Nitrates, Compt. rend.* 227: 1367 (1948).

98. Sutton, J., *The Hydrolysis of the Uranyl Ion, Part 1,* J. Chem. Soc. 1949, S275.

99. Ahrland, S., *On the Complex Chemistry of the Uranyl Ion. I. The Hydrolysis of the Six-valent Uranium in Aqueous Solution,* Acta Chem. Scand. 3: 374 (1949).

100. Robinson, R. A. and Lim, C. K., *The Osmotic and Activity Coefficients of Uranyl Nitrate, Chloride and Perchlorate,* J. Chem. Soc. 1951, 1840.

101. Ahrland, S., Hietanen, S. and Sillén, L. G., *Hydrolysis of the Uranyl Ion UO_2^{2+},* Acta Chem. Scand. 8: 1907 (1954).

102. Connick, R. E. and Hugus, Z. Z., Jr., *The Participation of f-Orbitals in Bonding in Uranium and the Transuranic Elements,* J. Am. Chem. Soc. 74: 6012 (1952).

103. Kraus, K. A. and Nelson, F., *The Acid Constant of U(IV) as a Function of Temperature,* J. Am. Chem. Soc. (in press).

104. Rossini, F. D., *et al., Selected Values of Chemical Thermodynamic Properties,* Circ. of the National Bureau of Standards, 500 (1952).

104a. Hedstrom, B. O. A., *The Hydrolysis of the Iron(III) Ion,* Arkiv Kemi 6: 1 (1954).

105. Powell, R. E. and Latimer, W. M., *The Entropy of Aqueous Solutes,* J. Chem. Phys. 19: 1139 (1951).

106. Latimer, W. M., *Single Ion Free Energies and Entropies of Aqueous Ions,* J. Chem. Phys. 23: 90 (1955).

107. Katz, J. J., *Oxide Systems of the Actinide Elements,* Record Chem. Progr. 12: 43 (1951).

108. Goeppert-Mayer, M., *Rare Earths and Transuranic Elements,* Phys. Rev. 60: 184 (1941).

109. Cap, F., *On the Problem of the Actinide Group,* Experientia 6: 291 (1950).

110. Paneth, F. A., *The Making of the Elements 97 and 98,* Nature 165: 748 (1950).

111. Coryell, C. D., *The Place of the Synthetic Elements in the Periodic System,* Record Chem. Progr. 12: 55 (1951).

112. Haissinsky, M., *On the Classification of the Last Elements in the Periodic Table,* J. chim. phys. 47: 415 (1950).

Effective Capture Cross Sections of Pa^{233} and Np^{239} for Thermal Reactor Neutrons

By J. Halperin,* R. W. Stoughton,* D. E. Ferguson,* C. V. Ellison,* D. C. Overholt* and C. M. Stevens,† USA

Pa^{233} and Np^{239} are intermediates in the conversion of Th^{232} into U^{233} and U^{238} into Pu^{239} in nuclear reactors. They play quite parallel roles in these two very similar systems. The capture cross sections of Pa^{233} and Np^{239} will affect both the neutron economy of the systems and the isotopic composition of the products. The contribution to 234 or 240 chain formation resulting from neutron absorption by Pa^{233} or Np^{239} during Th^{232} or U^{238} irradiations, respectively, will increase with irradiation time and gradually approach a constant value with a half-time equal to the beta decay half-life of the Pa^{233} or Np^{239}.

The ratio $\phi\sigma/\lambda$ is a measure of the loss by neutron capture while in the reactor compared to the product produced by beta decay, where ϕ is the average neutron flux, σ the effective capture cross section and λ the radioactive decay constant of either Pa^{233} or Np^{239}. The total contribution to the reactor system losses is then approximately $2\phi\sigma/\lambda$, since an otherwise useful neutron is lost as well as a potential product atom of either U^{233} or Pu^{239}. In order to evaluate these losses effective values for the capture cross sections of Pa^{233} and Np^{239} were obtained.

The work reported here is in essence an activation cross-section measurement (including a composite of neutron capture to all energy states) of the isotopes Pa^{233} and Np^{239} when produced during the course of a neutron irradiation. However, the measurement is made of the decay product of the 234 or 240 chain rather than the capture product itself. This method has the advantage of yielding the total capture cross section independent of a detailed knowledge of the decay scheme, and isomeric transitions; and the additional need for absolute beta counting. It is assumed here that no long lived isomeric states of Pa^{234} and Np^{240} have escaped detection. The principal analyses required by this method are the mass spectrographic determinations of the U^{234}/U^{233} and Pu^{240}/Pu^{239} ratios, the analyses of the U^{233} and Pu^{239} produced in the Th^{232} and U^{238} respectively, and the irradiation times. The Th^{232} samples were irradiated for periods of time varying from about two weeks to about six months such that the fraction of 234 chain arising from Pa^{233} capture varied from about 90 to 50 per cent. The U^{238} samples were irradiated for periods of time varying from 12 to 423 hours such that the fraction of Pu^{240} arising from Np^{239} capture varied from about 80 to 10 per cent. Although it is somewhat difficult to evaluate all the sources of error it is felt that the reported values of the cross sections are good to about 15 per cent.

When U^{238} is irradiated with neutrons, three paths exist for the formation of members of the 240 chain. The genetic relationship between the isotopes of interest is shown in the following diagram.

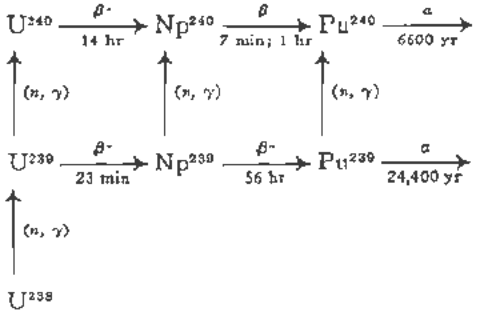

(1)

For the irradiation times used in this work (12 to 423 hr), the contribution to the 240 chain by U^{239} capture is small and only a minor correction need be made. For times up to about two days Np^{239} capture is the major contributor, and thereafter the Pu^{239} path predominates.

Uranium metal cylinders (99.97 per cent U^{238}) about 1.8 cm in diameter, 4.0 cm long, weighing about 190 grams and canned in aluminum were irradiated in a beryllium channel adjacent to the active lattice in the Low Intensity Test Reactor (LITR) of the Oak Ridge National Laboratory. Cobalt monitors were attached both above and below each slug in order to measure the integrated flux. Following the irradiation and about a one month cooling period, the uranium was chemically processed to determine the amount of plutonium produced and to prepare a purified sample for mass spectrographic analysis of the Pu^{240}. This latter measurement was made on a 12-in. 60-degree mass spectrometer of the type developed by Inghram. The multiple-filament ionization source[1] was used since this source produces highly efficient ionization of the plutonium as metal ions compared to the simple surface ionization source which produces PuO^+ ions.

* Oak Ridge National Laboratory.
† Argonne National Laboratory.

Table I. Pu^{239} and Pu^{240} Yields and Derived Cross Sections

	Length of irradiation (hr)	Pu^{239} Production, mg: Computed from Co monitor data*	Pu^{239} Production, mg: Observed†	$\frac{Pu^{240}}{Pu^{239}}$ %	$\sigma_c(Pu^{239})$ (barns)‡	$\sigma_c(Np^{239})$ (barns)‡
	12.00	0.95_0	0.85_5			
	12.00	0.85_9	0.80_1			
	11.47	—	0.84_8			
	12.00	0.87_8	0.84_7			
	12.00	0.88_0	0.82_1			
	12.00	0.87_7	0.86_4			
avg	11.9			0.0063 ± 0.0002	—	93
	24.00	1.73_5	1.64_2			
	24.07	1.69_8	1.62_1			
	24.00	1.75_4	1.66_9			
	24.00	1.71_4	1.62_4			
	25.17	1.70_9	1.61_9			
	24.00	1.63_1	1.58_5			
avg	24.2			0.0124 ± 0.0002	366	77
	48.0	3.42_7	3.29_5			
	48.0	3.46_8	3.33_4			
	48.0	3.53_3	3.35_1			
	48.0	3.41_4	3.21_4			
avg	48.0			0.0311 ± 0.0004	373	74
	96.0	—	6.42_2			
	95.45	6.50_0	6.30_7			
avg	95.7			0.081 ± 0.001	386	75
	192.0	13.6_8	13.2_4	0.228 ± 0.003	409	—
	423.0	27.3_9	27.0_5	0.590 ± 0.007	405	—

* Uncorrected for the depression in the uranium cylinder.

† Corrected for Pu^{240} alphas and burnout.

‡ Effective cross section.

A convenient formulation of the problem is shown in Equation 2 where the quantities to the left of the equality sign are the experimentally measured mass ratios.

$$\frac{Pu^{240}/Pu^{239}}{Pu^{239}/U^{238}} = \frac{\sigma_c(U^{239})}{\sigma_c(U^{238})} F_2 + \frac{\sigma_c(Np^{239})}{\sigma_c(U^{238})} F_3 + \frac{\sigma_c(Pu^{239})}{\sigma_c(U^{238})} F_4 \qquad (2)$$

F_2, F_3 and F_4 are functions of the irradiation time, and the production and destruction constants, a_i and b_i, of the set of differential equations, $dN_i/dt = a_iN_{i-1} - b_iN_i$, which describe the formation of the species in Equation 1. The solution is of the form of Equation 3

$$\frac{\sigma_c(_{n-1}Np^{239})}{\sigma_c(_{92}U^{238})} F_n = \frac{\prod_{i=1}^{n} a_i}{(\phi\sigma_c(U^{238})t)^n} \left[\frac{1}{\prod_{i=1}^{n} b_i} - \sum_{i=1}^{n} \frac{e^{-b_i t}}{b_i \prod_{\substack{j=1 \\ i \neq j}}^{n} (b_j - b_i)} \right] \qquad (3)$$

where $n = 2, 3, 4$; all $N_i = 0$ at $t = 0$, except $N(U^{238}) = N(U^{238})_0$.

for $n = 2$, $N_1 = U^{239}, N_2 = Pu^{240}$.

$n = 3$, $N_1 = U^{239}, N_2 = Np^{239}, N_3 = Pu^{240}$.

$n = 4$, $N_1 = U^{239}, N_2 = Np^{239}, N_3 = Pu^{239}, N_4 = Pu^{240}$.

The cross sections of the 239 chain members are all expressed relative to that of U^{238}, $\sigma_c(U^{238})$. All σ's are used here as effective cross sections (i.e., including both thermal and epithermal capture). The effective cross section accounts for all the product observed in neutron capture but is based on the thermal neutron flux. The thermal flux is taken as that measured by a $(1/v)$ absorber with the epicadmium contribution subtracted and based on the 2200 m/sec cross section.[2]

The irradiated cobalt and the plutonium produced (based on the thermal value of 2.80 barns[3] and a calculated value for the epithermal contribution such that $\sigma_c(U^{238}) = 3.5$ barns) independently serve as flux monitors. Their agreement is within 5%, and thus lies well within the experimental error. See Table I, columns 2 and 3.

A least square analysis of the data in terms of Equation 2 handled as a two parameter case yielded $\sigma_c(Np^{239}) = 81$ barns and $\sigma_c(Pu^{239}) = 402$ barns. For this purpose $\sigma_c(U^{239})$ was taken as 50 barns based on the work of M. H. Studier and co-workers of the Argonne National Laboratory and modified by a reinterpretation of their data. Actually due to the very small contribution to 240 chain formation by U^{239} capture, the derived cross sections are insensitive to the exact value chosen. In Table I, columns 5 and 6 show the value of $\sigma_c(Pu^{239})$ and $\sigma_c(Np^{239})$ where the least square values of $\sigma_c(Np^{239})$ and $\sigma_c(Pu^{239})$, respectively, were substituted into Equation 2. The error based only on the precision of the data reflects an uncertainty of about 2% in the average value. A more realistic appraisal of the numerous factors entering into such a measurement suggest an uncertainty of 10 to 20 per cent. Therefore the effective capture cross section of Np^{239} in our experiment is reported as 80 ± 15 barns and that of Pu^{239} as 400 ± 40 barns.

Pa^{233}

In the neutron irradiation of Th^{232} to produce U^{233} in a reactor, the following sequence of nuclear reactions will take place:

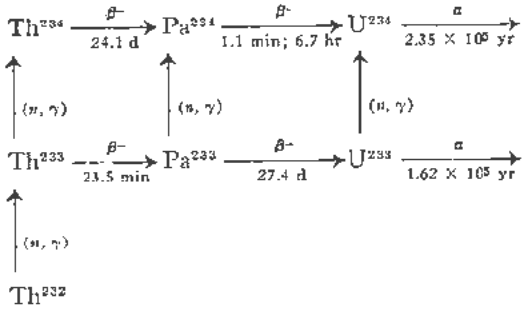

In 1946, Katzin and Hagemann of the Argonne National Laboratory obtained a value of 37 ± 14 barns for $\sigma_c(Pa^{233})_{eff}$ for graphite reactor neutrons by an alpha to neutron-fission ratio measurement in the uranium product following a thorium irradiation. More recently Katzin and Stevens of the Argonne National Laboratory reanalyzed mass spectrographically this same U^{233}–U^{234} product and thereby obtained a value of 55 ± 6 barns for this cross section exclusive of errors in the reported integrated flux-time. Smith of the Phillips Petroleum Company at Idaho Falls has measured $\sigma_c(Pa^{233}) = 60$ barns for thermal neutrons by counting the two isomers of Pa^{234} (UX_2 and UZ) formed during the neutron irradiation of Pa^{233}. He has further found a large absorption integral for resonance neutrons such that the effective cross section under his conditions (in a more thermalized flux than used in this work) was about 100 barns. In the present work an effective capture cross section, $\sigma_c(Pa^{233})_{eff}$, (i.e., including epithermal as well as thermal activation) has been measured for the LITR and a graphite reactor.

Thorium slugs, about 4 cm in diameter and 15 cm long, weighing about 1700 grams, were irradiated in both the LITR and in a graphite reactor. Following irradiation, cooling and processing, the isolated U^{233} in each case was mass spectrographically analyzed for its U^{234} content on a 6-in. 60-deg instrument by introducing the uranium as UF_6. The U^{234} arose from neutron capture by all three of the species, Th^{232}, Pa^{233} and U^{233}, although the predominant path of formation in these irradiations was via Pa^{233}. Corrections were made for neutron capture by Th^{232} and U^{233}.

The U^{233} produced acted as the neutron flux monitor. Using 12.5 barns for the resonance integral of thorium in the slugs as measured by Untermeyer of the Argonne National Laboratory, and 7.0 barns for the thermal capture cross section, the ratio of resonance to thermal absorption in thorium can be shown to be about 0.13 at the site of the irradiations in both reactors, and a value of $\sigma_c(Th^{232})_{eff}$ of 8.0 barns was taken for the current work. This latter value together with the experimental data yield an average value for the Pa^{233} effective capture cross section of 151 barns for the LITR (see Table II). An average value of 129 barns was obtained for five irradiations in the graphite reactor. A value of 140 ± 20 barns is therefore reported as the effective neutron capture cross section for Pa^{233} in these irradiations.

Table II. U^{233} and U^{234} Yields and Derived Cross Sections for LITR Irradiations

Time in reactor (days)	$10^6 \times \frac{233\ chain}{Th^{232}}$ cobalt monitor	$10^6 \times \frac{233\ chain}{Th^{232}}$ observed corrected	$\frac{234\ chain}{233\ chain}$ % observed corrected	$\sigma_c(Pa^{233})_{eff}$ (barns)
62	170.8	134.0	$.090_4$	138
113	457.0	329.0	$.202_4$	149
175	568.0	488.0	.259	145
35	46.4	36.7	$.032_9$	154
42	77.5	65.8	$.055_8$	152
63	131.6	107	$.078_1$	140
133	248.0	196	$.135_9$	172
			(LITR) weighted avg	151 b

In the LITR irradiations, cobalt monitors were placed in aluminum boxes at the two ends of each slug. The calculated yield of U^{233} from the cobalt monitor data (column 2, Table II) was about 20% higher on the average than the observed U^{233} yield. This discrepancy is larger than expected and may be due to a greater self shadowing in the thorium than in the cobalt. In this connection, a correction was made for the depression of flux within the slugs but not for the depression in the vicinity of the slugs.

ACKNOWLEDGEMENTS

The authors wish to express their appreciation to C. D. Cagle and W. H. Tabor in scheduling irradiations; to W. B. Howerton and R. C. Shipwash for their assistance in carrying out the U^{233} separation, and particularly to D. R. Hendrix for carrying out the Pu^{239} separation; to J. E. Cunningham and W. A. McNeish for making the depleted uranium metal slugs; to F. L. Moore, J. H. Cooper and L. T. Corbin for conducting very accurate U^{233} and Pu^{239} analyses; to A. R. Brosi for a cobalt sample accurately measured for its disintegration rate by the coincidence method; to H. O. Finley, R. F. Hibbs, L. E. Burkhardt, O. W. Briscoe and D. Mrkvicka for mass spectrographic analyses; and to R. A. Charpie and A. M. Weinberg for helpful advice and support of this work.

REFERENCES

1. Inghram, M. G. and Chupka, W. A., *Surface Ionization Source Using Multiple Filaments,* Rev. Sci. Instr., 24:518 (1953).
2. Hughes, D. J., *Pile Neutron Research,* p. 63, Addison Wesley Press, Inc., Cambridge, Mass. (1953).
3. *Neutron Cross Sections, A Compilation of the A.E.C. Neutron Cross Section Advisory Group,* AECU-2040, Published by the Office of Technical Services, Dept. of Commerce (1952).

The Formation of Higher Isotopes and Higher Elements by Reactor Irradiation of Pu^{239}; Some Nuclear Properties of the Heavier Isotopes

By W. C. Bentley, H. Diamond, P. R. Fields, A. M. Friedman, J. E. Gindler, D. C. Hess, J. R. Huizenga, M. G. Inghram, A. H. Jaffey, L. B. Magnusson, W. M. Manning, J. F. Mech, G. L. Pyle, R. Sjoblom, C. M. Stevens and M. H. Studier,* USA

The capture cross section of Pu^{239} for thermal neutrons is 340 barns,[1,2,3] a value little less than half the fission cross section, 805 barns.[1,2,3] The capture to fission ratio for neutron energies corresponding to Pu^{239} resonances is as high, or higher.[1] Consequently, when plutonium is generated or used in a reactor under conditions where an appreciable fraction undergoes slow neutron fission, such Pu^{240} is formed. Heavier isotopes will also be formed by successive neutron captures. In a fast reactor, the capture to fission ratio for Pu^{239}, particularly in the core, is substantially less than in a slow neutron flux,[4] and the influence of the heavier plutonium isotopes is somewhat less important. Nevertheless, appreciable production of heavier isotopes takes place, particularly in the outer or blanket zones, where the average neutron energy is diminished. In addition to their reactor aspects, the production and study of heavier plutonium and transplutonium nuclei is of basic scientific interest, making possible more extended studies of such fields as heavy element chemistry, nuclear systematics and fission.

The importance of instituting a program of Pu^{239} irradiations was recognized by Fermi, who initiated plutonium irradiations at Hanford in 1944 (the so-called CW samples). These and other early irradiations uncovered, among other things, Pu^{240} and its interesting spontaneous fission properties,[5] Pu^{241},[6] and Am^{241}.[7] Cm^{242} was also found, in this early period, among the products of neutron irradiation of plutonium.[8] Since 1948, a group at Argonne has carried on a plutonium irradiation program, making use of the reactors at Argonne, Hanford, Chalk River, and Idaho Falls, with the objectives of producing and studying the heavier plutonium and transplutonium nuclei.

Studies have been made of the properties influencing the behavior of plutonium in reactors, as well as less detailed studies of the nuclear properties of the many other nuclides formed in the irradiations. This paper summarizes some results of the Argonne program, with emphasis on previously unpublished results. Work of other groups is cited, but the literature is not reviewed comprehensively.

* Argonne National Laboratory.

NEUTRON CAPTURE CROSS SECTIONS OF Pu^{240}, Pu^{241} AND Pu^{242}

The pile[9] cross sections of the heavier plutonium isotopes have been measured by irradiating plutonium samples and by using the mass spectrometer to measure the growth and depletion of the various isotopes.[10]

The measurements reported here were made principally on three samples of plutonium irradiated in the Chalk River heavy water reactor for 6 months, 1 year, and 2 years. The starting material was one of the original irradiated Fermi samples and was designated as CW-3 (Table 1). The irradiated plutonium was separated from fission products, americium and curium through the use of ion exchange resins.

Following a procedure originally devised at the University of California Radiation Laboratory, the material was adsorbed on Dowex A-1 anion resin. This was followed by a thorough washing of the resin with concentrated hydrochloric acid, and elution of the plutonium from the resin using concentrated hydrochloric acid saturated with ammonium iodide and hydrazine hydrochloride.

The samples were purified by thenoyltrifluoroacetone (TTA) extractions just prior to the mass spectrometer analysis in order to remove americium which had grown in from Pu^{241} beta decay. The samples were then analyzed with a 12-inch, 60 degree single-focusing mass spectrometer. Table I gives the mass spectrometric analysis and the approximate integrated flux (nvt). In the cross-section calculations, Pu^{239} was used as an internal flux monitor. Although samples CR-1, 2, and 3 were re-irradiations of fractions of samples CW-3, for simplicity in calculation they were treated as though they had started as pure Pu^{239} and had been continuously irradiated to the final isotopic composition (corrected for Pu^{241} decay).

The values employed for the effective thermal neutron absorption cross section and the effective capture cross section of Pu^{239} were 1150 barns and 385

barns, respectively. These values are probably somewhat different from the cross sections to be expected within the Chalk River reactor, since the neutron "temperature" was undoubtedly above room temperature and resonance absorption probably occurred. Because of uncertainty in the required correction, no allowance was made for this effect in the calculations. Results are given in Table II. For reasons described later, $\sigma_F(Pu^{240})$[11] has been assumed to be zero.

The difference in $\sigma_a(Pu^{240})$ values obtained from CR-1 and CR-2 on the one hand, and CR-3 on the other, may be a result of experimental conditions. CR-1 and CR-2 were irradiated in similar positions in the Chalk River reactor, but CR-3 was placed in a different part of the reactor. Furthermore, CR-3 initially contained about 10 times as much plutonium as did CR-1 and CR-2, which may have resulted in different self-shielding factors. It is known that Pu^{240} has a very large resonance just above thermal energies,[1,12] and since neutron energy distributions vary with position within the reactor, the effective Pu^{240} cross section can vary considerably.

The neutron cross sections of Pu^{240} and Pu^{241} calculated from this series of samples agree fairly well with those obtained earlier from a similar series (but in a lower nvt range) measured in the Hanford graphite reactors. [Average, $\sigma_a(Pu^{240}) = 515$ barns and $\sigma_a(Pu^{241}) = 1420$ barns.] The most important errors lie in the calculation of nvt. The mass spectrometer errors, by themselves, would lead to errors of only a few barns, but the other errors raise the uncertainty in the Pu^{240} cross section to about 50 barns. Other uncertainties in addition to the flux determination (e.g., correction for Pu^{241} decay in intermittent radiations) serve to increase the error in the Pu^{241} cross section to perhaps 20%.

The capture cross section of Pu^{242} was determined by irradiating a known amount of sample CR-2 for a short time in the central thimble of the Argonne heavy water reactor. A pile neutron capture cross section of 30 ± 10 barns was obtained for Pu^{242} from the amount of Pu^{243} formed in the irradiation.[13]

FISSIONABILITY OF Pu ISOTOPES

Of the higher plutonium isotopes, Pu^{241} is the only long-lived one with a measurable thermal neutron fission cross section. Because of the large capture cross sections of Pu^{239} and Pu^{240}, quite appreciable concentrations of Pu^{241} may be built up in high flux reactors.

From a study of the systematics of fissionability, it was felt that Pu^{240} should not fission with thermal neutrons, so that the fissionability in excess of that ascribable to the Pu^{239} in irradiated plutonium could be assigned entirely to Pu^{241}. This assumption was proven in a separate experiment, in which it was shown that $\sigma_F(Pu^{240}) < 0.5$ barns.

The latter measurement could not be made on pile-irradiated plutonium samples, because all such samples had too high a concentration of either Pu^{239} or Pu^{241}. A sample relatively free of highly fissionable isotopes was isolated as the alpha decay product of a curium fraction formed in an extensive irradiation of plutonium.[14] The composition was: Pu^{240}—57.0 ± 0.3%; Pu^{238}—42.7 ± 0.3%; and Pu^{239}—0.285 ± 0.007%, the Pu^{240} and Pu^{238} coming from the alpha decay of Cm^{244} and Cm^{242}, respectively.[15] The upper limit given for $\sigma_F(Pu^{240})$ was set by the uncertainty in the cross-section value $\sigma_F(Pu^{238}) = 18 \pm 2$ barns.[16] No fissions ascribable to Pu^{240} were observed.

The same fissionability systematics would predict a zero cross section for Pu^{242}. This question was examined on a highly irradiated plutonium sample (for isotopic composition, see Table III, MTR-3). The Pu^{242} concentration predominates, so that it was possible to set a limit of $\sigma_F(Pu^{242}) < 0.3$ barns.[17]

The fissionability of highly irradiated plutonium samples containing Pu^{241} was examined by comparison of fission rates in a thermal beam with those of a pure fissionable nuclide. The earliest measurements were made on Hanford-irradiated plutonium containing less than 2% Pu^{241}, with the resulting value $\sigma_F(Pu^{241}) \cong 1700$ barns. This measurement was inherently inaccurate because of the large corrections necessary for the fission activity of Pu^{239}. As more enriched samples became available, the accuracy was improved. A sample of Hanford-irradiated plutonium with 6½% Pu^{241} yielded the value 1090 ± 90 barns. Our most recent and most accurate measurements were made on plutonium samples irradiated for two years in the Chalk River reactor. Two such samples contained 12.91 and 16.74% Pu^{241}, respectively;[18] the corresponding Pu^{239} concentrations were 30.3 and 23.8%. The non-fissioning Pu^{240} and Pu^{242} constituted the remaining mass.

Table I. Isotopic Composition (Atom Per Cent) of Plutonium Samples before and after Irradiation in the Chalk River Pile

Sample	*CW-3*	*CR-1*	*CR-2*	*CR-3*
Pu^{239}	92.63 ±0.07	74.31 ±0.22	53.3 ±0.3	23.82±0.16
Pu^{240}	6.96 ±0.07	21.96 ±0.20	35.6 ±0.2	49.35±0.40
Pu^{241}*	0.406±0.005	3.39 ±0.07	9.17±0.04	17.07±0.24
Pu^{242}		0.337±0.01	1.96±0.03	9.76±0.07
Approx. nvt	1×10^{20}	7×10^{20}	1×10^{21}	3×10^{21}

* The measured Pu^{241} concentration was corrected for decay and all the isotopic values were then readjusted to 100%.

Table II. Neutron Absorption and Capture Cross Sections of Pu^{240} and Pu^{241}

Based on Table I and $\sigma_a(Pu^{239}) = 1150$ b, $\sigma_\nu(Pu^{239}) = 385$ b, $\sigma_F(Pu^{240}) = 0$ and $\sigma_F(Pu^{241}) = 1100$ b.

Sample	$\sigma_a(Pu^{240}) = \sigma_c(Pu^{240})$ *(barns)*	$\sigma_a(Pu^{241})$ *(barns)*	$\sigma_c(Pu^{241})$ *(barns)*
CR-1	560	1450	350
CR-2	550	1450	350
CR-3	495	1450	350

For measuring the fission cross section, the enriched samples were exposed to thermal column neutrons (presumably with a room temperature Maxwellian energy distribution) from the Argonne heavy water reactor (CP-3') and the fission rates were compared to those of pure Pu^{239} in a double ionization chamber.[19] The Pu^{239} samples served as fission cross-section standards and also permitted corrections for Pu^{239} fission in the enriched samples.

Alpha counting was utilized to assay the weight of plutonium in each sample, through the use of mass spectrometer analysis and the known alpha half-lives for calculating the specific activity. A separate correction was made for Pu^{238}, which contributed about 25% to the alpha activity but very little to the mass, through pulse analysis with an alpha-energy spectrometer (ionization chamber plus multichannel pulse analyzer).[20]

The results for the two samples gave the average ratio (for fixed neutron flux):

$$\frac{\text{fission counts per } Pu^{241} \text{ atom}}{\text{fission counts per } Pu^{239} \text{ atom}} = 1.362 \pm 0.023$$

This is also the ratio of

$$\frac{f_{241}\,\sigma_F(Pu^{241})}{f_{239}\,\sigma_F(Pu^{239})}$$

where "f" is the factor by which σ_F (mono-ergic value at 2200 meter/sec) is multiplied in order to correct for the fact that the cross section is not inversely proportional to neutron velocity in the thermal region. The most recent values[1,2] of the Pu^{239} cross section are $\sigma_F(Pu^{239}) = 750 \pm 15$ barns and $f_{239} = 1.078 \pm 0.010$.

Thus, if Pu^{241} does not have a "$1/v$" fission cross section, $f_{241}\sigma_F(Pu^{241}) = 750 \times 1.078 \times 1.362 = 1100 \pm 30$ barns. If Pu^{241} does have a $1/v$ cross section, then $f_{241} = 1$, and 1100 barns is the 2200 m/sec fission cross section.

FISSION NEUTRONS PER FISSION (ν) FOR Pu^{241}

Because Pu^{241} builds up so rapidly in irradiated Pu^{239}, the attractiveness of using plutonium reactor fuel for long periods without removal from the reactor depends appreciably upon the fission properties of Pu^{241}. The quantities of interest are σ_F and η (fission neutrons produced per neutron absorbed). The latter quantity can be calculated from ν (fission neutrons produced per fission) and the ratio of σ_F to the total absorption cross section (σ_a).

The value of ν for Pu^{241} has been measured by comparison of the fission neutron yield from an enriched Pu^{241} sample with those of Pu^{239}, U^{235} and U^{233} standards. The sample used was plutonium irradiated in the Materials Testing Reactor (Sample MTR-1, Table III), containing 5.32% Pu^{239} and 21.8% Pu^{241} (the remainder being the essentially non-fissioning Pu^{240} and Pu^{242}).

The samples were exposed to a well-collimated thermal neutron beam. Surrounding the beam was a cylindrical cadmium shield, around which was placed a cylindrically symmetrical, long, annular BF_3 counter imbedded in paraffin moderator. Thermal neutrons scattered out of the beam were absorbed in the shield, but fission neutrons passed through the shield, were moderated and then counted in the BF_3 counter. Most of the samples were exposed to the same neutron flux, and small corrections were made where such exposure was not feasible. The counting efficiency for fission neutrons was the same for all samples. Thus, the counting rate for each substance, normalized to equal numbers of atoms, was proportional to the product $\sigma_F\nu$.

Using the best values[1] of σ_F and ν for the standard materials, the standards were found to agree among themselves well within the assigned errors, thus checking the accuracy of the method. Comparing the Pu^{241} neutron yield with those of the standards, $\sigma_F\nu(Pu^{241})$ was found to be 3200 ± 60 barn neutrons/fission. This value combined with $\sigma_F(Pu^{241}) = 1100 \pm 30$ barns, yields the value $\nu = 2.91 \pm 0.10$ neutrons/fission. Assuming the measurement of $\sigma_a(Pu^{241})$ described earlier can be treated as a thermal cross section, $\eta(Pu^{241})$ may be calculated as equal to $2.91(1100/1450) = 2.2$.

LONG-TIME VARIATION IN NEUTRON YIELD OF PILE PLUTONIUM

It is of some interest to consider the neutron economy of a system of thermal reactors employing plutonium fuel on a long-term basis. A special case is treated here, which, however, cannot be applied precisely to any actual reactor for the following reasons: (1) the effective pile cross sections are peculiar to individual reactor designs, since they are sensitive to the neutron "temperature" and to the neutron concentration in the resonance region; (2) the actual charge-discharge cycle for fuel elements may differ significantly from the "continuous feed" case considered here; and (3) the effect of accumulated fission-product neutron-absorbing poisons is not considered here. Nevertheless, the results give a semi-quantitative picture of the phenomenon.[21]

The case treated here represents a situation in which the Pu^{239} content is kept constant, i.e., it is fed in at a constant rate just balancing the rate of destruction, under conditions of a constant neutron flux of 3×10^{15} neutrons/cm^2/sec.[22]

Using the cross sections in Table IV, the growth and decay of the various nuclides in the main chain (Fig. 6) were calculated using an analog computer[23] to solve the differential equations involved.[24] The growth in the amounts of the various nuclides is shown in Fig. 1; the corresponding variation in the isotopic composition of the plutonium is shown in Fig. 2.

One method of demonstrating the long-time variation in neutron yield from pile plutonium is to determine the variation of the effective $\bar{\eta}$ as a function of time, where effective $\bar{\eta}$ is defined as the number of fission neutrons per neutron absorbed by all plu-

Table III. Products from Plutonium Irradiations in the Core of the Materials Testing Reactor

Sample number:	*MTR–1*	*MTR–2*	*MTR–3*
Mass of Pu^{239} inserted (mg)	350	350	170
nvt (neutrons/cm²)	4×10^{21}	1.1×10^{22}	1.4×10^{22}
Mass of Pu after irradiation (mg)**	~50	~20	~6
Isotopic composition of the Pu*			
Pu^{238}	—	0.216 ± 0.004	0.16 ± 0.02
Pu^{239}	5.33 ± 0.05	$0.087+0.002$	$0.068+0.004$
Pu^{240}	39.0 ± 0.4	2.02 ± 0.02	0.633 ± 0.006
Pu^{241}	21.6 ± 0.3	1.31 ± 0.01	0.308 ± 0.006
Pu^{242}	34.1 ± 0.3	96.33 ± 0.02	98.77 ± 0.03
Pu^{244}	0.0018 ± 0.0001	0.037 ± 0.002	0.052 ± 0.004
Composition of Pu by activity†			
Pu^{238} 5.5 Mev	26.06 ± 0.23	81.71 ± 0.3	81.9 ± 0.3
Pu^{239} and Pu^{240} 5.15 Mev	$72.6+0.25$	10.09 ± 0.24	5.3 ± 0.3
Pu^{241} and Pu^{242} 4.9 Mev	$1.35\pm.08$	8.20 ± 0.22	12.8 ± 0.2
Mass of Am recovered (mg)**	~5	~7	~3
Isotopic composition of Am*			
Am^{241}	13.8	0.05 ± 0.02	
Am^{242}		<0.002	
Am^{243}	86.2	99.95	
Mass of Cm recovered (mg)**	0.5	3	2.3
Alpha activity of recovered Cm (dpm)‡**	$\sim10^{12}$	$\sim10^{12}$	$\sim5\times10^{11}$
Cm spontaneous fission activity recovered (dpm)**	$\sim1.6\times10^{5}$	$\sim6\times10^{5}$	$\sim5\times10^{5}$
Isotopic composition of curium*¶			
Cm^{242}§	16.8 ± 0.3	1.84 ± 0.04	0.68 ± 0.01
Cm^{244}	82.1 ± 0.3	95.51 ± 0.07	96.29 ± 0.03
Cm^{245}	$0.93\pm^{0.1}_{0.02}$	1.27 ± 0.04	1.14 ± 0.02
Cm^{246}	0.24 ± 0.01	1.36 ± 0.04	1.86 ± 0.02
Cm^{247}	<0.004	0.016 ± 0.002	$0.028\pm^{0.003}_{0.020}$
Alpha energy distribution of Cm†			
Cm^{242} 6.1 Mev§	88	55	25
Cm^{243} and Cm^{244} 5.8 Mev	12	45	75
β activity of recovered Bk^{249} (dpm)§	—	—	4×10^{5}
Mass of Cf recovered (mg)**	—	3.5×10^{-7}	8×10^{-7}
Alpha activity of californium recovered (dpm)**	6	2.3×10^{5}	3×10^{5}
Isotopic composition of californium*			
Cf^{249}		4.3 ± 0.5	
Cf^{250}		49 ± 6	
Cf^{251}		11 ± 3	
Cf^{252}		36 ± 5	
Spontaneous fission activity recovered of Cf^{252} (dpm)**	0.07	6000	7.5×10^{6}
Alpha activity of 99^{253} recovered (dpm)	0.002	6.6×10^{4}	8×10^{4}
Alpha activity of 100^{254} recovered	—	trace	trace
Alpha activity of 100^{255} recovered	—	trace	trace

* Mole per cent, measured by mass spectrometer.

† Per cent of total alpha activity as measured by alpha pulse analyser.[30]

‡ Disintegrations per minute.

§ Measured soon after removal from the reactor.

¶ Cm^{243} was found to be less than 0.07% of MTR-3.

** Approximate yield. Efficiency of recovery not determined accurately.

Table IV. Nuclear Properties of Nuclides Resulting from MTR Irradiations of Plutonium

Nuclide	Type of decay	Partial half-life	Maximum partial energy (Mev)	Pile fission cross sections (barns)	Pile capture cross sections (barns)
Pu^{239}	α	24400 yr [64,65]	5.150[66]	805*[1]	340[1,5]
	S.F.†	5×10^{15} yr[5]			
Pu^{240}	α	6580 yr[30]	5.162[66]		530
	S.F.	1.2×10^{11}[5]			
Pu^{241}	β	13.0 yr[67]	0.0205[68]	1100*	350
	α	4×10^{3} yr[39]	4.893[69]		
Pu^{242}	α	3.9×10^{5} yr	4.898[72]		30[13]
	S.F.	$7.2_6\times10^{10}$ yr			
Pu^{243}	β^-	4.98 hr[70]	0.57[70]		170
Pu^{244}	α	$<7\times10^{7}$ yr			1.5
	S.F.	2.5×10^{10}			
Pu^{245}	β^-	10.1 hr			260
Pu^{246}	β^-	11.2 d[92]			
Am^{242}	α	8.8×10^{3} yr[71]	0.5341[72]		115[56]
Am^{244}	β^-	26 min[43]			
	E.C.‡	44.5 d			
Am^{245}	β^-	119 min	0.904[50]		
Am^{246}	β^-	25 min[52]	1.2[52]		
Cm^{244}	α	18.4 yr[14]	5.798[73]		20[56]
	S.F.	1.4×10^{7} yr[74]			
Cm^{245}	α	1.15×10^{4} yr[14]	5.34[75]	1800*	200[56]
Cm^{246}	α	4.0×10^{3} yr[14]	5.36		15[56]
Cm^{247}		long			180
Cm^{248}		long			4[76]
Cm^{249}	β^-	short			
Bk^{249}	β	290 d[58]	0.08[58]		1100[77]
	α	$\sim10^{5}$ yr[58]	5.405[78]		
Bk^{250}	β^-	3.13 hr[79]	1.9[79]		
Cf^{249}	α	470 yr[58]	5.81[58]	600[77]	270[77]
Cf^{250}	α	10 yr[58]	6.033[55]		1500[58]
	S.F.	1.5×10^{4} yr[58]			
Cf^{251}					3000[58]
Cf^{252}	α	2.2 yr[58]	6.117[58]		25[58]
	S.F.	66 yr[58]	6.08[58]		
Cf^{253}	β^-	18 d[58]			
Cf^{254}	S.F.	60 d			<2[77]
99^{253}	α	19.3 d[55]	6.61[55]		160[77]
99^{254}	β^-	37 hr[55]			<15[77]
	E.C.	150 d[67]			
99^{255}	β^-	~30 d[80]			
100^{254}	α	3.3 hr[55]	7.17[55]		
	S.F.	220 d[55]			
100^{253}	α	15 hr[80]	7.1[80]		

* Measured in thermal column of a reactor.
† S.F. = Spontaneous fission.
‡ E.C. = electron capture.

tonium isotopes (with a small correction for the effect of other nuclides in the chain, through Cm^{245}).[25] Combining the results shown in Fig. 1, the cross sections in Table IV and the ν values of Pu^{239} and Pu^{241}, the effective $\bar{\eta}$ was calculated and is shown in Fig. 3a.

The value of $\bar{\eta}$ is important in that it determines whether the fuel can be used to sustain a chain reaction. Neglecting neutron escape and non-plutonium neutron capture, $\bar{\eta}$ must exceed unity, since one neutron per cycle is needed for the chain reaction. Figure 3a shows that $\bar{\eta} > 1$ by a wide margin, which is not surprising considering the constant addition of new Pu^{239}. $\bar{\eta}$ starts at 2.02 (the value for pure Pu^{239}) and drops fairly rapidly to ~ 1.65 as Pu^{240} and Pu^{241} build up toward saturation. Beyond this region, $\bar{\eta}$ drops slowly as a result of increased neutron absorption in Pu^{242}. If Pu^{242} is allowed to reach saturation, $\bar{\eta}$ levels off at about 1.53, or at 1.60 if absorption by transplutonium nuclides is eliminated.[26]

Also of interest is the regenerative property of the system. If neutron absorption by U^{238} is utilized to supply the required Pu^{239}, then the reactor would be completely regenerative if as much Pu^{239} were made by this means as was destroyed by neutron absorption. Under these conditions, regeneration would only require constant addition of the fertile material U^{238}. Per neutron absorbed in plutonium, $\bar{\eta} - 1$ represents the number of neutrons in excess of those needed for the chain reaction. If $\theta = \Sigma_{49}/\Sigma_{Pu}$ is defined as the number of neutrons absorbed in Pu^{239} per neutron absorbed in all the plutonium isotopes, then $\pi_{49} =$

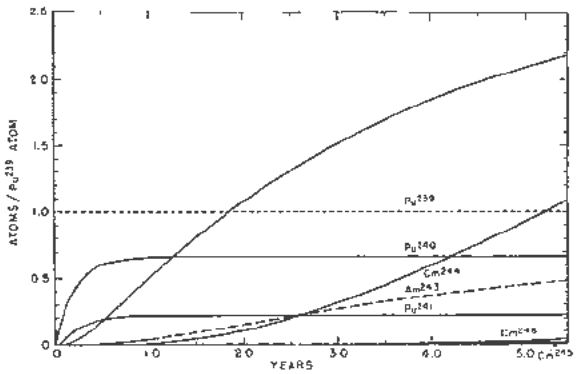

Figure 1a. Growth of higher mass nuclides when Pu^{239} is irradiated at a flux of 3×10^{14} neutrons/cm^2 for long-time periods. The case treated represents one in which the Pu^{239} level is kept constant by continuous feed-in of new material. The ordinates represent the amount of each nuclide relative to Pu^{239}.

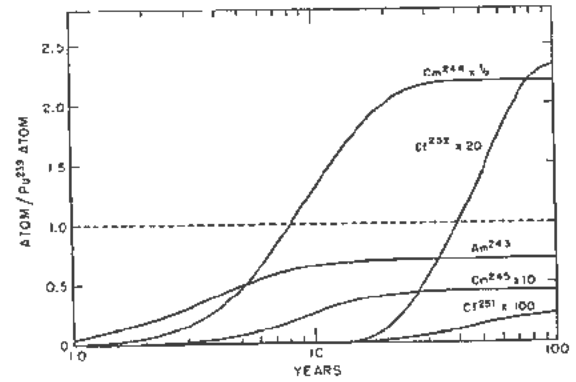

Figure 1b. Corresponding curves for several interesting nuclides over a longer period of time

$(\bar{\eta} - 1)/\theta$ is a measure of the regenerative property of the system, and is called the *productivity*. In this situation, the quantity π_{49} is also a *breeding ratio* for Pu^{239}. Neglecting neutron escape and parasitic absorption by structural materials and fission products, $\pi_{49} = 1$ corresponds to the "break-even" point. If $\pi_{49} < 1$, the Pu^{239} content cannot be kept constant solely by neutron absorption in U^{238}; some fuel must then be supplied from outside sources. The decrease in π_{49} after one year (solid line in Fig. 3b) is due to Pu^{242} absorption and could be minimized by withdrawing individual "spent" plutonium fuel elements from further irradiation after the plutonium in them becomes almost pure Pu^{242}. (See Fig. 5.) Figure 3b shows π_{49} as a function of time and indicates the somewhat surprising result that a system may be self-regenerative even though $\bar{\eta}$ is quite appreciably less than 2. This is a consequence of the fact that the parasitic neutron captures in plutonium are not entirely wasted, in that two neutron absorptions ($Pu^{239} \xrightarrow{n} Pu^{240} \xrightarrow{n}$) lead to the formation of the fissionable Pu^{241}. At 1.0 year, Pu^{239}, Pu^{240} and Pu^{241} are essentially in equilibrium, so that it is only necessary to feed in 63 Pu^{239} atoms (via U^{238} absorption) for every 100 neutrons absorbed by all the plutonium isotopes. Since the corresponding neutron yield in excess of the 100 neutrons required for the chain is 66, the system can be made regenerative.

LONG-TERM IRRADIATIONS OF PLUTONIUM IN THE MATERIALS TESTING REACTOR (MTR)

After the results of experiments on Chalk River irradiated plutonium were becoming known, the MTR began operation. The production of relatively large amounts of nuclides from very high order neutron reactions was feasible not only because of the high neutron flux ($nv = 3 \times 10^{14}$), but also because most of the nuclides involved had relatively high capture cross sections.

The desirability of irradiating considerable amounts of plutonium for extended periods of time was evident. However, at such high fluxes, heat generation in the plutonium was a serious problem, the initial rate being about 40 kw/gm Pu. Heat transfer was facilitated by dilution of the plutonium in an aluminum alloy; the alloy was clad with aluminum,[27] and the samples fabricated in a form designed for the rapid removal of heat with high velocity water during irradiation. At the time the MTR began operation in September, 1952, a large number of specimens, containing up to 350 mg plutonium each, were placed into the reactor.[28]

Following irradiation two immediate problems in the separations program were faced. A relatively large amount of aluminum was present in each plutonium sample—about 20 grams. In addition, each unit contained about 100 curies of fission product activity and one curie of heavy element alpha activity. The separation from the bulk of the fission product activity was performed in a heavily shielded "hot" laboratory.[29]

The aluminum was dissolved in a mixture of sodium hydroxide and sodium nitrate. The heavy elements and most of the fission products were centrifuged away from the sodium aluminate in the form of the hydrated oxides. The transplutonium elements were separated from plutonium and fission products by a combination of ion exchange, solvent extraction and precipitation techniques.[29,30] The transplutonium

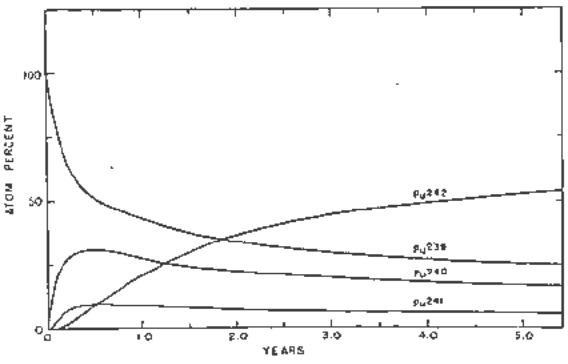

Figure 2. Isotopic composition of plutonium derived from curves of Fig. 1

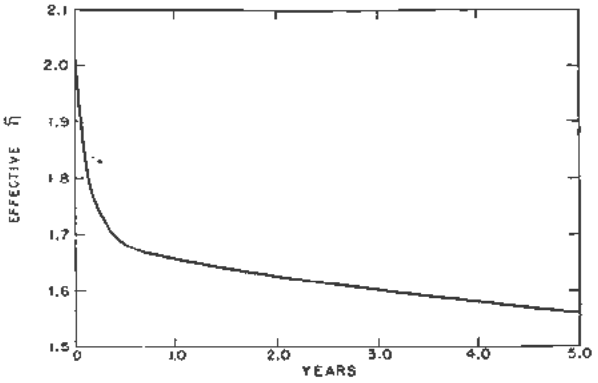

Figure 3a. Effective $\bar{\eta}$ as a function of time. Effective $\bar{\eta}$ is the ratio of the total number of neutrons produced to the number of neutrons absorbed in the plutonium isotopes (with small corrections for added absorption by nuclides through Cm^{245})

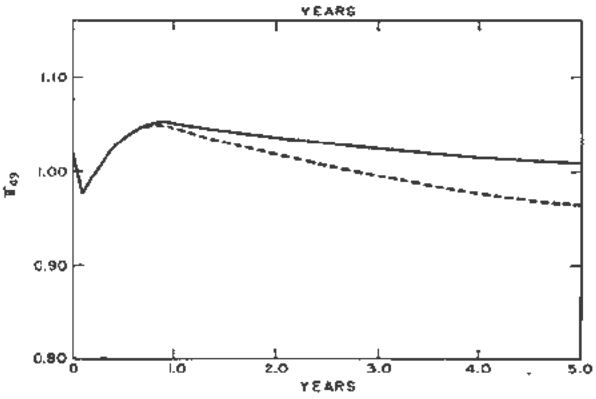

Figure 3b. Variation in π_{49}, the productivity, or breeding ratio for Pu^{239}, as a function of time (for definition of π_{49}, see text). $\pi_{49} = 1$ corresponds to the case where Pu^{239} is formed as rapidly from U^{238} as it is destroyed by neutron absorption, neglecting other sources of neutron loss (as neutron escape or parasitic absorption). The dashed curve includes the effect of Am^{243}, Cm^{244}, and Cm^{245}, while the solid curve represents only the plutonium isotopes

elements were then separated from each other by development on a cation exchange resin column with a citrate or glycolate eluting agent at carefully controlled pH.[29,31]

The products of these irradiations are listed in Table III and are described in greater detail in later sections. A summary of the nuclear properties is given in Table IV. Samples removed after irradiation for a year were found to contain all elements from atomic numbers 94 through 100, and nuclides with mass numbers up to 255. The tremendous effectiveness of such high fluxes in making possible very high order reactions is demonstrated by the fact that despite extensive reactor neutron irradiations since 1944, nuclei had not previously been built up beyond $Z = 96$ and $A = 244$.

Using the cross sections in Table IV, the growth and decay of the nuclides of the main chain were derived using the analog computer. In this case, of course, the initial conditions were different from those described previously in that single charges of Pu^{239} were considered to be placed in the reactor and samples withdrawn at various time intervals. In addition to the cross sections in Table IV, the fission cross sections for Cm^{247} and Cf^{251} were required for this computation. Values were estimated on the basis of fission-to-capture ratio estimates which were made by the method of Huizenga and Duffield[32] using binding energy systematics.[33] The estimated fission-to-capture ratios for these nuclides turns out to be small, around 10%.[34] In Fig. 4 is shown the calculated variation in amounts of the various nuclides; Fig. 5 shows the change in isotopic composition of the plutonium fraction.

NUCLEAR PROPERTIES OF PLUTONIUM AND AMERICIUM ISOTOPES FORMED IN THE MTR IRRADIATIONS

In these samples, a number of plutonium and americium isotopes ($A > 241$) have been made either for the first time or in greater purity than before.

Pu^{242}

Because the plutonium fractions of the longer irradiations were mostly Pu^{242}, it has been possible to make more accurate measurements of the alpha and spontaneous fission half-lives of this nuclide. Plutonium from irradiations MTR–2 and MTR–3 were utilized in these determinations. Mass spectrometric analyses and alpha pulse analyses of the two plutonium samples are given in Table III. Combining these two analyses, and making small corrections for the expected Pu^{239} and Pu^{241} alpha activities, the ratio of the Pu^{242} and Pu^{240} half-lives was determined. From the Pu^{240} half-life, 6580 ± 40 years,[35] the Pu^{242} half-life[36] was calculated as $(3.9 \pm 0.1) \times 10^5$ years. This value is to be compared with the values 3×10^5 years[37] and 4×10^5 years[38] previously reported.

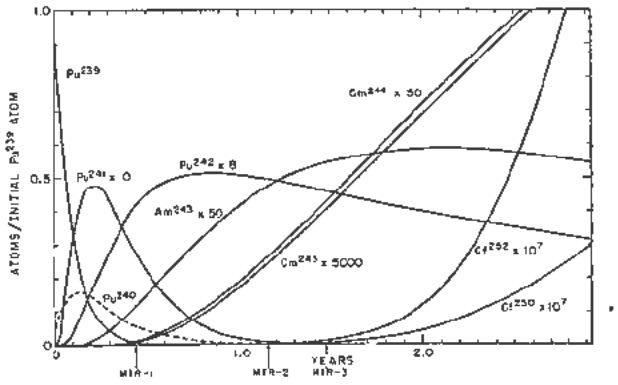

Figure 4. Production of heavier nuclides when Pu^{239} is irradiated at a flux of 3×10^{14} neutrons/cm^2 for long time periods. The case treated represents one in which an individual Pu^{239} sample is placed in a reactor and the composition calculated for various alternative times of withdrawal. This case corresponds to that of the MTR bombardments, and the arrows indicate the approximate withdrawal times for the MTR samples described in Table 3. It may be noted that within the period shown, only the nuclides through Am^{243} have reached saturation. Further irradiation would increase the amounts of the higher nuclides

The alpha activity and spontaneous fission activity of an MTR–3 plutonium sample were separately measured, and the ratio was found[39] to be $(1.86 \pm 0.05) \times 10^5$. Using the measured alpha half-life, the spontaneous fission half-life of Pu^{242} was found to be $(7.2_5 \pm 0.3) \times 10^{10}$ years, in good agreement with the previously reported approximate value.[40]

Pu^{243}

The pile neutron-capture cross section for Pu^{243} has been reported to be of the order of 100 barns.[33] This value was calculated from the Pu^{244}/Pu^{242} ratio in MTR–1 plutonium (Table III), assuming that all of the Pu^{244} was formed by the reaction $Pu^{243}(n,\gamma)Pu^{244}$. A more recent (and more accurate) mass spectrometric analysis of the plutonium yielded a higher Pu^{244}/Pu^{242} ratio, thus raising the cross-section value. However, as shown below, Pu^{244} is also formed by Am^{244} electron capture, approximately 10% of the final product coming through this path.[41] Correcting for both factors, the net change is an increase in the capture cross section to 170 ± 90 barns, the major error resulting from uncertainties in the neutron flux.

Am^{244}

A study of the Pu^{244}/Pu^{242} ratio (Table III) in several MTR irradiations showed that Pu^{244} was being formed more rapidly than might be expected from the path $Pu^{242} \xrightarrow{n} Pu^{243} \xrightarrow{n} Pu^{244}$. This result and the fact that Pu^{244} is apparently beta stable[18] suggested that Am^{244} might be unstable to orbital electron capture. This hypothesis was checked[42] by irradiating a sample of Am^{243} in the Argonne heavy water reactor (CP-5) and later in the MTR reactor. The isotopic compositions of the plutonium separated after these two irradiations, samples *A* and *B*, respectively, are given in Table V. The electron-capture/beta-decay branching ratio was obtained from the measured Pu^{244}/Cm^{244} ratio and was found to be 3.9×10^{-4}. The partial half-life for Am^{244} electron capture is then 46.0 days, using the reported twenty-six minute[13] Am^{244} beta decay half-life. Separate measurements have shown that less than 0.002% of the Am^{244} formed remained as a possible long-lived isomer.

Pu^{244}

Despite the short half-life of Pu^{243} (Table IV), the very high flux of the MTR made possible the

Table V. Isotopic Composition of Plutonium Produced by Irradiating Am^{243}

Isotope	*Sample A (CP-5)*	*Sample B (MTR)*
Pu^{238}	17.8 ±0.2%	<2.1%
Pu^{239}	13.0 ±0.2	8.1±0.2
Pu^{240}	67.5 ±0.3	70.4±0.4
Pu^{241}	0.052±0.004	1.7±0.1
Pu^{242}	1.63 ±0.09	4.2±0.2
Pu^{244}	0.058+0.004	13.5±0.3

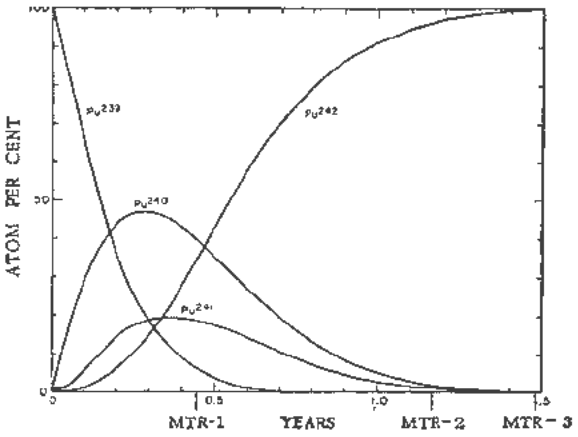

Figure 5. Isotopic composition of plutonium derived from curves of Fig. 4

formation[13] of Pu^{244} and higher plutonium isotopes. The possible importance of Pu^{244} in the history of the earth[44,45] led to an investigation of its alpha half-life. Its decay products, U^{240} and Np^{240}, were separated from the plutonium of sample MTR–3 and counted. These nuclides had been previously prepared through second-order neutron captures by U^{238} and the radiations characterized.[46,47] The decay chain is:

$$Pu^{244} \xrightarrow{\alpha} U^{240} \xrightarrow[\beta]{14.1\ hr} Np^{240} \xrightarrow[\beta,\ 0.56\ Mev\ \gamma]{7.3\ min}$$

These measurements yielded the value $(7 \pm 2) \times 10^7$ years for the Pu^{244} alpha decay half-life. Since U^{236} was used as a tracer to measure chemical yield and since the degree of isotopic exchange between the U^{240} daughter and the U^{236} tracer has not yet been determined, this value must be considered an upper limit for the Pu^{244} half-life. Thus, with this relatively "short" half-life, the probability of detecting Pu^{244}, or its U^{236} descendant, in the earth's crust is small.

The availability of a sample containing a relatively high Pu^{244} content (sample *B*, Table V) made possible spontaneous fission measurements on this nuclide. A portion of this sample, containing 0.0064 μg of Pu^{244}, was counted, a period of 50.356 minutes yielding 110 fissions. Corrections were made for background and the spontaneous fission contribution of the accompanying Pu^{240} and Pu^{242}. The net 40 fission counts corresponded to a spontaneous fission half-life for Pu^{244} of $(2.5 \pm 0.8) \times 10^{10}$ years.[42] This half-life is in excellent agreement with the extrapolated value taken from the correlations of Huizenga and Studier.[40a,48]

Pu^{245} and the Neutron Capture Cross Sections[49] of Pu^{244} and Pu^{245}

The Pu^{244} pile neutron-capture cross section was determined by measuring the amount of Pu^{245} formed by re-irradiation of some MTR–2 plutonium in CP–5. Because the Pu^{245} beta radiations were ob-

sured both by the Pu^{241} initially present and by the Pu^{243} formed in the irradiation, the activity of Pu^{245} was determined by measuring the amount of Am^{245} daughter activity formed by decay in a known period of time. The pile neutron-capture cross section of Pu^{244} obtained in this manner was 1.5 ± 0.3 barns, assuming the cross section of the gold foil monitor to be 98 barns.

The Pu^{245} beta half-life was found to be 10.1 ± 0.4 hours, using the technique of separating Am^{245} from the plutonium at two-hour intervals over a period of about a day. This value is in fair agreement with other reported half-lives of 12 ± 1 hours[50] and 11 hours.[51]

A half-life measurement of Am^{245} yielded the value 119 ± 1 minutes, in good agreement with other reported values, 125 ± 5 min[50] and 120 min.[51] Measurements on the radiations of Am^{245} have been reported elsewhere[49,50] and a complete decay scheme for Am^{245} has been proposed.[50]

The capture cross section of Pu^{245} in the MTR core was determined by measuring the amount of Pu^{246} in equilibrium with Pu^{244} in sample MTR–3. The details of the decay of Pu^{246} and Am^{246} are reported elsewhere.[52] The activities involved are

$$Pu^{246} \xrightarrow[11.2 \pm 0.2\ d]{0.15\ Mev\ \beta^-} Am^{246} \xrightarrow[25 \pm 0.2\ min]{1.2\ Mev\ \beta^-} Cm^{246} \xrightarrow[4000\ yr]{\alpha}$$

In the cross-section measurements, the plutonium activity was measured through the activity of its americium daughter. The resulting value for the Pu^{245} capture cross section was 260 ± 145 barns, most of the error arising from uncertainties in the neutron flux and in the value of $\sigma_c(Pu^{244})$ in the MTR reactor.

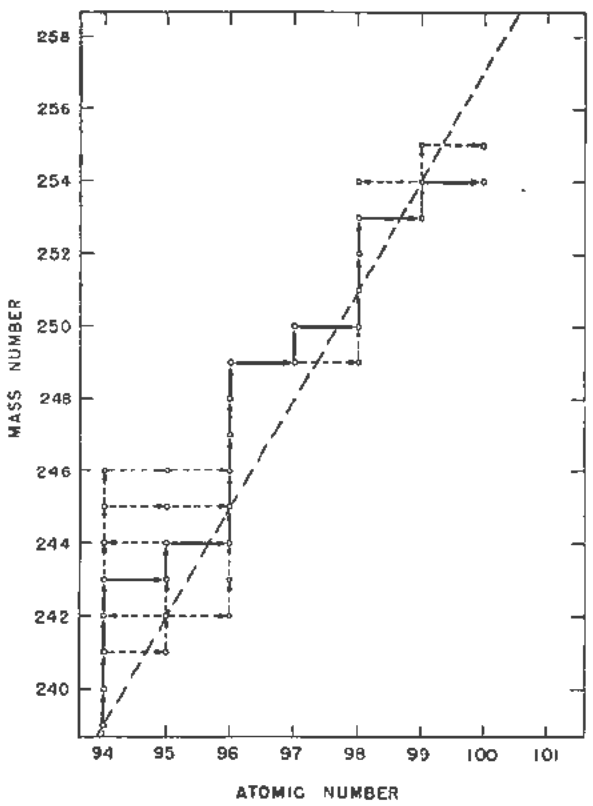

Figure 6. Chain of slow neutron capture reactions observed following irradiation of a plutonium sample in the MTR reactor. The heavy arrows represent the main chain (excluding fission) through which the bulk of the reactions go. Dashed arrows correspond to collateral branches, involving only a relatively small fraction of the reactions. A horizontal arrow corresponds to a beta or electron capture decay, while vertical arrows represent neutron capture. The diagonal dashed line corresponds to the position of maximum beta stability

ELEMENTS Cm THROUGH 100

At the neutron flux level of the MTR, very high order neutron reactions occurred. The arrows in Fig. 6 show the experimentally observed paths for the formation of isotopes of plutonium and transplutonium elements from Pu^{239} by processes of neutron capture, beta decay and electron capture. Much of the work done at Argonne on these nuclides has been recently published.[13,14,49a,53,58] The yields in the MTR bombardments are summarized in Table III, while the nuclear properties are presented in Table IV. In supplemental work, pure elemental fractions were re-irradiated with neutrons to prepare nuclides which were not clearly identified in the original MTR material.

In a re-irradiation not previously reported, a carefully purified sample of 99^{253} was bombarded and the resulting activities were chemically separated. In the californium fraction, a single isotope was found which decayed by spontaneous fission with a half-life of 60 ± 10 days. The activity was assigned to Cf^{254} formed by electron capture branching of 99^{254}. The electron capture to beta branching ratio of 99^{254} was calculated to be 0.001. Another bombardment of a 99^{253} sample gave an activity in the 100 fraction which decayed by the emission of 7.0-Mev alpha particles. The activity was assigned to 100^{255}.

The mass number ranges of isotopic nuclides formed by neutron capture depend primarily on beta stability. The trend of beta stability was predictable in an approximate manner from the beta-decay properties of the isotopes of americium, plutonium and lighter elements through the use of a modification of the Bohr and Wheeler[59] parabola method. The dashed diagonal line in Fig. 6 is drawn through the positions of maximum beta stability, Z_A according to Bohr and Wheeler, as determined by the beta decay energies of even Z, odd N nuclides and the electron capture energies of odd Z, even N nuclides in the "low" mass range 239–245.

The beta decay energies of odd Z, even N nuclides (e.g., Np^{239}) appear to be about 0.4 Mev more energetic than the values calculated from Bohr-Wheeler parameters established in this manner. The effect is ascribed by various authors to an excess of proton pairing energy over neutron pairing energy.[60–62] Including this pairing difference, the position of the Z_A line in the high mass region was determined from the beta-decay energy of Bk^{249}.

The resulting Z_A line of Fig. 6 indicates correctly that Cf^{253} should be beta unstable. No startling aberration in beta stability appears in the high mass region. However, a relatively small effect does appear near atomic number 96, which may be significant in the interpretation of properties of nuclides of higher Z. From separations of berkelium from irradiated curium, a lower limit of the order of 10^3 years may be placed on the beta-decay half-life of Cm^{247}. Since Cm^{247} appears to be beta stable, some sort of trend or discontinuity is suggested in the beta-stability relationship in the high mass region. Specifically, the beta instability of Pu^{241}, the stability of Cm^{247}, and the instability of Cf^{253} are not consistent with a linear Z_A representation.

Conspicuous evidence for irregular behavior near the same mass region is found in the alpha-decay energies of the californium isotopes. As a general rule, the alpha-decay energy at constant Z decreases with increasing A. The observed alpha-decay energy of Cf^{252} is about 80 kev more energetic than that of Cf^{250}. Ghiorso, Thompson, Higgins, Harvey and Seaborg[63] postulate a magic number subshell of 152 neutrons to explain the unexpectedly large alpha-decay energies of Cf^{252}, 99^{253} and 100^{254}.

The nuclear properties summarized in Table IV, with the exceptions of the anomalous decay energies already mentioned, conform to patterns characteristic of lighter mass nuclides. Even neutron nuclides have shorter alpha and spontaneous fission half-lives and smaller neutron cross sections than neighboring odd neutron isotopes.

One important development derived from studies of the transplutonium nuclides concerns the study of spontaneous fission behavior. The early fission theory of Bohr and Wheeler led to the correct prediction that the spontaneous fission decay rate would increase rapidly as a function of Z^2. Huizenga has observed that the spontaneous fission half-lives of even proton, even neutron isotopes (constant Z) appear to go through a maximum as A is increased.[48] The hypothesis is further confirmed by the results found for the curium and californium nuclides (Table IV).

In the high mass region, it may be seen that the spontaneous fission half-lives are relatively short, i.e., this mode of decay competes appreciably with other modes for even-even nuclides. For example, high Z and high A cause the heavy californium isotopes to decay prominently (Cf^{252}) or almost entirely (Cf^{254}) by spontaneous fission.

LONG TERM OUTLOOK

Formation of Higher Nuclides

The formation of nuclides with mass numbers much greater than 255 by neutron reactor irradiations will be made difficult by instability barriers. Extrapolation of the beta stability line (Fig. 6) indicates that 100^{259} should be the lightest isotope of element 100 which will decay by beta (β^-) emission. From Studier and Huizenga's correlation[40a] between Z^2/A and the ratio of spontaneous fission to alpha half-lives, the spontaneous fission half-lives of the heavier even-even isotopes, especially 100^{258}, may be predicted to be so short as to greatly limit the number of atoms that can be formed by further neutron capture. A further obstacle to mass increase is the likelihood that some of the odd neutron nuclides will have large fission cross sections.

The large number of nuclides in the high mass region with high spontaneous fission rates will be valuable in further nuclear research. Detailed studies of these nuclides should contribute to an understanding of the fundamental mechanism of the fission phenomenon.

The greater availability of low specific activity isotopes of plutonium, americium and especially curium will greatly facilitate investigation of chemical properties of these elements, by reduction of radioactivity hazards and of interfering radiation effects.

Some Useful By-Products of Long-Term Irradiation of Plutonium

Neutron emission from the fission fragments of the short-lived spontaneous fission emitters makes it possible to utilize them as neutron sources. For example, Cf^{252} has a neutron emission rate of 3×10^{12} neutrons per sec per gram. If sufficient californium were manufactured, portable neutron sources far more intense than any now available could be made. The calculated yield of Cf^{252} as a function of time is shown in Fig. 4 for the case in which a single charge of Pu^{239} is placed in a reactor, and the experimental yields from the MTR bombardments are given in Table III.

The anticipated yields for the situation in which the Pu^{239} is constantly replenished in a flux of 3×10^{14} n/cm^2/sec have been calculated for long time periods and are shown in Fig. 1. The long delay in building up considerable amounts of Cf^{252} is due to the fact that several of the capture cross sections in the chain (Fig. 6) are small. Because of the relatively short alpha half-life (Table IV), it would be most appropriate to extract the californium at periodic intervals, leaving the parent material in the reactor for further irradiation. The production rate of Cf^{252} has been calculated for these conditions for various time periods (Table VI). From Table VI, it can be seen that in a situation in which the average Pu^{239} consumption is 10 gm/day, after ten years of buildup of the parent material, the predicted Cf^{252} production rate is 1.3 mg/day. This corresponds to producing a neutron source of 10^{11} neutrons/second every 25 days. After 20 years, the Cf^{252} production rate would be almost tenfold greater. Of course, the predicted production rates are subject to experimental errors in the cross-section values. Also, the yields would be decreased by the inevitable imperfections in chemical processing and by Cf^{252} destruction through neutron absorption and decay, but these losses should be less than 50%.

Table VI. Predicted Ratio of Rate of Production of Cm^{244} and Cf^{252} to Rate of Consumption of Pu^{239}*,†

Flux: 3×10^{14} n/cm²/sec

Time (years):	0.5	1	2	5	∞	
$\frac{Cm^{244}\text{ production}}{Pu^{239}\text{ consumption}}$	5×10^{-4}	5×10^{-3}	1.7×10^{-2}	4.7×10^{-2}	7.4×10^{-2}	
Time (years):	2.5	4.5	10	20	30	∞
$\frac{Cf^{252}\text{ production}}{Pu^{239}\text{ consumption}}$	2.5×10^{-8}	7.4×10^{-7}	1.3×10^{-4}	1.1×10^{-3}	2.5×10^{-3}	6×10^{-3}

*Assumes condition in which the Pu^{239} level is kept constant by continuous feed-in (see Fig. 1). The Cm^{244} or Cf^{252} are extracted from the fuel material periodically; the parent materials are returned for re-irradiation. In the production of Cf^{252}, the Cm^{244} must remain in the reactor.

†Consumption of one gram of Pu^{239} is equivalent to production of 1.9×10^4 kilowatt hours when equilibrium is reached.

Another type of neutron source can be made from the highly alpha-active Cm^{244}. When mixed with beryllium, a gram of Cm^{244} would yield about 3×10^8 neutrons/second.[51] Yields for Cm^{244} are shown in Figs. 1 and 4, and in Tables III and VI.

REFERENCES

1. Reviewed by Hughes, D. J. and Harvey, J. A., *Neutron Cross Sections*, Brookhaven National Laboratory Report BNL-325 (1955).
2. *Neutron Cross Sections*, A Compilation of the AEC Neutron Cross Section Advisory Group, AECU-2040, Suppl. 3 (April, 1954).
3. These values include the correction for the non-$1/v$ variation of the Pu^{239} cross section.
4. Inghram, M. G., *et al.*, P/596, *Mass Spectrometric Methods for Determination of Nuclear Constants*, Volume 4, Session 16A.1, these Proceedings; Avery, R., Hummel, H., and Okrent, D., P/609, *A Survey of the Theoretical and Experimental Aspects of Fast Reactor Physics*, Volume 5, Session 22A.1, these Proceedings.
5. Chamberlain, O., Farwell, G. W. and Segré, E., *94^{240} and Its Spontaneous Fission*, LAMS-131 (September, 1944); Phys. Rev. *94*: 156 (1954).
6. Bartlett, A. A. and Swinehart, D. F., *Isotopic Constitution of Plutonium*, LA-561 (May, 1946).
7. Seaborg, G. T., James, R. A. and Morgan, L. O., *The New Element Americium (Atomic Number 95)*, Paper 22.1 in *The Transuranium Elements*, National Nuclear Energy Series, Division IV, Vol. 14B, McGraw-Hill Book Co., New York (1949), p. 1525.
8. Seaborg, G. T., James, R. A. and Ghiorso, A., *The New Element Curium*, Paper 22.2, in *The Transuranium Elements*, National Nuclear Energy Series, Division IV, Vol. 14B, McGraw Hill Book Co., New York (1949), p. 1554.
9. In this paper, "pile cross sections" refer to average or effective cross sections. They are measured in the neutron flux found in the body of the reactor (or pile), within or close to the active core. A pile neutron cross section may deviate quite appreciably from a thermal neutron cross section if the nuclide in question absorbs neutrons appreciably in the resonance region.
10. We are grateful to the staffs of the Hanford and Chalk River reactors for their aid in making these irradiations.
11. The conventional symbols σ_f and σ_a are used for the fission cross section and total neutron absorption cross section, respectively.
12. Havens, W. W. Jr., Melkonian, E., Rainwater, L. J. and Levin, M., *Slow Neutron Velocity Spectrometer Transmission Studies of Plutonium*, CUD-92 (May, 1951).
13. Studier, M. H., Fields, P. R., Sellers, P. A., Friedman, A. M., Stevens, C. M., Mech, J. F., Sedlet, J. and Huizenga, J. R., *Pu^{244} from Pile-Irradiated Plutonium*, Phys. Rev. 93: 1433 (1954).
14. Friedman, A. M., Harkness, A. L., Fields, P. R., Studier, M. H. and Huizenga, J. R., *Alpha Half-Lives of Cm^{244}, Cm^{245} and Cm^{246}*, Phys. Rev. 95: 1501 (1954).
15. The isotopic composition reported here is slightly different from that in Reference 14, due to the use of slightly different curium samples, which differed in their Am^{243} and Cm^{242} content.
16. Reed, G. Jr., Manning, W. M. and Bentley, W. C., ANL-4112 (March, 1948); referred to in *The Actinide Elements*, National Nuclear Energy Series, Division IV, Vol. 14A, McGraw-Hill Book Co. (1954), p. 202.
17. We wish to thank R. Barnes for aid in preparing samples for fission counting.
18. The second sample was CR-3, Table 1. The difference between 16.74% and the 17.07% shown in Table I is due to Pu^{241} decay.
19. Ghiorso, A. and Bentley, W., *High-Sensitivity Apparatus for Fission Counting*, Paper 22.29, in *The Transuranium Elements*, National Nuclear Energy Series, Division IV, Vol. 14B, McGraw-Hill Book Co., New York (1949).
20. Jaffey, A. H., *Radiochemical Assay by Alpha and Fission Measurements*, Chapter 16 in *The Actinide Elements*, National Nuclear Energy Series, Division IV, Vol. 14A, McGraw-Hill Book Co., New York (1954), p. 673.
21. Using preliminary or postulated values for some of the constants, related calculations have been made over a limited nvt range by Lewis, W. B. (Chalk River), Carter, J. C. and West, J. M. (Argonne National Laboratory), and Cohen, E. R. and Sehnert, R. H. (North American Aviation). These calculations treated the case of growth of Pu^{239} in natural uranium within a reactor and also considered the effect of fission product poisons.
22. This is a relatively high flux but it has been achieved in the Materials Testing Reactor. It may be presumed that some future reactors may have even higher fluxes.
23. REAC, Reeves Electronic Analog Computer.
24. We wish to thank Morehouse, N. F., Jr. and Dick, J. S. of the Computer Section, Argonne Laboratory, for carrying out these computations.
25. In the time period covered, the curve differs only slightly from that derived using only the plutonium isotopes.
26. For example, the plutonium may be processed periodically and returned to the reactors following separation from transplutonium elements.
27. We are grateful to Shuck, A. B., Morris, W. H. and Mikolajeski, B. J. of Argonne and to Coffinberry, A. S., Streubing, V. O., Tate, R. E. and Marshall, B. W. of

the Los Alamos Scientific Laboratory for their work in preparing the alloy and fabricating the samples.

28. We wish to express our thanks to the MTR staff for their aid in these irradiations.
29. Fields, P. R. and Youngquist, C. H., P/725, *Hot Laboratory Facilities for a Wide Variety of Radiochemical Problems*, Volume 7, Session 8B.2, these Proceedings.
30. Ketelle, B. H. and Boyd, G. E., *The Exchange Adsorption of Ions from Aqueous Solution by Organic Zeolites*, J. Am. Chem. Soc. 69: 2792 (1947); Hyde, E. K., *Radiochemical Separation of the Actinide Elements*, Chap. 15 in *The Actinide Elements*, National Nuclear Energy Series, Division IV, Vol. 14A, McGraw-Hill Book Co., New York (1954).
31. Stewart, D. C., P/729, *Rare Earth and Transplutonium Separation by Ion Exchange Resin Methods*, Volume 7, Session 10D.2, these Proceedings.
32. Huizenga, J. R. and Duffield, R. B., *Fission-to-Capture Cross-Section Ratio*, Phys. Rev. 88: 959 (1952).
33. Glass, Richard A., *Studies in the Nuclear Chemistry of Plutonium, Americium and Curium and the Masses of the Heaviest Elements*, UCRL-2560 (April, 1954).
34. The estimated values were also utilized in calculating the insert of Fig. 1.
35. Inghram, M. G., Hess, D. C., Fields, P. R. and Pyle, G. L., *Half-Life of Plutonium-240 by Determination of Its Uranium-236 Daughter*, Phys. Rev. 83: 1250 (1951).
36. Mech, J. F., Stevens, C. M., Diamond, H., Studier, M. H., Fields, P. R. and Huizenga, J. R., *Alpha Half-Life of Pu^{242}*, to be published (1955).
37. Asaro, Francesco, *The Complex Alpha Spectra of the Heavy Elements*, PhD thesis, University of California Radiation Laboratory Report UCRL-2180, (June, 1953) p. 99.
38. Thompson, S. G., Street, K., Jr., Ghiorso, A. and Reynolds, F. L., *The New Isotope Pu^{242} and Additional Information on Other Plutonium Isotopes*, Phys. Rev. 80: 1108 (1950).
39. Diamond, H., Barnes, R. F., Studier, M. H., Hirsch, A. and Fields, P. R., *Spontaneous Fission Half-Life of Pu^{242}*, to be published (1955).
40. Studier, M. H. and Hirsch, A., referred to in Ref. 40a.
40a. Studier, M. H. and Huizenga, J. R., *Correlation of Spontaneous Fission Half-Lives*, Phys. Rev. 96: 545 (1954).
41. This percentage will, of course, vary with time, since it depends upon the Am^{243}/Pu^{242} ratio in the irradiated plutonium.
42. Fields, P. R., Gindler, J. R., Harkness, A. L., Studier, M. H., Huizenga, J. R. and Friedman, A. M., *The Electron Capture Decay of Am^{244} and the Spontaneous Fission Half-Life of Pu^{244}*, to be published (1955).
43. Ghiorso, A., Thompson, S. G., Choppin, G. R. and Harvey, B. G., *New Isotopes of Americium, Berkelium and Californium*, Phys. Rev. 94: 1081 (1954).
44. Kohman, T. P., *Geochronological Significance of Extinct Natural Radioactivity*, Science, 119: 851 (1954).
45. Rosenblatt, D. B., *Effects of Primeval Endowment of U^{235}*, Phys. Rev. 91: 1474 (1954).
46. Knight, J. D., Bunker, M. E., Warren, B. and Starner, J. W., *The Radiations of U^{240} and Np^{240}*, Phys. Rev. 91: 889 (1953).
47. Studier, M. H. and Hyde, E. K., private communication (1948).
48. Huizenga, John R., *Spontaneous Fission Systematics*, Phys. Rev. 94: 158-60 (1954).
49. Fields, P. R., Studier, M. H., Friedman, A. M., Diamond, H., Sjoblom, R. and Sellers, P. A., *Production of Plutonium-245 and Americium-245 by Neutron Irradiation of Pu^{244}*, Journal of Inorganic and Nuclear Chemistry, in press (1955).
50. Brown, C. I., Hoffmann, D. C., Crane, W. T., Balagna, J. P., Higgins, G. H., Barnes, J. W., Hoff, R. W., Smith, H. L., Mize, J. P. and Bunker, M. E., *The Decay Chain — Pu^{245} — Am^{245} — Cm^{245}*, Journal of Inorganic and Nuclear Chemistry, in press (1955).
51. Fried, S., Selig, H. and Pyle, G., private communication.
52. Asprey, L., Browne, C., Engelkemeir, D., Fields, P. R., Fried, S. M., Pyle, G., Smith, L., Spence, R. and Stevens, C. M., *The New Isotopes Pu^{246} and Am^{246}*, to be published.
53. References to work on neutron capture products through mass 244 may be found in Hollander, J. M., Perlman, I. and Seaborg, G. T., *Tables of Isotopes*, Rev. Mod. Phys. 25: 469 (1953).
54. Studier, M. H., Fields, P. R., Diamond, H., Mech, J. F., Friedman, A. M., Sellers, P. A., Pyle, G., Stevens, C. M., Magnusson, L. B. and Huizenga, J. R., *Elements 99 and 100 from Pile-Irradiated Plutonium*, Phys. Rev. 93: 1428 (1954).
55. Fields, P. R., Studier, M. H., Mech, J. F., Friedman, A. M., Magnusson, L. B. and Huizenga, J. R., *Additional Properties of Elements 99 and 100*, Phys. Rev. 94: 209 (1954).
56. Stevens, C. M., Studier, M. H., Fields, P. R., Mech, J. F., Sellers, P. A., Friedman, A. M., Diamond, H. and Huizenga, J. R., *Curium Isotopes 246 and 247 from Pile-Irradiated Plutonium*, Phys. Rev. 94: 974 (1954).
57. Diamond, H., Magnusson, L. B., Mech, J. F., Stevens, C. M., Friedman, A. M., Studier, M. H., Fields, P. R. and Huizenga, J. R., *Identification of Californium Isotopes 249, 250, 251 and 252 from Pile-Irradiated Plutonium*, Phys. Rev. 94: 1083 (1954).
58. Magnusson, L. B., Studier, M. H., Fields, P. R., Stevens, C. M., Mech, J. F., Friedman, A. M., Diamond, H. and Huizenga, J. R., *Berkelium and Californium Isotopes Produced in Neutron Irradiation of Plutonium*, Phys. Rev. 96: 1576 (1954).
59. Bohr, N. and Wheeler, J. A., *The Mechanism of Nuclear Fission*, Phys. Rev. 56: 426 (1939).
60. Glueckauf, E., *Some Observations Concerning the Energy of Nuclei*, Proc. Phys. Soc. (London), 61: 25 (1948).
61. Kohman, T. P., *The Pairing Effect in Nuclei and the Beta-Labile Elements*, Phys. Rev. 85: 530 (1952).
62. Coryell, C. D., *Beta-Decay Energetics*, Annual Review of Nuclear Science, Vol. II, 305 (1953).
63. Ghiorso, A., Thompson, S. G., Higgins, G. H., Harvey, B. G. and Seaborg, G. T., *Evidence for a Subshell at $N = 152$*, Phys. Rev. 95: 293 (1954).
64. Wallmann, J. C., *Specific Activity and Half-Life of Various Isotopes of Plutonium*, UCRL-1255 (April, 1951).
65. Westrum, E. F., Jr., Hindman, J. C. and Greenlee, R., *Specific Alpha Radioactivity and Half-Life of Pu^{239}*, p. 1717, in *The Transuranium Elements*, National Nuclear Energy Series, Vol. 14B, McGraw-Hill Book Co., New York (1949).
66. Asaro, F. and Perlman, I., *Alpha Spectrum of Pu^{239} and Pu^{240}*, Phys. Rev. 88: 828 (1952).
67. MacKenzie, D. R., Lounsbury, M. and Boyd, A. W., *β^- Half-Life of Pu^{241}*, Phys. Rev. 90: 327 (1953).
68. Freedman, M. S., Wagner, F., Jr. and Engelkemeir, D. W., *Beta Spectra of Pu^{239}, Pu^{240} and Pu^{241}*, Phys. Rev. 88: 1155 (1952).
69. Asaro, F., Reynolds, F. L. and Perlman, I., *Complex Alpha-Spectra of Am^{241} and Cm^{242}*, Phys. Rev. 87: 277 (1952).

70. Engelkemeir, D. W., Fields, P. R. and Huizenga, J. R., *Radiations of Pu^{243}*, Phys. Rev. 90: 6 (1953).

71. Diamond, H., Fields, P. R., Mech, J. F., Inghram, M. G. and Hess, D. C., *The Half-Life of Am^{241}*, Phys. Rev. 92: 1490 (1953).

72. Asaro, F. and Perlman, I., *Table of Alpha Disintegration Energies of the Heaviest Elements*, Rev. Mod. Phys 26: 456 (1954).

73. Asaro, F., Thompson, S. G. and Perlman, I., *The Alpha Spectra of Cm^{242}, Cm^{243}, and Cm^{244}*, Phys. Rev. 92: 694 (1953).

74. Ghiorso, A., Higgins, G. H., Larsh, A. E., Seaborg, G. T. and Thompson, S. G., *Spontaneous Fission of Uranium-234, Plutonium-236, Curium-240 and Curium-244*, Phys. Rev. 87: 163 (1952)

75. Hulet, E. K., *An Investigation of The Isotopes of Berkelium and Californium*, UCRL-2283 (1953).

76. Seaborg, G. T., private communication to Huizenga, J. R.

77. Ghiorso, A. and Choppin, G. R., *Some Pile Neutron Cross Sections of Isotopes of Americium, Curium, Berkelium, and Element 99*, Phys. Rev. 95: 581 (1954).

78. Magnusson, L. B., private communication (1955).

79. Ghiorso, A., Thompson, S. G., Choppin, G. R. and Harvey, B. G., *New Isotopes of Americium, Berkelium and Californium*, Phys. Rev. 94: 1081 (1954).

80. Ghiorso, A. and Harvey, B. G., *Nuclear Properties of Some Isotopes of Californium, Elements 99 and 100*, Phys. Rev. 94: 1080 (1954).

81. These come primarily from Be(α,n); only 4% of the neutrons would come from spontaneous fission.

Record of Proceedings of Session 10B.1

FRIDAY AFTERNOON, 12 AUGUST 1955

Chairman: Mr. G. T. Seaborg (USA)

Vice-Chairman: Mr. D. I. Ryabchikov (USSR)

Scientific Secretaries: Messrs. J. Gaunt and D. J. Dewar

PROGRAMME

P/726 Thermodynamics of the heavy elements.....B. B. Cunningham
DISCUSSION

P/440 Electronic configuration of the actinide elements..J. K. Dawson and G. R. Hall
DISCUSSION

The CHAIRMAN: This session will be concerned with the chemical and some other properties of the heaviest or "actinide elements," a group which presently includes, besides actinium, twelve known elements. The discovery by Hahn and Strassman of the fission process paved the way for the opening of the field of transuranium elements with the discovery of the first of these elements, number 93, by McMillen and Abelson. Today nine transuranium elements are known: No. 93, neptunium; No. 94, plutonium; No. 95, americium; No. 96, curium; No. 97, berkelium; No. 98, californium; No. 99, einsteinium; No. 100, fermium; and No. 101, mendelevium. The eventual discovery of elements 102 and 103, ekaytterbium and ekalutetium should complete the heavy rare-earth series of fourteen elements and then if further elements are found they should be homologues of hafnium, tantalum, etc. The first four of the transuranium elements, that is, neptunium, plutonium, americium and curium, have been isolated in weighable amounts and the results of work with such macroscopic quantities will be included in this discussion.

It should be possible eventually to isolate the next three, that is, berkelium, californium, and einsteinium in weighable amounts, but it now seems that this will not be possible for the following elements because of their short half-lives. All of these elements have been investigated by the tracer method and the results of some such experiments will also be described here.

Mr. B. B. CUNNINGHAM (USA) presented paper P/726 as follows: Thermodynamic data that enable the engineer or technologist to predict by calculation alone whether a given chemical reaction can proceed under specified conditions of technological interest are of great practical value, and find extensive application in many phases of modern chemical industry.

The thermodynamic properties of such heavy elements as uranium, thorium and plutonium clearly are of concern to engineers and chemists interested in practical methods for the production of nuclear power.

The technological significance of studies of the rarer heavy elements, while less obvious, is not negligible in the sense that such investigations serve to reveal trends in thermodynamic properties, which furnish a basis for estimating quantities that have not been measured experimentally.

There is no attempt here to review in detail the mass of existing thermodynamic data pertaining to the heavy elements. It is the purpose of this paper rather: (1) to call attention to certain general problems of an experimental or theoretical character which in the opinion of the speaker, have not in the past received sufficient emphasis; (2) to summarize briefly some recent advances in heavy element thermodynamics; and (3) to illustrate trends in thermodynamic properties of the heavy elements as a function of atomic number.

Among the general problems encountered in the experimental study of the thermochemistry of the heavy elements perhaps the most persistent is that of securing substances in a state of high chemical and crystallographic purity. The latter requirement particularly is often overlooked. As an example one may cite the fact that most of the existing thermodynamic values for the heats and free energies of formation of plutonium ions and compounds refer ultimately to heat-of-solution measurements on samples of metal which were of doubtful crystallographic purity, and which also may have contained significant quantities of oxide.

Critical examination of the available literature for such elements as uranium and thorium reveals many similar ambiguities. It is to be hoped that future workers in this field will regard crystallographic as well as chemical purity of the utmost importance in thermochemical work involving the solid state.

At the present time in our Berkeley laboratories, methods of high vacuum distillation and subsequent

annealing are being used to prepare milligram quantities of chemically and crystallographically pure americium metal for thermochemical work.

Problems in experimental thermodynamics of a quite different kind arise because of the intrinsic radioactivity of the heavy elements. For example, self-heating effects preclude the possibility at the present time of third-law entropy measurements for any of the actinides except thorium, uranium and neptunium. The eventual production in quantity of longer-lived isotopes — the 500,000-year plutonium isotope of mass 242 for example — may solve this problem in some instances, but for many of the transuranium elements, third-law entropy measurements will remain forever inaccessible.

Self-heating effects may be quite spectacular for short-lived isotopes. For example, in attempting low-temperature measurements of the magnetic susceptibility of a ten microgram sample of curium-242, thermal isolation of the sample produced a rapid rise in temperature to approximately 800°C, as judged by the susceptibility. The calculated rise in temperature of thermally isolated curium-242 trifluoride is 17,000 degrees per minute, near room temperature.

In general, serious temperature ambiguities may appear in an alpha-active sample of half-life shorter than a few thousand years. The calculated self-heating of the trifluoride of americium-241 amounts to seventeen degrees per minute.

Aside from heating effects, radioactive disintegration may produce rapid destruction of crystal lattices and the breaking of chemical bonds. Such partially destroyed structures are, of course, unsatisfactory for thermodynamic measurements, and the possible cumulative effects of self-irradiation on the compounds under investigation must be kept in mind. An interesting example of what probably is an effect of radioactivity on chemical properties occurs in curium oxide. A detailed report on the curium-oxygen system is to be presented in a subsequent paper in this session. It will suffice to note here that a higher oxide of curium never was unambiguously identified with the short-lived curium isotopes of mass 242, in spite of many attempts to do so. Success in this undertaking was not realized until small quantities of the longer-lived isotope of mass 244 became available for study.

The disturbing effects of irradiation are not confined to the solid state. In aqueous solution there may be a rapid build-up of hydrogen peroxide, with the possibility of formation of complex ions. In addition oxidation-reduction reactions may occur which prevent the attainment of true thermodynamic equilibrium between oxidation states.

The production of hydrogen peroxide may be extremely rapid in the case of short-lived isotopes. It is found for example that 0.01 molar solutions of curium-242 form greater than 0.1 molar peroxide solutions in less than two hours.

As a third problem common to thermodynamic study of the heavy elements, one may note that in general there is a lack of an experimental or theoretical basis for assignment of that portion of the entropy of heavy element ions or compounds arising from the multiplet character of the electronic ground state. Some recent experimental work—to be mentioned later—as well as recent theoretical calculations have dealt with this problem, but neither experiment nor theory is adequate to clarify the situation in detail.

Turning now to the second topic to be considered in this paper, I wish to mention briefly some recent advances in heavy element thermodynamics which appear to me to be of special interest. Limitations of time preclude the possibility of discussion of all of the values tabulated in the printed version of this paper.

The unique position of actinium as the prototypic element of the heavy element series, according to the actinide hypothesis of Seaborg, makes that element of unusual interest. From the work of Farr, Giorgie, Money and Bowman, it is now known that the structure of the metal is face-centered cubic with coordination number twelve. The structure is similar to that of many of the so-called "normal" metals. The radius indicates that the metallic valance is three. In most of its properties actinium probably is rather similar to lanthanum. Estimates of the entropy of the metal and heats and entropies of fusion and vaporization have been estimated from trends of these properties in neighboring elements of the periodic system. Values of thermodynamic functions for the trifluoride, trichloride and oxyfluoride have been calculated or estimated by methods indicated in the printed paper.

Two recent studies on the thermodynamics of thorium which are of great interest are the third-law measurement of the entropy of the metal—which, unlike the case of cerium metal, failed to reveal any heat capacity anomaly down to 15°K—and the third-law measurement of the entropy of the dioxide. The latter is of special value as it may be taken to be representative of the lattice entropies of heavy element dioxides in general, leaving excess entropy to be assigned to contributions arising from the multiplet character of the ground state in the paramagnetic dioxides.

Heats of formation of thorium triiodide and trichloride have been calculated from existing values for the heats of formation of the corresponding tetrahalides and the assumption that the entropy of disproportionation of the trihalides is zero, within two or three entropy units.

Attention is re-directed to the measurement of the heat of formation of aqueous tetrapositive thorium, carried out by Westrum and Eyring some years ago. Although the work is of high caliber, these authors made only two measurements, using a single source of metal.

Substantial progress has been made in the last few years on the chemistry of protoactinium, from which it is possible to estimate a few quantities of thermodynamic interest. These are tabulated in the

paper. Of these values the most doubtful is the estimated entropy of aqueous protoactinium five. The structure for the aqueous ion may be quite unlike that of other heavy element pentapositive ions, with a corresponding difference in entropy.

The very recent measurements of the vapor pressure of uranium metal by Rauh and Thorn represent a contribution of great importance, not only because the work provides accurate thermodynamic data on the vaporization process for uranium but also because it has served to reveal the extreme sensitivity of the apparent vapor pressure to the presence of traces of oxygen.

It seems reasonable to expect that similar difficulties would be encountered in vapor pressure studies of other heavy element metals and that work of this kind must be carried out in extremely high vacuum if it is hoped to obtain reliable values.

The experiments of Jones, Gordon and Long on the heat capacity of uranium dioxide, although published some years ago, are cited here since it is to be anticipated that low temperature heat capacity anomalies will be found in the dioxides of all of the known heavy elements beyond thorium, as has indeed been found to be the case for neptunium dioxide.

Low temperature heat capacity effects are to be expected in other salts of tetrapositive uranium. Although no anomaly in the heat capacity of UF_4 was noted by Brickwedde, Hoge and Scott in measurements extending down to 20°K, Lohr, Westrum and Osborne believe that a hump in the heat capacity curve for UF_4 must lie below this temperature since they find no residual entropy after subtracting their curve for ThF_4 from the UF_4 heat capacity curve of the workers mentioned.

The measurement of the low temperature heat capacity of neptunium dioxide, carried out with only two grams of material, represented a remarkable technical achievement, and was of great interest in revealing an expected hump in the heat capacity curve at low temperature, due to the presence of unpaired electrons in the dioxide.

Relatively little work on the thermodynamics of plutonium has been reported in the last few years. Recent publications dealing with the allotropy of the metal, and with its magnetic behavior, while of great interest, do not yield thermodynamic information. However, the measurements of Phipps, Simpson and others on the vapor pressure of plutonium metal and the thermodynamic study of plutonium hexafluoride have been of great technical and scientific interest.

Paramagnetic resonance absorption measurements on sodium plutonyl acetate support the assignment of an f^2 rather than a d configuration for the plutonyl ion. This work is discussed more extensively in another paper in this session.

Recent work on the thermodynamic properties of americium, in part not hitherto published, include measurements of the heat of vaporization of the liquid metal and solid trifluoride as well as revised values for the heat of formation of aqueous ions, calculated from calorimetric measurements done by Gunn.

Entropies of the aqueous neutral ion of curium trifluoride, and CmF_2^+ have been calculated from solubility measurements at various temperatures. This last work is based on unpublished data of Feay.

No thermodynamic studies of trans-curium elements have been reported since the publication some years ago of an approximate value for the berkelium three-four potential.

It is realized that much of the work summarized in the printed version of this paper has been passed over hastily, or ignored entirely. Perhaps questions concerning these values can best be handled in private discussion.

Turning now to the final topic of this paper, I wish to point out certain trends in thermodynamic properties when the elements are arranged in the order of atomic number in Slide 1 (Fig. 1 of P/726).

The vertical axis gives the free energy of formation of the aqueous ion in kilocalories per mole. The energy of formation is based on the calorimetrically observed heat and estimated entropies.

The horizontal axis is a plot of atomic number from 89 to 95. The stability of the tripositive state increases rapidly with atomic number, as shown by the rapidly diminishing values for the free energy of formation. All of the higher oxidation states become less stable with increasing atomic number. In the case of elements of atomic number 93 and beyond, the aqueous tripositive state has the most negative free energy of formation, and in that sense, is the most stable that can be formed in aqueous solution.

In Slide 2 (Fig. 2 of P/726) somewhat similar data are displayed for the free energies of formation of the various higher oxidation states from the lower states.

The vertical and horizontal axes are free energies of the couples in kilocalories per mole, and atomic number respectively.

As may be observed, the figure displays a number of interesting regularities. The free energies of the 3-4, 3-5, and 3-6 couples all increase with increasing atomic number along roughly parallel lines, except for a marked deviation in the free energy of the uranium 3-6 couple, probably due to the exceptional stability of the noble gas structure of the U(VI). The free energies of the 4-5, 4-6 and 5-6 couples are less strongly dependent on atomic number, especially in the case of the former. It appears that the energies of oxygen bonding and hydration in the pentapositive ion differ by nearly a constant amount from the energy of ionization of the fifth electron, throughout the series.

It is to be hoped that future investigation will supply a deeper understanding of these relationships.

DISCUSSION ON PAPER P/726

Mr. G. S. Zhdanov (USSR): I should like to stress the great importance of thermodynamic and physicochemical research on plutonium and its alloys, for the

following reasons. Firstly, plutonium has a large number of modifications and, secondly, the chemical bond in the case of plutonium is covalent and directional. As a contribution to the exchange of scientific data, I should like to inform you that research on plutonium and a number of its alloys has been carried out in the Soviet Union under the direction of Mr. Konobeevsky. A study has been made of the equilibrium diagrams of plutonium with a number of other metals—vanadium, manganese, iron and nickel —and this study showed a regular change in the type of equilibrium diagram with the position in the periodic table of the alloying element. Six polymorphous modifications of plutonium were discovered. As an example, Slide 3 is an equilibrium diagram for plutonium with iron and osmium. Both elements are in the same column of the periodic table. The increasing complexity of the type of equilibrium diagram can be seen. These data were made public at the Moscow conference of July and may be consulted in the collection of Soviet papers submitted to that conference.

Mr. CUNNINGHAM (USA): Yes, I might say of course that there have been numerous studies of intermetallic systems involving plutonium. We have done no work of this kind at Berkeley, however, and I do not feel qualified as an expert to outline the work of this kind which has been done in the United States.

Mr. K. DAWSON presented paper P/440.

DISCUSSION ON PAPER P/440

Mr. V. M. KLECHKOVSKY (USSR): The regular sequence in which the electrons fill up the quantum levels, thus raising the atomic number of the element throughout the Mendeleev periodic table obeys the general rule that the direction of filling goes from groups of energy-levels having a lower value for the sum of the primary and orbital quantum numbers to groups of levels with higher values for $n + l$ and, within each $(n + l)$-group, from sub-states with lower n and higher l to sub-states with higher n and lower l.

This regularity was, apparently, first pointed out in 1946 in the work of Yu-Ta. As shown by the work of Reino Hakal and the work of Klechkovsky, a series of equations may be derived from the rule of consecutive $(n + l)$-group filling, expressing in mathematical form the relationship between the position of the element in the periodic table and the electronic configuration of its atoms. The fact that in the series of elements following radium, where $(n + l)$-group filling ends at the value $(n + l) = 7$, there is a transition to 5*f*-level filling is in full agreement with the rule of consecutive $(n + l)$-group filling and also with the general regularity which characterizes the whole periodic system.

As an example of a mathematical expression for the dependence between Z and the electronic configuration of atoms arising out of the rule of consecutive $(n + l)$-group filling, I should here like to give an expression for the Z_l-atomic number of an element in which the first electron must appear in the electron envelope of its neutral, unexcited atoms with a given value for its orbital quantum number l. The expression appears in this form:

$$Z_l = \tfrac{1}{6}(2l + 1)^3 + \tfrac{1}{6}(5 - 2l)$$

The form of this equation is close to that of similar equations derived by Sommerfeld from the Thomas-Fermi model and subsequently by Ivanenko and Larin from the Thomas-Fermi-Dirac model. The

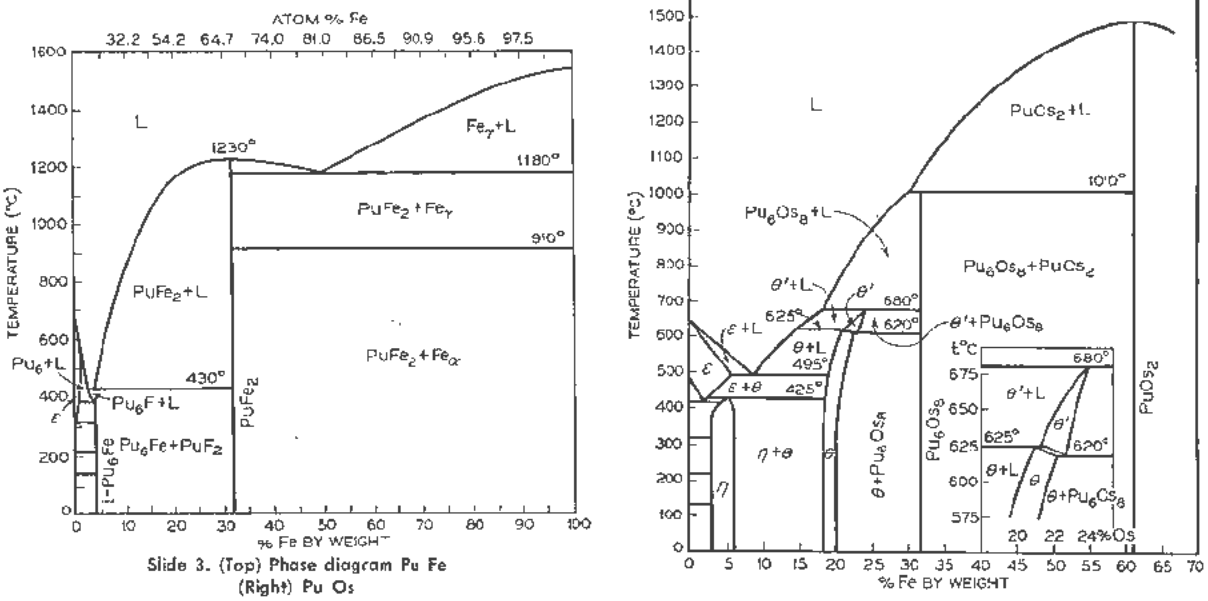

Slide 3. (Top) Phase diagram Pu Fe
(Right) Pu Os

expression given for Z_l, unlike equations derived from statistical theory, gives integral values for Z_l which completely coincide with the empirical values, thus: $l = 0 (Z_l = 1)$, $l = 1 (Z_l = 5)$, $l = 2 (Z_l = 21)$. For the value $l = 3$ the equation given yields $Z_l = 57$, which is lower by unity than the empirical value. It is necessary, however, in evaluating this discrepancy to bear in mind the fact that in the case of cerium ($Z = 58$) two 4*f*-electrons appear simultaneously and the further process of 4*f*-level filling is in agreement with the value $Z_l = 57$. Similarly, in accordance with the rule of consecutive $(n + l)$-group filling, the commencement of the filling of the 2*s*, 3*p*, 4*d*, and 5*f* levels corresponds with the values $Z = Z_l + 2(l + 1)^2$, and the 5*f*-levels must be filled in the case of the actinides, which is apparently closely in accordance with the facts.

Mr. CUNNINGHAM (USA): The published magnetic susceptibility measurements done at Berkeley on americium trifluoride indicate that the temperature magnetism of the ion becomes tempered at low temperatures, as is expected theoretically in the ground state, which is that calculated for sections of electrons and, therefore, is in that respect in excellent agreement with the actinide concept of Seaborg.

The CHAIRMAN: Mr. G. Racah (Israel) wishes to ask Mr. Dawson whether computations on the electronic configurations of the actinide elements have been made by the method of Hartree, and also have other quantum mechanical computations been made, for example, by the method of Slater.

Mr. DAWSON (UK): The calculations which have been made by Eisenstein and Pryce have been published elsewhere, and the written paper P/440 contains the reference where this information may be obtained.

Mr. RACAH (Israel): I should like to point out that the *s*-, *d*- and *f*-shells are filling up at the same time and the competition between the shells depends on the degree of ionization. (I am speaking about free atoms and ions, because I do not know anything about ions in crystals.) For example in Th^{++} there are two electrons outside closed shells, and it is not yet clear whether the fundamental level belongs to the *fd*- or to the d^2-configuration, because the two configurations are at about the same position. But in U^{++} it is almost sure that the two electrons are in the f^2 configuration. We know very well from the lanthanoides that the number of electrons which are not in the *f*-shell depends essentially on the degree of ionization and is almost independent of the total number of electrons.

If we consider the singly ionized lanthanide ions, we see that the fundamental level has always one *s*-electron and zero or one *d*-electron while the number of *f*-electrons increases from 0 to 14.

Session 10B.2

METHODS OF SEPARATING HEAVY ELEMENTS

LIST OF PAPERS

Radiochemical Separations Methods for the Actinide Elements

By Earl K. Hyde,* USA

The purpose of this paper is to review the radiochemical methods which have been developed to separate and purify the elements of atomic numbers 89 to 101.

The need for radiochemical analytical techniques arises in every stage of any program designed to employ a nuclear reactor for generation of industrial power or for the production of radioactive isotopes for widespread use for industrial, medical and scientific purposes. Large-scale processes for the purification of heavy elements such as uranium, thorium or plutonium before fabrication of fuel elements requires preliminary testing on the laboratory scale. Chemical plant processes for separation of uranium, plutonium and other heavy elements from the radioactive fission products have to be devised and tested on the laboratory scale. Heavy element samples may be used as flux monitors during reactor operation. Neutron reaction cross sections may have to be made by irradiating small samples and separating the products by radiochemical methods. These are just some of the problems which have to be solved by the application of laboratory scale radiochemical techniques.

A rather large fraction of the radiochemical techniques which were developed in the United States for the heavy elements during and since the war has been published in unclassified form in books, technical journals or in unclassified or declassified reports of the United States Atomic Energy Commission. References 1–4 can be consulted for considerable information or for references to detailed published information. The cumulative indexes of Nuclear Science Abstracts[5] provide an excellent guide to the published information. The purpose of this article is to review briefly those methods which have proved most useful in actual service and to emphasize newer methods which show excellent promise. In outline this article follows closely a review[3] on the same subject written by the author in 1951. Matters which were discussed there in considerable detail are treated much more briefly in the present article. On the other hand, there is a number of excellent chemical procedures involving solvent extraction, cation exchange and anion exchange which were not treated in the earlier review which are treated here.

The author has tried to summarize developments in this field from all laboratories in the United States Atomic Energy Commission. He has drawn freely on his own experience and on the experience of his professional colleagues at the Metallurgical Laboratory during World War II and at the Argonne National Laboratory and the University of California Radiation Laboratory since the war.

* University of California Radiation Laboratory, Berkeley, California.

RADIOCHEMICAL PURIFICATION OF ACTINIUM

Element 89, actinium, occupies the place in the periodic chart directly beneath lanthanum and bears the same relation to the tripositive states of the elements which succeed it that lanthanum bears to the tripositive lanthanide elements. In its chemistry actinium closely resembles the lanthanide elements with the small differences expected from the larger size of the actinium ion.

In practice, any precipitation or extraction process useful in the isolation of the rare earths will also be useful in the isolation of actinium. For the preliminary isolation of actinium from most elements, this similarity is a great convenience, but in some cases it makes the complete purification of actinium difficult. Frequently a solution from which the radiochemist wishes to isolate an actinium activity contains considerable amounts of rare-earth activities or of inert lanthanum. This is true, for example, in the preparation of actinium by the cyclotron bombardment of thorium and uranium, because of the simultaneous production of fission-product rare-earth activities. The isolation of Ac^{227} from natural sources is complicated by the presence of inert rare earths. In some cases, such as the isolation of Ac^{225} from neutron-irradiated radium (to be discussed), this difficulty is not present.

The radiochemical isolation of actinium, then, usually involves a two-step procedure: (1) the isolation of actinium and the rare earths as a group with or without the use of rare-earth carrier and (2) the separation of actinium from the rare earths.

The extensive classical literature on actinium and its isotopes up to 1940 is covered by Gmelin.[7] Hagemann[8] has reviewed the chemistry of actinium with particular emphasis on the literature of the period 1944–1951. Clarke[9] has provided a bibliography of unclassified project literature.

Coprecipitation Behavior of Actinium

The coprecipitation of actinium together with rare earths on such carrier precipitates as lanthanum flu-

oride, thorium fluoride, a number of insoluble hydroxides, zirconium iodate, bismuth phosphate, barium sulfate and lead sulfate has been discussed by McLane and Peterson.[10]

Solvent Extraction of the Thenoyltrifluoroacetone Complex of Actinium

A very useful method which is not based on the use of a carrier precipitate is the extraction of the thenoyltrifluoroacetone chelate complex of actinium into nonpolar organic solvents.[11] This extraction is strongly dependent on acidity, as shown by Fig. 1. It is decreased by the presence of inorganic ions in the aqueous phase which form strong complexes with actinium and by the presence of large quantities of cations which also form chelate complexes with thenoyltrifluoroacetone (TTA). In practice, the aqueous solution is intimately contacted with a dilute solution of TTA in benzene for a period of 10 to 20 minutes, and then the phases are separated. The actinium can be returned to an aqueous solution simply by contacting it for a few minutes with a dilute acid solution. This method is not specific in the sense that a single extraction will produce a pure actinium fraction, but it is possible to obtain almost any desired specificity by a combination of steps. There is a number of ions which will extract readily from solutions of lower pH; among these are the tetrapositive ions thorium(IV), zirconium(IV), plutonium(IV), neptunium(IV), etc., and other ions such as lead(II) and iron(III). If any of these ions are present in great quantity, they must be removed by some suitable preliminary separation. Trace quantities of these interfering elements can be removed by a preliminary TTA extraction at a pH adjusted below the point of appreciable extraction of actinium, e.g., a pH of 3.0. Afterward the acidity may be decreased to the point where the extraction coefficient for actinium is high (pH 5.5 or higher), and the actinium may be removed to the organic phase. The extraction of a few ions which extract under alkaline conditions may be minimized by adjusting the pH to a value just above the break in the extraction curve where the essentially complete extraction of actinium is achieved. A convenient method of adjusting the pH to the proper value is to use a buffer solution of ammonium acetate-acetic acid.

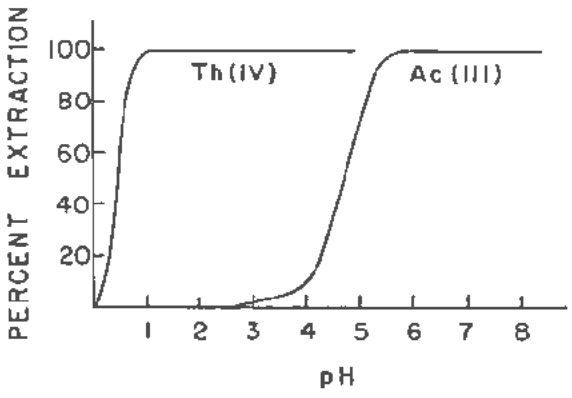

Figure 1. Extraction of trace amounts of actinium and thorium from a dilute nitric acid solution by an equal volume of a 0.25 M solution of TTA in benzene as a function of pH

Some work has been done on the separation of the tripositive actinide elements from the tripositive lanthanides by TTA extractions carried out under carefully controlled conditions. The separation of actinium from the rare earths should be the easiest but has received little study, and it is not clear whether it can be made as effective on a laboratory scale as the ion-exchange methods which are favored at present. Hall and Templeton[12] report the separation of rare-earth fission products from Ac^{226} by an extraction with a 3 *M* TTA-benzene solution with the pH maintained at 3.0 to 3.2. The Ac^{226} was subsequently extracted into a 0.15 *M* TTA-benzene solution at a pH maintained at 6.0 to 7.0.

Ion-Exchange Behavior of Actinium

The ion-exchange method has been applied with great success to the separation of the rare earths as is well known from numerous published articles. Most of these separations involve the adsorption from dilute acid of a mixture of the ions on top of a cation-exchange resin bed followed by the selective elution of the individual elements with solutions of ammonium citrate, ammonium lactate, ethylenediaminetetraacetic acid or some other complexing agent. These papers will not be reviewed in detail here.

In any of these rare-earth separations actinium may be expected to elute after the rare earths because of its larger ionic radius. Also it should be much easier to separate actinium from the rare earths than to separate individual rare earths from each other. A few publications deal specifically with the ion exchange separation of actinium using ammonium citrate.[4,13-15] Elution with nitric acid has been studied by Hagemann[5] who suggests 4 *M* HNO_3 for desorption of actinium from Dowex-50. Elution of actinium from Dowex-50 with hydrochloric acid of various concentrations is shown in Fig. 9 later in this report in the section on transplutonium elements. More complete data are given by Diamond, Street, and Seaborg[16] who have effected the separation of actinium from the rare earths by elution from Dowex-50 with 3 *M*, 6 *M*, and 9 *M* HCl.

Solvent Extraction of Actinium

Actinium is but poorly extracted into most organic solvents. Recently it has been found that the rare-earth elements are extractable into tributyl phosphate from very concentrated nitric acid or hydrochloric acid solutions.[17] The extraction of actinium has been investigated and found to be appreciable, but not high enough to be attractive as a separations method. For example, for 15.6 *M* HNO_3 the distribution coefficient into tributyl phosphate is approximately 0.1

and from 12 *M* HCl it is approximately 0.02.[18] However, if the aqueous phase is strongly salted with aluminum nitrate the extraction of actinium into tributyl phosphate is essentially quantitative.[19] Even from solutions saturated with ammonium nitrate and 0.3 *M* in nitric acid the extraction of actinium is quite high.[20] This property is quite useful in radiochemical problems involving actinium.

Difficulties in Radioactivity Measurement of Actinium

Most tracer work with actinium has been done with the isotope Ac^{227} which occurs in nature as the daughter of U^{235}. A ton of pitchblende contains about 0.15 milligram of actinium. Ac^{227} with a half-life of 22 years is the most stable of the actinium isotopes; the next most stable isotope is Ac^{225} with a half-life of only 10 days. Hence Ac^{227} is the only possible isotope for chemical studies on weighable amounts of material.

Unfortunately the nature of the radiations of Ac^{227} makes it difficult to do quantitative studies on either the tracer or the milligram scale. The beta-particle energy of Ac^{227} is only 40 kev and the alpha branching is only 1.2 per cent. Only under the most favorable conditions when working with highly pure and very thin samples can accurate measurements be made by direct counting of the Ac^{227} radiations. Two ways in which this problem can be met are the following:

The Ac^{227} sample can be allowed to come to equilibrium with its daughter activity and the hard beta and gamma radiation or the energetic alpha particles of the daughters can be counted. The objection to this is that the rate of build-up of the daughter activity is quite slow because the immediate daughter RdAc(Th^{227}) has a half-life of 18.9 days and the next chain member AcX(Ra^{223}) has a half-life of 11.2 days. The maximum in the daughter activity does not occur until 175 days have elapsed. This means that in any chemical step in which actinium is partially or completely separated from its daughters, the samples must be counted daily for at least a few weeks and the resulting growth curves compared with theoretical curves to determine the amount of actinium in the fraction under study.[8]

Those methods of assay which depend on the quantitative separation and quantitative measurement of radioactinium, or actinon, on the measurement of total heat liberated in a calorimeter from the equilibrium mixture suffer from the same disadvantage, i.e., the actinium must come to equilibrium with its daughters before assay.

Another method of actinium assay developed by Perey is based upon the fact that Ac^{227} decays by alpha emission in 1.2 per cent of its disintegrations to a short-lived isotope of francium called AcK. This AcK has a half-life of only 21 minutes and comes to equilibrium with a freshly purified Ac^{227} sample within a few hours. Perey pointed out that it should be possible to assay actinium samples by isolating AcK and counting the energetic beta particles which it emits. She has published details for doing this.[21] Hyde[22] has introduced a new coprecipitation and ion-exchange method for effecting this assay somewhat more easily. The AcK method requires that large enough samples of Ac^{227} be used to overcome the disadvantage of the small 1.2 per cent branching to the AcK product.

The difficulties and extra time required by these assay methods has had a great deal to do with the relative scarcity of published information of the solvent extractability, ion-exchange behavior and other chemical properties of actinium.

In tracer work one may avoid these difficulties by using shorter-lived isotopes having better radiation characteristics.

$MsTh_2$(Ac^{228}) is a 6.13-hour activity which occurs in the thorium decay chain as a daughter of $MsTh_1$(Ra^{228}). $MsTh_2$ emits hard beta particles and decays to a long-lived alpha-emitting daughter, RdTh (Th^{228}), so there are no counting difficulties other than the half-life correction which is not serious for experiments completed within one day. It is only necessary to have a strong source of 6.7-year $MsTh_1$ available from which $MsTh_2$ can be isolated for use as needed.

Ac^{225} has a half-life of 10 days for the emission of energetic alpha particles. A sample of Ac^{225} comes to equilibrium with its alpha-emitting daughters within a few hours, so that the total alpha activity is increased 4 fold.

A stock solution of Ac^{225} can be used for actinium tracer experiments for a few months. Such a stock solution may be prepared in two ways.

One approach is to isolate Ac^{225} from a large source of U^{233} which has been allowed to sit for a considerable period of time. In the U^{233} decay chain there is a long holdup at 7340-year Th^{229}, but nevertheless a one-gram source of U^{233} set aside for one year will contain 1.8×10^6 disintegrations per minute of Ac^{225}.

Alternatively, Ac^{225} can be prepared by bombarding thorium with high-energy protons in a cyclotron. The cross section for formation of Ac^{225} is about 5 millibarns for 100-Mev protons rising to about 20 millibarns at 340 Mev.[23] The 29-hour alpha emitter, Ac^{226}, is prepared in about equal yield on an atom basis so that the Ac^{225} will be appreciably contaminated with Ac^{226} activity until 10 days after bombardment.

RADIOCHEMICAL PURIFICATION OF THORIUM

The chemical and radiochemical properties of thorium are of very great importance in any nuclear reactor program and a vast amount of information has been collected on these properties. In this section no attempt will be made to review older information on thorium chemistry such as precipitation and coprecipitation behavior. A few topics of special interest for radiochemical separations will be treated.

Extraction of Chelate Complexes of Thorium

Thorium forms chelate compounds with a large number of reagents such as salicylic acid, cupferron, hydroxyquinoline, phenylarsonic acid and nitrobenzoic acid. The insolubility of these complexes in aqueous solutions and their extractability into organic solvents makes them of possible usefulness in radiochemical separations. Two beta diketones will be given special mention here.

The compound α-thenoyltrifluoroacetone (TTA) was found[24] to form a stable complex with thorium easily extracted into benzene when the pH was higher than 1 or 1.5.

Hagemann[13] has published a curve showing the extraction of thorium tracer into a 0.25 *M* solution of TTA in benzene as a function of the pH of a nitric acid solution. Above pH 1 the extraction is quantitative (see Fig. 1). In strongly acidic solutions the extraction is negligible. Careful studies on the effect of various inorganic ions in the reduction of thorium extraction by formation of competing complexes in the aqueous phase have been published.[25, 29]

In radiochemical separation of thorium from other radioactive elements the pH is adjusted to the range 1 to 2 to extract the thorium. The rare-earth elements, actinium and a few other elements which are extractable in the higher pH ranges are left in the aqueous phase as are a large number of elements which are not extracted under any conditions. The thorium is then stripped from the benzene phase by contacting the benzene with a 1 *M* acid solution. Other ions such as zirconium(IV), hafnium(IV), protactinium(V), plutonium(IV), neptunium(IV), and iron(III) are left in the benzene phase when the thorium is backextracted.

Thorium may be separated from uranium(VI) when both are present in small concentrations if the solution contains no great quantity of neutral salts but the pH must be regulated carefully. The extraction of thorium from concentrated solutions of uranium is not satisfactory and it is necessary to remove the bulk of the uranium by some preliminary step such as extraction into ethyl ether.

The solubility of the thorium-TTA complex in benzene is limited and in the extraction of gram quantities the volume of TTA-benzene required becomes excessive. In this case a more recently introduced beta diketone is more satisfactory, since the solubility of this thorium complex is many fold greater. This compound is 1-(3, 4-dichlorophenyl)-4, 4, 5, 5, 6, 6, 6 heptafluoro-1, 3 hexanedione and the structural formula is

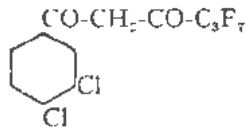

This compound has been made in research quantities by the Dow Chemical Company, Pittsburg, California. Iddings, Tellefson, and Osborne[29, 30] have studied the extraction of thorium with this reagent.

As an example of the application of this new diketone reagent, Iddings employed it in a study in which thorium metal foils weighing a few grams were bombarded in a cyclotron and it was desired to measure the yield of actinium isotopes. After dissolution of the thorium the acidity was adjusted to pH 1 with sodium hydroxide and extracted twice with a 0.6 *M* solution of the diketone in benzene to remove the thorium. Lanthanum fluoride was then precipitated from the aqueous phase to carry the actinium out of the salt solution.

The new reagent suffers from the disadvantage that in the presence of ammonium ion it tends to form an emulsion very difficult to centrifuge.

Solvent Extraction of Thorium

The extractability of thorium from aqueous solutions into organic solvents has been studied for dozens of representative solvents. Most of these studies have been concerned with hydrochloric acid systems, nitric acid systems or mixed nitric acid-neutral salt systems. Most of this work was originally published in classified reports and journal publication of the results has provided only scattered information. In this section a brief account will be given of several of the best solvents for application to laboratory radiochemical separations.

Ethyl ether does not extract thorium unless the aqueous phase acid and salt concentrations are so high that numerous other impurities would also extract.

Methyl isobutyl ketone will extract thorium with a distribution coefficient up to as high as 9 to 1 provided the aqueous phase nitric acid concentration is maintained at 1 *M* to 3 *M* and if in addition a high concentration of such strong salting agents as calcium, magnesium, or aluminum nitrate is maintained. The Ames, Iowa, laboratory purified large quantities of thorium from rare-earth impurities using an aqueous feed solution 3 *M* in calcium nitrate and 3 *M* in nitric acid.[31] In ordinary radiochemical analysis this solvent is of limited usefulness.

Pentaether (dibutoxytetraethylene glycol) will extract thorium from aqueous nitrate solutions under moderate salting conditions. For example, tracer amounts of thorium in a solution 2 *M* in nitric acid and 1 *M* or greater in calcium nitrate are removed to the extent of 90 per cent or more from the aqueous phase by an equal volume of this solvent. Fifty per cent is removed from a 4 *M* HNO_3 solution and 80 per cent from an 8 *M* HNO_3 solution by an equal volume of solvent. If the aqueous phase is 1 *M* in HNO_3 and saturated with ammonium nitrate the extraction is essentially complete.[32] Peppard[33] has reported the use of pentaether in the purification of ionium from pitchblende residues.

Mesityl oxide has been reported to be a useful solvent for thorium. Levine and Grimaldi[34] have

made use of it in an analytical procedure for thorium. Hiller and Martin[35] have used it to extract thorium away from rare-earth fission products in a thorium target solution.

Tributyl phosphate (TBP) is an excellent solvent for thorium. Undiluted TBP from which dibutylphosphate has been removed by alkaline scrubbing will not extract trace amounts of thorium from hydrochloric acid in the hydrochloric acid concentration range 0 to 6 *M* HCl. At concentrations 10 to 12 *M* HCl partition coefficients of 2 to 10 are observed.[19] In nitric acid solutions high partition coefficients are observed even at low acid concentrations. These range from about 5 to 10 at 1 *M* HNO_3 to values of 100 to 400 for nitric acid concentrations in the range 6 to 15 molar.[19] Mixed nitric acid-neutral nitrate salt solutions cause high extraction of thorium. For example, Peppard and co-workers[33] report that trace concentrations of the thorium are extracted in greater than 99.9 per cent yield from an aqueous phase 0.1 *M* in nitric acid and saturated with respect to calcium nitrate.

The viscosity and density of undiluted TBP make it somewhat troublesome to use. Hence it is frequently diluted to a 10 to 20 volume per cent solution in some other solvent such as *n*-butyl ether, benzene, carbon tetrachloride, or kerosene. This reduces the extraction coefficient for thorium but the extractability of a number of other ions is reduced below the point where they will extract appreciably.

With the diluted TBP the extraction coefficient of thorium has a maximum of about 4 in 4–8 *M* HNO_3. Below 0.5 *M* HNO_3 the extraction coefficient is low enough that very dilute acid solutions may be used to backextract thorium from TBP into an aqueous solution. Extraction of thorium into 10 or 20 per cent solutions of TBP in a diluent is much more complete if the nitric acid concentration is made 0.5 *M* and a neutral nitrate salt is added to raise the total nitrate ion concentration to 4–6 molar. Sodium nitrate is quite effective for this purpose.

The extraction of other heavy elements will be discussed later in this report. It will be shown that the ions uranium(VI), plutonium(VI), neptunium (VI), plutonium(IV), neptunium(IV), are also highly extracted. Zirconium(IV) and hafnium(IV) are highly extracted under most conditions. Cerium (IV) is extracted under some conditions.[36] The trivalent lanthanides and actinides are not extracted under most conditions, but from strong hydrochloric acid some of them are highly extracted. This will be discussed in the succeeding section on transplutonium elements.

Mono- and dialkyl phosphates such as mono-octyl phosphate or dibutyl phosphate show phenomenally high extraction coefficients for thorium even from dilute acid solutions. These coefficients can be as high as several thousand.[19] For special purposes these powerful solvents can be of great use, but when tributyl phosphate extraction cycles are being employed it is important that the TBP be free of the mono- and dibutyl derivatives to prevent trouble in the backextraction of the thorium into an aqueous solution.

Ion-Exchange Behavior of Thorium

In hydrochloric acid solution and in nitric acid solution of any concentration thorium forms no negatively charged complexes. Passage of a thorium solution through an anion exchange resin column will separate thorium cleanly from any elements which do form adsorbable negative ions. This is important in the separation of thorium from uranium, neptunium, plutonium, and protactinium among the heavy elements and from a large number of transition elements among the lighter elements.

On the other hand, thorium is strongly adsorbed on cation-exchange resins from acidic solutions and is not desorbed at any appreciable rate with any concentration of nitric or hydrochloric acid. A simple way to separate thorium from most other elements is to adsorb it on a cation-exchange resin column and wash it exhaustively with 6 *M* HCl or HNO_3. Anions and simple monovalent and divalent ions pass through the column immediately. Other ions such as trivalent rare-earth ions require a considerable volume of acid wash for their complete removal but the elution of thorium does not begin until long after the rare earths are gone. The recovery of the thorium from the column is done by elutions with a solution which forms a complex ion with thorium. Bane[37] separated small amounts of thorium from 0.15 *M* uranyl nitrate solution containing 0.1 *M* HNO_3 by passing the solution through a bed of Amberlite IR-1 resin. The column was thoroughly washed with 0.25 *M* H_2SO_4 to remove all the uranium. The thorium was then eluted with 1.25 *M* $NaHSO_4$. Dryssen[38] adsorbs UX1 from a 2 *M* HCl solution of uranium and later elutes the thorium with 0.5 *M* oxalic acid.

On occasion thorium is eluted with citric acid or lactic acid buffered to a suitable pH for rapid removal of thorium. This pH can be considerably lower than that needed to elute rare-earth ions. Asaro, Stephens, and Perlman[39] devised a method for the rapid purification of Th^{228}. The impure sample was adsorbed from dilute acid on a Dowex-50 resin column 3 mm diameter by 3 cm tall, jacketed to allow operation at an elevated temperature (87°C). Radium, lead, and bismuth fractions were eluted with several milliliters 4 *M* HNO_3 after which the thorium was stripped with one milliliter of a 50-volume per cent solution of lactic acid at pH 3. The elevated temperature was essential for rapid elution of the thorium.

RADIOCHEMICAL SEPARATION OF PROTACTINIUM

An excellent review of protactinium chemistry has been given by Elson.[40] The radiochemistry of protactinium has been reviewed by Hyde.[6] Hence pro-

tactinium chemistry will be summarized only briefly and some facts which have not been described in detail in the unclassified literature will be emphasized.

A number of excellent coprecipitatioa, solvent extraction, and ion-exchange methods is now available for effecting quantitative recovery of protactinium in high chemical and radiochemical purity. In practice these methods frequently fail until the chemist has worked with the element long enough to become acquainted with its special properties. In aqueous solutions, particularly in those of low acidity, protactinium has a pronounced tendency to undergo hydrolytic polymerization reactions of unknown nature which are not readily reversible. This can cause loss of protactinium by adsorption on the walls and by failure to duplicate the chemical behavior expected of simple aqueous ions. Frequently the conversion of the protactinium to the strong fluoride or oxalate complex will overcome these difficulties and detailed instructions to meet certain situations can be found in the literature. When the starting sample is of unknown composition and history, the difficulties of protactinium recovery can be rather formidable.

Coprecipitation Behavior

Compounds which have frequently been used in the past as carriers of protactinium from aqueous solutions include zirconium phosphate, zirconium iodate, manganese dioxide, lanthanum fluoride, and various insoluble hydroxides. Details can be found in the survey papers mentioned above[6,40] and in the references cited therein.

Solvent Extraction

Extraction by organic solvents from mineral acid solutions with or without neutral salting agents is one of the most useful methods for the purification of protactinium. This method was introduced by Hyde and Wolf.[41] The preliminary survey of a number of solvents indicated that the lower ethers and many other general solvent types are very poor solvents for protactinium but that some of the long-chain alcohols, such as heptanol and isopropyl ketone, are excellent solvents. Considerations of availability, stability, physical characteristics, and extractability of other elements led Hyde and Wolf to the selection of di-isopropyl ketone as the best solvent. Later work at Oak Ridge by Overholt, Steahly, and others[42] showed that di-isopropyl carbinol was also an excellent solvent for protactinium; in some respects it is to be preferred to di-isopropyl ketone.

To indicate the general characteristics of the extraction, a few curves are reproduced from the work of Hyde and Wolf on the extractability of Pa^{233} tracer from aqueous solutions by di-isopropyl ketone (see Fig. 2). In these experiments Pa^{233} tracer was added to aqueous solution and contacted with an equal volume of di-isopropyl ketone. Results are plotted as percentage extractions vs the initial composition of the aqueous phase.

An examination of the curves in Fig. 2 and others

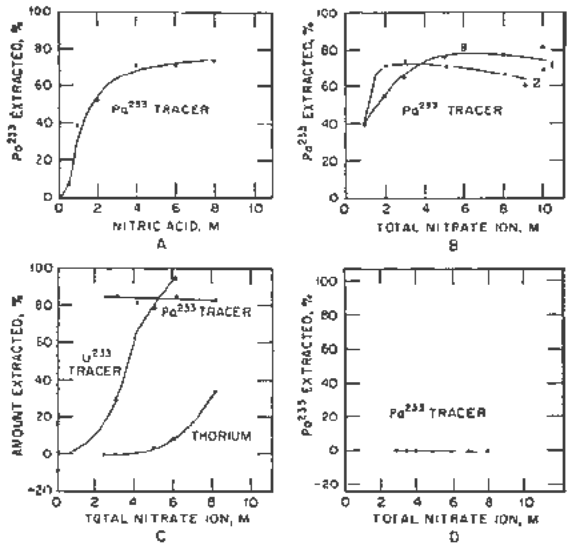

Figure 2. Extraction of protactinium tracer by an equal volume of diisopropyl ketone from an aqueous solution. Initial compositions (A) varying concentrations of HNO_3; (B) curve 1, 1 M HNO_3 and varying concentrations of NH_4NO_3; curve 2, 1 M HNO_3 and varying concentrations of $Ca(NO_3)_2$; (C) 1 M HNO_3, 1 M $Th(NO_3)_4$, and varying concentrations of $Mg(NO_3)_2$; (D) 0.75 M $Th(NO_3)_4$ and varying concentrations of $Mg(NO_3)_2$ with pH 1.5

given by Hyde and Wolf[41] reveals that a prominent feature of protactinium extraction is its great acid dependence. At low acid concentrations protactinium extraction is quite low and remains low even in the presence of high salt concentrations. Another feature is the steep rise of the extraction curves to a maximum at comparatively low total salt or acid concentration, provided that acidity is maintained at 1 *M* or higher. These characteristics are markedly different from the behavior of uranium, which can be extracted from solutions of low acidity by these ketones if neutral salts are added and which has extraction curves with a sigmoid shape not reaching a maximum until the aqueous solutions are nearly saturated with neutral salts. The extraction of thorium is typical of many impurities which are not appreciably extracted until quite high salting strengths are reached, particularly if neutral salts rather than nitric acid are used to raise the salting strength.

Hence, for protactinium extraction high acidities (greater than 1 *M*) and comparatively low total salt concentrations (3 *M* to 4 *M* NO_3^-) would be used in order to obtain high extractability and keep the extraction of unwanted impurities to a minimum.

Kraus and Van Winkle[43] have extended the study of di-isopropyl ketone to hydrochloric acid systems and find similar extractabilities. Some of their results are given in Table I. They found that hydrochloric acid was preferable to nitric acid for the extraction of macro amounts of Pa^{231}, presumably because of the greater strength of the chloride complexes and lower tendency to hydrolytic and precipitation reactions. For target work nitric acid sys-

Table I. Extraction of Protactinium from Hydrochloric Acid Solutions by Di-isopropyl Ketone

Initial aqueous HCl concentration, moles/liter	0.8	2.4	4.8	7.2	9.6
Pa^{233} tracer extracted into an equal volume of di-isopropyl ketone, %	10	55	72	71	73

tems are ordinarily to be preferred because the extraction of undesirable impurities, such as iron, is much lower in nitrate systems.

Kraus and Garen[44] studied di-isopropyl carbinol extraction in the presence of fluoride ion and found that the addition of aluminum ion, boric acid, or thorium ion tied the fluoride ion up in a competing complex and restored the protactinium extractability to normal. Elson and co-workers[45] have found that an important point of technique in this method is to stir the solvent and the aqueous solution as the aluminum ion is added so that the protactinium is drawn into the organic phase as soon as it is freed from the fluoride complex and before it has an opportunity to hydrolyze.

Moore[46] has described the separation of protactinium and niobium by solvent extraction. His studies show that di-isobutylcarbinol is a better solvent for protactinium under proper conditions than is di-isopropylcarbinol. Table II is based on information from his report.

Table II. Extraction of Pa^{233} Tracer from Aqueous Solutions of Acids into Various Organic Reagents

Aqueous phase	*Organic phase*	*Pa^{233} activity extracted (%)*
6 *M* HCl	5% MDOA*-xylene	95.0
6 *M* HCl	5% MDOA*-chloroform	88.5
6 *M* HCl	0.5 *M* TTA†-xylene	88.5
2 *M* HCl	0.5 *M* TTA†-xylene	95.8
6 *M* HNO_3	di-isopropylcarbinol (saturated with 6 *M* HCl)	89.5
6 *M* HCl	di-isopropylcarbinol (saturated with 6 *M* HCl)	99.6
6 *M* HCl	di-isobutylcarbinol (saturated with 6 *M* HCl)	99.9

* Methyldioctylamine.
† Thenoyltrifluoroacetone.

Another good solvent is tributyl phosphate (TBP). Peppard[19] reports that an extraction coefficient of about 1 into undiluted TBP is found when the aqueous phase is approximately 3 *M* HCl. This coefficient rises rapidly to about 20 for initial aqueous concentrations of 5 *M* HCl and to values in excess of 2000 for 11.8 *M* HCl solutions. The presence of fluoride ion in the aqueous phase drastically reduces the extraction of protactinium into TBP. Protactinium in TBP solution can be separated from other elements which show high extractability into TBP by washing the solvent layer with a mixture of hydrochloric acid and hydrofluoric acid. Protactinium is removed, leaving the other elements in the organic phase.

Still another solvent which can be used to extract protactinium is dibutoxytetraethylene glycol (pentaether). To achieve high extraction coefficients mixtures of nitric acid and neutral nitrate salts can be used.

Solvent Extraction of the α-Thenoyltrifluoroacetone Complex of Protactinium

The outstanding feature of the extraction of tracer amounts of protactinium into benzene solutions of TTA is the high extraction coefficients observed from strongly acidic solutions. Solutions of protactinium in 0.4 *M* solutions of TTA in benzene can be washed with strong mineral acid solutions without appreciable backwashing of the protactinium. This washing removes nearly every other possible coatamination ion including a large number which form extractable TTA complexes under conditions of lower acidity. Zirconium, hafnium, and iron are the principal elements likely to contaminate the protactinium.

Backextraction of the protactinium is easily achieved by contacting the benzene layer with a dilute hydrofluoric acid solution or oxalic acid solution.

Anion-Exchange Behavior of Protactinium

Kraus and Moore[47] have studied the separation of protactinium, uranium, and thorium by anion exchange. In strong hydrochloric acid solutions uranium and protactinium are strongly adsorbed by anion-exchange resins such as Dowex-1. (A copolymer of styrene and divinylbenzene containing quaternary ammonium groups.) The distribution coefficient K_d, defined as the amount of protactinium per gram of resin to the amount per milliliter of solution, is about 2 to 4 in the range 1 to 4 *M* HCl, rises abruptly to about 100 at 6 *M* HCl and to $>$ 1000 at HCl concentrations above 8.[48] In the concentration region below 8 *M* HCl distribution coefficients for uranium(VI) are considerably higher.

Kraus suggests two procedures for separating a thorium, uranium, protactinium mixture. In the first procedure the mixture in 8 *M* HCl is passed through a Dowex-1 column to adsorb uranium and protactinium at the top of the column. Thorium is not adsorbed at any hydrochloric acid concentration and passes through the column. The protactinium is eluted with 3.8 *M* HCl. It elutes rapidly. The uranium is also eluted but more slowly than the protactinium.

In the second method the protactinium is eluted with a mixture of 7 *M* HCl and 0.11 *M* HF leaving the uranium firmly bound to the resin. The presence of fluoride ion causes a dramatic decrease in the distribution coefficient for protactinium,[49] without affecting that for uranium. After the protactinium is off the column the uranium is rapidly desorbed with 0.5 *M* HCl.

Isolation of Protactinium by Distillation of Protactinium Chloride

Malm and Fried[50] have introduced a new method for the isolation of protactinium from irradiated

thorium oxide. The method consists in the treatment at 600°C of the thorium oxide with carbon tetrachloride vapor carried in a stream of nitrogen. The thorium and protactinium are converted to the chlorides and $PaCl_5$ distills out quantitatively. For further purification the $PaCl_5$ can be redistilled at 400°C. Other chlorinating agents such as phosphorus pentachloride at 200°C and aluminum chloride at 400°C have been used.

Cation-Exchange Behavior of Protactinium

No comprehensive study of the elution of protactinium from cation-exchange resins has been published. Sullivan and Studier[51] found that thorium and protactinium could be adsorbed completely from dilute (0.1 *M* to 2.0 *M*) nitric acid solutions. The thorium was then eluted with 0.2 *M* ammonium sulfate solution at pH 3.4 with no elution of protactinium.

Protactinium can be desorbed[52] with oxalic acid solutions at a pH of 3.0 to 5.0.

Radiocolloidal or polymerized protactinium can be filtered on to a Dowex-50 resin and treated with oxalic acid to convert it to a simple complex ion.

RADIOCHEMICAL PURIFICATION OF URANIUM

An enormous amount of work has gone into the development of extractive and analytical methods for uranium to meet the problems which have arisen in the extraction of uranium from ores, the purification of uranium, the reduction of uranium to the metal and the recovery of uranium from radioactive solutions after neutron irradiation.

Rodden[3,53,54] has written several reviews of the analytical chemistry of uranium which abstract much of the most significant wartime and postwar developments in the United States.

In the sections which follow a few characteristics of uranium which are particularly useful in the purification of small amounts of uranium ranging from a few grams down to trace amounts will be discussed.

Extraction of Uranium by Ethyl Ether

Ether Extraction

The extraction of uranium by ethyl ether from aqueous nitrate systems is applicable to a wide variety of problems because of its simplicity and specificity. There are but few elements which extract to nearly the same extent. From a mixture of fission products and heavy elements only the halogens, neptunium, and plutonium coextract with the uranium. The neptunium and plutonium can be reduced to lower oxidation states to keep them from extracting.

It is necessary to add inorganic nitrate salts ("salting agents") to the aqueous phase to get good extraction of the uranium, particularly if the uranium is in trace concentration. A wide variety of nitrate salts has been studied for this purpose. The most effective salts are magnesium, calcium, and aluminum nitrate. A minimum concentration of nitric acid of approximately 0.05 *M* is required. A high concentration of nitric acid improves the extraction but also markedly increases the extraction of certain impurities; hence in general the acidity is maintained below 1 *M*.

2.5 *M* magnesium nitrate in the presence of 0.5 *M* to 1 *M* HNO_3 can be recommended when quantitative extraction into a small solvent volume is required.

Sometimes a saturated solution of ammonium nitrate acidified to 0.05 *M* in nitric acid is used in spite of its relatively weak salting strength because the extraction of impurities is also relatively low and because any ammonium nitrate salt which finds its way by mechanical transfer or otherwise into the final uranium fraction can easily be destroyed by aqua regia or by volatilization. When samples of uranium absolutely free of extraneous solid matter are desired for a careful study of radiations this can be quite important.

The extraction of uranium from the aqueous phase can be made quantitative by repeated extraction with larger volumes of ether.

An idea of the effect of various salting agents on extraction of tracer uranium may be obtained from Table III.

Table III. Extraction of Tracer Uranium by Ethyl Ether*

Initial composition of the aqueous phase			
HNO_3 moles/liter	*Additional nitrate salt*	*Total NO_3^- moles/liter*	*Extraction by equal volume of solvent*
3	0	3	23
7	0	7	62
0.5	5 *M* NH_4NO_3	5.5	25
0.5	9.5 *M* NH_4NO_3	10	60
0.5	1.55 *M* $Mg(NO_3)_2$	3.6	38
0.5	2.5 *M* $Mg(NO_3)_2$	5.5	99

* Hellman, N. N. and Wolf, M. J., unpublished information, Metallurgical Laboratory, University of Chicago (1945).

The extraction of uranium may be considerably hindered in the presence of fluoride, phosphate and sulfate ions which form complex ions with uranium. The use of ferric nitrate will counteract this effect for phosphate and sulfate and aluminum nitrate effectively removes the fluoride ion.

The tendency of uranium to form complex ions may be taken advantage of when it is desired to backextract the uranium from the ether into a small aqueous volume. Ammonium sulfate, for example, may be used for this purpose.

Increased purification of the ether-extracted uranium can be achieved by washing the ether phase several times with small volumes of saturated magnesium nitrate. Impurities are backwashed into the aqueous phase if their partition coefficient into the ether phase is substantially less than that of the uranium.

Alternate Solvents for Uranium

A number of organic solvents has been shown to be as effective as, or considerably more effective

than, ethyl ether in the extraction of uranium from aqueous solutions. Dibutoxytetraethylene glycol (pentaether) and tributyl phosphate have been applied to routine analysis of uranium samples. Other solvents which are useful are dibutyl cellosolve, dibutyl carbitol, methyl isobutyl ketone and several dialkyl phosphates. Some of these are discussed in the next sections of this report.

Extraction of Uranium by Tributyl Phosphate

The solvent tributyl phosphate (TBP) is soluble in water only to a slight extent, is stable toward acidic solutions, and undergoes hydrolysis to the mono- and dibutyl compounds only slowly. In addition to these favorable chemical properties it shows a very high extractive power for uranium. The extraction is rather specific except for certain elements, principally cerium(IV), thorium(IV), plutonium(IV), zirconium(IV), and hafnium(IV) which also extract. The tributyl phosphate is frequently diluted to a 20 volume per cent solution with such solvents as carbon tetrachloride, hexane, benzene and *n*-butyl ether.

The mechanism of the extraction[55] is believed to be

$$UO_{2(aq)}^{++} + 2NO_3^-{}_{(aq)} + 2TBP_{(org)} \longleftrightarrow [UO_2(NO_3)_2(TBP)_2{}_{(org)}]$$

The equilibrium constant has been measured to be 7.70.[55]

The extraction of uranium requires the presence of nitric acid in the aqueous phase. For 2 *M* HNO_3 the partition coefficient, $E_{aqueous}^{organic}$, is of the order of 33 for 100 per cent of TBP.[56] If the acidity is raised the partition coefficient increases; for example, at 8 *M* HNO_3 it increases to 150.

Table IV. Comparison of Salting-Out Agents for Extraction of Uranium* by TBP and Pentaether

Salting-out agent	*Salt concentration (grams/100 ml)*	*Acid concentration (M)*	$E_{organic}^{aqueous}$ *for uranium*	
			TBP	*Pentaether*
$Al(NO_3)_3$	60	2	1000	83
NH_4NO_3	70	2	370	70
$Ca(NO_3)_2 \cdot 4H_2O$	58	2	370	32
$Fe(NO_3)_3 \cdot 9H_2O$	53	2	430	33
$NaNO_3$	66	0	1800	140
none	—	2	35	1.8

* 5 mg uranium/ml in original aqueous solution.

Neutral inorganic nitrate salts may also be used to increase the partition coefficient. Several of these are more effective than nitric acid, provided a certain minimum of nitric acid is present. Table IV taken from the data of Bartlett shows the high coefficients which can be achieved. From these data sodium nitrate appears to be the best salting agent.

In normal practice tributyl phosphate is diluted to a 10 or 20 volume per cent solution in a second solvent such as carbon tetrachloride, hexane, benzene or *n*-butyl ether.

The use of one of the diluents mentioned above reduces the uranium extraction several fold but may be desirable for several reasons. The extraction of other ions, particularly the quadrivalent ones mentioned above, may be reduced more drastically, thus permitting better separation from these elements. The density and viscosity properties of the organic phase may be more suitable. The eventual backextraction of the uranium into an aqueous phase can be handled more easily from the diluted solvent.

Small amounts of sulfate, phosphate and fluoride do not interfere seriously but when larger amounts are present iron or aluminum nitrate may be added to remove the interfering ions.

The backextraction of uranium into water is complicated because of the presence of nitric acid extracted from the original aqueous into the organic phase. Hence repeated water washes may be required to get complete recovery of the uranium. Alternatively, a solution of sodium carbonate, or ammonium sulfate may be used to remove the uranium from the TBP by complex formation.

Old samples of tributyl phosphate may contain an appreciable concentration of dibutyl phosphate (DBP). This compound is rather soluble in aqueous solutions but in the presence of tributyl phosphate or other organic solvents it remains in the organic phase. When it is present the partition coefficient for uranium increases markedly in favor of the organic phase. Usually, however, it is desirable to remove the dibutyl phosphate by repeated washing of the tributyl compound with alkali followed by distilled water. The reason for this is that the extraction of a number of impurities is increased when DBP is present and the backextraction of uranium into an aqueous phase is more difficult. Furthermore, with certain salts insoluble precipitates form. Occasionally the rather remarkable solvent properties of the dibutyl compound are of use. This will be discussed in the next section.

Uranium will extract into tributyl phosphate with a high partition coefficient from hydrochloric acid solutions of moderate strength. Peppard[19] reports a partition coefficient for uranium of about 40 into undiluted TBP from 5 *M* HCl. When the hydrochloric acid concentration is 11.8 *M* the partition coefficient is >2000.

Extraction of Uranium by Dialkyl Phosphates

The extraction of uranium by dialkyl phosphates and similar compounds has been studied at several US Atomic Energy Commission Laboratories. [University of California Radiation Laboratory (Stewart, Hicks, Crandall), Argonne National Laboratory (Peppard, and co-workers), and Oak Ridge National Laboratory (Higgins and co-workers) and others.]

Commercially available compounds are mixtures of the mono- and dialkyl compounds, but the pure

dialkyl compounds can be prepared by the method given by Stewart and Crandall.[57]

The dialkyl phosphates can be extracted from aqueous solutions with organic solvents such as hexane and carbon tetrachloride. They form very strong complexes with uranium which are highly extracted into the organic phase. The solvent power is so great that very dilute solutions can be used to extract small amounts of uranium from dilute acid solutions without the use of salting agents. It is possible to extract uranium from a large volume of aqueous phase into a small volume of organic solvent.

Some representative data are presented in Fig. 3 taken from the work of Stewart and Hicks.[58] The partition coefficient, $E^{aqueous}_{organic}$, for tracer amounts of uranium from an aqueous phase originally 1.98 *M* in nitric acid is shown as a function of the concentration of the dialkyl phosphate in hexane. Data are shown for 8 different phosphate compounds. It is observed that the dioctyl phosphate shows the highest extraction of uranium, but the extraction is quite high for all compounds studied. The mechanism of the extraction is believed to be

$$UO_{2(aq)}^{++} + 2HR_2PO_4 \longleftrightarrow UO_2(R_2PO_4)_{2(R_2O)} + 2H_{(aq)}^{+}$$

Additional data shown in Fig. 4 show that increased extraction can be achieved at lower acidity.

Equilibration of one volume of "sea water" containing U^{233} tracer with $\frac{1}{100}$ of its volume of 0.726

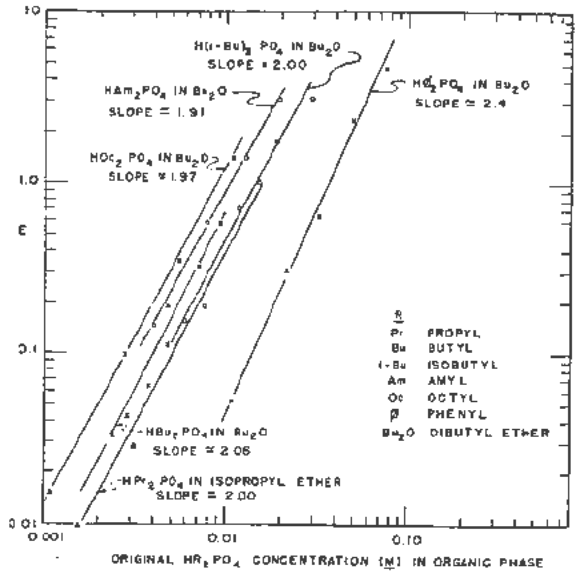

Figure 3. Partition coefficients, $E^{organic}_{aqueous}$ for trace concentrations of U^{233} extracted into dilute solutions of dialkylphosphates in butyl or propyl ether from 1.98 *M* HNO_3. (Stewart, D. C. and Hicks, T. E., University of California Radiation Laboratory Report, UCRL-861, August 1950.)

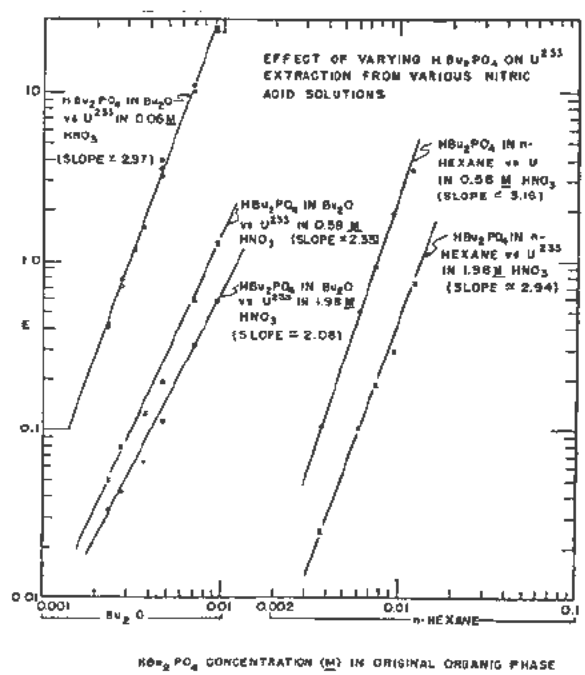

Figure 4. Extraction of uranium into a dilute solution of dibutyl phosphate in butyl ether or *n*-hexane. Effect of nitric acid concentration and of concentration of dibutylphosphate is shown. (Stewart, D. C. and Hicks, T. E., University of California Radiation Laboratory Report UCRL-861, August 1950)

M dibutyl phosphate in carbon tetrachloride followed by one wash of the water with carbon tetrachloride removed all of the uranium.[59]

The Extraction of Uranium by Dibutoxytetraethylene Glycol (Pentaether)

This solvent lies intermediate between ethyl ether and tributyl phosphate in its extractive power for uranium from nitrate-containing aqueous systems. Various groups within the United States have carried out extensive research on the effect of various conditions on the extraction of uranium by this solvent.[60-62]

To obtain high partition coefficients $E^{organic}_{aqueous}$, it is necessary to add nitric acid and nitrate salts to the aqueous solution. An idea of the effect of various salting agents on the extraction can be obtained by examining the data of Bartlett's presented in Table IV. Wright[63] has compared tributyl phosphate and pentaether for routine analysis of uranium.

Organic Compounds of Uranium: Solvent Extraction of Glycol (Pentaether)

Investigators interested primarily in finding new reagents for the detection and estimation of small quantities of uranium have reported literally hundreds of organic compounds which form precipitates or highly colored complexes with tetravalent or hexavalent uranium. Many of these complexes are of the chelate inner-complex type, and,

as would be expected, some of them are soluble in organic solvents. This makes them attractive for the radiochemical isolation of small quantities of uranium.

The only chelate complex which will be discussed in detail in this report is the uranyl complex of α-thenoyltrifluoroacetone.

The chelating agent, thenoyltrifluoroacetone (TTA), is used for the separation of many of the actinide elements and frequently the extraction is made from solutions in which uranium is present so that it is desirable to know to what extent uranyl ion is complexed and extracted. The group of Berkeley chemists[24] which introduced the reagent and studied its application to many elements, studied the behavior of uranium under many conditions. King,[63] for example, studied the extraction of uranyl ion at a concentration of approximately 0.1 *M* from lithium perchlorate-perchloric acid solutions of varying acidity by benzene solutions of TTA varying in TTA concentration from 1.53 *M* to 0.17 *M*. He found the extraction to be quite dependent on TTA concentration and acid concentration. At high acidities and low TTA concentration the ratio of uranium in the organic phase to that in the aqueous phase is quite low. For example, this ratio is 1.9×10^{-3} for a TTA concentration of 0.51 *M* and an aqueous composition of 1.24 *M* $HClO_4$, 1.45 *M* $LiClO_4$, and 0.10 *M* $UO_2(ClO_4)_2$. At higher TTA concentrations and lower acidities the extraction ratio is much larger. For example, at a TTA concentration of 1.53 *M* and an aqueous composition of 0.32 *M* $HClO_4$, 2.32 *M* $LiClO_4$, and 0.129 *M* $UO_2(ClO_4)_2$ the ratio is 0.27. A recent report by Day and Powers[65] gives data on the extraction of uranium(IV) from solutions of varying molarities of perchlorate, chloride and nitrate. Hyde and Tolmach[33] made a brief study of the extraction of trace concentrations of uranyl nitrate from dilute nitric acid solution using a TTA concentration in benzene of 0.2 *M*. Their results, shown in Fig. 5, indicate that near quantitative extraction is to be expected at pH's above 3.0. These investigators found that the extraction was markedly affected by the presence of high salt concentrations. This is shown for the case of solutions with a calcium nitrate concentration of 2.5 *M*. A similar effect was not observed for thorium extraction. Such ions as neptunium(IV), plutonium(IV), zirconium(IV) are readily separated from uranium by TTA extraction at relatively high acidities. The extraction of such ions as thorium(IV) from uranium is not so clean and requires more careful attention to choice of pH, TTA concentration and aqueous phase composition.

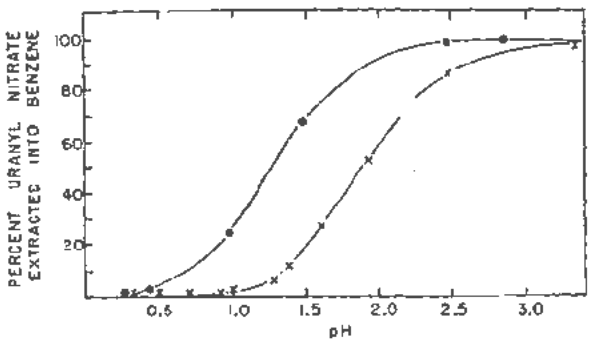

Figure 5. Extraction of trace amounts of uranyl nitrate by an equal volume of 0.2 M benzene solution of TTA from aqueous solutions of varying acidity: (x) dilute nitric acid; (o) dilute nitric acid plus 2.5 M $Ca(NO_3)_2$

Uranium in the tetravalent state has entirely different extraction characteristics, being extractable at higher acidities. In general, extractability of uranium(IV) falls between thorium(IV) and plutonium(IV).

An interesting recent study of the extraction of trace concentrations of uranium(VI) from nitrate systems into organic solvent solutions of TTA using solvents other than benzene has been made by Heisig and Crandall.[66] Their results show that if the nonpolar benzene is replaced by a polar solvent such as cyclohexanone, dibutoxytetraethylene glycol or methyl isobutyl ketone the extraction of the uranium(VI) in the form of the complex UO_2K_2 (where *K* represents the thenoyltrifluoroacetone molecule minus one proton) is markedly increased. The effect of this substitution of solvents on unoxygenated ions such as zirconium(IV) is the reverse. A consideration of these results suggests several applications to radiochemical separation of uranium(VI) from other ions.

Anion-Exchange Behavior of Uranium

Independent studies which have been carried out at several laboratories within the United States have shown that hexavalent uranium in strong hydrochloric acid solution forms a negatively charged chloride complex which may be readily adsorbed on an anion-exchange resin. Conditions are known under which the adsorption is quantitative and under which it is negligible. The behavior of nearly all elements in the periodic system has been studied and conditions are known for the separation of uranium from nearly every other element.

Quoting from the work of Kraus and his co-workers at Oak Ridge, the elements which are not adsorbed by Dowex-1 or 2 (commercial copolymers of styrene and divinylbenzene containing quaternary ammonium groups) are the alkali metals, the alkaline earths, the rare earths, aluminum, scandium, arsenic, nickel, and thorium. Among the elements which are strongly adsorbed are iron, zirconium, hafnium, niobium, zinc, cadmium, mercury, polonium, and antimony and uranuim. Among the elements which are moderately well adsorbed are cobalt, copper, lead, and bismuth.

Data on most of these elements except uranium can be found in a series of published articles by Kraus and co-workers.[67–69]

Published data on the behavior of uranium and higher elements is sparse but can be summarized thusly: uranium(VI), neptunium(VI), and plutonium(VI) are strongly adsorbed. Thorium(IV)

and uranium(IV) are not adsorbed. Neptunium(IV) is moderately well adsorbed and plutonium(IV) is strongly adsorbed. The (III) ions of the actinide elements are adsorbed but there are marked differences in adsorption in going up the series: the lower elements are poorly adsorbed while the higher elements (98–101) form much stronger complexes.

The separation of thorium, protactinium and uranium by anion exchange was discussed earlier. The behavior of higher elements will be discussed later.

Uranium(VI) will also form anionic complexes in nitric acid solution of greater strength than 9 *M*. These complexes are readily adsorbed on Dowex-1. The removal of iron impurity from uranium is easily done by adsorbing the uranium from concentrated nitric acid solution and washing the resin with excess nitric acid.

RADIOCHEMICAL PURIFICATION OF NEPTUNIUM AND PLUTONIUM

Neptunium can easily be converted to the oxidation state (IV), (V), or (VI) in aqueous solutions by proper choice of oxidizing or reducing conditions. Plutonium can easily be converted to the oxidation states (III), (IV) or (VI). These oxidation states have markedly different behavior in coprecipitation, complex formation, solvent extraction, organic chelate formation, cation exchange and anion exchange. Hence a wide variety of chemical treatments is possible in the isolation of these elements. When either of these elements is separated from a complex mixture of elements such as a fission product mixture advantage is taken of the differing behavior of the various oxidation states in the course of the purification. The philosophy behind most of these procedures is that those impurities which resemble and/or accompany the plutonium or neptunium in one of the oxidation states will show quite distinct behavior from them when they are converted to a different oxidation state. This very powerful method for the removal of impurities is not applicable to elements such as thorium, or curium, which exhibit but one oxidation state in aqueous solution. This principle will be illustrated repeatedly in the sections which follow.

Coprecipitation Behavior of Neptunium and Plutonium

This field has been covered rather thoroughly in published work on the second World War research of the American, British, and Canadian laboratories. A great deal of this literature can be found in the general references given at the beginning of this report.[1,2,4,6]

In this section the LaF_3 oxidation-reduction cycle, and the zirconium phosphate oxidation-reduction cycle will be briefly reviewed as examples of the method. These older methods are still frequently of considerable use in radiochemical analysis since it is often convenient to use a coprecipitation method to remove gross quantities of uranium or other elements before proceeding to the use of the ion exchange, solvent extraction or organic chelate compound extraction methods to be discussed in the later sections.

The Lanthanum Fluoride Oxidation-Reduction Cycle

Neptunium(IV) and plutonium(III) or plutonium(IV) are carried practically quantitatively by lanthanum fluoride precipitated under a range of acidities in hydrochloric acid, nitric acid, or sulfuric acid solution. Greatest decontamination (decontamination factor, greater than 1000) from uranium is obtained in sulfuric acid solutions because of the strong sulfate complexes of uranyl ion. In their hexapositive state neptunium and plutonium are not carried. A typical sequence is as follows.

A uranium metal or oxide cyclotron target or neutron irradiated sample is dissolved in concentrated nitric acid, evaporated partially to remove excess acid, and diluted to a final concentration less than 0.5 *M* uranium. Lanthanum carrier (0.1 to 0.5 mg/ml) is added, and sulfur dioxide is bubbled through the solution for a few minutes. With the solution in an HF-resistant container, enough HF to make the solution 1 *M* to 3 *M* is introduced, and the resulting LaF_3 precipitate is centrifuged and washed with a few milliliters of wash solution (1 *M* HNO_3 and 1 *M* HF, containing sulfur dioxide). The precipitate is dissolved in a small volume of concentrated nitric acid saturated with H_3BO_3 or with aluminum or zirconium ion (to complex the fluoride), diluted to a few milliliters with sulfur dioxide water, and reprecipitated by the addition of HF. The washed LaF_3 precipitate is converted to the hydroxide by treatment with a concentrated solution of potassium hydroxide (carbonate free) repeated twice. After being washed, the hydroxide is dissolved in 1 *M* HNO_3, and the neptunium and plutonium in solution are oxidized to the hexapositive state by the addition of $KBrO_3$ to a concentration of 0.15 *M* and heating at 95°C for 20 minutes. Then HF is added to precipitate LaF_3. An alternate oxidizing agent is argentic ion. This precipitate, which removes nearly all the activities, principally the rare-earth fission activities which coprecipitate with the LaF_3, is discarded. The HF used in this step is pretreated with a solution containing peroxydisulfate ion to remove reducing impurities. Gaseous sulfur dioxide is passed through the supernatant solution (or else the bromate solution is diluted several fold with sulfur dioxide solution) to destroy the excess bromate and reduce the neptunium and plutonium to LaF_3-carryable states. The reduction of neptunium to neptunium(IV) by sulfur dioxide in the presence of F^- is instantaneous, but, if plutonium is present, 15 to 30 minutes are allowed. Additional lanthanum is added and precipitated as LaF_3. After metathesis of the fluoride to the hydroxide as before, it is dissolved in whichever acid is suitable for the step next contemplated.

To modify this cycle for the separation of neptunium and plutonium, bromate is used as the oxidiz-

ing agent in the oxidation step, and the solution is not heated or allowed to stand for more than 20 minutes. The oxidation of plutonium(III) to plutonium(IV) is rapid, but the oxidation of plutonium(IV) or neptunium(V) to the hexavalent state is very slow in cold bromate solution. It has been shown, however, that the oxidation of neptunium(IV) by bromate is markedly catalyzed by fluoride ion, so complete oxidation occurs rapidly at the moment of precipitation of lanthanum fluoride. Plutonium(IV) does not show this marked catalysis and so precipitates with the lanthanum fluoride.

When a high separation factor from uranium is necessary, as in the separation of neptunium isotopes from a cyclotron bombardment of milligram quantities of U^{238}, the lanthanum fluoride cycle should be repeated, substituting 1 *M* H_2SO_4 for nitric acid and reducing the amount of lanthanum carrier to 0.2 mg/ml or less. The strong sulfate complex and the reduction in the amount of carrier reduce the coprecipitation of uranium greatly (only 0.01 to 0.1 per cent per precipitation even for uranium present in trace amounts).

The coprecipitation of a few elements such as zirconium and the alkaline earths which carry when present in trace amounts but not when present in milligram amounts may be eliminated by the addition of an inert holdback agent to the initial dissolver solution. Magnusson, Thompson, and Seaborg[70] also found it desirable to precede the lanthanum fluoride cycle by a manganese dioxide precipitation to remove protactinium which would otherwise coprecipitate on the initial lanthanum fluoride.

The lanthanum fluoride cycle constituted the principal means of purification in the isolation of the first weighable quantities of neptunium and plutonium.[71,72]

The Zirconium Phosphate Oxidation-Reduction Cycle

Neptunium and plutonium in the (IV) state resemble other (IV) ions, such as thorium(IV) and cerium(IV), in coprecipitation with zirconium phosphate. In the (VI) state they are not coprecipitated. These facts constitute the basis of a zirconium phosphate cycle similar to the lanthanum fluoride cycle. One formulation of the zirconium phosphate cycle, with particular application to neptunium, is as follows.[70]

A uranium target solution is adjusted to approximately 3 *M* HNO_3, 0.01 *M* Zr(IV), 0.001 *M* Ce(IV), and 0.02 *M* $NaBiO_3$. The solution is heated 1 minute to oxidize neptunium to neptunium(VI) and then made 0.5 *M* H_3PO_4 to precipitate zirconium phosphate. The solution is heated 1 minute to coagulate the precipitate and is centrifuged. The supernatant solution containing neptunium(VI) is reduced with excess $N_2H_4 \cdot H_2SO_4$ to destroy bromate and is then made 0.01 *M* $N_2H_4 \cdot H_2SO_4$ and 0.005 *M* iron(II) to reduce neptunium to neptunium(IV). This reduction is rapid. About 1 mg of zirconium(IV) per milliliter of solution is added, and the solution is heated and stirred. Zirconium phosphate precipitates, carrying neptunium(IV), and the precipitate is washed with 3 *M* HNO_3-0.5 *M* H_3PO_4 solution. Uranium remains in the supernatant solution. About 0.1 mg of lanthanum(III) as a nitrate solution is slurried with the zirconium phosphate (about 1 mg), and the zirconium is dissolved by forming a complex ion with fluoride by the addition of a 1 *M* HF–1 *M* HNO_3 solution. A precipitate of LaF_3 remains, bearing the neptunium.

In this procedure, plutonium is separated in the second precipitation of zirconium phosphate because plutonium is reduced to plutonium(III), which is not carried by zirconium phosphate.

In order to recover the plutonium, lanthanum carrier is added to the supernatant solution at this point and NH_4OH is added to precipitate $La(OH)_3$ which carries the plutonium. The $La(OH)_3$ is dissolved in nitric acid and heated to oxidize the plutonium to plutonium(IV). Zirconium carrier is added and precipitated as zirconium phosphate by addition of H_3PO_4. The plutonium(IV) is coprecipitated. About 0.1 mg of lanthanum(III) as nitrate solution is slurried with the zirconium phosphate. The zirconium is dissolved by the addition of 1 *M* HNO_3-1 *M* HF. A precipitate of LaF_3 remains bearing the plutonium.

Zirconium phenylarsonate is another compound which is very useful for removal of (IV) ions from solution. It can be used to analyze a mixture of plutonium(IV) and plutonium(III) because plutonium(III) is not coprecipitated.

Solvent Extraction of Neptunium and Plutonium

As might be expected from their chemical similarity to uranium, particularly in the hexapositive state, neptunium and plutonium may be extracted from an aqueous phase by ethyl ether and the other organic solvents which show the property of extracting uranyl ion.

The type of solvents which show high extraction of neptunium and plutonium from nitrate systems are in general the same ones we have mentioned as being good solvents for uranium, thorium, or protactinium, i.e., diethyl ether, tributyl phosphate, ketones such as di-isopropyl ketone, methyl *n*-amyl ketone or methyl isobutyl ketone and a number of the glycol-ether type of solvents, such as diethyl cellosolve, dibutyl carbitol, dibutoxytetraethylene glycol. The same general classes of solvents which show low extraction for uranium also show low extraction for plutonium and neptunium.

Solvent extraction of neptunium or plutonium is usually carried out from nitrate systems. Chloride systems have been used but extraction is lower and specificity not as great. Other systems which have been studied are virtually useless. Ions such as fluoride, sulfate and phosphate which form complex ions with the heavy elements inhibit their extraction.

Extraction shows a marked dependence on total nitrate ion concentration and to obtain a useful par-

tition coefficient for radiochemical work the aqueous phase is made several molar in nitrate ion. The higher-valent neutral nitrate salts are more effective in increasing the amount of neptunium or plutonium extracted by the aqueous phase. If fluoride ion is known or suspected to be in the solution, aluminum nitrate or calcium nitrate is used because of its fluoride complexing ability.

Nitric acid acidity needs to be somewhat higher for neptunium and plutonium extraction than the low minimum required for uranyl extraction and usually a concentration of 0.5 to 1 *M* HNO_3 may be necessary.

High extractability may be obtained from concentrated solutions of nitric acid (see Figs. 6 and 7) without the use of additional salting agent but this practice is not recommended for the three reasons that attack on the solvent is greater at higher acidities, extraction of impurities is greater and re-extraction from the solvent is complicated by the high coextraction of nitric acid into the solvent.

It has been shown that plutonium(III) is non-extractable. Plutonium(IV) is extracted well by some solvents such as dibutyl carbitol, methyl isobutyl ketone, but not very well by ethyl ether. High extractability of plutonium(IV) has been observed in tributyl phosphate. Neptunium(IV) presumably would show extractability similar to, if somewhat lower than, plutonium(IV) but is unstable in nitrate

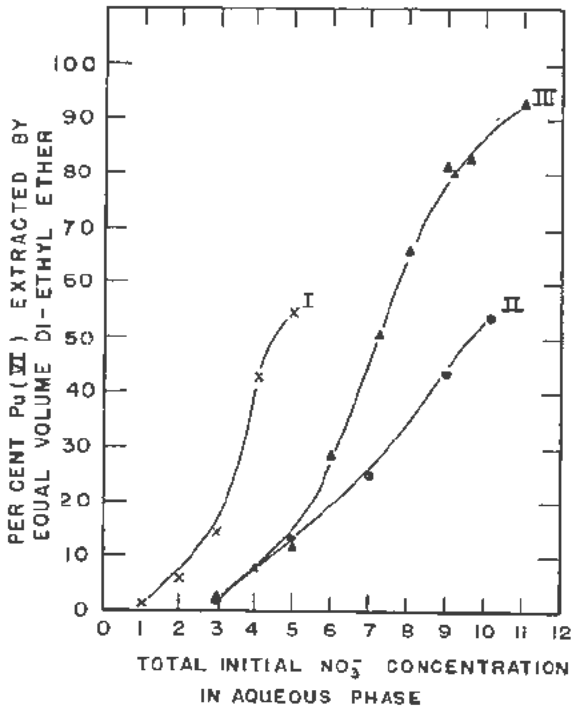

Figure 6. Effect of total nitrate ion concentration on the extraction of plutonium(VI) by diethyl ether: (curve I) HNO_3 only, (curve II) 1 M HNO_3 + NH_4NO_3, (curve III) 1 M HNO_3 + $Ca(NO_3)_2$. (Brody, Orlemann, Jensen, and Dixon, unpublished information, 1944)

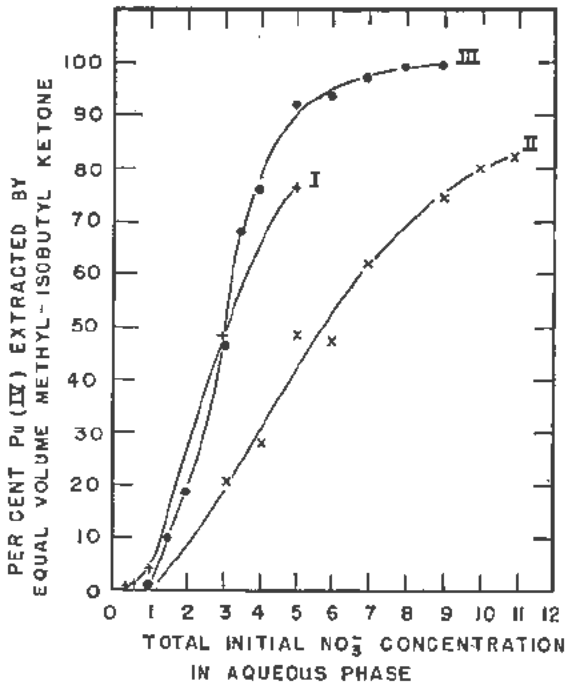

Figure 7. Effect of total nitrate on the extraction of plutonium(VI) by methyl isobutyl ketone: (curve I), HNO_3 only; (curve II), 1 M HNO_3 + NH_4NO_3; (curve III), 1 M HNO_3 + $Mn(NO_3)_2$. (Stewart, Brittain, Fineman, Jensen, and Dixon, unpublished information, 1944)

systems. The extraction of the (V) state has not received much study.

Figure 6 has been included to show the extractability of plutonium(VI) into ethyl ether from nitric acid solutions and from mixed nitrate salt-nitric acid solutions. The curves demonstrate the necessity for high nitrate concentrations and the greater "salting" effect of calcium nitrate over ammonium nitrate.

Figure 7 has been included to give an idea of the extractability of plutonium(IV) into methyl isobutyl ketone from nitric acid and nitric acid-nitrate salt solutions.

Tributyl phosphate is usually used as a 10 to 20 per cent solution in some diluting solvent such as carbon tetrachloride, benzene, or *n*-butyl ether. Distribution coefficients into the organic phase of the order of 2 to 4 are observed from nitric acid solutions as dilute as 1 to 2 *M*. Considerably higher distribution coefficients are observed from more acidic solutions or from nitrate salt-nitric acid mixtures. Extraction into the organic phase is appreciable at acidities as low as 0.1 *M* HNO_3 and backextraction of plutonium into an aqueous phase may require repeated washing with distilled water because of the nitric acid content of the tributyl phosphate phase. Alternatively, a reducing agent may be added to reduce plutonium(IV) to plutonium(III) which strips out immediately. The use of tributyl phosphate is undesirable in the presence of thorium or zirconium as these elements are highly extracted. The tributyl

phosphate should be washed with alkali and water before use, as previously mentioned in the uranium section, so that dibutyl phosphate is removed.

In working up uranium targets neptunium, plutonium, and uranium are frequently isolated together by solvent extraction as a first step in purification. Alternately a lanthanum fluoride cycle may be used as a first step and an ethyl ether extraction used secondly as a method of removing residual contaminants and of preparing carrier free solutions. In solutions where the level of contaminating radioactivity is quite high it is usually desirable to use a several-stage extraction incorporating the backwashing principle to remove residual coextracted impurities. One tenth molar BrO^- is added to the solutions to keep the neptunium and plutonium in the (VI) state.

A very sharp uranium-plutonium separation may be made by a solvent method involving the reduction of plutonium to the nonextractable (III) state, with some suitable reagent such as H_2O_2, N_2H_4, or ferrous ion and extracting exhaustively with ether or methyl isobutyl ketone to remove uranium.

A uranium-neptunium separation can be carried out in a similar fashion by contacting an ether solution of uranium and neptunium with a saturated ammonium nitrate solution containing 0.1 *M* HNO_3 and a small amount of ferrous ion and urea. The ferrous ion reduces neptunium(VI) to neptunium(V) which is unextractable at this acidity. The urea maintains the iron in the ferrous state.

Extraction of Neptunium and Plutonium as the Thenoyltrifluoroacetone Complex

Plutonium(IV) and neptunium(IV) are readily extracted by benzene solutions of α-thenoyltrifluoroacetone from dilute acid solutions free of interfering ions. High partition coefficients in favor of the organic phase are obtained in solutions acidic enough (e.g., 0.5 *M* H^+) that only a few other elements, notably zirconium(IV), cerium(IV), hafnium(IV), iron(III), protactinium(V), tin(IV), and uranium(IV) are readily extracted. Separation is easily made from thorium as thorium(IV) extraction is quite low at acidities above 0.1 *N*. TTA extraction is best employed after a preliminary isolation by a lanthanum fluoride cycle or by ether extraction and serves as an excellent final step to remove the remaining impurities as well as carrier material. TTA extraction has frequently been employed as a method of separation of neptunium and plutonium by taking advantage of the difference in stability of the neptunium(IV) and the plutonium(IV) states. A procedure developed by Magnusson, Hindman, and LaChapelle,[73] after a study of the kinetics of the reduction of neptunium in hydrochloric acid, is given below.

Starting with a solution containing trace concentrations of neptunium and plutonium and with or without macro concentrations of uranium, nitrate ion is eliminated by evaporations with concentrated HCl and the solution is made 5 *M* in HCl, 0.1 *M* in KI, 0.1 *M* in $N_2H_4 \cdot HCl$. This solution is heated in boiling water for 2 to 3 minutes. Under these conditions uranium(VI) is reduced, but very slightly, neptunium is rapidly reduced to neptunium(IV) and plutonium is reduced to plutonium(III) by the iodide ion. There is no danger of reducing neptunium to neptunium(III). To obtain a proper acidity for the extraction the solution is diluted tenfold. By heating the resulting 0.5 *M* HCl solution for 1 minute, any free iodine, which might cause a slow reoxidation of the neptunium is reduced to the iodide by the hydrazine present. This solution is equilibrated with an equal volume of a 0.15 *M* solution of TTA in benzene for a period of 20 to 30 minutes. The extraction of neptunium is nearly quantitative and less than 1 per cent of the uranium and plutonium is coextracted. Contact with a wash solution of the same composition as the original aqueous layer will remove most of the remaining uranium and plutonium.

The neptunium may be returned to an aqueous solution by contacting the benzene solution briefly with 5 *M* HCl. If separation factors greater than 100 from plutonium or uranium are required the neptunium solution should be oxidized, to convert uranium(IV) to uranium(VI) then put through the above sequence of reduction and extraction operations once more.

The plutonium(III) left in the aqueous phase may be oxidized to plutonium(IV) to prepare it for extraction. Oxidizing conditions must be chosen properly to prevent oxidation to plutonium(VI) which is not extracted. Potassium iodate at a concentration of 0.02 *M* has been used. After 20 minutes standing at room temperature the plutonium is nearly completely in the tetrapositive state and may be extracted with a fresh volume of 0.1 *M* TTA-benzene. The plutonium may be returned to an aqueous phase by contacting the benzene solution briefly with a 5 *M* HCl solution. Alternately the benzene solution may be contacted with a solution 0.5 *M* in hydrochloric acid and 0.2 *M* in $NH_2OH \cdot HCl$ which will reduce plutonium(IV) to plutonium(III) again and cause its return to the aqueous phase. This latter method has the advantage of providing an additional separation from neptunium or other coextracted impurities, if any, by leaving them in the benzene phase. It has the disadvantage that the reduction is slow.

A complete discussion of the application of the TTA cycle to the purification of neptunium is given in the report by Magnusson, Hindman, and LaChapelle.[73]

A paper which gives considerable detail on the extraction of plutonium(IV) by TTA has been published by Peppard *et al.*[74]

Some exact data on the extraction of neptunium(IV) by TTA from perchlorate and sulfate systems have been given by Sullivan and Hindman.[75]

Iddings and Hicks[76] have incorporated the TTA method into a radiochemical procedure for the extraction of neptunium from a complex mixture of fission products. Starting with a 6 *M* HCl solution formic acid is added and the solution is boiled to reduce neptunium to neptunium(IV). The solution is diluted to 1.5 *M* HCl and contacted with 0.4 *M* TTA in benzene for 15 minutes. The benzene layer is separated and washed once with a quarter volume of 2 *M* HCl. The neptunium is stripped from the benzene by two treatments with half volumes of 8 *M* HCl. The aqueous solution is again treated with formic acid, diluted to 1.5 *M* HCl and contacted with 0.4 *M* TTA in benzene. The benzene solution is washed with 2 *M* HCl, and with 0.1 *M* HNO_3. The neptunium is then removed from the benzene by two treatments of the benzene layer with 8 *M* HNO_3.

If the TTA method is used in the purification of milligrams of neptunium or tens of milligrams (as for example in the purification of a sample of Np^{237} bombarded in a cyclotron or a nuclear reactor to measure nuclear reaction cross sections), some difficulty will be experienced because of the limited solubility of the neptunium-TTA complex in benzene.

In this case the substituted hexandione reagent described in the section on TTA extraction of thorium is useful. Its main advantage is that the neptunium complex is several fold more soluble in benzene than is the corresponding TTA compound. It has the disadvantage that a long time (about one hour) must be allowed for formation of the complex.

Anion-Exchange Behavior of Neptunium and Plutonium

One of the most interesting recent developments in the radiochemistry of these elements in recent years has been the application of anion-exchange separations, particularly in HCl solutions.

It has been shown that readily adsorbed negative chloride complexes of neptunium and plutonium will form not only for the hexavalent ions in analogy with uranium, but also for the pentavalent and quadrivalent ions. Most experiments with which the author is acquainted have been done with the commercial resins Dowex-1 or Dowex-2 (a copolymer of styrene and divinyl benzene with quaternary ammonium functional groups). A brief summary of the adsorption behavior of the various oxidation states is given in the following few paragraphs.

Adsorption Behavior of Hexavalent Ions

Uranium(VI), neptunium(VI), plutonium(VI) are readily adsorbed from hydrochloric acid solution 6 *M* or greater in concentration. They are readily desorbed with 0 to 3 *M* HCl.

Uranium(VI) and plutonium(VI) are readily adsorbed from nitric acid solutions greater than 8 *M* in concentration.

Adsorption Behavior of Pentavalent Ions

Neptunium(V) is readily adsorbed above 4 *M* HCl. Uranium(V) and plutonium(V) are not stable enough to be of radiochemical interest. Protactinium(V) is readily adsorbed above 8 *M* HCl.[48,49]

Adsorption Behavior of Quadrivalent Ions

Thorium(IV) is not adsorbed at any HCl concentration.

Adsorption of the following in order of increasing adsorption is: uranium(IV) < neptunium(IV) < plutonium(IV). Uranium(IV) sticks only in very concentrated HCl. Neptunium(IV) is adsorbed above 4 *M* HCl. Plutonium(IV) is adsorbed strongly above 2.5 *M* HCl.

Adsorption Behavior of Trivalent Ions

Thorium(III), uranium(III) are not stable.

Plutonium(III) is not adsorbed at any HCl concentration.

Americium and higher actinide elements (see later discussion).

A consideration of these facts makes it readily apparent that the actinide elements can be cleanly separated from each other by a proper choice of oxidation states and hydrochloric acid concentration. The manipulations are simple, rapid and quantitative when small amounts or weightless amounts of the elements are used. The adsorption behavior of most of the fission product elements is known[68,69,77] and radiochemical procedures can be devised to decontaminate these elements.

The separation of neptunium from plutonium is easily and quantitatively effected by anion exchange. If both elements are in hydrochloric acid, iodide ion can be added and if the solution is heated for 1 minute the neptunium will be reduced to the (IV) state, the plutonium to the (III) state. The solution can then be drawn through a short resin bed of Dowex-1 resin and washed with concentrated hydrochloric acid. The plutonium passes through quantitatively while the neptunium is adsorbed quantitatively. The desorption of the neptunium with 0.5 *M* HCl can then be proceeded with.

An alternative procedure is to adsorb a mixture of plutonium(IV) and neptunium(V) or (VI) on the resin from concentrated hydrochloric acid. Then concentrated hydrochloric acid containing 0.1 *M* HI is drawn into the resin and allowed to stand for 20 minutes to reduce the plutonium to the (III) valence state. More concentrated hydrochloric acid is then drawn through the column to remove the plutonium. The reduction of the plutonium is complete within a minute if the anion resin is jacketed for operation at 80° to 90°C instead of at room temperature.[78]

Cation-Exchange Behavior of Neptunium and Plutonium

Uranium, neptunium, and plutonium in all valence states for which they are stable in acidic solution are readily adsorbed on cation-exchange resins such as Dowex-50. Trace amounts of these elements can be adsorbed on a small column of resin from rather

large volumes of dilute acid solution. This is useful for concentration purposes.

The elements can be desorbed by eluting them from the column with moderately concentrated solutions of hydrochloric acid or nitric acid as would be expected by the mass action influence of the hydrogen ion. However, the elution with hydrochloric acid is much speedier than would be expected from this effect alone because of the strong tendency toward the formation of chloride complexes. This complexing behavior which was discussed in the previous section on anion exchange is reflected in the elution behavior from cation-exchange resins. This is discussed rather completely in a recent publication by Diamond, Street, and Seaborg.[16]

A rough understanding of the effect of hydrochloric acid concentration on the elution of these elements can be obtained from Fig. 8 constructed from the data of these authors. The data were obtained in the following way. Tracer amounts of the elements were adsorbed on top of a Dowex-50 column 10 cm tall by 1 mm diameter prepared from 25 to 500 mesh resin particles. The hydrochloric acid was allowed to pass through at the linear flow rate of 0.1 cm per minute. The elution of the tracer ions was followed by alpha counting and alpha spectrum analysis of the successive fractions taken from the bottom of the column. The elution peaks as a function of volume of eluant were plotted. In Fig. 8 the volume of eluant passing through the column before the elution peak for a given ion was reached is shown. The scale is logarithmic to allow ions of widely varying elution behavior to be compared. The ions which are most readily eluted appear toward the left.

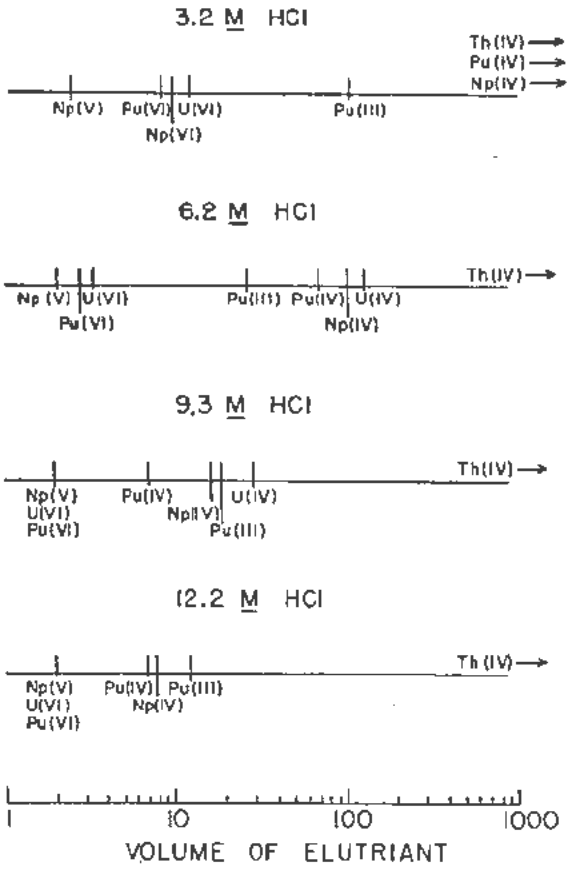

Figure 8. Summary of elution peak positions of thorium, uranium, neptunium and plutonium in various oxidation states showing effect of hydrochloric acid concentration on the elution of the elements. Data from reference 16

The behavior of the entire actinide series of trivalent ions will be discussed in a later section of this report.

It is to be noted that there are some rather remarkable changes in speed of elution and in relative elution positions shown by Fig. 8.

The case of the tetrapositive ions is particularly striking. Thorium(IV) is a comparatively large, highly charged, unoxygenated ion and adheres very strongly to the resin. In fact it is not eluted at any convenient rate by any concentration of hydrochloric acid. It is usual to resort to elution with oxalic acid, citric acid, lactic acid or other complexing agents in order to remove thorium. Uranium(IV), neptunium(IV) and plutonium(IV), however, show an increasing tendency toward chloride complex formation and plutonium in particular can be desorbed rather quickly with concentrated hydrochloric acid.

Extraction of Plutonium as Cupferron Complex

Plutonium(IV) readily forms a chelate complex with cupferron (phenyl nitroso hydroxylamine) in dilute hydrochloric acid or sulfuric acid which can be separated as a precipitate or extracted by chloroform. This is not a specific separation since iron, gallium, zirconium, hafnium, niobium, tin, antimony, titanium, vanadium, and tantalum also form chloroform-soluble complexes. However, it has proved of considerable use in radiochemical separations. For example, Nigon and Penneman[79] separated plutonium from americium by this method. Warren and Moore[80] have used this method to remove plutonium from solutions of neutron irradiated uranium. It is essential in this method to secure the plutonium in the (IV) oxidation state with an appropriate reducing agent such as hydroxylamine. The presence of ferrous iron is essential. The acidity of the solution is maintained at 0.6 ± 0.1 *M* HCl. The extraction is made quantitative by extracting the aqueous phase three times by means of a small portion of chloroform.

RADIOCHEMICAL PURIFICATION OF ACTINIDE ELEMENTS ABOVE PLUTONIUM (ELEMENTS 95–101)

In contrast to the situation with respect to neptunium and plutonium chemistry, every significant development in the chemistry of the transplutonium element group has been published in the standard

technical journals or in unclassified books and reports. Hence this section will merely outline the most significant radiochemical information and indicate where the complete information can readily be obtained.

The early work on americium and curium up to about 1951 was covered rather completely in the Volumes 14A and 14B of the National Nuclear Energy Series.[1,2] The tracer chemistry of americium and curium was reviewed by Thompson and co-workers.[81] Their discussion covered coprecipitation behavior and ion-exchange separation of americium, curium, and rare earths using Dowex-50 cation-resin columns and ammonium citrate elution as well as a number of other matters.

Perlman and Street[82] have reviewed the chemistry of americium, curium, berkelium, and californium.

Elution Separation of Transplutonium Elements from Cation-Exchange Resins

The great similarity of the trivalent transplutonium elements to each other and to the rare-earth elements has meant that the powerful ion-exchange method is relied upon heavily in chemical separation. The evolution of the ion-exchange method has followed this sequence.

The first separations were made by elution of the elements with ammonium citrate solutions of pH about 3.5 from a column of Dowex-50. To speed up and to sharpen the separations the total amount of material adsorbed on the column was kept below one milligram. Also the resin was wet screened to separate very small particles and the columns were operated at an elevated temperature. A detailed description of the method is given in a paper by S. G. Thompson and co-workers.[83]

It was later found[84–87] that somewhat sharper separations could be obtained by using buffered ammonium lactate solutions for elution. A very complete description of the experimental techniques in the ion exchange separation of the transplutonium elements with ammonium citrate and ammonium lactate elution is given in a recent paper by Thompson and his co-workers.[78]

Quite recently a new eluant, ammonium α-hydroxy-isobutyrate has been found to give much better separations even than ammonium lactate for actinide element and lanthanide element separations.[53]

Another ion-exchange method of considerable significance for the trivalent actinide elements is the one developed originally by Street and Seaborg.[16] They found that a group separation of the actinide and lanthanide elements is possible by elution with concentrated hydrochloric acid from Dowex-50 cation resin. The heavy elements have a tendency to form complex ions with chloride ion which decreases the concentration of trivalent ions in solution and speeds up the elution from the resin. Hence by eluting with 12 to 13 *M* HCl or with 20 per cent ethyl alcohol saturated with hydrochloric acid it is possible to strip the actinide elements as a group off the column ahead of the lanthanide elements. This separation was studied in detail by Diamond, Street, and Seaborg.[16] Figure 9 which is taken from their paper illustrates the dramatic shift of americium and curium with respect to representative rare earths as a function of hydrochloric acid concentration in the eluting solution. To obtain the data shown in this figure tracer ions were adsorbed from dilute acid solution on top of a 1 mm × 10 cm long column of Dowex-50 resin. Hydrochloric acid was then allowed to flow down through the column at a linear flow rate of 0.5 cm per minute. The eluant solution was collected in successive equal volume fractions and each fraction was analyzed radiochemically. Elution curves were plotted in the standard fashion. The volume of the eluant corresponding to the top of the elution peak for each element was plotted in Fig. 6 on a log scale. Those ions eluting rapidly appear to the left of the figure. The behavior of radium, barium, and cesium and of several oxidation states of neptunium and

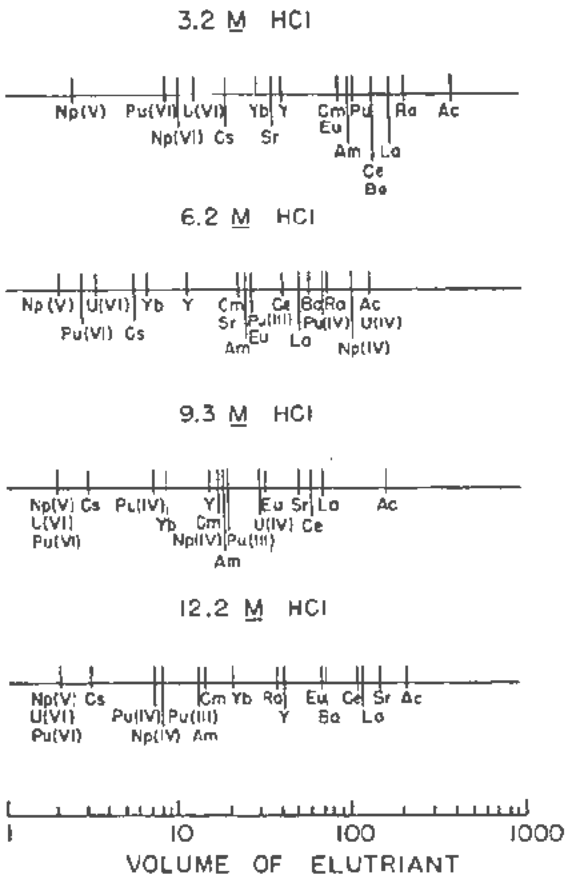

Figure 9. Elution peak positions of trivalent actinide and lanthanide elements showing pronounced shifts in elution positions of americium and curium as the concentration of the hydrochloric acid increases. Elution positions of representative monovalent and divalent ions and of higher valence states of actinide elements is also shown. Data from reference 16

plutonium was studied at the same time. Experiments were run with 3.2 *M* HCl, 6.2 *M* HCl, 9.3 *M* HCl and 12.2 *M* HCl. Detailed elution curves are shown in Diamond's paper.

The complexing of the trivalent actinide elements is greater as one goes up the series to the heavier elements and it is possible to make separations of the individual elements by careful control of the elution conditions. Figure 10 taken from the paper by Thompson[88] shows the separation of the elements 95–100 by elution from a 5 cm long by 3 mm diameter column of Dowex-50 (X-12 colloidal) resin with a 20 per cent ethyl alcohol solution saturated with hydrochloric acid. It can be seen that the complexing of elements 98–100 is greater than that of the earlier members of the series.

Anion-Exchange Behavior of Transplutonium Elements

The rapid elution of the actinide elements with hydrochloric acid suggests that negatively charged complexes may be formed in strong hydrochloric acid solution. This was tested by placing 13 *M* HCl solutions of the elements on top of a column of Dowex-1 anion resin and eluting the column with 13 *M* HCl.[89] The order of elution is shown in Fig. 10*b*. Americium and curium were held up only slightly. There was a definite delay in the elution of the higher elements indicating negative

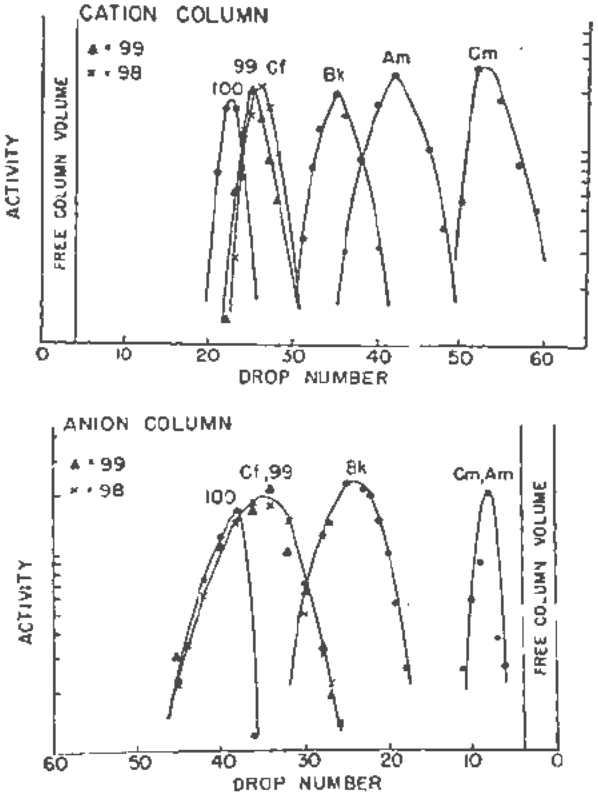

Figure 10. (top) Elution of actinides from Dowex-50 resin with 20 per cent alcohol-12.5 *M* HCl; (bottom) elution of actinides from Dowex-1 resin with 13 *M* Hcl. Figure reprinted from reference 88

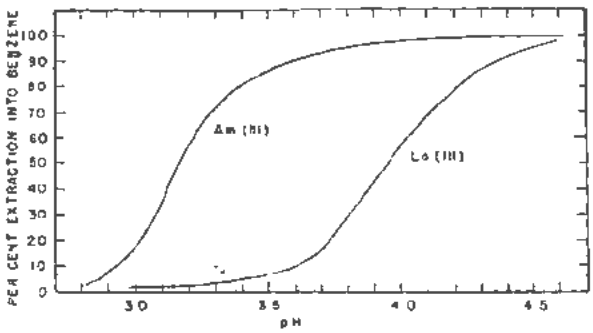

Figure 11. Extraction of Am^{241} tracer and lanthanum (approximately 0.1 mg/ml) by an equal volume of 0.2 *M* TTA in benzene as a function of pH. (Unpublished data of Werner and Perlman)

complex formation. Some separation of the elements was achieved with careful control of the conditions. All elements were eventually removed from the column when a few milliliters of 13 *M HCl* were passed through. When hydrochloric acid 10 *M* or less in concentration was used all the elements eluted immediately.

The elements 95 through 101 can be cleanly separated from uranium(VI) or from plutonium(IV), plutonium(VI), neptunium(IV), and neptunium(VI) by adjusting the hydrochloric acid concentration to 6 to 10 *M* and passing the mixture through a column of Dowex-1 resin. Complete adsorption of the uranium, neptunium, and plutonium occurs with no adsorption of the trivalent actinides.

Solvent Extraction of Thenoyltrifluoroacetone Complexes of Americium and Curium

Werner and Perlman[91] carried out a study of the extraction of americium into a benzene solution of α-thenoyltrifluoroacetone (TTA) as a means of purification from lanthanum. It was found that low acidities were required if appreciable extraction was to be obtained and that the extraction was in general similar to that of the rare earths (cf. section on TTA extraction of actinium above). Nevertheless the differences in the extraction curves obtained on plotting the amount extracted vs pH were sufficiently different that separation from some of the rare earths, particularly lanthanum, was quite feasible.

Magnusson and Anderson[92] have recently discussed the TTA complexes of elements 95 through 100.

Figure 11 shows the influence of pH on extraction of americium and lanthanum. These curves may be compared with the previously shown curves for actinium and thorium (Fig. 1). For highest extraction of americium one would adjust the pH to 4.0 or higher. For decontamination from lanthanum one would choose a pH around 3.3. For example, three extractions with an equal volume of 0.2 *M* TTA-benzene solution extracts 97 per cent of the americium and from 3 to 7.5 per cent of the lanthanum, from the aqueous solution at a pH of 3.27. The ex-

tracted americium may be removed from the benzene by brief contact with a solution of pH < 2.5. Since lanthanum is frequently used as a carrier for americium this separation has considerable importance. The separation of other rare earths is more difficult. Their extraction curves fall between those of americium and lanthanum.

Separation is also made from those elements which do not extract at this acidity. Contaminants such as neptunium(IV), plutonium(IV), protactinium(V), thorium(IV), iron(III), and zirconium(IV), may be removed by a preliminary extraction at a pH < 2.5.

The extraction curve for curium falls quite close to that for americium and preliminary attempts at americium-curium separation have not been promising. Separation of curium from lanthanum is possible although if microgram quantities of curium are involved some difficulties from the attack of the intense alpha radioactivity on the aqueous phase and the TTA are experienced.

Higher Oxidation States for Transplutonium Elements

The predominant valence state for the elements 95–101 is three. There are, however, three examples of higher oxidation states in aqueous solution among the elements in this group; namely, americium(V), americium(VI), and berkelium(IV).

Werner and Perlman[93] found that americium(III) in a 20 per cent potassium carbonate solution is slowly oxidized by 0.1 *M* NaOCl to americium(V). Some success in the separation of americium from curium(III) was attained using this oxidation, but the method was not developed and its application must be considered somewhat limited.

Asprey, Stephanou, and Penneman[94] succeeded in oxidizing 0.002 to 0.025 *M* solutions of americium(III) to the hexapositive state and in studying the properties of americium(V) and americium(VI). The oxidation was performed with peroxydisulfate ion or with argentic oxide. Complete details are given in their papers.

Naturally, these developments have considerable significance for the radiochemical purification of americium. In the isolation of americium from cyclotron bombardments or neutron irradiated samples, there is always the problem of the separation of rare-earth fission activities which exhibit marked chemical similarity to americium in the tripositive state. Also, in many instances it is necessary to separate americium and curium, which in their prevalent tripositive state exhibit the chemical similarities of adjacent rare earths. The ion-exchange procedures are quite capable of effecting these separations, but it is certainly desirable to supplement them with other methods whenever possible.

The existence of the hexapositive state and its chemical similarity to the corresponding state in the other actinide elements makes it possible in principle to apply to the separation of americium all the methods discussed for neptunium and plutonium which depend for their success on the differences in properties of the tripositive and hexapositive states, as for example, the lanthanum fluoride cycle or solvent extraction. However, experiments have shown that rate considerations seriously limit the applicability of these methods for trace concentrations of americium. The oxidation by peroxydisulfate is definitely a function of americium concentration; complete oxidation of trace concentration takes several hours, which is prohibitively long for many applications and, at any rate, makes the method more time consuming than the ion-exchange methods. This does not reject the possibility that a faster oxidation, involving perhaps some such specific catalysis as has been observed in the oxidation of neptunium, may be found.

When weighable amounts of americium are being dealt with, the situation is somewhat different. The rate of oxidation is sufficiently great that the use of the hexapositive state is definitely attractive. In the first experiments on the discovery of element 97, milligram amounts of americium were bombarded,[83] and the berkelium was isolated by ion-exchange methods. The resin-column operations were preceded, however, by an oxidation of the americium target material by making the solution 0.2 *M* in ammonium persulfate, 0.2 *M* in ammonium sulfate, and 0.1 *M* in nitric acid and heating for 1.5 hour at 75°C. The small fraction of the americium left unoxidized was precipitated by americium fluoride, which served as a carrier for curium, element 97, and the rare earths. This initial separation served the purpose of reducing sharply the bulk of material which needed to be separated and hence simplified and speeded up the ensuing column operations.

In the case of berkelium aqueous solution oxidation states of (III) and (IV) are known.[95] Trace concentrations of berkelium can be oxidized with the bromate ion, bismuthate ion, dichromate ion or ceric ion after a few minutes heating in a strongly acidic solution. Berkelium(IV) coprecipitates with zirconium phenylarsonate, zirconium phosphate or ceric iodate and can be separated from trivalent actinide ions which are not carried.

Extraction of Trivalent Actinide Ions into Tributyl Phosphate

The recent discovery[96] of the high order of extractability of the lanthanide rare-earth ions into tributyl phosphate from highly concentrated nitric acid or hydrochloric acid solutions naturally lead to the study of the extractability of the trivalent actinide elements under the same conditions. The extraction coefficients for the actinide elements are not as high as for the analogous lanthanide elements. However, the coefficients, particularly for the higher members of the series, are high enough to make the use of solvent extraction by this solvent very attractive. This is especially true of concentrated nitric acid solutions. Peppard has called attention to the remarkable analogies between the lanthanides and the

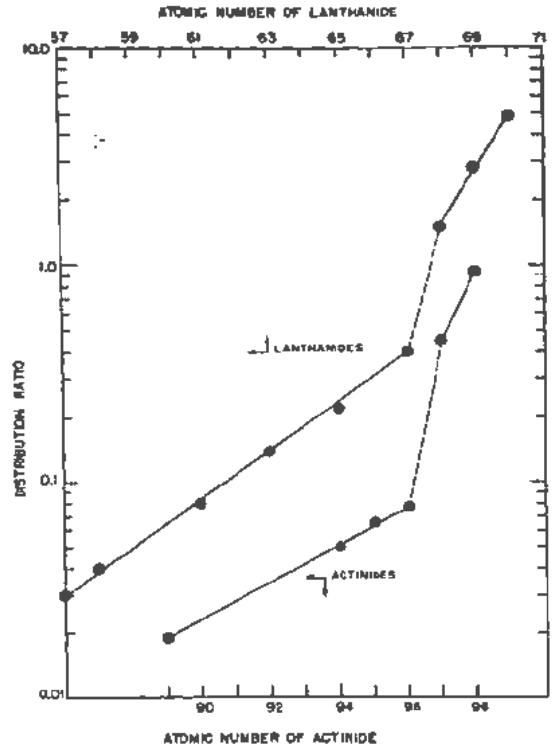

Figure 12. Solvent extraction behavior of trivalent lanthanide and actinide elements into tributyl phosphate from 12.0 N HCl

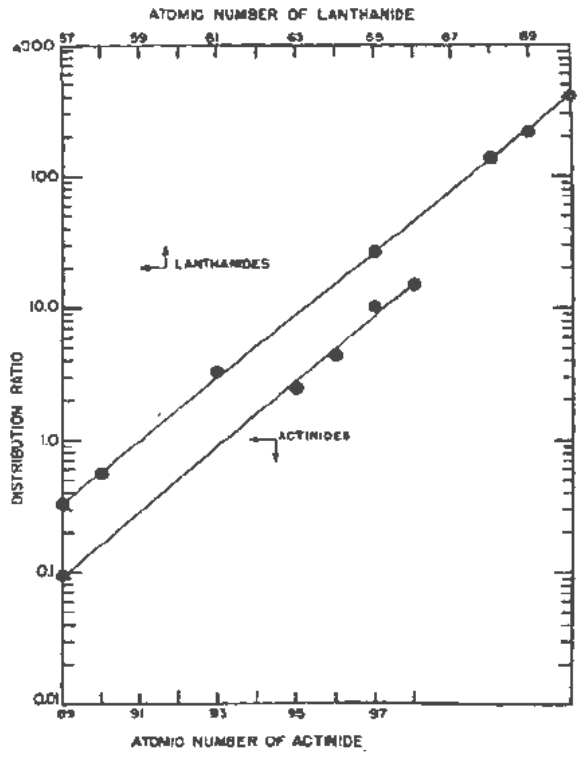

Figure 13. Solvent extraction behavior of trivalent lanthanide and actinide elements into tributyl phosphate from 15.6 N HNO_3

actinides in this solvent extraction behavior.[97] Gray[18] has prepared some curves showing the distribution ratio (i.e., the ratio of the amount of the element per unit volume TBP to the amount per unit volume of acid) for the two series of elements in 12 *M* HCl and 15.6 *M* HNO_3. These are reproduced here as Figs. 12 and 13.

Much higher distribution coefficients can be obtained by salting the aqueous phase strongly with powerful salting agents. For example, Peppard[19] found that curium(III) was extracted into undiluted tributyl phosphate with a distribution coefficient of aboue 100 from an aqueous solution 7.2 *M* $Na(NO_3)$ and 0.4 *M* HNO_3.

ACKNOWLEDGEMENTS

The author wishes to thank Miss Margot Carlson for her extensive and expert assistance in the preparation of this paper.

REFERENCES

1. Seaborg, G. T., Katz, J. J. and Manning, W. M., editors, *The Transuranium Elements: Research Papers*, Vol. 14B, Div. IV, National Nuclear Energy Series, McGraw-Hill Book Company, Inc., New York, (1949).
2. Seaborg, G. T. and Katz, J. J., editors, *The Actinide Elements*, Vol. 14A, Div. IV, National Nuclear Energy Series, McGraw-Hill Book Company, Inc., New York, (1954).
3. Rodden, C. J., editor, *Analytical Chemistry of the Manhattan Project*, Vol. 1, McGraw-Hill Book Company, Inc., New York, (1950).
4. Meinke, W. W., *Chemical Procedures Used in Bombardment Work at Berkeley*, US Atomic Energy Commission Declassified Document AECD-2738, (August 1949)
5. *Nuclear Science Abstracts*, a publication of the United States Atomic Energy Commission Technical Information Service, published twice monthly. Available in single copies or by subscription from Superintendent of Documents, US Government Printing Office Washington 25, D.C.
6. Hyde, E. K., *Radiochemical Separations of the Actinide Elements*, Chapter 15, pp 542 595, reference 2 this bibliography.
7. *Actinium and Its Isotopes*, Gmelin's Handbuch Der Anorganischen Chemie, 8, Auflage System Nummer 40, Verlag Chemie, Berlin, (1942). Available in English translation as US Atomic Energy Commission Report, AEC-TR 1734, (April, 1954).
8. Hagemann, F. T., *The Chemistry of Actinium*, Chapter 2, reference 2 this bibliography.
9. Clarke, R. W., *Actinium*. A bibliography of unclassified and declassified Atomic Energy Projects and References to the Published Literature (1906-1953), Atomic Energy Research Establishment Report (Britain) AERE-INF/Bib-95, (August 1954)
10. McLane, C. K. and Peterson S., *Tracer Chemistry of Actinium*, Paper 19.3, reference 1 this bibliography.
11. Hagemann, F. T., *The Isolation of Actinium*, J. Am. Chem. Soc. 72: 768, (1950).
12. Hall, K. L. and Templeton, D. H., *Beta Decay Energy of Ac^{226}*, University of California Radiation Laboratory Unclassified Report UCRL-957, (October 20, 1950).
13. McLane, C. K. and Peterson, S., *Separation of Actinium from Rare Earths Using Ion-Exchange Resin*, Paper 19.6, reference 1 this bibliography.

14. Yang, Jeng-Tsong and Haissinsky, M., *Chromatographic Separation of Actinium from Lanthanum*, Bull. Soc. Chim. France 16: 546, (1949).
15. Yang, Jeng-Tsong, *Separation by Ion Exchange of Traces of Ac^{227} from a Large Amount of Lanthanum*, J. Chim. Phys. 47:805, (1950).
16. Diamond, R. M., Street, K., Jr. and Seaborg, G. T., *An Ion-exchange Study of Possible Hybridized 5f Bonding in the Actinides*, J. Am. Chem. Soc., 76: 1461, (1954).
17. Peppard, D. F., Faris, J. P., Gray, P. R. and Mason, G. W., *Studies of the Solvent Extraction Behavior of the Transition Elements. I Order and Degree of Fractionation of the Trivalent Rare Earths*, J Phys. Chem. 57: 294, (1953).
18. Gray, P. R., unpublished information, University of California, Berkeley, California, (1954).
19. Peppard, D. F. and collaborators, unpublished information, Argonne National Laboratory, Lemont, Illinois, (1951).
20. Peppard, D. F., Mason, G. W., Gray, P. R. and Mech, J. F., *Occurrence of the (4n + 1) Series in Nature*, J. Am. Chem. Soc. 74: 6081, (1952).
21. Perey, M., *Measurement of Actinium by AcK*, Compt. rend. 214: 797, (1942).
22. Hyde, E. K., *Radiochemical Methods for the Isolation of Element 87 (Francium)*, J. Am. Chem. Soc. 74: 4181, (1952).
23. Skirvin, S. and Hyde, E. K., unpublished information, University of California, Berkeley, California, (1952).
24. Calvin, M., Reid, J. C., Connick, R. E., Crandall, H. W. and co-workers, unpublished work, University of California, Berkeley, California, (1944-1946).
25. Day, R. A. and Stoughton, R. W., *Chemistry of Thorium in Aqueous Solutions*, J. Am. Chem. Soc. 72: 5662, (1950).
26. Fry, A. J., Barney, J. E. and Stoughton, R. W., *Chemistry of Thorium in Aqueous Solutions. I The Thorium-Iodate System; Solubility and Complexes*, US Atomic Energy Commission Declassified Document AECD-2429, (1948).
27. Zebroski, E. L., Alter, H. W. and Heumann, F. K., *Thorium Complexes with Chloride, Fluoride, Nitrate, Phosphate, and Sulfate*, J. Am. Chem. Soc. 73: 5646, (1951).
28. Waggener, W. C. and Stoughton, R. W., *Chemistry of Thorium in Aqueous Solutions. II Chloride Complexing as a Function of Ionic Strength*, US Atomic Energy Commission Declassified Document AECD-3305, (1951).
29. Iddings, G. M., Tellefson, R. L. and Osborne, R. N., unpublished results, California Research and Development Corporation, (1952).
30. Lindner, M., compiler, *Radiochemical Procedures in Use at the University of California Radiation Laboratory (Livermore)*, University of California Radiation Laboratory Unclassified Report UCRL-4377, (August 1954).
31. Spedding, F. H. and collaborators, U.S. Atomic Energy Commission Classified Document CC-2393, (February 1945), as reported by Anderson, M. R., in *Distribution of Thorium Nitrate Between Water and a Mixture of Butyl Ether*, Iowa State College Unclassified Report ISC-116, (July 1950).
32. Hyde, E. K. and Tolmach, J., unpublished information, Argonne National Laboratory, Lemont, Illinois, (1947).
33. Peppard, D. F. and co-workers, *Isolation of Gram Quantities of Ionium from Pitchblende Residues*, J. Am. Chem. Soc. 75: 4516, (1953).
34. Levine, H. and Grimaldi, F. S., *Application of Mesityl Oxide to the Determination of Thorium*, US Atomic Energy Commission Declassified Document AECD-3186, (January 1952).
35. Hiller, D. M. and Martin, D. S., Jr., *Radiochemical Studies on the Photofission of Thorium*, Phys. Rev. 90: 581, (1953).
36. Warf, J. C., *Extraction of Cerium(IV) by Butyl Phosphate*, J. Am. Chem. Soc. 71: 3257, (1949).
37. Bane, R. W., unpublished information, Metallurgical Laboratory, University of Chicago, (1945).
38. Dyrssen, D., Svensk Kem. Tid. 62: 153-164, (1950).
39. Asaro, F., Stephens, F. S. and Perlman, I., *Complex Alpha Spectra of Radiothorium (Th^{228}) and Thorium-X (Ra^{224})*, Phys. Rev. 92: 1495, (1953).
40. Elson, R. E., *The Chemistry of Protactinium*, Chapter 5, reference 2 this bibliography.
41. Hyde, E. K. and Wolf, M. J., unpublished information, Metallurgical Laboratory, University of Chicago, (1946).
42. Overholt, D. C., Stehly, F. L. and co-workers, Oak Ridge National Laboratory, Oak Ridge, Tennessee, (1946).
43. Kraus, K. A. and Van Winkle, Q., unpublished information, Oak Ridge National Laboratory, Oak Ridge, Tennessee, (1949).
44. Kraus, K. A. and Garen, A., unpublished information, Oak Ridge National Laboratory, Oak Ridge, Tennessee, (1949).
45. Elson, R. E., Mason, G. W., Peppard, D. F., Sellers, P. A. and Studier, M. H., *Isolation of Protactinium from a New Source*, J. Am. Chem. Soc. 73: 4974, (1951).
46. Moore, F. L., *Separation of Protactinium and Niobium by Liquid-Liquid Extraction*, Oak Ridge National Laboratory Unclassified Report ORNL-1675, (February 1954).
47. Kraus, K. A. and Moore, G. E., unpublished information, Oak Ridge National Laboratory, Lemont, Illinois.
48. Kraus, K. A. and Moore, G. E., *Adsorption of Protactinium from Hydrochloric Acid Solutions by Anion Exchange Resins*, J. Am. Chem. Soc. 72: 4293, (1950).
49. Kraus, K. A. and Moore, G. E., *Anion Exchange Studies. III Protactinium in Some HCl-HF Mixtures: Separation of Niobium, Tantalum and Protactinium*, J. Am. Chem. Soc. 73: 2900, (1951).
50. Malm, J. and Fried, S., unpublished information, Argonne National Laboratory, as quoted by Elson, reference 40.
51. Sullivan, J. and Studier, M. H., unpublished information, Argonne National Laboratory, Lemont, Illinois, (1950).
52. Elson, R. E., Sellers, P. and John, R., unpublished information, Argonne National Laboratory, Lemont, Illinois, (1948).
53. Rodden, C. J., editor, Anal. Chem. 21: 327, (1949); *ibid* 25: 1598-1601, (1953).
54. Rodden, C. J., *Uranium Analysis in Ore and Source Materials*, U.S. Atomic Energy Commission Declassified Document AECD-2640, (1949).
55. Moore, R. L., *Mechanism of Extraction of Uranium by Tributyl Phosphate*, US Atomic Energy Commission Declassified Document AECD-3196, (no date).
56. Bartlett, T. W., unpublished information, Carbide and Carbon Chemical Company, (1951).
57. Stewart, D. C. and Crandall, H. W., *The Separation of Mixtures of Mono- and Di-Substituted Alkyl Phosphoric Acids*, J. Am. Chem. Soc. 73: 1377, (1951).
58. Stewart, D. C. and Hicks, T. E., University of California Radiation Laboratory Report UCRL-861, (August 1950).
59. Stewart, D. C. and Bentley, W. C., *Analysis of Uranium in Sea Water*, Science 120: 50, (1954).

60. Smellie, R. H., Jr. and Krause, D. P., unpublished information, Oak Ridge National Laboratory, Oak Ridge, Tennessee.
61. Kraus, K. A. and collaborators, Brown University, unpublished information, (1945-1946).
62. Orlemann, E. F. and collaborators, Y-12 Project, Oak Ridge, Tennessee, (1945-1946).
63. Wright, W. B., Jr., *Comparison of Tributyl Phosphate and Dibutoxytetraethyleneglycol as Extractants of Uranium*, Carbide and Carbon Chemicals Company Unclassified Report Y-884, (1952).
64. King, E. L., unpublished information, University of California, Berkeley, California, (August 1946).
65. Day, R. A., Jr. and Powers, R. M., *Extraction of Uranyl Ion from Some Aqueous Salt Solutions with 2-Thenoyltrifluoroacetone*, US Atomic Energy Commission Unclassified Report ORO-117, (1953).
66. Heisig, D. L. and Crandall, H. W., University of California Radiation Laboratory, unpublished information, (1950).
67. Kraus, K. A., Nelson, F. and Smith, G. W., *Anion Exchange Studies. IX Adsorbability of a Number of Metals in Hydrochloric Acid Solutions*, J. Phys. Chem. 58: 11, (1954).
68. Kraus, K. A. and Moore, G. E., *Anion Exchange Studies. VI The Divalent Transition Elements Manganese to Zinc in Hydrochloric Acid*, J. Am. Chem. Soc. 75: 1460, (1953); and *Anion Exchange Studies. I Separation of Zirconium and Niobium in HCl-HF Mixtures*, J. Am. Chem. Soc. 73: 9, (1951); and *Adsorption of Iron by Anion Exchange Resins from Hydrochloric Acid Solutions*, J. Am. Chem. Soc. 72: 5792, (1950).
69. Nelson, F. and Kraus, K. A., *Anion Exchange Studies XI Lead(II) and Bismuth(III) in Chloride and Nitrate Solutions*, J. Am. Chem. Soc. 76: 5916, (1954).
70. Magnusson, L. B., Thompson, S. G. and Seaborg, G. T., *New Isotopes of Neptunium*, Phys. Rev. 78: 363, (1950).
71. Magnusson, L. B. and LaChapelle, T. J., *The First Isolation of Element 93 in Pure Compounds and a Determination of the Half-Life of* $_{93}Np^{237}$, Paper 1.7, reference 1 this bibliography.
72. Cunningham, B. B. and Werner, L. B., *The First Isolation of a Synthetic Element: Pu*^{239}, Paper 1.8, reference 1 this bibliography.
73. Magnusson, L. B., Hindman, J. C. and LaChapelle, T. J., *Chemical Methods for the Purification and Isolation of Neptunium*, Argonne National Laboratory Report ANL-4066, (October 1947).
74. Peppard, D. F., Studier, M. H., Gergel, M. V., Mason, G. W., Sullivan, J. C. and Mech, J. F., *Isolation of Microgram Quantities of Naturally-occurring Plutonium and Examination of its Isotopic Composition*, J. Am. Chem. Soc. 73: 2529, (1951).
75. Sullivan, J. C. and Hindman, J. C., *Thermodynamics of the Neptunium(IV) Sulfate Complex*, J. Am. Chem. Soc. 76: 5931, (1954).
76. Iddings, G. M. and Hicks, H. G., as given in reference 30.
77. Samuelson, O., *Ion Exchangers in Analytical Chemistry*, Wiley and Sons, New York, (1953).
78. Glass, R. A. and collaborators, unpublished information, University of California Radiation Laboratory, Berkeley, California, (1955).
79. Nigon, J. P. and Penneman, R. A., *Quantitative Separation of Americium and Plutonium Using Cupferron*, U.S. Atomic Energy Commission Unclassified Document AECU-1006, (January 1951).
80. Warren, B. and Moor, E. B., Jr., unpublished information, Los Alamos Laboratory, Los Alamos, New Mexico, (1953).
81. Thompson, S. G., Morgan, L. O., James, R. A. and Perlman, I., *The Tracer Chemistry of Americium and Curium in Aqueous Solutions*, Paper 19.1, reference 1 this bibliography.
82. Perlman, I. and Street, K., Jr., *The Chemistry of the Transplutonium Elements*, Vol. II, Chapter 14, reference 2 this bibliography.
83. Thompson, S. G., Ghiorso, A. and Seaborg, G. T., *The New Element Berkelium (Atomic Number 97)*, Phys. Rev. 80: 781, (1950).
84. Wish, L., Freiling, E. C. and Bunney, L. R., *Relative Elution Positions of Lanthanide and Actinide Elements with Lactic Acid Eluant at 87°C*, J. Am. Chem. Soc. 76: 3444, (1954).
85. Mayer, S. W. and Freiling, E. C., *Column Studies of the Relative Efficiencies of Various Complexing Agents for the Separation of the Lighter Rare Earths*, J. Am. Chem. Soc. 75: 5647, (1953).
86. Glass, R. A., *Chelating Agents Applied to Ion-Exchange Separations of Americium and Curium*, J. Am. Chem. Soc. 77: 807, (1955).
87. Nervik, W. E., unpublished results, University of California, Berkeley, California, (1953).
88. Thompson, S. G., Harvey, B. G., Choppin, G. R. and Seaborg, G. T., *Chemical Properties of Elements 99 and 100*, J. Am. Chem. Soc. 76: 6229, (1954).
89. Choppin, G. R., Harvey, B. G. and Thompson, S. G., *A New Eluant for the Separation of the Actinide Elements*, to be submitted for publication in J. Am. Chem. Soc.
90. Street, K., Jr. and Seaborg, G. T., *The Separation of Americium and Curium from the Rare Earth Elements*, J. Am. Chem. Soc. 72: 2790, (1950).
91. Werner, L. B. and Perlman, I., unpublished information, Radiation Laboratory, University of California, Berkeley, California, (1946).
92. Magnusson, L. B. and Anderson, M. L., *Chelation of the +3 Ions of Elements 95 Through 100 with Thenoyltrifluoroacetone*, J. Am. Chem. Soc. 76: 6207, (1954).
93. Werner, L. B. and Perlman, I., *The Pentavalent State of Americium*, J. Am. Chem. Soc. 73: 495, (1951).
94. Asprey, L. B., Stephanou, S. E. and Penneman, R. A., *A New Valence State of Americium Am(VI)*, J. Am. Chem. Soc. 72: 1425, (1950); see also, *Hexavalent Americium*, J. Am. Chem. Soc. 73: 5715, (1951).
95. Thompson, S. G., Cunningham, B. B. and Seaborg, G. T., *Chemical Properties of Berkelium*, J. Am. Chem. Soc. 72: 2798, (1950).
96. Peppard, D. F., Faris, J. P., Gray, P. R. and Mason, G. W., *Studies of the Solvent Extraction Behavior of the Transition Elements*, J. Phys. Chem. 57: 294, (1953).
97. Peppard, D. F., Gray, P. R. and Markus, M. M., *The Actinide-Lanthanide Analogy as Exemplified by Solvent Extraction Behavior*, J. Am. Chem. Soc. 75: 6063, (1953).

On Methods of Separation of Neptunium from Plutonium

By I. K. Shvetsov and A. M. Vorobyev, USSR

During the operation of a nuclear uranium reactor weighable quantities of neptunium-237 are produced as by-product. The process may be written as:

$$U^{238}(n,2n)U^{237} \xrightarrow{\beta} Np^{237}$$
$$U^{235}(n,\gamma)U^{236};\ U^{236}(n,\gamma)U^{237} \xrightarrow{\beta} Np^{237}$$

The yield of neptunium from the first reaction is about 0.1 per cent of the number of fissions. Formation of neptunium by the second reaction is determined by the values of the slow neutron capture cross section for uranium-235 and uranium-236 ($\sigma_s^r = 101$ barns,[3] $\sigma_s^r = 24.6$ barns) and can lead to considerably greater amounts of neptunium in uranium piles operating with enriched uranium-235. Therefore, the question of quantitative separation of neptunium and plutonium is of great scientific and technical importance.

Separation of neptunium from the bulk of plutonium can be effected by the chlorination of their dioxides. The chlorination of neptunium and plutonium dioxides proceeds in different ways; for example, $PuCl_3$ and $NpCl_4$ are formed on chlorination with carbon tetrachloride. At 750–800° neptunium and plutonium trichlorides sublime at an appreciable rate. For tetrachlorides this temperature is considerably lower. For example, the complete sublimation of uranium(IV) and neptunium(IV) chlorides occurs quite rapidly at 500–530°C. The values of the separation coefficients of neptunium and plutonium are dependent upon the chlorination conditions and the apparatus used. At 620–650° more than 90 per cent of neptunium is sublimed as tetrachloride and concentrated in the sublimates. The presence of plutonium in chloride sublimates under these conditions is about 0.1 per cent of its original amount.

The methods for the following quantitative separations are based on difference between the neptunium and plutonium oxidation-reduction potentials. The oxidation-reduction potentials of neptunium and plutonium couples in 1 *M* HCl are summarized in the following schemes:[1]

$$Np(III) \xrightarrow{0.14\,v} Np(IV) \xrightarrow{0.74\,v} Np(V) \xrightarrow{1.13\,v} Np(VI)$$
$$\qquad\qquad\qquad\qquad\qquad\qquad\qquad\qquad\qquad\qquad \underset{0.94v}{\longrightarrow}$$

$$Pu(III) \xrightarrow{0.97\,v} Pu(IV) \xrightarrow{1.20\,v} Pu(V) \xrightarrow{0.91\,v} Pu(VI)$$
$$\qquad\qquad\qquad\qquad\qquad\qquad\qquad\qquad\qquad\qquad \underset{1.05v}{\longrightarrow}$$

The following ways of separating neptunium and plutonium were studied.

1. The potential difference of Pu(III/IV) and Np(III/IV) couples is 0.83 v, this makes it possible to obtain easily Np(IV) and Pu(III) in solution. Chaychorsky and Kondratov have investigated the extraction process of neptunium(IV) from nitric acid solutions by ethyl ether to follow the separation of neptunium(IV) from plutonium(III). Neptunium(IV) is extracted by ether as a complex with nitric acid. Its composition is $H_2[Np(NO_3)_6]$. This method, however, gave unsatisfactory results.

Pasvik and Ginsburg proposed an analytical method for separating neptunium and plutonium by coprecipitation of neptunium(IV) with zirconium phenylarsonate. Three reprecipitations from 1 *M* HCl produces radiochemically pure neptunium with a yield of about 97%.

For a similar purpose precipitation of neptunium(IV) by the sodium salt of benzenesulfonic acid was proposed by Borisova.

2. The separation of neptunium(V) and plutonium(IV) is based on ability of some reagents to oxidize Np(IV) to Np(V); at the same time plutonium is not affected and remains in tetravalent state. The separation of plutonium(IV) and neptunium(V) was investigated by precipitation of Pu(IV) as a fluoride or a double sulfate of plutonium and potassium; or the precipitation of a double carbonate of neptunium(V) and potassium. One precipitation did not provide analytical separation.

3. The difference in potentials of Pu(IV/VI) and Np(IV/VI) couples is only 0.11 v. In this case for neptunium and plutonium separation the decisive factor will be the rate of the corresponding oxidation-reduction reactions. $K_2Cr_2O_7$, $KMnO_4$, and $KBrO_3$ were used as oxidizing agents. The following separation of neptunium(VI) and plutonium(IV) was carried out by precipitation of Pu(IV) with potassium sulfate or hydrofluoric acid, or by precipitation of Np(VI) with sodium acetate. The best results were obtained by the use of potassium bromate.

Seaborg and Whal[3] have found that the treatment of neptunium and plutonium in tracer concentrations by 0.1 *M* $KBrO_3$ at 20° for 30 minutes in 1 *M* H_2SO_4 followed by precipitation of lanthanum fluoride

Original language: Russian.

makes possible a nearly quantitative coprecipitation of plutonium; neptunium remains in solution. This method was used by Magnusson and LaChapelle[4] to isolate weighable quantities of neptunium-237. As a result of performing this cycle a number of times, complete separation of plutonium was achieved. The distribution of neptunium and plutonium between the precipitate and solution and the yield of neptunium were not, however, given in the paper. In a later paper[5] it was shown that complete oxidation of weighable quantities of pure neptunium(IV) with potassium bromate at 25° can be achieved in several hours. The authors pointed out the important role of the fluoride ion as a catalyst in the oxidation reaction of neptunium(IV). The conclusion about the decisive role of fluoride ion in the oxidation of neptunium is not confirmed by our investigations. Even in the absence of fluoride ion, tracer quantities of neptunium are also separated completely from plutonium and lanthanum by coprecipitation of plutonium(IV) with the double sulfate of potassium and lanthanum; or precipitation of neptunium(VI) with sodium uranylacetate. The question of different oxidation rates for weighable and trace concentrations requires further investigation.

We have studied the oxidation of weighable quantities of neptunium and plutonium with potassium bromate, as a function of time and temperature. The investigation was carried out by spectrophotometric* and chemical methods. The oxidation rate of neptunium(IV) to neptunium(VI) is considerably increased with increase of temperature. The quantitative oxidation of 6 m*M* neptunium with 0.1 *M* $KBrO_3$ in 1 *M* H_2SO_4 requires: 7 hours at 20°; 5 hours at 22°; 2.5 hours at 25°; and 1 hour at 35°.

The oxidation of plutonium(IV) (concentration 5-6 m*M* per liter) to plutonium(VI) with 0.2 *M* $KBrO_3$ in 1 *M* H_2SO_4 at 20° is negligible; only about 1 per cent is oxidized in 48 hours. In nitric acid the rate of oxidation of neptunium and plutonium is increased.

The results of the oxidation of neptunium in the presence of large amounts of plutonium are shown in Table I.

Increasing the weight ratio of plutonium to neptunium considerably increases the oxidation rate of neptunium and at the ratio = 60:1 quantitative oxidation of neptunium is reached in one hour.

It can be assumed, that plutonium transfers oxygen and oxidizes neptunium(IV) due to the presence of traces of Pu(VI) according to reaction:

$$2Np(IV) + PuO_2^{++} + 2H_2O \rightleftarrows 2NpO_2^{+} + Pu(IV) + 4H^{+}$$

Neptunium(V) is instantly oxidized to neptunium(VI) by potassium bromate; therefore, the presence of potassium bromate shifts the equilibrium to the hexavalent state. This assumption is confirmed by the fact that in the presence of small amounts of plutonium(VI) the oxidation rate of neptunium(IV) is increased.

It is possible to use different variants of the bromate method. In addition to the fluoride method, the sulphate and acetate methods can also be successfully used to separate neptunium and plutonium. In both methods for the quantitative separation of neptunium the plutonium content in the neptunium fraction decreases 100-fold per cycle. In the use of all separation methods it is necessary to take into account the change in the oxidation rate of neptunium to the hexavalent state with the change in the relative concentrations of neptunium and plutonium in the original solution.

Table I. The Oxidation of Neptunium(IV) with 0.1 *M* $KBrO_3$ in 1 *M* H_2SO_4 at 20° in the Presence of Plutonium(IV). The Concentration of Neptunium is 2–6 m*M* per Liter

Weight ratio Np:Pu	The time of complete oxidation of Np in minutes
1: 0	420
1: 1.2	380
1: 13	240
1: 54	60
1:140	less 60

REFERENCES

1. Seaborg, G. T., "The Actinide Elements", NNES, Chapter 7, McGraw-Hill Book Company, New York, 1954.
2. Hughes, D. J., Pile Neutron Research, Addison-Wesley, Cambridge, 1953.
3. Seaborg, G. T. and Whal, A. C., Paper 1.6 of 2 "The Transuranium Elements", National Nuclear Energy Series, Division IV, Volume 14B, McGraw-Hill Book Company, New York, 1949.
4. Magnusson, L. B. and LaChapelle, T. G., Paper 1.7 of "The Transuranium Elements", National Nuclear Energy Series, Division IV, Volume 14B, McGraw-Hill Book Company, New York, 1949.
5. Magnusson, L. B., Hindman, J. C. and LaChapelle, T. J., Paper 15.11 of "The Transuranium Elements", National Nuclear Energy Series, Division IV, Volume 14B, McGraw-Hill Book Company, New York, 1949.

* Spectrophotometer SF-4.

Coprecipitation of Americium(V) with Double Carbonates of Uranium(VI) or Plutonium(VI) with Potassium

By G. N. Yakovlev and D. S. Gorbenko-Germanov, USSR

This report describes a new method of separation of americium and highly active rare-earth fission products in dilute solutions.

The published methods of separation of americium and rare-earth fission products may be divided into two general groups:

The first group is based on chromatographic separation of Am(III) and rare-earth elements with synthetic ion-exchange resins. The application of the chromatographic method is, however, impeded in the case of solutions of high specific activity, which cause considerable gaseous evolution due to the radiation decomposition of water.

The second group is based on the oxidation of americium to the hexapositive oxidation state in dilute acid solutions with the subsequent precipitation of rare-earth elements in the form of fluorides. Under laboratory conditions the separation of Am(VI) from the rare-earth elements gives satisfactory results. The difficulty of maintaining high oxidation potentials of the solutions prevents the application of the method on an extensive scale.

Oxidation potentials of americium couples in acid solutions are:[1]

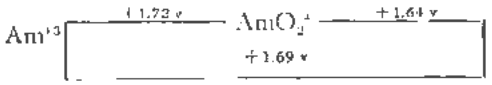

There are some indications which imply the possibility of oxidizing americium to the pentapositive state with sodium hypochlorite in concentrated potassium carbonate solutions, followed by the precipitation of the americium in the form of the slightly soluble double carbonate of Am(V) with potassium.[2] The separation of curium from considerable quantities of americium was carried out by this method. The authors, however, did not use this method for the separation of americium and rare-earth elements in their later work.

Oxidation potentials of americium couples in alkaline media are:[3]

$$Am(OH)_3 \xrightarrow{-0.4\ v} Am(OH)_4 \xrightarrow{(+0.7\ v)}$$

$$AmO_2OH^- \xrightarrow{(+1.1\ v)} AmO_2(OH)_2$$

The advantage of oxidizing americium in alkaline media lies in the removal of the oxidized americium in the form of a slightly soluble compound and in the decrease in the oxidation potentials of the solutions.

EXPERIMENTAL

The possibility of oxidizing americium to the pentapositive state in concentrated potassium carbonate solution in the form of a slightly soluble compound was used by the authors to develop a method for removing americium from dilute solutions and for separating americium and rare-earth elements by the formation of stable double carbonates.

The double carbonates of the rare-earths with potassium have sufficiently great solubility and this increases with increasing atomic number of the rare-earth element and with the concentration of potassium carbonate.

For the separation of small amounts of americium from weighable quantities of the rare-earths it was necessary to find a carrier for Am(V). Since the information about the carrier for Am(V) in alkaline media was limited,* calcium, barium and basic iron carbonate were examined. Positive results were not obtained with these compounds. In later work uranium was used for the following reasons:

1. The uranyl ions form slightly soluble precipitates of potassium uranylcarbonates in concentrated solutions of K_2CO_3.

2. The structure of the linear $(O–U–O)^{+2}$ ion is similar to that of the $(O–Am–O)^{+}$.

According to the published data the Am—O distance in the AmO^{+2} ion is 1.93Å; the U—O distance in the UO_2^{+2} ion is 1.93 ± 0.03Å.[4] This similarity allows us to assume that these ions will coprecipitate on the formation of slightly soluble compounds.

In fact, positive results were obtained for potassium uranylcarbonate and it was selected as a carrier for Am(V).

Further work required a preliminary study of the composition of potassium uranylcarbonate and the determination of the solubilities of potassium uranylcarbonate and double carbonates of rare-earths in solutions of K_2CO_3. The conditions for oxidation of

Original language: Russian.

*There are data concerning the possibility of use of hydrated Ta_2O_5 as a carrier for Am(V) in alkaline media. (L. Werner, Chem. Abstr., 45, 9390h, (1951)).

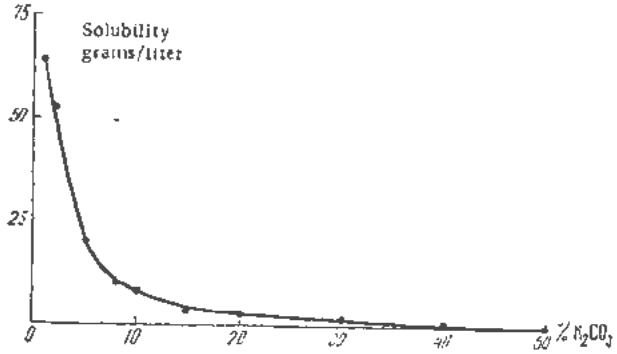

Figure 1. The solubility of potassium uranyltricarbonate in solutions of K_2CO_3 at 22°–23°C

americium and plutonium were studied. The compositions of double carbonates of Am(V) and Pu(VI) with potassium were also investigated.

THE INVESTIGATION OF COMPOSITION AND SOLUBILITY OF POTASSIUM URANYLCARBONATE

The following potassium uranylcarbonates are known:[4]

$$K_2[UO_2(CO_3)_2];\ K_4[UO_2(CO_3)_3];\ K_6[(UO_2)_2(CO_3)_5]$$

The above compounds have similar hexagonal structures.[4] When a concentrated potassium carbonate solution reacts with a solution of uranylnitrate, the uranium is precipitated in the form of potassium uranyltricarbonate $K_4[UO_2(CO_3)_3]$.

The solubility of $K_4[UO_2(CO_3)_3]$ was determined in solutions of K_2CO_3 of various concentrations at 22°–23°C. The results obtained are shown in Fig. 1.† The solubility of $K_4[UO_2(CO_3)_3]$ in a 50% solution of K_2CO_3 is 0.200 grams per liter.

THE DETERMINATION OF SOLUBILITIES OF DOUBLE CARBONATES OF LANTHANUM AND CERIUM WITH POTASSIUM IN CONCENTRATED SOLUTIONS OF K_2CO_3

The solubility of double carbonates of lanthanum and cerium with potassium was determined in 50% solution of K_2CO_3 at 22°–23°C. These compounds have the lowest solubilities for all the rare-earth elements. The solubility of the double carbonate of lanthanum and potassium corresponded to a concentration of lanthanum in solution of about 9 grams per liter and that of the double carbonate of cerium and potassium—to a concentration of cerium of about 13 grams per liter.

INVESTIGATION OF THE CONDITIONS FOR OXIDIZING AMERICIUM IN CONCENTRATED SOLUTIONS OF K_2CO_3

Besides hypochlorite, ammonium peroxydisulfate and ozone were used for the oxidation of americium. In all experiments the concentration of americium was 0.3 mg per ml.

The conditions for the oxidation of americium in concentrated carbonate solutions by the above-named oxidizing agents are:

1. Am(III) is oxidized to Am(V) by 0.1 *M* KClO in 10–15 min at 95°–100°C.
2. Am(III) is oxidized to Am(V) by ammonium peroxydisulfate in 2 hr at 75°–80°C with the concentration of $(NH_4)_2S_2O_8$—20 mg per ml.
3. Am(III) is oxidized to Am(V) by ozone in 15–20 min at 90°–100°C.

After oxidation, the precipitate which contained about 99 per cent of the americium was dissolved in 0.2 *M* HNO_3. The resulting solution was analyzed by a spectrophotometric method with a model SF-4 quartz spectrophotometer (made in USSR). The absorption bands of Am(III) (503 mμ and 811 mμ) and Am(VI) (668 mμ and 992 mμ) were not observed. The presence of absorption bands at 514 mμ and 717 mμ (Am(V)) indicates the complete oxidation of americium to the pentapositive state.

The solubility of double carbonate of Am(V) with potassium in saturated solution of K_2CO_3 is 5 mg per liter.

The precipitate of the double carbonate of Am(V) with potassium was analyzed for potassium, americium and CO_2.

Potassium was determined colorimetrically in the form of potassium dipicrylamine; americium was estimated by the usual α-counting method; CO_2 was determined by a volumetric method.

For analysis eight samples of the double carbonate of Am(V) with potassium were used (from 1.37 mg to 3.18 mg). This compound was dried to constant weight at 40°–50°C.

The composition of this compound corresponded to $K_5[AmO_2(CO_3)_3]$ and the analytical data are given in Table 1.

It was found by X-ray diffraction analysis that this compound was not isomorphous with $K_4[UO_2(CO_3)_3]$.

The absence of isomorphism of $K_5[AmO_2(CO_3)_3]$ with potassium uranyltricarbonate $K_4[UO_2(CO_3)_3]$ agrees with the published data of the presence of an orthorombic structure in the double carbonate of Am(V) with potassium (bisphenoid).[5]

INVESTIGATION OF THE CONDITIONS OF THE OXIDATION OF PLUTONIUM IN CONCENTRATED SOLUTIONS OF K_2CO_3 AND THE STUDY OF THE COMPOSITION OF THE DOUBLE CARBONATE OF Pu(VI) WITH POTASSIUM

Werner and Perlman[2] have pointed out that plutonium, like americium, would oxidize to the pentapositive state in concentrated solutions of K_2CO_3.

The oxidation of plutonium was studied by the authors in concentrated solutions of K_2CO_3 with the concentration of plutonium being 4.1 mg per ml.

After oxidation for 15–20 min at 95°–100°C a rich green compound was precipitated, which was

† The solubility of potassium uranyltricarbonate in water is 47 grams and 71 grams per liter at 0°C and 18°C respectively.[4]

Table I. Analysis of Double Carbonate of Am(V) with Potassium

Compounds	Potassium %		Americium %		CO_2 %	
	Calc.	Found	Calc.	Found	Calc.	Found
$K_5[AmO_2(CO_3)_3]$	30.1	30.5±1.5	37.2	35.8±1.5	20.4	21.2±0.8

Table II. Analysis of Potassium Plutonylcarbonate

Compound	Potassium %		Plutonium %		CO_2 %	
	Calc.	Found	Calc.	Found	Calc.	Found
$K_4[PuO_2(CO_3)_3]$	25.7	27.0±1.5	39.4	38.8±1.5	21.7	21.0±0.8

then dissolved in 0.2 *M* HNO_3 and analyzed by the spectrophotometric method. The optical density was measured between 400 mμ–1150 mμ and the characteristic absorption spectrum of Pu(VI) was observed with absorption bands at 833 mμ, 950 mμ and 982.5 mμ. Absorption bands of Pu(IV) and Pu(V) were not observed.

Therefore, plutonium had been oxidized to the hexapositive state under the same conditions as americium had been oxidized to the pentapositive state with the formation of a double carbonate of Pu(VI) and potassium.

The green precipitate of the double carbonate of Pu(VI) and potassium was analyzed for potassium, plutonium and CO_2 by the same methods as in the case of double carbonate of Am(V) and potassium.

Ten samples of the double carbonate of Pu(VI) and potassium (from 1.45 mg to 5.09 mg) were taken for analysis. This compound was dried to constant weight at 40° 50°C.

The composition of this compound corresponded to $K_4[PuO_2(CO_3)_3]$. Analytical data are given in Table II.

It was found by X-ray diffraction analysis that this compound was isomorphous with $K_4[UO_2(CO_3)_3]$.

COPRECIPITATION OF POTASSIUM Am(V) TRICARBONATE WITH POTASSIUM URANYL AND PLUTONYL TRICARBONATES

The oxidation of small quantities of americium by hypochlorite, ammonium peroxydisulfate and ozone and a further coprecipitation with potassium uranyltricarbonate were carried out under the conditions described above.

After oxidation of the americium, the solution of uranylnitrate (10 grams of uranium per liter) was added dropwise for 2 hr into the analyzed solution of americium and the rare-earth fission products in 50% K_2CO_3 solution. The mixture was agitated by bubbling with air. The precipitate of potassium uranyltricarbonate was separated after 12 hr. The precipitate and the filtrate were analyzed separately for the presence of americium and the rare-earth fission products. The precipitate of uranyltricarbonate contained 96–99% of the americium and 1–3% of the rare-earth elements.

Under the same conditions 99% of potassium plutonyltricarbonate is coprecipitated with potassium uranyltricarbonate.

Coprecipitation of Am(V) with potassium uranyltricarbonate has been successfully used by the authors for the separation of americium and the rare-earth fission products. For this purpose repeated reprecipitation of the tricarbonates is carried out in oxidizing media. With repeated reprecipitation, the percentage of the rare-earth fission products brought down is changed slightly. This provides a possible means of decontaminating americium from the fission products.

Similar results were obtained in the case of the coprecipitation of potassium Am(V) tricarbonate, and potassium plutonyltricarbonate.

The observed process for the coprecipitation of Am(V) with hexavalent compounds of uranium and plutonium is apparently connected with the formation of anomalous mixed crystals.

REFERENCES

1. Latimer, W., The oxidation states of the elements and their potentials in aqueous solutions. 2nd ed. Prentice-Hall, Inc., New York. (1952).
2. Werner, L. B. and Perlman, I., The transuranium elements. Pt. II, Paper No. 22.5, National Nuclear Energy Series, McGraw-Hill Book Co., Inc., New York. (1949); J. Am. Chem. Soc. *73*, 1, 495, (1951).
3. Ellinger, F. and Zachariasen, W., J. Phys. Chem., *58*, 5, 405, (1954).
4. Bachelet, Douis, Cheylan et Goulette. Bull. Soc. Chim. France, No. 2, 173, (1954).
5. Nigon, J. P., Penneman, R. A., Staritzky, E., Keenen, T. K. and Asprey, L. B., J. Phys. Chem., *58*, 5, 403, (1954).

A Tracer Study of the Partition of Neptunium between Nitric Acid Solutions and Three Organic Solvents

By J. Kooi,* The Netherlands

Up to now not much has been published about the extraction of any of the transuranium elements from aqueous solutions by organic solvents. In open literature there may be found descriptions of some actual procedures[1] and a few qualitative statements about the possible influence of the different oxidation states of neptunium and plutonium on their extraction.[2] However, no quantitative data seem to have been published.

On the other hand, the extraction of uranyl nitrate has been studied extensively for a large number of solvents, experimentally as well as theoretically.[3,4] Also for the case of thorium nitrate some data may be found in literature.[5] Therefore, apart from its obvious practical importance it seems to be of considerable interest to obtain quantitative data on the extraction, particularly of the two first transuranium elements.

In this paper some work on the extraction of neptunium in its different oxidation states from nitric acid by three of the most commonly used solvents (dibutyl carbitol, diethyl ether and methyl isobutyl ketone) will be described. It is believed that these data may also serve as an analogue for the behaviour of plutonium. To support and to complete the data obtained, measurements on uranyl and thorium nitrate have been included.

The method chosen is the following: A solution of the element in nitric acid in concentrations up to 10 *N* is equilibrated with an equal volume of the organic solvent. By determining the quantity of the element in equal volumes of both layers after phase separation, the partition coefficient α (= concentration in organic phase/concentration in water phase) is obtained. In this way the salting out effect of nitric acid on the extraction in trace or low concentrations may be found.

MATERIALS

Neptunium: In the experiments Np^{239} was used, half-life 2.33 days. This isotope can be easily obtained by irradiation of uranyl nitrate with reactor neutrons and separation from the uranium and the fission products, after allowing for decay of the primarily formed U^{239} ($t_{\frac{1}{2}}$ = 23.5 min). The extraction method, described by Fields[1] was used. It appeared that best results were obtained by using diethyl ether as an extracting agent. Essentially carrier free solutions of mainly Np(V) in approximately 2 *N* HNO_3 were obtained (2–5 mg solid residue from the used oxidants per 25 ml, containing in the order of 1 mc). The purity of the neptunium was excellent. The decay was purely exponential with the right half-life for more than 12 half-lives. The measured absorption is in agreement with literature values and with the average β-energy.

More detailed information on this, as well as on much of the following will be published elsewhere.[6]

Uranyl and thorium nitrate: High purity analytical grade $UO_2(NO_3)_2 \cdot 6H_2O$ and $Th(NO_3)_4 \cdot 4H_2O$ were used, the water content of which had been checked.

Nitric acid p.a.: This was distilled, diluted to approximately 10 *N* with distilled water, and immediately before use, boiled and diluted to the desired strength.

Diethyl ether: After removing peroxides possibly present and drying, the diethyl ether was distilled from $FeSO_4$ immediately before use. In the course of the investigation of Np(VI) this appeared to be necessary. Even after only a few hours standing of the ether, erroneous results were obtained.

Dibutyl carbitol (D.B.C.), $C_4H_9O-(C_2H_4O)_2-C_4H_9$: The pure commercial product was freed from peroxides and distilled in vacuo (1–3 mm Hg) before use. $n_D^{25} = 1.4221$.

Methyl isobutyl ketone (M.I.K.): The pure commercial product was distilled under normal pressure before use. $n_D^{25} = 1.3940$.

PROCEDURE: EQUILIBRATION

In the experiments 1 ml of Np solution was added to 14 ml of nitric acid of the desired strength, in 30 ml centrifuge tubes provided with a long ground stopper. After mixing, 15 ml organic solvent was added and by rotating top-bottom wise the contents were shaken in a waterbath at 25.0 ± 0.1°C.

Special runs were made to establish the proper shaking time. As longer shaking times resulted in irreproducible and erroneous results in the tracer experiments (contrary to those with the larger concentrations used in the cases of uranium, thorium and nitric acid alone)[3] these were chosen in the range from ½–3 minutes. In none of our experiments was

*Joint Establishment for Nuclear Energy Research, Kjeller, Norway.

α found to vary when the time of shaking was kept within these limits.

After shaking, 10 ml of both layers were taken out by pipetting. Those of the water layer were in all instances diluted to 50 ml, any dissolved diethyl ether being removed by evaporation. The diethyl ether was, after addition of some water, evaporated and the resulting water solution diluted to 50 ml. In the case of the other two solvents, the procedure differed for the different elements and will be described later.

ANALYSIS

Neptunium

In the case of D.B.C. and M.I.K. aliquots from the organic layer were shaken repeatedly with distilled water in a 100 ml flask. After back-extraction the volume was made up to 100 ml. No activity could be detected in the remaining organic layer.

From the ultimate water layers aliquots were taken, made approximately 2 N in HNO_3 and the neptunium reduced by means of SO_2. After addition of 50 mg $La(NO_3)_3 \cdot 6H_2O$ a precipitate was made of LaF_3 by addition of HF in a celluloid tube, centrifuged, washed and poured over in a glass tube. After a final centrifuging, the wet precipitate was finely divided in the adhering water and slurried in acetone. Part of this slurry was transferred onto a weighed Al-disk and evaporated to dryness, giving very fine and evenly distributed samples. After weighing, these were mounted on cardboard, covered with a thin polythene foil and counted, using essentially the set-up described by Pappas.[22] No corrections for self-absorption were shown to be necessary.

Uranium

Measurements with different concentrations of uranyl nitrate were carried out by using 50, 150, 450 and 1350 mg of $UO_2(NO_3) \cdot 6H_2O$ per 15 ml water layer respectively in the case of diethyl ether. 300 mg of $UO_2(NO_3)_2 \cdot 6H_2O$[2] per 15 ml water layer was taken in the experiment with D.B.C. and M.I.K.

In the 50 and 150 mg cases, uranium contents were determined by countiog the α-activity of small aliquots of both layers in a scintillation counter. In all other cases, samples from the ultimate water layers were evaporated carefully to dryness, ignited and weighed as U_3O_8.

The aliquots, taken from the D.B.C. and M.I.K. phases, were diluted to 25 ml with the solvents. From these a part was taken and the uranium backextracted into water, containing strong NH_4OH. After centrifuging the precipitate was dried, ignited and finally weighed as U_3O_8. In this way small losses occurred, but in general these values of α were used only for comparison with those found by calculating from the water phase content only.

Thorium

Thorinm was determined analogously to uranium. Instead of ammonia, however, oxalic acid had to be used, as it was almost impossible to separate the hydroxide precipitate from the interface between water and the organic phase by centrifugation.

CALCULATIONS

As only relative measurements were necessary, no corrections had to be applied to the countings, as care was taken always to prevent coincidence losses. Thus α was obtained directly from the activities per mg sample from both phases, allowing for possible differences that might occur in dilution of the original aliquots.

By using the known relation between the volumes of the water and organic phases after shaking,[7] a simple check on the measurements may be obtained by calculating the total amount of Np, U or Th recovered. For one series of measurements, using the same stock-solution of the element, this must be a constant. For Np the value of this may be found by treating an aliquot of this stock-solution in exactly the same way as the samples. The mean deviation from this constant was shown to be not more than a few per cent. When larger deviations were found, duplicate samples were taken. From the equilibrium measurements 97–99% of the Np was recovered. When excess uranyl nitrate was present, this figure was a few per cent lower, owing to the necessity of a Np-U separation.

MEASUREMENTS AND RESULTS

In the following, the methods for preparing the different oxidation states of neptunium, together with the proofs of their existence in the original solutions, will be described briefly. In addition, the main results will be presented as a number of curves. More details will be published elsewhere.[6]

Neptunium(VI)

The simplest way of preparing Np(VI) solutions appeared to be the oxidation of the stock-solution by means of potassium bromate, using NaF as a catalyst.[8] Satisfactory results were also obtained by using cerium-ammonium nitrate as an oxidant.[8] In both cases Np(VI) is produced instantaneously. The second method, however, could be used only in the diethyl ether experiments. With the other two solvents, no reproducible results could be obtained, probably due to fast reduction of the Ce(IV). This has also been reported by Wylie,[9] in his work on cerium extraction.

To prove the Np to be present in the (VI) state, it was coprecipitated with sodium uranyl acetate. The percentage carried was $90 \pm 5\%$. The solnbility of the sodium uranyl acetate under our conditions amounts tn 3–8%, depending on the nitric acid concentration.

With diethyl ether lower values for α were also found, if the cerium-oxidised solution had been standing for a longer period. α seems to approach the value for the (V) state, after the cerium solution has become colourless.

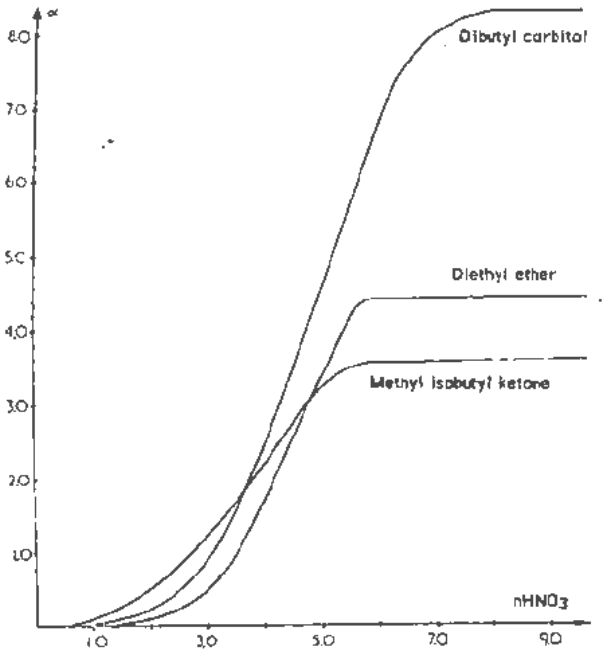

Figure 1. The partition of neptunium(VI) between nitric acid and diethyl ether, dibutyl carbitol and methyl isobutyl ketone

A limited number of experiments have been carried out with diethyl ether in the presence of a large excess of uranyl nitrate (50, 150, 450 or 1350 mg $UO_2(NO_3)_2 \cdot 6H_2O$ per 15 ml original water layer respectively). The α-values found, however, fall on the curve through the measured points, within the limits of experimental error.

Figure 1 presents the curves for the Np(VI) partition for the three solvents, plotted against the acidity of the original water layer.

Neptunium(V)

The first examples of values of α, definitely different from those found for Np(VI), were obtained by starting from Np stock solution, reduced by means of gaseous SO_2. Indeed a well defined curve was found in repeated experiments. Now, SO_2 may be expected to produce Np(V) under the conditions used.[10] The formation of Np(IV) in the presence of alkali and fluoride ions is suggested by Magnusson.[11] Addition of some NaF did not change our results.

As it is known that reduction by sodium nitrite is capable of producing Np(V) only, from Np(VI),[12] part of the Np stock-solution was heated for a longer time at nearly boiling temperature in ca 2 *N* HNO_3, oxidising all Np(IV) present to Np(V) and, partly, to Np(VI).[12] After dilution to about 1 *N* in nitric acid, $NaNO_2$ was added and the resulting solution used for α measurements. The same curve was found as that for SO_2-reduced Np.

A few additional points were obtained by using H_2O_2 as reducing agent.[13]

Furthermore, the presence of Np(V) and the absence of Np(VI) and Np(IV) in the starting solutions was shown by means of coprecipitation experiments, which were carried out as follows. From a solution of Np in dilute nitric acid, to which an amount of uranyl nitrate was added sufficient to produce a precipitate, together with Zr and La carriers, sodium uranyl acetate was precipitated, carrying with it the Np(VI). From the filtrate Zr-phenylarsonate was precipitated according to ref. 14 carrying Np(IV) (and UX_2). In the remaining solution a LaF_3 precipitate was formed, carrying all Np(V) and any residual Np left in solution by the two first (not totally quantitative) precipitations. In addition, it may be expected that part of the Np(VI) escaping the first precipitation is taken down by the Zr-phenylarsonate. So, these experiments cannot be expected to give clear cut separations;[15] it is believed, however, that the results nevertheless are giving decisive information regarding the presence of the different oxidation states of neptunium. All precipitates were converted to LaF_3, using the same amount of La carrier, and counted in the usual way. Sometimes the presence of the reducing agents interfered with the precipitation reactions, especially with the first one. In these cases this precipitation was left out. The results of these experiments were reproducible and in agreement with the assignment of the oxidation states as mentioned above.

The curves for Np(V) are given in Fig. 2.

Neptunium(IV)

The first indications for the possibility of obtaining a third and different curve were found by measuring α of a Np solution, oxidised to the (VI) state and subsequently treated with an excess of $NH_2OH \cdot HCl$. This reducing agent may produce Np(V) under the conditions used.[13] The same results were obtained by reducing with the same agent a stock-solution which had been treated with nitric acid, as mentioned earlier. Coprecipitation experiments, however, showed this neptunium to be carried by Zr-phenylarsonate.

So, a number of measurements were performed with Np solutions, treated so as to give Np(IV) according to several well established methods. First, the reduction was carried out by means of KI and N_2H_4, secondly by means of oxalic acid, both according to

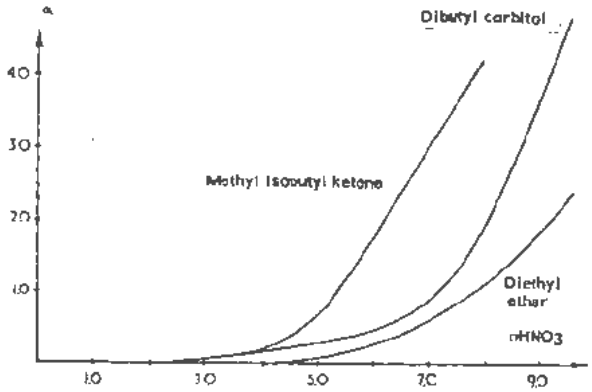

Figure 2. The partition of neptunium(V) between nitric acid and diethyl ether, dibutyl carbitol and methyl isohytid ketone

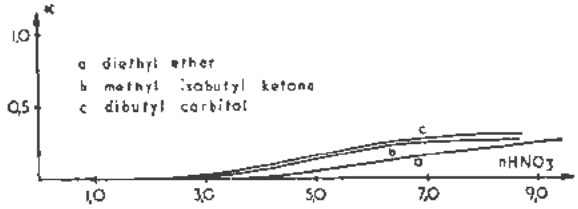

Figure 3. The partition of neptunium(IV) between nitric acid and diethyl ether, dibutyl carbitol and methyl isobutyl ketone

the procedures as described.[17] In the latter instance, the two first precipitates were not formed in the usual coprecipitation experiments. After reduction by KI, these experiments were not finally conclusive, but gave in any case relatively high Np(IV) contents.

The curves obtained are given in Fig. 3.

Uranium(VI)

In order to obtain data on some ions analogous to those used in the neptunium experiments, measurements were performed on the partition of uranyl nitrate and thorium nitrate in the same solvents.

Some data on uranyl nitrate and diethyl ether are given by Sillén and Norström,[18] Bock and Bock[19] and Katzin and Hellman.[20] Of those the results of the last two papers can be compared directly with ours. As the data of Bock and Bock, measured with a uranyl nitrate concentration of 0.1 mol and those of Katzin and Hellman, who used trace amounts, give somewhat different curves suggesting an influence of the uranyl nitrate concentration itself, a large number of measurements were carried out at the four concentrations mentioned above. Only the points obtained with 1350 mg $UO_2(NO_3)_2 \cdot 6H_2O$ per ml showed a definite deviation from those obtained with the three other concentrations.

Our results are presented in Fig. 4, including also the data from literature.

Thorium

The results of our measurements with thorium nitrate are shown in Fig. 5.

ADDITIONAL REMARKS

As may be seen from the figures, all the curves are of essentially the same general shape. Those for Np(VI) and U(VI) especially resemble those for nitric acid.[7] Some attempts have already been made towards a theoretical interpretation regarding the shape of the curves. Sutton[21] examined that for nitric acid and diethyl ether and presented a picture which also holds for the other two solvents.[6] Katzin and Hellman gave a discussion of the curve for uranyl nitrate and diethyl ether.[20] The work of McKay must also be mentioned.[3]

It is believed that at least a qualitative relationship between the partition coefficients and other properties of the different elements can be obtained. From a closer theoretical investigation one may also expect a better understanding of the fundamental processes occurring in these organic solvent extractions in the presence of nitric acid. Results of such investigations will be published elsewhere.[6]

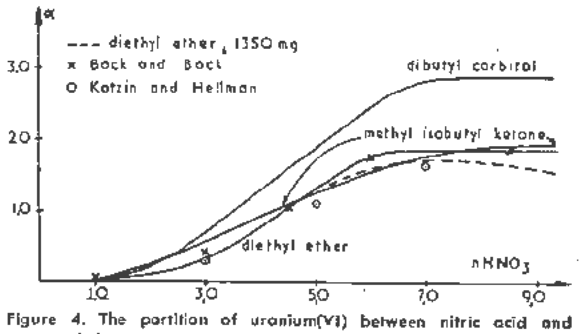

Figure 4. The partition of uranium(VI) between nitric acid and diethyl ether, dibutyl carbitol and methyl isobutyl ketone

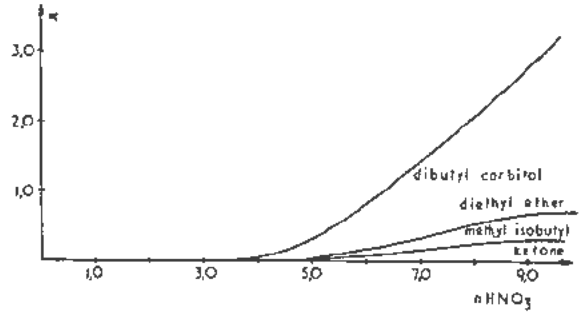

Figure 5. The partition of thorium between nitric acid and diethyl ether, dibutyl carbitol and methyl isobutyl ketone

ACKNOWLEDGEMENTS

My sincere thanks are due to Prof. Dr. A. H. W. Aten, Jr. for suggesting this investigation and for his continuous interest and criticism. The support given by Dr. T. J. Barendregt is gratefully acknowledged.

I am very indebted to Miss J. Koren for her assistance in the experiments and to Mr. J. E. Lundby for the many preparations he made.

REFERENCES

1. Fields, P., *The preparation and decontamination of $_{93}Np^{239}$ in trace concentrations*, paper 15.10 of: The Transuranium Elements, by G. T. Seaborg, J. J. Katz and W. M. Manning, McGraw-Hill Co., Inc., New York (1949).* Peppard, D. F., e.s., *Isolation in microgram Quantities of Naturally Occurring Plutonium and Examination of Its Isotopic Composition*, J. Am. Chem. Soc., 73: 2529, (1951).
2. Hyde, E. K., *Radiochemical Separations of the Actinide Elements*, Chapter 15 of: The Actinide Elements by G. T. Seaborg and J. J. Katz, McGraw-Hill Co., Inc., New York (1954).†
3. McKay, H. A. C., e.s., Several papers in Trans. Faraday Soc., see: Trans. Faraday Soc., 50: 107, (1954).
4. Katzin, L. I. and Sullivan, J. C., *The System Uranyl Nitrate — Water — Organic Solvent*, J. Phys. Chem., 55: 346, (1951).
5. Misciatelli, P., *The Separation of Thorium and Uranium by Means of Ether*, Phil. Mag. [7], 7: 670, (1929).

*Later on referred to as "The Transuranium Elements."
†Later on referred to as "The Actinide Elements."

6. Kooi, J., *Thesis*. University of Amsterdam, to be published.
7. Kooi, J., *The Partition of HNO_3 between Water and Three Organic Solvents*. Rec. Trav. Chim., 74: 137, (1955).
8. Cunningham, B. B. and Hindman, J. C., *The Actinide Elements*. Chapter 12: page 466.
9. Wylie, A. W., *Extraction of Ceric Nitrate by Solvents*. J. Chem. Soc., 1474, (1951).
10. Voigt, A. F., c.s., *The Transuranium Elements*, paper 15.9.
Magnusson, L. B., c.s., *The Transuranium Elements*, paper 15.11.
11. Magnusson, L. B., c.s., *The Transuranium Elements*, paper 15.11, page 1148.
12. Magnusson, L. B., c.s., *The Transuranium Elements*, paper 15.11, page 1147.
La Chapelle, T. J., *The Transuranium Elements*, paper 15.6.
13. Cunningham, B. B. and Hindman, J. C., *The Actinide Elements*. Chapter 12: page 464.
14. Voigt, A. F., c.s., *The Transuranium Elements*, paper 15.9, page 1121.
15. Hyde, E. K., *The Actinide Elements*, Chapter 15, page 575.
16. Hindman, J. C., c.s., *The Transuranium Elements*, paper 15.2.
17. Cunningham, B. B. and Hindman, J. C., *The Actinide Elements*, Chapter 12, page 462.
18. Norström, A., and Sillén, L. G., *On the Partition of Uranyl Nitrate between Diethyl Ether and Aqueous Nitric Acid*. Svensk Kem. Tidskr. 60: 227, (1948).
19. Bock, R. and Bock, E., Z. Anorg. Chem. 263: 146, (1950).
20. Katzin, L. I. and Hellman, N. N., *Theoretical Consideration of the Ether Extraction of Uranyl Nitrate from Aqueous Solutions Containing Various Metal Nitrate Salting Agents*. AECD — 2728: (1949).
21. Sutton, J., *Distribution of Nitric Acid between Water and Ether*, AERE C/R 438.
22. Pappas, A. C., *A Radiochemical Study of Fission Yields in the Region of Shell Perturbations and the Effect of Closed Shells in Fissions*, Techn. Rep. No. 63; Sept. 15, 1953, Laboratory for Nuclear Science, Massachusetts Institute of Technology.

Tri-*n*-butyl Phosphate as an Extracting Agent for the Nitrates of the Actinide Elements

By H. A. C. McKay,* UK

Tri-*n*-butyl phosphate (TBP) is becoming fairly well-known as an extracting agent for inorganic salts, especially nitrates. It is an essentially non-ionising solvent, having a dielectric constant of only about 8, so the nitrates most readily extracted are generally those which associate most readily into neutral molecules. These include the nitrates of the tri-, tetra- and hexavalent actinides, the first-named being moderately well extracted and the other two very well.

TBP extractions have considerable practical importance in purifying and analysing the actinides, because TBP is a solvent with very convenient properties. It is a commercial product, used as a plasticiser and readily obtainable in large quantities. Interfering impurities, particularly mono- and dibutyl phosphoric acids, can be removed by alkali treatment. It is liquid over a wide range, from $< -78°C$ to 289°C, and is involatile at room temperature. It is very little miscible with water. It is chemically stable, even to concentrated nitric acid, only being hydrolysed under quite vigorous conditions. Indeed its main drawbacks are its rather high viscosity (3.41 centipoises at 25°C) and the fact that its density (0.973) is similar to that of water, both of which disadvantages can be overcome by diluting with a suitable inert material; the extracting power is so high that we can usually afford to do this.

Our studies of the extraction of the actinide nitrates by TBP have had two aims in view: first, the collection of data of direct practical value for preparative and analytical purposes, and second, to understand the mechanism of the process. We have generally worked with trace quantities only of the actinides, in presence of larger amounts of nitric acid, sodium nitrate, etc.: this has been partly a matter of necessity and partly a matter of choice. Especially with uranyl nitrate, however, we have made a number of experiments with macro-quantities.

THE NATURE OF THE EXTRACTED SPECIES

Our evidence indicates that each nitrate occurs in one form only in the TBP; as the neutral, un-ionised molecule, unhydrated, but solvated by a definite number of TBP molecules. The formulae of the complexes in question are:

$$M(NO_3)_3 \cdot 3TBP$$
$$M(NO_3)_4 \cdot 2TBP$$
$$MO_2(NO_3)_2 \cdot 2TBP$$

in each of which the central metal atom is attached to six groups.

The first point, the lack of ionisation, follows from conductivity and viscosity measurements, which usually indicate less than 1% ionisation.

Solubility measurements provide evidence about hydration and solvation. A saturated solution of thorium nitrate at 100°C corresponds very nearly to the composition $Th(NO_3)_4 \cdot 2TBP$. Similarly uranyl nitrate at room temperature gives $UO_2(NO_3)_2 \cdot 1.99\ TBP \cdot 0.04H_2O$, i.e., very nearly $UO_2(NO_3)_2 \cdot 2TBP$. This by itself might be fortuitous. However the 1:2 ratio of uranium to TBP is maintained over a wide range of conditions, e.g., on adding an inert diluent to the TBP; moreover the saturated solution behaves like a pure compound on freezing and re-melting, having a sharp melting point of $-6.0 \pm 0.5°C$.

The TBP solvation numbers for thorium and uranyl nitrates have been confirmed by solvent extraction measurements, and those for neptunium(IV), neptunyl, plutonium(IV), plutonyl and americium(III) have been measured exclusively by this means. The procedure is to dilute the TBP with an inert substance, keeping the aqueous phase constant in composition, and to measure the partition coefficient during this process: only traces of the actinide element are used. It can be shown from the law of mass action that under these conditions there is a limiting law at high dilution of the TBP such that

$$\text{Partition coefficient} \propto (\text{TBP concentration})^q$$

where q is the solvation number. The limiting law is usually obeyed sufficiently accurately when the proportion of TBP in the solvent is below 5%. Two examples are given in Fig. 1.

Further information about the solutions comes from a study of the absorption spectra. Under all conditions uranyl nitrate gives substantially the same spectrum in TBP as in other solvents in which it is believed to exist primarily in neutral molecule form. Even in presence of large amounts of nitric acid there is no tendency to change towards the spectrum characteristic of trinitratouranyl complexes. Similarly

* Atomic Energy Research Establishment, Harwell.

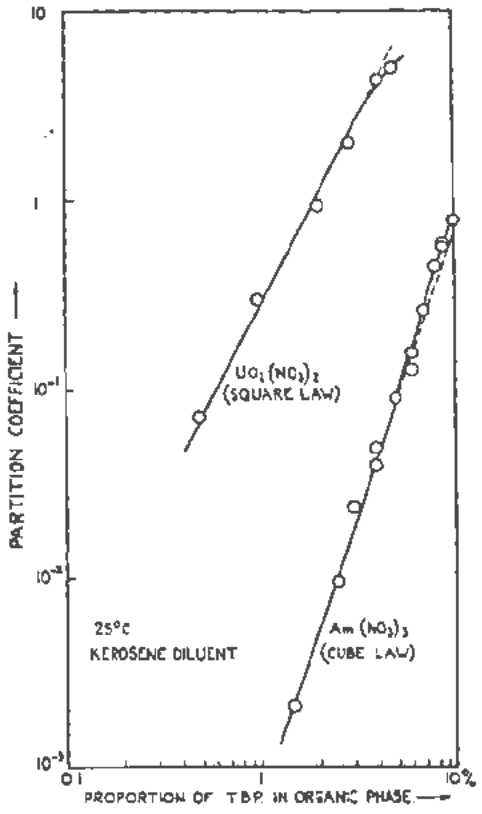

Figure 1. 25°C kerosene diluent

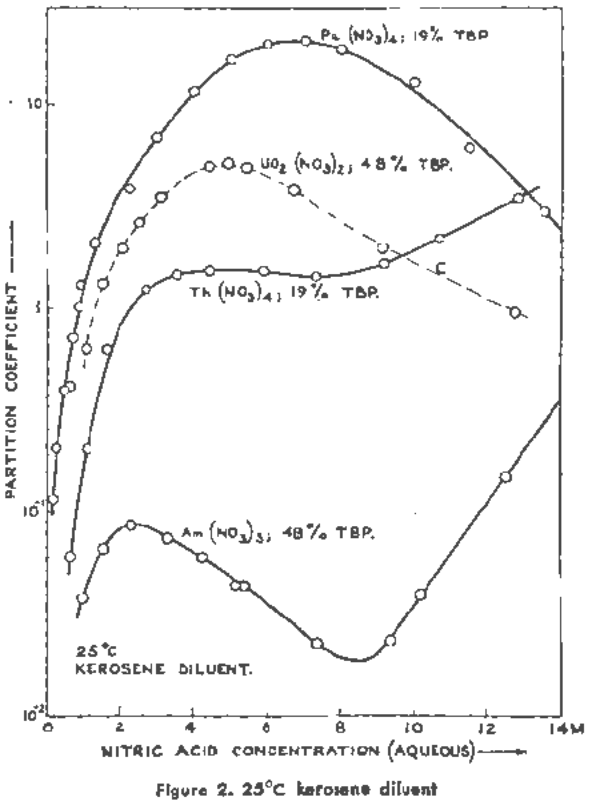

Figure 2. 25°C kerosene diluent

plutonium(IV) nitrate gives very nearly the same spectrum at all acidities, and this shows the features expected for neutral $Pu(NO_3)_4$ and definitely not those of hexanitratoplutonium(IV) complexes.

To conclude this section it is worth noting the contrast in extraction behaviour between TBP and ethereal or ketonic solvents, as illustrated in relation to uranyl nitrate. In ethers and ketones this compound is hydrated, giving a whole range of hydrates from the dihydrate upwards; moreover it very readily takes up a third nitrate group, and the solutions then acquire the characteristic trinitratouranyl absorption spectrum. In TBP, on the other hand, uranyl nitrate is unhydrated and apparently unable to take up a third nitrate group.

EXTRACTION FROM NITRIC ACID SOLUTIONS

When a trace of an actinide is extracted into TBP from nitric acid solutions of varying acidity, the partition coefficient (organic/aqueous) at first rises steeply with the acidity, then passes through a maximum and then falls again. In some cases there is also a further rise at high acidities, say $> 10M$. Some typical results are given in Fig. 2.

It is easy to give a qualitative explanation of such a curve. The concentration in the aqueous phase of the species actually extracted, the neutral nitrate, at first rises steeply: for a nitrate $M(NO_3)_p$ we should expect a p-power law initially. Later the rise becomes less steep, and ultimately gives place to a fall. However there is another effect also tending to check the rise, namely competition between the nitric acid and the actinide nitrate for the available TBP. At an aqueous acidity of $7M$ there is indeed very little free TBP left, most of it having been converted to $HNO_3 \cdot TBP$. In consequence of this, the actinide partition coefficient passes through its maximum much sooner than might have been expected from known nitrate complexity constants. A quantitative theory on these lines can be developed, but inevitably introduces activity coefficients, which are not known from independent experiments.

The rise sometimes observed at very high acidities is less amenable to theory, though it is not surprising in principle that high partitions should be obtained when the solvent contains large amounts of the highly polar substance, nitric acid.

THE EFFECT OF SALTING-OUT AGENTS

Much higher partition coefficients can be obtained if part of the nitric acid in the aqueous phase is replaced by sodium nitrate, or some other nitrate which is practically insoluble in the TBP phase. The main cause of the rise is the removal of nitric acid competition for the available TBP. At a total nitrate ion concentration of say $6M$, the effect is very striking, amounting to two or three orders of magnitude, in agreement with the corresponding large increase in the free TBP concentration. At say $2M$, on the other hand, we should expect only about a twofold

rise, which again agrees with experiment. Some results for thorium are given in Fig. 3.

The acidity must not, of course, be reduced too far, or hydrolysis will occur, and the partition coefficient will fall again, because the hydrolysis products are not extractable. The phenomenon has been noted with Th, Np(IV), Np(VI) and Pu(IV); it is most important in the last-named case. The measurements provide a possible method of studying the hydrolysis.

COMPARISON OF THE DIFFERENT VALENCY STATES

In the trivalent state, the actinides, like the lanthanides, are only moderately well extracted by TBP, though quite high partition coefficients can be obtained at low acidity with a salting-out agent. The separation factors for adjacent pairs, again like those of the lanthanides, are not very large, though they increase as the nitric acid concentration is increased and ultimately reach values of about 2 at an acidity of 16*M*.

In the tetravalent state the actinides are much more strongly extracted. The extraction increases in the order Th < Np(IV) < Pu(IV), and there are also a few data for U(IV) which seem to place it in its appropriate position in the series.

In the pentavalent state, extraction of the actinides is very weak.

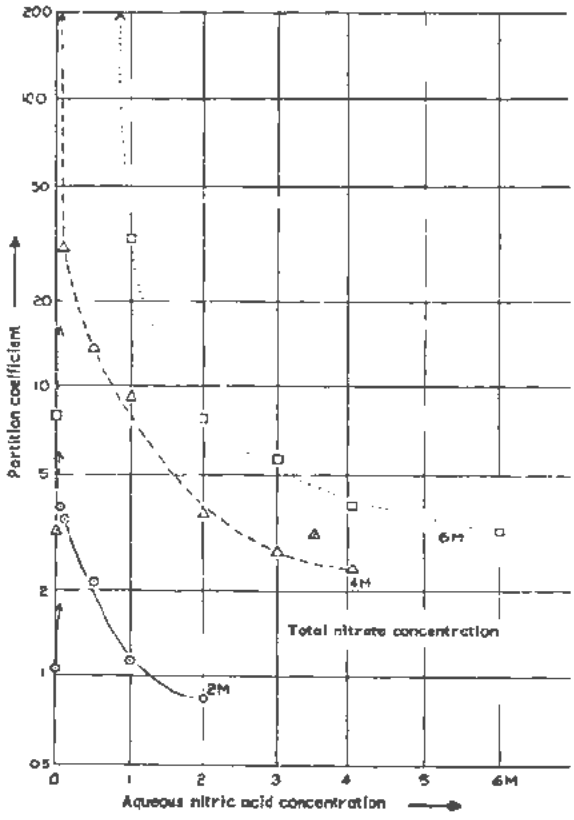

Figure 3. Salting-out of thorium by sodium nitrate into 19% TBP/kerosene

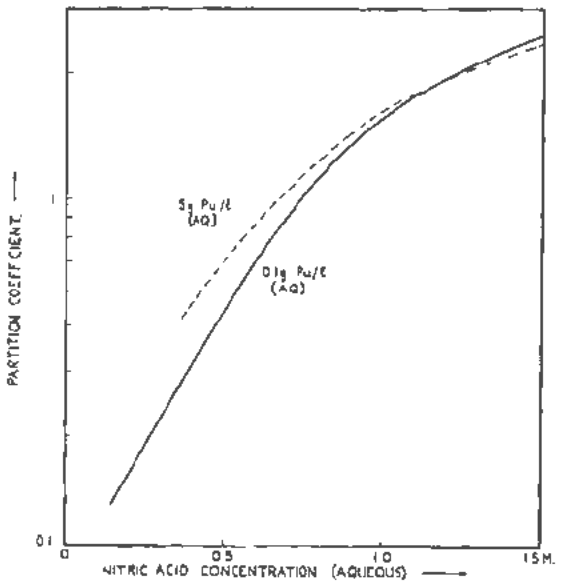

Figure 4

In the hexavalent state, extraction is again strong. The order is now Pu(VI) < Np(VI) < U(VI), i.e., the reverse of the order in the tetravalent state.

High extractability into TBP appears in general to be associated with cations of high polarising power, i.e., small size, as with Li^+ and Ca^{2+}, or high charge, as with the actinides. The high extractability of the hexavalent actinides is probably associated with a high positive charge on the central metal atom in the MO_2^{2+} ion, the oxygen atoms carrying a negative charge.

EXTRACTION OF MACRO-QUANTITIES

So far we have been chiefly concerned with the extraction of trace amounts of the actinides. When the quantity of actinide nitrate is increased, two effects occur. First, there is an increase in the aqueous nitrate ion concentration, and hence an increase in the salting-out due to the common ion effect. Second, there is greater usage of the available TBP by the actinide nitrate, i.e., a saturation effect, operating against the salting-out effect. Under some conditions the former is the more important, and the partition coefficient increases, as is illustrated by the data for plutonium(IV) in Fig. 4. Under other conditions the reverse is true, as can be seen from the high acidity end of Fig. 4.

The saturation effect, controlled ultimately by the formula of the TBP solvate concerned, sets a limit to the capacity of TBP for any given element.

There is also another complicating feature at high concentrations. The TBP solvates, especially of tetravalent nitrates, have only a limited solubility in the aliphatic hydrocarbons often used as diluents for TBP. Under appropriate conditions the organic phase splits into two, one consisting of the nearly pure solvate, and the other of a mixture of TBP and

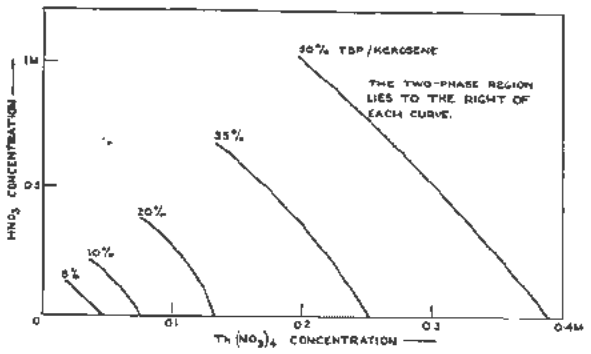

Figure 5. Limits of solubility of $Th(NO_3)_4$ in TBP/kerosene

diluent depleted in TBP. Some data for thorium are given in Fig. 5. The production of a third phase in this way must generally be avoided; its presence in an extraction column would, for instance, cause great difficulties. Methods of preventing its formation include limiting the actinide element concentration or the acidity, raising the temperature, and changing the diluent, e.g., to carbon tetrachloride.

SEPARATION OF THE ACTINIDES BY TBP

The differences in extractability between the different valency states make possible a number of separations of the lower actinides as nitrates with TBP. Uranyl nitrate, the most extractable hexavalent nitrate, can for example be extracted away from thorium nitrate, the least extractable tetravalent nitrate, in quite a short column, using say 5% TBP/diluent. A similar extraction of uranium from plutonium is possible if the plutonium is first reduced to the trivalent state, e.g., by ferrous ion; indeed the difference in extractability is so large that a single batch extraction with say 20% TBP/diluent may be adequate. Under such reducing conditions, neptunium becomes tetravalent, and therefore extracts with the uranium; americium and the higher actinides on the other hand, being trivalent, accompany the plutonium. Re-oxidation of the plutonium to the tetra- or hexavalent state would then render it extractable again, and hence separable from americium etc.

Separations based on the pentavalent state of neptunium (not extractable) or the hexavalent state of americium (extractable) might be worked out, but there would be difficulties in ensuring and maintaining the required state of oxidation.

When a group of elements are all in the same valency state, e.g., the trivalent higher actinides, then the separation factors available are smaller, though they may still be brought as high as 2 even in the worst cases. Separations then depend on using large numbers of stages. Under such conditions solvent extraction is not generally competitive with ion exchange either in speed or in simplicity of equipment; it may, however, be worth considering for handling relatively large amounts of material, and it may sometimes be advantageous on grounds of stability to radiation.

NOTE

A full account of this work will be published elsewhere, with references and all due acknowledgements to a rather large number of collaborators.

The Sulfate Method of Separating Plutonium and Neptunium

By B. V. Kurchatov, V. I. Grebenschikova, N. B. Chernyavskaya and G. N. Yakovlev, USSR

The sulfate method for separation of transuranium elements is based on the properties of Np(IV), Pu(III) and Pu(IV) to coprecipitate with the double sulfate of K and La.

This property for Pu was found by other investigators[1] but for Np our results are not in agreement with those of Hahn and Strassman.[2] In higher oxidation states, these elements do not coprecipitate with the double sulfate of K-La. This difference in chemical behavior of transuranium elements in different oxidation states may be used for an analytical determination of plutonium.

This method has been successfully used under plant conditions for analyzing certain industrial solutions. The method has proved to be applicable both to trace and weighable quantities of plutonium. This permitted its use not only for analysis but also for separating plutonium (as well as neptunium and americium) from dilute solutions.

The sulfate method consists of coprecipitation of neptunium and plutonium in reduced form with the double sulfate of La and K, separation from lanthanum by means of double sulfate precipitation after oxidation of the transuranium elements and subsequent reduction and coprecipitation of the transuranium elements with a smaller quantity of lanthanum.

By such a method, it is possible during one cycle to extract these elements from the initial solution as well as to reduce 10–15 fold the quantity of carrier and solution volume. At the same time a substantial decontamination of Pu and Np from fission products takes place.

The results of testing the sulfate method on tracer and weighable amounts of Pu with the L-Ka double sulfate are given in this paper.

For coprecipitation from the reduced solution, 5–7% HNO_3, containing 1% SO_2 and 0.2–0.3 mg La/ml was used.

After an hour's reduction at room temperature the solution was saturated with potassium sulfate, allowed to stand for 10–12 hours and then centrifuged. 95–99% of the Pa is coprecipitated for tracer and conventional amounts of Pu(IV).

For quantitative separation of Pu a new quantity of lanthanum is added to the solution and the double sulfate precipitation repeated.

Original language: Russian.

The effect of a more complete reduction of Pu was studied. Pu was reduced by means of SO_2 at 90–95°C for 30 minutes. Under these conditions Pu was reduced to the tri-positive state. 98% Pu was precipitated with the double sulfate i.e., there was no difference as compared with results of preceding experiments.

For the oxidation of Pu, potassium bichromate 10 gm/l at 95–98°C for an hour, or ammonium persulfate 10 gm/l, containing 1 gm/l of silver nitrate at 35–40° also for an hour were used.

After oxidation, lanthanum was precipitated by saturating the solution with potassium sulfate. Silver was precipitated as chloride. The double sulfate carried down about 2% of Pu, independent of the method of oxidation and of the amount of Pu. The quantity of precipitated La was equal to 3 gm per liter of solution.

For quantitative recovery of Pu, the precipitate of the double sulfate was dissolved in 0.5 *N* HNO_3 and reprecipitated from an oxidizing solution. To concentrate lanthanum with plutonium both were precipitated as hydroxides by means of NH_4OH solution.

As an analytical method, the sulfate method has certain advantages as compared with the known fluoride method: determination can be made in glass and therefore the sulfate method is more suitable for routine analysis and possibilities for erratic results, due to occasional reducing impurities from plastic test tubes, are excluded.

The influence of various factors on the completeness of precipitation was studied, and some preliminary investigations of the mechanism of coprecipitation of Pu with double sulfate crystals were made.

The coprecipitation of Pu with the La-K double sulfate was studied as a function of K_2SO_4 concentration, time of solid phase deposition and lanthanum quantity. The results are given in Table 1.

Table 1

La in mg/ml	*% of coprecipitated Pu for various times of precipitation*		
	10 min	*2 hours*	*12 hours*
0.2	83	–	98
0.4	88	93	99
0.6	88	99	–
1.2	98	–	100

The data are given for solutions saturated with potassium sulfate and are mean values from 3–4 determinations.

Results of the above determinations permit the choice of the best conditions for the separation of Pu by the sulfate method for various conditions of precipitation.

Decreasing the potassium sulfate concentration in solution has little influence on the completeness of Pu deposition, despite the fact that double sulfate solubility is much higher in less concentrated potassium sulfate solution. The quantity of Pu remaining in the solution 2 hours after the precipitation of the double sulfate (initial La concentration 0.6 mg/ml) was 0.9%, 3.7% and 4.5% for concentrations of potassium sulfate 1.5, 1.1 and 0.8 mol/l.

To investigate the mechanism of coprecipitation of Pu, the distribution coefficients of Pu between the solution and the precipitate were studied.

The composition of the K-La double sulfate and the solubility of that salt were studied first. It was found that in the range of potassium sulfate concentrations 0.2–1.5 mol/l the salt $K_3La(So_4)_3$ is precipitated independent of the order of reagent addition. In the final solution there was always an excess of potassium sulfate. X-ray analysis of the precipitates has shown that all precipitates have the same crystalline structure. The solubility of the double sulfate was determined in a thermostat at 20°C. Equilibrium was reached for 0.2 *M* K_2SO_4 solution after 8 hours, for 0.4 *M*, 0.8 *M* and 1.5 *M* solutions after 16 hours of saturation.

The solubility data are given in Table 2.

Table 2

K_2SO_4 mol/l	$K_3La(SO_4)_3$ (gm per 100 ml) in solution
0.2 *M* K_2SO_4 1.5 *M* HNO_3	2.241
0.4 *M* K_2SO_4 1.5 *M* HNO_3	0.172
0.8 *M* K_2SO_4 1.5 *M* HNO_3	0.0064
1.5 *M* K_2SO_4 1.5 *M* HNO_3	0.0003

The mechanism of coprecipitation of Pu with $K_3La(So_4)_3$ was studied by means of the three methods proposed by Chlopin.

1. Pu was coprecipitated with $K_3La(SO_4)_3$ from supersaturated solutions of the latter at 20°C with mechanical stirring (300 rpm).

The rate with which supersaturation of $K_3La(So_4)_3$ in 0.2 and 0.4 *M* K_2SO_4 could be eliminated with vigorous stirring was determined.

To eliminate supersaturation to the same degree after the same time period, the solution in 0.4 *M* K_2SO_4 must have a fivefold degree of supersaturation as compared with the solution in 0.2 *M* K_2SO_4. Crystallization of $K_3La(So_4)_3$ proceeds very slowly. In 0.4 *M* K_2SO_4 solutions containing 10 times more $K_3La(So_4)_3$ than corresponds to the solubility of this salt, a complete elimination of supersaturation required 15 hours. Slow crystallization of the double sulfate explains why it is so difficult to precipitate the last 2–3% Pu in analysis. The experiments on coprecipitation of Pu with double sulfate were conducted as follows: a quantity of double sulfate corresponding to a twofold supersaturation at 20°C for 0.2 *M* K_2SO_4 and to a tenfold supersaturation for 0.4 *M* K_2SO_4 was dissolved at 60°C in a measured volume of solution, containing a known quantity of Pu. A test tube with the solution was placed in a thermostat at 20°C and remained there until it reached the temperature of the thermostat. Then the double sulfate was precipitated by means of vigorous stirring. After the stirring came to an end the crystals settled and samples for analysis were taken from the clear supernatant solution. It was found in the first experiments, that in 0.2 *M* K_2SO_4 the first 10% of precipitated salt carried down 94% Pu, and 60% of salt carried down 100% Pu. In 0.4 *M* K_2SO_4 the first 15% of double sulfate carried down 69% Pu and when the supersaturation was diminished, 83%–100% Pu was carried down with crystals.

These results indicate that the distribution of Pu between crystals and solution is a nonequilibrium one, i.e., that we have here a distribution according to Doerner and Hoskins equation:

$$\ln\frac{x}{a} = \lambda \ln\frac{y}{b}$$

where a = total amount of microcomponent, x = amount of microcomponent in solution after crystallization, b = total amount of macrocomponent, and y = amount of macrocomponent after crystallization.

In all experiments (time of stirring—30 min) the coefficient λ was constant and equal to 27 for 0.2 *M* K_2SO_4 and 7 for 0.4 *M* K_2SO_4. After prolonged stirring the value of λ diminished due to recrystallization of the precipitate which led to equilibration of the crystals.

Dependence of λ on the K_2SO_4 concentration explains the small influence of K_2SO_4 concentration on the loss of Pu in solution.

2. Crystals of $K_3La(So_4)_3$ were being recrystallized for a long time in a solution containing Pu(IV). Hence the partition factor D was determined according to Chlopin's equation:

$$\frac{x(1-y)}{y(1-x)} = D$$

where x = fraction of microcomponent in solid phase; y = fraction of macrocomponent in solid phase; $(1-x)$ = fraction of microcomponent in solution; and $(1-y)$ = fraction of macrocomponent in solution.

True equilibrium was attained in 0.2 *M* K_2SO_4 for a freshly prepared suspension in 48–50 hours, and for a 2 month old suspension in 100 hours.

For both suspensions the partition factor D was found equal to 29—a value very near to the value of coefficient $\lambda = 27$ found by precipitation of the double sulfate.

3. Crystals of $K_3La(SO_4)_3$ containing Pu were recrystallized in an inactive 0.4 M K_2SO_4 solution for 125 hours. The value of the Doerner-Hoskins coefficient λ fell off to 1.7 while for the partition factor D the value 6.8 was found, in good agreement with the value of $\lambda = 7$ for that system in the case of precipitation from supersaturated solution.

The above data show that the Pu, in spite of different valency states of Pu(IV) and La(III), goes into the crystal lattice of $K_3La(SO_4)_3$, perhaps due to the formation of anomalous mixed crystals.

REFERENCES

1. Connick, R. E., McVey, W. H. and Sheline, G. E.; Voigt, A. F., Kant, A. and Hein, R. E., Metallurgical Project Report CN-1360 (Feb. 10, 1944), CN-1503 (June 10, 1944), quoted from Paper 3.8 of "The Transuranium Elements" part I, p. 163-167. McGraw-Hill, New York, 1949.
2. Strassmann, F. and Hahn, O., Naturwiss, *30*, 256, 1942.

Rare-Earth and Transplutonium Element Separations by Ion Exchange Methods

By D. C. Stewart,* USA

Surprisingly large number of variables are involved in the operation of an ion exchange resin column. As a result, while a number of elutriants have been suggested for use with such columns to separate the individual rare-earth and transplutonium plus-three ions, the prospective user may still find it difficult to make the cross comparisons required before a choice can be made of the most promising system available for the particular separation he has in mind. Because of this, the type of controlled experiment recently reported by Mayer and Freiling,[1] using a test system designed specifically to compare the efficiencies of various elutriants directly, is of unique value.

The present paper briefly describes another experimental arrangement for making similar comparisons, or for studying the effect of different operating variables within a single chosen elutriant system, using tracer quantities of radioactive nuclides of the elements of interest. To date, the experiments made with this test-column arrangement have all employed buffered glycolic acid as an elutriant. The various elution curves obtained in this study have been surveyed for the present report, and calculations have been made on the relative elution positions of the various rare-earth and rare-earth-like ions which have been used throughout the course of the work. In addition to presenting the author's data, a similar survey has also been made of a number of column runs performed by the Argonne National Laboratory heavy element nuclear chemistry group to separate the heavier actinides, also using glycolate-Dowex 50 separation systems. (The investigators in this group included M. H. Studier, J. F. Mech, J. E. Gindler, P. R. Fields, A. M. Friedman, H. Diamond, M. M. Petheram, R. K. Sjoblom and R. F. Barnes.) An attempt has also been made to review column separations of a similar type as reported in the literature by other investigators in this country, and, to the limited degree possible to do so with any certainty, to compare them to the data obtained for the glycolate elutriant system at Argonne.

Since the results of most macro-scale rare-earth separations are somewhat unsuited for such comparisons (quite different separation mechanisms are involved in some cases), very little is included about them in this review. Thus the early development of macro-scale column methods at Oak Ridge National Laboratory[2] and at Iowa State College[3] will not be considered in any detail. A review is available[4] of the various separations techniques developed at the latter site by Spedding and his associates, as well as a detailed development[5] of the theory of operation of their most extensively used separations technique (0.1%, high pH, citrate with hydrogen form cation resin columns). Also, the use of concentrated hydrochloric acid solutions to accomplish group separations of the lanthanides and actinides will not be discussed, since summaries are available[6-9] by the University of California investigators responsible for developing these methods.

In summarizing separations data, and in making literature comparisons, a useful concept is that of the separation factor, α. In ion exchange resin studies, this is defined as:

$$\alpha_b^a = \frac{(K_D)_a}{(K_D)_b} \qquad (1)$$

where $(K_D)_a$ and $(K_D)_b$ represent the distribution coefficients of the two ions whose separation is being considered. (The greater the difference of α from unity, the more readily the separation can be accomplished by column techniques.) The distribution coefficient, K_D, for a given ion is usually thought of as being the result of a batch-type experiment wherein the amount of the ion present in combination with the resin and the amount left in its associated supernatant solution are determined by some analytical means after the resin-solution-ion system has been allowed to reach equilibrium, or:

$$(K_D)_a = \frac{\text{conc. of solute "}a\text{" in resin phase at equilibrium}}{\text{conc. of solute "}a\text{" in solution phase at equilibrium}} \qquad (2)$$

Such batchwise determinations of K_D are quite feasible, of course, but may become tedious or difficult to apply if K_D values are sought for members of a large group of chemically very similar species, such as the rare-earth or transplutonium +3 ions. Fortunately, the plate-theory of Mayer and Tompkins[10,11] offers another approach. Where this theory applies, it permits a single experiment, simultaneous determination of the distribution coefficients for essentially any number of ions, purely

* Argonne National Laboratory.

Table I. Separation Factors in Glycolate Systems

Element M	"Thulium number" ($= \alpha_{Tm^M}$)				"Americium number" ($= \alpha_{Am^M}$)		
	Room temperature runs			87°C run	Room temperature		87°C run
	Mean of all runs		Run 38	Run 66	All runs	Run 38	Run 66
	Value	Number of determinations					
Sc	0.14±0.03	2	–	0.04	0.028	–	0.0056
Y	2.57±0.17	5	–	–	0.72	–	–
Lu	0.55±0.03	11	–	0.50	0.15	–	0.070
Yb	0.73±0.037	14	0.80	0.66	0.20	0.18	0.093
Tm	1.00± –	–	1.00	1.00	0.28	0.23	0.14
Er	1.40±0.06	12	1.49	1.38	0.39	0.34	0.19
Ho	1.79±0.16	4	1.90	2.06	0.50	0.44	0.29
Dy	2.20±0.18	2	2.38	2.56	0.61	0.55	0.36
Tb	2.29±0.23	11	2.74	3.56	0.64	0.63	0.50
Gd	–	–	–	~4.65	–	–	~0.66
Eu	2.47±0.32	13	3.17	4.93	0.69	0.73	0.69
Sm	2.67± –	1	–	6.04	0.75	–	0.85
Pm	3.55±0.31	13	4.42	7.78	0.99	1.02	1.09
Nd	6.49±0.71	3	6.69	9.82	1.81	1.54	1.38
Pr	8.9±0.23	2	9.15	13.5	2.48	2.10	1.90
Ce	19.5±3.0	2	22.5	18.9(?)	5.3	5.2	2.66(?)
La	32.0± –	1	>30	50.4(?)	8.9	>6.9	7.10(?)
100	–	–	–	–	–	–	–
99	1.13±0.03	3	1.10	–	0.315	0.254	–
Cf	1.34±0.04	3	1.36	–	0.373	0.313	–
Bk	–	–	–	–	–	–	–
Cm	2.86±0.26	15	3.32	5.76	0.800	0.765	0.809
Am	3.58±0.28	17	4.35	7.11	1.00	1.00	1.00
Na	2.57± –	1	–	–	0.72	–	–
K	7.5(?) –	1	–	–	2.1(?)	–	–
Rb	4.97± –	1	–	–	1.39	–	–
Cs	5.61± –	1	–	–	1.57	–	–

on the basis of the positions of their corresponding elution peaks. In the Mayer and Tompkins analysis, the K_D value of a given ion is simply:

$$(F_{max})_a = (K_D)_a\ (m/v) \qquad (3)$$

where $(F_{max})_a$ represents the number of free volumes of eluting solution which have passed through the column at the point where ion a reaches its maximum concentration in the eluant, and (m/v) is a correction factor involving the relative resin to liquid content of the column.[11] When the separation of two ions is considered, then:

$$\alpha_b^a = \frac{(K_D)_a}{(K_D)_b} = \frac{(F_{max})_a}{(F_{max})_b} \qquad (4)$$

This is a very useful relation, since most published data on resin column separations are presented in the form of elution curves. If, for such a curve, the flow rate, drop size, elutriant concentration, pH and temperature can be assumed to remain constant throughout the experiment, the separation factor for any pair of ions is simply the ratio of their elution peak positions after these have each been corrected by subtracting one column volume to compensate for the noneffective liquid present in the column at the beginning of the run. (A free column volume is that space in the column bed occupied by liquid, i.e., the non-resin volume.) The separation data obtained in the present work, as well as those derived from the literature, will be presented as α values calculated in the above fashion from elution curve data.

EXPERIMENTAL

Glycolate Elutriant Solutions

The separation factors in Table I are based on elution curves selected from a series of sixty-six column runs. In the case of the first twenty of these, elutriant solutions were prepared by direct weighing of crystalline Matheson, Coleman and Bell glycolic acid, followed by dilution to a calculated concentration of 0.25 M. In the balance of the runs, solutions of the acid were prepared, passed through a hydrogen form Dowex 50 resin bed to remove contaminating cations, titrated with standard base, and then adjusted to the desired 0.25 M concentration. The last few runs of the series (including Run 66, shown in Table I) employed elutriants prepared in this manner, but in these runs the glycolic acid had been first dissolved in boiling acetone, filtered, recrystallized five times from cold acetone and dried carefully before use. In all cases, the prepared 0.25 M glycolic acid solution was adjusted to the desired pH (as measured with a Beckman type G glass electrode pH meter) with ammonia gas.

Resin

The grading of the resin used has been previously described.[12] In essentially all cases, the resin em-

ployed was that portion of a ten-pound lot of minus 400 mesh, 12% cross-linked Dowex 50 which settled out in 2-18 hours after the resin had been suspended in two feet of distilled water. In all the runs examined in compiling the Table I data, the ammonium form of the resin was used. Dry resin density and settled-volume measurements were needed for calculation of free column volumes, and these were determined by modification of the methods recommended by Tompkins.[11] A density value of 1.37 was found for six-hour oven-dried resin. In 0.25 *M* glycolate systems, the free volume was 60% of the settled resin volume.

Radioactive Tracers

Known stocks of americium and curium, and of fission product cerium and promethium were already available. Californium and element 99 were furnished through the courtesy of members of the Argonne heavy element nuclear chemistry group.[13,14] All the other radioactive tracers were prepared by neutron irradiation in the Argonne Research Reactor, CP-5, of milligram amounts of the best stocks available of the element (as spectrographically pure oxides in most cases). On removal from the reactor, each material was dissolved in acid, diluted to a known volume and aliquots removed and plated so that radioactive decay and absorption curves could be taken. In preparing a column loading for a run or series of runs, appropriately sized volumes of the selected tracer stock solutions were combined in a small beaker and taken to dryness several times,

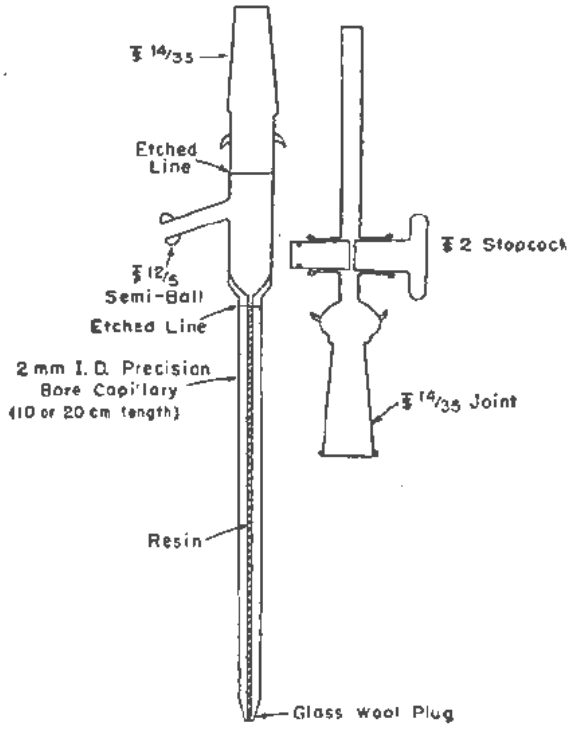

Figure 1. Unjacketed column and cap

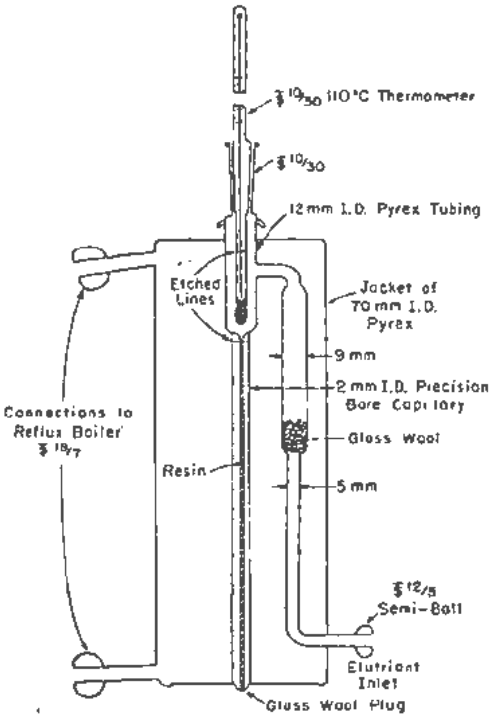

Figure 2. Jacketed column for non-room temperature experiments

following which the residue was taken up in weak (<0.1 *M*) hydrochloric acid. The column was loaded by forcing all or part of this acid solution through the top of the column bed, following it by an equal volume of wash water. The column walls above the resin were then carefully rinsed, and the elutriant solution was added to begin the run.

Experimental Arrangement and Procedure

The general features of these have already been described.[12] The mean α values of Table I include some data from the elution curves presented in that reference, which deals with techniques for the rapid separation of certain yttrium group rare earths by use of ultra-short resin columns. Most of the room temperature runs represented in Table I, however, were made with test columns of the type shown in Fig 1, whereas Run 66, which was performed at 87°C, and the results of which are also summarized in the same Table, was made with the jacketed test column shown in Fig. 2. (The jacket outlets were connected to a trichloroethylene reflux boiler in a manner analogous to that shown by Thompson, Harvey, Choppin and Seaborg.)[8] On receiving the columns, a glass wool plug was placed in the tip of each, and they were then calibrated for total volume by weighing the amount of mercury required to fill each to the lower of the etched lines indicated in Figs. 1 and 2. Resin was then slurried into each column, and, after it had settled, the upper resin surface was adjusted to the same etched line. Where a series of experiments was being performed to study

Table II. Very Heavy Element Separation Factors from Glycolate-Dowex 50 Column Runs*

Element (M)	Operating temperature (°C)	"Americium number" (α_{Am^M})			"Californium number" (α_{Cf^M})		
		Mean value	Standard deviation	Number of runs	Mean value	Standard deviation	Number of runs
99	Room temperature				0.838	±0.028	3
Cf		0.39		1	1.00		
Bk					1.49	±0.27	4
Cm		0.813	±0.018	8	1.87		1
Am		1.00			2.59		1
Pu(+3)		1.23	±0.03	2			
Pu(+4?)					0.28	±0.01	2
Pu(+5-6?)					0.07		1
100	87°				0.750		1
99					0.846	±0.017	2
Cf					1.00		
Bk							
Cm		0.806	±0.011	4			

* These data were taken from a series of fourteen column runs performed by M. H. Studier, J. F. Mech and J. E. Gindler for the specific purpose of studying heavy element separations in the glycolate system and from an equal number of elution curves available from process runs performed by these and other members of the Argonne nuclear group during their study of heavy element isotopes. The other investigators included P. R. Fields, A. M. Friedman, H. Diamond, R. F. Barnes, R. K. Sjoblom and M. M. Petheram.

the effect of one operating variable, the same column bed was used throughout the study in order to eliminate uncertainties due to possible differences between columns in total amount or size distribution of resin present. Between runs, each column was regenerated with 0.25 *M* ammonium citrate solution, followed by a water wash. This treatment also served to strip out any residual radioactivity.

In all runs, a 50-ml burette served as a reservoir for the elutriant solution. The tip of this burette was connected by tubing to the side arm of the column. Before and after a run, the elutriant level was brought to the upper of the etched lines shown in Figs. 1 and 2; the burette level was read and recorded, as was the elapsed time of the run. With these data, and a knowledge of the total number of drops passed, the mean drop size, drop rate and flow rate in terms of ml/cm²/min could readily be calculated.

The balance of the experimental arrangement was as previously described.[12] The drops from the column were collected in rotation on one-inch diameter stainless steel plates. After drying them under an infra-red lamp and heating briefly in a burner flame, the amount of radioactivity on each plate was measured, using a windowless, flow-type proportional counter for alpha-counting, and a similar instrument of the end window type for β-γ measurements. Elution curves of the radioactivity level versus drop number type were then drawn, and plates corresponding to the elution peak maxima were subsequently counted at intervals for half-life determinations. The β-γ emitting nuclides were identified by this means (and by absorption curves, where necessary). The alpha-emitters were identified primarily on the basis of the known relative amounts added, and, in the case of the californium peak, by its associated spontaneous fission activity.

RESULTS AND DISCUSSION

To date, the most commonly used elutriants for rare-earth separations have been buffered solutions of oxygenated carboxylic acids (citric, lactic, glycolic, etc.). Mayer and Freiling[1] have pointed out that for the monobasic acids of this type, the separation factor between any two rare-earths becomes equal to the ratio of the equilibrium constants for their respective adsorption reactions, and that, therefore, a separation factor as determined from a column run made at near-equilibrium conditions should be independent of the pH and concentration of the eluting agent. Ketelle and Boyd[15] had earlier reached the same conclusion for the citric acid system, if the pH was controlled within a range where the singly ionized citrate ion was effectively the only complexing species present. They developed an expression for the distribution coefficient of any given rare-earth in such a citrate system, showing that three different equilibria were involved: that for the exchange between the uncomplexed ion and the resin, that for the reaction between the rare-earth ion and the complexing ion, and that for the first hydrogen dissociation equilibrium of citric acid. They concluded that in the citrate system, temperature-induced shifts in the first of these equilibria appeared to be offset by opposing changes of the same magnitude in the second, and that ratios of K_D values (the separation factors) were essentially independent of temperature, as well as of eluting agent concentration and pH changes. This does not seem to be the case for glycolate systems, at least for the lanthanide series, so all the data shown in the tables are presented in terms

Table III. Separation Factors from Literature Data

a. Cold (20-30°C) citrate eluriant

Elements					Elements				
a	b	α_b^a	Reference	Comments‡	a	b	α_b^a	Reference	Comments‡
Lu	Tm	0.57	15	Calc. from Table II	Gd-Eu	Tm	2.12	21	"Standard curve"
		0.79	21	"Standard curve"	Sm	Tm	2.39	21	"Standard curve"
		0.82	21	Fig. 2	Pm	Am	0.97	5	Fig. 1
		0.59	21	Fig. 3	Pm	Eu	1.55	10	Fig. 4
Lu	Am	0.23	21	Fig. 1	Pm	Nd	0.9	30	Fig. 2. Amberlite IR 1
Yb	Tm	0.69	15	Calc. from Table II			0.69	28	
		0.92	21	"Standard curve"	Pr	Nd	1.39	28	
		0.73	21	Fig. 2	Pr	Ce	0.68	31	Fig. 6
		0.66	21	Fig. 3			0.53	31	Fig. 7
Er	Tm	1.55	15	Calc. from Table II			0.55	10	Fig. 3. Coarse Dowex 50
		1.44	15	Fig. 3. Amberlite IR 1			0.31–0.35	10	Fig. 3. Dowex 50 coll. agg. (4 runs)
		1.39	15	Fig. 4b					
		1.24	21	"Standard curve"	La	Ce	1.52	31	Fig. 7
		1.11	21	Fig. 2	Y	Tm	3.18	15	Calc. from Table II
Ho	Tm	2.44	15	Calc. from Table II			2.42	15	Fig. 3. Amberlite IR 1
		1.72	15	Fig. 3. Amberlite IR 1			2.10	21	"Standard curve"
		1.43	21	"Standard curve"	Y	Nd	0.35	30	Fig. 2. Amberlite IR 1
		1.40	21	Fig. 2	Y	Ce	0.53	3	Fig. 4. Amberlite IR 1
Dy	Tm	3.82	15	Calc. from Table II	Y	Cm	0.30	19	
		1.62	21	"Standard curve"	Ac	La	10–20	17	Batch expts.—Varying pH
		1.60	21	Fig. 2	Pm	Eu	0.77	32	Anion resin (Dowex 1) col.
Tb	Tm	1.89	21	"Standard curve"					

b. Hot (87-100°C) citrate eluriant

Elements					Elements				
a	b	α_b^a	Reference	Comments‡	a	b	α_b^a	Reference	Comments‡
Lu	Tm	0.57	15	Calc. from Table II	Nd	Ce	0.45	28	Run 1
		0.52	27				0.50	28	Run 1
Yb	Tm	0.69	15	Calc. from Table II	Pr	Ce	0.77	28	Run 1
		0.69	27				0.79	28	Run 4
Er	Tm	1.55	15	Calc. from Table II			0.58	28	Run 7
		1.68	27		Y	Tm	3.18	15	Calc. from Table II
Ho	Tm	2.44	15	Calc. from Table II			3.16	15	Fig. 5
		2.52	27				3.05	15	Fig. 6b
Dy	Tm	3.82	15	Calc. from Table II			3.24	15	Fig. 6a
		3.42	15	Fig. 6b	Y	Am	0.15	22	
		2.94	15	Fig. 6c after correction	Y	Eu	0.49	22	
		3.41	27				0.46	1	Fig. 1a
Tb	Tm	4.38	15	Fig. 6b	100	Am	0.24	8	
		4.49	15	Fig. 6c	100	Cf	0.90	13	
		5.35	27				0.72	14	
Tb	Am	0.29	18		99	Am	0.32	8	
Tb	Eu	0.65	22		99	Cf	0.94	13	
		0.59–0.83 (mean = 0.65)	1	Calc. from Table I. 0.25 to 1.0 *M* citrate			0.86	14	
					Cf	Am	0.38	8	
							0.34	19	
Gd	Tm	7.72	27		Bk	Am	0.43	22	
Gd	Am	0.48	18				0.51	19	
Gd	Eu	0.96	22				0.50	8	
Eu	Am	0.56	22		Bk	Cm	~0.63	20	
Sm	Tm	11.9	27		Cm	Am	0.82	18	
Sm	Am	0.69	22				0.80	33	
Sm	Eu	1.13–1.21 (mean = 1.17)	1	Table I. 0.25 to 1.0 *M* citrate			0.85	34	
							0.83	19	
Pm	Am	1.03	22				0.86	8	

of either room temperature (20–30°C) or high temperature (87–100°C) operations.

As far as other variables are concerned (resin size, flow rate within reasonable limits, etc.), practical experience has shown that, with modern high capacity resins, these will have relatively little effect on relative elution peak positions. (They may have a marked effect on the amount of cross contamination that occurs between neighboring peaks, however.)

All of the above considerations were in mind when the data shown in the tables were calculated. In Tables I and II particularly, it has been assumed that

Table III. Separation Factors from Literature Data (Continued)

c. Lactate elutriant (at 87°C unless noted)

Elements a	Elements b	a_b^a	Reference	Comments§
Er	Eu	0.21	8	
Ho	Am	0.14	26	Mean of runs at varying lactate conc.
Ho	Eu	0.29	8	
Dy	Am	0.20	26	Mean of runs at varying lactate conc.
Dy	Eu	0.37	8	
Tb	Am	0.27	27	Mean of runs at varying lactate conc.
Tb	Eu	0.53	8	
Tb	Eu	0.48–0.59 (mean = 0.52)	1	{7 runs—Lactate varies 0.2–1.33 *M*
Gd	Am	0.42	26	Mean of runs at varying lactate conc.
Gd	Eu	0.83	8	
Eu	Am	0.57	23	Room temp. run
		0.60	24	Room temp. run
Eu	Am	0.57	24	
		0.50	26	Mean of runs at varying lactate conc.
Sm	Am	0.64	26	Mean of runs at varying lactate conc.
Sm	Eu	1.23–1.31 (mean = 1.28)	1	{Lactate conc. varies 0.2–1.33 *M* (7 runs)
Pm	Am	0.96	23	Room temp. run
		1.00	24	Room temp. run
		1.02	24	
		1.03	26	
100	Am	0.23	8	
99	Am	0.31	8	
		0.20	26	Various lactate concs.
Cf	Am	0.38	8	
		0.32	26	Various lactate concs.
Bk	Am	0.56	8	
		0.44	26	Various lactate concs.
Cm	Am	0.83	23	Room temp. run
		0.88	24	Room temp. run
		0.84	8	
		0.76	26	
		0.84	24	
Cm	Y	~5.0	8	Series of runs at pH 4 to 5.

d. Miscellaneous elutriants

Elements a	Elements b	a_b^a	Reference	Comments§
Tb	Eu	0.50	1	0.30 *M* Glycolate at 87°C
		0.87	1	0.50 *M* Malate at 87°C
		0.81	1	0.70 *M* Malate at 87°C
		0.29	1	0.026 *M* EDTA* at 87°C
		0.26	1	0.017 *M* EDTA* at 87°C
Eu	Am	0.70	24	0.1 *M* Tartrate at R. temp.
		0.80	24	0.4 *M* Tartrate at 100°C
Sm	Eu	1.28	1	0.30 *M* Glycolate at 87°C
		1.15	1	0.50 *M* Malate at 87°C
		1.23	1	0.70 *M* Malate at 87°C
		1.60	1	0.026 *M* EDTA* at 87°C
		1.46	1	0.017 *M* EDTA* at 87°C
Sm	Nd	0.48	16	Hydrazinodiacetic acid† at R. T. with Dowex 50 resin
		0.33–0.39	16	{Same—with Amberlite 120 resin (4 runs)
Pm	Am	1.21	23	0.41 *M* Tartrate at 100°C
Pr	Nd	1.49	16	Hydrazinodiacetic acid† at R. T. with Dowex 50
		1.44–1.57	16	{Same—with Amberlite 120 (5 runs)
La	Nd	3.00	16	Same—Amberlite 120 resin
Y	Eu	0.59	35	2% TTA‡ in 38% Dioxane — 60% H_2O at R. temp.
Lanthanides	Am	<0.92	8	1.0 *M* Ammonium Thiocyanate on Dowex 1 (anion) resin at 87°C
100	Am	1.24	8	Same as above
99	Am	1.19	8	Same as above
Cf	Am	1.35	8	Same as above
Bk	Am	1.24	8	Same as above
Cm	Am	0.92	8	Same as above
		0.77	24	0.1 *M* Tartrate at R. temp.
		0.84	23	0.4 *M* Tartrate at 60°C
		0.84	23	0.4 *M* Tartrate at 87°C
		0.84	23	0.4 *M* Tartrate at 100°C
		0.87–0.91	24	{0.1 *M* and 0.8 *M* Tartrate at 87°C
Cm	Am	0.885	8	0.7 *M* Hydracrylate at R. temp.
		~1.0	23	0.025 *M* EDTA* at 87°C
		~1.0	23	0.0065 *M* EDTA* at 87°C

* Ethylenediamine tetraacetic acid.
† 0.5% solution + 1.5% ammonium acetate in H_2O.
‡ Thenoyltrifluoroacetone.

§ Table and figure numbers are those of the paper reviewed. Dowex 50 resin used unless otherwise noted.

mean values could be legitimately determined for any series of separation factors determined at the same temperature for a given elutriant-resin system, regardless of other variables.

Table I presents separation factors calculated from elution curves obtained by the author, using buffered glycolic acid elutriant. Table II shows similar factors for some of the elements of the actinide series as determined from elution data furnished by M. H. Studier and his associates in the Argonne heavy element nuclear chemistry group. Table III is a compendium of results calculated from the published reports of other laboratories in the United States. (A paper by Fitch and Russell[18] of Canada is included because the elutriant system they propose is of interest when compared to the others surveyed.)

The major difficulty met in presenting these separation factors was in deciding on the most informative basis of reference. In the author's work it was found that thulium was a very convenient reference

point to use because of the desirable qualities of the capture product that is formed when this element is neutron-irradiated to produce tracer. This nuclide, the 129-day thulium-170, has a stable daughter and decays by emission of β rays of easily measured energies; it is one of the first elements eluted from the columns, and has a half-life of sufficient length to permit use of the same stock solution of tracer for experiments done over a period of months, yet still short enough so that decay curve identifications are possible. Tm^{170} was used in all of the runs performed in the course of the present work, its elution position serving as an internal standard for comparing different runs. In Table I, therefore, the separation factors are presented as "thulium numbers," that is, as the ratio of the K_D of the element shown to that of thulium. Using these thulium numbers as a basis, "americium numbers" have also been calculated so as to expedite comparison with the data of Tables II and III, although americium may not have been actually present in some of the runs of Table I.

Mean separation factors were calculated for all of the rare-earth and similar type elements (except gadolinium) from the room temperature elution curves. It is realized that in some cases this probably gives a distorted picture of the relative elution positions, particularly where a thulium number calculated from only one available curve is compared to the value of a neighboring element where a dozen curves may have been suitable for use. The data are presented in this fashion only because there was no run at room temperature where all the elements of interest were present. Run No. 38 most closely approximated this condition, so data calculated from it are shown separately in Table I, as was also done for one run (No. 66) made at 87°C.

It will be seen that the thulium numbers based on Run No. 38 tend to be larger than the mean values calculated from all the room temperature runs. There are several reasons for believing that the Run No. 38 values are more accurate and that the other room temperature data should be used only to approximate the positions of lutecium, yttrium, scandium, etc., which were not in the Run No. 38 loading mixture. The mean values include data from the earlier runs, which were carried out before it was known that the glycolic acid elutriant contained considerable quantities of calcium ion, and also before the importance of keeping the amount of hydrogen ion to an absolute minimum in the loading solution was fully realized. In the earlier runs, eluting solution was often run through the columns for some hours before putting the tracers on the resin, and it is probable that some of the resin was occasionally thus inadvertently converted to the calcium form before the run, a factor which was later shown[12] to have considerable effect on the separations attained. (For later runs, the calcium was removed from the elutriant.)

The factor of high acidity in the loading solution would probably tend to decrease separation factors if these were calculated on the basis of an early eluting species, as is the case with the thulium numbers of Table I. Some of the resin would be converted to the acid form by a high acid tracer mixture, and as this hydrogen would be removed during the early part of the run by the mass action effect of the ammonium ion in the elutriant, the result would be lowering of the pH and the glycolate ion concentration. Thus the rare-earth bands would elute more slowly at the start of the run than they should, the error thus introduced being comparatively greater in terms of K_D values calculated for the early eluting elements than for those eluting in comparatively high drop number positions. Thus the thulium numbers would tend to be too low.

Perhaps the most interesting feature of the Table I data is that involving the effect of temperature on the separations. The thulium numbers for the lanthanide series (based on Run No. 66 at 87°C) are, in general, markedly higher than those from the room temperature runs. Several other preliminary runs which have been made at intermediate temperatures (but not reported here in detail) seem to bear out the fact of this being a real and quite substantial effect. On the other hand, the data of Table I for the actinides, and the similar values from the curve of Studier, *et al.*, shown in Table II, would indicate that similar temperature-induced changes in separation factors do not occur in the case of the heavy elements. Presumably the complex-forming reactions between glycolate and the plus-three ions are the major ones involved, and the fact that such a difference exists in the behavior of members of the lanthanide and actinide series is somewhat surprising in view of their presumed similarity in electronic structure. It is hoped to study this behavior further.

Gadolinium tracer was present in several of the room temperature runs, but it was never possible to distinguish its elution peak from that of europium. In the 87°C run shown in Table I, a shorter lived component was seen early after separation at the front of the europium peak and was assumed to be 18-hour Gd^{159}, some of which was still present at the time in the gadolinium tracer used. Further study will be required to be certain of the relative Gd position.

Unfortunately no runs have been made to date where europium and yttrium tracers were present at the same time. The thulium numbers shown in the first column of Table I would indicate that yttrium may elute *beyond* europium, which would be the furthest displacement from its usual separations chemistry "element 66½" position that has yet been reported. Yttrium definitely elutes in a position beyond terbium in room temperature glycolate systems.[12]

The thulium numbers shown in Table I for the alkali metals are based on a single run with a 10-centimeter column and pH 4.0, 0.25 *M* glycolate. Tracers of four of the alkali metals were in the original loading mixture, along with the usual Tm^{170} standard. The thulium and sodium peaks were

clearly separated and easily identified, but the remaining radioactivity appeared as one single very broad peak. Later recounting of the plates in this region permitted clear differentiation of the 19-day Rb^{86} and the 2.3-year Cs^{134} peak positions, but the only indication of the 12.4-hour K^{42} was in a short-lived activity that was seen briefly on the trailing edge of the cesium peak. The value of 7.5 for the thulium number of potassium is thus very tentative, particularly since this would put potassium out of order in the alkali metal series. Since presumably no glycolate-complexing of these alkali metals is occurring during the elution run, their relative elution portions should involve only their displacement from the resin by the mass action effect of the cations in the elutriant solution, and a Na-K-Rb-Cs elution order would appear more reasonable.

The data calculated from the separation runs of the Argonne heavy element group are presented in Table II, either as americium numbers or californium numbers, since no single element was present throughout all the experiments represented. By comparing Tables I and II, it is possible to derive a tentative placement of the relative positions of the individual members of the lanthanide and actinide series in room temperature glycolate systems:

Actinide	*Lanthanide*	*Certainty of assignment*
Element 100	Coincides with Tm	Fair
Element 99	⅓-way between Tm and Er	Good
Californium	Just before Er peak	Good
Berkelium	½-way between Ho and Dy	Fair to poor
Curium	Slightly past Sm	Fair to good
Americium	Coincides with Pm	Very good
Plutonium+3	⅓-way between Pm and Nd	Fair

By an extrapolation from the batch K_D values determinated by Hagemann[17] for lanthanum and actinium in citrate systems (see Table III), it would be predicted that actinium itself would give the appearance of being virtually inelutable by glycolate from columns of the length usually used.

In runs where plutonium was present, very early elution peaks of that element occurred in glycolate separation runs. The oxidation states of the plutonium in these peaks are uncertain and have been assumed in the case of the values shown in Table II. Plutonium +3 ion was shown by Studier and Mech to elute in the expected position beyond americium, as is also shown in Table II.

Table III represents an attempt to summarize a large mass of literature data in as compact a form as possible. Because of the wide variety of materials used in the reviewed experiments, the problem of the reference element to use for the separation factor calculations was a difficult one. It was finally decided to use the comparison order: thulium, americium, europium, californium, neodymium and cerium. If none of these elements were utilized in the experiment, the choice of a reference was arbitrarily made on the basis of those species which were present.

In calculating α values from the elution curves reported in the literature, several methods were used to correct the elution peak position for the initial inert column volume, if it was apparent that such a correction had not been previously made. If the authors had estimated the free volume in any manner, this value, of course, was used. Otherwise, if the elution curve showed an "anion" peak at the beginning, the volume to this point was taken as the correction to be applied. In some cases the total column volume was calculated, and the free volume obtained by assuming 60% free space (and a 30-microlitre drop size if it was necessary to express the free volume correction as drops).

Space permits the making of only a few general remarks about the experimental conditions used by the various authors. The techniques used in the University of California Radiation Laboratory work[8,18–24] (where they were largely developed), in the Argonne separations,[12,13,14] and in the Naval Radiological Defense Laboratory[1,25–26] experiments were somewhat similar. Generally, small diameter, relatively short columns were used to separate tracer or microgram amounts of materials, occasionally with comparatively high levels of fission product or alpha emitting elements of lesser interest also present. Often there was a high premium on speed of separation.

The work of Ketelle and Boyd[15,27] is still the most extensive of that which has been published dealing with heavy rare-earth separations in both hot and cold citrate systems. They used comparatively very long columns with milligram amounts of material present. Wilkinson and Hicks[21] prepared a "standard curve" for the separation of heavy rare-earths in room temperature citrate columns, using macro amounts of material so that the various peak positions could be set by spectrographic analyses. They have also reported several curves showing the separation of tracer amounts of some of the very heaviest members of the rare-earth series that were formed in cyclotron bombardments.

Hagemann's[17] batchwise K_D determinations for Ac and La in citrate systems have already been mentioned. This is the only separation value in Table III not derived from column data. Column separation of actinium from rare-earth elements apparently has not been performed to any extent in this country.

The work of Pressley and Rupp[28] is based on a number of experiments performed at the Oak Ridge National Laboratory for the production of fission product rare-earths for distribution by the Isotopes Division. Their curves are particularly useful for furnishing information on separations with citrate for rare-earths in the cerium region.

While only tentative conclusions can be drawn from the data presented thus far, a few general comments might be made. Comparison of the α values of Wish, Freiling and Bunney[26] with similar ratios in Tables I and II could make it appear that hot lactate is possibly a better elutriant for use in separating the actinides than is hot glycolate, while both are superior to either hot or cold citrate. The situation for the lanthanides, however, may be somewhat

different. The data of Ketelle and Boyd[15,27] for heavy rare-earth separations with citrate at 100°C show better factors than do either lactate or glycolate at 87°C. Glass[23,24] found that cold tartrate gave excellent curium-americium separation, but that this separation was decreased at higher temperature unless the total tartaric acid concentration and pH were modified to give a net increase in the amount of singly charged tartrate ion present. He pointed out that tartrate, like citrate, was very pH sensitive and that macro-loading of the column caused spreading of the peaks in tartrate systems.

Of the various systems reviewed in Table III, the ethylene diamine tetra-acetic acid elutriant (EDTA) would appear to be a particularly promising one, although Mayer and Freiling[1] have pointed out that certain precautions must be taken when it is used. (Spedding, Powell and Wheelwright[29] have described systems for using EDTA for macro-scale separations.) The work of Fitch and Russell on hydrazinodiacetic acid would also seem to indicate that this reagent would merit further study for application to radiochemical separations involving the actinides and lanthanides.

Unfortunately, very little work has been done with room temperature lactate elutriants, so it is not possible to decide whether or not high temperature operation produces any increase in the separation factors as is thought to be the case with the lanthanides and glycolate eluting agents. Glass[23,24] studied Am-Cm separation in room temperature and 87°C lactate runs, but found little difference in the separation factors calculated for these experiments.

ACKNOWLEDGEMENTS

Thanks have been previously extended to M. H. Studier and his associates for furnishing some of their elution curves and tracers to the author. Mention should also be made of the help of L. M. Porter in making the large number of radioactivity measurements involved in this study.

REFERENCES

1. Mayer, S. W. and Freiling, E. C., *Ion Exchange as a Separations Method. VI. Column Studies of the Relative Efficiencies of Various Complexing Agents for the Separation of Lighter Rare Earths*, J. Am. Chem. Soc., 75: 5647 (1953).
2. Tompkins, Edward R., Khym, Joseph X. and Cohn, Waldo E., *Ion Exchange as a Separations Method. I. The Separation of Fission-Produced Radioisotopes, Including Individual Rare Earths, by Complexing Elution from Amberlite Resin, ibid*, 69: 2769 (1947).
3. Spedding, F. H., Voight, A. F., Gladrow, E. M. and Sleight, N. R., *The Separation of Rare Earths by Ion Exchange. I. Cerium and Yttrium, ibid*. 69: 2777 (1947).
4. Spedding, F. H. and Powell, J. E., *Methods for Separating Rare Earth Elements in Quantity as Developed at Iowa State College*, ISC-444 (Jan. 25, 1954).
5. Spedding, F. H. and Powell, J. E., *The Separation of Rare Earths by Ion Exchange. VIII. Quantitative Theory of the Mechanism Involved in Elution by Dilute Citrate Solutions*, ISC-385 (August 6, 1953).
6. Street, Kenneth, Jr. and Seaborg, Glenn T., *The Separation of Americium and Curium from the Rare Earth Elements*, J. Am. Chem. Soc., 72: 2790 (1950).
7. Diamond, R. M., Street, K., Jr. and Seaborg, G. T., *An Ion Exchange Study of Possible Hybridized 5f Bonding in the Actinides, ibid*. 76: 1461 (1954).
8. Thompson, S. G., Harvey, B. G., Choppin, G. R. and Seaborg, G. T., *Chemical Properties of Elements 99 and 100, ibid*, 76: 6229 (1954).
9. Hicks, H. G., Gilbert, R. S., Stevenson, P. C. and Hutchins, W. H., *The Quantitative Anionic Behavior of a Number of Metals with an Ion Exchange Resin, "Dowex 2,"* LRL-65 (Dec. 1953).
10. Mayer, Stanley W. and Tompkins, Edward R., *Ion Exchange as a Separations Method. IV. A Theoretical Analysis of the Column Separations Process*, J. Am. Chem. Soc., 69: 2866 (1947).
11. Tompkins, Edward R., *Laboratory Applications of Ion Exchange Techniques*, J. Chem. Ed., 26: 32-38, 92-100 (1949).
12. Stewart, D. C., *A Rapid Separations Method for Tracer Amounts of Yttrium Group Rare Earth Elements*, Anal. Chem., (In press).
13. Studier, M. H., Fields, P. R., Diamond, H., Mech, J. F., Friedman, A. M., Sellers, P. A., Pyle, G., Stevens, C. M., Magnusson, L. B. and Huizenga, J. R., *Elements 99 and 100 from Pile Irradiated Plutonium*, Phys. Rev., 93: 1428 (1954).
14. Fields, P. R., Studier, M. H., Mech, J. F., Diamond, H., Friedman, A. M., Magnusson, L. B. and Huizenga, J. R., *Additional Properties of Elements 99 and 100*, Phys. Rev., 94: 209 (1954).
15. Ketelle, B. H. and Boyd, G. E., *The Exchange Adsorption of Ions from Aqueous Solutions by Organic Zeolites. IV. The Separation of the Yttrium Group Rare Earths*, J. Am. Chem. Soc., 69: 2800 (1947).
16. Fitch, F. T. and Russell, D. S., *Determination of Lanthanum in Rare Earth Mixtures*, Anal. Chem., 23: 1469 (1951).
17. Hagemann, F. T., *The Chemistry of Actinium*, Ch. 2 of Seaborg, G. T. and Katz, J. J., *The Actinide Elements*, National Nuclear Energy Series Div. IV. Vol. 14A, McGraw-Hill Book Company, Inc., New York (1954).
18. Thompson, S. G., Cunningham, B. B. and Seaborg, G. T., *Chemical Properties of Berkelium*, J. Am. Chem. Soc., 72: 2798 (1950).
19. Street, Kenneth, Jr., Thompson, S. G. and Seaborg, G. T., *Chemical Properties of Californium, ibid*, 72: 4832 (1950).
20. Thompson, S. G., Ghiorso, A. and Seaborg, G. T., *The New Element Berkelium (Atomic Number 97)*, Phys. Rev. 80: 781 (1950).
21. Wilkinson, Geoffrey and Hicks, Harry G., *Radioactive Isotopes of the Rare Earths. I. Experimental Techniques and Thulium Isotopes, ibid*, 75: 1370 (1949).
22. Higgins, G. H. and Street, K., Jr., *Note on the Ion Exchange Separation of Europium, Gadolinium and Terbium*, J. Am. Chem. Soc., 72: 5321 (1950).
23. Glass, R. A., *Studies in the Nuclear Chemistry of Plutonium, Americium and Curium and the Masses of the Heaviest Elements*, UCRL 2560 (April 20, 1954).
24. Glass, R. A., *Chelating Agents Applied to Ion Exchange Separations of Americium and Curium*, J. Am. Chem. Soc. (In press).
25. Freiling, Edward C. and Bunney, Leland R., *Ion Exchange as a Separations Method. VII. Near Optimum Conditions for the Separation of Fission Product Rare Earths with Lactic Acid Eluant at 87°, ibid*, 76: 1021 (1954).

26. Wish, Leon, Freiling, Edward C. and Bunney, Leland R., *Ion Exchange as a Separations Method. VIII. Relative Elution Positions of Lanthanide and Actinide Elements with Lactic Acid Eluant at 87, ibid,* 76: 3444 (1954).

27. Ketelle, B. H. and Boyd, G. E., *Further Studies of the Ion Exchange Separation of the Rare Earths, ibid,* 73: 1862 (1951).

28. Pressley, R. S. and Rupp, A. F., *Purification of Fissions Product Rare Earths by Ion Exchange,* ORNL 1313 (April 20, 1953).

29. Spedding, F. H., Powell, J. E. and Wheelwright, E. J., *The Separation of Adjacent Rare Earths with Ethylenediamine-tetra-acetic Acid by Elution from an Ion Exchange Resin,* J. Am. Chem. Soc., 76: 612 (1954).

30. Marinsky, J. A., Glendenin, L. E. and Coryell, C. D., *The Chemical Identification of Radioisotopes of Neodymium and of Element 61, ibid,* 69: 2781 (1947).

31. Harris, Darwin H. and Tompkins, Edward R., *Ion-Exchange as a Separations Method. II. Separation of Several Rare Earths of the Cerium Group (La, Ce, Pr and Nd), ibid,* 69: 2792 (1947).

32. Huffman, E. H. and Oswalt, R. L., *A Rare Earth Separation by Anion Exchange, ibid,* 72: 3323 (1950).

33. Crane, W. W. T. and Perlman, I., *New Studies in the Isolation and Properties of Curium,* AECD 2911 (August 3, 1950).

34. Higgins, G. H., *An Investigation of the Isotopes of Americium and Curium,* UCRL 1796 (June, 1952).

35. James, Ralph A. and Bryan, W. P., *The Use of Thenoyltrifluoroacetone in Ion Exchange Separations,* J. Am. Chem. Soc., 76: 1982 (1954).

Separation of Polonium with Diisopropylketone

By Arturo E. Cairo,* Argentina

The determination of polonium is usually made using the property which this element possesses of depositing spontaneously on silver plates, thus making it possible to separate it from solutions, after which the activity of the plate can be measured.

The method gives an approximation which is adequate for biological studies,[1] reproducibility being possible within ±5% and subject to increase if the solution contains no other dissolved substances, and the acidity of the hydrochloric acid is about 0.2 *N*.[2] In such a case, a preliminary separation of the components present in substantial quantities in this solution is made using tellurium as a carrier, effecting polonium deposition together with that of tellurium by reduction in an alkaline medium. The ultimate separation of tellurium is achieved by repeated precipitations in an acid medium in which polonium does not precipitate.

This method is not entirely satisfactory, since tellurium separation requires several precipitations, attended by losses of polonium, which reduces the already minute quantities of polonium to be separated.[3,4] A possible variant, to avoid the use of a carrier, is extraction by means of solvents.

There are several articles in the literature bearing on the solvent extraction of some polonium compounds. Guillot[5] found that chloroform could extract polonium diethyldithiocarbamate from alkaline solution to which bismuth had been added as a carrier. Servigne[6] describes a chloroform soluble acetylacetonate which is also soluble in other solvents and readily extractable from aqueous solutions.

More recently, the extraction of the polonium complex with dithizone has been applied to the separation of Po^{210} (RaF) from mixtures of it with RaD and RaE.[7,8] Hagemann[9] also determined the extractability in benzene of the complex with thenoyltrifluoroacetone, but this reagent, as well as dithizone, has the disadvantage of forming compounds with many other elements which are soluble in the solvents.

There are two references to solvent extraction of simple inorganic polonium compounds in aqueous solution. Boussieres[10] found that the residue from the evaporation of a solution of polonium in dilute hydrochloric acid is soluble in ethylene glycol, dioxane, methyl ethyl ketone and some other solvents which are partially miscible with water and he assumes that the polonium compound extracted is the oxychloride. Karracker and Templeton give a detailed description of a process for the separation of polonium from sulfuric acid solutions by extraction with mixtures of tributyl phosphate and dibutyl ether.[11]

It was observed, during the study of protactinium extraction,[12] that polonium dissolved in nitric or hydrochloric acid is readily extracted by diisopropylketone.

EXPERIMENTAL

The experiments were undertaken using Po^{210} separated from an RaD, RaE and RaF solution, by means of a silver plate. This plate was dissolved in 1:2 nitric acid and the silver was separated by precipitation with hydrochloric acid. The clear solution then was evaporated several times with hydrochloric acid until the nitrate ion had been eliminated, ending with a residual solution in 6*N* HCl.

Polonium was determined by its activity using a silver activated zinc sulfide screen and a photomultiplier tube. For this purpose, aliquots of the solutions to be measured were evaporated onto metal discs; the residue always remaining less than 0.5 mg/cm².

It was suspected, on the basis of the first results obtained that the polonium compound extracted by the solvent might possibly be volatile, which would cause losses during the preparation of the active discs. Several experiments were undertaken to check this by heating copper, silver, aluminum, platinum and glass discs for various lengths of time to different temperatures after evaporating portions of the ketone solution of polonium on the discs with an infrared lamp. Table I shows the results obtained with a series of discs. The values indicate counts per minute, the standard deviations of these measurements being in all cases under 1%.

It appears that the platinum discs retain the polonium somewhat less tenaciously than do the silver. In the case of the aluminum and glass discs, the polonium compound readily volatilizes and can be recovered on a cold surface placed over the discs.

The volatilization observed when the compound is on glass shows the true volatility of complex chloride extracted by the ketone. Thirty minutes heating at 112°C remove about one half of the polonium from the slide covers used for the purpose.

Original language: Spanish.

* Comisión Nacional de la Energía Atómica, Argentina. In collaboration with A. G. Maddock, Radiochemical Laboratory, Cambridge University.

Table I

Temp. °C	Time, minutes	Disc material: Silver	Aluminum	Glass	Copper	Platinum
Room	0	11,427	10,900	11,296	4401	4412
112	5	11,372				
112	10		8829			
112	12			7625		4379
112	15	11,379				
112	20		8047			
112	30			6470	4331	4325
178	5	11,193				
178	10		2436			
178	17	10,969				
178	20		1918			4200
178	27	11,279				
178	30				4306	4227
255	5	11,164				
255	10		1362			
255	16	11,181				

Silver was chosen since a series of experiments of longer duration at temperatures between 230 and 240°C indicated that the loss was lower than for copper discs. Under the same conditions the latter oxidize strongly, and it is suggested that the apparent loss in activity is in reality due to absorption consequent upon increase in thickness.

The advisability of slow evaporation of the solvent under an infrared lamp was demonstrated in an experiment in which aliquots of the ketone solution of polonium were evaporated on five copper discs. After measuring their activities, the discs were dried at 180°C for one hour, and there was no more than 1% reduction in activity.

The possibility of the polonium compound distilling with the solvent or the hydrochloric acid solution when distillation was carried out under atmospheric pressure was also investigated. Two experiments were undertaken for this purpose using 1 ml of the ketone solution and 1 ml of 6*N* hydrochloric acid solution. A micro-still, with a column about 6 cm long full of glass beads, was used to avoid mechanical entrainment of the active drops.

Some 90% of the acid solution was distilled, carrying with it only 0.3% of the polonium present, while the following 9% carried 0.5%. Diisopropylketone, on distillation, only carries half of these amounts.

Finally, a series of experiments proved that evaporation under infrared light of the solutions deposited on silver discs may be used both for the polonium solutions in sulfuric acid and for the diisopropylketone solutions obtained by extraction of the former, with volatilization losses of less than 1%.

Platinum discs were used for the polonium complexes with hydrofluoric or nitric acids, since nitric acid is slightly soluble in the ketone and will thus readily attack the copper and silver discs.

The elimination of polonium is often useful in the analysis of mixtures of natural alpha emitters, in order to determine it by difference; this elimination being achieved by volatilizing it from the discs onto which the mixtures have been deposited. Table II indicates the most notable differences observed in the case of polonium extracted from solutions containing ammonium fluoride or nitrate. The values express residual activity on the disc in percentage.

The practical conclusion from these experiments is that heating for 15 minutes at 850°C is sufficient to eliminate totally the polonium deposit.

The distribution of polonium between the diisopropylketone and the aqueous solutions of hydrochloric, nitric, hydrofluoric and sulfuric acids was determined as a function of the normality. The extractions were made by equilibrating a ketonic solution of the chlorine complex with the acid solution of the required concentration. The activity measurements in each phase were made on equal volumes of each after establishing equilibrium between equal volumes of the acid solution and the diisopropylketone solutions in sealed ampoules placed in a thermostat at 25°C ± 0.1°C and stirred with a vibratory stirrer. Experiments done with several stirring times, ranging from 6 minutes to 20 hours, showed that the equilibrium can be considered to be reasonably achieved after 2 hours provided that the stirring has been vigorous enough. Accordingly, all subsequent experiments were carried out with stirring times of this order of magnitude.

Table II

Salt present	Temp.°C	450	550	780	780	870
	Time in minutes	6	5	5	10	5
NH_4F		97	89	30	8	0
NH_4F		100	92	33	10	0
NH_4NO_3		60	50	12	0	0

The experiments on extraction from sulfuric and hydrofluoric acid solutions were made at room temperature: 19°C.

The amount of acid extracted by the ketone was determined by titration, and it was shown that neither the hydrochloric, nor the sulfuric acid, are extracted to an appreciable extent if the concentration is under 6*N*. This does not apply to hydrofluoric or nitric acid.

Figure 1 shows the results obtained for the extraction by diisopropylketone of polonium complexes with various acids as a function of acid normality.

In all these experiments, the stock polonium solution was prepared by extracting a solution of the element in 6*N* hydrochloric acid with diisopropylketone. The amount of hydrochloric acid passing into the solvent under these conditions is negligible.

In one case the stock solution was prepared by extracting polonium from a 6*N* nitric acid solution. Some of the acid was also extracted at the same time. The partition was determined with hydrochloric acid of different concentrations. It was found in these cases, that the quantity of polonium passing from the aqueous solution is greater than in the case of the stock solutions prepared from 6*N* hydrochloric acid, indicating the influence of the simultaneous presence

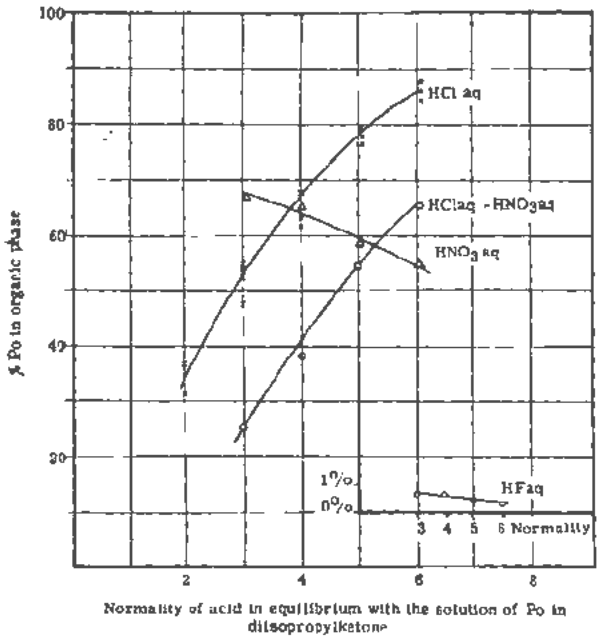

Figure 1. Normality of acid in equilibrium with the solution of Po in diisopropylketone

of hydrochloric and nitric acids on the partition coefficient. The behavior with mixtures of both acids was studied in greater detail. Figure 1 illustrates one of these experiments. It corresponds to a stock solution of polonium in diisopropylketone extracted from a 6*N* aqueous solution of hydrochloric acid and 0.5 *N* nitric acid, and then equilibrated with hydrochloric acid of different normalities.

The results suggest that the influence of reducing and oxidation agents on the extraction of polonium with diisopropylketone had to be investigated.

Table III shows some of the results obtained.

It was observed that polonium is deposited spontaneously on a silver plate immersed in the ketone solution of the complex chloride, a phenomenon similar to that known for aqueous solutions.

In another set of experiments, the extraction of other heavy natural radioactive elements dissolved in 6*N* hydrochloric acid was studied. It was shown that trivalent thallium and protoactinum are readily extracted (about 90%). Monovalent thallium is much less (about 17%). Uranyl ion extraction is very small (about 0.6%). The others do not extract in proportions higher than 0.5%. In particular RaD and RaE do not extract appreciably. Among the common elements, iron is easily extracted. It was also observed that no naturally radioactive element follows the polonium in its passage into the diisopropylketone if the extraction is carried out from a 12*N* sulfuric acid solution from which all the polonium passes into the solvent.

DISCUSSION

These experiments did not permit the identification of the ketone-soluble polonium compound, nor of the reaction whereby it is extracted from the aqueous acid stage, but it is worthwhile to view the whole in the light of what we know about the chemistry of polonium to date.

The only valence state of this element which is established without any doubt is that of Po(IV). Martin[15] has prepared $Po(NO_3)_4$ and PoO_2 in macroquantities and established the relevant formulae.

Numerous "tracer" experiments have established the existence of a series of tetravalent compounds.

A first possibility, therefore, as regards the nature of the species dissolved in diisopropylketone is that it may be $PoCl_4$, $Po(NO_3)_4$ or $Po(SO_4)_2$, according to the medium used. However, it is hard to defend this hypothesis if we draw a comparison with the behavior of $TeCl_4$ and postulate that polonium should behave similarly to its homologue. In effect, Elvins and Morgan[14] demonstrated that tellurium tetrachloride is neither extracted by diisopropylketone nor reacts, as it does with most of the higher order ketones.

The alternative assumption is that the extracted species are PoH_2Cl_6, $PoH_2(NO_3)_6$ or $PoH_2(SO_4)_3$. These species are cited in the literature as resulting from tracer experiments which indicate that the polonium is in the anion form if the acid solution has a concentration greater than 1*N*.[15]

It has been found, by coprecipitation, that the salts of $PoCl_6^{--}$ are isomorphous with the chloroplumbates, chloroplatinates and chlorotellurites[16] and, very recently, Staritzky[17] demonstrated the existence of the anion $PoCl_6^{--}$ as the principal species present in the solution of polonium in 2.5*N* hydrochloric acid, and further showed that potassium, rubidium, cesium, ammonium and tetramethylammonium are insoluble.

Our experiments in the extraction of hydrochloric acid in the presence of ammonium chloride (see Table III) give results which agree with these views and suggest that the extracted species is H_2PoCl_6, since a reduction of the extractability is to be expected if an insoluble salt is formed. The same hap-

Table III

Origin of the polonium solution in diisopropylketone	*Aqueous phase with which equilibrium was established*	*Percentage of polonium found in the solvent*
HCl 6 *N*	HCl 3*N*	54
HCl 6 *N*	HNO_3 3*N*	37.5
HNO_3 6 *N*	HNO_3 3*N*	71
HNO_3 6 *N*	HCl 3*N*	10
HNO_3 6 *N*	HCl 1.5*N*+HNO_3 1.5*N*	10
HCl 6 *N*	HCl 1.5*N*+HNO_3 1.5*N*	5
HCl 6 *N*	HCl 3*N*+KI 0.1*N*−I_2 0.1 *M*	87
HCl 6 *N*	HCl 3*N*+KI 0.5 *M*	97
HCl 6 *N*	HCl 3*N*+KI 0.25 *M*	85
HCl 6 *N*	HCl 3*N* sat. Cl_2	30
HCl 6 *N*	HCl 3*N*+$VOCl_3$ 0.1 *M*+ VCl_4 0.1 *M*	24
HCl 6 *N*,	HCl 3*N* sat. SO_2	3
HCl 6 *N*	HNO_3 3*N* sat. Cl_2	8
HCl 6 *N*	HCl 3*N*+CrO_3 (cold)	33
HCl 6 *N*	HCl 3*N*+NaCl 2*N*	61
HCl 6 *N*	HCl 3*N*+NH_4Cl 1*N*	33

pens when conducting experiments in the presence of iodine and potassium iodide. These were undertaken in the hope of observing a reduction of extractability, since the potential of the system I^-/I_2 should be enough to reduce the Po(IV) to a lower valence state, while an increase was actually observed. This may be interpreted by assuming that a more stable polonium iodine complex has been formed than the corresponding chlorine complex whose probable formula, by an extension of the same line of reasoning, would be H_2PoI_6.

In the case of VO^{++}/V^{+++}, on the other hand, the observed decrease in the extractability should correspond to a chemical reduction, as was confirmed by experiments in the presence of sulfur dioxide, which brings the element down to a lower valency, possibly Po^{++}, in which it is not extracted by diisopropylketone. The possibility of reduction to metallic polonium is excluded by measuring the activity distribution in a centrifuge after 4 hours of centrifugation which always gives uniform results, apart from statistical deviations.

The experiments made in the presence of strong oxidizing agents, such as chromic acid or chlorine, show a reduction of the amount of polonium passing to the solvent. This reduction is particularly noticeable in those cases in which the extraction is from an aqueous medium containing nitric and hydrochloric acid, either due to a mixture of them in the aqueous stage or to an addition of nitric acid originally present in the solvent.

Since the oxidizing power of the nitric and hydrochloric acids mixture is greater than that of the nitric acid by itself, we interpret these results as the passage of the element to a state of higher valency, possibly Po(VI), the corresponding species of which in this medium would be insoluble in the solvent.

Very little is known about a possible hexavalency of polonium. Possibly, the most convincing work of this nature is due to Samartzeva,[19] based on the apparent isomorphous incorporation of polonium when lead or potassium tellurates obtained by energetic oxidation are crystallized in its presence. Guillot[11] also found some evidence in the form of oxidation by chlorine which, in a weak acid medium, reduces the amount of polonium precipitated by ammonium chloroplumbate.

In our case, oxidation may be attributed to the presence of nitrosyl chloride, which is believed to account for the high oxidizing power of concentrated nitric and hydrochloric acid mixtures[20] and which might be present in our solutions.

Against this hypothesis, the findings of Hicks and Stevenson may be quoted;[21] they observed that, similar to Ti^{++}, Mn^{++}, Zr^{++}, Hf^{++} and Sn^{++}, Se^{++} is not extracted by diisopropylketone and that the Te^{++} is only sparingly extracted, while hexavalent compounds of tellurium and selenium are readily extracted under the same conditions, the nature of the compound soluble in the ketone being unknown.

Although the conditions under which Hicks and Stevenson developed their experiments are similar to ours, and although polonium is homologous with selenium and tellurium, these elements do not behave exactly alike. As shown in the literature by Escher-Desrivieres[22] and Guillot,[16] polonium behaves differently from tellurium in many instances. The insolubility of the hexavalent species in diisopropylketone may be one more difference from tellurium.

CONCLUSIONS

The behavior of polonium deposits in the form of chlorides, nitrates, fluorides and sulfates on platinum, copper, silver, aluminum and glass discs has been studied. It has been found that volatilization of these compounds begins at atmospheric pressure above 110°C in the case of aluminum and glass; copper, platinum and silver may be used if elimination of the solvent is carried out at a temperature not greater than 180°C and for no longer than 30 minutes.

The extractability of polonium with diisopropylketone in different media has been studied, and the following results have been obtained.

Where the pure hydrochloric, nitric or sulfuric acids are concerned, the extracted species are thought to be the following: H_2PoCl_6, $H_2Po(NO_3)_6$, $H_2Po(SO_4)_3$.

In hydrochloric acid at concentrations greater than $3N$, and containing nitric acid, the element probably passes to a hexavalent state in which it is not extractable.

It is extracted totally from a $12N$ sulfuric acid medium and, finally, not extracted from hydrofluoric acid solutions.

Extraction in the presence of several substances in a hydrochloric medium has also been studied, and shows that it is reduced by sulfur dioxide and ammonium chloride; the former by reduction, the latter by the formation of an insoluble compound.

The corresponding iodine complex, to which we ascribe the formula H_2PoI_6, is more soluble in diisopropylketone and more stable than the corresponding chlorine complex.

REFERENCES

1. Vittum, E. K., Minto, W. I. and Finch, R. M., *Biological studies with Polonium, Radium and Plutonium*. N.N.E.S. Div. VI, v.3 p. 18. McGraw-Hill, New York (1950).
2. Haissinsky, M., *Le Polonium*. Hermann, Paris (1937).
3. Karraçker, D. G., *Chemical procedures used in bombardment work at Berkeley*. A.E.C.D. 2738 — U.C.R.L. 432, W. W. Meinke, (editor) p. 245.
4. Rundo, J., A.E.R.E. Report HP/R 627. Dec. 1950.
5. Guillot, M., *Essai de mise en évidence d'un complexe non électrolite du polonium*. C. R. Acad. Sci., Paris. 190: 127, (1930).
6. Servigne, M., *Sur l'existence d'un acétylacétonate de polonium*. C. R. Acad. Sci., Paris. 196: 264-66, (1933).
7. Tomitaro Ishimore and Humihiko Sakaguchi, *Polonium dithizonate*. J. Chem. Soc., Japan Pure Chem. Sect. 71: 327, (1950).

8. Boussieres, G. and Ferradini, C., *Emploi de la dithizone pour séparer et purifier le radium D, le radium E et le polonium.* Anal. Chim., Acta 4: 610, (1950).

9. Hagemann, *The isolation of actinium.* J. Amer. Chem. Soc. 72: 768, (1950).

10. Boussieres, G., *Comportment de l'oxychlorure de polonium dans divers solvants organiques.* Bull. Soc. Chim. Fr. p. 536-38, (1952).

11. Karracker, D. G. and Templeton, D. H., *Polonium isotopes produced with energy particles.* Phys. Rev. (II) 81: 510, (1951).

12. Golden, J. and Maudock, A. G., *La aislación del protoactinio* (In press).

13. Martin, A. W., *Determination of the formula of an oxide of polonium.* J. Phys. Chem. 58: 911, (1954).

14. Morgan, G. T. and Elvins, *Interactions of tellurium tetrachloride and monoketones.* J. Chem. Soc. 127: 2625, (1925).

15. Haissinsky, M., *Recherche électrochimique sur le polonium.* J. Chim. Phys. 30: 27, (1933).

16. Guillot, M., *Sur les conditions de précipitation du polonium et sur quelques uns de ses dérivés complexes.* J. Chim. Phys. 28: 92, (1931).

17. Staritzky, E., *Some compounds of tetravalent polonium.* L.A. 1286, N.S.A. 5,5560.

18. Samartzeva, A. G., *Issledovanita po khimii poloniya. II. Poluchenie shestivalentnogo poloniya.* (The chemistry of polonium. II. Preparation of sexivalent polonium). Doklady Acad. Sci. U.R.S.S. 33: 498-501, (1941).

19. Guillot, M. (Reference 16).

20. Yost and Russel., *Systematic inorganic chemistry.* Prentice Hall p. 41, (1944).

21. Hicks and Stevenson, *Separation of tantalum and niobium by solvent extraction.* Anal. Chem. 25: 1517, (1933).

22. Escher-Desrivieres, J., *Contribution à l'étude de la chimie du polonium.* Ann. Chim. 5: 251-53, (1926).

Record of Proceedings of Session 108.2

FRIDAY AFTERNOON, 12 AUGUST 1955

Chairman: Mr. G. T. Seaborg (USA)

Vice-Chairman: Mr. D. I. Ryabchikov (USSR)

Scientific Secretaries: Messrs. J. Gaunt and D. J. Dewar

PROGRAMME

P/728	Radiochemical separations methods for the actinide elements	E. K. Hyde
P/674	On methods of separation of neptunium from plutonium	I. K. Shvetsov and A. M. Vorobyev
P/677	Coprecipitation of americium(V) with double carbonates of uranium(VI) or plutonium(VI) with potassium	G. N. Yakovlev and D. S. Gorbenko-Germanov
P/929	A tracer study of the partition of neptunium between nitric acid solutions and three organic solvents	J. Kooi

DISCUSSION

Mr. E. K. HYDE (USA) presented paper P/728 as follows: As an introductory topic, let us consider solvent extraction methods based on the formation of an organic chelate complex of one of the heavy elements and the removal of this complex from an aqueous solution into a nonpolar orgaoic solvent immiscible with water. A large number of chelating compounds have been used successfully, but the one which has demonstrated the most widespread applicability is the beta diketone called α-thencyltrifluoroacetone. This compound is conveniently referred to under the abbreviation TTA.

Slide 1 shows the structural formula of the compound. The compound was first synthesized and applied to heavy element extractions by Calvin and Reid and by their co-workers. The type of organic soluble metal chelate complexes that TTA forms is illustrated here by the actinium complex. TTA is in more widespread use than many other complexes because it is stable in strongly acidic solutions, it has a favarable keto-enol equilibrium, it is reasonable in cost, it has a low water solubility and because the complexes which it forms with various elements vary enormously in the equilibrium constant for their formation.

A typical equilibrium expression using actinium as a representative metal ion is:

$$Ac^{+3}_{(aq)} + 3HT_{(org)} \rightleftharpoons AcT_{3(org)} + 3H^{+}_{(aq)}$$

$$K_{(equil)} = \frac{(H^+)^3_{aq}}{(HT)^3_{org}} \times \left[\frac{AcT_{3(org)}}{Ac^{+3}_{(aq)}}\right]$$

$$\frac{AcT_{3(org)}}{Ac^{+3}_{(aq)}} = \text{distribution coefficient}$$

HT refers to thenoyltrifluoroacetone. The expression in brackets, labelled the "distribution coefficient," is the quantity in which the radiochemist is usually interested. This depends directly on the value of K which varies from 10^{10} to 10^{-15}, depending on the metal ion. However, it also depends—and this is a point which cannot be emphasized too strongly—to a high power on the acid concentration and to a high power on the concentration of the TTA in the organic solvent, usually benzene. This frequently makes possible very sensitive control of the course of the extraction. It makes it possible to direct a desired element into the organic phase, while leaving undesired elements in the aqueous phase.

The TTA extraction method is excellent for protactinium because the equilibrium constant is so great. Protactinium can be extracted from very strongly acidic solutions and the benzene phase can be washed repeatedly with aqueous acid solution in order to remove impurities.

The tetrapositive actinide element ions also are well extracted. Plutonium(IV) is particularly well extracted and can be removed from strongly acidic aqueous solutions, although not as easily as is protactinium. The equilibrium constant for thorium is about a factor of 1000 less, but good distribution coefficients are achieved if the acidity is dropped to a pH of 1 or 2. Uranium(IV) and neptunium(IV) lie between thorium and plutonium in extractability. Neptunium can be extracted away from plutonium by fixing the oxidation state of neptunium as the extractable (IV) state and of the plutonium as the unextractable (III) state before the extraction. The principal contaminants among the lighter elements

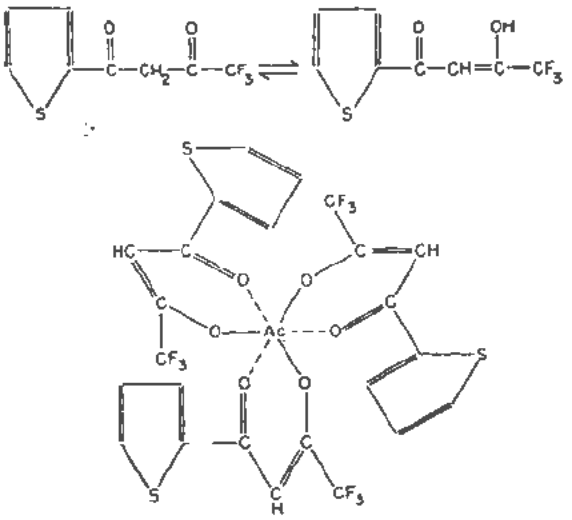

Slide 1. α-thenoyltrifluoroacetone

are zirconium(IV), hafnium(IV), iron(III), cerium(IV), tin(IV), and niobium(V).

The tripositive actinide elements do not have large equilibrium constants, but if the acidity is adjusted to somewhere in the pH range of 3.5 to 6, they too can be cleanly separated from a host of impurities. For example, Hagemann has removed milligram quantities of actinium from gram amounts of neutron-irradiated radium in this manner.

I should like to turn now to a consideration of the extraction of the nitrate or chloride salts of the heavy elements into certain organic solvents. The heavy-element group is rather outstanding in the readiness of the extraction of its members. I should like to make a few general remarks on the choice of solvents and choice of proper aqueous phase composition in order to get good extractions.

A number of organic compounds capable of extracting some or all of the heavy elements under suitable conditions are: ethyl ether; di-isopropyl ketone; methyl isobutyl ketone; dibutyl ether of ethylene glycol (dibutyl cellosolve); dibutyl or diethyl ether of diethylene glycol (dibutyl carbitol); dibutyl ether of tetraethylene glycol (pentaether); tri-*n*-butyl phosphate; and dialkyl phosphates.

Ethyl ether is chiefly useful for hexapositive uranium, neptunium, and plutonium. A large amount of research went into the study of the influence of nitric acid and of monovalent, divalent and trivalent neutral nitrate salts on the extractability of hexavalent uranium. It was found that extraction was low from dilute solutions. A high concentration of nitric acid increases the partition coefficient, but a greater increase is observed if the nitric acid concentration is in the range of 0.1 to 1 molar and if the salting strength is provided by a high concentration of such salts as ammonium nitrate, or, better still, magnesium nitrate or aluminium nitrate. The influence of the various salting agents holds true in a general way for the other solvents to be considered.

All the solvents listed are more powerful than ethyl ether, but for radiochemical laboratory scale work, ether is still frequently used because of its high specificity for the hexavalent actinide ions, because of the ease of removal of ether by evaporation and for other reasons.

The tetrapositive ions are poorly extracted by ether, but are well extracted by most of the other compounds. In general, extractability increases in going up the series from thorium(IV) to plutonium(IV). For a solvent such as methyl isobutyl ketone a rather high concentration of acid and nitrate salts in the aqueous phase is required. However, in the case of a solvent as excellent as tributyl phosphate, it is possible to obtain favorable partition coefficients with relatively low acid and salt concentration. This is well covered in other papers in this Conference such as McKay's paper P/441. In order to reduce the coextraction of undesirable impurities, the salt and acid concentrations are usually kept as low as possible, consistent with a workable partition coefficient for the desired element.

Protactinium(V) is the only pentapositive ion which has received much study. Protactinium is highly extracted into certain solvents from nitric acid or hydrochloric acid solutions. The effect of neutral salts is not quite the same for protactinium extraction, and in general neutral salts are not so necessary because of the high partition coefficients from moderately concentrated nitric acid or hydrochloric acid. Solvents which have proved effective for protactinium include di-isopropyl ketone, di-isopropyl and di-isobutyl carbinol, methyldioctyl amine, pentaether and tributyl phosphate. The tripositive actinide elements are extracted the least readily and in general are left in the aqueous phases.

As Slide 2 (Fig. 12 of P/728) shows, the extractability of the tripositive actinide and lanthanide elements into undiluted tributyl phosphate from very concentrated nitric acid is quite appreciable, particularly for the higher members of the series.

The data here are taken from the work of Peppard at the Argonne National Laboratory and of Gray and Thompson at California. Furthermore, if the acidity is made about 1 *M* in nitric acid and the solution is saturated with calcium or aluminium nitrate, even actinium, which is shown to have a low extraction, can be made to go into the tributyl phosphate with a very high distribution coefficient.

Separation of the heavy elements from each other can be achieved by taking advantage of differences in the behavior of the oxidation states. For example, uranium is quantitatively extracted from plutonium, which has been reduced to the tripositive state. Sometimes differences in complexing action with aqueous phase complexing agents may be useful. For example, the strong fluoride complex of protactinium can be made use of in removing protactinium from tributyl phosphate by washing the solvent with a mixture of hydrochloric acid and hydrofluoric acid.

Certain solvents have been found which have truly phenomenal extraction coefficients for some of the heavy elements even in the absence of salting agents. Examples of such solvents are the dibutyl or the dioctyl esters of phosphoric acid. Even dilute solutions of these compounds are powerful solvents. For various reasons these compounds will not replace the solvents we have already discussed for most radiochemical analysis work. However, for special purposes they are very helpful. For example, Stewart has concentrated the minute traces of uranium from a large volume of sea water into one hundredth the volume of organic solvent.

For my next topic I should like to say a few words about the application of cation exchange to the heavy elements. The adsorption of the tripositive lanthanide and actinide elements on a column of cation-exchange resin and the selective elution of the elements with buffered citric acid eluting solution is a procedure too well known to require review here. I wish only to call attention to a few developments. Many of these developments have arisen from the need for very rapid separation of the transcurium elements. The very great chemical similarity of berkelium to californium and to elements einsteinium, fermium and mendelevium, makes it obligatory to use the powerful cation-exchange method. The short half-lives of most isotopes of these elements make it equally important that the separations be effected as rapidly as possible, frequently within minutes.

One important point is to operate the column at an elevated temperature, such as 87°C rather than at room temperature. The column dimensions must be small and the resin carefully selected as to particle size and cross-linkage. The commercial resin presently preferred is Dowex-50, which is a co-polymer of vinyl benzene and divinyl benzene with nuclear sulfonic acid groups to provide exchangeable hydrogen ions.

Citric acid has been replaced by superior eluting agents.

Stewart has a paper in these Proceedings of this Conference (P/729, Session 10B.2, Volume 7) on the use of glycolic acid (α hydroxyacetic acid). Lactic acid also has been widely used. Slide 3 shows the clean cut separation of the actinide elements and of the lanthanide elements which can be achieved by using buffered lactic acid as the eluting agent. The California team of Thompson, Harvey and Choppin, responsible for the data shown on this slide, recently introduced the ammonium salt of α-hydroxy-isobutyric acid, which appears superior to all its predecessors for a fast separation of the actinide elements.

So much for the tripositive ions. The tetrapositive, pentapositive and hexapositive ions are readily adsorbed on cation-exchange resins. Data which have been published on this clearly indicate that a number of very promising new radiochemical separation techniques for thorium, protactinium, uranium, neptunium, and plutonium have not been fully explored.

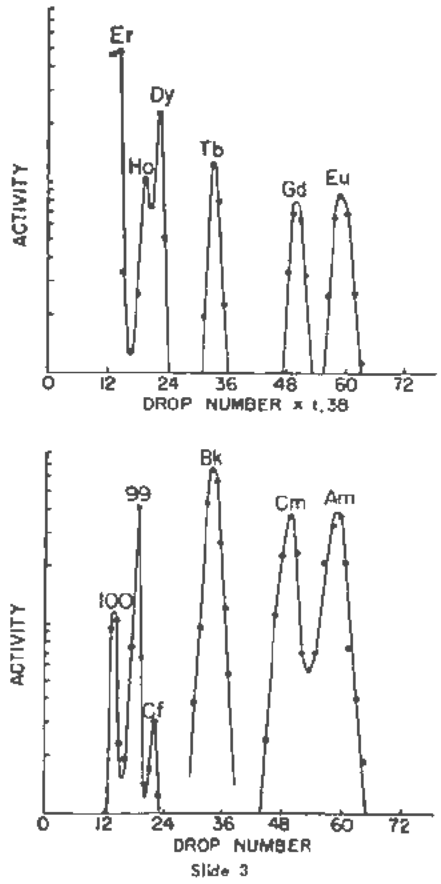

Slide 3

The case of the tetrapositive ions is particularly striking when hydrochloric acid of varying concentration is used to elute the elements from Dowex-50 cation-exchange resin. From dilute acid these ions are very strongly adsorbed. Thorium(IV), in fact, is strongly held even when elution with concentrated hydrochloric acid is attempted. But uranium(IV), neptunium(IV) and plutonium(IV), in that order, show an increasing tendency to form chloride complexes. Hence these ions and particularly plutonium(IV) are eluted rather quickly with concentrated hydrochloric acid. These facts are discussed in a paper by Diamond, Street, and Seaborg.

A consideration of the chloride complexes of the higher oxidation states of the actinide elements leads us into my next topic which is the anion-exchange behavior of the actinide elements.

One of the most interesting and certainly most useful developments of recent years has been the application of anion-exchange separations, particularly in hydrochloric acid solutions.

It has been found that negative chloride complexes of uranium, protactinium, neptunium, and plutonium are formed in concentrated solutions of hydrochloric acid and that these complexes are readily adsorbed on anion-exchange resins. Much work has been done on a commercial resin called Dowex-1 which is a co-

polymer of styrene and divinyl benzene with quaternary ammonium functional groups.

Adsorption behavior on anion-exchange resin from HCl can be summarized briefly as follows:

Hexavalent ions:	Pu(VI) < Np(VI) < U(VI) all strongly adsorbed
Pentapositive ions:	Pa(V) and Np(V) strongly adsorbed
Tetrapositive ions:	Th(IV) not adsorbed; U(IV) weakly adsorbed; Np(IV) and Pu(IV) strongly adsorbed
Tripositive ions:	Ac(III) and Pu(III) not adsorbed; elements 95–100 weakly adsorbed

Hexapositive uranium, neptunium and plutonium are readily adsorbed from hydrochloric acid solutions 6 molar or greater in concentration. They are readily desorbed with 0 to 3 molar hydrochloric acid. Plutonium(VI) can even be adsorbed from strong solutions of nitric acid. [In the written version of my paper an erroneous statement is made to the effect that uranium(VI) also adsorbs from concentrated nitric acid.]

Protactinium is readily adsorbed above 5 molar hydrochloric acid. Pentapositive neptunium is readily adsorbed above 4 molar HCl.

Thorium is not adsorbed at any HCl concentration at all. Tetrapositive uranium sticks only in very concentrated HCl, tetrapositive neptunium is adsorbed above 4 molar hydrochloric acid, plutonium(IV) is highly adsorbed and can be made to stick at any hydrochloric acid concentration above 2.5 molar.

Actinium(III), and the trivalent ions of the actinide series in general, do not adsorb although the elements beyond curium show a slight tendency to adsorb from aqueous solutions saturated in hydrochloric acid. Selective elution of these elements is possible.

A consideration of these facts makes it readily apparent that the actinide elements can be cleanly separated from each other by a proper choice of oxidation states and hydrochloric acid concentration. The laboratory manipulations are simple, rapid and quantitative when small amounts or when tracer amounts of the elements are used. The adsorption behavior of most of the fission products is known as was discussed by Kraus (P/837, Session 9B, this volume). Hence radiochemical procedures can be devised for decontamination.

This all too brief survey suggests the variety of excellent separations methods available in the heavy-element region. The variety is particularly striking in the case of neptunium and plutonium where several oxidation states can be obtained and stabilized in aqueous solution. These oxidation states have markedly different behavior in coprecipitation, in complex formation, in solvent extraction, in organic chelate complex extraction, in cation exchange and in anion exchange. When either of these elements is separated from a complex mixture of elements such as a fission product mixture it is usual to take advantage of the differing behavior of the various oxidation states in the course of the purification. The philosophy behind most of these procedures is that those impurities which accompany the plutonium or neptunium in one of the oxidation states will show quite distinct behavior from them when they are converted to a different oxidation state. This very powerful oxidation-reduction cycle method for the removal of impurities is not applicable to elements such as thorium or curium which exhibit but one oxidation state in aqueous solution.

Mr. V. N. Kosyakov (USSR) presented papers P/674 and P/677.

Mr. J. Koor (The Netherlands) presented paper P/929 as follows: As you may have seen from the paper submitted for this Conference we have carried out some experiments on the extraction of neptunium in its different oxidation states by means of organic solvents. We measured the partition coefficient α, defined as the ratio of the concentration of neptunium in the organic phase and in the water phase, as a function of the nitric acid concentration in the initial water layer. As solvents we have chosen diethyl ether, dibutyl carbitol and methyl isobutyl ketone. The neptunium tracer used was the 2.3 day Np^{239}.

The aim of the investigation was, apart from obtaining quantitative data possibly useful for extraction purposes of neptunium and gaining some insight into the solution chemistry of neptunium, to use the data obtained for this element as a first step for estimating the behavior of plutonium. For this reason too we carried out some additional measurements on uranium and thorium.

I should like to stress that our main interest has been to obtain as much quantitative experimental data as possible and that up to now we have not been able to go into detailed theoretical consideration of the curves obtained.

For the experimental procedure and the main part of the results, reference should be made to the paper. In this talk I should like to draw your attention especially for the results obtained with the (VI) state of the elements under consideration.

Slide 4 (Fig. 4 of P/929) shows the results for uranyl nitrate. The partition coefficient is plotted versus the concentration of nitric acid in the initial water layer for the three solvents mentioned. For diethyl ether some data may be found in literature, which have been included in the graph and which show a satisfactory agreement with our results. The curves have the typical S-shape so often found in extraction studies like this one, reaching an equilibrium value at higher nitric acid concentrations.

Slide 5 (Fig. 1 of P/929) gives the results ob-

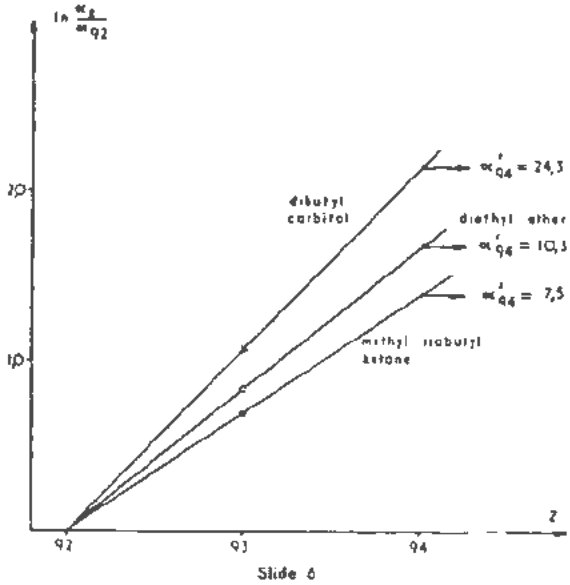

Slide 6

tained in the case of neptunium tracer in the (VI) state. It will be seen that for all solvents the partition coefficients are higher than for the uranium analogue.

Now it seems to be very tempting to try to predict, on the basis of these results, the values of α for the straight part of the curve for the (VI) state of plutonium. As a first, admittedly very rough, approximation—awaiting possible results of a closer examination of the different factors involved in the extraction process -one may plot the logarithm of the partition coefficient versus the atomic number of the element. In this way we may probably get an idea about the order of magnitude of the plutonium values by extrapolation from the presented data. This procedure is shown in Slide 6.

A plot of the logarithm of the ratio of the partition coefficients of the element and of uranium versus Z for the three solvents mentioned is shown here. Thus one arrives at the following values for the partition coefficient for plutonium(VI) at high nitric acid concentrations: 24.3 for dibutyl carbitol; 10.3 for diethyl ether; and 7.8 for methyl isobutyl ketone, respectively.

Now, during the last few weeks we have been able to obtain some preliminary data on the plutonium(VI) state. The plutonium solution used was of very low specific activity limiting seriously the accuracy of our results. It contained a 100-fold excess of uranium—a complication not believed to be serious in view of the results obtained with neptunium tracers in the presence of an even larger excess of uranium. The plutonium was oxidized to the (VI) state by means of silver nitrate and ammonium persulphate. The measurements were carried out at room temperature and the results at higher acid concentrations especially must be considered to be preliminary, in the sense that, owing mainly to the very low activity of the aqueous layers, the accuracy of the results is limited.

More accurate measurements are being carried out at present. However, our results, given in Slide 7, being somewhat lower than the predicted ones, are expected not to be too far off from the real values. We have, moreover, some reason to believe that the straight line values are probably a bit too high for dibutyl carbitol, and a bit too low for the other two solvents.

In Mr. Hyde's paper some values may be found for the extraction of plutonium(VI) by means of diethyl ether at nitric acid concentrations up to 5 *N*. As these data came to my knowledge only a few days ago, they could not be included in the graph.

Although they do fall a bit above our curve, it may be said, especially in view of the limited accuracy of our measurements, that they are in fair agreement with our data.

DISCUSSION OF P/728, P/674, P/677 AND P/929

The CHAIRMAN: Mr. J. J. Katz (USA) wishes to ask Mr. Kosyakov: "In the United States we have successfully separated Pa from Th by a volatilization procedure similar to that described by Shvetsov. Further, in P/823, submitted for this Conference, the United States describes volatility procedures for processing irradiated uranium. What is the general attitude of the scientists in the USSR towards volatility procedures of this kind?"

Mr KOSYAKOV (USSR): This method is certainly very valuable in that it yields such good results for a small engineering and economic outlay, as it is very simple and therefore easy to use. The application of

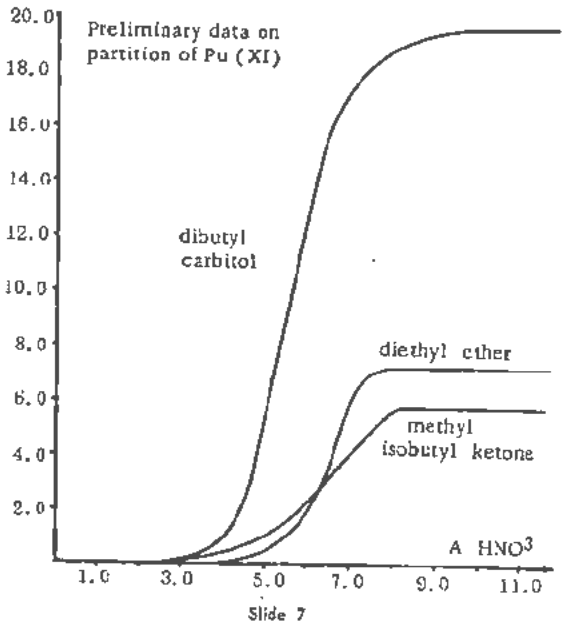

Slide 7

this method, not only to plutonium and neptunium, but also to the remaining elements is definitely of great importance and attention is being given to this question in our country as well as in all other countries, I should imagine.

The CHAIRMAN: The next question is from Mr. J. C. Hindman (USA) also to Mr. Kosyakov and he asks the following: "Have you made a direct chemical determination of the per cent yield of neptunium-237 compared to the plutonium? If so, what is your result?"

Mr. Kosyakov, you may have answered this during your comments when I heard you say that the amount is of the order of one-tenth of a per cent as much as undergoes the fission reaction. Is that right?

Mr. KOSYAKOV (USSR): In the paper I indicated that the ratio of neptunium to plutonium, i.e., the yield of neptunium, was 0.1 per cent, but this refers only to the first reaction, where the uranium has approximately its natural proportion of isotopes. In the case of uranium samples which have a greater enrichment of the light isotope, the neptunium proportion must be greater.

The CHAIRMAN: The next question is directed to Mr. Kooi in regard to his paper P/929 and it comes from Mr. E. K. Hyde (USA). The question reads as follows: "The extraction data for neptunium(IV) and neptunium(VI) presented by Mr. Kooi are very similar to unpublished data obtained in American laboratories. However, in the case of neptunium(V), I believe that the American data show much lower extraction. I wonder whether Mr. Kooi has made sufficient allowance for the rapid disproportionation of neptunium(V) in nitric acid solutions of greater than 5 molar concentration?"

I have a very similar question from Mr. H. A. C. McKay (UK). He asks the following: "What steps were taken to ensure that all the neptunium was in a single valency state? Could the same partition coefficients be obtained on extraction with two or more successive portions of solvent? A small admixture of a highly extractable species, for example Np(IV), can vitiate results with a less extractable species, for example Np(V)."

These are remarkably similar and I presume they could be answered at the same time.

Mr KOOI (The Netherlands): In answering these two questions I should like to say that we did our utmost to be sure that the solutions were given in the oxidation stage mentioned in the paper and that we checked it as far as possible by coprecipitation experiments. Secondly, we carried out our measurements as fast as possible, just to prevent changes in the valency state of the metal ions as well as we could, and in addition we varied the time of shaking by a factor of 4–10 in different experiments without finding any difference in the results. Therefore, I believe that our results are the best ones obtainable under the actual conditions under which we carried out our measurements. A more detailed discussion of these questions will be given later in one of the references, mentioned in the original paper.[5]

The CHAIRMAN: We have received another question directed towards Mr. Kosyakov in connection with paper P/677. The question comes from Mr. R. A. Penneman (USA) and it reads as follows: "You have given the stoichiometry of the orthorhombic $K_3AmO_2(CO_3)_2$. We have identified $KAmO_2CO_3$ as hexagonal. There are still one or more unidentified phases. Have you studied them?"

Mr. KOSYAKOV (USSR): An X-ray analysis of the compound $K_3AmO_2(CO_3)_2$ produced by the precipitation of americium from saturated carbonate solutions in an oxidizing medium has shown merely that it is not isomorphous with analogous compounds of hexavalent plutonium and uranium.

Session 10B.3

CHEMISTRY OF SPECIFIC HEAVY ELEMENTS

LIST OF PAPERS

Some Recent Developments in the Chemistry of Neptunium

By J. C. Hindman, Donald Cohen, J. C. Sullivan,* USA

The multiplicity of oxidation states exhibited by neptunium makes it one of the most interesting elements of the actinide series for chemical investigation. The early work on the aqueous chemistry of this element has been previously reviewed by Cunningham and Hindman.[1] It is the purpose of the present paper to summarize some of the more recent developments.

ISOLATION AND PURIFICATION OF NEPTUNIUM-237[2]

The recent work on the chemistry of neptunium has been aided by the isolation of gram quantities of the long-lived isotope, Np^{237}. Through the efforts of the Hanford Atomic Power Operations a quantity of Np^{237} was separated from uranium waste solutions by a precipitation process. The bulk composition of the composites as received is given in Table I. The neptunium was isolated from this material by solvent extraction.

Cycle I

The cycle I extraction equipment is shown in Fig. 1. The cycle I flowsheet is given in Fig. 2. The neptunium distribution was followed by the use of Np^{239} (β) tracer. The tracer solutions were reduced before addition to the feed make-up to insure isotope exchange equilibrium (see later summary). The total loss figures for the cycle I runs are summarized in Table II. The over-all recovery after the first hydroxide precipitation was 95.7%. The most serious losses occurred in runs 1-3 where a modification of the ferrous sulfamate process used in cycle II was utilized. This process was abandoned for the initial separation because: (*a*) the neptunium recovery was low (47%); (*b*) there was a carry-through of extraneous material, largely bismuth, into the strip (this caused serious interference in the hydroxide precipitation step); (*c*) the plutonium decontamination factor was low (2.5).

The following comment can be made about the stripping operation in cycle I. Difficulty was found in stripping the neptunium with small volumes of water or alkali solutions. This difficulty was eliminated after adoption of the nitrite strip. The effectiveness of this strip is presumably due to the reduction of the Np(VI) to Np(V).

* Argonne National Laboratory.

Table I. Composition of Concentrates
(Hanford Analyses)

Composite	HNO_3	*La*(III)	Pu^{239}	Np^{237}	*Volume*
1	2 *M*	0.65 *M*	18.85 gm	3.01 gm	25.8 l
2	2 *M*	0.65 *M*	20.71 gm	4.81 gm	26.2 l
		Total	39.56 gm	7.82 gm	52.0 l

Cycle II

The cycle II flowsheet is shown in Fig. 3. The most interesting aspect of the ferrous sulfamate process is the high acid concentration required for quantitative reduction. The behavior of neptunium in nitric acid solution appears similar to that in hydrochloric acid, where the rate of reduction of Np(V) to Np(IV) is favored by increasing hydrogen ion concentration.[3] It is probable that the poor yields in runs 1–3 of cycle I are related to this necessity to have high acid for quantitative reduction of the neptunium. Increasing the acid concentration in cycle I would have unduly increased the volume of solution to be handled.

The product recovery in cycle II is given in Table III. The total over-all yield through cycle II up to the hydroxide precipitation is $(95.7 \times 94.0) = 90\%$. The loss in the hydroxide supernatants was 0.46%. The total yield of cycles I and II was 89.5% of the original material. A pulse anaylsis of the cycle II product showed that the α content was $16 \pm 5\%$ Np^{237} and 84% Pu^{239}.

The increasing loss in the latter runs shown in Table III requires comment. The hydroxides before feed make-up in cycles II and III were dissolved in approximately 8.3 *M* HNO_3. Despite the fact that the hydroxides were heated to remove hexone before centrifugation, a considerable amount of organic matter carried through in the hydroxide. Very noticeable reaction was observed between this organic matter and the concentrated acid. It appears probable that the increasing losses can be attributed to complex formation between the end products of these reactions and the neptunium.

Cycle III

The cycle III flowsheet was the same as that in cycle II. Based on pulse analysis and alpha counts before and after this cycle, the losses were negligible. The product obtained from cycle III was $96.4 \pm 1.3\%$ $Np^{237}\alpha$ and 3.6% $Pu^{239}\alpha$. Based on the alpha count and pulse analysis of the cycle III material the original total neptunium was calculated to be 8.31 grams.

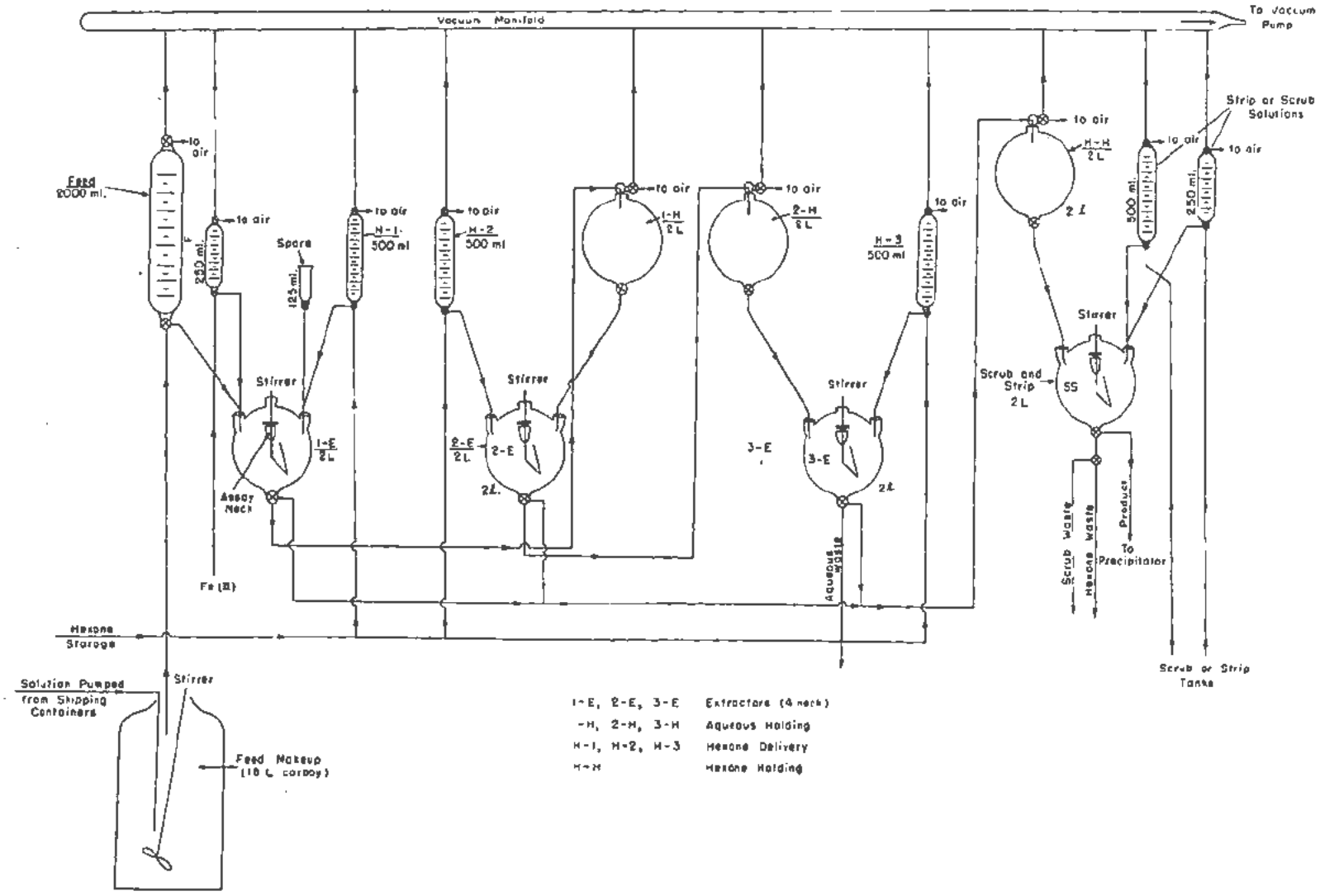

Figure 1. Cycle I: extraction equipment

Cycle IV

Preferential removal of neptunium from the product solution of cycle III was considered the best procedure for final purification. The principal gross metallic impurities in this stock were by weight, taking the Np as 100%, equal to: Bi 10%, Na 10%, Al 0.7%, Cu 0.7%, K 1.5%, Si 2%. The neptunium nitrate solutions from cycle III were converted to chloride by double hydroxide precipitation and then processed by the flowsheet shown in Fig. 4.

The resultant material from the cycle IV process analyzed (α content): batch 1, 4 gm Np^{237} (99.97% Np^{237}, 0.033 ± 0.033% Pu^{239}); batch 2, 3 gm Np^{237} (99.24% Np^{237}, 0.76 ± 0.3% Pu^{239}). No impurities were found spectrographically in greater quantities than shown by the reagent blanks.

The combined total of purified material was 7.08 grams. The over-all yield was 90.8% based on the Hanford analyses and 85.2% based on our estimate from the β yield after cycle III. In view of the experimental uncertainties, an average yield of 88 ± 3% was taken.

Table II. β Losses in Cycle I

(% of Total)

Runs	*Loss*	*Runs*	*Loss*
1,2,3	2.56%	24–28	0.06%
4–13	0.35%	29–57	0.43%
14-23	0.28%	OH^- supernatants	0.61%
		Total	4.29%

ELECTROCHEMISTRY OF NEPTUNIUM[4]

Studies of the electrolytic oxidation and reduction of neptunium ions have been undertaken for two reasons: (1) To establish conditions for the prepara-

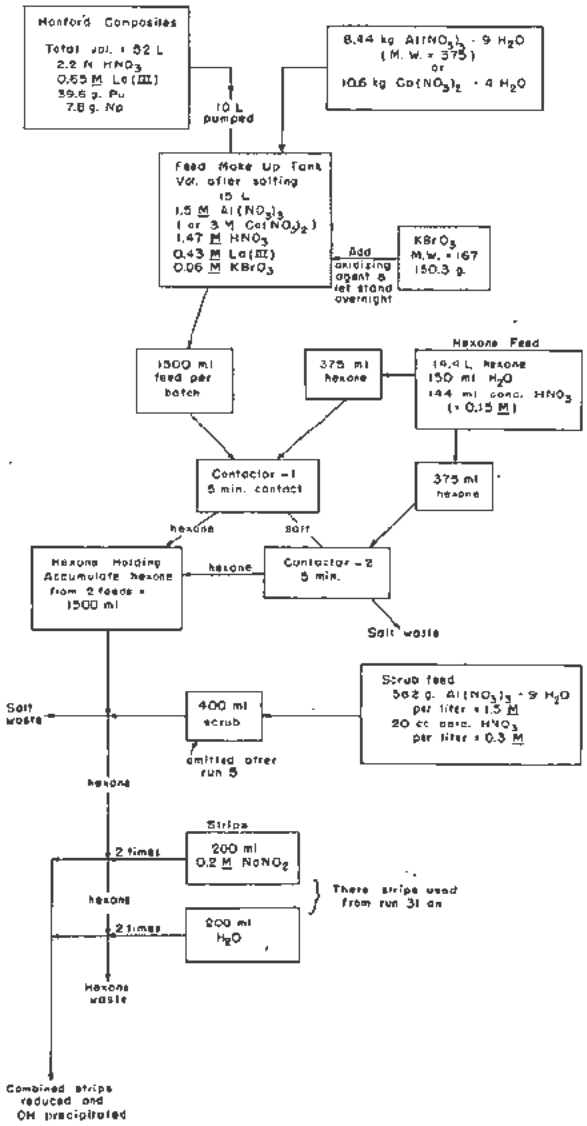

Figure 2. Cycle I: flowsheet 1B; (used for runs 4–57)

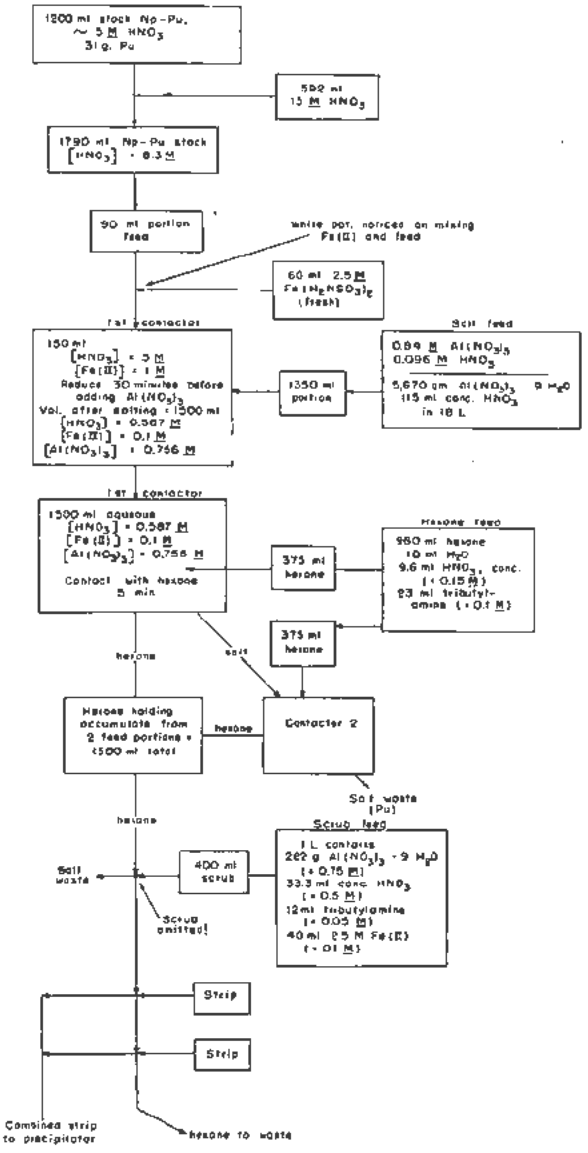

Figure 3. Cycle II: flowsheet II, Np-Pu separation

Table III. Product Recovery in Cycle II (β Loss)

% Cycle I product	Extraction loss (%)	Strip loss (%)	Yield %
0.88	0.78	0.64	98.6
0.88	2.31	1.40	96.5
0.88	1.84	0.25	97.9
0.88	2.65	0.22	97.1
0.88	2.34	0.11	97.7
0.88	3.12	0.10	96.8
0.88	4.31	0.03	95.7
0.88	6.67	0.17	93.2
4.94	10.8	0.10	89.1
2.68	8.28	0.10	91.6
1.27	6.90	0.10	93.0
	% Total product recovered		94.0

tion of a given oxidation state. The preparation of a desired oxidation state without the addition of extraneous oxidizing or reducing agents has obvious advantages in chemical studies. (2) To obtain knowledge about the type of processes involved in the electrode reactions. This aspect of the investigation is preliminary to a detailed investigation of the electrode kinetics.

Preparation of Oxidation States

The oxidation reduction reactions have been carried out using the controlled potential techniques.[5,6] The continuous control potentiostat and electrolysis cells were similar to those described by Wehner and Hindman.[7] Typical current voltage curves are shown in Fig. 5. Indicated in the figure are the thermodynamic oxidation potentials for the various couples. The Np(III)-Np(IV) and Np(V)-Np(VI) oxidations and reductions proceed readily near the thermodynamic oxidation potentials. Oxidation or reduction processes involving changes in state between Np(III) and Np(IV) or between Np(V) and Np(VI) are therefore readily carried out by appropriate adjustment of the electrode potentials according to Fig. 5.

On the other hand, preparation of lower states from Np(V) or higher states from Np(IV) require a more involved process. For example, because of the large overvoltage required for the reduction of Np(V) to Np(IV), Np(III) is produced. In the preparation of Np(IV) solutions, therefore, it is customary to reduce the neptunium completely to the +3 oxidation state and then reoxidize at the appropriate potential to give a Np(IV) solution. Similar remarks apply to the process for the preparation of Np(V) solutions from Np(IV).

The Electrode Reactions

From the fact that the Np(III)-Np(IV) and Np(V)-Np(VI) oxidations and reductions proceed readily near the thermodynamic oxidation potentials it is concluded that these reactions are essentially diffusion controlled processes. As expected, in these cases the diffusion current regions are well defined. To obtain a diffusion current for the reduction of Np(IV) to Np(III) it is necessary to use a mercury cathode. Diffusion currents proportional to the neptunium ion concentrations are obtained (see Fig. 6). Similarly, potential measurements by the zero-current method[8] give values of the oxidation potentials in reasonable agreement with those obtained by conventional electromotive force methods (see Table IV). The diffusion currents increase at a rate of 1–2 per cent per degree. This is similar to the temperature coefficient observed for polarographic diffusion currents.

An interesting phenomenon is observed in the reduction of Np(V). If a constant potential of −0.3 volt or less is applied, the current increases with time to a maximum at approximately the point where a coulometer indicates an average oxidation state of +4 and then falls off rapidly. This is illustrated in Fig. 7. These observations can be explained in terms of a mechanism involving the following reactions.

$$Np(V) + e^- \rightarrow Np(IV) \quad \text{slow} \quad (1)$$

$$Np(IV) + e^- \rightarrow Np(III) \quad \text{fast} \quad (2)$$

$$Np(III) + Np(V) \rightarrow 2\,Np(IV) \quad \text{very fast} \quad (3)$$

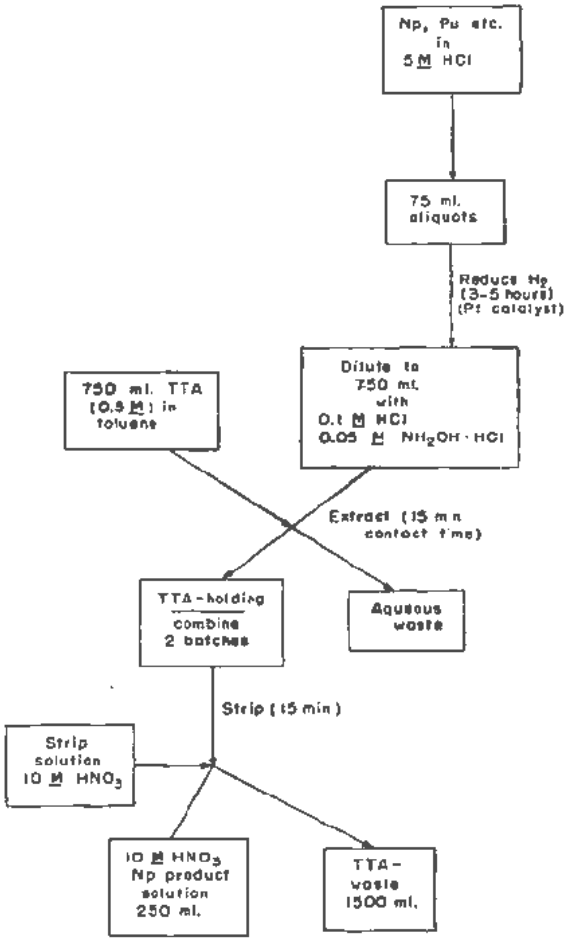

Figure 4. Cycle IV: flowsheet III

Table IV. Formal Oxidation Potentials of Neptunium Couples in 1 M $HClO_4$ at 25°

Couple	Oxidation potential (volts versus NHE)	
$Np^{+3}=Np^{+4}+e^-$	−0.15*	−0.155[9]
$NpO_2^+=NpO_2^{++}+e^-$	−1.17*	−1.137[9]

* From zero-current measurements.

After the initial reduction of part of the Np(V) by reaction (1), reaction (2) and (3) become dominant. A similar effect is not observed in the course of the oxidation of Np(IV) to Np(V), presumably because of the relative slowness of the Np(IV)-Np(VI) reaction.

KINETICS OF REACTIONS INVOLVING NEPTUNIUM IONS

There is at the present time an increasing amount of interest in both the experimental and theoretical aspects of the kinetics of reactions involving metal ions. The principal bar to future progress in this field is the lack of quantitative data. The number and relative stabilities of the oxidation states of neptunium are such as to offer a unique opportunity for such kinetic investigations. An extensive study of the reactions of neptunium ions has therefore been undertaken.

In addition to the fundamental aspects of these investigations, two practical considerations that make such investigations of interest should be noted. First, the application of tracer methods for following chemical reactions requires a knowledge of the rate at which isotopic equilibrium is established. Second, proper design of separation processes involving oxidation-reduction necessitates knowing the kinetics of the reactions involved.

The reactions of neptunium that have been studied to date include the net reaction of Np(IV) and Np(VI) to give Np(V),[10] the isotope exchange reaction between Np(IV) and Np(V),[11] and the isotopic exchange reaction between Np(V) and Np(VI),[12] all in perchlorate solution. In the latter case the experimental work has been extended to nitrate and chloride media.[13]

The Np(IV)-Np(VI) Reaction[10]

The rate law for the forward reaction, $Np(IV) + Np(VI) = 2\ Np(V)$, is given by

$$-d(Np^{+4})/dt = k_1^0\ [Np^{+4}]\ [NpO_2^{++}]\ [H^+]^2 \quad (1)$$

At 25°C and $\mu = 2.0$, $k_1^0 = 2.69 \pm 0.23$ mole-liter^{-1}-sec^{-1}. The single rate law is observed for hydrogen ion concentrations varying from 0.2*M* to 2.0*M*. The rate is not appreciably affected by change in ionic strength from $\mu = 0.5$ to $\mu = 2.0$.

The Arrhenius energy of activation, E, has been found to be 25.2 ± 1.6 kcal. The heat and entropy of activation for the reaction were calculated from the rate expression for the transition state theory:[14]

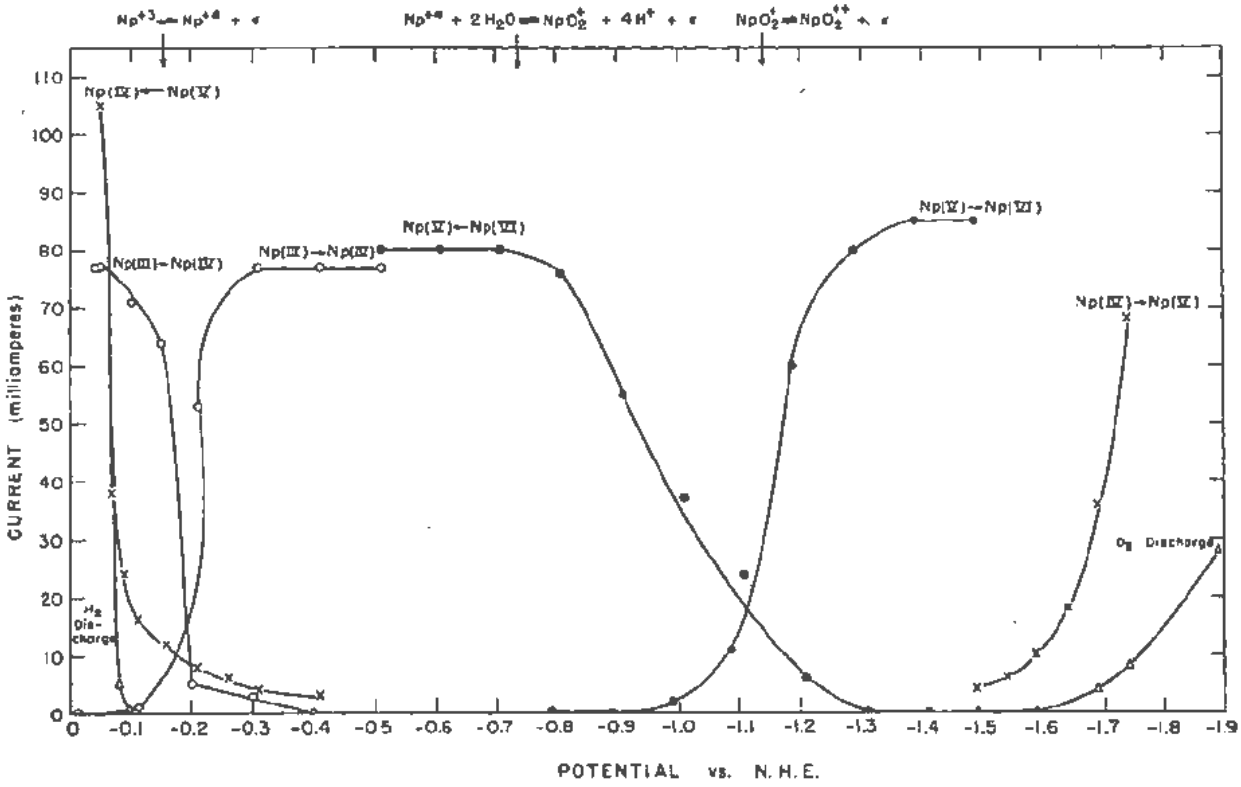

Figure 5. Current-voltage curves for oxidation-reduction reactions of neptunium

$$k_1^\circ = \frac{\rho kT}{h} e^{\Delta S^*/R} e^{-E/RT} = \frac{ekT}{h} e^{\Delta S^*/R} e^{-(\Delta H^* + RT)/RT} \quad (5)$$

The values are: $\Delta H^* = 24.6 \pm 1.6$ kcal, $\Delta S^* = 17.8 \pm 2.7$ cal-deg^{-1}, and $\Delta F^* = 19.3 \pm 1.6$ kcal.

Based on the observed stoichiometry, a number of mechanisms can be postulated for the reaction. Two of these are

$$Np^{+4}(aq) + H_2O \rightleftharpoons NpO^{++} + 2\ H^+ \quad \text{rapid equilibrium} \quad (6)$$

followed by

$$NpO^{++} + NpO_2^{++} \rightleftharpoons [O\text{-}Np\text{-}O\text{-}Np\text{-}O]^{+4} \rightarrow NpO_2^+ + NpO^{+3} \quad (7)$$

and then

$$NpO^{+3} + H_2O \rightleftharpoons NpO_2^+ + 2\ H^+ \quad \text{rapid equilibrium} \quad (8)$$

Alternatively we may write

$$Np^{+4}(aq) + 2\ H_2O \rightleftharpoons Np(OH)_2^{+2} + 2\ H^+ \quad \text{rapid equilibrium} \quad (9)$$

$$Np(OH)_2^{+2} + NpO_2^{++} \rightleftharpoons [O\text{-}Np\text{-}O\text{—}H\text{-}O\text{-}Np\text{-}O\text{-}H]^{+4} \rightarrow 2\ NpOOH^{+2} \quad (10)$$

and

$$NpOOH \rightleftharpoons NpO_2^+ + H^+ \quad \text{rapid equilibrium} \quad (11)$$

There is, at the present time, no experimental data that would indicate the most probable mechanism.

The Np(IV)-Np(V) Exchange[13]

The exchange reaction between Np(IV) and

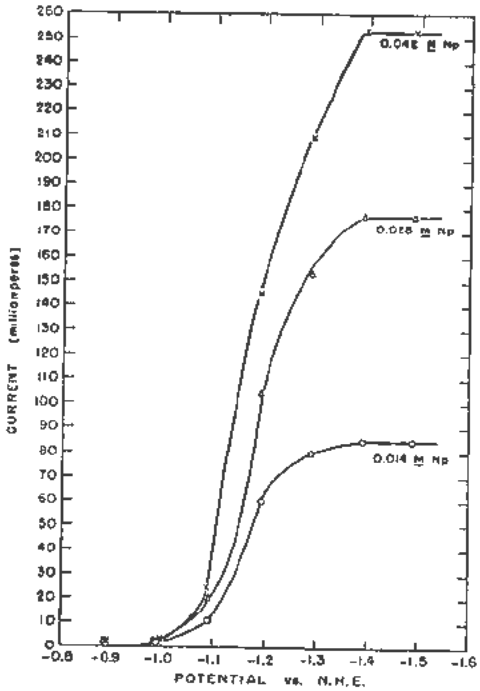

Figure 6. Current-voltage curve obtained in the oxidation of Np(V) to Np(VI)

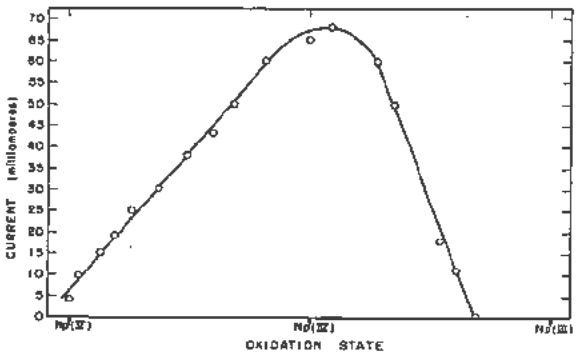

Figure 7. Current-time behavior in reduction of Np(V) at a cathode potential of approximately −0.15 volt.

Np(V) has been found to be complex. Figure 8 illustrates the division of the rate, R, into two paths depending on the acid concentration. The rate law for the high acid path involves a first power of the hydrogen ion and for the low acid path an inverse second power. The over-all rate equation can be expressed as

$$R = k_1 [NpO_2^+]^2 [H^+] + k_2 [Np^{+4}]^{1.5} [NpO_2^+]^{0.5} [H^+]^{-2} \quad (12)$$

The Arrhenius heat of activation, E, has been found to be 18.2 ± 0.2 kcal for the high acid path and 37.4 ± 0.5 kcal for the low acid path. The related quantities, ΔH^* and ΔS^* for the two mechanisms were calculated according to Equation 5. The experimental results are tabulated in Table V.

The mechanisms of the exchange reactions for both acid regions appear to be complex. The stoichiometry of the reaction for the high acid path is the same as that observed for the disproportionation of uranium(V).[15,16] This suggests that the exchange reaction may be

$$2\ Np^*O_2^+ + H^+ \rightleftharpoons [X^*]^{+3} \rightleftharpoons Np^*O_2^{++} + Np^*O_2H^+ \quad (13)$$

$$Np^*O_2H^+ + Np(OH)_2^{+4} \rightleftharpoons NpO_2H^+ + Np^*(OH)_2^{++} \quad (14)$$

The stoichiometry of the disproportionation reaction (13) does not have the same form as has been adduced from the over-all reaction

$$Np^{+4} + NpO_2^{++} + 2\ H_2O \rightleftharpoons 2\ NpO_2^+ + 4\ H^+ \quad (15)$$

and the kinetic data for the Np(IV)-Np(VI) reaction. However, it is possible that the disproportionation reaction should be written as

$$2\ NpO_2^+ + H^+ \rightleftharpoons [X^*]^{+3} \rightarrow NpO_2^{++} + NpO_2H^+ \quad (16)$$

followed by a series of reactions

$$NpO_2H^+ + H^+ \rightarrow Np(OH)_2^{++} \quad (17)$$

$$Np(OH)_2^{++} + H^+ \rightarrow Np(OH)^{+3} + H_2O \quad (18)$$

$$Np(OH)^{+3} + H^+ \rightarrow Np^{+4} + H_2O \quad (19)$$

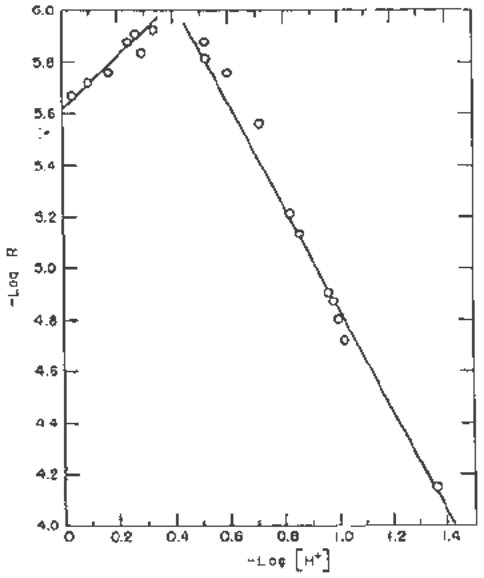

Figure 8. Plot of log [H+] against log R for Np(IV)-Np(V) exchange at 47.4°C with 0.0203 M Np(IV) and 0.0225 M Np(V); $\mu = 1.2$

with the rate determining step being reaction 16. Although the stoichiometry of the disproportionation reaction has not been experimentally verified, the free energy, heat and entropy of activation are known from the data on the Np(IV)-Np(VI) reaction[16] and on the over-all equilibrium (Equation 15).[17] In Table V are given the energetics of the disproportionation reaction calculated from these data. Although the activation energy for the exchange and disproportionation reactions are identical, the exchange proceeds at a much faster rate than does the gross reaction. It would appear that the activated state is not the same in the two cases. For example, the activated state corresponding to reaction[16] may be $[O\text{-}Np\text{-}O\text{-}H\text{—}O\text{-}Np\text{-}O]^{+3}$ while for the Np(IV)-Np(VI) reaction the activated state may be $[O\text{-}Np\text{-}O\text{—}Np\text{-}O]^{+6}$ or $[O\text{-}Np\text{-}O\text{-}H\text{—}O\text{-}Np\text{-}O\text{-}H]^{+4}$ (see Equation 7).

The mechanism for the exchange in the low acid region also presents an interesting problem. The observed rate (Equation 12) can be expressed in terms of the following simple reactions. First the equilibrium

$$Np^{+4} + Np^{*}O_2^{+} \rightleftharpoons Np^{*}O_2^{++} + Np^{+3} \qquad (20)$$

whence

$$[Np^{*}O_2^{++}] = [Np^{+3}] = K^{0.5}[Np^{+4}]^{0.5}[Np^{*}O_2^{+}]^{0.5} \qquad (21)$$

also the hydrolytic equilibrium (reaction 9) with exchange

$$Np(OH)_2^{++} + Np^{*}O_2^{++} \rightleftharpoons [X^{*}]^{+4} \rightarrow Np^{*}(OH)_2^{++} + NpO_2^{++} \qquad (22)$$

Reactions (9) and (22) correspond in stoichiometry to the rate law found for the formation of Np(V) from Np(IV) and Np(VI). In the exchange mechanism as written above, the reproportionation

Table V. The Free Energies, Heats and Entropies of Activation for the Np(IV)-Np(V) Exchange Processes at 25° C

Reaction path	ΔF^{*} kcal-mole^{-1}	ΔH^{*} kcal-mole^{-1}	ΔS^{*} cal-deg^{-1}-mole^{-1}
High acid (experimental)	24.2	17.6	−22.2
(calculated from disproportionation)	28.5	17.1	−38.1
Low acid (experimental)	27.2	36.8	32.1
(calculated from Np(IV)–Np(VI) reaction)	30.6	41.5	37.1

reaction (10) is the rate determining process. Both the values of the equilibrium constant in reaction (21) and the value of the rate constant for reaction (10) have been determined. Appropriate substitution gives

$$R = k_2[Np^{+4}]^{1.5}[NpO_2^{+}]^{0.5}[H^{+}]^{-2} = K^{0.5}k_1^{0}[Np^{+4}]^{1.5}[NpO_2^{+}]^{0.5}[H^{+}]^{-2} \qquad (23)$$

whence

$$\frac{k_1^{0}}{k_2} = \sqrt{\frac{1}{K}} \qquad (24)$$

but upon substitution of the measured values

$$\frac{2.69}{3.87 \times 10^{-6}} \neq \sqrt{\frac{1}{25 \times 10^{-10}}} \qquad (25)$$

As is shown by the data in Table V, the exchange reduction for the low acid path proceeds at a much faster rate than would be calculated assuming the same mechanism as observed in the net reaction of Np(IV) and Np(VI). The fact that in both cases the exchange reaction proceeds at a much more rapid

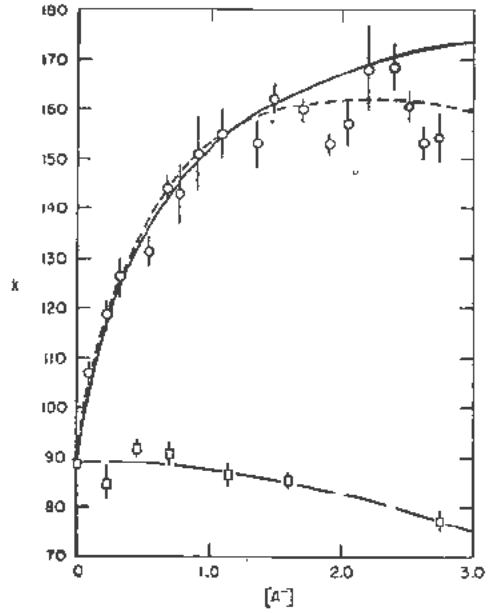

Figure 9. The effect of anions on the exchange rate $t = 0$°C, $\mu = 3.0$, $[H^{+}] = 3.0$: ——— single chloride complex, NpO_2Cl^{+}; – – – two chloride complexes, NpO_2Cl^{+} and NpO_2Cl_2; — — nitrate solution

rate than the formally related net reaction indicates the care that must be exercised in utilizing the results of exchange experiments in deducing the gross rate of reaction.

The Np(V)-Np(VI) Exchange[12,13]

The exchange reaction involving Np(V) and Np(VI) is of particular interest when considered in the light of recent theoretical proposals regarding the nature and the factors affecting electron transfer reactions in solution.[13,19,20] Both the Np(V) and Np(VI) ions are doubly oxygenated, with the Np-O distances reasonably close (~0.06 A). In this case it is expected that the primary hydration spheres are also very nearly identical. Calculation indicates that within the amplitude of the zero point energy vibration, the structures of the two ions will match. By application of the Franck-Condon principle,[19] this structural similarity is concomitant with a high probability for the electron transfer process.

The exchange reaction is first order in each of the metal ions and zero order in hydrogen ion. The bimolecular rate constant, k, is 29.8 liters-mole^{-1} sec^{-1} at 25°C and $\mu = 1.0$. The comparatively small difference between the heat and entropy of activation in the present case and that for the Fe(II)-Fe(III) exchange systems (Table VI) is surprising in view of the expected diminution on the barrier for exchange.

Table VI. Energies and Entropies of Activation for the Exchange Reactions of NpO_2^+ and NpO_2^{++}, and of Ferrous Ion with Various Ferric Species

	E_{act} (kcal-mole^{-1})	ΔS^* (cal-deg^{-1}-mole^{-1})
$NpO_2^+ - NpO_2^{++}$	8.3	−24
$Fe^{++} - Fe^{+++}$	9.9	−25
$Fe^{++} - Fe(OH)^{++}$	7.4	−18
$Fe^{++} - FeCl^{++}$	8.8	−24
$Fe^{++} - FeF^{++}$	9.1	−20

In an effort to further determine the factors affecting the exchange, the influence of nitrate and chloride ions on the rate have been determined. Figure 9 illustrates the results. If the slight decrease in the exchange rate at higher nitrate is attributed to the incipient formation of a nitrate complex of Np(VI), then the exchange rate through this path must be low. On the other hand the observed effect may be due solely to activity effects.

The exchange rate is markedly catalyzed by chloride. The data can be explained in terms of either one or two complexes of Np(VI). The energy, entropy and free energy values for the possible exchange paths are given in Table VII.

The effect of the halide complexing is much greater than observed in the Fe(II)-Fe(III) exchange studies.[21] If the similarity in the energetics in the iron systems are considered to indicate a single operative mechanism, then a change in mechanism

Table VII. Energy, Entropy and Free Energy of Activation for the Different Exchange Paths

Path	$t=0°C$ E_{exp} (kcal-mole^{-1})	$\mu=3.0$ ΔS^* (cal-deg^{-1}-mole^{-1})	ΔF^* (kcal-mole^{-1})
$NpO_2^+ - NpO_2^{++}$	10.6	−12.6	13.48
$NpO_2^+ - NpO_2Cl^+$	16.6*	10.9	13.06
$NpO_2^+ - NpO_2Cl^+$	15.4	6.7	13.02
$NpO_2^+ - NpO_2Cl_2$	15.3	5.0	13.52

* Assuming a single path through chloride.

between the chloride independent and chloride dependent paths appears likely for the Np(V)-Np(VI) system.

The argument can be advanced that if the NpO_2^+-NpO_2^{++} exchange proceeds by way of a hydrogen atom transfer, as suggested by Hudis and Wahl[21] to explain the iron data, then the NpO_2^+-NpO_2Cl^+ exchange probably proceeds by a chlorine atom transfer. If more than a single path through chloride is involved, the data suggests that the mechanism is the same in both cases.

Similarly, if the NpO_2^+-NpO_2^{++} exchange proceeds by a direct electron transfer via the tunneling mechanism of Marcus, Zwolinski and Eyring,[19] then the NpO_2^+-NpO_2Cl^+ exchange presumably proceeds by an atom transfer mechanism. This conclusion is based on the argument that, although it may be possible to fit the NpO_2^+-NpO_2^{++} data to the direct electron transfer process by appropriate adjustment of the empirical parameters in the equations, the positive entropy of activation precludes this mechanism for the halide dependent path if the electronic transmission coefficient, κ_t, is defined by the relation $\Delta S^* = R \ln \kappa_t$. The simplest explanation would be to assume that the halide dependent path involves a chlorine atom transfer:

$$NpO_2Cl^+ + Np^*O_2^+ = [O_2NpCl\text{—}Np^*O_2]^{++} - NpO_2^+ + Np^*O_2Cl^+ \quad (26)$$

It should be pointed out that the results of any calculations such as those of Marcus, Zwolinski and Eyring will depend on the model assumed for the activated complex. For example, a possible model for the activated complex involving the uncomplexed ions would be

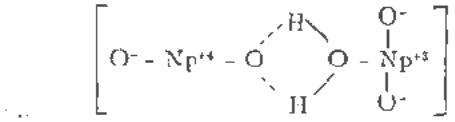

(A)

An alternative model for the activated complex involving chloride, or where the exchange in the uncomplexed species proceeds through water, would be

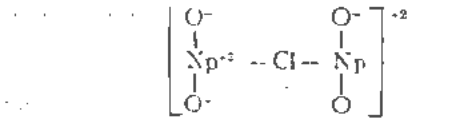

(B)

Assume that the bridging is through water molecules. In model (A) no rearrangement in the hydration spheres would be involved. In model (B) water would be unfrozen in the formation of the intermediate. Furthermore, because of the difference in charge distribution there would be a significant difference in the repulsion energy for the two models. Although direct electron transfer could presumably occur in either case there would be a marked difference in both energy and entropy values. A similar argument can be made if direct electron transfer occurs and the activated complex formed for the uncomplexed species is (A) and for the halide complexed species is (B). It would, therefore, appear naive to attempt to argue about the probable mechanism from the energetics alone.

THERMODYNAMICS OF SOLUTION

Distribution studies with the aid of the chelating agent theonyltrifluoroacetone, have been used to establish the existence of the $Np^{+4}(aq)$ ion as the predominant species in perchloric acid solution.[22] These measurements have been extended to a study of the association of Np^{+4} with sulfate ion. The kinetic data on the Np(V)-Np(VI) exchange has been used to obtain thermodynamic data on the Np(VI) chloride complex ions.[13]

The Sulfate Complexes of Np(IV)[22]

The thermodynamic data on the Np(IV) sulfate complexes were obtained at $\mu = 2.0$. No evidence was obtained for the presence of more than two complexes. The successive reactions may be written

$$Np^{+4} + HSO_4^- \rightleftharpoons NpSO_4^{++} + H^+ \qquad (27)$$

$$k_1 = \frac{[H^+][NpSO_4^{++}]}{[Np^{+4}][HSO_4^-]} \qquad (28)$$

$$NpSO_4^{++} + HSO_4^- \rightleftharpoons Np(SO_4)_2 + H^+ \qquad (29)$$

$$k_2 = \frac{[H^+][Np(SO_4)_2]}{[NpSO_4^{++}][HSO_4^-]} \qquad (30)$$

Values of the constants obtained at different temperatures are given in Table VIII.

From the temperature dependence of the association constants the partial molal heat and entropy changes of reactions (27) and (29) have been calculated. These are given in Table IX.

Combining these data with the value for the dissociation constant of bisulfate at $\mu = 2.0$[23] and the value for the heat of dissociation,[24] the thermodynamic constants for the reactions

$$Np^{+4} + SO_4^{--} \rightleftharpoons NpSO_4^{++} \qquad (31)$$

and

$$NpSO_4^{++} + SO_4^{--} \rightleftharpoons Np(SO_4)_2 \qquad (32)$$

are obtained. For reaction (31) we calculate $\Delta F = -4.79$ kcal-mole^{-1}, $\Delta H = 4.0$ kcal-mole^{-1} and $\Delta S = 30$ cal-deg^{-1}, and for reaction (32), $\Delta F = -2.89$ kcal-mole^{-1}, $\Delta H = 8.84$ kcal-mole^{-1} and $\Delta S = 39$ cal-deg^{-1}. The reactions proceed only because of the entropy changes.

Table VIII. Constants for the Stepwise Association of Np^{+4} and HSO_4^-

	10.2°C	25.2°C	35.3°C
k_1	296±30	270±27	250±25
k_2	8.11±1.62	11.0±2.2	13.7±2.7

The Chloride Complexes of Np(IV)[13]

Assuming that the catalytic effect of chloride on the rate of the Np(V)-Np(VI) exchange can be interpreted in terms of reaction paths involving chloride ion, the data can be analyzed to give values of the association constants of the chloride complexes. The kinetic data at 0°C can be fit up to a concentration of 1.5M Cl^- by the assumption of either one or two complexes. Despite the large experimental uncertainties at higher chloride the data are best represented in this region by a mechanism involving two chloride paths. The alternative possibility is that the slow falling off of the rate in the high chloride region and the similar effect at high nitrate in the nitrate-perchlorate solutions can be interpreted in terms of activity coefficient changes. In the absence of evidence favoring either one of these interpretations, the data have been analyzed both in terms of a single complex and two complexes of Np(VI).

For the association reactions

$$NpO_2^{++} + Cl^- \rightleftharpoons NpO_2Cl^+ \qquad (33)$$

$$K_1 = \frac{[NpO_2Cl^+]}{[NpO_2^{++}][Cl^-]} \qquad (34)$$

$$NpO_2Cl^+ + Cl^- \rightleftharpoons NpO_2Cl_2 \qquad (35)$$

$$K_2 = \frac{[NpO_2Cl_2]}{K_1[NpO_2^{++}][Cl^-]^2} \qquad (36)$$

the constants obtained at different temperatures are given in Table X.

Table IX. Values for the Free Energy, Heat and Entropy Changes in the Reactions of Bisulfate and Neptunium(IV)

Reaction	ΔF (kcal-mole^{-1})	ΔH (kcal-mole^{-1})	ΔS (cal-deg^{-1})
$Np^{+4}+HSO_4^-=$ $NpSO_4^{++}+H^+$	−3.3	−1.17	7.2
$NpSO_4^{++}+HSO_4^-=$ $Np(SO_4)_2+H^+$	−1.42	3.64	17.0

Table X. Association Constants for the Reaction of Cl^- and NpO_2^{++}

Temp. (°C)	K_1*	K_1	K_2
0.0	1.62	1.26	0.20
4.78	1.15	1.00	0.18
9.84	0.87	0.81	0.16

* Assuming the single complex of reaction (33).

Analysis of the data yields values for the change in heat content and entropy in the formation of the chloro complexes. If a single exchange path is assumed, then $\Delta H_{273} = -8.7$ kcal-mole^{-1} and $\Delta S_{273} = -32.2$ cal-deg^{-1} for reaction (33). The large negative quantities for the heat and entropy change in the formation of the complex is unexpected. Although the assumption of two chloride complexes leads to more positive values the difference is not marked. The computed values of the heat and entropy change are $\Delta H_{273} = -6.9$ kcal-mole^{-1} and $\Delta S_{273} = -21$ cal-deg^{-1} for reaction (33) and $\Delta H_{273} = 3.5$ kcal-mole^{-1} and $\Delta S_{273} = 16$ cal-deg^{-1} for reaction (35).

In magnitude, the association constant for the first Np(VI) chloride complex is very similar to that reported for U(VI).[25,26] At 10°, K, for the U(VI) chloride complex has been given as 0.58.[26] The two systems differ, however, in that the U(VI) complex is stabilized by increasing temperature, $\Delta H_{298} = 3.8$ kcal-mole^{-1} and $\Delta S_{298} = 12$ cal-deg^{-1}. The underlying cause of the difference in behavior is not obvious.

REFERENCES

1. Cunningham, B. B. and Hindman, J. C., *The Chemistry of Neptunium*, Chap. 12 "The Actinide Elements," McGraw-Hill Book Co., New York, N. Y., (1954).
2. Hindman, J. C., Wehner, Philip, Sullivan, J. C. and Cohen, Donald, unpublished report, *The Isolation and Purification of Neptunium-237 Obtained from Hanford Wastes.*
3. Magnusson, L. B., Hindman, J. C. and LaChapelle, T. J., *Kinetics and Mechanisms of Aqueous Oxidation-Reduction Reactions of Neptunium* Paper 15.11 "The Transuranium Elements," McGraw-Hill Book Co., New York, N. Y., (1949).
4. Cohen, Donald and Hindman, J. C., unpublished work.
5. Hickling, A., Studies in Electrode Polarization. Part IV., *The Automatic Control of the Potential of a Working Electrode*, Trans. Faraday Soc. 38:27 (1942).
6. Lingane, J. J., *Recent Applications of Controlled Potential Electrolysis*, Discussions of the Faraday Soc., No. 1, 203 (1947).
7. Wehner, P. and Hindman, J. C., *The Lower Oxidation States of Ruthenium in Acid Perchlorate Solutions*, J. Am. Chem. Soc. 72:3911 (1950).
8. Kolthoff, I. M. and Orlemann, E. F., *The Use of the Dropping Mercury Electrode as an Indicator Electrode in Poorly Poised Systems*, J. Am. Chem. Soc. 63:664 (1941).
9. Cohen, Donald and Hindman, J. C. *Oxidation Potentials of the Neptunium (III)-(IV) and the Neptunium (V)-(VI) Couples in Perchloric Acid*, J. Am. Chem. Soc. 74:4679 (1952).
10. Hindman, J. C., Sullivan, J. C. and Cohen, Donald, *Kinetics of Reactions between Neptunium Ions. The Np(IV)-Np(VI) Reaction in Perchlorate Solution*, J. Am. Chem. Soc. 76:3278 (1954).
11. Sullivan, J. C., Cohen, Donald and Hindman, J. C., *Isotopic Exchange Reactions of Neptunium Ions in Solution. II. The Np(IV)-Np(V) Exchange*, J. Am. Chem. Soc. 76:4275 (1954).
12. Cohen, Donald, Sullivan, J. C. and Hindman, J. C., *Isotopic Exchange Reactions of Neptunium Ions in Solution. I. The Np(V)-Np(VI) Exchange*, J. Am. Chem. Soc. 76:352 (1954).
13. Cohen, Donald, Sullivan, J. C. and Hindman, J. C., *Isotopic Exchange Reactions of Neptunium Ions in Solution. III. The Effect of Chloride and Nitrate Ions on the Rate of the Np(V)-Np(VI) Exchange*, J. Am. Chem. Soc., to be published
14. Glasstone, S., Laidler, K. and Eyring, H., "The Theory of Rate Processes," McGraw-Hill Book Co., Inc., New York, N. Y., 1941, pp. 197-199.
15. Kern, D. M. H. and Orlemann, E. F., *The Potential of the Uranium(IV), Uranium(VI) Couple and the Kinetics of Uranium(V) Disproportionation in Perchlorate Media*, J. Am. Chem. Soc. 71:2102 (1949).
16. Heal, H. G. and Thomas, J. G. N., *Unstable Ions of Quinquavalent Uranium*, Trans. Faraday Soc. 45:11 (1949).
17. Cohen, Donald and Hindman, J. C., *The Neptunium (IV)-Neptunium(V) Couple in Perchloric Acid. The Partial Molal Heats and Free Energies of Formation of Neptunium Ions*, J. Am. Chem. Soc. 74:4682 (1952).
18. Libby, W. F., *Theory of Electron Exchange Reactions in Aqueous Solutions*, J. Phys. Chem. 56:863 (1952).
19. Marcus, R. J., Zwolinski, B. J. and Eyring, H., (*a*) *The Electron Tunnelling Hypothesis for Electron Exchange Reactions*, J. Phys. Chem., 58:432 (1954); (*b*) *Inorganic Oxidation-Reduction Reactions in Solution*. Electron Transfers, Chem. Rev. 55:157 (1952)
20. Weiss, J., *On the Theory of Electron-transfer Processes in Aqueous Solutions*, Proc. Roy. Soc. A222:128 (1954).
21. Hudis, J. and Wahl, A. C., *The Kinetics of the Exchange Reactions between Iron (II) Ion and the Fluoride Complexes of Iron (III)*, J. Am. Chem. Soc. 75:4153 (1953).
22. Sullivan, J. C. and Hindman, J. C., *Thermodynamics of the Neptunium(IV) Sulfate Complex Ions*, J. Am. Chem. Soc. 76:5931 (1954).
23. Zebroski, E. L., Alter, H. W. and Heumann, F. K., *Thorium Complexes with Chloride, Fluoride, Nitrate, Phosphate and Sulfate*, J. Am. Chem. Soc. 73:5646 (1951).
24. Harned, H. S. and Owen, B. B., "The Physical Chemistry of Electrolytic Solutions," Reinhold Publ. Corp., New York, N. Y., 1943, p. 430.
25. Ahrland, S., *On the Complex Chemistry of the Uranyl Ion (VI). The Complexity of Uranyl Chloride, Bromide and Nitrate*, Acta. Chem. Scand. 5:1271 (1951).
26. Day, R. A., Jr. and Powers, R. M., *Extraction of Uranyl Ion from Some Aqueous Salt Solutions with 2-Thenoyltrifluoroacetone*, J. Am. Chem. Soc. 76:3895 (1954).

A Review of Americium and Curium Chemistry

By R. A. Penneman and L. B. Asprey,* USA

Americium and curium have now run the gamut of availability from early tracer quantities to the present gram amounts of americium and milligram amounts of curium. The bulk of work prior to about 1954 was with Am^{241} (470 year alpha)[1] and with Cm^{242} (162.8 day alpha).[2] The radiation from these materials not only constitutes a health hazard, but also produces remarkable chemical effects. For example, a solution of Am^{241} in the oxidation state (V) or (VI) reduces at a steady rate of a few per cent per hour by effects of its own alpha radiation.[3] The problem is magnified in solutions containing both americium and curium, since the specific activity of Cm^{242} is very nearly 10^3 times greater than that of Am^{241}.

In 1954, milligram amounts of Am^{243} (8800 year alpha)[4] and Cm^{244} (18.4 year alpha)[5] became available. In the case of curium, the importance of this longer-lived isotope is strikingly evident, since it allowed the use of 10–20 microgram samples for X-ray work, whereas X-ray work with Cm^{242} was restricted to sub-microgram amounts to avoid film blackening by the curium radiation itself.[6] With Cm^{244} it was possible for the first time to show unequivocally the existence of tetravalent curium in the oxide.[6]

The chemistry of americium and curium has been reviewed earlier.[7,8,9-13] This present review is based on recent work, as well as the earlier literature, and will touch on major characteristics of americium and curium.

The early data on americium and curium established some of the major chemical characteristics of these elements. However, results of work with larger amounts and, in some cases, other isotopes of these elements are now available. Consequently, tracer work is included here only if confirmed by work with macro quantities. This review will attempt to correct some errors in the literature.

The emphasis on theoretical interpretations of the properties of americium and curium has led to considerable interest in their chemisty. There is little question that americium and curium are members of the 5*f*, inner transition series.[14] There is discussion as to whether they are members of a "rare-earth-like" or "actinide" series as promulgated by Seaborg[14] or members of a "thoride" series as supported by Zachariasen.[15] These arguments will not be reprodnced here. However, from a chemist's viewpoint it would be well to state that strict application of the analogy between the 4*f* elements, europium and gadolinium, and the 5*f* elements, americium and curium, is primarily useful in comparison of properties of the (III) oxidation states and is an uncertain guide for prediction of valence state stability. While the (II) and (III) states of europium are well known, there is no reliable evidence for ionic componnds containing Am(II), and the existence of Am(III), Am(IV), Am(V), and Am(VI) has been well established. Gadolinium has the (III) oxidation state only, and, although Cm(III) is the only valence state known in aqueous solution, there is positive evidence for Cm(IV) in the oxide.

AMERICIUM METAL

Americium metal has been prepared by reaction of barium with AmF_3 at ~1200°C.[16,17,18] The metal is malleable and silver-gray; the density was measured to be 11.7 ± 0.3 gm/cm³.[16] The X-ray structure of americium metal has not been determined. The melting point is rather uncertain, since softening was observed about 850°C and apparently incomplete melting even at 1200°C.[16] The heat of reaction of americium metal with 1.5 *M* HCl was reported as -160 ± 4,[16] and -162.3 ± 2.7 kcal-mole^{-1} at 25°C.[17] The heat of formation at 25°C of Am^{+3}(aq) is calculated to be -163.2 ± 2.7 kcal-mol^{-1}.[17] The formal potential† of the half-reaction, Am(c) = Am^{+3}(aq) + $3e^-$, is estimated to be $+2.32 \pm 0.04$ volts.[7,17] Thus, americium metal is about as electropositive as the lighter rare earths,[19] and has approximately the expected density, assuming a light rare-earth atomic volume and adjusting for the increase in atomic mass.

Preliminary values for the vapor pressure of pure metallic americium were reported recently.[20] Over the temperature range 1103–1453°K, the observed pressures are best represented by $\log p = 7.563 - 13{,}162/T$. If a value of ΔC_p of vaporization of -2 cal mole^{-1} deg^{-1} is assumed, the equation $\log p = 11.092 - 13{,}700/T - \log T$ is obtained. The free energy of vaporization is then given by $\Delta F = 62{,}690 - 50.76T - 2.303(-2)T \log T$. Other reported quantities are: $\Delta H_{1273} = 60.2$ kcal-mole^{-1}; $T_p = 2880$°K;

*Los Alamos Scientific Laboratory, University of California, Los Alamos, New Mexico.

†The convention regarding sign in this paper is that used by W. M. Latimer, *Oxidation Potentials*, Prentice-Hall, Inc., New York, N. Y., 1938.

$\Delta H_{2850} = 57$ kcal-mole^{-1}; $\Delta S_{2850} = 20$ cal-mole^{-1}-deg^{-1}. This low value for ΔS_{2850} probably arises from uncertainty in the extrapolated value of the boiling point. Earlier studies on the vapor pressure of americium from dilute solution in plutonium metal[21] give higher americium vapor pressures; however, ideal behavior of the Am-Pu solution was assumed.

There are little data on reactions involving americium metal, although there are undoubtedly a great many reactions which such an electropositive metal would undergo.

The dissolution of americium in HCl was mentioned above. The measured evolution of H_2 was 1.5 ($\pm$ 10%) moles of H_2/mole of Am.[16] The reaction Am(c) with H_2 (g, 1 atm.) to form $AmH_{2.7(\pm 10\%)}$ was also reported.[16] The compound AmH_2(c) has been made in high vacuum.[18] Americium metal reacts with a deficiency of oxygen to yield AmO.[22] Americium amalgam has been prepared and is discussed under the section on Am(II).[18]

AMERICIUM(II)

There has been fragmentary evidence for the apparent production of Am(II) on a tracer scale.[9] However, subsequent work using milligram amounts and ~1/10 molar solutions of americium gave no supporting evidence for Am(II) in either the solid state or in aqueous solution. Treatment of $SmCl_3$ with H_2 yielded $SmCl_2$, whereas treatment of $AmCl_3$ with H_2 did not produce $AmCl_2$.[18] Electrolysis of samarium in acetic-sulfuric acid media, with a mercury cathode and separate anode compartment, yielded brick-red $SmSO_4$ immediately.[18] Electrolysis of ytterbium under similar conditions caused the immediate formation of green Yb(II) followed by precipitation of $YbSO_4$.[18] Electrolysis of similar americium solutions yielded americium amalgam but gave no color change or precipitate of $AmSO_4$.[18] Shaking americium amalgam (0.01 *M* Am) with $(NH_4)_2SO_4$ and with $(NH_4)_2SO_4$-H_2SO_4 solutions yielded only pink Am(III).[18]

The above evidence seems conclusive that Am(II) cannot be prepared under conditions where Sm(II) can be prepared. The first quantitative estimate of the potential was obtained polarographically from the failure to reduce Am(III) before reduction of hydrogen ion, thus demonstrating that the Am^{++}, Am^{+++} potential is more positive than +0.9 volts.[7,23] A higher limit (Am^{++}, Am^{+++} > 1.5 volts) can be assigned from the lack of reduction of Am^{+++} under conditions where both Sm^{+++} and Yb^{+++} are reduced. The Yb^{++}, Yb^{+++}[24] potential is +1.15 volts, and a recent estimate places the Sm^{++}, Sm^{+++} potential between +1.5 and +2.0 volts.[25]

As mentioned before, AmO and AmH_2 have been prepared. X-ray values for AmH_2, LaH_2, CeH_2, PrH_2, NdH_2, SmH_2, and GdH_2 give interatomic distances showing these compounds to be metallic and not ionic in character.[22] The compound, AmO[22] is metallic and is similar to NpO and PuO.[15] In the presence of excess metal, NdO has also been observed.[22] The early reported preparation of AmO by hydrogen reduction of Am_2O_3[10] has never been repeated successfully[26] and is considered unlikely.

AMERICIUM(III)

Trivalent americium has often been considered as the only stable state of americium in aqueous solution.[7] It is worth while to point out that Am(V) and Am(VI) are strong oxidizing agents in acid solutions, but no more so than Ce(IV) or MnO_4^-. It is thus only an accidental result of their reduction by effects of Am^{241} alpha radiation that makes AM(III) appear so relatively stable. The isotope Am^{243} with the longer half-life and smaller alpha energy will lower this self-reduction rate (by a factor of ~20) to a few per cent a day. Both Am^{243}(V) and Am^{243}(VI) should then show much greater chemical stability.

Treatment of americium metal and americium amalgam with acid (referred to in previous section) results in a solution of Am(III). The characteristic color of Am(III) is pink in 10^{-3} molar solution and gradually becomes yellow as the concentration increases to ~10^{-1} molar in americium. Absorption spectra of Am(III) in HNO_3, HCl, and $HClO_4$ and in K_2CO_3 have been studied.[27,28,29,30,31] It is interesting to note that only slight shifts of the major peaks occur in Am(III) spectra between acid and K_2CO_3 solution.[27,28] In contrast, the spectra of the rare earths, Eu(III) and Nd(III), show pronounced differences in the two media.[32] The absorption spectrum of Am(III) in $HClO_4$, obtained with the Models 11 and 14 of the Cary Recording Spectrophotometer[30,33] is reproduced in Fig. 1, and is characterized by sharp absorption peaks somewhat similar to Eu(III), but having much greater extinction coefficients. The peaks at 503 mμ and 812 mμ are useful for analytical purposes, but with the narrow 503 mμ peak, instrumental defects ordinarily cause deviations from the Beer-Lambert Law at high optical densities.[29,30]

Trivalent americium is precipitated by OH^-, F^-, $C_2O_4^{--}$, and PO_4^{---} ions to yield compounds of low

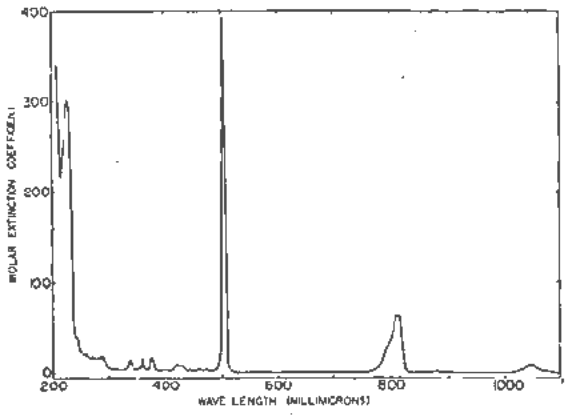

Figure 1. Absorption spectrum of Am(III) in 1M $HClO_4$

solubility.[7] In SO_4^{--} medium, Am(III) is precipitated if alkali ions are present; $NaAm(SO_4)_2 \cdot H_2O$ has been characterized.[34] Trivalent americium, in general, is precipitated by anions which precipitate the trivalent rare earths. A careful study of the fractionation of lanthanum(III) and americium(III) oxalates by precipitation from homogeneous solution showed americium oxalate to be much less soluble and that good separation could be obtained.[35] The crystal ionic radius of Am^{+3} is approximately that of Nd^{+3} ($Z = 60$),[16] although the complexing tendency of Am^{+3} causes it to behave like a rare earth of greater atomic number than Nd^{+3}; in citrate medium it closely resembles Pm^{+3} ($Z = 61$).[36]

A very useful group separation of rare earths from the 5*f* elements including americium and curium involves elution with saturated aqueous HCl and HCl-alcohol mixtures from Dowex-50 resin.[37a,37b] The 5*f* elements precede the rare earths. The reversal in elution position of Am(III) and Cm(III) as the concentration of HCl is varied (not shown by the rare earths) is interpreted as showing covalent bonding involving 5*f* orbitals.[37a] Another group separation of 5*f* elements and the rare earths is obtained by the use of ammonium fluosilicate and fluosilicic acid;[9] the HCl method is more widely used.

As discussed in the appropriate sections, there is no evidence for the reduction of Am(III) to a lower valence state in aqueous solution. The oxidation of Am(III) in acid solution yields Am(VI), while the oxidation in alkaline media usually yields Am(V), but Am(VI) can be obtained in special conditions.

Other solid compounds of Am(III) which have been characterized include the hydride (referred to earlier) and the following: AmF_3—the vapor pressure of AmF_3 has been reported recently;[38] $AmCl_3$;[39] $AmBr_3$;[39] AmI_3;[39] Am_2O_3,[26] Am_2S_3—like the rare earth sulfides, Am_2S_3 cannot be prepared by addition of H_2S to either acid or K_2CO_3 solutions of Am(III).[39] It is worth pointing out that the addition of H_2S to a solution of Am(III) in dilute K_2CO_3 solution is a very useful purification step, removing many elements, particularly lead, which follow americium in some purification procedures.

Americium Separation and Isolation

The major portion of the chemistry for isolating americium deals with the trivalent state. The extraction and separation of Am(III) and Cm(III) by alkyl phosphates are subjects of a recent patent.[40] The solvent extraction of rare earths on a kilogram scale using tri-*n*-butyl phosphate and nitric acid has been reported.[40a] Extraction of americium into tri-*n*-butyl phosphate has been used to concentrate americium on a gram scale.[41,42] It has recently been demonstrated that kilogram quantities of rare earths can be eluted from Dowex-50 in a series of head-to-tail bands, each band containing an essentially pure rare earth.[43] This technique was extended successfully to the large scale isolation of americium from kilogram quantities of lanthanum.[44]

Oxidation of Am(III) to Am(V) in carbonate solution by OCl^-, $S_2O_8^{--}$, or O_3 (as discussed later) is a very useful method of separating americium from rare earths and other carbonate-soluble impurities. Oxidation of Am(III) to Am(VI) in dilute acid solutions (as discussed later), followed by precipitation of fluoride-insoluble impurities, is another valuable purification method.

AMERICIUM(IV)

Americium(IV) has been found only in the anhydrous compounds discussed below. Estimation of the Am(III), Am(IV) couple from thermal data gives $E_f = -2.44 \pm 0.2$ volts,[45] which presumably accounts for the failure thus far to find Am(IV) in aqueous solution.

The oxide, AmO_2, has been prepared by ignition of the nitrate, hydroxide, sesquioxide, or oxalate in air.[7,26] At temperatures above 1000°C, the decomposition pressure of oxygen becomes appreciable.[26] The composition of AmO_2 has been established as $AmO_{1.98-0.02}$ by oxygenation of Am_2O_3.[26] Various lattice constants have been reported for the AmO_2 fluorite structure, depending upon the treatment and the purity of the starting material.[17,46] Very pure $Am_2(C_2O_4)_3$, ignited to 600°C and cooled slowly in an ozone-oxygen system gave $a_0 = 5.376 \pm 0.001$ A.[6] The dioxide may be reduced to Am_2O_3 by hydrogen at elevated temperatures.[7,26] The dioxide dissolves in acids to give Am(III).[45]

Americium tetrafluoride has been prepared by direct fluorination of AmF_3 or AmO_2 at 500°C and 1 atmosphere of fluorine;[47] $KAmF_5$ has been prepared similarly, using $KAmO_2CO_3$ as a starting material.[47] The monoclinic AmF_4 is isomorphous with UF_4, NpF_4, and PuF_4. It is orange-tan in color and reacts slowly with water to give a compound containing Am(III). The compound, $KamF_5$, is rhombohedral and isomorphous with $KPuF_5$. Both AmF_4 and $KAmF_5$ show sharp lines in their absorption spectra characteristic of "*f*" electronic structures.[48]

The disproportionation of Am(V) follows such a rate law that the presence of Am(IV) in solution can be inferred, but no absorption spectrum could be found which might be attributed to it.[49]

If a solution of Am(III) is made basic in the presence of a strong oxidizing agent such as H_2O_2, Cl_2, $S_2O_8^{--}$, or O_3 the precipitate which forms is black or deep brown, and not the usual light pink of Am(III).[25] A slurry of $Am(OH)_3$ when warmed and treated with ozone turns jet black.[33] Treatment of this material with K_2CO_3 solution dissolves some of the americium, leaving a black residue which is soluble in acid. The resulting solution yields a dark precipitate when treated with base.[33] The color of this precipitate could be due to the presence of AM(IV), but there is no specific evidence for this.

AMERICIUM(V)

A solid compound containing Am(V) was first prepared by oxidation of Am(III) in Co_3^{--} solution

by OCl$^-$,[28] $S_2O_8^{--}$ or ozone are equally satisfactory.[30,50] Dissolution of the compound in dilute acid (to avoid disproportionation) gives a solution of Am(V). A solution containing Am(V) may also be prepared by reduction of Am(VI) by Cl^- or Br^- ions[51] or by self-reduction of an Am(VI) solution.[3] Oxidation of an acid solution of Am(III) always yields Am(VI), not Am(V), since Am(V) is more easily oxidized to Am(VI)[52] than Am(III) is oxidized to Am(V).[52]

In acid solution, Am(V) occurs as the ion, AmO_2^+. Evidence for this is found from infrared structure,[54] the reversible oxidation-reduction for the Am(V), Am(VI) couple[52] and indirectly from solid compounds which contain the AmO_2^+ group.[55,56] Solutions containing Am^{241}(V) steadily reduce (~2%/hour) to Am(III) as a result of the alpha activity of Am^{241}.[3]

A measurement of the heat of reduction of Am(V) to Am(III) combined with other thermodynamic quantities, both estimated and measured, yield for the reaction $AmO_2^+ + 2H^+ + H_2 = Am^{+++} + 2H_2O$ the following values: $\Delta H = -92.1$ kcal; $\Delta S = -39.6$ cal-mole^{-1}-degree^{-1}; $\Delta F = -80.3$ kcal; $E_f^0 = +1.74$ v.[53,57]

Anhydrous $RbAmO_2CO_3$ and $NH_4AmO_2CO_3$ have been prepared by ozone oxidation of Am(III) solutions in the respective carbonates. These compounds have been analyzed and their hexagonal structure verified by X-ray analysis.[55,58] Other similar compounds of different crystal structure containing potassium or sodium have been prepared, but their structure has not been worked out. The compound, $KAmO_2F_2$, has been prepared by addition of KF to an acid solution of Am(V) and was identified by X-ray analysis.[59] Treatment of $KAmO_2CO_3$ with strong base gave a high americium solubility, indicating that Am(V) may be amphoteric or that americium(V) hydroxide is fairly soluble.[59]

An absorption spectrum of AmO_2^+ in $HClO_4$, taken on Models 11 and 14 Cary Recording Spectrophotometers, is given in Fig. 2.[30,34] The spectrum has also been measured in HCl[29] and H_2SO_4.[28] The

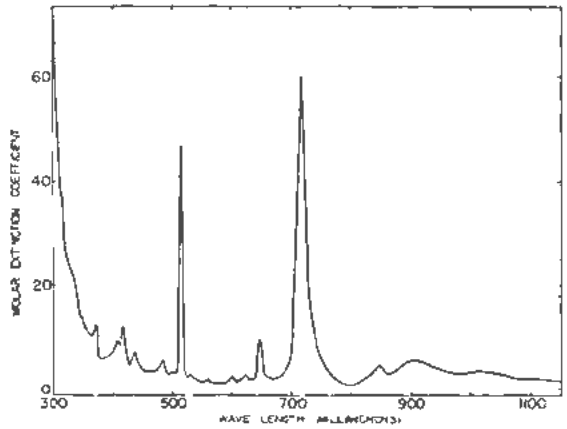

Figure 2. Absorption spectrum of Am(V) in 1M $HClO_4$

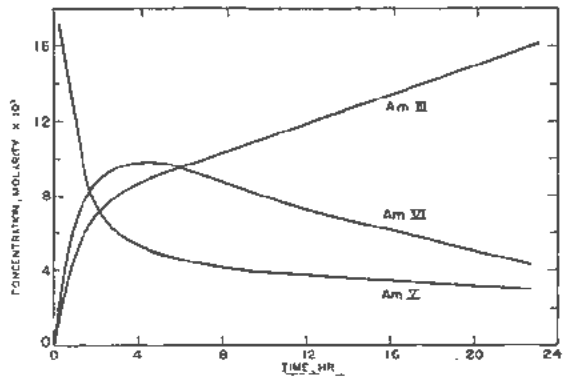

Figure 3. The disproportionation of Am(V) in 6M $HClO_4$

peak at ~717 mμ is used for determination of the concentration of Am(V).

One of the more interesting aspects of the solution chemistry of Am(V) is its disproportionation. The disproportionation reaction has been studied in perchloric acid[49,53] and in hydrochloric acid.[29]

In Fig. 3, rate curves of a disproportionation reaction in 6 *M* $HClO_4$ are given.[49] The reaction is bimolecular with respect to Am(V), and the results of experiments at 3 *M* and 6 *M* H^+ lead to the conclusion that the rate varies as the fourth power of the H^+ concentration. An equation and rate law are given:

$$2AmO_2^+ + 4H^+ = AmO_2^{++} + [Am(IV)] + 2H_2O$$

$$\frac{-d}{dt}[Am(V)] = k_1\,Am(V)^2\,(H^+)^4$$

$$k_1 = 0.04\ \frac{(\text{liters})^5}{(\text{moles})^5\,(\text{hours})}$$

The assumption is made that Am(IV) reacts with water to give Am(III) very rapidly since no spectrophotometric evidence for Am(IV) was found. However, the possibility of several per cent of Am(IV) existing transiently in solution during the course of the reaction cannot be excluded. The reaction $AmO_2^+ + Am(IV) = AmO_2^{++} + Am(III)$ is postulated to explain the observation that the Am(VI)-Am(III) ratio passes through a maximum between 1 and 2.

Further work has shown that the reaction of $Am^{+++} + 2AmO_2^+ + 2H_2O = 3AmO_2^+ + 4H^+$ does not occur in either 1 *M* or 6 *M* $HClO_4$, and that this may be construed as due to the high negative potential of the Am(III), Am (IV) couple.[53] Other evidence for this lack of equilibrium is given by the failure of Am(III) and Am(V) to exchange.[53a]

The disproportionation reaction in hydrochloric acid did not yield any evidence of Am(VI).[29] This is hardly surprising since chloride ion is rapidly oxidized by Am(VI).[51] In hydrochloric acid it was also found that the reaction is bimolecular with respect to Am(V) and that the rate varies as the fourth power of the hydrogen-ion concentration.[29]

The auto-reduction of Am(V) solutions by the effects of Am^{241} alpha radiation was mentioned.[3] It was concluded that the reaction was first order with respect to total americium, yielding the rate law:

$$\frac{d(Am^{+3})/dt}{(Am)} = \frac{-d(AmO_2^{+})/dt}{(Am)} = 0.023\ hr^{-1}$$

Reduction by hydrogen peroxide produced by alpha radiation effects on the aqueous solution was suggested. Additional studies using $Zr(ClO_4)_4$ to complex the peroxide caused the auto-reduction rate of Am(V) to be slowed by a factor of seven but had no effect on the auto-reduction rate of Am(VI).[53] Saturating a solution of 0.002 *M* Am(V) with chlorine reduced the Am(V) auto-reduction rate by a factor of ~60.[51] Measurement of the reduction rate of Am(V) by added hydrogen peroxide showed that the reduction rate was fairly slow and was first order with respect to H_2O_2.[53] The auto-reduction rate of Am(V) in HCl solutions is much lower than in $HClO_4$ solutions (0.007 hr^{-1} and 0.023 hr^{-1}, respectively).[3,20]

AMERICIUM(VI)

Oxidation of Am(III) to Am(VI) in dilute, nonreducing acids, i.e., below 1 *M*, may be accomplished by use of peroxydisulfate ion and less conveniently by argentic ion.[59] Ceric ion will only partly oxidize the Am(III) to Am(VI).[59] Ozone oxidation of Am(III) to Am(VI) was attempted without success using 0.001 *M* Am(III) in 8.76 *M* H_2SO_4.[50] No (<1%) oxidation of a solution of 0.02 *M* Am(III) in 0.2 *M* HNO_3 was observed using ozone; heating had no effect.[33] This is contrary to the results of a recent publication that Am(III) tracer can be partly oxidized to Am(VI) in 0.2 *M* HNO_3 by ozone.[59] Similarly, no oxidation with periodic acid was found.[59] Anodic oxidation of Am(III) to Am(VI) is successful.[33,59]

Oxidation of Am(V) to Am(VI) can be carried out in hot $HClO_4$ or HNO_3 solution very readily by ozone.[30] Strong oxidizing agents such as Ce(IV) or argentic ion will also oxidize Am(V) to Am(VI).[59] Disproportionation of Am(V) by strong acid may be used to prepare Am(VI).[49,59]

Quantitative oxidation of Am(III) to Am(VI) with peroxydisulfate ion has been carried out in solutions varying between 10^{-3} *M* and ~0.2 *M* in americium.[18,32] The fraction of americium oxidized is a constant over a given time interval, and from this it may be inferred that the reaction is no more than first order with respect to the concentration of americium. The hydrogen-ion concentration does not appear to affect the rate when it is below about 0.5 *M*, but *it is essential that the hydrogen ion concentration be kept low.* Peroxydisulfate ion in acidities of the order of 0.5 *M* and higher decomposes by a first order, acid-catalyzed path yielding peroxy-mono-sulfuric acid which in turn forms hydrogen peroxide,[61] a reducing agent for Am(VI). Thus, the oxidation goes incompletely or not at all at higher acidities.

Conditions yielding complete oxidation of Am(III) to Am(VI) are: hydrogen ion $\leq$0.1 *M*; $S_2O_8^{--}$ = 0.2 to 0.5 *M*; temperature = 90°C; time ~15 minutes. The anions may be ClO_4^-, NO_3^-, or SO_4^{--}, but Cl^- cannot be tolerated.

Removal of fluoride-insoluble impurities from a solution of Am(VI) may be carried out by the addition of KF to the hot solution. If HF is used, the solution must first be cooled, as the acid-catalyzed path for the decomposition of $S_2O_8^{--}$ becomes important at higher temperatures, causing reduction of the Am(VI).

Solutions of Am(VI) are gradually reduced to Am(V) at a constant rate of ~4–5% per hour,[3] due to the intense activity of Am^{241} (~7×10^{12} dm/gm).[1] Hence any long term equilibrium studies will be difficult to carry out until larger quantities of longer-lived isotopes become available.

In acid solutions, Am(VI) occurs as the ion AmO_2^{++}, americyl(VI), analogous to UO_2^{++}, NpO_2^{++}, and PuO_2^{++}. Infrared spectra support this assignment,[54] as does chemical evidence such as fluoride solubility, extraction into diethyl ether, and formation of $NaAmO_2(C_2H_3O_2)_3$.[50] No oxide such as AmO_3 or fluoride containing Am(VI) has been prepared.

The only compound of Am(VI) which has been characterized is sodium americium acetate, isomorphous with the analogous compounds of uranium, neptunium, and plutonium.[59] Attempted preparation of americanates by addition of strong bases results in immediate reduction to Am(V).[33,59]

The absorption spectrum of AmO_2^{++} in $HClO_4$, obtained on Cary Models 11 and 14 Recording Spectrophotometers, is given in Fig. 4.[30,33] The peaks at ~995 mμ and 667 mμ may be used to determine the concentration of Am(VI). Only a slight shift in the 995 peak in 1 *M* HF, HNO_3, and H_2SO_4 is observed.[32]

The potential of the AmO_2^{+}-AmO_2^{++} couple has been measured against Ce(III)-Ce(IV) in 1 *M* perchloric acid and against Hg_2^{++}-Hg^{++} in 1 *M*

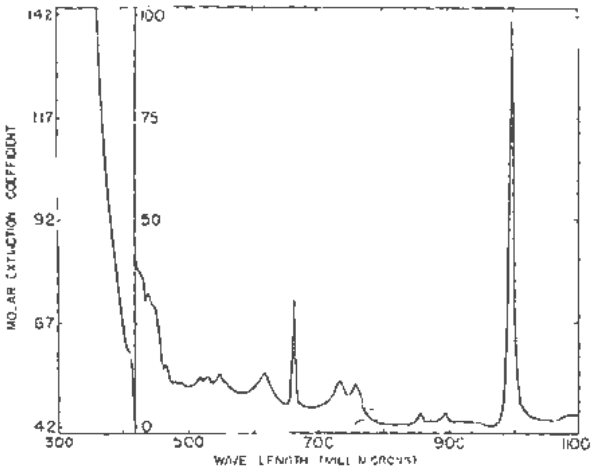

Figure 4. Absorption spectrum of Am(VI) in 1M $HClO_4$

$HClO_4$, using shiny platinum electrodes.[62] A value of $Ef = -1.60 \pm 0.01$ volts was found for the half-reaction $AmO_2^+ = AmO_2^{++} + e^-$. No hydrogen-ion dependence has been found for the U, Np, and Pu couples, and it is presumed that there is no hydrogen-ion dependence of the Am(V), Am(VI) couple.[62]

Measurements of the heat of reduction of Am(VI) to Am(III) by ferrous ion combined with measured and estimated values of other thermodynamic quantities for the reaction $AmO_2^{++} + H^+ + 3/2H_2 = Am^{+3} + 2H_2O$ yield the following values: $\Delta H = -128.9$ kcal; $\Delta S = -38.3$ cal-mole^{-1}-degree^{-1}; $\Delta F = -117.5$ kcal; $E^0 = 1.70$ v.[53,57]

An earlier estimate of the Am(III)-Am(VI) potential[70] was in error due to a misinterpretation of the effect of acidity on the oxidation of Am(III) to Am(VI) by $S_2O_8^{--}$. The lack of oxidation in 2 molar acid was erroneously attributed to the hydrogen-ion dependence of the reaction: $Am^{+++} + 2H_2O = AmO_2^{+} + 4H^+ + 3e^-$, rather than to the effect of H^+ ion on the $S_2O_8^{--}$ oxidation kinetics as discussed above. A study of the oxidation of Am(III) to Am(VI) by Ce(IV) ion yields the value of −1.67 volts for the above half reaction.[51]

Based on the values previously quoted, the following diagram giving the americium potentials in acid solution can be constructed:

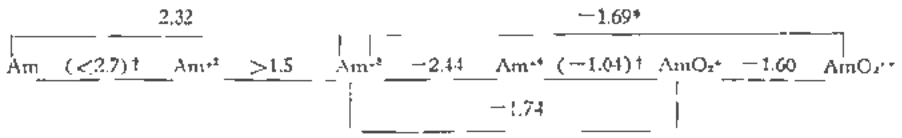

* The value of 1.69 volts is chosen rather than 1.70 or 1.67 volts for internal consistency.

† Values are determined by difference.

Reducing agents such as hydrazine, iodide ion, and hydrogen peroxide react with Am(VI) to give Am(III).

Sulfate ion was found to shift the potential of the Am(V)-Am(VI) couple in the positive direction by several hundredths of a volt, indicating substantial complexing of the americyl(VI) ion by sulfate.[62] Solution of 0.01 N Am(VI) in 1 M HNO_3, 1 M HF, 1 M H_2SO_4 are colored, respectively, light brown, yellow green, and deep brown, indicating complex ion formation, since AM(VI) is light yellow in $HClO_4$ solution.[32]

Early evidence of complexing by CO_3^{--} consisted of formation of a relatively stable, deep brown, or red brown color upon the addition of AmO_2^{++} to a carbonate solution.[69] This complex or complexes may be obtained readily by treatment of a slurry of $Am(OH)_3$ in $NaHCO_3$ solution with ozone.[33] The existence of Am(VI) in this solution was established by titration with hydrazine in basic solution and also by abrupt acidification which results in a solution containing primarily AmO_2^{++}.[33] Infrared spectra indicate that more than one species occur when the CO_2/AmO_2^{++} ratio is varied from 1.2 to 7.8.[33,62]

CURIUM

Curium exhibits only the plus three valence state in solution, and many attempts to oxidize curium in aqueous solution have failed.[6,7,9,13,63,64] An excellent separation from americium may be achieved by oxidation of the Am(III) to Am(VI) in acid solution by $S_2O_8^{--}$ (fast manipulation is quite important to success) and precipitation of the unoxidized Cm(III) by F^-.[63]

The radiation from Cm^{242} is of such magnitude that even americium cannot be completely oxidized if the concentration of curium is greater than about 0.0007 M.[63] However, even with Cm^{244}, an alpha emitter of ~18.4 years half-life,[5] no evidence for oxidation of curium was obtained.[6] Oxidation of Am(III) to an insoluble Am(V) compound in carbonate solution in the presence of curium gave no coprecipitation of curium.[13,63] These experiments rule out the existence of oxidation states such as Cm(V) and Cm(VI), but are not sufficient to rule out Cm(IV), since CmF_4 would be expected to be insoluble in the first case, and $Cm(OH)_4$ would probably be soluble in the second.

A mixture of CmF_3 and TbF_4 gave no evidence of oxidation of Cm(III) when heated together.[64] Heating CmF_3 in fluorine gas at 300–500°C gave no evidence of oxidation.[18] In the above fluorinations, Cm^{242} was used, and different results possibly may be obtained using the less radioactive Cm^{244}.

An important group separation of the rare earths from plutonium, americium and curium consists of elution of these elements from Dowex 50 resin with saturated HCl, as referred to in the section on Am(III).

Curium metal has been produced by the reduction of CmF_3 by barium vapor at 1275°C.[65] The metal is silvery and resembles plutonium metal in its malleability. It seems to tarnish more readily than plutonium in an atmosphere of nitrogen, probably due to its intense alpha radioactivity which heats the metal appreciably. The density of curium metal based on its weight and volume, estimated from microscopic measurements, was reported as 7 gm/cm^3;[63] this low value may be due to a void.

The solution chemistry of Cm(III) is much like that of Am(III), so much so that ion-exchange methods must be used to separate the two elements when both are in the trivalent state.[7,66] Slightly soluble compounds are formed with OH^-, F^-, $C_2O_4^{--}$, and PO_4^{---} which are useful in purification procedures.[7,13] A study of the solubility of CmF_3 at various temperatures has been made.[61] An X-ray pattern has been obtained for CmF_3, showing it to be isomorphous with LaF_3.[22] A soluble carbonate complex is formed in concentrated CO_3^{--} solutions, as is the case with americium.[13]

The absorption spectrum of solid CmF_3 has been photographed on a 21-foot spectrograph.[64] The spectrum of GdF_3 was also measured, and the prominent lines of both compounds are given in Table I for comparison.

Table I. Ultraviolet Absorption Spectra of Curium and Gadolinium in the Solid Trifluorides[64]

CmF_3 λ, Å	Relative intensity	GdF_3 λ, Å	Relative intensity
2826	2	2834	4
2774	10	2759	10
2680	6	2666	4
2368	4	2334	4

NOTE: The wavelengths are good to about 3 Å; the intensities are only relative, and the absorption in the curium is stronger than in gadolinium.

No absorption at wavelengths longer than 2850 Å was found in either curium trifluoride or gadolinium trifluoride. The fact that both curium and gadolinium show absorption only in this ultraviolet region of the spectrum supports the hypothesis that the electronic structure of curium is $5f^7$ analogous to the $4f^7$ structure of gadolinium.

The magnetic susceptibility of CmF_3 has been measured at 295°K and 77°K using samples of the order of 25 micrograms.[67] The value of χ of 22,500 ± 400 (cgs units × 10^6) at 295°K compares with the value of 26,000 which assumes a $5f^7$ configuration for Cm(III) and Russell-Saunders coupling. In a sample of CmF_3 diluted with 90% LaF_3, a value of 26,500 ± 700 cgs units was obtained at 296°K.[68] A difficulty, particularly important at the lower temperatures, arises from the Cm^{242} radiation which causes heating of the sample to an unknown degree.

Recently, with the availability of Cm^{244}, good X-ray patterns of some oxides of curium have been obtained, although a few measurements of compounds of Cm^{242} were made previously using, by necessity, samples of ≤½ microgram due to the intense radioactivity.[6] The white sesquioxide, Cm_2O_3, has been made by thermal decomposition of higher oxides and gives a value for $a_0/2$ of 5.50 Å.[6] Treatment with oxygen and ozone yielded a black compound with $a_0 = 5.372$ Å.[6] This low value indicates that the composition of this oxide must be nearly CmO_2, thus showing that quadrivalent curium exists as a solid compound. A preliminary measurement of the magnetic susceptibility of the higher oxides indicates that most of the curium was in the (IV) state.[69]

The basicity of curium is borne out by the great difficulty experienced in hydrolysis of $CmCl_3$ by H_2O vapor.[70]

REFERENCES

1. Harvey, B. G., *Alpha Half-Life of Am^{241}*, Phys. Rev., *85*: 482 (1950).
2. Trieman, L. H., Bevan, R. B., Jr., Stephanou, S. E. and Penneman, R. A., to be published, Los Alamos Scientific Laboratory.
3. Asprey, L. B. and Stephanou, S. E., *The Auto-Reduction of Am(VI) and Am(V) in Dilute Acid*, AECD-924 (1950).
4. Diamond, H., Fields, P. R., Mech, J., Inghram, M. G. and Hess, D. C., *The Half-Life of Am^{243}*, Phys. Rev., *92*: 1490 (1953).
5. Friedman, A. M, Harkness, A. L., Fields, P. R., Studier, M. H. and Huizenga, J. R., *The Alpha Half-Lives of Cm^{244}, Cm^{245}, and Cm^{246}*, Phys. Rev., *95*: 1501 (1954).
6. Asprey, L. B., Ellinger, F. H., Fried, S. and Zachariasen, W. H., *Evidence for Quadrivalent Curium: X-ray Data on Curium Oxides*, J. Am. Chem. Soc., *77*: 1707 (1955).
7. Perlman, I. and Street, K., Jr., *The Chemistry of the Transplutonium Elements*, The Actinide Elements, Chapter 14, National Nuclear Energy Series, Division IV, Volume 14-A, McGraw-Hill Book Co. Inc., New York, 1954.
8. Hyde, E. K., *Radiochemical Separations of the Actinide Elements, ibid.*, Chapter 15.
9. Thompson, S. G., Morgan, L. O., James, R. A. and Perlman, I., *The Tracer Chemistry of Americium and Curium in Aqueous Solution*, The Transuranium Elements, Paper 19.1, National Nuclear Energy Series, Division IV, Volume 14-B, McGraw-Hill Book Co., Inc., New York, 1949.
10. Cunningham, B. B., *The First Isolation of Americium in the Form of Pure Compounds; Microgram-Scale Observations on the Chemistry of Americium, ibid.*, Paper 19.2.
11. Seaborg, G. T., James, R. A. and Morgan, L. O., *The New Element Americium, ibid.*, Paper 22.1.
12. Seaborg, G. T., James, R. A. and Ghiorso, A., *The New Element Curium, ibid.*, Paper 22.2.
13. Werner, L. B. and Perlman, I., *The Preparation and Isolation of Curium, ibid.*, Paper 22.5.
14. Seaborg, G. T., *Correlation of Properties of Actinide Transition Series*, The Actinide Elements, Chapter 17, National Nuclear Energy Series, Division IV, Volume 14-A, McGraw-Hill Book Co., Inc., New York, 1954.
15. Zachariasen, W. H., *Crystal Chemistry of the 5f Elements, ibid.*, Chapter 18.
16. Westrum, E. F., Jr. and Eyring, L., *The Preparation and Some Properties of Americium Metal*, J. Am. Chem. Soc., *73*: 3396 (1951).
17. Cunningham, B. B. and Lohr, H. R., *Heat of Reaction of Americium Metal with Hydrochloric Acid, ibid., 73*: 2026 (1951).
18. Asprey, L. B., unpublished work, Los Alamos Scientific Laboratory.
19. Yost, D. M., Russell, H., Jr. and Garner, C. S., *The Rare Earth Elements and Their Compounds*, John Wiley and Sons, Inc., New York, 1947.
20. Carniglia, S. C. and Cunningham, B. B., *The Vapor Pressure of Americium Metal*, J. Am. Chem. Soc., *77*: 1502 (1955).
21. Erway, N. D. and Simpson, O. C., *Vapor Pressure of Americium*, J. Chem. Phys., *18*: 953 (1950).
22. Ellinger, F. H., private communication, Los Alamos Scientific Laboratory.
23. Cunningham, B. B. and Asprey, L. B., *First Isolation of Americium in the Form of Pure Compounds*, AECD-2946, July 20, 1950.
24. Laitinen, H. A., *Potential of the Ytterbic-Ytterbous Ion Electrode*, J. Am. Chem. Soc., *64*: 1133 (1942).
25. Onstott, E. I., private communication, Los Alamos Scientific Laboratory.

26. Asprey, L. B. and Cunningham, B. B., *Equilibria in the Oxide Systems of Praseodymium and Americium*, UCRL-329 (rev.), April 14, 1949.
27. Stephanou, S. E., unpublished work, Los Alamos Scientific Laboratory.
28. Werner, L. B. and Perlman, I., *The Pentavalent State of Americium*, J. Am. Chem. Soc., *73*: 495 (1951).
29. Hall, G. R. and Herniman, P. D., *The Separation and Purification of Americium^{241} and the Absorption Spectra of Tervalent and Quinquevalent Americium Solutions*, J. Chem. Soc., *1951*: 2214.
30. Stephanou, S. E., Nigon J. P. and Penneman, R. A., *The Solution Absorption Spectra of Americium (III), (V), and (VI)*, J. Chem. Phys., *21*: 42 (1953).
31. Stewart, D. C., *Absorption Spectra of Lanthanide and Actinide Rare Earths, II. Transition Probabilities for $+3$ Ions in the Two Series*, AECD-3551 (1952).
32. Penneman, R. A., unpublished work, Los Alamos Scientific Laboratory.
33. Coleman, J. S., unpublished work, Los Alamos Scientific Laboratory.
34. Staritzky, E. and Stephanou, S. E., unpublished work, Los Alamos Scientific Laboratory.
35. Hermann, J. A., *The Separation of Americium from Lanthanum by Fractional Oxalate Precipitation from Homogeneous Solution*, LADC-1667 (1954).
36. Thompson, S. G., Cunningham, B. B. and Seaborg, G. T., *Chemical Properties of Berkelium*, J. Am. Chem. Soc., *72*: 2798 (1950).
37. Street, K., Jr. and Seaborg, G. T., *The Separation of Americium and Curium from the Rare Earth Elements*, *ibid.*, *72*: 2790 (1950).
37a. Diamond, R. M., Street, K., Jr. and Seaborg, G. T., *An Ion Exchange Study of Possible Hybridized 5f Bonding in the Actinides*, *ibid.*, *76*: 1461 (1954).
37b. Thompson, S. G., Harvey, B. G., Choppin, G. R. and Seaborg, G. T., *Chemical Properties of Elements 99 and 100*, *ibid.*, *76*: 6229 (1954).
38. Carniglia, S. C. and Cunningham, B. B., *Vapor Pressure of Americium Trifluoride, Heats and Free Energies of Sublimation ibid*, *77*: 1451 (1955).
39. Fried, S., *The Preparation of Anhydrous Americium Compounds*, *ibid.*, *73*: 416 (1951).
40. Peppard, D. F. and Gray, P. R., *The Separation of Americium and Curium from Aqueous Solution*, U. S. Patent 2,683,655 (1954).
40a. Weaver, B., Kappelmann, F. A. and Topp, A. C., *Quantity Separation of Rare Earths by Liquid-Liquid Extraction, I. The First Kilogram of Gadolinium*, J. Am. Chem. Soc., *75*: 3943 (1953).
41. Brooksbank, R. E., Matherne, J. L., Rainey, R. H. and Whitson, W. R., unpublished work, Oak Ridge National Laboratory.
42. Armstrong, D. E., Coleman, J. S. Jones, L. H., Keenan, T. K., Maraman, W. J. and Penneman, R. A., unpublished work, Los Alamos Scientific Laboratory.
43. Spedding, F. H. and Powell, J. E., *A Practical Separation of Yttrium Group Rare Earths from Gadolinite by Ion Exchange*, ISC-349 (1953).
44. Armstrong, D. E., Keenan, T. K., LaMar, L. E. and Penneman, R. A., unpublished work, Los Alamos Scientific Laboratory.
45. Eyring, L., Lohr, H. R. and Cunningham, B. B., *Heats of Reaction of Some Oxides of Americium and Praseodymium with Nitric Acid and an Estimate of the Potentials of the Am(III)-Am(IV) and Pr(III)-Pr(IV) Couples*, J. Am. Chem. Soc., *74*: 1186 (1952).
46. Templeton, D. H. and Dauben, C. H., *Crystal Structure of Americium Compounds*, *ibid.*, *75*: 4560 (1953).
47. Asprey, L. B., *New Compounds of Quadrivalent Americium, AmF_4, $KAmF_5$*, *ibid.*, *76*: 2019 (1954).
48. Staritzky, E. and Asprey, L. B., unpublished work, Los Alamos Scientific Laboratory.
49. Stephanou, S. E., Asprey, L. B. and Penneman, R. A., *The Disproportionation of Americium(V)*, AECU-925 (1950).
50. Keenan, T. K., unpublished work, Los Alamos Scientific Laboratory.
51. Nigon, J. P., unpublished work, Los Alamos Scientific Laboratory.
52. Penneman, R. A. and Asprey, L. B., *The Formal Potential of the Am(V) Am(VI) Couple*, AECU-936 (1950).
53. Gunn, S. R., *Thermodynamics of the Aqueous Ions of Americium*, (Thesis, University of California), UCRL-2541 (1954).
53a. Keenan, T. K., Suttle, J. F. and Penneman, R. A., *Isotopic Exchange Reactions of Americium*, J. Phys. Chem., *59*: 381 (1955).
54. Jones, L. H. and Penneman, R. A., *Infrared Spectra and Structure of Aqueous Uranyl and Transuranyl (V) and (VI) Ions in Aqueous Perchloric Acid Solution*, J. Chem. Phys., *21*: 542 (1953).
55. Nigon, J. P., Penneman, R. A., Staritzky, E., Keenan, T. K. and Asprey, L. B., *Alkali Carbonates of Np(V), Pu(V), and Am (V)*, J. Phys. Chem., *58*: 403 (1954).
56. Asprey, L. B., Ellinger, F. H. and Zachariasen, W. H., *Preparation, Identification, and Crystal Structure of a Pentavalent Americium Compound, $KAmO_2F_2$*, J. Am. Chem. Soc., *76*: 5235 (1954).
57. Cunningham, B. B., private communication. See also Cunningham, B. B., *Thermodynamics of the Heavy Elements*. Section S.4.1 of these Proceedings.
58. Ellinger, F. H. and Zachariasen, W. H., *The Crystal Structure of $KPuO_2CO_3$, $NH_4PuO_2CO_3$, and $RbAmO_2CO_3$*, J. Phys. Chem., *58*: 405 (1954).
59. Asprey, L. B., Stephanou, S. E. and Penneman, R. A., *Hexavalent Americium*, J. Am. Chem. Soc., *73*: 5715 (1951).
60. Ward, M. and Welch, G. A., *The Oxidation of Americium to the Sexavalent State*, J. Chem. Soc., *1954*: 4038.
61. Kolthoff, I. M. and Miller, I. K. *The Chemistry of Persulfate. I. The Kinetics and Mechanism of the Decomposition of the Persulfate Ion in Aqueous Solution*, J. Am. Chem. Soc., *73*: 3055 (1951).
62. Jones, L. H., unpublished work, Los Alamos Scientific Laboratory.
63. Stephanou, S. E. and Penneman, R. A., *Observations on Curium Valence States; A Rapid Separation of Americium and Curium*, J. Am. Chem. Soc., *74*: 3701 (1952).
64. Feay, D. C., *Some Chemical Properties of Curium*, (Thesis, University of California), UCRL-2517 (1954).
65. Wallmann, J. C., Crane, W. W. T. and Cunningham, B. B., *The Preparation and Some Properties of Curium Metal*, J. Am. Chem. Soc., *73*: 493 (1951).
66. Glass, R. A., *Chelating Agents Applied to Ion-Exchange Separations of Americium and Curium*, *ibid.*, *77*: 807 (1955).
67. Crane, W. W. T., Cunningham, B. B. and Wallmann, J. C., *The Magnetic Susceptibility of Some Compounds of Americium and Curium*, UCRL-846 (1950).
68. Crane, W. W. T., *Some Physical and Chemical Properties of Curium*, AECD-3161 (1951).
69. Wallmann, J. C., private communication, Radiation Laboratory, University of California.
70. Fried, S., private communication, Argonne National Laboratory.

Spectrophotometric Studies of the Behaviour of Americium Ions in Solutions

By G. N. Yakovlev and V. N. Kosyakov, USSR

The present report concerns the spectrophotometric investigation of the complex formation of americium(III), the reduction of americium(V) and americium(VI) due to the products of the interaction of americium radiation with water and the mechanism of americium(V) disproportionation reactions. A preliminary study of the absorption spectra of americium ions in different valency states was carried out for this purpose.

This report has been compiled by research workers G. N. Yakovlev and V. N. Kosyakov from the data of research workers D. S. Gorbenko-Germanov, R. A. Zenkova, A. P. Korovin, Y. P. Sobolev and the authors. The data are available at the Academy of Sciences of the USSR.

EXPERIMENTAL

Measurements were carried out with the aid of a model SF-4 quartz spectrophotometer (made in USSR) using 1 cm quartz microcells and also cylindrical microcells with hermetic seals; the latter had a volume of 0.8 mm and a path length of 2 cm. A cell holder of special design permitted measurements to be made at a constant temperature. The absorption spectra of americium solutions were studied in the 300–1100 mμ range at 2.5 mμ intervals and at smaller intervals in the regions of absorption maxima. The americium concentration was determined radiometrically with a precision of ±1%.

Americium(III) solutions were prepared by dissolving americium(III) hydroxide in the desired acid.

Americium(V) was obtained by ozone oxidation of americium(III) in a 40% potassium carbonate solution at 80–90°C. The precipitate of the double americium(V)-potassium carbonate obtained was thoroughly washed with water and dissolved.

Americium(VI) was prepared by ozone oxidation of americium(V) in dilute acid solutions.

Specially purified chemicals were used in all experiments.

RESULTS AND DISCUSSION

The absorption spectra of americium(III), (V) and (VI) ions in aqueous solutions are described in a number of papers.[1,2,3,4]

The values of the molar extinction coefficients obtained by various authors for the most characteristic bands do not coincide.

Absorption spectra of americium(III) (V) and (VI) were studied and the molar extinction coefficients calculated for the whole spectral range from 300 to 1100 mμ (Figs. 1, 2, 4, 5).

For quantitative calculations use was made of the following values of the molar extinction coefficients for the most prominent bands in 0.1*M* $HClO_4$:

Original language: Russian.

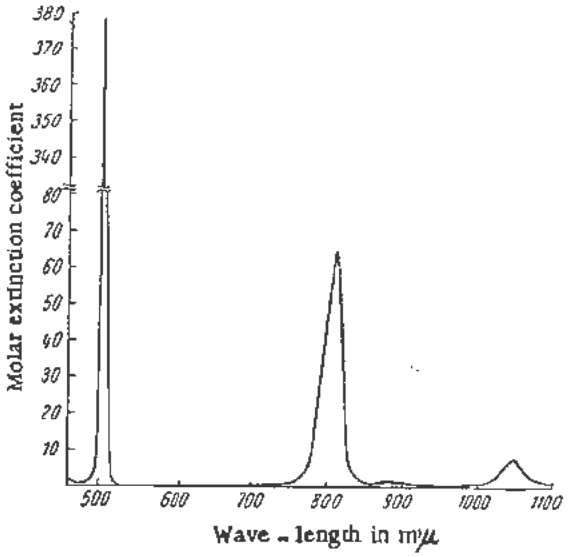

Figure 1. Absorption spectrum of americium(III) in 0.1M $HClO_4$ in the 460–1100 mμ range. Americium concentration 15.2 mM/l. The 480–520 mμ intervals were studied for a 3.86 mM/l americium concentration

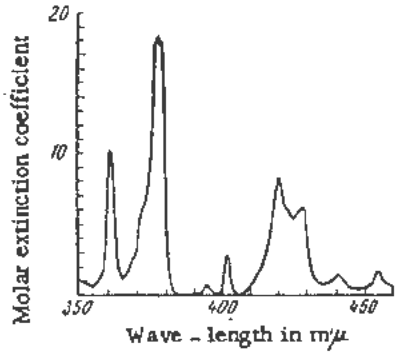

Figure 2. Absorption spectrum of americium(III) in 0.1M $HClO_4$ (short wage-length region); americium concentration 14.5 mM

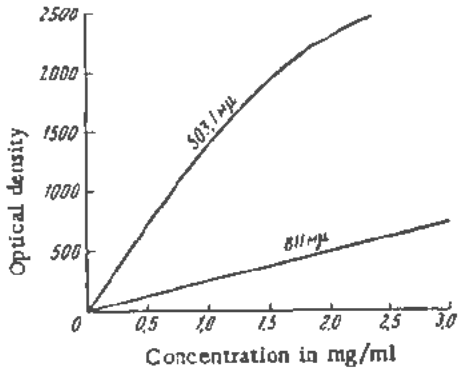

Figure 3. Applicability of Beer's law to 503.1 mμ and 811 mμ peaks: cell thickness, 1.0046 cm

	λ mμ	ε
Americium(III)	503.1	378
	811	64.4
Americium(V)	514	44.1
	718	59.6
Americium(VI)	666	24.6
	995	63.8

The optical densities of the absorption bands with the exception of the peak at 503.1 mμ (Fig. 3), light path within the range of concentrations studied (up to 16 mm/l for a cell length of 1 cm), obey Beer's Law, this being in agreement with other authors.[4,5]

FORMATION OF AMERICIUM(III) COMPLEX IONS

The formation of americium(III) complex ions was studied in perchloric, hydrochloric, nitric and sulphuric acids.

An increase in perchloric acid concentration alters the character of the spectrum only slightly. In 6*M* $HClO_4$ the values of the molar extinction coefficients for the 503.1 and 811 mμ peaks increase to 390 and 70.3 respectively, without a shift in the position of the maxima.

An increase in the concentration of hydrochloric acid from 0.20*M* to 6.04*M* also had only an insignificant effect on the height and position of the peaks in the visible and infrared spectral regions. $\varepsilon_{503.1\ m\mu}$ drops from 360 to 351; $\varepsilon_{811\ m\mu}$ from 63.7 to 61.2. In the ultra-violet region of the spectrum, however, highly substantial changes occur (Fig. 6).

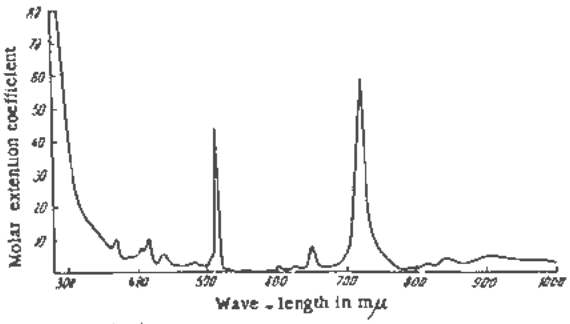

Figure 4. Absorption spectrum of americium(V) in 0.1M $HClO_4$: americium concentration 16.2 mM/l

With an increase in acidity there is a general rise of absorption in the ultra-violet region, accompanied by a flattening of some of the peaks, while others become more pronounced. However, the observed rise in absorption is less than that obtained by S. R. Hall, and P. D. Herniman for acid concentrations.[5]

The absorption spectrum in 0.2*M* nitric acid is very close to the spectrum in 0.1*M* perchloric acid, but an increase in acidity produces a marked change in the short wave-length region of the spectrum and a considerable shift of characteristic peaks in the visible and infra-red regions, accompanied by a decrease of molar extinction coefficients (Fig. 7). In 10*M* nitric acid the position of the 503 mμ peak is shifted to 505 mμ, whereas the molar extinction coefficient decreases to 168.

$\varepsilon_{811\ m\mu}$ diminishes to 43 and the band becomes broader. The 1048 mμ peak disappears.

The absorption spectra of americium(III) ions in 0.2*M* sulphuric acid, with the exception of the ultra-violet region, differ little from the spectrum in 0.1*M* perchloric acid, and an increase in acidity to 4*M* has no appreciable effect upon the character of

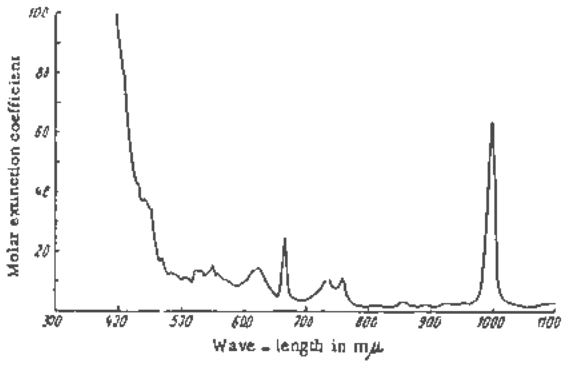

Figure 5. Absorption spectrum of americium(VI) in 0.2M $HClO_4$: americium concentration 10.2 mM/l

the spectrum. However, in 10*M* H_2SO_4 the spectrum experiences a marked change (Fig. 8). In the ultra-violet region a sharp increase is observed in absorption. $\varepsilon_{813\ m\mu}$ increases to 421. The peak maximum which formerly corresponded to 811 mμ shifts to 815 mμ, with a decrease in ε to 61.9. The 1048 mμ peak maximum moves to 1035 mμ with an increase in ε.

The character and magnitude of the alterations in the observed spectrum justify the assertion that sulphuric and nitric acids exhibit the greatest tendency towards complex ion formation with americium(III), while perchloric acid exhibits the least such tendency. This conclusion is in good agreement with experiments on the migration of americium(III) ions in different acids under the influence of electric fields.

Electromigration phenomena were studied with tracer quantities of americium in an electrolytic cell similar to that described by C. K. McLane, J. S. Dixon and J. C. Hindman,[6] the duration of electrolysis being 24 hours and current intensity 5–15 ma.

Table I. Americium(III) Electromigration

Solvent	Solvent concentration	% migration To cathode	% migration To anode	Solvent	Solvent concentration	% migration To cathode	% migration To anode
$HClO_4$	0.2*M*	100	—	H_2SO_4	1.0*M*	100	—
	1.0*M*	100	—		2.0*M*	98	2
	3.7*M*	99	1		4.0*M*	82	18
HCl	1.0*M*	100	—		6.0*M*	75	25
	6.0*M*	94	6		8.0*M*	21	79
	8.0*M*	93	7		10.0*M*	8	92
	10.0*M*	32	68				
HNO_3	2.0*M*	100	—	K_2CO_3	10%	—	100
	4.0*M*	78	22		40%	3	97
	6.0*M*	33	67		50%	2	98
	8.0*M*	32	68				
	10.0*M*	24	76	NaAc	25%	22	78

The results obtained (Table I) do not give a sufficiently accurate quantitative picture of the complex formation process, owing to the superposition of diffusion phenomena, difference in ion mobility, etc., but they do make it possible to form a conclusion on the sign of the complex ion charge and the relative strength of the complexing agents.

Comparison of the data obtained in a study of the formation of plutonium(III) complex ions in hydrochloric and sulphuric acids[6] reveals a certain difference in the behaviour of plutonium and americium. In hydrochloric acid media americium(III) exhibits a greater ability to form complexes, whereas in sulphuric acid a noticeable migration of plutonium(III) to the anode is already observed in 1*M* H_2SO_4.

With carbonate and acetate ions americium(III) produces rather stable complexes. A study of electromigration reveals that in a 10% solution of potassium carbonate the americium is already in the form of a complex anion. The formation of complex ions of americium in other valency states was not the subject of a special study, but random observations of changes in absorption spectra and the chemical behaviour of certain compounds furnish evidence of a pronounced tendency of americium(VI) to form complexes in sulphuric acid media and americium(V) in hydrochloric acid media, which is confirmed by data available in the literature.[3,5]

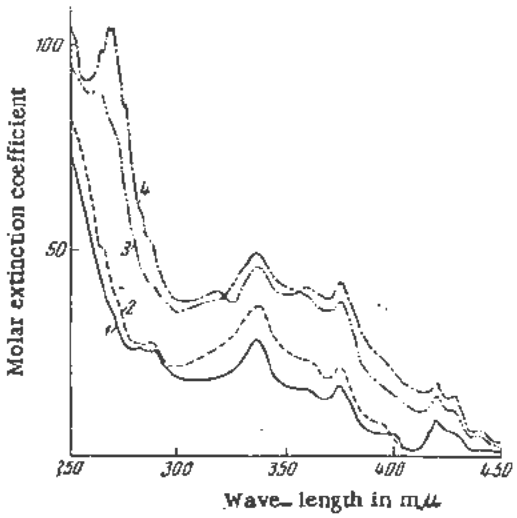

Figure 6. Short-wage region of spectrum of americium(III) in hydrochloric acid: (1) 0.20 *M* HCl, (2) 1.00 *M* HCl, (3) 4.02 *M* HCl, (4) 6.04 *M* HCl

AUTO-REDUCTION OF AMERICIUM(V)

In dilute acid solutions americium(V) is reduced to americium(III) by the products of the decomposition of water under the influence of americium radiation.[5,7]

The reduction process was studied by observing the decrease in americium(V) concentration and the increase in americium(III) concentration (Fig. 9). The complete reduction of americium(V) at 23°C takes place in 66 hrs: there is an almost linear dependence of the reduction rate on the total concentration of the americium in the solution.

The decomposition of water under the influence of ionising radiation may take place according to the reactions:[8]

$$H_2O \rightarrow H + OH \qquad (1)$$

$$H_2O \rightarrow H + \tfrac{1}{2}H_2O_2 \qquad (2)$$

$$H_2O \rightarrow \tfrac{1}{2}H_2 + \tfrac{1}{2}H_2O_2 \qquad (3)$$

If it is assumed that under the influence of α-radiation decomposition follows only reaction (3)[9,10] and

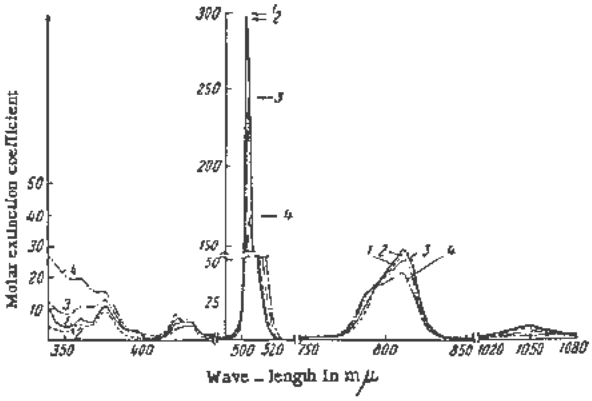

Figure 7. Absorption spectrum of americium(III) in nitric acid: (1) 0.20 M HNO_3, (2) 1.00 M HNO_3, (3) 5.02 M HNO_3, (4) 10.04 M HNO_3

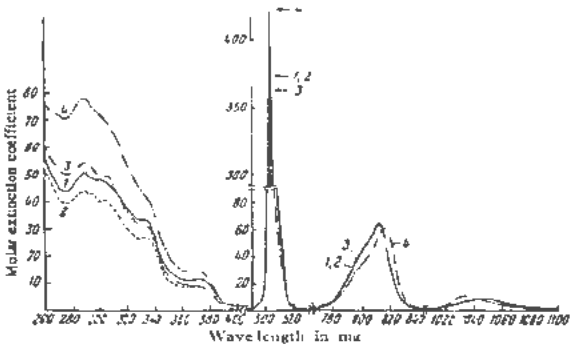

Figure 8. Absorption spectrum of americium(III) in sulphuric acid: (1) 0.20 M H_2SO_4, (2) 1.0 M H_2SO_4, (3) 4.0 M H_2SO_4, (4) 10.0 M H_2SO_4

that the rate of the formation of hydrogen peroxide is far slower than the rate of the reduction of americium(V) (the latter is true for a very broad range of concentrations), the rate of the reduction of americium(V) may be calculated approximately according to the formula:

$$\frac{d\ [\mathrm{Am(V)}]}{dt} = k_a\ [\mathrm{Am}] = -\frac{\lambda_{\mathrm{Am}} \cdot Q}{W \cdot n} \cdot [\mathrm{Am}]$$

where λ_{Am} is the Am^{241} decay constant; Q is the total energy per disintegration; W is the energy of the formation of 1 pair of ions; and n is the change in valency.

The accuracy of the calculation is determined by the value of W for aqueous solutions (different authors quote different values). We adopted $K_a = 1.76 \times 10^{-2}$ hr^{-1}, obtained experimentally from the accumulation of hydrogen peroxide in the americium(III) solution.* It is possible, however, that the decomposition of water partially follows reaction (2).[11,12] In this case the rate constant of the reduction reaction increases, and the time of the complete reduction of americium(V) will be less than 57 hr, provided there are no americium ions in other valency states at zero time. The long duration of the process of complete reduction and the non-rigid linearity of the reduction process in time, both of which were established experimentally, may be attributed in these conditions, to side processes one of which is evidently the reaction of americium(V) disproportionation. The very low value of the rate constant of the auto-reduction reaction (7.4×10^{-3} hr^{-1}) obtained in 0.5*M* HCl (Hall and Herniman[5]) is apparently partly due to the same causes.

*The quantitative determinations of hydrogen peroxide were carried out spectrophotometrically from measurements of the absorption of the titanium complex at 400 mμ.

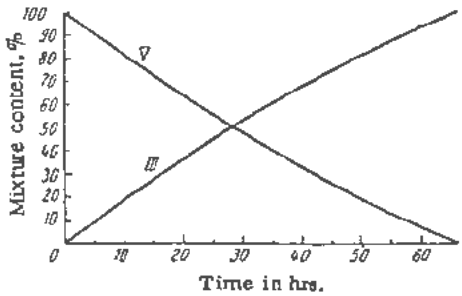

Figure 9. Reduction of americium(V) in 0.1 M $HClO_4$ at 23°C; initial concentration of americium(V) 16.2 mM/l

AMERICIUM(V) DISPROPORTIONATION

A study of the auto-reduction of americium(V) in solutions of higher acidity reveals that the process of reduction is in this case retarding, leading to other parallel reactions. The complete reduction of americium(V) in 1*M* sulphuric acid at 23°C takes place in 98 hr. When americium(V) is dissolved in 2*M* H_2SO_4 after a certain period of time an appreciable quantity of americium(VI) is detected in the solution, besides americium(III). The concentration of the americium(VI) 5 hr after dissolving reaches 30% of the total americium concentration. This gives evidence of the disproportionation reaction taking place under these conditions (Fig. 10). With an increase

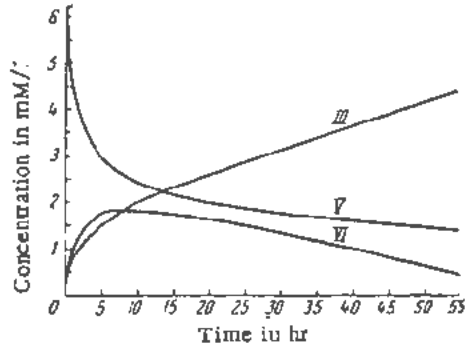

Figure 10. Disproportionation of americium(V) in 2M H_2SO_4: molar extinction coefficients for americium(III) at 811 mμ — 63; for americium(V) at 718 mμ — 60; for americium(VI) at 996 mμ — 103

in acidity the rate of this reaction increases markedly, and in 4*M* H_2SO_4 at 23°C, 2½ hrs after the americium(V) is dissolved, the solution contains more than 50% of americium(VI) (Fig. 11).

Owing to the parallel reaction of the reduction of americium(VI) to americium(V) the reaction of disproportionation does not attain stable equilibrium. The composition of the reaction mixture changes with an increase in the concentration of americium(III), which is the sole final product of the overall reaction.

If the reaction of disproportionation is represented in its general form as

$$n\mathrm{Am(V)} \underset{R_2}{\overset{R_1}{\rightleftharpoons}} (n-1)\ \mathrm{Am(VI)} + \mathrm{Am(III)} \qquad (4)$$

and the reaction of reduction as

$$\mathrm{Am(VI)} \xrightarrow{R_3} \mathrm{Am(V)} \qquad (5)$$

the rate laws for each of the valency states of americium (both reactions proceeding) will be:

Table II. Calculation of the Stoichiometric Coefficient n of the Disproportionation Reaction of Americium(V) in 2M and 4M H_2SO_4

Acid concentration	Time, hr	Concentration of Am(V) in mM/l	Concentration of Am(VI) in mM/l	Concentration of Am(III) in mM/l	K_a	n
	20	2.00	1.65	2.62	2.42×10^{-2} hr^{-1}	2.8
2M	30	1.76	1.33	3.14		2.9
H_2SO_4	40	1.60	1.02	3.64		2.9
	50	1.49	0.63	4.15		3.0
	20	0.57	3.63	3.95	2.36×10^{-2}hr^{-1}	2.9
4M	30	0.52	3.06	4.58		2.9
H_2SO_4	40	0.48	2.48	5.22		3.0
	50	0.42	1.90	5.85		3.0
	60	0.36	1.34	6.48		3.0

$$\frac{d[\mathrm{Am(III)}]}{dt} = R_1 - R_2 \qquad (a)$$

$$\frac{d[\mathrm{Am(V)}]}{dt} = nR_2 - nR_1 + R_a \qquad (b)$$

$$\frac{d[\mathrm{Am(VI)}]}{dt} = (n-1)R_1 - (n-1)R_2 - R_a \qquad (c)$$

where R_1 and R_2 are the rates of the forward and back reactions, and R_a is the rate of the reduction reaction.

By combining Equations a and c and integrating the expression obtained, we get:

$$(n-1)\,[\mathrm{Am(III)}] - [\mathrm{Am(VI)}] = R_a t = K_a[\mathrm{Am}] \cdot t$$

therefore

$$n = \frac{K_a[\mathrm{Am}] \cdot t + [\mathrm{Am(III)}] + [\mathrm{Am(VI)}]}{[\mathrm{Am(III)}]}$$

The value of K_a can easily be calculated from the change in the average oxidation number of the americium with time. The values of K_a obtained in this way for $2M$ and $4M$ H_2SO_4 are 2.42×10^{-2} and 2.36×10^{-2} hr^{-1}.

On the basis of the value obtained for the stoichiometric coefficient, the reaction of disproportionation of americium(V) may be represented as follows:

$$3AmO_2^+ + 4H^+ \rightleftharpoons 2AmO_2^{++} + Am^{+++} + 2H_2O \qquad (6)$$

As a rule, such reactions are multi-staged. Therefore, a more detailed picture of its mechanism may be given by the following equations:

$$\mathrm{Am(V)} + \mathrm{Am(V)} \rightleftharpoons \mathrm{Am(VI)} + \mathrm{Am(IV)} \qquad (7)$$

$$\mathrm{Am(IV)} + \mathrm{Am(V)} \rightarrow \mathrm{Am(VI)} + \mathrm{Am(III)} \qquad (8)$$

with reaction (8) taking place instantaneously, since americium(VI) is not detected in the solution.

Asprey and Stephanou suggest a different mechanism of disproportionation reactinn in $6M$ $HClO_4$, considering it to be a second order reaction:

$$\mathrm{Am(V)} + \mathrm{Am(V)} \rightleftharpoons \mathrm{Am(VI)} + \mathrm{Am(IV)} \qquad (9)$$

$$\mathrm{Am(IV)} \rightarrow \mathrm{Am(III)} \qquad (10)$$

$$2\,\mathrm{Am(V)} \rightleftharpoons \mathrm{Am(VI)} + \mathrm{Am(III)} \qquad (11)$$

However, analysis of the experimental curves obtained by these authors show that in $6M$ perchloric acid the stoichiometric coefficient of the disproportionation reaction (11) exceeds two.

Evidently reactions (8) and (10) are competing reactions. In sulphuric acid, which is a strong complex-forming agent for americium(VI) and, apparently, for americium(IV), reaction (8) is the dominant one.

AUTO-REDUCTION OF AMERICIUM(VI)

In aqueous solutions americium(VI), under the influence of its own radiation, reduces to americium(V). The reduction process was studied by the change in the concentration of americium(VI) and (V) (Fig. 12).

As long as the concentration of americium(V) is below 4 mM/l only oue reaction takes place:

$$AmO_2^{++} + \vec{e} \xrightarrow{K_a} AmO_2^+$$

This proceeds at a constant rate, dependent upon the total americium concentration and independent of the concentration of americium(VI). When the concentration of americium(V) exceeds 4 mM/l, the dispro-

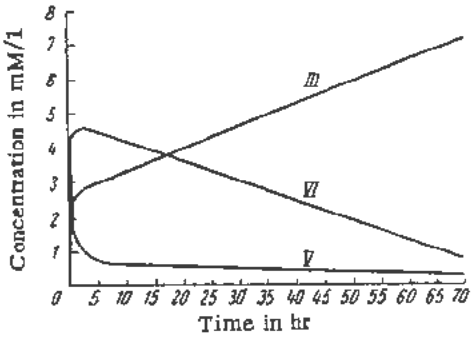

Figure 11. Disproportionation of americium(V) in 4M H_2SO_4: molar extinction coefficients for americium(III) at 811 mμ — 65; for americium(V) at 718 mμ — 60; for americium(VI) at 996 mμ — 105

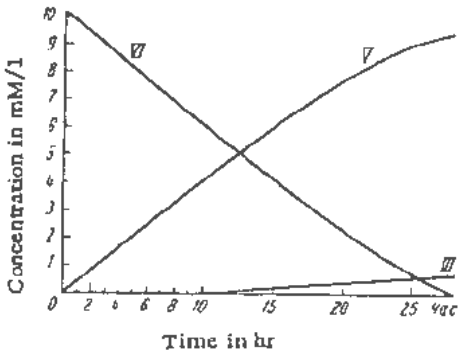

Figure 12. Reduction of americium(VI) in 0.2M $HClO_4$ at 23°C: initial concentration of americium(VI) 10.14 mM/l

portionation reaction of americium(V) becomes significant and retards reduction. As a result of this reaction americium(III) appears in the solution. The complete reduction of americium(VI) took place in 28 hr under the conditions of the experiment (in 0.2*M* $HClO_4$ at 23°C and a 10.1 mM/l initial concentration of americium(VI)). If the formation of 0.7 mM/l americium(III) is assumed to follow reaction (6), the rate constant of the reduction reaction in these conditions will be equal to 4.0×10^{-2} hr^{-1}. The lower rate constants for this reaction (2.42×10^{-2} hr^{-1} and 2.36×10^{-2} hr^{-1}) obtained in 2*M* and 4*M* H_2SO_4, seem to testify the influence of complex formation on the rate of the reaction of reduction.

If we assume that the decomposition of water follows reaction (3) exclusively, the value of K_a for the reduction of americium(VI) is equal to 3.5×10^{-2} hr^{-1}. The higher value of this constant obtained in studying the reduction of americium(VI), confirms that under these conditions the decomposition of water takes place according to reaction (2).

REFERENCES

1. Stover, B. J. and Conway, J. G., Journ. Amer. Chem. Soc., *73*: 491 (1951).
2. Werner, L. B. and Perlman, J., Journ. Amer. Chem. Soc., *73*: 495 (1951).
3. Asprey, L. B., Stephanou, S. E. and Penneman, R. A., Journ. Chem. Soc., *73*: 5715 (1951).
4. Stephanou, S. E., Nigon, J. P. and Penneman, R. A., Journ. Chem. Phys., *21*: 42 (1953).
5. Hall, S. R. and Heruiman, P. D., Journ. Amer. Chem. Soc., 2214 (1954).
6. McLane, C. K., Dixon, J. S. and Hindman, J. C., *The Transuranium Elements*, National Nuclear Energy Series, New York (1949).
7. Perlman, J. and Street, K., *The Actinide Elements*, Ch. 14, New York (1954).
8. Allen, O., Hochanadel, C. J., Gormley, J. A. and Davis, T. W., Journ. Phys. Chem., *56*: 575 (1952).
9. Bonet-Maury, D. P. and Lefort, M., Nature, 4114, 381 (1952).
10. Lefort, M., Journ. Chem. Phys., *51*: 351 (1954).
11. Rowbottom, J., Science, *119*: 904 (1954).
12. Miller, N. and Wilkirson, J. Trans. Faraday Soc., *50*: 690 (1954).

Electrodeposition of Plutonium, Americium and Curium

By V. B. Dedov and V. N. Kosyakov,* USSR

Electrodeposition of transuranium elements from solutions of their salts is a good method for obtaining uniform films which show no signs of flaking. These films can be used for studying nuclear properties and for other experimental purposes.

This paper describes a method for the electrodeposition of plutonium, americium, and curium and gives some information about the behaviour of these elements during the electrolysis and about the kinetics of the process.

Owing to their great electronegativity the elements of the actinium series cannot be deposited in the form of metals. It is characteristic of these elements that they can be deposited on the cathode as the hydroxides or other insoluble compounds, depending on the conditions of electrolysis. Considering that in their tripositive state plutonium, americium and curium are chemically analogous to the rare earth elements it was reasonable to suppose that their electrochemical behaviour would be similar to that of the latter. By their chemical properties plutonium(IV) and plutonium(VI) resemble respectively thorium and uranium, whose electrochemical properties have been investigated by a number of authors.[1,2,3,4,5] A peculiar feature of the electrolysis of aqueous thorium solutions is hydrolysis in the layer immediately adjacent to the cathode[6,7] which causes precipitation of either the hydroxide or basic compounds. This can be avoided by electrolysis in acid media,[1] in non-aqueous solvents[1] or in media of complex salts of organic[3] or inorganic[2] acid solutions.

Uranium can be deposited on metal surfaces in the form of uranyl ions[4,5,8,9,10] from solutions of its compounds.

Considering the above analogy of the chemical properties of uranium(IV, VI) and plutonium(IV, VI), the electrodeposition methods for uranium have been used also for the deposition of plutonium. Existing practices of plutonium electrodeposition may be divided into two groups.

The first group consists of normal methods based on the isolation of plutonium from solutions containing plutonium in the form of plutonyl ions. It includes electrolysis of buffered solutions of complexes with organic acids, also methods based on the formation of insoluble compounds during the process of the cathodic reduction of plutonium to the tetrapositive oxidation state.

* Original language: Russian.

The second group consists of methods of electrolysis of plutonium in the lower oxidation states.

Like uranium, plutonium(VI) salts were electrolysed in acetone, carbonate and basic solutions.[11–16] Though plutonium(VI) and uranium are quite similar in a number of properties, the methods applicable to uranium did not yield sufficiently satisfactory results for plutonium. This was not unexpected, as plutonium and uranium behave differently in electrolysis due to the great difference in their oxidation-reduction potentials and the properties of the resulting compounds.

In the reported work[12] on electrodeposition of plutonium from solutions with carrier containing plutonium in the lower oxidation state, the authors have erroneously proceeded on the assumption that absolute absence of water and free acid in the electrolyte was necessary and therefore carefully avoided plutonium(IV). But it is known[17] that the media need not be absolutely neutral and non-aqueous for the electrodeposition of lanthanum and thorium, whose chemical properties are very much like those of plutonium(III) and (IV) respectively. It therefore hardly seemed probable that plutonium would behave essentially differently under these conditions.

The authors of this paper investigated the influence of various factors on the electrolysis of chlorides of transuranium elements in the tripositive state and of plutonium(IV) chloride for the purpose of working out a simple and reliable method for obtaining uniform and adherent films.

The preliminary investigation of the electrodeposition method was carried out on the rare earth elements; cerium and samarium, because their chemical properties are similar to those of transuranium elements in the tripositive state.

EXPERIMENTAL

Apparatus

Special equipment was designed and built for the investigations to solve the problems connected with the practical application of the electrodeposition method.

In the main two kinds of electrolytic cells were used: (*a*) glass and quartz electrolytic cells with a flat cathode and rotating anodes, (*b*) electrolytic cells with cylindrical cathodes and rotating anodes for deposition of films on the outside and inside surfaces of the cylinders.

Table I. The Influence of Alcohol on the Current Efficiency and the Quality of Cerium and Samarium Deposits

Solvents	Oxides obtained, mg	Current efficiency, %	Quality of deposits
Water	5.1	50.5	Friable, crumbles when dry
25% alcohol	7.7	76	
50% alcohol	7.9	78	
75% alcohol	8.2	81	
99% alcohol	8.8	87	Adherent, cracks when dry

Reagents

For the work with rare earth elements commercial $CeCl_3 \cdot 7\ H_2O$ and Sm_2O_3 were used. Samarium chloride was prepared by dissolving samarium oxide in hydrochloric acid with subsequent vacuum drying. Carefully purified plutonium(IV) chloride was used directly. Plutonium(III) chloride was prepared from it by hydrogen reduction on platinized platinum. Contamination of the plutonium and americium samples did not exceed 1 per cent. The curium samples were obtained by irradiation of americium in a pile with subsequent quantitative separation by cation-exchange-resin.

THE PRELIMINARY INVESTIGATION

The composition and quality of cathode films are determined chiefly by electrolyte composition and current density. Since published works hardly touch on the influence of these factors we undertook systematic research in this field. Experiments were carried out on the electrolysis of cerium and samarium chlorides in aqueous media, ethyl alcohol, and alcohol-acetone-water mixtures.

Flaking films, obtained by electrolysis of aqueous samarium chloride solutions, adhered only slightly to the cathode surface.

Decrease of current density improves the quality of the film. When the current density, however, is less than 0.5 ma/cm² the hydroxide is not formed.

The influence of the alcohol content in the electrolyte on the current efficiency and the quality of the film is shown in Table I.

Table II. The Influence of Current Density on the Current Efficiency and Deposit Quality of Cerium and Samarium Oxides. (The Solvent Is 99% Alcohol.)

Current density, ma/cm²	Oxide obtained, mg	Current efficiency, % mg	Quality of deposit
1.0	8.8	8.7	Adherent, cracks when dry
0.5	4.6	91.0	Cracks when heated
0.2	2.0	100.	Adherent, readily rubs off
0.1	1.0	100.	Adherent, readily rubs off

The data in Table I were obtained at a current density of 1 ma/cm² and electrolysis time of 40 min.

Alcoholic media are more convenient for electrolysis since they make it possible to decrease the current density with the result that the quality of the deposit improves and gas evolution is completely excluded.

As seen from Table II the most suitable current density for electrolysis in 99% alcohol is 0.2 ma/cm². Further decrease of current density increases the electrolysis time, but does not appreciably improve the quality of the deposit.

Various mixtures of alcohol with acetone and water were tried for improvement of the film quality. These tests showed that the addition of a small quantity of water (up to 15%) considerably improves the quality of the electrolysis film. The most adherent film was obtained by using a mixture consisting of 50% alcohol, 45% acetone, and 5% water with a current density of 0.2 ma/cm². Acetone evidently facilitates dehydration which in turn is conducive to the formation of adherent cathode films.

Analysis of the cathode deposits shows that the hydroxide produces crystalline compounds with alcohol and water as constituents.

The composition of the deposits depends upon the water and alcohol ratio in the electrolyte and can be expressed by the general formula: $Sm(OH)_3 \cdot nH_2O \cdot mC_2H_5OH$. The composition of the cerium deposits differs from that of the samarium one, since cerium is partially oxidized to the tetrapositive state by the products formed at the anode.

ELECTRODEPOSITION OF PLUTONIUM(III)

For the deposition of plutonium by the rare earth element method it was found that the electrolysis under these conditions should not be carried out for more than 10–15 min. Prolonged passage of the current leads to the precipitation of plutonium(IV) hydroxide. However, if the concentration of plutonium does not exceed 0.03 mg per ml precipitation may not occur.

Table III. Electradeposition of Plutonium from Neutral Media

Current density, ma/cm²	Time, min	Current efficiency, %	Film density in mg of Pu/cm²
0.2	4	93.7	0.037
0.2	8	92.2	0.073
0.27	15	81.0	0.14
0.2	40	36.0	0.16

Table III gives the results of the electrodeposition of plutonium from neutral media.

The dependence of the deposit on the electrolysis time in acid media (pH = 1.5–2.0) is shown in Fig. 1. The points on the curve represent average results of a number of experiments.

The initial quantities of plutonium in each experiment were 1.5 mg, the cathode surface was 16 cm². Electrolysis was carried out with a current density

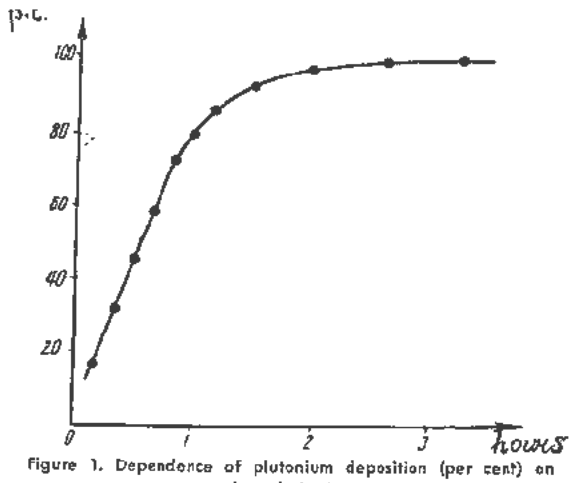

Figure 1. Dependence of plutonium deposition (per cent) on electrolysis time

of 5–10 ma/cm². Practically all the plutonium was separated with a film density of up to 0.25 mg/cm². The plutonium films obtained were sufficiently adherent.

ELECTRODEPOSITION OF PLUTONIUM FROM SOLUTIONS OF PLUTONIUM(IV)

Good films can be obtained by increased acidity and high current density. Thus, electrolysis at a current density of 40 ma/cm² of an alcohol-acetone-water solution of plutonium(IV) with 0.1 *N* acidity removed 97% of the plutonium from the solution in 3 hr as a uniform yellow-brown deposit with a film density of up to 0.3 mg/cm².

ELECTRODEPOSITION OF CURIUM AND AMERICIUM

Electrodeposition of tracer amounts of curium and americium was carried out from solutions having americium and curium concentrations of 2×10^{-10} gm/ml and 2×10^{-7} gm/ml respectively (the disintegration rate for both elements was 10^6 α particles/ml-min) at a current density of 20 ma/cm². From

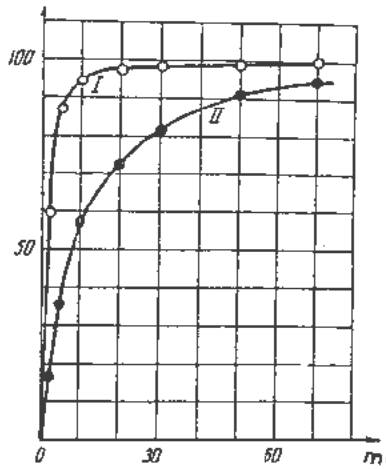

Figure 2. Dependence of percentage of element isolation upon electrolysis time in min.: curve 1, curium; curve 2, americium

nitric acid solutions at pH = 2.0–2.5, 99.6% of the americium was deposited on the cathode in 30 min and 99.7% of the curium in 3 hr.

Quantity dependence of the deposited material on electrolysis time under the above conditions is shown in Fig. 2, where the *x*-axis represents time in minutes and the *y*-axis represents americium deposition in per cent. Investigation of the dependence of total deposition upon pH revealed that a fixed maximum percentage of isolation corresponds *to each pH value* irrespective of the initial concentration of the element in the electrolyte (Fig. 3).

Thus, under certain conditions n_{max}/N_0 = constant, where n_{max} is the maximum deposit on the cathode and N_0 the initial concentration in the electrolyte. With increasing pH, the percentage deposition increases. In neutral solutions, however, the losses due to adsorption on the vessel walls may essentially account for some loss of material. In nitric acid the pH is constant throughout the electrolysis,

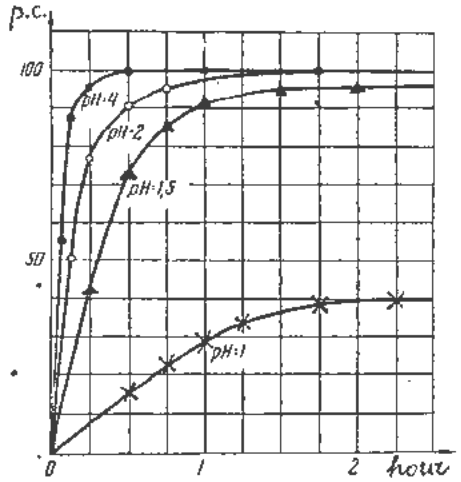

Figure 3. Dependence of percentage of americium isolation upon electrolysis time and pH of nitric acid media

whereas in hydrochloric acid solutions it increases due to acid decomposition.

Electrodeposition of weighable amounts of americium yielded better results, as in this case losses due to adsorption are negligible, and electrolysis can be carried out in a less acidic medium (pH = 3) with a lower current density, which is conducive to the formation of a more adherent fine crystalline deposit.

From a solution initially containing 400 μg of americium 399 μg (99.8%) of it was deposited on the cathode in 3 hours with a current density of 15 ma/cm².

RESULTS

Considering that plutonium(III) and the rare elements have similar electrochemical properties it might have been assumed that the electrodeposition method worked out for cerium and samarium would also be suitable for plutonium(III). This, however, was not the case as it was found that oxidation of plutoni-

um(III) by chlorine formed at the anode resulted in the precipitation of plutonium(IV) hydroxide from the electrolyte. In this case the anode processes can be expressed by the reactions whose oxidation-reduction potentials are given in Table IV.

As is koown, the oxidation-reduction potential of the plutonium(III/IV) couple is +0.96 volts[19] and in the pH range 0 1 5, does not depend on the hydrogen-ion concentration, as oxidation occurs according to the scheme:

$$Pu^{+3} \rightarrow Pu^{+4} + e^-$$

In the pH range 1.5–7.0 the potential of the system due to hydrolysis of the plutonium(IV) greatly depends on pH, since oxidation corresponds to the scheme:

$$Pu^{+3} + 4H_2O \rightarrow Pu(OH)_4 + 4H^+ + e$$

In this acidity range the potential change on the negative side is 0.236 volts per pH unit. As may be seen from Table IV, the oxidation-reduction potentials of the above systems are more positive than that of the plutonium(III/IV) couple even in acid media. In the neutral range this difference is even greater and plutonium oxidizes to the tetrapositive state. The plutonium(IV) thus produced is hydrolized and precipitated from the solution in the form of hydroxide. Work on this problem showed the necessity for studying electrodeposition of non-metallic deposits Though non-metallic deposition is a complex process and is rather scantily discussed in the literature, it still may be explained to some extent from the standpoint of existing concepts regarding electrode process kinetics.[21] Plutonium deposition rate depending on electrolysis time in concentrated solutions may be characterized by the curve in Fig. 1. Examination of this curve shows that initially the process proceeds at an approximately constant rate, up to a deposition of about 80 per cent of the plutonium in the solution, and then slows down. This

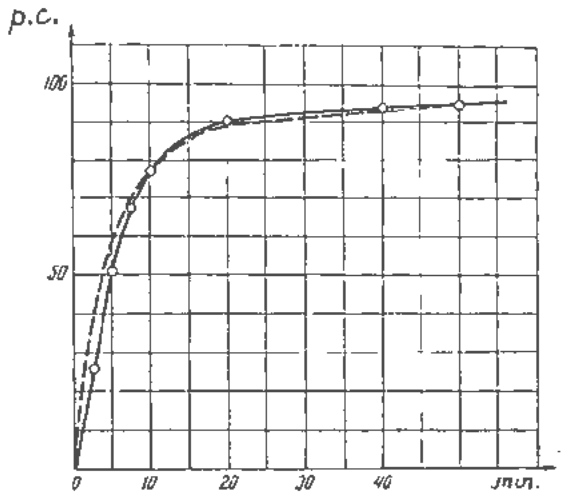

Figure 4. Dependence of deposited substance on electrolysis time

Table IV

System	E_0 volts*
$Cl^- \longrightarrow Cl_2 + e^- \ldots$	1 36
$\frac{1}{2} Cl_2 + H_2O \longrightarrow HClO + H^+ + e^-$	1.63
$Cl^- + H_2O \longrightarrow HClO + H^+ + 2e^-$	1.49

* The potential signs are given according to the European system.

slowing down may be attributed both to the considerable decrease of plutonium concentration in the solution, as a result of its deposition on the cathode and to the oxidation of plutonium(III) to the tetrapositive state.[22]

Thus, in the electrolysis of relatively large amounts of plutonium, the process becomes complicated due to the secondary process, caused by the chemical properties of plutonium. A much better concept of deposition kinetics may be developed by an analysis of the curves representing the electrodeposition process of tracer amounts of americium and curium (Fig. 2). The deposition process of these elements may be regarded as being the results of decomposition of water according to the following reactions:

$$3HOH + 3e^- \rightarrow \tfrac{3}{2}H_2 \uparrow + 3OH'$$

$$R^{+3} + 3OH' \rightarrow R(OH)_3$$

$$R^{+3} + 3HOH + 3e^- \rightarrow \tfrac{3}{2}H_2 \uparrow + R(OH)_3$$

Consequently the formation of the hydroxide precipitate in the layer immediately adjacent to the cathode layer is related to the electrolytic decomposition of water and precipitation occurs at the electrode potential corresponding to hydrogen evolution. Investigation of the electrodeposition curves of tracer amounts of americium and curium revealed that the formation of the deposit on the cathode obeys for some time an exponential law which can be expressed by the following equation:

$$n = n_{max}(1 - e^{-kt}) \qquad (1)$$

where n is the amount of substance deposited on the cathode in time t, and k is a constant.

From the values of the constant k during the electrolysis (Table V) and from Fig. 4 where the solid curve passes through the experimental points and the dotted curve corresponds to Equation 1 when $k = 0.163$, we conclude that the above process obeys Equation 1 only after a certain time—in our case 10 min.

Table V

Minutes	Experimental data	Δk
2.5	0.124	....
5	0.150	....
10	0.163	0.000
15	0.165	+0.002
20	0.163	0.000
30	0.160	−0.003
40	0.165	+0.002
Average data	0.163	±0.002

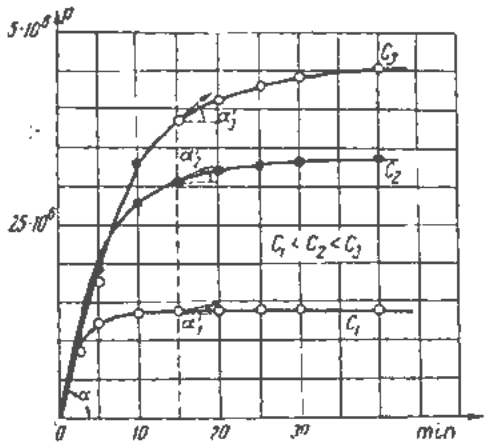

Figure 5. Dependence of electrodeposition on initial element concentration C in the electrolyte

The exponential form of the electrodeposition curve was noted in earlier reports on the electrodeposition of small quantities of substances[23,24,26] during investigations of the process of total element isolation. This phenomenon was explained from the viewpoint of electrodeposition diffusion kinetics by Joliot[25] using the example of the deposition of polonium on gold. He found the following empirical formula expressing this deposition rate:

$$\frac{dn}{dt} = \alpha(N_0 - n) - \beta n \qquad (2)$$

where n is the amount of polonium deposited on the cathode, N_0 is the initial amount of polonium in the electrolyte, α and β are empirical constants which depend on the experimental conditions.

Ultimately the deposition process obeys the exponential law.

In our case the deposition rate is determined not only by the diffusion rate of the cations, but also by the inverse reaction of hydroxide dissolution. The latter explains the influence of pH on the limiting percentage of deposition (Fig. 3). It will be remembered from Fig. 4 and Table V that the empirical Equation I is valid only for that section of the curve where k = const, i.e., for the end of the process. As for the beginning of the process, the experimental data indicate a linear dependence (Fig. 1). Special experiments were carried out to investigate the dependence of electrodeposition on the initial concentration in the electrolyte using cerium labelled with radioactive Ce^{144}. The results obtained are presented graphically in Fig. 5 and show that when the initial concentration of the element in the electrolyte is not too low, the deposition (denoted by α) does not depend on the concentration.

Thus the conclusion can be drawn that, at the start, electrodeposition proceeds at a constant rate and only at the end of the process, when the concentration of the substance in electrolyte has decreased, does the diffusion process begin to play an increasing role, as a result of which the rate dependence becomes exponential.

REFERENCES

1. Tödt, F., Z. Phys. Chem., *113*: 329 (1924).
2. Casto, C. C., "Analytical chemistry of the Manhattan project," National Nuclear Energy Series, Div. 8. *1*, New York, 1950.
3. Koizumi, Katsunaga, Japan, *172*: 375, Feb. 12 (1946).
4. Fischer, A., Z. Anorg. Chem., *81*: 170 (1913).
5. Casto, C. C., "Analytical chemistry of the Manhattan project," National Nuclear Energy Series, Div. 8, *1*: New York, 1950.
6. Dennis, L. M. and Lemon, B. J., J. Am. Chem. Soc., *37*: 131-37 (1915).
7. Bayer, O. v., Hahn, O. and Meitner, L., Physik. Zschr. *15*: 649 (1914).
8. Franciset, M., Tcheng-Da-Tchang, C. R., *206*: 1024 (1935).
9. Smith, E. F., Ber., *13*: 751 (1880).
10. de Coninck, F. W. O. and Camo, M., Bull. Acad. Belg., *106*: 321 (1901).
11. Cook, O. A., "The Transuranium Elements," National Nuclear Energy Series, Div. 4, *14B*, New York, 1949.
12. Seaborg, G. T. and Whall, A. C., "The Transuranium Elements," National Nuclear Series, Div. 4, *14B*, New York, 1949.
13. Hufford, D. L. and Scott, B. F., "The Transuranium Elements," National Nuclear Series, Div. 4, *14B*, New York, 1949.
14. Müller, M. L., Suppl. Los Alam. Rep. LAMS-100, July 11, 1944.
15. Müller, H. W. and Brouns, R., Anal. Chem., *24*: 537 (1952).
16. Dodson, R. W., Graves, A. C., Helmholz, L., Hufford, D. L., Potter, R. M. and Povelites, J. G., "Miscellaneous Physical and Chemical Techniques of the Los Alamos Project," National Nuclear Energy Series, Div. 5, *3*, New York, 1952.
17. Cetele, S. and Haissinsky, M., C.R., *206*: 644 (1938).
18. Glasstone, S., "An Introduction to Electrochemistry."
19. Howland, J. J., "Transuranium Elements," National Nuclear Energy Series, Division 4, *14B*, New York, 1949.
20. Isgarishev, N. A. and Gorbachev, S. V., Studies in Theoretical Electre-Chemistry, page 29, State Chemical Publishing House, Moscow - Leningrad (1951).
21. Frumkin, A. N., "Kinetics of Electrode Processes," Moscow, University Press, 1952.
22. Kraus, K. A., "The Transuranium Elements," National Nuclear Energy Series, Div. 4, *14B*, New York, 1949.
23. Töpelman, H. and J. prakt. Chem. *121*: 239 (1929).
24. Tammann, G. and Wilson, C., Z. Anorg. Chem., *173*: 137 (1928).
25. Joliot, F., J. Chim. Phys., *27*: No. 3, 133 (1930).
26. Flagg, J. F. and Bleidner, W. E., J. Chem. Phys., *13*: 269 (1945).

Plutonium Hexafluoride: Preparation and Some Physical and Chemical Properties

By C. J. Mandleberg, H. K. Rae, R. Hurst, G. Long, D. Davies and K. E. Francis,* UK

Several observations by workers at A.E.R.E., Harwell suggested that plutonium forms a volatile compound, possibly a fluoride. For example, milligram quantities of plutonium trifluoride, plutonium(IV) oxalate or plutonium dioxide were completely volatile in a stream of hydrogen fluoride and oxygen.[1] By analogy with the reaction

$$UF_4 + O_2 \rightleftharpoons UO_2F_2 + UF_6$$

it was assumed that plutonium hexafluoride had been produced, and milligram quantities of a volatile plutonium compound were in fact obtained by passing oxygen over plutonium tetrafluoride at 850°C.[2] Consequently the action of fluorine on plutonium compounds was investigated, with successful production of plutonium hexafluoride. The method of preparation and some physical and chemical properties of the hexafluoride are presented below.

PREPARATION

Plutonium hexafluoride has been prepared by the direct fluorination of the dioxide, trifluoride and tetrafluoride of plutonium. The sample was contained in a nickel boat and heated in a horizontal nickel furnace (1.2 in.) i.e., to a temperature in the range 370 to 720°C. Fluorine gas at 1 atmosphere pressure was passed through the furnace, and the volatile hexafluoride condensed from the fluorine stream in a nickel cold-trap immersed in liquid oxygen. On cooling the furnace, the fluorine was displaced with argon, the whole furnace evacuated to 10^{-3} mm Hg and the PuF_6 distilled into a reservoir of nickel or glass. Quantities of up to 5 gm of hexafluoride have been prepared in this manner, with yields $\sim$ 90%.

The fluorination of the dioxide and trifluoride appeared to proceed with the tetrafluoride as an intermediate; consequently the fluorination of plutonium tetrafluoride was studied in greatest detail, the influence of temperature, fluorine flow-rate, doration of reaction and the nature of the tetrafluoride.

Temperature

Samples (ca 3.0 gm) of plutonium tetrafluoride were fluorinated for four hours at various temperatures and the amount converted to hexafluoride determined by weighing the residues of tetrafluoride. The amount converted varies from 40 mg/hr/gm PuF_4 at 320°C to 200 mg/hr/gm PuF_4 at 620°C. It is interesting to note that under identical conditions at 400°C the rate of fluorination of uranium tetrafluoride is 20 times that of plutonium tetrafluoride.

Effect of Fluorine Flow-Rate

When the fluorine flow-rate falls below 0.2 millimole/min the reaction rate is considerably reduced, but an increase from 1 millimole/min to 20 millimole/min brings about no significant increase in the reaction rate. Even the lowest flow-rate corresponds to a large excess of fluorine over plutonium tetrafluoride, and a very inefficient conversion of fluorine. In this work a flow-rate of 1 millimole/min was used.

Duration of Reaction

The extent of conversion to plutonium hexafluoride at 720°C of a series of 3.0-gram charges of plutonium tetrafluoride was determined after varying intervals of time, and as may be expected the meau reaction rate decreased with increasing time. Assuming that the rate of reaction is proportional to the surface area of the tetrafluoride and as this is roughly proportional to the mass of tetrafluoride then a logarithmic relation holds between the mass of tetrafluoride and the time This relation has been demonstrated over the range 0 to 65% conversion of the PuF_4.

The effect of initial charge of plutonium tetrafluoride on the reaction rate was investigated; below about a 3-gram charge the rate was approximately proportional to the charge (as assumed above) but with larger charges the rate of reaction fell off, presumably because with a deep bed of PuF_4 the diffusion of fluorine into and PuF_6 out of the bed became rate determining.

Effect of the Plutonium Tetrafluoride

The tetrafluoride from which the hexafluoride was prepared was made by precipitating the oxalate at 80–90°C from a solution of quadrivalent plutonium nitrate, igniting the oxalate to oxide in a stream of argon and oxygen, and then converting to tetrafluoride in a stream of hydrofluoric acid gas and oxygen. The effects on the rate of fluorination of the tetrafluoride, of the temperature of ignition of the oxalate and fluorination of the oxide, were studied and it was found that the most reactive tetrafluoride was produced by low-temperature (350°C) ignition and hydrofluorination.

* A.E.R.E., Harwell, England.

The Residue Remaining After High-Temperature Fluorination of Plutonium Tetrafluoride

Plutonium tetrafluoride, when prepared as described above, is pale pink in colour when viewed in white light, and the residue remaining after partial conversion to hexafluoride at temperatures below 500°C is of similar colour. As the fluorination temperature is increased, however, the residue appears darker in colour, the proportion of darker material and the depth of colour increasing with increasing temperature and time of fluorination. At 600°C some apparently unaltered pink material still remains overlying the darker residue. These dark residues have been analysed for fluorine by the pyrohydrolytic method, the average value for a series of fluorinations at different temperatures being 25.9 ± 0.3% F (cf PuF_4 24.1%; Pu_4F_{17} 25.3%; Pu_2F_9 26.3% F). The X-ray diffraction pattern of the residues is clearly defined, and the majority of lines compare closely with those of plutonium tetrafluoride, with a number of extra lines, which make the pattern for the residue similar to the "distorted UF_4" lattice which Agron *et al.*[3] reported (cf fluorine analysis above).

Analysis of the Volatile Fluoride

Although there is little doubt as to the formula of the volatile fluoride of plutonium, it was felt desirable to confirm its composition by chemical analysis. This was carried out by hydrolysis and subsequent determination of the Pu:F ratio. Because of the vigorous nature of the hydrolysis at room temperature (see below) the hydrolysis was carried out by condensing PuF_6, which had been pumped at −70°C for some hours, on to ice on a glass cold finger at −180°C, sealing off the cold-trap and allowing the system to warm up to room temperature. The hydrolysis took place smoothly under these conditions to give an orange-pink solution. The glass-trap was cracked open and washed out with dilute sulphuric acid. The solution was examined spectrophotometrically and the plutonium found to be substantially in the hexavalent state.

The solution was analysed for fluorine by distillation of hydrofluoric acid from the acid solution and subsequent titration, and plutonium by the counting of aliquots. The ratio Pu:F was found to be 1:6.26 ± 0.38; thus confirming the formula PuF_6.

PHYSICAL PROPERTIES

Appearance and Melting Point

Plutonium hexafluoride, when condensed in a dry Pyrex or silica tube at −180°C and sealed in vacuo, is a white crystalline solid, similar in appearance to uranium hexafluoride. On warming to room temperature the solid turns pale brown which deepens as the temperature is increased, the solid melting at 54 ± 1°C to a limpid dark-brown liquid. Vapour at melting point is pale brown and at 70°C deep brown.

Vapour Pressure

This was determined at various temperatures by means of a bellows manometer which was used as a null-point instrument, the backing pressure required to return the bellows to the fiduciary mark being observed on a mercury in glass manometer by means of a cathetometer. Before making any readings, the reservoir of hexafluoride was maintained at −70°C and evacuated continuously for 60 hours to remove traces of hydrofluoric acid. When this precaution was not taken, appreciably higher values of the vapour pressure were obtained. The series of measurements extended over three weeks, and it was found that, although the apparatus was free from leaks a pressure of a gas, which was incondensible at −80°C, slowly developed. This was attributed to the decomposition of PuF_6 to a lower fluoride and fluorine under its own α-bombardment (see below). Consequently, before making a series of measurements the reservoir was cooled to −70°C and pumped to remove the incondensible gas. The vapour pressure was measured over the temperature range −29.5 to +21°C (vapour pressure range 0.8 to 97.4 mm Hg) and the points are closely represented by the equation

$$\log_{10} p_{mm} = 11.45 - 2778/T$$

DECOMPOSITION OF PLUTONIUM HEXAFLUORIDE

On standing for several days in a sealed container, plutonium hexafluoride produces a free-flowing pink solid (from which residual hexafluoride can be removed by pumping) and a corresponding rise in pressure occurs. This is attributed to disruption of the molecule under the bombardment of the plutonium α-particles. The nature of the solid product and rate of decomposition are reported upon below.

NATURE OF THE SOLID DECOMPOSITION PRODUCT

Immediately on coming in contact with moist air the pink powder darkens slightly. This compound (*A*) was examined on a quartz helix balance and a thermogravimetric curve obtained, on which a distinct plateau was observed at 150 to 230°C for all the samples. On cooling from 200°C an increase in weight of 1% occurs, giving compound *B*. At higher temperatures both compounds lose weight and at 500°C in air are completely converted on the dioxide.

Compound *A* gives no X-ray diffraction pattern, presumably because of the small size of the particles deposited during the decomposition of the hexafluoride. The diffraction pattern of compound *B* was found to be identical to that of a compound reported by Dawson and D'Eye[4] which was shown to be a hydrate of plutonium tetrafluoride containing between 0.5 and 1.5 molecules of water (cf the analyses below). Both compounds were analysed for plutonium by ignition to the dioxide and for fluorine by pyrohydrolysis, giving the following results:

	Compound A	*Compound B*
Plutonium	70.0%	72.4%
Fluorine	22.2%	23.4%
Water (?) by difference	7.8%	4.2%
F:Pu atomic ratio	3.99	4.3
Formula	$PuF_4 \cdot 1.5\ H_2O$	$PuF_4 \cdot 0.8\ H_2O$

Thus the product of the decomposition of plutonium hexafluoride is the tetrafluoride and the darkening on bringing the product into contact with air is attributed to the rapid formation of hydrate.

Rate of Decomposition

The rate of decomposition was determined by two methods, namely (*a*) by weighing the amount of solid decomposition product produced and (*b*) by observing the pressure rise during the decomposition.

(*a*) Solid Formation

The amount of solid produced by decomposition of the hexafluoride was determined by weighing as $PuF_4 \cdot 1.5\ H_2O$. Vessels of nickel and glass were used, the latter being kept at —70°C during the experiment. Sufficient hexafluoride (~1 gram) was introduced into the vessels to ensure that some solid hexafluoride was remaining at the end of the experiment. The amount of tetrafluoride produced after different times, varying from 6 to 36 days, was determined, giving an average value for the decomposition rate of about 10 mg of hexafluoride decomposed per day for the particular vessel used (i.e., about 1% per day).

(*b*) Pressure Rise

The rise in pressure during the decomposition was observed in the same apparatus that was used to determine the vapour pressure of plutonium hexafluoride. The reservoir of hexafluoride was kept at room temperature during the experiment, but when readings of pressure were made the reservoir was cooled in ice. The experiment covered a period of 34 days; during the first 11 days, while, by mass balance, solid PuF_6 was estimated to be still present, the pressure rise was linear with time, but after the 11th day the rate of rise in pressure decreased, following an exponential law. Under the conditions of the experiment the total rate of decomposition in the vapour was 2% per day. However, the estimated range of plutonium α-particles in the vapour (approx. 5 cm) was so much greater than the size of the reservoir (cylinder, 1 cm diameter, 20 cm long) that the greater part of the energy of the α-particles would be lost to the walls.

REACTIONS OF PLUTONIUM HEXAFLUORIDE

Reaction with Water

Plutonium hexafluoride can be stored at room temperature in carefully dried Pyrex glass for long periods, and with undried glass there is no reaction at —180°C unless the glass is unusually moist. On warming from —180°C a brown flaky stain spreads rapidly over the whole of the inside of the tube, accompanied by considerable etching. The reaction does not appear to go to completion as readily as that of uranium hexafluoride, for after some period of hydrolysis a considerable quantity of plutonium hexafluoride can be distilled from the tube. The product of this hydrolysis is plutonyl fluoride, PuO_2F_2, as demonstrated by X-ray diffraction and thermogravimetric analysis.

On hydrolysis with water or moist air at room temperature a violent reaction takes place accompanied by flashes of light. The resulting solution contains a variable amount of precipitate which has been shown by X-ray analysis to contain PuF_4 hydrate and PuO_2, demonstrating further the high temperatures occurring during the hydrolysis. By spectrophotometry no evidence was found for the presence of valency states other than (VI) in the solution resulting from the hydrolysis.

Reaction with Sulphuric Acid

During the fluorination of the tetrafluoride the effluent fluorine was passed through a bubbler of 98% sulphuric acid, which served to prevent the diffusion of water vapour into the apparatus. After a time this acid became pink in colour and eventually threw down a flocculent pink precipitate which on standing separated out as a pink crystalline solid. If the acid and precipitate were left standing in moist air the precipitate redissolved to give a bright red solution.

The crystalline precipitate was filtered under suction on a porous disc, but could not be washed as it dissolved in sulphuric acid or water. On standing, however, it dried to a friable brick-red powder. The X-ray diffraction pattern of this powder is very complex, and agrees closely with that of $U(SO_4)_2 \cdot 2H_2O$. The powder was analysed after dissolving in dilute nitric acid, the plutonium being determined by α-counting and the sulphate by precipitation as barium sulphate, giving the following values: Pu 41.8%; SO_4, 37.0%; water (?) by difference 11.2%. This corresponds to $Pu(SO_4)_2 \cdot 2H_2SO_4 \cdot 3.5H_2O$ which represents the formula of the air-dried sample of the precipitate. The solution in 98% sulphuric acid was examined in the spectrophotometer[5] and the absorption spectrum agrees closely with that for Pu(IV) in 16*M* sulphuric acid.[6]

Thus the analytical, X-ray diffraction and spectrophotometric evidence make it highly probable that the pink precipitate produced when plutonium hexafluoride is passed into sulphuric acid is plutonium(IV) sulphate, although the mechanism of the reaction:

$$PuF_6 \xrightarrow[H_2SO_4]{F_2} Pu(SO_4)_2$$

is obscure.

REFERENCES

1. Dawson, J. K. and Truswell, A. E., A.E.R.E. C/R-662 (1951).
2. Mandleberg, C. J., Davies, D. and Francis, K. E., A.E.R.E. C/M-157 (1952).
3. Agron, P., *et al*, M.D.D.C., 1588.
4. Dawson, J. K., D'Eye, R. W. M. and Truswell, A. E., J. Chem. Soc., 3922 (1954).
5. The authors are indebted to Messrs. Hall, G. R. and Walter, A., for these measurements.
6. Hindman, J. C., N.N.E.S., IV-14A, Chapter 9.

The Properties of Plutonium Hexafluoride

By B. Weinstock and J. G. Malm,* USA

Plutonium hexafluoride is the volatile plutonium analogue of uranium hexafluoride. Its existence was suggested in the nineteen-forties by many experimenters because of the high volatility observed for plutonium in fluorinating gas streams at elevated temperatures. The first successful isolation and identification of this compound was reported by A. E. Florin of the Los Alamos Scientific Laboratory in October, 1950. Subsequently, plutonium hexafluoride has also been prepared and studied at the Atomic Energy Research Establishment (Harwell, Berks., England), the Knolls Atomic Power Laboratory and the Argonne National Laboratory. This paper will deal principally with the studies that have been made at the Argonne National Laboratory. It is our understanding that papers are in preparation for publication that will describe the work of the other laboratories.[1,2,3]

METHOD OF PREPARATION

Plutonium hexafluoride can be readily prepared by the reaction between plutonium tetrafluoride and fluorine gas at elevated temperatures. The reactor that we have used for this purpose (Fig. 1) was modeled after that developed by Florin, Tannenbaum and Lemons.[1] Plutonium tetrafluoride contained in a shallow nickel dish is heated in a fluorine atmosphere (300 mm Hg pressure) by the work coil of an induction heater that is located within the reactor. This coil, which is made of copper tubing, is cooled by the passage of liquid nitrogen and therefore also serves as the condenser for the plutonium hexafluoride produced. The proximity of the heated and cooled zones provides an efficient convection mechanism for the removal of the volatile product from the hot crucible to the condensing surface. The reaction is observed (through the fluorothene window) to proceed very rapidly at about 700°C and appears to be completed in a few minutes. The plutonium hexafluoride is subsequently recovered from the condenser by vacuum distillation and stored in a nickel reservoir as vapor. During this procedure a careful attempt is made to completely remove hydrogen fluoride from the product in order to permit the eventual study of PuF_6 in Pyrex glass and quartz equipment without hydrolytic decomposition. Starting with about one gram of PuF_4, a yield of purified PuF_6 corresponding to 90 per cent or more of the theoretical amount is generally obtained.

*Argonne National Laboratory.

In one experiment 2 mg of americium as the oxide was added to 860 mg of PuF_4 in an attempt to produce americium hexafluoride together with the plutonium hexafluoride. Although it would have been preferable to have started with americium fluoride rather than the oxide, the fluorine gas that was used contained sufficient hydrogen fluoride to assure the rapid conversion of the oxide to the corresponding fluoride under the conditions of the experiment. About 90 per cent of the plutonium was recovered as plutonium hexafluoride in this experiment, but americium was not detected in an aliquot taken from this gas. This result indicates either that americium hexafluoride cannot be produced or that much more vigorous treatment is required for its formation than for the formation of plutonium hexafluoride.

In a somewhat different type of reactor neptunium hexafluoride has been produced at a very rapid rate at a temperature of 500°C.[4] Under similar conditions one would expect uranium hexafluoride to be produced rapidly at about 300°C.[5] Thus the hexafluorides are produced with increasing difficulty as one

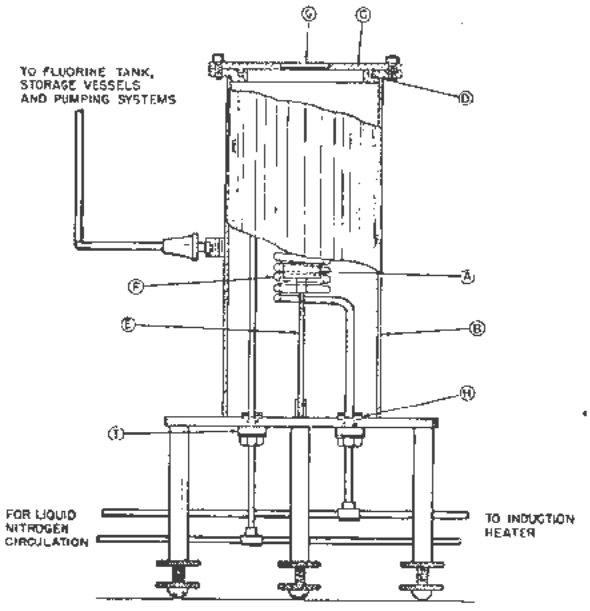

Figure 1. Reactor for plutonium hexafluoride: (A) nickel dish filled with PuF_4; (B) brass reactor can; (C) removable cover for loading reactor; (D) tongue and groove, teflon gasket for closure; (E) nickel supporting rod for nickel dish; (F) coil of 3/16-in. copper tubing; (G) fluorothene window; (H) teflon seal and insulator; (I) micalex insulator

proceeds through the series uranium, neptunium, plutonium and americium, with the possibility that americium hexafluoride cannot be prepared. This behavior is analogous to the increasingly negative value found for the (IV)-(VI) oxidation potentials of these elements in 1-molar aqueous solutions,[6] which G. T. Seaborg has suggested is partial evidence for an actinide series.

IDENTIFICATION AND CHEMICAL COMPOSITION

The similarity in volatility between the plutonium compound and uranium hexafluoride suggests that the two compounds are of similar chemical composition. This has been confirmed by a chemical analysis of a carefully purified sample of PuF_6. In this experiment a weighed amount of PuF_6 was condensed in the bottom of an evacuated glass tube at the sublimation temperature of solid carbon dioxide and hydrolyzed by admitting an ammoniacal solution through a break seal in the top of the tube. The hydrolysis occurred with considerably greater vigor than had been our experience with uranium hexafluoride. The chemical assay for plutonium and fluorine in the solution formed corresponded to the formula $PuF_{5.83}$ and accounted for 97.3 per cent of the weight of the sample. Within the experimental uncertainty of this determination the volatile gas under study was determined to be PuF_6. The purity of the material has been established by infrared measurement where absorption bands due to other known volatile fluorides were not found. Further evidence for the similarity of this material with UF_6 has been obtained from X-ray powder photographs, taken in a thin-walled Pyrex capillary, which showed it to be isostructural with UF_6.[7]

PHYSICAL PROPERTIES

Solid plutonium hexafluoride varies in color from dark red to yellow brown. The vapor is brown in color resembling nitrogen tetroxide. The melting point of a freshly distilled sample was found to be 50.75°C in an experiment carried out in a glass capillary. The vapor density has been roughly determined at 25°C and found to agree with the monomeric formula, PuF_6. Semi-quantitative dew point measurements of the vapor pressure indicate that PuF_6 is slightly less volatile than UF_6.[8]

RADIATION DECOMPOSITION

The study of plutonium hexafluoride is influenced to some degree by the high specific alpha activity of plutonium. Aside from the extreme health hazard presented by this volatile compound of plutonium, the alpha-particle emission results in a significant amount of radiation decomposition. When PuF_6 is stored principally as the solid phase the amount of this decomposition corresponds to the destruction of about 1.5 per cent of the volatile material per day. Assuming that the total alpha-particle energy is absorbed in the condensed PuF_6 it is estimated that an average of 31 electron volts are used in the decomposition of one molecule of plutonium hexafluoride. The products of decomposition have been identified as fluorine and plutonium tetrafluoride. All attempts to identify a plutonium compound of intermediate valence between four and six have thus far been unsuccessful.

In order to decrease the loss of PuF_6 due to radiation decomposition, we generally store the compound as vapor in a nickel container. In this state, dependent on the geometry of the container and the pressure of the gas, a large fraction of the alpha-particle energy is absorbed by the walls of the container and does not result in the decomposition of the compound. In general our decomposition losses during storage as vapor are found to be of the order of 0.1 per cent per day.

CHEMICAL PROPERTIES

Plutonium hexafluoride is a very powerful fluorinating agent. It has been found to effect fluorination reactions with greater rapidity than has been observed for fluorine gas.

The reaction between BrF_3 and PuF_6 has been studied in collaboration with I. Sheft and H. H. Hyman. PuF_6 was condensed onto the surface of solid BrF_3 contained in a Fluorothene tube at the temperature of liquid nitrogen. As the tube was allowed to warm up to room temperature the PuF_6 was observed to react at the surface of the BrF_3 and form an insoluble green precipitate. Subsequent distillation of the BrF_3 at 100°C yielded 0.1 per cent of the plutonium in the distillate. The non-volatile precipitate appeared to contain two solid phases under microscopic examination. One of the solid phases gave an X-ray pattern that showed it to be isostructural with PuF_4; the other solid phase did not produce an X-ray pattern and was presumably amorphous PuF_4. The probable reaction is summarized by the equation:

$$PuF_6 + BrF_3 = PuF_4 + BrF_5 \qquad (1)$$

This fluorination of BrF_3 to BrF_5 by PuF_6 apparently occurs with greater ease than the corresponding reaction between fluorine and BrF_3.[9] It is also of interest to compare this result with the fact that BrF_3 is usually used as a fluorinating agent[10] and, in particular, is used to convert uranium compounds to UF_6 quantitatively.[11]

An attempt to dissolve PuF_6 in BrF_5 has been made. The experiment was performed by condensing 40 mg of PuF_6 onto 6 cm³ of BrF_5 frozen in a fluorothene tube at the temperature of liquid nitrogen. As the surface of the BrF_5 was warmed a yellowish brown solution was at first observed to form; subsequently, however, the plutonium precipitated out. Since BrF_5 is the highest known fluoride of bromine the probable explanation for this result is that small amounts of BrF_3 in the BrF_5 reacted with the PuF_6 to form the insoluble PuF_4.

An 0.5 per cent solution of PuF_6 in *n*-perfluoroheptane (C_7F_{16}) has been prepared with some difficulty. Although the fluorocarbon sample used had

been carefully purified and various tests had indicated complete fluorination, it was observed to react rapidly with PuF_6 upon mixing. This suggested that some undetected carbon-hydrogen bonds still present in the fluorocarbon had reacted rapidly with PuF_6. The hydrogen fluoride produced from this reaction was then separated and a successful solution of PuF_6 in the now purified C_7F_{16} was obtained.

A preliminary investigation of the reaction between PuF_6 and PuF_3 has been undertaken. A quartz boat containing 55.2 mg of PuF_3 was exposed to 138 mg of PuF_6 vapor (pressure = 85 mm Hg) at room temperature in a glass system. The purple PuF_3 in the boat was observed to be partially converted to PuF_4 (light pink in color) very rapidly and pressure-volume calculations showed that 10 mg of PuF_6 had reacted. No further reaction was detected by pressure measurement after 16 hours of further exposure. The system was subsequently heated to 118°C for one hour and an additional 18 mg of PuF_6 was decomposed at this temperature. The weight change of the boat and its contents accounted for 26.3 mg of the reacted PuF_6. A sample of the contents of the boat did not give an X-ray pattern, but on heating this sample in the X-ray capillary for 16 hours at 305°C the pattern for PuF_4 (with a trace of PuF_3) was obtained. Neither solubility measurements with the product in neutral aqueous solution nor spectrophotometric examination of an acidic aqueous solution indicated the presence of an oxidation state higher than the tetravalent. The probable course of the reaction is summarized by the equation:

$$2PuF_3 + PuF_6 = 3PuF_4 \qquad (2)$$

On the basis of this equation 80 per cent of the PuF_3 initially present was converted to PuF_4.

In another experiment the reaction between PuF_3 (from the same source as that used above) and fluorine gas at 300 mm Hg pressure was observed at room temperature. Reaction took place very rapidly, although it did not go to completion. A sample of the pink reaction product (after heating at 230°C for 12 hours in a thin-walled Pyrex capillary) showed the PuF_4 X-ray pattern. On the basis of the equation

$$PuF_3 + \tfrac{1}{2}F_2 = PuF_4 \qquad (3)$$

the reaction had proceeded to 61 per cent of completion.

Reactions (2) and (3) offer promising systems for the determination of the heat of formation of PuF_4 and PuF_6. Although they did not proceed to completion with the sample of PuF_3 that was used, reaction (3) had previously been found by one of us to go to completion at room temperature with a more reactive sample of PuF_3.

A quartz boat containing 88.4 mg PuF_4 was exposed without evidence of reaction to 100 mg PuF_6 (70 mm Hg pressure) in a glass system at room temperature. The system was then heated to 180–210°C for an hour, and by pressure measurement 27 mg of PuF_6 were determined to have decomposed. Subsequent measurement of the increase in weight of the boat accounted for 19.4 mg of this material. X-ray analysis of a sample of the contents of the boat revealed only PuF_4 to be present. The conclusion is that the PuF_6 did not react with PuF_4 but decomposed on the surface of the PuF_4 in the following manner:

$$PuF_6 = PuF_4 + F_2 \qquad (4)$$

This conclusion is substantiated by the following experiment.

Plutonium hexafluoride (25 mg) was heated in a glass tube at 50 mm Hg pressure in order to determine the non volatile solid phase that results from its thermal decomposition. Heating for 30 minutes at 208°C revealed little, if any, thermal decomposition. Heating for 1 hour at 280°C resulted in rather complete decomposition of the PuF_6. The solid decomposition product deposited on the walls in red, single crystals (about 1 mm in size) and was identified as PuF_4 by X-ray analysis. Equation 4 describes the course of this decomposition although the fluorine was not identified in this experiment.

The reaction between UF_4 and PuF_6 was studied in a Pyrex glass system. In this experiment, 56 mg UF_4 contained in a quartz boat was contacted with 56 mg of PuF_6 gas (35 mm Hg pressure). The section of the apparatus containing the boat was then heated for 20 minutes at 200°C. At the end of this time PuF_6 was determined to be present by condensation of the vapor in a side arm and observation of the colored condensate. The heating was then continued for 30 minutes at 225°C, and condensation of the vapor indicated that the brown PuF_6 had been substantially replaced by a condensable white solid (UF_6). The heating was then continued for another 3.5 hours at 223°C and the vapor and contents of the boat analyzed. The vapor was determined to contain 14.3 mg UF_6 (11 mm Hg pressure in the experiment) and 2.7×10^{-5} mg PuF_6. The boat contained three differently colored solids which upon X-ray analysis gave the following results: pink compound, PuF_4; black compound, U_2F_9; greenish-black compound, U_2F_9. The equations representing the course of the reaction are:

$$4UF_4 + PuF_6 = 2U_2F_9 + PuF_4 \qquad (5)$$

$$U_2F_9 + \tfrac{3}{2}PuF_6 = 2UF_6 + \tfrac{3}{2}PuF_4 \qquad (6)$$

The presence of U_2F_9 as the only solid uranium phase under these conditions is in agreement with the phase diagram for the uranium-fluorine system.[5]

MAGNETIC SUSCEPTIBILITY

The magnetic susceptibility of solid PuF_6 has been measured in collaboration with D. M. Gruen at 81° and 295°K by the Faraday method. For this experiment 62 mg of PuF_6 were condensed into a thin-wall, 4.2-mm diameter quartz bulb and its 1-mm quartz connecting tube sealed off about 8 mm above the

bulb. Due to the small vapor volume available in the ampoule, the fluorine pressure build-up due to radiation decomposition was very rapid. This greatly increased the hazard of the experiment and the quartz ampoule was enclosed in a capped copper container during the magnetic measurements as a precautionary measure. It was estimated that the fluorine pressure would increase at the rate of one atmosphere per day in the ampoule so that at the end of the third day after filling the experiment was discontinued and thereafter the ampoule kept under water until it exploded on the tenth day.

The magnetic apparatus and experimental procedure were similar to that described by Gruen and Hutchinson.[12] The molal susceptibility was found to be 290 $\times$ 10^{-6} at 295°K and 330 $\times$ 10^{-6} at 81°K. This small, relatively temperature-independent susceptibility found for PuF_6 is very surprising, since other compounds that are isoelectronic with PuF_6 [U^{+4}, Np^{+5}, and $(PuO_2)^{+2}$] have susceptibilities[12,13] of magnitude 3000–4000 $\times$ 10^{-6} at room temperature that are strongly temperature dependent. It seems likely that the two non-bonding electrons in PuF_6, unlike those in U^{+4}, Np^{+5}, and $(PuO_2)^{+2}$ compounds, have paired spins and that the electronic ground state is non-degenerate.

RAMAN SPECTRUM

An unsuccessful attempt to obtain the Raman spectrum of PuF_6 vapor at two atmospheres pressure using a mercury arc source has been made in collaboration with H. H. Claassen. The Raman tube was filled with gas rather than liquid because the absorption of PuF_6 in the spectral region of interest is of such intensity that a greater density would be impractical. The general difficulty of obtaining the Raman spectrum for colored gases[14] is perhaps increased to the point of impossibility with PuF_6 because of photochemical decomposition. Under the conditions of irradiation (with the ultra-violet light completely filtered out) the sample of PuF_6 had decomposed by 50 per cent after 10 minutes of exposure. By comparison a vapor sample of UF_6 showed no evidence of photochemical decomposition after 72 hours of exposure in the mercury arc source.

INFRARED SPECTRUM

The infrared spectrum of PuF_6 vapor has been measured in collaboration with H. H. Claassen. A double beam infrared spectrophotometer equipped with KBr, CaF_2 and NaCl optics was used for the measurements. The PuF_6 was contained in a nickel cell fabricated with AgCl windows, and its pressure was maintained at values between 0.6 and 600 mm Hg pressure by adjustments of the temperature of a side arm.

The observed infrared spectrum is very similar to that obtained for UF_6[15,16,17] and on this basis the molecular structure of PuF_6 is also believed to be a regular octahedron. Without this comparison with UF_6 the infrared spectrum would be very difficult to interpret since only one of the two infrared active fundamentals is observed (ν_3)[14] and the three Raman active fundamentals probably cannot be obtained directly. Fortunately all of the fundamentals can be derived from the observed combination bands in the infrared, and the values derived are given in Table I together with Gaunt's[17] assignment of the UF_6 fundamentals.

From these frequencies and the Pu-F bond distance of 1.98 Å given by Zachariasen[6] the thermodynamic functions of PuF_6 have been calculated on the simple harmonic oscillator approximation.

The entropy (exclusive of nuclear spin) calculated for PuF_6 is 1.55 cal-deg^{-1}-mole^{-1} smaller than that calculated for UF_6[17] between 150° and 500°K. In this calculation the ground state of PuF_6 was taken to be non-degenerate in view of the magnetic susceptibility measurements.

Table I. Fundamental Vibration Frequencies (cm^{-1})

Assignment	*Symmetry*	*UF_6*	*PuF_6*
ν_1	A_{1g}	668	631
ν_2	E_g	532	523
ν_3	F_{1u}	626	615
ν_4	F_{1u}	189	202
ν_5	F_{2g}	202	210
ν_6	F_{2u}	144	173

ABSORPTION SPECTRUM

The absorption spectrum of PuF_6 vapor has been investigated in collaboration with J. K. Brody, F. S. Tomkins and M. S. Fred. The PuF_6 was contained in a quartz cell, 10 cm in length, at a pressure of 100 mm Hg. The spectrum was photographed over the region of wavelength 5000–12,000 Å, using a Jarrell-Ash spectrograph with a dispersion of 5 Å/mm and the Argonne 30-foot spectrograph with a dispersion of 1.8 Å/mm. In order to obtain sufficient absorption for the weaker bands, multiple traversal of the light through the cell was used with the number of passes varying from one to eight. Below 4500 Å the absorption intensity increases greatly and hence the photographic observations were limited to wave lengths greater than 5000 Å to avoid possible rapid photochemical decomposition. Beyond 12,000 Å, the photographic limit in the infrared, the spectrum was examined with a conventional infrared spectrophotometer.

Over the range 5000–25,000 Å the spectrum consists of about 6 groups of bands, each group evidently corresponding to a different electronic transition, as in the rare-earth spectra. Each group of bands consists of 3 or 4 bands of various intensities and separations. These separations are of the order of 100 Å and evidently form a vibrational spectrum that is superimposed on the electronic transition. The bands in these groups have a width of about 50 Å that is probably due to unresolved rotational structure with the exception of one weak sharp band at 9371 Å. Some of the separations in individual bands recur

from group to group. Under high dispersion, fine structure is found in many of the bands that consists of a great many sharp absorption lines of which some are arranged in obvious sequences of about 10–15 cm^{-1} and others without obvious regularity. This structure is too fine to be due to vibrational lines and too coarse to be due to rotational lines. It is being investigated further in high orders of the 30-foot spectrograph.

THERMODYNAMIC STABILITY

As has been previously mentioned, PuF_6 has been found to be unstable relative to dissociation into fluorine and PuF_4 (Equation 4). A preliminary measurement of the equilibrium constant for this dissociation has been made at 220°C. In this experiment, a mixture initially containing 141 mm Hg of fluorine and 5 mm Hg of PuF_6 was maintained at a temperature of 220°C for seven days in a seasoned nickel container. The amount of PuF_6 present in the mixture was then measured and the ratio of F_2 to PuF_6 calculated to be 1.86×10^3. The standard free energy change

$$\Delta F^\circ = -RT \ln (F_2)/(PuF_6) \qquad (7)$$

calculated from this result at 493°K was −7.4 kcal-mole^{-1}. At 298°K the values of $\Delta F^\circ = -7.6$ kcal-mole^{-1}, $\Delta H^\circ = -8.3$ kcal-mole^{-1}, and $\Delta S^\circ = -2.3$ cal-mole^{-1}-deg^{-1} were calculated from this result and from the entropies of PuF_6 (this report), fluorine,[19] and PuF_4 (estimated from the entropy of UF_4).[18]

Although the instability of PuF_6 toward dissociation accounts for its ability as a fluorinating agent, the rate of its thermal dissociation is fairly small under some conditions. For example, the quartz cells in which the absorption spectrum of PuF_6 (100 mm Hg pressure) is being studied show only a small amount of decomposition although they were filled over a year ago. In another instance a mixture of F_2 and PuF_6 has been kept at a temperature of 120°C for seven days without a measurable change in the amount of PuF_6 (±1.4 per cent). Further increase in temperature, however, does lead to observable thermal decomposition, and at 280°C the decomposition is found to be complete in one hour.

ACKNOWLEDGEMENTS

The authors are particularly indebted to Stanley Siegel for the many X-ray determinations that were made to identify the reaction products. Acknowledgement is also made to J. C. Hindman for his help in interpreting the spectrophotometric data and in the attempts to identify an intermediate fluoride between +4 and +6; to Ralph Bane and Mary Lou Rauh for fluorine analyses; to James H. Patterson, Harold Evans and Robert Hornbeck for plutonium analyses; to Charles M. Stevens for mass spectrometer analyses; to Laurids Ross for uranium analyses; to John Faris for spectrochemical analyses; and to Stanley J. Rymas and Dale Henderson for alpha-pulse analyses.

REFERENCES

1. Florin, A. E., Tannenbaum, I. R. and Lemons, J. F., (Los Alamos Scientific Laboratory), *Preparation and Properties of Plutonium Hexafluoride*, Paper in preparation by these authors.
2. Hurst, R., informs us that a paper dealing with the work done on the preparation and properties of plutonium hexafluoride at Harwell is in preparation for publication. The following have been contributors: Hurst, R., Mandleberg, C. J., Rae, H. K., Davies, D., Francis, K. E. and Brooks, R.
3. Hawkins, N. J., of the Knolls Atomic Power Laboratory is preparing a paper describing the work with plutonium hexafluoride done there. Co-workers in this include Maltraw, H. C. and Sabol, W. W.
4. Malm, J. G and Weinstock, B, unpublished work.
5. Katz, J. J. and Rabinowitch, E., *The Chemistry of Uranium*, Part 1, National Nuclear Energy Series, Division VIII, Vol. 5, McGraw Hill Book Co., Inc., New York (1951).
6. Seaborg, G. T. and Katz, J. J., *The Actinide Elements*, National Nuclear Energy Series, Division IV, Vol. 14A, McGraw-Hill Book Co., Inc., New York (1954).
7. Hoard, J. L. and Stroupe, J. D., *X-ray Crystal Structure of Uranium Hexafluoride*, A-1296 (1944).
8. Weinstock, B. and Crist, R. H., *The Vapor Pressure of Uranium Hexafluoride*, J. Chem. Phys., *16*: 436-441 (1948).
9. Ruff, O. and Menzel, W., *Bromine Pentafluoride*, Z. anorg. u. allgem., Chem., *202*: 49 (1931).
10. Gutmann, V., *Die Chemie in Bromtrifluorid*, Angew. Chem., *62*: 312-315 (1950).
11. Emeleus, H. J., Maddock, A. G., Miles, G. L. and Sharpe, A. G., *Fluorides of the Natural Radioactive Elements*, J. Chem. Soc., 1948; 1991.
12. Griven, D. M. and Hutchison, C. A., Jr., *Magnetic Susceptibilities of Np^{+4}, Np^{+5}, and Np^{+6}*, J. Chem. Phys. *22*: 386-393 (1954).
13. Dawson, J. K., *Electronic Structure of the Heaviest Elements*, Nucleonics, 10, No. 9: 39-45 (Sept. 1952).
14. Herzberg, G., *Infrared and Raman Spectrum of Polyatomic Molecules*, D. Van Nostrand Co., New York (1946).
15. Bigeleisen, J., Mayer, M. G., Stevenson, P. C. and Turkevich, J., *Vibrational Spectrum and Thermodynamic Properties of Uranium Hexafluoride Gas.*, J. Chem. Phys., *16*: 442-445 (1948).
16. Burke, T. G., Smith, D. F. and Nielsen, A. H., *The Molecular Structure of MoF_6, WF_6 and UF_6 from Infrared and Raman Spectra*, J. Chem. Phys., *20*: 447-454 (1952).
17. Gaunt, J., *The Infrared Spectra and Molecular Structure of Some Group 6 Hexafluorides*, Trans. Far. Soc., *49*: 1122-1131 (1953).
18. Osborne, D. W., Westrum, E. F. and Lohr, H. R., *The Heat Capacity of Uranium Tetrafluoride from 5 to 300°K*, J. Am. Chem. Soc. (in press).
19. Murphy, G. M. and Vance, J. E., *Thermodynamic Properties of Hydrogen Fluoride and Fluorine from Spectroscopic Data*, J. Chem. Phys., *7*: 806 (1939).

Vapor Pressure of Liquid Plutonium

By T. E. Phipps,* G. W. Sears,† R. L. Seifert,‡ and O. C. Simpson,§ USA

The research which forms the basis for the present paper was carried out at the Chicago Metallurgical Laboratory in the summer and fall of 1944.

INTRODUCTION

The vapor pressures of substances having very low volatility are conveniently measured by the Knudsen effusion method. In this method a sample of the volatile material is placed in a small oven which is closed except for a thin-edged orifice of known area. The area of the orifice must be small compared to the evaporation surface of the sample to insure that the pressure of the vapor in the oven will closely approximate the saturation pressure. To insure "molecular flow" the largest dimension of the orifice must be small compared to the mean free path of vapor molecules in the oven. When the oven is maintained at a constant temperature in a vacuum the number of molecules of vapor effusing from the orifice in unit time is directly proportional to the pressure of the vapor in the oven. The pressure can be calculated quite simply from the measured total effusion rate by application of the kinetic theory of gases, if there is no backscattering of vapor molecules from the walls of the orifice. Though the orifice edge can usually be made quite thin it still has a finite thickness and there exists some backscattering of molecules, which reduces the total effusion rate into 2π ster-radians. If, however, one measures the partial effusion rate into a small solid angle about the axis normal to the plane of the orifice, the effect of backscattering is largely avoided.[1,2]

Measurement of the effusion rate within a small solid angle normal to the plane of the oven orifice is accomplished by collecting on a cold target the vapor that effuses from the oven orifice and passes through a collimating orifice. The planes of collimator orifice and oven orifice are mounted parallel, with the centers of the two orifices on the same normal. If circular orifices are used the weight of vapor arriving at the target is the fraction, $D^2/(D^2 + 4r^2)$, of the total weight of vapor effusing from an ideal oven orifice of area equal to that of the given orifice.[1] D is the diameter of the collimating orifice and r is the distance from oven orifice to collimator, which must be large compared to D.

The efficiency of condensation of plutonium vapor on the cold targets could be tested as follows. If vapor, after passing through the collimating orifice, should fail to condense on the cold targets, it would accumulate upon the colder inner walls of the target chamber where it could be detected because of its radioactivity. Tests showed that if any scattering occurred it amounted to less than 0.1% of the vapor collected on the targets.

From the kinetic theory of gases and the geometry factor determined by the diameter and position of the collimating orifice, the following Equation is obtained for N, the number of moles of vapor striking the target in τ minutes,

$$N = \frac{60\tau p A D^2}{(D^2 + 4r^2)(2\pi MRT)^{1/2}} \qquad (1)$$

In this equation p is the pressure of vapor in the oven in cgs units, A is the area of the oven orifice, T is the oven temperature in degrees Kelvin, and M is the molecular weight of the effusing molecule. Under the counting conditions used in this investigation the activity per microgram of Pu^{239} was 7.10×10^4 registered disintegrations per minute. If it is assumed that plutonium vaporizes as a monatomic gas the following Equation is obtained for its vapor pressure in millimeters of mercury,

$$p = \frac{2.603 \times 10^{-13} c(D^2 + 4r^2)T^{1/2}}{A\tau D^2} \text{ mm Hg} \qquad (2)$$

In this equation c is the number of alpha disintegrations registered per minute for a target deposit obtained during an exposure for τ minutes with oven at temperature T.

APPARATUS

Measurements were made with two different experimental units. The major differences between the two units were in design of the effusion oven, method of measuring oven temperature, type of target material, number of measurements that could be made without breaking the vacuum, and fraction of effusing vapor collected. These two experimental units, which were constructed of Pyrex, have been described elsewhere.[2]

In each apparatus tantalum effusion ovens were used and were heated by induction. Each oven consisted of a top and bottom section which fitted to-

* University of Illinois.
† General Electric Research Laboratory.
‡ Indiana University.
§ Argonne National Laboratory.

gether by means of a finely-ground taper joint. Liquid plutonium wets tantalum and has a tendency to creep over large areas. This results in a large evaporation surface even with small samples of plutonium and insures saturation of the vapor phase.

The following observations indicated that tantalum does not have a significant solubility in liquid plutonium under the conditions of these experiments. A layer of plutonium that had spread to cover the inner surface of a tantalum crucible became oxidized. The oxide layer flaked easily away from the tantalum surface. The original machine marks on the inner surface of the oven remained clear and sharp. Furthermore the plutonium oxide showed no trace of tantalum under X-ray crystallographic examination.

In the first apparatus (see Fig. 2 of reference 2) a 1.0-in. high tantalum oven (see Fig. 2 of reference 1), machined from 0.5-in. rod, was supported by a 4-in. tungsten rod 0.100 in. in diameter, ground down to a diameter of 0.060 in. over a length of 0.5 in. A round orifice was formed in 0.005-in. tantalum foil, which was then spot-welded to the cover of the oven. A platinum, platinum-rhodium thermocouple was mounted in the bottom of the oven and held in a thermocouple well by a tantalum screw. The junction was surrounded by a section of platinum tubing to prevent direct contact with tantalum. Inside the well the thermocouple wires were insulated from each other and from the wall by a short section of a two-hole alundum insulator. The oven was surrounded by a 0.005-in. tantalum foil radiation shield that was curved as one loop of a spiral so that the shield would not be heated by induction. In a preliminary experiment with a "dummy" oven made of nickel three thermocouples were attached to the top, middle, and bottom outside surfaces. At 1000°C it was observed that the bottom surface was 10°C cooler than the top, with approximately a constant gradient. In the tantalum oven used for the vapor pressure measurements the thermocouple junction came within 0.2 in. of the bottom inside surface of the oven, which was the coolest surface in the oven.

A target strip, 0.7 by 9 in., was bolted to a Pyrex holder that could be moved back and forth above the oven inside a horizontal target chamber by the action of a permanent magnet outside the evacuated apparatus. The target chamber was double-walled and was cooled by liquid nitrogen between the walls. The target strip was marked into ten sections which in turn could be placed in position above the collimating orifice. A thin-edged, round collimating orifice was machined in a nickel collimator piece that was held by tungsten wire clips in an opening through the double wall of the target chamber. A magnetically-operated shutter passed between the oven and the collimator. Two types of target strips were used; nickel foil, which was found to be heated somewhat by induction, and mica sheet that had been sputtered with nickel to increase the probability of condensation of plutonium vapor. With this apparatus it was necessary to break the vacuum after every ten target exposures.

The diameter of the oven orifice was 0.0137 cm and that of the collimating orifice was 0.5512 cm. The distance between the two orifices was 3.02 cm.

A second apparatus (Fig. 3 of reference 2) was built to improve the precision of measurement. More uniform oven temperature was achieved by using a more massive oven.[8] The oven, 0.75-in. diameter by 1.0-in. high, with 0.13-in. minimum wall thickness, was supported on three 0.040-in. diameter tungsten legs that tapered to a point at the bottom and rested on a quartz table. In the top of the quartz table was ground a conical cavity, a V-groove, and a flat-bottomed groove to support the three legs of the oven in a steady and reproducible position. The oven temperature was determined with a calibrated optical pyrometer focused on a "black-body" hole in the center of the oven bottom. The oven was surrounded by a nickel-coated quartz radiation shield (see Fig. 3 of reference 2). The shield was designed with two concentric quartz tubes, each with four vertical slots, sealed together so that there were eight vertical breaks in the nickel surface that was evaporated onto the inner surface of the quartz. The more uniform oven temperature thus achieved increased the danger of creepage of plutonium over the entire inner surface of the oven and out of the orifice. To avoid this the plutonium sample was placed in the innermost of two concentrically nested, sharp-edged tantalum cups placed in the oven. The oven orifice was formed in 0.005-in. tantalum foil that was spot-welded to the cover of the oven.

The collimator piece in the second apparatus was constructed of Pyrex and was supported in an opening through a horizontal, double-walled, liquid-nitrogen-cooled target chamber by a flared section that rested on the inner surface of the target chamber.

As in the first apparatus a target holder was provided that could be moved back and forth within the target chamber by the action of magnets outside the evacuated apparatus. The target holder consisted of a Pyrex glass plate 1.3 × 27 × 0.12 inches through which were drilled 18 holes to hold the targets. The targets were 0.75-in. diameter disks of 0.005-in. platinum foil. These targets were held in aluminum holders (see Fig. 4 of reference 2), which were 1.0-in. diameter and 0.125-in. in thickness, by circular phosphor-bronze springs. A disk of 0.020-in. nickel foil was placed between the platinum target and the aluminum holder to make the entire assembly ferromagnetic and to permit the movement of targets in the vacuum by magnets held outside the apparatus. A hundred such targets, each marked by a number, were placed inside the apparatus and, as needed, were loaded into the Pyrex target holder by the action of external magnets.

A seal-off manifold was attached to the apparatus for removing exposed targets without breaking the vacuum. The exposed targets were magnetically removed from the target holder and maneuvered

through partially flattened sections of glass tubing into a part of the tube that could then be sealed off at one of the flattened places. A magnetically-operated shutter was provided between oven and collimating orifice, as in the first apparatus.

In this second apparatus the diameter of the oven orifice was 0.01571 cm and that of the collimating orifice was 0.5182 cm. The distance between the two orifices was 8.103 cm. These values are the lengths at 25°C. They were corrected to proper experimental temperatures by use of known values of thermal expansion coefficients.

Each apparatus was evacuated by a vacuum system capable of maintaining a pressure of less than 10^{-6} mm Hg while the oven was heated.

EXPERIMENTAL PROCEDURE

Because of the ease of oxidation of the plutonium surface, precautions had to be taken to exclude oxygen and water from the apparatus. The tantalum ovens were initially outgassed by heating them in an auxiliary vacuum system to 2000°C for two or three hours or until the pressure in the system had fallen to about 1×10^{-5} mm Hg. After the oven had cooled, dried nitrogen was admitted to the system and the oven was removed to a nitrogen-filled desiccator. Before being placed in the desiccator the oven top was inspected with a microscope for possible change in orifice size during the outgassing procedure. No change in orifice size was ever observed. The thermocouple was attached to the oven of the first apparatus after the outgassing. The vapor pressure apparatus, with targets in place, was evacuated and the glass walls were torched until the pressure had been reduced to less than 1×10^{-5} mm Hg with all walls hot. While the apparatus was being torched the radiation shield was outgassed by use of a "stand-in" oven that was heated inductively to a temperature considerably higher than that to which the oven was to be heated. Dried nitrogen was admitted to the apparatus just prior to the introduction of the oven.

Each pellet of plutonium had previously been cleaned anodically or by brush-burnishing and stored in a sealed glass tube under an inert atmosphere. The pellet to be used for vapor pressure measurements was transferred from the tube to the outgassed oven in an atmosphere of dried nitrogen. The top was put on the oven and tapped into good contact with the tapered surface of the bottom section. The oven was rapidly transferred to the glass apparatus. A slight positive pressure of dry nitrogen was maintained in the apparatus until the last closure was made. The apparatus was immediately evacuated.

Except for the difference in the method of measuring oven temperature and for the slight variation in the method of moving the target holder and operating the shutter, the exposure procedure was the same with both experimental units. With the shutter between oven and collimator the oven was heated and its temperature was observed and recorded over a considerable interval of time. When the temperature appeared to be stable the shutter was opened and a timing device started. Temperature readings were taken at frequent intervals during the exposure. Finally, as the shutter was closed, the timer was stopped. The temperatures recorded during the exposure were averaged to obtain the oven temperature. The target holder was moved to place a new target in position, the oven temperature was adjusted to a new value, and the process was repeated. Exposure times varied from 200 minutes at the lowest to 2 minutes at the highest oven temperature.

With the first apparatus it was necessary after ten exposures to cool the oven, admit dry nitrogen, and replace the target strip. With the second apparatus the exposed targets were removed by means of the "seal-off manifold" without breaking the vacuum. New targets, previously stored in the apparatus, were transferred to the target holder by manipulation with external magnets.

The exposed target strips from the first apparatus were cut to separate the ten exposures. The exposed platinum foil targets used with the second apparatus were removed from the aluminum holders. The amount of plutonium deposited on each target was determined by standard counting procedure. When the time involved was not prohibitively long, the counting of each target was continued until about 10,000 counts had been recorded.

EXPERIMENTAL RESULTS

Thirty exposures, ten on nickel and twenty on nickelized mica, were made in the first apparatus. For these measurements the oven was charged with a 5.5-mg sample of plutonium, which had been prepared at the Chicago Metallurgical Laboratory by reduction in a beryllia crucible and had been purified by remelting on tantalum. These measurements covered the temperature interval 1338°K to 1838°K. The resulting vapor pressures, as calculated by Equation 2, are shown in Fig. 1 by partially shaded circles. These data scatter badly, due most probably to uncertainties in the temperature measurements since considerable erratic behavior of the thermocouple was experienced. Least squares treatment of these data gave the following equation for p:

$$\log_{10} p_{mm} = -(17{,}600 \pm 900)/T + (8.08 \pm 0.15) \quad (3)$$

Fifty-six exposures were made on platinum targets in the second apparatus. For these measurements the oven was charged with a 30-mg sample of plutonium which had been prepared at the Los Alamos Laboratory and had been remelted twice in a calcium oxide crucible. These measurements covered the temperature range 1392°K to 1793°K. The resulting vapor pressures are shown in Fig. 1 as circles. The equation obtained from these data by least squares treatment is as follows:

$$\log_{10} p_{mm} = -(17{,}587 \pm 73)/T + (7.895 \pm 0.047) \quad (4)$$

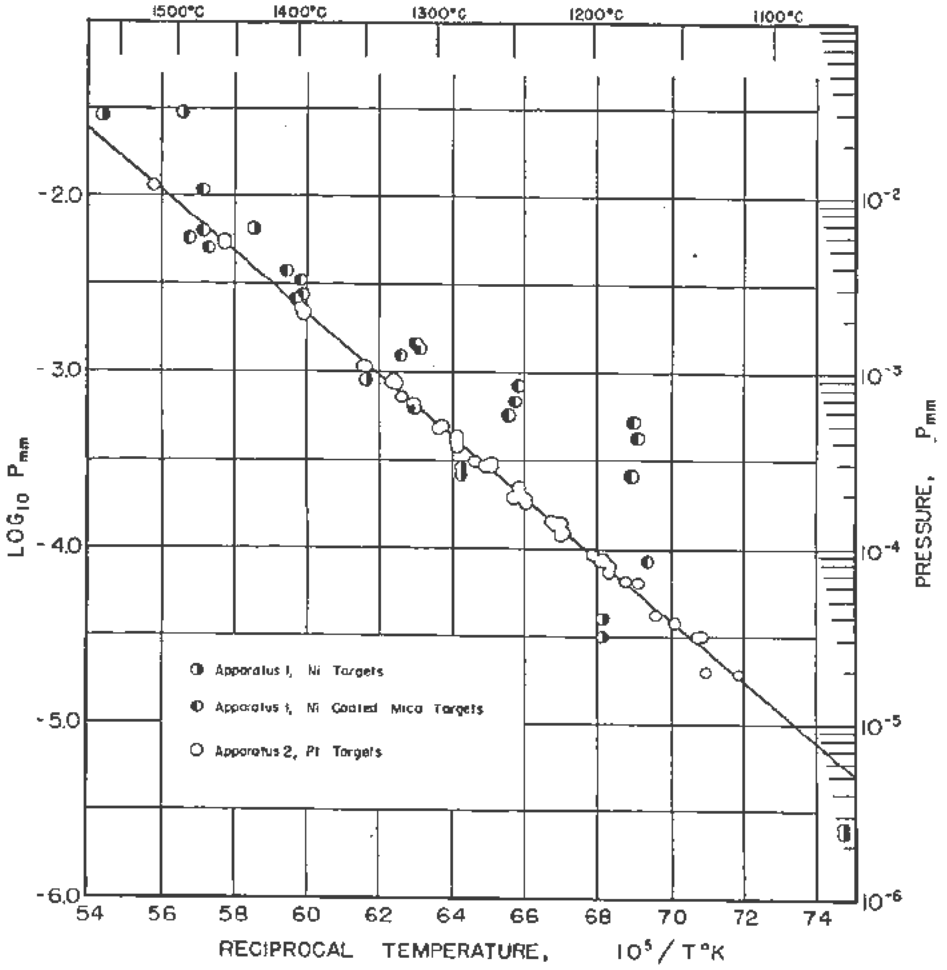

Figure 1. The vapor pressure of liquid plutonium

The probable errors given for the constants in Equations 3 and 4 were calculated from the residuals of the experimental points from the lines defined by the Equations. The relative values of these probable errors in the two equations and the distribution of points in Fig. 1 show the marked improvement in precision of measurement by the second apparatus.

Systematic errors in the geometry of the apparatus and in the measurement of oven temperature would shift the position of the log p vs $1/T$ curve but would not contribute to the probable errors as calculated for the constants in Equations 3 and 4. Estimates of the maximum possible error in each of the various quantities (e.g., the geometric parameters of Equation 1) whose errors might contribute to a systematic error, led to the conclusion that values of vapor pressure calculated by Equation 4 are correct within $\pm 5\%$.

The average molar heat of vaporization of liquid plutonium in the temperature range 1392°K to 1793°K is 80.46 $\pm$ 0.34 kcal/mole. Extrapolation of the linear Equation 4 gives a normal boiling point of 3508 $\pm$ 19°K.

ACKNOWLEDGEMENT

We are greatly indebted to E. F. Westrum who carried out the reduction and to H. L. Robinson and Zene Jasaitis who did the remelting purification of the 5.5-mg Chicago sample. We are also greatly indebted to the Los Alamos Scientific Laboratory for furnishing the 30-mg sample. To Mr. L. O. Gilpatrick we express our sincere gratitude for his able assistance with many of the measurements.

REFERENCES

1. Phipps, T. E., Sears, G. W., Seifert, R. L. and Simpson, O. C., *The Vapor Pressure of Plutonium Halides*, J. Chem. Phys., *18*: 713 (1950), or *The Vapor Pressure of Plutonium Halides*, Paper 6.1a of "The Transuranium Elements," National Nuclear Energy Series, Div. IV, Vol. 14B, McGraw-Hill Book Company, New York (1949).
2. Phipps, T. E., Sears, G. W. and Simpson, O. C., *The Volatility of Plutonium Dioxide*, J. Chem. Phys., *18*: 724 (1950), or *The Volatility of Plutonium Dioxide*, Paper 6.1b, *ibid.*
3. Erway, N. D. and Simpson, O. C., *The Vapor Pressure of Americium*, J. Chem. Phys., *18*: 953 (1950).

Some Aspects of Polonium Chemistry

By K. W. Bagnall,* UK

Although polonium was discovered by Pierre and Marie Curie[1] nearly 60 years ago, the literature, until recently, has contained little definite information about the element and its compounds. This is due to the fact that only very minute amounts of polonium were available, since the only sources of the element were pitchblende (containing 0.1 mg of Po^{210}/ton) and, later, radon ampoules containing the radium decay series RaD-E-F. Consequently much of the early literature was devoted to procedures for the separation of the element. Fundamental studies of its spontaneous deposition on to silver,[2] copper,[3] nickel[4] and some other metals were made, together with some work on the electrodeposition of polonium on to platinum[5,6] and on to gold.[5,6,7]

The deposits obtained by these procedures were usually dissolved off the substrate for tracer experiments, although some vapourization studies were made which showed that the volatilization of tracer polonium was somewhat erratic,[8] the problem being further complicated by the fact that the chemical nature of the sublimates was uncertain.

There is evidence for the formation of a polonide, $Na_2Po \cdot xH_2O$,[9] formed by the reduction of tracer polonium together with tellurium under conditions suggesting isomorphism, and, under similar conditions, evidence for polonium dimethyl and dibenzyl was obtained. Tracer work has also indicated the existence of an unstable and volatile hydride,[10] presumably PoH_2 and evidence for the existence of tetravalent compounds of the type M_2PoCl_6 was obtained by co-precipitation studies.[11]

The evidence concerning the valency states of polonium is conflicting. By analogy with the other Group 6 elements and tellurium in particular, polonium should exhibit valencies of 2, 4 and, possibly, 6. In the last case, however, it has been shown[11] that polonium is not precipitated with tellurium after oxidation by chromic oxide, indicating that polonium is not oxidised to the hexavalent state under these conditions and the only evidence for the existence of hexavalent polonium is the possible formation of the trioxide by anodic oxidation[7] and co-crystallisation studies of tracer polonium with hydrated potassium tellurate.[12]

Diffusion studies[13,14] indicate the presence of divalent ions in solution, but these could be complex ions of the form $PoCl_6$ or possibly PoO^{++} and the evidence obtained by co-precipitation studies has also suggested trivalency in solution.[11] Much of this tracer work has been summarised in a monograph by Haissinsky.[15]

Now that intense neutron fluxes are available in nuclear reactors, larger amounts of polonium can be prepared by neutron irradiation of bismuth.

$$Bi^{209}\ (n,\gamma) \rightarrow Bi^{210} \xrightarrow[5d]{\beta} Po^{210} \xrightarrow[138d]{\alpha} Pb^{206}$$

Due to the high specific activity of this isotope (4.5 curies/mg, i.e., 10^{13} disintegrations per min per mg) the hazard from contamination is high, so that work with milligram amounts must be carried out in dry-box systems. The maximum permissible ingested dose is only 0.02 μc (4.5×10^{-12} gm) and since rubber dry-box gloves are rapidly penetrated, it is necessary for workers in this field to wear surgical gloves for additional protection against contamination and this tends to make for clumsiness in manipulation. More recently, work with synthetic rubber gloves (e.g. neoprene) has shown that these have increased resistance to penetration.

Work with milligram quantities of the element is complicated by the scattering and decomposition of the solid preparations under the intense α bombardment. The high internal temperatures of the specimens, due to the heat evolved in the stoppage of the disintegration α particles within the sample (equivalent to 27.4 calories/hour/curie)[16] is an additional complicating factor. It is also necessary to exclude air from the preparations to prevent oxidation of the sample and, since nitrogen dioxide is formed under the α bombardment, to prevent the subsequent reaction of this gas with the preparation.[17,18] Preparations of organic compounds are rapidly charred and consequently analytical work must be carried out very quickly. In solution, the problem is aggravated by the continuous (and, at concentrations of the order of 500 mc/ml, visible) radiation decomposition of the solvent accompanied by strongly oxidising effects.

Most of the preparative work reported recently in the literature has been carried out on the 100–500 microgram scale and even at the lower of these levels it is frequently difficult to assign a colour to a new compound due to the blue glow emitted by the preparation and to the fluorescence induced in the containing tube by the α bombardment.

In our work in this field the main effort has been directed to the solid state chemistry of the element

* Atomic Energy Research Establishment, Harwell.

and for this purpose X-ray powder photography has been used for identification purposes.

The primary requirement was a quick method of preparing pure polonium metal as the starting point for each preparation. Due to the short half-life of Po^{210} lead grows into the preparation at the rate of approximately 0.5% per day. The self-deposition of milligram amounts of polonium on to silver, copper and nickel[17] and the electrodeposition on to platinum[17] and on to gold[18] was therefore investigated. The deposits were then sublimed off the substrates under vacuum and examined by X-ray powder photography and by spectroscopic analysis. It was found that, with the exception of the copper deposits, very pure polonium metal was obtained.

For convenience the electrodeposition on to gold was used since it was found that reproducible deposits of high density could be obtained on gold wires 0.010 in. in diameter. This led to the technique[18] of preparing the specimens by solid/gas reactions in X-ray capillaries. One curie (0.2 mg) of polonium, electrodeposited on a one-inch length of gold wire, was sealed into the open end of an X-ray capillary attached to a ground glass joint. The polonium was sublimed under high vacuum into the centre of the capillary and the stripped gold wire was then sealed off and discarded. The required reagent gas was then admitted to the evacuated capillary or fed through it in a slow stream. The product could then be sealed off for X-ray powder photography and analysis or subjected to reaction with a second gas by evacuating the capillary and repeating the above procedure.

A micro-filter stick which could be used as an X-ray capillary[18] was devised for work with insoluble compounds, since the normal centrifugation technique for preparing X-ray capillaries could not be applied in the case of polonium due to the disruption of the precipitate by the vigorous radiation decomposition of the solvent.

The first published study on "weighable" amounts of polonium was by Beamer and Maxwell[19] who determined the crystal structures of the two modifications of the metal by means of X-ray powder photography of 0.1 mg samples. The low temperature (α) form was found to be simple cubic with a phase transformation at about 75°C to the high temperature (β) form, which is simple rhombohedral. Due to the high internal temperature of the sample, freshly prepared specimens are always the β form unless subjected to prolonged cooling in liquid air. Maxwell[20] has determined a number of the physical properties of the element, including the melting point, found to be 254°C, considerably lower than the theoretical calculations which had suggested 1300°C[21] and 1785°C.[22]

The physical properties of the metal resemble those of thallium, lead and bismuth, its neighbours in the period table, more closely than those of the sulphur (Group VI) family to which it belongs.

The metal reacts with oxygen at 250°C to form a dioxide, identified by Martin[23] and found to exist in two crystal modifications, tetragonal (apparently red) and face centred cubic (yellow). It appears to be a UO_2- type oxide with variable oxygen content, the phase-change tetragonal face-centred cubic being temperature dependent and reversible, with the cell constant of the face centred cubic modification varying from 5.626 to 5.687 kX.

The metal also reacts with chlorine[24,18] and bromine[24,25,26] to form the corresponding tetravalent halides, which can be degraded thermally under vacuum to the dichloride[24,18] and to the dibromide[26] respectively. These compounds are brightly coloured, the tetrachloride being bright yellow and the tetrabromide bright red. The dichloride is a dark ruby-red and the dibromide dark purple-brown. The tetrachloride melts (in chlorine) to a straw-coloured liquid which becomes scarlet about 60° above the melting point, the vapour being purple-brown below 500°C and blue-green above this temperature[18]—changes which indicate either changes in association in the vapour state, or decomposition to a series of lower halides.

The dihalides can also be prepared by reduction of the tetrahalide by hydrogen sulphide or sulphur dioxide gas.[18,26] Even the dioxide degrades to metal under vacuum at 500°C[17] showing the instability of the tetravalent state.

In solution the tetrahalides are readily reduced to the pink divalent state by sulphur dioxide gas, hydrazine, etc., but are rapidly re-oxidised by the oxidising effects of the intense α bombardment.[18] There is also some evidence for the existence of an intermediate trivalent state in the case of the chlorides.

The ions formed in halogen acid solution are certainly complex and, like tellurium, salts of the type $M_2\,Po\,X_6$ (X = Cl, yellow,[18,28] and Br, brick-red[26]) are readily precipitated by addition of a solution of the corresponding caesium halide.

According to one report[24] iodine does not react with polonium metal, but we have found[27] that a grey-black tetraiodide of metallic appearance can be prepared by direct combination of the elements, by the action of hydriodic acid on the dioxide or by precipitating a solution of the tetrachloride in hydrochloric acid with potassium-iodide solution.[27] The precipitate is soluble in excess potassium-iodide solution to give a dark red solution from which caesium iodide precipitates black caesium hexaiodopolonite.[27]

Solvent extraction work has led to the isolation[26] of polonium organic compounds which appear to be analogous to those of tellurium, formed by condensation of polonium tetrachloride with mono- and diketones. The yellow initial products have two atoms of chlorine per molecule, which are lost, as elementary chlorine, on heating and can also be removed by potassium hydroxide solution, the product being a purple-violet, volatile crystalline solid. Work is still in progress on these compounds.

The chemistry of the halides is therefore seen to be analogous to the chemistry of tellurium, as indi-

cated by Marckwald,[29] with the divalent state rather more stable than is the case with tellurium.

REFERENCES

1. Curie, P. and Curie, M., Compt. rend., *127*: 175 (1898).
2. Marckwald, W., Ber., *38*: 593 (1905).
3. Russell, A. and Chadwick, J., Phil. Mag. (6), *27*: 112 (1914).
4. Tammann, G. and Wilson, C., Z. anorg. Chem., *173*: 137 (1928).
5. Joliot, F., J. Chim. phys., *27*: 9 (1930).
6. Wertenstein, M., Compt. ren. soc. sci. Varsovie, *10*: 771 (1917).
7. Haissinsky, M., J. Chim. phys., *29*: 453 (1932).
8. Bonet-Maury, P., Ann. Phys., *11*: 253 (1929).
9. Chlopin, V. G. and Samarzewa, A. G., Compt. rend. acad. sci., URSS, *4*: 433 (1934).
10. Paneth, F., Ber., *51*: 1704 (1918).
11. Guillot, M., J. Chim. phys., *28*: 92 (1931).
12. Samarzewa, A. G., Compt. rend. acad. sci., URSS, *33*: 498 (1941).
13. Hevesy, G., Phys. Z., *14*: 49 (1913).
14. Paneth, F., Koll. Z., *13*: 297 (1913).
15. Haissinsky, M., Le Polonium, Hermann et Cie, Paris (1937).
16. Beamer, W. and Easton, W. E., J. Chem. Phys., *17*: 1298 (1949).
17. Bagnall, K. W. and D'Eye, R. W. M., J. Chem. Soc., 4295 (1954).
18. Bagnall, K. W., D'Eye, R. W. M. and Freeman, J. H., J. Chem. Soc. (in press).
19. Beamer, W. and Maxwell, C., J. Chem. Phys., *14*: 569 (1946).
20. Maxwell, C., J. Chem. Phys., *17*: 1288 (1949).
21. Proszt, J. and Vendl, M., Mitt. berg. Nuttenmann Abt. Ungar. Hochscule Berg Forstwesen, 319 (1930).
22. Vinassa, P., Atti R. Acad. Lincei (6), *8*: 123 (1928).
23. Martin, A. W., J. Phys. Chem., *58*: 911 (1954).
24. Burbage, J. J., *The Chemistry of Some Alpha-Emitters*, American Report MLM-885 (1953).
25. Joy, E. F., Chem. and Eng. News, *32*: 3848 (1954).
26. Bagnall, K. W., D'Eye, R. W. M. and Freeman, J. H. (in press).
27. Bagnall, K. W., D'Eye, R. W. M. and Freeman, J. H. (in press).
28. Staritzky, E., *Some Tetravalent Compounds of Polonium*, American Report LA-1286 (1951).
29. Marckwald, W., Ber., *35*: 2285 (1902).

On the Vapour Pressure of Polonium at Room Temperature

By Josef S. Ausländer and Iulia I. Georgescu,* Romania

PRINCIPLE OF THE METHOD

In two previous papers,[1,2] it was shown that nuclear research plates could be used as measuring instruments for extremely low pressures, especially partial, and/or vapour pressures, if the gas considered were radioactive or contained a radioactive component, e.g. an unstable isotope in the case of chemically homogeneous vapours.

Consider a vessel of some arbitrary rotational symmetrical form and, on its internal wall, an elementary area, covered with an emulsion sensitive to ionizing particles. Let the vessel be filled with a radioactive gas (vapour) of such low partial pressure that the equation of state of perfect gases applies.

Then, it is easy to show, that the partial pressure p of the radioactive substance is given by

$$p = \frac{k\,T}{V G\,\theta} \cdot \nu \qquad (1)$$

where k is the Boltzmann constant, T the absolute temperature, ν the number of tracks per unit area of the emulsion, V the volume of the vessel (or in some cases, see below, the part of it which contributes to the formation of tracks), while G, called the geometry factor, depends on the form of the vessel, and on the position of the sensitive emulsion in it, and θ is a quantity, called the time factor; the last two quantities, G and θ, are defined as follows:

If the radioactive gas is in equilibrium with an equally radioactive condensed phase, then

$$\theta = \lambda t \qquad (2a)$$

where λ is the disintegration constant and t the time of exposure; if necessary, λ may be supposed to include an abundance factor of the radioactive isotope.

If there is no such equilibrium, then

$$\theta = 1 - \exp\,(-\lambda t) \qquad (2b)$$

Under the assumption of a low enough total gas pressure in the vessel, such that the range R of the ionizing particle in the gas may be considered as infinite, the geometry factor G has been calculated[1] for spherical vessels as:

$$G = \frac{A}{3V} \qquad (3)$$

where A is the radius of the sphere. Under the same assumption it has been calculated for hemispherical and cylindrical vessels.[2]

If the total gas pressure is large, so that R is smaller than the smallest of the linear dimensions of the vessel, then G becomes, under certain conditions,[2] independent of the vessel form and for V in Equation 1 the volume of the hemisphere with radius R_0 has to be substituted.

EXPERIMENTAL

Preliminary experiments have been carried out with a (nearly) spherical vessel of radius $A \cong 14.2$ cm (Fig. 1). At A the nuclear plate could be brought in or taken out. At B a glass tube with stopcock could be connected to a vacuum pump. At C there was a brass tube, which contained the source Po (a silver foil with polonium). As seen in Fig. 2, the polonium foil was placed in such a way that the direct impact on the plate of α-particles from the source could be excluded for geometrical reasons. The glass tube at E was provided with a simple Hg manometer and contained $CaCl_2$ in order to prevent humidity and subsequent fading. The vessel was closed at A_2, B, C, D, and E by greased rubber stoppers. At the bottom it contained a small piece (~3–5 cm²) of a nuclear research plate.

All manipulations were carried out in a dark room, where the vessel, previously evacuated to ~3–4 mm Hg, was stored during exposure.

Each exposure was duplicated by a control exposure, under as far as possible identical conditions except for the absence of the orifice C and the polonium.

The plates used, which were similar in type to Ilford C2 plates, were prepared in the laboratory by one of the authors,[3] and exposed at room temperature (18–22°C, i.e., 294°K). Their shrinkage factor was determined by weighing as 1.99.

Four plates (and four control plates) were exposed for different exposure times (see Table I on following page).

The vessels were evacuated again during exposure, as soon as the manometer showed a pressure higher than ~30 mm Hg. Such operations became necessary once with the vapour vessel in experiment 1 (see Table I), once with the control vessel in experiment 4, and daily after the seventh day with the vapour vessel in experiment 4; in this last case it also happened twice that the vapour vessel remained for ~½ day under a pressure of 50–60 mm Hg.

* Polytechnical Institute, Bucharest.

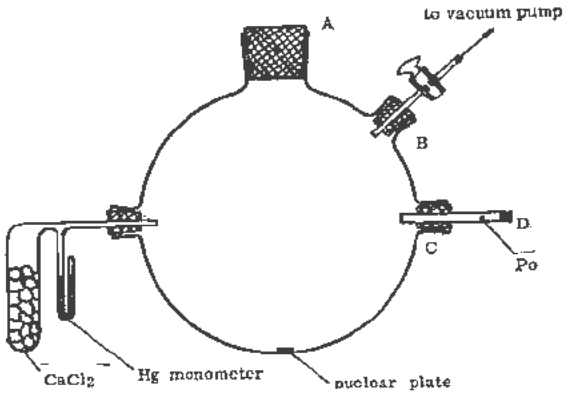

Figure 1

Scanning was performed by means of a binocular "Me-Opta" microscope with total magnification of ~840 × (oil immersion objective).

PRELIMINARY RESULTS AND DISCUSSION

The results given below are to be considered as preliminary, firstly because the experimental technique employed is subject to improvement, and, secondly, because the area of the plates could not yet be scanned to the full extent.

Substituting Equations 2 and 3 in Equation 1, introducing the corresponding numerical values, with $\lambda = 5.011 \times 10^{-3}\ d^{-1}$,[4] and expressing p in mm Hg, we get:

$$p = 1.28 \times 10^{-15} \cdot \frac{\nu}{t}\ [\text{mm Hg}] \qquad (4)$$

Table I gives an over-all view of the results obtained. Most of its columns need no explanation. Column (e) gives the number of radioactive stars which appeared in the scanned area. All of them are two-pronged; their number is negligibly small and will not be taken into account in the following. The numbers ν from column (h) are the differences between the upper and the lower numbers, ν', of column (g). Column (i) contains the pressure p, calculated by Equation 4 from ν of the preceding column. The last column (j) gives pressure values p', calculated in the same way from the upper values ν' for the vapour vessel.

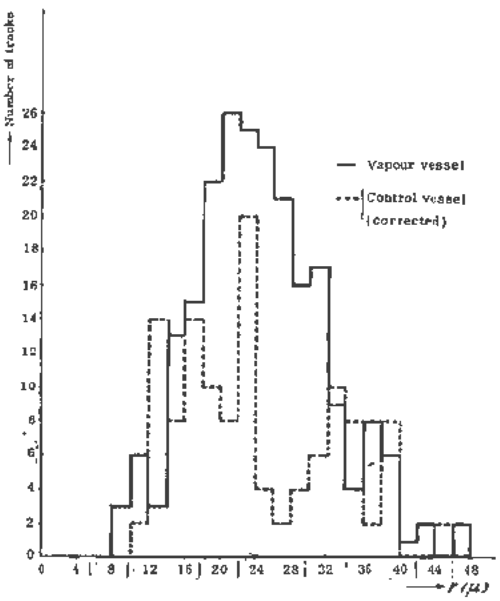

Figure 2

The most reliable measurements are those of experiments 1 and 3. In experiments 2 and 4 the scanned area is very small. The most unreliable is experiment 4, where fading may be of great influence because of the vacuum accidents mentioned above, and the long time of exposure.

Figure 2 shows a histogram of the range, r, in the emulsion for experiment 3. The dotted histogram refers to the control plate. It is corrected for the difference of scanned area, i.e., the number of tracks plotted is recalculated to the same area as the vapour vessel plate. The peak of the histogram is at ~21 μ, as is to be expected for polonium tracks in the plates used. The histograms of all other plates show the same character.

In order to make sure that the tracks recorded actually belong to atoms in the vapour phase and not to atoms adsorbed on the walls of the vessel and on the plate, or to impurities on the plate, a histogram

Table I

Experiment	Time of exposure (days)	Vapour or control vessel	Scanned area (cm^2)	Number of stars	Number of single tracks	Single tracks per cm^2 ν'	ν (cm^{-2})	p (10^{-14} mm Hg)	p' (10^{-14} mm Hg)
a	b	c	d	e	f	g	h	i	j
1	11.4_8	Vapour	1.40_4	0	159	114	41	0.4_8	$1._2$
		Control	0.80_1	0	62	73			
2	14.0_0	Vapour	0.78_5	1	91	116	25	0.2_3	$1._1$
		Control	0.77_0	2	70	91			
3	15.0_5	Vapour	1.76_5	2	223	127	56	0.4_6	$1._3$
		Control	0.86_6	1	61	71			
4	30.2_3	Vapour	0.65_1	2	55	84	43	0.1_8	0.3_6
		Control	0.76_6	3	31	41			

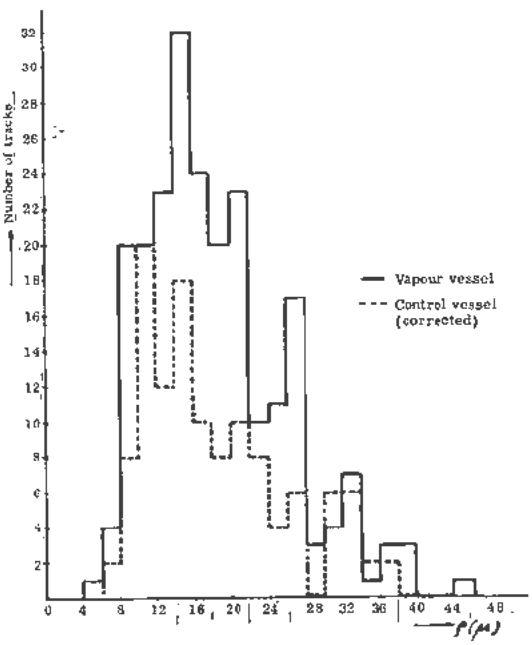

Figure 3

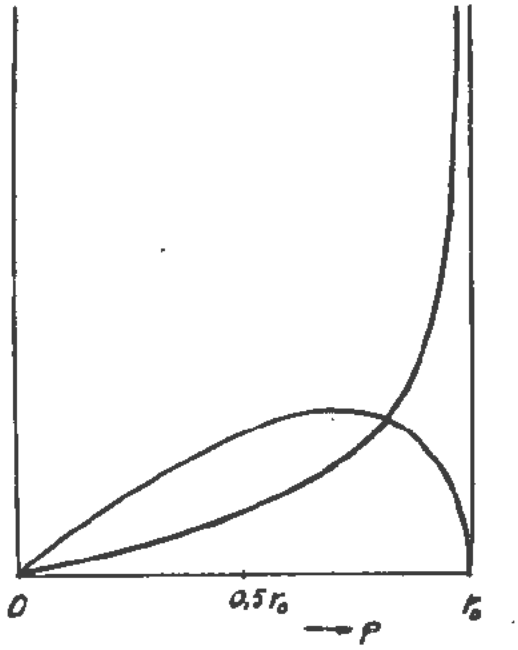

Figure 4

of the lengths ρ of horizontal track projections was traced in Fig. 3, which refers to experiment 3, too. The dotted lines represent numbers of tracks in the witness plate, corrected in the same way as in Fig. 2. Here, too, all histograms of this kind show the same essential features.

It has been shown[2] that the distribution function $f(\rho)$ of the horizontal projections enables one to distinguish statistically between tracks issuing from disintegrations of atoms adsorbed on the walls of the sphere and on the plate, and those issuing from disintegrations in the volume of the vessel. These distribution functions[2] were calculated with range fluctuations neglected. These functions are plotted in Fig. 4, where r means the range in the emulsion of the α-particles. One of the plots shows a maximum at $0.71\ r$; it refers to the atoms from the volume of the vessel. The other plot has a vertical asymptote at r; it refers to the disintegration of adsorbed atoms. As far as we are interested here, the form of the plots would not change essentially, if the fluctuations were not neglected.

Figure 3 shows a well pronounced maximum at $\sim 16\ \mu$, which is in satisfactory agreement with $0.71 \times 21\ \mu = 15\ \mu$.

The fact that the dotted plots showed the same form as the full ones, suggests the possibility that the tracks in the control plate may originate, at least to some extent, from polonium vapours leaking in from the vacuum pump. Under the hypothetical assumption that all the control tracks have this origin, in column (j) are given the values p' of the pressure, calculated by Equation 4 from ν' for the vapour-vessel plate. It is more probable that the above assumption is only partially true, and thus part of the control tracks has to be subtracted from the ν' values of the vapour vessel plate.

The very small number of tracks from radioactive contamination can be explained by the fact that only tracks which begin at the emulsion surface play any role.

In spite of the preliminary character of the results we feel entitled to assert, that the vapour pressure of polonium at room temperature is $\sim 0.5 \times 10^{-14}$ mm Hg.

FINAL REMARKS

It is not intended to claim a greater precision for our results than the order of magnitude. Notwithstanding the small total numbers of tracks, the small scanned areas and the vacuum imperfections mentioned, all four experiments lead to vapour-pressure values of the same order, no matter whether we compute p (column i) or p' (column j) under the respective assumptions. Therefore, we can say that the order of magnitude is well established.

It must be pointed out, that the method can be most valuable in many respects, especially if used with electron sensitive plates and radioactive tracers.

REFERENCES

1. Ausländer, J., Com. Acad. R.P.R., *1*: 1033 (1951).
2. Ausländer, J., Bul. St. Acad. R.P.R., s. şt. Mat. Fiz., *3*: 533 (1951).
3. Georgescu, I., Rev. Univ. C. I. Parhon, şi a Politehnicii Bucureşti, *2*: 67 (1953).
4. Nesmeianov, A. N., Lapitzky, A. V. and Rudenko, N. P., Poluchenie radioactivnykh isotopov (in Russian), Moscow, 1954, p. 136.

A Natural Isotope of Element 84 With a Very Long Half-Life

By R. Ripan, R. Paladi, H. Hulubei, Romania

During the course of previous research into the possible existence of long-lived or very long-lived isotopes of the radioactive elements of the periodic system, one of us, in collaboration with Y. Cauchois,[1] observed in some gold ores of the petzite type from Transylvania (in 1940 and 1947) the existence of a naturally occurring element of atomic number 84 which appeared likely to have a very long half-life.

Element 84 had previously been identified by the L lines of its X-ray spectrum. At that time we knew well the L spectrum of polonium-210 which had been recorded with a double focusing X-ray spectrometer.[2]

This research also enabled us to shed some light on the detecting power of our methods (the α activity of polonium deposited on the anticathode gave a measure of the quantity of the substance which was used for the analysis; and we could also detect 10^{-10} gm of Po which was contaminated with other substances such as Au, Ag, Bi, Pb).

After conventional chemical treatment of the petzites, X-rays still showed the existence of element 84 in the extracted product.

The activity of the product thus obtained, a few contaminatiog particles, was very weak.

We then came to the conclusion (see above) that there existed a very long-lived isotope of element 84.

The petzites are very rare in Transylvania. In order to confirm the results mentioned, we analyzed other Transylvanian tellurium minerals in the hope of finding this element in larger concentrations and in minerals less scarce than the petzites.

Ultimately, we identified the same long-lived isotope of element 84 in the altaites, minerals containing tellurium, gold and lead, from Staaija (Transylvania).

The chemical treatment, briefly described here, was as follows: The mineral was treated with aqua-regia—the lead sulfate was separated after the nitric acid had been eliminated. The product was filtered and chemical treatment continued as follows:

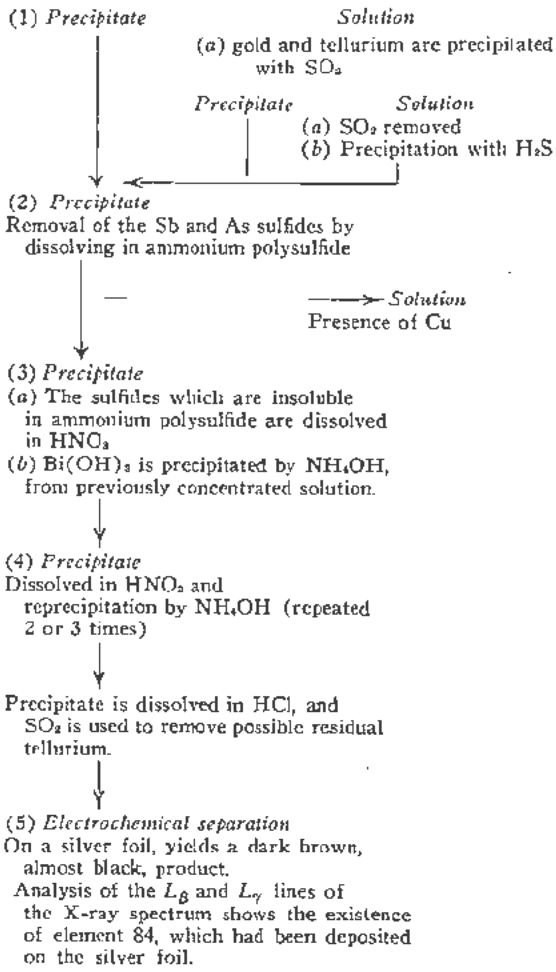

Analysis was made by the spectrographic methods mentioned above, and $L_{\beta,\gamma}$ region was chosen for practical reasons: e.g., fewer rays coming from the elements in the mineral.

The efficiency of the chemical treatment has been

Original language: French.

checked with a small quantity of mineral using Po^{210} as a tracer.

Control of large-scale treatment was achieved with the aid of the typical X-ray spectrum.

Since our first publication in 1940, Tempelton, Howland and Perlman[3] published their work on artificial radioisotopes of Po.

It would be interesting to try to place the long-lived natural isotope which we found in 1940 among those obtained artificially.

Preliminary research with nuclear emulsions indicates very weak α-activity, which would bear out the persistence of this isotope in our mineral.[1] The mineral does not contain any trace of uranium or thorium and does not contain any rare earths.

The systematic study of α radioactivity made by Perlman, Ghiorso, and Seaborg[4] seems to show that this isotope might well be found, as we expected, in the region of isotopes deficient in neutrons.

Research in this direction is continuing.

REFERENCES

1. Hulubei, H. and Cauchois, Y., C.R., *210*: 1940, p. 761; *224*: 1947, p. 1265.
2. Hulubei, H., Cauchois, Y. and Cotelle, S., C.R., *207*: 1938, p. 1204; Hulubei, H. and Cauchois, Y., Disquitiones Math. and Physicae (Bucarest), tome I fas. 3-4; pp. 467-490 (1941).
3. Tempelton, D. H., Howland, I. I. and Perlman, I., Phys. Rev., *72*: 1947, p. 758, *73*: 1948, p. 1211.
4. Perlman, I., Ghiorso, A. and Seaborg, G. T., Phys. Rev., *77*: 1950, p. 26.

Recent Developments in the Chemistry of the Uranium-Oxygen System

By Henry R. Hoekstra and Stanley Siegel,* USA

The uranium-oxygen system, as well as binary oxide systems of uranium, have been the subject of intensive study during recent years. In addition to the interest purely in the basic chemistry of the uranium oxides, a great deal of work has been done on use of the oxides as reactor fuels, as well as the possibility of high-temperature processing of metallic fuels by oxide slagging techniques. A comprehensive survey of all phases of investigations on these systems would require more space than is available here. This paper, therefore, will be concerned almost exclusively with the dry chemistry of the oxide systems. Literature citations are restricted to the period 1945–1955.

URANIUM-OXYGEN SYSTEM

U–UO_2

The region between uranium metal and the dioxide is relatively simple; the solubility of oxygen in the metal is very slight (0.4 atom per cent at 2000°C). A monoxide of uranium has been reported.[1] The structure is given as cubic (NaCl type) with lattice parameter (4.92 kX) intermediate between that of uranium mononitride and the monocarbide. Uranium monoxide has never been prepared in bulk, appearing only as an impurity on uranium metal in a system containing "oxygen as the chief contaminant." Cubicciotti[2] and Loriero[3] found no indication of a monoxide in their studies on the low-temperature oxidation of uranium metal. The inability to prepare uranium monoxide in bulk suggests that the pure compound is stable only at elevated temperatures, or that it is thermodynamically stable towards disproportionation only when carbon and nitrogen are present to stabilize the NaCl structure. If the problems of technique can be solved, X-ray studies at elevated temperatures are indicated here. The system might also be studied by the gradual addition of oxygen to the well-established monocarbide or mononitride.

The structure of uranium dioxide (fluorite, $a = 5.458$ kX) is well known, as is the fact that the structure is maintained over a considerable composition range with oxygen/uranium greater than 2. Less well-established is the ability of the fluorite structure to exist at oxygen/uranium ratios less than 2. Several studies[4,5] based on X-ray evidence indicate the fluorite structure is stable at $UO_{1.75}$, but no analytical data have been given to substantiate the discovery. At present the existence of both UO and $UO_{1.75}$ must be considered as questionable.

UO_2–$UO_{2.25}$

The uranium-oxygen system between UO_2 and $UO_{2.6}$ has been studied in detail by Anderson and his associates[6,7,8] in England and by Perio and Hering[5,9] in France. The first portion of this composition range (to $UO_{2.25}$) is comparatively straightforward. Oxidation of UO_2 has been found to begin at a temperature as low as —183°C. At these temperatures chemisorption of oxygen equivalent to a monomolecular half-layer of oxygen is found. The adsorption energy is very high, approximately 50 kcal/mole, but there is practically no activation energy.[10] Above —140°C further oxidation occurs equivalent to several complete monolayers (~10 kcal activation energy). The mechanism of the oxidation process has not been determined. The oxidation rate shows little temperature dependence, and is a logarithmic function of time. On the basis of these findings, it should be remembered that uranium dioxide which has been exposed to air at room temperature will have a composition approximating $UO_{2.04}$.

Above 50°C a third oxidation process, which follows a parabolic law, becomes important. This process is diffusion controlled, has an activation energy of about 30 kcal, and represents the actual bulk oxidation of uranium dioxide. Anderson, on the basis of density measurements, considers the diffusion-controlled oxidation to involve the random addition of interstitial oxygen atoms into the flunrite lattice. The composition limit in which the fluorite structure is retained is indefinite. Anderson estimates the limit at $UO_{2.20}$, while Perio reports the preparation of $UO_{2.35}$ in which the cubic structure is retained. The random addition of interstitial oxygen results in a gradual decrease in unit cell dimensions, but when oxidation is followed by annealing in a closed tube at 200°C or above, a rearrangement occurs with the interstitial oxygen placing itself at the center of the unit lattice to give an oxide with the composition $UO_{2.25}$. Thus, any oxide in the composition range UO_2–$UO_{2.25}$ will disproportionate to two cubic structures on annealing, UO_2 and $UO_{2.25}$. The unit cell of $UO_{2.25}$ is given as 5.430 ± 0.003 kX with four uranium atoms per unit cell (U_4O_9).

* Argonne National Laboratory.

$UO_{2.25}$–$UO_{2.5}$

The usual result of oxidation beyond $UO_{2.25}$ is a conversion from cubic to tetragonal symmetry with c/a increasing as oxidation proceeds. This increase is believed to be stepwise rather than continuous as would be observed with a solid solution region. Jolibois[11] and Gronvold and Haraldsen[12] were the first investigators to report the formation of a tetragonal structure on oxidation of uranium dioxide.

Anderson finds two tetragonal structures at approximately $UO_{2.31}$ ($c/a = 1.016$), and $UO_{2.37}$ ($c/a = 1.030$), for which he suggests the formation of a superstructure of the type $(U_4O_9)_4O_n$ where $n = 1$ and 2. A third phase, with $n = 3$, might be expected. Perio does report a third tetragonal phase, but it does not fit into the Anderson picture, since its composition is such that $n < 1$, with $c/a = 1.010$.

The tetragonal forms show a rather limited temperature stability range which decreases from about 500°C at $\sim UO_{2.3}$ to 400°C at $\sim UO_{2.4}$. Above 500°C the tetragonal phases disproportionate to form $UO_{2.25}$ and U_3O_8. Their exact composition boundaries are difficult to ascertain since the low temperatures required for the annealing process result in very slow diffusion and equilibration. Furthermore, the tetragonal phases are almost never obtained in a pure state. The usual experience is to observe the coexistence of two phases in varying quantities. Within the quoted composition limits for their stability, these mixtures are believed to represent equilibria by Perio. He reports the preparation of tetragonal phases from heated mixtures of UO_2 and U_3O_8. Anderson believes that the tetragonal phases are formed only by oxidative processes and that true equilibria do not exist. The end point in the oxidation of the tetragonal forms above $UO_{2.4}$ is always U_3O_8.

We have found that a reactive form of UO_2, prepared by the thermal decomposition of uranyl oxalate in a closed, evacuated system, follows a very different oxidation path. Exposure to air at room temperature results in oxidation to nearly $UO_{2.6}$. The X-ray pattern remains cubic, although poorly crystalline, with a unit cell somewhat smaller than $UO_{2.25}$. Annealing studies on this material may prove worthwhile. Complete oxidation results in the formation of amorphous UO_3, with no indication of the formation of U_3O_8 as an intermediate.[13] The different oxidation pattern may be due to the extremely small particle size which does not permit nucleation of the U_3O_8 phase. We have observed that exposure to oxygen, rather than air, results in the formation of some U_3O_8. Evidently the heat of oxidation in pure oxygen is sufficient to cause some nucleation of the U_3O_8 phase. It is also possible that the tetragonal phases may play some role in the nucleation of the U_3O_8 phase.

$UO_{2.5}$ to $UO_{2.67}$

Our recent work has been concentrated on the next portion of the system.[15] Biltz and Muller, on the basis of tensimetric measurements, had indicated a lower limit of the U_3O_8 phase at approximately $UO_{2.6}$. Rundle,[1] on the basis of X-ray measurements, reported the existence of an orthorhombic phase related to U_3O_8 and extending to $UO_{2.52}$. Gronvold[12] had indicated $UO_{2.56}$ as the lower limit, while Hering and Perio's investigation[5] was in agreement with the results obtained by Rundle.

One factor which may play some part in the disagreement as to the lower limit of the orthorhombic phase is the lack of a precise analytical means for analyzing the products for oxygen. We have utilized a procedure[14] which permits the direct determination of oxygen in all uranium oxides to ±0.4%. The method involves the use of bromine trifluoride to liberate molecular oxygen which is then measured tensimetrically. In addition, a careful tensimetric study of the thermal decomposition of U_3O_8 has revealed that the composition of heated samples reverts exactly to U_3O_8 on cooling to room temperature, provided the oxygen pressure above the sample does not fall below 100 mm. At lower pressures a certain amount of hysteresis in oxygen absorption results in the formation of an oxide deficient in oxygen relative to U_3O_8. We feel that the lack of agreement on the position of phase boundaries in the past may have resulted in part from the low-temperature oxidation of UO_2 discussed earlier and from the inability to measure oxygen content with sufficient accuracy. The two methods outlined above should solve most analytical problems.[16]

Our results on ignited mixtures of UO_2 and U_3O_8 place the lower limit of the orthorhombic phase (Rundle's U_2O_5) at $UO_{2.56}$, in agreement with Gronvold. Samples were analyzed both by reaction with bromine trifluoride and by oxidation to U_3O_8. The possibility remains that the solubility range is greater at elevated temperatures, but since all results have been reported in terms of room temperature X-ray measurements, there should be agreement on phase boundaries. The upper limit of the orthorhombic phase (which we have termed the $UO_{2.6}$ phase) is at $UO_{2.65}$. There is no measurable variation in lattice dimension over the composition range.

We have succeeded in preparing single crystals of an oxide with the composition $UO_{2.64}$ by ignition of U_3O_8 at 1150°–1400°C in air. If these crystals are cooled rapidly, oxidation is negligible. At 1150°C needle-like crystals, approximately one mm in length, are formed in a week. At higher temperatures volatilization becomes appreciable. Pseudo-hexagonal blocks of oxide with the composition $UO_{2.61}$ condense at a slightly cooler portion of the furnace tube. Single crystals of U_3O_8 were obtained by heating the $UO_{2.64}$ in oxygen to 500°. In performing this oxidation, it was observed that the U_3O_8 so formed was of a different crystalline modification. This new phase, the β-phase, has been identified as orthorhombic, with $a = 7.04$ kX, $b = 11.40$ kX, and $c = 8.27$ kX. This leads to 4 molecules in the unit cell and an X-ray density of 8.38 gm/cm³. The β-form can be converted to the conventional, or α form, of U_3O_8 by

heating to 750°C. No measurable change in oxygen content is observed as a result of the phase transformation.

High temperature X-ray studies were initiated in order to determine the phase transformation temperature (α to β) and the decomposition temperature (β to $UO_{2.64}$). For purposes of technique, it was desirable to confine the U_3O_8 in a closed and evacuated capillary. However, since it was known that α-U_3O_8 loses oxygen below 750°C under these conditions, a second set of data was obtained using an open-ended capillary, thus permitting the sample to equilibrate with atmospheric oxygen.

Upon heating the α-U_3O_8 to 975°C in either an open or a closed capillary, the β-U_3O_8 form was not observed. We conclude that (1) the β-form may occur near the U_3O_8 decomposition temperature, (2) the β-form cannot occur in a closed capillary because the structure of the α-form is too modified by the oxygen loss, or (3) the β-form is a metastable modification of U_3O_8 which appears when the $UO_{2.6}$ phase is oxidized to U_3O_8 at low temperatures. Although the β-modification was not observed, other phase changes were detected, and one in particular has been identified.

The following applies only to results obtained with a closed and evacuated capillary of α-U_3O_8. Between room temperature and 400°C, the orthorhombic cell undergoes dimensional changes which arise from the oxygen loss as well as the temperature coefficient of expansion. At about 400°C, a new phase appears and persists up to about 600°C; beyond 600°C, an additional phase occurs.

The phase between 400°C and 600°C can be interpreted on the basis of a hexagonal cell with dimensions $a = 6.801 \pm 0.001$ kX, and $c = 4.128 \pm 0.001$ kX. The cell contains one molecule and the calculated X-ray density is 8.41 gm/cm³ at the transition temperature. The main features of the X-ray pattern of this phase can be accounted for by placing uranium atoms at (000), (⅓ ⅔ 0), and (⅔ ⅓ 0). This structure is related to α-U_3O_8 reported by Zachariasen,[17] and the uranium positions are derived as follows: (000) orth → (000) hex, (½ ⅙ 0) orth → (⅓ ⅔ 0) hex, and (0 ⅓ 0) orth → (⅔ ⅓ 0) hex.

If the ratio a/b for α-U_3O_8 is plotted as a function of temperature, it is found that this ratio approaches the value $\sqrt{3}/3$ near the transition temperature. This change to the hexagonal symmetry is so continuous as to indicate that the oxygen atoms as well as the uranium atoms show similar structural relationships. Thus, the oxygen positions in the hexagonal cell become

$$⅓\ 0\ z;\ 0\ ⅓\ z;\ ⅓\ ⅓\ \bar{z};\ ⅓\ ⅔\ ½$$

$$⅔\ 0\ \bar{z};\ 0\ ⅔\ z;\ ⅔\ ⅔\ z;\ ⅔\ ⅓\ ½$$

For $z = 0.1$, the oxygen contributions are approximately of the correct sign and magnitude, indicating that the oxygen positions are approximately as given. On the basis of the assigned oxygen position, the structure must be considered as trigonal.

If a sample of U_3O_8 is pre-heated to 675°C, the X-ray pattern at room temperature indicates that the sample composition is between $UO_{2.65}$ and $UO_{2.67}$ (U_3O_8). High-temperature studies of this material reveal that there may be a transition near 375°C but the new phase may not necessarily be hexagonal. For an open capillary, a transformation occurs near 300°C, but again the transformation is not well-defined. This indicates that for compositions with oxygen content slightly less than occurs in U_3O_8, the phase may be maintained up to about 300°–400°C, but at higher temperatures the transformations may involve order-disorder phenomena.

$UO_{2.67}$ to UO_3

This portion of the system is generally considered to consist of a solid solution. The upper limit, UO_3, is known to exist in at least four crystalline modifications in addition to the amorphous form. Three crystal types are encountered in the high-temperature high-pressure oxidation of U_3O_8.[18] Phase I, the first to form, is hexagonal[17] ($a = 3.963$ kX, $c = 4.16$ kX). Phase I then converts to phase II, whose structure is unknown. This in turn forms phase III, or Mallinckrodt UO_3, which Perio[19] has tentatively indexed as orthorhombic with $a = 12.98$ kX, $b = 10.70$ kX, and $c = 7.49$ kX. Phase IV, formed by the oxidation of U_3O_8 by nitrogen dioxide, may also be converted to the Mallinckrodt oxide by prolonged heating in air at 500–550°C.

Very little appears to be known of the phase relationships in converting U_3O_8 to UO_3, or vice versa. It is possible that at least two paths exist between these composition limits.

Zachariasen[20] has shown that the orthorhombic U_3O_8 can be derived from the hexagonal UO_3 by referring the UO_3 to orthohexagonal axes and choosing an axis three times longer than required. The transformation would involve only slight shifts in the uranium positions. Fried and Davidson[21] reported that $UO_{2.82}$ and $UO_{2.96}$ prepared by thermal decomposition of amorphous UO_3 at 620–630°C in an atmosphere of oxygen were orthorhombic, but their lattice parameters were not intermediate between those of U_3O_8 and UO_3. Perio[19] reports the preparation of a hexagonal form of $UO_{2.83}$, whose dimensions are given as $a = 3.85$ kX, $c = 4.16$ kX. Perio's compound was also prepared by thermal decomposition of amorphous UO_3,[22] but it is not stated whether decomposition occurred in vacuum, air, or oxygen. The phases encountered may be a function of decomposition conditions. Milne[23] has prepared, by thermal decomposition of uranyl nitrate in air at 220°C, a compound which he assumes to be U_3O_8. The fact that UO_3 is routinely prepared from uranyl nitrate at somewhat higher temperatures, coupled with the reported structure (hexagonal, with $a = 3.93$ kX, $c = 4.14$ kX) suggest that the composition was actually much nearer to UO_3.

BINARY OXIDE SYSTEMS

The binary oxide systems of uranium are characterized by extensive regions of solid solution much as the uranium-oxygen system itself. Mixed oxides of di- and trivalent elements with uranium oxide reflect the stability of the cation lattice in the fluorite structure. Oxides containing less than the required amount of oxygen for the perfect MO_2 lattice show anion vacancies, while those containing oxygen in excess of the required 2:1 ratio add the extra oxygen at interstitial positions in the lattice. Complete oxidation of uranium to the hexavalent state with the formation of uranates is encountered only with mono- or divalent metal oxides. In mixtures of tri- or tetravalent oxides with uranium oxides, the uranium is not oxidized beyond U_3O_8. Attempts to stabilize tetravalent uranium by the addition of other oxides have, in general, been successful only in decreasing the rate of oxidation. As was indicated earlier, the fluorite lattice of uranium dioxide is capable of adding interstitial oxygen. Retention of this phenomenon in binary oxide systems of uranium has prevented effective valence stabilization. The data on binary oxide systems with UO_2 and U_3O_8 are summarized in Table I.

Oxides of the metals of small ionic radius (Be, Al, and Ti) show no compound formation or solid solution with uranium oxides. The slightly larger magnesium ion does not form compounds or solid solution with uranium dioxide, but does form compounds and solid solutions with uranium at higher valences.

GROUP I OXIDES

The work reported in this category is concerned almost exclusively with compounds formed between the alkali metal oxides and uranium(VI) oxide—the uranates. Recent investigations have been confined for the most part to the constitution of the uranates of the alkali metals formed on precipitation from aqueous solution[24-27] and to the determination of crystal structures of the ortho-uranates (M_2UO_4) of potassium, sodium, and lithium.[28] Potassium uranate is reported to crystallize in an orthorhombic structure ($a = 7.96$ kX, $b = 6.90$ kX, and $c = 19.74$ kX with 12 molecules per unit cell). The sodium and lithium compounds are isomorphous.

GROUP II OXIDES

Magnesium Oxide-Uranium Oxide

As mentioned above, no compound or solid solution is formed in the magnesium oxide-uranium dioxide system. As uranium is oxidized above the tetravalent stage, we have observed a solid solution region which extends from at least 25–50% MgO. The structure is fluorite and extends on either side of the perfect fluorite (MO_2) lattice– (anion vacancies,

Table I. Binary Oxide Systems with UO_2 and U_3O_8

Metal oxide	*Ionic radius**	*Reaction with†*	*Observations*	*Reference*
BeO	0.30	UO_2	(Theoretical; eutectic at 2060°C; no compound or solid solution)	35
MgO	0.65	UO_2	Eutectic at 2100°C; no compound or solid solution	7, 36
		$UO_{2.5}$	Fluorite structure 25–50% MgO; oxidizes to uranates in air	7, 28
CaO	0.94	UO_2	Eutectic at 2080°C; solid solution 0–47% CaO at eutectic; $CaUO_3$, Ca_2UO_4 stable below 1850°C	7, 31
		$UO_{2.5}$	Fluorite structure at 33% CaO; oxidizes to uranate in air	28
SrO	1.10	$UO_{2.5}$	Fluorite structure at 33% SrO; oxidizes to uranate in air	28
BaO	1.29	$UO_{2.5}$	Fluorite structure at 33% BaO; oxidizes to uranate in air	28
Al_2O_3	0.55	UO_2	Eutectic at 1930°C; no compounds or solid solution	37
Sc_2O_3	0.68			
Sm_2O_3	0.97	U_3O_8	Fluorite structure at 50% M(III)	38
Yb_2O_3	0.85			
Y_2O_3	0.88	UO_2	Almost complete miscibility at 2000°C fluorite to rare-earth C	7
La_2O_3	1.04	U_3O_8	Fluorite 33–70% $LaO_{1.5}$; to rare-earth C type above 70% $LaO_{1.5}$	38
Pr_6O_{11}	1.00(III) 0.90(IV)	U_3O_8	Fluorite 30–60% PrO_x to rare-earth C type above 60% PrO_x	39
Nd_2O_3	0.99	UO_2	Solid solution 0–60% $NdO_{1.5}$	40
		U_3O_8	Fluorite 25–65% $NdO_{1.5}$ to rare-earth C type above 65% $NdO_{1.5}$	38
Er_2O_3	0.89	U_3O_8	Fluorite 27–67% $ErO_{1.5}$ to rare-earth C type above 67% $ErO_{1.5}$	41
TiO_2	0.60	U_3O_8	No compounds or solid solution at 25% TiO_2	40
ZrO_2	0.77	UO_2	No compounds, fluorite 0–52% ZrO_2, tetragonal 53–100% ZrO_2	42
CeO_2	0.92	UO_2	Continuous solid solution	43, 44
		U_3O_8	Fluorite 50–100% CeO_2	45
ThO_2	0.99	UO_2	Continuous solid solution	46
		U_3O_8	Fluorite 44–100% ThO_2	47
		$UO_x + xO_2$	Fluorite 50–100% ThO_2, maximum stable U valence +5	48

* Ionic radii are taken from Zachariasen's compilation in Seaborg, G. T. and Katz, J. J., *The Actinide Elements*, National Nuclear Energy Series, Division IV, Vol. 14A, p. 775, McGraw-Hill Book Co., New York (1954).

† Reactions with UO_2 are in vacuum or in an inert atmosphere; with U_3O_8 in air. Reactions with $UO_{2.5}$ represent reduction of uranium in uranates by thermal decomposition to U(V). Reactions with $UO_2 + XO_2$ were controlled oxidation experiments.

and interstitial oxygen). The upper limit of the phase with respect to oxygen has been fairly well established, while the lower limit is less well known. Observed ranges are: 50% MgO($XO_{1.}$–$XO_{1.75}$), 33% MgO ($XO_{1.5}$–XO_2), and 25% MgO(XO_2–$XO_{2.13}$), where X = Mg + U.

Two magnesium uranates have been prepared: Mg_2UO_4 and MgU_3O_{10}. The diuranate,[28] MgU_2O_7, has been shown to be an equimolar mixture of the mono- and triuranate. We find that thermal decomposition of the triuranate occurs at ~1050°C in air to form $MgUO_4$ and U_3O_8($MgU_3O_{9.3}$). At 1200°C further oxygen is lost and the fluorite structure is formed at the empirical composition $MgU_3O_{8.5}$. Vacuum heating at 1150°C causes further oxygen loss to MgU_3O_8 with retention of the fluorite structure. The monouranate is stable in air to ~1250°C at which temperature oxygen is lost to form a fluorite phase with the composition $MgUO_{3.5}$. Vacuum heating at 1100°C results in a further slight oxygen loss to $MgUO_{3.4}$. Above 1100°C loss of uranium from magnesium uranates becomes appreciable. We have not identified the volatile species, but it is probably the same compound responsible for volatilization losses in the uranium-oxygen system itself. Whether the end product of the volatilization process is magnesium oxide, or whether another refractory binary oxide is being formed, is unknown.

The structure of $MgUO_4$ has been determined by Zachariasen.[25] It is orthorhombic body-centered with four molecules per unit cell. The compound contains co-linear uranyl groups joined together by the remaining oxygen atoms to form long chains, indicating that crystallographically the formula should be written $Mg(UO_2)O_2$. Zachariasen[30] has also suggested that the simplest way in which polyuranates could be formed would be to join two or more of these chains by means of shared uranyl oxygen atoms (O-U-O-U-O, etc.).

Calcium Oxide-Uranium Oxide

The calcium ion has nearly the same ionic radius as the U^{+4} ion. As a result, the anion deficient rare-earth C type structure is stabilized sufficiently to permit extensive solid solution at the eutectic temperature (2080°C), with Ca(II) + U(IV) replacing the two trivalent rare-earth atoms in the structure.[31] The CaO solubility decreases rather rapidly with temperature, but below 1850°C two compounds are formed, $CaUO_3$ and Ca_2UO_4.

The effect of addition of oxygen to the CaO-UO_2 system has been studied only in the vicinity of the composition of CaU_2O_6, where the fluorite structure is obtained.[28] Further oxygen addition results in loss of the fluorite structure.

We find that calcium uranate is more stable than the corresponding magnesium compound. Ignition in air to 1350°C causes no change in composition. Zachariasen[32] has reported the structure of $CaUO_4$ to be rhombohedral with one molecule per unit cell. The structure contains co-linear uranyl groups. In this compound the $(UO_2)O_2$ arrangement is such as to form a layer structure rather than the chain structure observed with $MgUO_4$. It is interesting to note that $CaUO_4$ can be regarded as having a deformed fluorite type of structure.

Calcium diuranate (CaU_2O_7) can be decomposed to CaU_2O_6 by heating to 900°C under vacuum. The intervening region is largely diphasic, but there is some solid solution near the diuranate composition. Its crystal structure has not been determined.

Strontium Oxide-Uranium Oxide

No data have been reported for the SrO-UO_2 system. At the composition $SrU_2O_{5.9}$, prepared by heating SrU_2O_7 in 1100°C in a vacuum, a fluorite structure is obtained. We have observed an unusual reaction for this composition in that it oxidizes in air at room temperature to give ~$SrU_2O_{6.2}$. Complete oxidation to the diuranate requires heating at 600°C.

The structure of $SrUO_4$ is isomorphous[32] with $CaUO_4$; its thermal stability has not been measured.

Barium Oxide-Uranium Oxide

We have obtained the composition BaU_2O_6 (fluorite structure) by heating barium diuranate in a vacuum at 1200°C, but the reaction is accompanied by a slow loss of uranium.

Barium uranate ($BaUO_4$) is orthorhombic with four molecules per unit cell.[32,33] The $(UO_2)O_2$ layering observed with calcium and strontium uranates is also seen here. We have not measured the thermal stability of $BaUO_4$ above 1200°C, at which temperature no decomposition was observed.

GROUP III OXIDES

Yttrium oxide and neodymium oxide show extensive solubility in uranium dioxide. The remainder of the rare-earth oxides should show very similar properties. The crystal structure encountered here is a transition, from fluorite to the type C rare earth. When the rare-earth oxides are ignited with U_3O_8 in air, opportunity for the formation of both anion-deficient and interstitial oxygen containing structures exists. The work of Hund and his associates illustrates this phenomenon in their plots of cell radius vs composition for the Nd, La, and Pr systems. The Pr_6O_{11}–U_3O_8 system might be expected to show the interstitial oxygen to oxygen deficient transformation at higher percentage of the rare-earth metal than the other lanthanides, but at the temperature (1200°C) used in their work, the composition of the praseodymium oxide was probably considerably below $PrO_{1.83}$.[34] The approximate composition range observed for the fluorite structure in the rare-earth uranium-oxide systems is $MO_{1.94}$–$MO_{2.25}$. At lower oxygen-metal ratios the rare-earth type C structure is obtained. In general, it can be said that the addition of rare-earth oxides to uranium oxides results in the stabilization of the fluorite structure, but does not appreciably affect the resulting uranium valence.

No uranates have been reported for trivalent metals, although the possibility exists that a ternary oxide of the type $M(I)M'(III)(UO_4)_2$ can be prepared. We are beginning an investigation of systems of this type at the present time.

GROUP IV OXIDES

A continuous solid solution over the entire composition range is found for the CeO_2-UO_2 and ThO_2-UO_2 systems, as expected, since the oxides are isomorphous. The addition of cerium or thorium dioxide to uranium oxide again tends to stabilize the fluorite structure. Anderson reports the inability to form the U_3O_8 phase when the uranium oxide concentration falls below 50%. Measurements of lattice dimensions indicated shrinkage of the fluorite lattice with addition of oxygen until the uranium valence reaches +5. Further oxidation (maximum achieved was 5.38) results in expansion of the lattice, indicating a maximum stable valence of +5 for isolated uranium atoms in the fluorite lattice. A very similar situation is encountered in the $CeO_2 \cdot U_3O_8$ system. Rudorff and Valet report uranium valences to 5.2 with retention of the fluorite structure. They report a fluorite composition range from 55–100% CeO_2. Hund, Wagner, and Peetz indicate a somewhat greater stability range—37 to 100% CeO_2.

REFERENCES

1. Rundle, R. E., Baenziger, N. C., Wilson, A. S. and McDonald, R. A., *Structures of the Carbides, Nitrides, and Oxides of Uranium*, J. Am. Chem. Soc., *70*: 99-105 (1948).
2. Cubicciotti, D., *The Reaction between Uranium and Oxygen*, J. Am. Chem. Soc., *74*: 1079-81 (1952).
3. Loriers, J., *The Oxidation of Metallic Uranium*, Compt. rend., *234*: 91-93 (1952).
4. Zachariasen, W. H., private communication.
5. Hering, H. and Perio, P., *Equilibria of Uranium Oxides between UO_3 and U_3O_8*, Bull. Soc. Chim. France, 351-57 (1952).
6. Alberman, K. B. and Anderson, J. S., *The Oxides of Uranium*, J. Chem. Soc., Suppl. 303-11 (1949).
7. Anderson, J. S., *Recent Work on the Chemistry of Uranium Oxides*, Bull. Soc. Chim., France, 781-88 (1953).
8. Roberts, L. E. J., *The Chemisorption of Oxygen on UO_2*, J. Chem. Soc., 3332-3339 (1954).
9. Perio, P., *Considerations on the Uranium Oxides between UO_3 and U_3O_8*, Bull. Soc. Chim., France, 840-41 (1953).
10. Chemisorption of hydrogen on uranium dioxide equivalent to a complete monolayer has been observed at 553°C. This hydrogen is difficult to remove even by pumping at considerably higher temperatures.
11. Jolibois, P., *On a New Oxide of Uranium, U_3O_7*, Compt. rend., *224*: 1395-96 (1947).
12. Gronvold, F. and Haraldsen, H., *Oxidation of Uranium Dioxide*, Nature, *162*: 69-70 (1948).
13. Boulle, A., Jary, R. and Domine-Berges, M., *Oxides of Uranium Resulting from the Decomposition of Uranyl Oxalate*, Compt. rend., *230*: 300-02 (1950).
14. Hoekstra, H. R. and Katz, J. J., *Direct Determination of Oxygen in Less Familiar Metal Oxides*, Anal. Chem., *25*: 1608-12 (1953).
15. Hoekstra, H. R., Siegel, S., Fuchs, L. H. and Katz, J. J., oxides, it cannot be used for all oxide combinations. A Chem., *59*: 136-138 (1955).
16. Although bromine trifluoride will evolve oxygen quantitatively from uranium oxides as well as many binary oxides, it cannot be used for all oxide combinations. A procedure using salts of bromine trifluoride ($KBrF_4$ or BrF_2SbF_6), has been successful in giving quantitative evolution of oxygen from all oxides tested. (Sheft, I., Martin, A. F. and Katz, J. J., to be published.)
17. Zachariasen, W. H., *New Structure Types in the 5f Series of Elements*, Acta Cryst., *1*: 265-68 (1948).
18. Sheft, I., Fried, S. and Davidson, N., *Preparation of Uranium Trioxide*, J. Am. Chem. Soc., *72*: 2172 (1950).
19. Perio, P., *Crystalline Varieties of UO_3*, Bull. Soc. Chim., France, 776-77 (1953).
20. Zachariasen, W. H., private communication.
21. Fried, S. and Davidson, N. R., private communication.
22. Freymann, M., Langevin, S., Rolland-Bernard, M. T., Perio, P. and Kleinberger, R., *Hertzian Spectra of Uranium Oxides*, J. Phys. Rad., *15*: 82-91 (1954).
23. Milne, I. H., *Studies of Radioactive Compounds: UO_3*, Am. Min., *36*: 415-420 (1951).
24. Guter, H., *Potentiometric Titration of Uranyl Nitrate and Acetate with Sodium Hydroxide*, Bull. Soc. Chim., France, 403-04 (1946), 275-76 (1947).
25. Tridot, G., *Sodium and Potassium Uranates*, Ann. Chim., *5*: 369-82 (1950).
26. Wamser, C. A., Belle, J., Bernsohn, E. and Williamson, B., *Constitution of the Uranates of Sodium*, J. Am. Chem. Soc., *74*: 1020 (1952).
27. Sutton, J., *Hydrolysis of Uranyl Ion and Formation of Sodium Uranates*, Journal of Inorganic and Nuclear Chemistry, *1*: 68-74 (1955).
28. Hoekstra, H. R. and Katz, J. J., *Studies on the Alkaline Earth Diuranates*, J. Am. Chem. Soc., *74*: 1683-90 (1952).
29. Zachariasen, W. H., *The Crystal Structure of Magnesium Ortho-uranate*, Acta Cryst., *7*: 788-91 (1954).
30. Zachariasen, W. H., *The Crystal Chemistry of Uranyl Compounds and of Related Compounds of Transuranic Elements*, Acta Cryst., *7*: 795-99 (1954).
31. Alberman, K. B., Blakey, R. C. and Anderson, J. S., *The Binary System UO_3-CaO*, J. Chem. Soc., 1352-56 (1951).
32. Zachariasen, W. H., *The Crystal Structure of $Ca(UO_3)O_2$ and $Sr(UO_3)O_2$*, Acta Cryst., *1*: 281-85 (1948).
33. Samson, S. and Sillén, L. G., *The Crystal Structure of Barium Uranate*, Ark. Kemi. Min. Geol., *25*: 21 (1948).
34. Guth, E. D., Holden, J. R., Baenziger, N. C. and Eyring, L., *Praseodymium Oxides*, J. Am. Chem. Soc., *76*: 5239-42 (1954).
35. Epstein, L. F. and Howland, W. H., *Binary Mixtures of UO_3 and Other Oxides*, J. Am. Ceram. Soc., *36*: 334-35 (1953).
36. Lambertson, W. A. and Mueller, M. H., *UO_3-MgO Phase Equilibrium Systems*, J. Am. Ceram. Soc., *36*: 332-34 (1953).
37. Lambertson, W. A. and Mueller, M. H., *UO_3-Al_2O_3 Phase Equilibrium Systems*, J. Am. Ceram. Soc., *36*: 329-331 (1953).
38. Hund, F. and Peetz, U., *Research on the Systems La_2O_3, Nd_2O_3, Sm_2O_3, Yb_2O_3, Sc_2O_3 with U_3O_8*, Z. anorg. allgem. Chem., *271*: 6-16 (1953).
39. Hund, F. and Peetz, U., *The Fluorite Phases in the Praseodymium Oxide-Uranium Oxide System*, Z. Electrochem., *56*: 223-28 (1952).

40. Lambertson, W. A. and Mueller, M. H., *Uranium Oxide Phase Equilibrium Systems*, ANL-5312 (1954).

41. Hund, F. and Peetz, U., *The Fluorite Phase in the System U_3O_8-Er_2O_3*, Z. anorg. allgem. Chem., *267*: 159-97 (1952).

42. Lambertson, W. A. and Mueller, M. H., *UO_2-ZrO_2 Phase Equilibrium Systems*, J. Am. Ceram. Soc., *36*: 365-68 (1953).

43. Rudorff, W. and Valet, G., *On Cerium-Uranium Blue and Solid Solution in the System CeO_2-UO_2-U_3O_8*, Z. anorg. allgem. Chem., *271* 257-72 (1953).

44. Brauer, G. and Tiessler, R., *On Cerium-Uranium Blue*, Z. anorg. allgem. Chem., *271*: 273-80 (1953).

45. Hund, F., Wagner, R. and Peetz, U., *Anomalous Solid Solution in CeO_2-UO_2 System*, Z. Electrochem., *56*: 61 (1952).

46. Lambertson, W. A., Mueller, M. H. and Gunzel, F. H., *UO_2-ThO_2 Phase Equilibrium System*, J. Am. Ceram. Soc., *36*: 397 99 (1953).

47. Hund, F. and Niessen, G., *Anomalous Solid Solution in the System ThO_2 - $UO_{2.67}$*, Z. Electrochem., *56*: 972-79 (1952).

48. Anderson, J. S., Edgington, D. N., Roberts, L. E. J. and Wait, E., *The System UO_2-ThO_2-O*, J. Chem. Soc., 3324-31 (1954).

On Some Precipitation and Coprecipitation Systems of Thorium and Uranium Salts

By Božo Težak,* Yugoslavia

The precipitation and coprecipitation of inorganic substances from dilute solutions (in concentrations ranging from a few micrograms to a few thousand micrograms per milliliter) are nowadays very frequently used unit operations. In the field of nuclear chemistry many extractions, refining procedures, purifications, and other nperations in connection with technological treatment of low-grade ore, nuclear fuel separation, radioactive waste disposal, etc., and analytical techniques, are based on processes controlling the appearance of a new solid phase from solution.

From this point of view it seems worth-while to discuss certain general and specific features of the precipitation and coprecipitation phenomena as exemplified by some thorium and uranium salts. It is expected also that the results obtained can be fitted into the framework of the systematic survey of precipitation systems in general.[1]

For the characterization of such systems we are using the so-called typical precipitation curves obtained by making the concentration of one of the precipitating components reasonably small and constant, and varying systematically the concentration of the other component. Such diagrams with tyndallometric values, or amount of foreign substance (or the constitutent ion in excess) occluded, or effect of peptization, or any other characteristic element for the precipitate, as ordinates, plotted against the logarithm of concentration of the varying precipitation component are well suited for accurate description of the systems.[2]

We intend to illustrate here, by using typical precipitation curves of some sparingly or moderately soluble thorium and uranium salts, some important interactions between the heteropolar crystals in *statu nascendi* and their environment.

For the description and discussion of various critical regions and limits it is necessary to distinguish between various maxima of precipitation (the isoelectric or equivalency maxima, the crystallization maximum, the coagulation maximum, von Weimarn's maximum, the aggregation maximum, and others).[3]

THE PRECIPITATION SYSTEMS OF THORIUM SALTS

Figures 1–4 present systems of thorium maleate, fumarate, oxalate and phthalate obtained by mixing aqueous solution of the sodium or potassium salt of the corresponding acid with 5×10^{-3} N thorium nitrate solution. The concentrations of anionic components are plotted on the abscissa. The technique of mixing and observation was the same as before. With the exception of thorium fumarate, all typical precipitation curves show a pronounced isoelectric or equivalency maximum. Similar diagrams were obtained when the concentration of the anionic component was constant while the concentration of thorium nitrate varied.

The diagram is somewhat different for the thorium iodate system; Fig. 5 gives both the tyndallograms with constant thorium nitrate and with constant potassium iodate concentration. In the latter case only, there was a wide isoelectric maximum; with excess of potassium iodate it was impossible to obtain stable systems.

Although on each side of a maximum in systems on Figs. 1–4 there are usually clear solutions, there is also the possibility (in the vicinity of the maximum at least) for the solid phase to be "thrown out" by the action of neutral salts.

Figure 6 shows the critical concentrations of lanthanum nitrate which "coagulate" thorium phthalate in the presence of varying excess of potassium phthalate. Similar effects are found with sodium, magnesium, and calcium nitrate: an over-all picture of the "coagulation" effects of these ions on clear solutions of thorium phthalate as a function of the excess of potassium phthalate is given in Fig. 7. An analogous situation is observed with the coagulation effect of sodium sulfate on thorium phthalate in excess of thorium nitrate. Figure 8 gives the results over a large concentrational region of sodium sulfate; with increasing excess of thorium nitrate the precipitation becomes more and more incomplete.

THE PRECIPITATION SYSTEMS OF URANIUM SALTS

Usually the separation of uranium salts is performed by alkali hydroxide or carbonate. In order to follow the completeness of the precipitation, the uranium content was determined polarographically in the clear mother liquor and expressed in percentage of the original content. The polarographic method for uranium determination was described earlier.[4]

Figures 9, 10 and 11 show the results of mixing uranyl nitrate solutions with sodium hydroxide, am-

* In collaboration with M. Branica, H. Füredi, and N. Simunović, Institute "Rudjer Bošković," Zagreb, and Laboratory of Physical Chemistry, Faculty of Science, University of Zagreb, Yugoslavia.

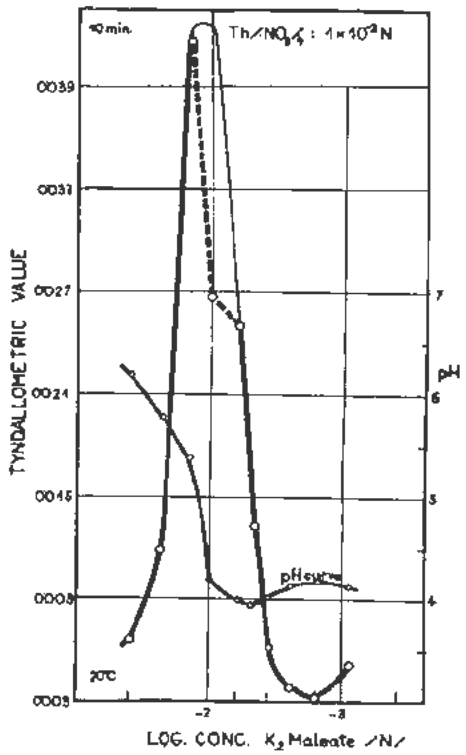

Figure 1. Typical precipitation curve (10-min tyndallogram and pH curve) for the systems: 1×10^{-2}N thorium nitrate and 2×10^{-2}–3×10^{-3}N potassium maleate

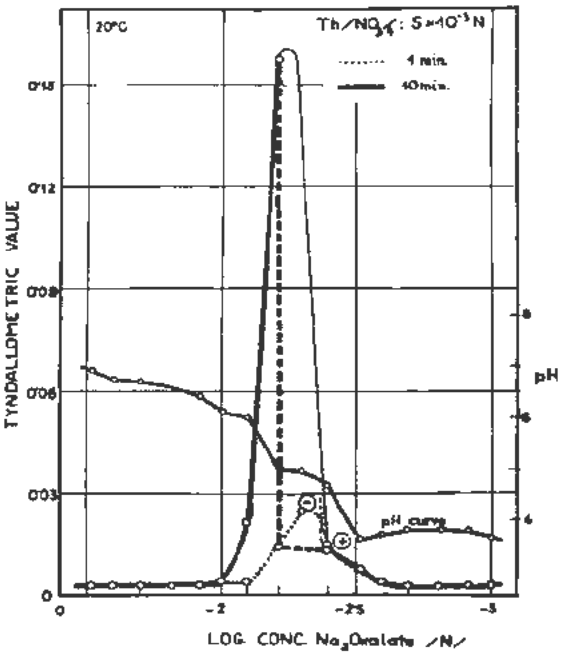

Figure 3. Typical precipitation curve (1 min and 10 min tyndallograms and pH curve) for the systems: 5×10^{-3}N thorium nitrate and 3×10^{-2}–1×10^{-3}N sodium oxalate

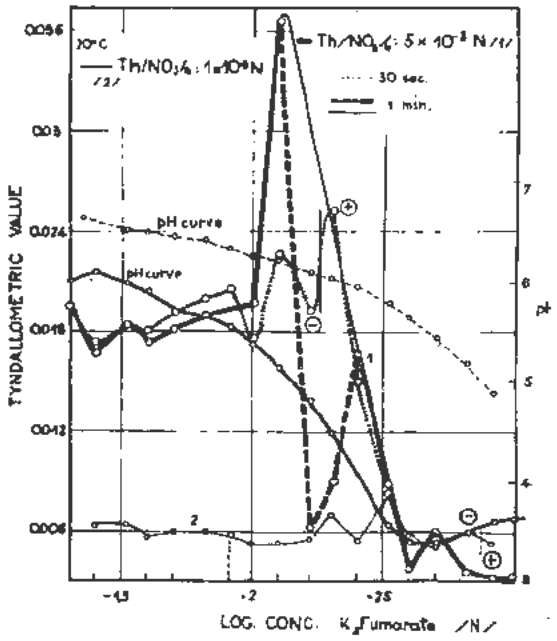

Figure 2. Typical precipitation curve (30 sec. and 1 min tyndallograms and pH curves) for the systems: 5×10^{-3}N (1) and 1×10^{-2}N (2) thorium nitrate, and 5×10^{-2}–1×10^{-2}N potassium fumarate

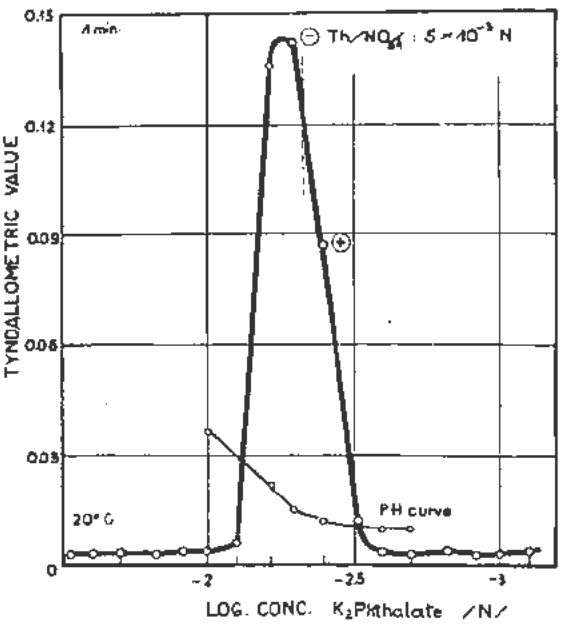

Figure 4. Typical precipitation curve (1 min tyndallogram and pH curve) for the systems: 5×10^{-2}N thorium nitrate and 3×10^{-2}–8×10^{-4}N potassium phthalate

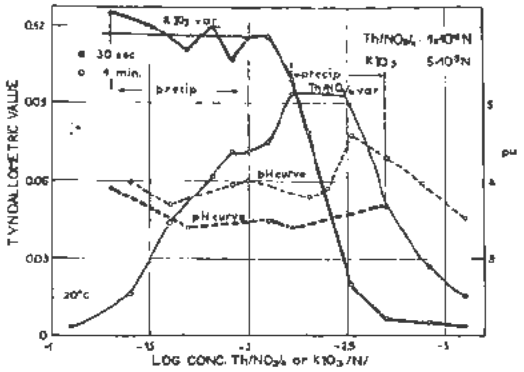

Figure 5. Typical precipitation curves (30 sec and 1 min tyndallograms and pH curves) for the systems: (1) (thick lines) 1×10^{-3}N thorium nitrate and 5×10^{-2}–8×10^{-4}N potassium iodate; (2) (thin lines) 5×10^{-3}N potassium iodate and 8×10^{-2}–8×10^{-4}N thorium nitrate

monium carbonate and sodium carbonate solutions respectively. On some of these figures there are remarks describing the precipitate formation; on others the tyndallometric values are given as a measure of precipitation; the corresponding pH-values, and the uranium content in the filtrate are marked in all figures.

The possibility of precipitating uranium more completely by addition of neutral salts was demonstrated in the case of uranyl nitrate—sodium carbonate systems. Figure 12 presents a series of coagulation effects of sodium, magnesium, calcium, barium, and lanthanum nitrate on equivalent "bodies" of uranyl carbonate; all coagulation curves were obtained by using sols in *statu nascendi*.[5] The series of coagulation values is in accordance with the rule of Schulze and Hardy. However, the great differences between the effects of magnesium, calcium and barium indicate the influence of solubilities of alkaline earth—uranyl—carbonates. It will be of interest, therefore, to examine the precipitation and coprecipitation curves of such mixed systems.

THE PRECIPITATION AND COPRECIPITATION IN SYSTEMS OF URANYL NITRATE-BARIUM CHLORIDE-SODIUM CARBONATE

Figure 13 gives the precipitation curve of barium chloride together with an equivalent amount of uranyl nitrate; the concentration of barium chloride and uranyl nitrate was constant, while the concentration of sodium carbonate solutions varied. It should be noted that the precipitation was more complete than in the case of uranyl carbonate; the minimum amount of uranium in mother liquor did not exceed 2%. It may be concluded, therefore, that the best conditions for the precipitation of uranyl ion are obtained by performing the precipitation with carbonate ion concentration equivalent to the sum of barium and uranyl ion, which are also in equivalent concentrations.

This is demonstrated again in Fig. 14 where the precipitation was performed with the concentration of carbonate ion equivalent to the sum of barium and

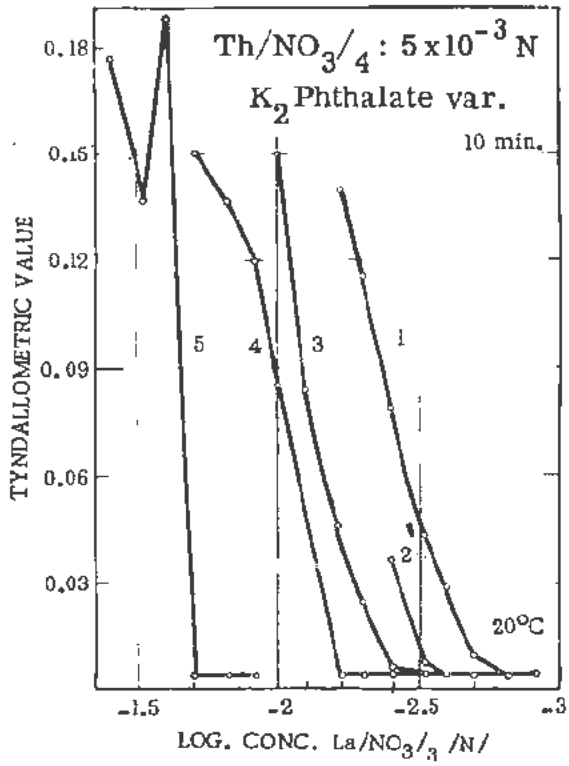

Figure 6. Critical "coagulating" concentrations (10 min concentration tyndallograms) of lanthanum nitrate for the systems: 5×10^{-3}N thorium nitrate and 1×10^{-3}N (1), 1.2×10^{-3}N (2), 1.5×10^{-3}N (3), 2×10^{-3}N (4), and 4×10^{-3}N (5) potassium phthalate

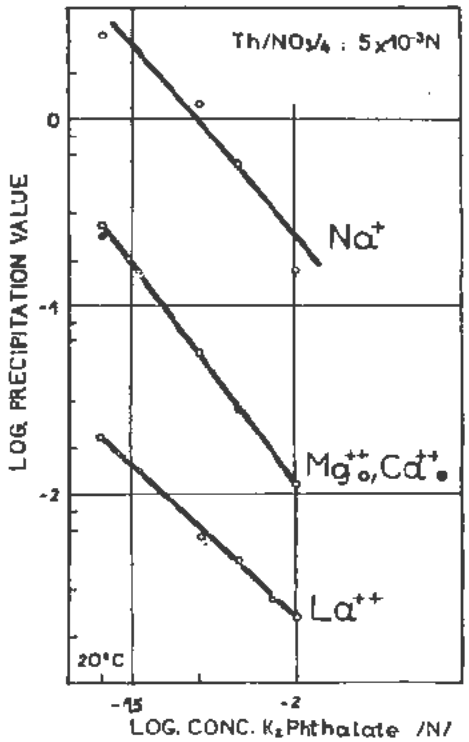

Figure 7. Effect of the concentration of potassium phthalate on precipitation values ("coagulation" values) of sodium, magnesium, calcium, and lanthanum nitrate for the sysems of horium phthalate in *statu nascendi*

uranyl-ion concentrations, but with systematic variation of barium ion; while the concentration of uranyl ion was kept constant. On both sides of the barium chloride "gradient" there is a region where the precipitation of uranyl ion is nearly complete; the remaining amount in the mother liquor was under 1% of the original concentration.

When the ratio between barium and uranyl ion was 2:1, a sharp peak was obtained with the consequence that about 50% of the original amount of uranyl ion remained in the solution. It should be noted that the concentration of the remaining uranyl ion is dependent upon the time elapsing between the moment of mixing and that of taking the sample of supernatant mother liquor for the analysis. This fact reflects the changes in the composition of the precipitate. Nearly complete removal of uranyl ion from solution in the range of great excess of barium carbonate (more than 100 Ba/1 U) is certainly due to coprecipitation.

THE COPRECIPITATION OF URANIUM WITH BARIUM CARBONATE AND CALCIUM HYDROXIDE

It has been shown already that the effect of coprecipitation in systems of barium nitrate-sodium carbonate-sodium hydroxide depends on the concentration of carbonate and hydroxide as much as on the Ba/U ratio. Therefore some experiments in this direction were performed.

The solution of barium nitrate was added as precipitating component to solutions containing from 1 to 50 micrograms of uranium per milliliter, 0.03 to 1.0 *N* sodium hydroxide, and 0.02 to 0.5 *N* sodium carbonate. The systems were filtered, the precipitate dissolved in nitric acid, evaporated to dryness and treated with perchloric acid. After repeated evaporation the samples were dissolved in suitable electrolyte and polarographed. When the ratio Ba/U was greater than 600 the coprecipitation was nearly complete in all cases where the excess of carbonate was less than four times the concentration of barium ion.

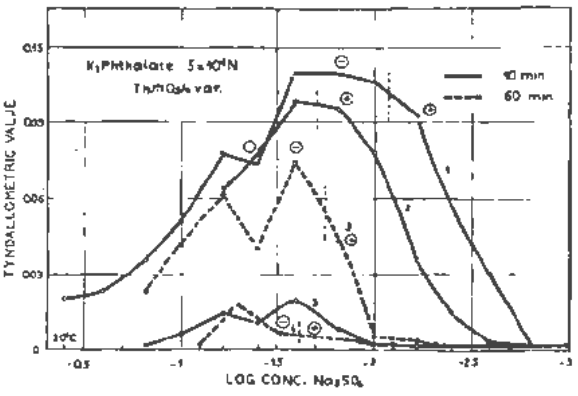

Figure 8. 10 min and 60 min concentration tyndallograms for the systems: 5 × 10^{-3}N potassium phthalate, 1.2 × 10^{-2}N (1); 1.5 × 10^{-2}N (2); 2 × 10^{-2}N (3); 2.4 × 10^{-2}N (4); thorium nitrate, and 6 × 10^{-1}–1 × 10^{-3}N sodium sulfate

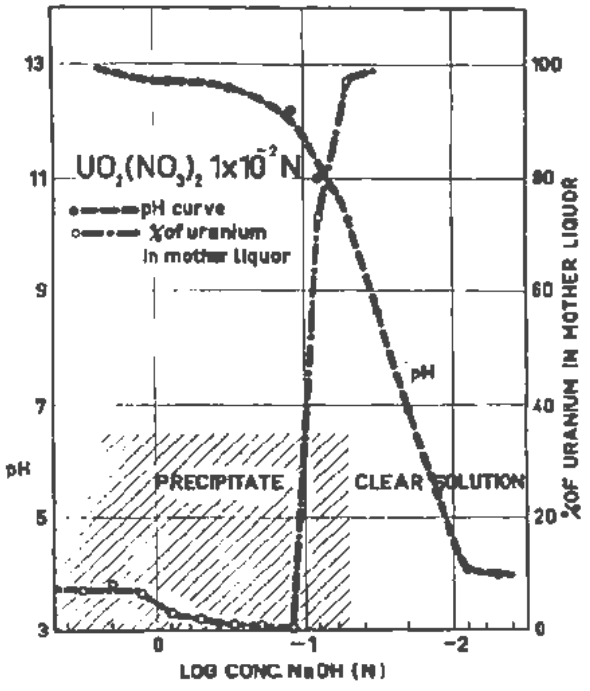

Figure 9. Precipitation systems: 1 × 10^{-2}N uranyl nitrate and 5 × 10^{-5}–5 × 10^{-2}N sodium hydroxide, indicating the region of precipitation, pH curve, and the percentages of original uranium amount which remain in mother liquor

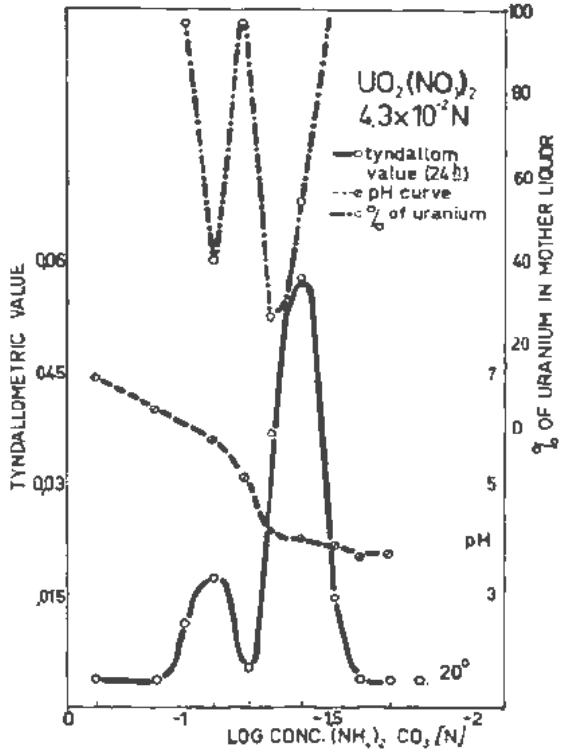

Figure 10. Precipitation systems: 4.3 × 10^{-2}N uranyl nitrate and 2 × 10^{-1}–2 × 10^{-3}N ammonium carbonate, indicating 24 hour tyndallogram, pH curve, and the percentages of original uranium amount which remain in mother liquor

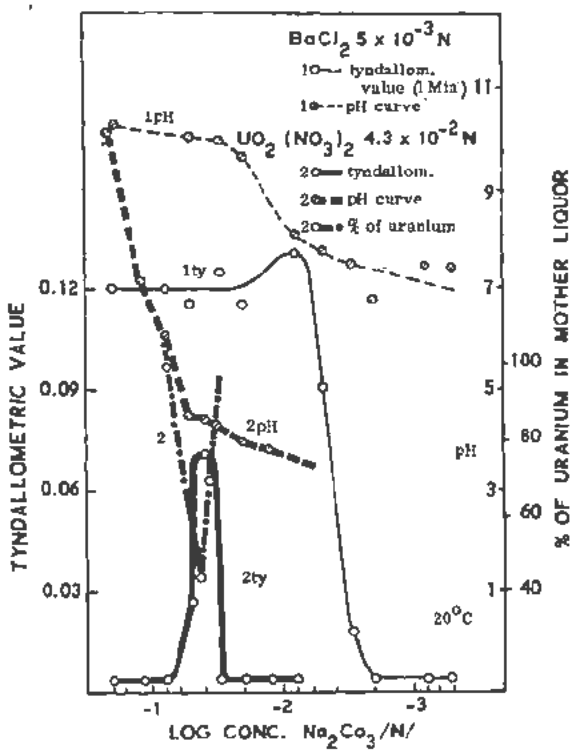

Figure 11. Precipitation systems. 5 × 10^{-3}N barium chloride and 2 × 10^{-1}–5 × 10^{-4}N sodium carbonate (1 min tyndallogram and pH curve, drawn with thin lines); and 4.3 × 10^{-2}N uranyl nitrate and 2 × 10^{-1}–8 × 10^{-3}N sodium carbonate (tyndallogram, pH curve, and percentages of the original uranium amount which remain in mother liquor, drawn with thick lines)

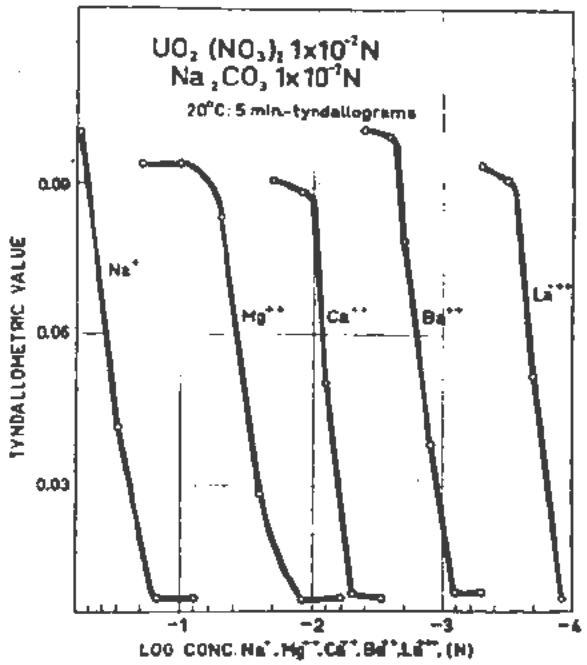

Figure 12. Critical coagulating concentrations (5 min tyndallograms) of sodium, magnesium, calcium, barium, and lanthanum nitrate for the precipitation systems: 1 × 10^{-2}N uranyl nitrate and 1 × 10^{-2}N sodium carbonate

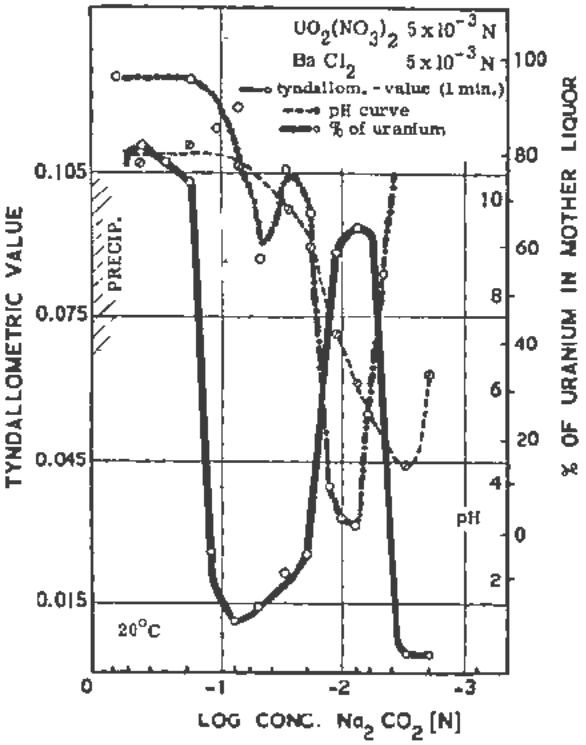

Figure 13. Precipitation systems: 5 × 10^{-3}N uranyl nitrate, 5 × 10^{-3}N barium chloride, and 6 × 10^{-1}–2 × 10^{-3}N sodium carbonate (1 min tyndallogram, pH curve, and percentages of original uranium amount which remain in mother liquor)

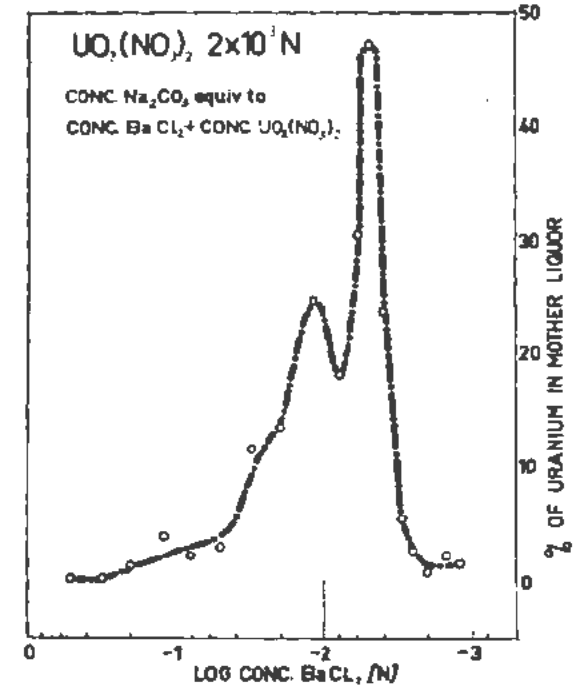

Figure 14. Precipitation and coprecipitation systems: 2 × 10^{-3}N uranyl nitrate, 5 × 10^{-4}–1.1 × 10^{-2}N barium chloride, and sodium carbonate equivalent to the sum of uranyl and barium ions. Plot of the percentages of original uranium amount which remain in mother liquor against the concentration of barium carbonate acting as precipitating (mixed salts) and coprecipitating component

These results may be compared with the results obtained with the calcium-nitrate sodium-hydroxide system. To obtain a similar effect of coprecipitation to that with barium carbonate, the ratio Ca/U had to be 3000, with the most convenient concentration of sodium hydroxide about 0.5 *N*. With the ratio 600, about 70% of the uranium was found in the precipitate. When aluminium ions were present (in concentration of about 5×10^{-2}N) the effect of coprecipitation was much smaller. With the barium-carbonate system such an effect was not noticed. In the presence of sodium carbonate the coprecipitated amounts of uranium were smaller.

With these examples we have tried to demonstrate that similar systems are very well-suited for obtaining an insight into the character of the effect of various salts, and other factors, which are responsible for the appearance of a new phase. It had already been shown by similar investigations that it was possible not only to describe the behaviour of the systems with regard to practical applications, but also to obtain valuable information for a theoretical approach to the mechanism of nucleation, crystal growth, aggregational crystallisation, coagulation, and all phenomena connected with the sensitive structures on the boundary between the solid and liquid phases.

REFERENCES

1. Težak, B., Kolloid-Z. *68* (1934) 60; Z. physik, Chem., A *175* (1935) 219; A *190* (1942) 257; A *191* (1942) 270; *192* (1943) 101; A *175* (1936) 284; B *32* (1936) 46, 52; Arhiv kem. *20* (1948) 16; *21* (1949) 96; *23* (1951) 30.
2. Težak, B. and co-workers, J. Amer. Chem. Soc. *73* (1951), 1602, 1605; J. Phys. Chem. *55* (1951) 1558, 1567; *57* (1953) 301; *59* (1955) in press; J. Polymer Sci. *12* (1954) 221. Arhiv kem. *21* (1949) 109; *22* (1950) 75; *23* (1951) 44, 59; *24* (1952) 67; *25* (1953) 39. Kolloid-Z. *136* (1954) 74; Trans. Faraday Soc. *50* (1954) 65.
3. Težak, B. and co-workers, Arhiv kem. *19* (1947), 9, 19; J. Colloid Sci. Suppl. *1* (1954) 118; Discus. Faraday Soc. *18* (1954).
4. Vouk, V. B., Branica, M. and Weber, O. A., Arhiv kem. *25* (1953) 225.
5. Težak, B. and co-workers, J. Phys. Chem. *57* (1953) 301.

Recent Developments in the Chemistry of Thorium

By L. I. Katzin,* USA

Before 1940, the main industrial use of the element thorium had been in the incandescent gas mantle industry. The advance of electrification had already cut deeply into that use of thorium. Other potential uses were still uncertain, and the study of the chemistry of the element was stagnated. With the discovery, within the last 15 years, of U^{233} and its slow-neutron fission properties, a new stimulus has been given to the detailed study of thorium chemistry. It is the purpose of this paper to discuss some of the more significant achievements of the newer studies, namely, (*a*) the production of massive thorium metal, (*b*) the development of thorium hydride as a raw material for the synthesis of thorium compounds, (*c*) preparation of volatile compounds of thorium, (*d*) development of extraction and purification procedures for the element based on the solubility of thorium nitrate in oxygenated organic solvents, and (*e*) the preparation of compounds in which thorium has an apparent oxidation number less than four.

THORIUM METAL

In his original work on the element thorium, Berzelius[1] treated both potassium thorium fluoride and thorium chloride, with potassium to obtain metallic thorium. Later workers used these compounds and the double chloride in various arrangements, with potassium or sodium metal.[2-7] Calcium was also tried as a reductant for the chloride,[8,9] and some experiments on reduction of thorium oxide with sodium, magnesium and calcium have been reported.[10-13] A characteristic feature of all of these reduction processes is the powdery or granular nature of the metallic product; massive metal is not produced. Other techniques which have been tried include the vapor phase decomposition of thorium iodide on a hot tungsten filament,[14] which is best suited for production of small amounts of high-purity material, and electrolysis of thorium chloride in molten NaCl and KCl.[15-17]

The production of powdery and granular metal in thermochemical reduction processes is clearly a consequence of the high melting point of thorium metal. Formation of impurity (oxide) surface films may be a secondary complicating factor. Spedding, Wilhelm, Keller, Iliff and Neher developed a method of producing massive metal by both raising the temperature of the reacting system and lowering the melting temperature of the metal formed so that it would flow together. The first part of this was accomplished in part through choice of thorium fluoride and calcium metal as the reactants. The heat of formation of calcium fluoride gives a maximum heat evolution in the reaction. Additional heat could be supplied by means of a side reaction, such as that of iodine, bromine, or the halides of volatile metals with excess calcium in the system. Zinc chloride proved to be the most effective of such "boosters." Its success is based upon a double action—in addition to the heat released through the reaction of zinc chloride with calcium, the zinc metal formed alloyed completely with the thorium, lowering its melting point and giving coherent massive metal that separated well from the slag. Vacuum fusion of the cleaned alloy billet gives sound metal completely free of the volatile zinc.

The production of pure solid metal is of great importance because of its relationship to the chemistry of thorium compounds formed from the metal. When only powdered metal of unverified purity was available for synthetic work, stoichiometry of reaction products could not be correctly verified from either the starting proportions or from analysis. This difficulty was exaggerated by the large atomic weight of thorium in comparison with the elements with which it was caused to react. Much of the early descriptive chemistry and thermochemistry of the compounds of thorium with hydrogen, nitrogen, sulfur, etc., now should be or has been repeated.

THORIUM HYDRIDES

Typical of the compounds whose nature was uncertain before the advent of massive pure thorium are the thorium hydrides. The uptake of hydrogen by freshly prepared thorium (mixed with much other material) was demonstrated by Winkler[18] in 1891. Later work failed to define the composition.[19,20] With the massive metal as starting material, Nottorf, Wilson, Rundle, Newton and Powell[21,22,23] were able to demonstrate positively that there were two thorium hydrides, with the formulae ThH_2 and $ThH_{3.75}$ verified by X-ray diffraction and neutron diffraction studies[24,25,26] of the crystal structure of the solids.

The reaction between either massive thorium or thorium turnings and hydrogen gas can be initiated by heating at 300–350°C, though somewhat higher temperatures may be used for convenience. Powdered thorium (e.g., formed from high-temperature decom-

* Argonne National Laboratory.

position of hydride) reacts immediately with hydrogen at room temperature, becoming red hot. At room temperature ThH_2 reacts very slowly with hydrogen, but the rate gradually increases, and after a few minutes the sample begins to get warm, which in turn increases the rate rapidly. Heating in vacuo at 900°C completely decomposes the hydrides.

The total amount of hydrogen absorbed by a sample of thorium is greatly affected by impurities. Thus, thorium recast in BeO crucibles formed hydride to a maximum hydrogen content of 3.19 atoms per thorium atom; thorium heated to 1100°C in high vacuum (residual Zn, 0.03 per cent) took up 3.52 hydrogen atoms per thorium, and metal which had been heated to 1600°C in vacuum took up 3.62 atoms of hydrogen per thorium atom. The detailed dissociation pressure curves of the hydrides were also affected by purity, the best curves being given by the purest material. The vapor pressure relation[27,25,29] for the Th-ThH_2 system is

$$\log P \text{ (mm)} = -7700/T + 9.54$$

for the higher hydride, in equilibrium with ThH_2,

$$\log P \text{ (mm)} = -4220/T + 9.50$$

The most significant feature of the thorium hydrides (or possibly the finely divided metal in equilibrium with them) from the standpoint of the present discussion is their use in synthesis of anhydrous compounds of thorium. This is done in analogy with the corresponding use of uranium hydride[30] and is due primarily to the work of Lipkind and Newton.[31,32]

The general technique is to pass the desired gas or vapors over thorium hydride (there seems to be no important differentiation between them, though the starting material more often is the higher hydride) at 350°C or sometimes 400°C. The gases are usually at low pressure, and the vapors may be carried with an inert gas such as nitrogen, so that reaction is kept to a reasonable rate. Typically, 3 to 4 hours of reaction time are allowed for from 10 to 25 g thorium in the starting material. In all cases, production of the desired product is quantitative, with the exception of the few per cent ThO_2 which may be in the original metal.

The most common type of gaseous reagent used is the hydrogen compound—HF, HCl, HBr, Hi, PH_3, and H_2S. The compositions of the products in all of these cases correspond to tetravalent thorium; the phosphide has the composition Th_3P_4, and the sulfide is ThS_2. Water vapor at 100°C converted an original 12.7 grams of metal to ThO_2 in six hours. Even at 500°C, methane produced no reaction product (other than bringing all the hydride down to ThH_2). Others,[33,34] however, have used the reaction between powdered metal produced from thorium hydride and ammonia gas to produce both ThN and a thorium nitride, tan in color, which has been identified[34,36] as Th_2N_3. This reaction was carried out at 700–1100°C.

Reaction between chlorine or bromine and thorium hydride also takes place under the same conditions to give the corresponding halides. In these instances an important factor is probably the simultaneous reaction with the hydrogen to give gaseous hydrogen halide. Carbon dioxide at 350°C, even after 47 hours, gave neither carbide nor oxide visible to X-ray investigation, and the apparent weight change, if real, was only from 11.9 gm of hydride to 12.0 gm.

The technique possibilities cannot be considered exhausted and further work would show syntheses and institute the method for preparation of known materials.

VOLATILE THORIUM COMPOUNDS

In 1896, Urbain[37] reported synthesis of thorium acetylacetonate and that the compound sublimed at temperatures around 170°C. For over 50 years this compound remained the single example of what could be called a "volatile" compound of thorium. As a result of experience with the wartime preparation of metal borohydrides and their properties, Hoekstra and Katz[38] were able to prepare thorium borohydride, $Th(BH_4)_4$, and to demonstrate that it sublimed at temperatures lower than does the acetylacetonate. The reaction used for the synthesis was

$$ThF_4 + 2Al(BH_4)_3 = Th(BH_4)_4 + 2AlF_2BH_4$$

The vapor pressures as measured were 0.05 mm Hg at 130°C, and 0.20 mm Hg at 150°C. On passing through a tube at 300°C, thorium borohydride decomposes to a bright metallic mirror on the walls, which seems to be amorphous ThB_4. Thorium borohydride was found soluble in diethyl ether to the extent of 47 gm per 100 gm of ether, and in tetrahydrofuran the solubility was 23.6 gm per 100 gm of solvent. Benzene did not seem to dissolve the borohydride compound. From diethyl ether, a complex of the probable formula $Th(BH_4)_4 \cdot 2Et_2O$ could be obtained at ice-bath temperature.

Very recent work by Bradley, Saad and Wardlaw[39] has disclosed a whole class of relatively volatile thorium compounds. These are the alkoxides of tertiary alcohols, with the general formula $Th(OCXYZ)_4$, where X, Y and Z are organic radicals attached to the carbinol carbon, and in the published work have been methyl, ethyl, *n*-propyl and *i*-propyl, in various combinations. The dimethylpropyl alkoxides have been unstable to heating above 120°C, and the tetraisopropoxide, parent substance for synthesis of the others, is not volatile. The most volatile compound, according to the experimenters, has been the tetra-methylethylisopropoxide, which may be written $Th(OCMeEtPr^i)_4$. It boils at 139°C under a pressure of 0.05 mm Hg. This seems slightly less volatile than the borohydride which Hoekstra and Katz report boils at 130°C under the same pressure.

THORIUM NITRATE IN ORGANIC SOLVENTS

Péligot[40] reported the ether solubility of uranyl nitrate in 1842, and Imre[41] in 1927 used ether to

extract a thorium isotope from strong nitric acid solutions, but it took the war-time atomic energy program to give the needed impetus toward exploration of solvent-extraction procedures as a common purification and isolation procedure for inorganic salts. One of the earliest surveys of organic solvents suitable for solvent extraction of thorium nitrate was carried out in 1944–45 under the writer's direction by Hyde and Wolf. Without giving their results in detail, the following summary may be presented.

Using a standard arbitrary aqueous composition of 2*N* thorium nitrate, 1*N* HNO_3 and 3*N* ammonium nitrate, and equal volumes of aqueous and organic phases, the simple ethers (diethyl, di-*n*-propyl, dibutyl) showed essentially zero extraction of thorium nitrate. (Imre, it will be remembered, had found it necessary to go to acid concentrations greater than 5*N* to obtain detectable extraction with diethyl ether.) Polyethers or hydroxylic ethers were better, the diethyl ether of ethylene glycol giving some 24% extraction, and the monobenzyl ether of ethylene glycol, 21%. Alcohols were better than the simple ethers as a group, with *n*-butanol (5%) and methyl *n*-amyl carbinol (4.7%) appearing to show most promise. Dimethyl dioxane was also a little better than the simple ethers (3.8%). Halogenated hydrocarbons (trichlorethane, trichlorethylene, chloroform) were no good, and the nitro compounds (2-nitropropane, nitrobenzene, *o*-nitroanisole) showed no promise. The best of a dozen esters were the two propyl acetates, with extraction of 1.2–1.3%.

As a class, the most outstanding group of extracting solvents, with the arbitrary conditions set, were the ketones. Almost any liquid member of the class did well as a solvent. Examples are methyl ethyl ketone (15% by volume xylene added to diminish water solubility), 22%; methyl *n*-propyl ketone, 11%; methyl isobutyl ketone, 20%; cyclohexanone, 11%; isophorone, 27%; and mesityl oxide, 12.7%.

Taking a given solvent and varying the conditions, for a given thorium concentration, nitric acid was more effective than ammonium nitrate in promoting extraction into the organic phase, and higher total nitrates gave better results than lower concentrations. For the same total nitrate concentration, higher concentrations of thorium gave better distribution into the organic phase than lower concentrations. With both thorium and acid concentrations fixed, added salts such as calcium nitrate and especially magnesium nitrate promoted thorium extraction much more than did ammonium nitrate of the same normality. Aluminum nitrate also promoted the extraction of thorium better than did ammonium nitrate.

With proper detailed choice of aqueous composition and solvent, very favorable single-contact distribution coefficients can be obtained for thorium nitrate. With the exception of uranyl nitrate, no other nitrate salt extracts as well. Particularly, the rare earths are extracted very poorly. Incorporating the extraction into a many-stage counter-current flow-column process, one has an extremely practical mode of isolation of thorium from other metallic cations and, in particular, of freeing it completely from the rare earths which are found with it in nature. Such a process has been worked out by Spedding, Johnson, Tucker, Kant, Wright, Warf, Powell, Newton, Fisher and Lipkind and was embodied into an operating plant about 10 years ago. The thorium feed solution is 3 *M* in calcium nitrate, 3 *M* in nitric acid, and 0.445 *M* in thorium nitrate. Methyl isobutyl ketone is used as the extracting agent. The extraction column has operated satisfactorily to give consistently at least 99.7 per cent recovery of thorium, but the exact separation factors from the impurities in the starting thorium nitrate are not known, if only because their final concentrations cannot be measured. Since the war there have been a number of publications from various laboratories over the world dealing in one manner or another with thorium nitrate and organic liquids as solvents which do not alter what has been said above concerning the extraction procedure, and which will, for brevity's sake, not be discussed at this point.

Our understanding of the nature of solutions of inorganic salts in organic solvents is still limited, and thorium nitrate furnishes a desirable test material. In collaboration with Ferraro, we have established that the important hydrates of thorium nitrate at ordinary temperatures are the pentahydrate and tetrahydrate,[42] and we have measured the heats of solution of these hydrates in a variety of organic solvents. A summary of the findings appears in Table I. We have also prepared anhydrous thorium nitrate[43] and measured its heat of solution in water (it is very difficultly soluble in other solvents), finding an evolution of —34.7 kcal/mole at a dilution of 1:2500.

The solubility and rates of solution of the hydrates in the various solvents were not equal, so it was not practical to measure all the heats in Table I for equally concentrated solutions. There is, nevertheless, a marked trend from high heat evolution for solution in the strongest electron donors to low heat absorption for solution in some of the esters, the weakest donors. Of significance seems to be the extremely high heat of solution in tributyl phosphite, which suggests that there is in this instance coordination to the lone electron pair of the phosphorus, whereas in the other solvents listed the electrons shared come from oxygen.

Another point of interest is the heat of solution values in isobutyl alcohol, which come almost at the end of the list rather than with the strong bases. In similar work with 2-1 nitrate hydrates[44,45] it was shown that this probably corresponded to partial displacement of anions by alcohol groups. When isobutyl alcohol diluted with a weak base like acetone was used, a value approximating that for the other alcohols was found. With tertiary butyl alcohol, elimination of anions from the coordination sphere[46-48] is attended by formation of insoluble hexasolvated solids; with thorium nitrate, insolubility is also found. A series of measurements of thorium nitrate tetra-

Table I. Heats of Solution (ΔH) of Thorium Nitrate Hydrates in Water and in Various Organic Solvents at 25° (kcal/mole)*

Solvent/Solute	$Th(NO_3)_4 \cdot 4\,H_2O$	$Th(NO_3)_4 \cdot 5\,H_2O$
Tributyl phosphite	−42.9 (480)	−44.2 (80) −37.2 (480)†
Dimethyl formamide	−25.2 (150)	−21.6 (150) −20.0 (293)†
Dibutyl butylphosphonate	−18.8 (450)	−14.2 (80) −15.5 (450)
Tetrahydrofuran	14.2 (80)	− 9.4 (80) − 8.9$_7$ (138)† − 5.9$_5$ (300)†
Tributyl phosphate	−12.1 (80)	− 7.6$_5$ (80)
Ethylene glycol diethyl ether	−11.1 (150)	− 6.6$_0$ (150)
Diethyl ether	− 9.5$_3$ (80)	− 4.8$_3$ (80) − 4.5$_9$ (110)† − 3.2$_5$ (218)†
Ethylene glycol monoethyl ether	9.4$_0$ (150)	− 7.0$_5$ (150)
Dibutyl "carbitol"	− 8.4$_0$ (450)	− 3.3$_0$ (450)
Water	− 7.6$_2$ (350)	− 3.5$_3$ (350)
Acetone	− 6.6$_3$ (80)	− 3.3$_5$ (80)
Methyl ethyl ketone	− 5.9$_8$ (130)	− 1.50 (130)
Ethyl acetate	− 1.41 (200)	3.10 (165) 1.04 (200)† 1.74 (100)
Methyl isobutyl ketone	− 1.19 (300)	0.37 (300)† 4.4$_3$ (150)
Ethyl propionate	1.05 (150)	4.7$_0$ (300)
Ethyl chloroacetate	1.38 (300)	4.6$_2$ (130)
n-amyl acetate	1.10 (200)	5.0$_7$ (200)† 6.3$_5$ (180)
Isobutyl alcohol	1.65 (180)	9.8$_5$ (700)
Diethyl malonate		

* The numbers in parenthesis indicate the solvent/solute mole ratios.

† Single determinations.

hydrate heats of solution in isobutyl alcohol mixed with acetone shows an effect identical in type as with the 2-1 salts (see Table II). A similar sort of explanation for the heats of solution in the pure alcohol may therefore be considered.

Table II. Heats of Solution of $Th(NO_3)_4 \cdot 4H_2O$ in Mixtures of Isobutyl Alcohol or Water with Acetone

Solvent	Vol %*	ΔH (kcal/mole)
Water	0	− 6.6$_5$
	40	−12.0
	50	− 9.1$_8$
	75	− 7.4$_5$
	100	− 7.6$_5$
Isobutyl alcohol	50	− 8.0$_5$
	75	−11.4
	87.5	− 7.90
	100	1.65

* Percentages determined from the respective volumes used in the solvents.

The explanation cannot be identical, however. With the dihydrate of a 2-1 nitrate of a cation whose coordination number is 6, it is clear that there are two places at least to be occupied by solvent groups (6-2 anions—2 waters) when the solid is dissolved. The ordering of solvents by base strength and the effects of alcohol diluted with acetone, and even of dilute solutions of water in acetone, in giving high heats of solution, can readily be related to the effects of groups entering the two obviously vacant positions. Since the energy change on replacement of a water group by an oxygenated solvent group is much less than that on adding a totally fresh group, the effects of such replacement should be small, similar to the differences between two solvents for the 2-1 salt dihydrate case.

Thorium nitrate tetrahydrate contains four anions per thorium and four water groups, a total of 8 groups available to fill coordination positions. There is some evidence, as from crystallographic studies[49-52] of $ThCl_4$, $ThBr_4$, $Th(OH)_2SO_4$ and $Th(OH)_2CrO_4 \cdot H_2O$, that the coordination number of thorium may be 8. If this is so, thorium nitrate tetrahydrate already contains sufficient groups to satisfy the coordination requirements of the cation. That the heat effects for the solution of tetrahydrate differ by 20 kcal between solvent dibutyl butylphosphonate and solvent n-amyl acetate suggests that more than water replacement may be involved. For addition to a formerly vacant coordination position, one may consider that either a coordination number greater than 8 is achieved, or that some of the crystal water not coordinated to thorium is diluted out in the solution process, and the vacant coordination position is thus made available without having coordination greater than 8 and without displacing a water group. A somewhat similar and perhaps more attractive way of attaining the same effect is by systematically excluding one of the anions from the coordination sphere. With isobutyl alcohol, a second anion could be competitively excluded in pure alcohol and re-admitted in the acetone-diluted solvent. More experimental work from different approaches is required to clear up this question.

THORIUM OF "SUBNORMAL" VALENCE STATE

Salts of thorium, in solution or in the solid state, thorium dioxide, and volatile compounds such as thorium acetylacetonate all contain thorium clearly in the oxidation state 4+. Compounds such as ThS and Th_2S_3 are known only in the solid state. They would appear to represent compounds with thorium in subnormal oxidation states. Crystallographic study[53] of ThS and Th_2S_3, on the other hand, appear to offer convincing proof that the binding and interatomic distances are characteristic of thorium atoms in the metallic state, rather than in some ionic state. The physical properties[54] of these sulfides in many ways agree with such a characterization—they show metallic luster, have no significant vapor pressures at their melting points (2000°C and higher), can be machined or filed like a metal, and conduct electricity fairly well. To perhaps confuse the issue, it may be pointed out that, although actinium, uranium, nep-

tunium and plutonium all show a tripositive state in solution, and form sulfides of the formula X_2S_3, only those of actinium and plutonium are definitely ionic —the uranium and neptunium sulfides are crystallographically metallic, like Th_2S_2.

Against this background, there have been reported in recent years by Hayek, Rehner and Frank,[55,56] and by Anderson and D'Eye,[57] the preparation of compounds with the stoichiometry ThI_3 and ThI_2. The technique is to heat together thorium tetraiodide and thorium metal in the proper proportions. The colors of the compounds have been reported as dark metallic grey with violet or brownish tinge. Hayek, Rehner and Frank report that the iodides are sensitive to X-rays and that crystallographic study is not possible. Anderson and D'Eye claim to have obtained a pattern for the diiodide and two different patterns for the triiodide. They characterize the diiodide structure as a hexagonal layer-lattice structure, like that of common diiodides. Unfortunately, detailed crystallographic data have not been given for either of the iodides, and no confirmation or check of the interpretation has been possible. In contrast to the behavior of the metallic sulfides mentioned earlier, the "subnormal" iodides are very sensitive to water. Hayek and Rehner report ThI_4 and Th as the products of the reaction with water. Anderson and D'Eye give Th^{4+} and gaseous hydrogen. This apparent difference might be one between acidified and non-acidified water but it is not clear from the descriptions given. There is not complete agreement apparent between the two groups concerning the temperature stability relations between the phases $Th\text{-}ThI_2\text{-}ThI_3\text{-}ThI_4$.

Experiments of our own have dealt with another type of compound which apparently contains thorium in subnormal valence. It has been known since early work with thorium metal that it will dissolve on treatment with HCl. A residue is usually left. This residue has customarily been ascribed to ThO_2 present in the starting material or produced during the reduction procedure. At least one investigator,[58] however, has proposed that this residue was a lower oxide formed in the reaction process. The most recent suggestion[59] has been that it is finely divided metal, coated with oxide, which reacts only slowly with the acid. Our results make the last suggestion rather improbable, and give support to the guess of von Bolton;[58] the residue is probably ThO. Pieces of good quality massive thorium metal, 11–14 gm in weight, were used as starting material. Excess hydrochloric acid (concentrated acid may be used, 3–4*N* acid will do also) is allowed to react with the metal in a flask to which a water-cooled condenser is attached. The spontaneous reaction drives the solution to boiling, and the metal becomes dispersed to a black suspension. When gas evolution has largely terminated, the solution may be heated to boiling for short periods until ebullition stops when the source of heat is removed. If allowed to stand, the black matter settles out fairly rapidly. To free it from dissolved thorium, the solid is slurried, transferred to centrifuge tubes, and separated from the supernatant liquor. Several washes with fresh HCl and separation of the wash liquid by centrifugation give good removal of soluble thorium. Thorium dioxide originally present in the metal appears in these manipulations as a white, dense, finely granular material, which settles out faster than the dark reaction product. Some can be made to adhere to the original reaction vessel, in transferring to the centrifuge tubes, and is thus eliminated, but it is usually still visible as a small white ring near the bottom of the centrifuge tube. In mass it represents but a few per cent of the total thorium in the residue. The residue itself contains some 20–25% of the thorium in the original metal.

The mean oxidation state of the thorium in the residue, other than ThO_2, is obtained by catalytically promoting the reaction between the residue and HCl. The catalyst is a small concentration[60] of HF—a few drops of 6*N* HF in 10–20 ml of 5*N* HCl (an acid concentration chosen for convenience). The hydrogen evolved is measured by determining the volume of water displaced at atmospheric pressure. When the reaction is complete, the ThO_2 originally present in the metal remains as a small white residue at the bottom of the solution and can be separated off. The amount of thorium in the solution is determined gravimetrically, and the number of moles of hydrogen evolved per mole of thorium entering the solution is calculated. Typical values are 0.99, 1.04, 1.03, 1.01 and 1.02 moles hydrogen gas per mole of thorium dissolved. This corresponds formally to the reaction $Th^{2+} + 2H^+ = Th^{4+} + H_2$. In the cold, the decomposition rate of the material is quite slow, and an appreciable portion remains after even six weeks. A sample of this sort gave a hydrogen-thorium ratio of 0.92, with a perhaps larger residue of oxide than normal.

In other experiments, washed and centrifuged residue, separated from supernatant liquor, was connected to a vacuum pump and trap, and the water and excess HCl pumped off. The ratio of hydrogen evolved to thorium dissolved was not distinguishably different from a portion of the same residue which had not been so dried. In other experiments, washed residue which had been pumped dry was analyzed for hydrogen, oxygen, chloride and thorium. Material balances were effectively 100%, confirming that no other element formed a significant portion of the material. Hydrogen was determined by igniting a portion of residue in a train and capturing the water in magnesium perchlorate (Anhydrone). Oxygen was determined by the $KBrF_4$ procedure.[61] Samples for thorium analysis were dissolved in dilute sulfuric acid, with fluoride catalysis, and the thorium was precipitated with oxalic acid. Chloride was determined gravimetrically in the supernatant liquor.

A sample which had been pumped for 16 hours showed the following analysis: hydrogen, 0.75%; chloride, 7.72%; oxygen, 10.12%; thorium, 82.36%; material balance, 100.95%. The critical hydrogen analysis, unfortunately, probably represents an upper

limit, inasmuch as in the ignition of the residue, which explodes spontaneously when heated to about 110°C, some hydrogen appears as HCl as well as H_2O. The fraction of the hydrogen represented by the HCl is small, and it can be trapped at the end of the analytical train and measured. However, its mass hydrogen equivalent is over 4 times that of H_2O, so that any small amounts of HCl that are trapped in the magnesium perchlorate lead to erroneously high hydrogen values. The atomic ratios, per thorium, in the above analysis, are hydrogen, 2.12, chloride, 0.61, oxygen, 1.78. Assuming all the chloride to be HCl, and all the residual hydrogen to be water, the thorium-oxygen composition may be represented as $ThO_{1.03}$. A small percentage of ThO_2 is known to be in the dried solid, so the oxygen may be expected to be a little high for ThO, but the closeness of agreement with expectation is fortuitous. As there is but 0.75 water molecule per thorium, the material is probably not $Th(OH)_2$.

As already stated, the dried residue, heated to 110-115°C, will decompose explosively to white ThO_2. Warmed in an inert gas atmosphere, some permanent gas is evolved (hydrogen?). If the original residue in contact with acid is centrifuged, or allowed to settle, so that its upper surface extends somewhat along the length of a centrifuge tube, with the passage of time a yellow zone will be seen to progress from the direction of the liquid surface downwards. This is an indication of reaction with atmospheric gases, probably with oxygen (since the analytical material balances do not seem to be affected by the reaction). Handling of damp residues in the air brings the yellowing reaction on quickly. Residues which have been pumped dry quickly have the yellowing very greatly inhibited, although they are exposed to the air after drying. Even in samples which have reached a canary-yellow condition, the hydrogen evolution-thorium solution ratio is still close to unity, though the amount of residual oxide may be somewhat increased. More investigation of the nature of the yellowing reaction and its end-product is in progress.

Characterization of the residue by X-ray diffraction is hampered by the largely amorphous character of the material. With long exposures, a weak pattern with diffuse lines is obtained. Though there may be contributions from the small amount of crystalline ThO_2 which is present, or from any small metal fragments that might have survived the acid treatment, the pattern is not the characteristic sharp-lined structure of either of these. As thorium metal, ThO and ThO_2 all have cubic structures with similar unit cell dimensions careful investigation is called for. Means of improving crystallization will be tried. At such time as the identification with ThO may be made, it will be appropriate to again refer to the question whether this is thorium in the 2+ state or an "inter-metallic" compound formed in aqueous solution.

ACKNOWLEDGEMENTS

Deep indebtedness should be expressed to Mrs. Mary-Lou Rauh for general analytical assistance, to Irving Sheft for the oxygen analyses, and to Stanley Siegel for X-ray assistance.

REFERENCES

1. Berzelius, J. J., *Untersuchung eines neuen Minerals und einer darin enthaltenene zuvor unbekannten Erde*, Ann. d. Physik, (2) *16*: 385-415 (1829).
2. Chydenius, J. J., *Ueber die Thorerde und deren Verbindungen*, Ann. d. Physik (2) *119*: 43-55 (1863).
3. Nilson, L. F., *Ueber metallisches Thorium*, Ber., *15*: 2537-46 (1882).
4. Matignon, C. and Délépine, M., *Composition de l'hydrure et de l'azoture de thorium*, Compt. rend., *132*: 36-8 (1901).
5. Matignon, C. and Délépine, M., *Chlorure, oxychlorure, hydrure et azoture de thorium*, Ann. chim. phys. (8) *10*: 130-44 (1907).
6. Moissan, H. and Hönigschmid, O., *Sur la préparation du thorium*, Ann. chim. phys. (8) *8*: 182-92 (1906).
7. Von Bolton, W., *Ueber das Thorium*, Z. Elektrochem., *14*: 768-90 (1908).
8. Moissan, H. and Martinsen, M., *Préparation et propriétés du chlorure et du bromure de thorium*, Compt. rend., *140*: 1510-15 (1905).
9. Marden, J. W. and Rentschler, H. C., *Metallic thorium*, Ind. Eng. Chem., *19*: 97-103 (1927).
10. Winkler, C., *Ueber die Reduktion von Sauerstoffverbindungen durch Magnesium*, Ber., *24*: 873-99 (1891).
11. Matignon, C., *Combinaison directe de l'azote avec les métaux du groupe des terres rares*, Compt. rend., *131*: 837-9 (1900).
12. Kohlschütter, V., *Ueber die Vorkommen von Stickstoff und Helium in Uranmineralien*, Ann., *317*: 158-89 (1901).
13. Ruff, O. and Brintzinger, H., *Reduktion von Thor-, Zirkon- und Titandioxyd*, Z. anorg. allgem. Chem., *129*: 267-75 (1923).
14. Van Arkel, A. E. and de Boer, J. H., *Darstellung von reinem Titanium-, Zirkonium-, Hafnium- und Thoriummetall*, Z. anorg. allgem. Chem., *148*: 345-50 (1925).
15. Moissan, H. and Hönigschmid, O., *Sur la préparation du thorium*, Ann. chim. phys., (8) *8*: 182-92 (1906).
16. Von Wartenberg, H., *Ueber Thorium*, Z. Elektrochem., *15*: 866-72 (1909).
17. Driggs, F. H. and Lilliendahl, W. C., *Preparation of metal powders by electrolysis of fused salts. II. Thorium*, Ind. Eng. Chem., *22*: 1302-3 (1930).
18. See reference 10.
19. See reference 4.
20. Sieverts, A. and Roell, E., *Zirkonium, Thorium und Wasserstoff*, Z. anorg. allgem. Chem., *153*: 289-308 (1926).
21. Nottorf, R. W., Wilson, A. S., Rundle, R. E., Newton, A. S. and Powell, J. E., private communication.
22. Nottorf, R. W., *Some problems in chemistry of uranium and thorium of interest to the development of atomic power*, Iowa State Coll., J. Sci., *26*: 255-7 (1952).
23. Newton, A. S. and Johnson, O., *Thorium compounds*, U. S. Patent Appl., 787,850, Official Gaz., *651*: 615-6 (1951).
24. Rundle, R. E., Wilson, A. S., Nottorf, R. and Rauchle, R. F., *The crystal structures of ThH_1 and ZrH_1*, AECD-2120 (July 19, 1948).

25. Rundle, R. E., Shull, C. G. and Wollan, E. O., *The crystal structure of thorium and zirconium dihydrides by X-ray and neutron diffraction,* Acta Cryst., *5*: 22-6 (1952).
26. Zachariasen, W. H., *Crystal chemical studies of the 5f-series of elements. XIX. The crystal structure of the higher thorium hydride, Th_4H_{15},* Acta Cryst., *6*: 393-5 (1953).
27. See reference 21.
28. See reference 22.
29. Mallett, M. W. and Campbell, I. E., *The dissociation pressures of thorium dihydride in the thorium-thorium dihydride system,* J. Am. Chem. Soc., *73*: 4850-2 (1951).
30. Newton, A. S., Warf, J. C., Spedding, F. H., Johnson, O., Johns, I. B., Nottorf, R. W., Ayres, J. A., Fisher, R. W. and Kant, A., *Uranium hydride - II. Radiochemical and chemical properties,* Nucleonics, *4* (2): 17-25 (1949).
31. Lipkind, H. and Newton, A. S., *Preparation of binary compounds of thorium from thorium metal,* unpublished data.
32. See reference 23.
33. Foster, L. S., *et al., The preparation of crucibles from nitrides,* AECD-2942 (March 23, 1950).
34. Chiotti, P., *Experimental refractory bodies of high-melting nitrides, carbides, and uranium dioxide,* J. Am. Ceram. Soc., *35*: 123-30 (1952).
35. Zachariasen, W. H., *The crystal structure of Th_3N_4,* AECD-2090 (June 28, 1948).
36. Zachariasen, W. H., *Crystal chemical studies of the 5f-series of elements. XII. New compounds representing known structure types,* Acta Cryst., *2*: 388-90 (1949).
37. Urbain, G., *Contribution a l'étude du thorium,* Bull. soc. chim. (3) *15*: 347-9 (1896).
38. Hoekstra, H. R. and Katz, J. J., *The preparation and properties of the Group IV-B metal borohydrides,* J. Am. Chem. Soc., *71*: 2488-92 (1949).
39. Bradley, D. C., Saad, M. A. and Wardlaw, W., *Tertiary alkoxides of thorium,* J. Chem. Soc., 3488-90 (1954).
40. Péligot, E., *Rercherches sur l'uranium,* Ann. chim. phys. (3) *5*: 5-47 (1942).
41. Imre, L., *Beiträge zur Chemie des Aktiniums,* Z. anorg. allgem. Chem., *166*: 1-15 (1927).
42. Ferraro, J. R., Katzin, L. I. and Gibson, G., *The system thorium nitrate-water-nitric acid at 25° and the hydrates of thorium nitrate,* J. Am. Chem. Soc., *76*: 909-10 (1954).
43. Ferraro, J. R., Katzin, L. I. and Gibson, G., *The reaction of thorium nitrate tetrahydrate with nitrogen oxides. Anhydrous thorium nitrate,* J. Am. Chem. Soc., *77*: 327-9 (1955).
44. Katzin, L. I., Simon, D. M. and Ferraro, J. R., *Heats of solution of uranyl nitrate hydrates in water and in organic solvents,* J. Am. Chem. Soc., *74*: 1191-4 (1952).
45. Katzin, L. I. and Ferraro, J. R., *Heats of solution of the cobaltous nitrate hydrates in water and in certain organic solvents and binding energies of molecular ligands,* J. Am. Chem. Soc., *74*: 6040 (1952)
46. Katzin, L. I. and Ferraro, J. R., *The systems cobaltous nitrate-water-acetone and cobaltous nitrate-water-t-butyl alcohol at 25°,* J. Am. Chem. Soc., *72*: 5451-5 (1950).
47. Katzin, L. I. and Sullivan, J. C., *The system uranyl nitrate-water-organic solvent,* J. Phys. and Colloid Chem., *55*: 346-74 (1951).
48. Katzin, L. I. and Ferraro, J. R., *The system cobaltous chloride- water-t-butyl alcohol at 25°,* J. Am. Chem. Soc., *75*: 3825-7 (1953).
49. Mooney, R. C. L., *The crystal structure of $ThCl_4$ and UCl_4,* Acta Cryst., *2*: 189-91 (1949).
50. D'Eye, R. W. M., *The crystal structure of thorium tetrabromide,* J. Chem. Soc., *1950*: 2764-6.
51. Lundgren, G. and Sillén, L. G., *The crystal structure of $Th(OH)_2CrO_4 \cdot H_2O$,* Arkiv f. Kemi, *1*: 277-92 (1949); Naturwiss., *36*: 345-6 (1949).
52. Lundgren, G., *The crystal structure of $Th(OH)_2SO_4$,* Arkiv f. Kemi, *2*: 535-49 (1950).
53. Zachariasen, W. H., *Crystal chemical studies of the 5f-series of elements. X. Sulfides and oxy-sulfides,* Acta Cryst., *2*: 291-6 (1949).
54. Eastman, E. D., Brewer, L., Bromley, L. A., Gilles, P. W. and Lofgren, N. L., *Preparation and properties of the sulfides of thorium and uranium,* J. Am. Chem. Soc., *72*: 4019-23 (1950).
55. Hayek, E. and Rehner, Th., *Thoriumtrijodid,* Experentia, *5*: 114 (1949).
56. Hayek, E., Rehner, Th. and Frank, A., *Halogenide des zwei - under dreiwertigen Thoriums,* Monatshefte f. Chem., *82*: 575-87 (1951).
57. Anderson, J. S. and D'Eye, R. W., *The lower valency states of thorium,* J. Chem. Soc., Suppl., *2*: S244-S248 (1949).
58. See reference 7.
59. Rodden, C. J. and Warf, J. C., *Thorium,* in Rodden, C. J., *Analytical Chemistry of the Manhatlan Project,* NNES., Division VIII, Volume 1, McGraw-Hill Book Company, Inc., New York (1950).
60. Steahly, F. L. and Stoughton, R. W., U. S. Patent No. 2,546,933 (March 27, 1951).
61. Sheft, Irving, Martin, A. F. and Katz, J. J., *High temperature fluorination reactions of inorganic substances,* American Chemical Society Meeting, Cincinnati, Ohio, April 6, 1955.

Record of Proceedings of Session 10B.3

FRIDAY AFTERNOON, 12 AUGUST 1955

Chairman: Mr. G. T. Seaborg (USA)

Vice-Chairman: Mr. D. I. Ryabchikov (USSR)

Scientific Secretaries: Messrs. J. Gaunt and D. J. Dewar

PROGRAMME

P/736 Some recent developments in the chemistry of neptunium ..... J. C. Hindman *et al.*

P/838 A review of americium and curium chemistry ..... R. A. Penneman and L. B. Asprey

P/676 Spectrophotometric studies of the behaviour of americium ions in solutions ..... G. N. Yakovlev and V. N. Kosyakov

DISCUSSION

Mr. J. C. HINDMAN (USA) presented paper P/736.

Mr. R. A. PENNEMAN (USA) presented paper P/838 as follows:

Americium and curium are now about 10 years old. During this time they have increased in availability to the present gram amounts of americium and milligram amounts of curium. Most of the americium work has been done with Am^{241}, a 470-year alpha emitter. The long-lived Am^{243}, with a half-life of 8800 years, should make future investigations easier, particularly because the self-induced reduction of the higher americium valence states will be less by a factor of about 20 compared with Am^{241}. Curium has received much less study than americium, primarily because of the simpler curium chemistry and the difficulty in working with the short half-life of the usual isotope of curium, Cm^{242}, a half-life of 162.8 days. A relatively long-lived isotope of curium, Cm^{244}, with a half-life of 18.4 years, recently became available, and with it it was possible for the first time to have evidence of tetravalent curium in the black oxide. Since americium-243 and curium-244 are formed by high neutron irradiation of plutonium, it is reasonable to expect that these long-lived isotopes will become more available as the use of plutonium in power reactors becomes widespread.

I shall present today only the highlights of americium and curium chemistry and will be unable to reference each work which has been done by a great many workers. These references are in the paper which will appear in the proceedings of this Conference.

Americium is known in the formal valence states of (0), (III), (IV), (V), (VI), but only americium(III), (V) and (VI) have been characterized in solution. Metallic americium (Slide 1) has been prepared by reduction of AmF_3 with barium metal at 1100-1200°C in high vacuum. The vapor pressure of americium metal has been measured recently and is 1.7×10^{-3} mm mercury at 1000°C. The heat of the reaction of americium with 1.5 *M* HCl is −162.3 kcal-mol. This, combined with entropy estimates, yields E_f^0 of $Am(c) = Am^{+3}_{(aq)} + 3e^- = +2.32$ volts. Americium metal reacts with excess oxygen to form AmO_2. With a minimum of oxygen, as long as americium metal is present, AmO is formed. Americium also reacts with a minimum of hydrogen to give AmH_2.

It is interesting that the ionic radius of Am^{+3} is 0.99Å, which is the same as that of Nd^{+3}. If one assumes that the two elements have the same atomic volume or trivalent metallic structure, the calculated density of americium metal (Table I on next page) would be 11.7 gm/cm³, based on neodymium and 11.6 gm/cm³ based on praseodymium. If, however, americium had the europium metallic structure, its density would be only 8.3 gm/cm³. It is the inference of this qualitative argument that americium is not divalent in the metal. Note here also the low density of curium metal—about 7 gm/cm³. Based on the gadolinium radius the density would be around 12. The reported density of curium metal is low, approximately that of the light rare-earth metals, and may be due to a void.

With macro quantities of americium, it has not been possible to demonstrate the existence of divalent americium in compounds. If one reduces anhydrous $SmCl_3$ with hydrogen at 500°C to 800°C, $SmCl_2$ is readily obtained (Slide 2). A similar reaction in the case of $AmCl_3$ gives no reduction. Electrolysis in aqueous acetic acid-sulphuric acid media with a mercury cathode and separate anode compartments was then tried. Whereas $SmSO_4$, which is red, and $YbSO_4$, which is green, are readily formed, in the case of americium there is no color change observed

AmF_3 + BARIUM $\xrightarrow{1100-1200°C}$ $Am_{(c)}$

Am VAPOR PRESSURE 1000°C, 1.7×10^{-3} mm Hg

$Am^{+3}_{(aq)}$; $\Delta H = -163.2$ Kcal mol^{-1}

$Am_{(c)} = Am^{+3}_{(aq)} + 3e^-$, $E_f^\circ = +2.32$ VOLTS

$Am_{(c)}$ → AmO_2 (O_2 EXCESS)
$Am_{(c)}$ → AmO (O_2 (MINIMUM)) (PRESENCE OF Am METAL)
$Am_{(c)}$ → AmH_2 (H_2 (MINIMUM))

Slide 1. Americium metal

and no precipitate. Americium amalgam, however, is formed under these conditions. If one treats americium amalgam with either ammonium sulphate or sulphuric acid, a pink Am^{+3} solution is obtained and no precipitate.

We conclude that Am(II) is not an easily attainable state and that americium is not europium-like in its behaviour.

Trivalent americium has often been considered as the only stable state of americium in solution. It is worth while pointing out that the valence states of Am(VI) and Am(V) are strong oxidizing agents

Table I

Element	*Observed density*	*Estimated density*
Np	20.46	
Pu	19.7	
Am	11.7	11.6 Pr 11.7 Nd 8.3 Eu
Cm	~7.0	12.2 Gd
La	6.19	
Pr	6.80	
Eu	5.24	

in acid solution, though not appreciably stronger than permanganate or tetravalent cerium, for instance. Thus, it is only an accidental result of the reduction of higher valence states of americium by Am^{241} alpha radiation that makes Am(III) appear so relatively stable. The isotope Am^{243} will lower this self-reduction rate of Am(V) and Am(VI) to only

$SmCl_3 + H_2 \xrightarrow{500-800°} SmCl_2$; $AmCl_3 + H_2$ = NO REDUCTION

$Sm^{+3}_{(aq)} + e^- \xrightarrow[HC_2H_3O_2-H_2SO_4]{Hg\ CATHODE} SmSO_4$ (RED)↓

$Yb^{+3}_{(aq)} + e^-$ (·) → $YbSO_4$ (GREEN)↓

$Am^{+3}_{(aq)} + e^-$ (·) → NO COLOR CHANGE NO PPT.

Am (AMALGAM) + H_2SO_4 + $(NH_4)_2SO_4$ = Am^{+3} (PINK SOL'N.) (NO PPT.)

Slide 2. Reactions not yielding Am(II)

a few per cent per day, and at this time the higher oxidation state should then show a more significant chemical stability.

The three states, Am(III), Am(V), and Am(VI), which are stable in aqueous acid solution, have very sharp and characteristic spectra and high molecular extinction coefficients, Slide 3 (Fig. 1 of P/838). The exact value of the molecular extinction coefficient depends somewhat on the resolution of the instrument. This spectrum was obtained on the Model 14 of the Cary Recording Spectrophotometer. For each of the americium-valence states there is one or more peaks which can be used to estimate the concentration of americium in a mixture which contains all three valence states. The characteristic color of americium(III) in dilute solution is pink. The color changes to yellow as the americium concentration is increased. Only slight shifts in the major peaks of americium(III) occur on going from acid solution to K_2CO_3 solution. This is in contrast to the behaviour of the absorption spectra of Nd(III) and Eu(III) in acid and carbonate media.

Information on complexes of americium(III) by spectrophotometric studies by Yakovlev and Kosyakov will be presented in the next paper by Kosyakov.

Since the major portion of the chemistry for isolating americium deals with the trivalent state, a brief discussion will be included at this point. It has recently been demonstrated that kilogram-scale separations of rare earths can be achieved by elution from the cation-exchange resin, Dowex-50, using 0.1% ammonium citrate at pH 8 at very high flow rates (5 cm per minute). Under these conditions,

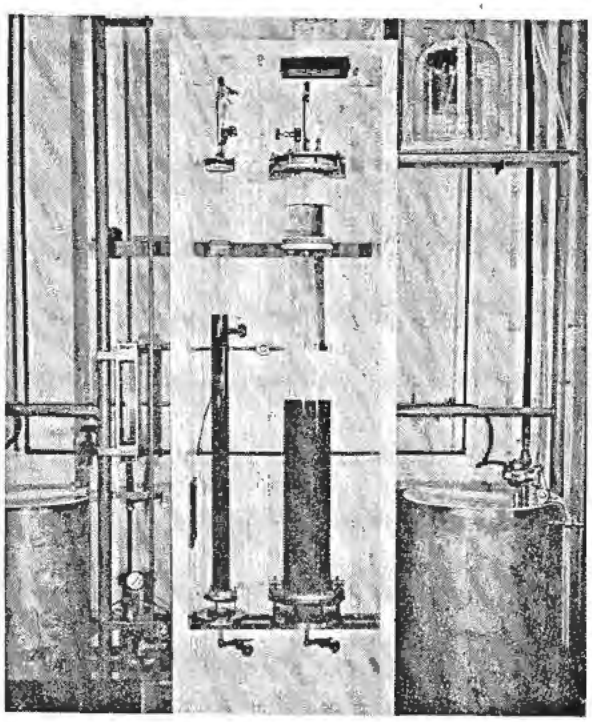

Slide 4

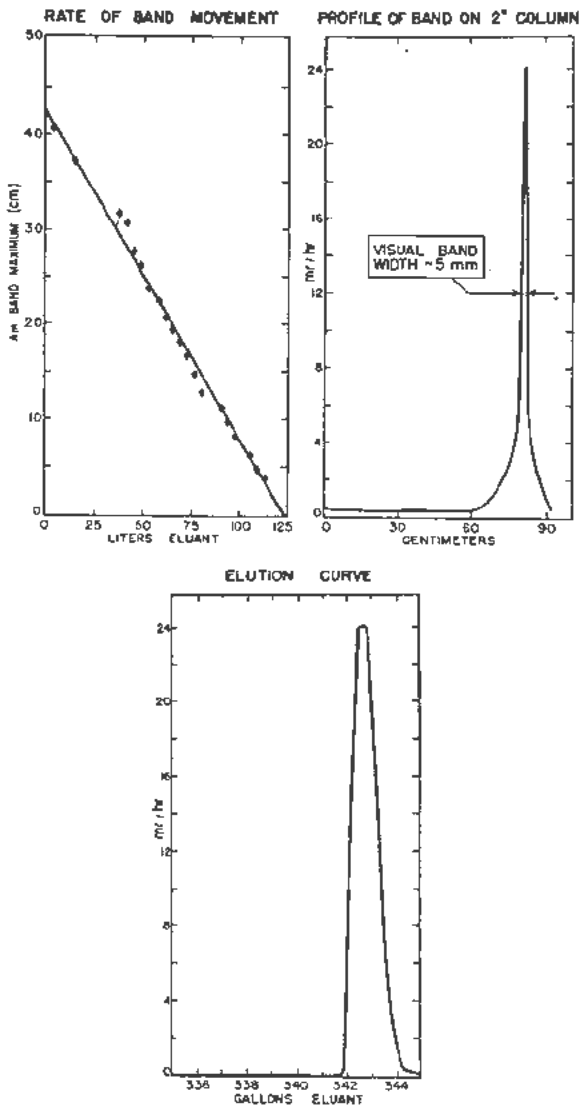

Slide 5. Separation of Am from rare earths. Resin: H^+ form Dowex 50; eluant: ammonium citrate, pH 8

the rare earths separate and form a series of head-to-tail bands, each band containing an essentially pure rare earth.

This procedure was utilized to separate gram amounts of americium from several hundred times its weight of lanthanum. Slide 4 depicts the apparatus which consists of a 6-inch Pyrex pipe filled with Dowex-50 and a 2-inch Pyrex pipe filled with the same resin.

The original americium-lanthanum band occupied a linear foot of this column. By the time the elution had proceeded, and the americium was at the bottom of the 2-inch column it had formed a narrow band approximately 5 mm wide.

Slide 5 depicts the linear rate of band advance of the americium, and depicts also the gamma scan of

Am (IV)

Am (IV) IS KNOWN ONLY IN SOLID COMPOUNDS

AmO_2 (AIR IGNITION OF NITRATE, OXALATE)

$$\left.\begin{matrix} AmO_2 \\ AmF_3 \end{matrix}\right\} + F_2\ (g,\ 1\ atm) \rightarrow AmF_4$$

$$Am^{+3}_{(aq)} = Am^{+4}_{(aq)} + e^-, \quad E_f^\circ = -2.44 \text{ VOLTS}$$

Slide 6

the americium activity at the bottom of the 2-inch column, width about 5 mm. Large volumes were needed here—more than 300 gallons—and the americium was eluted in approximately 8 liters.

With respect to column separation if only small amounts of light rare earths are present the elution of americium from Dowex-50 using saturated hydrochloric acid is a very useful separation technique.

Tetravalent americium is known only in the solid state (Slide 6). Typical compounds are the dioxide AmO_2 and tetrafluoride AmF_4; the tetrafluoride is prepared by treating AmO_2 or AmF_3 with fluorine at one atmosphere at a temperature of around 500°C. Cunningham has calculated, on the basis of heat measurements and entropy, the formal potential of the Am(III) and Am(IV) couple to be —2.44 volts.

Pentavalent americium is readily prepared and is precipitated (Slide 7) if a solution of Am(III) in an alkali carbonate solution is warmed with OCl^-, $S_2O_8^{--}$ or O_3. Under some conditions the precipitate phase has the composition $KAmO_2CO_3$. By dissolution of this precipitate in dilute acid, a solution containing pentavalent americium-AmO_2^+ is obtained. If an acid solution of Am(V) is warmed or treated with ozone Am(VI) is obtained. Solutions of Am(V) made from the isotope Am^{241} undergo zero-order reduction to Am(III) at a rate of about 2 per cent per hour from alpha radiation effects. It is interesting

Am (V)

Am (III) IN $K_2CO_{3(aq)} \xrightarrow[S_2O_8^{=}]{OCl^-;\ O_3} KAmO_2CO_3\downarrow$

$KAmO_2CO_3$ + DILUTE ACID $\longrightarrow AmO_2^+_{(aq)}$

$AmO_2^+_{(aq)} + O_3 \xrightarrow[WARM]{} AmO_2^{++}$

$AmO_2^+_{(aq)} \xrightarrow{Am^{241}\ ALPHA} Am^{+3}_{(aq)}$; ~ 2 % PER HOUR

Slide 7

AM(VI)

Acid media

Am^{+3}, HNO_3 0.1 M, $\xrightarrow[\text{Hot}]{S_2O_8^{--}}$ $Am\ O_2^{++}$

$-d\ (S_2O_3^{--})/dt = k\ (S_2O_8^{--}) + k'\ (S_2O_8^{--})\ (H^+)$

$AmO_2^{++} \xrightarrow{-} (Br^-, Cl^-) = AmO_2^+$

$AmO_2^{++} + I^- = Am^{+3}$

$AmO_2^{++} \xrightarrow[4\%\ HR^{-4}]{} AmO_2^+$ (Am^{241} Alpha radiation)

Alkaline medium

$Am(OH)_3 \xrightarrow[NaHCO_3 + O_3]{\text{Heat}}$ $Am_2(VI)$ complex deep red brown

Slide 9

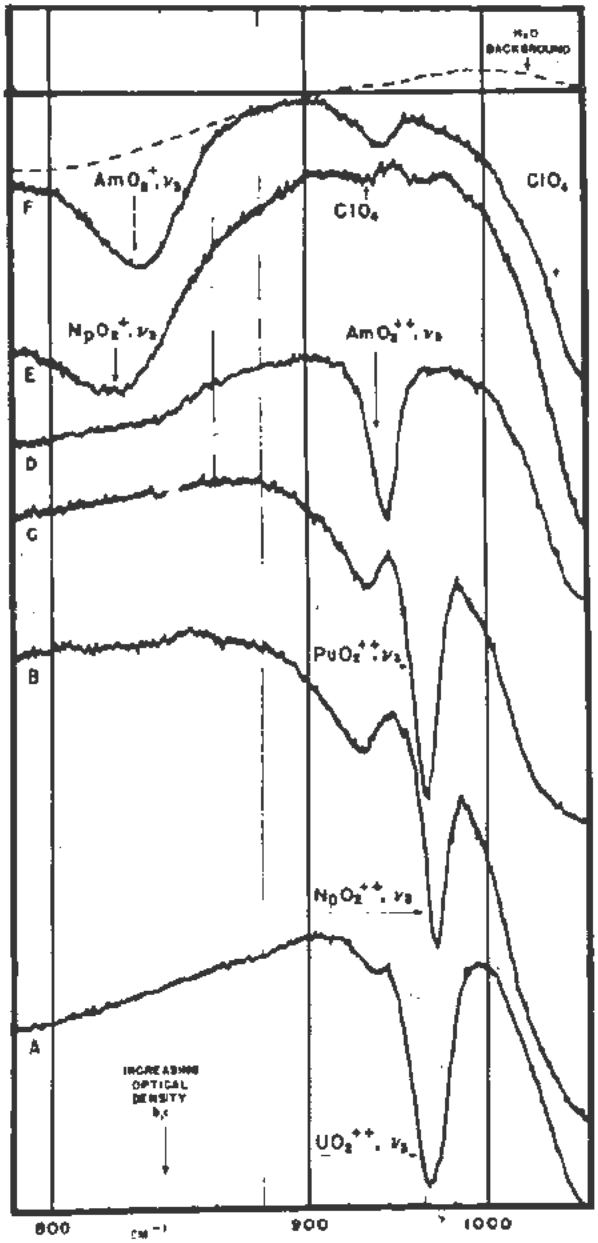

Slide 11

that the addition of zirconium slows this self-reduction rate, and the addition of chlorine to the solution slows the reduction rate to less than 1 per cent per day. The absorption spectrum of Am(V) in $HClO_4$ is shown in Slide 8 (Fig. 2 of P/838).

A very prominent peak of very high molecular extinction coefficient can be seen and also a sharp band around 514 millimicrons which is overlapped by the absorption peak of trivalent americium at 503 mμ. One of the more interesting aspects of the chemistry of Am(V) is the disproportionation in fairly concentrated acid solution. The disproportionation is not reversible since any arbitrary mixture of Am(V), Am(VI) and Am(III) is apparently stable and undergoes no change. The only change is that caused by alpha radiation. The disproportionation is complicated by the continuous reduction due to alpha radiation effects, but one can state that it is definitely bimolecular in Am(V).

Preparation of Am(VI) can be achieved (Slide 9) by ozone oxidation of a solution of Am(V) in a non-reducing acid, as mentioned earlier. Quantitative oxidation of Am(III) to Am(IV) by peroxydisulphate is achieved by heating in dilute acid, preferably 0.1 *M* or less. Higher acidities are bad since $S_2O_8^{--}$ decomposes by a H^+ ion catalyzed path forming peroxy-mono-sulphuric acid, a reducing agent for americium(VI); at acidities much above 0.5 *M* H^+ ion, no oxidation is observed.

Americium(VI) in acid solution is reduced to Am(V) by chloride and bromide ions. The reduction with bromide is very rapid, but the reduction by chloride is measurable at room temperature and apparently second order in americium. It may involve a complex such as AmO_2Cl^+. Iodide ion reduces Am(VI) to Am(III) rapidly.

In dilute perchloric acid solution, the alpha radiation causes reduction of Am(VI) nearly quantitatively to Am(V) at a rate of about 4 per cent per hour. Some Am(III) is formed, but only a fraction.

When an acid solution of Am(VI) is made alkaline, formation of Am(V) occurs. If a solution of Am(VI) is injected rapidly into a solution of carbonate, a deep color persists. This complex (or complexes) of Am(VI) in alkaline solution can be pre-

CURIUM

Cm^{+3}, Am^{+3} (0.1M HNO_3, $S_2O_8^{=}$) $\longrightarrow AmO_2^{++} + Cm^{+3}$ (?)

Cm^{+3}, Am^{+3} (K_2CO_3 aq) $\xrightarrow[S_2O_8^{=}]{}$ Am (V) $\downarrow$ $+ Cm^{+3}$ (?)

$CmF_3 \xrightarrow[TbF_4\ \ HEAT]{} CmF_3$

$CmO_{2(?)}$(BLACK) $\xrightarrow[VAC.]{HEAT}$ Cm_2O_3 (WHITE)

Slide 12

pared by heating a slurry of $Am(OH)_3$ in $NaHCO_3$ with ozone.

The absorption spectrum of Am(VI) in $HClO_4$ is shown in Slide 10 (Fig. 4 of P/838). Americium(VI) complexes with sulphate, nitrate, and fluoride, since each of these ions cause a color change: deep brown with sulphate, light brown with nitrate, and green with fluoride. The major change in spectrum occurs at wavelengths shorter than the prominent peak which is not appreciably shifted.

That AM(VI) is "uranyl-like" in aqueous solution is borne out by the infrared absorption spectra of all the hexavalent ions from uranium to americium, Slide 11.

The main thing that I should like to bring out about curium is that many attempts to oxidize curium in acid and alkaline solution have failed to produce evidence of Cm(V) or Cm(VI). However, Cm(IV) has not been completely ruled out. Recently, with the availability of Cm^{244}, good X-ray patterns of curium oxides were obtained. The sesquioxide, Cm_2O_3 is white; and a black oxide having X-ray constants approaching those expected for CmO_2 was obtained, Slide 12. Heating the black oxide in high vacuum yields the white Cm_2O_3. Magnetic measurements showed that more than half the curium in the black oxide was in the tetravalent state.

I should like to sum up and state that failure to find Am(II) and the evidence of Cm(IV) must mean that the $5f^7$ configuration is not as energetically stable as the corresponding $4f^7$ structure appears to be in the rare earths.

Mr. V. N. Kosyakov (USSR) presented paper P/676.

DISCUSSION OF P/736, P/838 AND P/676

The CHAIRMAN: We have one question directed to Mr. Kosyakov by Mr. Penneman (USA): "Do you have any actual constants for the formation of complex ions between americium and various anions?"

Mr. KOSYAKOV (USSR): We do not yet have a reliable constant that we could publish for complex combinations of trivalent americium. We have confined ourselves to a semi-quantitative interpretation of the process itself, which is confirmed by both the spectrophotometric and the electromigration methods.

Session 11B

EFFECT OF RADIATION ON REACTOR MATERIALS

LIST OF PAPERS

Radiation Damage in Reactor Materials

By D. S. Billington,* USA

The structural damage observed in metamic minerals is probably the first good example of radiation damage in a solid. This type of damage is introduced by alpha particle bombardment in certain minerals such as zircon through the presence of natural radioactive impurities. The extent of the alpha particle bombardment in many cases has been sufficient to render the internal crystal structure of the mineral amorphous. This phenomenon was first studied by Des Cloizeaux and Damour in 1860.

Present day interest in radiation damage is not the result of continued interest in these early experiments but came as a result of an observation by Wigner during wartime research on nuclear reactor development. Wigner realized that the energetic neutrons, born in the fission process, would have the ability to displace atoms from equilibrium positions in the crystal lattices of solids that might be far removed from the fuel, and as a consequence would have deleterious effects on many properties that would be of engineering interest in reactor construction. This observation plus the obvious realization that considerable damage to the fuel from fission fragments would result during fissioning prompted an immediate program of theoretical and experimental study of the magnitude of the effects to be expected. A brief account of some of these early studies has been given by Burton[1] and Wigner.[2] A further theoretical analysis of the problem was made by Seitz.[3] He discussed the type of defects one might expect and their probable effect on the various properties that would influence the design of a reactor. It was at this time also that Seitz conceived the idea of a "thermal spike" and the possible consequences of such a mechanism in creating radiation damage. An early concept of point heating was postulated by Dessauer[4] in 1922 but this did not appear appropriate to the present problems.

The early experimental studies confirmed Wigner's prophesy and the studies mentioned above led to suitable action by the reactor designers to allow for the damage expected to result from reactor operation. Moreover, it soon became obvious that radiation damage was to be expected in all solid materials and that the susceptibility of a material to neutron and fission fragment effects would be a function of that particular solid. It was also apparent that the magnitude of the effect was a function of the flux, the temperature, the environment and other variables such as stress.

The above observations led the Atomic Energy Commission to establish research programs designed to study the basic mechanisms of radiation damage, to make a comprehensive study of the effect of neutron irradiation on the physical properties of various solids and to survey, in so far as possible, radiation damage in a wide variety of materials of interest under conditions appropriate to possible use. This program has been active for many years. While progress has been considerable, it cannot be said that the need for further research has been satisfied. It is not now possible to give the reactor designer all the information he needs in a quantitative form. However, it is recognized that it will be possible eventually to derive engineering formulas that will enable a designer to calculate probable effects as a function of time, flux, temperature.

Experimental work in the radiation damage field is difficult and slow due to the fact that the problem of performing suitable in-pile experiments requires a great deal of ingenuity in instrumentation. Moreover, care must be taken to insure that the instrumentation transmits valid information about the material in question and does not reflect changes induced by radiation on any component of the measuring system itself. The other important problem in experimentation revolves around the fact that most materials as removed from a reactor are highly radioactive. Thus, suitable shielding of the experimenter from the lethal radiation is required. Performing even the simplest of manipulations of a sample remotely is slow and laborious.

In addition to experimental difficulties, the present shortage of reactors suitable for radiation damage studies and the lack of hot lab facilities also considerably hamper the progress of the work in this field of research. In spite of the above limitations, a great deal of knowledge has been gained in the past several years.

This paper will deal with the general subject of radiation damage to reactor materials but can only do so in a limited fashion since neither space nor time permits one to make a comprehensive and critical review. Consequently, the plan is to discuss representative materials and situations encountered relative to solid reactor materials with the hope that some insight into the problem can be gained. Later papers in this

* Oak Ridge National Laboratory. A brief review including work done at Argonne National Laboratory; Battelle Memorial Institute; Brookhaven National Laboratory; California Research and Development Corporation; Hanford Atomic Production—General Electric; Knolls Atomic Power Laboratory; Oak Ridge National Laboratory; Westinghouse Atomic Power Division.

session and in Sessions 12B and 13B will provide many details which, of necessity, must be neglected here.

ORIGIN OF RADIATION DAMAGE

Let us briefly discuss the origin of radiation damage in a solid. This may arise in three ways: first through the interaction of the fission fragments with atoms of the parent fuel lattice. This type of damage is usually confined to the fuel-bearing material because the range of the fission fragments is only of the order of microns even in the most transparent solids (in graphite the range is less than twenty microns). The second way in which radiation damage is created is through the elastic collision of a neutron with atoms of a lattice. This type of damage may occur at relatively great distances from the source of the neutron since the probability of capture of a fast neutron is very low at high neutron energies. This means that parts of a reactor other than the fuel will be affected, and hence the moderator, shield, or structural components of the reactor can be damaged. The third manner of introducing radiation damage is by ionization effects. These effects arise through ionization caused by fission fragments traversing the material or by ionization caused by the neutron "knocked-on" atoms or by beta and gamma rays. Ionization effects will be discussed very briefly since they are only of consequence in those solids that are of auxiliary value to a reactor such as plastics. Furthermore, a detailed discussion of the matter properly belongs under radiation chemistry.

The physical consequences of the above interactions are that several types of defects are introduced which affect the properties of a solid. These defects are: vacant lattice sites, interstitial atoms, thermal spikes, ionization effects and impurity atoms (fission fragments and impurities created by neutron capture).

Vacancies

Vacant lattice sites may be created either by collisions of fission fragments or energetic neutrons with the atoms in a solid lattice. The energy transferred in these collisions is usually sufficient to permit the recoiling atom to create further vacant lattice sites by subsequent collisions. Thus for each primary collision, a cascade of collisions resulting in vacancies is initiated.

Interstitial Atoms

The atoms that are displaced from their equilibrium positions in the lattice in general will stop in an interstitial or nonequilibrium position provided they do not immediately recombine with a nearby vacancy.

Thermal Spikes

This concept in its modern form originated with Seitz, who took into account the lattice oscillations that would be set up in the wake of either a fission fragment or a charged knocked-on atom of the lattice. Calculations by Brooks and others indicated that the possible duration of a high temperature region of approximately 1000°K involving some 5000 atoms might be 10^{-10} to 10^{-11} seconds.

Impurity Atoms

The fission process, which introduces foreign fission products, and the capture of the neutron by a nucleus which results in a different atomic species are the means of introducing impurity atoms. The fission fragment effect is most pronounced, though both mechanisms are often insignificant compared to the other effects.

Ionization Effects

The passage of charged particles through a lattice may cause extensive ionization and electronic excitation, which in turn leads to bond rupture, free radicals, etc. in many types of solids. These effects are most important in plastics, elastomers, etc. It is not intended to consider these effects in this paper. Rather, reference is made to papers in Session 12B that deal with radiation chemistry, where the subject will be treated in some detail.

BRIEF REVIEW OF SOME BASIC EXPERIMENTS

Metals

Before discussing some of the experiments on reactor materials it is appropriate to review briefly some of the experiments of a more general nature that have been done in order to provide some insight into the interpretation of data on more complex materials. In order to avoid any uncertainty in interpretation, only that work which has been done using neutron bombardment will be considered here. In addition to such work, however, bombardment experiments using cyclotron particles have, in a number of cases, also yielded interesting and similar results.

First it has been shown by a number of investigators[5–8] that most metals and alloys become harder and stronger as a result of bombardment particularly if the temperature of bombardment is sufficiently low.

The most striking effect on mechanical properties is the increase in critical shear stress of copper single crystals that has been observed by Blewitt and Coltman.[6] The critical shear stress was observed to rise from an unirradiated value of 0.2 kg/mm² to 7.5 kg/mm². However, it was also seen that once the sample began to flow plastically its behavior began to resemble that of an alloy rather than a cold worked material, suggesting that alloying with interstitial atoms was taking place, even though the values of the critical shear stress obtained far exceeded those obtainable by alloying. Making a number of assumptions concerning the stability of the defects involved, Blewitt estimated that one interstitial atom was forty times as effective as a Zn atom in raising the critical shear stress. Holden and Kunz,[7] performed similar studies on iron and zinc single crystals and were able to obtain similar increases in the critical shear stress. McReynolds[8] made studies on copper and aluminum after bombardment at 80°K and found that the effects

in aluminum annealed out before reaching room temperature while temperatures of 300°C were required to anneal out the increase in the flow stress of copper in agreement with Blewitt and Coltman's observations.

Besides the plastic behavior, the effects of neutron bombardment on a number of other properties of copper have been studied. The elastic constants of copper have been measured by Thompson who found rapid increases in the apparent elastic constants and a sharp reduction in internal damping. This has been attributed by Eshelby to the pinning down of dislocation loops. These measurements would appear to indicate that dislocations are not introduced as a result of neutron bombardment. Slight increases in the electrical resistivity of irradiated copper have been observed at room temperature with substantial increases at low temperature.[6,8] The large resistance increase found in copper at 80°K by McReynolds confirmed earlier observations by Blewitt and Coltman, who have since performed irradiations at approximately 20°K. They report even larger increases by a factor of 2–4 in copper. Only very slight density decreases are reported. There seems to be no broadening of X-ray diffraction lines. There are no observable dimensional changes. The thermal conductivity is relatively unaffected at room temperature.

Studies of a variety of metals indicate strongly that there is a relationship between activation energy for self diffusion and the temperature stability or radiation effects in pure metals, radiation effects being greater the lower the rates of self-diffusion at a given temperature. The above experiments tend to show that interstitial atoms play an important role in radiation effects. Furthermore, the creation of dislocations seems unlikely, and the temperature stability of radiation effects is a function of the diffusional characteristics of the solid.

Another series of observations has been made by several investigators. These show the influence of the excess vacancies introduced by bombardment. The ability of reactor radiation to order rapidly a sample of disordered Cu_3Au[9] at temperatures at which in the absence of radiation the rate is negligible is attributed to enhanced diffusion on a micro-scale resulting from excess vacancies.

Neutron bombardment has been shown to accelerate precipitation[13] in unstable supersaturated solid solutions. The effect of the irradiation is equivalent to raising the temperature 50–150°C. Neutron bombardments performed at liquid nitrogen temperatures show that the radiation effect in copper beryllium is influenced by a thermally activated process.[14] The rate of disordering of Cu_3Au was substantially altered for the same reasons.

Taylor and Murray[13] have shown that nucleation of a new phase can be inaugurated by neutron bombardment. Also the grey tin transformation appears to be nucleated by bombardment according to Dienes and Fleeman.

A phase transformation in black phosphorus has been observed by Warren *et al.*[15]

The disordering of ordered Cu_3Au and Ni_3Mn by bombardment[10,11] at room temperature lends some credibility to the concept of a thermal spike mechanism since displacements by collision would not appear to disorder these samples as rapidly as observed. However, a replacement collision mechanism has recently been proposed by Kinchin and Pease[12] which might account for the observed rates and not require a thermal spike or displacement spike.

Molybdenum has been shown by Burch, McHugh and Hockenbury[16] (Knolls Atomic Power Laboratory) to become embrittled after neutron irradiation. After irradiation to an estimated exposure of approximately 10^{20} n/cm^2, the molybdenum exhibited brittle behavior in tensile tests. The transition temperature was also increased from −30°C to ~70°C. This is an example of the importance of crystal structure in determining radiation resistance, the molybdenum occurring as a body centered crystal. This embrittlement appears to be characteristic of body centered cubic structures.

Stability of the shear transformations of a cadmium-gold alloy under irradiation has been shown by Wechsler to be excellent. However, this is in agreement with expectation since the process is not diffusion controlled.

Non-Metals

Considerable attention has been devoted to non-metals in view of their potential interest for high temperature applications in nuclear technology. A summary of the many basic experiments in this field is presented by Crawford and Wittels (see Session 13B, P/753, this Volume).

We will concern ourselves here with a few representative examples of those property changes that are of direct engineering interest. For example, thermal conductivity and dimensional and structural stability.

Those non-metals that are characterized by covalent bonding appear to be most susceptible to dimensional changes as a result of neutron irradiation. Primak[17] first reported a lattice expansion in diamond after bombardment.

Wittels[18,19] and others have studied quartz in some detail. They find large decreases in density (14.7% for an exposure of 2×10^{20}). The internal crystal structure has become amorphous but interestingly enough no macroscopic defects were developed in a single crystal and the surface integrity was maintained.

Berman[20] shows that the room temperature thermal conductivity of quartz drops by a factor of ten after moderate irradiation.

The ionic structure, though more stable, is not capable of adjusting to high internal strain. Experiments by Binder and Sturm, Warren and Tucker all show that LiF crystals will shatter after moderate exposures due to the strain induced by the release of helium and tritium from the (n, α) reaction in Li^6.

The specific heat of irradiated quartz approaches that of vitreous silica. Post irradiation annealing above 850°C results in recrystallization and eventually leads

in Brazilian quartz to macroscopic development of small holes parallel to the *c*-axis which results from the recovery of the pre-irradiated density.

The mineral beryl ($3BeO \cdot Al_2O_3 \cdot 6SiO_2$) behaves in a similar fashion to quartz though the loss in density is only about ¼ the rate exhibited by quartz.

A sample of chrysoberyl which is less covalent and, in addition, is close-packed shows only 1% dimensional changes and maintains its crystal structure. Thus it appears that high crystal stability is shown by crystals exhibiting ionic binding and low stability for covalent binding.

URANIUM

A fuel material is subjected to both fast neutron and fission fragment damage, thus the damage observed is unusually severe. Most of the damage appears in the form of embrittlement, distortion and growth. A great deal of attention has been directed to this problem. However, an accurate analysis of the effects is complicated by the fact that uranium exhibits a high degree of anisotropy in many of its properties that are of engineering interest. For example, the coefficients of thermal expansion vary from slightly negative values to large positive values as a function of crystal orientation. A further complication is that uranium exists in three allotropic modifications in the temperature range from room temperature to approximately 800°C. Thus it can be seen that appropriate combinations of heat treatment might very well lead to growth and distortion even in the absence of irradiation and this is indeed the case. Growth of uranium as a function of thermal cycling was first observed at Battelle Memorial Institute. Dahlen and Rankin (Hanford Atomic Products Operations) first reported distortion in massive uranium as a result of neutron irradiation.

The superficial resemblance between thermal cycling and irradiation distortion led to a great deal of study of thermal cycling at a number of laboratories, particularly at Argonne National Laboratory, Battelle, and Knolls Atomic Power Laboratory.

A review by Kelman (Argonne National Laboratory) summarized much of this work. He reported that preferred orientation, grain size, microstructure and time temperature relationships all play an important role in determining the amount of distortion as a result of thermal cycling. A review of later work by Burke, Howe and Lacy (Knolls Atomic Power Laboratory) revealed that the kind of distortion obtained under irradiation is related to the size and preferred orientation of the metal grains. Fabrication techniques and subsequent heat treatment were also found to be important factors in determining resistance to irradiation distortion.

They proposed a "ratchet" mechanism that depended upon the ease of grain boundary flow versus crystallographic slip as a function of temperature, coupled with the anisotropy of the thermal expansion coefficients of uranium to explain thermal cycling in the absence of neutron irradiation. Efforts to apply this mechanism to distortion during irradiation have not been entirely successful, the principal difference being that single crystal uranium samples are unaffected during thermal cycling but are greatly affected by irradiation.

Several other properties of uranium have been shown to be affected by irradiation: e.g., density decreases of the order of 1%. Small hardness changes after moderate irradiation have been observed by Siegel and Billington (Oak Ridge National Laboratory) and Madsen (Harwell) while O'Keefe (Hanford Engineering Works—General Electric) reports large changes after extended irradiation.

In-pile measurements of thermal conductivity by Woods and Jones gave a 10–15% decrease and a post-irradiation measurement by Siegel and Billington showed a similar decrease.

The electrical resistivity increases approximately 1% after 2×10^{-4} per cent of the total atoms have fissioned according to Royal (Argonne National Laboratory). X-ray line broadening has been observed by Tucker and Senio (Knolls Atomic Power Laboratory). They attribute this to fission fragments since they did not observe broadening in a sample of pure U^{238} after irradiation.

Reynolds (Knolls Atomic Power Laboratory) has shown that severe embrittlement takes place in uranium when only one atom in 10^5 has fissioned in a uranium wire. Additional data have been obtained in a more quantitative form by Hueschen and Kemper (Hanford Atomic Products—General Electric) who conducted several mechanical property measurements on irradiated uranium. They find that there is a marked decrease in ductility. The ultimate strength decreases while the yield strength increases by large amounts. Their inability to anneal out these effects at 400°C leads them to conclude that fission fragment alloying must play the dominant role.

Thus we can see that there are many differences between the two methods of producing distortion. Accordingly it is not too surprising that the proposed ratchet mechanism is not too successful. Alternate schemes have been reported that rely on twinning instead of grain boundary motion by Calm and others (Harwell). Recent Knolls Atomic Power Laboratory work suggests that diffusional effects may play an important role.

Simple models of the ratchet mechanism have been reported by Burke and Turkalo,[21] and Boas and Honeycombe.[22]

The inability to resolve completely the radiation damage problems encountered in uranium has led to studies of uranium alloys which will be considered in a later section.

THORIUM

The superior isotropic nature of thorium as contrasted with uranium would indicate that one would expect less radiation damage in thorium. In general, the effects that have been observed thus far do indicate the excellent radiation stability of thorium.

Kernohan (Oak Ridge National Laboratory) reports no growth and only slight hardness increases after a neutron exposure of 10^{19} n/cm². Paine and Murphy (Argonne National Laboratory) confirm the lack of growth and report a hardness increase from 40.5 unirradiated to 67 after irradiation (Rockwell 30T scale) after extensive bombardment. An increase in the yield strength of a factor of two has been reported by Wilson, Berggren and Adams (Oak Ridge National Laboratory). However, they report a decrease in impact strength, which is surprising in a face centered cubic metal.

URANIUM ALLOYS

The severe radiation damage observed in metallic uranium has led to studies of various alloys such as uranium-aluminum, uranium-beryllium, uranium-chromium, and uranium-zirconium, it being recognized that the crystal structure of many of these alloys would be much less susceptible to radiation damage.

Aluminum-Uranium

One of the first alloy systems to be studied was that of uranium and aluminum containing up to 30% uranium by weight. The microstructure of these alloys is such that, at all uranium concentrations, the aluminum furnishes the continuous matrix and therefore the uranium can be considered as dispersed in the aluminum. There is a eutectic reaction occurring at approximately 13% uranium so that for uranium concentrations near this figure the uranium shows the highest degree of uniform dispersion.

Alloys of aluminum containing 5.7, 15 and 17.2% uranium in the form of strips 9 cm × 1 cm × 0.1 cm were irradiated and a series of measurements made after irradiation by Siegel and Billington.

No changes as great as 1% were observed in the original dimensions. The changes in electrical resistivity, thermal conductivity and hardness are shown in Figs. 1, 2, 3. Feldman (Oak Ridge National Laboratory) reports similar hardness increases to those reported in Fig. 3.

The effect on thermal conductivity and hardness appears to be a function only of the total exposure while the electrical resistivity appears to be influenced by the microstructure. That is, the 5.7% uranium sample microstructure does not permit uniform irradiation of the aluminum matrix by the fission fragments. The hardness and electrical resistivity increase annealed at approximately the same temperatures are shown in Fig. 4.

The retention of fission gases was measured by collecting the radioactive krypton (10-year half-life) as a function of annealing temperature. At temperatures up to 550°C only 0.2% of the krypton present was released and most of this in the first two hours of a 20-hour anneal at each temperature. Complete melting was required to remove all krypton present.

Later measurements on 5, 15 and 30% uranium-aluminum alloys showed a maximum density decrease

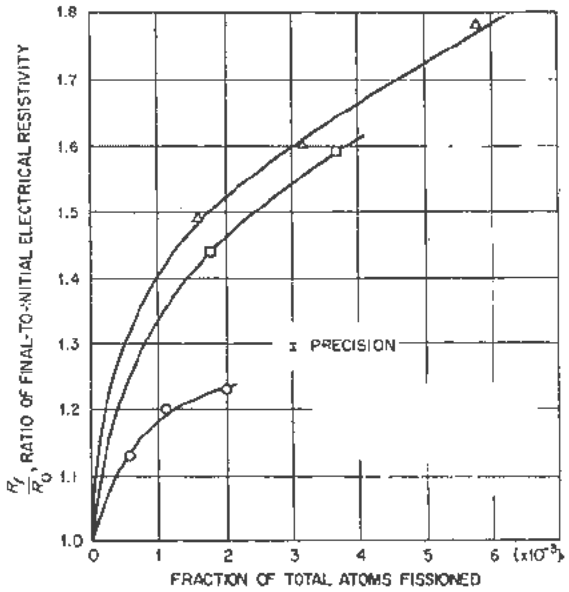

Figure 1. Effect of fission in Al-U alloys: Wt.% U: circles, 5.7; squares, 17.2; triangles, 15

of 3% at 0.05% total burn-up (Templeton, Bredig and Dismuke).

Mechanical property measurements by Wilson, on the 5.7, and 15% samples previously mentioned show interesting changes. Tensile tests made on samples of the 5 and 15 per cent alloys showed sharp increases in yield strength (0.2% offset) and in ultimate strength with an attendant loss in ductility. The data are presented in Figs. 5 and 6.

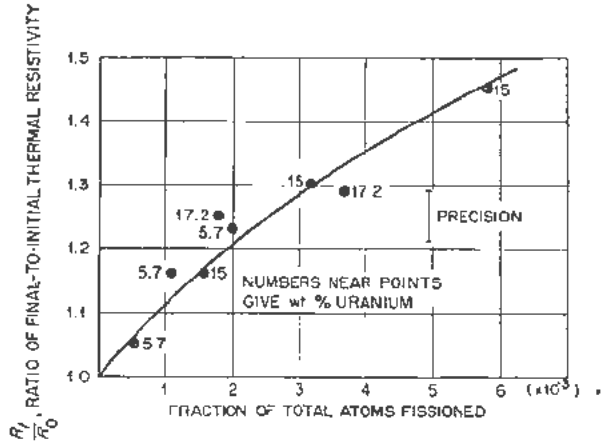

Figure 2. Effect of fission in aluminum-uranium alloys upon ratio of final-to-initial thermal resistivity

It should be observed that in this alloy no serious changes occurred even after 1 atom in 10^3 had fissioned, while in uranium metal severe damage is observed after 1 atom in 10^4 has fissioned. This better behavior can be attributed to the dispersion of the uranium in a metal well suited to absorb the damage from the fast neutrons and the fissioning process.

Beryllium-Uranium

Alloys of beryllium containing 0.5, 1.0 and 3% uranium after 0.06% burn-up of total atoms show an electrical resistivity increase of 1½ to 9% depending upon the uranium concentration. The changes in dimensions and in density were trivial according to Castleman, Jones and Jones (Westinghouse Atomic Power Division).

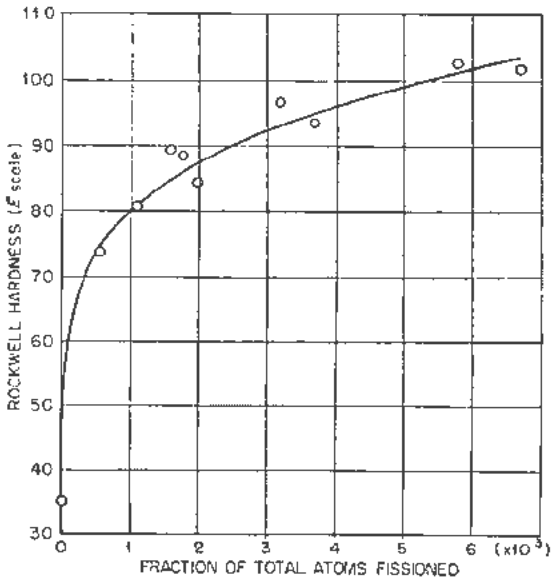

Figure 3. Effect of fission in aluminum-uranium alloys upon hardness

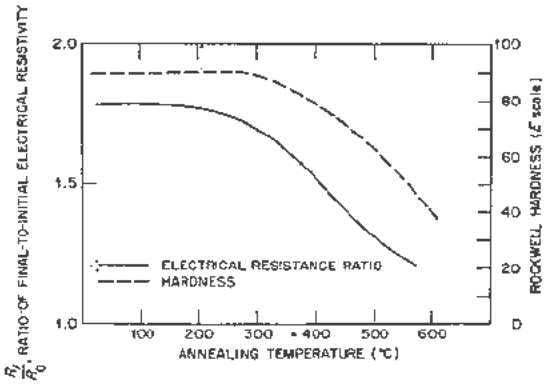

Figure 4. Annealing of radiation-produced changes of aluminum-uranium alloys

In-pile measurements of the thermal conductivity of a beryllium-20% uranium sample showed no significant change at 100°C as reported by Monaweek, Webb and Sutton of Argonne National Laboratory.

Zirconium-Uranium

Alloys of zirconium-uranium have been studied extensively. There appears to be little change in hardness and in thermal conductivity (see beryllium-uranium) and the dimensional stability appears good. There does appear to be a density decrease of the order of 1% according to Johnson, Castleman and others (Westinghouse Atomic Power Division).

The effect of having the uranium dispersed as uranium nitride particles as contrasted to uniform dispersion was studied by Castleman, Jones and Jones (WAPD). Density decreases were identical.

Chromium-Uranium

Tucker and Senio studied the effect of fission on a 2 atomic per cent chromium-uranium alloy and showed that the thermal spike mechanism would not transform the beta quenched phase to the alpha phase nor in the reverse direction for alpha to beta. The time duration of a thermal spike was too short to permit nuclei to grow.

This brief summary should indicate that alloys of uranium with inert metals represent a means of avoiding some of the undesirable properties of metallic uranium. Most of future progress will probably be found in the development of uranium alloys.

However, it is not possible to neglect the possibility of utilizing uranium in a non-metallic form. Several studies have been undertaken that indicate the possibility of ceramic fuels.

THORIUM ALLOYS

Thorium alloys containing 1–5% uranium have been studied by Paine, Murphy (Argonne National Laboratory) and Carroll (Oak Ridge National Laboratory). They both report only slight changes in dimensions and density with small hardness increases being noted.

CERAMIC FUELS

Several studies have been undertaken that involve mixtures of uranium oxide and a moderator such as graphite or BeO.

Uranium-Graphite

Hunter (Oak Ridge National Laboratory) studied graphite-uranium mixtures that had been prepared in two ways: (1) impregnation of the graphite with an aqueous solution of uranyl nitrate, followed by drying and high temperature firing which converted the uranium to U_3O_8 and (2) molded coke pitch and U_3O_8 mixture which was baked and fired at high temperature. The latter technique resulted in large particle sizes of U_3O_8.

In-pile thermal conductivity measurements of the two types of samples made at 630–775°C revealed that the thermal conductivity of the impregnated sample was reduced by orders of magnitude while the molded graphite dropped by only one-third. This difference was attributed to a particle size effect. The U_3O_8 in the impregnated sample was so finely dispersed that fission recoils were able to damage all portions of the graphite matrix while in the molded sample most of the fission fragments were retained in the U_3O_8 particles due to their larger size. Subse-

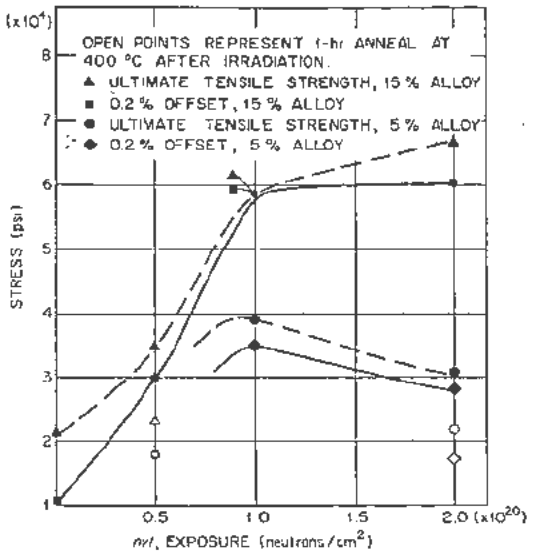

Figure 5. Effect of fission in aluminum-uranium alloys upon the tensile strength at 30°C

quently Berggren and Primak report even larger decreases in thermal conductivity as the temperature of irradiation is lowered.

Kernohan investigated this particle size effect in more detail using samples of molded and baked graphite-UO_2 samples prepared by Battelle Memorial Institute which contained particle sizes ranging from 586 microns to less than 40 microns. After less than 0.01% total atom burn-up he showed that an abrupt decrease in thermal conductivity resulted in the 44 micron particle size samples. An abrupt increase in elastic modulus and electrical resistivity was also observed at this particle size. The results indicated the importance of avoiding complete damage to the matrix material. A suitable size appears to be of the order of 100 microns. Post-irradiation annealing studies up to 750°C showed recovery of most of the neutron damage to the graphite but no recovery of fission damage. Fission damage in the graphite was found to be inversely proportional to the diameter of the imbedded UO_2 particle.

Work by Gilbreath, Wohlberg and Simpson at Argonne National Laboratory on the impregnated graphite as a function of total dose showed pronounced changes in dimensions and electrical resistivity. Resistivity changes saturated with continued exposure while dimensional changes did not. Post-irradiation annealing at 1250°C gave recovery of length changes but no recovery of resistivity.

Kierstead and Negy (Argonne National Laboratory) studied elastic modulus as a function of uranium concentration and dosage. They found a 4.7 per cent increase in modulus per milligram of U^{235} per gram of graphite for low concentrations. For 16 milligrams of U^{235} per gram of graphite the change saturated at approximately 150% of the original value.

The results on the graphite-uranium mixtures in general reveal serious damage to a number of properties. This appears to result from the undesirable, anisotropic nature of the graphite (see below), and is to be contrasted with the effects observed in a uranium-aluminum alloy where the properties of the aluminum are well suited for resisting radiation damage.

Beryllium Oxide-Uranium Oxide

An excellent comprehensive study of the UO_2:BeO combination was made by Gilbreath and Simpson (Argonne National Laboratory). They studied samples containing 2% and 10% UO_2. The largest changes were found in the thermal conductivity which did not saturate after a drop by a factor of six. The linear dimensions increased by 1% while the compressive strength and elastic modulus decreased by 30%.

All these changes occurred after only 5×10^{-6} of the total atoms had fissioned. The difference in uranium content did not result in pronounced differences in the two types of samples. This is regarded as being due to the higher irradiation temperature of the 10% UO_2 samples. Consequently, some annealing during irradiation may have occurred.

Stainless Steel–UO_2

A strong effect of particle size of the UO_2 on hardness of the stainless steel matrix is reported by Feldman. A particle size of the UO_2 which was less than 3 microns gave larger hardness increases and retained more hardness as a function of temperature than a sample containing UO_2 with a particle size in the range 15–44 microns.

Uranium Oxide

X-ray diffraction studies of irradiated U_3O_8 and UO_2 by Tucker and Senio (Knolls Atomic Power Laboratory) show pronounced line broadening for burn-up that are of the order of 3×10^{-6} per cent. At a burn-up of 3×10^{-4} the lines in U_3O_8 are removed completely according to Chalk River investigators. Presumably the rate of change in UO_2 is less than in U_3O_8. Other property measurements have not been made on this material. It would appear worthwhile considering in some detail.

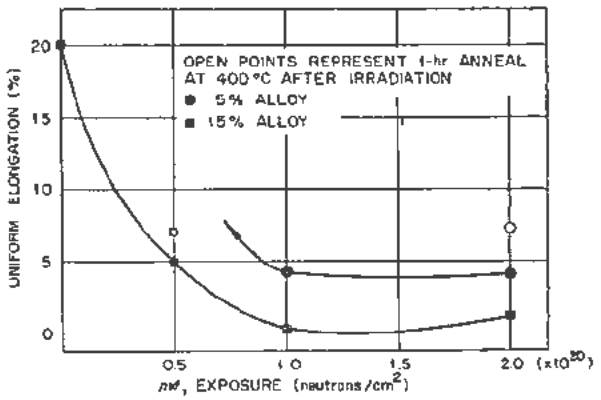

Figure 6. Effect of fission in aluminum-uranium alloys upon elongation at 30°C

MODERATORS AND STRUCTURAL METALS

Moderators

An essential component of nuclear reactors is the moderator or reflector-moderator system. Although there has been an increasing tendency to use liquid moderators (D_2O and H_2O) because of their great effectiveness, solid moderators are by no means outmoded and, in fact, offer many desirable characteristics. In many reactor designs, the moderator-proper may also serve a structural function, as is indeed the case with many of the early reactors. Consequently, the effect of radiation on the mechanical properties of such materials may be of critical importance. Perhaps the most widely used solid moderator today is graphite. Besides fulfilling the moderating function adequately and having excellent nuclear properties from the standpoint of neutron economy, artificial graphite of suitable purity is easily fabricated and available in the necessary quantities.

From the standpoint of radiation damage, graphite has considerable historical significance. It was one of the first materials in which radiation damage was observed and extensively investigated. In fact, the extensiveness of radiation effects on its physical properties constitutes the major disadvantage in using graphite in both its moderating and structural capacities. It has been observed that in anisotropic, covalent materials fast neutron disordering effects tend to make the structure more isotropic. This results usually in an anisotropic expansion of the crystal lattice which is greater the larger the initial anisotropy of the lattice. Even though artificial graphite is composed of extremely small crystallites, it possesses a considerable amount of preferred orientation. Consequently, prolonged exposure to fast neutrons causes an anisotropic expansion. In order to use the structural function of graphite, it is, therefore, necessary either to take account of this behavior in the reactor design or to devise production techniques which will reduce the degree of preferred orientation. Besides dimensional effects, irradiated graphite also suffers a reduction in thermal conductivity which also has important consequences in reactor utilization. Other properties which are affected are electrical conductivity, thermoelectric power and hardness. Moreover, considerable energy is stored in the matrix as a result of damage to crystallites. These problems will be dealt with in detail in other papers presented at this conference.

Another moderator of interest is metallic beryllium. This material, though expensive and difficult to fabricate, has excellent radiation stability. Measurements of dimensions, X-ray structure, density and hardness made by experimenters at Oak Ridge National Laboratory and Argonne National Laboratory showed negligible changes even after extensive bombardment.

In contrast, beryllium oxide shows serious decreases in thermal conductivity and compressive strength at room temperature after bombardment at $\sim 10^{19}$ n/cm^2. Dimensional changes were of the order of 1%. Gilbreath and Simpson indicated that the compound was chemically stable as they were unable to observe any oxygen evaluation by chemical or magnetic susceptibility measurements.

The thermal conductivity and dimensional stability of a wide variety of ceramic materials have been studied by Bopp and Towns and collaborators. They found a substantial decrease in the room temperature thermal conductivity of spinel, HfO_2, mica, ZrO_2, plate, Pyrex, and lead glass and porcelain after fast neutron exposures of 10^{19} n/cm^2. Silica glass and single crystal Al_2O_3 appeared unaffected. X-ray studies of zircon, SiC, BeO, $BaTiO_3$, and ZrO_2 showed 0.2–0.3% lattice expansion.

Studies of materials such as B_4C have been studied by Tucker *et al.* They report behavior very similar to that observed in quartz.

A great deal more work is required in this class of materials before an understanding of the effects can be gained.

Structural Metals

The moderator in a reactor often serves as the main structural component but in cases where this is not possible then one is required to make use of certain of the conventional structural metals to make up this deficit. Consequently, these metals may be in high fast neutron flux regions. The thermal neutron absorption cross section of metals such as the carbon steels, while not ideally low, may still be sufficiently low to warrant consideration in reactor design.

An increasing amount of attention is being paid these materials in regard to their resistance to radiation damage, particularly in regard to strength and ductility characteristics. An early survey[5] revealed that most of the conventional alloys become harder and stronger. Recently Sutton and Leeser[23] described radiation effects on a wide variety of alloys. One important observation on carbon steels revealed that the impact strength was reduced appreciably. In addition, the temperature of transition from brittle to ductile fracture was raised 50–100°C after a bombardment of approximately 10^{19} n/cm^2. Bombardments at 300°C for the same exposure gave only a 25°C increase in transition temperature. These observations become of importance when it is realized that the carbon steels they examined were pressure vessel type. These carbon steels as well as stainless steels, nickel and cobalt base alloys showed higher yield strengths and a reduction in ductility. Electrical resistivity and density changes were slight for all alloys examined. Several of the stainless steels showed an increase in magnetic susceptibility. Low and coworkers (Knolls Atomic Power Laboratory), and Carroll (Oak Ridge National Laboratory) had also observed this phenomenon. The magnetic susceptibility increase indicates possible precipitation of ferrite from the metastable austenite. A careful study by Reynolds, Low and Sullivan[24] indicates that the amount of ferrite precipitated is probably insufficient to cause concern in regard to the stainless character of these alloys. However, additional attention to this

effect is warranted in view of its possible importance.

Wilson and Berggren[25] have recently made a number of measurements on carbon and alloy steels. They were able to confirm the observations of Sutton and Leeser. An additional measurement of the maximum contraction below the notch after impact rupture of the carbon steel samples showed good agreement with the tests made by the more conventional type of measurement. It is not clear whether these property changes in the carbon steels are beginning to saturate at 10^{20} n/cm^2 at 100°C.

The yield strength of the stainless steels at 10^{20} n/cm^2 is very close to the ultimate strength. They observed too an indication of a yield point suggesting an approach to carbon steel behavior. A small amount of cracking was observed during impact tests made at liquid nitrogen temperature.

A metallic property of engineering interest is creep. This property has been studied as a function of neutron bombardment by a number of laboratories. Wilson, Zukas and Davis (Oak Ridge National Laboratory) have seen a decrease in the creep rate of nickel and Inconel at low temperature in agreement with observations by Coffin (Knolls Atomic Power Laboratory) on stainless steel and by Witzig (Westinghouse Atomic Power Division) on zirconium and by Morgan on aluminum. However, if the temperature was raised high enough, a slight increase in the creep rate was observed by Wilson *et al.* The temperature at which the increase occurs appears to be a function of the stress level.

Steele and Wallace studied irradiation effects in the aluminum alloys 2S, 52S, 61S and A 54S. They found a uniform increase in the yield stress with an attendant loss in ductility after an exposure of 10^{21} n/cm^2. Klein and McGinnis (Massachusetts Institute of Technology) had earlier shown similar results for 2S aluminum.

Cohen obtained no increase in thermal conductivity of Inconel and nickel using in-pile measurements.

Density and dimensional changes are reported by Argonne National Laboratory as being absent in titanium and tantalum after exposure to 10^{19} n/cm^2. Tungsten showed a 0.2% reduction in density.

Columbium, titanium and tantalum-7.5% tungsten alloy gave hardness increases of + 35 (Brinnell Hardness number).

Tantalum and tungsten of 99+% purity showed no change after 10^{19} n/cm^2.

Solid solution alloys of copper with aluminum, zinc, gallium, germanium, arsenic and manganese have been shown by Kernohan and Billington to yield an anomalous decrease in electrical resistivity of 1–3%. An adequate explanation is not presently available. The hardness and strength in these alloys increases upon irradiation.

Though many of the effects mentioned above can be qualitatively understood in terms of the experiments mentioned under the review of basic experiments, it is highly desirable that more detailed attention be devoted to these and other important alloys of a similar nature.

AUXILIARY REACTOR COMPONENTS

Although they are not reactor components in the strictest sense of the word, electrical and electronic accessories are quite important in reactor-control and monitoring systems. Moreover, in the case of research reactors, electronic instrumentation is quite often an integral part of experimental equipment for in-pile measurements. Consequently, information regarding the radiation stability of various electrical materials and components is valuable to both reactor engineers and scientists.

In recent years considerable emphasis in circuit development has been given semiconductor devices, both diodes and transistors. The chief advantage of these units is their very small space and power requirements. The very marked sensitivity, however, of the electrical properties of germanium and silicon as well as other diamond-lattice semiconductors to fast neutron bombardment[26] precludes the use of these miniature components inside nuclear reactors. Germanium point-contact and junction diodes become ohmic after an exposure of 10^{15} fast neutrons/cm^2 and transistor action in p-n-p junction transistors is essentially destroyed by 10^{12} fast neutrons/cm^2. Consequently, when using these units in electronic equipment near a reactor, careful account of their radiation sensitivity should be taken. Although the rate of deterioration is somewhat slower than in the case of germanium diodes, other semiconductor rectifiers (silicon, copper-cuprous oxide and selenium) also tend to become ohmic when exposed to fast neutrons.

In addition to components, considerable attention has been given an even more important electrical material, namely, lead-wire insulation. The commercially available wire isolations include both inorganic and organic materials. These cover a wide range of radiation stability. Some deterioration, both chemical and electrical in nature, is observed with all insulations studied. In evaluating the effects on the usefulness of a given insulation, it is necessary to take into account the over-all impedance of the electrical circuit in which it is to be used. Low impedance networks require a much lower insulation stability than those with high impedances. Besides simple resistance changes, variation of dielectric constant and loss-tangent have been observed in the dielectric materials employed in high-frequency transmission cable (coaxial cable) by Pigg and Weeks (ORNL).

A comprehensive study of elastomers and plastomers has been carried on by Sisman and Bopp for several years. They have been able to correlate radiation stability with chemical structure. The unclassified reports ORNL-928 and ORNL-1373, give the details of this excellent study. Other studies of interest have been made by Charlesby[27], Little[28] and Ross[29] (Harwell) and Ryan and Mannal (Knolls Atomic Power Laboratory).

Some insulation materials available commercially have been studied. It was found that there is a large difference in insulation resistance depending on whether the reactor is operating (dynamic conditions) or not (static condition). In many instances, the dynamic resistance measurements indicate a value lower by two orders of magnitude than pile-off values. The breakdown exposure of the insulation materials studied is listed in Table I. Here breakdown exposure is arbitrarily defined following Pigg (Oak Ridge National Laboratory) as that value at which there is an accelerated decrease in the dynamic resistance of the material in question.

Table I. Break-Down Exposures of Insulating Materials

Insulation material	*Break-down exposure (neutrons/cm²)*
Polyethelene	$> 10^{18}$
Selastic 80 (dimethyl silicone)	10^{19}
Sil-X	9×10^{17}
Teflon (tetrafluorethylene)	5×10^{18}
Silicone rubber	4×10^{19}
Neoprene	$> 3 \times 10^{19}$
Formvar (polyvinyl formal)	$> 2 \times 10^{18}$
Polyvinyl chloride	1.9×10^{18}
Glass cord covered by glass braid	1.9×10^{17}
Rubber	1.3×10^{19}
Kel-F (monochlortrifluorethylene)	10^{19}
Surprenant A-10 (polyvinyl)	10^{17}
Surprenant B-2 (polyvinyl)	5×10^{19}

TECHNIQUES THAT CAN BE EMPLOYED TO MINIMIZE RADIATION EFFECTS

Some rather obvious but useful suggestions are presented:

1. Adjustment of Bombardment Temperature

(*a*) In cases where excessive hardening due to irradiation appears undesirable, an increase in bombardment temperature would certainly reduce the magnitude of the effect. This is well illustrated in the instance of reduction in impact strength of carbon steels.

(*b*) Where diffusional effects play an important role in radiation damage, for example in metastable solid solutions, then a decrease in bombardment temperature would prove beneficial by decreasing the mobility of the irradiation generated defects. In this connection, decrease of the precipitation rate in copper-beryllium alloys has been effected by bombardment at 80°K.

(*c*) A careful selection of bombardment temperature of order-disorder alloys would presumably lead to a balance between ordering and disordering effects resulting from bombardment.

2. Alloying

(*a*) It appears reasonable to consider alloying to reduce phase instability and anisotropic effects in uranium. The superior performance of an aluminum-uranium alloy over unalloyed uranium has been demonstrated.

(*b*) Care should be taken to avoid alloys or other solids that transmute to new atomic species, particularly under conditions of extremely long bombardments. The transmutation of manganese to iron is a case in point. Deleterious property changes could easily develop through this mechanism.

3. Dispersion

Adjustment of the particle size of fissionable material appears to be an effective means of controlling the damage rate in a uranium mixture by confining most of the fission fragment damage to the volume of the particle.

4. Material Selection

It would appear wise to choose those materials that do not exhibit any high degree of anisotropy in their important properties.

Metallic bonding appears best for radiation resistance, ionic binding next for most applications, then covalent and finally molecular binding.

It appears desirable to avoid materials that possess unstable phases at or near the bombarding temperature, particularly if the phase transformations are diffusion controlled.

The importance of a close-packed crystal structure has been recognized in determining radiation stability.

Studies reveal that close-packed structures have the highest radiation stability, and in general, simple structures of high symmetry have better radiation characteristics than anisotropic structures.

COMMENTS ON FUTURE RESEARCH

Research programs currently active on radiation damage in solid reactor materials seem to be composed of the following parts:

1. A concerted basic effort designed to understand in a quantitative fashion the fundamental mechanisms involved in neutron and fission fragment interactions with solid matter is in progress. Such studies are aimed at providing accurate information on the kinds and numbers of defects introduced into a solid.

2. Studies are made to determine the effect of the bombardment generated defects on typical reactions such as diffusion, precipitation, nucleation, phase transformations that are common to many classes of solids. The studies include an examination of these effects as determined by the type of solid such as metals, semiconductors, ionic crystals, covalent crystals and molecular crystals. A representative number of physical, chemical, thermal, electrical, magnetic and mechanical property measurements should be made.

3. Appropriate engineering property measurements are made on those materials that appear most suitable for immediate reactor application under conditions that approximate the proposed operating conditions.

4. An active program of construction and irradiation of appropriate combinations of the various reactor components that constitute the essential features of the proposed reactor system is under way.

In spite of the number of research programs that

seem to follow the above outline, there is still a large number of unanswered problems facing those concerned with radiation damage.

Accurate knowledge of the number of defects introduced by bombardment is not yet available. The temperature stability of the defects is imperfectly understood. In addition the relative importance of the several types of defects introduced by bombardment is not known.

The relative merits of the thermal spike mechanism, the displacement spike, the replacement collision theory and the direct collision theory are not understood. Are they mutually exclusive or are they all operative to some degree? Do cyclotron and other charged particle machines provide experimental information that has direct validity in terms of nuclear reactor radiation damage problems in spite of the difference in the mechanism of introducing defects and the low range of charged particles in solids?

Are the present experimental determinations of the energy required to displace an atom from its equilibrium position as determined by electron bombardment correct or are the present values a factor of 2-5 too high?

The neutron flux distribution in radiation damage facilities is not sufficiently well known.

The effect of irradiation on many important properties is not known. For example, an understanding of the mechanism responsible for decrease in impact strength, increase in creep rate and related mechanical properties is not available.

Our knowledge of the solid state in the absence of irradiation is far from complete.

Too few experiments have been performed with appropriate care and statistics on most materials of interest. Insufficient qualitative data have been obtained on the many solids of possible interest to reactor designers.

CONCLUSIONS

1. Radiation damage in solid reactor components is a problem that seriously affects the operation of a reactor.

2. Radiation damage is imperfectly understood at the present and one can not reduce the problem to an engineering calculation.

3. Radiation damage is intimately connected with other important variables that influence the performance of solids. Thus one must take account of the temperature, the environment, the stress as well as the flux level when meaningful experiments are to be performed.

4. Our knowledge of basic mechanisms is not at present adequate.

5. More reactors designed specifically for materials testing are needed.

6. Hot laboratories are at present inadequate in both number and function.

It is my belief, that, once we do understand all the facets of radiation damage, the world will gain a bonus over and above an improved reactor technology. This will come about because radiation damage studies are in themselves a technique for manipulating and studying the solid state and will undoubtedly make many important contributions to our knowledge of solid matter.

ACKNOWLEDGEMENTS

It is a pleasure to acknowledge the assistance rendered in the preparation of this paper by O. C. Simpson (Argonne National Laboratory), J. E. Burke (Knolls Atomic Power Laboratory), B. Lustman and W. E. Johnson (Westinghouse Atomic Power Division), and to J. H. Crawford, T. H. Blewitt, J. C. Wilson, J. T. Howe, W. E. Busby, Margaret Stewart and the staff of the Solid State Division, Oak Ridge National Laboratory.

I regret that the brief nature of the paper has made it necessary to defer discussion of much of the excellent research presently being done in the field of radiation damage by a number of very fine scientists of the United States and abroad. The decision to eliminate discussion of charged particle experiments, where pertinent, was not easily made.

REFERENCES

1. Burton, Milton, *Radiation Chemistry,* Phys. Colloid Chem., 51: 611 (1947).
2. Wigner, E. P., *Theoretical Physics in the Metallurgical Laboratory of Chicago,* J. Appl. Phys., 17: 857 (1946).
3. Seitz, Frederick, *On the Disordering of Solids by Action of Fast Massive Particles,* Discussions of the Faraday Soc., 5: 271 (1949).
4. Dessauer, F., *Über einige Wirkungen von Strahlen I,* Z. Physik, 12: 38 (1923).
5. Billington, D. S. and Siegel, S., *Effect of Nuclear Radiation on Metal,* Metal Progress, 58: 847 (1950); Sutton, G. R. and Leeser, D. O., *How Radiation Affects Structural Materials,* Iron Age, 174: 97 (1954).
6. Blewitt, T. H. and Coltman, R. R., *The Effect of Pile Irradiation on the Stress Strain Curve of Copper,* Phys. Rev., 82: 769 (1951).
7. Kunz, F. W. and Holden, A. N., *The Effect of Short-time Moderate Flux Neutron Irradiations on the Mechanical Properties of Some Metals,* Acta Metallurgica. 2: 816 (1954).
8. McReynolds, A. W., Augustyniak, W., McKeown, Marilyn, and Rosenblatt, D. B., *Neutron Irradiation Effects in Cu and Al at 80°K,* Phys. Rev., 98: 418 (1955).
9. Blewitt, T. H. and Coltman, R. R., *The Effect of Neutron Irradiation of Metallic Diffusion,* Phys. Rev., 85: 384 (1952); Blewitt, T. H. and Coltman, R. R., *Radiation Ordering in Cu_3Au,* Acta Metallurgica, 2: 549 (1954).
10. Siegel, S., *Effects of Neutron Bombardment on Order in the Alloy Cu_3Au,* Phys. Rev., 75: 1823 (1949).
11. Aronin, L. R., *Radiation Damage Effects on Order-Disorder in Nickel-Manganese Alloys,* J. Appl. Phys., 25: 344 (1954).
12. Kinchin, G. H. and Pease, R. S., *The Mechanism of the Irradiation Disordering of Alloys,* J. Nuclear Energy, 1: 200 (1955).
13. Murray, G. T. and Taylor, W. E., *Effect of Neutron Irradiation on a Supersaturated Solid Solution of Beryllium in Copper,* Acta Metallurgica, 2: 52 (1954).
14. Cleland, J. W., Billington, D. S., and Crawford, J. H., *Low Temperature Fast Neutron Bombardment of Copper-Beryllium Alloy,* Phys. Rev., 91: 238 (1953).

15. Chipman, D. L., Warren, B. E., and Dienes, G. J., *X-ray Measurements of Radiation Damage in Black Phosphorus*, J. Appl. Phys., 24: 1251 (1953).

16. Bruch, C. A., McHugh, W. E., and Hockenbury, R. W., *Embrittlement of Molybdenum by Neutron Radiation*, Trans. AIME, 203: 281 (1955).

17. Primak, W., Fuchs, L. H., and Day, P., *Radiation Damage in Insulators*, Phys. Rev., 92: 1064 (1953).

18. Wittels, M. C., *Lattice Expansion of Quartz Due to Fast Neutron Bombardment*, Phys. Rev., 89: 656 (1953).

19. Wittels, M. C., and Sherrill, F. A., *Radiation Damage in SiO_2 Structures*, Phys. Rev., 93: 1117 (1954).

20. Berman, R., *The Thermal Conductivity of Some Dielectric Solids at Low Temperature*, Proc. Roy. Soc., A 208: 90 (1951).

21. Burke, J. E. and Turkalo, A., *The Ratchet Mechanism*, AECU-1639 (1951).

22. Boas, W. and Honeycombe, R. W. K., *The Anisotropy of Thermal Expansion as a Cause of Deformation in Metals and Alloys*, Proc. Roy. Soc., A 188: 427 (1947).

23. Sutton, C. R. and Leeser, D. O., *How Radiation Affects Metals*, Iron Age, 174: 97-100: 128-131 (1954).

24. Reynolds, M. B., Low, J. R. and Sullivan, L. O., *Study of the Radiation Stability of Austenitic Type 347 Stainless Steel*, Jour. Metals, 7: 555 (1955).

25. Wilson, J. C. and Berggren, R. G., *Effects of Neutron Irradiation in Steels*, ASTM Bulletin No. 206 (1955).

26. Cleland, J. W., Crawford, J. H., Lark-Horovitz, K., Pigg, J. C. and Young, F. W., *The Effect of Fast Neutron Bombardment on the Electrical Properties of Germanium*, Phys. Rev., 83: 312 (1951); Cleland, J. W. and Crawford, J. H., *Neutron Irradiated Indium Antimonide*, Phys. Rev., 95: 1177 (1954).

27. Charlesby, A., *How Radiation Affects Long Chain Polymers*, Nucleonics, 12: 18 (1954); Charlesby, A., *The Crosslinking of Rubber by Pile Irradiation*, Atomics, 5: 12, 27 (1954).

28. Little, K., *Some Effects of Irradiation on Nylon and Polyethylene Terephthalate*, Nature, 173: 680 (1954).

29. Ross, M., *Changes in Some Physical Properties of Polyethylene by Pile Irradiation at 80°C*, AERE-M/R-1401 (1954).

Effect of Irradiation on Structure and Properties of Fissionable Materials

By S. T. Konobeevsky, N. F. Pravdyuk and V. I. Kutaitsev, USSR

The study of radiation changes in fissionable materials, first and foremost in uranium, is of great scientific and practical importance.

Uranium as a metal with a high anisotropy of mechanical and physical properties provides the possibility of enlarging and making more complete the knowledge of the behaviour of anisotropic metals and alloys affected by deformation, thermal effects, etc.

On the other hand, the use of uranium as a nuclear fuel for power reactors necessitates a detailed study of how uranium is affected by temperature, stresses and irradiation.

There is a marked difference between radiation damage of uranium and that of usual non-fissionable materials in two aspects. First, the higher density neutron flux in uranium should be taken into consideration, because not only fast but also slow neutrons, which as a rule hardly affect non-fissionable materials, are absorbed and damage uranium. Secondly, the major effect of irradiation in the metal is caused by fission fragments. As a result of the relatively low velocity of the fission fragments, the latter interact strongly with atoms, dissipating energy of the order of 100 Mev in a limited volume. Thus, the thermal effect (thermal impact) must be much stronger in a fissionable material than in a non-fissionable one.

HIGH PLASTICITY OF URANIUM UNDER IRRADIATION

One should differentiate between the properties of uranium during irradiation and after it. There are many data at our disposal indicating that uranium assumes high plasticity at the moment of irradiation in a neutron flux. Specially conducted experiments showed that uranium creep increased approximately by the order of 1.5–2.

This property is still more pronounced in uranium enriched by U^{235}. This is apparent from the following experiment. A sheet of cold-rolled and annealed uranium (75% enrichment) 0.28–0.34 mm thick was placed on a magnesium core. The core and the sheet were pressed into a tube of Cr18Ni9Ti stainless steel. The specimen was exposed to an integrated neutron flux of 10^{19} nvt. After irradiation it was cut and examined. The uranium sheet between the magnesium core and the stainless-steel tube was found to have become strongly wrinkled. The surface of the sheet adjacent to the steel remained smooth and that adjacent to the magnesium became undulated (see Fig. 1).

Measurements of the sheet thickness showed that its average value was 0.3 mm in the smooth parts while the observed sheet thickness varied from 0.07 to 0.45 mm in the undulated sections.

INCREASE IN HARDNESS AND BRITTLENESS OF URANIUM, CHANGES IN ITS STRUCTURE AND ELECTRICAL RESISTIVITY DUE TO IRRADIATION

Despite the apparent plasticity displayed by uranium during irradiation, its hardness is increased and plasticity decreased after exposure. The average value of the microhardness of the uranium sheet described above was found to be 492 kg/mm^2, thus considerably exceeding the hardness of uranium in its original condition.

The increase in hardness of irradiated uranium was determined for different initial conditions of casting, mechanical treatment and heat treatment. The data of Table I give quantitative values for these changes. The samples for investigation were cut from cylindrical uranium rods exposed to an integrated neutron flux of 10^{19}–10^{20} nvt.

Table I shows that all samples, irrespective of preparation technology, became very brittle after irradiation. This is apparent from the sharp decrease in impact strength and from a zero elongation. All samples were found to have increased in hardness.

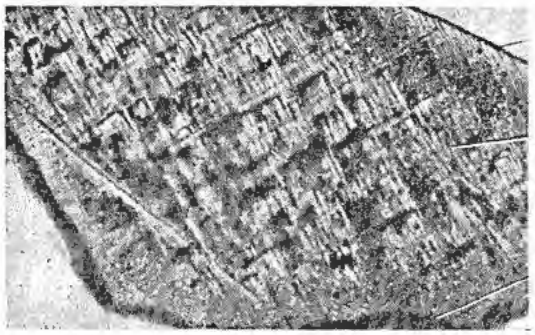

Figure 1. Uranium sheet after irradiation: (1) surface adjacent to steel; (2) sheet; (3) surface adjacent to magnesium

Original language: Russian.

Table I. Properties of Irradiated Uranium (10^{19} nvt)

No.	Metal condition	Micro-hardness H_k kg/mm²		Ultimate tensile strength σ_b kg/mm²		Relative elongation δ %		Impact strength α_k kg/cm²	
1	Cast (with increased carbon contents)	327		55		Zero Elongation (brittle)		2.1	
1a	The same after exposure		416		21				0.6
2	Cast	333		45.2				2.92	
2a	The same after exposure		413		13.4				0.76
3	Heat-treated	368		55.3				2.2	
3a	The same after exposure		440		28.4				0.71
4	Hot-rolled	351		41.1				3.7	
4a	The same after exposure		417		27				0.94

A decrease in ultimate tensile strength instead of the expected increase is explained by the presence of many inner cracks developed in the material during the exposure. The cracks were detected microscopically.†

The microstructure of irradiated uranium is characterized by the presence of a large amount of twinning. Contrary to the twinning of ordinary metals uranium twinning exhibits a wavy structure (see Figs. 2 and 3).

The peculiar globular structure of a uranium grain may be observed at a higher (4000–15,000 times) magnification obtainable in an electron microscope (see Figs. 4a and 4b).

Uranium carbide grains undergo certain changes (see Figs. 5–8). Some photographs illustrate a phenomenon similar to destruction or gradual "thawing" of carbides.

The change in electrical resistivity of uranium was determined to study the nature of the uranium changes during irradiation.

Specimens were investigated during and after irradiation. Strips of uranium foil (60 × 2 × 0.2 mm) were taken as specimens. Thin nickel and constantan wires, which served as current and potentiometer conductors, were soldered to them. A nickel-constantan pair also served as a thermocouple.

The specimens were mounted in a quartz ampoule filled with helium, the ampoule in its turn being placed in an aluminium tube in the channel of a reactor. Measurements showed that the maximum temperature during irradiation did not exceed 80°C.

Electrical resistivity was recorded. The maximum increase in the electrical resistivity of a foil under these conditions was about 4%.

To judge the nature of the structural changes caused by irradiation it is essential to know the temperature stability of the changes obtained. To determine this, uranium wires (1 mm diameter and 40 mm long) were annealed after an exposure in a reactor.

† The 3–4% decrease in density observed in unirradiated uranium may be due to the cracks.

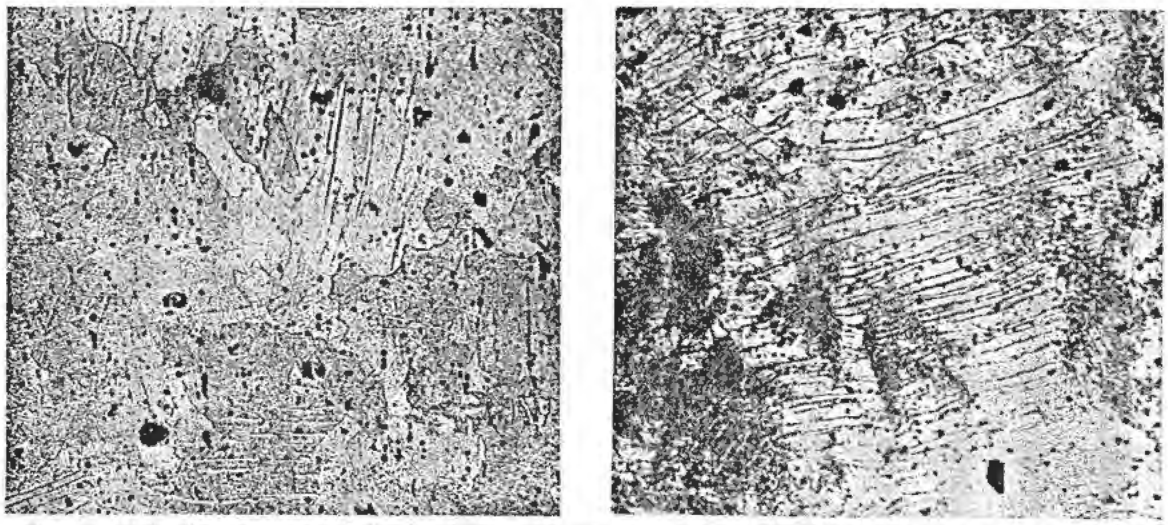

Figure 2. (a) Uranium microstructure before irradiation, obtained from a replica (× 240); (b) uranium microstructure after irradiation, obtained from a replica (× 240)

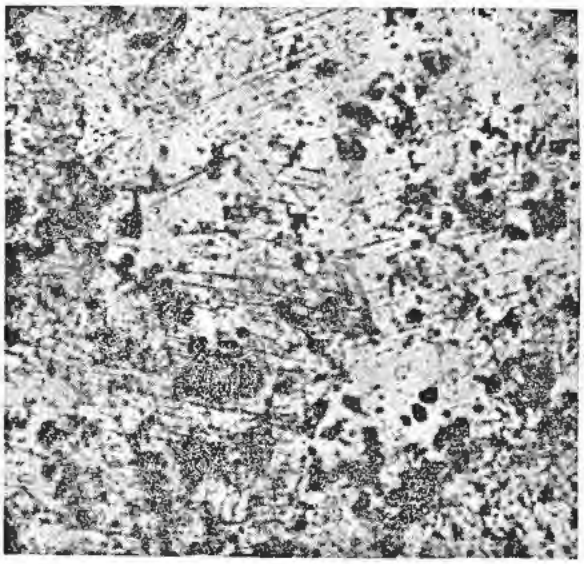

Figure 3a. Uranium microstructure before irradiation (× 200)

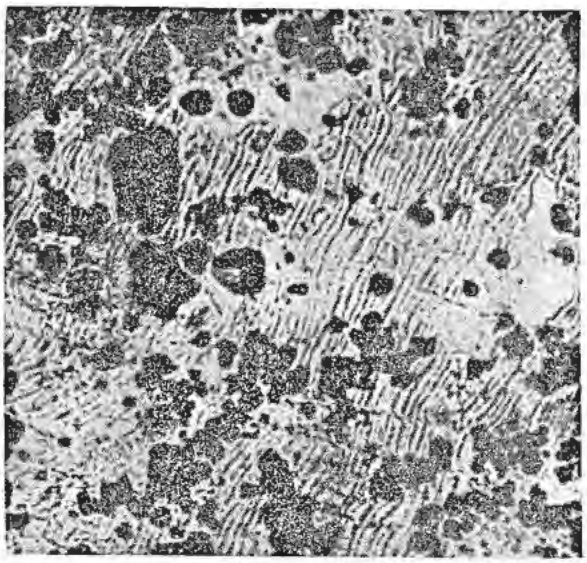

Figure 3b. Uranium microstructure after irradiation (× 200)

the average value of the integrated flux being 3×10^{18} nvt.

The annealing curves, plotted in Figs. 9 and 10 as "additional resistivity vs time," cannot be represented by an exponential or by any other simple relationship. The annealing was step-wise, the exposure at every temperature being 10 minutes. A comparison of annealing curves for several temperatures made it possible to calculate the activation energy (see Table II).

Table II

Temperature °C	*Activation energy kcal/mol*
171	45.3
209	52.5
218	62.7

The increase in activation energy with increase in temperature shows that changes caused by irradiation are non-homogeneous and exhibit a different degree of stability. When the temperature is increased, the activation energy approaches the value characteristic of the activation energy for the salt-diffuson of a heavy metal.

ROLE OF CRYSTAL ANISOTROPY OF URANIUM IN ALTERATION OF PROPERTIES, DIMENSIONS AND SHAPE OF COLD-ROLLED SHEET CAUSED BY IRRADIATION OR THERMAL CYCLING

As is known, crystals of metallic uranium possess a high anisotropy. Cold worked (for instance, rolled) uranium develops a texture and becomes macro-anisotropic. The anisotropy of the electrical resistivity of a cold-rolled uranium sheet (20 × 1.5 × 2 mm) is apparent from the plot (Fig. 11).

It cites the values of specific electrical resistivity, ρ, across and along the rolling direction. The electrical resistivity was measured after annealing at the temperatures given in the figure. Both curves are parallel up to 650° and drop more abruptly in the region of 400–450° (recrystallisation). However, the texture obtained in the process of rolling is preserved up to the $\alpha \rightarrow \beta$ transition. An average de-

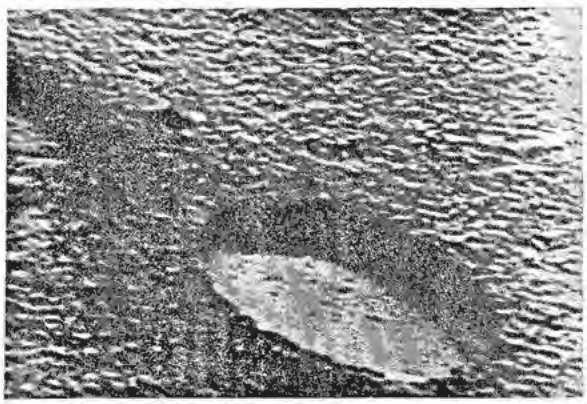

Figure 4a. Uranium microstructure before irradiation (× 15,000)

Figure 4b. Uranium microstructure after irradiation (× 15,000)

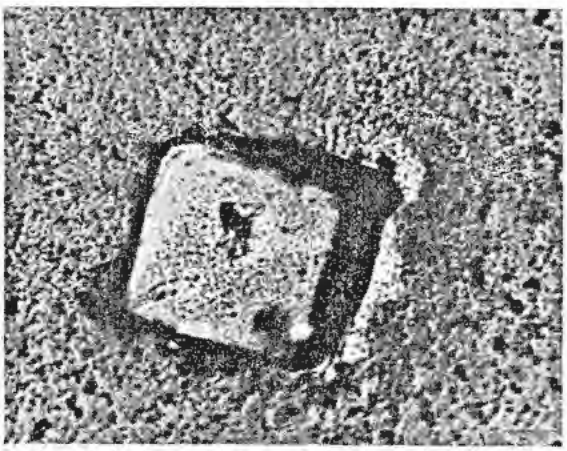

Figure 5. Uranium carbide grain before irradiation (× 4500)

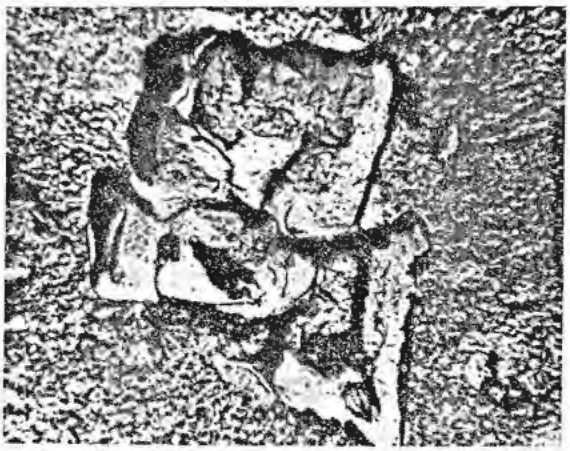

Figure 6. Uranium carbide grain after irradiation (× 4500)

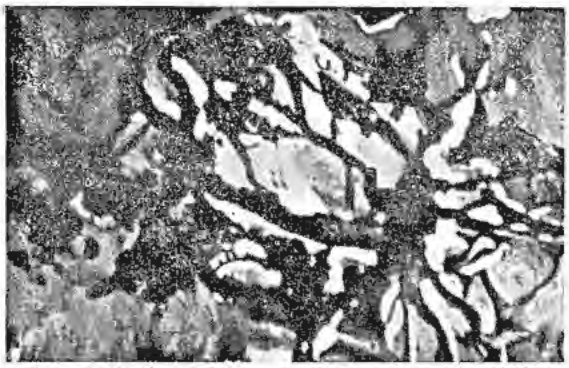

Figure 7. Uranium carbide grain after irradiation (× 15,000)

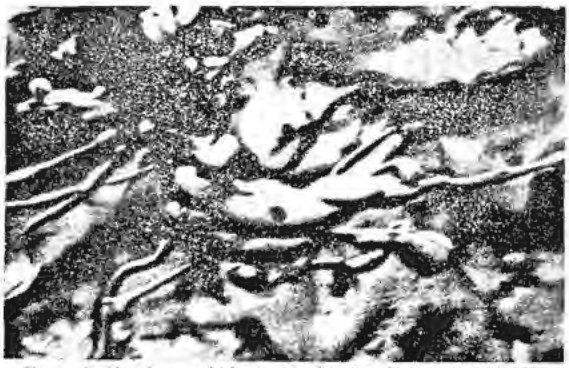

Figure 8. Uranium carbide grain after irradiation (× 15,000)

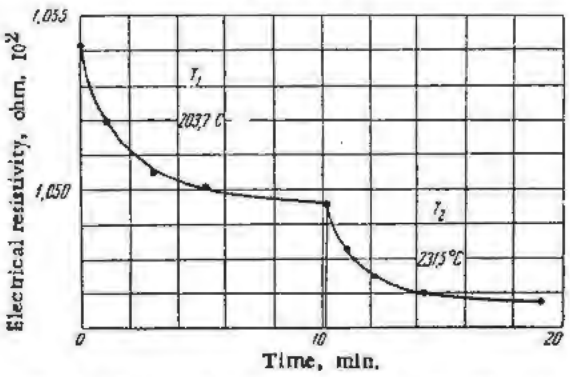

Figure 9. Plot of change in electrical resistivity of specimen No. 1 under annealing

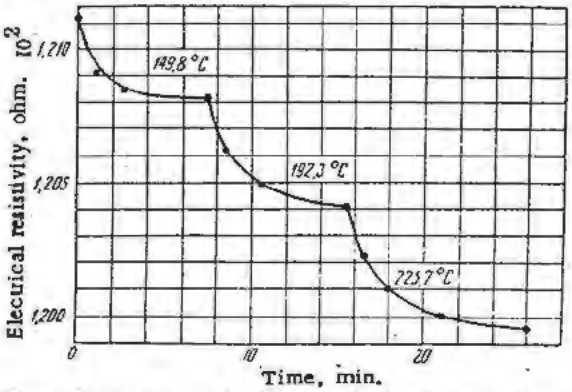

Figure 10. Plot of change in electrical resistivity of specimen No. 2 under annealing

crease in the specific electrical resistivity amounts to 3.5–4% after annealing at 600°C.

The crystal axes of the cold-rolled strip texture and the degree of its scattering were determined by X-ray methods. The orientation is represented in Table III.

The analysis of the texture and the electrical resistivity measurements along and across the rolling direction made possible the calculation of the approximate value of specific resistivity along the uranium crystal axes.

Table III

Deformation axes	*Crystallographic axes normal to plane*
Rolling direction	(061)
Transverse direction	(312)
Normal direction	(114)

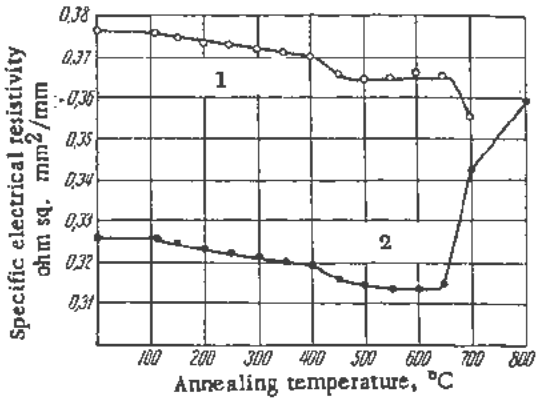

Figure 11. Specific electrical resistivity across and along rolling direction: (1) across rolling, (2) along rolling

It was found that ρ_2 along the b axes = 28.2 μ ohm-cm, and $\rho_{1,3}$ (average) along the a and c axes = 40.2 μ ohm-cm.

The cold-rolled material texture is shown by a peculiar phenomenon of "growth" of uranium products, that is, by their elongation in the rolling direction occurring under irradiation.

The tests were run using a cold-rolled foil 60 × 2 × 0.1 mm and 7 × 7 × 0.1 mm in size. The degree of cold deformation of the foil was 50%.

The foil specimens were placed between two magnesium half cylinders and pressed in an aluminium envelope. Thus, a thermal contact was secured. During the experiment (irradiation) the temperature of the specimen did not rise above 60°C.

Table IV summarizes the data on the properties of rolled uranium foils and uranium alloys containing 0.61 and 9.0% of molybdenum before and after irradiation. The materials listed in column 2 were exposed to an average neutron flux of 0.25 × 10^{20} nvt. The thermal expansion coefficient was determined for uranium and for a 0.61% Mo alloy in irradiated and unirradiated states. The results of the determination (column 3) indicate the anisotropy of thermal expansion and consequently the presence of a texture in samples cold-rolled and annealed at 600°C. After irradiation at 60° the specific electrical resistivity (columns 5, 6, 7) was increased approximately 3–4%, with the exception of the alloy containing 9% Mo which had received a preliminary anneal for 100 hours at 500°. Its specific electrical resistivity was increased 14.2%. The reason for this very appreciable change will be explained later.

The change in the outer dimensions of cold rolled and irradiated foils (col. 8, 9, 10) is most striking. According to the data of the table the change in the length amounts to 8–9% for a 0.25 × 10^{20} nvt. The dimensions across the rolling direction have not changed appreciably. The same foils first annealed for an hour at 600° have elongated less (~1%) though according to thermal expansion measurements and X-ray data their texture is preserved. The foils of a uranium 9% Mo alloy consisting of a cubic γ-phase structure have not changed in length at all.

Testing of "growth" of the rolled foils was repeated, increasing the time of exposure (to 0.50 × 10^{20} nvt). Foil specimens of a uranium alloy containing 0.61% Mo 50 mm long were subjected to irradiation after preliminary annealing at various temperatures. The results are given in Table V. This

Table V. Elongation of Foils of Uranium Alloys Containing 0.61% Molybdenum after Irradiation

Temperature of preliminary annealing	*Elongation δ after irradiation, %*
20	12.9
120	18.5
215	5.8
300	12.6
412	15.4
500	2.0

Table IV. Properties of Uranium and Its Alloys After Irradiation

No.	*Material*	*Linear expansion coefficient 100–300° C × 10^6*		*Specific electrical resistivity ohm × mm² × m⁻¹*			*Length and width of specimens in mm*		
		Before	*After*	*Before*	*After*	*Change %*	*Before*	*After*	*Change %*
1	*2*	*3*	*4*	*5*	*6*	*7*	*8*	*9*	*10*
1	Rolled uranium foil	8.05(∥) 16.6(⊥)	7.5(∥) 15.5(⊥)	0.303	0.305	+0.7	60.0(∥) 6.78(∥) 7.15(⊥)	64.8(∥) 7.40(∥) 7.15(⊥)	+8 +9 0
1a	The same annealed at 600° C	6.1(∥) 16.5(⊥)	.. ..	0.288	0.299	+3.8	60.0(∥)	60.5(∥)	+8
2	Cold-rolled 0.6% Mo alloy	8.3(∥) 16.1(⊥)	8.9(∥) 15.4(⊥)	0.330	0.340	+3.0	60.0(∥) 7.28(∥) 7.21(⊥)	64.5(∥) 7.90(∥) 7.21(⊥)	+7.5 +8.5 0
2a	The same annealed at 600° C	8.9(∥) 14.5(⊥)	.. ..	0.337	0.353	+4.7	60.0(∥)	60.7(∥)	+1.2
3	Quenched and cold-rolled 9% Mo alloy	12.1(⊥) 11.6(∥)	.. ..	0.660	0.685	+3.7	60.0(∥)	60.0(∥)	0
3a	The same annealed for 100 hours at 500° C	..	..	0.523	0.603	+14.2	..	..	..

Note: Symbol (∥) means that properties were measured along the rolling direction, symbol (⊥)—across it. Electrical resistivity was measured along the rolling direction only.

gives the temperatures of preliminary annealing and the per cent elongation caused by irradiation. The appearance of the foils before and after irradiation is shown in Fig. 12.

In some cases the elongation was up to 18.5%.

If the annealing at 500°C, at which temperature recrystallization should take place, is neglected, the variations in elongation can be assigned to the method of applying pressure to the foils (between magnesium blocks) which could hinder the development of elongation in different ways. The average value of $\Delta l_2 = 13.0\%$ may be obtained from the first five elongation values of the table. From the comparison of the average value of $\Delta l_1 = 7.5\%$ obtained during half as much exposure, it is evident that the "growth" of a foil proceeds almost linearly up to the 0.5×10^{20} nvt.

X-ray diffraction patterns were obtained from the specimens of a rolled uranium foil before and after irradiation (see Table IV) by a method described in the report "Metal Research 'Hot' Laboratory" (Session 8B.2, P/673, this Volume). Figure 13 represents the record of one of the lines of α-uranium.[114] The almost equal intensity of the X-ray line before and after irradiation is indicative that the texture has not changed after the exposure.

The width of the line, however, has changed appreciably ($B_1 = 27$ mm instead of $B_1 = 35$ mm for

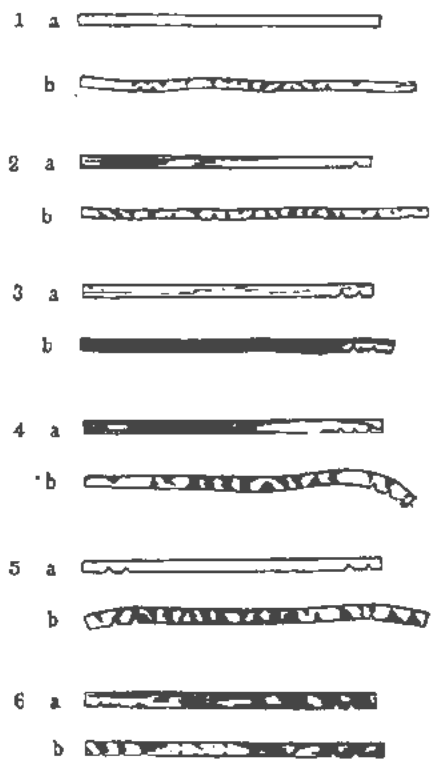

Figure 12 The appearance of foil strips of uranium alloy containing 0.61% molybdenum before (a) and after (b) irradiation: (1) cold-rolled; (2) annealed at 120°; (3) at 215°; (4) at 300°; (5) 412°; (6) 500°

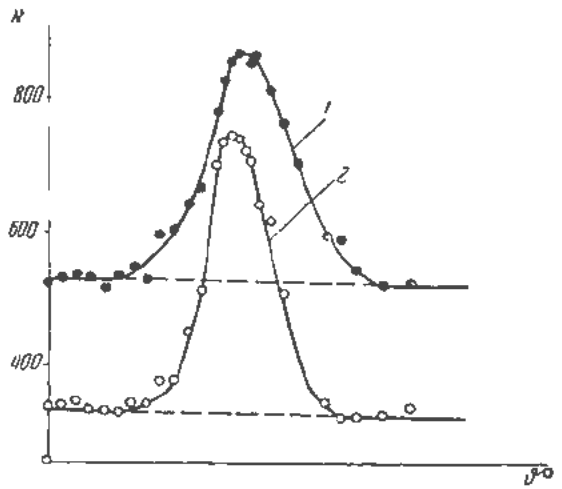

Figure 13. Lines (114) of α uranium X-ray diffraction pattern: (1) before irradiation; (2) after irradiation

the original condition in arbitrary units). This result indicates that non-uniform inner distortion, bringing about the expansion of the X-ray lines (elastic stresses of the second kind), disappears with the "growth" of the foil.

Changes in dimensions and shape analogous to those pointed out above for rolled uranium specimens under irradiation may be reproduced by alternately heating and cooling an unirradiated specimen (thermal cycling).

Plastic deformation caused by thermal cycling in the temperature range of α-phase (20–500°C) was investigated using uranium plates cold rolled with 20, 30, 40, 50 and 60% reduction in the area.

Uranium specimens in sealed quartz ampoules were heated to 500°C, exposed for 20 minutes at this temperature and cooled rapidly in water. The dimensions of the specimens were measured before the test and after 100, 200 and 500 cycles. Examination (see Fig. 14) showed a marked residual deformation which is displayed in elongation. It is increased with the degree of the area reduction and is accompanied by a large change in the shape of the specimens. An almost 35% elongation as a result of thermal cycling is astonishing and is of great importance in the theory of anisotropic metals and alloys.

Changes in dimensions of textured uranium were studied using flat specimens (the degree of cold rolling was 70%). They were cut out parallel and perpendicular to the rolling direction.

The results of the change in the shape and the dimension of these specimens in the temperature range of 20–500°C after 500 cycles are shown in Figs. 15 and 16. They indicate that the longitudinal specimen has been elongated almost 15%, the transverse specimen has been shortened almost 9%.

From the comparison of the deformations caused by irradiation and thermal cycling the conclusion may be drawn that both the phenomena have the same cause, namely uranium anisotropy. Instantane-

Table VI. Properties and Microstructure of Uranium Alloys Under Irradiation

No.	Heat treatment	Specific weight		Specific electrical resistivity ohm·mm²·m⁻¹		Thermal coefficient of electrical resistivity × 10³		Microstructure	
		Before	After	Before	After	Before	After	Before	After
1	Quenching (homogeneous state)	17.26	17.23	0.686	0.682	0.01	0.01	Homogeneous	Homogeneous
2	Quenching, annealing at 500°C for 100 hrs (heterogeneous state)	17.35	17.20	0.531	0.682	1.5	0.01	Heterogeneous	Homogeneous
3	The same (as in 2 foil)	..	..	0.523	0.603	1.14	0.39		

ous local increases in the temperature in the submicroscopic volumes of uranium as a result of the nuclear fission of U^{235} are likely to be equivalent to thermal cycling.

CHANGES IN STRUCTURE OF URANIUM ALLOY CONTAINING 9% OF MOLYBDENUM EXPOSED TO IRRADIATION

The data on the accelerated creep rate, stress relaxation and spontaneous deformation of exposed uranium, pointed out above, testify to the fact that in some respects the irradiation of uranium is analogous to thermal treatment. This is confirmed by the behaviour of a uranium-9% Mo alloy. As is known, an alloy containing 9% of molybdenum may be in two states. The alloy heated above 600° and not too slowly cooled is found to be in a homogeneous state of a solid solution of molybdenum in γ-uranium.

Annealing at the temperature below 600° (for instance 100 hours at 500°, see Table IV) brings about its transition into a heterogeneous state; eutectoid in the form of a fine mixture of α-uranium with the inter-metallic compound γ!

The experiment showed that while the specimens of a homogeneous alloy preserve their phase state under irradiation, the specimens of a heterogeneous alloy are found to have become partly or completely homogeneous after irradiation. This is apparent from the following experiment. Wires 60 mm long and 2 mm diameter of a uranium (enriched 5% in U^{235}) alloy with 9% of Mo were pressed in lead blocks and exposed at the outer temperature of about 50°C to a neutron flux of the order of 10^{19} nvt.

The alteration of their properties after irradiation is shown in Table VI. It lists changes in density, microstructure, electrical resistivity and its temperature coefficient.

On the basis of the property measurements and the examination nf microstructure, the conclusion may be drawn that after irradiation the alloy in wire

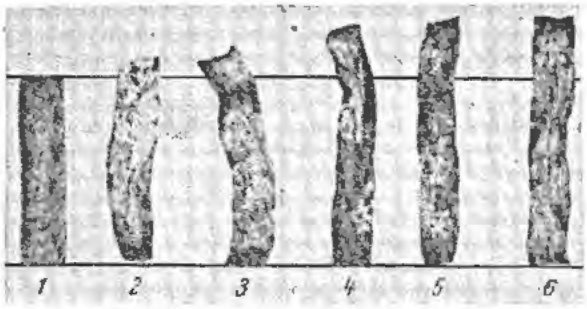

Figure 14. Specimens of cold-rolled uranium strip after 500 cycles of heating and cooling 20°C-500°-20°C: (1) original specimen; (2) rolled 20%; (3) at 30%; (4) at 40%; (5) at 50%; (6) at 60%

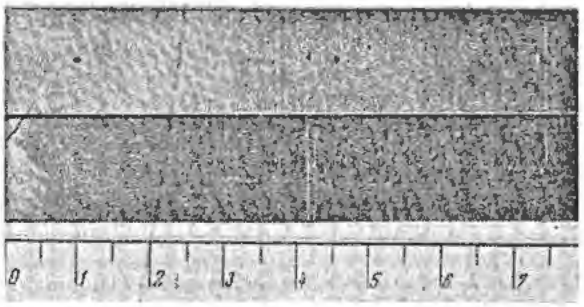

Figure 15. Specimens of cold-rolled uranium strip (70% area reduction) natural size, before thermal cycling: (above) across the rolling direction; (below) along the rolling direction

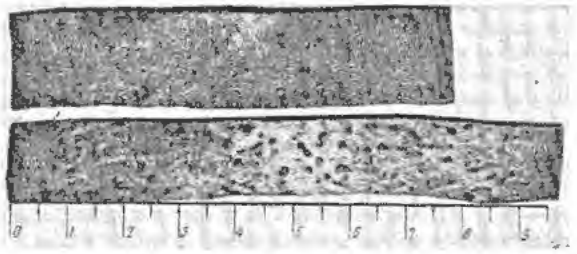

Figure 16. The same specimens as in Fig. 15 after 50 cycles of heating and cooling 20°C-500°C-20°C, natural size: (above) across the rolling direction; (below) along the rolling direction

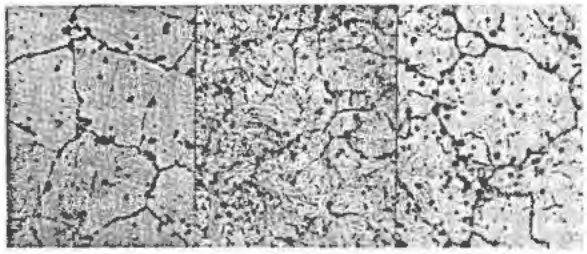

Figure 17. Microstructure of uranium alloy with 9% Mo: (left) homogeneous state; (center) after annealing at 500°C, 100 hr; (right) after irradiation

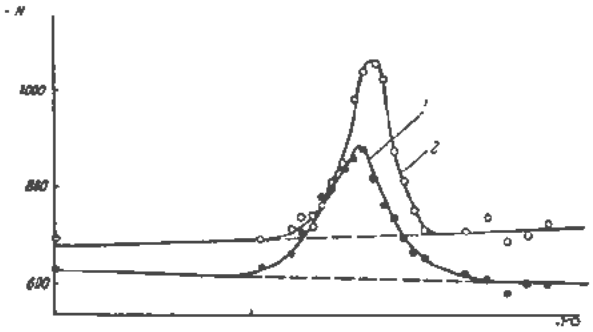

Figure 18. Lines (112) of X-ray diffraction pattern obtained from uranium alloy with 9% Mo in homogeneous state: (1) before irradiation; (2) after irradiation

No. 2 has been transformed from a heterogeneous to homogeneous state. For the state of comparison Fig. 17 illustrates microstructure of an alloy before and after irradiation.

Table VI lists the data on a foil irradiated under conditions completely eliminating any heating above 50°C. In this case partial transformation to a homogeneous state is undoubted. The X-ray diffraction pattern (Fig. 18) obtained from a homogeneous specimen of a cold worked foil shows the result of irradiation. It is seen in a decrease of the width of a line (from 36 mm to 24 mm) and a slight displacement (about 4′–5′) corresponding to the relaxation caused by elastic stresses of the first kind present in a rolled foil.

The tests indicate that irradiation change at a low macroscopic temperature of uranium is similar to the effect of heat treatment.

ACKNOWLEDGEMENTS

The work is compiled from the communications of K. R. Dubrovin, V. M. Golyanov, B. M. Levitsky, N. T. Chebotarev, G. Y. Sergeev and others available at the Academy of Sciences of the USSR.

Damage Occurring in Uranium during Burn-up

By S. F. Pugh,* UK

The efficient operation of a power reactor requires both the highest rate of heat output per unit mass of uranium and the lowest possible consumption of power in circulating the coolant. This is best achieved by using rapidly circulating liquid coolants in narrow channels: an arrangement that has the least volume of coolant in the reactor, which is an advantage if the coolant absorbs neutrons. To avoid blocking of the coolant channels the dimensions of the fuel must remain constant during burn-up. Two distinct phenomena cause change in dimensions of uranium under irradiation, "growth" and "swelling"; these will be discussed separately. To obtain a high heat flux from the fuel requires a steep temperature gradient which causes internal stress due to uneven thermal expansion. If the fuel is embrittled by irradiation the internal stress may produce cracking. The mechanical properties of fuel elements both before and after irradiation must therefore be investigated.

GROWTH OF URANIUM UNDER IRRADIATION

The term "growth" is used to describe the change in shape that occurs in uranium under irradiation. Growth occurs in polycrystalline uranium having preferred orientation and in single crystals, and is not necessarily accompanied by an increase in volume.

Before the results of any single crystal experiments were known, a mechanism was developed theoretically at A.E.R.E., Harwell, whereby uranium might grow under irradiation.[1] Growth was ascribed to a combination of the effects of fission spikes which cause local expansion of the uranium lattice, and the anisotropic plastic properties of alpha-uranium deduced by Cahn[2] from the observed slip and twin systems. This mechanism was used to predict that single crystals of alpha-uranium would grow, that the increase in length would be in the [010] direction and that growth would not occur above about 500°C. These predictions have since been confirmed by experiment.[3]

The proposed mechanism was as follows: around the site of fission in a single crystal of alpha-uranium there is a region of uniform compressive stress which causes local plastic yielding by twinning, preferentially in the longitudinal [010] direction. When the site of fission cools, the outer region is subjected to a uniform tensile stress and therefore yields plastically, this time in the [100] and [001] directions by twinning. The net result is a local increase in length in the [010] direction of the outer region. In a more recent extension of the mechanism[4] it was suggested that the local extension in the [010] direction throws a stress on the surrounding matrix, which is relieved by equal amounts of slip on both the {110} planes in the appropriate $<1\bar{1}0>$ directions to cause extension in the [010] direction. Since tension in the [010] direction produces no resolved shear stress on the (010) plane, slip on this plane does not occur although it is usually the major slip mode. The macro-deformation of the crystal being now by $\{1\bar{1}0\}$ $<110>$ shears, the resulting deformation agrees with that found by experiment, in that extension occurs in the [010] direction, contraction in the [100] direction and the [001] direction remains unchanged in length. The direction of the contraction was not specified in the original model except to say that it lay somewhere on the zone passing through the (100) and (001) poles. Lloyd and Chiswick[5] in an investigation of the deformation modes of alpha-uranium did not find the {110} slip mode but their samples were deformed in compression when an alternative twin mode could probably operate. It has also been realised[4] that the very fine twins lying in the region round the site of fission are unstable, so that when a hot spot due to fission occurs in a finely twinned region the twins anneal back onto the parent lattice. Since annealing takes place by individual atomic migration, no change in shape occurs although the crystal is restored to its original twin-free condition. The above model imposes no limit on the extent of growth.

Slip, being a reversible process in the geometrical sense, could not be the basis of a ratchet mechanism. It was therefore predicted that growth rates would diminish above 350°C and be practically zero at 600°C because at the higher temperature slip would occur rather than twinning and slip. On the other hand, below 200°C growth diminishes with diminishing temperature due to a corresponding increase in yield strength. Observations on variations of growth rate with temperature[3] are in striking agreement with these predictions.

Arguments against the twinning mechanism of growth can be based on the supposition that fission spikes are too small or too short in duration to cause plastic deformation. The two recoiling fission fragments will dissipate the energy of fission along a line 10^{-4}–10^{-3} cm long. Calculation indicates that at distances greater than 500 atoms from this line the yield stress will not be exceeded, assuming a yield strength

* A.E.R.E., Harwell, England.

of 4 tons per square inch. According to Cottrell, a radius of about 1000 atoms is usually necessary to cause operation of a Frank Read source. The radius of the spike might be increased effectively by two fission spikes sometimes occurring sufficiently close for their stress fields to overlap. For the latter effect to occur a significant number of times, the life-time of the fission spike must be about 10^{-4} seconds. The heat pulse associated with the fission spike is probably dissipated initially at the speed of sound and this part of the energy release is unlikely to cause plastic deformation. A part of the energy release, however, is temporarily stored as interstitials and vacancies which also cause a local expansion and the rate at which these recombine diminishes exponentially with diminishing temperature. A rough estimation indicates that at 600°C recombination is almost as fast as the rate at which the thermal energy is dissipated, but below 500°C, namely in the temperature range in which the growth occurs the fission spike remains expanded by interstitials and vacancies. In a fission spike about 10^4 atoms in length and 500 atoms in radius there are 10^{10} atoms. Since only 10^5 interstitials and vacancies are produced per fission, the strain due to the latter at a radius of 500 atoms is only 10^{-5} and is therefore too small to cause plastic flow. If flow occurs, therefore, it must occur very rapidly unless there is some other delaying mechanism, but these objections are not sufficient to allow any definite decision on the validity of the twinning mechanism.

DIFFUSION MECHANISMS OF GROWTH

Seigle has suggested that growth of uranium under irradiation may be due to the anisotropic diffusion of interstitials or vacancies in the alpha-uranium lattice. The grain boundaries act as a sink for the vacancies leading to a change in shape of each grain. In a variant of this growth model Seitz has suggested that the vacancies diffuse to dislocation lines.

The simplest way of obtaining the observed change in shape is by rearrangement of atoms in the [001] planes, which are composed of close-packed rows parallel to the [100] direction. Assuming that the effect of irradiation is to knock atoms out of these close-packed rows, the lattice can be maintained in the correct alpha-structure by forming extra interstitial close-packed pairs of [100] rows giving an extension of the crystal in the [010] direction, and by the vacant sites in the original close-packed [100] rows diffusing along the [100] rows to the grain boundary giving a contraction of the grain in the [100] direction.

If the vacancies diffuse to dislocation lines of the (010) [100] slip system, thus removing (100) planes, while the interstitials form extra planes between the (010) corrugated planes, this combination of changes produces a change of shape in agreement with that observed under irradiation. Both diffusion mechanisms giving the observed mode of growth are similar to the Wigner growth of graphite on irradiation in that the favoured interstitial sites are assumed to be between the slip planes.

It was next shown[4] that the correct variation of growth rate with temperature can be obtained from a diffusion mechanism. This mechanism is most efficient when the lowest proportion of the vacancies and interstitials recombine and are mutually annihilated. The growth rate is therefore highest when the vacancy concentration under irradiation is lowest. The rapid decrease of growth rate with temperature from 400° to 500°C may therefore be due to the rapid increase in the equilibrium concentration of thermal vacancies over this temperature range, so that interstitials are absorbed by vacant sites before they can form "extra planes" which are large enough to be stable. Annealing occurs in uranium at 500°C and it is therefore reasonable to suppose that the supply of very mobile vacancies is large enough to prevent the build-up of extra interstitial planes under irradiation at this temperature. On the other hand, the decrease in growth rate below 200°C is due to an increase in concentration of vacancies with decrease in temperature being caused by a decrease in the mobility of the vacancies so that they do not fall to the equilibrium concentration which would be present in the absence of irradiation.[7] Moreover, at low temperatures, vacancies due to their low mobility would contribute less to the growth process. Since below 200°C the vacancies arise from the fission process, then increase in flux will increase the vacancy concentration and so decrease the efficiency of the growth process; while above 200°C the vacancies arise from the thermal vibrations and are at the equilibrium concentration, therefore change in flux does not in this range change the growth for a given burn-up.

In experiments on the growth of single crystals of uranium under irradiation, undertaken by A.E.R.E., Harwell, two batches of uranium samples 1.5 × 0.08 × 0.01 in. were prepared in the form of single crystals by the phase transformation method.[6] By electropolishing and examining under polarised light the position of any grain boundaries could be determined. The crystallographic orientation of the crystals was determined from microbeam back-reflection Laue X-ray diffraction patterns[6] taken at three positions along the specimen. The crystals had a marked mosaic structure in which the spread in orientation of the individual crystallites was 5 degrees.

The first batch was irradiated[8] at 200°C and the second at 500°C to a burn-up of about 0.03%. The increase in length resolved in the [010] direction of the first batch was about 15% while no growth was detectable in the samples irradiated at 500°C. Cold-rolled uranium sheet having an [010] fibre texture also grew about 15% in the [010] direction after the same burn-up.[3] These and other experiments indicate that 0.1% fission may cause up to 100% growth. On the diffusion mechanism 100% growth is obtained when 50% of the atoms have taken up interstitial positions and an equal number of vacancies have diffused along [100] rows, therefore one fission must produce 500

permanent interstitials and 500 vacancies which diffuse to grain-boundaries or to dislocations. It is estimated that about 50,000 vacancies and interstitials are produced per fission so that the process only needs to have at best a 1% efficiency.

An experiment that would clearly indicate whether the mechanism of growth is based on plasticity or diffusion has not yet been found. It is suggested that determination of the effect of rate of burn-up on growth per unit burn-up at low temperatures might settle this point since on the diffusion mechanism the growth per unit burn-up might diminish with increase in rate of burn-up while on the twinning mechanism it might increase.

There is no evidence of any fundamental difference between growth of single crystals under irradiation and growth of polycrystalline aggregates. Thus each crystal in the aggregate will tend to grow in the [010] direction and contract in the [100] direction but will be more or less constrained by the surrounding grains, the effect of such constraint apparently being much greater in fine grained material of random grain orientation. The growth of the sample can therefore be predicted from a knowledge of the preferred orientation.

WRINKLING OF URANIUM UNDER IRRADIATION

Wrinkling is the term used to describe the roughening of the surface of uranium during burn-up. It is most marked in coarse-grained uranium and occurs because the individual grains grow in different directions in the sample as they have different orientations. Wrinkling is not appreciable in very fine-grained material, the size of the wrinkles being related to the grain size. Wrinkling does not occur in single crystals or in polycrystalline samples consisting of a single texture, but such samples will grow under irradiation. Cast uranium or uranium slowly cooled from the beta range consists of grains about ½ mm diameter having a fine substructure with 5 degree mis-orientation. In the wrinkling phenomenon these large clusters behave as single crystals so that these materials develop large wrinkles on irradiation.

The grain size of uranium may be refined by any of the following three methods. If the uranium is quenched in water from the beta range, preferably above 720°C, a grain size of between 0.05–0.08 mm is obtained. This method is not effective if the uranium is very pure; about 0.05% of impurities such as iron, silicon or aluminium appear to be necessary. A more elaborate procedure which can produce a finer grain size than the above is the isothermal transformation of beta to alpha-uranium at an elevated temperature in the alpha range. An alloying addition such as ½% to 1% chromium or molybdenum which tends to stabilise the beta phase[8] is necessary for this method. The temperature at which such an alloy will transform to a fine grained alpha is very dependent on the impurities present and therefore varies from one batch of uranium to the next. The effectiveness of this treatment is also dependent on the size of the sample. If these alloys are quenched to room temperature they are liable to crack due to the retention of beta-uranium which is brittle. The third method of obtaining a fine grained uranium is by use of an alloying addition which produces a finely divided second phase in the gamma range which may diminish the grain size resulting from the phase transformation on cooling. This method, to be effective, requires a large proportion of the second phase and therefore rather higher additions than those used in the second method are necessary. Grain sizes as small as 0.002 mm have been obtained. The fine grain obtained by these methods is stable for a few months at temperatures up to 500°C.

Slow thermal cycling in the alpha range also causes growth and wrinkling.[9] For this growth a double fibre texture is necessary,[10] which is different from the requirement for growth on irradiation. For wrinkling the severity of the damage depends on the grain size as for wrinkling on irradiation. These effects on thermal cycling arise from the anisotropic thermal expansion of uranium single crystals so that in aggregates an internal stress develops due to change in temperature. In aggregates therefore deformation is by twinning at low temperatures on cooling while grain boundary relaxation occurs on heating. The mechanism is therefore not related to that of irradiation growth.

INCREASE IN VOLUME ON IRRADIATION

The change in dimensions of uranium due to increase in volume is much smaller than that which can be encountered due to growth. The increase in volume is due to a different mechanism from that of growth and is in the UK referred to as swelling. At 0.1% burn-up an increase in length due to growth of a single crystal may be about 40%, while that due to swelling is unlikely to exceed 4% even in the worst case. One of the causes for the increase in volume is the formation of small holes which are believed to be blown up by the volatile fission products, particularly the inert gases. Calculation[11] of the swelling expected from the pressure in the bubbles and the creep behaviour of the uranium gives a value that is much less than that observed experimentally at temperatures in the alpha range, indicating that another mechanism is also playing a part in swelling. The scatter in the amount of swelling observed for the same burn-up and at the same temperature and the uneven distribution of microporosity observed in individual specimens after irradiation indicates that at least one of the swelling mechanisms is structure sensitive. The condensation of vacancies on existing holes may be such a process.

Examination of uranium after burn-up by X-ray diffraction shows that the lattice parameters are only very slightly increased[12] and the crystal structure is not severely distorted. These observations confirm that the swelling on irradiation is mainly due to internal porosity.

MECHANICAL PROPERTIES OF URANIUM AFTER IRRADIATION

For some time it has been realised that uranium becomes more brittle after only say 0.03% burn-up.

Part of the increase in yield strength is presumably by the same mechanism as that which raises the yield strength of non-fissile metals on irradiation. In addition there are the effects due to growth, fission products and formation of internal porosity. Annealing restores the mechanical properties but only partially by ensuring a better distribution of fission products and by removing internal strains due to growth and irradiation hardening. Thermal stress might cause embrittled fuel elements to crack in service, a hazard which is more severe in reactors operating at low temperatures and high rates of burn-up.

SUMMARY

Changes in the dimensions and other properties of uranium occurring during burn-up of up to 0.1% have been described and tentative mechanisms to explain these changes have been discussed. It has not yet been decided which mechanism operates in each case. The phenomena have to be considered in the design and manufacture of fuel elements for power reactors.

ACKNOWLEDGEMENTS

The author wishes to thank colleagues for criticism and discussion of this report during its preparation, in particular, Dr. W. M. Lomer and Dr. A. H. Cottrell.

APPENDIX

1. Classical heat flow calculations on the duration of a thermal spike. Neglecting end effects for a cylinder

$$t = R^2/4K$$

where t is the time at which the temperature at a radius R has reached its maximum value; K is the thermal diffusivity $= K'/\rho c$ where K' is the heat conductivity, ρ the density and c the specific heat. For uranium $K' = 0.07$ cal/cm/sec °C at 200°C; $c = 0.03$ cal/gm/°C at 200°C; $\rho = 18.9$ gm/cm³; and $K = 0.1$ cm²/sec, approximately.

When $R = 10^{-5}$ cm then $t = 2 \times 10^{-10}$ sec.

Since the thermal conductivity is mainly electronic, this is a reasonable value for the life of the spike. The elastic waves involved in the movement of dislocations will however move more slowly. Dislocations will not therefore move far before being overtaken by the heat flow.

2. In the following rough calculation of the stress due to thermal expansion caused by local absorption of 100 Mev of fission energy, it has been assumed that the expansion is linear with temperature. The distribution of the heat has therefore been ignored and it has been assumed that a cylinder containing the fission spike as axis is raised to a uniform temperature. Neglecting end effects the stress will be uniform over a cylindrical surface. If the length of the spike is 10^4 atoms, then at a radius of 1000 atoms the stress is obtained as follows:

$$100 \text{ Mev} = 3.8 \times 10^{-12} \text{ cal}$$

The spike contains 3×10^{10} atoms, i.e., 1.2×10^{-11} gm uranium. Therefore temperature rise is 10°C; taking coef. of exp. 16×10^{-6} per °C, thermal expansion is 1.6×10^{-4}. Stress therefore is

$$\frac{1.6 \times 10^{-4} \times FM}{2(1-n)}$$

where FM is Young's Modulus and n Poisson's ratio. The stress at 1000 atoms radius is therefore approximately 1 ton per square inch.

Since the stress varies as $1/R^2$ at 300 atoms radius it is 10 tons per square inch which is above the yield stress.

The stress is maintained from the moment of fission until some of the energy has escaped from the cylinder under consideration. A linear expansion coefficient has been assumed but it is likely that at the high temperature in the spike the average expansion will be greater than 16×10^{-6} per °C. Since the atomic radius of uranium is about 3Å the size of the cylindrical surface where the stress is 10 tons per square inch is: radius 0.1μ and length 3μ.

REFERENCES

1. Pugh, S. F., *The growth of alpha-uranium on irradiation*, A.E.R.E. report to be published.
2. Cahn, R. W., *Plastic deformation of alpha-uranium; twinning and slip*. Acta Met *1*, 1, 49-70 (1953).
3. Plail, O. S., *Some experimental irradiation tests on natural uranium*. A.E.R.E. report to be published.
4. Pugh, S. F., *The growth, wrinkling and fission product damage of uranium and its alloys during irradiation*. A.E.R.E. report to be published.
5. Lloyd, L. T. and Chiswick, H. H., *Deformation mechanisms of alpha-uranium single crystals*. U.S.A.E.C. report ANL-FGF-2, 1955.
6. Cahn, R. W., *The preparation of alpha-uranium crystals*. Acta Met., *1*, 2, 175-184 (1953).
7. Johnson, R. D. and Martin, A. B., *The effect of cyclotron bombardment on self-diffusion in silver*. J. app. Phys. 23 (11) 1245-54 (1952).
8. Mott, B. W., *The transformation from beta to alpha in uranium alloys*. A.E.R.E. report to be published.
9. Pugh, S. F., *The mechanism and kinetics of the growth and wrinkling of uranium on slow thermal cycling in the alpha range*. A.E.R.E. report to be published.
10. Burke, J. E. and Turkalo, A. M., *Thermal ratchetting*. U.S.A.E.C. report A.E.C.U. 1639, 1-20 (1951)
11. Foreman, A. J. E., *Calculations on the rate of swelling of gas bubbles in uranium*. A.E.R.E. report to be published.
12. Pease, R. S., *Diffraction data from active materials*. A.E.R.E. report to be published.

Irradiation Effects in Uranium and Its Alloys

By S. H. Paine, and J. H. Kittel,* USA

Stability of the fuel configuration is perhaps the most important practical problem in the engineering and operation of a heterogeneous reactor. Any general dimensional changes have an important bearing on the nuclear behavior of the reactor and its efficiency as a power producer, and any localized changes may cause local overheating with attendant serious consequences. The fuel materials, therefore, must be fabricated and heat removal must be managed in such a manner as to conserve the lattice arrangement and, in particular, to minimize as much as possible the occurrence of nonreversible changes in the spacings and dimensions of the fuel elements.

Uranium is the only fissionable reactor fuel readily obtainable and is, quite unfortunately, anisotropic in its properties. Its erratic behavior under thermal cycling and neutron irradiation has made it the object of much close study by engineers and scientists in the USA. This paper presents a summary of available information on the changes which have been observed in the base metal and some of its alloys. Of primary interest are the dimensional changes, following discussion of which some data are given on miscellaneous properties changes, such as strength, hardness, thermal conductivity, solid diffusion and corrosion resistance.

CHANGES IN LINEAR DIMENSIONS

A most spectacular effect of irradiation upon uranium metal is manifested by radical changes in dimensions of test specimens. The magnitude of the effect is found to have a close relationship to variables in fabrication technology. Before discussing these, however, it would be well to review briefly what has been learned concerning fundamental behavior and the theories which appear pertinent to its explanation.

The Phenomenon of Radiation Growth in Uranium

It has been possible to study the basic anisotropy of deformation by irradiating true single crystals of alpha uranium, produced by Fisher (Argonne National Laboratory) and observing the dimensional changes in the three lattice directions. Figure 1 shows a series of photographs of such a crystal originally nearly a right circular cylinder 0.125 inch (0.32 cm) in diameter. It will be seen that considerable lengthening has occurred and that the circular cross section has become elliptical. Careful measurements after irradiation give the three lattice growth coefficients shown in Table I. The dimensionless unit, G_i, expressed in microunits of growth per unit length for one fission per million total atoms, has been found convenient to use. Its exact value is based upon the well-known exponential relationship between initial and final measurements, L^0 and L,

$$G_i = \frac{\log_e (L/L_0)}{(\text{Ratio of fissions to total atoms})} \qquad (1)$$

For small elongations the following approximation may be used:

$$G_i = \frac{\text{Per cent growth}}{\text{Per cent burnup}} \qquad (2)$$

Imperfect lineage crystals, made by gradient transformation from the beta to the alpha phase, have the same relative behavior under irradiation. They elongate in the [010], shorten in the [100], and remain approximately unchanged in the [001] directions. However, the magnitude of elongation is always greater and the geometric regularity of the distorted specimens is distinctly less than observed in true single crystals.

Cylindrical polycrystalline specimens in which the grains are not randomly oriented also deform under irradiation. They retain their circular cross section, however, if the longitudinal axis coincides with the rolling direction. As will be seen from evidence presented later, the magnitude and character of deformation, including surface distortions, depend upon structural factors. Longitudinal growth rates more

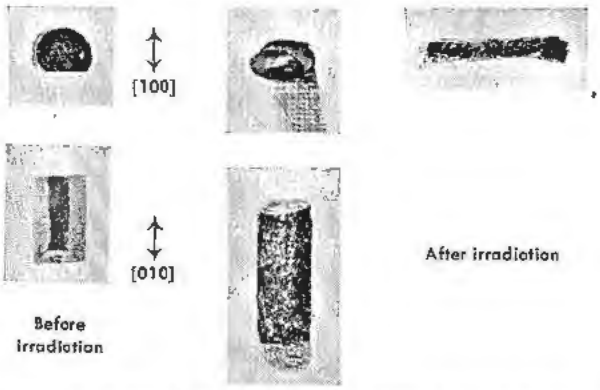

Figure 1. Aspects of a cylindrical single crystal of alpha uranium before and after irradiation in a reactor (0.1% atom burn-up)

*Argonne National Laboratory.

Table I. Comparison between the Irradiation Growth Coefficients of a True Crystal of Uranium and the Thermal Expansion Coefficient along the Major Crystallographic Axes in the Uranium Lattice

Direction axis	Irradiation growth coefficient (G_3)*	Thermal expansion coefficient (10^{-6} per °C)†		
		25° – 125°C	25° – 325°C	25° – 650°C
(100)	−420 ± 20	21.7	26.5	36.7
(010)	+420 ± 20	−1.5	−2.4	−9.3
(001)	0 ± 20	23.2	23.9	34.2

* Argonne National Laboratory. Specimen irradiated to 0.1% burnup at approximately 100°C.
† Battelle Memorial Institute. Compound from X-ray lattice expansion data.

than double those measured in single crystals have been observed in highly oriented polycrystalline specimens irradiated at the same temperature. Appreciable shrinkages have also been observed.

Comparison with Thermal Cycling Growth

Uranium also exhibits marked deformation as the result of thermal cycling. The visual appearance resulting from cycling has a strong resemblance to that of irradiated material, suggesting that the two effects may depend, at least in a measure, on the same basic mechanisms.

Thermal cycling growth has been studied extensively in the USA. A comprehensive paper devoted to this topic is being presented at this Conference by Chiswick and Kelman (ANL).[1] Therefore, it will suffice to present only a brief tabulation outlining the respects in which growth by irradiation and by thermal cycling seem to be similar to each other, and also the important respects in which they are known to differ.

Similarities

1. Irradiation and thermal cycling both induce progressive alterations in the dimensions of polycrystalline uranium specimens. Elongation is the most common manifestation of these phenomena but shrinkage has also been observed.

2. The characteristic surface distortions—roughening, humping, etc.—are qualitatively the same for both phenomena.

Differences

1. Although the direction and magnitudes of the growth phenomena often have a loose correlation, it is by no means consistent. Specimens which elongate in thermal cycling sometimes shrink in irradiation.

2. Irradiation deforms single crystals and lineage crystals as well as polycrystalline uranium, whereas thermal cycling deforms the latter only.

Many ideas have been advanced to explain the basic mechanism of thermal cycling growth, and because of the similarities mentioned above an effort has been made to link this type of deformation to that which occurs during irradiation. It seems advisable to include in this paper, comparative data emphasizing some of the similarities observed. The differences in behavior are definitive enough, however, to show that there must be a basic difference in the causative mechanisms. In the following discussion only those ideas directly related to the irradiation growth phenomenon will be considered; the Chiswik and Kelman paper should be consulted for a detailed account of thermal cycling growth theory.

Fundamental Considerations

In any basic thinking concerning irradiation growth, some primary or predisposing anisotropy of properties must be called upon to permit differential strains, some driving force must be postulated to activate such properties, and there must be cooperating mechanisms which make the strains in some measure irreversible.

The Role of Thermal Expansion

In line with this analysis, an obvious choice for consideration as a predisposing anisotropy is the known difference between coefficients of thermal expansion in the three lattice directions (see Table I). Most of the growth theories are based on this property in some way and postulate as the driving force the high temperature spikes resulting from fission events.

The main differences in thinking relate to the matter of cooperating mechanisms. Thus, Burke, Howe and Lacy (GE-KAPL) proposed, before the radiation growth of single crystals had been demonstrated, that the fission thermal spikes at grain boundaries activate the same "ratchet" mechanisms which give rise to thermal cycling growth. This model is not disproved by the single crystal results, although inadequate to explain them. It is possible that the accentuated growth of polycrystalline material is due in part to a real effect of this type.

Bettman (CRD) proposed a model which makes elongation of single crystals the result of residual compression stresses in the [010] direction and tension stresses in the (010) plane after the thermal spike cools down. His development does not explain the elliptical deformation noted in the (010) plane of single crystals, although it does account fairly well for their elongation.

A somewhat similar but more extended model has been proposed by Burke and Turkalo (GE-KAPL) based on a localized slip mechanism previ-

ously discussed by Last and McLachlan (GE-HAPO). They suggest that the thermal spike volume change buckles the structure perpendicular to the (010) [100] major slip direction,[2] in a manner analogous to distortions resulting from ball indentations normal to the basal slip planes of zinc crystals.[3] It is assumed that the [010] expansion would be balanced by [100] and [110] slip and that the deformation would be nonreversing in some measure.

This model makes provision for elliptical deformation of single crystals in the (010) plane, and Bettman's model provides a satisfactory argument for nonreversibility in deformation. Putting these complementary ideas together we have a reasonable growth mechanism based on anisotropy of thermal expansion. It does not depend upon the presence of grain boundaries, and is independent of grain size. However, experimental verification will be exceedingly difficult, and the elementary concepts need further quantitative elaboration.

The Role of Diffusion

Seigle and Opinsky (SEP, Inc.) have proposed a mechanism of dimensional instability which is based upon anisotropic diffusion of displaced atoms and vacancies created in the crystal lattice by fission recoils. The idea that a crystal can suffer alteration of shape due to preferential diffusion was first discussed by Nabarro[4] and later used by Herring[5,6] to explain experimental sintering results obtained by Alexander.[7] Buttner, Baluffi and others[8] have produced additional experimental confirmation on brass and copper investigations.

The theoretical treatment of the alpha uranium lattice by Seigle and Opinsky arrives at the conclusion that interstitial uranium atoms would migrate with some preference for the [010] direction, while vacancies would migrate entirely in the [100] and [001] directions in the computed ratio 5:4. In fitting this result to the observed behavior of single crystals, the assumption is made that diffusion of interstitials and of vacancies in the [001] direction is almost exactly balanced; this leaves a net shrinkage in the [100] direction. The theory predicts that the rate of growth in the [010] direction will vary directly with the 3/4th power of the neutron flux and the square root of the diffusion coefficient for interstitial atoms. A temperature dependence, of course, should be found. A grain size effect is also expected because of the role of grain boundaries as vacancy sinks; however, it is pointed out that random dislocations and other lattice imperfections are also available as internal sinks.

The anisotropic diffusion model is partly supported by the work of Kunz and Holden (GE-KAPL) who showed that the deformation rate of cold-rolled uranium foil is greatly reduced when irradiation is done in a liquid air cryostat. Other predictions are capable of experimental check, and will doubtless be subjected to careful test.

The Role of Grain Boundaries

Grain boundaries are classically considered as restraints upon deformation mechanisms, hindering the free propagation of strains in polycrystalline structures. In irradiation growth, however, it is apparent that they provide a medium whereby the distortions produced in single crystals may be sharply accentuated. It may be pointed out that this effect is to be expected if the diffusion mechanism discussed above is operative, and it is doubtless true that grain boundary restraints multiply the population of sinks for vacancies and interstitials both at the grain boundaries and within the bodies of the grains. However, in thermal cycling growth the presence of grain boundaries is required in order that the deformation may proceed; moreover, it is evident that the mechanism does not depend upon the anisotropic disposal of large numbers of interstitials and vacancies by diffusion.

Therefore, the inference may be valid that irradiation growth is not entirely a diffusion phenomenon, but may be induced by more than one combination of stress activations with mechanisms of anisotropic strain relief. Thus, the cooperative role of grain boundaries in both irradiation and thermal cycling growth may be identical although the respective driving stresses are dissimilar.

VARIABLES WHICH AFFECT DIMENSIONAL STABILITY

We will now consider in greater detail the variables which are found to have an influence upon irradiation growth in uranium. A practical understanding of these is needed in order to predict the over-all behavior of fuel configurations in reactors. It has been found that structure of the metal, its fabrication history and its composition are sensitive variables, as well as the environmental conditions under which irradiation proceeds.

Structural Variables

Early in the investigation of the thermal cycling behavior of uranium, it was found that the rolling texture of the material and its grain size had an important bearing upon the character and magnitude of the effects observed. Investigators at ANL have spelled out the relationship between growth and these variables in the case of cold-worked (300°C) alpha recrystallized (575°C) material, and the results are shown as smoothed curves in Fig. 2.

The greatest growth for each degree of cold work occurs at the smallest grain size, and the greatest growth for each grain size occurs in the material with greatest preferred orientation. Decrease of growth rate with increase in grain size is quite pronounced, coarse-grained 70% cold-worked material being about equivalent in growth to fine-grained 10% cold-worked material.

Some of the specimen materials from this study were available for a comparative irradiation growth test. The results are shown in Fig. 3. Scatter of data

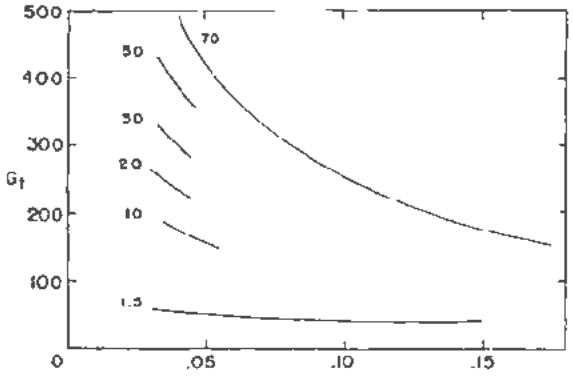

Figure 2. Combined effect of grain size and cold work upon growth rate (G_t) of uranium under thermal cycling: (curve numbers denote per cent reduction in area by rolling after which the specimens were recrystallized at 575°C, G_t = micro in./in./cycle)

makes the comparison somewhat uncertain for the coarser grain sizes, but the curve has been drawn to favor the minimum growth numbers. The deduction, therefore, appears valid that as the grain size of 70% cold-worked metal is increased, the irradiation growth rate does not decline as rapidly as is the case in thermal cycling. A further comparison is given in Fig. 4, where irradiation growth and thermal cycling growth of fine-grain material are shown as functions of cold work. The ordinates have been arbitrarily normalized so that the two effects coincide at 70% reduction in area. Here again it is seen that the phenomena do not exactly correspond. The difference might be described as an inequality in saturation tendencies. It is also observed that changes in degree of cold work are more sharply effective in altering irradiation growth than are changes in grain size.

It should be pointed out that in the figures the ordinates for thermal cycling and irradiation growth are given in G_t and G_i units. These are empirical scales which have no more than an arbitrary correspondence. G_i has already been defined in terms of burnup (Equation 1), whereas G_t is given in microunits of elongation per unit length resulting from an arbitrary heating and cooling cycle.

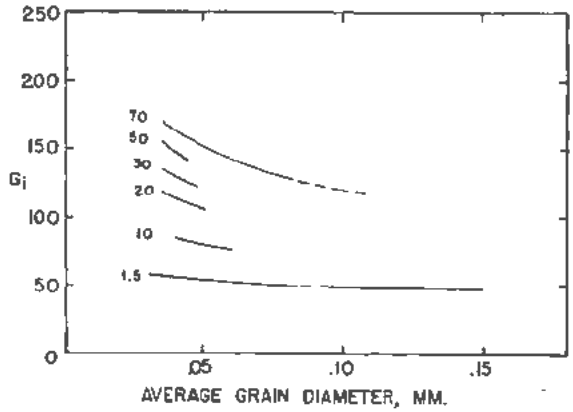

Figure 3. Combined effect of grain size and cold work upon growth rate (G_i) of uranium under irradiation: (curve numbers denote per cent reduction in area by rolling after which the specimens were recrystallized at 575°C, G_i = micro-in./in./ppm burn-up)

At one time it had been hoped that a direct ratio between the magnitudes of the thermal cycling and irradiation effects might be found so that the effect of burnup, for example, could be expressed in terms of equivalent thermal cycles. Apparently no simple relationship between the two different units exists, either for variable grain size at constant texture, or for variable texture at constant grain size. The grain size result is not unexpected when it is recalled that thermal cycling growth is entirely dependent upon the presence of grain boundaries, whereas irradiation growth can proceed without them. The texture result is doubtless also a reflection of basic differences in the over-all mechanisms of growth.

Fabrication Variables

The magnitude of linear distortion in irradiated uranium is quite sensitive to previous mechanical fabrication procedure and thermal treatment. In general, the effect of these metallurgical factors may be understood in terms of resultant grain size and type and degree of preferred orientation, structural variables which have been discussed previously.

Alpha rolling of uranium is successfully accomplished in the range from 300°C (cold work) to 640°C (hot work). The irradiation growth reaction in cold-worked and recrystallized material has already been seen in Fig. 4. The starting stock in this experiment has been heated into the beta region and water quenched to produce a moderately fine-grained, random structure so that textures produced by previous fabrication would be erased. This is an important consideration for work at ANL has shown that the effects of rolling the same material successively at

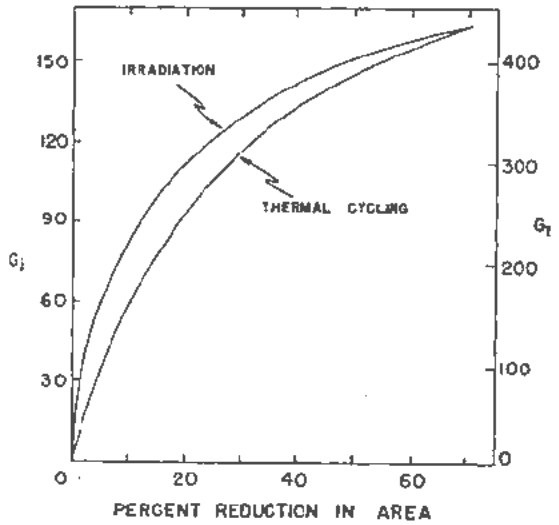

Figure 4. Effect of cold work upon the irradiation growth rate (G_i) and thermal cycling growth rate (G_t) of uranium: (specimens were recrystallized at 575C before testing; G_i = micro-in./in/ppm° burn-up, G_t = micro-in./in./cycle)

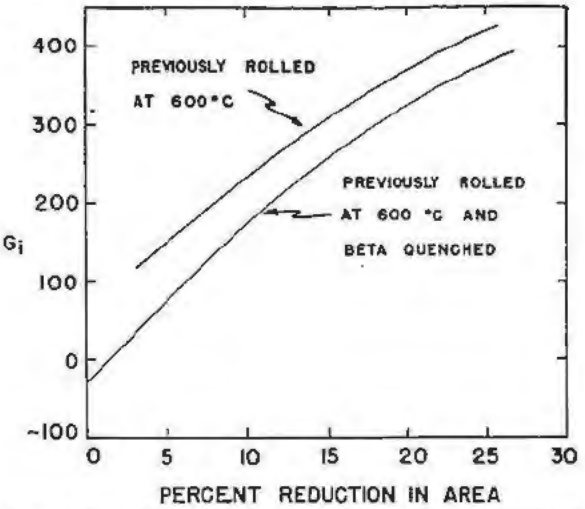

Figure 5. Effect of additional cold work (at 300°C) on the irradiation growth rate of uranium (previously rolled at 600°C)

different temperatures are roughly additive. Figure 5 illustrates the point by comparing the growth resulting from superposing cold work upon previous hot work with that resulting from cold-working identical material randomized by beta quenching. Figure 6 shows the beta quenched and cold-worked specimens from this test as they appeared after 0.1% burnup of total atoms.

Before proceeding with a description of the effect of rolling temperature upon growth rate, a comment should be made concerning the rolling technique itself as affected by the behavior just described. It is impossible to conduct a rolling operation strictly at constant temperature. The thermal fluctuations normally are dependent on degree of reduction per pass, speed of rolling, surface oxidation rate and radiative losses, and may be quite large. As far as irradiation growth is concerned, therefore, each bar may be considered as having been partially rolled at a number of different temperatures, all of these contributing to its final texture and irradiation behavior. Thus, the rolling procedure itself is a variable which has a definite effect upon the reaction of uranium to irradiation.

Cold rolling produces essentially a (010) texture in uranium bar. As the rolling temperature is raised

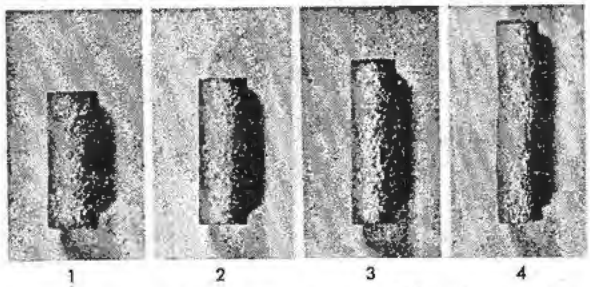

Figure 6. Effect of 0.1% atom burnup on 600°C rolled and beta quenched uranium after further cold work at 300°C: (1) no cold work; (2) 5% red. at 300°C; (3) 10% red. at 300°C; (4) 25% red. at 300°C

above the recrystallization threshold (~400°C), however, a strong (110) component becomes activated and at higher temperatures even the (100) fiber is brought into play. The original (010) component meanwhile becomes progressively weaker. This means that irradiation growth is greatly attenuated in material rolled at the higher temperatures, and may even become negative. Figure 7 shows this behavior graphically. Irradiation growth coefficients are listed in Table II, together with thermal cycling results for comparison. The bars used in this experiment were carefully soaked at the indicated temperatures before each pass through the rolls, in order to standardize the results as much as possible.

When the roll-pass design is changed there is a further variation of irradiation behavior, illustrated by comparing Figs. 7 and 8. The rolling technique was held constant in rolling two identical lots of test bars, but one went through round passes and the other through oval passes. The latter apparently work the material more drastically at higher temperatures than do the former.

The effect of heat treatment has already been mentioned briefly. Beta or gamma recrystallization of alpha rolled material almost completely removes the preferred orientation and reduces the growth rate to $G_i = 15$–20. Recrystallization in the high alpha range does not radically modify the texture. The growth rates, however, are appreciably reduced, as shown in Figs. 7 and 8 and Table II. The small shift in texture, coupled with grain coarsening, is probably responsible.

Variations in Composition

It is common metallurgical knowledge that the properties of base metals may be altered and improved by the addition of alloying elements. Uranium

Table II. Growth Coefficients of Polycrystalline Uranium Round Rolled to 75% Reduction in Area at the Indicated Temperatures*

Rolling temperature °C	*Subsequent heat treatment*	*Growth coefficients*	
		Irradiation (G_i)	*Thermal cycling (G_i)*
300	As rolled	–	540
	2 hours at 630°C	294	358
400	As rolled	475	577
	2 hours at 600°C	204	467
500	As rolled	321	519
	2 hours at 600°C	163	446
600	As rolled	4	278
	2 hours at 575°C	6	296
640	As rolled	–22	224
	2 hours at 575°C	–55	183

*Compiled from data by Mayfield, Kittel and Mueller (ANL).

is no exception to this principle, and a study of the binary constitution diagrams reveals several ways of inducing such changes.

1. A composition may be selected which is so low in uranium that the irradiation characteristics of the diluent control the behavior of the alloy. For example, aluminum, beryllium and zirconium are dimensionally stable under irradiation, and continue to be relatively stable in alloys containing uranium as a minor constituent.

2. In the high-uranium alloys, combinations of additives may be sought which by proper heat treatment will refine and stabilize the grain and thereby bring about desirable improvements in the properties of the base metal. For example, one- or two-tenths of a per cent of chromium in uranium permits refinement of the grain so that randomly oriented material has excellent stability under irradiation. Other elements, such as molybdenum, niobium and zirconium, and combinations of two, are equally effective, but the quantities required are somewhat higher. The homogenized compound, U_3Si, is also stable.

3. In the uranium alloy systems which have large ranges of solid solubility in the gamma phase, compositions may be sought which retain the body-centered cubic lattice at room temperatures. The most notable systems of this type are the binaries of molybdenum, niobium and zirconium. Titanium and vanadium in combination with uranium also have large gamma regions. The gamma phase in these systems is not in stable equilibrium at room temperature; therefore, the alloy content must be great enough

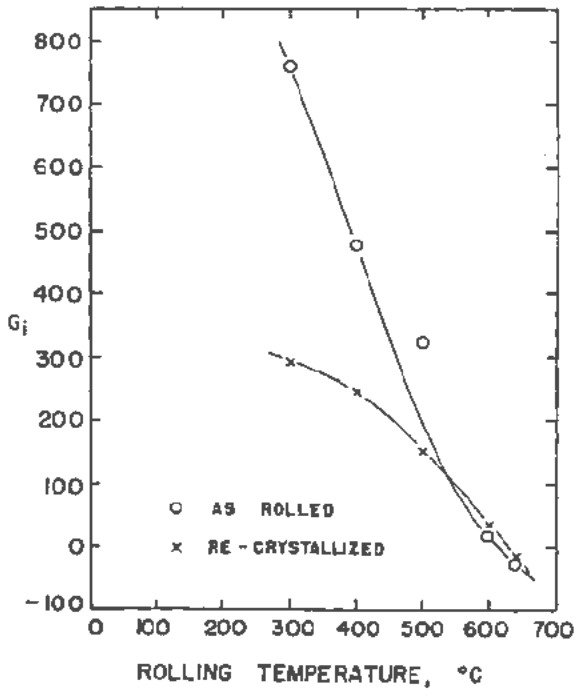

Figure 7. Effect of rolling temperature on the irradiation growth rate of round-rolled uranium

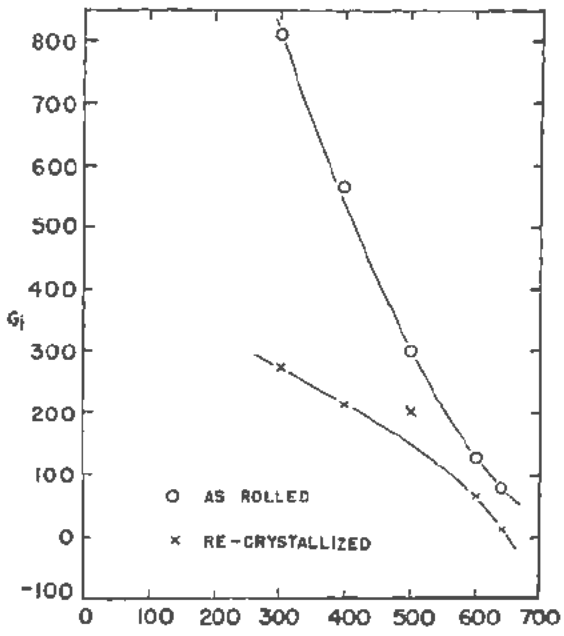

Figure 8. Effect of rolling temperature on the irradiation growth rate of oval-rolled uranium

to inhibit transformation after initial solution heat treatment. For example, approximately 10% of molybdenum in uranium gives excellent dimensional stability when the alloy is irradiated in the gamma condition.

The presence of variable quantities of carbon in uranium has a small and somewhat anomalous effect upon the observed rates of irradiation growth. In low chromium or zirconium alloys in the rolled and alpha recrystallized condition the growth is somewhat enhanced, whereas it is retarded in the same material after it has been quenched from the beta phase. Unalloyed uranium does not seem to react to variations in carbon content.

Irradiation Variables

In general, the growth of uranium specimens under irradiation is found to be an exponential function of the burnup, which depends upon total integrated flux (see Equation 1). However, total flux is the product of time and instantaneous flux, which chiefly determines the temperature at which the irradiation proceeds. The higher is the instantaneous flux, the higher also is the burnup rate and temperature, if other conditions remain constant.

Some of the growth rate data obtained from identical specimens irradiated under different flux conditions when plotted against burnup have enough scatter to strongly suggest a secondary dependence upon irradiation temperature. The degree of scatter is considerably reduced when a semilogarithmic plot of growth rate against inverse temperature is made (see Fig. 9), although a straight-line relationship does

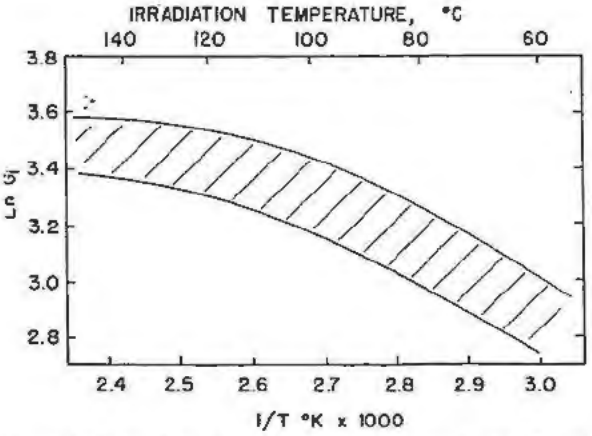

Figure 9. Effect of irradiation temperature on growth rate (G_ϵ) of 300°C-rolled and beta quenched uranium

not result from this treatment. It is not unlikely that the activation energy required for the growth phenomenon should vary with temperature, as the mechanisms resulting in growth are doubtless in competition with other temperatures sensitive healing mechanisms such as recombination of vacancies and interstitials.

There is a great scarcity of accurate data whereby the complete relationship between the irradiation variables and property damage in fuel metals may be deduced, but the effect of temperature will probably prove to be a fruitful field of investigation. Further definitive work needs to be done in this area.

MISCELLANEOUS PROPERTY CHANGES

Thus far our discussion has been devoted to the striking changes in dimensions which certain variable conditions are able to induce in uranium under irradiation. It is understandable that this phenomenon is of primary interest from the engineering viewpoint. We shall now consider briefly other interesting irradiation effects which have been observed, most of them dealing with properties of the metal which have an important bearing on its performance as fuel in a reactor. In general, available information is quite limited and much work needs yet to be done to complete our understanding of the effect of irradiation upon these properties.

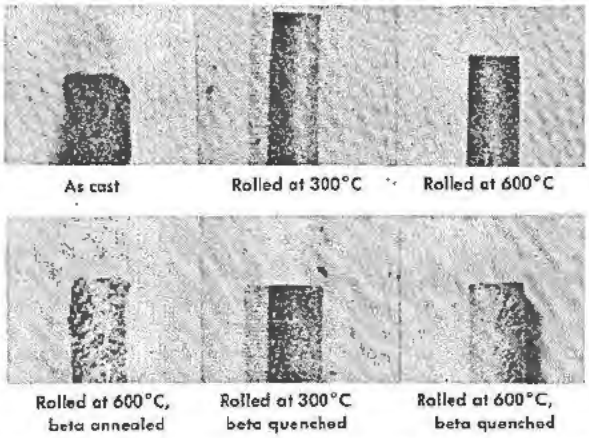

Figure 10. Relative appearance of various uranium specimens after irradiation to 0.1% atom burn-up

Surface and Volume Effects

A second order, but none the less characteristic, result of the dimensional instability of uranium is the distortion of the surface which occurs. The roughening becomes progressively worse as burnup increases, but its distinctive appearance is a function of the grain size and degree of preferred orientation. Figure 10 shows the extremes of this behavior.

In large-grain random material, such as gamma recrystallized or as-cast uranium, the surface is distorted by an "orange-peel" effect which is so gross that the contours of the specimen are rapidly destroyed. Fine-grain random material, such as uranium which has had a fast beta cycle and quenching after alpha rolling, roughens with a fine surface irregularity which does not radically change the specimen shape. The effect is intermediate in coarseness for intermediate grain sizes which result from beta annealing or from beta quenching hot rolled uranium.

In alpha worked or alpha worked and recrystallized material the effect is quite different. Although the same dependence upon grain size is shown, the surface remains much smoother than for comparable random-grained specimens. Roughening is not equiaxed, but develops as longitudinal striations and ridges into a characteristic woody appearance.

In spite of radical changes in dimensions and shape during irradiation, the volume of uranium specimens experiences only a very nominal shift. This change is remarkably independent of differences in metallurgical history and composition, and is equal in per cent to about twice the burnup which has occurred. Only half of this change can be accounted for by the creation of fission products. Figure 11 shows the change in immersion density as a function of burnup, and indicates the degree of scatter which has been observed in testing many different specimens.

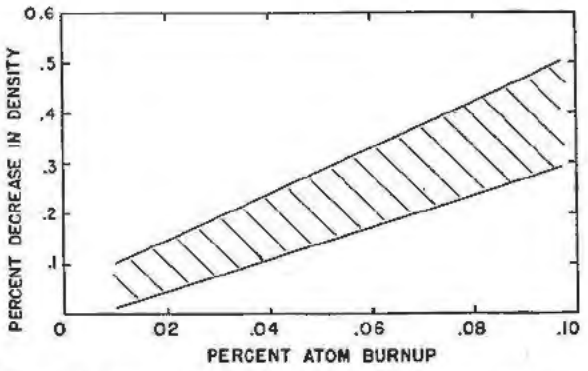

Figure 11. Decrease in density in uranium and uranium-rich alloys as a function of atom burn-up

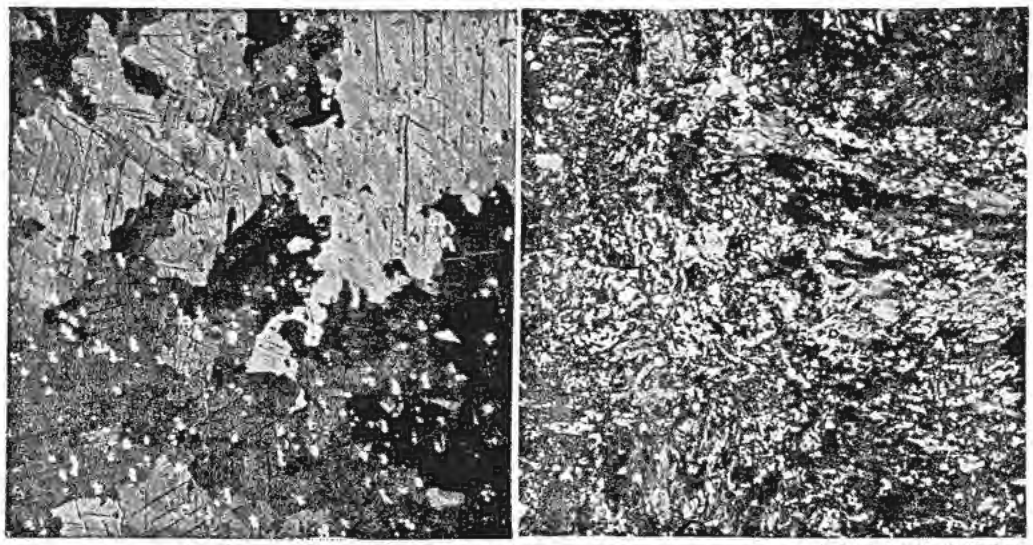

Figure 12. Effect of irradiation on the metallographic structure of uranium, (100 diameters, polarized light): (left) beta quenched uranium before irradiation; (right) beta quenched uranium after irradiation

Table III. X-ray Diffraction Line Broadening in Uranium at 0.1% Total Atom Burnup*

Crystallographic lattice plane	*Per cent increase in X-ray line width at half height*	*Ratio of line intensities in irradiated and control specimens*
(110)	36	1.4
(021)	26	0.9
(111)	20	1.0
(131)	48	0.9

* Cummings and Hurst (GE-HAPO).

Metallographic and X-ray Behavior

The metallographic appearance of polycrystalline uranium is altered by irradiation. Photomicrographs in Fig. 12 illustrate the change which occurs in beta quenched material. Whereas the pre-irradiation structure is fully recrystallized and the grains sharply outlined by polarized light, the structure after irradiation appears to be badly distorted as if by cold work and almost unable to give any distinctive rotation to polarized light. The "cold work" is the result of internal adjustment of the structure by the interference of randomly oriented grains which have been restrained from growing about 50% longer in the [010] direction.

As should be expected, the X-ray structure of equiaxed polycrystalline uranium is also affected by irradiation. Tucker and Senio (GE-KAPL) were the first to identify line-broadening in the X-ray diffraction spectrum, using very lightly irradiated material as the subject of their study. Cummings and Hurst (GE-HAPO) later used a special shielded double crystal spectrometer to examine more heavily irradiated material which had suffered a burnup of 0.1% of total atoms. Working on cross sections of rolled and alpha recrystallized bar they obtained pre- and post-irradiation comparisons from four lines. The degree of broadening, shown in Table III, is similar to what might be expected from moderate cold working of the structure.

Tensile Properties and Hardness

The tensile properties of uranium are strongly affected by moderate irradiation. Hueschen and Cadwell (GE-HAPO) report that 0.035% atom burnup

Table IV. Effect of Irradiation on the Strength Properties of Standard 0.250" Diameter Uranium Tensile Bars*

Description of specimen	*Ultimate strength*		*Yield strength*		*% Elongation*		*Young's Modulus*
	(1000 psi)	*% Change*	*(1000 psi)*	*% Change*	*(1 in. Gauge)*	*% Change*	*(10^6 psi)*
Control specimen	104	–	33	–	17	–	25
Irradiated at 120°C to 0.035% atom burnup	76	—27	71.5	117	0.36	—97.9	28
Irradiated, annealed 15 hours at 400°C in vacuo	65	—38	52	58	0.54	—96.8	–
Irradiated, hot tensile at 285°C	71	—32	70	112	0.7	—95.9	12

* Tabulated from data by Hueschen and Cadwell (GE-HAPO).

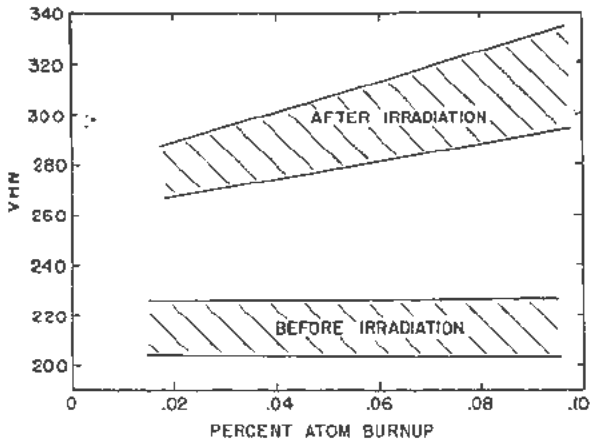

Figure 13. Change in Vickers hardness of uranium as a function of burnup (recrystallized before irradiation)

at 120°C is sufficient to decrease the ultimate strength by one-fourth, to double the yield strength, and to practically destroy the ductility of the metal. Data reported by these investigators are presented in Table IV. The ductility is not significantly restored by long-term annealing at the alpha recrystallization threshold (~400°C), although ultimate strength is attenuated still further by this treatment. These results are believed to indicate that damage to the strength and ductility of uranium by irradiation is in the main due to the presence of fission product atoms as impurities rather than to the disordering of the uranium lattice by thermal spikes.

Appreciable hardness changes occur during the irradiation of uranium. The behavior of rolled and alpha recrystallized metal, shown graphically in Fig. 13, is a good illustration of this effect. In a large groups of tests the average pre-irradiation hardness Vickers Hardness Number 214 ± 12 increases to averages of 275 ± 10 at 0.01% burnup and 315 ± 20 at 0.10% burnup. The individual tests in this group were made on the Rockwell A hardness scale and converted to Vickers by use of a series of uranium test blocks. Hardoess changes in as-rolled material are of the same order of magnitude, but with a trend to much greater scatter.

Thermal Conductivity

Of special importance to reactor engineering is a knowledge of the thermal conductivities of fuel materials. This is a difficult property to measure directly with accuraey, and the normal difficulties are greatly aggravated by irradiation of the subject material. For this reason, electrical conductivity measurements are usually taken and considered as an analog from which may be gained a rough idea concerning thermal conductivity changes.

A recent thermal measurement has been made on irradiated material by two teams of investigators: Deem, Calkins *et al.* (BMI), and Paine and Rothman (ANL), using a heat-wave method and an equilibrium method, respectively. The results are in good agreement and indicate that a low zirconium alloy of uranium suffers a loss of approximately 5% in thermal conductivity at a burnup of 0.1% of total atoms. This preliminary result may be taken to indicate the order of magnitude of irradiation-induced change which may be expected in uranium and high-uranium alloys.

Diffusion Couples

Contact of fuel uranium and its alloys with structural metals in the fuel configuration of a reactor is essential. If no barriers exist, such as oxide films, interdiffusion oay occur at the proper temperature levels. The possibility that the presence of energetic neutrons and fission product atoms will enhance solid-solid diffusion has been investigated.

Results obtained thus far indicate that the dynamics of uranium-structural metal systems are probably not appreciably affected by irradiation. For example, interdiffusion of uranium-235 with stainless steel at temperatures approaching the eutectic has been shown by Weil (ANL) to be indifferent to the presence of fluxes in the order of 10^{12} n/cm²-sec. There are indications that the uranium-aluminum system is equally insensitive. Interdiffusion at elevated temperatures may itself be a serious problem in eogineering of the reactor core, but the present data permit the reasonable conclusion that the problem is not aggravated by a radical irradiation effect.

Aqueous Corrosion Resistance

The incompatibility of uranium with water is well known. Therefore, much interest has been attached to a search for uranium alloy systems which will resist aqueous corrosion at the reactor temperatures necessary for efficient power production.

The addition of at least 3% niobium or 5% zirconium and proper heat treating is necessary in order to achieve a significant lowering of the corrosion rate. The fully homogenized epsilon U_3Si compound is also known to have good properties when tested outside of a reactor. However, when such materials are tested after irradiation or while irradiation is proceeding, the corrosion resistant properties are found to be adversely affected at temperatures below 300°C. Gamma-queoched U-5 wt % Zr-1.5 Nb alloy

Table V. Exomples of Pre- ond Post-Irradiation Corrosion Resistance in Uranium Alloys, Compiled from ANL Data

Composition	*% atom burnup*	*Corrosion resistance (cracking and weight loss)*
3% Nb, gamma quenched	None	No failure after 2000 hours at 260°C. Avg. weight loss rate, 4.3 mg/cm²-day.
	0.1	Disintegrated after 1 hour at 260°C.
5% Zr-1.5%	None	No failure after 360 days at 265°C. Avg. weight loss rate, 2.7 mg/cm²-day.
Nb, gamma quenched	0.04	Cracking after 63 hours at 260°C. Avg. weight loss rate, 23 mg/cm²-day.

specimens have somewhat better properties in unirradiated tests, but they also are damaged by irradiation so that the corrosion rates are considerably increased. Some comparative data are given in Table V.

Alloys of uranium containing 9% molybdenum or more have greatly improved temporary corrosion resistant properties. The resistance during test, however, finally ends and sudden failure occurs. After irradiation the behavior is qualitatively quite similar, but the period of time during which the corrosion rates are low is appreciably shortened and the final failure occurs sooner.

It may be concluded that the ability of uranium alloys to resist corrosion is impaired by irradiation. Martensitic zirconium, niobium and zirconium niobium alloys and the homogenized U_3Si compound are more adversely affected than molybdenum alloys in which the gamma phase has been stabilized.

CONCLUSION

Objectively, it is recognized that in the foregoing account only the framework of knowledge concerning irradiation effects in uranium and its alloys has been reviewed, condensed in some areas and showing large gaps in others. Because of the difficulties peculiar to irradiation experimentation, filling and integrating these gaps will take much more time than ordinary physical metallurgy research.

From the subjective viewpoint, it is impossible to have worked with such a material as uranium for several years without forming some distinct reactions concerning its unconventional behavior. Candidly, it is not a very satisfactory engineering material for use in a nuclear reactor. It refuses to retain its dimensions and shape during irradiation unless treated with the utmost consideration, and assumes a defiant attitude toward the best efforts to surmount its idiosyncrasies and make it behave like a proper metal. Its only virtue is that it fissions. Some success has been achieved in bending it to the will of the reactor engineers, and we are confident that the problems of doing so are not all insurmountable. The headaches which may be involved in their solution are offset by the fascination of studying a truly unusual metal.

REFERENCES

1. Chiswick, H. H. and Kelman, L. R., P/557, *Thermal Cycling Effects in Uranium*, Volume 9, Session 18B.1, these Proceedings.
2. Lloyd, L. T. and Chiswick, H. H., (ANL), *Deformation Mechanisms of Alpha Uranium Single Crystals*, (to be published).
3. Jillson, D. C., (New Jersey Zinc Company of Pennsylvania), *An Experimental Survey of Deformation and Annealing Processes in Zinc*, Trans. AIME, *188*: 1009 (1950).
4. Nabarro, F. R. N., *Deformation of Crystals by the Motion of Single Ions*, Rep. Conf. Strength of Solids, Phys. Soc., London, 75 (1948).
5. Herring, C., *Surface Tension as a Motivation for Sintering*, Physics of Powder Metallurgy (W. E. Kingston, Editor), p. 143 (McGraw-Hill Book Co., N.Y.C., 1951).
6. Herring, C., *Diffusional Viscosity of a Polycrystalline Solid*, J. Appl. Phys., *21*: 437 (1950).
7. Alexander, B. H. and Balluffi, R. W., *Experiments in the Mechanism of Sintering*, Trans. AIME, *188*: 1219 (1950).
8. Buttner, F. H., Funk, E. R. and Udin, H., *Viscous Creep of Gold Wires Near the Melting Point*, Trans. AIME, *194*: 401 (1952).

Irradiation Damage to Artificial Graphite

By W. K. Woods, L. P. Bupp and J. F. Fletcher,* USA

The properties of artificially manufactured graphite make it a very suitable material for use in a nuclear reactor, both as a moderator and as a structural component. Of particular advantage are its mechanical strength, moderating properties, low neutron absorption cross section, refractory and heat conducting properties, and availability in large quantities at low cost. However, irradiation in a reactor produces basic changes in the crystalline structure of graphite which result in large changes in its physical properties.

There exists a vast quantity of experimental data, largely empirical, on irradiation damage effects in graphite. The results obtained from irradiation of a given sample are in many instances dependent upon the fabrication history of the graphite and are very sensitive to the temperature at which the sample is irradiated; reproducible results are obtained only if these factors are kept under close control.

The bulk of the data has been obtained from irradiation of graphite samples in the production reactors at Hanford. In addition to limited amounts of data from other reactors with lower neutron flux intensities, the data have recently been augmented by irradiations in the high flux of the Materials Testing Reactor at the National Reactor Testing Station.

This report consists of a compilation of representative data on the effects of irradiation on graphite. Particular attention is given to those effects most pertinent to the evaluation of graphite as a reactor material. The source material for this report consists of a large body of hitherto classified reports which have not yet been made available for public release.

THE MANUFACTURE OF GRAPHITE

Artificial graphite is produced by the partial recrystallization, at high temperature, of suitable carbonaceous materials. The raw materials for graphite manufacture consist of various grades of petroleum cokes, used as fillers, and coal tar pitch binders. The coke is calcined, ground and/or milled, mixed to produce the desired particle size distribution, and mixed with the pitch until a fairly uniform plastic mass is obtained. This mixture may then be formed into the desired shapes by extrusion or pressure molding; most of the reactor grade graphite has been made to date by the extrusion method.

The formed shapes are given a preliminary bake at about 900°C to remove volatile components. Following the preliminary bake the shapes may be impregnated with additional pitch, if desired, to increase the bulk density of the graphite.

The shapes are then given a final graphitizing bake in an Acheson electric resistance furnace in which the graphite is heated, normally, to 2800°C. Alternatively, the shapes may be graphitized in the so-called GBF furnace, a controlled-atmosphere electric resistance furnace in which a graphitizing temperature of about 2500°C is usually employed.

Additional information on the subject of graphite manufacture is given in the paper by Currie, Hamister, and MacPherson.[1]

The various grades of extruded graphites considered in the United States as reactor grade are designated in this report according to the nomenclature of Table I. Special or non-standard types are described in the text.

The physical properties of artificial graphite may be varied over a wide range by selection of raw materials and by variations in the manufacturing process; the term "graphite" is analogous to the term "steel" in this respect.

Table I. Nomenclature of Graphites

Designation	*Filler*	*Binder*	*Manufacturing process*
CSF	Cleves*	Standard¶	Acheson Process
CS-GBF	Cleves	Standard	GBF Process
KC	Kendall†	Chicago**	Acheson Process
KS	Kendall	Standard	Acheson Process
WSF	Whiting‡	Standard	Acheson Process
WS-GBF	Whiting	Standard	GBF Process
TS-GBF	Texas§	Standard	GBF Process

* Petroleum coke (mid-continent crudes) from the Gulf Oil Company refinery at Cleves, Ohio.

† Petroleum coke (Pennsylvania crudes) from the Kendall Oil Company refinery at Bradford, Pennsylvania.

‡ Petroleum coke (mid-continent crudes) from the Standard Oil Company (Indiana) refinery at Whiting, Indiana.

§ Petroleum coke (mid-continent crudes) from the Texas Company refinery at Lockport, Illinois.

¶ No. 2 medium-hard coal tar pitch manufactured by the Barrett Company.

** Barrett-Chicago No. 7HO coal tar pitch manufactured by the Barrett Company.

* General Electric Company, Richland, Washington. Including work by Argonne National Laboratory; Battelle Memorial Institute; Brookhaven National Laboratory; General Electric Co., Hanford Atomic Products Operation; General Electric Co., Knolls Atomic Power Laboratory; North American Aviation, Inc., Nuclear Engineering and Manufacturing Department.

Graphite exhibits anisotropy in varying degrees owing to the varying orientation of crystallites. In extruded graphite, the planes of the crystals tend to be oriented parallel to the direction of extrusion, whereas in molded graphite the orientation of the crystal planes is at right angles to the direction of applied pressure. Orientation of the graphite crystallites occurs during the forming process and the degree of orientation is dependent upon the geometry of the coke filler particles and the amount of forming pressure used.

In addition to the varying anisotropic behavior, wide variations in the physical properties of graphite may be obtained, dependent mainly on the crystal lite properties. These physical properties may be controlled by selection of raw materials and by variations in the manufacturing process, particularly the temperature and time of graphitization.

IRRADIATION OF GRAPHITE

The size of graphite samples irradiated in a reactor is dictated by the requirements of the facility in which they are placed. Although sample dimensions vary somewhat for various facilities, the "standard" sample used in most cases is a cylinder about one-half inch in diameter and four inches long. Physical properties are normally measured with respect to the long axis of the sample; it is important to know the orientation of the sample with respect to the bar from which it was cut. This orientation is designated as the "cut" of the sample, and is specified as transverse or parallel depending on whether the sample axis is oriented perpendicular or parallel to the long axis of the extruded bar.

Unless otherwise specified, all irradiations discussed in this report were conducted in cooled test hole facilities at Hanford. A cooled test hole facility consists of a tubular aluminum shell containing a bundle of smaller tubes which contain the samples. Water circulates between the shell and the tube bundle to cool the facility. Temperatures vary from 20°C to 40°C, averaging 30°C. The facility is installed between and perpendicular to the uranium-filled process tubes; small differences in neutron flux are encountered depending on the proximity of the sample to the process tube.

Some samples have been irradiated in a process tube facility at Hanford. In this facility an inner tube which contains the samples is fitted into a process tube, replacing the usual uranium charge. This inner tube also contains an electric resistance heater for regulating the temperature of the graphite samples. Cooling water flows in the annulus between the inner tube and the process tube.

For "capsule" exposures at Hanford, the samples are encased in water-tight aluminum cans and loaded into process tubes between pieces of uranium. These samples are subjected to a more energetic neutron flux and the temperature of the sample is less well established.

For irradiation in the Materials Testing Reactor, graphite samples are encased in aluminum cans, the cans are inserted into the reactor immediately adjacent to the active lattice, and cooling water is circulated around the cans. Heat generation rates in these facilities are high enough that sample temperatures are strongly dependent on the design of the sample cans.

Conventionally, exposures in the Hanford reactors have been reported in terms of "megawatt-days per ton of uranium," abbreviated Mwd/t. This unit is defined as the irradiation exposure received by the sample during the period required for the (2000-lb) ton of uranium metal in the immediate vicinity of the sample to generate one megawatt-day of fission heat. For Hanford cooled test hole irradiations one Mwd/t of exposure is equivalent to an integrated neutron flux (total nvt) of 6.46×10^{17} neutrons/cm^2. Other conversion factors apply for other facilities.

The exposure received by graphite samples irradiated in the Materials Testing Reactor are reported in units of reactor megawatt-days. Conversion of these units to neutrons/cm^2 is difficult not only because of uncertainties in the neutron energy spectrum but also because of the extreme variations in neutron flux intensity which exist within a facility. In practice, one reactor megawatt-day is considered equivalent to 1.15×10^{18} thermal neutrons/cm^2 or about 1.25×10^{15} total neutrons/cm^2. Materials Testing Reactor exposures as presented in this report actually are in terms of thermal nvt.

EFFECTS OF IRRADIATION ON PHYSICAL PROPERTIES

Damage to the crystallite structure of graphite is incurred during irradiation in a reactor, causing significant and often severe changes in the over-all physical properties of the graphite. The mechanical properties are improved; the hardness and strength of the graphite are increased. Other physical properties are detrimentally affected. Thermal and electrical conductivities decrease; graphite shapes exhibit changes in their gross dimensions; and several other effects, such as the storing of potential energy, are encountered. All effects are decreased in magnitude when the temperature of the graphite during irradiation is increased.

None of the data obtained to date from irradiations in the Hanford reactors indicates any dependence on the neutron flux intensity, or the rate at which exposure is accumulated. Such a dependence on flux intensity, if present, is masked by the effects of small temperature variations in the samples during irradiation and by small differences in the initial properties of presumably duplicate samples. However, recent irradiations in the Materials Testing Reactor have produced some results which are in quite poor agreement with the results obtained from Hanford irradiations. Whether these differences are caused by the higher neutron flux intensity in the Materials

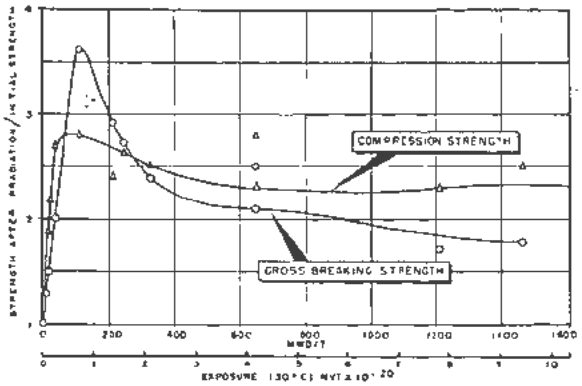

Figure 1. Changes in mechanical strength as function of exposure for parallel cut KC graphite

Testing Reactor, by differences in the neutron energy spectra in the different reactors, or by other factors has not been ascertained as yet.

In general, observations of the physical properties of irradiated graphite are made at room temperature (about 25°C).

Mechanical Properties

The effects of irradiation upon the mechanical properties of graphite are to produce a stronger, harder, and more brittle material. Consequently, irradiation effects on the mechanical properties of graphite have been of little immediate concern in the operation of graphite moderated reactors, and the amount of reliable data obtained under controlled conditions is limited.

The variation in compression strength and cross-breaking strength of parallel cut KC graphite as affected by irradiation is shown in Fig. 1, and variation in Young's modulus for the same samples is shown in Fig. 2. The property changes are shown as ratios of the values after irradiation to the average values for pre-irradiated KC graphite. Pre-irradiation values are: Compression strength, 4050 lb/in^2; cross breaking strength, 1420 lb/in^2; Young's modulus, 1.71×10^6 lb/in^2.

Irradiation of graphite produces a tougher, harder graphite which is more difficult to machine. This is

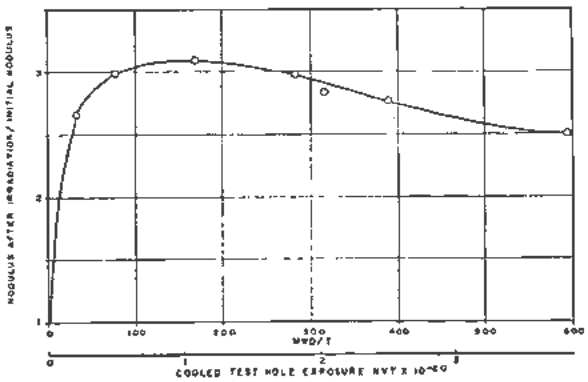

Figure 2. Change in Young's modulus with exposure for parallel cut KC graphite

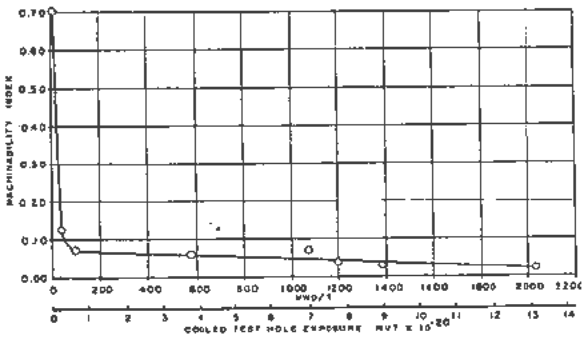

Figure 3. Machinability of CSF graphite as a function of exposure

illustrated in Fig. 3, in which the machinability index is the depth of penetration of a carbide-tipped drill in a standardized drilling test.

Thermal Conductivity

Brief irradiations produce large decreases in the thermal conductivity of graphite, or large increases in the thermal resistivity. The conductivity continues to decrease, though less rapidly, with prolonged irradiation.

Figure 4 shows the exposure dependence of thermal resistivity for parallel cuts of several grades of graphite, while Fig. 5 shows the corresponding variation for transverse samples. Initial values of thermal conductivity for these graphites are shown in Table II. The values for conductivity shown in Table II have in some instances been reduced by factors greater than 50 by irradiation.

Table II. Thermal Conductivity of Unirradiated Graphite

Grade	*Parallel conductivity cal/cm/sec/°C*	*Transverse conductivity cal/cm/sec/°C*
KC	0.43	0.27
CSF	0.40	0.26
TS-GBF	0.20	0.18

Changes in the thermal conductivity of transverse cut CSF graphite as affected by the temperature of irradiation are shown in Fig. 6. The data at low exposure temperature are the same data plotted in different form on Fig. 5. The remainder of the data were obtained by the irradiation of graphite samples at controlled temperatures in a Hanford process tube facility. The effects induced by irradiation are markedly reduced at higher temperatures of irradiation.

Irradiation at 30°C results in a change of the temperature coefficient of thermal conductivity from a negative to a positive value. This is illustrated in Fig. 7, which shows the change in thermal conductivity with temperature for unirradiated parallel cut KC graphite and for samples of the same material irradiated to 6.35×10^{20} neutrons/cm^2. If plotted to the same ordinate scale, the two lines in Fig. 7 are convergent and would presumably meet at some high temperature.

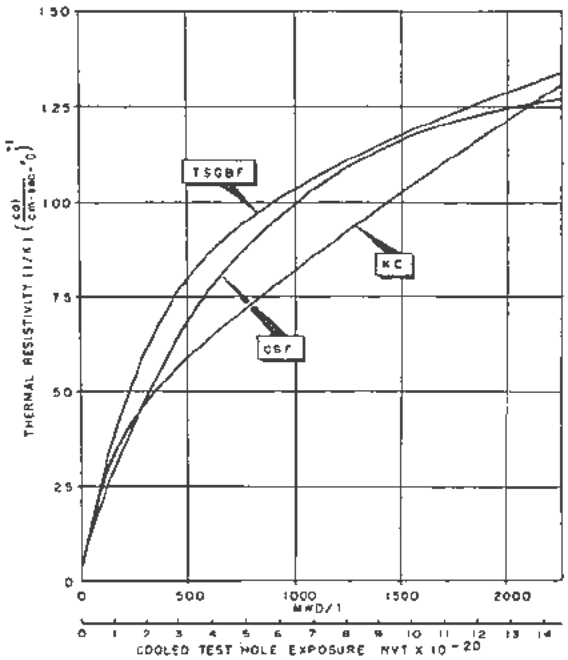

Figure 4. Radiation damage to thermal conductivity of parallel cut graphites

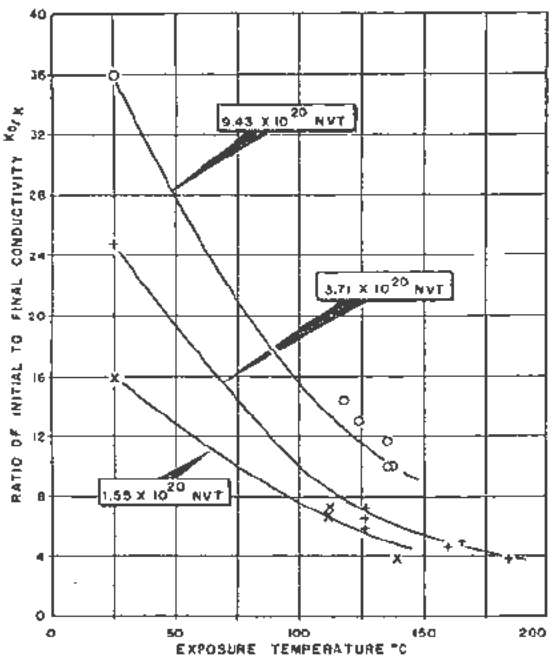

Figure 6. Variations in thermal conductivity of transverse cut CSF graphite with exposure temperature

Electrical Resistivity

The electrical resistivity of graphite is not of importance in the evaluation of graphite as a reactor component. The measurement of electrical resistivity, however, is useful as an index of radiation damage and is important in theoretical studies of damage. In addition, the simplicity and high accuracy of electrical resistance measurements makes them attractive for theoretical irradiation damage studies.

The electrical resistivity of graphite changes rapidly during the early stages of irradiation. Figures 8 and 9 show, respectively, the electrical resistivities of parallel and transverse cuts of two grades of graphite after irradiation. Initial values of electrical resistivity for these graphites are shown in Table III. The resistivity rises quickly to a maximum at about 2×10^{20} neutrons/cm^2, decreases slightly, and begins a slow increase at exposures above about 10×10^{20} neutrons/cm^2.

The dependence of electrical resistivity changes upon the temperature of exposure is shown in Fig. 10. These data were obtained from the same samples

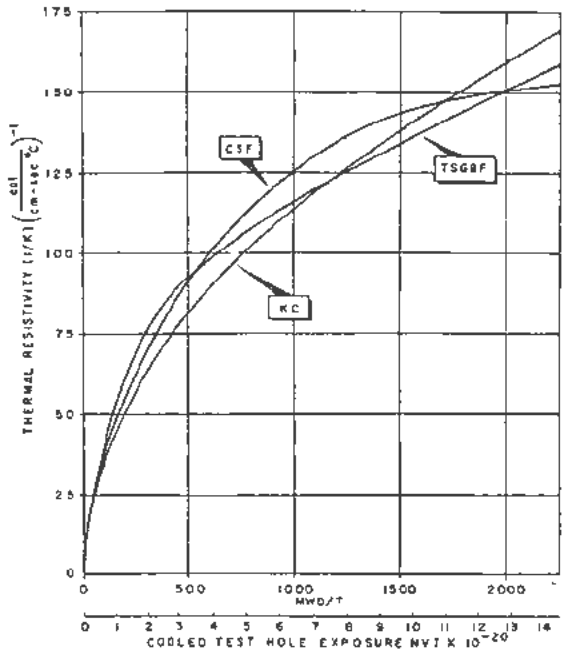

Figure 5. Radiation damage to thermal conductivity of transverse cut graphites

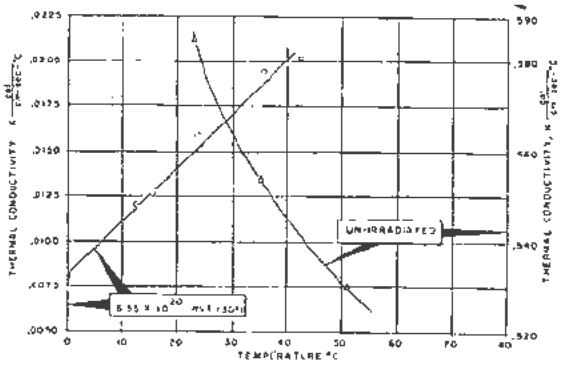

Figure 7. Variation of thermal conductivity with temperature parallel cut KC

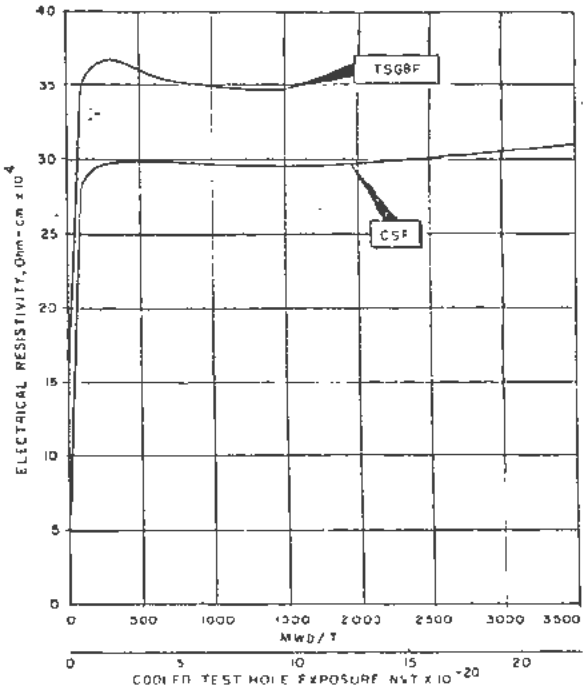

Figure 8. Radiation damage to electrical resistivity of parallel cut graphite

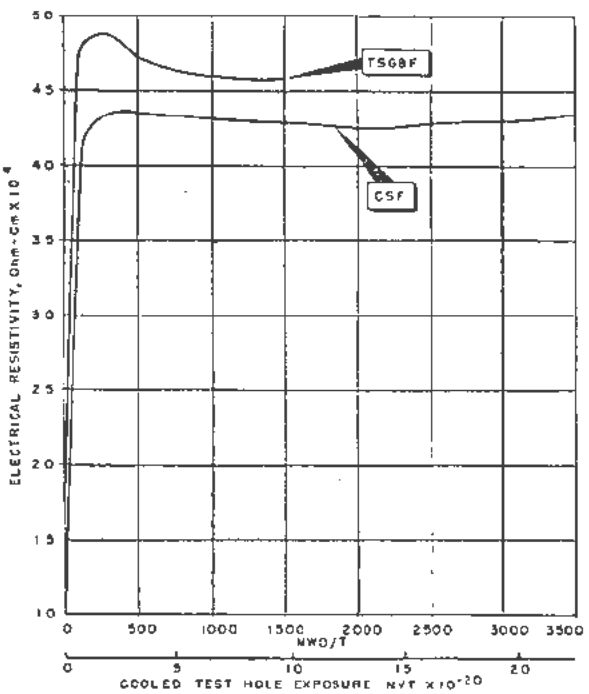

Figure 9. Radiation damage to electrical resistivity of transverse cut graphite

from which data for Fig. 6 were taken. Comparison of Fig. 6 and Fig. 10 leads to the conclusion that electrical resistivity effects are less sensitive to changes in temperature of irradiation than are thermal conductivity effects.

Crystallite Properties

The major effects of radiation upon the crystallite structure of graphite are distortion of the crystal lattice and eventual breakup and disorder of the crystal structure with a trend toward amorphous form. The distortion of the lattice takes the form of an expansion in the C_0, or interplanar, dimension and a shrinkage or warping of the a_0 dimension along crystal planes. Refer to Fig. 11.

These distortions are caused primarily by collisions between atoms of carbon in the graphite lattice and impinging energetic particles, particularly fast neutrons. These collisions result in the displacement of carbon atoms from normal positions within the lattice and the production of lattice vacancies. In addition the displaced atoms, in losing kinetic energy, may produce further lattice distortions.

The crystallite changes induced in graphite by irradiation have been studied extensively by X-ray diffraction techniques. Figure 12 shows typical 002 reflection peaks obtained for graphite irradiated at low temperature. (Note: the C_0 spacing is inversely proportional to the sine of half the angle of diffraction plotted as an abscissa in Fig. 12.) Low expo-

Table III. Electrical Resistivity of Unirradiated Graphite

Grade	*Parallel resistivity ohm-cm × 10⁴*	*Transverse resistivity ohm-cm × 10⁴*
CSF	7.1	11.8
TS-GBF	13.7	18.5

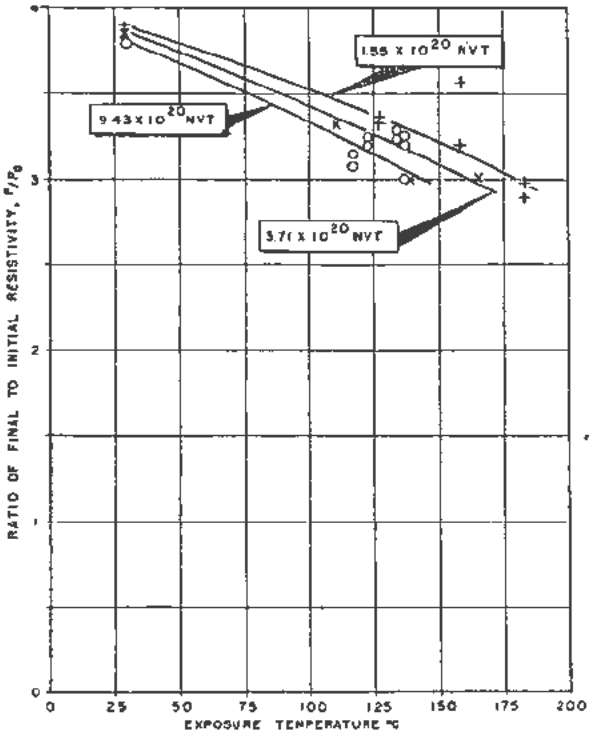

Figure 10. Variations in electrical resistivity of transverse cut CSF graphite with exposure temperature

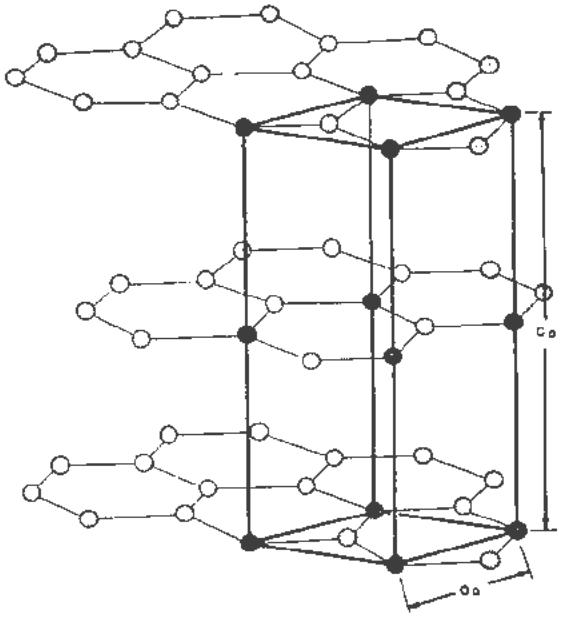

Figure 11. The crystalline structure of graphite: unit cell accented. Normal cell dimensions; $C_0 = 6.70$ Å, $a_0 = 2.46$ Å

sures cause a decrease in the peak intensity and a shift in the angle of diffraction but the peak shape remains essentially constant. At exposures above 4×10^{20} to 6×10^{20} neutrons/cm^2 the peak is broadened progressively at its base until at high exposures the peak becomes very diffuse.

The C_0 spacing of graphite samples is the most readily obtained of the crystallite parameters and is useful as an index of radiation damage. Figure 13 shows the variation of C_0 spacing with exposure for two typical grades of graphite. The C_0 values as reported are uncorrected for small angle scattering and other minor effects. The highest uncorrected C_0 spacing observed to date as a result of irradiation damage is around 8.0 (refer to Fig. 23). This was obtained after irradiation to 20×10^{20} neutrons/cm^2 in the Materials Testing Reactor.

The effect of exposure on the C_0 spacing of graphite crystallites is decreased markedly at higher exposure temperatures. Figure 14 shows the effect of exposure temperature on the change in C_0 spacing.

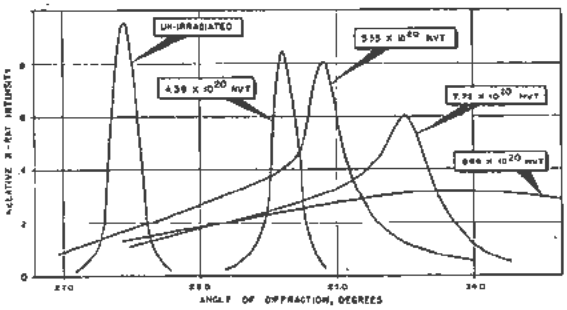

Figure 12. X-ray diffraction line shapes; graphite 002 reflection: effect from irradiation in cooled test holes

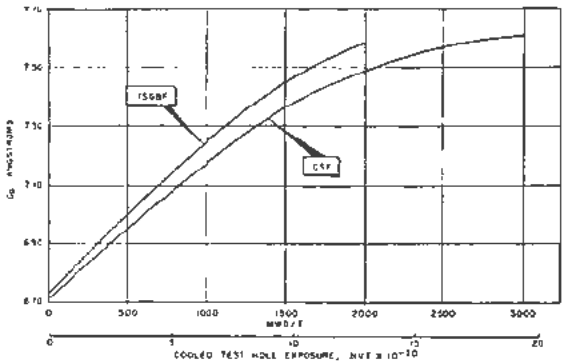

Figure 13. C_0 displacement in irradiated graphite

These data were obtained from the same samples from which data for Fig. 6 and 10 were taken. Figure 15 shows additional data on the variation of C_0 spacing with exposure for various exposure temperatures. The data shown in Fig. 15 came from capsule samples; the temperatures shown are estimated and are probably accurate to within ± 10°C.

The a_0 spacing of irradiated graphite samples has not been studied extensively, both because the experimental data are more difficult to obtain and because the irradiation-induced changes in the a_0 spacing are an order of magnitude smaller than those in the C_0 spacing. The meager data which are available indicate that the a_0 spacing decreases as a result of irradiation.

The increase in C_0 spacing is believed to be caused by the retention of displaced carbon atoms in inter-

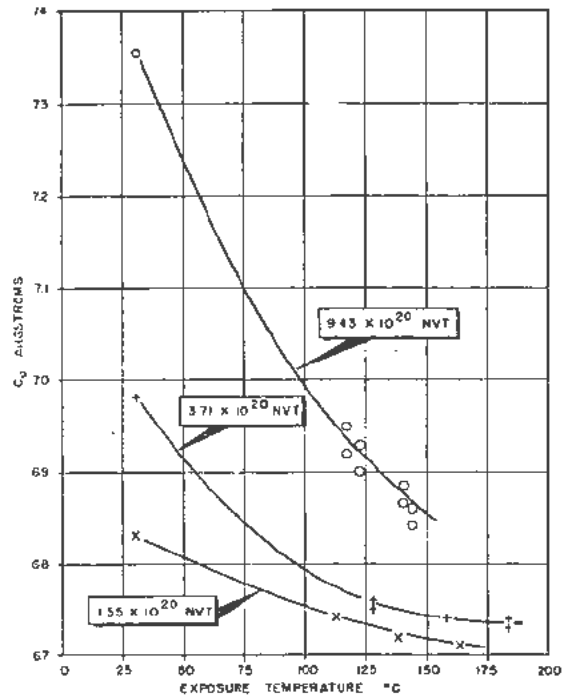

Figure 14. Variations in C_0 displacement of CSF graphite with exposure temperature

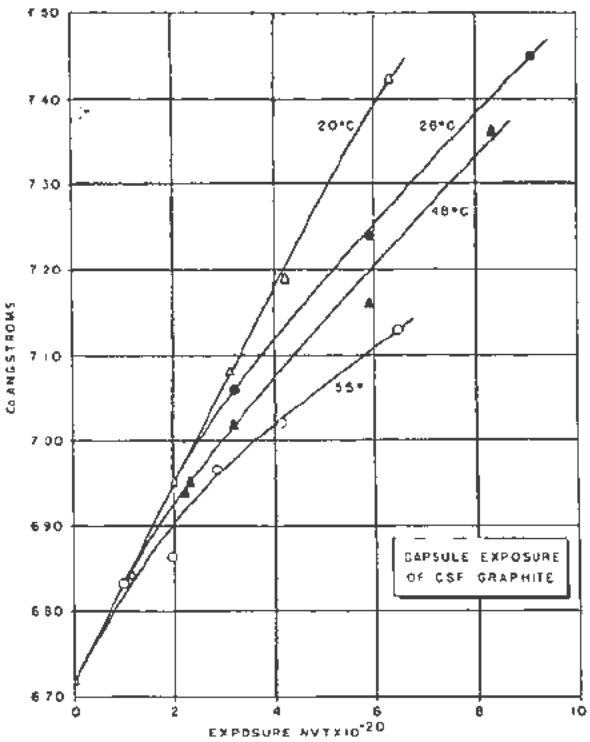

Figure 15. Temperature effects on Co displacement: capsule exposure of CSF graphite

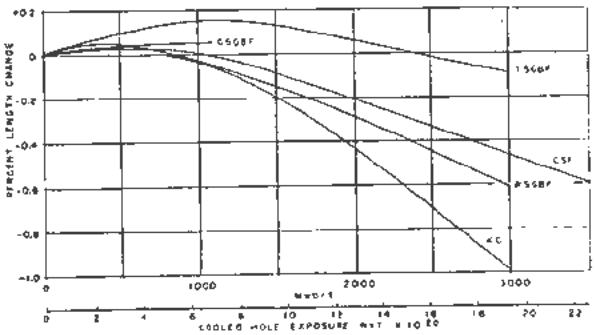

Figure 17. Physical distortion of parallel cut graphites with irradiation

stitial positions within the lattice, as well as by the corresponding lattice vacancies created by the displacement of these atoms. The broadening of the X-ray diffraction line peak shapes after extended irradiation (above 6×10^{20} neutrons/cm^2) is attributed to bending and slippage of the crystal planes as the crystallites begin to break up. At high exposures (above 13×10^{20} neutrons/cm^2) the crystal structures appear to have reached a state similar to that found in carbon blacks and decomposed organic solids.

Dimensional Stability

The dimensional stability of graphite under irradiation is a property of major interest in the design and operation of a graphite-containing reactor. In general, graphite tends to expand along planes transverse to the preferred axis of crystal orientation and

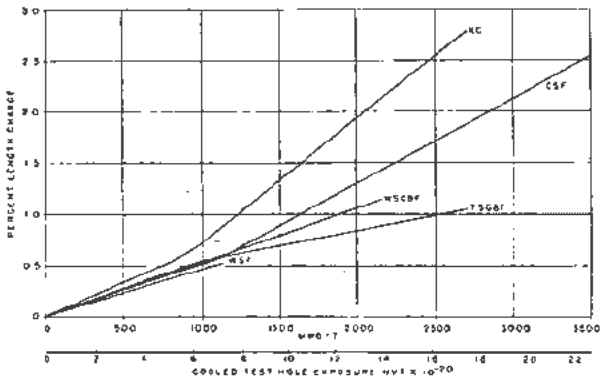

Figure 16. Physical expansion of transverse cut graphites with irradiation

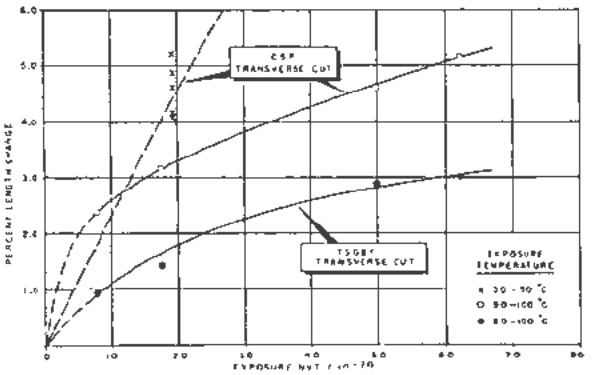

Figure 18. Physical expansion of graphites irradiated in Materials Testing Reactor

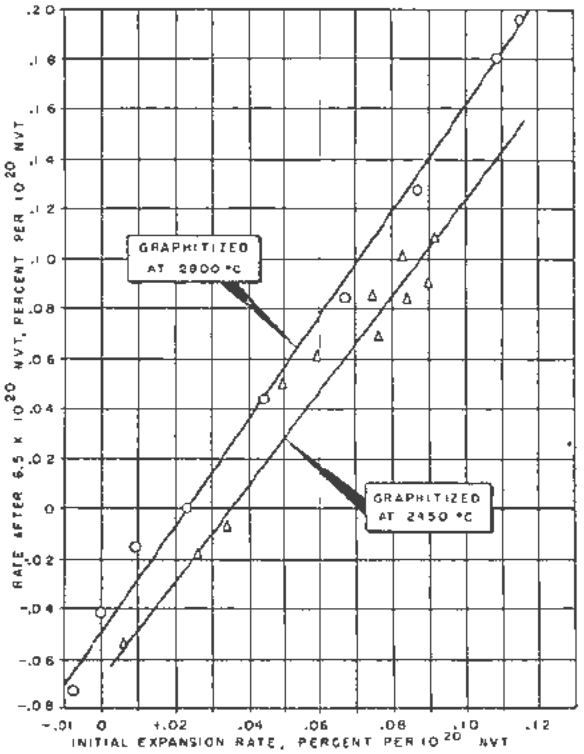

Figure 19. Correlations of expansion rates

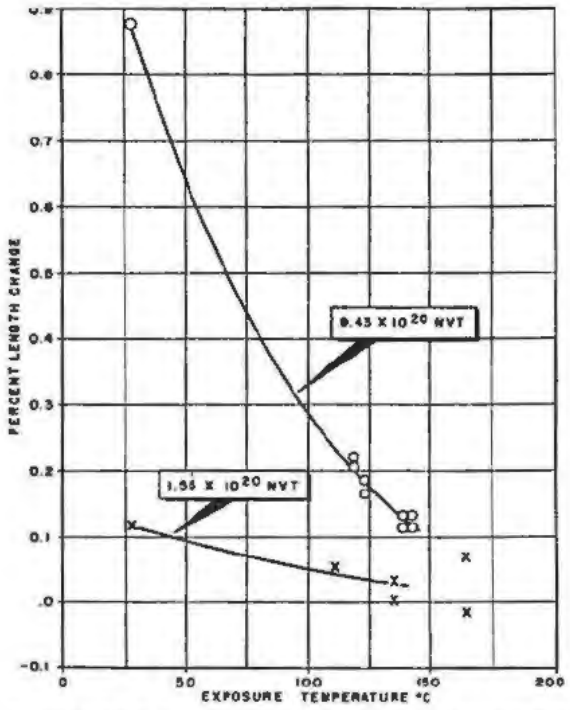

Figure 20. Effects of temperature on physical expansion; transverse cut CSF

to contract along planes parallel to this axis. The behavior varies widely, however, with the degree of orientation attained in the graphite. The over-all dimensional changes are only qualitatively related to the crystallite changes. Some of the variation in performance can be accounted for but other factors remain unknown.

Figures 16 and 17 show the changes in dimensions of several grades of graphite after irradiation. In Fig. 16 note the rather abrupt change in the rate of linear distortion at about 6×10^{20} neutrons/cm^2; it is believed that this may be associated with the broadening of the X-ray diffraction line peak shapes above this exposure. Several parallel cut samples show an expansion at low exposures (refer Fig. 17), followed by a contraction after continued irradiation. This behavior has not yet been explained. The values

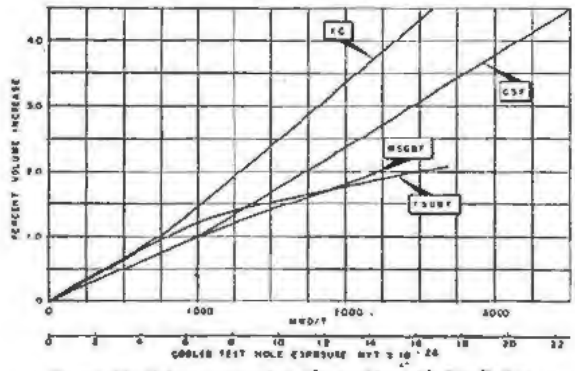

Figure 21. Volume expansion of graphite with irradiation

shown in Figs. 16 and 17 are the averages of a large number of samples; considerable scatter exists in the data.

In striking contrast to the data shown in Fig. 16, a transverse cut sample of graphite made from large natural flake graphite instead of petroleum coke expanded 24 per cent during an irradiation to 25×10^{20} neutrons/cm^2. This rate is an order of magnitude greater than that observed in artificial graphites.

Figure 18 shows data on the physical expansion of graphite after irradiation at low temperature in the Materials Testing Reactor. The temperatures of the samples were not monitored but are estimated to be in two ranges of, respectively, 30 to 50°C and 90 to 100°C. Study of the data shown in Figs. 16 and 18 reveals important differences which have not yet been explained.

The relationship between the low-exposure and the high-exposure expansion rates of several grades of graphite is shown in Fig. 19, which was derived from data used in preparing Figs. 16 and 17. The major variable as shown here appears to be the temperature of graphitization during manufacture of the graphite. Figure 19 suggests the feasibility of using brief irradiations of graphite samples as a measure of the behavior of the material upon extended irradiation. It also indicates that graphite intended to be relatively free of expansion effects upon prolonged irradiation should be characterized by small positive expansion rates during initial periods of irradiation.

The physical distortion of irradiated graphite is dependent on the temperature of exposure. Representative data are shown in Fig. 20. These data were obtained from the same samples used in preparing Figs. 6, 10, and 14.

The volumetric expansion characteristics of several grades of graphite are shown in Fig. 21. These curves were derived from the data shown in Figs. 16 and 17. Every reactor grade graphite investigated to date has shown positive volumetric expansion after irradiation at temperatures of about 30°C.

An interesting direct correlation has been obtained between the physical distortion characteristics of graphite under irradiation in a cooled test hole and the thermal expansion coefficient of unirradiated graphite. Figure 22 shows this relationship, which holds for a number of reactor grade graphites. Representative values for the thermal expansion coefficient of various graphites are given in Table IV.

Table IV. Thermal Expansion Coefficient of Unirradiated Graphite

Grade	*Thermal expansion coefficient, (1/°C × 10⁶)*	
	Parallel	*Transverse*
KC	0.9	5.5
CSF	1.1	4.8
TS-GBF	2.2	4.2
WSF	1.4	4.3

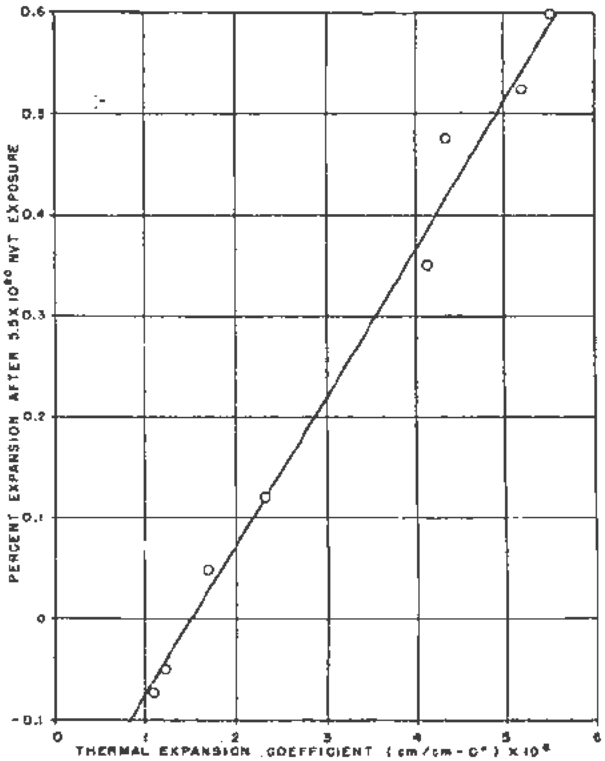

Figure 22. Correlation of physical expansion with thermal expansion coefficient

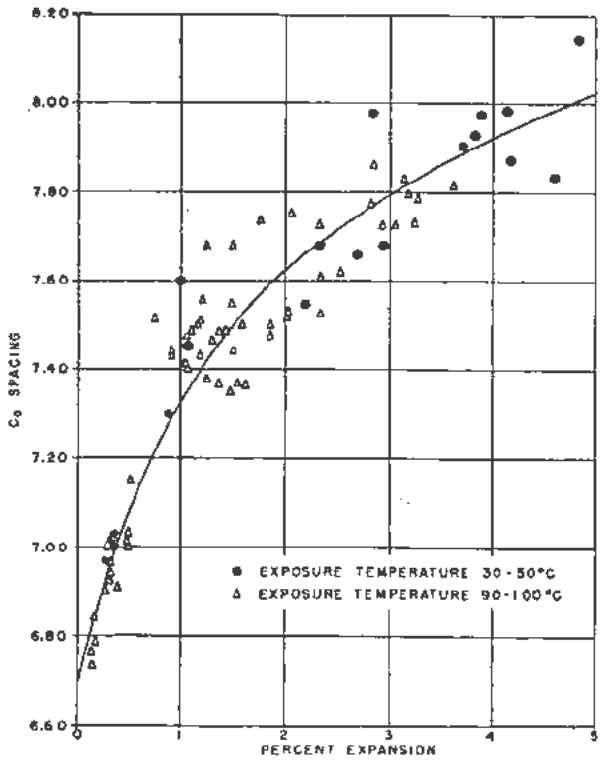

Figure 23. Expansion correlations for materials testing reactor irradiation; transverse cut CSF

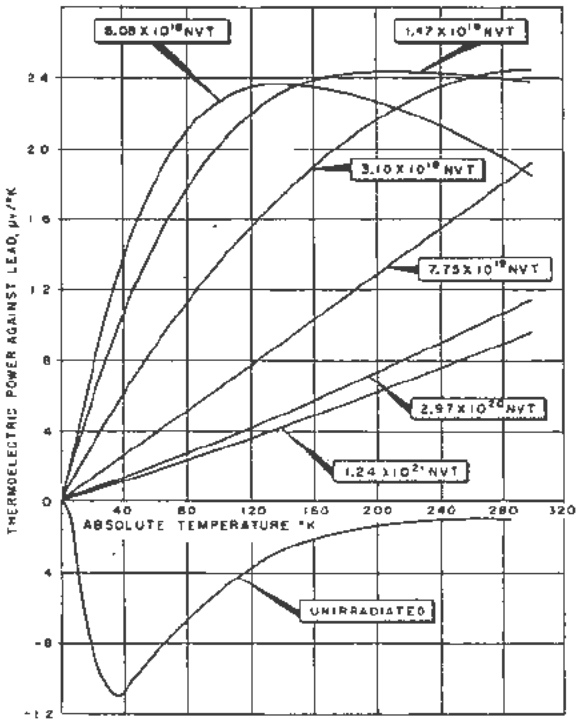

Figure 24. Thermoelectric power of parallel cut XC graphite irradiations at 30°C

Figure 23 shows the relationship between macroscopic expansion and C_0 crystal lattice expansion for CSF graphite samples irradiated in the Materials Testing Reactor. These samples were irradiated under varying conditions of neutron flux intensity, and the exposure received by individual samples is usually not known.

Thermal Expansion

Although conflicting information exists in the literature, most recent data indicate that irradiation has a negligible effect on the temperature coefficient of thermal expansion of reactor grade graphite. In this connection it is sometimes necessary to distinguish the irreversible effects caused by annealing of the radiation-induced distortion from the reversible effects normally considered as thermal expansion.

Specific Heat

Irradiation induces a small increase in the specific heat of graphite when measured at temperatures below the temperature of irradiation. Specific heat determinations were made on one sample of graphite before and after irradiatioo. Although the exposure history of the sample is not known, its total stored energy value (475 cal/gm) indicates an exposure equivalent to about 15×10^{20} neutrons/cm^2 in a cooled test hole. The specific heat at room temperature was increased about 0.006 cal/gm/°C (about 3 per cent) as a result of irradiation.

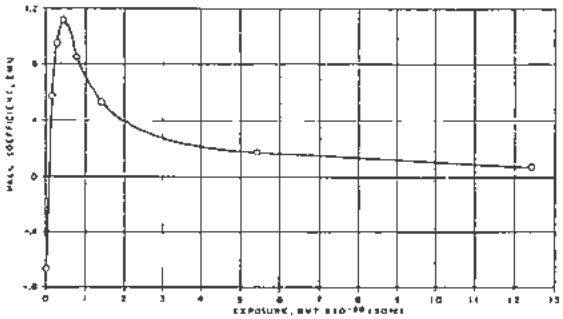

Figure 25. Variations in Hall coefficient of parallel cut KC graphite

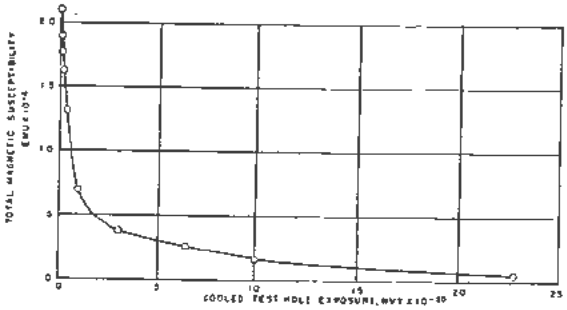

Figure 27. Magnetic susceptibility of KC graphite

Thermoelectric and Magnetic Properties

Considerable work has been done on the determination of the thermoelectric and magnetic properties of irradiated graphite. Typical values of several of these properties are given for KC graphite in Figs. 24 through 27. Although these properties are not important in the engineering consideration of the merits of graphite for nuclear reactor use, they are extremely useful in the theoretical studies directed toward determining a mechanism of irradiation damage. Discussion of these effects is given in a paper by Hennig and Hove.[2]

STORED ENERGY

Irradiation of graphite in a reactor increases the energy content of the crystal lattice. This increase in energy is referred to as "stored energy." The total stored energy in a graphite sample represents an increase in enthalpy, and is observed as an increase in the heat of combustion of the material. Numerous such measurements have been made by the National Bureau of Standards.

Of greater interest than the total stored energy, however, is the nature of the release of stored energy during annealing. Figure 28 shows the total stored energy in irradiated graphite and the stored energy which remains after prolonged annealing at 1000°C. By difference one obtains the amount of stored energy which was released during the annealing, shown as a dotted line on Fig. 28. The first thing to notice is that these stored energy effects are large; 500 calories per gram of stored energy represents the energy required to raise the temperature of a gram of graphite more than 1200°C. The second observation is that all of the stored energy accumulated during brief irradiations can be released by annealing at a temperature of 1000°C, but essentially none of the incremental amounts of stored energy accumulated after exposures greater than 13×10^{20} neutrons/cm² can be released by annealing at a temperature of 1000°C.

An illustration of the effect of annealing highly irradiated graphite at other temperatures is shown in Fig. 29. Twenty-one graphite samples were irradiated under presumably identical conditions, and heat of combustion measurements were made on each sample after annealing at various temperatures. It is noted that the results of Fig. 29 are not in quantitative agreement with those shown in Fig. 28, for annealing at 1000°C did not decrease the residual stored energy as shown in Fig. 29 as much as would

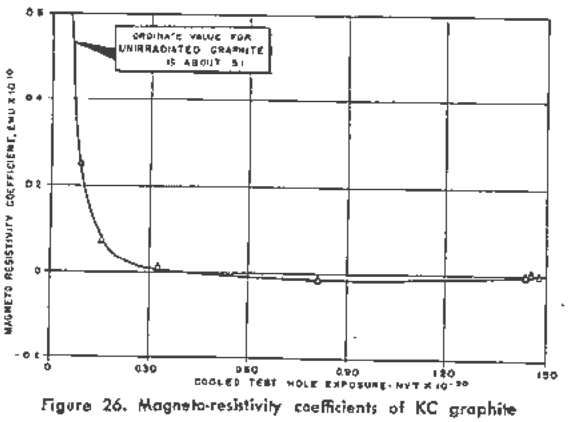

Figure 26. Magneto-resistivity coefficients of KC graphite

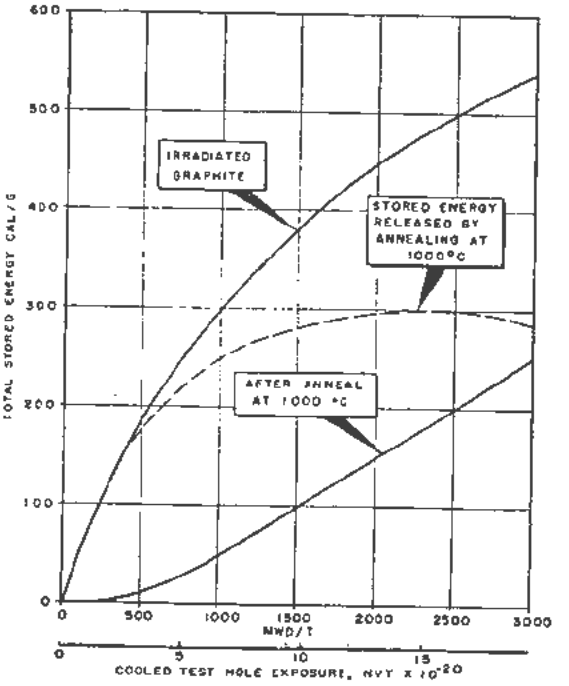

Figure 28. Build-up of total stored energy in irradiated graphite

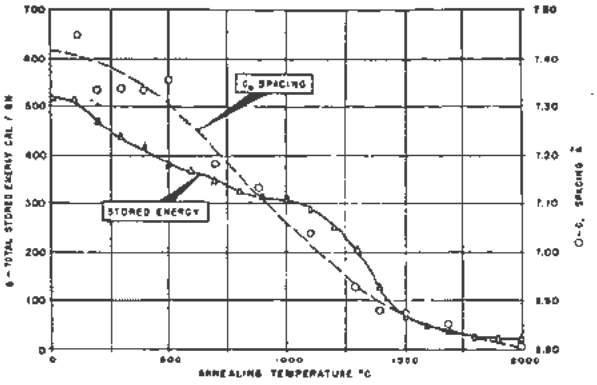

Figure 29. Annealing of total stored energy

he predicted from the curves shown in Fig. 28. Whether this difference is caused by difference in samples, by incomplete annealing, or by experimental error is not known.

Superimposed on Fig. 29 is a plot of the C_0 spacing as measured for the annealed samples. The release of stored energy is associated with a decrease in C_0 spacing back toward normal values observed for unirradiated graphite. However, the sample must be heated close to graphitization temperatures in order to effect complete recovery of either stored energy or lattice distortion for these highly irradiated samples. Other information from the X-ray diffraction studies indicates that accompanying the release of stored energy and the decrease of C_0 interplanar spacing is an increase in the crystallite thickness in the C dimension.

The slope of the curve for stored energy as shown in Fig. 29 is the stored energy release per unit change in annealing temperature. For these samples the average stored energy release is about 0.22 cal/gm/°C over the range from 100° to 1100°C. The release then increases to about 0.6 cal/gm/°C, and subsides to a value of about 0.1 cal/gm/°C at annealing temperatures above 1500°C.

Particular attention has been paid to this stored energy release at low annealing temperature. Experimentally it is more satisfactory to conduct calorimetric measurement of the apparent decrease in specific heat of one sample than to attempt to measure small changes in the heat of combustion of a large number of samples. Rather than attempt to get complete annealing after each small rise in temperature, current techniques are based upon measuring the stored energy release as the sample temperature is increased at a standard rate, usually established empirically at 10°C/min.

The results of experimental measurement of the release of stored energy by calorimetric technique is shown in Fig. 30. The ordinate of Fig. 30 is equivalent to the (negative) slope of a curve such as that shown in Fig. 29, but exact agreement would not be expected because of the more rapid change in annealing temperature in the calorimetric experiment. If the calorimetric experiments were continued to sufficiently high temperature, the area under the curve would represent the total stored energy of the sample.

In some cases values of stored energy release are sufficiently high to give an apparent negative specific heat for the graphite—the sample spontaneously increases in temperature. This occurs whenever the stored energy release exceeds the true specific heat of the sample. Values of specific heat for unirradiated graphite are superimposed as a dotted line on Fig. 30.

The data shown in Fig. 30 were obtained from graphite irradiated at about 30°C. Of special interest is the large peak in the stored energy release at about 200°C, which increases in intensity with exposures up to about 4.2×10^{20} neutrons/cm^2. At higher exposures this release peak is diminished, and increasing proportions of the stored energy are released only at higher temperatures. The similarity of this phenomenon to the crystallite expansion characteristics is noted by comparing Figs. 12 and 30. The exposure at which the shape of the C_0 X-ray diffraction peak begins to broaden corresponds to the exposure at which the 200°C stored energy release decreases in magnitude.

The accumulation of stored energy which can be released by annealing at low temperature decreases rapidly as the temperature of irradiation is increased. Figure 31 shows data on calorimetric measurement of three samples which had been given the same low exposure at three different temperatures. It is observed consistently in both calorimetric and combus-

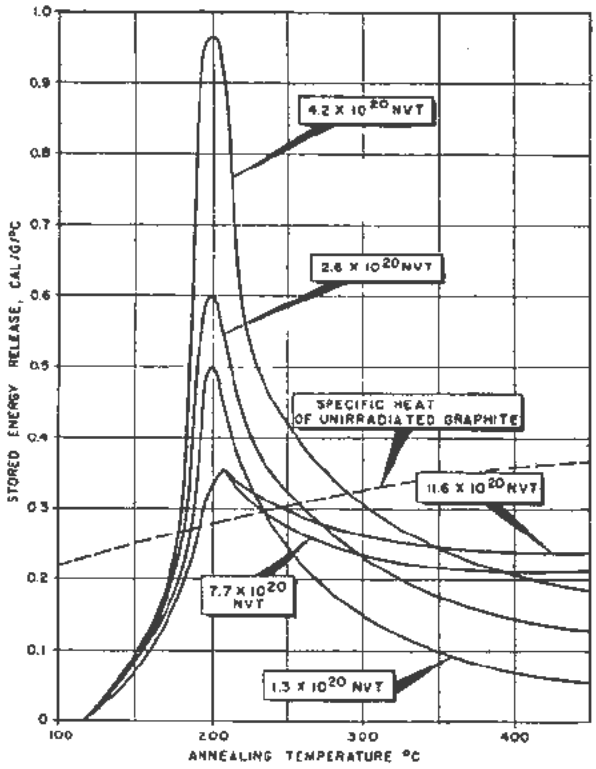

Figure 30. Stored energy annealing spectra in irradiated graphite

tion experiments that irradiated graphite must be annealed at temperatures substantially above the irradiation temperature (exceeding the latter temperature by the order of 100°C) before any release of stored energy is encountered. Hence, as shown in Fig. 31, irradiation at 111 to 164°C instead of 30°C effectively eliminates the 200°C peak observed in Fig. 30. (Negative ordinate values shown at low temperatures in Fig. 31 are due to experimental error.

With regard to annealing of stored energy at low temperature (<300°C), results comparable to raising the temperature of irradiation can be obtained by irradiating at low temperature and then annealing thermally at a higher temperature. For example, one sample irradiated in a cold test hole to an exposure of 1.0×10^{20} neutrons/cm² was annealed at 155°C for 50 hours. The sample at the end of that time showed no measurable release of stored energy below a temperature of 300°C. These results are in reasonably good agreement with the data shown in Fig. 31 for the sample which had been irradiated for substantially the same exposure at an irradiation temperature of 164°C.

The accumulation of stored energy is a function of crystallite size. Figure 32 shows stored energy release rates for CSF graphite and for two forms of microcrystalline carbon. The large crystallites in the fairly well-ordered CSF graphite accumulate stored energy during irradiation more rapidly than do the microcrystallites in the amorphous carbon.

Results of experimental measurements of stored energy release by calorimetric methods are sensitive to experimental techniques, and substantial improvements have been made in recent years in the resolution of this type of experiment. In consequence, care must be exercised in comparing the results obtained by different workers with different equipment at different times. The much higher stored energy release rate for artificial graphite shown in Fig. 32 than in Fig. 30 is attributed to the improved techniques developed for the more recent data shown in Fig. 32.

ANNEALING OF PHYSICAL PROPERTY DAMAGE

Physical property damage to graphite is removed to a greater or lesser degree upon heating the graphite. The rate of annealing and the ultimate degree to which the damage may be removed depend on the annealing temperature and the amount of damage; quantitative recovery of changes in physical properties may be attained as graphitization temperatures are approached.

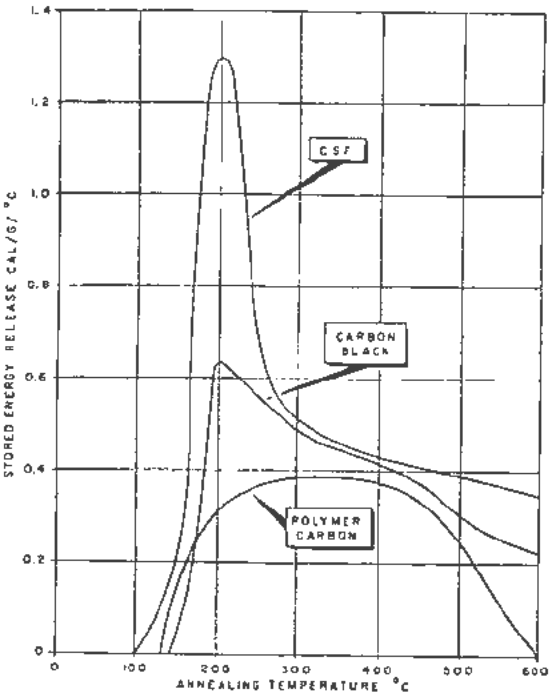

Figure 32. Stored energy in special carbons: exposure 3.42 × 10^{20} nvt (30°)

The thermal annealing characteristics of irradiated graphites have been studied by four methods:

1. Isothermal annealing, or annealing for varying lengths of time at a fixed temperature.

2. Asymptotic annealing, or annealing for extended periods of time at a fixed temperature.

3. Tempering, or the heating of samples at prescribed rates, with measurement of physical properties being made periodically at annealing temperature.

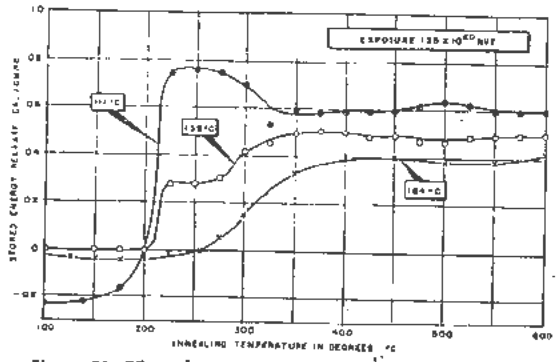

Figure 31. Effect of exposure temperature on stored energy

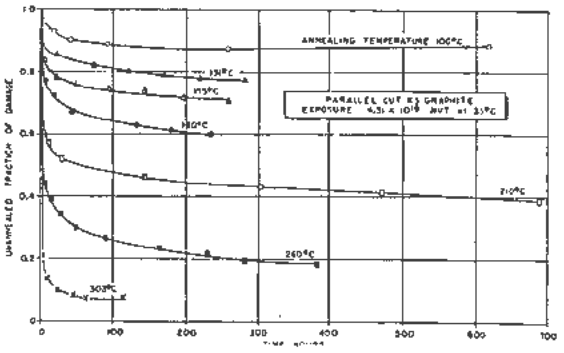

Figure 33. Isothermal annealing of Young's modulus changes

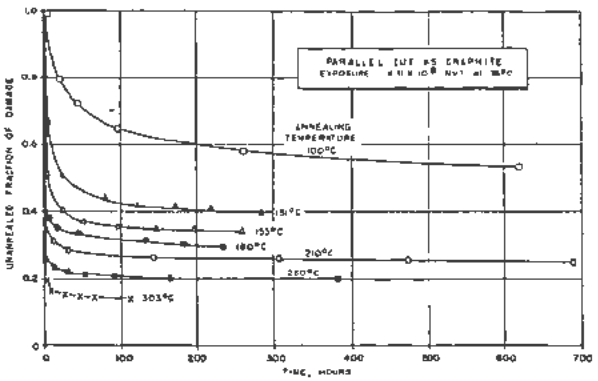

Figure 34. Isothermal annealing of electrical resistivity

4. Pulse annealing, or heating for short lengths of time to successively higher temperatures, with the samples being cooled and measured between pulses.

In addition, some of the irradiation damage previously incurred by irradiation at low temperature will be annealed if the temperature of irradiation is increased during the course of the irradiation. This is called nuclear, or radiation, annealing. Nuclear annealing can effect recovery of damage to many physical properties at temperatures substantially lower than those required to obtain equivalent recovery by thermal annealing.

Isothermal Annealing

Figures 33 to 35 illustrate the type of data obtained from isothermal annealing experiments. Figure 33 shows isothermal annealing curves for Young's modulus for parallel cut KS graphite which had been irradiated to an exposure of 4.3×10^{18} neutrons/cm^2 in the Clinton (X-10) reactor at a temperature of 35°C. Figure 34 shows isothermal annealing curves for the electrical resistivities of the same samples shown in Fig. 33. Figure 35 shows additional isothermal annealing curves for electrical resistivity of graphite irradiated to higher exposure in a Hanford reactor and annealed for comparatively short periods of time.

Asymptotic Annealing

Asymptotic annealing studies are normally preceded by at least cursory isothermal annealing studies to establish the approximate time-temperature relations needed to assure approach to terminal values.

The results of annealing on some mechanical properties of parallel cut CSF graphite after irradiation to an exposure of 1.1×10^{20} neutrons/cm^2 are shown in Fig. 36. The data of Fig. 36 can be expressed in terms of change in ultimate compressive strength, changes in (effective) Young's modulus, etc.

Results of asymptotic annealing studies on the thermal conductivity of transverse cut CSF graphite after various exposures are shown in Fig. 37 and are replotted in different form in Fig. 38. Figure 39 is analogous to Fig. 38 except that it shows data obtained during study of electrical conductivity instead of thermal conductivity.

An unusual effect has been observed during annealing of electrical resistivity effects at high temperatures, as shown in Fig. 40. These data were obtained on several samples of parallel cut WSF graphite irradiated to the very low exposure of only 8.4×10^{18} neutrons/cm^2 in the Clinton reactor. The behavior at high annealing temperatures is unexpected; lower electrical resistivity was obtained after annealing at 1000°C than was obtained by annealing at 1300°C. The data of Fig. 40 also suggests that the curves drawn on Fig. 39 are inaccurate for very small abscissa values.

Figures 41 and 42 present representative data on the results of studies of annealing of changes in C_0 spacing and annealing of physical expansion.

Tempering

The major use of the tempering technique has been in determining the nature of the release of stored energy. The technique has not been used extensively for determining the annealing characteristics of other physical properties because of the difficulties in maintaining predetermined rates of temperature increase, in making physical property measurements at elevated temperatures, and in eliminating purely thermal effects from the data.

The results of one application of tempering techniques in the study of annealing of physical property damage is shown in Figure 43. Interferometric meas-

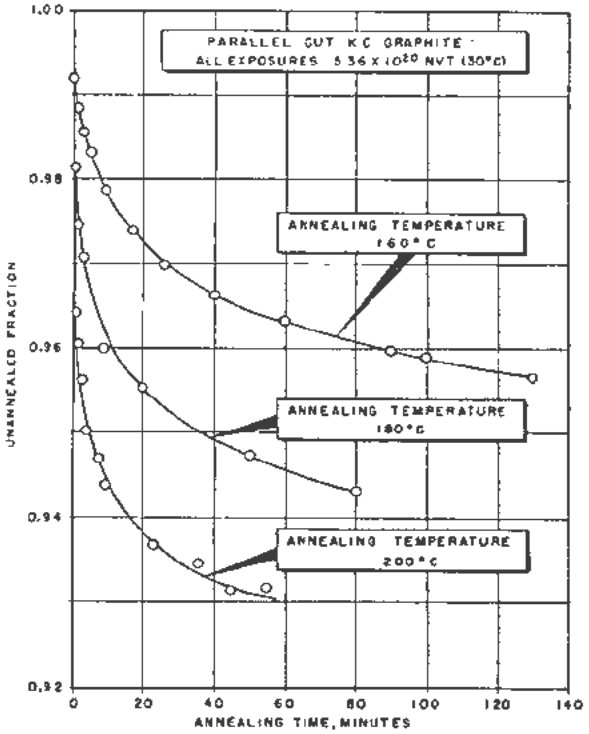

Figure 35. Isothermal annealing of electrical resistivity: short periods. Parallel cut KC graphite: all exposures 5.36×10^{20} nvt (30°C)

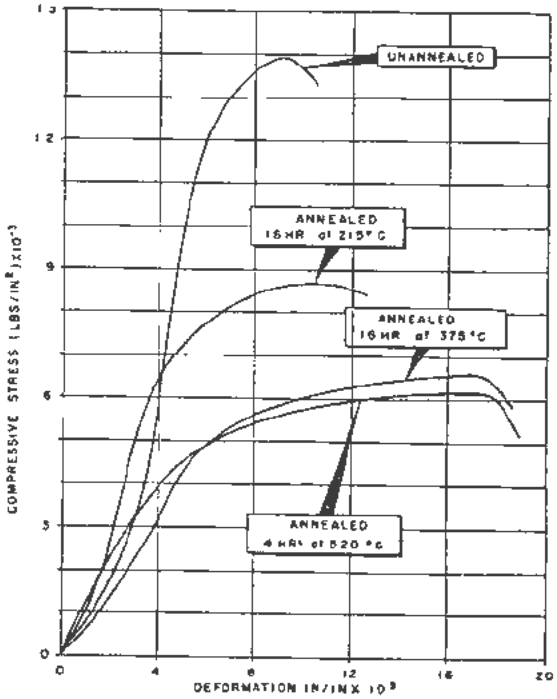

Figure 36. Stress-strain curves for annealed CSF graphite: exposure 1.14×10^{20} nvt

urements were made on changes in length of transverse cut CSF graphite samples during the course of the annealing, and the data presented in Fig. 43 have been corrected for the purely thermal expansion of the graphite. The slight expansion shown at low annealing temperature is a real effect which has also been observed in other studies.

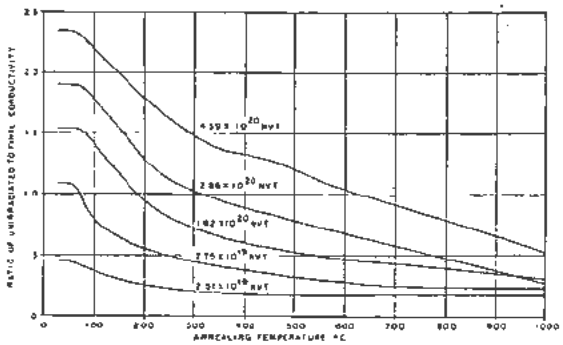

Figure 37. Effect of annealing temperature on thermal conductivity: all exposures 30°C

Pulse Annealing

Pulse annealing provides a comparatively simple means of determining rates and activation energies during annealing and of obtaining very high annealing temperatures. Pulse annealing is essentially a discontinuous tempering with thermal effects being eliminated by measuring the physical properties at a fixed base temperature. The temperature pulses are usually of short duration (about one minute) and of such characteristic that in each pulse the annealing is essentially isothermal after a rapid rise to temperature.

Typical results for the pulse annealing of damage to thermal conductivity are shown in Fig. 44. The material under study is a molded petroleum-coke graphite. The initial increase in thermal resistivity

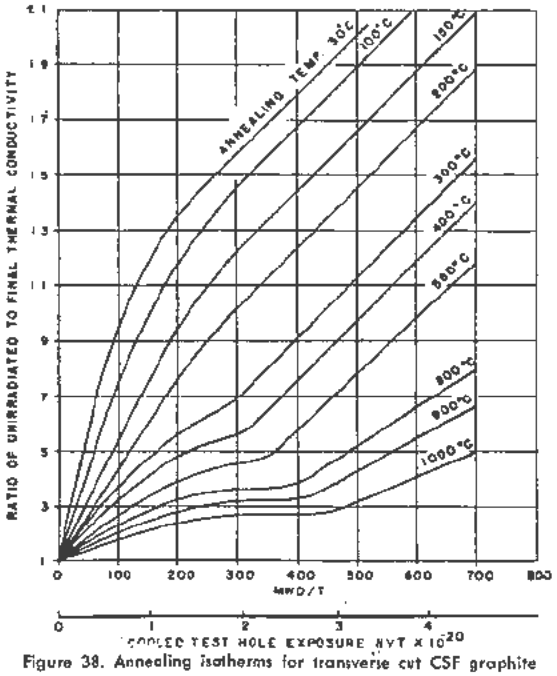

Figure 38. Annealing isotherms for transverse cut CSF graphite

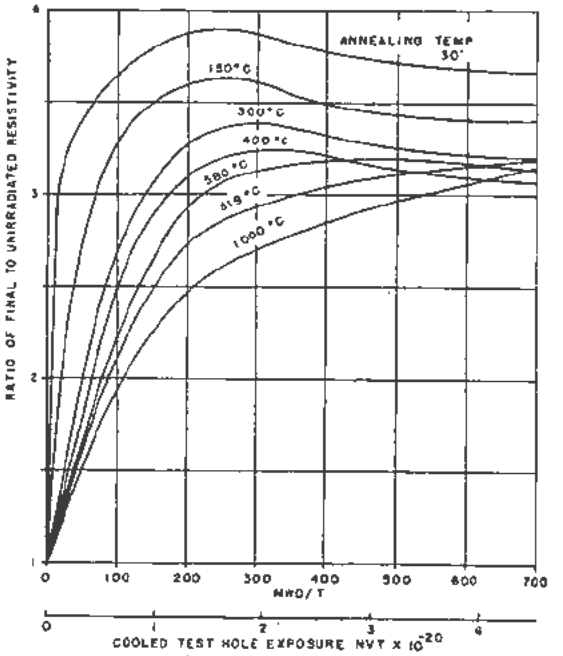

Figure 39. Annealing electrical resistivity: transverse cut CSF graphite

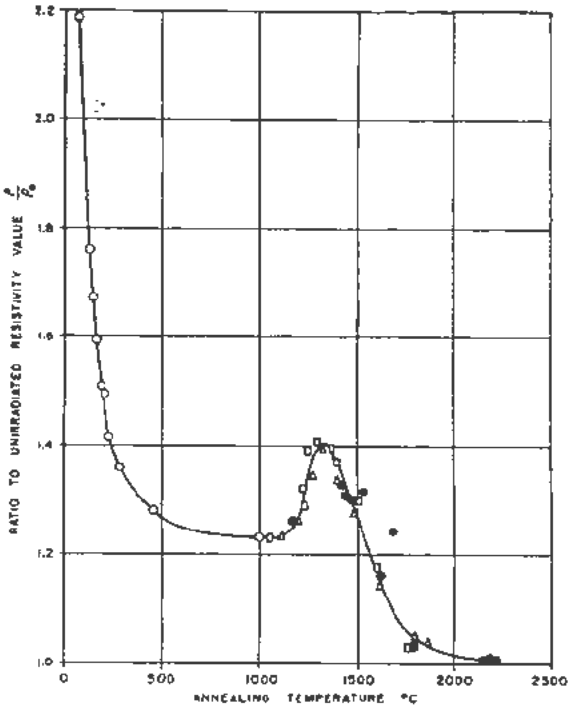

Figure 40. High temperature annealing effects on electrical resistivity: exposure 9.61 × 10^{19} nvt

for low-temperature pulses is believed to be related to the similar effect shown in Fig. 43. The data in Fig. 44 are expressed in terms of the ultimate conductivity observed after annealing to 2100°C and it is reported that the conductivity after annealing to 2100°C was in reasonably good agreement with the conductivity of the unirradiated graphite.

Kinetic Relations in Thermal Annealing

Several models have been proposed for the thermal annealing of radiation damage to graphite, no one of which is completely successful in explaining the experimental data. These models usually propose rather complex mechanisms involving high-order reaction rates, continuous spectra of activation energies, or diffusion limiting or chain inhibiting effects.

Activation energies derived from analysis of isothermal annealing data and apparent reaction orders

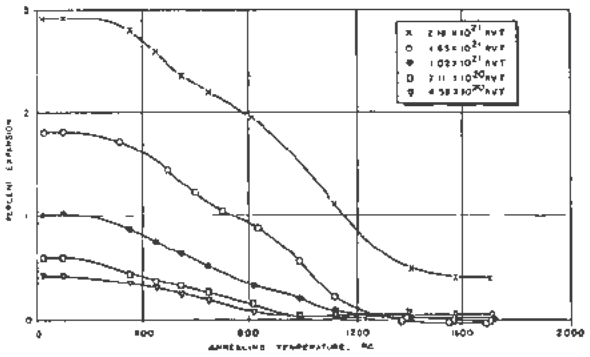

Figure 42. Annealing physical expansion: transverse cut CSF

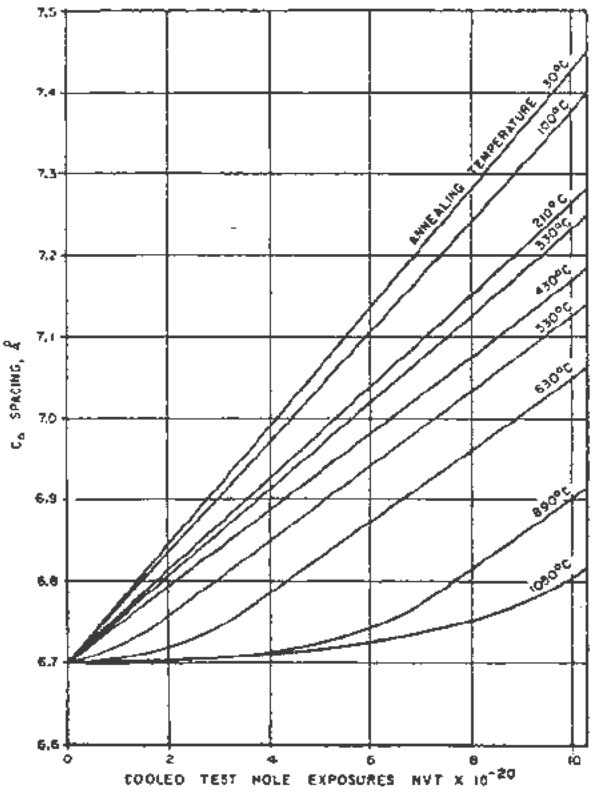

Figure 41. C_0 annealing isotherms

derived from analysis of pulse annealing data for irradiation-induced changes in electrical resistivity of graphite are shown in Table V.

Reaction rates associated with the annealing of crystallite expansion in damaged graphite are shown in Table VI. Samples were annealed isothermally while held in an X-ray diffractometer and rates of annealing of the C_0 displacement were observed. The annealing rate approximated first order kinetics.

Table V. Activation Energies for Annealing of Damage to Electrical Resistivity (kcal/gm-atom)

Annealing temp. (°C)	*150–200*	*1100–1200*	*1400–1500*
Exposure (neutrons/cm²)			
8.1 × 10^{18}	23.8	69.5	123.2
1.5 × 10^{19}	29.2	58.2	100.5
5.4 × 10^{20}	39.6		120.3
Apparent reaction order	6	1	4

Table VI. Reaction Rates for C_0 Annealing of TS-GBF Graphite, Previous Irradiation 3.59 × 10^{20} nvt (30°C)

Temperature of anneal, °C	*Temperature of previous anneal, °C*	*First order reaction rate, min^{-1}*
124	99	0.03
150	100	0.17
225	150	0.11
329	225	0.13
449	329	0.12
650	524	0.08

Nuclear Annealing

The phenomenon of nuclear annealing, with its enhancement of annealing effects through the influence of concurrent neutron irradiation, is presumably the result of the formation of small regions of extremely high temperature within the crystallites of the graphite. The energy absorbed by carbon atoms in the moderation of neutrons is largely dissipated as heat; only a very small fraction appears as potential energy of dislocated crystal structure. An atom after collision with a neutron of more than thermal energy may have a kinetic energy equivalent to a temperature of thousands of degrees Centigrade. As this energy is dissipated to the surrounding atoms a very small region of the crystallite is momentarily heated to high temperature, annealing any distortion present in that region.

The most suitable illustrative example of nuclear annealing is taken from data developed in Britain,[3] and shown in Fig. 45. Measurements of changes in physical length were made on a graphite sample irradiated first at a temperature of 30°C and then at 150°C. Irradiation at 150°C effected a 40 per cent recovery of the expansion incurred at the low temperature irradiation. A second sample having the same exposure at 30°C was annealed thermally at 150°C and was found to expand slightly; this is consistent with the data shown in Fig. 43. Figure 43 also indicates that to obtain a recovery of 40 per cent of this amount of physical expansion by thermal annealing it would have been necessary to heat the sample to a temperature of several hundred degrees Centigrade.

The expansion curve for graphite irradiated only at 150°C is also shown on Fig. 45. The curves for

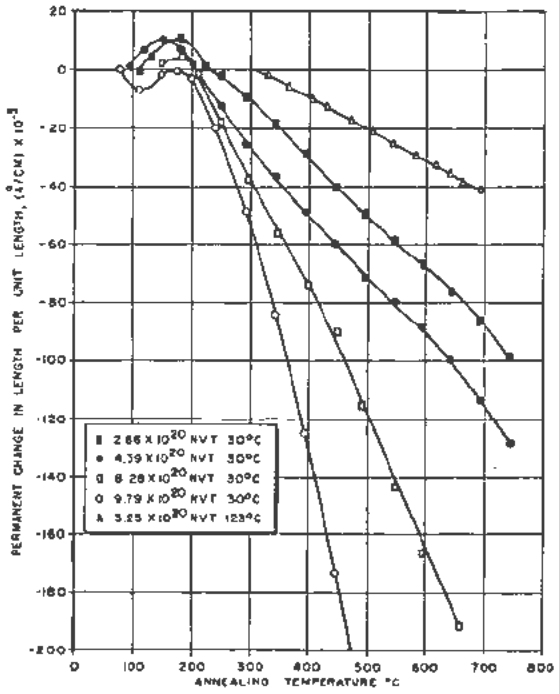

Figure 43. Physical expansion annealing: interferometer measurements

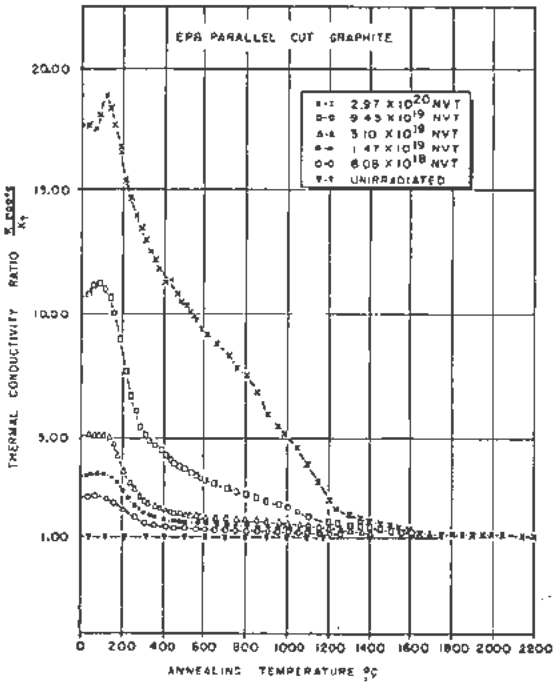

Figure 44. Pulse annealing of thermal conductivity damage

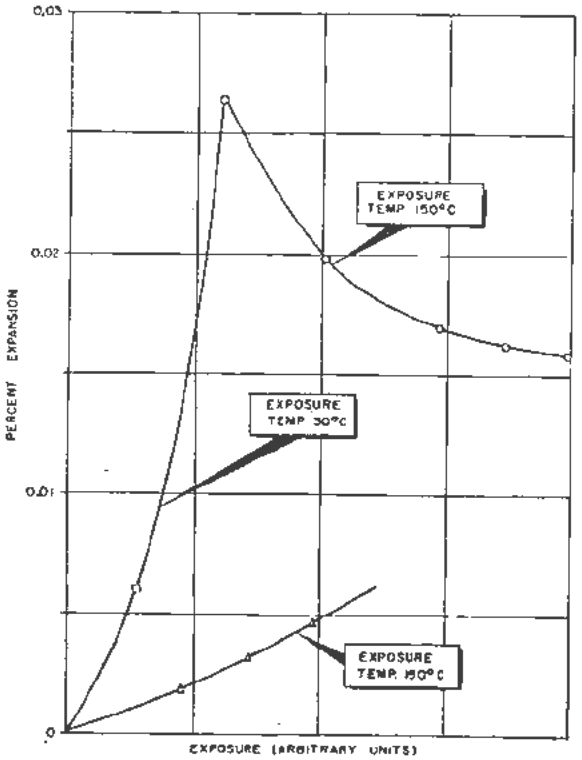

Figure 45. Nuclear annealing of physical distortion of graphite

the two irradiations at 150°C appear to approach each other and may meet at higher exposures.

CONCLUSION

Artificial graphite is subject to major changes in its physical properties by irradiation in a nuclear reactor at low temperature. Of particular engineering interest are the doubling of mechanical strength, the fifty-fold reduction in thermal conductivity, the linear physical expansion in excess of 3 per cent, and the accumulation of more than 500 calories of stored energy per gram—all of which have been observed to result from irradiation of Acheson type graphites at temperatures of about 30°C to exposures on the order of 2×10^{21} neutrons/cm^2.

These effects which result from low-temperature irradiation are difficult to remove by thermal annealing and in most cases annealing temperatures above 2000°C are required to effect substantially complete recovery. The magnitude of the effects can be reduced, however, both by changes in the method of manufacture of the graphite and especially by an increase in the temperature of irradiation. Irradiation at 150°C effects an order-of-magnitude reduction in the changes of most physical properties compared with those incurred by irradiating at 30°C.

The physics of the solid state is not sufficiently advanced as a science to enable us to understand all the mechanisms involved in irradiation damage to graphite. Study of changes in electrical resistivity, investigation by X-ray diffraction techniques, analysis of annealing rates, and observation of changes in electromagnetic properties are contributing to an understanding of the phenomenon. It is possible that the contributions to knowledge resulting from study of irradiation effects in materials such as graphite may eventually become one of the most important products of the development of atomic energy.

REFERENCES

1. Currie, L. M., Hamister, V. C. and MacPherson, H. G., P/534, *The Production and Properties of Graphite for Reactors*, Volume 8, Session 16B.2, these Proceedings.
2. Hennig, G. R. and Hove, J. E., P/751, *Interpretation of Radiation Damage to Graphite*, Volume 7, Session 13B, these Proceedings.
3. Sheard, H., personal communication.

The Effects of Irradiation on Graphite

By G. H. Kinchin,* UK

Because of variations in the size and orientation of the crystals, the physical properties of polycrystalline graphite depend to a great extent on the method of manufacture. Consideration of the effects of fast neutron irradiation will be restricted to one particular extruded graphite, the properties of which are given in Table I. Single crystals of graphite, which consist of widely spaced planes of carbon atoms, are extremely anisotropic and the anisotropy of extruded polycrystalline graphite is due to the fact that the crystals tend to be aligned with the planes of atoms parallel to the extrusion direction. The figures for the elastic moduli are arbitrarily determined from stress-strain ratios at about half the breaking strain, since stress-strain curves are non-linear and exhibit hysteresis phenomena. Because of the anisotropy, there are three values of Poisson's ratio, all of them low.

The effects to be discussed are due to lattice defects (interstitial atoms and vacancies) produced through the displacement of atoms by fast neutrons; a recent review of this subject has been given by Kinchin and Pease.[1] The doses in this paper are expressed in terms of integrated thermal neutron flux, and are referred to a position in BEPO for which the fast neutron flux up to about 5 Mev is given by

$$\phi(E)dE = 0.06\ \phi_t\ dE/E \qquad (1)$$

where E is the neutron energy and ϕ_t is the thermal neutron flux.

ELECTRICAL PROPERTIES

Irradiation

Changes in the resistivity and Hall coefficient of graphite irradiated at 30°C have been previously reported;[2] the dose scale differed from the one used in the present paper in that the constant in Equation 1 was 0.03. Graphite is a semi-metal in which charge is carried both by electrons and positive holes, and the resistivity is governed by the concentrations of charge carriers and their mean free path. The electrons and positive holes are scattered by the defects introduced by irradiation, and the mean free path decreases, while at the same time Hall coefficient measurements show that electrons are trapped at the defects. The net result is that at low doses, when the increase of positive hole concentration is almost balanced by the decrease of free electron concentration, the increase of resistivity is almost proportional to the concentration of defects, while at high doses, when there are few free electrons, the increasing positive hole concentration counteracts the decreasing mean free path and leads to a saturation of the resistivity change.

Figure 1 shows the resistivity changes caused by irradiation at different temperatures; specimens cut perpendicular to the extrusion direction show slightly smaller changes of ρ/ρ_0 because of their smaller effective crystal size.[2]

The rate of change of Hall coefficient varies with irradiation temperature in much the same way as the rate of increase of resistivity but, as may be seen from Table II, when the resistivity changes of specimens irradiated at 30 and 150°C are the same, the Hall coefficients are not identical. This suggests either some difference in the distribution of defects or the presence of different types of defects in the two cases.

Recovery

The main features of recovery are demonstrated in Fig. 2, which shows the resistivity of irradiated specimens after annealing for one hour at successively higher temperatures.

For short irradiations there is rapid recovery at temperatures up to 400°C, and little further change between 400 and 1000°C. The activation energy of the recovery process, derived from isothermal experi-

Table I. Physical Properties of a Polycrystalline Graphite

Density (gm-cm^{-3})		1.60
Electrical resistivity (ohm cm)	para.*	1.05×10^{-3}
	perp.	1.25×10^{-3}
Thermal conductivity (cal-°C^{-1}-cm^{-1}-sec^{-1})	para.	0.33
	perp.	0.28
Thermal expansion coefficient −190 to + 20°C (°C^{-1})	para.	1.18×10^{-6}
	perp.	2.25×10^{-6}
Crystal size (cm)		10^{-5}
Young's modulus (dyne-cm^{-2})	para.	8.9×10^{10}
	perp.	6.2×10^{10}
Torsional modulus (dyne cm^{-2})	para.	3.2×10^{10}
	perp.	3.6×10^{10}
Poisson's ratio		0.1

* Relative to the extrusion direction.

* Atomic Energy Research Establishment, Harwell

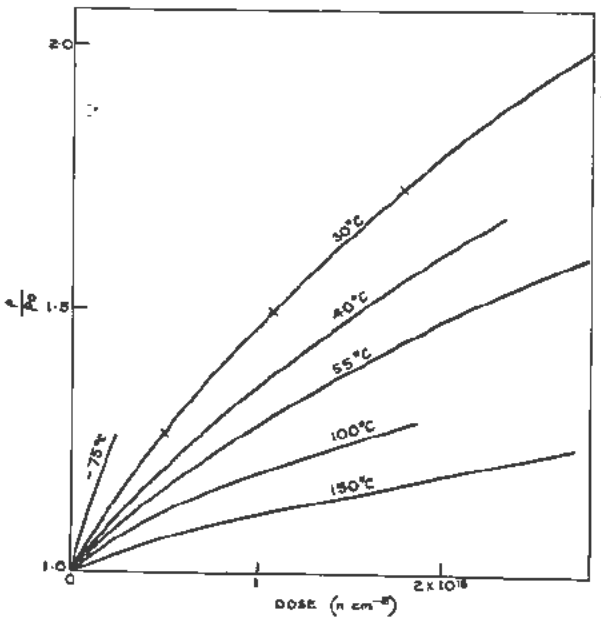

Figure 1. Changes of electrical resistivity at different irradiation temperatures

ments by comparing the rates of recovery at different temperatures, has a constant value of 1.2 ev at temperatures up to 200°C and thereafter rises rapidly. Figure 3 is a composite curve obtained from isothermal measurements in the range of constant activation energy, showing the variation of resistivity with time at a constant temperature; the extremely wide range of time over which recovery takes place should be noted.

At higher doses recovery is continuous up to 1000°C; the activation energy starts at about 1.2 ev in the early stages of recovery, but rises gradually to 3 ev at 900°C as annealing proceeds. Above 1000°C there is a rapid decrease of resistivity which overwhelms the remarkable increase observed in specimens with low doses.

There is a marked difference in the temperatnre variation of Hall coefficient between graphite irradiated at 30°C and graphite which has subsequently been annealed at a higher temperature.

Relation between Recovery and Accumulation of Damage

It is clear from Fig. 1 that there is simultaneous recovery and production of damage at temperatures above —75°C, while the form of the curves suggests that the regions of damage produced by individual fast neutron collisions are annealing independently; if the rate of recovery were dependent on the average concentration of defects, as might be expected if the defects were randomly distributed, it may easily be shown that the curves of Fig. 1 should all start with the same slope and saturate at different levels.

If it is assumed that the regions of damage produced by fast neutron collisions anneal independently, and that an instantaneously produced change of resistivity $d\rho$ decays to $d\rho\ F(T, t)$ after a time t at

Table II. Hall Coefficient of Irradiated Graphite

	$\frac{\rho}{\rho_0}$	Hall coefficient (cm^3-coulomb^{-1}) 300°K	195°K	77°K
Unirradiated	1.00	−0.060	−0.083	−0.155
0.9×10^{19} neutron-cm^{-2} at 30°C	1.44	−0.018	+0.021	+0.202
6.3×10^{19} neutron-cm^{-2} at 150°C	1.44	−0.005	−0.012	+0.116

temperature T, the function $F(T, t)$ may be determined experimentally by annealing after irradiation at low temperatures. If damage is produced at a constant rate which would give rise to a rate of change of resistivity $d\rho/dt$ in the absence of recovery, then the resistivity change produced by irradiating for a time t^1 at temperature T would be

$$\Delta\rho = \frac{d\rho}{dt}\int_0^{t^1} F(T, t^1 - t)dt \qquad (2)$$

There is a good agreement between the curves of Fig. 1 and curves calculated from annealing data at low doses using Equation 2. Without any consideration of the detailed mechanisms of recovery, Equation 2 throws light on the dependence on neutron flux, time and temperature of the irradiation changes in graphite at low doses. The change of resistivity is not quite proportional to the time of irradiation, and it is evident that an irradiation is completely defined only when both flux and time are specified. Nevertheless, the changes after a given product of flux and time (integrated flux) are not very different if the irradiation is carried out in a high flux for a short time instead of in a low flux for a long time, and for practical purposes the integrated flux is an adequate measure of an irradiation.

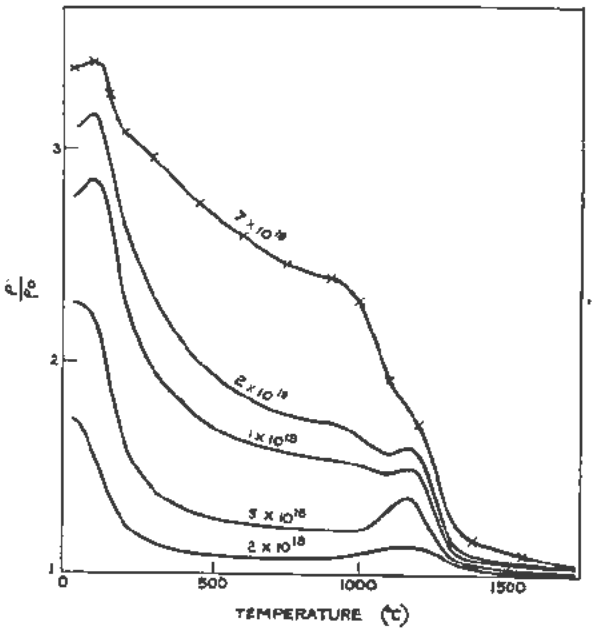

Figure 2. Recovery of resistivity changes: one hour anneals

Model

An energetic carbon atom moving through the lattice as a result of a fast neutron collision at first loses practically all its energy by electronic excitation and ionization. Below some ill-defined energy L_e, energy is lost mainly by elastic collisions, and the cross section for these collisions increases as the energy falls. The result is a pear-shaped region of damage with vacancies in the centre and a high concentration of interstitial atoms and interstitial-vacancy pairs at the surface. Assuming that L_e is 1.2×10^4 ev, and that the minimum energy needed to displace a carbon atom is 25 ev, the fraction of displaced atoms produced by unit integrated thermal flux in a neutron flux with an energy spectrum given by Equation 1 is 2.4×10^{-22} cm^2-neutron^{-1}. With the assumption that each interstitial + vacancy may trap one electron, the maximum value of this fraction, determined from Hall coefficient measurements after irradiation at 30°C, is 7×10^{-23} cm^2-neutron^{-1}. Bearing in mind the recovery at 30°C implicit in the data presented in Fig. 1 and the inherent difficulties in estimating L_e, agreement is satisfactory.

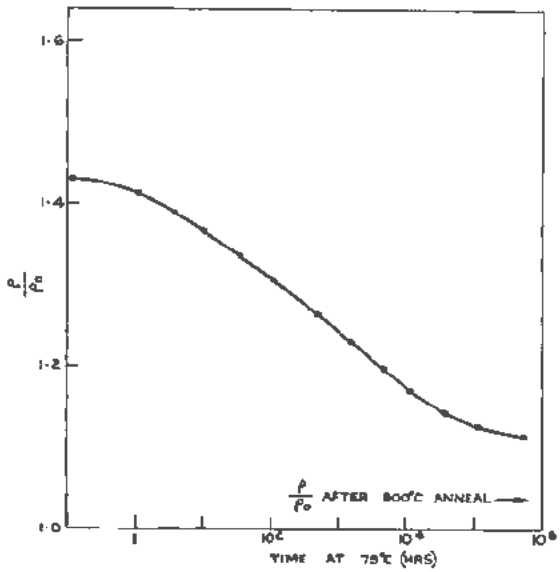

Figure 3. Recovery of resistivity changes: composite curve from data at temperatures up to 200°C; constant activation energy of 1.2 ev

The interstitial atoms occupy sites between in planes of carbon atoms[3] and their diffusion is limited to motion in two dimensions. The annihilation of separate interstitial-vacancy pairs by the two-dimensional diffusion of interstitials adequately explains the greater part of the recovery curve shown in Fig. 3. Detailed fitting may not be significant, since grouping may cause some departures from the assumed linear relationship between concentration of defects and change of resistivity, but these departures cannot be very great and many of the simpler processes, such as the recombination of *randomly* distributed interstitials and vacancies can be ruled out. As the interstitials diffuse over greater distances, interaction between adjacent pairs would be expected to affect the kinetics of recovery, although this effect is mitigated by the restrictions on the motion of interstitials. After all the interstitials have been removed by recombination with vacancies or by migration to crystal boundaries, only vacancies, some of which are in planes inaccessible to interstitial atoms, remain; it is postulated that the recovery process which is operative at about 1100°C is due to the migration of vacancies. The increase of resistivity may be tentatively explained by changes in the trapping levels as the groups of vacancies spread out in the early stages of diffusion. The decreasing interaction between vacancies may raise the energy of the trapping levels and release electrons; the number of electrons trapped by a given number of defects may also be altered by changing the temperature, and experiments of this kind show that a decrease in the number of trapped electrons gives rise to an increase in the scattering cross section of the defects.[2]

At higher doses, interaction between different groups of displaced atoms becomes possible during annealing, and the recovery which takes place between 400 and 1000°C may reasonably be attributed to the formation and breaking up of groups of interstitial atoms. The diffusion of vacancies still gives marked recovery at 1100°C and only a few of the most stable groups remain at higher temperatures.

By analogy with the saturation observed in irradiation effects in boron nitride,[4] which has a structure similar to that of graphite, the fraction of single interstitial atoms would be expected to saturate at about 1%, although the electrical properties are not suitable for observing this phenomenon because of the non-linear relation between resistitivity and defect concentration at high doses. The relation between recovery and accumulation of damage, which assumed no interaction between groups of displaced atoms, breaks down at the onset of saturation which is essentially caused by such interactions.

Changes in other properties of graphite will be discussed in relation to the model described above.

THERMAL CONDUCTIVITY

Irradiation

The thermal property normally measured is the conductivity K, but the thermal resistivity $1/K$ has more significance in this context. K_0/K which is equal to the ratio of the thermal resistivities after and before irradiation, is shown in Fig. 4 as a function of dose at different irradiation temperatures. The marked knee which appears in the curve for irradiation at 30°C is taken to correspond to the saturation of the concentration of single interstitial atoms, referred to in the previous section, while the subsequent steady increase is due to the accumulation of vacancies and groups of interstitials.

Recovery

The recovery of thermal resistivity changes is shown in Fig. 5. Activation energies determined from thermal and electrical measurements on the same specimen agree within the limits of experimental error. The relation between thermal and electrical resistivity which holds for specimens irradiated at 30°C is not greatly altered by annealing at temperatures up to 800°C; at higher temperatures the anomalous increase in the electrical resistivity is not observed in the thermal resistivity, and the relation is changed. The thermal conductivity of electrical conductors is composed of two parts—lattice conductivity and electronic conductivity. In graphite the electronic conductivity is negligible so that any purely electronic changes, such as have been suggested to explain the increase of electrical resistivity at 1000°C, have little effect on the thermal resistivity. The migration of vacancies therefore leads to a decrease in the thermal resistivity at temperatures above 1000°C.

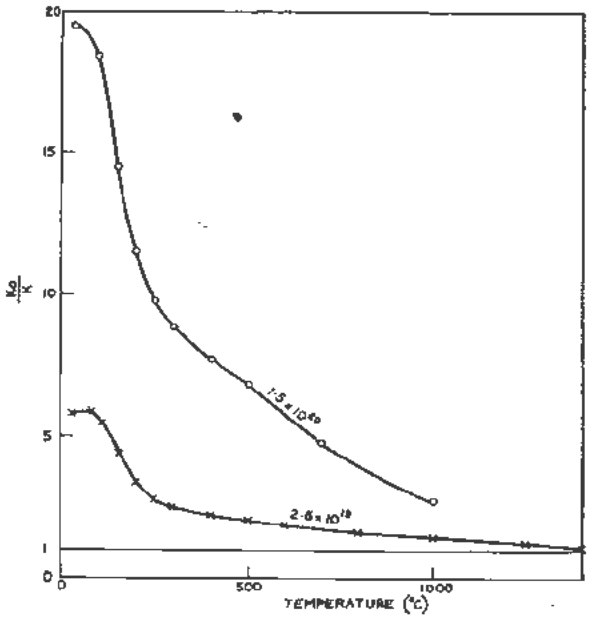

Figure 5. Recovery of thermal resistivity changes: two hour anneals

LATTICE PARAMETER AND DIMENSIONS

Irradiation

The interstitial atoms produced by irradiation cause an increase in the spacing between the planes of carbon atoms (c-spacing). Owing to the porous structure, the fractional increase of volume observed by dimensional measurements on polycrystalline graphite is appreciably smaller than that of the crystals. The c-spacing may be determined by X-ray measurements and is found to increase almost linearly with dose at the rate of 1.3% per 10^{20} neutrons-cm^{-2} at 30°C; at high doses the X-ray lines are broad and asymmetrical, so that the average and most probable values of the c-spacing are no longer identical. Changes in length (bulk growths) of polycrystalline graphite perpendicular to the extrusion direction are shown in Fig. 6; parallel to the extrusion direction the growths are smaller and there may be an initial slight contraction.

In order to explain the remarkable linearity of the greater part of the growth curves, it must be assumed that a group of interstitial atoms has a greater

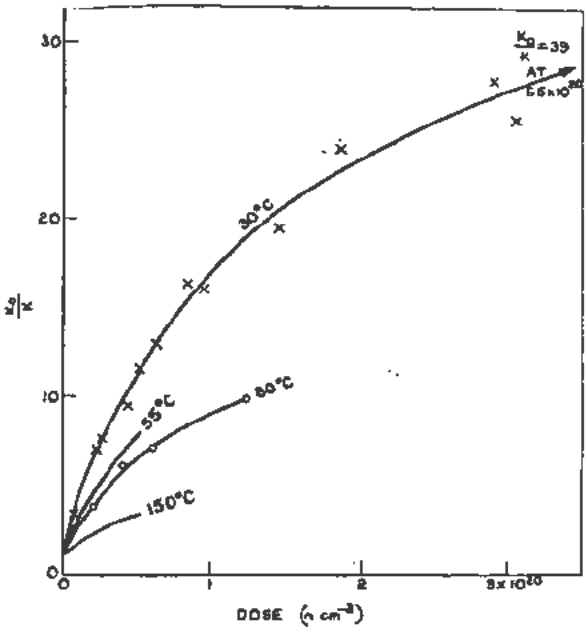

Figure 4. Changes of thermal resistivity at different irradiation temperatures

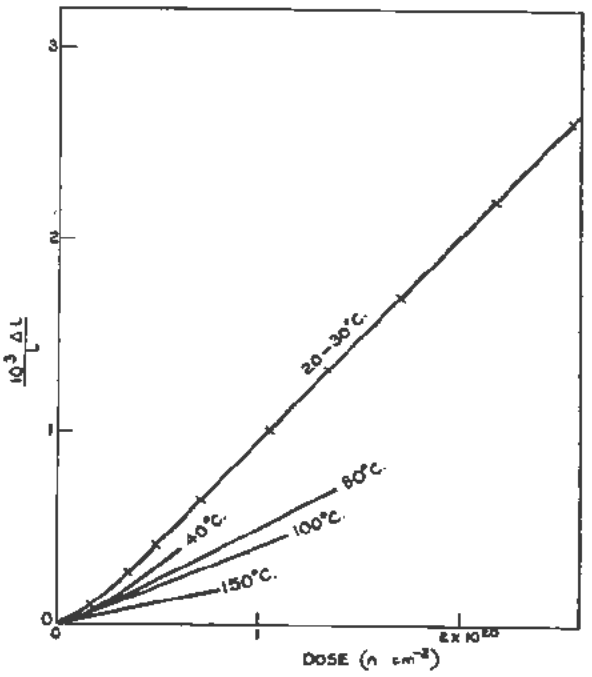

Figure 6. Growth perpendicular to extrusion direction at different irradiation temperatures

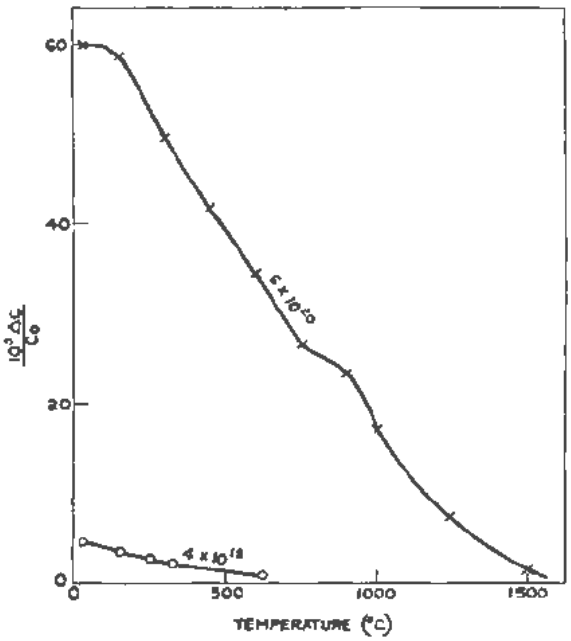

Figure 7. Recovery of c-spacing changes: eight hour anneals

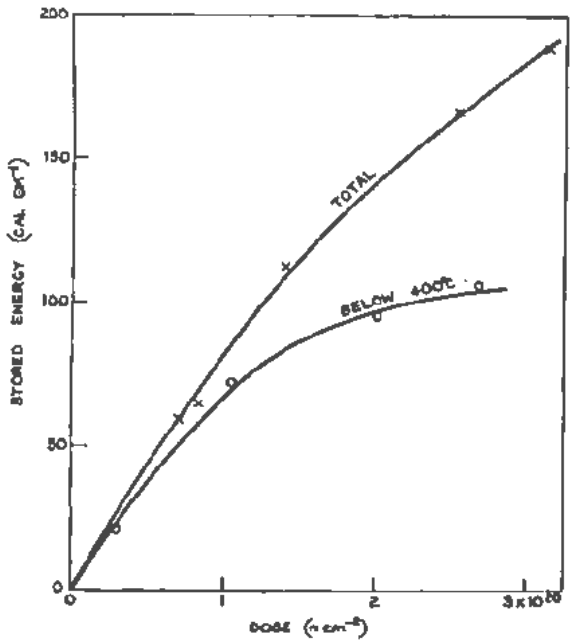

Figure 8. Total stored energy and energy released below about 400°C: irradiation temperature 30°C

effect on the *c*-spacing than the same number of separate interstitials. The initial non-linearity of the bulk growth may be explained in terms of the hysteresis observed in the stress-strain curves of unirradiated graphite; a change of internal stresses caused by crystal growth will not become evident as a dimensional change until the internal stresses are overcome.

Recovery

The recovery of *c*-spacing changes is shown in Fig. 7. These curves give a measure of the number of interstitial atoms present after annealing at different temperatures since it is probable that, unlike the electrical and thermal resistivities, *c*-spacing is not affected by the presence of vacancies. The recovery of *c*-spacing changes at temperatures up to 200°C is relatively less than that observed in other physical properties, in agreement with the contention that single interstitials are not very effective in increasing the *c*-spacing; the bulk growth may show no change at all, or even a slight increase at 200°C. Here again, this behaviour may be accounted for by the internal friction.

STORED ENERGY

Irradiation

In Fig. 8 both the total stored energy (determined from heats of combustion) and the energy released up to about 400°C are shown as a function of dose for irradiation at 30°C. The low-temperature stored energy, which is due largely to the recombination of single interstitials and vacancies, saturates in a manner consistent with the proposed model, and the change in slope of the total stored energy curve occurs at the same dose as that observed in the thermal resistivity curve.

With the assumption that the energy released when an interstitial atom returns to a vacancy is 10 ev, the fraction of displaced atoms produced by unit integrated flux is 4×10^{-20} cm^2-neutron^{-1}, in reasonable agreement with the figures given in a previous section.

Recovery

Figure 9 shows the rate of energy release from irradiated graphite when the temperature was raised at a constant rate of 20°C per minute. Increasing the temperature in steps approximates to raising the temperature at a steady rate and the rates of change of thermal and electrical resistivity derived from such step anneals closely resemble the curve shown in Fig. 9.

MECHANICAL PROPERTIES AND THERMAL EXPANSION

Irradiation

Changes of Young's modulus are shown in Fig. 10 and similar results are obtained for the torsional modulus. Stress-strain curves become more linear after irradiation, and the magnitude of the residual strain which remains after the application and removal of stress diminishes. The thermal expansion coefficient does not increase by more than 5% for an irradiation of 10^{20} neutrons-cm^{-2} at 30°C.

Recovery

The recovery of Young's modulus changes is shown in Fig. 11. The general similarity between this recovery curve and those for the other properties

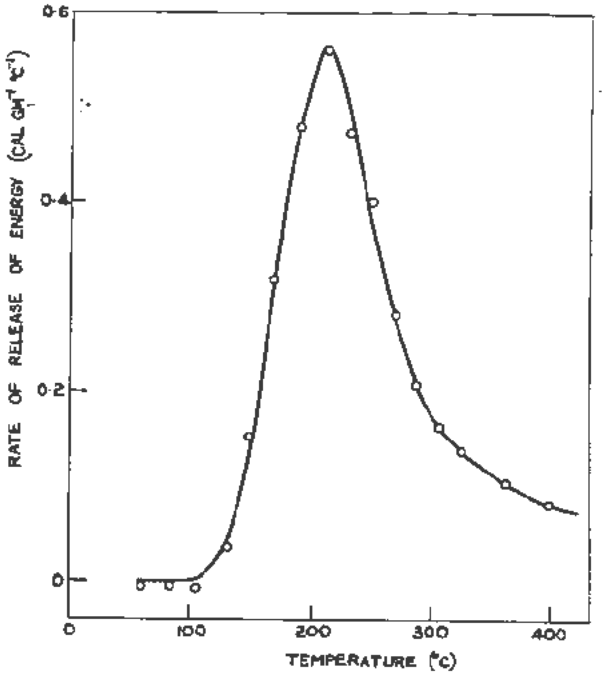

Figure 9. Rate of release of energy: linear rise of temperature (20°C min^{-1}); irradiation ~2 × 10^{20} at 50° C

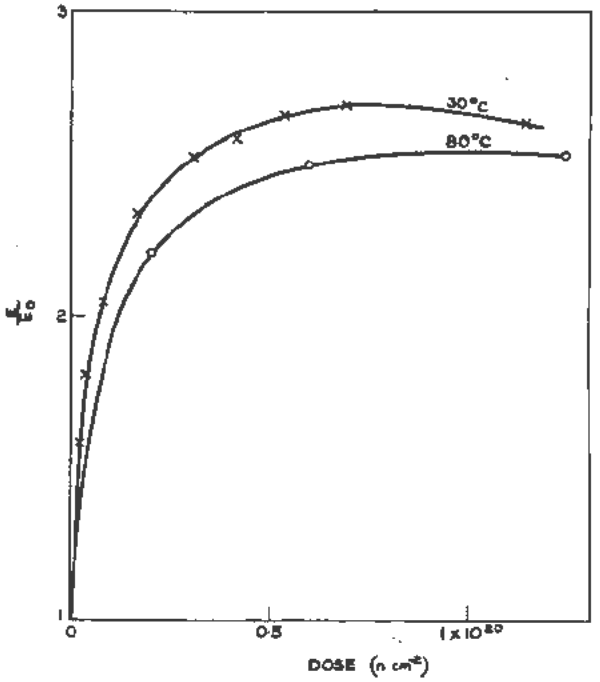

Figure 10. Changes of Young's modulus at different irradiation temperatures

suggests that we are concerned with changes in the crystalline properties rather than changes in the bonds between crystals. The strains produced in the individual crystals by the application of tensile or compressive stresses to polycrystalline graphite are difficult to visualize. It is improbable that the effects in polycrystalline graphite are due to changes in the

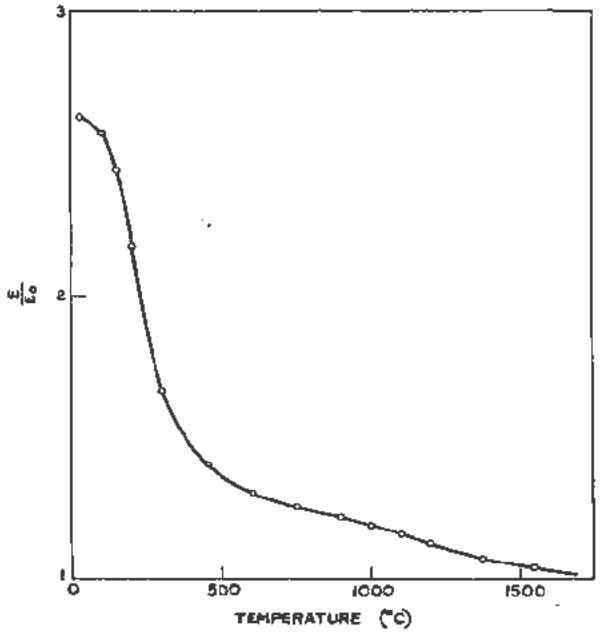

Figure 11. Recovery of Young's modulus changes: one hour anneals; irradiation 1.1 × 10^{20} at 30°C

Young's moduli of the single crystals either parallel or perpendicular to the c-axis, since the concentrations of defects are very small, and it would be difficult to reconcile the small increase of thermal expansion with such changes. It may plausibly be argued that the increased difficulty of shearing the planes of carbon atoms is responsible, but the changes are not well understood.

CONCLUSIONS

Irradiation effects in graphite have been ascribed to the presence of three types of defect-vacancies, single interstitial atoms and groups of interstitials. The difficulties of ascribing changes of physical properties to specific defects are well known and no special immunity to the onslaughts of fresh experimental evidence is claimed for the proposed model. The model accounts qualitatively, and in some cases quantitatively, for the observed changes, but there are many unanswered questions. What sizes are the groups of interstitials? Are the smaller groups mobile or do they disintegrate? These questions underline the complexity of the conglomeration of defects which has been referred to as a group of interstitials, and serve to emphasise the gaps in our knowledge concerning the irradiation behaviour of graphite.

ACKNOWLEDGEMENTS

Many of the results presented in this paper were obtained by other workers. The X-ray measurements of lattice parameter were made by G. E. Bacon and the majority of the growth measurements by H. Sheard and N. J. Pattenden. T. M. Fry was responsible for much of the early irradiation work on graphite. The author is particularly grateful to

J. H. W. Simmons both for a large proportion of the data and for the most helpful discussions.

REFERENCES

1. Kinchin, G. H. and Pease, R. S., *The displacement of atoms in solids by radiation*, Reports on Progress in Physics (1955).
2. Kinchin, G. H., *Changes in the electrical properties of graphite due to neutron irradiation*, J. Nuclear Energy, *1*: 124 (1954).
3. Dienes, G. J., *Mechanism for self-diffusion in graphite*, J. Applied Physics, *23*: 1194 (1952).
4. Pease, R. S., *X-ray examination of irradiation effects in boron nitride*, Acta Crystallographica, *7*: 633 (1954).

The Effect of Irradiation on the Structure and Properties of Structural Materials

By S. T. Konobeevsky, N. F. Pravdyuk and V. I. Kutaitsev, USSR

The effect of radiation on materials is one of the most interesting new problems. It is as important for the design and operation of nuclear reactors as for the general science of matter.

Structural materials used in nuclear reactors are subjected to a high flux of fast neutrons, slow neutrons and intense radiation of gamma rays. Peculiar changes take place in the structure and properties of a material as a result of these radiations, combined with the effects of an elevated temperature and mechanical stresses. These changes of structure and properties are chiefly due to collisions of fast neutrons with nuclei which knock out ionized atoms from their normal positions.

Radiation effects in matter must be taken into consideration in designing and operating reactors. Tests dealing with the behaviour of materials exposed to radiations as well as the study of irradiated materials will lead to the development of new materials less sensitive to radiation and also to the development of a new branch in the science of metals.

Among new metallurgical problems the following should be noted in this field: (*a*) the specific nature of hardening and other changes in properties and structure of metals and alloys caused by irradiation; (*b*) age-hardening at low temperatures; (*c*) phase transformations; (*d*) ordering in solid solutions at low temperatures; and (*e*) formation of supersaturated solid solutions caused by radiation.

This paper gives an accounnt of the results of a research on item (*a*).

RADIATION DAMAGE OF PURE METALS

Results of Irradiation of Cubic Metals

The metals studied were annealed copper, nickel, iron-armco and aluminium. Copper and iron were annealed at 700°C, nickel at 800° and aluminium at 400°C. In all cases the annealing exposure was one hour. These metals were irradiated at temperatures from 250 to 300°C. The integrated neutron flux was 1.1 to 1.4 $\times$ 10^{20} nvt.

Changes in the mechanical properties of irradiated materials are given in Table I.

An analysis of the data in Table I shows that, in spite of the high temperature at which irradiation took place, all the materials studied were hardened (with the exception of aluminium). This is shown by: (*a*) an increase in ultimate strength; (*b*) a decrease in relative elongation and in a reduction in area; (*c*) a decrease in impact strength; and (*d*) an increase in microhardness.

The most pronounced change was observed in iron (its elongation was decreased three-fold and the impact strength ten-fold); the least change of the three hardened metals was shown by copper. This may be explained by the fact that copper has a lower temperature of recovery and recrystallization than iron or nickel. This also accounts for slight changes observed in the properties of aluminium, for which the irradiation temperature of 250 to 300°C is above its recrystallization temperature.

Specific Nature of Radiation Hardening

The changes in mechanical properties of copper, nickel and iron are somewhat similar to those in the hardening of metals effected by plastic deformation. The cause in both instances can be considered to be due to the appearance of defects, that is, to disturbances in the arrangement within a crystal lattice. It can be shown, however, that radiation hardening differs essentially from mechanical hardening. This is apparent, for example, from a plot of the microhardness of irradiated metals vs the degree of preliminary deformation.

Data on copper and iron are represented in Fig. 1.

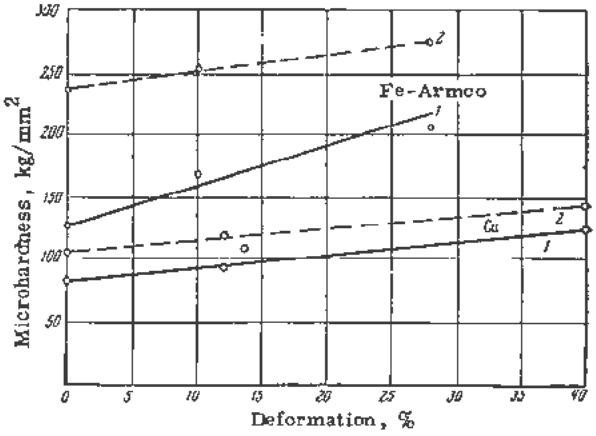

Figure 1. Change in microhardness of metals as a function of degree of preliminary deformation; (1) before irradiation; (2) after irradiation

Original language: Russian.

Table I. Mechanical Properties of Copper, Nickel, Iron and Aluminium Before and After Irradiation

No.	Material	Ultimate tensile strength σ_β kg/mm²			Relative elongation δ in %			True tensile strength S_k kg/mm²			Reduction of area ψ %			Impact strength a_k kg/cm²*			Microhardness H_0 kg/mm²		
		Before	After	Change in %	Before	After	Change in %	Before	After	Change in %	Before	After	Change in %	Before	After	Change in %	Before	After	Change in %
1	2	3	4	5	6	7	8	9	10	11	12	13	14	15	16	17	18	19	20
1	Copper annealed	22.2	24.7	+11	58.7	34.8	−40	69.5	63.7	− 9	81.4	78.5	− 4	14	5.95	−59	82	105	+28
2	Nickel annealed	40.0	62.4	+56	63.5	28.7	−55	187	178	− 5	86.0	81.0	− 6	4.3	3.3	−23	114	207	+ 82
3	Iron (Armco) annealed	35.5	57.7	+61	40.0	13.1	−67	89.9	97.5	+ 8	76	63	−15	3.4	0.35	−90	126	237	+88
4	Aluminium annealed	7.1	7.3	+ 3	33.7	32.0	− 5	70.0	53	−24	96.3	93.4	− 3	3.65	5.9	+62	33	29	−12

*Impact strength a_k was determined using round nonstandard specimens. Hence values should be considered relative.

Table II. Mechanical Properties of Steel Specimens Before and After Irradiation

No.	Material and its condition	Integrated neutron flux n/cm²	Ultimate strength σ_β kg/mm²			Yield strength $\sigma_{0.2}$ kg/mm²			$\frac{\sigma_\beta - \sigma_{0.2}}{\sigma_\beta}$		Relative elongation δ, %			Impact strength a_k kgm/cm²			Microhardness H_0 kg/mm²		
			Before	After	Change in %	Before	After	Change in %	Before	After	Before	After	Change in %	Before	After	Change in %	Before	After	Change in %
1	2	3	4	5	6	7	8	9	10	11	12	13	14	15	16	17	18	19	20
1	X18H9T stainless steel quenched from 1100°C	2.43×10^{20}	62.5	80.0	+ 29	22.3	65.5	+ 192	0.65	0.19	71.3	37	− 48	24.1	8.2	− 65	163	250	+ 53
2	The same stabilised (850°C)	3.2×10^{20}	64.0	70.5	+ 10	27.0	58.5	+ 116	0.58	0.17	66.5	36.5	− 45	–	–	–	184	306	+ 66
3	ЭИ-588 quenched from 1100°C	2.43×10^{20}	65.8	66.5	+ 1.5	20.7	51.3	+ 148	0.69	0.23	76.0	56.0	− 26	18.6	3.35	− 55	161	268	+ 66
4	ЭИ-211 quenched from 1100°C	3.2×10^{20}	60.0	72.2	+21.0	28.2	55.2	+ 96	0.53	0.23	60.5	38.4	− 36.5	–	–	–	183	330	+ 80
5	Steel 50XΦ normalised at 850°C	2.43×10^{20}	109.5	138.0	+27.0	82	130	+ 58	0.30	0.17	17.2	9.2	− 46.5	3.26	1.84	− 43.3	380	384	–
6	Stainless Steel X13 with Mo and Nb	2.43×10^{20}	48.0	69.0	+44	31.7	69	+ 116	0.34	0.0	36.5	1.2	− 97.0	–	–	–	258	327	+ 26

(1,2) X18H9T—18% Cr; 9% Ni; 0.6% Ti; 0.1% C.
(3) ЭИ-588—18% Cr; 9% Ni; 0.06% C.
(4) ЭИ-211—20% Cr; 14% Ni; 2.5% Si.
(5) 50 XΦ—1.0% Cr; 0.25% V; 0.5% C.
(6) X 13—13% Cr; 0.5% Mo; 0.12% C; 7.5% Ni.

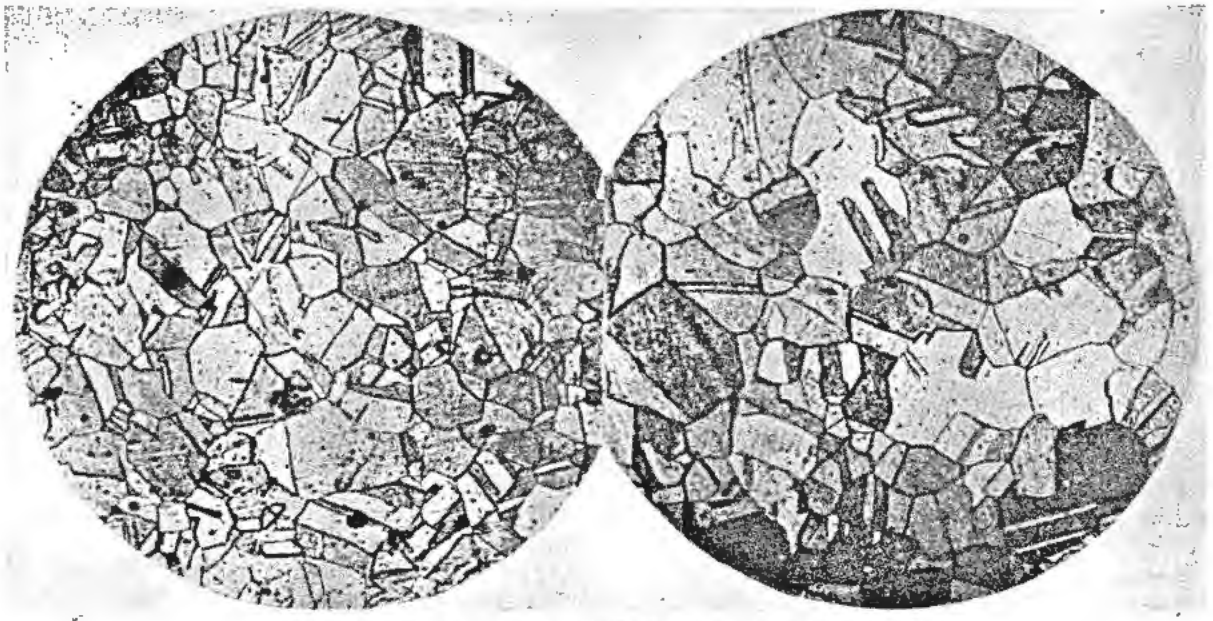

Figure 2. Microstructure of copper: (left) before irradiation; (right) after irradiation

Although the rate of change in microhardness with the degree of deformation is somewhat different for irradiated and unirradiated materials, there is no evident convergence of both curves before 40% deformation. Such a convergence would be observed if the nature of irradiation hardening were similar to that caused by deformation.

A second difference can be seen from the microstructure of irradiated materials. Micrographs of irradiated copper, nickel and iron show slight differences from those of metals in the original annealed condition. No changes inherent to cold-worked metals (such as slip lines, twins, etc.) are evident in this case. The grain size is increased in copper and nickel. Thus, prior to irradiation copper grains were 32 μ average diameter and after irradiation 43 μ, the average diameter of nickel being 68 μ and 103 μ, respectively. The average grain size of iron did not change.

The microstructures of copper and nickel before and after irradiation are shown in Figs. 2 and 3.

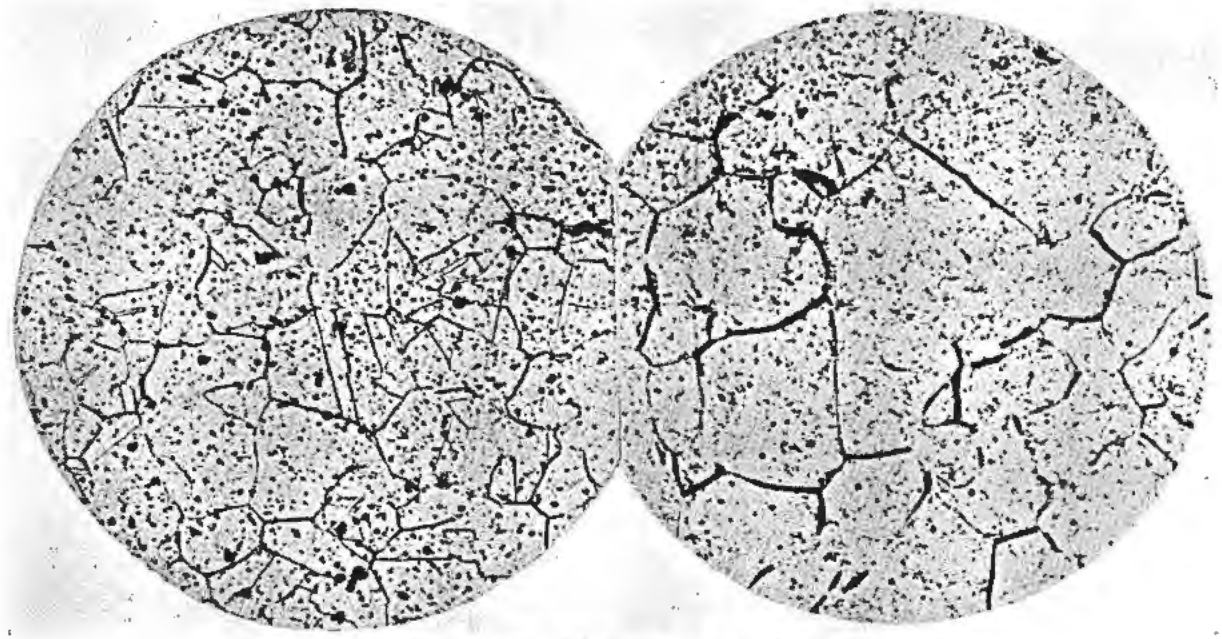

Figure 3. Microstructure of nickel: (left) before irradiation; (right) after irradiation

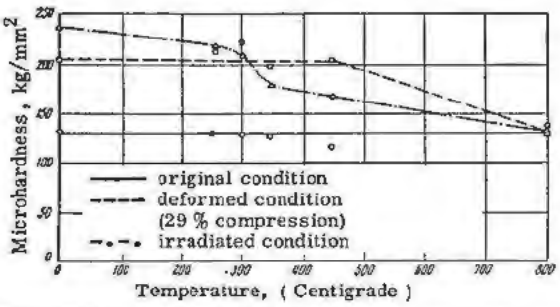

Figure 4. Change in the microhardness of iron-armco specimens as a function of annealing temperature

Thus, grain growth (recrystallization *in situ*) is observed in copper and nickel when subjected to radiation at temperatures of 250 to 300°C.

This recrystallization leads to increasing grain size without appreciable formation of new crystals. Such grain growth is not encountered in the metals under consideration in an annealed state under ordinary conditions. It shows that their ability to recrystallize is greatly increased due to irradiation.

Of interest is the fact that, contrary to the ordinary behaviour of a metal which softens when recrystallized, recrystallization in this case is accompanied by an increase in hardness.

An increase in tensile properties of iron, where recrystallization of this sort is not observed, is still larger.

Curves for the annealing of irradiated materials (see Fig. 4) are different from those for cold-worked and hardened metals. Stress relaxation occurs at a lower temperature and extends over a greater temperature range. This may be due to a lower value of the activation energy and the lower stability of the changes resulting from irradiation, compared with those produced by plastic deformation.

Changes in Zirconium under Irradiation

Zirconium was exposed to an integrated flux of 2×10^{20} nvt at a temperature ranging from 180° to 240°C. Its properties and structure changes are somewhat similar to the metals considered above. Microhardness of zirconium, first annealed for one hour at 900°C, is raised from 120 to 146 kg/mm². Specific electrical resistivity changes from 0.446 to 0.456 ohm-mm²/m, and the temperature coefficient of electrical resistivity is decreased from 3.88 to 3.78×10^{-3}. Its density remains practically unchanged from its original value.

The changes in microstructure (see Fig. 5) are of interest. Simultaneous processes of inner distortions, accompanied by the appearance of deformation twinning, as well as processes of recrystallization take place in zirconium under the influence of radiation. Recrystallization of zirconium during irradiation at a temperature not exceeding 250°C apparently is possible because of crystal lattice distortions caused by neutron effect.

RADIATION HARDENING OF CARBON AND ALLOY STEELS

Austenitic, martensitic, pearlitic and ferritic steels were selected to study the effect of radiation on iron alloys. Iron-armco was also investigated for the sake of comparison. This study of tensile properties of steels exposed to radiation shows that various types of steel behave more or less similarly to iron and nickel.

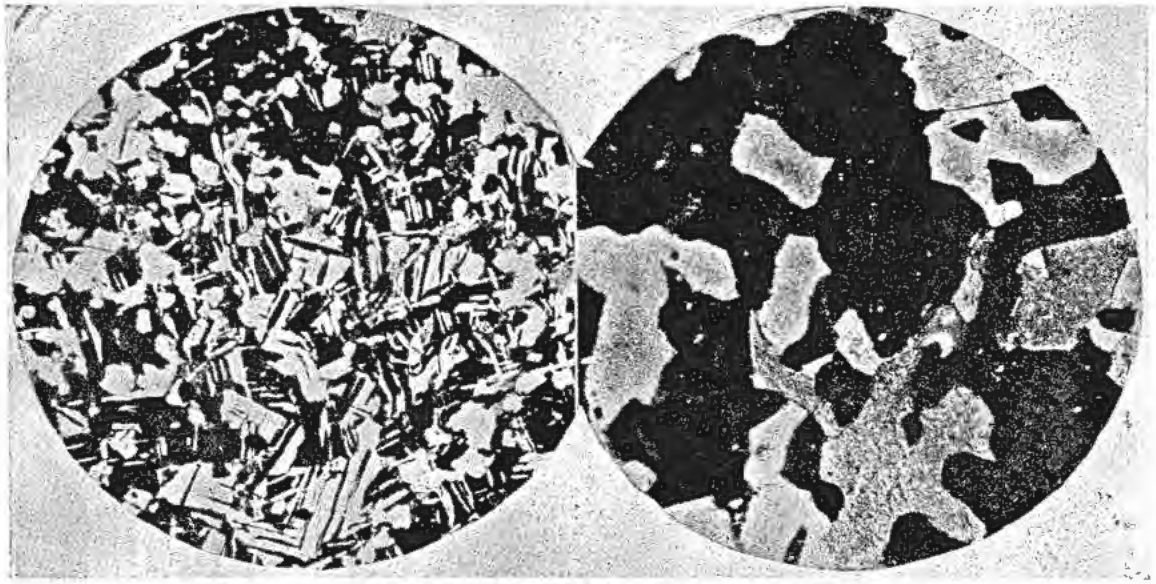

Figure 5. Microstructure of zirconium: (left) before irradiation; (right) after irradiation

Results of Irradiation

The steels under the study were normalised or quenched to austenite according to their composition. They were exposed to an integrated flux of 1 to 3 × 10^{20} nvt at 80°.

The composition of steels and the results of mechanical tests before and after radiation are given in Table II. An increase in strength and a decrease in ductility are particularly apparent from the change in impact strength as well as from an increase in conventional yield strength $\sigma_{0.2}$. The values of $(\sigma_\beta - \sigma_{0.2})/\sigma_\beta$, listed in columns 10 and 11 of Table II, best characterize the decrease in plasticity. This value is reduced from 2.5 to 3-fold for certain types of steel. As a rule the hardness of steel is increased after irradiation.

The measurement of the hardness of steels before and after radiation is shown in Table III. The Table shows that significant radiation hardening is a property common to various types of steels.

Irradiation Effects on Properties of Steel Subjected to Preliminary Cold Working

In many cases after mechanical working steel is not subjected to heat treatment, and therefore steel is in a strain-hardened condition. It was of interest to study the hardness of steel after preliminary cold-working and additional "radiation treating" in a neutron flux. Curves showing the hardness of specimens of austenite stainless steel X18H9T, deformed in compression are given in Fig. 6 as a function of the degree of deformation (in %) for unirradiated and irradiated samples. The curve for the irradiated specimens lies above that for the unirradiated ones and shows no tendency to saturation.

This shows the peculiarity of the hardening process under the influence of irradiation, and corresponds to the data given above for copper and iron (Fig. 1). This hardening is quite different from the ordinary mechanical hardening process.

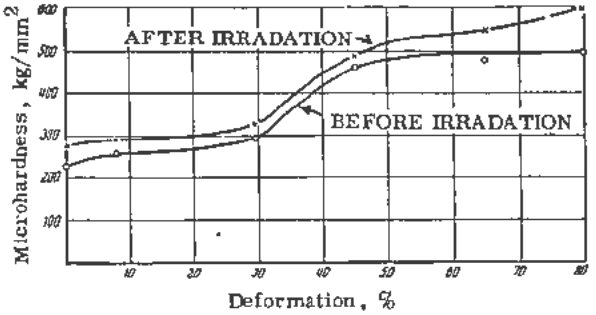

Figure 6. Change in hardness of type X18H9T stainless steel specimens as a function of degree of preliminary deformation: O, before irradiation; X, after irradiation

Magnetic measurements were made on several samples of type X18H9T stainless steel. The object of these measurements was to ascertain whether austenite decomposes to form a ferritic constituent during irradiation, the latter phenomenon accompanying plastic deformation of this type stainless steels. The specimens were placed in a non-uniform magnetic field and measured on a microbalance by estimation of specific force of separation. If certain measures were taken to preserve specimens from plastic deformation, ferromagnetism was not observed to appear.

Thus, the present study showed that due to irradiation steels, including industrial austenitic types, display an increase in their strength and an essential decrease in their plasticity.

This work is compiled from the communications of Amaev, A. D., Ivanov, A. N., Pokrovski, U. I., Golanov, V. M. and others available at the Academy of Sciences of the USSR.

Table III. Microhardness of Steel Specimens Irradiated at 80°C

No.	Type of steel	Microhardness H_0 in kg/mm² Before	After	No.	Type of steel	Microhardness H_0 in kg/mm² Before	After
1	15/15	151	289	9	ЭЖ-27	177	300
2	25/10	237	367	10	Iron-Armco	148	272
3	ЭИ-595	211	319				
4	ЭИ-626	237	360	11	ЭЖ-18	159	277
5	ЭИ-627	269	340	12	1X18H9T	223	280
6	ЭИ-401	122	300	13	Steel-10	151	266
7	ЭИ-402	150	300	14	ЭЖ-2	293	411
8	ЭИ-403	160	320				

Composition of Steels

(1) 15/15—15% Cr; 14% Ni; 2% Nb.
(2) 25/10—25% Cr; 11% Ni; 2% Nb.
(3) ЭИ-595—25% Cr; 6% Al with addition of small amounts of other elements.
(4) ЭИ-626 | 40% Cr; 10% Al with addition of
(5) ЭИ-627 | small amounts of other elements.
(6) ЭИ-40—18% Cr; 10% Ni; 2% Mo.
(7) ЭИ-402—18% Cr; 12% Ni; 1.5% Nb.
(8) ЭИ-403—18% Cr; 12% Ni; 2%Co; 1.5% Nb.
(9) Эж-27—28% Cr.
(11) ЭИ-18—18% Cr; 0.6% Ti; 0.06% C.
(12) ЭИ-18—18% Cr; 9% Ni; 0.6% Ti.
(13) Steel-10—0.1% C.
(14) Эж-2—12% Cr.

The Effects of Irradiation on Structural Materials

By F. E. Faris,* USA

The purpose of this paper is to provide a survey of United States investigations in the field of radiation effects on structural materials. In order to maintain a reasonable length an attempt has been made to give results which are typical rather than to provide a very detailed summary of the work. Although there is some discussion of the nature of defects in metals, the paper consists primarily of a presentation of experimental results. Theoretical work in the field is presented in at least two other Conference papers.[1,2]

The proper specification of irradiation conditions is of importance in the study of irradiation effects. In the case of a beam of charged particles, the energy of the particles leaving the accelerator, the beam current and the thickness of the sample being bombarded are sufficient for the specification of the radiation exposure. In the case of neutrons in a reactor the neutron flux and the neutron-energy spectrum are required. Because of the difficulties associated with fast-neutron monitoring and the variable conditions often encountered in a reactor, the neutron exposures quoted are often incomplete and in general are less reliable than the charged-particle exposures. A flux of neutrons having an energy greater than a certain value is to be taken as meaning an exposure in a region of a reactor having this flux plus a flux of lower-energy neutrons which is not specified. The temperature of the samples during exposure is also a parameter of significance. In this paper the radiation exposure and the temperature are quoted without qualification if actual measurements were made during the irradiation. The number is preceded by the symbol "~" to indicate an approximate value if the exposure or the temperature is merely an estimate.

All results reported are for measurements in the vicinity of room temperature unless otherwise stated.

DEFECTS IN METALS

Defects in metals have been produced by fast electrons, cyclotron particles, and fast neutrons. The use of several different kinds of particles is desirable for two reasons, namely:

1. Each type of radiation source has certain unique advantages from an experimental standpoint.
2. More information is gained regarding the effects of specific defects on the physical properties.

The latter circumstance arises because of the differences in the kinds of defects produced by particles having different masses and different types of interaction with the atoms of the material being exposed. That one might expect a considerable difference in the nature of the defects produced may be seen by considering the average energy which is transferred to the atoms of a metal by various particles. In the case of zirconium, for example, the average energy of the atoms knocked from their normal sites by 1-Mev electroos, protons, and neutrons is approximately 32 ev, 180 ev, and 21,000 ev, respectively, if the energy required to displace an atom from its normal lattice position is assumed to be 25 ev. Because of the small amount of energy given to the atoms, bombardment with electrons produces primarily single vacancies and interstitials, in other words, Frenkel defects. As the amount of energy transferred increases, it appears that other, more complicated defects besides the Frenkel defects may be produced in metals having a sufficiently large atomic number.[3] In addition, when relatively large amounts of energy are transferred, atomic rearrangements, as in the disordering of ordered alloys and the annealing of defects previously produced, may be important. The passage of heavy, high-energy particles such as fission fragments produces results similar to those along the paths of fast knock-on atoms.

An example of a physical-property change under

* North American Aviation, Inc., Nuclear Engineering and Manufacturing, Los Angeles, California. Including work by A. H. Barnes, W. F. Murphy, S. H. Paine, Jr., F. A. Smith, R. Weil, G. K. Whitham, Argonne National Laboratory; W. Augustyniak, D. H. Gurinsky, A. W. McReynolds, M. McKeown, M. Montag, D. B. Rosenblatt, E. E. Walsh, Brookhaven National Laboratory; W. S. Kelley, R. S. Kemper, Hanford Works; C. A. Bruch, L. F. Coffin, Jr., R. W. Hockenbury, J. R. Low, Jr., W. E. McHugh, M. B. Reynolds, L. O. Sullivan, Knolls Atomic Power Laboratory; J. L. Klein, W. B. Nowak, Massachusetts Institute of Technology; J. A. Brinkman, J. M. Denney (now at the General Electric Research Laboratory), Pol Duwez (Consultant), R. R. Eggleston, F. L. Fillmore, F. E. Faris, W. S. Gilbert (now at the University of California Radiation Laboratory), R. D. Johnson (now at the Battelle Memorial Institute), H. M. Kenworthy, A. B. Martin, M. M. Mills (now at the University of California Radiation Laboratory), North American Aviation, Nuclear Engineering and Manufacturing; R. G. Berggren, D. S. Billington, W. W. Davis, R. H. Kernohan, S. Siegel (now at the North American Aviation, Inc., Nuclear Engineering and Manufacturing), J. C. Wilson, J. C. Zukas, Oak Ridge National Laboratory; M. H. Bartz, Phillips Petroleum Company, Atomic Energy Division M. L. Bleiberg, L. S. Castleman, L. A. Cook, R. H. Fillnow, W. E. Johnson, Westinghouse Atomic Power Division.

conditions in which little energy is transferred to the atoms of a metal is given in Fig. 1. This figure, prepared from data gathered by Kenworthy, shows the change in the electrical resistance of nickel as a function of exposure for various energies. It is to be noted that a threshold exists, below which insufficient energy is transferred to produce any defects. From this threshold, as first suggested by Mills, the energy required to displace an atom from its normal position in the lattice may be calculated. Values obtained to date for various metals are given in Table I.

Figure 2, obtained by Brinkman and Gilbert, shows that annealing can be produced by irradiation when sufficient energy is available. The curve was obtained by first bombarding thorium with 9-Mev protons, which do not produce fission, until the electrical-resistivity change had saturated and then bombarding with 18-Mev deuterons, which do produce fission. It is seen that the fission fragments, which have a much higher energy than the atoms removed from the lattice by either the protons or the deuterons, produce a decrease in the saturation value of the electrical resistivity.

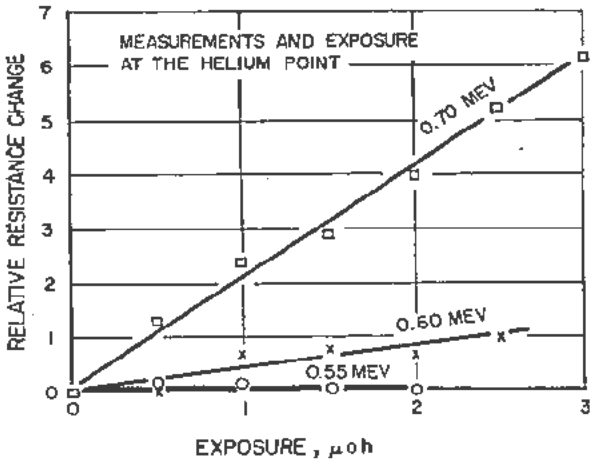

Figure 1. The change in the electrical resistance of a 0.0001 cm thick nickel foil as a function of exposure for various electron energies

Appreciable recovery occurs in irradiated metals below room temperature, a result which shows that migration of certain of the defects is possible even when the amount of thermal energy available is small. In the case of zirconium, for example, Eggleston and Fillmore find that 60 per cent of the electrical resistivity change produced by bombarding at an average temperature of —147°C with 18-Mev deuterons is removed by annealing for 5-minute intervals at successively higher temperatures up to 0°C. McReynolds, Augustyniak, McKeown and Rosenblatt report complete recovery to the pre-irradiation values of the electrical resistivity and the critical shear stress of reactor-irradiated aluminum as a result of annealing near —60°C (activation energy = 0.55 ev). The samples were exposed at 80°K to an integrated fast-neutron flux (energy >0.5 Mev) of $\sim 3 \times 10^{18}$ n/cm². Most reactor exposures have been at room temperature or higher. The physical-property changes under such conditions are the result of some secondary state produced by irradiation plus a significant amount of annealing.

Table I. The Energy Required to Displace an Atom from Its Normal Lattice Position in Various Metals

Metal	*Displacement energy, ev*	*Investigators*
Copper	25 ± 1	Eggen and Laubenstein[4]
Iron (fcc)	27 ± 1	Denney
Nickel	35 ± 2	Kenworthy

GENERAL CHANGES IN THE PHYSICAL PROPERTIES

In general a reactor exposure or an exposure to fast charged particles produces an increase in the hardness and the strength and a decrease in the ductility of metals. The changes are similar to those produced by cold work; but detailed annealing studies on copper have demonstrated the existence of significant differences, which may be interpreted in terms of the types of defects produced by each treatment. In the case of zirconium Kemper and Kelley find that 75 per cent of the change produced in the tensile properties by exposure in a reactor at ~50°C is removed by annealing for 100 hours at 250°C, although some of the radiation-induced change still remains after 100 hours at 300°C. Higher annealing temperatures are required for comparable recovery in the case of cold-worked zirconium samples.

The percentage change in the properties of metals as a result of irradiation is appreciably smaller for cold-worked samples than for annealed samples. Klein's results on aluminum, given in Table II, illustrate this point. Saturation of the radiation-induced changes, a result which is also typical, is apparent in the data.

Klein and Nowak, using X-ray measurements, find evidence that irradiation ($\sim 2 \times 10^{20}$ neutrons per cm² having an energy greater than 0.5 Mev) at ~30°C produces lattice distortion in addition to that already present from cold working 2S (commercially pure) aluminum to a partially hardened condition. Klein also finds for the same samples a 15 per cent increase in the hardness, a 26 per cent increase in the ultimate tensile strength, and a 22 per cent increase in the yield strength (0.2 per cent offset).

In addition to their dependence on cold work the changes in the physical properties as a result of a given exposure vary with a number of factors, among which are the atomic number, the melting point, and the crystallographic structure of the sample being exposed. The atomic number influences the changes because of its effect on the number and the types of the defects produced. The melting point is related to the ease with which the defects migrate and hence influences the amount of recovery occurring at a given temperature of exposure. In so far as the effect of crystallographic structure is concerned, Bruch,

Table II. The Effect of Fast Neutrons (Temperature of Exposure ~30°C) on the Tensile Properties of High-Purity Aluminum in Various Conditions of Cold Work

Exposure, neutrons per cm² having energies > 0.5 Mev	Initial sample condition	Property change, per cent		
		Offset yield strength	Ultimate strength	Per cent elongation
~7.5 × 10^{19}	Annealed	+ 100	+ 60	− 67
	Half-hard	+ 10	+ 6	0
	Extra-hard	Very small		
~15 × 10^{19}	Annealed	+ 100	+ 70	− 67
	Half-hard	+ 10	+ 6	0
	Extra-hard	Very small		

McHugh and Hockenbury find larger changes in the tensile properties of body-centered-cubic metals than in the corresponding properties of face-centered-cubic and hexagonal-close-packed metals.

Figure 3 from the work of Bruch, McHugh, and Hockenbury illustrates the significant changes often observed in the stress strain curves of metals. Some other typical changes are as follows:

Beryllium (Initial Rockwell "B" Hardness = 69)

No significant changes in the length, the density, the hardness, the modulus, the decrement, the electrical resistivity, or the thermal conductivity of beryllium are found as the result of an exposure at ~30°C to an integrated fast-neutron flux (energy >0.5 Mev) of ~5 × 10^{18} n/cm² (Siegel).

A 27 per cent increase in the hardness of beryllium results from an exposure at ~30°C to an integrated fast-neutron flux (energy >1.0 Mev) of ~3 × 10^{20} n/cm² (Bartz).

Molybdenum (Initial Rockwell "B" Hardness = 99; 5000 Grains/mm²)

An increase of approximately 50 per cent in the tensile strength and the yield point, a decrease from approximately 40 per cent before irradiation to zero after irradiation in the elongation to rupture, and a decrease from approximately 65 per cent before irradiation to zero after irradiation in the reduction in area are found in molybdenum for an exposure to an integrated fast-neutron flux (energy >1.0 Mev) of ~10^{20} n/cm² at a temperature of ~80°C (Bruch, McHugh and Hockenbury).

Nickel (Initial Rockwell "B" Hardness = 43)

An increase of 120 per cent in the hardness, an increase of 50 per cent in the ultimate tensile strength, and a decrease of 45 per cent in the elongation at rupture are reported in the case of nickel for an exposure at ~180°C to an integrated fast-neutron flux (energy >0.5 Mev) of ~2 × 10^{20} n/cm². Annealing data are given in Table III (Murphy and Paine).

Cold-Worked Type 347 Stainless Steel (Initial Rockwell "C" Hardness = 34.7)

A 10 per cent increase in the hardness and a 2 per cent increase in the electrical resistivity result from an exposure at ~80°C to an integrated fast-neutron flux (>1.0 Mev) of ~10^{20} n/cm² (Bruch, McHugh and Hockenbury).

CREEP

The sensitivity of creep to temperature and the rather large variations which are often observed in the creep rate of samples of the same metal make even laboratory creep tests somewhat difficult. The performance of such tests in a reactor is a difficult task, and it is not surprising that the results are sometimes non-reproducible. The data from in-pile creep experiments on various structural metals are summarized at the end of this paragraph. It is interesting to note that with the exception of the data on zirconium and some of the data on Type 347 stainless steel, irradiation appears to have little effect on the creep rate.

Aluminum

One preliminary test indicated a reduction in the creep rate of aluminum at 350°C and 62.6 kg/cm² by approximately a factor of two as the result of an exposure to a fast-neutron flux (energy >0.6 Mev) of ~8 × 10^{11} n/cm²/sec. It is now believed by the investigators that the observed change can be explained as a temperature effect rather than a radiation effect. Additional experiments are being performed in order to check this point (Gurinsky, Walsh, and Montag). It is interesting to note that cyclotron irradiation is reported to have no effect on the creep rate of aluminum.[5]

Nickel

Exposure to a fast-neutron flux (energy >0.5 Mev) of ~3 × 10^{11} n/cm²/sec produces little change

Table III. The Annealing of Hardness Changes in Irradiated Nickel

Annealing temperature °C	Annealing time, days	Rockwell "B" hardness
As irradiated		96
200	1	96
	8	97
400	1	94
	8	78
600	1	48
	8	46

in the creep rate at 700°C of nickel loaded as a beam with a maximum fiber stress of 141 kg/cm² (Wilson, Davis and Zukas). Exposure to a fast-neutron flux (energy >0.5 Mev) of ~6 × 10^{12} n/cm²/sec produces no change in the creep rate of nickel at 500°C (Coffin).

Zirconium

The exposure of zirconium to a fast-neutron flux (energy >0.5 Mev) of ~3 × 10^{12} n/cm²/sec appears to produce a marked decrease in the creep rate of zirconium as indicated in Table IV (Fillnow, Cook and Johnson).

Constantan

Irradiation with a fast-neutron flux of ~3 × 10^{13} n/cm²/sec has no effect on the creep rate of constantan at 300°C and 1270 kg/cm² (Barnes, Smith, and Whitham).

Inconel

Preliminary results indicate little change in the creep rate of Inconel at 705°C with beam loading to a maximum fiber stress of 420 kg/cm². The exposure was to a fast-neutron flux (energy >0.1 Mev) of ~5 × 10^{12} n/cm²/sec (Wilson, Davis, and Zukas).

Type 347 Stainless Steel

It appears that the effect of fast-neutron irradiation on the creep rate of stainless steel may be to produce a slight increase in the rate above 760°C and a decrease in the rate below this temperature. It is interesting to note that the hardness of Type 347 steel samples irradiated at 760°C does not increase, whereas that of samples irradiated at lower

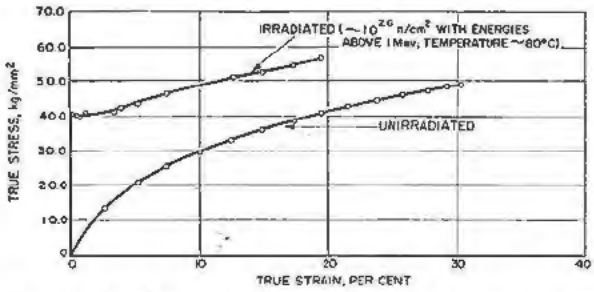

Figure 3. The effect of reactor exposure on the stress-strain curve of nickel

temperatures does. The temperature dependence of the creep rate of irradiated and unirradiated samples loaded as beams with a maximum fiber stress of 562 kg/cm² is compared in Fig. 4. The fast-neutron flux (energy >0.5 Mev) was ~3 × 10^{11} n/cm²/sec (Wilson, Davis, and Zukas). The exposure of small, Type 347 stainless steel tubes at 600°C under a hoop stress of 2000 kg/cm² to a fast-neutron flux (>0.5 Mev) of ~6 × 10^{12} n/cm²/sec has no significant effect on the creep rate (Coffin). The reason for the discrepancy between the results of Coffin and those of Wilson *et al.* is not clear at the present time. The cause may lie either with experimental difficulties or with differences in the creep mechanisms at the two different stress levels used.

IMPACT STRENGTH

In the case of those metals which exhibit a brittle behavior below a certain temperature and a ductile behavior above the same temperature, the effect of irradiation is to increase the brittle-ductile transition temperature. In addition it is often found that irradi-

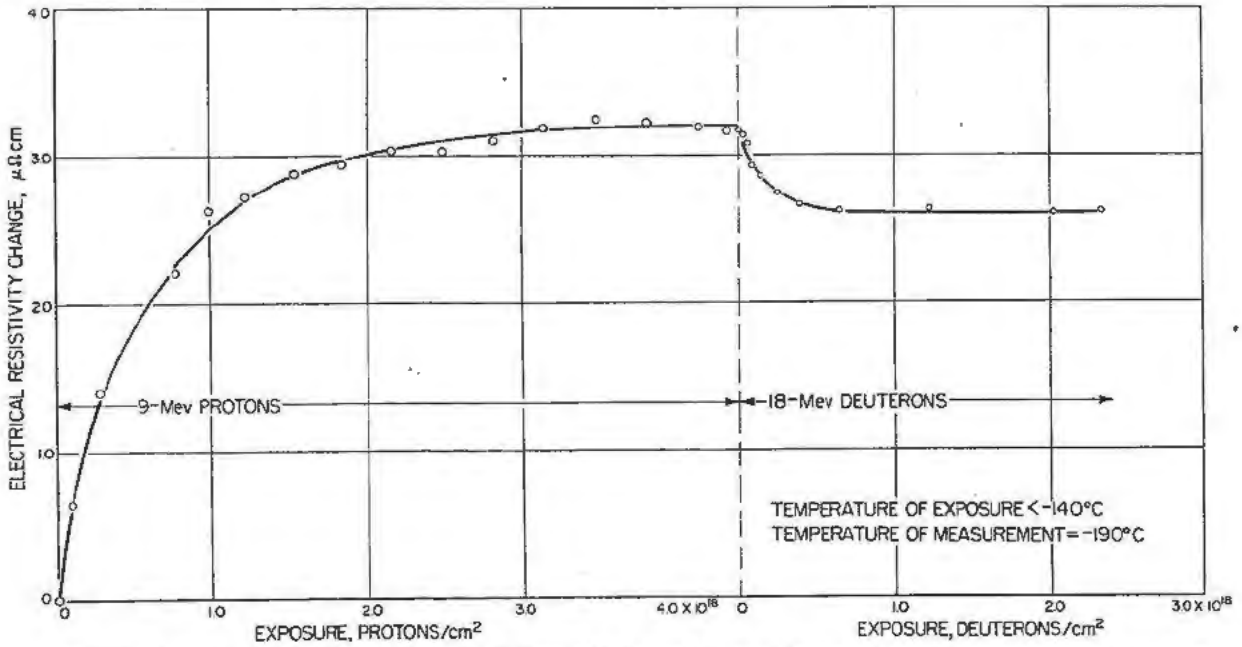

Figure 2. The change in the electrical resistivity of 0.0005 cm thick thorium foil as a function of exposure to protons and deuterons

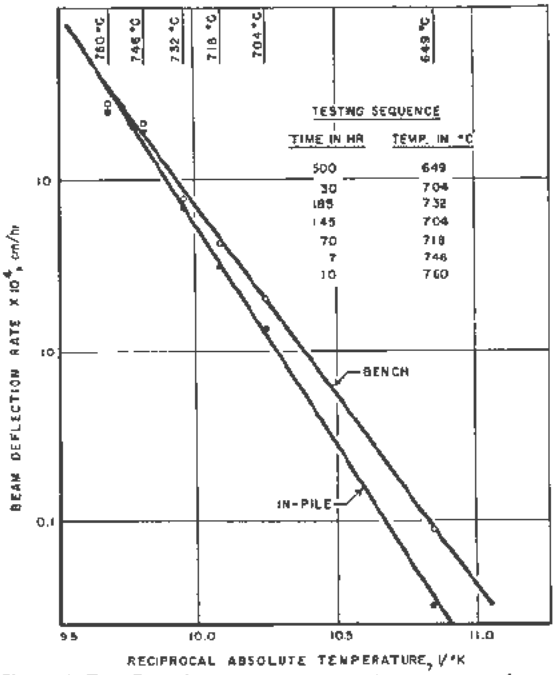

Figure 4. The effect of reactor exposure on the creep rate of type 347 stainless steel beams

ation decreases the energy required to fracture the material in the ductile region. Evidence to date indicates that irradiation will not induce brittle behavior in metals which exhibit no such behavior in the unirradiated state.

SA-70 pressure-vessel steel and molybdenum are examples of body-centered-cubic systems which suffer significant changes in their impact properties as a result of irradiation. The curves of Berggren and Kernohan in Fig. 5 illustrate the changes produced in the impact properties of SA-70 steel by exposure. Similar effects are observed to result from the deuteron bombardment of mild steel.[6] In the case of molybdenum Bruch, McHugh, and Hockenbury find that exposure of molybdenum at ~80°C to an integrated fast-neutron flux (energy >1 Mev) of 10^{20} n/cm² increases the brittle-ductile transition temperature from an initial value of approximately —30°C to a final value of approximately 70°C.

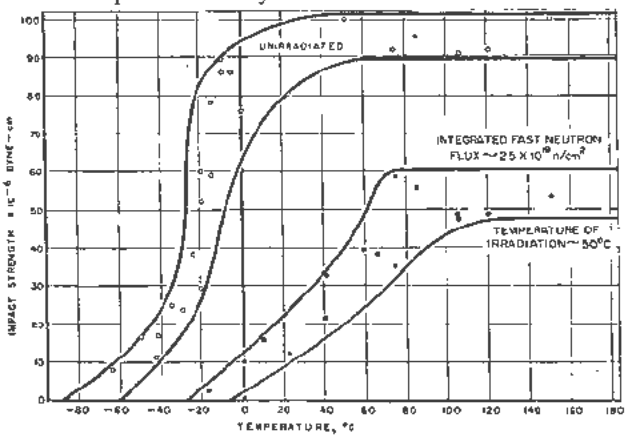

Figure 5. The effect of reactor irradiation on the impact strength of SA-70 pressure vessel steel

The hexagonal-close-packed metal zirconium exhibits ductile behavior in impact tests even at —196°C according to Bleiberg and Castleman. They also report that studies over the temperature range from —78°C to 250°C show that irradiation at ~50°C increases the energy required to fracture the material. The increase is particularly noticeable below 150°C. For impact tests conducted at —78°C they find that an integrated fast-neutron flux (energy >1 Mev) of ~3 × 10^{19} n/cm² increases the energy required to fracture by approximately 200 per cent and that subsequent irradiation produces a decrease until the pre-irradiation value is attained at ~6 × 10^{19} n/cm².

PHASE TRANSITIONS

Irradiation is observed to produce phase transitions in certain cases. The transformation from white to gray tin as a result of an exposure to fast neutrons has been reported.[7] Denney finds in studying a 2.4 weight per cent alloy of iron in copper that bombardment with fast electrons produces a transition from the metastable face-centered-cubic phase of iron to the stable body-centered-cubic phase. Magnetic measurements on the copper-iron samples after electron bombardments at various energies are the bases for the displacement-energy figure quoted for face-centered-cubic iron in the section entitled "Defects in Metals." Reynolds, Low and Sullivan observe that irradiation increases the saturation magnetic induction of Type 347 stainless steel, a result indicating some transition from austenite to ferrite. Their data are given in Fig. 6. The results in Fig. 6 plus some subsequent studies indicating saturation lead the investigators to the conclusion that the effect is due to the enhanced growth of existing ferrite nuclei in the presence of radiation.

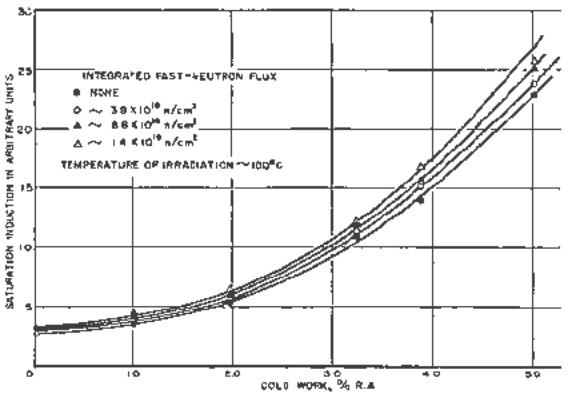

Figure 6. The effect of reactor irradiation on the saturation value of the magnetic induction of type 347 stainless steel

Table IV. The Effect of Exposure on the Creep Rate of Zirconium at 260°C

Run no.	Stress in kg/cm²	Rate before exposure, 10^{-4} %/hr	Rate during exposure, 10^{-4} %/hr	Rate after exposure, 10^{-4} %/hr	Ratio of creep rate with pile off to that with pile on in per cent
1	1265	1.0	<0.045		2000
	2530		0.23	4.6 (3 hr after)	2000
2	1265	2.8	<0.22		1300
3	1090	2.0	<0.20	13.0	1000
	1300		2.0	(30 hr after)	650

DIFFUSION

All results to date indicate that irradiation has no influence on the macroscopic diffusion rate of metals. Martin and Johnson find that an exposure to $\sim 10^{13}$ proton/cm²/sec (proton energy = 9 Mev) has no effect on the self-diffusion of silver; and Duwez, Martin, and Johnson find no effect of similar exposures on the inter-diffusion of copper-gold and copper-nickel samples. Duwez, Martin, and Johnson also report a slight increase in the inter-diffusion rate of copper-gold and copper-nickel powder samples in the presence of a fast-neutron flux (energy >0.5 Mev) of $\sim 6 \times 10^{12}$ n/cm²/sec. They point out that the effect observed can probably be explained by a small underestimate of the temperature of the reactor exposure. Paine and Weil observe that any increase in the diffusion at a stainless steel-U^{235} interface as the result of exposures in the range from 500°C to 675°C to a thermal-neutron flux of 3×10^{12} n/cm²/sec is less than the error of measurement.

ACKNOWLEDGEMENT

The data presented herein represent the work of investigators at many different laboratories. The author wishes to take this opportunity to thank the contributors for permission to use previously unpublished results.

REFERENCES

1. Seitz, F. and Koehler, J. S., P/749, *The Theory of Lattice Displacements during Irradiation*, Volume 7, Session 13B, these Proceedings.
2. Dienes, G. J., P/750, *Theoretical Aspects of Radiation Damage in Metals*, Volume 7, Session 13B, these Proceedings.
3. Brinkman, J. A., *On the Nature of Radiation Damage in Metals*, Journal of Applied Physics, *25*: 961 (1954).
4. Eggen, D. T. and Laubenstein, M. J., *Displacement Energy for Radiation Damage in Copper*, Physical Review, *91*: 238(A) (1953).
5. Jeppson, M. R., Mather, R. L., Andrew, A. and Yockey, H. P., *Creep of Aluminum under Cyclotron Irradiation*, Journal of Applied Physics, *26*: 365 (1955).
6. Meyer, Robert A., *Influence of Deuteron Bombardment and Strain Hardening on Notch Sensitivity of Mild Steel*, Journal of Applied Physics, *25*: 1369 (1954).
7. Fleeman, *The β–α Transformation in Tin*, Physical Review, *94*: 1422(A) (1954).

Radiation Damage to Radiochemical Processing Reagents

By G. I. Cathers,* USA

An important factor in reprocessing nuclear reactor fuels is the radiation damage to process reagents. The magnitude of the chemical changes produced by radiation is sufficient to affect the performance, and even the feasibility, of some radiochemical processes used to recover uranium and other materials from irradiated reactor fuels. This is true especially in the case of short-cooled fuels, where the fission product radiation is very intense. Organic materials are usually rather sensitive to radiation, the effects being complicated and not well understood. In radiochemical processing, however, interest is in the effects of radiation damage on, first, the recovery of fissile or fertile material and the decontamination of this material from fission products, and, second, on the process cost. In this paper are presented results of radiation damage studies on several ion-exchange resins; on tributyl phosphate, an organic compound useful in solvent extraction; and on one chelating agent, sodium ethylenediamine tetraacetate.

NATURE OF RADIATION IN RADIOCHEMICAL PROCESSING

The magnitude of radiation damage in chemical processing is dependent on the nature and concentration of the radioactivity and the length of time process reagents are exposed to the radiation. In processing of reactor fuel containing fission products, the β activity generally produces more chemical damage than the γ. Beta activity is almost totally absorbed in process materials in contrast to the γ radiation which has comparatively low absorption coefficients and is usually negligible when accompanied by an equivalent amount of β activity. Damage resulting from absorption of α radiation is similar to that resulting from β, since absorption is total in a few millimeters. In all three types of radiation, excitation and ionization processes produce the chemical damage.

For experimental radiation studies, γ radiation, for example, from Co^{60}, is a convenient activity and easy to handle. Its effects are similar enough to those of β activity to warrant its use in experimental work. Theoretical radiation chemistry indicates that the dissipation of absorbed γ energy proceeds by the same mechanisms as that of β radiation, at least to the accuracy usually required in process development. The energy received in any experiment with a Co^{60} γ source can be calculated on the basis that a roentgen is equivalent to 93 ergs of energy dissipation per milliliter. This is approximately correct for most organic materials as well as for water.

A useful plot of the specific power of β radiation from gross fission products as a function of decay time is presented in Fig. 1.[1] The specific power, which is defined as watts per gram of gross fission products, varies with the irradiation time. Although the accuracy of this plot is limited, it can be used in estimating the β activity power present when uranium or other fuels are separated from gross fission products in any process. The plot emphasizes that a brief irradiation period with a short decay period leads to a high specific power for the gross fission products. A correction factor of 0.8 was included in the calculation of the values plotted in Fig. 1 to account for the absence of the activity due to the volatile fission product gases, since they are not present in most chemical processing solutions.

The radiation specific power as calculated from the disintegration schemes of some radioisotopes encountered in processing varies greatly (see Table I).

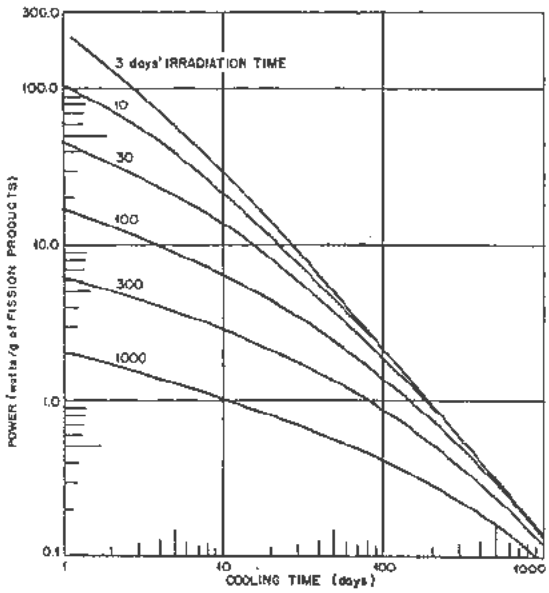

Figure 1. Specific beta radiation power of gross fission products

* Including work by R. E. Blanco, G. I. Cathers, D. E. Ferguson, I. R. Higgins, A. H. Kibbey, R. G. Mansfield and R. P. Wischow, Oak Ridge National Laboratory.

Table I. Specific Power of Certain Radioisotopes

Element	*Half-life*	*E (Mev)**	*Specific power (watts/gm)*
Plutonium-239	24,300 yr	5.1 α	0.0019
Protactinium-233	27.4 d	0.16 β	19
Zirconium-95	65 d	0.16 β	20
Niobium-95	37 d	0.06 β	13
Barium-140	12.8 d	0.32 β	138
Lanthanum-140	40 hr	0.60 β	1980

* Based on 0.4 of maximum energy in case of β emission.

However, the radiation damage from even long half-life isotopes of low specific power is occasionally great when highly concentrated materials are processed.

ION-EXCHANGE RESINS

Preliminary work has established the order of magnitude of radiation damage to ion-exchange resins as shown by a loss in capacity. This capacity loss is possibly the most important factor in the use of ion-exchange resins for radiochemical processing at high activity levels. However, other effects that must be considered include changes in the physical and chemical character of the resin. The swelling behavior, as well as the chemical selectivity toward various ions, is probably affected by radiation. Another question that arises is whether radiation of an ion-exchange resin results in organic material being dispersed as a contaminant in the aqueous stream.

The radiation work described was carried out with a Co^{60} γ source or with Ce^{144} and Pr^{144} sorbed on the resin whose effects are chiefly due to β emission.

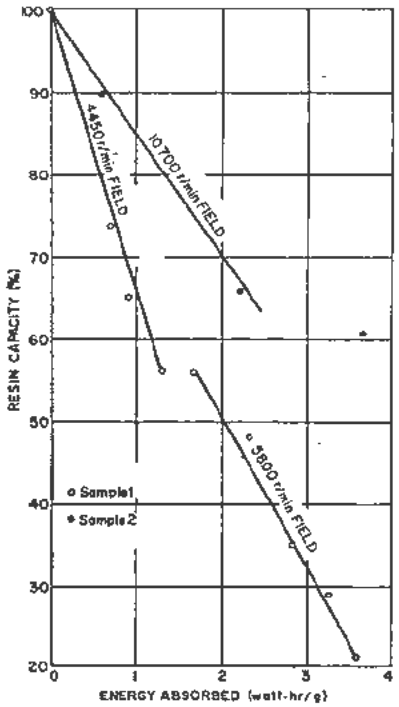

Figure 2. Capacity loss of Dowex-50 cation-exchange resin (sulfonated polystyrene) as a result of Co^{60} gamma irradiation

The rate of capacity loss with either method was the same within the experimental accuracy of the work. Dowex-50 resin exposed to a Co^{60} source lost from 15 to 35% of its capacity per watt-hr of energy absorbed per gram of dry resin (see Fig. 2). These data indicate that the capacity loss was inversely dependent on the rate of irradiation, since the lower rate of capacity loss was obtained with the more intense source. However, two different lots of resins were used in the tests and variations such as percentage of cross-linking in the original resin samples may account for the difference in capacity loss. Therefore, this should be interpreted only as an order of magnitude estimate of the rate of capacity loss. Dowex-50 is a sulfonated polystyrene resin. Capacity changes were determined by measuring the capacity of the resin for uranyl ion. Dowex-1, an anion-exchange resin of the quaternary amine polystyrene type, lost 40% of its capacity per watt-hr of energy absorbed per gram, definitely more than did the sulfonated

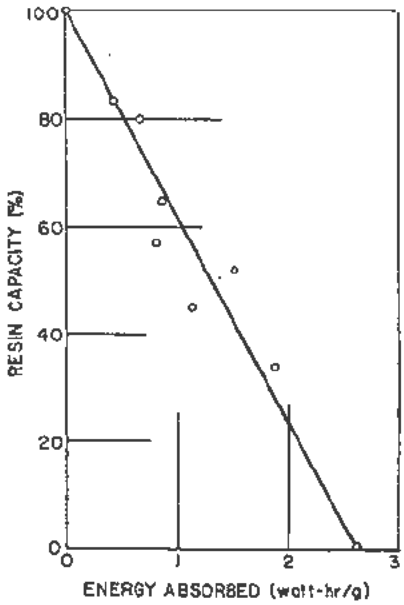

Figure 3. Capacity loss of Dowex A-1 anion-exchange resin (quaternary amine polystyrene) as a result of Co^{60} gamma irradiation

polystyrene resin (Fig. 3). These results were also obtained with a Co^{60} source; the capacity was determined by measuring the capacity of the resin for chloride ion. A third resin, Dowex-30, a sulfonated phenolic cation-exchange resin, showed a capacity loss of only 1% per watt-hour of energy absorbed per gram with both the Co^{60} and Ce^{144}-Pr^{144} irradiation methods.

The variation in capacity loss, especially in the case of Dowex-30 and Dowex-50, demonstrates that radiation damage can perhaps be minimized with the proper choice of ion-exchange resin. However, this criterion is not the only one to be considered. For example, the high radiation stability of the phenolic type resin is counterbalanced by relatively poor chemical stability.

TRIBUTYL PROSPHATE IN NAPHTHA SOLVENT

The use of tributyl phosphate as an extractant for uranium, plutonium, and thorium has been reported,[2,3] usually at a concentration of 30–40 vol % in petroleum naphtha. The usefulness of this solvent is limited by radiation damage. For instance, a radiation exposure of 0.5 watt-hr/liter results in a two-fold decrease in the ruthenium decontamination factor when thorium and uranium are separated from fission products by a tributyl phosphate solvent extraction process. The process fails completely at about 10 watt-hr/liter owing to emulsification and the formation of insoluble thorium compounds.

Radiation damage to tributyl phosphate probably includes the same processes occurring in organic solvents generally. For example, the gas produced by the irradiation of tributyl phosphate, as well as the naphtha diluent, is 70–80% hydrogen. While gas production and polymer formation are considerations in the use of tributyl phosphate and naphtha at high radiation levels, specific radiation effects, such as hydrolysis, peroxide formation, and production of unsaturated compounds, appear more important.

The hydrolysis of tributyl phosphate under irradiation is believed to be the primary factor in limiting its use in radiochemical processing. After standing, tributyl phosphate has to be carefully conditioned with caustic, to remove traces of any mono- and dibutyl phosphate formed by hydrolysis, before it can be used. Even at low concentrations these hydrolysis products markedly affect the extraction properties of tributyl phosphate. Radiation apparently accelerates

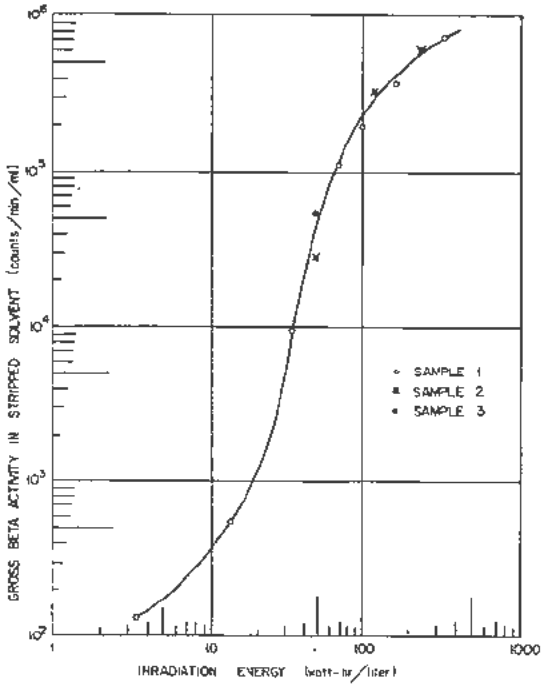

Figure 4. Gross fission product beta activity retention in irradiated 30% tributyl phosphate in naphtha solvent

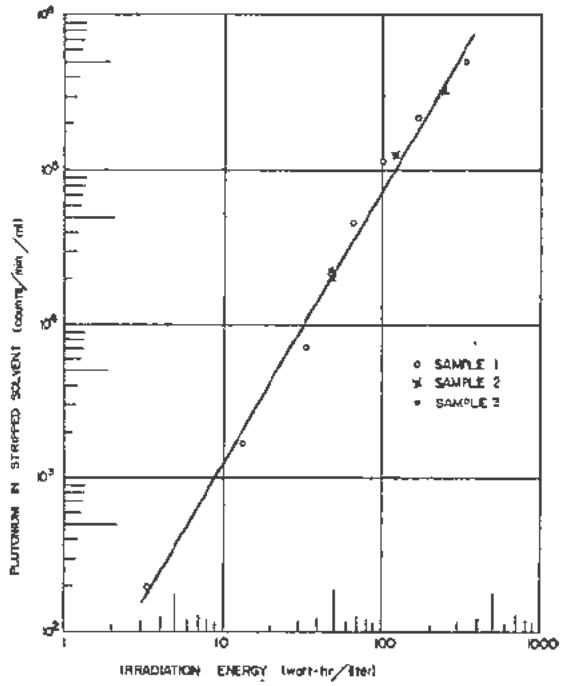

Figure 5. Plutonium retention in irradiated 30% tributyl phosphate in naphtha solvent

the hydrolysis rate, resulting in the extraction of fission products with the uranium, plutonium, or thorium and leads to difficulty in stripping these materials from tributyl phosphate. A caustic treatment after irradiation will remove the hydrolysis products.

Increased unsaturation, acidity, and a tendency toward emulsion formation are some of the other effects noted in irradiated tributyl phosphate solvent. The unsaturation probably plays some role in the formation of peroxidic material, while the acidity is due both to hydrolysis and oxidation processes. The formation of unsaturated compounds is particularly undesirable in processing of short-cooled fuel since these components combine with the large amounts of I^{131} present and carry this radioactive material over into the recovered solvent.

Batch extraction tests of 30% tributyl phosphate in naphtha showed two results of the effects of radiation, namely, extraction of fission product activity and poor stripping efficiency for plutonium (Figs. 4 and 5). The extraction test consisted in equilibrating the solvent with a 1.2 *M* uranyl nitrate—2 *M* nitric acid solution containing gross fission product and plutonium activity, scrubbing twice with an equal volume of 3 *M* nitric acid, and then stripping with two five-fold volumes of water. Three irradiations were made in a Co^{60} γ source of approximately 10^6 r/hr. Two of the irradiated samples were diluted at various ratios with nonirradiated material to achieve lower concentrations of the chemical products of radiation. The final gross β and plutonium activities in the organic phase after the extraction test were

determined and corrected for the activities found in a nonirradiated control sample.

The dependence on irradiation energy of retention of gross β activity is complex owing to the presence of more than one fission product, and possibly more than one radiation product. A plot of plutonium retention versus the irradiation energy absorbed is approximately linear and indicates that the dependence of plutonium retention on absorbed energy is nearly second order.

A rough estimate of the amount of mono- and dibutyl phosphates needed to produce the effects in Figs. 4 and 5 was obtained by adding trace quantities of these materials to tributyl phosphate—naphtha solvent. The presence of 0.02% monobutyl phosphate in 30% tributyl phosphate in naphtha solvent resulted in the same plutonium retention as in a 50 watt-hr/liter irradiation, while 0.1% dibutyl phosphate was required to duplicate the uranium stripping behavior measured in the same series of tests. Therefore, approximately 0.090 millimole of tributyl phosphate is hydrolyzed per watt-hour of absorbed energy. The corresponding G value, or molecules affected per 100 ev of energy absorbed is 0.24.

The results of several countercurrent extraction tests with 30% tributyl phosphate in naphtha show some of the adverse radiation effects obtained in a process developed for the separation of uranium and plutonium from fission product activity (see Table II). The changes are similar to those expected with the hydrolytic reaction. Irradiation exposures of 2–4 watt-hr/liter resulted in a decrease of uranium decontamination from fission products, and in a lower uranium and plutonium stripping efficiency. An irradiation exposure of 30 watt-hr/liter led to a marked increase of the activity left in the solvent after use.

Ruthenium decontamination as a function of irradiation exposure was studied with 40% tributyl phosphate—naphtha solvent in a thorium—U^{233} extraction process.[2] An irradiation of only 0.5 watt-hr/liter of solvent caused a twofold decrease in the ruthenium decontamination factor (see Fig. 6). Since normally ruthenium is the chief contaminant in the recovered

Table II. Effect of Radiation Damage from Co^{60} Source in Solvent Extraction with 30% Tributyl Phosphate

Feed: 3 volumes of 1.35 M $UO_2(NO_3)_2$—2 M HNO_3 spiked with plutonium and fission product activity.
Scrub: 2 volumes of 3 M HNO_3.
Extractant: 10 vol of 30% tributyl phosphate in naphtha.
Strip: 2 vol of H_2O.

Radiation exposure (watt-hr/liter)	*U Decontamination factor*	*Pu loss in strip column (%)*	*U loss in strip column (%)*	*β activity of used solvent (counts/min/ml)*
0	5000	0.08	0.0004	550
2.4	1300	0.05	0.007	225
4.3	2200	0.31	0.02	110
27	220	0.22	0.2	4×10^3
30	600	...	0.6	1.3×10^5
280	21	0.62	2.1	1.4×10^6

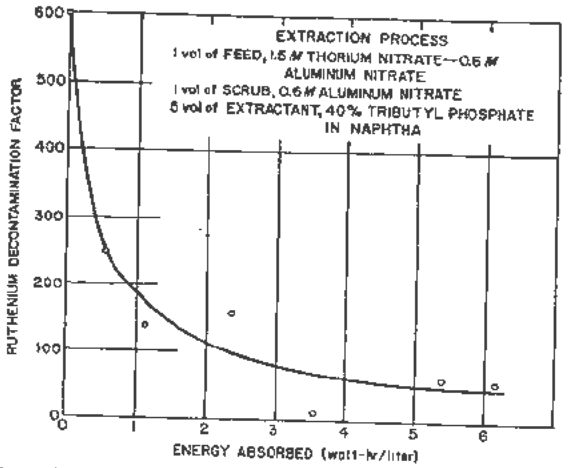

Figure 6. Dependence of ruthenium decontamination on irradiation in tributyl phosphate solvent extraction process

thorium and U^{233} from this process, operation of the process under conditions which expose the solvent to more than 0.5 watt-hr/liter will seriously impair the separation efficiency. However, if maximum decontamination is not desired, the solvent can be permitted to absorb up to 10 watt-hr/liter before it is unsuitable for use as a result of emulsification and the formation of insoluble thorium compounds.

Another radiation effect in tributyl phosphate—naphtha solvent is the production of peroxide (see Fig. 7). When the oxidizing normality value, obtained by titration with ferrous sulphate, is plotted against irradiation energy, the relation is linear and a G value of 0.2 is indicated; this is comparable with the G value obtained for the hydrolysis of tributyl phosphate.

ETHYLENEDIAMINE TETRAACETATE

Chelating compounds, such as ethylenediamine tetraacetate acid, have proved to be valuable reagents in the separation of fission products at low radiation levels. The radiation stability of sodium ethylenediamine tetraacetate was studied to determine its usefulness at high radiation levels.

The sodium ethylenediamine tetraacetate solutions used, containing barium, strontium, and lead, were exposed to Co^{60} γ sources with intensities of 5400 and 14,000 r/min. The irradiated solutions were analyzed for metallic ion concentrations, pH, and the amount of ethylenediamine tetraacetate remaining. The metal ion concentrations were determined radiochemically while the ethylenediamine tetraacetate content was determined spectrophotometrically.

The results shown in Fig. 8 were obtained by irradiating a solution of 0.065 M ethylenediamine tetraacetate, 0.33 M Na^+, 9×10^{-4} M Ba^{2+}, 1.6×10^{-3} M Sr^{2+}, 0.03 M Pb^{2+}, 0.018 M diethanolglycine, and 0.16 M NO_3^-. The initial rate of disappearance of the ethylenediamine tetraacetate ion corresponded to 0.62 millimole per watt-hour of absorbed radiation. This is equivalent to a G value of 1.7, indicating that

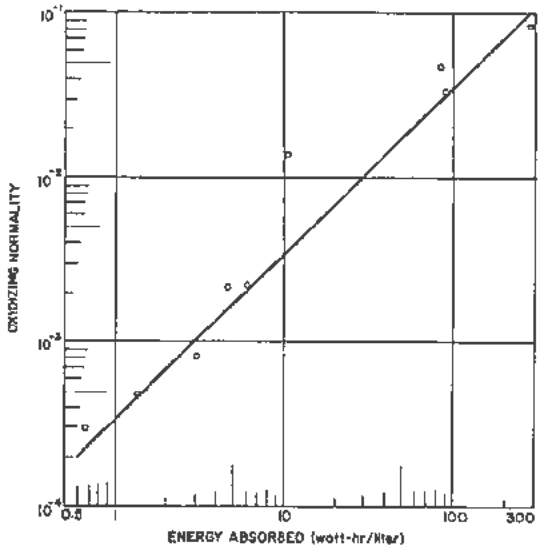

Figure 7. Oxidizing power of irradiated 40% tributyl phosphate in naphtha solvent

the rate of destruction is the usual order of magnitude encountered with many organic materials. Two runs were also made in the absence of ions other than sodium and nitrate. Initial destruction rates of 0.69 and 0.55 millimole per watt-hour were obtained at the radiation levels of 5400 and 14,000 r/min respectively. The average of 0.62 millimole per watt-hour was the same as the value observed in Fig. 8.

The extent of metallic ion precipitation and changes in pH, quantities of much interest in process solutions, are also indicated in Fig. 8. The pH changed very fast with the initial destruction of ethylenediamine tetraacetate, then leveled out. The Pb^{2+} ion precipitation rate was less than that of the Sr^{2+} ion, owing possibly to the latter being carried down with the first ion. The work demonstrated that radiation exposures have to be less than 0.1 watt-hr per milliliter of solution to avoid excessive radiation damage effects.

RADIATION DAMAGE IN THORIUM BREEDER REACTOR PROCESSING

Chemical processes designed for use with a thorium breeder reactor illustrate the radiation damage problem which arises in the use of organic solvents or ion-exchange resins. For processing thorium breeder reactor fuels, a solvent extraction process is suited to the separation of U^{233} from the thorium blanket, while ion-exchange resins can be used in removing neutron poisons and replenishing the U^{233} concentration in the core or fuel solution.[4] Radiation damage effects on the process reagents must be considered in each case. The high radiation level is avoided only with long decay and a corresponding increase in inventory and storage costs. Use of short-cooled material requires a careful study of the radiation effect since this can affect the cost as well as the process performance.

The blanket of a 360-Mw thorium breeder reactor when discharged from the reactor contains 1.2 gm of Pa^{233} and 3 gm of U^{233} per kilogram of thorium. A solvent extraction process developed for the continuous processing of this blanket uses 1 volume of feed of 1.5 *M* thorium nitrate concentration with 1 volume of scrub and 5 volumes of 40% tributyl phosphate in naphtha. The aqueous phase would therefore have 0.21 gm of Pa^{233} per liter. If the specific β radiation power of Pa^{233} is taken as 19 watt/gm, the β radiation energy in the aqueous phase of the solvent extraction process is calculated as 4.0 watts/liter. A contact time of 10 min would result in the solvent being given an exposure of 0.66 watt-hr/liter. This is raised to about 0.8 watt-hr/liter by the fission product β radiation level which is about one-fourth of the Pa^{233} activity after a decay period of approximately one day. It should be emphasized, however, that such a short decay period would result in a much higher irradiation if the blanket process is used also as part of the core process. In this case a blanket decay period of 60 days would be required to obtain a solvent irradiation of only 0.5 watt-hr/liter.[4]

It was stated earlier that radiation effects begin to be very evident at radiation exposures of about 2 watt-hr/liter. In Fig. 6 the ruthenium decontamination was shown to be significantly affected at a level of 0.5 watt-hr/liter. The solvent extraction process for a thorium breeder reactor blanket therefore operates close to the maximum permissible radiation level, and, if radiation-induced impurities build up with solvent recycling, the performance of the process may be seriously affected.

The radiation problem is important in the use of an ion-exchange process for core processing in a thermal breeder reactor. In the case of a 360-Mw reactor with a core volume of 10^4 liters, 300 liters of core solution at room temperature, or 0.8 kg of uranium, is processed per day to remove about 400 gm of gross fission products.[4] Reference to Fig. 1 shows that the specific β radiation power is approximately 30 watts/gm with a reactor residence time of 24 days and a cooling period of 5 days. About one-half of this radiation energy, or 6 kw, will be absorbed in a cation-exchange bed. Use of a 2-liter ion-exchange bed would result in about 1 kg of resin

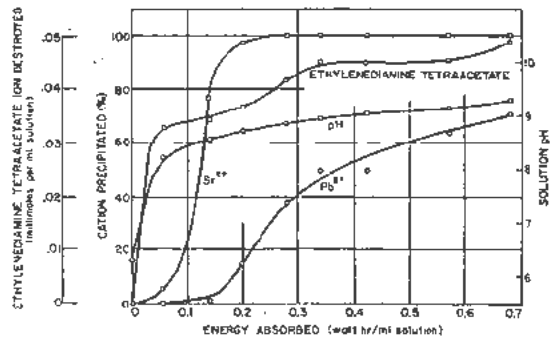

Figure 8. Radiation stability of ethylenediamine tetraacetate solution

(on a dry basis) being given a total exposure of 10 kwh in 3 hr. Since sulfonated phenolic resins, which are the most stable to radiation, lose 1% of their capacity per watt-hour of exposure per gram, the total capacity loss in this core would be about 10%. If a polystyrene resin, which has a capacity loss of at least 15% per watt-hr per gram, was used, a decay period of 100 days would be required to limit the capacity loss to 10%. This would greatly increase the inventory of uranium required for operation of the reactor.

SUMMARY

The use of organic reagents in radiochemical processes is limited by the destructive effects of radiation. The loss of capacity, encountered in ion-exchange resins that have been irradiated, is apparently dependent on the nature of the material. A quaternary amine polystyrene resin showed the most effect with a 40% loss of capacity per watt-hour absorbed energy per gram. A 15–35% loss per watt-hr/gm was found in the case of a sulfonated phenolic resin with a capacity loss of only 1% per watt-hr/gm.

Exposure of ethylenediamine tetraacetate to more than 0.1 watt-hr/ml radiation results in decreasing effectiveness of the material as a complexing agent for metallic ions. This is indicated by the observed G value of 1.7 for the destruction of ethylenediamine tetraacetate ion in solution.

The radiation damage to tributyl phosphate appears unique in that a radiation-induced hydrolytic reaction produces products that are deleterious in a solvent-extraction process. The G value, 0.2, for the hydrolytic reaction is not unusual. A G value of 0.2 was also found in the production of peroxidic material in irradiated tributyl phosphate—naphtha solvent.

In a tributyl phosphate solvent-extraction process for a thermal breeder reactor blanket after a 1-day decay period, about 0.8 watt-hr of β radiation would be absorbed in the solvent. The decontamination of thorium and U^{233} from ruthenium activity at this radiation level would be less than one-half that obtained at much lower radiation levels. No information is available, moreover, as to whether the solvent in a process at this radiation level could be continuously recycled without encountering the more serious type of damage noticed in an irradiation of 10 watt-hr/liter. In a core process employing an ion-exchange resin, approximately 10% of the capacity of a sulfonated phenolic resin would be destroyed with a processing cycle of about 24 days and a fuel decay period of 5 days.

REFERENCES

1. Murray, R. L., *Introduction to Nuclear Engineering*, Prentice-Hall, Inc., New York (1954).
2. Gresky, A. T., P/540, *The Solvent Extraction Separation of U^{233} and Thorium from Fission Products by Means of Tributyl Phosphate*, Volume 9, Session 21B, these Proceedings.
3. Flanary, J. R., P/539, *Solvent Extraction Separation of Uranium and Plutonium from Fission Products by Means of Tributyl Phosphate*, Volume 9, Session 21B, these Proceedings.
4. Ferguson, D. E., P/551, *The Chemical Processing of Aqueous Homogeneous Reactor Fuels*, Volume 9, Session 21B, these Proceedings.

Record of Proceedings of Session 11B

SATURDAY MORNING, 13 AUGUST 1955

Chairman: Mr. J. H. de Boer (Netherlands)

Vice-Chairman: Mr. J. P. Howe (USA)

Scientific Secretaries: Messrs. B. Prakash and D. J. Dewar

PROGRAMME

P/744	Radiation damage in reactor materials	D. S. Billington
P/681	Effect of irradiation on structure and properties of fissionable materials	S. T. Konobeevsky *et al.*
P/443	Damage occurring in uranium during burn-up	S. F. Pugh
	Discussion	
P/746	Irradiation damage to artificial graphite	W. K. Woods *et al.*
P/442	The effects of irradiation on graphite	G. H. Kinchin
	Discussion	
P/680	The effects of irradiation on the structure and properties of structural materials	S. T. Konobeevsky *et al.*
	Discussion	

Mr. D. S. Billington (USA) presented paper P/744 as follows: The fact that the energetic neutrons born in the fission process have the ability to change the properties of materials which they might penetrate has created a new type of materials problem for those persons concerned with the development of materials for nuclear reactor use.

Radiation damage is conceived to take place in a solid by the introduction of excessive numbers of vacant lattice sites, interstitially placed atoms, transmutation effects, fission fragment effects, the so-called "thermal spike" and, in certain types of solids, ionization effects. The first two effects appear to be most important in non-fissile materials, while in uranium-containing materials fission fragment effects become very important. All of the components of a reactor, such as the fuel, the moderator, the shield, are subject to some degree of radiation damage.

The principal materials demand of a reactor is usually upon metals and alloys just as it is in other fields. However, the materials requirements are so diversified that we find that it is necessary to study all types of solids for their susceptibility to radiation damage.

Since it is not possible in the time available to discuss in proper detail the many solids with the different properties of interest, I should like to present a few brief examples of data that have been obtained in certain materials on properties of interest to reactor technology.

I should like to refer first to the effect of neutron irradiation upon the mechanical properties of metals and alloys.

It has been long known that one general effect of neutron irradiation on metals and alloys is that there is a general increase in the hardness and strength.

Slide 1 describes an experiment by Blewitt and Coltman who studied the effect of radiation upon the critical shear stress of copper single crystals. The data show that the critical shear stress increases rapidly with exposure. However, once the metal begins to flow plastically, there is a decrease in the stress and the ultimate shape of the stress strain curve strongly resembles the unirradiated copper which is shown by the solid curve. In this particular experiment the crystals were not of the same orientation; thus, there is not a superposition of the curves in the later stages of the deformation. The data in this slide are important because, along with other data, such as the fact that one does not observe line broadening or asterism in X-ray diffraction pictures but does observe a lowering of internal friction and an initial increase in the apparent elastic constants after irradiation, they indicate quite clearly that radiation damage in metals should not be considered analogous to cold work. It is not clear that radiation damage is analogous to any other technique for changing the properties of a metal such as alloying, heat treatment, or cold working. Slide 2 does indicate, however, a superficial resemblance to alloying wherein the effect of radiation on the critical shear stress is contrasted with the effect of adding zinc to copper. However, it can readily be seen that neutron irradiation is much more effective than alloying with zinc in raising the critical shear stress. By making several assumptions regarding the stability of defects Blewitt calculated

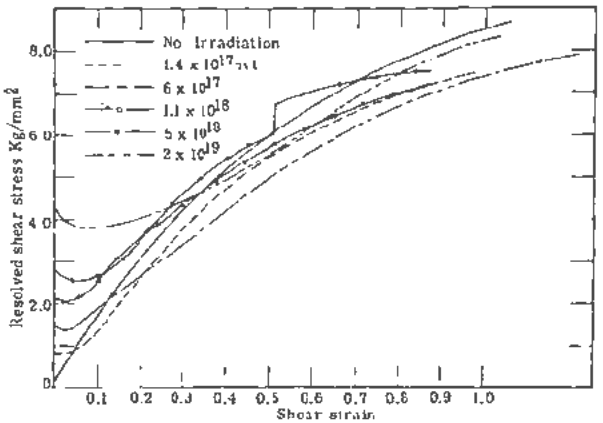

Slide 1. Stress-strain curves of neutron-irradiated copper single crystals

that an interstitial copper atom was approximately 40 times as effective as a zinc atom in raising the shear stress.

Slide 3 shows the effect of change in critical shear stress as a function of temperature of measurement and neutron exposure. It would appear that the more extensive the bombardment, the more prononnced is the effect of temperature. This slide also shows higher room temperature values of the critical shear stress than had been obtained previously.

The effect of radiation on critical shear stress has been verified by other workers, notably Holden and others at Knolls Atomic Power Laboratory who studied the effect in iron and zinc single crystals and by McReynolds at Brookhaven who studied copper and aluminum after low temperature irradiation.

Thompson, Holmes and Blewitt of Oak Ridge have studied the change in Young's modulus and internal damping in copper single crystals after very modest irradiations; they find pronounced decreases in internal damping and corresponding increases in Young's modulus. The data are shown on Slide 4.

It is interesting to note that the internal damping is reduced sufficiently so that an irradiated sample will ring like a bell when properly struck. The interpretation of these data is that the defects introduced by irradiation pin down the dislocations originally present in the metal so that they cannot move. This interpretation is consistent with the ideas of Esbelby.

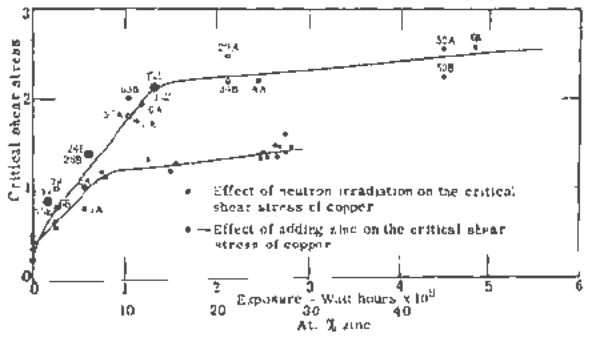

Slide 2

I'd like to mention next some data that have been recently obtained on metallic beryllium.

Wilson of Oak Ridge and Bartz of Phillips Petroleum Company have reported that they observe an increase in the ultimate tensile strength of beryllium from 35,000 psi to 51,000 psi after an exposure of 1×10^{21} nvt (fast). They noted also that the % elongation dropped from 1.4% to 0.2%. Early experiments had shown little or no effect in metallic beryllium after moderate irradiation at room temperature. It was thought that the low mass of the beryllium might be responsible in that fewer secondary and tertiary collisions would result, even though the higher activation energy for self-diffusion argued that any effect created should be preserved at room temperature. Thus the present data are consistent with the feeling that the activation energy for self-diffusion plays an important role in determining the temperature stability of irradiation effects.

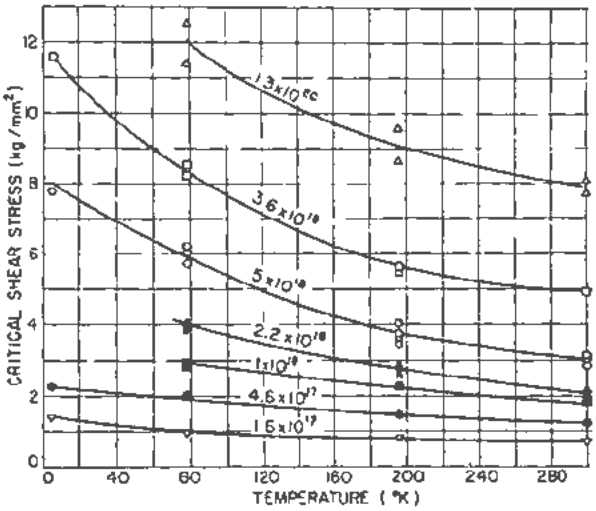

Slide 3. Effect of temperature on the critical shear stress of irradiated copper crystal

An alloy that may have considerable reactor application is low carbon pressure vessel silicon steel. This material has been shown by several investigators to show a lowering of impact strength and an increase in the transition temperature for brittle fracture. Slide 5 gives a summary of recent data that have been collected by Wilson and Berggren of Oak Ridge. Note the large increase in yield strength and the pronounced reduction in % elongation and reduction in area. The transition temperature has increased from approximately 20°C to 125°C after a room temperature bombardment of 1×10^{20} nvt (fast). If the impact tests employed are valid in determining service behavior, then serious problems will be posed when this alloy is exposed to extended high intensity radiation. However, several preliminary results obtained by bombarding at elevated temperatures (300°C) indicate that the rate of change of property is greatly reduced.

These investigators also have studied type 347 stainless steel. The data of Slide 6 show drastic increases

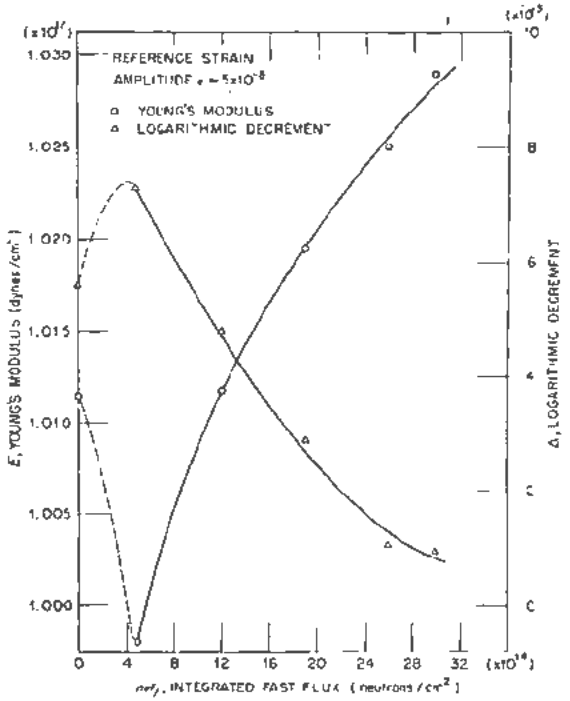

Slide 4. Young's modulus and logarithmic decrement vs integrated flux for copper single crystals

in the yield strength—the upper two curves being the irradiated samples and the lower curve being an unirradiated sample. The inset at the lower right shows the development of a yield point, thus indicating perhaps an approach to the behavior of the carbon steels, which are characterized by definite yield points in the absence of irradiation. In any event, the effects are serious enough to warrant further study.

In connection with the carbon steels, I'd like to mention a transmutation effect that may be of importance. This is the transmutation of manganese to iron which takes place at an appreciable rate. If the manganese has already served its purpose in the alloy during its heat treatment, then we need not worry. However, if it plays a continuing role, then its subsequent removal by transmutation may alter appreciably some of the important properties of the alloy. It is conceivable that other alloying elements may be appreciably depleted after sufficiently long irradiation.

One other effect that has been observed that can be of interest is the observation by Reynolds, Low and Sullivan that the ferritic content of stainless steel increases after irradiation. The effect they observed was not considered serious; however, if the effect is proportional to exposure then this effect should be investigated in more detail where concern with preservation of the "stainlessness" of the alloy is required.

I would now like to discuss briefly the effect of neutron irradiation on certain reactions that take place in metallic alloys.

There are many reactions, such as precipitation-hardening, order-disorder, etc. that are diffusion-controlled and that occur in many alloys of technological importance. I'd like to refer to the precipitation-hardening and order-disorder reactions in simple systems to illustrate the effect that neutron irradiation has on diffusion-controlled reactions.

Siegel first pointed out that a Cu_3Au alloy in the ordered state is rapidly disordered but a disordered alloy is not ordered when bombarded at room temperature. Similar results were obtained by Aronin on the Ni_3Mn system. However, Slide 7 shows some of the effects of bombardment on a disordered alloy at 150°C. It can be seen that the rate of ordering at this temperature is exceedingly slow in the absence of radiation. However, once the sample is placed in the reactor, the resistance drops rapidly, indicating an increase in the degree of order. It is argued here that the excess vacancies or interstitials permit diffusion to proceed at an accelerated rate when the temperature is high enough to give mobility to the defects. This does not mean that the activation energy for diffusion has been decreased but the effect is due only to the excessive number of vacancies present as a result of irradiation.

Recent experiments by Kernohan and the speaker on the precipitation hardening alloy nickel-2½% beryllium have shown quantitatively that neutron irradiation does enhance precipitation from supersaturated solid solution. Slide 8 shows how this was done. The ferromagnetic Curie temperature was measured before and after irradiation, and the difference in Curie temperatures shows directly the excess beryllium in the form of the compound Ni-Be that precipitated as a result of irradiation because the ferromagnetic Curie temperature is a linear function of the beryllium content in solid solution.

The importance of the above experiments is that in interpreting radiation effects in complex engineering alloys for reactor use, it is important to keep in

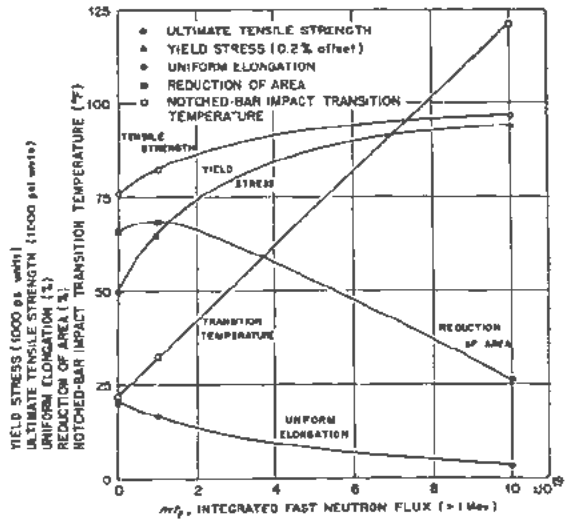

Slide 5. Integrated fast-neutron flux dependence of several mechanical properties of A-212B carbon-silicon steel

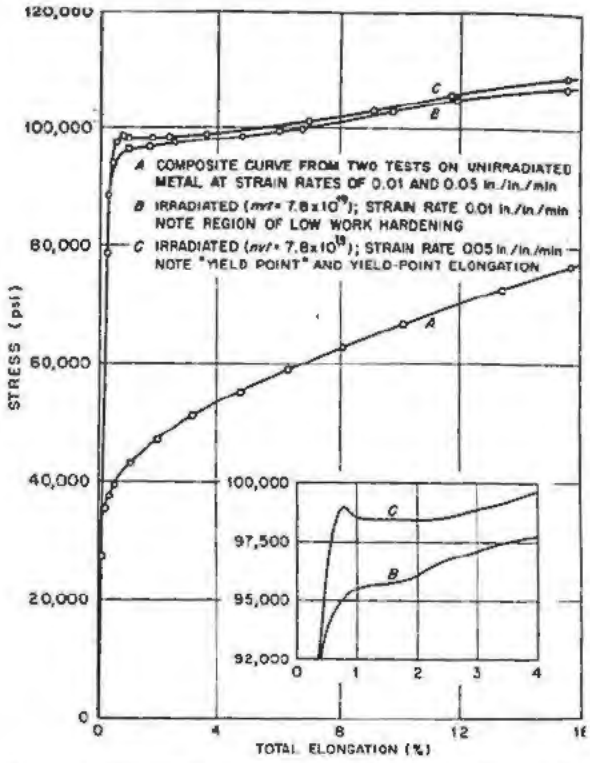

Slide 6. Conventional tension stress-strain curves for annealed austenitic stainless steel type 347

mind the possibility of enhancing diffusion controlled reactions, particularly at elevated temperatures. Thus, raising the temperature does not necessarily mean that the effect will be annealed out.

Let us now turn our attention to the fissionable materials. Most attention has been given to metallic uranium and we find that radiation effects are quite severe with growth and distortion being the principal problems. This should probably be expected because of the very anisotropic nature of the material. This characteristic is so pronounced that one can obtain gross distortion in uranium by appropriate thermal cycling. One would not voluntarily choose uranium as a fuel but would prefer to work with a more symmetrical structure. In fact, thorium does have a high degree of symmetry and most of the observations that have been made up to the present indicate that radiation damage in metallic thorium is indeed minor compared to uranium.

One of the ways of correcting the bad characteristics possessed by uranium is to alloy it with a suitable metal. Alloys of uranium and aluminum have been successfully employed and I now wish to show some slides that show the behavior of these alloys.

Slide 9 (Fig. 3 of P/744) shows how the hardness increases as a function of the burn-up of the uranium atoms. The arbitrary hardness scale employed is roughly equivalent to the Brinnell scale and, while the changes shown are appreciable, the material is still relatively soft. However, in Slide 10 (Fig. 5 of P/744) we see that other mechanical properties have changed quite severely. The exposure however is quite excessive. The 15% alloy shows substantial increases in both yield and ultimate tensile strength; the decrease in the 5% alloy is not understood. Slide 11 (Fig. 6 of P/744) shows the decrease in elongation. The open circles show results of annealing at 400°C. Slide 12 (Fig. 2 of P/744) shows the effect of fission upon the thermal conductivity. A 40% increase in resistance can be observed for the maximum burn-up of approximately 0.6% of all atoms.

The effect of fission on the electrical conductivity, as shown in Slide 13 (Fig. 1 of P/744), is quite large and also appears to be structure sensitive, that is, the 15 and 17% uranium samples are close to the eutectic composition and, as such, show maximum dispersion of the uranium in the form of UAl_4 throughout the aluminum, thus causing more damage to the alloy as a whole than is shown in 5.7% alloy.

Slide 14 (Fig. 4 of P/744) shows that much of

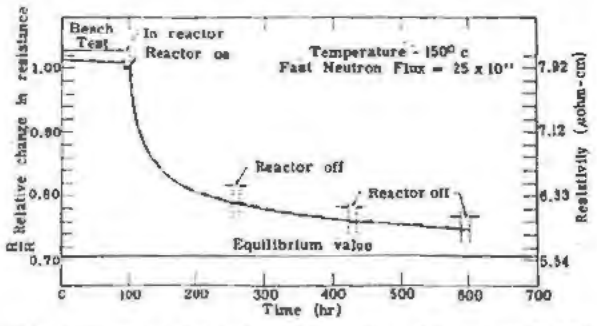

Slide 7. Change of electrical resistivity vs time of CuAu sample 15A

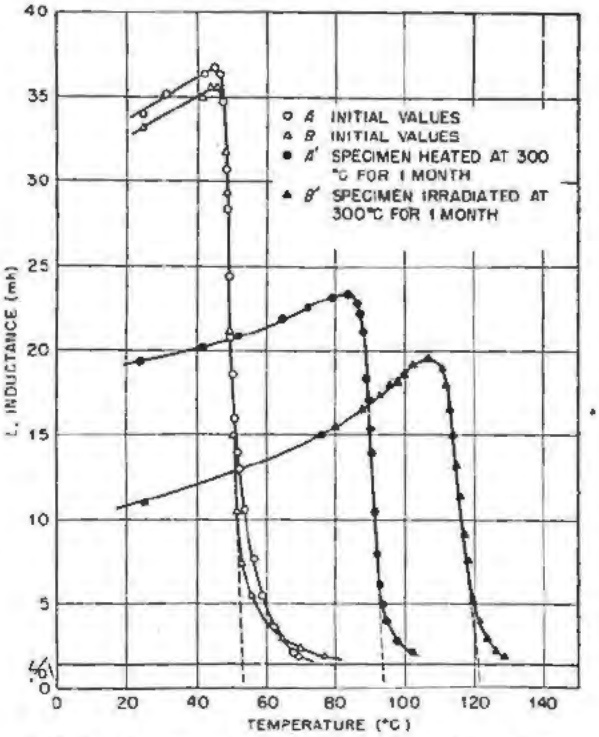

Slide 8. Inductance vs temperature curves for nickel-beryllium

the damage to these alloys begins to anneal out at 300°C, though it is not complete even at 600°C. Due to the fission fragments present it is probable that the material cannot be returned to its pre-irradiated values.

The degree of dispersion and the particle size of the uranium in an alloy or ceramic mixture is important because it will determine the degree of damage to the element. We had a suggestion of this effect in the uranium-aluminum alloys. Kernohan made a thorough study of this problem in a UO_2-graphite mixture. He found that an abrupt increase in change of properties occurred as the particle size was decreased to 44 microns or less. He was able to show that at these particle sizes the fission fragments from the UO_2 were able to penetrate all regions of the graphite and thus maximize damage. The problem is to protect the load-bearing part of the mixture, in this case, graphite.

Hunter made in-pile determinations on thermal conductivity of molded and impregnated UO_2 graphite mixtures at 600–700°C. He found order of magnitude increases in the thermal conductivity and also observed that the impregnated samples (smaller particle size) gave the biggest changes in comparison with the molded sample.

Simpson and others at Argonne have studied BeO-UO_2 mixtures and again find drastic changes in thermal conductivity substantially larger than are found in metallic samples.

Thus it appears that at low temperature of operation, metallic alloys of uranium are definitely superior. However, at extremely high temperatures ceramic samples are definitely needed so it is suggested that many more studies be started wherein elevated in-pile measurements are made.

Before concluding, let me mention several other materials problems encountered in a reactor.

Solids, such as quartz, which is a combined covalent ionic structure, are quite sensitive to radiation damage. Slide 15 shows a quartz crystal that has been extensively irradiated by Wittels of Oak Ridge. The density has decreased approximately 15% and now is the same as vitreous silica. The internal structure is completely amorphous. In spite of this dimensional

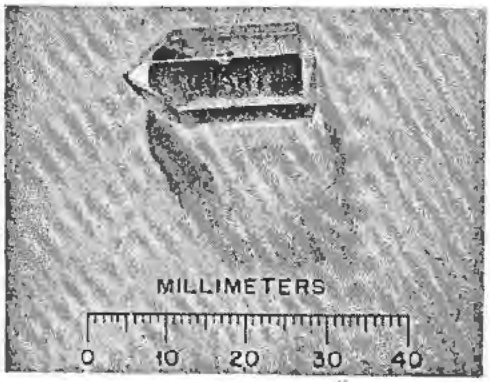

Slide 15

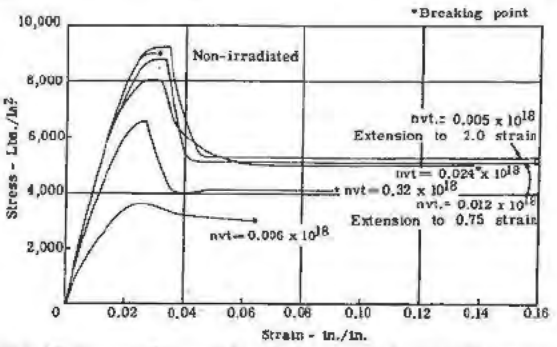

Slide 16. Stress-strain curves for pile irradiated vinyl chloride acetate

instability, the gross integrity of the single crystal has been maintained.

Semiconductors are extremely sensitive to neutron damage and pose a serious problem in connection with the use of transistors in radiation fields.

Plastics are also sensitive to ionization damage as well as neutrons as is shown in Slide 16. Since plastics are useful in a variety of ways as electrical wire insulation, gaskets, etc., means of developing radiation stability in this class of materials are to be encouraged.

I have very inadequately reviewed some of the problems that confront the reactor designer but I think I have pointed out that it is important to continue studies in radiation damage both from a basic standpoint and an engineering standpoint, for as higher fluxes, long time use, higher temperatures and other unusual conditions are proposed, then the need for understanding and for developing radiation stability will be greatly increased.

Mr. G. S. Zhdanov (USSR) presented paper P/681.

Mr. S. F. Pugh (UK) presented paper P/443 as follows: It is not surprising that uranium should undergo distortion of many kinds under irradiation, since the atoms are undergoing fission, but the first phenomenon to be described, growth, is most peculiar; it has not been found in any other material, but seems to be peculiar to alpha-uranium. Not only that, but it is peculiar to alpha-uranium over a very limited range of temperature. Experiments have shown that the growth which occurs—by which I mean a change in shape without any accompanying change in volume—is at a maximum at about 200°C and is absent above 500°C. It is most noticeable in uranium samples which have preferred orientation or in single crystals. In coarse-grained alpha-uranium the growth of individual large grains is revealed as wrinkling.

Growth and wrinkling also occur by an entirely different mechanism during thermal-cycling of alpha-uranium, and the appearance produced by thermal-cycling is similar to that produced by irradiation.

In my first slide (Slide 17) a series of uranium bars is shown after 300 cycles between 600°C and 60°C. The bars were all smooth and of equal length before cycling. The bar on the left consists of cast uranium and therefore has a coarse grain size; this bar after

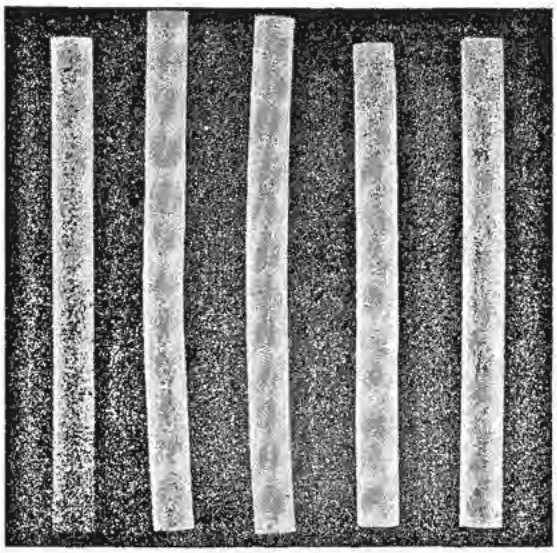

Slide 17

cycling has wrinkled badly but is unchanged in length. The second bar to the left was hot-rolled and therefore had preferred orientation of the grain. The third was hot-rolled and swaged. Both these bars have preferred orientation and therefore elongated during cycling and warped slightly. Beta annealing removed most of the preferred orientation but gave a coarse grain size. It can be seen that the fourth bar from the left has wrinkled badly but is unchanged in length. The bar on the right was quenched from the beta range and remained smooth and unchanged in length. This bar had been hot-rolled and therefore before treatment contained preferred orientation. We see that a beta quenching or annealing removes the preferred orientation, and beta quenching has the additional advantage that it also produces a fine grain size and so prevents wrinkling.

These bars would behave similarly on irradiation. The cast bar and the beta-annealed bars would be heavily wrinkled after a 0.05 per cent burn-up, and the hot-rolled and cold-swaged bars would change in length, but not necessarily in the same way that they change in length on thermal-cycling. On working these materials we obtain a mixture of (010) and (110) in the texture, and there is almost invariably an increase in length after thermal-cycling, but with an excess of (110) after hot-rolling one can get a bar which will increase in length after thermal-cycling and decrease after irradiation. A beta-quenched bar should be fairly stable when irradiated at low burn-up.

The similarity between the effects of thermal-cycling and of irradiation on alpha-uranium was somewhat misleading, as it has since been shown that the mechanisms causing these are quite different.

Slide 18 shows lead replicas taken from a uranium bar which has been irradiated to about 0.06 per cent burn-up. This was a coarse-grained bar, and it will be seen on the replica that the surface has become very wrinkled.

The difference between the mechanism of growth on irradiation and that of growth on thermal-cycling became apparent when experiments on the effect of irradiation on single crystals were performed. Thermal-cycling has no effect on single crystals, but irradiation has a very large effect. Single crystals grow on irradiation. It is now clear that the mechanism causing growth of uranium on irradiation is not primarily a grain boundary mechanism, and our experiments have shown—and I refer particularly to those of Plail—that the change in length of single crystals is an increase in length in (010) direction, a decrease in length in the (100) direction, while (001) direction remains unchanged.

It then follows immediately that wrinkling in a coarse-grained aggregate arises because each of the crystals during irradiation in that aggregate grows in a different direction. The experiments on the growth of single crystals are described in the report.

Slide 19 shows three of the specimens after irradiation. The top two samples consisted essentially of single crystals, and the main change is an increase in length of 15 per cent in the (010) direction for a burn-up of 0.03 per cent at 200°C. The orientation of the crystals was determined by using a micro-beam back reflection Laue technique. We measure the change in length of these crystals along the crystal axes, and then by examining a large number of crystals we can analyse the results and so discover which is the growth direction and which is the contraction direction. The lower crystal in the slide contained 3 or 4 grains of different orientation, so that it has distorted. This is shown more clearly in Slide 20.

Here the two grain boundaries will be seen. We have thus a kind of bi-metallic effect, in that these two crystals are growing in different directions, and the result is that the crystal bends over.

Two mechanisms have been proposed to explain the growth of alpha-uranium on irradiation, and these

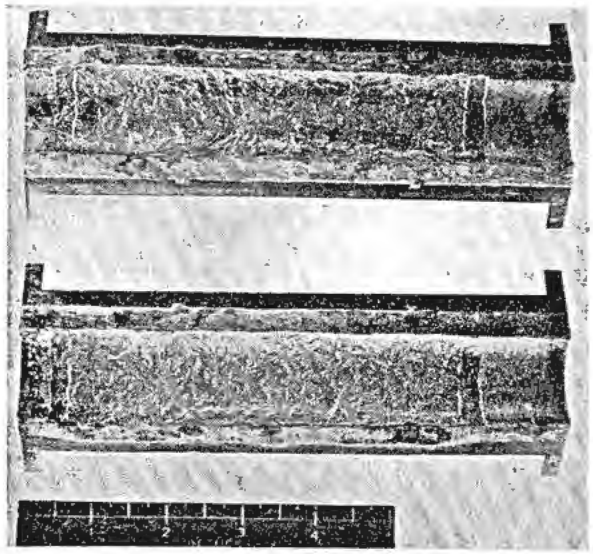

Slide 18

Slide 19

I have discussed in my paper. The twinning mechanism is based on the restrictions on twinning determined by Cahn.

Slide 21 is part of a stereogram showing the twinning restrictions in uranium. They are such that in directions close to (010) there is no twinning in tension, and in directions close to the zone running through (001) and (100) there is no twinning in compression. One might expect deformation to go in a different direction during heating from the direction during cooling, so that a rachetting effect would be obtained. The main argument against this mechanism is that the lifetime of a hot-spot is estimated mathematically to be between 10^{-10} and 10^{-12} seconds. It is not clear whether during this time dislocations could move permanently. Little is known about deformation at these high rates. The amount of deformation required at each fission site would be extremely small, so that it is possible that this might happen.

This mechanism was used to predict that the growth of single crystals would occur in the (010) direction and not above 500°C, because at that temperature there is a change-over from twinning to slip. It so happened that experiments supported the predictions.

Slide 22 shows 3 single crystals after the same burn-up as the previous three, namely 0.03%, but this time at 500°C. No growth and no distortion have occurred.

The second mechanism proposed to explain growth is based on anisotropic diffusion of interstitials and vacancies. There are numerous ways of filling in the details of this mechanism, depending on which sinks are chosen for the interstitials or vacancies to go to.

Slide 23 represents an alpha-uranium lattice, and the lines represent the close-packed (100) rows in

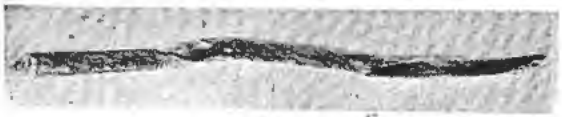

Slide 20

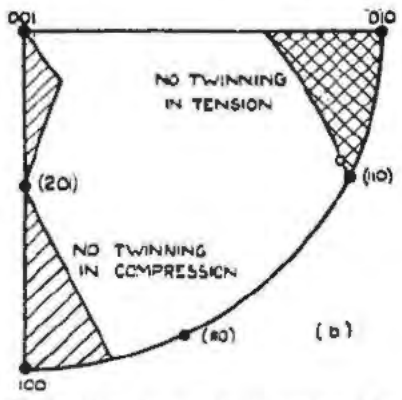

Slide 21. Restrictions on twinning in uranium: (after Cohn)

that lattice. If we assume that vacancies diffused along these rows to the grain-boundaries, that would give a decrease in length in the (100) direction. The interstitials we could pack into extra (100) rows and so increase the length in the (010) direction.

It is also possible to explain most of the variables between growth and temperature by this mechanism, although the drop in growth between 200°C and room temperature is surprisingly small, and possibly more in accordance with change in mechanical properties than change in diffusion rates.

To prevent growth and wrinkling it is necessary to remove preferred orientation and to refine the grain size. Beta annealing will remove most of the preferred orientation, and beta quenching will go some way towards refining the grain size. There are other basic ways in which grain size can be reduced. There is the interrupted quench of uranium containing a small percentage of beta-stabilizer. I think that the 0.6 per cent molybdenum alloys shown in the previous paper have been grain-refined by a critical cooling rate, and so they behaved very well under irradiation. That has the same effect as an interrupted quench. One can do this more efficiently by quenching to a temperature of 400–500°C and holding at that temperature. Finally one can make a larger alloying addition such that during cooling the alloy will split up into two phases

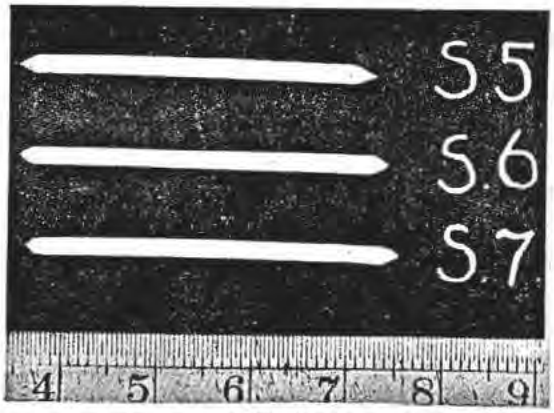

Slide 22

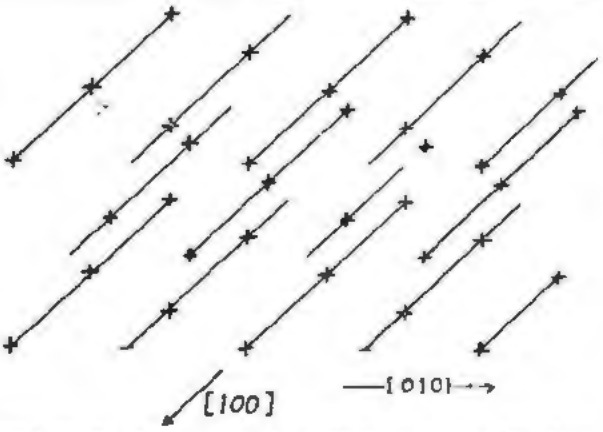

Slide 23. Growth of uranium by a diffusion mechanism: (slip plane is [010] and direction [100])

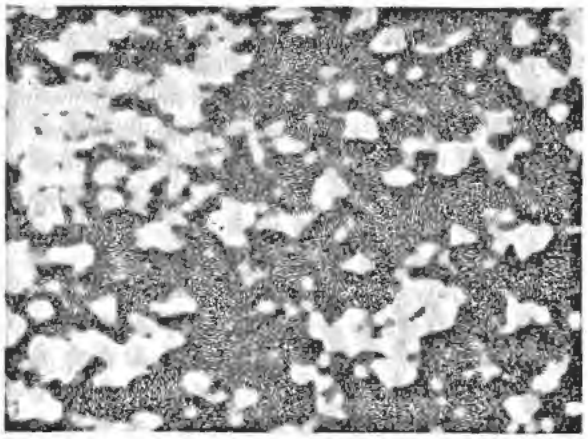

Slide 25

during the transformation. This requires a moderate alloying addition of something which will cause transformation to alpha plus a fine dispersion of intermetallic compound on cooling, and this compound during precipitation will restrict the growth of the alpha-grain.

An entirely different mechanism often occurring in uranium is swelling. This is far more important at high temperatures and high burn-ups. For example, in the high gamma range one might obtain an increased volume of, say, 30 or 40 per cent for a burn-up of 0.1 per cent.

Slide 24 shows a section near the surface of a small sample of enriched uranium, which was taken to a burn-up of 0.1 per cent. There is a 38 per cent drop in density. The magnification is 1000 times. This slide shows that the increase in volume, or swelling, is caused by the formation of very small holes in the sample. Near the centre the porosity was less. This is shown in the next slide.

Slide 25 shows, amongst other things, that in doing experiments of this kind one has to be very careful in taking average values. The swelling appears to be structure-sensitive to a very large extent. The samples used in this experiment consisted of arc-melted buttons of uranium.

Slide 26 shows the buttons before (left) and after (right) irradiation. These are two samples irradiated at different temperatures and illustrate that essentially this is an isotropic change. They have increased in volume without a change in shape.

The explanation of swelling of uranium when irradiated at high temperatures which has received the most support is based on the assumption that the inert gases and volatile fission products blow up the uranium in much the same way as, for example, in the blistering of aluminium during heat treatment. At high temperatures, where the creep strength of uranium is low, the bubbles are able to grow more rapidly. The swelling calculated from the creep strength of uranium on this basis, by Lomer and Foreman and also by Wyatt, is in agreement with that determined experimentally, but a similar calculation based on the creep rates to be expected at 500 or 600°C gives a result not in agreement with the swelling ob-

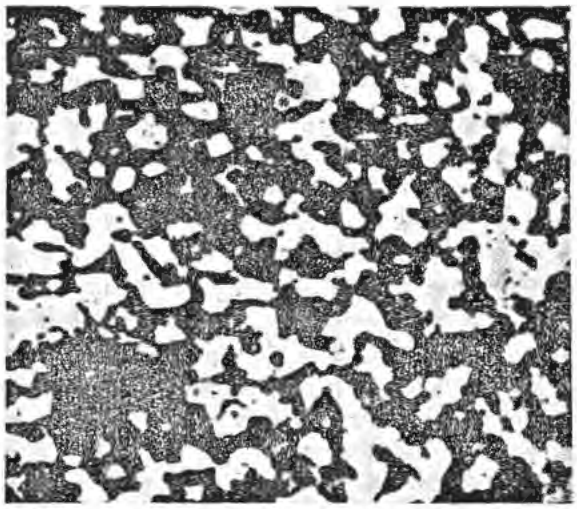

Slide 24. Specimen having 38% decrease in density on irradiation

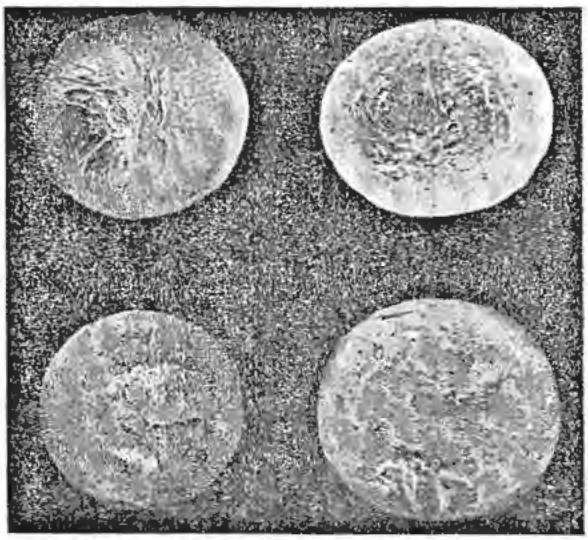

Slide 26. Effect of irradiation on alloy specimens

tained in irradiation experiments at these temperatures. One way of explaining this discrepancy would be to assume that under irradiation the creep rate of uranium is increased by two orders of magnitude. There are other ways in which this discrepancy could be accounted for, and these will be discussed in a later paper. It may, for instance, arise from the retention of some of the vacancies formed by the fission fragments during their movement through the lattice. Each fission yields about 10^5 vacancies, and only about 50 need be retained per fission to give the amount of swelling observed. Another form of damage which is particularly significant in power reactors, where, due to the large temperature gradients in the uranium, big internal stresses are found, is the change in mechanical properties. The first speaker showed changes in the mechanical properties of non-fissile materials by irradiation of something like 10^{19} neutrons per square centimetre. To show that the effect is in orders of magnitude greater in the case of uranium, I want to show you a stress-strain curve of natural uranium after an exposure of 10^{17}, which is 100 times less.

We have seen quite a lot of examples of the effects of irradiation of 10^{19} neutrons per square centimetre on uranium. Slide 27 shows an irradiation of 10^{17} and the effect on the stress strain curve here is quite as big as one gets in copper with an irradiation of 10^{19}. From this one can compute, or guess, the number of interstitials and vacancies which are formed during irradiation for each atom which undergoes fission. It has been calculated that in copper a fast neutron will produce about 500 atomic displacements, and since the effect of fission in uranium is 100 times greater, then one can say immediately that the number of displacements produced in uranium must be about five times 10^4. This is in agreement with a direct estimate of the number one would expect to get in uranium. At the higher temperatures existing in a power reactor, of course, the fission products are the main cause of damage to the fuel element, both causing swelling already described and embrittlement. The effect shown in Slide 27 would anneal out at high temperatures and would not be important.

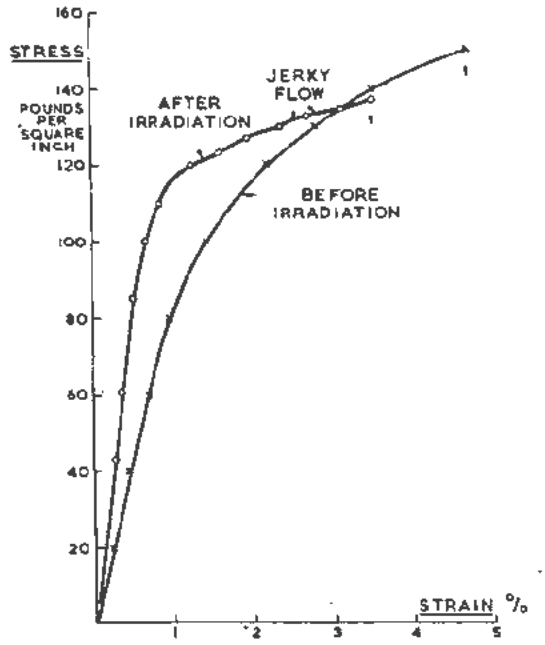

Slide 27. Effects of a short irradiation on the stress-strain characteristics of uranium

DISCUSSION ON PAPERS P/744, P/680 AND P/443

Mr. C. S. Smith (USA): I wish to compliment the USSR workers on the excellent photomicrographs and electron-micrographs of fissionable materials that they produced, including micrographs of irradiated uranium samples. Can Mr. Zhdanov give some more details on the technique of polishing, etching and replication? Also, are the most interesting globular features shown in Fig. 4 observed on samples polished prior to fission or were they after irradiation?

Mr. Zhdanov (USSR): The structures shown in a number of microphotographs were obtained from microsections with an electron microscope by the replica method. The globular structure of the uranium was observed on samples polished after irradiation.

Mr. C. E. Weber (USA): The uranium wrinkling caused plastic flow of the magnesium, but not the steel. Does this mean that the strength of the uranium is between that of magnesium and steel? I should also like to ask that more details be given on the bearing this observation has on the ductility of uranium under irradiation.

Mr. Zhdanov (USSR): The uranium sheet was located between the stainless-steel tube and the magnesium core. In this experiment there was practically no wrinkling of the steel tube. The pronounced wrinkling of the uranium sheet after irradiation indicates the great plasticity of the uranium during the irradiation process. What can be seen is the result of the mutual deformation of uranium and magnesium.

Mr. H. M. Finniston (UK): I am very interested in Mr. Zhdanov's statement about the decrease in the creep strength of uranium during irradiation. In normal creep testing it is very difficult to achieve results to within 50 per cent, yet Mr. Zhdanov is claiming an accuracy of something between 1.5 and 2. I wonder if we could have more details of the tests on the creep of uranium and would Mr. Zhdanov say what accuracy is claimed for those?

The Chairman: A similar question has been put in by Mr. Billington, who I hope will be satisfied with the question asked by Mr. Finniston.

Mr. Zhdanov (USSR): The data on the plastic flow of uranium were obtained in supplement to the basic material of the paper and show that the rate of flow increases under conditions corresponding to those which obtain in a reactor. I referred to an increase in uranium creep during irradiation of the order of 1.5–2, and not of 1.5–2 per cent. This confusion is very likely due to a mistake in the English interpretation.

Mr. F. SEITZ (USA): I would like to ask Mr. Zhdanov if the investigators have made self-diffusion measurements in fissionable materials, particularly uranium, and if the activation energies for diffusion are available.

Mr. ZHDANOV (USSR): The data on the activation energies were obtained from our study of the curves for the variation of the electrical conductivity. The activation energies measured increase with the annealing temperature and as regards order of magnitude show correspondence with the co-efficient of self-diffusion of the metal.

Mr. PERIO (France): In connection with the structural effects, whether in uranium-carbide or in heterogeneous alloys, reported in document P/681, could Mr. Zhdanov tell us what part of this effect can be attributed to purely thermal phenomena?

Mr. ZHDANOV (USSR): No, I am sorry; I cannot.

Mr. H. BROOKS (USA): In connection with Mr. Pugh's computations of the duration of a thermal spike, I should like to point out that one should actually use only the lattice conductivity in this calculation, since the coupling between the electrons and the lattice is so weak that in the short spikes there is no opportunity for equilibration of electrons and lattice. This would tend to increase it by a factor of the order of 10. How would this affect Mr. Pugh's conclusions regarding the mechanism of growth?

Mr. PUGH (UK): A factor of 10 would not help very much; it is a factor of 10^6 that I would be more interested in.

Mr. F. G. FOOTE (USA): We have observed these growth rates in single crystals of about 400 micro-inches/inch/parts per million burn-up quite comparable with those of Mr. Pugh. We have, however, in heavily worked crystal material observed growth rates of as high as 800 micro-inches/inch/parts per million burn-up. In other words, polycrystalline materials heavily worked can grow at rates of twice those observed in single crystals. I would like to ask if Mr. Pugh would like to comment on those observations, and whether he feels that his mechanism can explain this effect in polycrystalline material.

Mr. PUGH (UK): I have not tried to incorporate that observation. I knew of the observation and that there is a factor of 2 difference, but I do feel that in these irradiation experiments factors of 2 can be lost and found very easily. I think the same applies to the creep measurements. Therefore, I think that until one observes bigger effects than factors of 2, one should not really try to stretch the theories to fit them.

Mr. WEBER (USA): In regard to the excessive swelling at lower temperatures, I would like to point out the phenomenon of cracks which develop in uranium around inclusions. These, together with the embrittlement that you get on irradiation, could be responsible for the excessive cracking and therefore the swelling which occurs. Would Mr. Pugh care to comment on this?

Mr. PUGH (UK): We are preparing a paper on the matter of swelling, and we have included in this discussion phenomena based on cracking. I should say that this one comes fairly low down in the list of mechanisms which we do favour to account for the increased swelling; but we have considered this explanation.

Mr. W. K. WOODS (USA) presented P/746 as follows: The subject of irradiation damage to graphite has been under extensive experimental investigation by a variety of laboratories in the United States. There are several reasons why this program has developed on a large scale. Graphite was used as the moderator for the initial plutonium production reactors, and it was important to increase our knowledge regarding the behavior of this graphite as affected by irradiation. Irradiated reactor-grade graphite, unlike uranium, is only mildly radioactive, and investigation can proceed without the need for heavily shielded "caves" and elaborate remote handling equipment. Finally, the interest of many investigators has been attracted to this field because irradiation effects in graphite are so remarkable and so dramatic.

On the other hand, there are some important handicaps associated with the study of irradiation damage to graphite. Most important is the fact that the solid state of unirradiated graphite is quite complex and incompletely understood. Artificial graphite is not a single substance but comes in many varieties, dependent on the raw materials used and upon the fabrication history. These different graphites have various degrees of anisotropy, various densities, various crystallite sizes, and various amounts of disorder in their initial structure.

It is the purpose of this paper to summarize the experimental data which have been obtained by many different investigators in the United States on irradiation damage effects in artificial graphite. A theoretical discussion of some of the observed facts will be presented by both Mr. Kinchin in the paper immediately following, and also in paper P/751 during Session 13B of this Conference.

First, a word about exposure units. For many years laboratories all over the United States have conducted irradiations in the production reactors at Hanford, because these were the prime source of neutrons. The basic data on exposure comes from measurement of the amount of heat generated by the uranium metal in the immediate proximity of the graphite samples. We therefore can express exposure in terms of megawatt-days of heat per ton of adjacent uranium, and we abbreviate this Mwd/t. Now the physicists can take these basic data and express them in terms of integrated neutron flux, or nvt, but the conversion factors change as reactor physics theory improves; the factors we use today are different from those we have used yesterday and may be still different tomorrow. So generally we express our exposures in Mwd/t and then attach a companion nvt curve for those of you who prefer to think in those terms.

Now let us run quickly through a series of slides showing what happens to various physical properties of graphite as a result of irradiation in a Hanford reactor at a temperature of about 30°C.

Our first slide, Slide 28 (Fig. 1 of P/746) shows that these particular samples of artificial graphite are about doubled in strength as a result of irradiation. This effect might be referred to as radiation beneficence rather than radiation damage. Since the mechanical properties of graphite do not deteriorate under the influence of radiation but are improved, these radiation effects have not been studied intensively and there are limited amounts of reliable data.

Irradiated graphite is less flexible than virgin graphite, that is, it has a higher Young's modulus of elasticity. Not only is irradiated graphite more rigid and stiff than is virgin graphite, as shown on Slide 29 (Fig. 2 of P/746), but irradiated graphite is much harder than virgin graphite and is difficult to machine.

Slide 30 (Fig. 4 of P/746) shows three different curves, designated by the weird combination of letters *TSGBF*, *KC* and *CSF*. These letters refer to three different kinds of reactor-grade graphite, the descriptions of which are given in the full text of this paper. These different kinds of graphite were made from different raw materials and were graphitized at different temperatures.

The slide before you is labelled "Thermal Conductivity," but it actually plots as an ordinate the reciprocal of the thermal conductivity or the thermal resistivity. The conductivity is comparable initially to that of brass, but with continued irradiation the conductivity decreases (that is, the resistivity increases) to values comparable to that of marble. Conductivity ratios as high as fifty have been observed.

A considerably different phenomenon is encountered when we measure the change in electrical resistivity. Resistivity climbs rapidly to a value three or four times as large as its initial value, and then effectively saturates. Note that conventional ideas regarding the relationship between thermal conductivity and electrical conductivity are no longer applicable; comparing Slide 31 (Fig. 8 of P/746) with the previous slide, continued exposure causes the thermal resistivity to increase while at the same time the electrical resistivity may even be decreasing slightly.

Graphite crystals consist of stacks of parallel planes, and irradiation effects in graphite have been studied extensively by X-ray diffraction techniques. Slide 32 (Fig. 13 of P/746) shows the change in distance between the crystal planes, as measured by the C_0 spacing. At low exposures the planes merely separate. At high exposures the reflection peaks become very diffuse, and there is a trend toward the lack of pattern associated with amorphous carbon.

For comparison with the next slide, note that thn C_0 spacing increases about 10 per cent after an exposure of 1500 Mwd/t.

There are very few data on the distance between atoms within a crystal plane, that is the a_0 spacing. Changes in the a_0 spacing are much smaller than those for the C_0 spacing and appear to be opposite in sign.

The changes in crystal lattice spacing cause changes in the gross dimensions of the graphite specimens, and it is here that fabrication history of the graphite is especially critical. The crystals in extruded graphite tend to assume a preferred orientation such that the planes of the crystals are parallel to the direction of extrusion of the bar. Consequently, irradiated graphite usually increases in the transverse dimension perpendicular to the axis of extrusion, and decreases in longitudinal dimension parallel to the extrusion axis.

Changes in transverse dimension for various grades of graphite are shown in Slide 33 (Fig. 16 of P/746). Note that an exposure of 1500 Mwd/t now gives an expansion of about 1 per cent, which is an order of magnitude less than the expansion of the crystal as shown by the C_0 spacing.

Data for changes in the longitudinal dimension are shown in Slide 34 (Fig. 17 of P/746). The various grades of graphite expand slightly and then begin to shrink, with the magnitude of the effect strongly dependent upon the type of graphite under study.

Combining the data shown in the last two slides we can compute the change in specific volume as shown in Slide 35 (Fig. 21 of P/746). All samples of reactor grade graphite investigated to date show increases in specific volume during irradiation at 30°C.

Finally, irradiation produces an effect which is commonly referred to as accumulation of "stored energy." This is basically an increase in the enthalpy of the material, and it can be measured as an increase in the heat of combustion of the graphite. Slide 36 (Fig. 28 of P/746) shows the effect of irradiation on the build up of stored energy in graphite as measured by change in heat of combustion. The slide shows stored energy values greater than 500 cal/gram, with little tendency to approach saturation.

Now let us take a brief look at the effect of changing the temperature at which the graphite was irradiated. The data for the following four slides are based upon one particular type of graphite. Slide 37 (Fig. 6 of P/746) shows the effect of irradiation temperature on the change in thermal conductivity or thermal resistivity. Irradiation at 30°C causes the thermal resistivity to increase, as we noted previously. On the other hand, with irradiation at a temperature at 130°C, rather than 30°C, the change in the thermal resistivity is of the order of only about one-third as much.

Slide 38 (Fig. 14 of P/746) shows that similar results are obtained for change in C_0 lattice spacing; the amount of irradiation damage decreases rapidly as the temperature of irradiation is increased.

Slide 39 (Fig. 20 of P/746) shows that similar results are also obtained for transverse expansion; the rate of expansion decreases rapidly as the temperature of irradiation, or exposure temperature, is increased.

The change in electrical resistivity is less sensitive to change in temperature of irradiation, as shown in

Slide 40 (Fig. 10 of P/746), at least after irradiation has been continued long enough to reach this saturation value. We encounter almost as much change in electrical resistivity when we irradiate at 130°C as we do when we irradiate at 30°C.

In all of the work reported above, based on irradiations in the Hanford reactors, there has been no conclusive evidence of any effects resulting from variation in rate of exposure, or neutron flux intensity. However, recent data from the Materials Testing Reactor at higher fluxes than are obtainable in the Hanford reactors have shown a transverse expansion rate about twice as great as that experienced at Hanford; this may be a flux effect. It is under study.

Time does not permit of a discussion of the many experimental studies on thermal annealing of irradiation damage, and so we will restrict ourselves to a brief discussion of the type of data obtained from low temperature annealing of stored energy. Stored energy is gradually released as irradiated graphite is slowly raised in temperature, and this evolution of stored energy can be measured calorimetrically.

Illustrative data on the annealing of stored energy from graphite which had been irradiated at 30°C are shown in Slide 41 (Fig. 30 of P/746).

Let us start by following the curve for the graphite sample which had received the smallest exposure. The graphite was irradiated at 30°C. As we heat the graphite up nothing happens until we reach a temperature of about 120°C. Further heating then causes the release of stored energy at rates which increase until we get up to a temperature of about 200°C. At this point we get a peak release rate of about 0.5 cal/gm/°C. This means that in heating the graphite from 200°C to 201°C 0.5 calories of energy are released per gram of sample. Further heating causes the stored energy release rate to decline, but measurable amounts of stored energy are still being evolved after heating to a temperature of 450°C. If we could continue this curve to sufficiently high temperatures, the area beneath the curve should be equal to the total stored energy as obtained by change in heat of combustion measurements.

Much the same type of curve is obtained from annealing of graphite which had received the intermediate exposure, except that for temperatures greater than 120°C the curve is displaced upward, and peak release rates of almost one cal/gm/°C are obtained in the neighborhood of 200°C.

Now when we look at the annealing curve for the graphite which had received the highest exposure we find a very surprising effect. The amount of energy which is being released at temperatures below 200°C has been decreased, but there is a continued increase in the amount of energy which can only be released by heating to temperatures above 400°C.

Superimposed on this curve is a dotted line representing the specific heat of unirradiated graphite. When the rate of stored energy release exceeds the specific heat of the graphite, the graphite then exhibits an apparent negative specific heat and it can spontaneously increase in temperature.

For all physical damage, the rate of annealing and the ultimate degree to which the damage may be removed depend on the annealing temperature and on the amount of damage. Quantitative recovery of changes in physical properties may be attained as graphitization temperatures are approached.

Substantial annealing of previously damaged graphite can also be obtained by only moderate increase in the irradiation temperature. This phenomenon is referred to as "nuclear annealing."

The most suitable illustrative example of nuclear annealing is shown in Slide 42 (Fig. 45 of P/746), based on data obtained by Mr. Sheard in Great Britain. The sample of graphite is expanded by irradiation at 30°C. The sample is then irradiated at 150°C and this causes a 40 per cent recovery in the amount of the expansion. It would have been necessary to heat the expanded sample to a temperature of several hundred degrees to have obtained the same effect by oven annealing. To anneal out 40 per cent of the damage in an oven would require a temperature of several hundred degrees centigrade in the oven.

The expansion curve for graphite irradiated only at 150°C is also shown on this slide. The curves for the two irradiations at 150°C presumably meet at higher exposures.

Gentlemen, irradiation of materials such as graphite produces new solids with combinations of physical properties not previously encountered. In consequence, knowledge of the physics of the solid state should be greatly accelerated. This new scientific knowledge may eventually prove to be one of the most important products of the development of atomic energy.

Mr. G. H. KINCHIN (UK) presented paper P/442.

DISCUSSION ON PAPERS P/746 AND P/442

Mr. O. C. SIMPSON (USA): I should like to ask Mr. Kinchin to make additional comments on the fact pointed out in his paper that two samples irradiated respectively at 30°C and at 150°C to the same resistivity have very different Hall coefficients. For example, does he conclude that the simpler interstitials presumably present at the lower temperature are more effective electron traps than the more complex interstitials?

Mr. KINCHIN (UK): I do not know whether one would say that they are more effective electron traps, but they certainly appear to be different. There is a difference in the temperature coefficient of the Hall coefficient between the 30°C and the 150°C samples. This presumably indicates a difference in the energy levels of the electron traps.

Mr. HERING (France): My first questions I should like to address to Mr. Woods. Judging by Fig. 32 and what is said in his paper, it seems to me that microcrystalline graphites accumulate much less energy than graphites with well-developed crystals. But

I should like to ask him whether his "polymer carbon" and his "carbon black" have been exposed to high temperatures and whether they are laboratory or industrial products.

I should also like to ask him whether the less perfect structure of the carbon which should be reflected by a larger C parameter would, in his opinion, facilitate the accumulation of interstitials without any appreciable increase in the C parameter.

Lastly, assuming that these products can be produced industrially, does Mr. Woods consider that they have much of a future as moderators in graphite nuclear reactors?

Mr. Woods (USA): I will try to remember the various questions that were asked. I should like to point out, at first, that on Fig. 32 the lamp black is ordinary industrial lamp black; it is a sample, not a graphite. The polymer carbon came from the Bell Telephone Laboratories in small hollow spheres about 1 millimeter in diameter. It was really a powder. These materials were irradiated. They cannot be thought of as being moderator materials because, as I say, it was merely a powder sample.

I believe your second question was with regard to prospects for taking advantage of this kind of phenomenon to develop a more-radiation-resistant graphite. There are considerable studies under way in the United States but the results are inconclusive at the present time. In particular, one research worker is making up a wide variety of experimental samples, trying to get various crystallite sizes to work in, and he is also exploring the use of different raw materials. Some of the workers in the field are very optimistic, and they take the view that they can develop a graphite which will not expand when irradiated at room temperature, despite the statement made in my talk, but whether they will succeed or not I do not know.

Mr. Hering (France): What Mr. Woods has just said answers my second question. I asked him whether the linear relationship between the thermal expansion coefficients of unirradiated and irradiated products also applies in the case of carbons of bad structure, seeing that these carbons are pulverulent. I am quite sure that it has been difficult to measure these expansion coefficients. But I should also like to ask Mr. Woods whether that relationship holds good for industrial graphites whatever the direction of the section, i.e., for transverse as well as longitudinal sections.

One of Mr. Woods' diagrams clearly shows that in parallel sections expansion varies a great deal according to the dose. This being so, I should like to ask Mr. Woods the dose to which these expansion figures correspond.

Mr. Woods (USA): The dosage to which these expansion figures correspond is 5.5×10^{20} nvt. This is defined in the ordinate title of Fig. 22.

We are extremely interested in the correlation that has been developed in Fig. 22, for it indicates that the thermal expansion coefficient is apparently a very good measure of the rate of expansion under irradiation for this group of artificial graphites. I do not have a theoretical explanation for the correlation, but I would like to point out that the correlation applies to both parallel cut and transverse cut samples.

Mr. Hering (France): We were glad to see from Fig. 23 that there is a linear correlation at the beginning of exposure between the variation of the C parameter and the global expansion during exposure. Mr. Woods' paper does not, however, show whether there is any correlation between the variation of the crystallographic parameter and the energy accumulated in the graphite. Does such a correlation exist?

Mr. Woods (USA): May I suggest that I would be most happy to spend all the afternoon discussing this with you.

Mr. Hering (France): Figure 19 shows that graphitization at higher temperature increases the ratio between heavy-dose expansion and weak-dose expansion. The reason might be that treatment at lower temperature increases the initial expansion, or that it reduces expansion under a heavy dose, or again that weak-dose expansion is greater than the increase in heavy-dose expansion.

Mr. Woods (USA): To answer your question, I would refer you to Fig. 16, because the empirical correlation in Fig. 19 came from the type of data shown in Figs. 16 and 17. In Fig. 16 we see one case of graphite which was made with *WS* — that particular combination of raw materials. The *WS/GBF* was graphitized at a lower temperature than was the *WSF*. Figure 16 suggests that graphitizing at a lower temperature increases the initial expansion rate. That is all we can draw from this picture, because we do not have sufficiently high data on *WSF*, but my intuitive answer is that graphitizing at the higher temperature for the same material would cause increased expansion rates.

Mr. Hering (France): Your diagram giving the relation between the C parameter and the relative macroscopic expansion shows, as you yourself have pointed out, that a large part of the expansion is absorbed by the voids in the graphite. It may therefore be wondered whether the ratio of the variation of C to the variation in macroscopic length would not change as one passes from graphites of normal apparent density to those of high apparent density with a much smaller proportion of voids.

Mr. Woods (USA): All the graphites discussed in the paper today had densities very close to the 1.6 to 1.65 range. Consequently we did not observe any density effect because the density was not varied. One would truly expect that raising the density would increase the expansion rate, and that lowering the density would cause the expansion rate to be decreased. The reason this was not discussed in the paper was because the experimental data obtained so far are so scattered. We do have information where we have impregnated and successfully varied the density. We also have experimental samples from our laboratories

in the United States where we have varied the density by changing the pressure of molded graphite, but we have not got a good correlation. True, in general the data are so inconsistent and erratic that we have not been able to draw firm conclusions. In this connection, we know that paper P/620 presented yesterday talked about graphite with a density of 1.8, and I was hoping that some time during the morning Mr. Zhdanov might be able to tell us whether at a density of 1.8 the results were significantly different from what we had been getting at 1.6.

Mr. HERING (France): My first question to Mr. Kinchin concerns Fig. 1 in P/442. This shows the effect of healing by irradiation. It would seem, therefore, that account should be taken of this in your Equation 2 by introducing a more complex function of temperature and time.

Mr. KINCHIN (UK): I think that the relation in Equation 2 only holds for very low doses. When one has reached doses of the order of 10^{20} or greater and overlapping between the adjacent groups will occur, then this is no longer correct. It would be in principle possible to put in this effect if one knew the properties of the so-called groups of interstitials. In fact it is extremely complex to do this.

Mr. HERING (France): Now my second question: How do you obtain the value $L_c = 1.2 \times 10^4$ ev, which you give in your paper?

Mr. KINCHIN (UK): I think Seitz gives a value in his 1949 paper of something of this order of magnitude. We have taken rather a crude criterion. One cannot treat graphite either as a metal or as an insulator for determining this cut-off energy, so we have treated it more or less as if it were a metal and have taken the value which we would have got if it were a pure metal, but this is a thing which is almost impossible to calculate very accurately and is responsible for the large possible errors in the calculations of the numbers.

Mr. HERING (France): What is the unit regarding the thermal flux which you quote—would it be 10^{18}?

Mr. KINCHIN (UK): No; the unit is one neutron per square centimetre.

Mr. G. S. ZHDANOV (USSR) presented paper P/680.

DISCUSSION ON PAPER P/680

Mr. J. H. CRAWFORD (USA): I would like to ask whether the integrated neutron flux refers to thermal neutrons or to fast neutrons. If the former, could you please give an estimate of the integrated fast flux flow stating the position of the specimens with regard to fuel elements in the reactor during exposure?

Mr. ZHDANOV (USSR): The data on the integrated neutron flux pertain to both fast and slow neutrons. The specimens were placed in special channels in the reactor.

Mr. G. J. DIENES (USA): There are two interesting observations in this paper. The first I would like to comment upon is the transformation of austenite to ferrite. It was observed that this transformation was not accelerated by irradiation. We have recently completed some work on tin transformation of supercooled metallic tin to grey tin, and have found this transformation is very much accelerated by a prior lower temperature irradiation. It appears to me that phase transformation is an interesting field of study. It looks as if there is sensitivity not only to radiation but also to the detailed nature of the phase transformation itself.

The second point is on the very interesting observation of grain growth. I would very much appreciate some further details on this observation.

My first question is, were any control samples run for the same length of time at the same temperature in the absence of any irradiation?

My second question is, how was the temperature of the sample measured, and by how much did it fluctuate during exposure to the reactor?

Mr. ZHDANOV (USSR): As regards the first comment, I agree with Mr. Dienes that irradiation may influence the process of phase transformations. However, in the grades of steel investigated, no noticeable irradiation effects were observed. I should like to ask Mr. Dubrovin to answer the questions.

Mr. K. P. DUBROVIN (USSR): No control specimens were used. The influence of prolonged exposure on the irradiation temperature was not studied. As was indicated, the irradiation temperature was approximately 250–300°C.

Mr. ZHDANOV (USSR): These data refer to a series of observations under the conditions obtaining in the reactor. I want to call attention to the fact that in the case of similar irradiation of zirconium there occurs a decrease, rather than an increase, in grain size.

Mr. C. E. WEBER (USA): I should like to refer to the question of ferrite transformation. Reynolds, Lowe and Sullivan, in the Transactions of the American Society for Metals, report very little ferrite transformation when the stainless steel type 347 was annealed, but as the amount of prior cold work is increased more and more ferrite transformation occurs. It was not clear to me from your paper whether you were talking of average lack of increase in magnetism because the samples were annealed beforehand or not; and I would like to ask the question, is this lack of transformation due to the samples not being annealed, or did you have prior cold work samples which also did show a transformation in contrast?

Mr. ZHDANOV (USSR): Our results show that irradiation does not cause any direct transformation of unannealed austenite steels or the appearance of the ferromagnetic component. Plastic deformation may perhaps account for the effects observed in a number of studies.

Mr. D. H. GURINSKY (USA): The authors have noted a reduction in impact strength as a result of irradiation. Have they made any measurement on transition temperature and impact?

Mr. ZHDANOV (USSR): The reduction in impact strength noted was due primarily to irradiation. The effect on transition temperature was not studied.

Mr. GURINSKY (USA): Have you made any measurements on the change in transition temperature as a result of irradiation in steels?

The CHAIRMAN: I will ask these gentlemen to get together after the meeting.

Mr. H. M. FINNISTON (UK): I find this paper very interesting and very mystifying. There seem to be a number of inconsistencies in the hardness measurements, and what one would have expected to account for these, and the microstructures. The differences between copper, nickel and iron do not seem to give a consistent picture. Have the authors any theory or model which would account for the types of defect which they would have expected in these materials?

Mr. ZHDANOV (USSR): In this little-investigated field we might expect to discover new facts which do not fully jibe with present ideas. I do not think there is any internal inconsistency between an increase in grain size on the one hand and an increase in hardness on the other in the same case, although at first glance this may appear to be in conflict with what occurs in annealing plastically deformed metals.

As for a theory of radiation effects, this question is attracting an increasing amount of attention among Soviet investigators.

The CHAIRMAN: We have now come to the end of this session, but on Monday morning we shall have what is more or less a continuation. What we have heard this morning is, for people who want to be pessimistic, something which may tend to increase their pessimism, because we have learned that the fuels and the moderators and the construction materials, and also the construction materials for the instrumentation, will all suffer immensely from irradiation. Unfortunately we cannot place all these materials outside the biological shield; they have to be inside and so they have to suffer.

When you see all these changes, and especially in the materials for the instrumentation, you might doubt whether a reactor could be constructed and worked. Fortunately we know that it can do so, and that this is a little damping for the pessimists! The best attitude to take is this, that the more we study all these forms of damage and understand them—so that the theoretical side is very important—the better we shall all be prepared first of all to make the best of it and then to improve the materials.

I am very glad to know that all this work will stimulate a further increase in the study of solid materials. Just prior to the advent of atomic energy the study of solid materials was to some extent on the decrease, and inorganic chemistry was very much on the decrease. The impetus of all this work is that both are rising in importance again. I do not want to say anything to offend organic chemists, but I am very glad that inorganic chemistry is coming into its own again. I ought to say that I was originally an organic chemist myself!

With these words I bring this session to a close. On Monday morning many of these problems will come up again, but after everybody has thought about them, and perhaps we can then hear some of the results of the lobby discussions which have now been arranged.

Session 12B

EFFECTS OF RADIATION ON LIQUIDS

LIST OF PAPERS

A Survey of Recent American Research in the Radiation Chemistry of Aqueous Solutions

By Augustine O. Allen,* USA

The subject of chemical effects of radiations on aqueous solutions is well-covered in the generally available scientific literature, and several reviews of the field have appeared from different countries in the last few years.[1-8] To present still another at this time is justified chiefly because of the rapid state of development of the subject. Many basic questions, which have troubled workers in the field for a long time, now appear to be on the way to resolution in the light of current research. Much of this work, simply because of the normal delays in scientific publication, could not be published until late this year or some time next year. The present paper affords a welcome opportunity for discussion of some of the important current American work. A complete explanatory review of the field will not be attempted here, nor will the applications of radiation chemistry in engineering and in biology be indicated: such discussions may be found among the references.

The immediate problem in the radiation chemistry of aqueous solutions is to correlate all the various reactions observed in different solutions in terms of the current free radical theory of water decomposition. Great quantitative success is being met with in explaining reactions in solutions of various simple inorganic substances. A complete account of the decomposition of pure water itself, and the behavior under irradiation of solutions of the decomposition products, oxygen, hydrogen peroxide and hydrogen, appears to be more difficult to attain, but progress is being made. Determining radiation-chemical reaction yields with precision is a difficult matter, and present techniques, though apparently simple, are the result of years of experiment at many laboratories. With certain basic points of manipulation, material purity and dosimetry now settled, good precise information is presently appearing at a great rate. Behind the chemical theories lies the problem of working out a molecular-dynamical model, based on physical analysis of the processes resulting from absorption of high-energy radiation in a solution, to serve as a basis for the chemical theories.

THE FREE RADICAL THEORY AND REACTION KINETICS

The theory in its usual form applies to solutions so dilute that direct action of radiation on the solute is negligible. Then the radiation acts on the water to give four products: the free radicals H and OH, and the molecules H_2 and H_2O_2. The radicals are manifested by their reactions with solutes; the molecules by their appearance in the solution when a solute is present to protect them from action of the radicals. With radiations of low ion density, such as gamma rays, radicals predominate; with those of high ion density, such as alpha rays, molecules predominate.

A free radical is perhaps best defined as a molecule which possesses an odd number of electrons. Radicals act on solutes by one-electron transfer processes. With an inorganic solute, such as nitrite, the initial reaction products are oxidized and reduced compounds which may often react with one another to regenerate the original solute. In such cases, which are more usual than not in the inorganic field, the H and OH radicals contribute little or nothing to the observed reaction; the amount of net oxidation or reduction occurring is determined by the yield of molecular products, H_2 or H_2O_2. To bring out the full radical yield, a mixture of solutes may be used, one reacting readily with OH, the other with H; the resulting radicals must then undergo clear and well-defined reactions. A classical example is the reaction in solutions containing hydrogen and oxygen, discussed below. Addition of acid also allows the full radical yield to appear as oxidizing power, since H as well as OH can act as oxidant in the presence of acid.

Since the interactions involved are somewhat complicated, the notation used to express them is unavoidably somewhat complicated also. Reaction rates in radiation chemistry are usually expressed as a "yield" G, the number of molecules of a given product formed per 100 ev of energy given to the material by the radiation. The rate of formation of the four products from water can thus be expressed as G_{H}, G_{OH}, $G_{\mathrm{H_2}}$ and $G_{\mathrm{H_2O_2}}$. These four yields are however connected by an equation of material balance:

$$G_{\mathrm{OH}} + 2G_{\mathrm{H_2O_2}} = G_{\mathrm{H}} + 2G_{\mathrm{H_2}}$$

so that three quantities are sufficient to specify the system. We express the water decomposition by three numbers, which (to avoid subscripts) we call F, E and R, all in units of molecules per 100 ev, and defined thus: $G_{\mathrm{H_2}} = F$, $G_{\mathrm{OH}} = R$, $G_{\mathrm{H_2O_2}} = F + E$. From the above equation, we see that $G_{\mathrm{H}} = R + 2E$.

* Brookhaven National Laboratory.

This set was originally chosen to emphasize the fact that more H_2O_2 than H_2 usually forms, so that E is usually positive. There is no inherent reason, however, why E should not sometimes be negative. It may on occasion be helpful to think of F, E and R as yields of three different stoichiometric modes of water decomposition:

$$2H_2O = H_2 + H_2O_2 \qquad (F)$$

$$2H_2O = 2H + H_2O_2 \qquad (E)$$

$$H_2O = H + OH \qquad (R)$$

These equations are merely intended to represent the overall result of the water decomposition reactions, and do not necessarily represent actual elementary processes occuring in the water.

The writer formerly hoped that F, R and E would prove to be constants, the same in all dilute water solutions for each given type of radiation. However, recent precise work, to be detailed more fully below, has shown that, at least for gamma rays, the molecular peroxide yield $F + E$ is appreciably decreased in solutions of reducing agents, while the hydrogen yield F is decreased in solutions of oxidizing agents, to an extent which increases with increasing solute concentration. The effect is readily understandable if the H_2 and H_2O_2 are formed at least in part by combination of like radicals, produced close to one another in the solution. Presence of reactive solute molecules tends to interfere with the combination, hence to lower the molecular yields. The effect is small, however, and in working out reaction kinetics of any given system F, R and E may usually be taken as constant to a good approximation.

The feature of simplicity in present thinking on radiation kinetics is that each radical escaping initial combination eventually reacts with a solute, even when the solutes are very dilute (10^{-4} M or less). The yield of any reaction is simply the yield of radicals, unless, as often happens, another process occurs that reverses the effect of the first reaction. It is perhaps the prevalence of such opposing reactions which has led some people to suppose that bimolecular recombination of radicals is continually in competition with radical-solute interactions. This if true would indeed lead to very complicated kinetics, and to a dependence of observed yields on the radiation intensity. Fortunately there is no evidence favoring such a state of affairs. Among all the numerous reactions which have been studied, a dependence of the yield on intensity has been shown only for a few chain reactions, where the mechanism is clearly such as to make this dependence inevitable. It is of course true, if the solute concentration is reduced far enough and the water is maintained unusually free from impurities, that radical-radical interaction must eventually become rate-determining. Experiments of this kind may in the future lead to valuable knowledge. Most experiments available at present, however, appear to fall in the higher concentration category in which reactions between radicals are not rate-determining.

The chief feature of radiation kinetics is "competition" or "protection," resulting from the presence of two or more solutes which can react with the same radical. Even if only one solute is initially present, the molecular products H_2 and H_2O_2 may compete with the added solute for reaction with the radicals. The yield then takes the following characteristic form as a function of the concentrations. Let radicals, formed with a yield R, react with either A or B, present at respective concentrations (A) and (B). Then if k_A and k_B are the respective reaction rate constants, the probability that a radical reacts with A is $k_A(A)/[k_A(A) + k_B(B)]$, or $1/[1 + k_B(B)/k_A(A)]$, and the yield for destruction of A is $R/[1 + k_B(B)/k_A(A)]$.

YIELDS OF OXIDATION AND REDUCTION REACTIONS

Sulfates of iron, copper, cerium and thallium, chromate and formate ions, and certain mixtures of the above, are among the substances, solutions of which are being or have recently been studied in detail. The results of all these studies fit together beautifully. Many of the studies have been made in 0.8 N H_2SO_4 solutions, and all these appear to be consistent with the values $F = 0.39$, $E = 0.39$, $R = 2.92$ (applying strictly speaking only to extremely dilute solutions of the various solutes).[9] At higher pH the values of the primary yields change, the values of F, E and R at pH 7 being given by one source[9] as 0.42, 0.33 and 2.12, by another[10,11] as 0.45, 0.25 and 2.16, respectively.

Ferrous sulfate in solutions with oxygen reacts according to the scheme:

$$H_2O = H,\ OH,\ H_2,\ H_2O_2$$

$$OH + Fe^{++} = Fe^{+3} + OH^-$$

$$H + O_2 = HO_2$$

$$H_2O_2 + Fe^{++} = Fe^{+3} + \overline{OH} + OH$$

$$H^+ + HO_2 + Fe^{++} = Fe^{+3} + H_2O_2 \quad k_{+2}$$

$$HO_2 + Fe^{+3} = Fe^{++} + O_2 + H^+ \quad k_{+3}$$

The last reaction does not occur in 0.8 N acid. In that case, each H atom leads, through HO_2, to the oxidation of $3Fe^{++}$; each OH oxidizes one, and each H_2O_2, two. The yield (15.5) is then given by $2F + 8E + 4R$. At lower acid concentrations the *initial* yield is still given by the same expression, and drops only slightly because of the decrease of R with increasing pH; but the yield falls as the reaction proceeds, the more rapidly the higher the pH, because of the occurrence of the last reaction (reduction of ferric iron by HO_2).[12] However, the net reaction is always one of oxidation, and the oxidation always goes to completion, because even if every HO_2 reduces one equivalent of iron, the oxidizing power of OH plus H_2O_2 is greater than the reducing power of H by an amount equivalent to the molecular hydrogen formed; the minimum oxidation yield in the

presence of ferric ion is $2F$. Older work in which incomplete oxidation was reported in the presence of air may have been vitiated by impurities. At the lower acid concentrations (pH 1–3), each H still forms HO_2; a fraction $1/(1 + W)$ of the H atom yield $R + 2E$ (where $W = k_{+3}(Fe^{+3})/k_{+2}(Fe^{++})$) therefore leads to oxidation of 3 molecules of Fe^{++}, while the remaining fraction $W/(1 + W)$ leads to reduction of one molecule of Fe^{+3}. The yield of Fe^{++} oxidation is therefore given by $2F + 2E + R + (R + 2E)(3 - W)/(1 + W)$. The expression has been thoroughly verified by experiment, with k_{+3}/k_{+2} found to increase with decreasing acidity in the way expected from studies of thermal reaction kinetics in the ferrous-ion peroxide reaction. Copper sulfate acts like ferric salt when mixed with ferrous sulfate at pH = 2. Hart has shown[13] that the copper ion oxidizes HO_2:

$$Cu^{++} + HO_2 = Cu^{+} + H^{+} + O_2$$

The resulting Cu^{+} reduces part of the Fe^{+3} formed by action of OH and H_2O_2 on the ferrous salt, so that again the net oxidation is simply $2F$, equivalent to the H_2 formed.

In the absence of oxygen, ferrous ion is oxidized by both H and OH, as well as H_2O_2:

$$Fe^{++} + H + H^{+} = H_2 + Fe^{+3}$$

$$Fe^{++} + OH = Fe^{+3} + OH^{-}$$

$$Fe^{++} + H_2O_2 = Fe^{+3} + OH^{-} + OH$$

The first reaction, originally proposed by Weiss, met with some incredulity when first introduced, but is now well established. The yield should be $2F + 4E + 2R$, or, in 0.8 N H_2SO_4, 8.18; the ratio of the yields in aerated and deaerated solution should be 1.90. The latest determinations of this ratio gave 1.88[14] and 1.91.[15] As ferric salt builds up in the solution, the rate falls, slightly in 0.8 N H_2SO_4 and quite sharply at lower acidities. The fall-off is obviously due to competition of Fe^{+3} for the H atoms:

$$Fe^{+3} + H = H^{+} + Fe^{++}$$

which will have kinetic consequences similar to the reaction of Fe^{+3} with HO_2 in the aerated solutions. A major difference from aerated solutions results from the formation of H_2 gas in high yields in the air-free reaction. If the H_2 is allowed to remain in the solution, it exerts (at H_2SO_4 concentrations below 0.1 N) an additional reducing effect, so that the iron is never completely oxidized, but attains on long irradiation a steady state with ferrous and ferric salt both present. In agreement with this result, it is found that solutions of ferric salts are partly reduced by radiation when saturated with hydrogen, but are not reduced when saturated with nitrogen. The hydrogen effect must be due to the reaction

$$OH + H_2 = H_2O + H$$

which competes with the reaction of OH with Fe^{++}. With competition for both H and OH, the complete kinetic expression is complicated; it is

$$G_{Fe^{+3}} = F + E + (F + E + R)\left[1 - \frac{1}{1+p}\left(1 - \frac{1-q}{1+q}\right)\right] + (R + 2E)\frac{1-q}{1+q}$$

where $p = k_{OH,Fe^{++}}(Fe^{++})/k_{OH,H_2}(H_2)$; $q = k_{H,Fe^{+3}}(Fe^{+3})/k_{H,Fe^{++}}(Fe^{++})$. Experiments at pH 2 have confirmed this expression in complete detail.[15] Solutions containing various concentrations of ferrous and ferric sulfates and of hydrogen gas were irradiated, and not only the initial yields of oxidation or reduction, but also the steady-state concentration levels attained on long irradiation, and the complete course of the reaction from the beginning to the steady state, agreed with those predicted, assuming $k_{H,Fe^{+3}}/k_{H,Fe^{++}} = 7$ and $k_{OH,Fe^{++}}/k_{OH,H_2} = 5$. At Fe^{+3} concentrations of 0.01 M or more, where the rate is chiefly determined by the H_2 yield F, the value of F was found to drop with increasing Fe^{+3} concentration, as found also with Cu^{++} ion (see below).

The reduction of ceric sulfate has long been known to proceed with considerably lower yield than corresponds to use of all the radicals. Sworski has recently found[16] that if thallous sulfate is added and the mixture irradiated with γ-rays, the cerium is reduced with a yield $G = 8.05$, equal to the yield of oxidation of $FeSO_4$ in oxygen-free solution. (In the absence of radiation Ce^{IV} does not react at an appreciable rate with Tl^{I}.) All the radicals are therefore being used by the mixture, and the obvious mechanism is:

$$Ce^{+4} + H = Ce^{+3} + H^{+}$$

$$Tl^{+} + OH = Tl^{+2} + OH^{-}$$

$$Tl^{+2} + Ce^{+4} = Tl^{+3} + Ce^{+3}$$

$$2Ce^{+4} + H_2O_2 = 2Ce^{+3} + O_2 + 2H^{+}$$

Tl^{II}, being (unlike Tl^{I}) a one-electron reducing agent, reacts readily with Ce^{IV}.

In the absence of added Tl^{+} or other reducing agent, the relatively low yield (2.5) of Ce^{+4} reduction by gamma rays had been ascribed[7] to oxidation by OH of Ce^{+3}, so that net reduction occurs only to the extent that the initial yield of free H from water exceeds that of OH (plus the reduction by molecular peroxide). This explanation was confirmed by Challenger and Masters[17] who showed that when radioactive Ce^{+3} was mixed with Ce^{+4} (in H_2SO_4 solution) and the mixture irradiated with X-rays, radioactivity appeared in the Ce^{+4} at a rate (over and above the thermal exchange rate) equal to that expected for production of OH radicals by the X-rays. They find also[18] an acceleration of the exchange reaction between Tl^{+} and Tl^{+3} much greater than the rate of radical production, and dependent on dose rate—clearly a chain reaction. The obvious mechanism involves reduction of Tl^{III} and oxidation of Tl^{I} to Tl^{II} by the radicals, with subsequent exchange occurring freely between Tl^{II} and both Tl^{III} and Tl^{I}—the chain

being broken only by the disproportionation of Tl^{II}. The observations thus confirm the existence of Tl^{II}, postulated by Sworski to explain the reaction with cerium.

Another reducing agent which can be mixed with ceric sulfate and has the effect of increasing the yield of cerium reduction is formic acid. This is less reactive to OH than Tl^{+}, and according to Sworski,[16] a considerable excess of HCOOH is required to bring the Ce reduction yield up to its limiting value of 8.1 with γ-rays; lower concentrations of HCOOH give intermediate yields which drop as Ce^{III} builds up in the solution. Similar results are reported for X-rays of longer wave-length by Spencer and Rollefson;[19] the elaborate system of reaction kinetics favored by these authors seems unnecessary.

Chromate in acid solution was found by Hochanadel and Davis[20] to act like Ce^{IV} with γ-rays; in solutions containing oxygen both are reduced with the same yield (2.5), and presence of hydrogen gas at 1 atm pressure increases the yield in both to about 5.2 (not all the way to the limiting value of 8.1). Both solutes readily oxidize hydrogen peroxide, and the mechanism in both cases involves reduction by H_2O_2 and H, and re-oxidation by OH, with the net reduction yield (in terms of atom-equivalents per 100 ev) equal to the excess of H over OH, plus twice the primary H_2O_2 yield, or $2F + 4E$. When H_2 is present, some of the OH reacts with it instead of with reduced Cr, causing an increase in net Cr^{VI} reduction. In agreement with expectation, the addition of Cr^{III} sulfate slightly decreased the reduction yield in the presence of H_2. In neutral solutions, chromate is not reduced by peroxide, and in this case there is no reduction by γ-rays in the presence of oxygen either, although radiation does cause reduction in the presence of hydrogen. Hochanadel and Davis[20] have also studied the reactions of Cr^{VI} and Cr^{III} at pH 3 and 7, and find their observations to be in good agreement with expectations from the assumed reaction mechanisms.

The work of Schwarz and the writer[21] on γ-ray oxidation of nitrite solutions showed good agreement with expectations based on the theory outlined above. The main initial effect is to form H_2 and H_2O_2, the effect of radicals on the nitrite ion mostly cancelling one another. Oxidation of nitrite to nitrate occurs later and results from a radical-induced reaction between nitrite ion and peroxide.

VARIATIONS IN THE MOLECULAR YIELDS; THE RADICAL DIFFUSION MODEL

The first definite evidence that molecular yields change with solute concentration was provided by Sworski,[9] who showed that the peroxide yield in aerated water containing bromide decreased by about 20% in going from dilute solutions to 0.01 M KBr. Since the observed peroxide yield is always given by $F + 2E$ and thus depends only on the molecular yields, the assumption was made that the yield of peroxide coming directly from the water, $F + E$, was decreased by the presence of the bromide. Later Sworski's experiments were verified exactly by Holroyd and the writer.[10] A similar effect was found by Sworski with chloride ions in acid solution[22] and by Schwarz and the writer with nitrite.[21] It thus appears that reducing agents which readily react with OH radicals lower the molecular yield of hydrogen peroxide. The presence of oxidizing agents meanwhile has been shown to lower the molecular yield of hydrogen; thus Schwarz[23] showed that the hydrogen yield is reduced by 30% in 0.02 M $CuSO_4$, and by the same amount in 0.06 M KNO_2. Ghormley and Hochanadel showed[24] that the yield of hydrogen is decreased by the presence of oxygen or hydrogen peroxide. Thus substances which react readily with atomic H lower the yield of molecular hydrogen.

Qualitatively, such an effect is to be expected on the radical diffusion model for formation of these molecules. In this model, H and OH radicals are formed initially in small groups located close together. As they diffuse outward a certain fraction will meet and combine with one another. The remainder will escape by diffusion into the main body of the solution, where their presence is made known by their reaction with a solute. If the solute is present in sufficiently high concentration so that radicals can act upon it while still near the site of their formation, such radicals may be prevented from meeting other like radicals and the yields of the resulting H_2 or H_2O_2 molecules may be reduced. The question is whether a quantitative analysis of the diffusion process could be made to confirm the experimental results. Analysis of the diffusion process when recombination is also occurring is mathematically difficult and can be carried out only approximately. Such an approximation had been carried through by Samuel and Magee for the case where solute concentration was negligible; their equations were found to give reasonable division of water decomposition products between free radicals and molecules if one assumed reasonable values of the various physical parameters involved.[6] Their calculation was extended to the case where solutes are present by Fricke,[25] who derived a curve connecting the drop of the molecular yield with solute concentration for the case that every radical-solute encounter led to reaction; if the reaction were less probable, the solute concentration must be correspondingly increased to obtain the same effect. A similar expression was obtained by Schwarz[23] with somewhat different approximations. Schwarz finds that both Fricke's theory and his own agree very well with available data on the effect of bromide and chloride on the peroxide yield and of nitrite, copper ion, oxygen and hydrogen peroxide on the hydrogen yield. The relative concentrations of the different substances required to produce equal effects on the molecular yields are about what would be expected from our knowledge of the relative reactivities towards the free radicals, except possibly in the case of the oxygen effect on the yield of H_2 (see below). The observations of Schwarz and the writer on the effect of nitrite

on the peroxide yield[14] do not fit the other observations at the higher nitrite concentrations and should probably be repeated. Recent observations of the effect of ferric sulfate on the hydrogen yield[15] and of thallous sulfate on the peroxide yield[16] have not yet been compared with theory.

EFFECT OF IONIZATION DENSITY

It has been known for a long time that with gamma rays most of the water decomposition leads to free radicals, while with alpha rays the products are chiefly the molecules H_2 and H_2O_2. With rays of intermediate ionization density the relative values of the radical and molecular yields should vary smoothly from one extreme to the other. Fission recoils are now found[26] to give about the same yield of molecular hydrogen as the natural alpha rays from polonium or radon, although the energy expended per unit track length is much greater for the fission recoils. Presumably the radicals are already so crowded together in the α-ray track that they practically all combine with one another, so that further crowding in the fission recoil track makes little difference. According to the results of McDonell and Hart,[27] however, the radical yield increases noticeably with increasing energy (and hence decreasing ionization density) of the α particles. Their results check exactly with the independent work of Ehrenberg and Saeland.[28] There appears to be an internal inconsistency if one compares the yield quoted for $FeSO_4$ oxidation by Po α's with that given by the $Li^6(n,\alpha)H^3$ reaction occurring in the $FeSO_4$ solution. Clearly the H^3 particle has a much lower ionization density than the Po α and should therefore give more free radicals and a higher $FeSO_4$ oxidation yield, but the experiments give a higher yield for the Po α. More work needs to be done on this question. Comparisons of this type are very difficult since each determination with a different type of radiation must be made on a separate absolute scale of dosimetry.

The cyclotron is well-suited to the study of α particle yields in the energy range lying somewhat above that of the natural α-rays, and can also be used for producing beams of deuterons and protons of still lower ionization densities. Studies of the ferrous sulfate yields as a function of particle energy for both alphas and deuterons are now being carried out at the Brookhaven National Laboratory by Schuler and the writer and at the Argonne National Laboratory by Hart. The measurements are not yet final and the preliminary results published by Schuler and the writer[20] require slight revision. Our present results can best be expressed in terms of the "instantaneous yield" G_i. When a particle of initial energy E expends all its energy in a material and converts a total of M molecules, G_i is defined as the rate of change of M with E, dM/dE, while the "over-all yield" G_0 is given by M/E. Thus $G_0E = \int_0^E G_i dE$. G_i is the yield which would be given by particles which entered the solution at an energy near E and then left the solution before they had been appreciably slowed down. Our results for the yield as a function of energy for deuterons and alpha particles can be expressed by equations giving G_i as a function of dE/dx, the rate of energy loss by the particle. The results for both deuterons and α's within experimental error, are: $G_i = 3.4 + 12.1/(1 + 0.38\ dE/dx)$. This means that at low energies the yield approaches 3.4; at very high particle speeds where dE/dx is small the yield approaches 15.5, the γ-ray value; in between the variation with ionization density is about the same for the two particles, though theoretically a slight difference might be expected. The increase in yield is due to the escape of hydrogen atoms from recombination in the particle track; the OH radicals each oxidize one molecule of iron whether they combine with one another or not. If we assume that in considering tracks at different densities the concentration of H atoms (for any given fraction of H atoms reacted) is approximately proportional to the initial ionization density, and we consider the yield as determined by a competition between reaction of H atoms with O_2 and with one another, an expression of the form given above is obtained if the O_2 concentration is constant. An exact theory of the variation of radical yields with ionization density would be very complicated since the tracks are actually made up of numerous relatively dense "spurs" or "hot spots" located at random distances along the track. Fricke[25] has considered the problem but has assumed that the spurs are all of the same size and evenly spaced, which can hardly be the case.

KINETICS OF WATER DECOMPOSITION

The decomposition of water under radiation is important to the design of water-cooled or water-moderated nuclear reactors. The writer has discussed this subject elsewhere.[8] Here it will suffice to say that water decomposition by radiation, which is due to the molecular part of the primary decomposition yield, is reversed by a back reaction brought about by the action of free radicals on the decomposition products. The back reaction is inhibited by the presence of impurities in the water and by an excess of hydrogen peroxide or of oxygen in the decomposition products, but is favored by the presence of excess hydrogen. Since the decomposition reaction is proportional to the molecular yield and the back reaction depends on the free radical yield, the amount of decomposition occurring in a given situation depends critically upon the ionization densities of the radiations present. Since the reactions observed depend upon so many different factors, much experimental work has been and is being done on irradiation of solutions of oxygen, hydrogen and hydrogen peroxide under various conditions. The results, although complicated, can be correlated qualitatively by the following rather simple mechanism:

$$H_2O = H_2,\ H_2O_2,\ H,\ OH$$

$$OH + H_2 = H_2O + H \qquad (1)$$

$$H + H_2O_2 = H_2O + OH \quad (2)$$

$$OH + H_2O_2 = H_2O + HO_2 \quad (3)$$

$$HO_2 + HO_2 = H_2O_2 + O_2 \quad (4)$$

$$H + O_2 = HO_2 \quad (5)$$

Reactions (1) and (2) constitute a chain, which is the chief factor in bringing about the back reaction in water decomposition. Reactions (3) and (5) break this chain, as do reactions of the radicals with any foreign solutes present; hence the effect of oxygen, peroxide and foreign matter in increasing water decomposition. When oxygen alone is present, peroxide formed by (5) and (4) is mostly destroyed by (3) so that the net yield observed is merely the amount of molecular peroxide formed from the water, plus one molecule of O_2 reduced to H_2O_2 for each two H atoms produced in excess of OH radicals, giving a total yield of $F + 2E$. Actually as hydrogen forms in the solution along with peroxide it will be drawn into reaction, so that the net yield of peroxide will be slightly greater; but it can be made to equal $F + 2E$ by the addition of a little bromide ion, which protects the hydrogen from radical attack. When hydrogen and oxygen are both initially present, reactions (1) and (5) occur, followed by (4), leading to formation of one molecule of peroxide for every two radicals of either type generated, in addition of course to the molecular peroxide formed from the water, giving a total yield of $R + F + 2E$.

When we attempt to treat quantitatively existing data for cases when oxygen and peroxide are both present some inconsistencies appear. The general expression for the kinetics of peroxide formation deduced from the above mechanism is

$$G_{H_2O_2} = F + R + 2E - \frac{1}{1+x}\left[Rx + \frac{(1+2x)[2E + 2R + x(R+2E)]}{x + y + xy}\right]$$

where $x = k_{OH,\,H_2O_2}(H_2O_2)/k_{OH,\,H_2}(H_2)$ and $y = k_{H,\,O_2}(O_2)/k_{H,\,H_2O_2}(H_2O_2)$. When the O_2 concentration is kept very low (y small) the expression reduces to $G_{H_2O_2} = F - (2R + 2E)(1 + 1/x)$. This condition should correspond experimentally to the case in which hydrogen is bubbled continuously through an irradiated solution of peroxide, so that any oxygen formed is swept away. Under this condition, Hochanadel[30] has found exact agreement with the above expression for gamma irradiation down to the lowest peroxide concentrations measurable, if $k_{OH,\,H_2O_2}/k_{OH,\,O_2} = 3.13$. The decreases in rate at lower peroxide levels, and lower value for the ratio of rate constants, found in the earlier work of Hochanadel[31] and the more recent work of Gordon[32] are now ascribed to the presence of small quantities of oxygen. It is encouraging to note that Hochanadel has studied the photolysis of H_2O_2 in the presence of bubbling H_2 and finds the same ratio for the rate constants,[30] indicating that the OH radicals formed by peroxide photolysis and by water radiolysis are the same. However, if we calculate the same ratio from the decrease in peroxide yield in aerated water caused by addition of bromide as measured either by Sworski[9] or by Holroyd and the writer,[10] a value is obtained in the neighborhood of 1.

More serious discrepancies occur in the attempted evaluation of the ratio $k_{H,O_2}/k_{H,\,H_2O_2}$. The rate of growth of peroxide in oxygen-bubbled solutions, interpreted in terms of this ratio, leads to values of the order of unity. A similar conclusion may be reached by comparison of the yields of the oxidation of nitrite ion by peroxide and by oxygen.[21] However, if we look at the curve showing the growth and subsequent decline of peroxide in a sealed vessel containing initially hydrogen, together with relatively small amounts of oxygen, as published originally by Hochanadel[34] and recently verified in this laboratory by Barr,[11] the conclusion is reached that the ratio has a very large value—that is, H atoms go on reacting almost exclusively with O_2 until it is practically gone, although peroxide is present. A very large value of the ratio is also obtained by comparing data of Hart on oxygen-formic acid mixtures[33] with his earlier data on peroxide-formic acid mixtures.[34] On the other hand, the suppression of the molecular hydrogen yield by a given concentration of oxygen and of hydrogen peroxide is almost the same, which would lead one to conclude that the ratio must be close to unity.

Gordon and Hart[35] irradiated ordinary water saturated with deuterium gas. They found conversion of D_2 to HD resulting from the radical reactions:

$$H + D_2 = HD + D$$

$$OH + D_2 = HOD + D$$

$$D + D = D_2$$

In agreement with expectation the yield of HD was about as expected from the H atom yield, and they give interesting data on the variation of this yield with pH. However they also find yields of H_2 in amount almost equal to the molecular yield of H_2 from water. Now it is very hard to understand why this H_2 should not be attacked by the D atoms present. Near-equilibrium of H_2 with the HD and D_2 present would be expected, but the amounts of H_2 reported are much larger than correspond to this equilibrium. One would almost suspect that the H_2 determination was in error, but the result has been confirmed by Zeltmann independently in a different laboratory. Zeltmann[36] has also measured the yield of conversion of para-hydrogen dissolved in water to ortho-hydrogen by gamma rays which occurs with a yield of about 70 corresponding to a chain length of about 20. The yield is independent of radiation intensity, and it is not clear what sort of reaction terminates the chain.

Evidently the situation in solutions of the water decomposition products is not as satisfactory as with the solutions of inorganic salts discussed in an earlier

section. Further work is clearly required. It is gratifying however to find that the very intricate phenomenology of water decomposition can be completely expressed qualitatively by as simple a mechanism as that given here.

AQUEOUS SOLUTIONS OF ORGANIC COMPOUNDS

Interest continues in the study of solutions of compounds thought to be of particular concern to biology. Solutions of glycine, previously studied with X-rays by Maxwell and co-workers,[37] have now been studied with heavy particle radiation by Weeks and Garrison.[38] Maxwell and co-workers have continued[39] with the study of another amino acid, alanine, while Barron and co-workers[40] have studied the yields for production of ammonia in solutions of a whole series of amino acids. Loss of ammonia, with oxidation of the residue of the molecule to a keto acid, is the main reaction occurring in these solutions, but many other products are also found. Some products increase linearly with amino acid concentration, indicating that they are produced by direct action of radiation on the solute. In aqueous solutions of methanol, according to McDonell,[41] formaldehyde is a product of direct action, while ethylene glycol is a chief product of indirect action.

Interest continues in the deactivation by radiation of large molecules such as enzymes. In such reactions the concentration of unchanged material generally falls exponentially with the amount of radiation given, instead of linearly as with smaller molecules. A recent study by Okada[42] of the inactivation of desoxyribonuclease by X-rays provides a model for the study of kinetics of this type. The exponential character of the reaction is basically due to the fact that radicals react as readily with enzyme molecules after they have been deactivated as before. However, the initial deactivation rate is much smaller than the rate of radical production, and in order to explain the observed kinetics, radicals must be assumed to disappear both by reactions with enzyme molecules which do not lead to deactivation and by other reactions, presumably with foreign substances present in the solution in a constant amount. Okada finds that the process competing with reaction of the enzyme for destruction of radicals is first order with respect to radical concentration. It is then legitimate to assume a mean radical concentration x, and we can write the equation

$$aI = k'xE_0 + k_1x$$

where I is radiation intensity, aI the rate of radical formation, and E_0 the initial concentration of enzyme. The rate of deactivation of the enzyme, on the other hand, is $-dE/dt = k_0xE$, where E is the concentration of enzyme at any time t. Eliminating x, we find that

$$\frac{dE}{dt} = \frac{-k_0aIE}{k'E_0 + k_1}$$

If $It = D$, the dose, we find on integration

$$E = E_0e^{-KD}$$

where

$$K = \frac{a}{\frac{k'}{k_0}E_0 + \frac{k_1}{k_0}}$$

K is readily measured as the reciprocal of D_{37}, the dose required to reduce enzyme activity to $1/e$ (37%) of its initial value. The variation of D_{37} with enzyme concentration was found to fit the above expression very well. Assuming that $a = 2$ per ion pair (i.e., about 3 radical pairs for 100 ev), Okada finds $k_1/k_0 = 2.8 \times 10^{15}$ molecules/ml and $k'/k_0 = 9.3$. The meaning of the last number is that only one radical out of 9.3 which reacts with enzyme material causes deactivation. The identification of the side competing reaction k_1 as first order is particularly interesting, and may help dispose of the old idea that reactions between radicals are important in radiation kinetics.

REFERENCES

1. Faraday Society Discussions No. 12, *Radiation Chemistry* (1952).
2. Hart, E. J., *Radiation Chemistry*, Ann. Rev. Physical Chem., *5*: 139-162 (1954).
3. Vereshchinskii, I. V., *Radiation Chemistry*, Uspekhi Khim, *20*: 288-308 (1951).
4. Haissinsky, M. and Lefort, M., *Radiolysis of Water and of Aqueous Solutions: A Critical Survey*, Symposium on Chemical Transformations, Milan and Rome (1953).
5. Hart, E. J., *Molecular Product and Free Radical Yields of Ionizing Radiations in Aqueous Solutions*, Radiation Research, *1*: 53-61 (1954).
6. Dewhurst, H. A., Samuel, A. H. and Magee, J. L., *A Theoretical Survey of the Radiation Chemistry of Water and Aqueous Solutions*, Radiation Research, *1*: 62-84 (1954).
7. Allen, A. O., *The Yields of Free H and OH in the Irradiation of Water*, Radiation Research, *1*: 85-96 (1954).
8. Allen, A. O., *Radiation Damage to Water*, Chem. Eng. Progress Symposium Series, *50*, No. 12: 238-242 (1954).
9. Sworski, T. J., *Yields of Hydrogen Peroxide in the Decomposition of Water by Cobalt γ-Radiation. I. Effect of Bromide Ion*, J. Am. Chem. Soc., *76*: 4687-92 (1954).
10. Allen, A. O. and Holroyd, R. A. *Peroxide Yield in the Gamma-Irradiation of Air-Saturated Water*, presented at Am. Chem. Soc. Meeting, Cincinnati, Ohio, April 1955.
11. Barr, N., unpublished work at Brookhaven National Laboratory.
12. Hogan, Virginia and Allen, A. O., unpublished work at Brookhaven National Laboratory.
13. Hart, E. J., *Radiation Chemistry of Aqueous Ferrous Sulfate-Cupric Sulfate Solutions. Effect of γ-Rays*, Radiation Research, *2*: 33-46 (1955).
14. Barr, N. and King, C. G., *The Radiation-Induced Oxidation of Ferrous Ion*, J. Am. Chem. Soc., *76*: 5565 (1954).

15. Allen, A. O. and Rothschild, W., *Reactions Induced by Gamma Rays in Oxygen-Free Ferrous Sulfate Solutions*, presented at meeting of the Radiation Research Soc., New York, May 1955.
16. Sworski, T. J., unpublished work at Oak Ridge National Laboratory.
17. Challenger, G. E. and Masters, B. J., *Radiation-Induced Ce(III)-Ce(IV) Exchange in Aqueous Nitric and Sulfuric Acids*, J. Am. Chem. Soc., *77*: 1063 (1955).
18. Challenger, G. E. and Masters, B. J., unpublished work at Los Alamos Scientific Laboratory.
19. Spencer, H. E. and Rollefson, G. K., *The Effect of X-Rays on Solutions which Contain Formic Acid and Ceric Ion*, J. Am. Chem. Soc., *77*: 1938-43 (1955).
20. Hochanadel, C. J. and Davis, T. W., unpublished work at Oak Ridge National Laboratory.
21. Schwarz, H. A. and Allen, A. O., *The Radiation Chemistry of Nitrite Ion in Aqueous Solution*, J. Am. Chem. Soc., *77*: 1324-30 (1955).
22. Sworski, T. J., *Yields of Hydrogen Peroxide in the Decomposition of Water by Cobalt γ-Radiation. II. Effect of Chloride Ion*, Radiation Research, *2*: 26-32 (1955).
23. Schwarz, H. A., unpublished work at Brookhaven National Laboratory.
24. Ghormley, J. A. and Hochanadel, C. J., *The Effect of Hydrogen Peroxide and Other Solutes on the Yield of Hydrogen in the Decomposition of Water by Gamma Rays*, presented at meeting of the Radiation Research Soc., New York, May 1955.
25. Fricke, H., *Track Effect in Isochemistry of Aqueous Solutions*, Ann. N.Y. Acad. Sci., *59*: 567-73 (1955).
26. Boyle, J. W., *Decomposition of Water by Fission Recoils*, paper submitted to International Conference on Peaceful Uses of Atomic Energy, Geneva, 1955.
27. McDonell, W. R. and Hart, E. J., *Oxidation of Aqueous Ferrous Sulfate Solutions by Charged Particle Radiations*, J. Am. Chem. Soc., *76*: 2121-24 (1954).
28. Ehrenberg, L. and Saeland, E., *Chemical Dosimetry of Radiations Giving Different Ion Densities. An Experimental Determination of G Values for Fe^{++} Oxidation*, JENER Publications, No. 8 (1954).
29. Schuler, R. H. and Allen, A. O., *Radiation-Chemical Studies with Cyclotron Beams*, J. Am. Chem. Soc., *77*: 507 (1955).
30. Hochanadel, C. J., *The Photolysis of Dilute Hydrogen Peroxide in the Presence of Dissolved Hydrogen and Hydrogen Plus Oxygen*, presented at meeting of the Radiation Research Soc., New York, May 1955.
31. Hochanadel, C. J., *Effects of Cobalt Gamma Radiation on Water and Aqueous Solutions*, J. Phys. Chem., *56*: 587-93 (1952).
32. Gordon, S., McDonell, W. R. and Hart, E. J., unpublished work at Argonne National Laboratory.
33. Hart, E. J., *Gamma-Ray Induced Oxidation of Aqueous Formic Acid-Oxygen Solutions. Effect of Oxygen and Formic Acid Concentrations*, J. Am. Chem. Soc., *76*: 4312-15 (1954).
34. Hart, E. J., *Mechanism of the Gamma-Ray Induced Oxidation of Formic Acid in Aqueous Solution*, J. Am. Chem. So., *73*: 68-73 (1951).
35. Gordon, S. and Hart, E. J., *Gamma-Ray Induced Deuterium Gas-Water Exchange*, J. Am. Chem. Soc. in press.
36. Zeltmann, A. H., unpublished work at Los Alamos Scientific Laboratory.
37. Maxwell, C. R., Peterson, D. C. and Sharpless, N. E., *The Effect of Ionizing Radiation on Amino Acids. I. The Effect of X-Rays on Aqueous Solutions of Glycine*, Radiation Research, *1*: 530 (1954).
38. Weeks, B. M. and Garrison, W. M., *Indirect and Direct Action of Heavy-Particle Radiation on Glycine in Aqueous Solution*, presented at meeting of the Radiation Research Soc., New York, May 1955.
39. Sharpless, N. E., Blair, A. E. and Maxwell, C. R., *The Effect of Ionizing Radiation on Amino Acids. II. The Effect of X-Rays on Aqueous Solutions of Alanine*, Radiation Research, *2*: 135-44 (1955).
40. Barron, E. S. G., Ambrose, J. and Johnson, P., *Studies on the Mechanism of Action of Ionizing Radiations. XIII. The Effect of X-Irradiation on Some Physico-Chemical Properties of Amino Acids and Proteins*, Radiation Research, *2*: 145-59 (1955).
41. McDonell, W. R., *Decomposition of Methyl Alcohol-Water Solutions by Co^{60} Gamma Radiation*, J. Chem. Phys., *23*: 208-9 (1955).
42. Okada, S., *Inactivation of Desoxyribonuclease by Ionizing Radiation. I. The Kinetics of Inactivation in Aqueous Solution*, unpublished work at U. of Rochester, School of Medicine and Dentistry.

The Radiation Induced Reaction of Hydrogen and Oxygen in Water at 25°C to 250°C

By C. J. Hochanadel,* USA

Hydrogen peroxide is produced on irradiating water containing dissolved hydrogen and oxygen with gamma rays at 25°C. Initially, each free radical (H and OH) produced as an intermediate in the radiolysis of water, reacts with hydrogen or oxygen and is converted to peroxide. The initial reaction can be described by the sequence

$$H_2O \xrightarrow{\gamma\text{-rays}} a\ H_2 + b\ H_2O_2 + c\ H + d\ OH \quad (1)$$

$$H_2 + OH \rightarrow H_2O + H \quad (2)$$

$$O_2 + H \rightarrow HO_2 \quad (3)$$

$$HO_2 + HO_2 \rightarrow H_2O_2 + O_2 \quad (4)$$

The initial rate of peroxide formation is equal to the sum of the rates of formation of H_2 and H ($a + c$) in reaction (1). As the peroxide builds up in solution, it competes for the free radicals by reactions (5) and (6), thereby leading to steady-state concentrations of H_2O_2, H_2 and O_2.

$$H_2O_2 + H \rightarrow H_2O + OH \quad (5)$$

$$H_2O_2 + OH \rightarrow HO_2 + H_2O \quad (6)$$

The reaction of hydrogen and oxygen in water irradiated at high temperatures is of practical importance in the technology of water-moderated atomic reactors operated at high temperatures. Results could not be reliably predicted from studies of the reaction at low temperatures partly because of the thermal instability of peroxide. The reaction was therefore studied at 100°C, 200°C and 250°C in order to elucidate the mechanism in terms of present theories of the radiation decomposition of water. Results of a further study of the reaction at 25°C are also reported.

EXPERIMENTAL

Irradiations at 25°C

Solutions were irradiated with cobalt gamma rays using the source described previously.[1] During irradiation at 25°C, either hydrogen, oxygen, hydrogen plus oxygen or helium was bubbled through solution. This served the twofold purpose of maintaining constant concentrations of gases and of maintaining essentially zero concentrations of either hydrogen, oxygen or both. Solutions were irradiated in a Pyrex vessel as shown in Fig. 1. The gas was introduced into the vessel at *a*, and entered the solution after passing through the sintered glass disc *d*. Periodically the irradiation was interrupted and samples taken for analysis by closing *b* and expelling the sample at *c*. This allowed removal of samples without danger of contaminating the remaining solution. Purification of materials and peroxide analyses were carried out as described previously.[2] During irradiation the reaction vessel was surrounded by cobalt[2], and the solution was irradiated at a dose rate of about 5.5×10^{17} ev-gm^{-1}-min^{-1}. Dosage measurements are based on the ferrous sulfate dosimeter with a yield of 15.6 Fe^{+3}/100 ev.[3]

Irradiations at High Temperatures

Solutions were irradiated at 100°C to 250°C in ampoules constructed of 10-cm lengths of 8-mm silica tubing as shown in Fig. 2. The pressure of gases in an ampoule was measured without opening the ampoule by the method described previously.[4] The pressure change could therefore be measured as a function of radiation dosage using a single sample. In preparing the ampoules, carefully purified water[2] was introduced and the gas space adjusted to the minimum required to accommodate thermal expansion of the water. This afforded maximum pressure changes on irradiation. After degassing on a vacuum line with the ampoule in a vertical position, the neck of the ampoule was heated and the ampoule bent upward slightly beyond the horizontal position. Hydrogen was then added at pressure of 40 cm over the water in the main body of the ampoule. Water was then frozen in the neck of the ampoule and the vacuum line reevacuated. Oxygen was then introduced at a pressure of 60 cm and the ice plug melted in order to allow the gas to enter the ampoule. This gave a total pressure in the ampoule consisting of 40 cm of hydrogen and 20 cm of oxygen. The capillary neck was then sealed off without danger of explosion. The ampoules were heated in a furnace during irradiation with cobalt gamma rays at a dosage rate of 1.4×10^{17} ev-gm^{-1}-min^{-1}. Periodically the irradiation was interrupted and, after cooling the ampoules in

*Oak Ridge National Laboratory. Including work by T. W. Davis, Oak Ridge National Laboratory on leave from New York University, 1954.

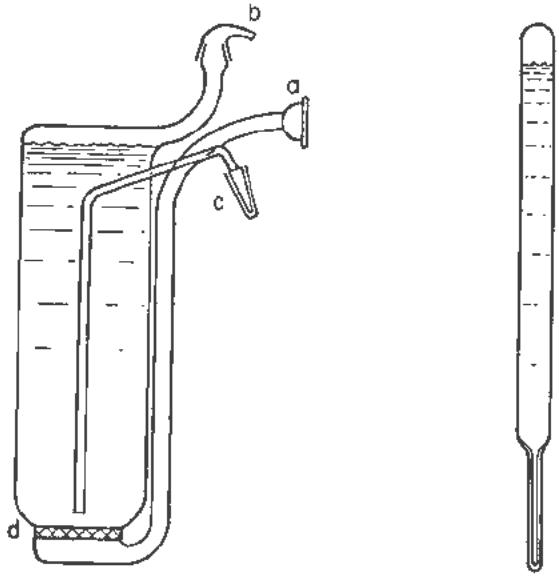

Figure 1. (left) Reaction vessel for irradiating solutions with gamma rays. Figure 2. (right) Reaction vessel for irradiating solutions with gamma rays at temperatures up to 250°C

room temperature and equilibrating the gas and liquid using a pneumatic shaker, the pressures were measured. It was not convenient to maintain equilibrium by shaking the ampoules during irradiation. However, the radiation dosages administered between equilibrations were kept sufficiently low so that the gases dissolved in solution were not depleted. At the higher temperatures this condition was more easily met because of the higher gas solubilities. For the irradiations at 200°C and 250°C the hydrogen and oxygen reacted stoichiometrically to form water. The total number of moles of both gases used up (Δn) was calculated from the measured pressure change (ΔP) using the Equation

$$\Delta n = \frac{3\Delta P\ (V_g + \alpha_{O_2} V_l)\ (V_g + \alpha_{H_2} V_l)}{RT\ [3V_g + (\alpha_{H_2} + 2\alpha_{O_2})\ V_l]} \qquad (7)$$

where V_g and V_l are the gas and liquid volumes, α_{O_2} and α_{H_2} are solubility coefficients, T is the absolute temperature, and R is the appropriate gas constant.

In ampoules heated at 250°C out of radiation, a drop in pressure occurred at a rate not exceeding 15 per cent of the rate under irradiation. In three different ampoules the rates were 1.2, 1.4 and 1.5 cm-hr^{-1}. On heating at 250°C with only hydrogen present over the water at a pressure of 60 cm, the pressure dropped 0.5 cm the first hour, 2.3 cm in five hours and 5.8 cm in twenty-one hours. The rates are considerably greater than the diffusion rate of hydrogen through fused silica as given by Barrer,[5] and may be due to reaction with impurities or reaction catalyzed by the wall or impurities. The results at 250°C are corrected for the thermal reaction. Measurements of yields in ampoules with widely differing gas to liquid volume ratios indicated that reaction in the gas phase was negligible.

RESULTS AND DISCUSSION

Reaction of Hydrogen and Oxygen in Solution at 25°C

At 25°C hydrogen and oxygen react in solution under gamma radiation to form peroxide as shown in Fig. 3. The peroxide reaches a steady state concentration which depends on the relative concentrations of hydrogen, oxygen and peroxide as shown by the several curves of Fig. 3. The peroxide decomposes to water and oxygen as shown by curves A and B of Fig. 4 and reacts with hydrogen to form water as shown by curve C of Fig. 4. These results can be explained reasonably well by reactions (1), (2), (3), (4), (5) and (6), although some unresolved discrepancies still exist. Reaction (8), which is postulated as an important reaction in the decomposition of hydrogen peroxide solutions under certain conditions, is known to be relatively slow at 25°C.

$$H_2O_2 + HO_2 \rightarrow H_2O + OH + O_2 \qquad (8)$$

The velocity constant for this reaction at 25°C has been reported[6] as 3.7 l-mol^{-1}-sec^{-1} and for reaction (4), 3.4×10^6 l-mol^{-1}-sec^{-1}. Under the conditions of concentration and intensity employed in the radiolysis experiments, the contribution of reaction (8) is expected to be negligible. Further evidence for this derives from studies of the photochemical decomposition of peroxide at 25°C.[6,7,8] It was shown that at high light intensities and low peroxide concentrations a limiting quantum yield is obtained, indicating the absence of a chain reaction and a negligible contribution by reaction (8). These results were also confirmed in this study.

Assuming homogeneous kinetics (reactions are known to occur to some extent in the particle tracks) and steady state concentrations of free radicals, reactions (1), (2), (3), (4), (5) and (6) give the rate equation

$$\frac{d\ (H_2O_2)}{dt} = a + c + d - \frac{\dfrac{k_2\ (H_2)}{k_6\ (H_2O_2)}\left[c + d + \dfrac{d\ k_3\ (O_2)}{k_5\ (H_2O_2)}\right] + \dfrac{2d\ k_3\ (O_2)}{k_5\ (H_2O_2)} + 2c + 2d}{\dfrac{k_3\ (O_2)}{k_5\ (H_2O_2)}\left[\dfrac{k_2\ (H_2)}{k_6\ (H_2O_2)} + 1\right] + 1} \qquad (9)$$

The letters a, c and d represent rates of formation of H_2, H and OH in reaction (1). The initial rate of peroxide formation ($H_2O_2 \approx 0$), in the presence of both dissolved hydrogen and oxygen, is $a + c$.

With oxygen bubbling through solution during irradiation ($H_2 \approx 0$) the rate equation reduces to:

$$-\frac{d\ (H_2O_2)}{dt} = a + c - d - \frac{2c}{1 + \frac{k_3\ (O_2)}{k_5\ (H_2O_2)}} \qquad (10)$$

The initial rate of formation is $a + c - d$. From the initial peroxide yields in these two systems along with hydrogen yields in solutions with a scavenger present to prevent reaction (2), the values obtained[2,9] were $a = 0.41$, $b = 0.76$, $c = 2.8$ and $d = 2.1$ in terms of molecules per 100 ev of energy adsorbed.

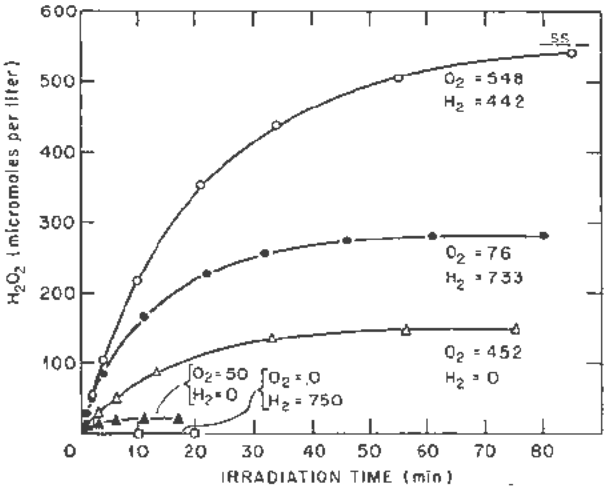

Figure 3. Peroxide formation in the gamma irradiation of water through which either hydrogen, oxygen or a mixture of both gases was bubbled during irradiation at 25°C. Dose rate 5.53 × 10^{17} ev-gm^{-1}-min^{-1}

The value for b agrees with that obtained from studies of bromide solutions.[10] With oxygen in various proportions with helium bubbling through solutions during irradiation, the steady state concentrations were $O_2 = 50$, $H_2O_2 = 21$; $O_2 = 250$, $H_2O_2 = 88$; $O_2 = 450$, $H_2O_2 = 150$; $O_2 = 1260$, $H_2O_2 = 356$. The steady-state peroxide concentration varied from 0.30 to 0.37 times the oxygen concentration. From Equation 10 the ratio of rate constants, k_3/k_5, is then 1.2 to 1.5.

With hydrogen bubbling through solution during irradiation ($O_2 \approx 0$) the rate equation becomes:

$$-\frac{d\ (H_2O_2)}{dt} = c + d - a + (c + d)\frac{k_2\ (H_2)}{k_6\ (H_2O_2)} \qquad (11)$$

The reaction as shown in curve C, Fig. 4 can be approximated using a ratio of rate constants $k_2/k_6 = 0.25$.

With helium bubbling through solution during irradiation ($H_2 \approx O_2 \approx 0$) the rate equation becomes:

$$-\frac{d\ (H_2O_2)}{dt} = c + d - a \qquad (12)$$

According to this mechanism the rate of peroxide decomposition should be independent of peroxide concentration under the conditions employed. However, as shown by curve B in Fig. 4, the rate of decomposition increases continuously with increasing concentration. The extrapolated yield at zero concentration is about 3.6 molecules per 100 electron volts. The value predicted ($c + d - a$) from the yields given previously is 4.5. These discrepancies may indicate that other radical combination reactions are important and also that reaction (8) is important even under these conditions. Including reaction (8), the rate equation for helium swept solutions becomes:

$$-\frac{d\ (H_2O_2)}{dt} = c + d - a + 2k_8 \times \left[\frac{c + d}{2k_4}\right]^{1/2} (H_2O_2) \qquad (13)$$

This indicates a dependency of rate both on concentration and on radiation intensity. A small intensity dependence has been observed. These results will be discussed more fully elsewhere.

The Reaction of Hydrogen and Oxygen in Water Irradiated at 100°C to 250°C

On irradiating solutions of hydrogen and oxygen at 200°C or 250°C, no peroxide ($<10^{-6}$ M) could be detected in solution immediately after irradiation. The gases reacted stoichiometrically to form water at a rate independent of total dose and of pressure. Typical experiments showing pressure changes as a function of radiation dosage at several temperatures are shown in Fig. 5. In six experiments at 200°C, the average total yield for hydrogen plus oxygen removal was 6.8 ± 0.7 molecules per 100 electron volts. The average yield in three experiments at

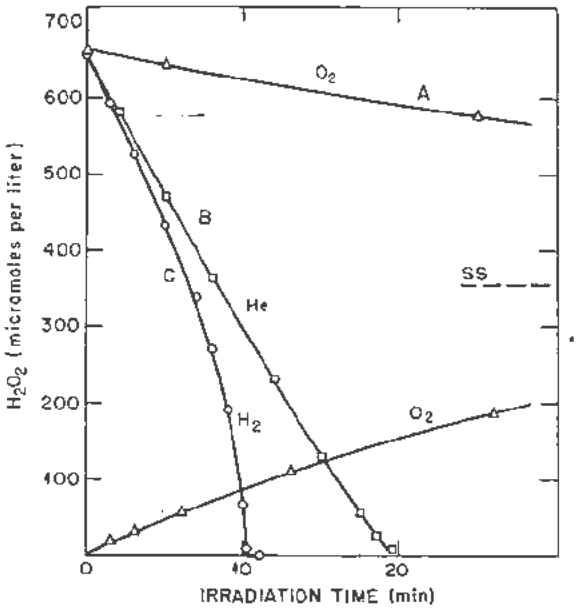

Figure 4. Peroxide disappearance or formation in the gamma irradiation of solutions through which either hydrogen, oxygen, or helium was bubbled during irradiation at 25°C. Dose rate 5.53 × 10^{17} ev-gm^{-1}-min^{-1}

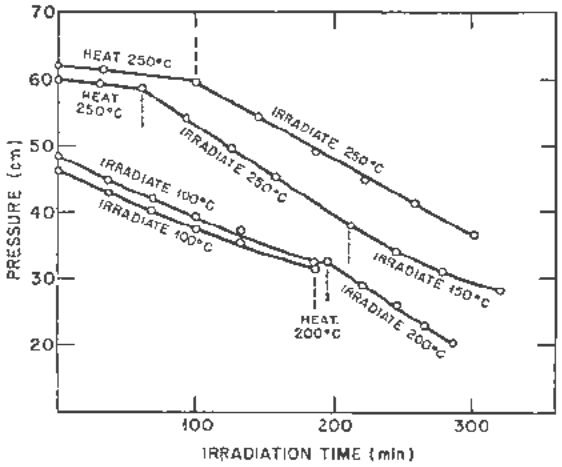

Figure 5. Changes in pressure of hydrogen and oxygen over water irradiated with cobalt gamma rays at high temperatures. Dose rate 1.4×10^{17} ev-gm^{-1}-min^{-1}

250°C was 7.7 ± 0.6 molecules per 100 electron volts. A mechanism which can explain these results includes reactions (1), (2), (3), (4) and (8). By this mechanism the peroxide is removed by reaction (8) as fast as it is formed. The predicted yield for hydrogen plus oxygen depletion is equal to $\frac{3}{2}(c + d)$. Taking the yields of c and d as given above, the predicted yield for hydrogen plus oxygen removal is 7.35 molecules per 100 ev. The over-all reaction can be written

$$4.9\ H_2 + 2.45\ O_2 \xrightarrow[100\ ev]{\gamma} 4.9\ H_2O \qquad (14)$$

The agreement between observed and predicted yields would indicate no large effect of temperature on the yields in reaction (1).

At 200°C and 250° C, where the peroxide steady state concentration is less than 10^{-6} M, the most likely competition of the peroxide formed is with HO_2 in reactions (4) and (8) rather than with hydrogen and oxygen in reactions (2) and (6), and (3) and (5). Participation of reaction (5) would have no effect on the yield, whereas reaction (6) would lower the yield. At room temperature, reaction (8) is known to be relatively slow. However, it is usually postulated as a chain propagating step in the photolysis and radiolysis of solutions at higher concentrations and for irradiations at lower intensities. The activation energy for reaction (8) was estimated to be 6 to 10 kcal in solution,[6] and 14 kcal in the gas phase.[11] On the basis of the mechanism proposed herein, and from the estimated maximum steady state peroxide concentration, an activation energy of 15 to 20 kcal is indicated.

For irradiations at lower temperatures where reaction (8) is sufficiently slow, the peroxide can build up in solution and compete with hydrogen and oxygen in reactions (2) and (6), and (3) and (5). Peroxide was present in solution after the termination of the irradiations at 100°C and 150°C. For the experiments shown in Fig. 5 for example, the concentrations were 50 micromoles per liter at 100°C and 25 micromoles per liter at 150° C. The concentrations change continually as the hydrogen and oxygen concentrations change. At these temperatures the yield for hydrogen plus oxygen removal decreased with increasing dose (decreasing pressure) and depends on the relative concentrations of hydrogen, oxygen and peroxide. The average yields were estimated to be 3.0 molecules per 100 ev at 100°C and 5.5 molecules per 100 ev at 150°C.

Other reactions which might become significant at still higher temperatures are:

$$H_2O_2 \xrightarrow{\Delta} 2\ OH \qquad (15)$$

$$H_2 + HO_2 \rightarrow H_2O_2 + H \qquad (16)$$

$$H_2 + HO_2 \rightarrow H_2O + OH \qquad (17)$$

Reaction (15) represents the thermal decomposition of peroxide to form two OH radicals and along with reactions (2), (3), and (4) would provide a chain reaction of hydrogen and oxygen. Reaction (15) was shown to occur by measuring the stoichiometry in the thermal decomposition of peroxide at 100°C in the presence of dissolved hydrogen. Peroxide at a concentration of 3×10^{-3} molar was thermally decomposed in silica ampoules containing hydrogen at a pressure of 60 cm. In the reaction, under these conditinns, about 20 per cent of the peroxide reacted with hydrogen, presumably via OH radicals produced by reaction (15). The thermal decomposition of peroxide in vacno at 100°C and 150°C appeared to be first order. The rate constants were 3.3×10^{-5} min^{-1} and 6.3×10^{-2} min^{-1}, giving an estimated activation energy of 18 kcal. From the low peroxide concentrations present in irradiated hydrogen-oxygen solutions at the higher temperatures, and from the rates given above, it is concluded that reaction (15) is relatively unimportant. Reactions (16) and (17) are unimportant at low temperatures since they would provide a chain reaction of hydrogen with oxygen to form either peroxide or water and this was not observed.[2] However, they are often postulated[11] to occur in gas phase reactions at higher temperatures and would provide a chain reaction of hydrogen with oxygen. The results observed at temperatures up to 250°C indicate no chain reaction and can be satisfactorily explained by the mechanism proposed. At still higher temperatures, reactions such as (15), (16) and (17) may become important and lead to higher rates of reaction.

Since the yield for hydrogen and oxygen reaction at 200°C to 250°C is given by $3/2\ (c + d)$, it should be dependent on the type of radiation considered. As the specific energy loss along the particle track increases, the yields a and b increase, and c and d decrease. Therefore the yield in the hydrogen-oxygen reaction is expected to be lower for particles giving high specific energy loss. For example, reactor radiation which provides energy both from gamma rays

and fast neutrons (proton recoils) is expected to give a lower yield than gamma rays alone. For those radiations such as α particles for which c and d are small compared to a and b, reaction (15) will probably become more important.

REFERENCES

1. Ghormley, J. A. and Hochanadel, C. J., *A Cobalt Gamma Ray Source Used for Studies in Radiation Chemistry*, Rev. Sci. Inst., *22*, No. 7: 473 (1951).
2. Hochanadel, C. J., *Effects of Cobalt γ-Radiation on Water and Aqueous Solutions*, J. Phys. Chem., *56*: 587 (1952).
3. Hochanadel, C. J. and Ghormley, J. A., *A Calorimetric Calibration of Gamma Ray Actinometers*, J. Chem. Phys., *21*, No. 5: 880 (1953).
4. Allen, A. O., Hochanadel, C. J., Ghormley, J. A. and Davis, T. W., *Decomposition of Water and Aqueous Solutions Under Mixed Fast Neutron and Gamma Radiation*, J. Phys. Chem., *56*: 575 (1952).
5. Barrer, Richard M., *Diffusion in and Through Solids*, Cambridge University Press (1941).
6. Dainton, F. S. and Rowbottom, J., *The Primary Radical Yield in Water. A Comparison of the Photolysis and Radiolysis of Solutions of Hydrogen Peroxide*, Trans. Far. Soc., No. 370, *49*: 1160 (1953).
7. Lea, D. E., *The Termination Reaction in the Photolysis of Hydrogen Peroxide in Dilute Aqueous Solutions*, Trans. Far. Soc., *45*: 81 (1949).
8. Hunt, John P. and Taube, Henry, *The Photochemical Decomposition of Hydrogen Peroxide, Quantum Yields, Tracers and Fractionation Effects*, J.A.C.S., *74*: 5999 (1952).
9. Ghormley, J. A. and Hochanadel, C. J., *The Yields of Hydrogen and Hydrogen Peroxide in the Irradiation of Oxygen Saturated Water with Cobalt Gamma Rays*, J.A.C.S., *76*: 3351 (1954).
10. Sworski, T. J., *Yields of Hydrogen Peroxide in the Decomposition of Water by Cobalt Gamma Radiation. I. Effect of Bromide Ion*, J.A.C.S., *76*: 4687 (1954).
11. Lewis, B. and Von Elbe, G., *Mechanism of the Thermal Reaction Between Hydrogen and Oxygen*, J. Chem. Phys., *10*: 366 (1942).

The Chemical Reactions Induced by Ionizing Radiation in Various Organic Substances

By L. Bouby,* A. Chapiro,† M. Magat,‡ E. Migirdicyan,§ A. Prevot-Bernas,* L. Reinisch,* and J. Sebban,* France

Even though it was thanks to the chemical action of the radiation emitted that radioactivity was discovered by Becquerel, a systematic study of the reactions brought about by the various forms of ionizing radiation was not begun until a fairly late date. As a matter of fact, for a long time, all the efforts made were concentrated on a study of the reactions in an aqueous phase. The ever developing use of radiation therapy required some understanding of the chemical reactions in tissues, of which water is the main component. Only a few authors, such as Kailan, Mund, Gunther and Lind, made a study of the radiochemical reactions taking place in an organic medium.

The situation has changed over the last few years. The development of atomic energy gives reason to believe that intense sources of beta and gamma radiation, consisting in the main of fission products, will become available in the near future. Since the fission products are, at the present time, in the nature of a liability, the economically worthwhile utilization of some of them might make a contribution to lowering the cost of atomic energy itself.

The use of ionizing radiation to bring about chemical reactions is a possibility which has to be explored. It is not surprising then, that we have been witnessing, for the last few years, a rapid development in the radiation chemistry of organic compounds. It is just as logical that our present knowledge of this field should still be so spotty. For instance, while we know that the chemical action of X, γ and β rays is brought about mainly through the secondary electrons they produce, the mechanism of this action is but very vaguely known to us. In particular, there is no theory which enables us to predict either the number, or the nature, of the fragments formed from a given compound. The very fate of the slow electrons is much debated.

On the experimental plane, various methods have been put forward to determine the number of free radicals formed per unit of energy absorbed: some results make it possible to get some idea of the order of magnitude. However, neither the chemical nature of these radical fragments nor their initial spatial distribution are known as yet.

Similarly, while there is a great deal of circumstantial evidence available to the effect that the radicals, rather than the ions, are responsible for secondary reactions,[1] and while it is known that, in many cases, these radicals act as would those produced by any process whatsoever, it is not known for certain that this will always be so.

One would thus be very far away from any possibility of industrial application unless there existed a whole series of reactions of considerable practical interest for which a knowledge of the nature of the radicals produced by radiolysis is not essential. These are chain reactions in which the radicals from radiolysis only serve to unleash a succession of secondary reactions, thus transforming a whole series of molecules. On the other hand, since the amounts and activity of the sources available in the course of the next few years will still be limited, it will be legitimate to use them only to trigger reactions of this type.

Our work, of which we shall show the most significant results in this paper, was concerned with two aspects of radiation chemistry, firstly the determination of the number of radicals obtained by radiolysis from a certain number of organic compounds and secondly a particularly simple chain reaction, the polymerization of vinyl compounds. We shall also say a few words about a radiochemical reaction which can even now be envisaged, namely the cross-linking of polymers.

NUMBER AND SPATIAL DISTRIBUTION OF THE PRIMARY FREE RADICALS PRODUCED BY RADIOLYSIS

Theoretical Data

Number of Radicals Formed

The rate constant of the monomolecular thermal dissociation reactions, which makes it possible to compute the number of molecules decomposed per time unit, dN/dt, has been given by the absolute rate theory:

Original language: French.

* Attaché de Recherches au Centre National de la Recherche Scientifique. Physical Chemistry Laboratory of the Paris Faculty of Sciences.

† Chargé de Recherches au Centre National de la Recherche Scientifique. Physical Chemistry Laboratory of the Paris Faculty of Sciences.

‡ Maitre de Recherches au Centre National de la Recherche Scientifique. Physical Chemistry Laboratory of the Paris Faculty of Sciences.

§ Chercheur libre. Physical Chemistry Laboratory of the Paris Faculty of Sciences.

$$\frac{dN}{dt} = 10^{13}\, e^{-D/kT} \cdot N \qquad (1)$$

where D is the heat of dissociation and N the number of moles present.

A similar computation can be made for the case of photochemical reactions by using Einstein's law of equivalence; each molecule degraded or decomposed corresponds to one quantum absorbed.

The same does not apply to radiolysis. Indeed the photon or electron does not give up the whole of its energy to a single molecule, the fraction given up depending, among other things, on the probabilities of electronic transitions and on the energy of the impinging particle. Now this energy decreases along the trajectory of this particle in an irregular fashion according to the nature of the collisions. In addition, the excitation curves, and often even the position and nature of the excited states, are not known. No *a priori* estimate of the number of radicals formed can be made.

Spatial Distribution of the Primary Radicals

The probability of a γ- or an X-ray photon, or a fast electron, ionizing a molecule and producing a secondary electron is very small. On the other hand, where electrons are concerned, this probability increases as they slow down. As a result, the secondary and tertiary electrons, which are responsible for most chemical effects, are absorbed close to the point of their production. The path of the incident photon thus will be delineated by a series of radical "spurs" of varying importance, relatively far apart. A fraction of the radicals recombine inside a given spur, others diffuse in the space between the spurs, in which their concentration becomes very low, and their recombinations rarer. One must thus distinguish between a continuous background of radicals at a concentration C_f, and local accumulations, spurs, in which the concentration C_p is much higher.[2,3] The concentration inside the spurs will vary as a function of time, due to the scattering and recombination of the radicals. The mathematical description of these changes was given, in the case of the ions, by Jaffé,[4] Kramers,[5] and Magee and Samuel.[6] Magee took up the problem for the case of a simple competitive reaction between free primary radicals.[6] However, the practical applications of the proposed expressions are limited, due to the fact that we know neither the diffusion constants of the various radicals formed nor the rate constants of the elementary reactions.

All we can now state is that the spatial distribution of the radicals will not be uniform, except if the intensity of radiation is such that the spurs belonging to different paths partially overlap before free radicals they contain have reacted in significant numbers.

Experimental Determination of the Number of Radicals Formed

Usually, the number of radicals formed per 100 ev of absorbed energy is designated by symbol G_R. The energy absorbed is measured, in practice, by actinometry with ferrous sulfate. In our experiments, we have taken for this reaction $G_{Fe^{+++}} = 20.8$, and have made the corrections needed to allow for the difference in electronic density between the aqueous solution of ferrous sulfate and the compound under review. Many authors currently recommend a value $G_{Fe^{+++}} = 15.8$. If this were to be taken, all our figures for G_R should be multiplied by $15.8/20.8 = 0.76$.

Three methods have been put forward to date, for the determination of G_R: (*a*) the dosage and composition of the final products; (*b*) interception by very active substances; and (*c*) initiation of reactions of known kinetics.

Before the results are given, a brief review will be made of the advantages and limitations of the three methods.

Dosage and Analysis of the Final Compounds

This method is based on the assumption that the final products are derived exclusively from a recombination of the primary radicals or from their reaction with the irradiated substance, without any intervention of chain processes. On the other hand, the only radicals detected are those which combine and give products different from the initial one. Now, a fraction of the primary radicals always recombines in such a way as to reconstitute the initial molecule and thus escapes detection, so that the values of G_R determined by this method generally are too small. The error so made may be very substantial. Thus, for CH_3I, the dosage method of the final products shows $G_R = 5.08$, while the real value is 20.2.[7,8] Obviously, the difference is not always so large, but it can never be left out of the computations.

Scavenging (Interception by Reactive Substances)

The method, in essence, consists of adding to the irradiated compound a substance which reacts very rapidly with some radicals, and this in quantity sufficient to intercept the primary radicals before they have had time to recombine. The scavenger must fulfill a certain number of conditions. It must: (*a*) be readily measured in low concentrations; (*b*) recombine with the radicals in a known proportion; (*c*) react with the radicals in a non-selective fashion, but react neither with the substrate, nor with the ions, nor with the excited molecules; (*d*) be sufficiently reactive to afford complete interception at concentrations low enough for the direct effect of radiation on the interceptor to be negligible; and (*e*) have no protective or sensitizing action.

Two scavenging agents have been used with success to date: triphenylmethane[9] and diphenylpicrylhydrazyl (DPPH), the routine use of which, suggested by one of us,[10] gave a certain number of important results. This compound, a "stable" crystallizable free radical, is entirely dissociated both in the solid state and in solution. It reacts quickly with thermal radicals by decolorizing.[11] Its very intense violet or purple hue makes colorimetric dosages pos-

sible at concentrations of the order of 10^{-6} mol/cm^3. No protective effect has been observed with DPPH, following the recrystallization in an ether-chloroform mixture.¶ Its applications are limited, however, to compounds which have neither a mobile hydrogen (acids, hydroquinone, hydroperoxides, amines, etc. . . .) nor double vinyl bonds.[13,14] (For a more detailed discussion of the limitations of the method, see reference 8.)

Since there always is some competition between the scavenging or intercepting reaction:

$$R^{\cdot} + \mathrm{DPPH} \xrightarrow{k_2} R{\cdot}\mathrm{DPPH}$$

and the recombining reaction between the primary radicals

$$R^{\cdot} + R^{\cdot} \xrightarrow{k_1} A$$

the speed of formation of which is given by:†

$$\frac{dR^{\cdot}}{dt} = G_R I$$

interception can be complete only for an infinite concentration of the interceptor.

By assuming the existence of a quasi-stationary state for $R^{\cdot}$, the rate of DPPH disappearance, V, will be:

$$V = k_2/(k_1)^{\frac{1}{2}}(G_R I)^{\frac{1}{2}}\mathrm{DPPH} \qquad (2)$$

for low concentrations of the intercepter or scavenger, and

$$V = G_R I \qquad (3)$$

for sufficiently high concentrations.[15]

On the other hand, a "critical" concentration, DPPH_{crit}, can be defined, such that the fraction of the $R^{\cdot}$ radicals which escape interception is constant. We arbitrarily set the value of this fraction to 2.5%.[15,16] Equations 2 and 3 have been verified for solutions of DPPF in chloroform and methyl acetate in concentrations ranging from 0.3 to 1500 r/min. In each and every case, it was found that DPPH_{crit} was under 5×10^{-3} M. In these circumstances, it is permissible to assume that the direct effect is negligible and that the protective and sensitizing effects, if any, are weak. The ultimate determination of V under high DPPH concentrations consequently gives G_R directly.

Some difficulties, which do not affect the orders of magnitude of G_R, still persist. On the one hand, the values of G_R determined in that fashion are, in some cases, influenced by the presence of oxygen. On the other hand, a post effect often is observed: the decoloration continues to persist after irradiation is concluded.[12]

¶ DPPH, when recrystallized in benzene, with which it forms mixed crystals, has a protective action in chloroform, probably due to benzene.[2]

† I is given in units of 100 ev/sec.

Influence of Initial (Non-Homogeneous) Distribution of the Radicals

From the kinetic mechanism proposed, one can deduct that, for the case in which the radicals due to radiolysis are uniformly distributed in space, one should have:

$$\mathrm{DPPH}_{crit} \propto I^{\frac{1}{2}} \qquad (4)$$

The same no longer obtains for a non-uniform distribution. In fact, to achieve a given degree of interception, the ratio of scavenger concentration to the concentration of radicals to be intercepted must reach a certain value in the elements of volume where it is highest, namely, in the spurs. Thus, Equation 4 will hold good only if the intensity is high enough for the average concentration of the continuous background C_f to be equal to concentration C_g in those spurs. Since, on the other hand, the latter is independent of the intensity, one must expect to find, for low intensities, a nearly constant value of DPPH_{crit}. This has effectively been observed by one of us[10] for chloroform and methyl acetate (Fig. 1).

Initiation of a Chain Reaction

If the primary radicals are used to start a chain reaction, the propagation and termination rates of which are known, the number of active centers produced can be derived from the quantity of substance transformed for a given dose. By adding a substance which does not take part in the subsequent reactions, but contributes to the production of active centers, this contribution, and thus the G_R of the added substance can be computed.

Utilization of the method is based on the following assumptions: (a) the reaction is started only by the free radicals; (b) all the radicals created are used for the purpose of starting the reaction; (c) the kinetic laws are known; and (d) the various

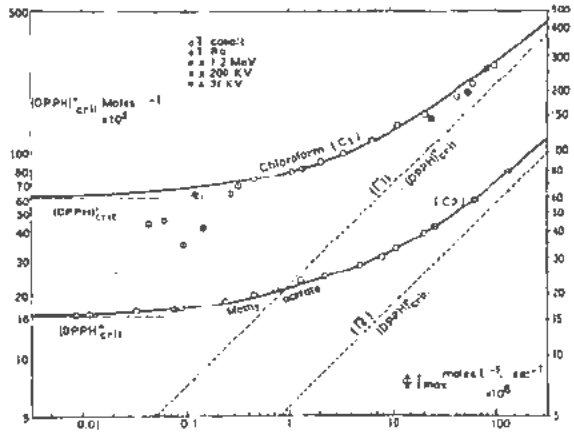

Figure 1. Variation of the critical concentration as a function of radiation intensity. The Γ curves (dashed lines) represent the variation of $(\mathrm{DPPH})_{crit}$ (namely of a magnitude proportional to the concentration of radicals in the continuous background). The (C) curves (solid lines) were developed point by point from the Γ curves, by adding to the ordinates 60×10^{-5} in the case of chloroform, and 16×10^{-5} in the case of methyl acetate, respectively

constituents of the mixture have no mutual sensitizing or protective action on each other.

We chose, for our chain reaction, the polymerization of styrolene.[17] This is brought about entirely by a radical mechanism,[18] since the ions which may be present do not start any chains, presumably due to their short life.[3] The monomer and polymer are soluble** in a great many organic solvents, and the reaction follows the customary laws of kinetics. The rate is proportional to $I^{\frac{1}{2}}$ over a wide range of intensities (Fig. 2) and concentrations, which indicates that the kinetics are not influenced by the non-uniform distribution of primary centers, and that all radicals produced are used to initiate the chain reaction.

However, the propagation and termination rate constants k_p and k_t, which seemed to be well established when the work was carried out, are now being questioned, since the differences between the findings of the various authors[19] lead to an uncertainty of a factor 2 as regards the values of G_R. On the other hand, Burton and his group[20] and Bouby and Chapiro[12] showed that benzene had a strong protective action on more highly saturated compounds and halides, while the latter, on the contrary, acted as sensitizers on benzene. From some indications[18] the same applies in the case of styrolene.

Thus, the use of the method is limited to good solvents of the polymer and to substances having a structure close enough to that of the monomer, for protection and sensitization effects to be negligible.

If such conditions are fulfilled, kinetics give for the over-all rate of polymerization:

$$V = -\frac{dM}{dt} = \frac{k_p}{k_t^{\frac{1}{2}}}[M]^{3/2}(\phi_M I)^{1/2}\left\{1 + \frac{\phi_S [S]}{\phi_M [M]}\right\}^{\frac{1}{2}} \quad (5)$$

in which $[M]$ and $[S]$ are the concentrations of the monomer and solvent in mole/l, ϕ_M and ϕ_S the kinetic constants directly connected with the radiochemical yields G_R^M and G_R^S (see below). This Equation makes it possible to compute the ratio of G_R^S/G_R^M independently of the k_p, k_t, and the absolute G_R values if these constants be known.

Experimental Results. Correlation between the Values of G_R and Chemical Structure

Table I gives a compilation of the values of G_R for a series of organic compounds obtained by the various methods mentioned above. For styrolene, we give the limiting values obtained by taking constants k_p and k_t of Melville and Valentine, and those of Matheson and coll.,[19] respectively; for methyl methacrylate, these computed from the Mackay and Melville figures[21] and those of Matheson and coll.[22] The G_R of acrylonitrile was determined with respect to styrolene through methanol.[23] The values on which there is most doubt are between brackets. In view of the many sources of error inherent in the various methods, the agreement seems satisfactory.

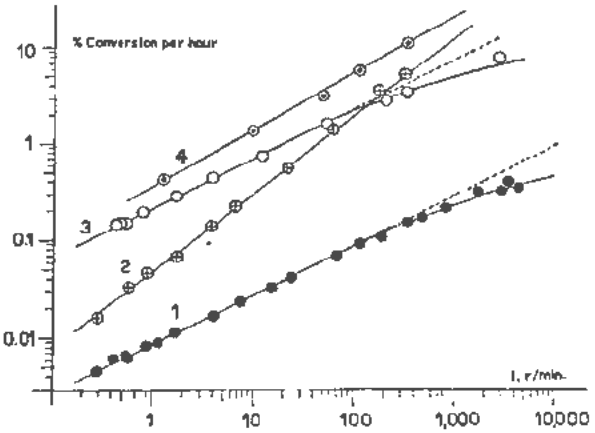

Figure 2. Rate of polymerization of pure monomers as a function of γ-ray intensity: (1) styrolene, (2) acrylonitrile, (3) methyl methacrylate, (4) vinyl chloride

Some qualitative rules may be deduced as regards the correlation between the chemical structure of the various components and their radiostability.[8,24]

Among the hydrocarbons, the aromatic compounds are most stable, and stability is increased by an extension of the system of double conjugate bonds,

Table I

Compounds	G_R			
	Polymerization		DPPH	
			Air	Vacuum
CS_2	0.8	1.9	0.69	
Benzene	0.79	1.92	0.75 to 1.2	0.96
Styrolene	0.7	1.7		
Toluene	1.2	2.90	2.6	
m-Xylene	3.06	7.4	...	
Ethylbenzene	4.4	11.1	...	
Acrylonitrile	(1.1)	(2.6)	...	
Propionitrile	...	...	3.2	
Nitrobenzene	...	...	3.8	
n-Heptane	(1.74)	(4.15)	8.1	
n-Octane	...	...	9.35	
Cyclohexane	(3.48)	(8.4)	11.7	
Ether	7	16.9	20.3	
Dioxane			16.4	
Methanol	...	...	19.7	
Propanol	...	...	24.6	
Methanol-d_4	...	...	18.9	
Me acetate	...	...	16.5	9.0
Me acetate-d_6	...	...	21.6	
Ethyl acetate	...	...	26.2	
Me-methacrylate	15.9	21.6	...	
Acetone	(44)	(10.6)	41	
Chlorobenzene	8.35	19.6	14.4	
o-dichlorobenzene	...	...	24.6	
Cyclohexyl chloride	...	...	27	
CH_3Cl	...	...	22	
CH_2Cl_2			36	
$CHCl_3$	(30)	(72.4)	50	32.8
CCl_4	(89)	(214)	33	24.5
1,2-dichlorethane	...	...	24.6	
Ethyl bromide	13.1	31.5	23	
Bromoform	...	...	59	

**Where the polymer is not soluble in the added compounds, complications appear, which will be mentioned elsewhere.

while it is reduced by introducing the aliphatic chains; G_R is greater for the alicyclic compounds than for the paraffins.

By adding atoms which can form negative ions (O, halogens), G_R is very markedly increased. Their accumulation brings about only a smaller increase.

Possibility of Using Ionizing Radiation for Organic Synthesis

The fact that radiolysis breaks up organic compounds, which gives certain radicals, and that these radicals can either recombine to form new molecules or else be used for substitution, may, on principle, be used to carry out organic syntheses. However, this only represents a remote possibility for, on the one hand, we do not know the nature of the compounds formed in each case and, on the other hand, the amounts of products which can thus be obtained are small. In addition, the cost is, and will probably remain, too high: a 1000 curie source of Co^{60} emits 3.7×10^{13} 1.1 and 1.3 Mev photons per second. Assuming that they are entirely absorbed, that G_R is about 20, that the yield is maximal (50%), and that the molecular weight of the final product is approximately 200 gm, the hourly production would be only:

$$\frac{3.7\times10^{13}\times1.2\times10^{4}\times20\times0.5\times3.6\times10^{3}\times200}{6\times10^{23}} \approx 5 \text{ gm}$$

Thus, in five years, one would have some 200 kg of the product and, at the end of that period, the intensity of the source, and thus its price, would be reduced to one-half (1-million French francs).

It will be seen, from this discussion, that the use of radiation for conventional chemical synthesis can not currently be envisioned.

The situation is very different for chain reactions (halogenizing, oxidizing, polymerizing, etc. . . .) and those which take place between macromolecules. We shall consider two typical instances of such reactions: the polymerization of vinylic compounds, and the cross-linking of polyethylene.

RADIOCHEMICAL POLYMERIZATION

General Kinetic Laws. Rate of Polymerization

As already indicated, polymerizations started by radiation proceed by a radical mechanism. It is possible, in such a case, to draw up the following reaction mechanism, which makes allowance for all such reactions as may determine the over-all rate of polymerization.[25]

(1)
$$\left.\begin{array}{l} M \xrightarrow{MI} \\ S \xrightarrow{SI} \end{array}\right\} R^{\cdot} \quad \text{production of radicals by radiolysis}$$

(2)
$$R^{\cdot} + R^{\cdot} \xrightarrow{k_2} B \quad \text{recombination of primary radicals}$$

(3)
$$R^{\cdot} + R \xrightarrow{k_3} RM^{\cdot}$$
Initiation or start of chains

(4)
$$RM_n^{\cdot} + M \xrightarrow{k_p} RM_{n+1}^{\cdot} \qquad \text{Propagation}$$

(5)
$$RM_n^{\cdot} + RM_m^{\cdot} \xrightarrow{k_t} P \text{ (or } 2Q)$$
Mutual termination of chains

(6)
$$RM_n^{\cdot} + R^{\cdot} \longrightarrow P^{\cdot}$$
Termination by primary radicals

If the mutual termination is predominant, namely if reactions (2) and (6) are negligible as compared to reaction (5), and if a nearly stationary condition is reached from the very beginning of the reaction, Equation 5 was the over-all rate V, which is proportional to $I^{1/2}$.*

The values of ϕ_M and ϕ_S in the case of γ rays, if I is given in r/min, are given by:

$$\phi_M = \frac{G_R^M}{d_m N_A} 58 \times 10^{19} \text{ and } \phi_S = \frac{G_R^S}{d_s N_A} 58 \times 10^{19} \qquad (6)$$

in which d_m and d_s are the specific gravities of the monomer and solvent, and N_A is Avogadro's number.

If a stationary condition is not reached, the solution is a little more complicated; it has been given, for the case of catalytic initiation, by one of us.[26]

In the case of radiochemical initiation for a pure monomer and assuming that the polymer is eliminated as it is being formed, in order not to have it contribute to the initiation, the expression then becomes:

$$-\frac{dM}{dt} = \frac{k_p}{k_t^{1/2}} (\phi_M I)^{1/2} M^{3/2} \times \tanh\left[(k_t \phi_M I [M])^{1/2} t\right] \qquad (7)$$

namely, we no longer have a simple relationship between the rate and intensity.

However, the situation changes if the concentration of $R^{\cdot}$ radicals becomes important, as in the case for very strong radiation intensities. Reactions (2) and (6) cease to be negligible and, at the limit, reaction (5) is the one which becomes negligible as against (6), i.e., termination is entirely by primary radicals. By applying the hypothesis of a quasi-stationary state, it will be found, in this case, that the rate of polymerization becomes independent of the intensity, i.e., proportional to I°.[25] If the two termination mechanisms (5) and (6) are coexistent, the formula which gives the rate, as a function of intensity, will be more complex[25] but an approximation of it can be obtained by a I^{α} law, in which $0 \leqslant \alpha \leqslant \frac{1}{2}$.

Thus, in the cases in which the hypothesis of a quasi-stationary state applies, the speed of polymeri-

*As already indicated, Equation 5 assumes the absence of protection and sensitization phenomena.

zation will be proportional to $I^{1/2}$, and will tend to become independent of I at the very high intensities. It can readily be shown,[25] that the deviation from the $I^{1/2}$ law will appear for intensities so much weaker as: the monomer concentration is smaller, the temperature is lower, the reactivity of the monomer is smaller, and the G_R value for the medium is higher.

It will be seen below that all these forecasts are confirmed by experience.

If a quasi-stationary state is not reached, and if the termination takes place by primary radicals, it is envisioned by the theory[27] that the speed of polymerization will be proportional to I^β, in which $\frac{1}{2} < \beta < 1$, where β can be a function of the degree of conversion. This is the situation which appears to be found in some cases of polymerization in a precipitating medium (acrylonitrile).

Molecular Weight

In the absence of any transfer, the mean degree of polymerization, $\overline{DP}_0$, is equal to the length of the kinetic chain, namely to $(dP/dt)/(dR/dt)$. In the case of radiochemical initiation, the degree of polymerization will thus vary as $I^{-1/2}$ if the speed or rate is proportional to $I^{1/2}$. Thus, if a polymer having a distribution of molecular weights similar to that obtained with a catalytic initiation is required, the radiation field must be as uniform as possible.

Nothing is known from the start about the molecular weights of the polymers produced in a precipitating medium. Our experiments have shown, however, that they are greater than in a system in which the polymer remains in solution.[25] Furthermore, they decrease more slowly with the intensity than in the case just covered.

Experimental Results

We made a study of the rate of polymerization of a certain number of monomers, both pure and in solution. The polymer formed is either soluble, or insoluble, in the reacting medium.

Our experiments were conducted at 19°C with two sources of γ rays: one of 0.27 curie of Ra, used in the 0.29 r/min–4.05 r/min range, and a 25 curie source of Co^{60} for the 6 r/min–435 r/min range. The significant results are shown on Figs. 2 (pure monomers) and 3 (styrolene solutions). Our results for styrolene and methyl methacrylate were completed by those of Ballantine and Manowitz,[28] which were obtained with higher intensities. The data of these authors were recomputed for our temperature and dosimetry. It can be seen that agreement with the theoretical predictions is most satisfactory.

For the polymers which are soluble in their monomer (styrolene and methyl methacrylate—Fig. 2), the rate of polymerization is proportional to $I^{1/2}$ between 0.29 and 100 r/min approximately, while, for the higher intensities, an increase in the rate of polymerization with intensity decreases.

The deviation appears for methyl methacrylate at lower intensities than for styrolene, and this for two reasons: in the first place G_R is higher for methacrylate than for styrolene and, in the second place, the double bond of styrolene is more reactive than that of methacrylate (see, for instance, Mayo and his group).[29]

Finally, the deviation from the $I^{1/2}$ law appears for lower intensities for styrolene in solution in toluene than for pure styrolene (dilution effect) (Fig. 3).

Agreement between the experimental results and the theoretical forecasts, particularly as regards the $I^{1/2}$ law, justify, after the fact, the implicit assumption that the non-uniform distribution of the primary radicals does not disturb the kinetics or, again, that, for polymerization, everything takes place as though the distribution of the primary radicals were homogeneous. Let it be stated again that this was not the case for the interception of the primary radicals by DPPH. A possible explanation for this is as follows: homogenization of the concentration of the primary radicals takes place by diffusion and the rate of diffusion is increased by the polymerization process, which ensure a transfer of the free valency. Nothing similar happens where interception is concerned. On the other hand, since the termination of growing or developing chains is a relatively uncommon reaction, the life of the chains is long, which favors homogenization by diffusion.

For polymerization in a precipitating medium (vinyl chloride and acrylonitrile, Fig. 2) or styrolene in propanol (Fig. 3) the rate of polymerization is proportional to I^β, in which β is somewhere between ½ and 1. The same applies to the polymerization of acrylonitrile containing 7% water or methanol[30] (not shown). Values of β of the same order of magnitude have been observed for the polymerization of acrylonitrile by chemical catalysts.[31,32] The deviation from the law in $I^{1/2}$ thus is not characteristic of polymerization initiated by ionizing radiation, as had been thought by some writers.[33] It is no longer connected

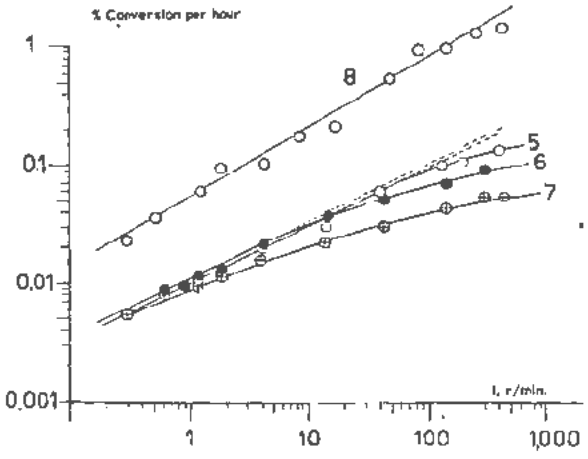

Figure 3. Rate of polymerization of styrolene in solution as a function of γ-ray intensity: curve 5, 40% styrolene (in moles) in toluene; curve 6, 20% styrolene (in moles) in toluene; curve 7, 10% styrolene (in moles) in toluene; curve 8, 10% styrolene (in moles) in propanol

with the nature of the monomer, since the polymerization of styrolene, both pure and in a concentrated solution in toluene, and the polymerization of acrylonitrile in dimethylformamide (solvent of the polymer), follow an $I^{1/2}$ law.

On the other hand, this deviation seems to be related to the fact that the polymer precipitates in the medium. It is attended, at any rate, by two characteristic phenomena: the rate of reaction is a function of the degree of conversion up to fairly high levels,[23,31,32,34] which indicates that the stationary condition is not reached; and polymerization continues, with a decreasing speed, at times for a fairly long time (two months in the case of acrylonitrile),[23,24] which indicates that the termination reaction is slow, and accounts for the absence of a stationary condition. Let it be noted that the conversion in the course of post-polymerization may exceed 50% of that obtained during irradiation.

It is likely that, as is the case with all homogeneous polymerizations, exponent β will go down with high intensities. We have not been able to observe this phenomenon with the intensities available to us.

In view of the difference in the exponents of I for the polymerizations taking place in a homogeneous medium and a precipitating one, it is possible to have conditions such that, for a given monomer, the speed of polymerization is greater in a precipitating than in a homogeneous medium. In some cases, the weight of polymer formed per unit time is greater for dilute solutions in a precipitating medium than in the pure monomer. This is the case, for instance, of styrolene in dilute solution in alcohol.[23]

Influence of the Temperature

On the Rate of Polymerization

The activation energy of the over-all reaction, in the case of a catalytic or thermal initiation, is given by:

$$E_g = E_p + \tfrac{1}{2}E_a - \tfrac{1}{2}E_t$$

in which $E_p \approx 5$ kcal is the activation energy of the propagation reaction, $E_a \approx 30$ kcal that of the initiating reaction, and $E_t \approx 0$ kcal that of the terminating reaction. By using the values just given, one finds $E_g \approx 20$ kcal. A temperature rise of 10° between 300° and 310°K causes the rate to increase by a factor of 2.5.

In the case of photochemical initiation, the rate of the initiating reaction is independent of the temperature, and the over-all activation reaction reduces, to all practical purposes, to $E_p \approx 5$ kcal. The same temperature rise increases the speed by only 32%. Thus, the danger of a polymerization reaction "running away" is less in the case of polymerization by radiation than in that of catalytic polymerization.

Two complications may arise, but have not been seen as yet:

On the one hand, if it is found that, in the intensity range in which the rate develops less rapidly than as a function of $I^{1/2}$, a temperature rise, by favoring reaction (3) as over reactions (2) and (6), increases the value of α, and thus the reaction rate. This acceleration adds to the normal acceleration mentioned above. This effect will rarely be important.

On the other hand, if polymerization is carried out in a precipitating medium, and if the temperature is brought above the critical dissolution temperature, the higher temperature reaction will take place in a homogeneous medium, and a rather sudden decrease in the rate will be observed.

On the Mean Molecular Weight

Two cases have to be distinguished, according to whether the molecular weight is determined by the propagation or the transfer reaction.

If the amount of transfer is negligible, one will find, for thermal or catalytic polymerization:

$$DP_0 \propto e^{-(E_p - E_a^{1/2} - E_t^{1/2})/RT} \approx e^{+10{,}000/RT} \qquad (8)$$

which means that the molecular weight decreases as the temperature increases. Thus, it is impossible simultaneously to accelerate the conversion rate and the molecular weight.

For photochemical or radiochemical initiation, one finds, in this case:

$$DP_0 \propto e^{-(E_p - E_t^{1/2})/RT} \approx e^{-5000/RT} \qquad (9)$$

in other words, the mean molecular weight increases with the temperature. These initiating techniques thus make it possible simultaneously to increase the molecular weight and the rate of conversion. Such an increase in the rate and mean molecular weight with the temperature actually was observed by Ballantine and Manowitz[23] for the radiochemical polymerization of styrolene and methyl methacrylate.

If the transfer reaction to the monomer is not negligible, one can write:

$$\frac{1}{\overline{DP}} = \frac{1}{\overline{DP}_0} + \frac{k_f}{k_p} \qquad (10)$$

in which k_f is the rate constant of the transfer reaction. The variation in the degree of conversion with the temperature then is described, for the case of radiochemical initiation, by:

$$\overline{DP} = [A\, e^{+(E_p - \frac{1}{2}E_t)/RT} + B\, e^{-(E_f - E_p)/RT}]^{-1} \qquad (11)$$

Since, in general, $E_f > E_p$, the two terms vary in opposite directions and according to the exact values of constants A and B and the activation energies. $\overline{DP}$ may decrease or increase with the temperature. In the general case, there will be a temperature for which $\overline{DP}$ will be at a maximum.[35] One must expect to find such a situation in the case of chlorinated monomers.

Influence of Solvents

While in all other initiation techniques the solvent which may be present only plays the part of a chem-

ically inert diluent, the addition of which only causes a reduction in monomer concentration, and possibly a change in the state of the polymer (precipitation or solubilization), radiochemical initiation gives entirely different results. Since the action of ionizing radiation is not selective, the radicals from solvent radiolysis will take part in the initiation.[17,23]

It is often possible to find solvents having a G_R sufficiently larger than that of the monomer for their addition to bring about an acceleration of the polymerization, despite the decrease in monomer concentration. Examples of such accelerations are provided by the polymerization of styrolene in various organic solvents,[21] and by that of acrylonitrile in water.[33] Let us remember, however, that the solvent and the polymer have mutually protective or sensitizing actions, and that the total number of radicals produced in the mixture is not equal to the sum of the radicals which would be produced in the components taken separately.[12,18,20]

Influence of the Polymer Formed

As soon as the concentration of the polymer produced ceases to be negligible during polymerization, the latter begins to play a role equivalent to that of a solvent, since the radicals formed from the polymer participate in the initiation of the reaction.[36] The values of G_R are not yet known, but they can be expected to be markedly higher than those of the corresponding monomers. The monomers, for the same structure, contain one more double bond than the polymer does, and double bonds stabilize substances with respect to radiolysis, particularly where one is dealing with conjugate systems (see, for instance, styrolene and ethylbenzene, Table I).

Two types of radicals may be formed from the polymer, according to whether one is dealing with breaking of the main chain or the side chains.

In the first case, the chains initiated by macro-radicals will be linear, but longer, by the length of the macro-radical, than the average length of the "normal" chains initiated by short radicals. In the second case, one will obtain branched chains.

During the polymerizations initiated by radiation, one should observe an increase in the molecular mass with the degree of conversion. Such an increase indeed was observed by Ballantine and Manowitz,[28] in the polymerization of styrolene and methyl methacrylate by gamma rays, as well as by Landler[37] for the polymerization of styrolene by the mixed radiation from the reactor.

Formation of "Grafted" Copolymers

The initiation of polymerization by macro-radicals can also be demonstrated and utilized in another fashion. If polymer A_n be added to monomer B, and the mixture be irradiated, there will be a polymerization of monomer B, part of which gives polymer B_m and the other a "grafted" copolymer A_nB_m. By the proper choice of A_n and B_m pairs, and of the experimental conditions, it will be possible to favor the formation of the "grafted" polymer at the expense of the simple B_m. It is a well known fact that, as against what happens with the usual copolymers, in which A and B are distributed at random, which are endowed with properties intermediate between those of the simple polymers A_n and B_m, the "grafted" copolymers combine some properties of A_n with some others which pertain to B_m, and present considerable practical interest. The radiation "grafting" process has the advantage over other processes of making it possible to carry out "grafts" on finished or semi-finished objects which, in some cases, may make it easier to use this method of preparation.[38]

Advantages and Drawbacks of Radiochemical Polymerization

On the basis of what has just been stated, it is possible to draw up a table of the advantages and technical drawbacks of initiating polymerization by ionizing radiation, as compared to the other techniques. We shall consider in turn the advantages shared by the radio- and photochemical initiation over the catalytic method, and then the advantages of radiochemical initiation over the photochemical method. Thereafter, we shall go into the drawbacks.

Common Advantages of the Radiochemical and Photochemical Initiation Methods

Polymerization by radicals can be effected at a very low temperature.

The speed of polymerization does not depend much on temperature. The latter thus does not have to be checked as strictly as in the case of catalytic initiation.

It is possible, in some cases, simultaneously to increase the speed of polymerization and the length of the chains.

No fragment of a foreign body is introduced into the polymer (catalyst fragment, metal atoms, oxygen), which may be of advantage, for instance from the dielectric standpoint.

Specific Advantages of Radiochemical Initiation

Photochemical initiation is possible only with monomers which absorb in the regions of the spectrum for which intense sources are available. Otherwise, it would be necessary to add a photosensitizer to the monomer. There is no limitation of this type to radiochemical initiation. This is due to the non-selective nature of the absorption of ionizing radiation.

Since gamma rays are more penetrating than ultraviolet rays, it is possible to irradiate volumes of greater thickness.

Optical heterogeneity or opacity of the medium is no obstacle. Irradiation can be carried out through metal walls.

Radioactive sources are stable, and require neither maintenance nor repairs.

Up to a certain point, the degree of ramification may be adjusted.

"Grafted" polymers may be prepared by relatively simple methods.

The Main Drawbacks

These are as follows:

The need for protection, which may make the facility more cumbersome.

The decrease in the intensity of the radioactive sources with time. This notable drawback for Co^{60} sources practically does not exist for Cs^{137} sources (25 years). However, this effect is decreased due to the fact that the rate of polymerization is proportional to a fractionary power of the intensity.

The existence of an intensity gradient in the reactor, which implies a variation in the mean molecular weight with the distance from the source. This inconvenience can be averted (it does not present itself at all if the length of the chains is determined by transfer) by using, rather than a single source, an array of adequately arranged sources.

Economic Aspects

Knowing the rate of polymerization as a function of intensity, the production of the reactor may be evaluated by using a source, or set of sources, of a given power and thus the "cost" of radiochemical initiation can be estimated.

We carried out this computation[39] for the case of a linear source of Co^{60} having an activity of 100 curies, placed along the axis of a cylindrical vessel of the same height as the source (h=20 cm). Methyl methacrylate was chosen as a typical monomer. If self-absorption is neglected, one may compute the intensity, at each point of the vessel, by using the formula given by Sievert:[40]

$$I_Q = \frac{P}{l_a}\int_{\phi_1}^{\phi_2} e^{-\frac{\mu a}{\cos\phi}}\, d\phi = \frac{P}{l_a}\left[F(\mu a\ \phi_2) - F(\mu a\ \phi_1)\right] \tag{12}$$

where a is the distance of the point considered to the axis of the cylinder, μ the absorption coefficient (0.055), ϕ_1 and ϕ_2 the angles between the perpendicular drawn from point Q to the axis and the straight lines connecting Q to the ends of the source. Functions F are tabulated by Sievert.

Intensity of the radiation varies, not only with the radius, but also with the position h of the plane with respect to the center of gravity of the source.

In order to simplify all calculations, we assumed that we were working with an average intensity independent of h and only allowed for the variation with a, which is much more important. Figure 4 shows the circles of iso-intensity. They are sufficiently close to one another to warrant the assumption that, inside each cylindrical layer that they mark off, the intensity is constant and equal to the arithmetic mean of the intensity at the boundary surfaces. The hourly amount of conversion was read on Fig. 2, and multiplied by the weight of the monomer present in each cylindrical layer.

Figure 5 [curve I (100)] shows the weight in grams of methyl polymethacrylate produced in each hour as a function of the reactor radius. It will be seen that this value tends toward a limit which is practically reached for $r = 50$ cm.

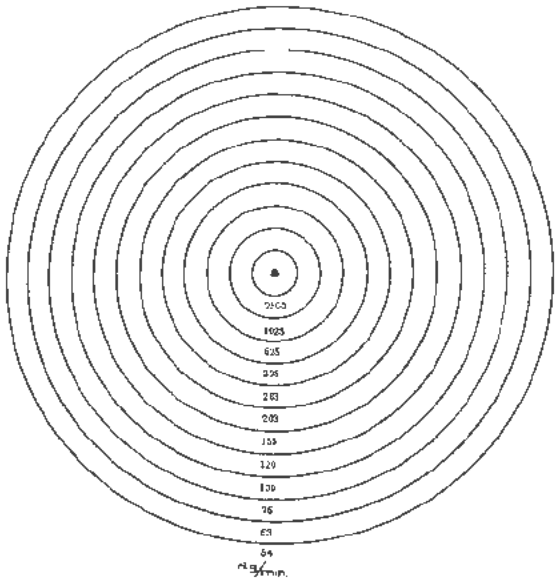

Figure 4. Iso-intensity circles (r/min) for a linear 100 curie source of Co^{60}, 20 cm high, immersed in methyl methacrylate. The values correspond to an average for variations with height of the point considered

At 19°C, the yearly production of a reactor 50 cm in radius reaches 5.35 tonnes. At 60°C, if we assume an activation energy of 6 kcal, the production would be about 21 tonnes. Allowing for the decay of the source which has a 5 year half-life, the five year production of the polymer may be estimated at 22.5 and 90 tonnes respectively. The price differential, between a 100 curie and a 50 curie source, being currently some 100,000 French francs, the cost of radiochemical initiation may be estimated at 4.50 French francs and 1.10 French francs per kilogram of polymer respectively. With Cs^{137} sources, the prices would be approximately three times lower. On the other hand, since the cost of radiochemical initiation is all the lower as the speed of reaction is greater, the cost of initiation can be reduced substantially while increasing production, by carrying out polymerization in an

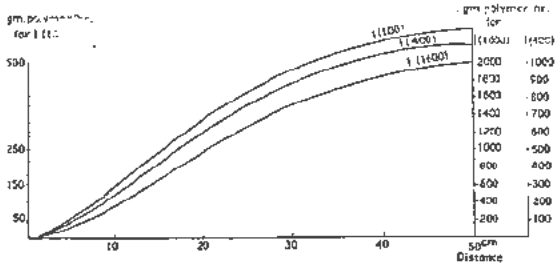

Figure 5. Hourly production in grams of polymethyl methacrylate as a function of the reactor radius, at 19°C, for a linear source 20 cm high, placed on the axis of a cylindrical reactor. The curves have reference to sources of 100, 400 and 1600 curies respectively

emulsion or precipitating medium. However, even now, the cost of radiochemical initiation is of the same order of magnitude as that of the chemical catalysts.*

Let it finally be noted that, currently, the number of sources available makes it possible to contemplate the use of radiochemical initiation only for special polymers, the yearly consumption of which is not unduly high.

Optimal Activity of the Sources. Near-Homogeneous Fields

The reactor mentioned in the above paragraph is far from being the optimum device. Indeed, since the rate of polymerization is proportional to $I^{1/2}$, total production is increased by 40% if one breaks up the source into two 50 curie units, which are placed in two independent reactors with radii of 50 cm.

On the other hand, if the activity of the sources is brought up to 400 or 1600 curies, the production is less than doubled or multiplied by four [see Fig. 5, curve I (1600)]. This is due to the fact that, at the high intensities, the rate increases more slowly than the square root of the intensity.

In the case of polymerization in a homogeneous medium, this makes it of no interest to use single sources having an activity greater than 50 or 100 curies.

The situation may be different in the case of polymerizations in a precipitating medium, in which the exponent of I varies from one case to the next, and is greater than ½. A computation of the optimal activity of the sources must be made for each individual case.

Another characteristic of the cylindrical reactors using a single axial source, which may be a drawback in some instances, is the considerable variation of the intensities along the reactor radius. In the case considered earlier for instance, the intensity varies from 2000 to 1 r per minute. If the transfer reaction is negligible, the average molecular weight varies, as we have noted, as $I^{1/2}$, and the device envisioned would give a polymer having a very wide distribution of mean molecular weights ($\overline{DP}$ varying by a factor of 40) superimposed on the normal distribution.

To alleviate this drawback, various arrangements of weaker sources can be envisioned, making possible more uniform radiation fields. Figure 6 shows, as an example, iso-intensity curves for 7 sources of Co^{60} of 14.3 curies each, arranged at the apices and at the center of a hexagon. The computation was carried out for a vessel having a radius of 12 cm, with a separation of 6 cm between sources. In such a reactor, the yearly production would be 1.7 tonnes, with a single source and 2.0 tonnes with the seven-source arrangement.

It will be noted that, with the last mentioned arrangement, the efficiency of the reactor is increased while a product of more uniform molecular weight is obtained.

*The cost of the shielding has not been considered in this estimate.

RADIOCHEMICAL CROSS-LINKING OF POLYMERS

Influence of Oxygen and Intensity

As against the situation found for the polymerization reaction, the cross-linking of polymers is not a chain reaction. However, in so far as the chemical entities which come into play are macro-molecular chains made up of several thousands of monomeric elements, and since it is enough, on the average, to form one bridge per polymer chain in order to modify profoundly some of the over-all properties, this reaction, as well as polymerization, requires but a few primary events in order to bring about the transformation of large quantities of products.

The action of radiation on polymers has been studied very actively for about three years, mostly by Charlesby,[41] and Lawton and his group.[42,43] From the very beginning, these authors observed that some polymers, such as polymethyl methacrylate, polyisobutylene, the cellulose derivatives and polytetrafluoroethylene, are degraded by irradiation, while others, such as polyethylene, nylon, the polyesters and the rubbers, are cross-linked (vulcanized).[41,42] In so far as the cross-linked polymers have new qualities, in particular better resistance to heat and solvents, and since it is difficult, not to say impossible, to cross-link some polymers by conventional chemical methods, radiochemical cross-linking may be considered an economically worth-while operation.

In our laboratory, we undertook the study of the irradiation of polymers for the double purpose of shedding light on the mechanism of the reactions which come into play, and of determining the most favorable conditions for achieving cross-linking. Our study was essentially concerned with the influence of

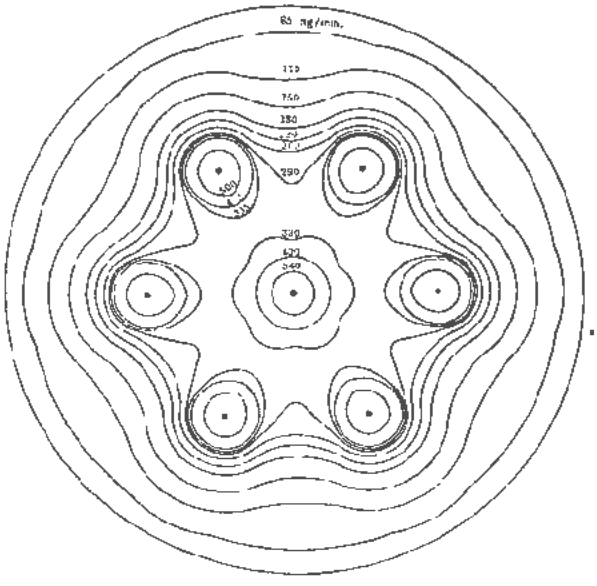

Figure 6. Average (with respect to height) iso-intensity curves in r/min for 7 linear sources of Co^{60} of 14.3 curies each, arranged at the apices and center of a hexagon having 6 cm sides. Absorbing medium: methyl methacrylate. Radius of reactor 12 cm

dose, the intensity of radiation, and the presence or absence of oxygen during irradiation.[44]

In order to follow the development of the reaction, we measured the temperature at which a small sample of the polymer became sufficiently fluid to break under a very low tension (0.7 gm/mm²). This temperature, which has been called the "melting point" for the polymer first increases slowly with the dose, then more and more rapidly. Beyond a critical dose in some cases, a polymer is obtained which is no longer fusible. Figures 7 and 8 show the results obtained with polyethylene irradiated in the presence and absence of air respectively. Figure 7 shows that, in the absence of air, the increase in the melting point for small doses is a function of the intensity of radiation, and that it is all the larger as the intensity is smaller. This is true only for intensities under 500 r/min. For higher intensities, the effect observed is independent of said intensity.

On the same figure, it will be seen that, for low intensities, the melting point of the samples goes through a maximum for a given dose, while for intensities greater than 500 r/min, polyethylene becomes infusible, following a dose of 2.5 megaroentgens. If irradiation is carried out in the absence of air (under a vacuum or in an inert atmosphere), the increase in the melting point for a given dose is independent of the intensity of the radiation, and infusibility is reached after a dose of 1 megaroentgen only (Fig. 8). On the same figures may be seen the limit elongation under the load used (0.7 gm/mm²) for samples which had become infusible (Curves *B* on Figs. 7 and 8). It will also be seen that, in order to obtain a given degree of "thermal reinforcement," a dose 2.5 times greater in the presence of air than under a vacuum is needed.

The role of oxygen present during irradiation is still more striking in the case of the irradiation of polyvinyl chloride. In fact, we found that this polymer[45] is degraded if irradiated in the presence of air while under a vacuum cross-linkage is achieved. This observation might account for the disagreement between the results obtained by Charlesby,[41] according to whom polyvinyl chloride is cross-linked by irradiation, and those of Lawton and his group,[42] who found that this polymer is degraded. None of these authors specified the experimental conditions of irradiation.

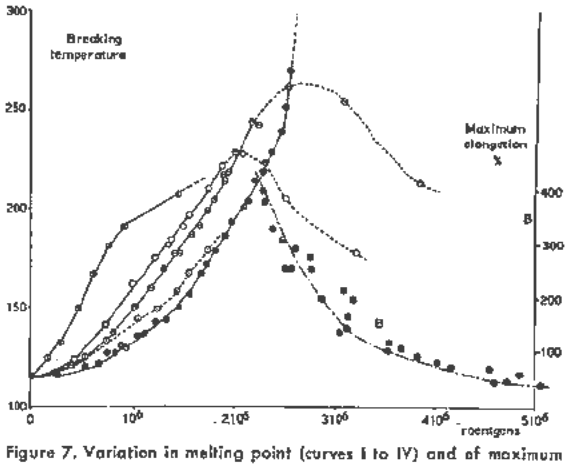

Figure 7. Variation in melting point (curves I to IV) and of maximum elongation of samples (curve B) as a function of the irradiation dose in the presence of air. Curve I, intensity 432 r/min; curve II, intensity 113 r/min; curve III, intensity 42.3 r/min; curve IV, intensity 7.3 r/min

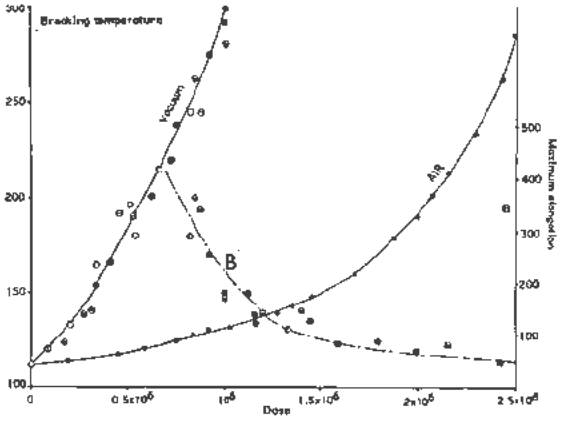

Figure 8. Variation in melting point (curve II) and maximum elongation of samples (curve B) as a function of the irradiation dose in the absence of air. (The dotted curve is a reproduction of curve I of the preceding figure)

The results already given indicate that, in order to carry out radiochemical cross-linking of polymers under optimum conditions, it is necessary to exclude oxygen during the irradiation. Without this precaution, cross-linking will be accompanied by oxidizing degradation of the polymer.[46]

Second Process for the Preparation of "Grafted" Polymers

A more detailed study of the elongation curves as a function of temperature[44] for polyethylene samples irradiated in the presence of air shows that they have acquired better thermal resistance for temperature lower than about 150°C, but that this increase in resistance ceases at higher temperatures. Nothing similar to this was observed with samples irradiated under a vacuum. The fact was interpreted[44] by the formation during irradiation of intermolecular peroxide bridges which break at temperatures higher than 150°C, the resulting fragments being free macro-radicals. This hypothesis was verified by the following experiment: if a sample of polyethylene irradiated in the presence of air be immersed in a monomer of a different constitution, for instance acrylonitrile, and if the whole be heated to a temperature sufficient to break the peroxide bonds, acrylonitrile polymerization will be observed, the polyacrylonitrile chains being chemically attached (grafted) to the macro-radicals of polyethylene. It has thus been possible to fix up to 30 times its weight

of acrylonitrile on a polyethylene film without any change in the geometric form of the polyethylene sample.

We thus have here a radiochemical "grafting" process[47] which is different from that described in paragraph 11. This method makes it possible to prepare "grafted" copolymers starting from finished or semi-finished objects which, in some cases, may present appreciable technical advantages.

CONCLUSIONS

The irradiation of solid polymers may lead, in some cases, to the cross-linking (vulcanization) of these polymers. This cross-linking requires a substantially smaller dose in the absence of air than in its presence.

In the presence of air, some of the bridges formed very likely are oxygen bridges, which break down at higher temperatures. The radicals so produced can initiate the polymerization of an added monomer and lead to the formation of grafted copolymers.

We have here two possible utilizations of ionizing radiation which even now lend themselves to industrial development.

REFERENCES

1. Eyring, H. and co-workers, 5ème Réunion annuelle de la Société de Chimie-Physique, Paris 1955.
2. Magee, J. L., J. Am. Chem. Soc., *73*: 3270 (1951).
3. Samuel, A. M. and Magee, J. L., J. Chem. Phys., *21*: 1080 (1953).
4. Jaffé, G., Ann. Phys. (4), *42*: 303 (1913).
5. Kramers, H. A., Physica, *18*: 655 (1952).
6. Magee, J. L., 5ème Réunion de Chimie-Physique, Paris 1955.
7. Petry, R. C. and Schuler, R. H., J. Am. Chem. Soc., *75*: 3716 (1953).
8. Magat, M., Colloque "Transformazioni radiochimiche," Roma 1953.
9. Schuler, R. H. and Hamil, W. H., J. Am. Chem. Soc., *4*: 6171 (1952).
10. Chapiro, A., C. R. 233,792 (1951).
11. Bawn, E. H. and Mellish, S. F., Trans. Far. Soc., *47*: 1216 (1951).
12. Bouby, L. and Chapiro, A., 5ème Réunion de Chimie-Physique, Paris 1955.
13. Chapiro, A. and co-workers, J. Chim. Phys., *50*: 482 (1953).
14. Russel, K. E. and Tobolsky, A. V., J. Am. Chem. Soc., *75*: 5052 (1953).
15. Chapiro, A. and co-workers, J. Chim. Phys., *50*: 468 (1953).
16. Chapiro, A., J. Chim. Phys., *51*: 165 (1954).
17. Chapiro, A. and co-workers, Rec. Trav. Chim. Netherlands, *68*: 1037 (1949).
18. Chapiro, A. and co-workers, 5ème Réunion de Chimie-Physique, Paris 1955.
19. Melville, M. W. and Valentine, L., Trans. Far. Soc., *46*: 210 (1950). Bamford, E. H. and Dewar, M., Proc. Far. Soc., *3*: 310 (1947). Matheson, M. S. and coll., J. Am. Chem. Soc., *73*: 1700 (1951). Valentine, L., Dis. Far. Soc., *12*: 131 (1952).
20. Manion, J. P. and Burton, M., J. Phys. Chem., *56*: 560 (1952).
21. Mackay, M. H. and Melville, M. W., Trans. Far. Soc., *45*: 323 (1949).
22. Matheson, M. S., Auer, E. E. and coll., J. Am. Chem. Soc., *71*: 497 (1949).
23. Chapiro, A., J. Chim. Phys., *47*: 747 and 764 (1950).
24. Prévot-Bernas, A. and coll., Disc. Far. Soc., *12*: 98 (1952).
25. Chapiro, A. and coll., Congrès intern. de chim. macromoléculaire, Milan-Turin 1954.
26. Magat, M., J. Polymer Sciences, *16*: 491 (1955).
27. Durup, J. and Magat, M. To be published.
28. Ballantine, R. and Manowitz, B., BNL., *27*: 141 (1951).
29. Mayo, F. R., Lewis, F. M. and Walling, C., Far. Soc. Disc., 2285 (1947).
30. Bensasson, R. Unpublished results.
31. Bamford, C. H. and Jenkins, A. S., Proc. Roy. Soc., A216, 515 (1953).
32. Thomas, W. M. and Pellon, J. J., J. Polym. Sc., *13*: 329 (1954).
33. Collinson, E. and Dainton, F. S., Far. Soc. Disc., *12*: 212 (1952).
34. Prévot-Bernas, A. and Sebban, J. To be published.
35. Landler, Y., Rev. gén. du Caoutchouc., *30*: 647 (1953).
36. Chapiro, A., Cousin, C., Landler, Y., Prévot-Bernas, A. and Magat, M., XIIème Congrès de I.U.P.A.C., New York (1951).
37. Landler, Y., Thesis, Paris (1952).
38. Chapiro, A. and coll., B. F. No. de dépôt 692,736 (1955).
39. Magat, M. and Reinisch, L. To be published.
40. Sievert, R. M., Acta Radiol Snppl. XIV (1932).
41. Charlesby, A., Proc. Roy. Soc., A.215,187 (1952). Plastics, *18*:142 (1953).
42. Lawton, E. J. and his group, Nature, *172*: 76 (1953).
43. For a complete bibliography regarding this matter see Ref. 44.
44. Chapiro, A., J. Chim. Phys., *52*: 246 (1955).
45. Chapiro, A., J. Chim. Phys. To be published.
46. Chapiro, A. and Magat, M., B. F. No. de dépôt, 676,716 (1954).
47. Chapiro, A., Magat, M. and Sebban, J., B. F. Provisional numbers 690,659 and 692,735 (1955).

Radiolytic Oxidation of Organic Compounds

By Nathalie Bach, USSR

The production of useful compounds by chemical reactions taking place under the action of radiations is one of the important branches of atomic energy utilization. In this respect the action of radiations on organic compounds is a particularly promising field.

The specificity of ionizing radiations action is manifested in the formation in an irradiated system of a large number of free radicals with excess of kinetic energy and of molecules excited to various levels at all temperatures, down to the very lowest. Charged particles (ions) may also play a certain part in the reactions but this part is usually much less important due to the shortness of their lives.

Molecular oxygen is a very efficient acceptor for most organic radicals. Reactions involving the formation of peroxide radicals possess the advantage that their final products are easily identified and can readily be quantitatively determined. A study of radiation chemical processes in organic systems in the presence of molecular oxygen allows us to ascertain the role of the primary radicals in the basic mechanism of these processes, and at the same time opens new ways of producing oxidation products of practical interest from chemically inert substances.

Molecular oxygen plays an important part in the radiolytic oxidation of organic compounds not only as such, but in aqueous solution as well. In the latter more complicated case the efficiency of the radiation energy absorbed may be substantially increased by the presence of inorganic components, particularly by ions of variable valency.

In the present report are discussed the results of experimental studies of the radiolytic oxidation of various systems, carried out in the Soviet Union. Attention is focused mainly on elucidation of the nature of the primary radiation chemical reactions, under conditions when the action of radiation on the oxidation products formed is still of minor importance.

The chemical individuality of the end products of radiation chemical processes depends primarily on the nature of the active particles formed under the action of the radiation. These primary uncharged particles may be divided into three groups:

(*a*) Free radicals resulting from the ionization of molecules and showing no tendency to combine into the initial molecule at the moment of their formation.

Original language: Russian.

(*b*) Free radicals, formed as a result of the dissociation of an excited molecule and showing a marked tendency to recombine into the initial molecule, particularly in the liquid state. Radicals of this type play a substantial part in radiation chemical processes only in the presence of acceptors which bind one of them, freeing the other for subsequent reactions.

(*c*) Excited molecules, which decompose into molecular products or react with other molecules without dissociating into radicals.

Free radicals may react with non-excited molecules of the substrate, initiating chains or may enter into non-chain reactions with each other. The non-chain mechanism is also characteristic of reactions between excited molecules which do not dissociate into radicals.

Experimental data show that the predomination of reactions of one type or another in chemical systems subjected to the action of radiation depends on the structure and properties of the irradiated compounds. The general regularities governing this relationship are one of the important problems of radiation chemistry.

Some information on the primary radicals of the first type can be had from mass-spectrometric data. In the great majority of cases these data are obtained with electron energies not exceeding 100 ev, which is much lower than the energy of the ionizing particles dealt with in radiation chemistry. It should, however, be taken into account that a considerable part of the ionization acts occurring under the action of high energy ionizing particles are due to secondary electrons with energies not over several hundred volts. The influence of the electron energy on mass-spectra has been studied by Tunitsky and co-workers[1] within a range of 20 to 1000 v. Experimenting on a number of halogen substituted hydrocarbons, they showed that as the energy of the electrons increases up to 1000 ev the amount of low-mass fragmentary ions, whose contribution to the spectrum is relatively small, decreases somewhat, thus causing a corresponding increase in the importance of the main ions. The change in the relative quota of the latter does not exceed a few per cent. It is thus permissible to use mass-spectrometric data for drawing conclusions regarding the nature of the primary ions formed in radiation chemical processes.

With their charge neutralized the radical ions become free radicals, which may retain the structure

of the initial ion if the conditions for energy dissipation are favourable. Mass-spectrometric data may be used also, as shown by Stevenson[2] to draw conclusions as to the structure of the free radicals formed simultaneously with ions when molecules dissociate under impact.

Data on possible reactions involving molecules excited to energy levels too low for ionization and on their dissociation into radicals may often be obtained from studies of photochemical processes.

The radiation chemical processes considered below include both reactions involving primary radicals and reactions with the participation of excited molecules.

THE ACTION OF IRRADIATION ON INDIVIDUAL ORGANIC COMPOUNDS IN THE PRESENCE OF MOLECULAR OXYGEN

There are almost no data in the literature on the action of irradiation on individual organic compounds in the presence of O_2. The only system studied in some detail is the system chloroform-oxygen.[3] In the studies reported here the objects selected were hydrocarbons of various structure: *n*-heptane, isooctane (2,2,4-trimethylpentane), cyclohexane, toluene, benzene, acetic acid and ethyl and benzyl alcohols.

Irradiation was carried out with 75 kv X-rays at a dose rate of ~1000 r per sec with an electron beam of 900 kv at a dose rate of 10^{17}–10^{18} ev/cm³ per sec and with γ-rays from Co^{60} at a dose rate of 30 r per sec. The dose rates were determined by ferrous ion dosimetry.

The experiments were carried out in glass cells of various types in an atmosphere of O_2, and in some cases N_2 and H_2, at different temperatures. Reaction products appeared both in the liquid and in the gaseous phase. The liquid was analyzed for peroxides, carbonyl compounds, acids and water. Based on differences in the kinetics of this oxidation and the reaction with titanium it was possible to determine three types of peroxides: R_1OOR_2, $ROOH$ and H_2O_2.[4] Quantitative determinations mainly characterized functional groups; in some cases individual compounds were identified. The gas phase was analysed in the studies of ethyl alcohol and acetic acid. The amounts of H_2, CO, CH_4, and CO_2 liberated were determined, as well as O_2 absorbed.

In general it may be stated that under the action of ionizing radiations, both peroxides and the end products of oxidation including carbonyl compounds, acids, phenol (in the case of benzene), etc. are formed in all systems. The products are for the most part similar to those produced in photochemical and auto-oxidation reactions, but the differences in the relative yields and, in some cases, in the nature of the compounds formed are specific for the action of ionizing radiation.

In this connection the peroxide compounds are the most characteristic. A typical picture of the formation of peroxides is shown in Fig. 1 for *n*-heptane.

It can be seen that di-substituted peroxides of the type $ROOR$ are formed in largest amounts; concentration increase shows no tendency to diminish within the range of doses studied. In Table I are given the peroxide yields for all the hydrocarbons studied calculated from the initial slopes of the curves.

Table I. Radiation-Chemical Yields (molecules per 100 ev)

	n-heptane	*isooctane*	*cyclo-hexane*	*toluene*	*benzene*
R_1OOR_2	2.2	1.3	0.2	1.2	0.2–0.3
$ROOH$	1.2	0.7	1	0.4	0
H_2O_2	0.3	0.3	0	0.2	0.2–0.3
Total peroxides	3.7	2.3	1.2	1.8	0.5

The predominant type of peroxide in all the hydrocarbons with the exception of cyclohexane is R_1OOR_2. This is an essential difference between the radiation chemical process and photochemical or auto-oxidation reactions. In the latter cases only hydroperoxides are formed;[5] whereas peroxides of the R_1OOR_2 type can usually be obtained only synthetically from hydrogen peroxide. Another characteristic feature is the independence of the yield on temperature and intensity of irradiation in the case of the radiation chemical formation of peroxides.

When hydrocarbons are irradiated in the presence of oxygen, all three classes of peroxides are formed as a rule. The same is true of acetic acid[6] but not of ethyl alcohol.[7] In the latter case peroxides of the R_1OOR_2 type are absent, and the only peroxides found are hydrogen peroxide or oxyethylhydroperoxide.

The formation of carbonyl compounds and acids in saturated hydrocarbons may be illustrated by Fig. 2, which shows the data obtained for *n*-heptane at 0°, 25°, and 60° under the action of X-rays with dose rates from 6×10^{15} to 6×10^{17} ev/cm³ per sec.

The amount of acids formed is much smaller than in the case of carbonyl compounds. During the ini-

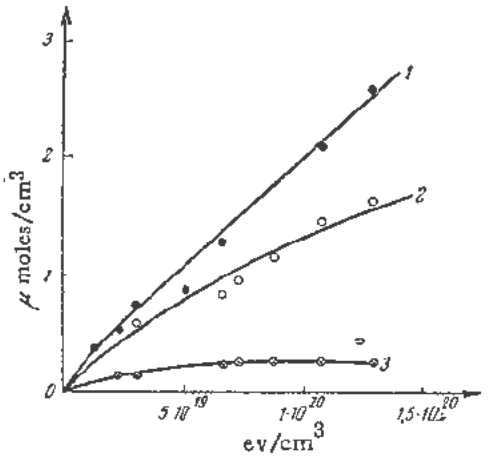

Figure 1. Peroxide compounds in n-heptane irradiated under saturation with oxygen: (1) R_1OOR_2; (2) $ROOH$; (3) H_2O_2

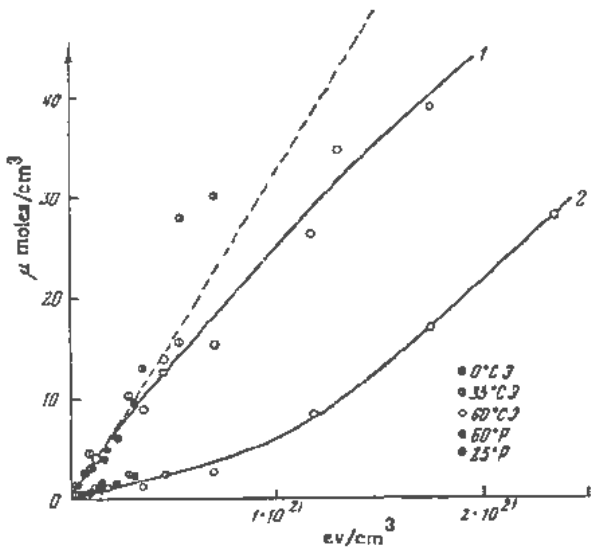

Figure 2. Formation of carbonyl compounds (1) and acids (2) in n-heptane irradiated under saturation with oxygen. Electron flux: 3×10^{16}–6×10^{17} ev/cm³ per sec. X-rays: 6×10^{16}–10^{18} ev/cm³ per sec

tial stages of irradiation the yield is constant and depends neither on the temperature nor on the intensity of irradiation. It may be concluded from Figs. 1 and 2 that the formation of peroxides, carbonyl compounds and acids commences simultaneously from the beginning of irradiation. The slope of the curves changes only after the absorption of a certain amount of energy. In the case of peroxides the yield decreases due to decomposition reactions; with acids at 60°, on the contrary, additional amounts begin to form apparently as a result of secondary reactions of aldehyde oxidation.

The total yield of similar oxygen-containing products formed under the action of irradiations in hydrocarbons of various structures is a measure of their susceptibility to radiolytic oxidation. Characteristic yield values are given in Table II.

Table II. Total Yield of Oxidation Products (molecules per 100 ev)

	n-heptane	*isooctane*	*cyclohexane*	*benzene*
Peroxides	3.7	2.3	1.2	0.5
Carbonyl compounds	2.0	1.2	0.6	0.45
Acids	0.4	0.6	0.2	0
Total	6.1	4.1	2.0	~1.0

These data show that the difference in behaviour between saturated hydrocarbons and benzene is much less in the case of oxidation reactions than in decomposition processes leading to gas evolution. The same is true for polymerization reactions.

The simultaneous appearance of the various reaction products from the beginning of irradiation may be due to their being formed independently or to their being derived from the same labile primary compound and transformed in different ways. In the case of the oxidation reaction this primary labile product is the peroxide radical $R\dot{O}_2$. Owing to the relative inertness of hydrocarbons, $R\dot{O}_2$ reacts predominantly with other radicals, forming di-substituted peroxides as follows:

$$R_1\dot{O}_2 + \dot{R}_2 \rightarrow R_1OOR_2 \qquad (1)$$

and not with the hydrocarbon molecules according to the reaction

$$R_1\dot{O}_2 + RH \rightarrow R_1OOH + \dot{R} \qquad (2)$$

which would lead to the development of chains.

A reaction alternative to (1) involving the radical $R\dot{O}_2$ is its isomerization and subsequent decomposition according to the well known schemes of carbonyl compounds and alcohol formation in the case of alkyl and alkene radicals C_nH_{2n+1} and C_nH_{2n-1}. With the alkylidene biradicals $R\ddot{C}H$ the addition of molecular oxygen may result in the formation of acids according to the scheme:

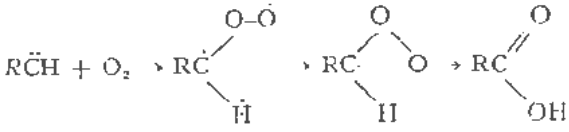

(3)

The isomerization of the peroxide

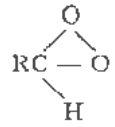

into the acid is promoted by an increase in temperature.[8] In this case the acid is formed independently of the aldehyde.

A reaction between oxygen and excited molecules, resulting in the direct formation of a hydroperoxide by "introduction" of oxygen without detachment of hydrogen atoms, is also possible. This is apparently how the hydroperoxide is formed in the cases cited above, since the low yield values and the independence on the temperature and intensity make the chain mechanism corresponding to scheme (2) improbable. In the mechanism suggested above the number of radicals necessary to obtain the observed yields must be supplied by the ionization acts. An estimate on the basis of the number of ion pairs formed per 100 ev known for the vapour state, and of the per cent of radical ions as derived from mass-spectrometric data shows that in the case of hydrocarbons the number of primary radicals formed is high enough for the reactions considered to take place with the yields observed.

The behaviour of acetic acid in this connection is similar, its molecule being stable towards radiolytic oxidation.[6] Table III shows the initial yields of the products in the presence of oxygen compared to those obtained without oxygen.

Table III

Reaction products	Yield, molecules per 100 ev: In the presence of O_2	Yield, molecules per 100 ev: Without O_2
Hydrogen peroxide and acetyl hydroperoxide	0.36	0
R_1OOR_2 (acetyl peroxide)	0.78	0
ROOH (methyl hydroperoxide)	1.1	0
Formaldehyde	1.1	0
Acetone	0.45	0.45
Total gases liberated	2.4	5.4
Carbon dioxide	2.4	2.4

It is a characteristic feature that if the acetic acid is saturated with oxygen no methane, hydrogen or carbon monoxide form during the initial phase of irradiation, though these gases constitute more than half of the total gases liberated when oxygen is absent. This points to the conclusion that the radicals which lead to their formation react very efficiently with oxygen to form peroxide radicals. A parallel analysis of the liquid and gaseous phases shows that in the beginning, when the peroxides are accumulating, the formation of CO_2 is balanced by the absorption of oxygen, so that no liberation of gas is observed. At a definite dose the peroxides begin to decompose, liberating CH_4 and additional CO_2 and upon further irradiation a steady state concentration of peroxides is established. This explains the induction periods in the evolution of gases observed on irradiation of different organic systems in the presence of oxygen.

The picture presented by alcohols when subjected to oxidizing radiolysis is substantially different from that of hydrocarbons and acetic acid. As already mentioned, in the case of ethyl alcohol[7] the total amount of products formed is considerably higher. Data on the yields obtained under various conditions are given in Table IV. If the concentration of oxygen is kept constant the yields remain constant throughout the range of doses studied up to $\sim 1.5 \times 10^{21}$ ev/cm^3.

As can be seen from the table, irradiation of oxygen-free alcohol also leads to the formation of a considerable amount of radiolysis products, including aldehydes, water, hydrogen. In the presence of oxygen the yields of all these products increase and new products—acids and peroxides—are formed.

The considerable increase in the amount of hydrogen liberated is particularly striking.

In this case the total yield of products can no longer be obtained by the free radicals formed due to ionization, and the participation of excited molecules in the reactions cannot be disregarded.

The increase in the yield of hydrogen from 6 to 12 molecules per 100 ev can be explained most simply by assuming that hydrogen is formed by two different mechanisms: as a result of molecular dehydrogenation of excited molecules in the absence of oxygen with a yield $G = 6$, and secondly in the presence of oxygen as a result of the reaction between H atoms and alcohol molecules, also with a yield $G = 6$. The liberation of molecular hydrogen in the radiolysis of air-free alcohol is accompanied by the formation of aldehyde, but since the yield of the latter is much lower than that of hydrogen, this reaction is evidently not the only one leading to the molecular dehydrogenation of alcohol. Considering that the behaviour of excited molecules must be similar in radiolysis and photolysis it may be supposed that, as was shown by Farkas and Hirschberg for the photochemical decomposition of ethyl alcohol in aqueous solutions,[8] Ketene is formed beside the aldehyde according to the reactions:

$$CH_3CH_2OH \xrightarrow{h\nu} CH_3CHO + H_2 \qquad (4)$$

and

$$CH_3CH_2OH \xrightarrow{h\nu} CH_2 = CO + 2H_2 \qquad (5)$$

Assuming, in accordance with the energy of the quanta in the photochemical experiments, that the necessary excitation energy is 6 ev, we find that to an absorption of 100 ev, with the simultaneous formation of ~4 ion pairs requiring ~50 ev for the work of ionization and dissociation, about 8 molecules of alcohol can become sufficiently excited for reactions (4) and (5) to take place.

The excited molecules may also decompose according to the scheme:

$$CH_3CH_2OH \longrightarrow (CH_3CH_2OH)^* \rightarrow CH_3\dot{C}HOH + H \qquad (6)$$

but in the liquid phase in the absence of acceptors the radicals easily recombine. In the presence of oxygen a peroxide radical is formed and an atom of hydrogen is liberated, allowing the following reactions to develop:

$$CH_3\dot{C}HOH + O_2 \rightarrow CH_3\underset{\displaystyle OH}{\overset{\displaystyle H}{\underset{|}{\overset{|}{C}}}}\text{-O-O-} \qquad (7)$$

$$H + CH_3CH_2OH \rightarrow CH_3\dot{C}HOH + H_2 \qquad (8)$$

$$CH_3\underset{\displaystyle OH}{\overset{\displaystyle H}{\underset{|}{\overset{|}{C}}}}\text{-O-O-} + CH_3CH_2OH \rightarrow \qquad (9)$$

$$CH_3\underset{\displaystyle OH}{\overset{\displaystyle H}{\underset{|}{\overset{|}{C}}}}\text{-OOH} + CH_3\dot{C}HOH$$

Reactions (8) and (9) in which the radicals form without the action of radiation lead to the development of chains and result in an increase in the yield.

Oxyethylhydroperoxide $CH_3\underset{\displaystyle OH}{\overset{\displaystyle H}{\underset{|}{\overset{|}{C}}}}\text{-OOH}$

can decompose into acetaldehyde and hydrogen peroxide, or into acetic acid and water. This mode of aldehyde formation is confirmed by the equality of the initial yields of acetaldehyde and peroxide formed in the presence of oxygen. The latter value is found by subtracting the yield of aldehyde in oxygen-free alcohol $G = 1$ from the total yield $G = 3.6$, and making use of polarographic data showing that the aldehyde appearing under these conditions is a mixture of 90 per cent acetaldehyde and 10 per cent formaldehyde. The fact that two different mechanisms of aldehyde formation exist, with and without the participation of oxygen, is confirmed by the different behaviour of the corresponding systems when the temperature is varied. In the presence of oxygen the reaction is temperature dependent, while no such dependence is observed in the experiments without oxygen, as can be seen from Figs. 3 and 4.

Table IV

Dose rate ev/cm³ per sec / Products	Molecules per 100 ev: saturated with O_2		without O_2	
	2×10^{18}	10^{17}	2.9×10^{17}	2.9×10^{17}
Peroxides	6.0	3.6	2.3	0
Aldehyde	7.5	4.2	3.6	1.0
Acid	3.6	4.8	7.2	0
Water	4.8	–	7.2	2.1
H_2	–	12	–	6.0
CO	–	1.8	–	0.3
CH_4	–	0.9	–	0.2
CO_2	–	0.1	–	0.03
O_2 absorbed	–	11.3	–	0

The yield of water increases with the yield of acid, but since from stoichiometrical considerations such a relationship should hold for any reaction leading to the transformation of alcohol into acid with the participation of molecular oxygen, this fact cannot be regarded as confirming a definite mechanism. In the experiments with oxygen the yields of both aldehyde and acid depend not only on the temperature, but also on the intensity of irradiation. This may be considered as due to the participation of chain reactions in some phases of the process.

The available experimental information is as yet insufficient to choose between the possible reaction mechanisms. In particular it is necessary to obtain a satisfactory balance between the oxygen-containing reaction products and the oxygen absorbed, and to identify all the final products not functionally but individually.

The much larger part played by the alcohol molecules in radiolysis and radiolytic oxidation, as compared with that of hydrocarbon and acetic acid molecules, is doubtless connected with the increase in the reactivity of the hydrogen atoms in the $-CH_2OH$ group in comparison with the methyl group. A further increase in the mobility of this hydrogen resulting in a corresponding growth in the yields of the oxidation reactions may be expected if the methyl group in ethyl alcohol is substituted by an unsaturated group.

Proskurnin and Barelko[10] have shown that if a phenyl group is present in the alcohol (irradiation of benzyl alcohol) a very large yield of oxidation products is obtained, leaving no doubt as to the chain mechanism of the reaction.

Combining iodometric and polarographic methods they showed that under the action of radiation on benzyl alcohol, through which oxygen is continuously passed, peroxide compounds were formed consisting in equal parts of hydrogen peroxide and unhydrolyzed organic peroxides. With the intensity used (Co^{60} γ rays, ~22 r per sec) the initial yield under the action of the irradiation was ~50 molecules per 100 ev.

From the point of view stated above this means that the peroxide radical formed in the benzyl alcohol according tn the scheme:

$$C_6H_5\cdot CH_2OH \rightarrow (C_6H_5CH_2OH)^* \rightarrow C_6H_5\dot{C}HOH + H \qquad (10)$$

$$C_6H_5\underset{\underset{OH}{|}}{\overset{\overset{H}{|}}{C}}\cdot + O_2 \rightarrow C_6H_5\underset{\underset{OH}{|}}{\overset{\overset{H}{|}}{C}}\text{-O-}\dot{O} \qquad (11)$$

reacts readily with an unexcited alcohol molecule as follows:

$$C_6H_5\underset{\underset{OH}{|}}{\overset{\overset{H}{|}}{C}}\text{-O-O-} + C_6H_5CH_2OH \rightarrow C_6H_5\underset{\underset{OH}{|}}{\overset{\overset{H}{|}}{C}}\text{-OOH} + C_6H_5\underset{\underset{OH}{|}}{\overset{\overset{H}{|}}{C}}\cdot \qquad (12)$$

promoting the development of chains.

Thus, in the case of the radiolytic oxidation of benzyl alcohol the presence of a benzene ring not only fails to decrease the yield, in comparison with aliphatic compounds, as is the case with hydrocarbons, but actually increases it pronouncedly.

As is well known from the studies of a number of authors,[11] the stability of aromatic compounds under radiolysis is very high and is interpreted as being due to a distribution of the absorbed energy among the conjugate bonds followed by deactivation. There are no grounds to assume that this effect is absent in benzyl alcohol. It probably causes a low yield of primary radicals, but the essential point in the system considered is the fact that the reaction proceeds at the expense of chain development and does not require a large number of initiating radicals. In this case it is precisely the presence of the phenyl radical that ensures a favourable course for the non-radiation phase of the process.

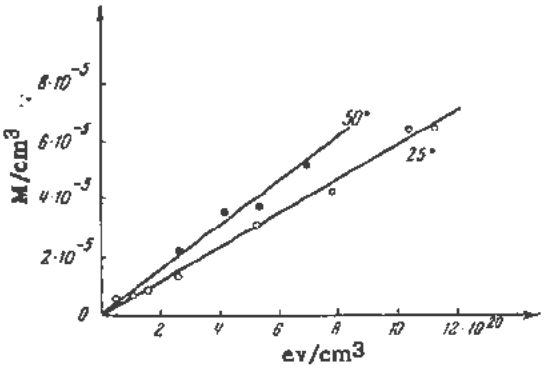

Figure 3. Formation of aldehyde upon irradiation of ethyl alcohol in the presence of oxygen at 25°C and 50°C

The examples cited show that in reactions of radiolytic oxidation, even more than in pure radiolysis, the individual properties of the irradiated molecules, depending on their structure and on the presence of definite functional groups, play a decisive part in determining the trend of the various processes and the yields.

THE ACTION OF IRRADIATION ON HIGH POLYMERS IN THE PRESENCE OF OXYGEN

The changes which take place in the mechanical properties of high polymers under the action of irradiation were explained in a number of papers published in recent years[12] as being due to ruptures of the C-H bonds and a subsequent recombination of the free radicals to form new bonds between the molecules cross-linking or to rupture of the C-C bonds (destruction). Charlesby found that the changes observed when polyethylene is irradiated in the presence of air are connected with oxidation reactions which take place at the surface.[13]

It is of substantial interest to establish the functional nature of these products, since it is necessary to ascertain the character of the new bonds that form in order to determine their role in the changes that take place in the physical properties of the polymer.

Karpov and Slovokhotova[14] studied the red and ultraviolet spectra of thin films of polyethylene subjected to irradiation by fast electrons under vacuum and in air. Definite changes are observed in the spectra, which increase regularly with the dose of energy absorbed. Analysis of the absorption bands has shown that, besides the appearance of double bonds and branched chains and the transition from the crystalline to the amorphous state, irradiation in the presence of air leads to the formation of carbonyl, carboxyl and ether groups. The latter account for the increase in the rigidity of the polymer by cross-linking it with "oxygen bridges". The main mechanism of the formation of these oxidation products is the same as in the case of low molecular hydrocarbons, i.e., it is based on the addition of molecular oxygen to the free radicals formed under the action of the irradiation and the subsequent transformations of the peroxide radicals. The particular course of these reactions in polymers is connected with the limited mobility of the macromolecules.

RADIOLYTIC OXIDATION OF ORGANIC COMPOUNDS IN AQUEOUS SOLUTIONS

In the absence of oxygen, organic compounds in aqueous solution are oxidized by irradiation at the expense of the OH radicals formed in the water together with H atoms in the processes of ionization and excitation. It is also of interest to use molecular oxygen for oxidation by saturating the solution during irradiation.

The oxidation of inorganic compounds under the action of irradiation is often markedly increased by the presence of oxygen. It is generally assumed that this effect is due to the participation of HO_2 radicals in the oxidation processes, these radicals forming as a result of the addition of H atoms according to the reaction:

$$H + O_2 \rightarrow HO_2 \qquad (13)$$

The existence of HO_2 radicals in the gaseous phase has been proved experimentally by mass-spectrometric[15] and infra-red spectral[16] methods. These are sufficient grounds to postulate that these radicals exist also in the liquid phase.

HO_2 is a good oxidant for ions of variable valency, particularly for ferrous ions owing to the ease of electron transfer following the well known scheme:

$$Fe^{2+} + HO_2 \rightarrow Fe^{3+} + HO_2^- \qquad (14)$$

and

$$HO_2^- + H^+ \rightarrow H_2O_2 \qquad (15)$$

$$Fe^{2+} + H_2O_2 \rightarrow Fe^{3+} + OH^- + OH \qquad (16)$$

according to which the relatively weak oxidant HO_2, formed at the expense of atomic hydrogen, is transformed by the ferrous ions into a stronger oxidant OH.

Weiss and Stein have shown[17] that the irradiation of oxygen-free aqueous solutions of benzene results in the formation of phenol, diphenyl, terphenyl and hydrogen. The occurrence of these products is explained by the formation of phenyl radicals as a result

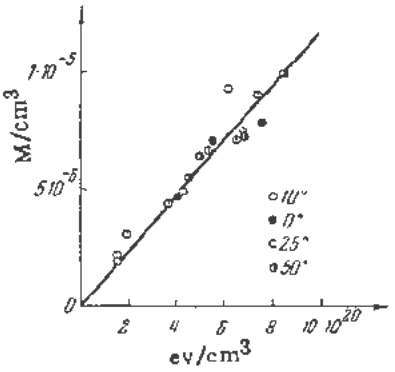

Figure 4. Formation of aldehyde upon irradiation of oxygen-free ethyl alcohol at various temperatures

of the reaction between benzene and the OH radicals and the subsequent intercombination of C_6H_5 radicals with OH. Thus, the consumption of OH radicals corresponds to the total yield of phenol and di- (ter-) phenyl, OH radicals being required for each molecule of the product. Stein and Weiss demonstrated that in the presence of oxygen the yield of phenol increases to twice its usual value. However, at the same time the yield of diphenyl falls, and the total yield remains almost unchanged and equal to $G = 2$. Thus, although the presence of oxygen results in a certain redistribution of OH radicals between the phenyl radicals and benzene after a mechanism which is not clear as yet, the total quantity of primary water radiolysis products engaged in the reaction does not increase. The yield of the phenyl products, approximating 2 molecules per 100 ev, corresponds to the consumption of about 4 OH radicals, i.e., all the radicals formed as a result of the ionization processes in water on absorption of 100 ev. As to the HO radical, these data show that it does not take part in the oxidation at all.

Proskurnin and Barelko attempted to increase the utilization of the primary water radiolysis products in oxidation reactions by increasing the oxidizing power of the HO_2 radicals towards organic, in particular aromatic compounds.[13] They showed that if ferrous ions are introduced into aqueous benzene solutions the yield of phenol in the presence of oxygen increases by about 2.7 times, while in the absence of oxygen ferrous ions do not influence the reaction at all.

This effect may be explained[14–16] by the reactions between HO_2 and Fe^{2+}. In this case each H atom gives rise to one OH radical and the phenol yield should increase twofold. Actually the yield increase is much larger. In this connection the authors consider the possibility of the activation of HO_2 by Fe^{2+} ions according to the reaction:

$$HO_2 + C_6H_6 + Fe^{2+} + H^+ \rightarrow C_6H_5OH + Fe^{3+} + H_2O \qquad (17)$$

which results in the formation of 1 molecule of C_6H_5OH for each hydrogen atom, i.e., in a threefold increase of the yield compared to that of the reaction in the absence of ferrous ions.

The efficiency of the ferrous ions depends on their concentration between 10^{-4} and 10^{-3} M and reaches a maximum value at 10^{-3} M. The phenol yield is also increased by ferric ions, though not so effectively.

The radiolytic oxidation of organic compounds in aqueous solutions can thus be sensitized by cations of variable valency, which are themselves oxidized during the reaction. This method is of general interest and can be applied to numerous systems.

When the molecule contains a benzene ring and a side chain it is important to know whether oxidation displays any particular trend. This problem was studied by Proskurnin and Barelko for aqueous solutions of benzyl alcohol.[10] They showed that the irradiation of 5×10^{-4} to 5×10^{-2} M solutions, through which a continuous stream of oxygen is passed gives rise to hydrogen peroxide, benzyldehyde and phenol, the yields being 3, 1.6 and 1.2 molecules per 100 ev respectively. As can be seen, the yields of oxidation reaction involving the benzene ring and the side chain are close in value. Contrary to the radiolytic oxidation of pure benzyl alcohol, large yields of peroxide corresponding to a chain mechanism are not observed in this case. The simultaneous appearance of hydrogen peroxide, which was identified polarographically, and benzaldehyde, may be explained by the hydrolytic decomposition of initially formed oxyhydroperoxide according to a scheme similar to that for ethyl alcohol:

$$C_6H_5CH_2OH + OH \rightarrow C_6H_5\dot{C}HOH + H_2O \qquad (18)$$

$$C_6H_5\dot{C}HOH + O_2 \rightarrow C_6H_5\underset{\displaystyle OH}{\overset{\displaystyle H}{\overset{|}{\underset{|}{C}}}}\text{-O-O}\cdot \qquad (19)$$

$$C_6H_5\underset{\displaystyle OH}{\overset{\displaystyle H}{\overset{|}{\underset{|}{C}}}}\text{-O-OH} + C_6H_5CH_2OH \rightarrow C_6H_5\underset{\displaystyle OH}{\overset{\displaystyle H}{\overset{|}{\underset{|}{C}}}}\text{-OOH} + C_6H_5\dot{C}HOH \qquad (20)$$

$$C_6H_5\underset{\displaystyle OH}{\overset{\displaystyle H}{\overset{|}{\underset{|}{C}}}}\text{-OOH} + H_2O \rightarrow C_6H_5\underset{\displaystyle OH}{\overset{\displaystyle H}{\overset{|}{\underset{|}{C}}}}\text{-OH} + H_2O_2 \qquad (21)$$

$$C_6H_5\underset{\displaystyle OH}{\overset{\displaystyle H}{\overset{|}{\underset{|}{C}}}}\text{-OH} \rightarrow C_6H_5\overset{\displaystyle H}{\overset{|}{C}}{=}O + H_2O \qquad (22)$$

The OH radical reacts with the benzene ring with an almost equal probability, oxidizing it to phenol according to the mechanism described above. Oxidation of both ring and side chain in the same molecule was not observed.

The particular behaviour of benzene derivatives observed in the radiolysis of pure substances and manifested in a stabilization of the molecules owing to redistribution and dissipation of the absorbed energy, does not appear in dilute aqueous solutions, since the energy is absorbed by the water and not by the solute. The reactions develop in this case mainly as a result of interaction of the solute with the radicals H and OH, and only to a minor extent as a result of the transmission of excitation energy to the organic molecule.

The development of the application of reactions of radiolytical oxidation of organic compounds in aqueous solution is connected with the utilization, not only of all the free radicals in H and OH appearing in the ionization disintegration of H_2O, i.e., ~4 pairs of H+OH per 100 ev, but of the molecule excitation energy as well.

Proskurnin and collaborators demonstrated that the radiation energy is very efficiently utilized when solutions of potassium nitrate containing glucose are irradiated.[19] The nitrate is reduced to nitrite at the expense of atomic hydrogen, and at the same time the glucose is oxidized at the expense of the OH radicals. It was found that for every 100 ev of absorbed energy 12–13 molecules of water were involved in the reaction. The use of conjugate oxidation-reduction reactions for the production of definite products in aqueous solutions under the action of radiations is one of the different methods of radiolytic synthesis.

REACTIONS IN MIXTURES OF ORGANIC COMPOUNDS UNDER THE ACTION OF RADIATION

Methods of synthesis under the action of radiation may not only be used to obtain oxidation products. Irradiating mixtures of organic compounds may lead to the formation of new compounds, which often represent derivatives of one of the components formed by the introduction of a radical detached from another of the constituents. Thus, Zimin and co-workers showed[20] that aniline is formed if a mixture of ammonia and benzene is irradiated under a pressure of 10 atm. They studied the dependence of yield on the composition of the mixture and found that the results are best at an equimolecular ratio of the components. The aniline yield, which under such conditions equals about 0.4 molecules per 100 ev, increases in the presence of insignificant amounts of oxygen, corresponding to the introduction of ~0.1% of air into the system, to ~2 molecules per 100 ev. In this case the oxygen apparently plays the part of a stabilizing acceptor as is the case in the oxidation reactions discussed above. Liberation of radicals promotes the synthesis.

Similarly, irradiation of carbon tetrachloride and benzene mixtures results in the formation of benzene trichloride according to the reaction:

$$CCl_4 + C_6H_6 \rightarrow C_6H_5CCl_3 + HCl \qquad (23)$$

Irradiation of a two-component mixture may give rise to radicals due to the dissociation of the two kinds of molecules as a result of both ionization and excitation. Nikitina and Bagdasaryan showed[21] that a satisfactory quantitative treatment of the effects observed under irradiation of mixtures cannot be carried out if only the radiolytic products formed as a result of direct absorption of energy by each of the components are considered separately. Energy transfer from the excited molecules of one of the components to molecules of the other must also be taken into account.

The opportunities for intercombination of radicals and for the participation of excited molecules in the reactions are much larger in mixtures than in one-component systems. The available experimental data on the formation of aniline and benzene trichloride are, however, as yet insufficient to permit consideration of reaction mechanisms in some detail.

The examples given in this report of the production, under the action of radiation, of new compounds in organic systems as a result mainly of oxidation, but also of direct substitution, are demonstrative of an interesting field of the utilization of the energy of radiation for chemical purposes. The results obtained allow us to expect that a proper selection of objects and conditions should lead to chemical processes under the action of ionizing radiation, which may be difficult to realize with other agents usually employed in overcoming the chemical inertness of systems.

REFERENCES

1. Tonitsky, N. N., Kupriyanov, S. E., Tikhomirov, M. V. (Collection of Papers on Radiation Chemistry), USSR Academy of Sciences, Publ. H. (in press).
2. Stevenson, D. P., Trans. Far. Soc., *49*, 867 (1953).
3. Schulte, J. W., Suttle, J. F., Wilhelm, R., J. Am. Chem. Soc., *75*, 2222, (1953).
4. Bach, N. A., Collection of Papers on Radiation Chemistry . . . see ref. 1; Bach, N. A. and Popov, N. I., *ibid* . . . see ref. 1.
5. Ivanov, K. I., Intermediate Products and Intermediate Reactions in the Auto-Oxidation of Hydrocarbons, M–L., (1949) (in Russian).
6. Bach, N. A., Sarayeva, V. V. . . . see ref. 1.
7. Bach, N. A., Sorokin, Y. I. . . . see ref. 1.
8. Rieche, A., Meister, Ber. deutsch. Chem. Ges., *64*, 2335 (1931).
9. Farkas, L., Hirschberg, J., J. Am. Chem. Soc., *54*, 2450 (1937).
10. Proskurnin, M. A. and Barelko, E. V. . . . see ref. 1.
11. Burton, M., Gordon, S., Henz, R., Journ. Chimie phys., *48*, 190 (1951).
12. Charlesby, A., Proc. Roy. Soc. *A*, *215*, 187 (1952); Lawton, E. J., Bueche, A. M., Balwitt, J. S., Nature *172*, 76 (1953).
13. Charlesby, A., Nature *171*, 167 (1953).
14. Karpov, V. L., Slovokhotova . . . see ref. 1.
15. Foner, S. N., Hudson, R. L., J. Chem. Phys., *21*, 1608 (1953).
16. Giguere, P. A., J. Chem. Phys., *22*, 2085 (1954).
17. Stein, G., Weiss, J., J. Chem. Soc. Lon., 3245 (1949).
18. Proskurnia, B. A., Barelko, E. V. . . . see ref. 1.
19. Orekhov, V. V., Chernova, A. I., Proskurnin, B. A., . . . see ref. 1.
20. Zimin, A. V., Churmantayev, S. V. and Verina, A. A. . . . see ref. 1.
21. Nikitina, G. S., Bagdasaryan, K. S. . . . see ref. 1.

Organics as Reactor Moderator-Coolants: Some Aspects of Their Thermal and Radiation Stabilities

By R. O. Bolt and J. G. Carroll,* USA

The idea of cooling a nuclear reactor with a hydrocarbon has great appeal. An important advantage is that these compounds generally are not corrosive to construction metals. Hydrocarbons also exhibit low residual radioactivity from neutron capture, thereby permitting a minimum of coolant shielding external to the reactor. Moreover, hydrocarbon species of interest for the coolant use have low vapor pressures at useful temperatures, which would allow a reduction in the size (and cost) of reactor pressure vessels. The aforementioned features have resulted in the serious consideration of organics for reactor moderator-coolants.

Broad areas needed further definition before the attractive aspects of organic compounds for the reactor use could possibly be realized. Thus, a search for the best organic structures to withstand maximum temperatures and radiation dosages was rendered necessary.

Information was needed on the effects of these irradiation variables on radiation damage to such materials and on their rates of decomposition under selected conditions. Data on the identity of products of irradiation were desired. Also of primary concern was the relation of deposition on heat transfer surfaces to coolant composition and conditions of operation.

These problems were studied in strictly thermal and in irradiation tests under various conditions. The majority of the experimental work was with capsules or small cells in which selected materials were exposed and subsequently analyzed to determine changes in physical properties and to establish the nature of the products formed. In a study of deposition characteristics, data were also obtained from circulating fluid loops exposed to high temperatures both alone and in a reactor.

The information obtained in the experimental work is discussed in sections to follow under *Thermal Stability* and under *Radiation Stability*.

The presentation of the data concludes with a treatment of the *Significance of the Results in Reactor Design*.

* California Research Corporation, Richmond, California. Including work done by: W. K. Anderson, S. Greenberg, L. W. Fromm, Argonne National Laboratory; R. O. Bolt, J. G. Carroll, B. J. Fontana, J. R. Wright, California Research Corporation; E. L. Colichman, R. F. Fish, R. H. J. Gercke, North American Aviation, Inc.

THERMAL STABILITY

Introduction

From purely thermodynamic considerations, all hydrocarbons are unstable at high temperatures with respect to decomposition into their component elements. On this basis also, increased instability with increasing molecular weight is predicted.[1] Probably more significant is the fact that the latter is to be expected on the grounds of statistical mechanics.[2] Actually, organic materials do not tend to decompose into their elements on pyrolysis. Instead, they stop at an intermediate point where the solid product is a high condensed aromatic.[3] These observations suggest that the problem of stability at elevated temperatures is basically a kinetic one. There would appear to be some hope, then, for finding an ideal structure of maximum stability to thermal attack.

The present work on the thermal stability of organic compounds was undertaken in order to establish: (1) the best types of chemical structures and organic combinations for subsequent irradiation studies; (2) the upper temperature limits beyond which the most promising organics could not be used for reasonable periods of time; and (3) the degree of pyrolytic breakdown of the best organic compounds and their tendencies to deposit decomposition products on heat transfer surfaces. Aromatic hydrocarbons were favored in the work because it has long been known that this class of organics is most stable to high energy radiation.[4] Some data are available on the thermal cracking of aromatic hydrocarbons,[5,6] but the conditions given are too varied to allow intercomparisons of stabilities or of applications to proposed enviroaments. Initial studies of the temperature effect in the new research were made on biphenyl and naphthalene. This approach was followed because the available thermodynamic information already cited led to the conclusion that the simplest structures probably would be the most stable.

Approach

In the present pyrolysis work, samples were exposed in containers from which air had been removed. This allowed the study of the role of temperature without oxidation effects. The latter were eliminated because of their well known unfavorable influence on the decomposition of organics. The main cri-

terion of thermal stability was gas evolution. The gaseous products of pyrolysis were recovered and analyzed by mass spectrometric methods. Results are reported as ml of gas per gram of organic charged. The data are also presented, for theoretical use, as moles of gas (hydrogen and C_1 to C_5 hydrocarbons) per mole of original material. Experience has shown that, as the value of this latter index approaches unity, extensive damage to the organic is indicated.

A second criterion used in the capsule tests was residue formation. This material was the relatively nonfusible or nonvolatile fraction of the pyrolysis mixture. In most cases, this was insoluble in the mixture and was recovered by a simple manual method. In other cases, the residue was soluble and was recovered through the use of single-stage, high-vacuum (1 micron pressure), "molecular" distillations. The residue values are regarded as a less satisfactory index of stability than gas evolution. However, they may be of more practical interest in evaluations for reactor coolant use.

The tendency of organics to deposit carbonaceous matter on heated surfaces was investigated with a fluid circulating loop. The hot organic was pumped in a simple closed hydraulic circuit past an element maintained at a desired surface temperature. The element was examined for deposition at the end of a test. Less significant information on this subject was derived from casual observations in the capsule tests.

The data presented in the following section typify some 400 pyrolytic tests on about 40 different aromatic hydrocarbons. Most of the materials studied were of high quality commercial grade and were used without further purification. Others were synthesized and purified by crystallization or distillation.

Results

Initial Survey

The first step in the work on thermal stability was to screen the aromatic class of organics so that the most promising members might be chosen for more intensive study. Table I gives results on a few selected compounds. The amount of decomposition was estimated by observing the color change and the amount of residue formed and by measuring the pressure of the gas generated.

Data in Table I attribute superior thermal stability to biphenyl, the three terphenyl isomers, and naphthalene. The polyphenyls were certainly more promising than any of the fused ring aromatics, except naphthalene. It was noted, however, that partially pyrolyzed naphthalene tended to form a hard, brittle residue, resembling coke, in a separate phase, while the polyphenyls reduced to resins which, though nonvolatile, tended to remain in solution. Such information is pertinent to the choice of an organic for the reactor coolant use.

Several substituents for hydrogen atoms in the naphthalene structure were studied in order to note any stabilizing influence of such groups. Included were alkyl side chains as typified by the methylnaphthalenes and acenaphthene. Fluoronaphthalenes were also pyrolyzed to ascertain the contribution of the C-F bond. In these and other instances, the substituents markedly reduced thermal stability as indicated by larger quantities of gas and/or more copious formations of residue.

Table I. Thermal Stability* of Selected Aromatic Compounds

Compound	Relative thermal stability
A. *Polyphenyls*	
1. Biphenyl, *o*-terphenyl, *m*-terphenyl, *p*-terphenyl	Good
2. *p*-quaterphenyl	Fair
B. *Fused Ring Aromatics*	
1. Naphthalene	Good
2. Anthracene, Phenanthrene, Chrysene, Pyrene	Poor
C. *Other Materials*	
1. 2,2'-binaphthyl	Fair
2. 1,1'-binaphthyl, tetraphenylsilane, tetrabenzylsilane	Poor

* Tests in Vycor capsules; 10 microns initial pressure; 465°C; various times.

Selection of the Best Class

Additional tests were made to compare naphthalene and biphenyl as representatives of their respective organic classes. In one such comparison, the two compounds were exposed for two different periods of time at 493°C. These results are summarized in Table II.

Table II. Thermal Stability* of Typical Polyphenyl and Fused Ring Compounds

Compound	Time, hours	Gas evolution		Per cent residue†
		ml/gram	moles/mole	
Naphthalene	24	3	0.018	0.1
	72	121	0.69	63
Biphenyl	24	4	0.02	1.4
	72	21	0.13	41

* Stainless steel (AISI Type 304) vessels; about 22 kg/cm² initial N_2 pressure; 493°C.
† Recovered by vacuum distillation.

For the shorter exposure, naphthalene was more interesting on the basis of both gas evolution and residue formation. However, for the longer term, it showed less stability than did biphenyl. Because an organic chosen for use as a moderator-coolant must exhibit stamina at the highest possible temperature for extended periods, biphenyl was considered superior to naphthalene. This preference extended generally to polyphenyls as the most desirable single class of aromatic hydrocarbons.

Tests were next conducted to study the temperature sensitivity of the polyphenyls. Exposures at different temperatures strikingly illustrated the dependence of stability on temperature. Typical data

Table III. Dependence of Stability* of Polyphenyls on Temperature

Compound	Temperature, °C	Gas evolution ml/gram	Gas evolution Mole/mole	Per cent residue†	
1. Biphenyl	526	28	0.18	77	M
	510	16	0.10	(2-4)	M
	493	4	0.02	1.4	D
2. *o*-terphenyl	510	37	0.37	92	M
	493	9	0.08	39	D
3. *p*-terphenyl	510	27	0.27	98	M
	493	7	0.06	56	D

* Stainless steel (AISI Type 304) vessels; about 22 kg/cm² initial N_2 pressure; 24-hour exposure.
† *M* = manual recovery, *D* = vacuum distillation recovery.

for three polyphenyls are shown in Table III. From these and similar data, it was concluded that about 490°C is the highest practical temperature at which these organics may be used for a reasonable period of time. Fused ring aromatics, including naphthalene, were increasingly less stable than the polyphenyls at the higher temperatures.

Role of Additives

It is generally accepted that a free radical mechanism predominates in the thermal decomposition of hydrocarbons.[7] A fruitful approach to the problem of increasing the thermal stability of these materials would appear to be that of arresting pyrolysis through the use of chemical inhibitors. The thermal stability of the inhibitor itself would then become a concern. Several additives were tried in various fluids, but none was found to be beneficial. The type of effect observed is noted in Table IV for several inhibitors contained in biphenyl. The lack of inhibiting effect of nitric oxide is surprising in view of its known behavior in this regard with paraffins.[5,7] Acridine is known to function as an inhibitor in catalytic cracking,[8] but it was not effective in the present study. Iodine is known to act in certain situations as a radical chain stopper and in others as a radical reaction accelerator.[9] It was found to augment the pyrolysis of biphenyl in the present study. From these and similar results, the possibility of finding a beneficial additive did not appear hopeful.

Circulating Loop Tests

Work of particular interest in the thermal part of the reactor coolant study was conducted with biphenyl in a fluid circulating loop. Figure 1 is a simplified sketch of the system used. In this closed circuit, biphenyl was pumped through a reaction chamber at a bulk temperature of 315°C. A nichrome ribbon heating element within the chamber was maintained at an estimated surface temperature of 420°C. A heat flux of about 22 cal/sec/cm² (292,000 BTU/hr/ft²) was delivered to the fluid from the heating element under the test conditions used. This heat flux is in the range expected from fuel elements in the reactor coolant application.

The nichrome ribbon was inspected for deposits after 145 hours of operation. No deposit was in evidence; only a slight darkening was observed which was attributed to the sustained operation at 420°C. No deposits appeared on the surface of the strainer, which comprised a 100-mesh screen. A sample of the pyrolyzed biphenyl was carefully distilled to separate starting material from polymeric product. By this means, it was shown that about 10% of the biphenyl had been converted to other materials, probably higher polyphenyls.

During the course of the experiments with the loop, it was learned that certain improper operating conditions produced heavy boiling on the surface of the ribbon element, causing its temperature to rise rapidly. This heavy boiling over long periods promoted vapor phase and liquid phase cracking of the organic, both of which encouraged carbon deposition. Short periods of surface boiling did not seem to cause deposition.

Table IV. Effects of Additives on Thermal Stability* of Biphenyl

Additive, weight per cent	Compound	Gas evolution cm³/gram	Gas evolution Mole/mole	Per cent residue†
	None	21	0.13	41
1.5	Nitric oxide	23	0.15	81
2.4	Thianthrene	21	0.14	61
2.4	Triphenylmethane	113	0.7	77
2.4	Iodine	164	1.09	69

* Stainless steel (AISI Type 304) vessels; about 22 kg/cm² initial N_2 pressure; 493°C; 72-hour exposure.
† Recovered manually.

Although these experiments were somewhat limited in scope, they demonstrated certain levels of polyphenyl performance in a circulating system. For the specified time, biphenyl was observed neither to undergo excessive pyrolysis nor to promote catastrophic deposition on heat transfer surfaces. For the high heat fluxes used, these tests established that this type of organic could be used at temperatures which are considered attractive for the reactor coolant application.

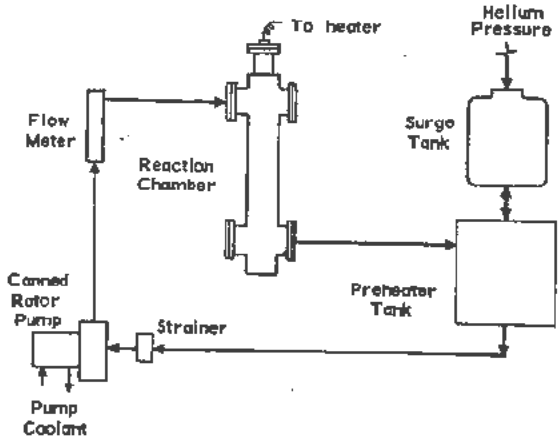

Figure 1. Flow diagram of thermal test loop

Conclusions

Based on the formation of gas and residue, polyphenyls show less damage from extreme high temperatures than other types of aromatic hydrocarbons. About 490°C seems to be an upper limit beyond which the use of organics is not feasible for reasonable periods of time. Selected additives hold little promise of extending this thermal ceiling. At somewhat lower temperatures, a simple polyphenyl demonstrated acceptable levels of deterioration and surface fouling tendencies when pumped past a surface transmitting a high heat flux. Strictly from the standpoint of thermal stability, polyphenyls hold promise for use as coolants in an atomic reactor and warrant emphasis in studies on radiation stability.

RADIATION STABILITY

Background and Purpose

Early investigators,[4] using 170 kv cathode rays, indicated that aromatic hydrocarbons are more stable to radiation than aliphatic hydrocarbons. Their work also suggested, by showing less evolution of gas for biphenyl than benzene, that the higher polyphenyls are perhaps the more stable. Other workers[10] have pointed out that molecular symmetry and resonance are responsible for the enhanced radiation resistance of benzene molecules. Various aspects of the relation of organic structure to the primary and the secondary radiation decomposition mechanisms were also investigated.[11–14] A detailed radiolysis study[14] on hydrocarbon mixtures shows that benzene tends to protect less stable aliphatic hydrocarbons. This same report confirms the high order of stability of aromatic compounds previously noted in earlier work.[4]

It was shown in the previous section that polyphenyl materials, such as the terphenyls, exhibit unusually high resistance to pyrolysis. The effect of combined thermal and radiation exposure compared to thermal exposure alone is of interest. For *p*-terphenyl, Fig. 2 shows graphically that the temperature effect is eclipsed by the radiation factor. To appraise this decomposition due to radiation in the light of the background of thermal and radiation studies already cited, new irradiation tests were undertaken. It was hoped that these tests might determine the choice of organic structures most nearly suitable for service as reactor coolants and their limiting conditions of temperature and radiation dosage. Supporting analyses were provided to gain an insight into the mechanism by which the most stable organic materials decompose in the presence of radiation. A continuing search for evidence of fouling of heat transfer surfaces was also maintained during the work.

Approach

The new work on radiation stability included static or capsule tests in reactors to study effects of exposure to varying temperatures and radiation

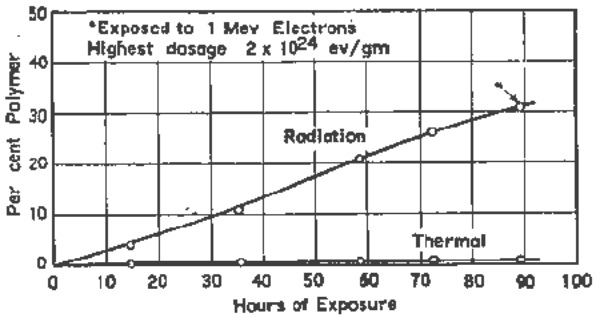

Figure 2. Relative damage to p-terphenyl at 400°C from thermal and radiation exposures

dosages. An especially extensive survey was made of the terphenyl isomers with 1 Mev electrons in a Van de Graaff electrostatic generator. Also, dynamic tests were made with a circulating loop in a reactor, and rough correlations between damage to organics in static and in dynamic tests were established. Analyses of many of the samples available from this research contributed information on the composition of irradiated products. This was then related to possible modes of deterioration and to methods of purifying the degraded organics. These items are all discussed in turn in the sections to follow.

In the present description, polymer formation and gas evolution were employed as criteria of damage. Polymer formation was measured both indirectly by viscosity change and directly by careful vacuum microdistillation of irradiated samples. In the latter case, everything boiling above the original starting material was assumed to be polymer. Corrections were made, based on ultraviolet analyses, for contaminants in either the distillate or residue. Viscosity determinations were made by the Zeitfuchs method.[15] Evolved gas was collected for mass spectrometric analysis, and the total gas pressure under standard conditions was measured.

All of the irradiations were conducted in the nearly complete absence of oxygen because of the harmful effect of this agent on organic materials in the presence of radiation. Figure 3 illustrates this with *n*-butylbenzene. In both instances portrayed, the organic fluid was blanketed with helium; however, in one case, air entered through a leak in the system to produce the major effect noted. Air dilution was confirmed by infrared analysis, which revealed oxidation products in the more viscous sample. Figure 3 is typical of the fashion by which decomposition of organic materials is accelerated by oxygen in the presence of radiation.

Screening Tests in a Nuclear Reactor

Stainless steel capsules were employed in this work. These containers were of 22 ml capacity and were charged with 10 ml of sample at room temperature. The sealed, oxygen-free vessels were contained in ovens (18 to an oven) which were inserted in a reactor. Automatic temperature control was provided.

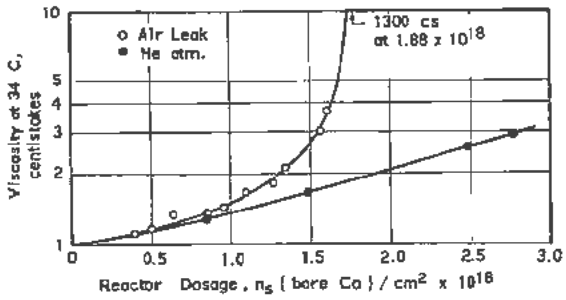

Figure 3. Acceleration of radiation damage to n-butylbenzene at 140°C due to air

After the exposure, the containers were allowed to decay in radioactivity for a few days and then were opened to measure total gas pressure generated and to recover the products.

The irradiations were conducted in the Brookhaven Reactor (Hole E-25). Work was undertaken to determine the important components of the combined flux existing in this facility. For fast neutrons, neptunium-237 and uranium-238[16] fission monitors were employed. Small aluminum disks, containing about 0.5% cobalt, were used to measure slow and resonance neutrons by exposures in the bare or cadmium shielded condition. The gamma flux in the Brookhaven facility was measured with a simple calorimeter which consisted of a lead rod insulated everywhere but on one end. The temperature difference between two points in the rod depended upon the heat input from gamma radiation.

By these means, the resonance neutron flux (about 0.5 ev to 0.6 Mev) was determined to be approximately 10% of the subcadmium slow neutron flux (below about 0.5 ev). Similarly, the fast neutron flux (above about 0.6 Mev) was shown to be approximately 25% of the subcadmium slow neutron flux. With the assumption of 1 Mev as the average energy of a reactor gamma photon, this flux was found to be about 45% of the subcadmium slow neutron flux. As these ratios hold for the various positions used in this particular facility, the combined reactor dosage or integrated flux will generally be expressed in terms of the more easily measured slow and resonance neutrons, even though these components are not the major contributors to damage. Thus, where dosage is shown as slow plus resonance neutrons/cm², n_s (bare Co)/cm², gamma radiation and fast neutrons were also present in the ratios cited.

Effects of Irradiation Variables

Knowledge as to the basic roles of temperature and radiation dosage in the damage of organics is of primary importance in any situation in which such materials are to be used under varied exposure conditions. This is particularly true of the proposed reactor coolant application. Here the meaningful selection of exposure temperature and dosage even for screening test work depends upon this knowledge. Thus, work on this facet of the problem preceded the main search for materials of optimum stability for the projected use.

Figure 4 illustrates the role of temperature in radiation damage to a typical aromatic compound, naphthalene, at a single radiation dosage. It is seen that polymer formation, as indicated by viscosity change, remains essentially constant up to about 400°C. For the radiation dosage shown in Fig. 4 (representing a 10-day exposure in the E-25 Brookhaven facility), an abrupt dependence of damage on temperature occurs above 400°C. At 425°C, samples were completely coked.

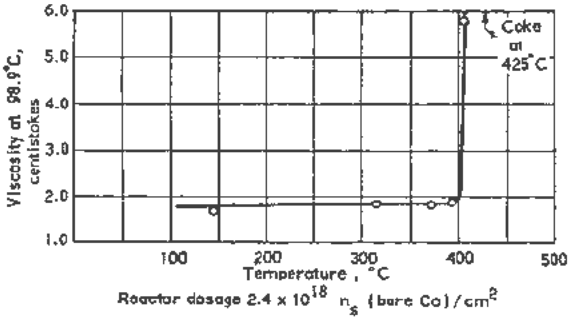

Figure 4. Role of temperature in radiation damage to naphthalene

Figure 5 illustrates effects of both temperature and radiation dosage. The data for butylbenzene show the general shape of the log viscosity-dosage curve for a given temperature. The straight line out to about 3×10^{18} n_s (bare Co)/cm² should be noted as should the accelerated damage, as measured by the viscosity change, after that point. A similar situation exists for the biphenyl irradiations at various temperatures. This again shows the lack of influence of exposure temperature on damage in terms of viscosity change in the region below about 380°C. The difference in slopes of the butylbenzene and biphenyl curves reflects the greater stability of the latter.

Figures 4 and 5 illustrate the sensitivity of stability to temperature in the 400–500°C range and the relative temperature independence of damage below this range. These effects have been observed generally in comparable tests with the most stable organics. In the sensitive region, temperature and radiation dosage have proved to be interdependent variables

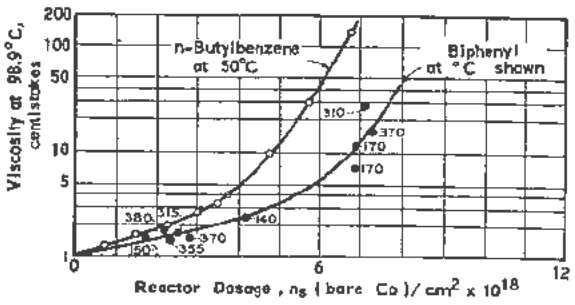

Figure 5. Effects of radiation dosage and temperature on organic materials

in relation to damage; thus, to reach a given point of damage, dosage may be increased while the temperature of exposure is lowered and vice versa. However, the ultimate reactor dosage possible at any temperature without complete decomposition is in the range of 10 to 12 $\times$ 10^{18} n_s (bare Co)/cm^2.

The approximate straight-line relationship between the log function of viscosity and reactor dosage out to about 3 $\times$ 10^{18} n_s (bare Co)/cm^2 was used in the screening work with various organics. Dosages near this value were employed to avoid a region of accelerated damage as indicated by the viscosity change method. Threshold temperatures above which the particular organics were temperature sensitive were then determined at these dosages.

Temperature Limits for Practical Application

Many different aromatic compounds, some containing elements other than carbon and hydrogen, were screened in this temperature threshold work. Table V summarizes typical data and illustrates the general superiority of the polyphenyl class of hydrocarbons. It is noteworthy that susceptibility to radiation damage does not appear to increase in higher members of the homologous series, as was predicted and shown (see Table I) in the thermal work.

The performance of materials containing sulfur, as typified by dibenzothiophene, is particularly striking. Unfortunately, the radioactivity induced in sulfur compounds by neutron capture is undesirable in a reactor coolant. However, the stability of sulfur (and selenium) compounds to radiation damage prompted interest in using these and similar compounds as stabilizing additives in other organics. Small quantities (up to 5%) of these additives were found to be of value in this regard. Further investigation revealed mixtures of hydrocarbons which exhibited a similar improved stability. This finding was of particular interest to the coolant application because it furnished a means of improving stability of organic materials without increasing the induced radioactivity due to sulfur, selenium, etc.

Table V. Typical Temperature Thresholds* for Aromatic Compounds in a Reactor†

Compound	Threshold temperature, °C
Fused ring	
Naphthalene	400
Phenanthrene	415
Chrysene	415
Pyrene	400
Polyphenyl	
Biphenyl	400
o-terphenyl	415
m terphenyl	415
p-terphenyl	450
m-quinquephenyl	445
Other	
Carbazole	400
Amylbiphenyl	370
Diphenylacetylene	415
Dibenzothiophene	455

* Approximate point above which damage is temperature sensitive at the test dosage.
† Radiation dosage: about 2.5 $\times$ 10^{18} n_s (bare Co)/cm^2.

Table VI. Mixtures of Organics for Improved Radiation Stability*

Mixture	Threshold† temperature, °C
A. 1. Biphenyl (0.5% phthalocyanine)	425
2. Biphenyl (5% triphenylmethane)	440
B. 1. Terphenyl eutectic‡	440
2. Terphenyl eutectic‡ (5% thianthrene)	455
C. 1. Phenanthrene (30%)—*o* terphenyl (70%)	425
2. Phenanthrene (30%)—*o*-terphenyl (70%) (5% naphthacene)	440
3. Phenanthrene (23%)—*o*-terphenyl (77%) (5% dibenzyl selenide)	455
D. Dibenzothiophene	455

* Radiation dosage: about 2.5 $\times$ 10^{18} n_s (bare Co)/cm^2.
† Approximate point above which damage is temperature sensitive at the test dosage.
‡ 50% meta, 25% ortho, 25% para by weight.

Table VI contains data on the most promising mixtures of organics for the reactor coolant use as determined from the temperature screening tests. The performance of phenanthrene is of interest since the thermal stability work had predicted poor resistance for this compound. It can be seen (with reference to Table V as well) that certain mixtures showed stability which was better than that of the components alone. Also, small percentages of certain additives improved less stable materials to a markedly greater extent than would be expected from a straight dilution effect. Thus, "protection" of the more susceptible compounds actually took place. From these data, it appears possible for the best organic combinations to operate at an upper limit of 440–450°C at the screening dosage of about 3 $\times$ 10^{18} n_s (bare Co)/cm^2.

Work with 1 Mev Electrons

Within the preferred polyphenyl class, the terphenyl isomers possess boiling points (ortho, 332°C; meta, 363°C; and para, 376°C; compared to 255°C for biphenyl) of particular interest for the reactor coolant use. They also are prepared more easily than higher members of the series and therefore are less costly. For these reasons, the terphenyls were made the subject of an intensive study with electron radiation from a Van de Graaff electrostatic generator. With this machine, it was possible to secure large energy inputs in relatively short times. It has already been established that damage suffered by organics as a result of electron bombardment generally differs from that resulting from reactor exposure in degree, not in kind.[17]

In the research with the Van de Graaff machine, 1 Mev electrons were beamed at 15 to 25 microamperes into an organic specimen contained in a cell as shown in Fig. 6. Dosimetry was conducted for cells of this sort by substituting an electrically isolated

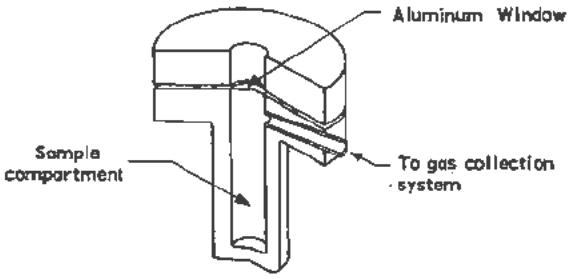

Figure 6. Steel exposure cell for electron irradiations

aluminum plug for the organic in the sample compartment and measuring the electron current absorbed. By this procedure, it was determined that for 1 Mev electrons 55% of the total electron beam was entering the cell of Fig. 6.

Figure 7 compares the performance of the terphenyl isomers at 400°C by the rate of polymer formation criterion. The superiority of the para compound was thus demonstrated, together with the approximate equivalence of the ortho and meta isomers. The tendency of the three materials to approach one another in stability at higher dosages reflects the increasing stability of the *m*- and *o*-terphenyls with increasing dosage. This indicates that products formed at this dosage are predominantly more resistant to radiation than the starting material.

Figure 8 shows the effect of increasing temperature on the radiation resistance of *p*-terphenyl. The improved stability at the higher dosage values is illustrated for this isomer at 450°C. The higher equilibrium values for rate of polymer formation at the higher temperature show that the range of 400–450°C is in the temperature sensitivity region for *p*-terphenyl.

The per cent polymer values equivalent to the rate points of Fig. 8 are shown in Fig. 9. The polymer produced by irradiation was a mixture of species comprising four or more phenyl groups. In the exposures of Fig. 9, the polymer was definitely not coked.

The effect on stability of adding a small amount of *p*- to *m* terphenyl is illustrated in Fig. 10. The stability of the mixture containing 4.35% by weight of the para isomer was much closer to that of the more stable component than would be predicted from percentage composition. The physical properties of the mixture compared to those of the components are also of practical significance. Thus, the melting point of the mixture (110°C) is only slightly higher than that of *m*-terphenyl (89°C) and is much below that of the high melting para compound (213°C). Similar improved radiation stability has been observed for other combinations. For example, 5% *p*-quaterphenyl in *m*-terphenyl showed stability much closer to that of the very resistant *p*-quaterphenyl than to that of *m*-terphenyl.

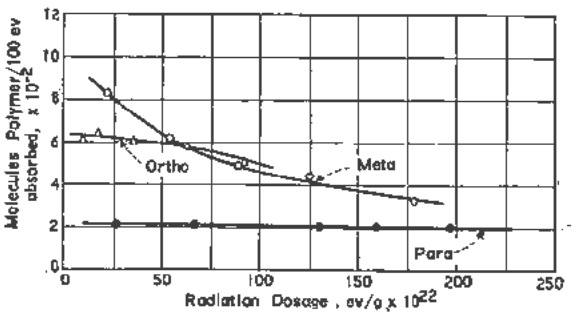

Figure 7. Relative radiation resistance of terphenyl isomers at 400°C

Dynamic Tests in a Reactor Loop

In screening tests already cited, the temperature in the capsules was maintained by an external oven. No internal heat, except that from the absorption of radiation, was provided. These conditions resulted in no deposits on the capsule surfaces for the varied types of exposure used in the work until temperature thresholds were exceeded and the entire sample was reduced to coke. Although this lack of deposition was encouraging, information was needed on the tendencies of organics to deposit on heated surfaces in a dynamic system in a reactor. Work was undertaken

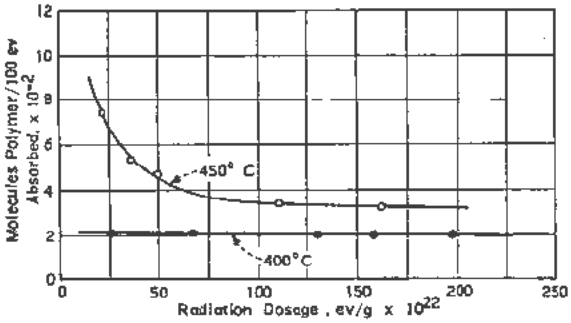

Figure 8. Effect of temperature on radiation stability (rate of polymer formation) of *p*-terphenyl

with a fluid circulating loop to secure such information. Here, test conditions could be more carefully controlled to permit observations before the occurrence of the massive coking which was the end point in capsule tests. Confirming evidence on the degree of radiation damage to organics as a function of neutron dosage was also possible from the loop experiments.

A hydraulic system similar to that of Fig. 1 was used to circulate the lowest member of the polyphenyl series, biphenyl. The reaction chamber consisted of concentric stainless steel tubes arranged so that the test liquid passed down into the irradiation zone through the annular space between the inner and outer tubes and returned through the inner tube. An aluminum sheathed immersion heater was placed in the center of the inner tube. Heat generation from this source was limited by space and design considerations to about 0.11 cal/sec/cm² (1500 BTU/hr/ft²). Although this was far from the 22

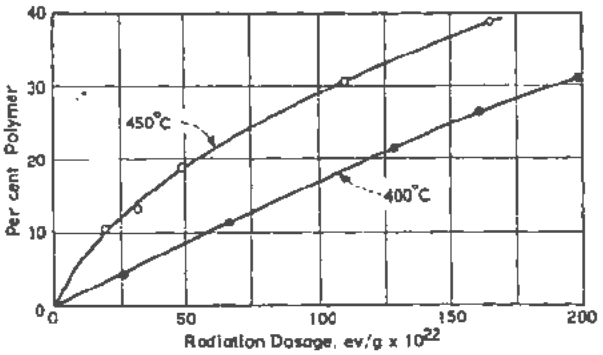

Figure 9. Effect of temperature on radiation stability (per cent polymer) of p-terphenyl

cal/sec/cm² (292,000 Btu/hr/ft²) used in the thermal loop, it made possible a preliminary study of the deposition problem in reactor equipment.

Two runs were completed, Run I for 25 hours and Run II for 74 hours, at average operating temperatures of 190–196°C. Samples were taken periodically for analytical work, and the heater was removed from the reactor for visual observation at the end of each run.

In the 25-hour experiment, no deposition of any sort was observed on the heater. However, because of equipment limitations, there was no heat generation in the portion of the heater in the maximum flux region. In Run II, this was corrected, and heat generation took place even in this region. In this longer test, the entire length of the heater showed adherent black deposits which were more concentrated in the maximum flux zone. During the 74-hour run, two periods of essentially static (no flow) operation occurred. In both of these, observed bulk temperatures increased appreciably, and it is very probable that a large rise in the temperature of the heater surface also took place. With this likelihood during the periods of no coolant flow, the deposition cannot be attributed to irradiation alone. It may be concluded, therefore, that carbonization of biphenyl on heat generation surfaces during irradiation may occur, but such deposition certainly cannot be considered as catastrophic.

Table VII summarizes the data on polymer formation from the dynamic runs in comparison with

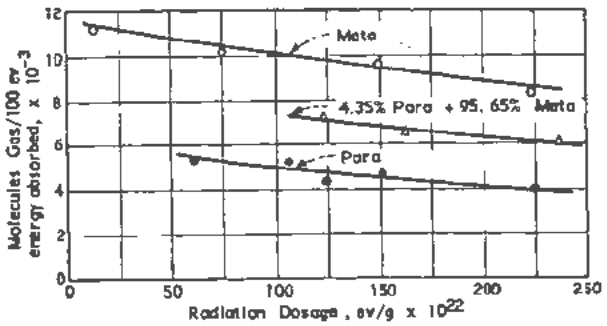

Figure 10. Improved radiation stability of terphenyl mixtures at 350°C

similar information from static irradiations. The reasonable agreement between the two is important as it attests to the validity of evaluation techniques and supports the appraisal of the temperature effect previously made.

Structural Changes on Irradiation

A general idea of the products formed in the irradiation of the most stable aromatic materials is important in the present study. Such information relates directly to the design of a purification system. By means of this system, the composition of the organic coolant might be kept more constant during irradiation, and the tendency to form deposits on heat transfer surfaces thereby reduced. How the organic materials change is also of concern for a better understanding of the over-all problem. The present section is concerned with a discussion of these items.

Table VII. Comparative Radiation Damage to Biphenyl in Static and Dynamic Systems

	Capsule test	*Loop run I*	*Loop run II*
Temperature of exposure, °C	355	190	196
Per cent polymer formed	21	3.4	11
Neutron dosage, nvt* × 10^{17}	7.6	1.2	4.5
Per cent polymer/10^{18} nvt*	28	28	25

* Neutrons > about 0.5 ev.

When materials such as biphenyl or the terphenyls change under the influence of radiation, considerable gas is formed. Liquids and solids of both higher and lower molecular weight than the starting materials also are formed. In the present study, the higher molecular weight products are those which have been termed "polymer." They are present in irradiated materials generally in much larger amounts than the lower molecular weight products. The gas evolved consists primarily of hydrogen with smaller amounts of low molecular weight hydrocarbons. A typical gas sample analysis from electron irradiation of biphenyl showed 98 mole per cent hydrogen, 1.5% methane, and 0.4% ethane. Traces of propane, butane, and toluene were also present.

Several of the irradiated polyphenyl and fused ring compounds were analyzed insofar as possible with infrared, ultraviolet, and high temperature mass spectrometric methods. These methods are less reliable as the exposed materials become more damaged. In this situation, the best approach is to fractionate the samples carefully and then to analyze the fractions. The many types of unsaturated materials present contribute high backgrounds which interfere in the ultraviolet, while the many products complicate the infrared method. The mass spectrometric procedure is limited by volatility considerations, although this limitation can be lessened to a certain degree with a heated inlet manifold.

By these analytical means, samples of biphenyl from the reactor loop experiment described in the

previous section were analyzed qualitatively. The polymer fraction was found to be predominantly polyphenyl materials, including terphenyls and quaterphenyls. Mono- and dialkylaromatic compounds were also present. Alkyl groups attached to aryl nuclei amounted to one, two, and three carbon atoms each and contained unsaturation. These products all typify materials formed by free radical reactions as expected in a radiation environment. Indeed, this probably explains the effectiveness of inhibitors, such as those containing sulfur, in improving the resistance of less stable compounds. Such additives are known to interfere with the free radical mechanism by acting as chain stoppers.[9]

The analytical results indicate that the decomposition of aromatic materials by radiation apparently proceeds by the two main routes of "ring doubling" and "ring cleavage." This is illustrated for biphenyl in Fig. 11, where R represents an unsaturated alkyl group.

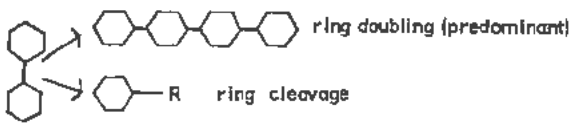

Figure 11

The quaterphenyl can then undergo additional doubling, loss of rings, or ring cleavage as a result of further irradiation. The unsaturated alkylaromatics can proceed in like manner; however, with these materials, further polymerization would be expected as the principal reaction in the same manner in which styrene derivatives form high polymer in the presence of free radicals.

This simple scheme explains the reaction products found through analytical work. It also explains why the rate of decomposition with some materials decreases with increasing radiation dosage. Here, the doubled-up products formed by the predominant reaction are more stable to radiation than the starting materials.

The finite rate of decomposition of even the best organic materials in the presence of radiation and the final end result of complete coking make the use of a purification system a necessary part of the reactor coolant scheme. The identity of the reaction products indicates that this purification may be accomplished either by a distillation or by an adsorption technique on a side stream of coolant. Both of these means have been found satisfactory.

Conclusions

From the work on the radiation stability of organic materials, certain conclusions can be drawn pertinent to the reactor coolant use. These are listed as follows:

1. Polyphenyls, particularly the terphenyls, are the preferred class of organics for exposure to maximum radiation dosage at elevated temperature.

2. The radiation stability of aromatic mixtures has been shown in many instances to be markedly better than that of any of the individual components. Additives further enhance the stability of the mixtures.

3. Radiation damage is due directly to the interrelated variables of irradiation temperature and dosage. Below about 400°C, damage to the most stable materials is independent of temperature. Above this point, marked dependence exists.

4. Regardless of exposure temperature, a dosage of about 1.1×10^{19} neutrons† (bare Co)/cm^2 converts the best organics to coke.

5. For a neutron dosage (bare Co) of 3 to 4 $\times$ 10^{18}/cm^2, a log function of viscosity is approximately a straight line function of radiation dosage. In this dosage range, it appears possible to use the best organic combinations at 440–450°C.

6. Radiation degrades polyphenyls by two processes: "ring doubling" (predominant) to form stable products and "ring cleavage" to form undesirable products.

7. Due to the predominaut ring doubling process and the improved stability of doubled-up polyphenyl molecules, certain polyphenyls become more stable with increasing radiation dosage.

8. Deposition tendencies on heat transfer surfaces have not been thoroughly investigated. However, reasonable estimates from static and from dynamic tests indicate that they will not prove to be insurmountable problems.

SIGNIFICANCE OF THE RESULTS IN REACTOR DESIGN

The effect of radiation on organic materials, which is of most importance in reactor design, is the formation of compounds of higher molecular weight than the starting material. These products have a direct bearing on the over-all operation of the reactor because at some point in the radiolysis process they become sufficiently unstable to deposit a residue on heat transfer surfaces. The flow of heat to the coolant is thereby impeded. The utilization of organics as reactor coolants is then a problem of balancing the removal of degraded products against the addition of fresh organic. Deposition, on the one hand, must be avoided, but the make-up requirements, on the other hand, must not become prohibitive on an economic basis.

The deposition on heat generating surfaces is a function of at least two principal variables in the reactor: the temperature of operation and the radiation dosage delivered to the organic. The average dosage can be reduced by increasing the make-up rate, but the temperature cannot likely be reduced because this must be high enough to permit an operationally competitive plant. In this regard, it has been established that, even in the absence of radiation, 490°C is about the upper limit of usefulness of the best organic materials. Exposure to radiation would

† Defined in section entitled "Screening Tests in a Nuclear Reactor."

decrease this figure to 400–450°C in the reactor application. Only a few organic species, such as *p*-terphenyl and certain mixtures, are able to withstand the combined effects of both radiation and temperatures of this order; most materials would give much poorer performance. In the 400–450°C region, the best organic coolants would be about 30% converted to polymer by a neutron* dosage of 10^{18}/cm². It is believed that such a radiolysis mixture would not exhibit deposition tendencies, although this point has yet to be established firmly.

Beyond the stage of about 30% polymer formation, deposit-free operation would necessarily require that certain polymer constituents be removed continuously and replaced with fresh organic. The make-up rate would be about 10% to 15% of the material in the flux zone for each 10^{18} neutron*/cm² dosage increment. This lowered rate of decomposition over that existing initially reflects the increasing stability of the high molecular weight polyphenyls formed during irradiation.

From the foregoing, it is seen that nuclear reactors moderated and cooled with organic materials appear to be entirely feasible. This has been shown strictly from the chemical approach. The next steps in applying this basic information, together with economic concepts, to prototype reactor designs require a nuclear engineering approach. These steps are currently being taken.

* Greater than 0.5 ev.

REFERENCES

1. Franklin J. L., *Prediction of Heat and Free Energies of Organic Compounds,* Ind. Eng. Chem. 41, 1070-6 (1949).
2. Obreimov, I. F., *Thermal Stability of Complex Molecules,* Zhur. Eksptl. Teoret. Fiz. 19, 396-406 (1949); Chem. Abstr. 46, 9906f (1952).
3. Hadzi, D., *Structure of Possible Intermediates in Carbon Formation During Pyrolysis of Organic Compounds,* Fuel 32, 112-3 (1953).
4. Schoepfle, C. S. and Fellows, C. H., *Gaseous Products from Action of Cathode Rays on Hydrocarbons,* Ind. Eng. Chem. 23, 1396-8 (1931).
5. Sachanen, A. N., *Conversion of Petroleum,* p 87-110, Reinhold Publishing Corp., New York (1948).
6. Tilicheev, M. D., *Kinetics of Cracking of Hydrocarbons under Pressure,* J. Applied Chem. USSR 12, 105, 735, 741, (1939).
7. Brooks, B. T., Kurtz, S. S., Boord, C. E. and Schmerling, L., *The Chemistry of Petroleum Hydrocarbons.* Vol. II, p 1-25, 113-36, Reinhold Publishing Corp., New York (1955).
8. Voge, H. H., Good, G. M. and Greensfelder, B. S., *Catalytic Cracking of Pure Compounds and Petroleum Fractions,* Proceedings of the Third World Petroleum Congress, The Hague, Section IV, p 124-37 (1951).
9. Bailey, K. C., *The Retardation of Chemical Reactions. X. The Choice of Retarders in Liquid Phase Oxidations,* Proceedings of Royal Irish Acad. 45, Section B, No. 16, 373-412 (1939).
10. Burton, M., *Effects of High-Energy Radiation on Organic Compounds,* J. Phys. and Colloid Chem. 51, 786-97 (1947).
11. Burton, M., *Radiation Chemistry. IV. An Interpretation of the Effect of State on the Behavior of Some Organic Compounds and Solutions,* J. Phys. and Colloid Chem. 52, 564-78 (1948).
12. Burton, M., *Radiation Chemistry, V. Effects of Molecular Size,* J. Phys. and Colloid Chem. 52, 810-19 (1948).
13. Magee, J. L. and Burton, M., *Elementary Processes in Radiation Chemistry. II. Negative Ion Formation by Electron Capture in Neutral Molecules,* J. Am. Chem. Soc. 73, 523–32 (1951).
14. Manion, J. P. and Burton, M., *Radiolysis of Hydrocarbon Mixtures,* J. Phys. Chem. 56, 560-69 (1952).
15. Zeitfuchs, E. H., *Kinematic Viscometer for Opaque and Very Viscous Liquids,* Oil Gas J. 44, 99-102, Jan. 12 (1946).
16. Keller, R. N., Steinberg, E. P. and Glendenin, L. E., *Yields of Fission Products from U^{238} Irradiated with Fission Spectrum Neutrons,* Phys. Rev. 94, 969 73 (1954).
17. Calkins, V. P., *Radiation Effects on Reactor Materials,* Nucleonics 12, No. 9, 9-12 (1954).

Experience with Heavy Water Systems in the NRX Reactor

By R. F. S. Robertson, Canada

Before the NRX reactor was brought into operation in 1947 it was feared that the D_2O would prove unstable under the intense ionizing radiation. It was expected that about 9000 litres of electrolytic gas (at NTP) would be generated per hour with the reactor operating at 30 megawatts. Experience has shown these fears to be groundless and we now know that under the proper conditions the net decomposition rate of the D_2O is negligible.

This paper will discuss the radiation stability of the D_2O in NRX and in two large scale irradiation experiments in which D_2O was recirculated in a closed loop. It will be shown that experimental results are in accord with presently accepted theories of the radiation chemistry of water.

EXPERIENCE IN NRX[1]

Figure 1 shows a *schematic* representation of the D_2O system in NRX. The reactor vessel, or calandria, holds about 15,000 litres of D_2O under normal operating conditions. A continuous flow of about 25 litres per minute is maintained to the storage tanks, the D_2O being pumped from there back to the calandria. A fraction of the return flow (about 5 litres per minute) is fed through ion-exchange columns to remove ionic impurities. These columns also serve as a filter. The ion exchange resins used at present are a mixture of a strong base anion exchange resin and a strong acid cation-exchange resin. In another circuit the D_2O is pumped through heat exchangers and back to the reactor at about 900 litres per minute. With the reactor operating at 40 megawatts the temperature of the D_2O is kept at about 50°C.

At any place in the NRX system where there is a free surface the D_2O is in contact with an atmosphere of purified helium. The helium system (not shown in Fig. 1) is provided with a purification unit in which any gaseous impurities may be removed by adsorption on active charcoal at liquid nitrogen temperatures. This unit is operated intermittently when analyses of the helium show too high a concentration ($> 0.2\%$) of gaseous impurities such as nitrogen or when fresh helium is added to replace that lost through leakage. There is also a recombination unit consisting of a bed of alumina impregnated with palladium through which the calandria helium is blown at about 300 litres per minute. This unit is operated continuously.

The operation of NRX may be divided into three periods. Table I shows the pH, specific conductivity and composition of calandria gases normally observed during these periods. It can be seen that the addition of the ion-exchange resins improved the purity of the D_2O considerably. This improvement in purity was also reflected in the concentrations of such ions as Cl^- and NO_3^- which fell from values of 1 to 3 parts

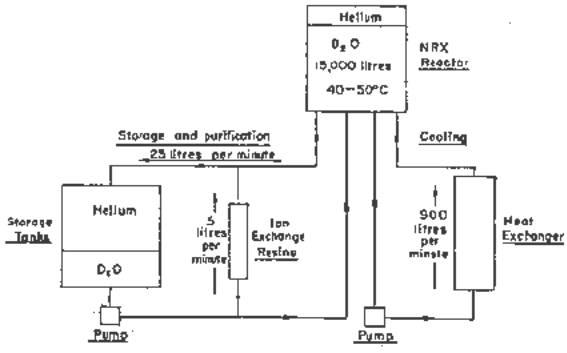

Figure 1. D_2O system in the NRX reactor

Table I. Operating Conditions of D_2O in NRX

Period	*Reactor power (Mw)*	*D_2O temp °C*	*pH*	*Specific conductivity ohm^{-1} cm^{-1}*	*D_2O_2 concentration*	*Composition of calandria He* % D_2	% O_2	% N_2	*Remarks*
July 1947 to Feb. 1949	Slowly raised to 10 Mw	~40°C	Started at 6 gradually fell to 4	$>5 \times 10^{-6}$		~1%	<0.2%		No ion exchange resins present. D_2O distilled once in Dec. '48 when pH dropped to 4.
Feb. 1949 to Dec. 1952	30	~40°C	5.5	1 to 2 $\times 10^{-6}$	1–4 ppm (30–120μM)	~0.3%	<0.05%	~0.1%	Ion exchange resins added
Feb. 1954 to present	40	~50°C	5.8	0.5×10^{-6}	0.5–4 ppm (15–120μM)	<0.2%	<0.2%	<0.1%	

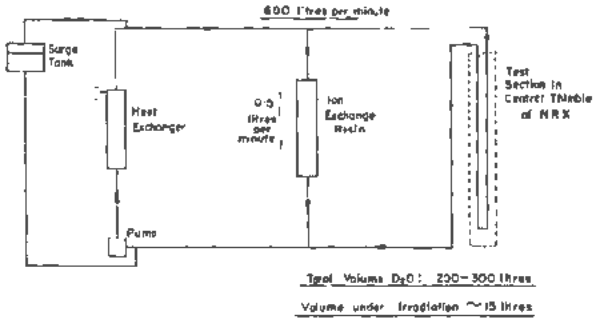

Figure 2. Loop circuit

per million (ppm) to less than 0.1 parts per million when the resins were installed.

In August 1948 a measurement of the decomposition rate of the D_2O at 10 megawatts power showed that about 2 grams were decomposing per hour. This corresponds to an evolution of about 2 litres of electrolytic gas per hour. In January 1951 with the reactor at 26 megawatts the decomposition rate was found to be 0.8 gm D_2O per hour, a factor of 8 less if calculated at the same reactor power. This drop in rate may be attributed to the improved D_2O purity.

D_2O_2 concentrations fluctuate considerably but are never greater than 5 ppm (150 μM) and are usually less than 1 ppm (30 μM).

EXPERIENCE WITH LOOPS

In the centre of NRX there is a vertical irradiation position about 6 inches in diameter which extends the full depth of the calandria. This position, known as the "Central Thimble", is of such a size that quite large scale assemblies may be irradiated in a high thermal neutron flux (5×10^{13} n/cm²/sec). Such an assembly consists of a prototype fuel rod, inserted in the central thimble, and cooled by a stream of D_2O (or H_2O) recirculating in a closed loop. Many such loop experiments have been performed in the central thimble, two of which will be described here.

The first of the experiments, usually referred to as the "Cold Loop",[2] was a joint US, Canadian experiment and was primarily a performance test of a fuel element for a proposed US reactor. The second experiment, the "NRU Loop"[3] was primarily a performance test of a fuel rod for the new Canadian reactor, NRU. In both experiments we were able to obtain valuable information regarding the stability of D_2O under reactor irradiation.

Figure 2 shows a schematic representation of the circulating system normally used in loop circuits. A pump recirculates the D_2O through the test section inserted in the central thimble. Since in most cases the test section consists of a fuel rod, the D_2O is passed through a heat exchanger to keep the temperature in the range 60–70°C. The total volume of circulating D_2O is usually 200–300 litres passing through the test section at about 600 litres per minute. A fraction of the flow, usually 0.5 to 2 litres per minute, is by-passed through ion-exchange columns to maintain the D_2O purity. The surge tank acts as a reservoir to accommodate any fluctuations in the D_2O volume because of changing temperature. This unit may also be used to apply any desired pressure to the circuit. In both experiments the test section, which contained aluminium-sheathed uranium rods, was made from aluminium. The remainder of the circuit was fabricated from stainless steel.

The Cold Loop

This loop operated with a mean D_2O temperature of about 60°C. A continuous flow (~0.5 litres per hour) was maintained through the surge tank, the liquid phase of which was continuously purged by a stream of pure helium at a known flow rate. From analyses of the effluent helium the production rate of gases such as O_2 and D_2 in the loop could be measured. At the start of the experiment, because the proper ion-exchange resin was not available, the specific conductivity of the D_2O was high ($\sim 40 \times 10^{-6}$ ohm^{-1}-cm^{-1}), and the Cl^- ion concentration was found to be 5 parts per million (3×10^{-5} M). At this time the D_2 evolution rate was found to be about 380 cm^3 D_2 (STP) per litre D_2O per day (1 cm^3 gas/l $\equiv$ 45 μ mols/l). The O_2 evolution rate was found to be just half this. When proper resins were added to the circuit the specific conductivity fell rapidly to less than 1×10^{-6} ohm^{-1}-cm^{-1}, and the D_2 evolution rate fell to about 6 cm^3/l/day. Conductivity and D_2 evolution rates remained at these values for the remainder of the experiment. After the clean up of the D_2O the O_2 evolution rate fell to and remained at an unmeasurably low value of less than 0.1 cm^3/l/day. D_2O_2 concentrations were high when gas evolution was high, but fell to below 0.1 ppm (3 μM) when the proper resin was installed. Table II shows the results obtained under steady conditions.

The NRU Loop

This loop operated with a mean D_2O temperature of about 70°C. The flowing D_2O was sampled and analysed directly for dissolved gases, and gas accumulation rates could be measured directly. Data are presented in Table II. The normal D_2 accumulation rate was found to be about 1 cm^3/l/day. On a bypass in this loop there was a unit in which dissolved gases could be stripped from solution by a stream of helium. When this unit was operating the D_2 concentrations fell to a steady value of ~1 cm^3/l (45 μM). Knowing the flow rate of D_2O to the stripper, a production rate for D_2 of 7 cm^3/l/day could be calculated. Throughout this experiment O_2 concentrations remained at 0.1 cm^3/l or less, and D_2O_2 concentrations were normally below 0.2 ppm (6 μM).

During one part of the experiment H_2 was injected into the flowing D_2O to a concentration of 12 cm^3/l. A stoichiometric amount of O_2 was injected into the loop and the resulting gas concentrations followed with time. It was found that two minutes after the O_2 addition the D_2 concentration

had fallen to 7 cm^3/l and eight minutes later it was 0.6 cm^3/l. Since the D_2O was recirculated about twice per minute, the complete recombination must have occurred in under 20 cycles of the D_2O through the test section.

The results of the tests in NRX and in the loops may be summarized as follows:

1. If the purity of the D_2O is maintained at a high level (specific conductivity $\sim 1 \times 10^{-6}$ ohm^{-1}-cm^{-1}) radiation decomposition is negligible.
2. Under these conditions a slow accumulation of D_2 may be observed in the D_2O. If, by some means, D_2 is continuously removed from solution, the resulting D_2 formation rate is higher.
3. O_2 and D_2O_2 concentrations are always extremely low.
4. If the D_2O is allowed to become impure, evolution of electrolytic gas at quite a high rate will be observed.
5. If H_2 and O_2 are injected into D_2O under irradiation extremely rapid recombination will take place.

DISCUSSION

We will now show that the observed experimental results are in agreement with currently accepted theories regarding the radiation chemistry of water. An excellent review has been given by Allen.[4]

Under reactor irradiation we believe that two reactions are occurring simultaneously; the "Forward Reaction," the net result of which is the formation of D_2, D_2O_2 and O_2 and the recombination reaction in which the decomposition products are recombined to form water.

The forward reaction may be represented by

$$2D_2O \longrightarrow D_2 + D_2O_2 \qquad (F)$$

This reaction is usually referred to as reaction F. The D_2O_2 undergoes partial decomposition to O_2. Concurrently, free radicals D and OD are also believed to be formed.

$$D_2O \longrightarrow D + OD \qquad (R)$$

The radicals D and OD are very reactive species, and the recombination reaction is brought about by their reaction with the D_2 and D_2O_2 by a chain reaction,

$$D_2 + OD \rightarrow D_2O + D$$
$$D_2O_2 + D \rightarrow D_2O + OD$$
$$\overline{D_2O_2 + D_2 \rightarrow 2D_2O}$$

the net result of which is recombination of D_2 and D_2O_2 to reform D_2O.

The yield of reaction F thus determines the rate of the forward reaction while the yield of R determines the rate of the recombination reaction. These yields are usually expressed in terms of G, the number of molecules decomposed (or recombined) per 100 ev of energy absorbed. The magnitude of G_R and G_F depend on the type of ionizing radiation. In water irradiated by γ rays G_R is much greater than G_F and hence no net decomposition is observed, but low steady state concentrations of D_2, D_2O_2 and O_2 occur. Under bombardment by heavily ionizing radiation such as α particles, reaction F predominates and hence a net evolution of D_2 and D_2O_2 is observed. In a D_2O moderated reactor the effective radiation is a mixture of γ and fast deuteruns (recoils from fast neutron interactions). Evidently the yield G_R from the γ irradiation is enough to counterbalance the yield G_F from the deuteron bombardment. That is, excess of D and OD are produced, large enough that any D_2 and D_2O_2 produced along the denteron tracks are recombined to D_2O. Hart[5] has shown that in water under γ irradiation, of the H_2O molecules decomposed, 80% will be by reaction R and 20% will be by reaction F. For water irradiated in a heavy-water moderated reactor Hart finds the same relative yields of reactions R and F.

Table II. Operating Conditions of D_2O in Loops

	Cold loop	*NRU loop*
Volume D_2O	300 litres	235 litres
Volume under irradiation	15 litres	11 litres
Reactor power	30 Mw	30 Mw
Mean temperature	60°C	70°C
pH	6.0	5.7
Specific conductivity	0.5×10^{-6} ohm^{-1}-cm^{-1}	$1–2 \times 10^{-6}$ ohm^{-1}-cm^{-1}
D_2 accumulation rates		
Stripping	6 cm^3/l/day	7 cm^3/l/day
No stripping	not measured	1 cm^3/l/day
O_2 evolution rate	negligible	negligible
O_2 concentrations	not measured	<0.1 cm^3/l
D_2O_2 concentrations	~ 0.1 ppm (~ 3 μM)	~ 0.2 ppm (~ 6 μM)

The existence of the recombination reaction was strikingly demonstrated in the NRU loop experiment where H_2 and O_2 added to the loop water were recombined very rapidly. The existence of the recombination reaction may also be demonstrated in another manner. If some reactive substance is added to the D_2O which will remove free radicals from solution, then the recombination reaction will be stopped and the net effect of the forward reaction may be observed. Halide ions are known to be efficient scavengers for D and OD and it is known that the presence of only a few parts per million in solution is sufficient to cause a rapid decomposition of water under reactor irradiation.[6] It will be recalled that when the high decomposition rate was observed in the cold loop the specific conductivity of the D_2O was high and about 5 ppm of Cl^- ion were observed in solution. Assuming an energy absorption rate of about 0.2 watts per gram by the D_2O under irradiation, the yield of the forward reaction may be calculated to be about 0.3 molecules of D_2 produced per 100 ev of energy absorbed, i.e., $G = 0.3$. The usually accepted yield of the forward reaction for water under γ irradiation is $G = 0.5$.[7]

The processes postulated above account in the main for the radiation stability of the D_2O in NRX, but do not completely explain some experimental observations. First, D_2 concentrations may not remain steady, but increase slowly with time and second, the required material balance

$$[D_2] = [D_2O_2] + 2[O_2]$$

is never observed, D_2O_2 and O_2 concentrations being much smaller than D_2. To explain this we must assume two more reactions.

The first is the reaction between D_2O and the metal surfaces,

$$M + D_2O \rightarrow MO + D_2$$

In NRX and the loops M is undoubtedly Al since the corrosion rate of stainless steel at these temperatures is negligible. In the NRU loop an aluminium corrosion rate of about 0.3 mg/dm²/day (4×10^{-4} cm penetration per year) can be calculated from the D_2 accumulation of 1 cm³/l/day. This is in good agreement with the measured rate of Al corrosion in distilled water at 70°C.

The second reaction is the removal of O_2 from solution by various processes

$$X + O_2 \rightarrow \text{removal of oxygen}$$

The most probable process is formation of Al_2O_3, but other processes such as CO_2 formation, NO_3^- formation, etc., undoubtedly occur.

On the basis of the above reactions one would expect, when D_2O is irradiated in a metal system, a net build-up of D_2 in solution and low steady state concentrations of D_2O_2 and O_2. This condition was found in the NRU loop. Conditions will be changed if another reaction occurs in which D_2 is removed continuously from solution, for example by operation of the gas stripper in the NRU loop. Because D_2 is being removed, the recombination chain is being interfered with and the effect of the forward reaction will be more apparent. A steady state D_2 concentration will be observed but the net rate of D_2 removal from the system may be high. In the NRU loop under normal conditions D_2 collected in solution at a rate of about 1 cm³/l/day. When D_2 was removed in the stripper a steady state D_2 concentration of 1 cm³/l was observed but the net D_2 evolution rate from the system was 6 cm³/l/day.

In NRX, D_2 escapes from solution to the helium and one would expect a steady D_2 accumulation there. The reason why D_2 concentrations do not increase in the helium but stay at low steady values is probably due to the fact that D_2 is removed in the recombination unit by reaction with O_2 which may enter the helium system through small air leaks in the blowers, etc.

EXPERIMENTS AT HIGHER TEMPERATURES

An extensive co-operative programme between Canada, USA and Great Britain is now under way at Chalk River, in which several large scale loop experiments are under irradiation in NRX. These loops are similar in principle to those already described but are operated with light water, H_2O, up to temperatures of 300°C and under pressures of about 130 atmospheres. Stainless steel is used throughout as a construction material. The following observations and interpretations have resulted from the operation of these loops:

1. At high temperatures water is no less resistant to reactor radiation than at lower temperatures provided it is kept pure. Actually there is reason to believe that water should show even less radiation decomposition at higher temperatures. Reactions F and R are believed to be temperature independent but the rate of the radical catalysed recombination reaction increases with increasing temperature.

2. Higher rates of H_2 evolution are observed, and dissolved O_2 concentrations are vanishingly small. Peroxides are unstable at these temperatures.

3. An additional reaction, the thermal recombination of H_2 and O_2 becomes important at these temperatures. This is believed to be surface-catalysed.

4. At high temperatures an entirely new problem arises. This is the problem of mass transfer in which corrosion products from the metal piping are selectively deposited in some regions. Deposition may depend on small differences such as temperature and electro-potential gradients and on small amounts of dissolved or suspended materials. In a reactor it has been found also to depend on the radiation intensity. The deposition may be so great that flow channels may be obstructed and heat transfer rates decreased. Because of the selective nature of this deposition the normally observed corrosion rates of stainless steel in pure water at these temperatures, low though they are, produce enough corrosion product to produce this effect.

The corrosion product is normally Fe_3O_4 containing variable amounts of Cr_2O_3 and NiO in solution. The mechanism of its deposition is not yet understood and deserves active investigation. At present it appears that the most promising way to prevent this deposition is to decrease the corrosion rate of the stainless steel. Promising corrosion inhibitors are now being studied.

REFERENCES

1. Unpublished report (July 1951)
2. Heal, H. G., Van Dyken, A. R., Hardwick, T. J. and Robertson, R. F. S., unpublished report (1952).
3. Kreuz, F. H. and Robertson, R. F. S., unpublished report (June 1953).
4. Allen, A. O., *Nuclear Engineering, Part II*, 239-242, (1954). Published by AIChE; Chem. Prog. Symposium Series No. 12, Vol. 50.
5. Hart, E. J., McDonell, W. R., Gordon, S., unpublished report (1952).
6. Allen, A. O., Hochanadel, C. J., Ghormley, J. A. and Davis, T. W., *Decomposition of Water and Aqueous Solutions under Mixed Fast Neutron and Gamma Radiation*, J. Phys. Chem., *56*, 575 (1952).
7. Allen, A. O., *The Yields of Free H and OH in the Irradiation of Water*, Radiation Research *1*, 85 (1954).

Effect of Radiation on Heterogeneous Systems of Air or Nitrogen and Water

By J. Wright, J. K. Linacre, W. R. Marsh and T. H. Bates,* UK

Heavy water and light water are both used extensively in reactors as moderators and coolants, and it is found that close control of purity and acidity is essential to avoid excessive water decomposition and excessive corrosion of metals in the water circuit. Thus, it is undesirable for the pH to remain below about 5 for prolonged periods in a system containing aluminium, whereas for steels at high temperatures, modern boiler practice indicates that pH 10 leads to minimum corrosion. This control cannot be achieved by using buffered systems since excessive radiation decomposition of the water would result from the high salt concentrations, and it is usual to maintain the required purity and acidity by passing a fraction of the circulating water through a suitable ion-exchange unit. Any regular production of acid or alkali is important in the operation of such a system.

Air may leak into the reactor system, and its complete exclusion during periods of maintenance and of fuel rod changing often presents practical engineering difficulties. In view of the well-known effects of electrical discharges on wet and dry air, it is clearly important to see whether acid is produced by the effect of reactor radiation on the heterogeneous system of air and water.

From a practical point of view, three questions may be asked.

1. Is the rate of acid production in a given reactor system so high that it will govern the size of ion-exchanger unit required to maintain a given water purity?

2. Since some systems have no free surface within the reactor itself, while others have a mixture of gas and water under radiation, what are the relative contributions to acid production of air in the gas phase and air in solution?

3. Is it possible to replace the expensive helium normally used in the gas space of low temperature water reactors by nitrogen? (Air would normally be unacceptable because of enhanced corrosion in the presence of oxygen.)

In the course of studies designed primarily to answer these questions, the systems showed features of interest in themselves, and some of the work described below was carried out from a more basic standpoint. Investigations are still in progress, but much of the data required for practical application to reactor systems is now available.

* Atomic Energy Research Establishment, Harwell.

EXPERIMENTAL

Nitrogen and water, and air and water samples have been irradiated in the Harwell pile, B.E.P.O. Samples were prepared from specially purified water which had been distilled first from alkaline potassium permanganate solution and then from acid potassium dichromate solution to remove organic impurities, and finally distilled from a silica flask and stored before use in silica vessels. Nitrogen was freed from small amounts of oxygen by passage through a column of kieselguhr impregnated with activated copper[1] and maintained at 160°C, resulting in an oxygen content less than 1 part per million. Air was washed successively with concentrated sulphuric acid, concentrated alkali, and purified water, before admission to the irradiation vessels.

In all the work described below, the irradiation vessels were sealed silica tubes of 2.0 cm diameter and approximately 50 ml volume. These tubes, containing a known quantity of air or nitrogen and a known volume of water, were irradiated for various times in one of the vertical experimental holes of the Harwell pile. The thermal neutron dose to which the tube was exposed was determined from the activity of an accompanying cobalt foil which was measured against a standard cobalt foil of known activity. From the thermal neutron dose it was possible to calculate the energy deposition in any component of the sample by using the results of a separate investigation[2] in which energy deposition in various materials has been measured calorimetrically as a function of thermal neutron dose in various positions in the reactor.

Chemical changes resulting from irradiation were determined by analysis of solutions as soon as possible after removal from B.E.P.O. This minimum time was dictated by the radioactivity of the aluminium containers in which the tubes were held, but determinations of the more labile species, such as hydrogen peroxide, were usually completed within 3 hours of the end of irradiation. Hydrogen peroxide was measured by the catalysed liberation of iodine from potassium iodide;[3] nitrate was determined colorimetrically, using the phenol-disulphonic acid reagent;[4] Nessler's reagent was used for ammonium ion by a method adapted for the use of a spectro-

photometer;[5] and hydrogen ion was determined from the pH of the solution as measured by a glass electrode. Tests for hydroxylamine and for hydrazine were made using the resorcinol—potassium periodate test[6] for the one and paradimethylaminobenzaldehyde[7] for the other, but neither substance was found in any of the experiments. Hyponitrous acid, which would have been detected in the test for hydroxylamine, was also absent. The accurate determination of nitrite in acid solutions containing excess hydrogen peroxide is difficult because of reaction between the two substances, but any nitrite which might have been present at the end of irradiation would have been detected by the colorimetric method using *N*-1-naphthylethylenediamine dihydrochloride and sulphanilamide.[8] No nitrite was ever observed when the irradiation vessel contained liquid water during irradiation.

RESULTS

For doses up to 10^{18} thermal neutrons per cm^2, the only products found in solution after irradiation of systems containing water and air or nitrogen were nitric acid and hydrogen peroxide. The hydrogen-ion concentration calculated from the measured pH agreed, within experimental error, with that corresponding to the observed nitrate ion concentration. At higher doses, ammonium ion was formed in the nitrogen-water case but not in the air-water systems. Nitrite, hydrazine, and hydroxylamine were not found in concentrations greater than about 2 micromolar under any conditions so far studied.

In order to obtain reproducible results for hydrogen peroxide production, it was necessary to take extreme care over the condition of the silica surface, and pre-irradiation of the vessels filled with water was essential. Such pre-treatment had no effect on the nitrate yield which was reproducible and quite independent of the value obtained for hydrogen peroxide. Since the present paper is concerned primarily with the nitrogenous products, it is sufficient to note that the hydrogen peroxide concentrations obtained at the higher doses were comparable with the observed nitrate concentrations and considerably greater than the nitrate concentrations at the lower doses.

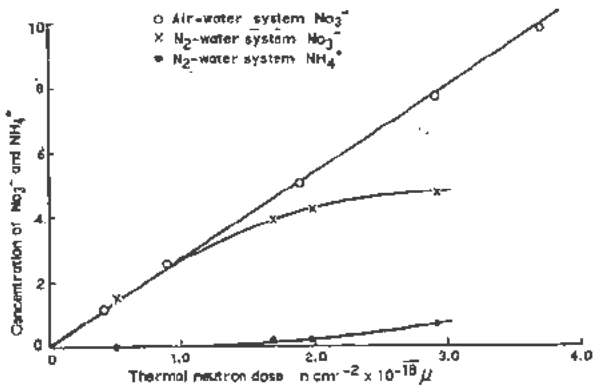

Figure 1. Variation of dose at constant gas/liquid volume ratio of 2.0. Concentration in μM × 10^{-3}

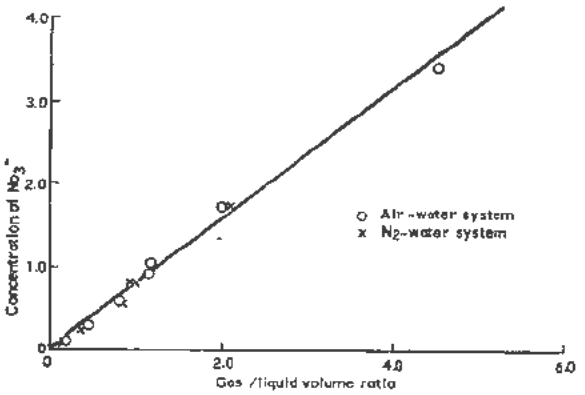

Figure 2. Variation of gas/liquid volume ratio at constant thermal neutron dose of 0.55 × 10^{18} n-cm^{-2}. Concentration in μM × 10^{-3}

The yield of nitrate is shown as a function of dose for the air-water and nitrogen-water systems in Fig. 1 which includes also some points showing the production of ammonium ion in the case of heterogeneous systems of nitrogen and water. The results illustrated in this figure were obtained with tubes filled so that the ratio of gas volume to liquid volume was about 2, and have been corrected where necessary to correspond precisely with the value of 2.0.

The concentration of nitrate was found to depend markedly on the ratio of gas volume to liquid volume, and Fig. 2 gives results for the two systems air-water and nitrogen-water at a comparatively low dose where the ammonium-ion production in the nitrogen-water system was negligible. The corresponding diagram for a higher dose, showing also the behaviour of ammonium ion is given in Fig. 3.

DISCUSSION

It will be seen that all three curves in Fig. 3 extrapolate to zero concentration at low ratios of gas volume to liquid volume, indicating that there is no appreciable reaction in the complete absence of a gas phase. At the lower doses, the nitrate concentration is a linear function of the ratio of gas volume to liquid volume to a first approximation, and this suggests that the yield of the radiation chemical reaction is constant if the calculation is based on the energy deposition in the gas phase only while the much greater energy deposition in the liquid phase is ignored. Both systems give essentially the same results at low doses corresponding to a *G* value (nitrate ions produced per 100 ev of energy absorbed by the gas phase alone) of about 1.1. This agreement in initial yield for systems in which the oxygen concentration differed by a factor of more than 10^3 suggests that the nitrate does not arise from the reaction of nitrogen and oxygen in the gas phase, but rather between nitrogen and water vapour.

In the air-water system, the linear relation between the nitrate concentration and the gas to liquid volume ratio persists to higher doses, but linearity breaks down in the nitrogen-water case at the point where ammonium ion production becomes appreciable. The

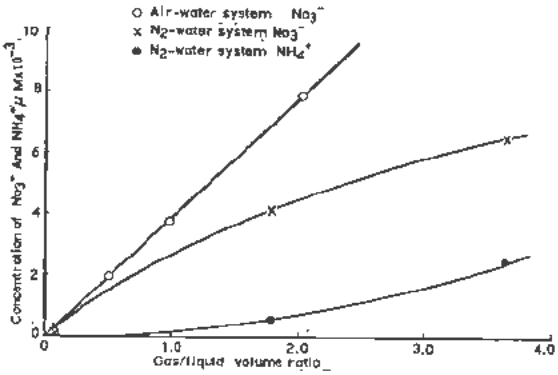

Figure 3. Variation of gas/liquid volume ratio at constant thermal neutrol dose of 2.92×10^{18} n-cm^{-2}

form of the curves in Fig. 3 suggests that there is competition between the processes leading to nitrate ion and those leading to ammonium-ion production.

The relationship between nitrate and dose indicates that this product arises from substances already present at the start of the irradiations, but the asymptotic nature of the ammonium ion curve with respect to the dose axis in Fig. 1 shows that this is a secondary product which must await the formation of some intermediate substance. It is natural to suppose that appreciable ammonium ion production occurs only after hydrogen has accumulated in the gas phase.

A closer examination of the relationship between the absolute amount of nitrate produced and the volume of gas under irradiation, indicates that the two are not related strictly linearly. The departure from linearity is small but real, and is associated with the fact that the diameter of the tubes used in these experiments is comparable with the range of the protons produced by the nuclear reaction, $N^{14}(n,p)C^{14}$, which makes a major contribution to the total energy deposition in the gas phase. This observation is receiving further study, but does not materially affect the application of the above results to practical reactor systems.

APPLICATION TO REACTOR SYSTEMS

It is clear from the results outlined above that calculations of acid production in a reactor system should be based on the energy deposited in the irradiated gas. The yield, $G = 1.1$, corresponds to 0.11 micromoles of nitrate for every watt-second of energy absorbed in the gas. In order to deal with the case of small nitrogen impurities in helium, we shall assume that the yield is independent of nitrogen partial pressure at all concentrations of practical interest. It will also be necessary to assume that all energy absorbed by the main constituent, helium, is available by energy or ionization transfer for the essential steps which lead to nitrate formation.

In the general case of a reactor containing a total of V litres of water in the whole circulating system, and a gas space in which energy is deposited by radiation at the rate of w watts, the rate of acid production is 0.11 w micromoles per sec or 4×10^{-4} w moles per hr, and the rate of increase of acid concentration, p, is given by

$$p = 4 \times 10^{-4} \frac{w}{V} \text{ gm-moles/litre per hr} \qquad (1)$$

If the rate of flow of water through the ion-exchange unit is f litres per hour, and the acid concentration is c gm-moles/litre at time t, the rate of acid removal will be fc gm-moles per hr, and the rate of decrease of acid concentration, r, is given by

$$r = \frac{fc}{V} \text{ gm-moles/litre per hr} \qquad (2)$$

The net rate of change of acid concentration in the system, dc/dt, is then

$$\frac{dc}{dt} = p - r = p - \frac{fc}{V} \qquad (3)$$

which, on integration and applying the condition that no acid is present when the reactor starts up ($c = 0$ when $t = 0$) gives

$$c = \frac{pV}{f}(1 - e^{-ft/v}) \qquad (4)$$

The steady-state concentration finally reached is pV/f, which, substituting for p, gives

$$c_{max} = 4 \times 10^{-4} \frac{w}{f} \text{ gm-moles/litre} \qquad (5)$$

By adjusting f, the amount of the total circulating water which goes through the ion-exchange unit every hour, this concentration must be brought to a value acceptable from corrosion considerations.

As a typical example, we may consider a water-moderated reactor into the 6×10^4 litre helium circuit of which there leak 350 litres of air when the reactor fuel elements are changed. The gas composition when the reactor next operates will be 86.2% He, 13.2% H_2O, 0.5% N_2, 0.1% O_2, and, if the gas space under irradiation is 600 litres, and the thermal neutron flux into this space is 6×10^{11} n-cm^{-2}-sec^{-1}, the total rate of energy deposition into the gas may be assumed to be about 1 watt. With a flow rate through the ion exchanger of 100 litres/hr, Equation 5 indicates that the steady-state concentration of nitrate will be 4 micromolar and, starting with a neutral system, the pH will fall to 5.4, and remain at this value until all the nitrogen is consumed. In the present case in which 12.4 moles of nitrogen were admitted, and conversion to nitrate is only 2×10^{-4} moles per hour, we must consider continuous production for as long as the reactor operates. Most anion exchange resins have capacities in the region of 1 gram equivalent per kilogram, so that a unit containing about 2 kg would have satisfactory performance for several months without regeneration so far as nitrate production was concerned. The flow rates and size of ion exchanger required to deal with this system are not excessive.

It is worth noting that the nitrogen conversion in a reactor system of the type considered above is only about 5 cm^3 per hour. Quite apart from any admission of air which may occur as a result of fuel rod charge and discharge, any steady leakage into the system at a rate greater than 5 cm^3 per hour during operation would lead, ultimately, to the same water conditions as those calculated above. The leak rate is seldom the controlling factor in rate of acid production.

If we consider using pure nitrogen in a reactor of the above type, the energy deposition in the gas space increases to about 7 watts, partly as a result of the greater density, but also because of the marked increase in the energy contribution made by the nuclear reaction, $N^{14}(n,p)C^{14}$. In order to maintain a pH above 5, the flow rate through the inn exchange unit would need to be 280 litres per hour, which is still reasonable, but an ion exchange unit holding at least 7 or 8 kg of anion resin is now required for three months' continuous operation, and this is beginning to approach the limit of convenient size. As a limiting case, a reactor in which 10 ft^3 (280 litres) of nitrogen was exposed to a thermal neutron flux of 10^{13} n-cm^{-2}-sec^{-1} would produce nitric acid at a rate of 0.022 moles per hour, flow rates of 2200 litres per hour (8 gallons per minute) would be required to maintain a pH above 5.0, and an ion-exchange unit containing 16 kg of anion resin would need to be replaced every month.

In high-pressure water systems it is often desirable to limit the number of free surfaces, and the reactor part of such a system may contain no gas space in the radiation field. Nitric acid production in such a system should be quite negligible. In practice, however, local boiling may occur at the surfaces of the fuel elements, and any nitrogen in solution would be brought into the gas phase and react to form nitrate under the influence of the intense radiation at these positions. This behaviour cannot be predicted quantitatively with the data at present available, and more work is needed on such systems.

CONCLUSIONS

Nitric acid production in water reactors to which nitrogen has access may be considerable, and could in certain cases control the size of ion exchange unit required. It is possible to reduce the rate of acid formation by restricting the volume of gas in the radiation field, since reaction occurs only as a result of energy deposited in the gas phase. If the gas space is restricted in this way, it is possible to use nitrogen itself as "blanket" gas in place of the more expensive helium.

REFERENCES

1. Meyer, F. R. and Ronge, G., *Removal of Oxygen from Gases by Means of Active Copper*, Agnew. Chemie, 1939, *52*, 637-8.
2. Anderson, A. R., private communication.
3. Aller, A. O., Hochanadel, C. J., Ghormley, J. A. and Davis, T. W., *Decomposition of Water and Aqueous Solutions under Mixed Fast Neutron and Gamma Radiation*, J. Phys. Chem., 1952, *56*, 575-586.
4. Taras, M. J., *Phenoldisulphonic Acid Method of Determining Nitrate in Water*, Anal. Chem., 1950, *22*, 1020-2.
5. Thompson, J. F. and Morrison, G. R., *Determination of Organic Nitrogen: Control of Variables in the Use of Nessler's Reagent*, Anal. Chem., 1951, *23*, 1153-7.
6. Gopala Rao, G. and Sandara Rao, W. V. B., *A Test for Hydroxylamine and Hyponitrous Acid*, Analyst, 1938, *63*, 718.
7. Watt, G. W. and Chrisp, J. D., *A Spectrophotometric Method for the Determination of Hydrazine*, Anal. Chem., 1952, *24*, 2006-8.
8. Shinn, Martha B., *Colorimetric Method for Determination of Nitrite*, Ind. Eng. Chem. (Anal.), 1941, *13*, 33-4.

Radiolysis of Water in the Presence of H_2 and O_2 due to Reactor Radiation, Fission Fragments and X-Radiation

By P. I. Dolin and B. V. Ershler, USSR

Radiolysis of water is an undesirable process accompanying the operation of reactors, especially heavy-water reactors. The rate of this process should depend considerably on the concentration of H_2, O_2 and impurities dissolved in the water, on the temperature and on other factors. The present paper gives the results of several investigations aimed at determining, on the one hand, the influence of these factors on the rate of radiolysis in an operating reactor itself, and on the other hand, at verifying the mechanism of radiolysis in solutions of H_2 and O_2.

THE RATE OF THE RADIOLYSIS OF WATER DUE TO THE ACTION OF FAST NEUTRONS AND γ RADIATION UNDER STATIONARY REACTOR OPERATION CONDITIONS*

The explosive mixture that is formed in a reactor as a result of radiolysis demands special apparatus and a gas circuit that ensure removal of it from the liquid. This complicates the design of the reactor. Since the size of this circuit depends on the rate of radiolysis, this value is of obvious interest. A determination of this value was the aim of the present investigation.

To a first approximation the rate of radiolysis should be proportional to the amount of radiation absorbed by the water, and, consequently proportional to the reactor power. It may easily be seen, however, that the coefficient of proportionality K, which may be called the specific rate of radiolysis, is itself a function of power, and, in addition, depends on the design of the apparatus.

Indeed, as is well known, the specific rate of the radiolysis of water diminishes with concentration of dissolved H_2 and O_2, and at certain concentration values it becomes equal to zero (details are given below).[1,2] Therefore, in the absence of impurities, this rate for water circulating in a reactor must depend upon the concentration of H_2 and O_2 in the water, and diminishes with the concentration. The steady-state concentration that is established with time depends on the rate of degasification of water, i.e., upon the type of apparatus; in addition, it will obviously vary with the power, and K will thus be dependent on the power.

The character of this relationship may be predicted qualitatively. Indeed, the speed of the transition of an explosive mixture from the liquid to the gas phase of the reactor, all other conditions being equal (i.e., given the same speed for the circulation of the liquid and of the inert gas), is proportional to the concentration of $D_2 + \frac{1}{2}O_2$ in the liquid. On the other hand, the total rate of formation of $D_2 + \frac{1}{2}O_2$ should rise with the power. Since in a steady state both of these rates must be equal, the steady-state concentration of $D_2 + \frac{1}{2}O_2$ being established in the circulating water should also rise with the power. From this it follows that the specific rate of radiolysis of water in an operating reactor should fall with the power. There are no data in the literature that confirm this important conclusion.

EXPERIMENTAL

The investigation was performed on the heavy-water reactor of the Academy of Sciences. In it, degasification of the liquid results from its circulation through a closed liquid circuit including a heat exchanger. During circulation, the liquid comes in contact with a stream of helium. The latter circulates through a gas circuit which has a chamber for the catalytic burning of the explosive mixture. Circulation of the gas may also be achieved when the chamber is not operating. A more detailed description of the equipment is given in the report of A. I. Alichanow *et al.*[3]

The liquid and gas in the equipment was first carefully freed of O_2 and D_2 with the aid of water and helium circulation when the chamber was working. Simultaneously the content of $D_2 + \frac{1}{2}O_2$ in the liquid was determined. When the latter fell sufficiently, the reactor was started up, and, after a definite power was established, the water was periodically analyzed for the $D_2 + \frac{1}{2}O_2$ in it. The typical curves of gas accumulation in the liquid with operation time thus obtained are given in Fig. 1. Here the Y-axis is the content of the explosive mixture in the liquid, and the X-axis the time from the beginning of the experiment. The initial horizontal sections of these curves give the detonating mixture content in the liquid prior to the beginning of operation of the equipment. The curve rises the moment the power is turned on. The curves show that gas accumulation in the liquid is at first linear with time,

---

Original language: Russian.

* This work was conducted in 1950 by M. P. Anikina, B. A. Medzhibovsky, and B. V. Ershler.

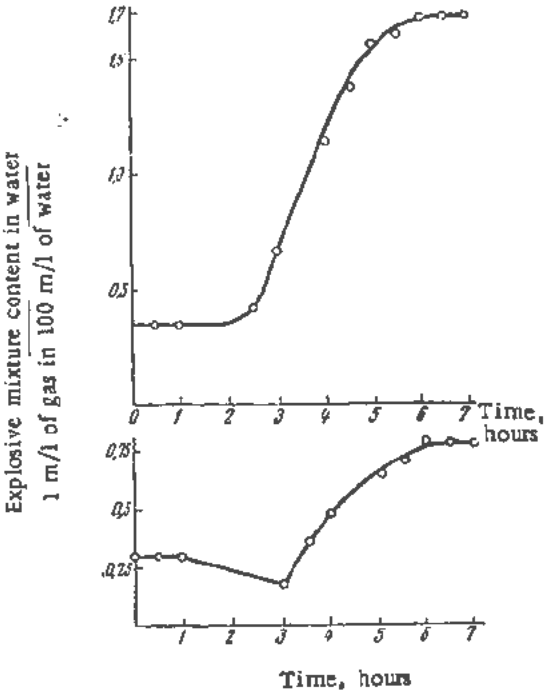

Figure 1. Variation of explosive mixture concentration in liquid with time at a power of 50 kw (lower curve) and 100 kw (upper curve)

and then it slows down and the gas concentration tends to a definite limit, the value of which rises with power.

Table I gives data on the values of saturated concentrations of an explosive mixture measured in such experiments at various power levels.

As may be seen from Table I, the process of radiolysis (depending upon the power and given established operation conditions) takes place in the presence of extremely varied quantities of the dissolved explosive mixture.†

In evaluating the influence of this factor on the specific rate of radiolysis, one should simultaneously consider the accumulation of the explosive mixture in the liquid and gas phases of the equipment. Curves showing such accumulation, obtained at 42, 50, and 105 kw (when the combustion chamber was not working), are given in Figs. 2, 3, and 4.

The lower curve shows the quantity of explosive mixture (in liters) in the gas circuit of the equipment, the second curve shows its quantity (in the same units) in the liquid of the equipment, and the third curve shows the total quantity.

From the lower curves it may be seen that accumulation of the explosive mixture in the gas at first proceeds slowly, after which the rate of accumulation increases, and after a period becomes constant. By the time this constant speed has been established,

† The steady-state values of concentrations of explosive mixture in the liquid depend of course on the efficiency of the system used to remove the gas from the liquid, i.e., on the design of the equipment. The figures given in Table I refer only to the design we studied.

Table I. The Saturation of an Explosive Mixture in the Liquid under Various Operation Conditions

Power (kw)	*Temperature of liquid (°C)*	*Content of explosive mixture in liquid (milliliters of gas/100 milliliters of water)*
38	30	0.85
50	36	1.10
50	60	0.78
100	40	1.69
450	*	3.1

* The temperature varied considerably during the experiment.

accumulation of the explosive mixture in the liquid has virtually ceased. It is this state that corresponds to a steady-state condition.

Table II gives the values of the coefficient K found from such curves, i.e., the quantity of explosive mixture forming per kwh in a reactor under steady-state conditions at various powers.

Table II. The Dependence of the Specific Rate of Radiolysis K (the Rate of Explosive-Mixture Formation in the Reactor in liters/kwh) on the Power

Power in kw	*20*	*50*	*100*	*200*	*400*
K (formation rate of $D_2 + \frac{1}{2}O_2$ in liters per kwh)	0.070	0.052	0.048	0.029	0.016

As may be seen from the table K decreases sharply with power.

From the initial slopes of the uppermost curves in Figs. 2, 3 and 4, calculations may be also made of K for a more or less degassed liquid. The results of such calculations are given in Table III.

The values of K given in the last column of this table depend only slightly on the power, as was to be expected. These values are the maximum possible values since they are measured in degassed water. The mean value of this specific rate, 0.4 liters/kwh,

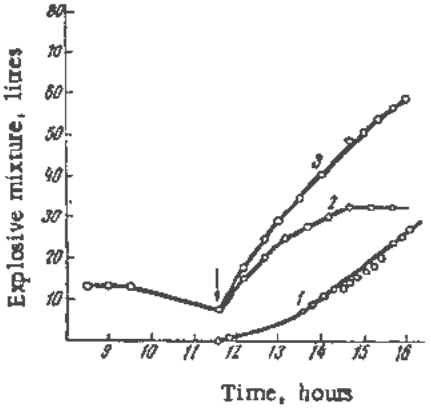

Figure 2. Accumulation of explosive mixture in liquid and gas at 42 kw: (curve 1) accumulation in gas; (2) in liquid; (3) total accumulation

Table III. Rate of Explosive-Mixture Formation in Liters/kwh in Equipment with Degassed Liquid

Temperature °C	Power in kw	Accumulation rate of $D_2 + \frac{1}{2}O_2$ liters/hour	K, specific accumulation rate of $D_2 + \frac{1}{2}O_2$ liters/kwh
35	50	22	0.44
55	42	17.5	0.42
40	105	36.5	0.35

should correspond to "initial yield" of gas during radiolysis, the yield determined in ordinary laboratory experiments with degassed water.[3]

As the data of Fig. 2 show, the actual specific rate of formation of the explosive mixture in the reactor investigated was considerably below this value. At 20 kw, it is 0.18 of the maximum, and at 400 kw it is only 0.04 of the maximum.

THE RADIOLYSIS OF CONTAMINATED WATER AT ELEVATED TEMPERATURES

Since power reactors operate at elevated temperatures and since their construction material is stainless steel, the problem of the radiolysis of water under such conditions is a matter of interest. The literature does not contain any relevant data, with the exception of the important work of Hochanadel[4] in which it is shown that back-reactions of the radiolysis of pure water are accelerated in the case of a temperature rise from 30 to 65°C. In the present work, a qualitative study was made of the influence of temperature on saturation pressures of the explosive mixture. These pressures arise under the action of reactor radiation and fission fragments in water contaminated with certain impurities.

Since radiolysis of water in the reactor takes place chiefly through the energy of fast neutrons, use was made in these experiments of a neutron converter which increased the portion of fast neutrons in the ampoules undergoing irradiation. The converter was a section of a thick-walled cylindrical uranium pipe 120 mm in length with an inside diameter of 32 mm and an outside diameter of 72 mm. The converter was

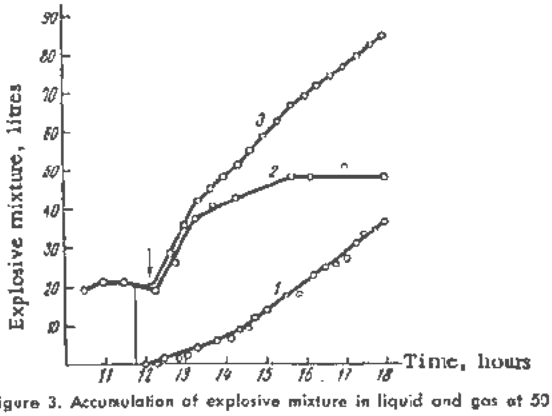

Figure 3. Accumulation of explosive mixture in liquid and gas at 50 kw: (curve 1) accumulation in gas; (2) in liquid, (3) total accumulation

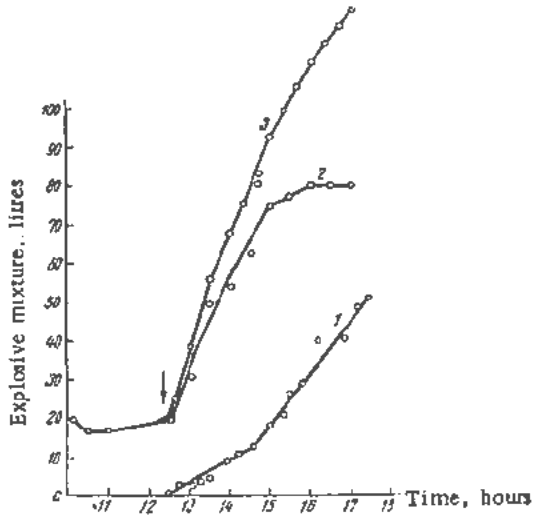

Figure 4 Accumulation of explosive mixture in liquid and gas at 105 kw: (curve 1) accumulation in gas; (2) in liquid; (3) total accumulation

lowered into the experimental hole of the reactor. The specific rate of the radiolysis of water in the converter, as a number of measurements showed, was of an order above the average for the reactor.

Experimental Part

The degassed solutions being investigated were put into small ampoules shown in Fig. 5. The ampoules were sealed in a vacuum. In each ampoule, a noticeable gas space (about ⅓ of the total volume) was left. The ampoule was then placed in a small aluminium test tube of diameter 12 mm and length 100 mm. A spiral that could be heated by an electric current was wound around the test tube, which was then placed in the above-mentioned converter. The temperature in the test tube could be raised to 300°C and could be measured by a thermo-couple. After exposure, the ampoule was cooled, and the pressure of the accumulated detonating mixture was measured by the method of Allen and co-workers.[5]

Figure 5. Ampoule for experiments in irradiation at elevated temperatures

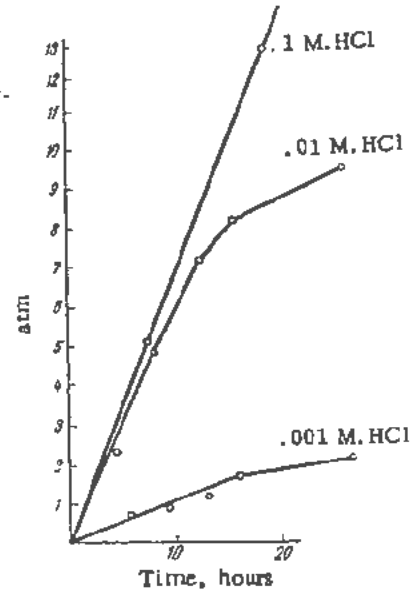

Figure 6. Pressure growth during irradiation in solutions of hydrochloric acid

Figure 6 gives the results of experiments conducted with 0.001 *M*, 0.01 *M*, and 0.1 *M* HCl at a temperature of 40–50°C. Here, and later, the value of the pressure in the ampoule in atmospheres is plotted as a function of exposure time in hours. The power of the apparatus during these experiments was constant (200 kw) and, therefore, the exposure gives the dose value (in conventional units) directly. The curves show the usual inhibiting influence of impurities on back-reactions. The influence is seen in the increase, with impurity concentration, of the saturation pressure of the explosive mixture. In 0.1 *M* HCl, a steady state was not attained at 50°C, even when the pressure of the explosive mixture reached 19 atmospheres.

Figure 7 shows the influence of temperature on the formation of an explosive mixture in 0.01 *M* HCl.

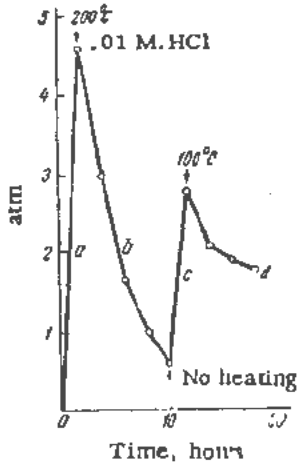

Figure 7. Influence of temperature on radiolysis of hydrochloric acid solution

The initial section of the curve corresponds to irradiation at 50°; here we find the usual linear growth of pressure with time as in Fig. 6. The arrows show the heating start time. Section *b* shows that in passing to a temperature of 200°C the pressure begins to diminish with exposure. On section *c* the temperature again becomes 50°C and the pressure rises; and finally on *d* section the temperature goes up to 100°C and the pressure again diminishes. Such inhibition of the radiolysis of contaminated water produced by temperature, was observed in the case of all the impurities that we studied.

Technically, the most important impurities are those of iron, manganese, chromium, and uranium which may get into the water of the apparatus.

Figure 8 gives data for solutions of 0.01 *M* iron sulfate to which 0.1 and 0.5 *N* sulfuric acid is added to eliminate hydrolysis. In the first case, the pressure reached 3.5 atmospheres, but fell off noticeably at 100°C; as the temperature rose to 200°C it fell to 0.3 atmosphere; in this case, iron hydroxide was precipitated.

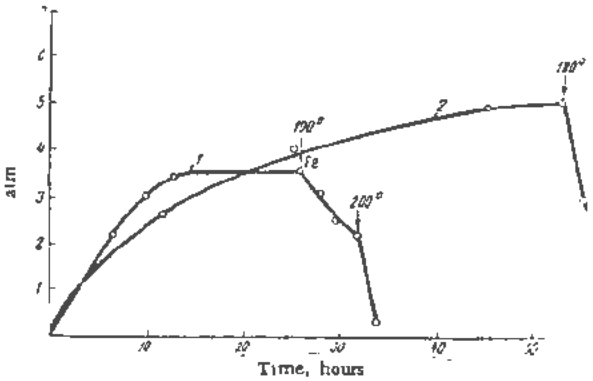

Figure 8. Influence of temperature on radiolysis of water in the presence of ions of iron: (curve 1) 0.01 *M* $FeSO_4$ + 0.1 *N* H_2SO_4; (curve 2) 0.01 *M* $FeSO_4$ + 0.5 *N* H_2SO_4

In a more acid solution, the temperature could be raised to 200°C without hydrolysis; in this case also the pressure in the ampoule fell.

Figure 9 gives the data for a 0.002 *M* solution of chromium sulfate and for a 0.0025 *M* manganese sulfate in the presence of 0.1 *N* sulfuric acid. As may be seen from the curves, heating to 200°C sharply reduces the pressure in the presence of chromium and noticeably in the presence of manganese.

Figure 10 gives the results for a 0.1 *M* solution of uranyl sulfate. At 40°C there is an increase in pressure, and at 180°C it falls sharply. The same may be observed in the case of 0.1 *M* solutions of boric acid (dotted line).

Curves of pressure increase, obtained for the 0.1 *M* solution of uranyl sulfate are also of interest when irradiation of the ampoule was conducted without the converter, i.e., directly in the experimental hole. Under these conditions heating up to 200°C did not even slow down the pressure rise of the mixture ($H_2 + \frac{1}{2}O_2$) in the ampoule, although the pressure

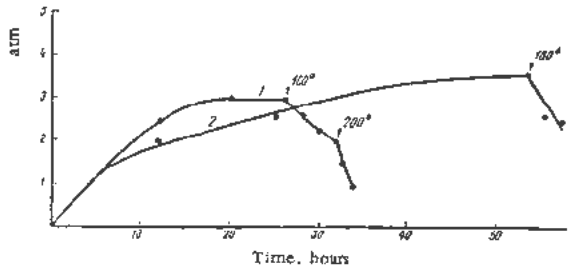

Figure 9. Influence of temperature on radiolysis of water in the presence of ions of manganese: (curve 1) 0.002 M $Cr_2(SO_4)_3$ + 0.1 N H_2SO_4; (curve 2) 0.0025 M $MnSO_4$ + 0.1 N H_2SO_4

reached 30 atmospheres (Fig. 11). It should be noted that under these conditions the radiolysis of water in the ampoule is due, to a great extent, to the energy of fission fragments.

The difference in the radiolysis of solutions containing uranium, when they are irradiated in the converter and also without it, is due to the fact that the uranyl-ion produces a double action in radiolysis. On the one hand, it inhibits back-reactions as any mixture does; on the other hand it accelerates radiolysis through fission. This latter process in general increases saturation pressures. Judging from the behaviour of such solutions during irradiation in a converter, when the fission process is relatively slow, the inhibiting action of the uranyl-ion on the back-reactions of radiolysis of water is light. This is confirmed also by experiments at low temperature in the irradiation of ampoules with a solution of uranyl fluoride, containing H_2 and O_2 at a large pressure. These ampoules were wrapped in cadmium foil so that the fission process in them was virtually excluded. The initial pressure of H_2 in these experiments was five atmospheres, and of O_2 two atmospheres. As may be seen from Fig. 12, the pressure even in a 1 *M* solution of uranyl fluoride during irradiation at 50°C falls, though slowly, to a value close to that reached under these conditions in an ampoule with pure water.

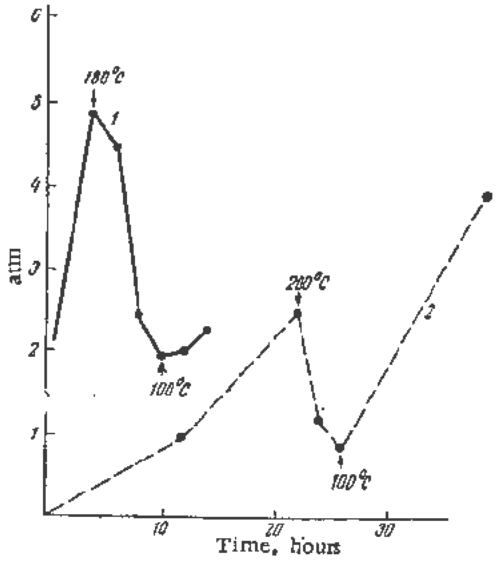

Figure 10. Influence of temperature on the radiolysis of water in the presence of boric acid and uranyl-ion in the converter: (curve 1) 0.1 M uranyl sulfate; (2) 0.1 M boric acid

The experiments described above are not quantitative. However, they show very convincingly that when the water is contaminated with iron, manganese, and chromium (to a value of 100 mg per liter), the saturation pressures of $H_2 + \frac{1}{2}O_2$ in the liquid at temperatures above 200° will be of the order of one atmosphere. Since such extreme contamination of water is excluded in operation conditions, the saturation pressures of the explosive mixture will be extremely small in heterogeneous power reactors with a temperature above 200°C. The behaviour of solutions of uranium is also of practical interest in the case of heterogeneous power reactors, since when the shield shell breaks the metal may get into the water. The course of radiolysis in solutions contaminated with uranium is more complicated, since in such solutions it is due partly to the energy of γ-rays and fast neutrons, and partly to fission fragments.

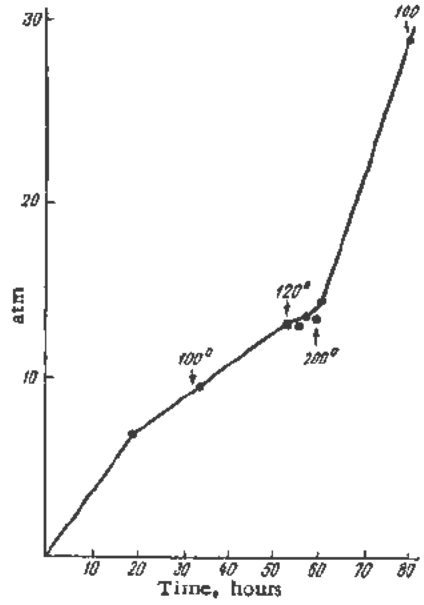

Figure 11. Radiolysis of 0.1 M solution of uranyl sulfate in the experimental hole (outside the converter)

The data of this work showed that an explosive mixture of a stoichiometric composition does not inhibit reactions of radiolysis due to fragments even at a pressure of 30 atm and a temperature of 200°C.

However, the results of the irradiation of concentrated solutions of uranyl fluoride in ampoules wrapped in cadmium foil show that the uranyl ion is a but relatively slightly effective impurity with respect to its inhibitory influence on back-reactions of radiolysis proceeding under the action of fast neutrons.

THE MECHANISM OF THE RADIOLYSIS OF WATER IN THE PRESENCE OF H_2 AND O_2§

D_2 and O_2 dissolved in water influence considerably the process of gas generation in a heavy-water reactor. As is shown above, D_2 and O_2 may, in technical conditions, lower the rate of this process by one order. It was in connection with these observations that the present investigation of the radiolysis of aqueous solutions of H_2 and O_2 was begun.

The influence of dissolved O_2 and H_2 on the radiolysis of water was studied by many investigators,[1,2,4,5] especially by Allen, who proposed an extremely fruitful theory of radiolysis.

However, data concerning the influence of dissolved O_2 on the saturation pressures of H_2, as well as the influence of acidity on the rate of direct reactions of radiolysis is lacking in the literature, apparently because of the difficulties of such measurements.

We worked out a method of determining the quantity of hydrogen being formed in the radiolysis of water in the presence of oxygen in a cell nearly totally filled with the solution, without the cell being opened. One end of the cell (Fig. 13) was a tightly-drawn glass membrane capable of being bent in the case of pressure variation in the cell. The degree of bend of the membrane was determined by measuring changes in the length of the gas bubble placed in the gas-measuring tube soldered to the other end of the cell. An analysis of the gas as to the presence in it of a detonating mixture was done within the cell itself, without its being opened by a spark passed between platinum electrodes soldered into the lower part of the gasometric tube. The gas bubble was equilibrated with the liquid phase by energetic shaking.

A sectional X-ray tube working on a voltage of 65 kv and with an anode current of 200 ma served as the radiation source.

Irradiation was carried out in equal intervals of 15 minutes each. After each of the first five intervals of irradiation, the gas bubble was exploded in order to determine the detonating mixture. Subsequent irradiation was done without exploding the gas. The results obtained are represented graphically in Figs. 14 and 15.

The curves in Fig. 15 have a small horizontal plateau due to the fact that after the first intervals of irradiation the gas in the bubble was exploded. After a certain total dose, the quantity of hydrogen removed from the liquid phase into the bubble (after the regular irradiation period) became constant. The partial pressure of hydrogen fluctuated in a certain range but remained, on the average, constant. As irradiation without explosion of the gas continued, the pressure of the hydrogen again increased until it reached a constant, so-called limit value, depending on the concentration of the dissolved oxygen. The initial yield of hydrogen may easily be found from the

§ This work was conducted in 1951–53 by P. I. Dolin, and S. A. Brusentseva with I. D. Kudryavtsev and A. A. Orlova participating.

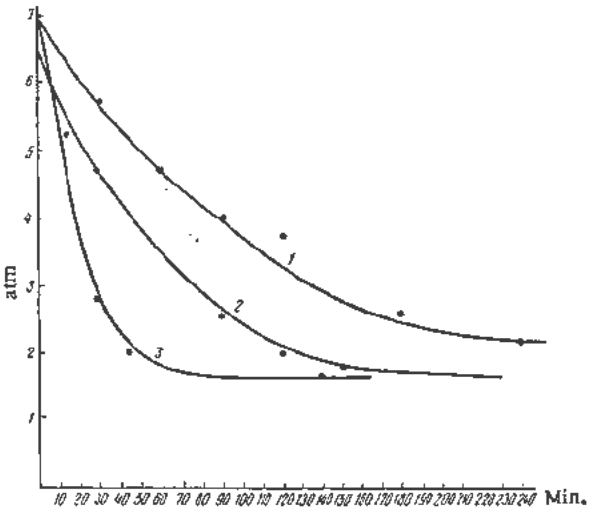

Figure 12. Recombination of explosive mixture during irradiation of ampoules with solutions of uranyl fluoride wrapped in cadmium foil: (curve 1) 1 M uranyl fluoride; (2) 0.01 M uranyl fluoride; (3) water

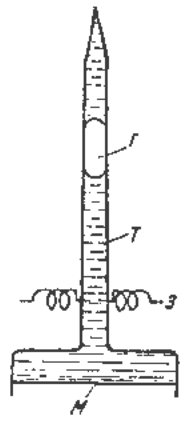

Figure 13. Cell membrane: (M) membrane, (T) gas-measuring tube, (3) platinum electrodes, (1') gas bubble)

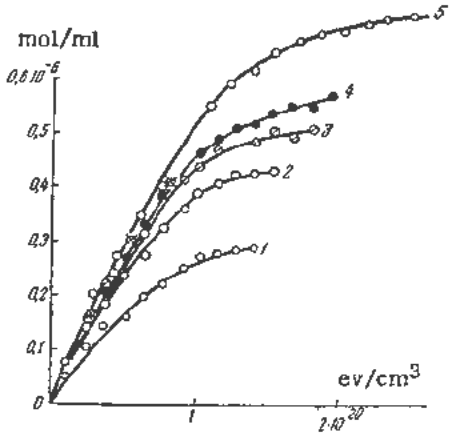

Figure 14. The dependence of the quantity of evolved hydrogen on the dose, given oxygen content in the water in the following concentrations: (1) 0.23 × 10^{-3} mole/liter, (2) 0.53 × 10^{-3} mole/liter, (3) 0.98 × 10^{-3} mole/liter, (4) 1.34 × 10^{-3} mole/liter, (5) 1.88 × 10^{-3} mole/liter. The results obtained from Co^{60} radiation are marked with stars

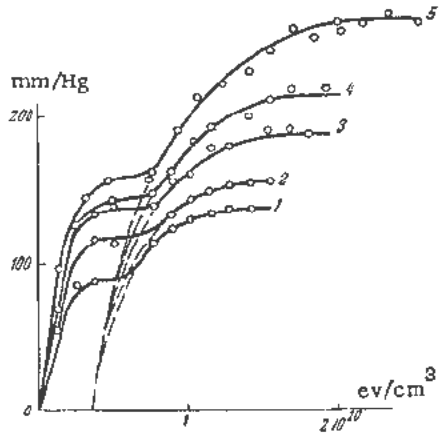

Figure 15. The dependence of the pressure of the evolved hydrogen upon the dose at concentrations of oxygen given in the preceding figure

initial slope of the curve value in Fig. 15 at the end of irradiation. These values, together with the value of the steady-state concentration of hydrogen peroxide, are given in Table IV.

Table IV

Concentration of O_2 m/liter	*Equilibrium pressure of O_2, atmospheres*	*Initial yield of H_2, molecules H_2 per 100 ev*	*Equilibrium pressure of H_2 (mm of mercury)*	*Steady-state concentration of H_2O_2 (M/liter)*
0.23×10^{-3}	0.20	0.26	138	0.28×10^{-3}
0.53×10^{-3}	0.41	0.31	160	0.41×10^{-3}
0.98×10^{-3}	0.70		190	0.70×10^{-3}
1.34×10^{-3}	1.00	from 0.32	220	0.93×10^{-3}
1.88×10^{-3}	1.39	to 0.35	270	1.14×10^{-3}
5.76×10^{-3}*	4.24		370	1.40×10^{-3}

* The experiment was carried out in a glass sphere.

The data of Table IV show that in the concentration range of oxygen from 0.23 to 5.76×10^{-3} M the initial yield of hydrogen increases only by 30%, whereas the saturation pressure of hydrogen increases by three times and the steady-state concentration of hydrogen peroxide by five times.

At gas pressures above two atmospheres, the experiments were conducted in glass spheres. Gas analysis in this case was conducted in a gas analysis apparatus by burning hydrogen on a platinum contact. Measurements were taken when the dose was sufficient to reach a steady state. The oxygen concentration range in which the experiments were conducted corresponded to an equilibrium pressure of from 1 to 23 atmospheres.

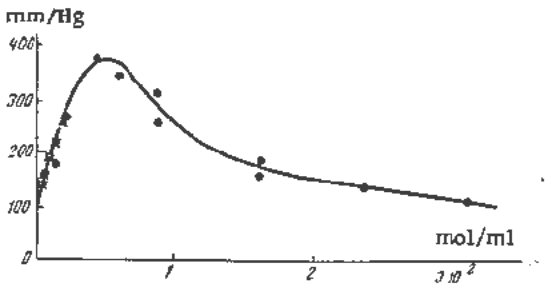

Figure 16. The dependence of the saturation pressure of hydrogen on the concentration of oxygen. The experimental results in spheres are designated by points, in cell membranes by crosses

The results of these experiments are given in Fig. 16. From the figure it may be seen that the initial portion of the curve corresponds to a linear dependence of the saturation pressure of hydrogen on the concentration of dissolved oxygen. For this range of oxygen concentrations there also exists a linear dependence between the saturation pressure of hydrogen and the steady-state concentration of hydrogen peroxide, as may be seen from Fig. 17. In the case of higher concentrations of oxygen, the saturation pressure of hydrogen passes through a maximum and then diminishes without however reaching zero even in the case of an oxygen concentration corresponding to a pressure of 23 atmospheres. Interesting results were obtained from experiments when a solution mixture of oxygen and hydrogen in water was irradiated. As Hochanadel[4] showed, the initial yield of hydrogen peroxide evolution is in this case higher than for a solution of oxygen alone.

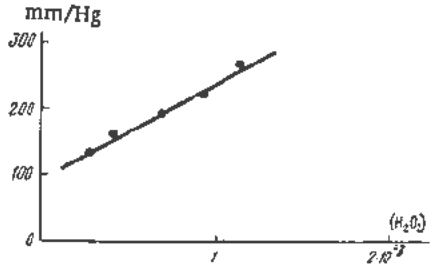

Figure 17. The dependence of saturation pressure of hydrogen on the steady concentration of hydrogen peroxide

We measured the yield of hydrogen peroxide in water containing a saturated mixture of O_2 and H_2 in various ratios. The results are given in Fig. 18. It may be seen from these results that the initial yield of hydrogen peroxide does not depend upon the ratio of concentrations of O_2 and H_2 and is equal to 3.5 molecules/100 ev. This means that a maximum quantity of OH radicals and H atoms is used in the formation of hydrogen peroxide. It should be noted that the initial yield of H_2O_2 is 11 times higher than the initial yield of hydrogen.

The experimental dependence of the pressure of the hydrogen being formed upon the dose, and the connection between the initial yield of hydrogen, its saturation pressure and the steady concentration of hydrogen peroxide for concentrations of oxygen corresponding to the initial linear section of the curve in Fig. 16, may be found theoretically if we take the following mechanism of the radiolysis of water:

$$2H_2O \text{ — ~ —} \rightarrow H_2O_2 + H_2 \qquad (A)$$

$$H_2O \text{ — ~ —} \rightarrow OH + H \qquad (B)$$

$$H_2O_2 + H \rightarrow H_2O + OH \quad (1)$$

$$H_2 + OH \rightarrow H_2O + H \quad (2)$$

$$H + O_2 \rightarrow HO_2 \quad (3)$$

$$OH + H_2O_2 \rightarrow H_2O + HO_2 \quad (4)$$

$$HO_2 + HO_2 \rightarrow H_2O_2 + O_2 \quad (5)$$

In this scheme, reactions A and B give molecular and radical products of the radiolysis of water distributed throughout the whole volume; 1 and 2 are so-called back-reactions, and reactions 3, 4, and 5 suppress the back-reactions and carry out the mutual transition between O_2 and H_2O_2. These reactions together with others were proposed by Allen[5] to explain the radiolysis of water. Here, we limit ourselves to those reactions that are most probable under the given conditions.

From this mechanism it is easy to obtain the following kinetic equation by using the method of steady concentrations for intermediate products and taking account of the fact that the yield of hydrogen peroxide is much greater than that of hydrogen:

$$\frac{d[H_2]}{dt} = K_A J - \frac{K_2 K_B J [H_2]}{K_4 [H_2O_2]_{st}} \quad (1)$$

or in the integral form:

$$[H_2] = \frac{K_A K_4 [H_2O_2]_{st}}{K_2 K_B} \left(1 - e^{-\frac{K_2 K_B J t}{K_4 [H_2O_2]_{st}}} \right) \quad (2)$$

where the various K's are constants of the respective reactions, J is the dose, t the time, and $[H_2O_2]_{st}$ is the steady-state concentration of H_2O_2.

From Equation 2 it may be seen that with the growth of dose Jt, the concentration of H_2 or its pressure tends to the limit

$$(p_{H_2})_{lim} \approx [H_2]_{lim} = \frac{K_A K_4 [H_2O_2]_{st}}{K_2 K_B} \quad (3)$$

A comparison of results computed from Equation 2 with experimental results (the H_2 concentration was recalculated to its corresponding pressure) is given

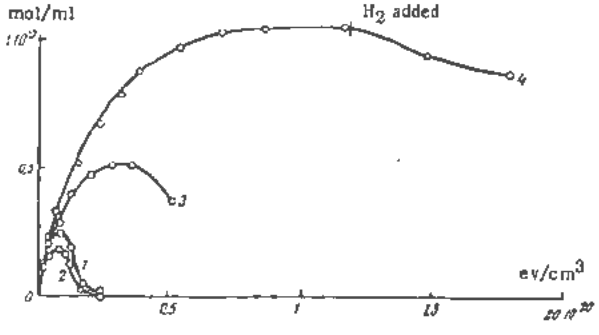

Figure 18. The dependence of the concentration of H_2O_2 evolved on the dose in solutions of a mixture of O_2 and H_2 in water. The initial concentration is: (1) O_2 0.135 × 10^{-3} M/liter, H_2 0.695 × 10^{-3} M/liter; (2) O_2 0.178 × 10^{-3} M/liter, H_2 0.674 × 10^{-3} M/liter; (3) O_2 0.475 × 10^{-3} M/liter, H_2 0.448 × 10^{-3} M/liter; (4) O_2 0.728 × 10^{-3} M/liter, H_2 0.298 × 10^{-3} M/liter

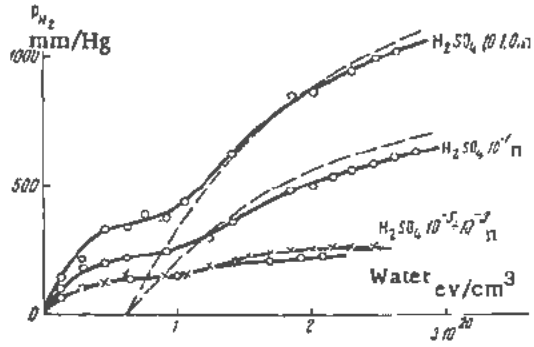

Figure 19. The dependence of hydrogen pressure on the dose in solutions of H_2SO_4 saturated with oxygen. Solid curves describe experiment results, dotted lines the results calculated from Equation 2

in Fig. 15. The solid curves in the upper part and the dotted curves in the lower part were computed from Equation 2; the points represent experimental results. In comparing experimental results with calculated results the small horizontal plateaus on the experimental curves must be excluded; then the calculated curves coincide with the experimental curves with good accuracy. This result is a convincing confirmation of the mechanism of the radiolysis of water given above. However, in the case of a high concentration of dissolved oxygen corresponding to a maximum and to the falling branch of the curve in Fig. 16, Allen's mechanism is insufficient and must be supplemented. But we shall not dwell on that.

Equation 2 also gives good agreement with experiment in solutions of H_2SO_4 from 10^{-5} to 1 N concentration (Fig. 19) if account is taken of the fact the constant K_A and $(H_2O_2)_{st}$ may in this case have other values than those in water because of the influence of the SO_4^{2-} ion on back-reactions. For 10^{-5}–10^{-3} N solutions of H_2SO_4 the calculated curves fully coincide with the experimental curves, whereas for 10^{-2} N and 1 N the experimental and calculated curves do not diverge in the upper part more than 7–10%.

In solutions of KOH, beginning with a concentration 10^{-3} N and higher, there is observed an increase in the initial yield of hydrogen as compared to pure water.

Interesting results are obtained by considering the material balance between the absorbed and evolved oxygen, the hydrogen peroxide formed, and the hydrogen evolved.

The results of this consideration in solutions of H_2SO_4 and KOH are given in Tables V and VI.

From Table V it follows that the material balance in solutions saturated with oxygen is satisfied with an accuracy within experimental error for 0.1 N and 1.0 N solutions of H_2SO_4 only. Its greatest disagreement in excess absorption of oxygen is observed in alkaline solutions of high concentration. As was shown later in a Beckker KOH preparation with which the experiments were performed, there are traces of organic impurities which influence the ab-

Table V. Solutions of H_2SO_4 and KOH Saturated with Oxygen

Solution	Concentration (Normality)	Initial yield of H_2 (molecules/100 ev)	$[H_2O_2]$ st (M/liter)	$[-2O_2+H_2]$ (M/liter)	Excess absorption of O_2 (M/liter)
Water	–	0.33	0.93×10^{-3}	1.59×10^{-3}	0.66×10^{-3}
H_2SO_4	10^{-5}	0.33	1.08×10^{-3}	1.79×10^{-3}	0.71×10^{-3}
H_2SO_4	10^{-3}	0.33	1.25×10^{-3}	1.97×10^{-3}	0.72×10^{-3}
H_2SO_4	10^{-1}	0.47	4.16×10^{-3}	4.32×10^{-3}	0.16×10^{-3}
H_2SO_4	1.0	0.67	5.00×10^{-3}	5.24×10^{-3}	0.24×10^{-3}
KOH	10^{-4}	0.27	1.00×10^{-3}	2.04×10^{-3}	1.04×10^{-3}
KOH	10^{-3}	0.58	1.02×10^{-3}	2.10×10^{-3}	1.08×10^{-3}
KOH	10^{-2}	0.58	0.99×10^{-3}	2.28×10^{-3}	1.29×10^{-3}
KOH	10^{-1}	0.58	1.02×10^{-3}	2.56×10^{-3}	1.54×10^{-3}
KOH	1.0	0.78	0.93×10^{-3}	4.12×10^{-3}	3.19×10^{-3}

Table VI. Solutions of H_2SO_4 and KOH Saturated with Nitrogen

Solution	Concentration (Normality)	Initial yield of H_2 (molecules/100 ev)	$[H_2O_2]$ st (M/liter)	H_2 evolved (M/liter)	O_2 evolved (M/liter)	Excess H_2 generated (M/liter)
H_2SO_4	10^{-5}	0.06	0.0	0.024×10^{-3}	–	0.024×10^{-3}
H_2SO_4	10^{-4}	0.06	0.0	0.026×10^{-3}	–	0.026×10^{-3}
H_2SO_4	10^{-3}	0.10	0.0	0.045×10^{-3}	–	0.045×10^{-3}
H_2SO_4	10^{-2}	0.18	0.04×10^{-3}	0.10×10^{-3}	–	0.060×10^{-3}
H_2SO_4	10^{-1}	0.51	0.11×10^{-3}	0.31×10^{-3}	–	0.20×10^{-3}
H_2SO_4	1.0	1.14	1.09×10^{-3}	1.47×10^{-3}	–	0.37×10^{-3}
KOH	10^{-4}	0.15	0.0	0.05×10^{-3}	–	0.05×10^{-3}
KOH	10^{-3}	1.15	0.16×10^{-3}	1.29×10^{-3}	0.65×10^{-3}	0.48×10^{-3}
KOH	10^{-2}	1.15	0.17×10^{-3}	0.91×10^{-3}	0.27×10^{-3}	0.47×10^{-3}
KOH	10^{-1}	1.45	0.73×10^{-3}	1.10×10^{-3}	0.09×10^{-3}	0.28×10^{-3}
KOH	1.0	0.71	0.83×10^{-3}	0.76×10^{-3}	0.0	0.07×10^{-3}

sence of material balance. However, even in experiments with KOH purified from organic impurities, absence of material balance towards excess absorption of oxygen is observed.

In solutions of KOH saturated with nitrogen (Table VI) absence of balance is observed for those concentrations of KOH for which oxygen is evolved during radiolysis. In concentrated solutions of H_2SO_4 (10^{-1} N and 1.0 N) a deviation of the balance is connected with oxidation of nitrogen; in alkaline solutions oxidation of nitrogen does not take place.

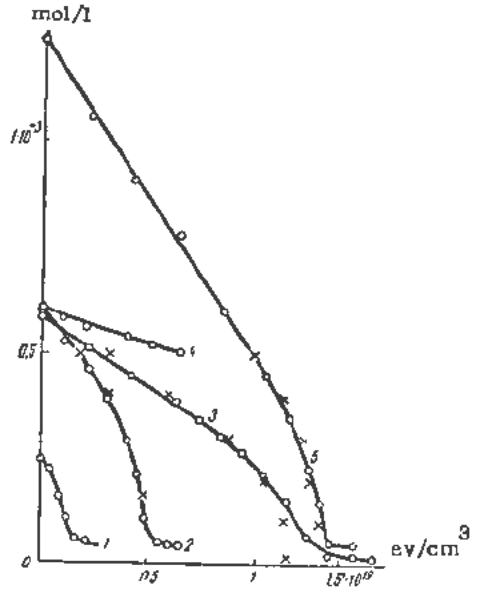

Figure 20. Dependence of concentration of H_2O_2 on the dose: (1, 2 and 5) concentration of $H_2 = 0.84 \times 10^{-3}$ M; (3) 0.42×10^{-3} M; (4) solution saturated with air. Circles designate experimental results, crosses designate calculated results

Deviation in the material balance may be explained by the accumulation in the solution (during radiolysis of water) of a superoxide-like compound of the HO_2 type or of its complex with H_2O_2, and by the electrolytic dissociation of the radicals HO_2 and OH in alkaline solutions.

$$HO_2 \rightleftarrows H^+ + O_2^-$$

$$OH \rightleftarrows H^+ + O^-$$

Apparently, these products are more stable in the dissociated form and therefore will participate more slowly in back-reactions.

Allen and collaborators[1,4,5] were the first to study the reaction of H_2O_2 with H_2 under the action of reactor radiation and γ-rays from Co^{60} in a narrow range of H_2O_2 concentrations. In our work, this range was considerably extended, and, in addition, the concentration of H_2 during the experiment was maintained by constant passage of H_2 bubbled through the solution.

The experimental results are given in Figs. 20, 21, and 22. An analysis of these data shows that the whole investigation range of concentrations of H_2O_2 is divided into four regions, for which the decomposition kinetics of H_2O_2 are different. The empirical kinetics formulae found for these regions are given in Table VII.

For region I, the empirical equation coincides with the equation deduced by Allen and Hachanadel:[5]

Table VII. Kinetic Equations of Decomposition Reactions of H_2O_2

	Region concentration range of H_2O_2 (M/liter)	Kinetic equation	K_1	K_2
I	$0.05–0.5 \times 10^{-3}$	$-\frac{d[H_2O_2]}{d(tJ)} = K_1 + \frac{K_2}{[H_2O_2]}$	$\frac{0.33 \times 10^{-2} \text{ molecule}}{\text{ev}}$	1.3×10^{10} molecule/ev
II	$0.5–2 \times 10^{-3}$	$-\frac{d[H_2O_2]}{d(tJ)} = K = 4.26$ mol./100 ev	–	–
III	$2 \times 10^{-3}–1 \times 10^{-2}$	$-\frac{d[H_2O_2]}{d(tJ)} = K_1 + K_2[H_2O_2]$	$\frac{1.5 \text{ molecule}}{100 \text{ ev}}$	1.8×10^3 molecule/100 ev-mole
IV	$10^{-2}–1.15$	$-\frac{d[H_2O_2]}{d(tJ)} = K_1 + K_2[H_2O_2]^{\frac{1}{2}}$	$\frac{17 \text{ molecule}}{100 \text{ ev}}$	60 molecule/100 ev-(mole)$^{\frac{1}{2}}$

$$-\frac{d[H_2O_2]}{dt} = -K_4 J + \frac{K_2 K_B J[H_2]}{K_4[H_2O_2]}$$

and for regions III and IV deduced by Hart and Matheson.[5] For region II, the mechanism of back-reaction of Allen-Hochanadel must be supplemented by reaction (5).

The kinetic equation for region I coincides accurately, if we disregard its sign, with the equation for the direct reaction of the formation of hydrogen in the radiolysis of water. This permits comparison of the constant K_4 and of the ratio K_2K_B/K_4 (entering into both equations) according to the results related to direct processes and back-processes. In both cases the constants K_4 practically coincide, and the ratio K_2K_B/K_4 in the first case is equal to 2.2 pairs of radicals/100 ev, and in the second case of 2.7 pairs of radicals/100 ev. Such a coincidence of these values, considering the complexity of the experiments, is one more convincing proof of the correctness of the mechanism of water radiolysis used here. If we know the value of $[H_2O_2]_{st}$, it makes possible the calculation (according to the back-reaction) of the value of the saturation pressure of hydrogen in the direct reaction, given any dose.

The measured results of the rate of the reaction of H_2O_2 with H_2 in solutions of H_2SO_4 and KOH are given in Figs. 23 and 24.

These results confirm the fact that an increase in the hydrogen yield during radiolysis in these solutions is connected with retardation of the back-reaction.

There are no data in the literature concerning the influence of temperature on the radiolysis of water in a broad temperature range. We investigated radiolysis due to X-rays and a so-called mixed reactor radiation (fast neutrons plus γ-rays) at

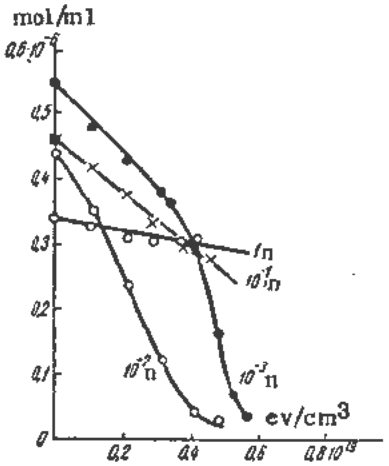

Figure 23. The kinetics of the reaction $H_2O_2 + H_2$ in solutions of H_2SO_4. Variations of H_2O_2 concentrations with dose

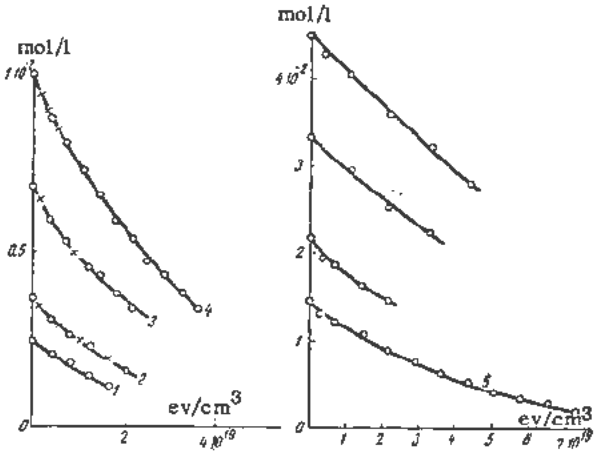

Figure 21. The dependence of H_2O_2 concentration on dose for solutions with various initial concentration of H_2O_2: concentration H_2 = 0.84×10^{-3} M

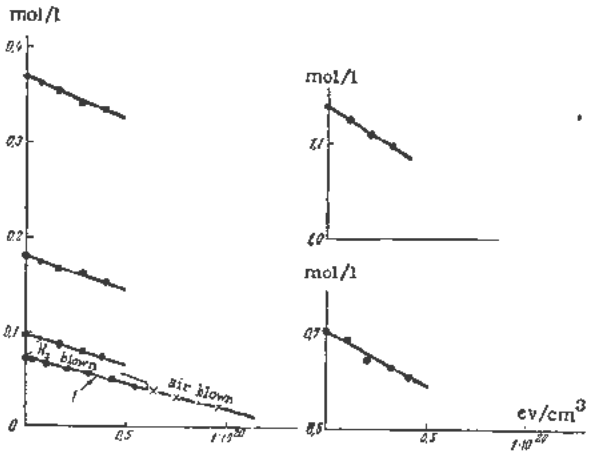

Figure 22. Dependence of H_2O_2 concentration on dose. All solutions, with the exception of 1, are saturated with air

temperatures up to 280° in water saturated with oxygen in a solution of 10^{-3} KBr. The experiments were conducted in quartz spheres. The dose corresponded to that of the steady-state reaction. The results, recalculated to the quantity of hydrogen evolved in moles per cm^3 of solution, are given in Figs. 25 and 26.

As may be seen from the figures, the evolution of hydrogen ceases (under the action of X-rays) at a temperature of 100°; and at a temperature of about 200° in the case of reactor radiation. In the presence of KBr, suppression of explosive mixture evolution is not achieved at 200° for X-rays and 280° for reactor radiation.

The influence of temperature on hydrogen evolution during radiolysis of water is connected with a reduction of the activation energy of the slowest back-reactions (1) and (2). Since the concentration of OH radicals and H atoms (distributed throughout the body of the solution) in the case of "heavy" radiation (fast neutrons) is less than for "light" radiation, given a comparable value of the dose power, a greater temperature rise is obviously necessary in order to accelerate the back-reactions in the same degree. In this case, the effect of an addition of KBr, which lowers the concentration of radicals in the body of the solution, is similar to changing from "light" to "heavy" radiation.

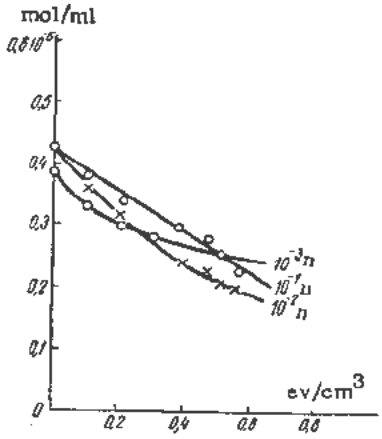

Figure 24. The kinetics of reaction $H_2O_2 + H_2$ in solutions of KOH. Variation of H_2O_2 with dose

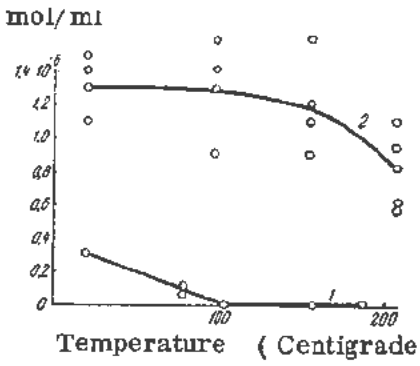

Figure 25. Dependence of the quantity of hydrogen evolved on temperature during irradiation with X-rays: (1) water saturated with oxygen; (2) 10^{-3} M KBr solution saturated with air

CONCLUSION

The investigation of the radiolysis of moderator water in an operating reactor showed a one-order reduction in the formation rate of $D_2 + \frac{1}{2} O_2$ per unit of power with the growth of the total reactor power; this is due to acceleration of back-reactions with growth of D_2 and O_2 concentrations in the circulating water. In other investigations it was shown that a temperature rise of 200°C reduces considerably the saturation pressures of H_2 and O_2 during the radiolysis of water proceeding from reactor radiation, but not, however, from fission fragments.

Thus, saturation pressure values and the rate of radiolysis in the presence of various quantities of H_2 and O_2 is of obvious practical interest; however, the existing data in the literature are insufficient for their determination.

To verify these values and also the mechanism of the radiolysis of water, the latter was studied in aqueous solutions of O_2 under the action of X-rays. It was found that the saturation pressure of H_2 at first grows linearly with an increase in the concentration of dissolved O_2; it then passes through a maximum after which it diminishes. These data show that the accepted schemes of the radiolysis of water for more concentrated solutions of O_2 are incomplete. An equation has been introduced for calculating saturation pressures of H_2 in the presence of O_2 in the region of a linear dependence of the saturation pressure of H_2 on the concentration of O_2.

It is shown that in alkaline solutions there takes place an accumulation of noticeable quantities of superoxide compounds.

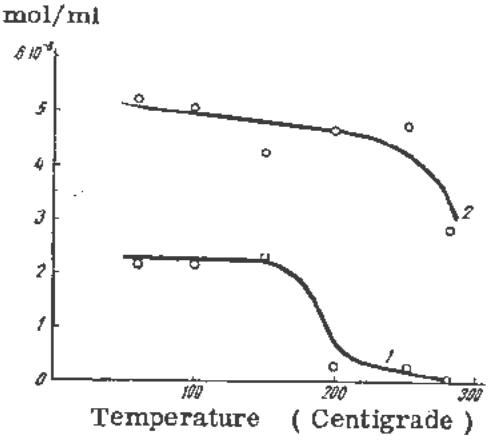

Figure 26. Dependence of the quantity of hydrogen evolved on temperature from reactor radiation: (1) in water saturated with air; (2) in 10^{-3} M KBr solution saturated with air

REFERENCES

1. Allen, A. O., J. of Phys. and Coll. Chem, *52*, 479, (1948).
2. Dainton, F. S., *ibid*, *52*, 490, (1948).
3. Alichanow, A. I. *et al.*, P/623, "Experimental heavy water physical reactor," Volume 2, Session 9A, these Proceedings.
4. Hochanadel, C. J., *ibid*, *56*, 587, (1952).
5. Allen, A. O., Hochanadel, C. J., Ghormley, J. A. and Davis, T. W., *ibid*, *56*, 575, (1952).
6. Hart, E. J. and Matheson, M. S., Discussions of the Faraday Society, N 12, 169, (1952).

The Decomposition of Water by Fission Recoil Particles

By J. W. Boyle,* C. J. Hochanadel,* T. J. Sworski,* J. A. Ghormley* and W. F. Kieffer,† USA

The fission recoil particle is a relatively new radiation entity whose effects are to be studied and compared with those of γ-rays, electrons, α-particles, etc. The primary purpose of this investigation was to obtain reliable values of gas yields for the reactor engineer since the effects of fission fragments on water are of prime importance in the design of any aqueous homogeneous reactor. The radiation chemistry associated with the fission process is of particular interest because the rate of energy loss in a fission track is over an order of magnitude greater than that for any other known radiation.

In this paper are presented initial yields of gas production for aqueous solutions of UO_2SO_4, UO_2F_2, $UO_2(NO_3)_2$ and $U(SO_4)_2$ determined as a function of uranium concentration, isotopic enrichment, temperature and hydrogen ion concentration. Effects of the oxidation state of the uranium, of different anions, and of added solutes also have been considered.

EXPERIMENTAL

The majority of irradiations were made on 0.5 ml samples of solution in fused silica ampoules drawn from 4–5 mm diameter silica tubing. The liquid occupied about half the ampoule volume. All samples were carefully degassed on the vacuum line before sealing. Each ampoule was provided with a tip which could easily be broken off in the vacuum line for gas analysis. Samples highly depleted in U^{235} were larger so as to provide more gas for analysis. Concentrated samples highly enriched in U^{235} were much smaller to prevent any appreciable self-shadowing. Pile irradiations were made in a cooled hole of the Oak Ridge Graphite Reactor. Sample temperatures of 120°C and above were maintained by a controlled electric furnace.

After irradiation the samples were allowed to stand for a period of about one day to allow decay of induced radioactivity and permit safe handling of samples during analysis. Yield values may be a few per cent low because the post irradiation back reaction induced by fission product activity predominates over the forward reaction. With Br^- present the back reaction would be observed.

Ampoules were broken open in a vacuum system and evolved gases were analyzed using the Saunders-Taylor[1] semi-micro technique in which H_2 and O_2 were burned on a platinum filament.

Peroxide in solution was determined both from the stoichiometric excess of H_2 and also by direct analysis using a spectrophotometric method to detect IO_3^- formed by the oxidation of I^- by peroxide.[2] The optical density was measured at 3750 Å instead of 3500 Å, the wave length of maximum absorption for the triiodide ion. At 3750 Å the absorption of uranyl ion does not interfere as much as it does at 3500 Å. The molar extinction coefficient at 3750Å and 250°C was 17,500. The absorption followed Beer's law over the forty-fold range of concentration studied from 10^{-4} to 4×10^{-3} *M*.

Some irradiations were made in micro ampoules (only about 0.1 ml of solution required) which permitted measurement of total pressure without opening. The method of determining pressure in an ampoule by measuring the boiling temperature of the solution has been described previously.[2]

Irradiations in a Co^{60} source[3] at an intensity of about 4000 r per minute were made in pressure indicating ampoules (approximately 30 mm ID by 50 mm over-all length). These ampoules also contained a platinum filament for combusting gases. The composition of the hydrogen-oxygen gas, and by difference the peroxide present in solution could be determined at any time during the irradiation sequence.

RADIATION DOSIMETRY

The energy absorbed in pile irradiated uranium solutions is contributed by fission recoil particles, beta-particles, fast neutrons and gamma-rays. The majority of the energy absorbed in most of the samples studied was from fission recoils.

As a rough measure of relative dose, the product of pile power and irradiation time may be used. It was found, however, that for a given pile power and position, the thermal flux as determined by monitors, varied as much as 5% from day to day. A monitor (~25 mg of Al-Mn-Co alloy, 0.7% Mn) was included with each irradiation in order to measure relative dose. The Mn^{56} activity was measured in a 4 π ionization chamber after allowing short lived activities, such as 2.4 min Al^{28}, to decay for about two hours. It was assumed that the activity as measured with the manganese monitors was a relative measure of total dose.

* Oak Ridge National Laboratory.
† College of Wooster, Wooster, Ohio.

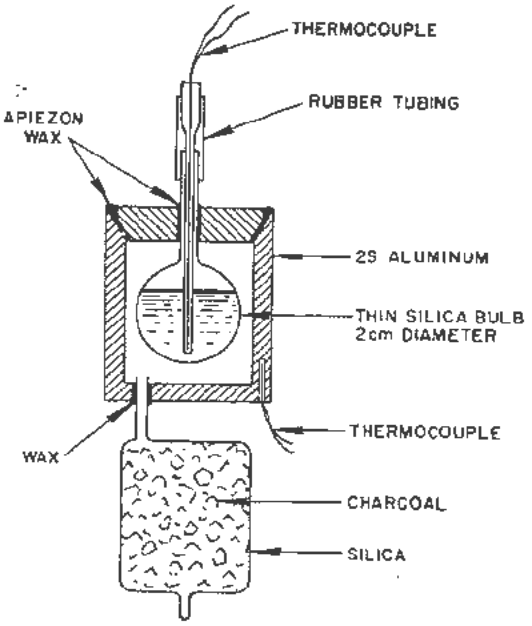

Figure 1. Calorimeter for measuring reactor radiation absorbed in water and uranium solutions

The absolute measure of energy absorption in solution was based on adiabatic calorimetric measurements of rate of energy absorption in pure water and in uranyl sulfate solutions containiog natural uranium at two concentrations.

The fission energy absorbed in solution, as calculated from activity induced in a manganese monitor irradiated with the calorimeter, agreed with the calorimetric measurement within 0.5%. The values for constants used in this calculation were σ_f for $U^{235} = 549$ barns, σ_a for $Mn^{55} = 13$ barns, $t_{1/2}$ for $Mn^{56} = 2.59$ hr with the decay scheme proposed by Mitchell[4] and the energy absorbed in solution per fission = 173 Mev.

The calorimeter, shown in Fig. 1, consisted of a cylindrical aluminum jacket in which was placed the water or solution contained in a silvered, thin-walled silica bulb insulated by a vacuum. The charcoal getter was baked out, the system evacuated and sealed off immediately prior to irradiation. Copper-constantan thermocouples were placed in both the sample and in the aluminum jacket and temperatures were followed with a potentiometer during irradiation. Typical time-temperature curves for sample and jacket during irradiation are shown in Fig. 2. The rate of energy absorption in the sample was calculated from the heat capacity of the sample plus silica bulb and the rate of temperature rise of the sample when the temperatures of sample and jacket were identical. This required 68 minutes irradiation time for 44.6 gm U/l solution and 30 minutes for the 297 gm U/l solution. The calorimetric data are summarized in Table I. It was assumed that energy absorption in the silica bulb was negligible compared with absorption in solution. However, some gamma and neutron energy was expended in the silica and for measurements on pure water this correction could amount to a few per cent. The result obtained for pure water is in good agreement with that obtained by Richardson,[5] 0.0209 cal-ml^{-1}-Mw^{-1}-min^{-1}, using an isothermal method. The work of Richardson also indicated that about 34% of the pile energy absorbed in H_2O is by gamma-rays and 66% by neutron scattering. In estimating the ratio of fission energy to total energy absorbed in pile irradiated solutions, it was assumed that gamma absorption and neutron scattering was the same for solutions as for pure water. This assumption is obviously not strictly valid, but for this estimate a detailed and laborious calculation was not warranted.

Yields reported for gamma-rays were based on a yield for ferrous sulfate oxidation of 15.6 Fe^{++} per 100 ev which had been calibrated both by calorimeter and by ion chamber measurements.[6]

PRODUCTS OF IRRADIATION

The products found were mainly those resulting from the decomposition of water: H_2 and O_2 gases and peroxide. In all cases where the temperature of the sample was maintained at 100°C or above during irradiation, the H_2/O_2 was nearly 2/1, indicating that nearly all of the peroxide assumed to be intermediate to O_2 production had been thermally decomposed. In one series of samples (natural UO_2SO_4, 44 gm U/l), direct measurement of peroxide gave a yield within 10% of the gas analysis yield for H_2. This was found to be true only if the samples were frozen immediately after irradiation and analyzed quickly upon thawing. One hour's waiting between the thawing and analyzing further lowered the yield by 15%, indicating the significance of the room temperature decomposition of the peroxide.

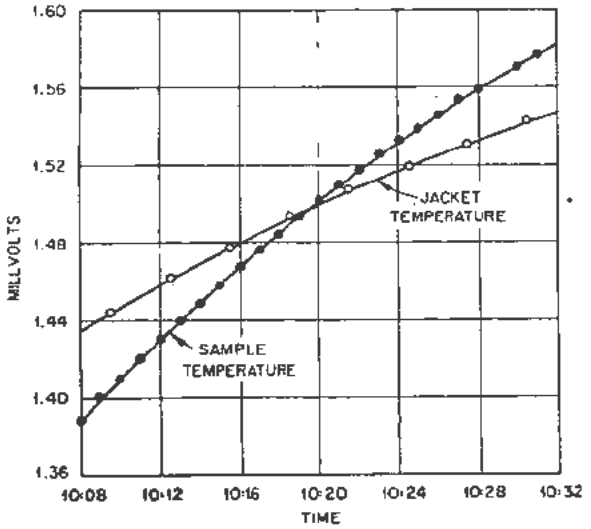

Figure 2. Typical time-temperature curves of calorimetric measurements in the reactor

Table I. Calorimeter Results for Rate of Energy Absorption in Water and Uranyl Sulfate Solutions

		Solutions natural UO_2SO_4	
	Water	44.6 gm U/l	297 gm U/l
U^{235}, gm/l	0.0	0.321	2.14
Pile power, Mw	3.85	3.70	3.55
Temperature, °C	38	37	33
Temperature rise, °C-min^{-1}	0.076 ± .0015	0.201 ± .002	0.888 ± .009
Weight solution, gm	2.04	1.90	2.49
Weight silica, gm	0.25	0.44	0.41
Solution C_p, cal-gm^{-1}-deg^{-1}	1.00	0.95	0.73
Heat capacity, cal-deg^{-1}	2.09	1.89	1.90
Energy absorbed, cal-min^{-1}	0.159	0.380	1.69
cal-ml^{-1}-min^{-1}	0.078	0.212	0.943
cal-ml^{-1}-Mw-min^{-1}	0.0202	0.0572	0.265

In nearly all ampoules analyzed, a small amount of CO_2 was found, probably resulting from oxidation of trace organic impurities in the solutions.

In none of the investigations of uranyl sulfate or fluoride solutions was there any evidence for the decomposition of the solute species. It was found that during irradiation with Co^{60} gamma-rays, SO_2 could be swept out of 18 *M* H_2SO_4 and 11 *M* H_2SO_4 solutions, but none could be detected from 0.4 *M* H_2SO_4 or 297 gm U/l UO_2SO_4 solutions. On analyzing solutions after irradiation, during which there was no sweeping, no SO_2 was detected. These results would indicate that back reaction (oxidation of SO_2) is very rapid and therefore the steady state concentration of reduction products of the anion is very low.

The gases found in irradiated ampoules containing uranium in the (IV) oxidation state were all deficient in O_2. After the ampoules had been opened and the gases analyzed in the usual manner, samples of the remaining solution were removed and analyzed. By comparing the resulting U(IV)/U(VI) ratio with the corresponding value for the solution before irradiation, the amount of U(IV) oxidation to U(VI) could be calculated. The values thus found for 10 samples accounted for the difference between the observed amount of O_2 gas and that expected from the stoichiometric ratio of ½ the H_2 gas produced. The fact that some O_2 gas was found, even in the presence of sufficient U(IV) to completely remove it, can probably be explained by the decomposition of the peroxide intermediate into O_2 gas and its diffusion into the gas phase before it had opportunity to react with the solute U(IV). This was tested by irradiating ampoules filled with solution to leave a negligible amount of free gas space. The gases from these contained only 2.2% of the stoichiometric amount of O_2 gas, whereas in ampoules where the gas volume/liquid volume ratio was about unity, the O_2 gas was 17.2% of the stoichiometric amount. The solutions with little gas space showed a correspondingly larger amount of U(IV) oxidation.

It was concluded from the stoichiometry found for H_2, O_2 and peroxide on irradiating uranyl solutions in the pile that U(VI) was the stable valence state under radiation and that at the steady state the concentrations of other valence states were very small. These studies with U(IV) solutions confirmed this conclusion. It was also shown that U(VI) was the stable form in irradiating solutions with gamma-rays. By spectrophotometric analysis, it was shown that 10^{-3} *M* and 10^{-2} *M* U(IV) in 0.1 *M* H_2SO_4 irradiated with cobalt γ-rays were oxidized completely to U(VI).

Two sets of ampoules containing concentrated $UO_2(NO_3)_2$ solutions were found to give other than the typical electrolytic ratio of hydrogen to oxygen. Natural $UO_2(NO_3)_2$ (318 gm U/l) and 8.8% enriched $UO_2(NO_3)_2$, (420 gm U/l) were found to give relatively large amounts of non-condensable gas which was inert to combustion with either added excess O_2 or H_2. Its identity as N_2 was established by spectroscopic examination. In these cases H_2 and O_2 were present in nearly equal amounts. Irradiated dilute $UO_2(NO_3)_2$ solutions, highly enriched in U^{235}, yielded only H_2 and O_2 in stoichiometric amounts.

These data suggest that nitrate ion was decomposed by pile irradiation when present in concentrations of 318 gm U/l or greater. Such decomposition of nitrate ion was not unexpected since it was known that during irradiation with X-rays or gamma-rays, both oxidized and reduced forms exist at equilibrium.[7] It was surprising to note that nitrate was reduced all the way to N_2. A more thorough study of nitrate radiation stability is in progress.

FACTORS WHICH AFFECT H_2 GAS YIELD

The extent of net decomposition of water by radiation is most reliably indicated by the amount of H_2 gas produced, since the oxidant from water decomposition is usually divided among a variety of products. The yield of gas per energy input is expressed in terms of the *G* value, defined as the number of molecules of H_2 gas produced by the absorption of 100 ev of energy. It was found that G_{H_2} depended on a number of variables: type of radiation, concentration of uranium, and pH of the solution.

Table II. Initial Rates of H_2 Production from Reactor Irradiated Uranium Solutions

	Concentration gm U/l	Enrichment gm U^{235}/l	Fission energy / Total energy	pH	G_{H_2}
UO_2SO_4	0.399	Enrichment over 90% U^{235}			1.61
	4.03	Enrichment over 90% U^{235}		3.26	1.66
	18.6	1.63	0.906	2.90	1.48
	38.1	0.274	0.619		0.95
	40.7	Enrichment over 90% U^{235}		2.42	1.53
	102.1	37.4	0.995	2.00	1.35
	105.2	38.9	0.995	0.10*	1.20
	108.4	40.1	0.995		1.35
	202.3	0.063	0.273		0.69
	202.5	37.6	0.995	1.61	1.11
	203.4	Enrichment over 90% U^{235}			1.11
	227.0	1.63	0.906		0.98
	310.4	0.096	0.364		0.62
	386.0	1.63	0.906		0.80
	431.3	37.8	0.995	1.32	0.77
	436.8	3.10	0.949		0.73
	477.2	0.148	0.467		0.56
	713.5	33.5	0.995		0.56
	796.0	37.4	0.995	1.03	0.49
UO_2F_2	4.25	Enrichment over 90% U^{235}		4.25	1.63
	40.1	Enrichment over 90% U^{235}		3.32	1.58
	118.8	37.1	0.995	2.98	1.36
	272.0	37.2	0.995	2.64	1.11
	377.0	39.3	0.996	1.35*	0.84
	405.7	42.3	0.996	2.41	0.95
$UO_2(NO_3)_2$	4.24	Enrichment over 90% U^{235}			1.63
	42.3	Enrichment over 90% U^{235}		2.05	1.5
	318.0	2.29	0.932	1.03	0.6
	420.1	36.0	0.994	0.60	0.55
$U(SO_4)_2$	42.2	Enrichment over 91% U^{235}		1.95	1.45
	92.5	35.1	0.996	0.1	1.25
	350.0	32.0	0.995	0.1	0.75

* pH was adjusted by adding acid.

The data which are pertinent to demonstrating the effect of variables on G_{H_2} are summarized in Table II. These figures represent the average of from three to six determinations for each point. The results of individual experiments agreed within 2% or better. In cases where H_2 gas yield was not linear with doses employed (as discussed in the following section), the tabulated value is either for an extrapolated initial yield or for G_{H_2} obtained from samples containing added Br^- ion.

In Fig. 3 the yield of H_2 is shown as a function of energy input for various types of radiation. The fission energy contribution is >99.5% in the enriched solutions, 90.6% in the natural uranium solutions, and only 27.8% of the total energy in the depleted solutions. The rest of the energy is contributed by γ-rays and fast neutrons. Fission energy as used in this paper only includes the energy from the fissioning taking place in the sample solution. Probably 95% of this energy comes from fission fragment recoils and the rest from radioactive fission products, prompt neutrons, etc. It is immediately evident from the graph that the hydrogen yield is less for lower ratios of fission energy to total energy.

A leveling off with increased dose was observed for all solutions of pure UO_2SO_4 except those in which essentially all the energy was from fission. This suggests that a radiation-induced back reaction occurred in the former solutions. It has been shown[2] that bromide ion effectively inhibits radiation-induced reactions involving H and OH free radicals. The dotted lines in Fig. 3 show that the yield in the presence of Br^- does not fall off, but maintains the initial

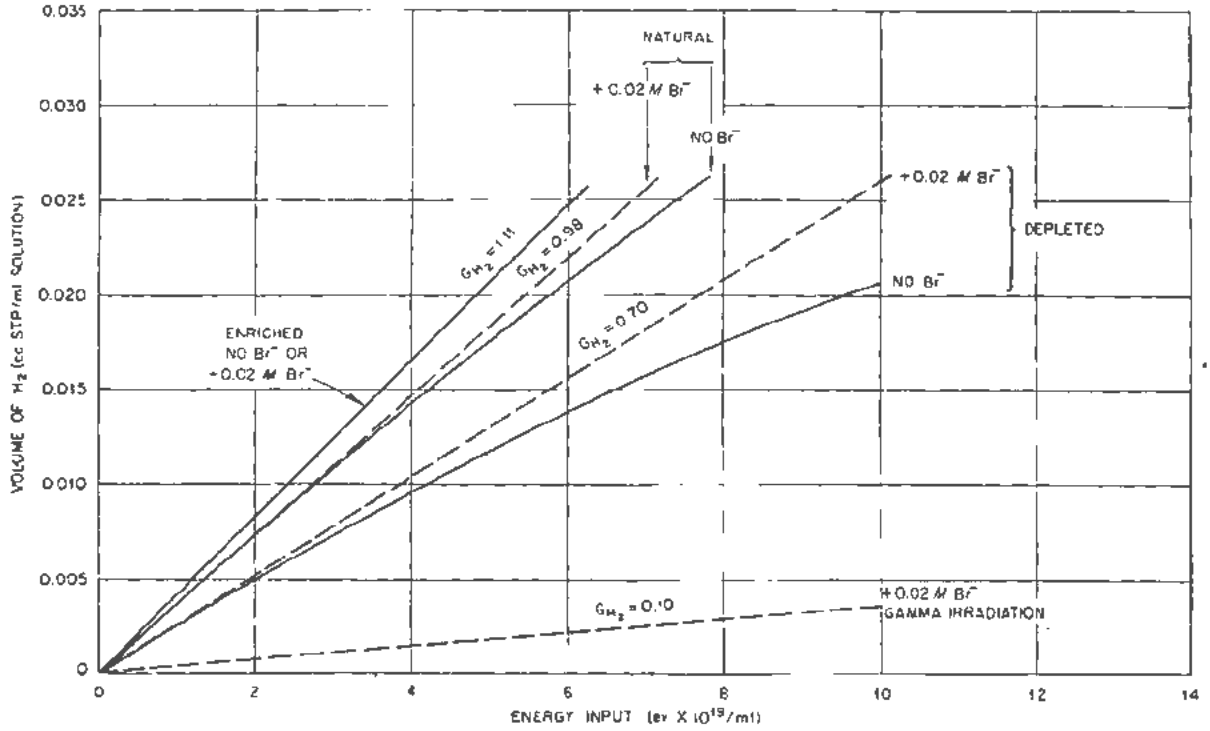

Figure 3. Effect of type of radiation on hydrogen yield from irradiated UO_2SO_4 solutions (concentration ~200 gm U/liter)

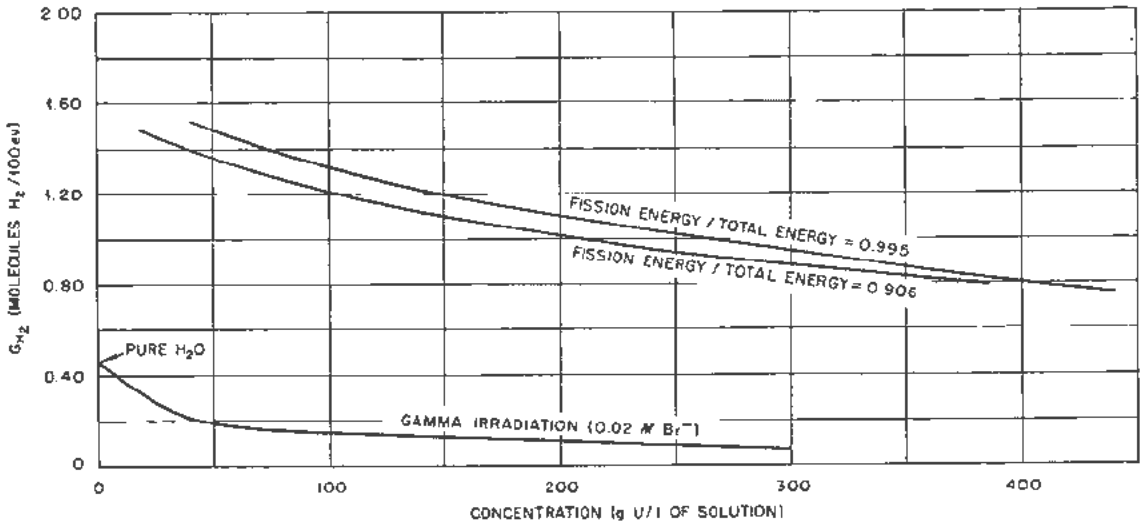

Figure 4. Effect of uranium concentration on hydrogen-gas yields from irradiated UO_2SO_4 solutions

rate of gas production up to the highest dose given. The yield without Br^- for Co^{60} γ-irradiations was so low that it could not readily be shown on the same scale as the other data of the figure. The linear H_2 yield for solutions in which fission contributed 99% or more of the total energy implies that the radical back reaction during irradiation is not appreciable at these doses. Therefore Br^- would not be expected to have much effect.

It can be seen from Fig. 4 that the presence of increased amounts of uranium in solution lowers the G_{H_2} for all types of radiations here reported. The decrease in yield by the solute is greater at lower solute concentrations and also at lower fission energy/total energy ration.

The data for UO_2F_2, UO_2SO_4, and $U(SO_4)_2$ solutions in which essentially all the energy is from fission fit the equation: $G_{H_2} = 1.83 - k(C)^{1/2}$; k for the three salts is respectively 0.043, 0.048, 0.059. $(C)^{1/2}$ is the square root of the uranium concentration in grams of uranium per liter. The concentration effect is due to more than a change in the solution pH as is shown in Table II by a comparison of the G_{H_2} for UO_2SO_4 solutions of low uranium concentrations with those for the UO_2F_2 solutions of higher uranium concentrations but similar pH.

The acidity of the solution was found to have an effect on G_{H_2} when uranium concentration and type of energy absorbed were not variables. A plot of the data in Table II shows that when H_2SO_4 was added to a UO_2SO_4 solution (105 gm U/l—marked with *), to adjust the pH to a value equal to that for a comparable solution of $U(SO_4)_2$, the G_{H_2} value for the acidified UO_2SO_4 solution agreed with that for the $U(SO_4)_2$ solution. Similarly, aqueous HF was added to a UO_2F_2 solution (377 gm U/l—marked with *) to lower the pH to a value equal to that for a UO_2SO_4 solution of comparable uranium content. Again a plot shows the G_{H_2} values to agree. This implies that the difference between the G_{H_2} for the various solutions at the same uranium concentration is mainly due to a pH effect and is dependent neither on the species of anion present nor on the oxidation state of the uranium. It further implies that alterations in the chemical species of uranium by the different complexing tendencies of the anions is not particularly important.

The very low G_{H_2} for $UO_2(NO_3)_2$ at 420 gm U/l (Table II) may reflect the fact that there was nitrate decomposition which may have produced oxidizing intermediates. These could have reacted with H radicals or dissolved H_2 gas.

To determine whether the change in G_{H_2} with increasing UO_2SO_4 concentration is related to mass of solute material, two solutions were made consisting of mixtures of UO_2SO_4 and Cs_2SO_4. Cs_2SO_4 was chosen because (1) cesium is an alkali metal and would be expected to behave as a chemically inert material; (2) its neutron capture cross section is low enough not to appreciably alter the fissioning characteristics of the solution; (3) the ratio of masses of Cs to SO_4 in Cs_2SO_4 is 265.8/96 and the ratio of UO_2 to SO_4 in UO_2SO_4 is 267.0/96, so that in relation to SO_4 the cation mass is very nearly equal. The results of irradiating these solutions compared with those for pure UO_2SO_4 (calculated from the data of Table II) are presented in Table III.

It can be seen that the addition of cesium as a solute cation does not have the same depressing effect on G_{H_2} as the addition of an equivalent mass of uranium. This experiment has a second implication. The addition of such large amounts of sulfate ion would be expected to have considerable effect on the degree of complexing of the UO_2^{++} ion at these concentrations. That the G_{H_2} is not thereby lowered lends further support to the conclusion that G_{H_2} is virtually independent of changes in the chemical species of the uranium present in solution.

Table III. Effect of Cesium Sulfate on the Hydrogen Yield from Reactor Irradiated Uranyl Sulfate Solutions

I	*II*	*III*	*IV*	*V*
4.63	0	0	1.66	1.66
6.74	155.3	102.2	1.63	1.32
6.23	324.2	213.3	1.64	1.06

I. Concentration of uranium (gm U/l), enrichment over 90% U^{235}.
II. Concentration of Cs_2SO_4 (gm Cs_2SO_4/l).
III. Concentration of uranium equivalent to Cs_2SO_4 (gm U/l).
IV. G_{H_2} observed for solution of composition column I + II.
V. G_{H_2} calculated for solution of composition column I + III.

It was found that the forward reaction (the decomposition of water by irradiation with an initial rate measured as G_{H_2}) was independent of temperature. Figure 5 shows that in highly enriched uranyl sulfate, the rate of pressure increase is the same at 150°C and 250°C. It also demonstrates that the presence of bromide ion has only a small positive effect, where essentially all the energy is from fission. The rate of gas production is seen to be large compared with the rate of thermal recombination. This conclusion was also confirmed by the identical H_2 yields measured by direct analysis for ampoules filled with highly enriched UO_2SO_4 at a concentration of 40 gm U/l irradiated at 30°, 120°, 190° and 210°C. Figure 6 shows the contrasting behavior of irradiated ampoules containing natural uranyl sulfate (fission energy/total energy = 0.925). In the Br^- containing ampoules where the radical back reaction is minimized, the rate of decomposition again is seen to be temperature independent. The slope of the line for 30°C agrees with that for 150° and 250° when the precaution of decomposing peroxides to produce gaseous O_2 was observed. The variation with temperature of the slopes of the lines for the bromide-free ampoules indicates that the radiation-induced back reaction does have a positive dependence on temperature.

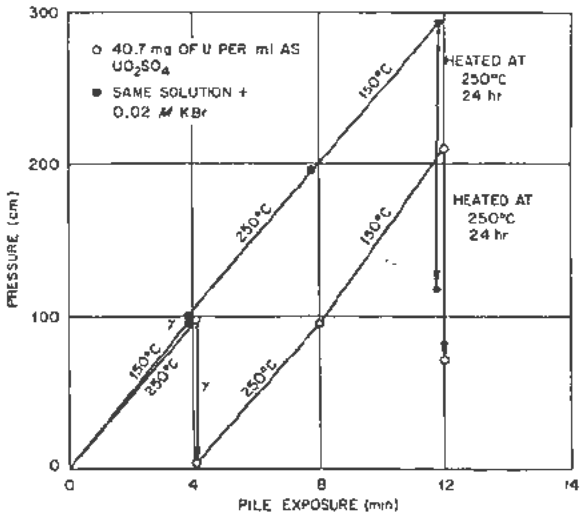

Figure 5. Pressure changes in capillary ampoules containing highly enriched UO_2SO_4 solutions

DISCUSSION

Water, when subjected to ionizing radiation, has been generally considered to behave as though two reactions are occurring simultaneously:[2]

$$H_2O \rightleftharpoons H + OH \quad (1)$$

$$2H_2O \rightleftharpoons H_2 + H_2O_2 \quad (2)$$

In reaction (2), H_2 and H_2O_2 result from the combination of many of the H and OH radicals in the regions of high ionization density before these radicals have time to separate by diffusion and become available for reactions with solute molecules. Although these two reactions are written as if stoichiometry applies, it is evident from this presentation that reaction (2) can be deficient in one or the other product and then reaction (1) would be deficient in the required corresponding product. An excess of H_2O_2 over H_2 in reaction (2) has been clearly demonstrated for cobalt gamma radiation.[8]

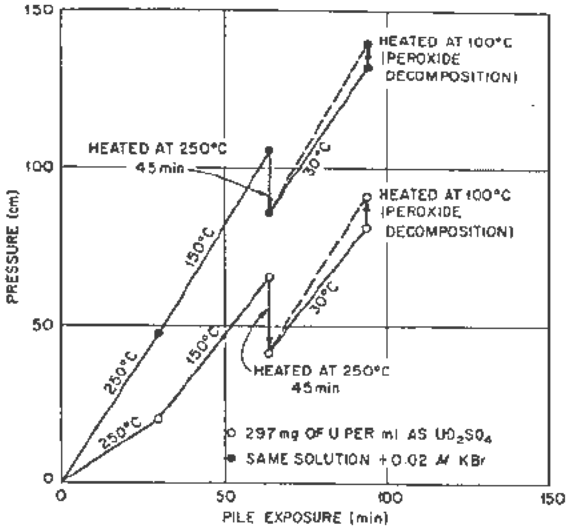

Figure 6. Pressure changes in capillary ampoules containing natural UO_2SO_4 solutions

The addition of solutes such as Br^- inhibits the radiation-induced recombination of H_2 and H_2O_2 and allows the yield of H_2 in reaction (2) to be measured.[9] The relative yields for reactions (1) and (2) depend on the ionization density or energy density along the particle track; reaction (2) is favored by high ion density (alpha particles and fission recoils) and reaction (1) by low ion density (fast electrons). The absolute yields for the products of reaction (2) are dependent upon the concentration of solutes reactive to H or OH radicals. For cobalt gamma radiation, the H_2O_2 yield has been demonstrated[10,11] to be dependent upon the concentration of Br^- and Cl^- while the H_2 yield has been demonstrated to be dependent upon the concentration of H_2O_2.[12]

The effects of the variables on H_2 yield reported here are consistent with this interpretation of the processes that occur. Varying the type of radiation by altering the U^{235} content of the solutions changed the yield as expected. When type of radiation was not a variable, i.e., in solutions where fissions contributed more than 99% of the total energy, the yield was independent of intensity. When neither uranium concentration nor type of radiation was a variable, the small differences accompanying changes in anion were traced apparently to differences in solution pH. For cobalt gamma radiation, an 18% decrease in H_2 yield has been found on going from pH 7 to 0.4.[13] The mechanism for this pH effect has not been elucidated.

The most striking effect on the H_2 yield is the decrease with increased uranium concentration. This cannot be explained by changes in solution pH; variation of pH from 2 to 0.1 for solutions containing about 100 gm of uranium per liter decreased the yield only from 1.35 to 1.20 (see Table II) whereas for solutions containing about 800 gm of uranium per liter at an intermediate pH of 1.03 the H_2 yield was 0.49. The addition of comparable amounts of cesium sulfate to the solutions had no marked effect on the H_2 yield, indicating that this decrease in H_2 yield cannot be attributed to energy absorption in the mass of solute present.

The mechanism by which uranium lowers the H_2 yield is not clearly understood. It was found for cobalt gamma radiation that uranium, which had a large effect on the H_2 yield, had little effect on reaction (1). This conclusion was based on the observation that the yield for H_2O_2 in water containing dissolved H_2 and O_2 during irradiation was decreased by uranium (at any particular uranium concentration) by only about the same amount as the H_2 yield was known to be decreased. This indicates that the action of uranium occurs only in regions of high energy density.

ACKNOWLEDGEMENTS

The authors wish to acknowledge their indebtedness to the following: C. H. Secoy and H. F. McDuffie for many valuable discussions during the course of this investigation; T. H. Handley, A. C. Stewart and P. F. Thomason for help in obtaining some of the analytical results.

REFERENCES

1. Saunders, K. W. and Taylor, H. A., *The Photolysis of Acetone in Presence of Mercury*, J. Chem. Phys. *9*, 616-25 (1941).
2. Allen, A. O., Hochanadel, C. J., Ghormley, J. A. and Davis, T. W., *Decomposition of Water and Aqueous Solutions Under Mixed Fast Neutron and Gamma Radiation*, J. Phys. Chem. *56*, 575-86 (1952).
3. Ghormley, J. A. and Hochanadel, C. J., *A Cobalt Gamma-Ray Source Used for Studies in Radiation Chemistry*, Rev. Sci. Inst. *22*, 473-5 (1951).
4. Mitchell, A. C. G., *Spectroscopy of Some Artificially Radioactive Nuclei*, Rev. Mod. Phys. *22*, 36-55 (1950).
5. Richardson, D. M., Allen, A. O. and Boyle, J. W., *Dosimetry of Reactor Radiations by Calorimetric Measurements*. To be presented at this Conference.
6. Hochanadel, C. J. and Ghormley, J. A., *A Calorimetric Calibration of Gamma-Ray Actinometers*, J. Chem. Phys. *21*, 880-5 (1953).
7. Lefort, M., *Action of Ionizing Radiations on Water and Aqueous Solutions*. J. Chimie Physique *47*, 776-94 (1950).
8. Dainton, F. S. and Sutton, H. C., *Hydrogen Peroxide Formation in the Oxidation of Dilute Aqueous Solutions of Ferrous Sulfate by Ionizing Radiations*, Trans. Faraday Soc. *49*, 1011-25 (1953).
9. Hochanadel, C. J., *Effects of Gamma-Rays on Water and Aqueous Solutions*, J. Phys. Chem. *56*, 587-94 (1952).
10. Sworski, T. J., *Yields of Hydrogen Peroxide in the Decomposition of Water by Cobalt Gamma Radiation I Effect of Bromide Ion*, J. Am. Chem. Soc. *76*, 4687-92 (1954).
11. Sworski, T. J., *Yields of Hydrogen Peroxide in the Decomposition of Water by Cobalt Gamma Radiation II Effect of Chloride Ion*, Radiation Research, *2*, 26-32 (1955).
12. Ghormley, J. A. and Hochanadel, C. J., *The Effect of Hydrogen Peroxide and Other Solutes on the Yield of Hydrogen in the Decomposition of Water by Gamma Rays*. Paper presented at the 3rd annual meeting of the Radiation Research Society at New York, N. Y., May 16-18 (1955).
13. Johnson, E. R. and Allen, A. O., *The Molecular Yield in the Decomposition of Water by Hard X-rays*. J. Am. Chem. Soc., *74*, 4147-50 (1952).

The Effects of Reactor Radiation upon High Temperature Static Water Systems

By J. R. Humphreys,* USA

An important consideration in the design of a water-cooled, closed system reactor is the steady-state concentration of decomposition products which are generated in water by reactor radiation. The hydrogen and oxygen thus formed in a high temperature power reactor may give rise to local boiling on the fuel element surfaces resulting in hot spot formation and bulk density variation in the core coolant. In addition to the heat transfer and control problems arising from local boiling, the presence of dissolved oxygen in the water can introduce a corrosion problem.

Previously reported work has shown that the concentrations of the decomposition products of pure water due to reactor irradiation will rise to a steady-state level where the back reaction of the decomposition products is equal in rate to the radiation breakdown of the water. The variation in the decomposition product concentrations at this steady-state condition with such variables as temperature, radiation intensity, and ionic impurities has been studied extensively at the lower temperatures, but very little work has been reported in the 300–500°F temperature range.

An experimental program was devised to determine the steady-state concentrations of the gaseous decomposition products of pure water systems at the higher temperature levels and to determine the effects of temperature, radiation intensity, and systemic impurities on these steady-state concentrations.

The reaction vessel used in this investigation consisted of a horizontal stainless steel autoclave with a 120-cm³ capacity as shown in Fig. 1. Two $\frac{1}{16}$-inch id capillary lines entered the autoclave at the top (vapor phase) and at the bottom (liquid phase). A schematic drawing of the pressure system, including the pile face manifolding and pressurizing arrangement, is shown in Fig. 2. The entire pressure system was fabricated of AISI type 347 stainless steel.

A schematic diagram of the instrumentation and control of the experiment is shown in Fig. 3. Two platinum-platinum-10 per cent rhodium thermocouples were used to indicate the temperature in the autoclave. A platinum resistance element, positioned within the autoclave, actuated an ac bridge-controlled, proportional heater power supply for autoclave temperature control. System pressure was indicated by a bourdon tube-type, 15-inch Heise precision pressure gage. Its range was −15 to +800 psia; the minor scale divisions were one psi.

For one portion of the experimental program the autoclave was surrounded by a cylindrical, uranium flux converter containing approximately 9 kilograms of natural uranium. The function of this converter was to transform part of the thermal neutron flux to fast neutron radiation by the fission of the U^{238} isotope.

Neutron monitoring foils of neptunium in a nickel-cadmium sandwich for the fast neutron flux and cobalt in aluminum for thermal flux were mounted in the annulus between the autoclave and converter. Analysis of these foils indicated that the average epithermal neutron flux was $2.05 \pm 0.4 \times 10^{12}$ neutron/cm²/sec at full reactor power with a thermal neutron flux of $2.7 \pm 0.5 \times 10^{12}$ neutrons/cm²/sec.

An estimation of the average neutron flux to which the autoclave was exposed without the neutron converter was $1.2 \pm 0.5 \times 10^{12}$ fast neutrons/cm²/sec and $5 \pm 2 \times 10^{12}$ thermal neutrons/cm²/sec.

Three types of water systems were exposed in this facility. They are designed Type A, Type B, and Type C runs.

The Type A runs were those in which the autoclave was completely filled with water and in which the autoclave was externally pressurized to insure a completely liquid phase. Type A runs were made only in the autoclave facility without the neutron converter.

The Type B runs were those in which both liquid and vapor phases were present, usually in equal volume. Type B runs were made both in the first autoclave without the neutron converter and in the second autoclave facility with the neutron converter.

The Type C runs were those in which gaseous hydrogen and oxygen were added to two-phase water system in the autoclave. Type C runs were also made both with and without the neutron converter.

All water used in these experiments was first distilled and then passed through an ion exchange column. This was followed by a boiling step to remove dissolved atmospheric gases before irradiation.

Autoclave total gas samples were taken at the conclusion of each run and analyzed for H_2, O_2, and

*Argonne National Laboratory. Including work done by Y. Solomon, Westinghouse Electric Corporation.

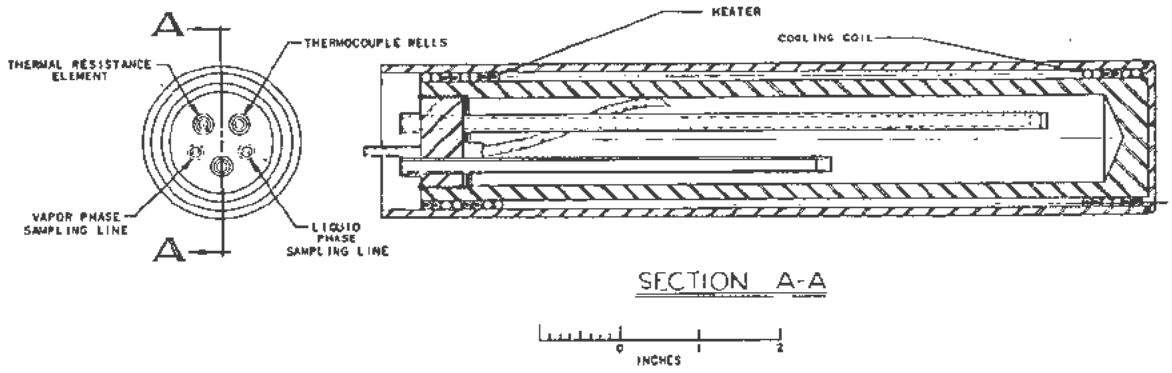

Figure 1. Cutaway of autoclave

CO_2. For the Type A and Type B runs, this resulted in direct measurement of the amounts of gaseous decomposition products, H_2 and O_2, existing in the autoclave under steady-state conditions. The sampling and analytical equipment used in this determination are shown in Fig. 4.

The data for all Type A and Type B runs are presented in Tables I and II. The notation used for individual run consists of type of run (A or B), general temperature level, and series number. For example, run B3-2 indicates a Type B, or two-phase, run at approximately 300°F, the second run in that series, without converter. Following the series number, a C represents the use of the duplicate autoclave with the neutron converter. A notation P.D. indicates a "pile down" run.

In Tables I and II hydrogen, oxygen, carbon dioxide, and inert gas analyses are reported both as the total cm^3 (STP) of each gas found in the autoclave, and as concentrations, cm^3 (STP)/liter volume. In the case of the Type B runs, the concentration of each gas was calculated for liquid-phase and vapor-phase concentrations, as based on the known solubility factors[1] with the exception of CO_2, for which solubility factors have not been reported for the higher temperatures. The inert gas was assumed to be nitrogen introduced by atmospheric contamination of the charge water or to atmospheric leakage during sampling.

The values for material balance were reported as oxygen deficiencies, expressed both quantitatively and as rates. Oxygen deficiency (*O.D.*) values were calculated by the following formula, using gas volumes corrected to standard temperature and pressure:

$$O.D.\ (cm^3\ O_2) = \frac{(cm^3\ H_2) - (cm^3\ CO_2)}{2} + \frac{(cm^3\ N_2)}{4} - (cm^3\ CO_2) - (cm^3\ O_2) \qquad (1)$$

In correcting the material balance for the presence of carbon dioxide, it was assumed that the oxidized organic impurity was originally of the C_nH_{2n} type. Little is known of the exact nature of the trace organic impurities introduced by the ion exchange water treatment step. Neither the anion exchange resin (quaternary amino groups) nor the cation exchange resin (sulfonated polystyrene) was chemically pure. Organic reagents and washes were undoubtedly occluded in the active resins and contributed to the organic-impurity content of the water. Errors from assuming impurities of the form C_nH_{2n} will therefore be greatest for the runs with the higher CO_2 product concentrations.

It was also assumed in these calculations that oxygen was introduced with the nitrogen (inert) in atmospheric proportions due either to incomplete degassing of the charge water or to leakage of air during charging or sampling.

THE EFFECT OF AUTOCLAVE CORROSION ON DECOMPOSITION PRODUCT CONCENTRATIONS

There is sufficient evidence to indicate that corrosion of the reaction vessel played an important part in generating some of the gas found at the conclusion of these experiments. As the corrosion of stainless steel is a metal oxidation process, the effect of this process is to increase the amount of hydrogen and to decrease the amount of oxygen present in the autoclave at the conclusion of a run. Two possible mechanisms for the corrosion process are:

$$4H_2O + 3Fe \rightarrow Fe_3O_4 + 4H_2 \qquad (2)$$

$$2O_2 + 3Fe \rightarrow Fe_3O_4 \qquad (3)$$

Some evidence for both of these reactions is found in the experimental results. In out-of-pile and pile-down experiments with the first autoclave, hydrogen was detected in approximately the same quantities as in corresponding irradiation experiments. This finding indicates that water supplies the oxygen for oxidation of the autoclave walls, producing free hydrogen by the first mechanism.

Also, in these out-of-pile tests and pile-down runs, the final oxygen content was well below the 25 per cent of the inert content which must necessarily have been added with the inert (N_2) as either air leakage or as incomplete gas removal of atmospheric solution in the charge water. Since this condition is also characteristic of the irradiation experiments, in which higher concentrations of inert gas existed, oxygen consumption by the second mechanism is indicated.

Table I. All-Liquid-Phase Irradiations, Analytical Results

Run no.	Temp, °F	Time at flux, hr	Time at temp, hr	Gas content: H_2 cm³	H_2 cm³/l	O_2 cm³	O_2 cm³/l	CO_2 cm³	CO_2 cm³/l	Inert cm³	Inert cm³/l	Total gas content, cm³	Total gas content, cm³/l	O_2 deficiency cm³	O_2 deficiency cm²/day	Water resistivity, megohm-cm Charge	Drain
A1–1	140	39.3	42.8	0.18 ±0.01	1.4	0.062±0.002	0.50	0.090±0.002	0.72	0.27	2.1	0.6	4.8	0.03	0.02	0.60	0.32
A1–2	140	65.2	68.1	0.29 ±0.01	2.32	0.145±0.002	1.12	0.080±0.001	0.64	0.34	2.7	0.85	6.8	0.03	0.01	0.20	0.12
A3–1	300	21.3	21.3	0.60 ±0.03	4.8	0.060±0.000	0.48	0.060±0.002	0.48	0.48	3.8	1.2	9.6	0.27	0.30	0.21	0.14
A3–2	300	22.3	22.3	0.43 ±0.04	3.4	0.050±0.001	0.40	0.090±0.002	0.72	0.93	7.5	1.5	12.0	0.26	0.28	0.36	0.18
A4–1	400	19.0	26.0	0.585±0.04	4.7	0.088±0.003	0.70	0.052±0.002	0.40	0.63	5.0	1.35	10.8	0.28	0.26	0.61	0.20
A4–2	400	19.9	21.3	0.592±0.005	4.7	0.071±0.001	0.57	0.031±0.002	0.25	0.28	2.2	0.97	7.8	0.25	0.28	0.58	0.29
A4–3	400	41.4	41.4	0.675± –	5.4	0.058±0.001	0.46	0.060±0.002	0.48	0.31	2.5	1.1	8.8	0.27	0.16	0.61	0.28
A5–1	500	20.5	20.6	0.60 ±0.01	4.8	0.089±0.003	0.72	0.045±0.012	0.4	0.35	2.7	1.1	8.6	0.24	0.28	0.70	0.16
A5–2	500	21.1	21.1	0.80 ±0.02	6.4	0.105±0.000	0.84	0.050±0.002	0.40	0.28	2.3	1.24	9.9	0.30	0.34	0.76	0.20
A5–3	500	21.8	21.8	0.675±0.02	5.4	0.076±0.003	0.61	0.118±0.003	0.94	0.25	2.1	1.1	9.0	0.15	0.16	0.57	0.20
A1–1PD	140	0.0	0.9	0.062±0.001	0.50	0.059±0.002	0.47	0.035±0.001	0.26	0.34	2.8	0.5	4.0	0.01	0.26	0.12	–

Table II. Irradiations with Vapor Phase, Analytical Results

Run no.	Temp, °F	Time at flux, hr	Time at temp, hr	Vap/liq. vol.	H_2 cm³ in autoclave	H_2 L.P. cm³/l	H_2 V.P. cm³/l	O_2 cm³ in autoclave	O_2 L.P. cm³/l	O_2 V.P. cm³/l	CO_2 cm³ in autoclave	Inert cm³ in autoclave	Inert L.P. cm³/l	Inert V.P. cm³/l	Total gas, cm³	O_2 deficiency cm³	O_2 deficiency cm²/day	Resistivity, megohm-cm Charge	Drain
B1–1	145	30.8	30.8	1:1	0.270±0.005	0.10	4.33	0.030±0.001	0.015	0.48	0.034±0.001	0.32	0.07	5.17	0.65	0.13	0.10	0.80	0.31
B3–1	300	21.1	21.1	1:1	0.175±0.003	0.08	2.79	0.067±0.001	0.03	1.07	0	0.32	0.09	5.15	0.56	0.19	0.22	0.32	0.32
B3–2	300	25.4	25.6	1:1	0.196±0.001	0.09	3.13	0.003±0.001	–	0.05	0.010±0.002	0.02	0.006	0.32	0.23	0.086	0.08	0.58	0.50
B3–3	300	42.5	42.5	3:1	0.200±0.001	0.06	2.16	0.045±0.001	0.015	0.50	0.009±0.001	0.025	0.005	0.27	0.28	0.05	0.03	–	0.16
B5–1	500	5.3	5.3	1:1	0.230±0.001	0.33	3.44	0.003±0.000	0.005	0.05	0.012±0.001	0.02	0.02	0.31	0.265	0.09	0.41	0.33	0.32
B5–2	500	14.7	14.7	1:1	0.240± –	0.35	3.59	0.087±0.001	0.13	1.29	0.003±0.000	0.33	0.34	5.07	0.66	0.11	0.18	0.41	0.25
B5–3	500	20.5	20.5	1:1	0.311±0.004	0.45	4.65	0.088±0.005	0.13	1.31	0	0.75	0.76	11.53	1.15	0.26	0.30	0.20	0.10
B5–4	500	31.8	31.8	1:1	0.557±0.004	0.80	8.33	0.052±0.001	0.08	0.77	0.032±0.003	0.05	0.05	0.77	0.69	0.20	0.15	0.26	0.32
B5–5	500	21.9	21.9	3:1	0.333±0.003	0.345	3.58	0	0	0	0.014±0.001	0.02	0.015	0.22	0.37	0.15	0.16	0.90	–
B5–6	500	23.1	23.1	∞	0.11 ± –	–	0.88	0	0	0	0	0.025	–	0.14	0.135	0.06	0.06	0.77	–
B3–1C	300	16.0	16.0	1:1	0.84 ±0.02	0.37	13.4	0.02 ±0.01	0.01	0.32	0.29 ±0.02	0.07	0.07	1.13	1.22	0.015	0.02	0.60	0.12
B3–2C	300	42.0	42.0	1:1	1.02 ±0.01	0.45	16.3	0.05 ±0.01	0.02	0.79	0.225±0.005	0.08	0.03	1.29	1.35	0.14	0.08	0.77	0.08
B3–3C	300	5.6	5.6	1:1	0.359±0.002	0.16	5.73	0.016±0.002	0.08	0.25	0.033±0.002	0.04	0.012	0.65	0.45	0.12	0.51	0.91	0.39
B5–1C	500	20.6	20.6	1:1	2.310±0.006	3.33	34.5	0.152±0.005	0.23	2.26	0.15 ±0.01	0.07	0.07	1.08	2.68	0.80	0.93	0.54	–
B5–2C	500	16.7	16.7	1:1	1.59 ±0.02	2.29	23.8	0.14 ±0.01	0.21	2.08	0.032±0.003	0.02	0.02	0.31	1.78	0.62	0.39	0.65	0.19
B3–1PD	325	0	15.6	1:1	0.116±0.002	0.08	2.64	0.004±0.001	0.002	0.06	0.001±0.001	0.10	0.03	1.61	0.27	0.10	0.15	–	–
B3–1aPD	325	0	1.1	2:1											0.045				
B3–2PD	300	0	16.0	1:1	0.052±0.001	0.023	0.83	0.052±0.008	0.023	0.83	0.005±0.002	0.16	0.05	2.57	0.27	0.01	0.015	0.97	–
B3–2aPD	300	0	.8	2:1	0.025± –	0.01	0.31	0	0	0	0.005± –	0.015	0.003	0.19	0.04	0.014	0.42	–	–

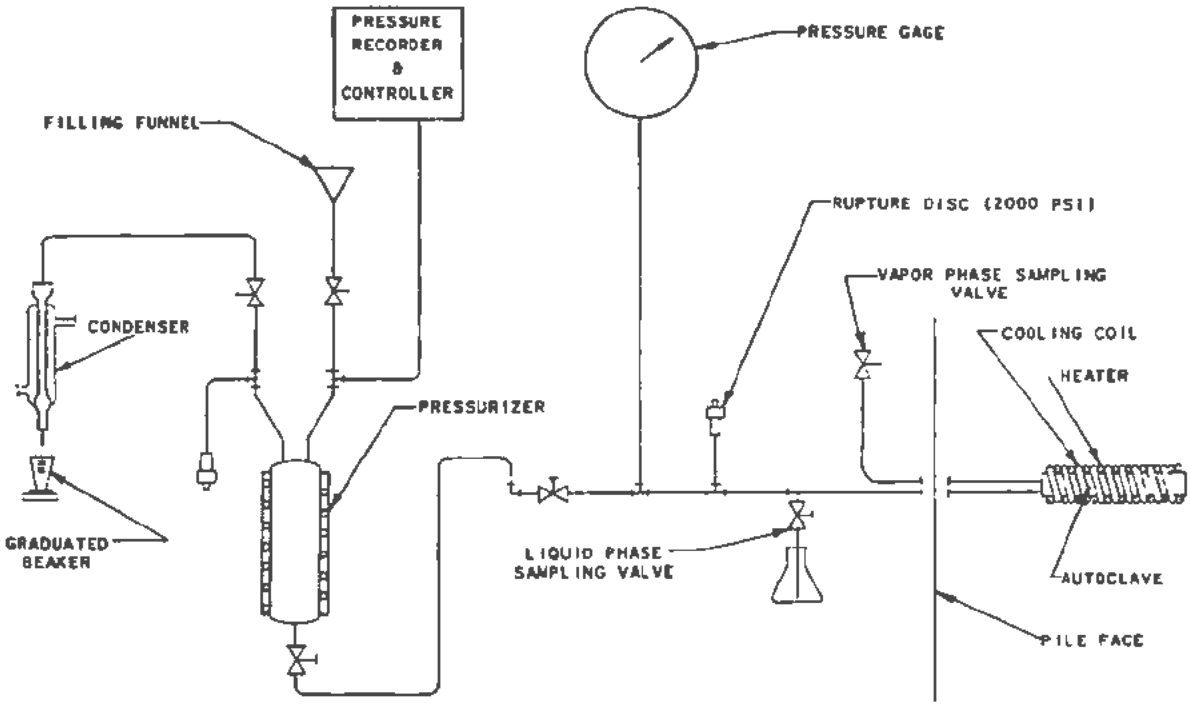

Figure 2. Pressure system

A study of gas product material balances for the in-pile experiments provides further evidence for the existence of a corrosion process and may also be used to estimate its approximate magnitude. These results are marked by an oxygen deficiency in almost every case, indicating corrosion, the extent of which is a function of the magnitude of the oxygen deficiency and of the duration of the run. Using these factors the corrosion rate of the autoclave is calculated by the equation:

$$\text{Corrosion rate (mg Fe/cm}^2\text{/mo)} = 10.5\left(\frac{\text{O.D., cm}^3\text{(STP)}}{\text{Run time (hours)}}\right) \qquad (4)$$

The constant, 10.5, includes the necessary conversion factors and the surface area of the autoclave.

The calculated corrosion rates for the first stainless steel AISI type 347 autoclave are presented in Table III.

Table III. Autoclave Corrosion Rate Calculations, Type A Runs

Run no.	*Run time, hr*	*Corrosion rate, mg Fe/cm²/mo*
A1–1	39.3	0.00
A1–2	65.3	0.00
A3–1	21.3	0.13
A3–2	22.3	0.12
A4–1	19.0	0.15
A4–2	19.9	0.13
A5–1	20.5	0.12
A5–2	21.1	0.15

Runs A1-1 and A1-2 in Table III show essentially no corrosion at 140°F. All other runs from 300°F to 500°F indicate corrosion rates of 0.12 to 0.15 mg Fe/cm²/mo. This range of values is in agreement with other values for the corrosion rate of AISI type 347 stainless steel at 500°F determined by the standard weight change methods.

The results of corrosion calculations for the Type B runs are listed in Table IV.

As the results include both liquid and vapor phase corrosion processes, they are not directly comparable with those reported in Table III for the Type A runs.

However, Table IV may be used for a comparison of the corrosion rates in the first autoclave with those in the second autoclave (with converter). Both at 300°F and 500°F the second autoclave corrosion rates are between 2 and 3 times those for the first autoclave for two-phase operations. The effect of reactor radiation on steel corrosion mechanisms is

Table IV. Autoclave Corrosion Rate Calculations, Type B Runs

Run no.	*Run time, hr*	*Corrosion rate, mg Fe/cm²/mo*
B5–1	5.3	0.18
B5–2	14.7	0.08
B5–3	20.5	0.13
B5–4	31.8	0.07
B5–1C	20.6	0.41
B5–2C	16.7	0.39
B3–1	21.1	0.09
B3–2	25.4	0.04
B3 3C	5.6	0.22

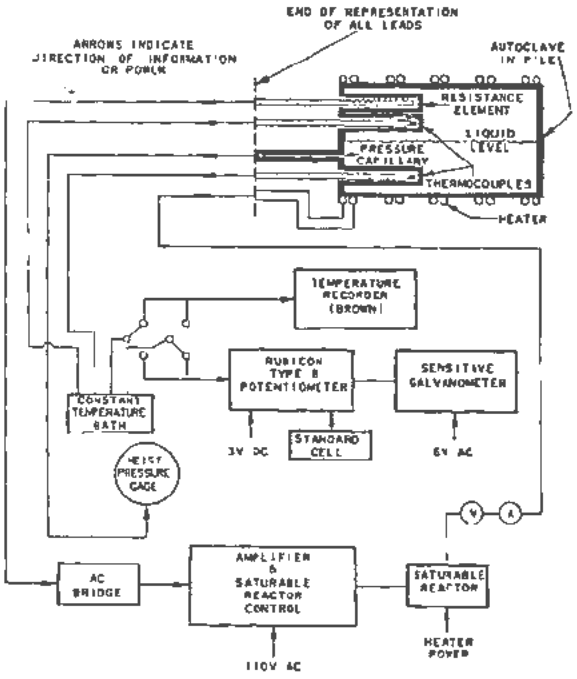

Figure 3. Schematic diagram of instrumentation and control

unknown, but it is unlikely that the 70 per cent increase in epithermal neutron flux could account for so much increase in the corrosion of the second autoclave. More likely it primarily represents a difference in corrosion rates between two specimens of the same material.

In contrast with the Type A corrosion insensitivity to temperature between 300°F and 500°F, the Type B results indicate a higher rate of corrosion at 500°F for both autoclaves. The effect of the vapor phase in the Type B runs upon corrosion is twofold. First, a vapor phase corrosion mechanism is superimposed upon the liquid phase corrosion process. Secondly, the dissolved oxygen in the liquid phase of the Type B runs is of a much lower order of magnitude than that present in the Type A runs. One or both of these differences appear to make the over-all corrosion process more temperature sensitive.

The variation of corrosion rate with time is another relationship illustrated in Table IV for the B5 series of runs. The data indicate that the corrosion rate may decrease initially with time (run B5-1) and eventually approach a level off value (runs B5-2 and B5-4).

THE EFFECTS OF TEMPERATURE ON THE LIQUID-PHASE DECOMPOSITION PRODUCT CONCENTRATIONS

It is only in the liquid-phase or Type A runs that variables other than temperature remain sufficiently constant to permit the identification of a reproducible temperature effect. Table V lists Type A runs of comparable duration, radiation intensity, and water purity, but characterized by different operational temperatures.

Table V. Variation of Decomposition Product Concentration with Temperature

Run no.	Temp, °F	Run time, hr	Gas sample - cm³ (STP)/l			Oxygen deficiency, cm³ (STP)
			H_2	O_2	CO_2	
A1-1	140	39.3	1.4	0.5	0.7	−0.03
A1-2	140	65.2	2.3	1.1	0.6	−0.03
A3-1	300	21.3	4.8	0.5	0.5	0.27
A3-2	300	22.3	3.4	0.4	0.7	0.26
A4-1	400	19.0	4.7	0.7	0.4	0.28
A4-2	400	19.9	4.7	0.6	0.25	0.25
A5-1	500	20.5	4.8	0.7	0.4	0.24
A5-2	500	21.1	6.4	0.8	0.4	0.30
A5-3	500	21.8	5.4	0.6	0.9	0.15

It may be seen in Table V that of the three gaseous products, H_2, O_2 and CO_2, only the yield of hydrogen appears to vary in a determinate manner with change in temperature. The greatest change in hydrogen concentration occurs between 140°F and 300°F. There appears to be only a slight increase in the hydrogen concentration between 300°F and 500°F.

A material balance, in this series of experiments, is most closely approached in the two 140°F runs. In the rest of the Series A experiments at 300, 400, and 500°F, for run times of about 20 hours, there is little variation in the oxygen deficiency. Discounting run A5-3, which is clearly inconsistent with the other runs, the other six experiments show an oxygen deficiency of 0.27 ± 0.03 cm³ (STP).

The variation of the hydrogen concentration and oxygen deficiency with temperature, considered with the relative independence of oxygen concentration

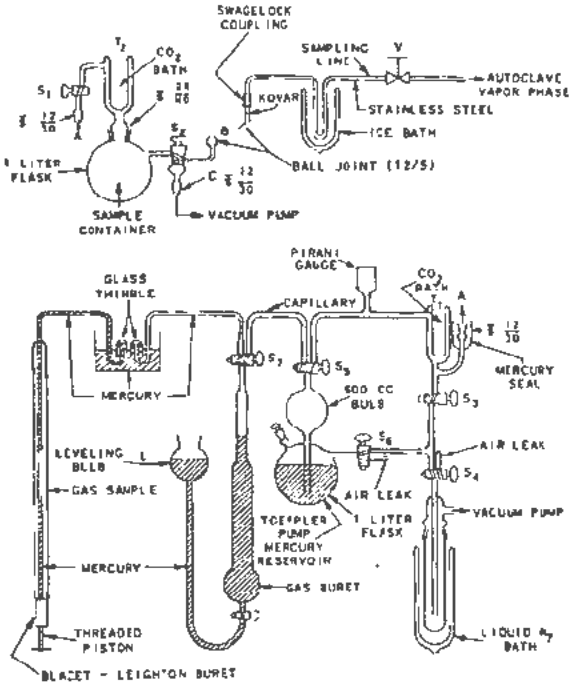

Figure 4. Gas sampling, transfer and analysis apparatus

and the uniform contribution of carbon dioxide formation, suggests the predominance of the corrosion reaction in the production of gaseous products.

As corrosion is a rate process, resulting excess hydrogen would progressively depress the oxygen concentration by mass law action. This oxygen repression continues until a very low level of oxygen is present in the system. The hydrogen concentration would then quantitatively approach that resulting from the integrated corrosion process from the system time zero. The resulting hydrogen and oxygen concentrations will be affected by the radiation-decomposition-recombination reactions only insofar as the sustained presence of a very low concentration of oxygen and the presence of free radicals affect the corrosion characteristic of the container materials.

The oxygen concentrations cannot successfully be used in analyzing the data for decomposition product steady-state equilibrium conditions since oxygen is present in such small amounts that any leakage or extraneous additions of air during charging or sampling operations mask the true steady-state condition.

THE EFFECTS OF EXCESS HYDROGEN OR OXYGEN ON DECOMPOSITION PRODUCT CONCENTRATION

The operational methods for the Type C experiments were developed so that the hydrogen and oxygen gases would be added in approximately stoichiometric mixtures to the autoclave. However, there were several Type C runs in which either a hydrogen excess or an oxygen excess resulted. The final steady-state conditions for these runs are listed in Table VI.

These results indicate that the concentration of hydrogen is suppressed in the presence of a slight excess of oxygen. The suppression of hydrogen is apparently sufficiently effective so that the total amount of hydrogen from all contributing sources—gas addition, corrosion, CO_2 formation, and water decomposition—is considerably lower than that found in the corresponding series of Type B steady-state runs. In the case of run C5-1 no hydrogen was found at 501°F. It was in this run that the largest excess of oxygen was present.

C3-2C was the only Type C run in which an excess of hydrogen was maintained for a sufficient time to approach a steady-state condition. The oxygen concentration reported for this experiment is greater than that which would be predicted from the results listed in Table II. The Type B runs resulted in considerably lower oxygen concentrations for much smaller excess hydrogen conditions. It can only be assumed that run C3-2C was sampled before a true steady-state was established in the system.

Table VI. Effects of Excess Oxygen or Hydrogen

Run no.	Temp, °F	Final gas analysis, cm³ (STP)	
		H_2	O_2
		Oxygen excess	
C3–1	327	0.14	3.9
C3–2	327	0.20	5.8
C5–1	501	0.00	16.8
		Hydrogen excess	
C3–2C	345	30.1	0.4

THE EFFECTS OF INORGANIC IMPURITIES ON DECOMPOSITION PRODUCT CONCENTRATIONS

Impurities present in the test water were of two general types: (1) foreign material added by the water handling and degasifying vessels, and (2) corrosion products occurring in a high temperature water-stainless steel system.

In determining the effect of inorganic impurities on the steady-state total gas concentrations, the specific resistance values were used as the index of water purity. As indicated in Table I, the residual water in the autoclave ranged in specific resistance from 0.08 to 0.50 megohm-cm. Within this range no relationship between specific resistance and gas yield was noted from 300°F to 500°F. Thus it appears that, in this temperature range, the total gas content of the autoclave is rather insensitive to a variation of impurity concentration within the range 0.08 to 0.50 megohm-cm.

However, run A1-2 at 140°F showed a rise in both hydrogen and oxygen concentrations over those for run A1-1, also at 140°F. The resistivity determinations on the autoclave drain water for the two runs were 0.32 and 0.12 megohm-cm for runs A1-1 and A1-2, respectively. The duration of run A1-2 was longer than run A1-1, but hydrogen produced by corrosion at 140°F must be negligible since the material balance of oxygen and hydrogen showed the same excess of oxygen in both runs. It seems, therefore, that the factor determining the difference in decomposition product concentrations for these two runs must be primarily an effect of ionic impurity.

To investigate the possibility that nitrogen in the autoclave was being oxidized to nitric acid, the water remaining in the autoclave at the completion of runs A1-1 and A3-2 was analyzed for nitrate ion. However, the determined concentrations of 0.06 and 0.09 ppm were negligible.

Therefore, while the 140°F runs exhibit a marked influence of water purity in agreement with previously published low temperature data, the higher temperature operation appears to be much less sensitive both to the presence of systemic inorganic impurities and to variations in their concentrations.

OXIDATION OF ORGANIC CONTAMINANTS IN WATER

Carbon dioxide was detected in almost all of the experiments with both autoclaves. The amount of this gas present bore no relationship to temperature or duration of run, resistivity of the charge water, or to the amount of any other gas in the autoclave.

This suggests that carbon dioxide, or an organic compound which could be oxidized to carbon dioxide, was added in varying amounts to the charge water used in each run. Since, in most of the experiments,

the quantities of carbon dioxide present were much greater than the amount of carbon dioxide present in water saturated with air (at room temperature), the carbon dioxide found in these experiments must have resulted from the oxidation of an organic contaminant in the charge water. One step in the purification of charge water consisted of passing the water through an ion exchange resin column. It seems quite likely that this was the source of the organic contaminant.

To investigate this possibility, five gallons of charge water were recirculated for one week through a two-inch ion exchange column. This water, saturated with the organic compound, was then used as charge water in runs B3-1C and B3-2C. As is shown in Tables I and II, the carbon dioxide yields for these runs were considerably higher than those for any of the others. Since the amount of carbon dioxide formed in 42 hours (run B3-2C) was not greater than that formed in 16 hours (run B3-1C), it may be assumed that the organic impurity was oxidized completely within 16 hours.

It will be noted in Table II that a significantly greater amount of carbon dioxide was found in runs B3-3C, B5-1C, and B5-2C. These runs were the first to be made following a replacement of the resin in the ion exchange column. The fresh resin very probably contained a greater portion of the more soluble organic compounds.

In a Type A run, the autoclave contained twice as much water and hence twice as much organic impurity as was present in a corresponding Type B run. During the initial phase of a Type B run, the autoclave was filled completely with water and irradiated for a period of from 30 minutes to 2 hours before the selected operating temperature was established and before a vapor phase was formed in the autoclave. As water was removed from the autoclave to form the vapor space, the gases stripped from solution and swept from the autoclave included some carbon dioxide formed during the preliminary irradiation period.

A comparison of oxygen deficiencies for runs B3-1C and B3-2C for which resin-saturated charge water was used, reveals an interesting condition with respect to run duration. Run B3-1C had evidenced an oxygen deficiency of zero after 16 hours at 300°F, while run B3-2C, with the same charge water, showed an appreciable oxygen deficiency after 42 hours at 300°F (Table II), indicating significant autoclave corrosion in the latter case and none in the former. This difference suggests the possibility that the organic oxidation reaction not only proceeds much faster than the corrosion reactions, but also that the corrosion reactions may actually be inhibited by the organic oxidation process until the latter has proceeded to completion.

THE EFFECT OF A VAPOR PHASE ON DECOMPOSITION PRODUCT CONCENTRATIONS

Table VII tabulates product gas variations with vapor-liquid volume ratio at different temperature levels for a number of comparative Type A and Type B experiments.

Table VII indicates that the presence of a vapor phase will decrease both the oxygen deficiency and the total product gas content of the autoclave, and that the amount of this decrease is dependent upon the vapor-liquid volume ratio. This reduction in total product gas concentration was most evident at 300°F in the range of minimum gas solubility.

The reported concentrations of the dissolved gas in the liquid phase decrease precipitously with the introduction of a vapor phase and continue to decrease as the vapor space is increased. These are calculated values for the two-phase experiments using measured total gas quantities and known solubility factors and are based on an assumed equilibrium condition.

These results suggest the existence of a predomi-

Table VII. Product Gas Variation with Vapor-Liquid Volume Ratio

Run no.	Vap./liq vol. ratio	Temp, °F	Liq. phase, cm³ (STP)/liter H_2	Liq. phase, cm³ (STP)/liter O_2	Vap. phase, cm³ (STP)/liter H_2	Vap. phase, cm³ (STP)/liter O_2	Total H_2+O_2, cm³ (STP)	O_2 def.
A1–1	0	140	1.4	0.5	–	–	0.24	−0.03
A1–2	0	140	2.31	1.1	–	–	0.43	−0.03
B1–1	1:1	145	0.1	0.02	4.3	0.5	0.30	0.13
A3–1	0	300	4.8	0.5	–	–	0.66	0.27
A3–2	0	300	3.4	0.4	–	–	0.48	0.26
B3–1	1:1	300	0.08	0.03	2.8	1.1	0.25	0.19
B3–2	1:1	300	0.09	0	3.1	0.05	0.20	0.08
B3–3	3:1	300	0.06	0.02	2.2	0.5	0.24	0.05
A5–1	0	500	4.8	0.7	–	–	0.69	0.24
A5–2	0	500	6.4	0.8	–	–	0.90	0.30
A5–3	0	500	5.4	0.6	–	–	0.76	0.15
B5–3	1:1	500	0.4	0.1	4.6	1.3	0.40	0.26
B5–4	1:1	500	0.8	0.1	8.3	0.8	0.61	0.20
B5–5	3:1	500	0.3	0	3.6	0	0.33	0.15
B5–6	∞	500	–	–	0.9	0	0.11	0.06

nant hydrogen and oxygen combination reaction in the vapor phase (H_2O-H_2-O_2) system at 300 to 500°F. This vapor phase combination reaction must be considerably more significant than liquid-phase back-reactions in order to effect a net reduction in the total quantity of product gas. This conclusion is strengthened by noting the smaller quantities of total gas which were formed in the quarter-filled runs that were produced in comparable half-filled runs. B5-6 was the only run in which an all vapor-phase water system was exposed to reactor radiation and in which the decomposition products were measured directly. The product gas in this experiment contained only a trace of hydrogen and no detectable oxygen. The hydrogen is attributed to corrosion. The absence of oxygen indicates that the equilibrium concentrations of water decomposition products in the vapor phase at 500°F is below the experimental limits of detectability.

Therefore, the product gases measured for the two-phase experiments must have been generated in the liquid phase. This results in a constant effusion of dissolved product gases from the liquid phase into the vapor phase, as the equilibrium partial pressures of these gases are never attained due to the vigorous vapor phase combination reaction. Thus the true product gas concentrations in the liquid phase of the Type B runs would be higher than those calculated for Table VII and the vapor phase concentrations would be lower. The degree of deviation from equilibrium distributions would be a function of the hydrogen and oxygen effusion rates from the liquid phase and the combination rates of these gases in vapor phase. The system steady-state condition then exists when the rate of effusion equals the rate of vapor phase combination of the hydrogen and oxygen generated in the liquid phase by the reactor radiation.

EFFECTS OF TEMPERATURE ON THE COMBINATION RATES OF ADDED HYDROGEN AND OXYGEN

Excess hydrogen and oxygen gases were added to two-phase static water systems in the presence of reactor radiation in order to investigate the effects of temperature and radiation intensity on the back-reaction. As the back-reaction is the radiation-induced combination of hydrogen and oxygen, a study of the combination of an added excess of these gases at different operating temperatures and flux conditions should yield direct information concerning the effect of these variables on the back-reaction in a two-phase water system.

The rate characteristics of the hydrogen and oxygen combination reactions may be seen in Fig. 5 for operation without the neutron flux converter and in Fig. 6 for operation with the flux converter. In all experiments the rate of combination is constant throughout the initial stage of the reaction. This is a direct measure of the vapor-phase combination reaction rate. This phase of reaction is characteristically followed by a gradual reduction in the measured combination rate as the vapor-phase reaction is progressively influenced by contribution of product gases from the liquid phase.

In Fig. 5, the three combination experiments conducted without the neutron converter show essentially the same initial combination rates for two runs at 327°F and one run at 501°F, indicating very little effect of temperature on the vapor-phase reaction in this range.

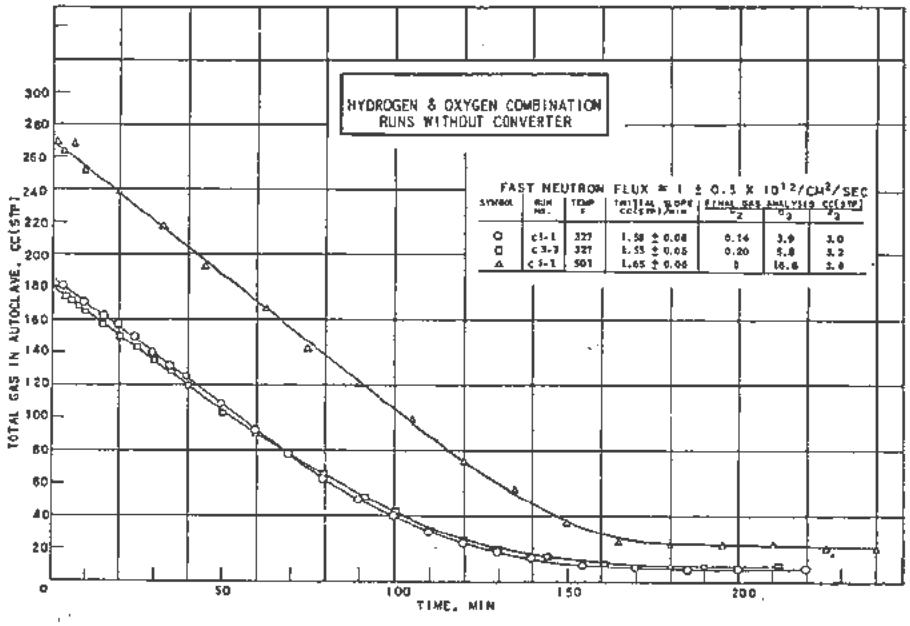

Figure 5. Hydrogen and oxygen combination runs without converter

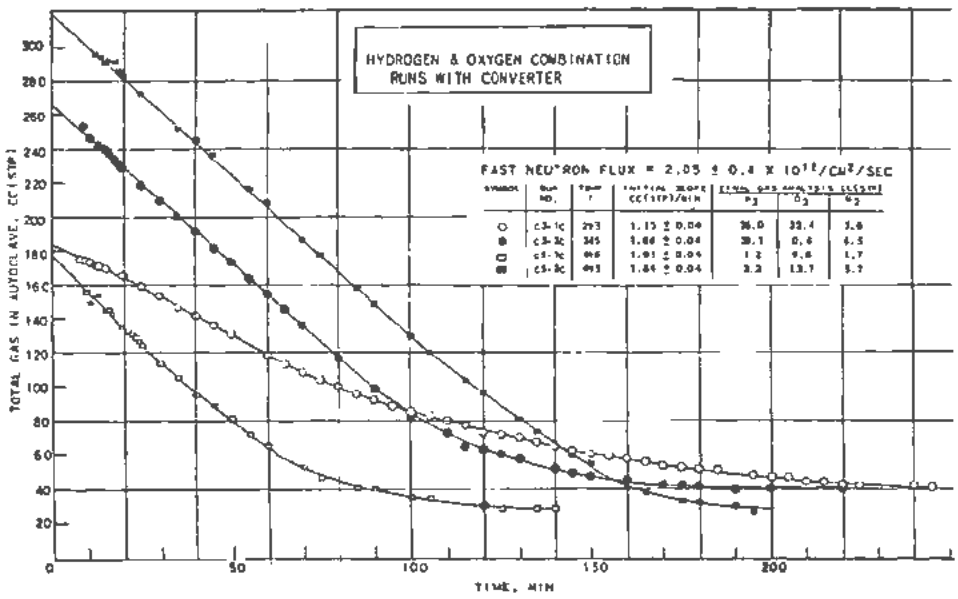

Figure 6. Hydrogen and oxygen combination runs with converter

In Fig. 6 three of the combination experiments with the neutron converter show essentially the same initial combination rates for run C3-2C at 345°F and for runs C5-1C and C5-2C at 495°F. However, for run C3-1C at 293°F, the initial combination rate suggests a definite effect of temperature on the combination rate at this lower temperature level.

Therefore, it appears that there is little change in combination rates between 327°F and 501°F. However, between 293°F and 327°F there is a temperature below which variation in temperature will have significant effect on the vapor-phase combination rates. It is possible that this sensitivity to temperature is due to a dependency of the vapor-phase combination reaction on the concentration of water vapor.

THE EFFECTS OF RADIATION INTENSITY ON THE COMBINATION RATES OF ADDED HYDROGEN AND OXYGEN

Operation without the neutron converter and with the neutron converter offered two levels of fast neutron flux with which to study the effects of reactor flux variation on hydrogen and oxygen combination rates. The fast neutron flux with the converter, as measured with a neptunium foil, was 2.05 ($\pm$0.4) $\times$ 10^{12} neutrons/cm^2/sec. The fast neutron flux without the neutron converter was estimated to be 1.2 (+0.5) $\times$ 10^{12} neutrons/cm^2/sec.

From Fig. 5 the hydrogen and oxygen combination rate was found to be 1.6 cm^3 (STP) ($2H_2 + O_2$)/min for 327°F to 501°F in a fast neutron flux of about 1.2 $\times$ 10^{12}. From Fig. 6, the combination rate was calculated to be 1.9 cm^3 (STP) ($2H_2 + O_2$)/min for 345°F to 496°F in a fast neutron flux of 2.05 $\times$ 10^{12}. Therefore, for an estimated two-fold increase in fast neutron flux, the combination rate rose from 1.6 to 1.9 cm^3 ($2H_2 + O_2$)/min. The values differ so little in magnitude and are known with such poor precision that a quantitative estimate cannot possibly be made of the effect of neutron flux variation.

POINTS OF DEVIATION FROM CONSTANT REACTION RATE IN COMBINATION CURVES

An interesting feature of Figs. 5 and 6 is the initially constant combination rate which is exhibited in all Type C experiments. This condition shows that the rate-determining variable is radiation intensity and that the combination process is independent of hydrogen and oxygen concentrations above a minimum concentration level. The points of deviation from constant reaction rate in the hydrogen and oxygen combination curves are listed in Table VIII. This precludes the possibility of a chain mechanism for the combination reaction in the vapor phase.

The quantities of hydrogen and oxygen which combined to form water after the autoclave contents reached the point of deviation from constant reaction rate ranged from about 55 to 80 cm^3 (STP) and showed little variation with temperature or with

Table VIII Points of Deviation from Constant Reaction Rate in Combination Curves

Run no.	Temp, °F	Point of deviation from constant rate, Total gas, cm^3 (STP)	Final steady-state autoclave gas, total, cm^3 (STP)	Autoclave gas combined after deviation point, cm^3 ($2H_2+O_2$) (STP)
C3–1	325	65±5	10	55±5
C3–2	325	85±5	10	75±5
C5–1	500	75±5	20	55±5
C3–1C	295	105±5	40	65±5
C3–2C	345	100±5	40	60±5
C5–1C	500	95±5	30	65±5
C5–2C	500	110±5	30	80±5

varying excess of either added gas. Thus, the point at which flux is no longer the sole rate-determining factor and diminishing reactant concentration becomes significant in the combination process is about 1 cm^3 (STP) ($2H_2 + O_2$)/cm^3 in the vapor phase with a corresponding 25 to 50 cm^3/l in the liquid phase for the temperature range of 300 to 500°F.

The constant initial combination rate and the independence of the reaction to reactant concentrations above a definite point indicate that the initial phase of the combination reaction is zero order. This precludes the possibility of a chain mechanism for the combination reaction in the vapor phase.

REFERENCE

1. Pray, H. A., Schweickert, C. E. and Minnich, B. H., *The Solubility of Hydrogen, Oxygen, Nitrogen, and Helium in Water at Elevated Temperatures*, BMI-T-25, (1950).

The Decomposition of Light and Heavy Water Boric Acid Solutions by Nuclear Reactor Radiations

By Edwin J. Hart,* William R. McDonell,† and Sheffield Gordon,* USA

Ionizing radiations such as X-rays, γ-rays and nuclear pile radiations fail to cause the decomposition of pure, air-free liquid water. However, heavy particle radiations, such as α-rays from radium or polonium, cause the continuous decomposition of water even at low intensities. This behavior of water toward ionizing radiations is explained by the following two radiation-induced reactions:[1-5]

$$H_2O = H + OH \qquad (1)$$

$$H_2O = \tfrac{1}{2}H_2 + \tfrac{1}{2}H_2O_2 \qquad (2)$$

Reaction (1) identifies those radicals escaping primary recombination in the track, and reaction (2) refers to the products of decomposition of water formed in the track and resulting from pair-wise recombination of H and OH radicals. If the proportion of radicals which are formed via (1) is sufficiently high, recombination of hydrogen and hydrogen peroxide formed in (2) by these radicals is effected. As a result, no decomposition of water is observed. However, if this ratio is low enough, continuous decomposition of the water results.

In general, reaction (1) is favored by light particle radiations, whereas reaction (2) is favored by heavy particle radiations.

As a result of the nuclear reaction $B^{10}(n,\alpha)Li^7$, water containing boric acid may decompose in reactors. An extensive study of hydrogen peroxide formation upon irradiation of boric acid and borate solutions in the French reactor Zoé, has been reported by Bonét-Maury and Deysine[6] and Pucheault, Lefort and Haissinsky.[7] This work was carried out at relatively high concentrations of boric acid, the main emphasis being on hydrogen peroxide formation and decomposition.

Light and heavy water boric acid solutions in the concentration range from zero to 0.2 *M* have been irradiated in the Argonne Heavy Water Reactor CP-3'. The irradiated solutions were analyzed for hydrogen peroxide, hydrogen, and oxygen.

The present report also deals with experiments on the effect of addition agents such as potassium indide, hydrogen peroxide, hydrogen, and deuterium.

* Argonne National Laboratory.
† duPont Company.

EXPERIMENTAL

The light and heavy water used in these experiments was purified by a triple distillation procedure previously described.[8] An additional initial alkaline permanganate distillation was found necessary for the heavy water in order to remove organic impurities. Isotopic analysis of the heavy water thus purified showed it to be 99.60 ± 0.02 per cent deuterium. Exhaustive γ-ray irradiation of air-free samples of this purified water liberated approximately 10^{-6} mole of hydrogen and carbon dioxide per liter of water. This radiation stability test was also applied to 0.10 *M* boric acid solutions. The absence of carbon dioxide in these irradiated solutions demonstrated that organic matter was not present in the water or in the boric acid. Regular tank hydrogen and deuterium (99.5% purity) were used after passage through a liquid nitrogen trap.

The hydrogen peroxide was prepared from 90% (CP) hydrogen peroxide, diluted to 0.06 *M* with triply-distilled light water, then further diluted to approximately 0.6 m*M* with triply-distilled normal or heavy water, as the case required. Since the heavy water was 99.6% isotopic purity, the 100-fold dilution from the 0.06 *M* stock solution reduced the deuterium content to 98.6%.

Irradiation Procedure

Cylindrical quartz cells, 2 cm in diameter and of 12-ml capacity, were evacuated, filled with air-free solution, and sealed with standard tapered ground glass joints.[8] The sealed quartz cells containing the evacuated solutions were then placed in 15-inch aluminum cans, two cells per can for irradiation in the core of the CP-3' heavy-water moderated reactor. After irradiation, the total amount of gas was measured and analyzed using the Van Slyke[9] or Saunders-Taylor[10] microgas analysis techniques. Hydrogen peroxide was determined by the triiodide ion procedure developed by Ghormley.[8] Boric acid was determined by the mannitol method described by Scott.[11]

Dosimetry

Gamma-Ray Flux

A complete spectrum of γ-rays originating from fission, capture gammas from aluminum, silica, hydrogen, and other components of the pile and cell

Table I. Relative Amounts of Dissociation and Recombination Reactions for Ionizing Radiations

Type of Radiation	Fraction of water molecules decomposed	
	Reaction (1)	Reaction (2)
Co^{60} γ-rays	80	20
CP-3′	80	20
B^{10} (n, α) Li^7 (0.02 M H_3BO_3)	4	96
B^{10} (n, α) Li^7 (0.05 M H_3BO_3)	6	94
β-rays (tritium water)	70	30

* Measured by the formic acid-oxygen method.[5]

assembly is expected. However, the ionizing radiations absorbed in aqueous solutions irradiated in CP-3′ behave exactly like radiation from a Co^{60} γ-ray source. This fact was demonstrated by the formic acid-oxygen technique previously employed to measure the relative proportions of reactions (1) and (2).[5] The results are contained in Table I. Since chemical effects of the radiation present in the core of the reactor are identical to those of Co^{60} γ-rays, use of the ferrous-sulfate dosimeter calibrated for γ-rays is warranted. On the basis of the Hochanadel value[4] of 15.5 ferric ions/100 ev it is found that the rate of energy absorption in our irradiation cells is 11.9×10^{20} ev/liter-minute.

Energy Absorption Due to the $B^{10}(n, \alpha)Li^7$ Reaction

The rate of energy absorption due to the $B^{10}(n, \alpha)$ Li^7 reaction in an aqueous solution containing one molar boric acid exposed to pile radiation is calculated from the equation

$$dE/dt \text{ (ev/sec)} = E_r f \sigma N$$

where $E_r = 2.33 \times 10^6$ ev, effective total energy of the α and Li^7 recoil nuclei;[12] $f = 1.39 \times 10^{12}$ n/cm²-sec, thermal neutron flux obtained by gold activation experiments,[13] and independently checked by gas evolution experiments from boric acid solutions;[14] $\sigma = 7.55 \times 10^{-22}$ cm², cross section of natural boron,[16] and $N = 60.2 \times 10^{23}$ molecules/mole.

The experimental rate of production of free radicals and stable decomposition products was measured by the formic acid-oxygen method[5] and is given in Table II for aqueous solutions of boric acid. In this table the absolute amount of the products formed in millimoles/liter-min are given for the γ-ray and B^{10} reactions in aqueous solutions irradiated in the pile. In obtaining the data for Table II it was assumed that the γ-ray flux in the pile was independent of the boric acid concentration. The contribution of free radicals from the $B^{10}(n, \alpha)Li^7$ reaction is extremely small, and consequently the relative proportion of free radicals to hydrogen and hydrogen peroxide decreases as the concentration of boric acid increases.

RESULTS AND DISCUSSION

Effect of Boric Acid Concentration

The rate of hydrogen evolution in air-free water irradiated in the reactor is shown in Figs. 1 and 2. In Figs. 1, linear decomposition curves are obtained at boric acid concentrations of 0.05 and 0.10 M after four minutes irradiation. Decomposition is not observed at 0.010 and 0.015 M boric acid concentrations but hydrogen evolution appears to set in at 0.020 M boric acid. In Fig. 2 the linear rates of hydrogen evolutions are plotted as a function of the concentration of boric acid. Noteworthy is the fact that these rates are linear beyond 0.02 M boric acid for light water and 0.04 M boric acid for heavy water. In this part of the core a thermal flux of 8.34×10^{13} n/cm²-min and a γ-ray flux of 11.9×10^{20} ev/liter-min exists.

Table II. Rate of Production of Free Radicals and Decomposition Products of Boric Acid Solutions in the Core of CP-3′*

Boric acid concentration (M)		0	0.02	0.05
Reaction	Radiation	Millimolar products/minute		
$H_2O = H + OH$	γ-rays	0.054	0.054	0.054
$H_2O = \frac{1}{2}H_2 + \frac{1}{2}H_2O_2$	γ-rays	0.007	0.007	0.007
$H_2O = H + OH$	$B^{10}(n, \alpha)Li^7$	0.0	0.003	0.012
$H_2O = \frac{1}{2}H_2 + \frac{1}{2}H_2O_2$	$B^{10}(n, \alpha)Li^7$	0.0	0.038	0.099

* Measured by the formic acid-oxygen method.[5]

Using 0.02 M boric acid, a slow steady decomposition of light water to form hydrogen, hydrogen peroxide, and oxygen may be detected. As the concentration of boric acid is increased beyond this point, the decomposition of water is increased linearly at a rate of 1.83 mM hydrogen per minute per molar boric acid. This result agrees satisfactorily with the rate of hydrogen evolution (1.94 mM hydrogen per minute per molar boric acid) deduced from Table II, which is based on the formic acid-oxygen method. Using the value of 1.83 mM hydrogen per minute per molar boric acid, it is deduced that 1.25 hydrogen and hydrogen peroxide molecules are produced per 100 ev. This means that 2.50 water molecules are decomposed per 100 ev of energy absorbed.

Since aqueous boric acid solutions below 0.02 M are not decomposed in the core of the reactor, it is

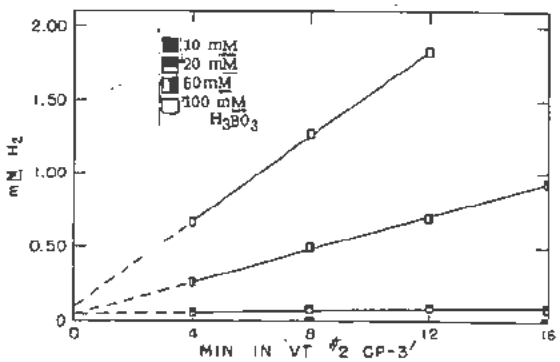

Figure 1. Effect of pile radiation on boric acid solutions in H_2O

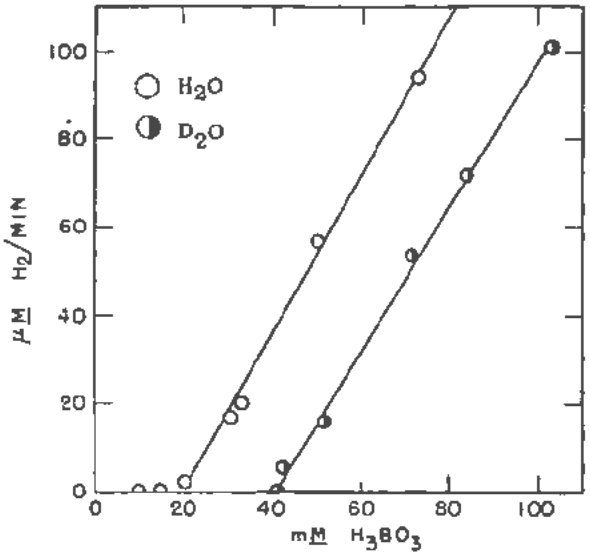

Figure 2. Effect of boric acid concentration on hydrogen production in air-free solutions irradiated in CP-3'

concluded that the free radicals formed in reaction (1) are capable of recombining the hydrogen and hydrogen peroxide formed in reaction (2). At 0.02 *M* boric acid, Table II shows that 0.057 m*M* hydrogen and hydroxyl radicals and 0.045 m*M* hydrogen and hydrogen peroxide are formed per minute. Since decomposition of water begins at 0.02 *M* boric acid it is calculated from the above results that 1.3 water molecules must be dissociated in reaction (1) to combine the stable products formed in reaction (2).

The γ-ray flux is substantially more effective in causing the recombination of the decomposition products for the heavy water, since the inception of water decomposition is delayed to about 0.04 *M* boric acid. In this case, assuming the same rates of formation of products in reactions (1) and (2), it is estimated that 0.8 molecule of heavy water dissociating in reaction (1) are required to recombine the products formed in a dissociation of one molecule of heavy water in reaction (2).

In the concentration range of boric acid where linear decomposition rates of water are observed, oxygen appears to be a primary product of the decomposition. Characteristic curves for 0.10 *M* boric acid solutions are given in Fig. 3. Here it is observed that oxygen is produced linearly and that hydrogen peroxide formation is less than that of hydrogen production. In general the stoichiometry of this reaction is such that hydrogen formed is equal to hydrogen peroxide plus two times oxygen formed. There is some uncertainty in the interpretation of these results since it is not known whether oxygen is liberated during irradiation or during post-irradiation. Also, it is possible that a small amount of hydrogen peroxide could decompose into oxygen during the course of the analysis. In any case hydrogen production appears unaffected by these results and the decomposition rates of the water are based on the rate of hydrogen production.

Table III gives the rates of hydrogen, hydrogen peroxide, and oxygen formation for a series of irradiations in light and heavy water. From these results it is observed that the uncertainty inherent in oxygen production is rather high.

Effect of Hydrogen and Hydrogen Peroxide

Hydrogen added initially to aqueous boric acid solutions has the effect of shifting water decomposition curves to higher boric acid concentrations. It has been found that 0.081 m*M* hydrogen causes a shift in the curve of some 0.014 *M* boric acid (see Fig. 4).

At higher initial hydrogen concentrations this process becomes even more efficient, proving that hydrogen/hydrogen peroxide ratios greater than one cause a chain recombination as demonstrated by Allen and co-workers.[3] Difficulty was found in obtaining reproducible results at concentrations above 0.081 m*M* hydrogen. The difficulty is inherent in the problem of getting identical hydrogen concentrations in successive irradiations containing variable concentrations of boric acid. In addition, as the concentration of hydrogen is increased to its saturation point in water there is strong tendency for hydrogen to be removed from solution and to form bubbles in the cells. It would appear that up to 0.150 *M* boric acid solutions at one atmosphere pressure of hydrogen can be irradiated in CP 3' without decomposition.

Hydrogen peroxide promotes the decomposition of water at boric acid concentrations below 0.02 *M*. Typical dosage curves appear in Fig. 5, and the rates of hydrogen evolution appear in Fig. 6. It is to be noted that the effect of hydrogen peroxide is particularly pronounced in the region of low concentrations of boric acid. Under these conditions, the hydrogen peroxide/hydrogen ratio existing during irradiation is high at all times. At high concentrations of boric acid the high rate of hydrogen and hydrogen peroxide

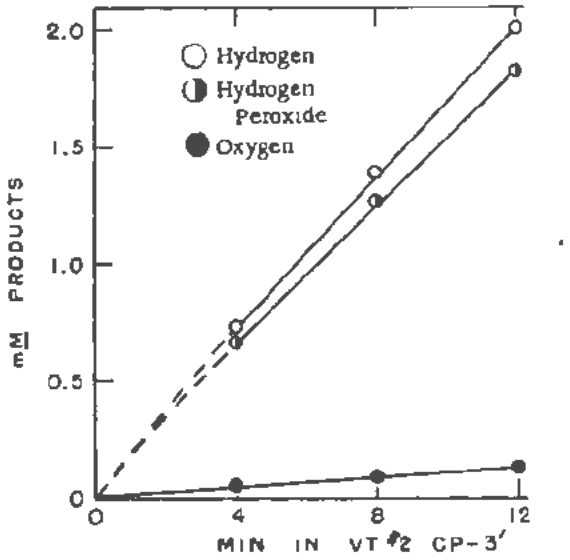

Figure 3. Decomposition products of the irradiation of 0.10 M boric acid in light water

Table III. Rates and Steady States of Formation of Decomposition Products of Pile Irradiated Light and Heavy Water Solutions of Boric Acid

	Boric acid conc.	Rate of formation, μ moles/l-minute				Steady state, μ moles/l	
		Total gases	Hydrogen peroxide	Hydrogen	Oxygen	Total gases	Hydrogen peroxide
Light water	0.00 *M*	0	–	0	0	5–10	0
	0.01	0	–	0	0	5–10	0
	0.02	0	0	0	0	90	80
	0.0313	23±1	18±1	21±2	2±2	–	–
	0.05	57±2	–	53±2	5±1	–	–
	0.0732	101±4	77±3	93±5	8±5	–	–
	0.10	160±2	–	147±2	11±1	–	–
Heavy water	0.00 *M*	0	0	0	0	20–30	0
	0.0104	–	0	–	–	–	0
	0.0209	–	0	–	–	30–40	2–3
	0.0312	0	0	0	0	50–60	3–4
	0.0410	0(+1)	0	0(+1)	0	100	40
	0.0422	6.0±0.5	5.5±0.5	5.8±0.8	(0)	–	–
	0.0515	17±3	14±1	16±3	(1)	–	
	0.0716	56±2	50±3	54±4	(2)	–	–
	0.0839	75±2	67±2	72±3	(3)	–	–
	0.1029	106±5	90±3	101±6	(5)	–	–
	0.1032	–	95±3	–	–	–	–

production rapidly decreases the hydrogen peroxide-hydrogen ratio. The effect of the initially added hydrogen peroxide is therefore less pronounced and the two curves approach each other.

Effect of Iodide Ions

The result of adding boric acid to 0.10 m*M* potassium iodide solutions is shown in Fig. 6. One notes in these potassium iodide irradiations that the free radical induced reaction of hydrogen and hydrogen peroxide has been eliminated entirely. Furthermore, the decomposition of water increases linearly at a rate of 1.80 m*M* hydrogen per minute per molar boric acid. This rate is nearly identical with the rate of water decomposition at higher boric acid concentrations in the absence of potassium iodide.

Isotope Effect in Heavy and Light Water

Heavy water is more stable than light water to pile radiations in CP-3' (see Fig. 2). It is possible that the γ-ray component of the radiation causes a more efficient recombination of $D_2 + D_2O_2$ than of $H_2 + H_2O_2$. The validity of this explanation was demonstrated by measuring the relative rates of the recombination reactions induced by Co^{60} γ-rays for different isotopic permutations of hydrogen and hydrogen peroxide. The systems studied were:

$$H_2 + H_2O_2 \xrightarrow{H_2O} 2H_2O \qquad (A)$$

$$D_2 + H_2O_2 \xrightarrow{H_2O} 2HOD \qquad (B)$$

$$D_2 + D_2O_2 \xrightarrow{D_2O} 2D_2O \qquad (C)$$

$$H_2 + D_2O_2 \xrightarrow{D_2O} 2HOD \qquad (D)$$

The relative rates of these reactions is illustrated by Fig. 7, the circles representing the experimental points. The rates observed are in the order $k_D > k_C > k_A > k_B$.

MECHANISM

The experimental results deal with complex phenomena involved in pile irradiations. However, it is clear that the major features of these results may be explained by current ideas regarding dissociation and recombination reactions in water.[3,4] An equation suitable for expressing the rate of oxygen production as a function of boric acid concentration may be derived from the following mechanism:

	Rate constants	
$H_2O = H + OH$	γ_d	(1)
$H_2O = 1/2\ H_2 + 1/2\ H_2O_2$	γ_r	(2)
$H_2O = H + OH$	B_d	(1a)
$H_2O = 1/2\ H_2 + 1/2\ H_2O_2$	B_r	(2a)
$OH + H_2 = H_2O + H$	k_3	(3)
$H + H_2O_2 = H_2O + OH$	k_4	(4)
$OH + H_2O_2 = H_2O + HO_2$	k_5	(5)
$H + HO_2 = H_2O_2$	k_7	(7)

Reactions (1) and (2) refer to the dissociation and recombination reactions respectively for γ-rays whereas (1a) and (2a) refer to these reactions induced by by the $B^{10}(n,\alpha)Li^7$ disintegration in the solutions.

The rate law for the formation of hydrogen derived from the above mechanism is:

$$\frac{dH_2}{dt} = \frac{\gamma_r + B_r}{2} - \frac{k_3(\gamma_d + B_d)(H_2)}{k_5(H_2O_2)} \qquad (8)$$

The constants $\gamma_r/2$ and γ_d may be obtained from Table II and are 0.007 and 0.054 m*M*/min, respectively. $B_r/2$ and B_d are functions of boric acid concen-

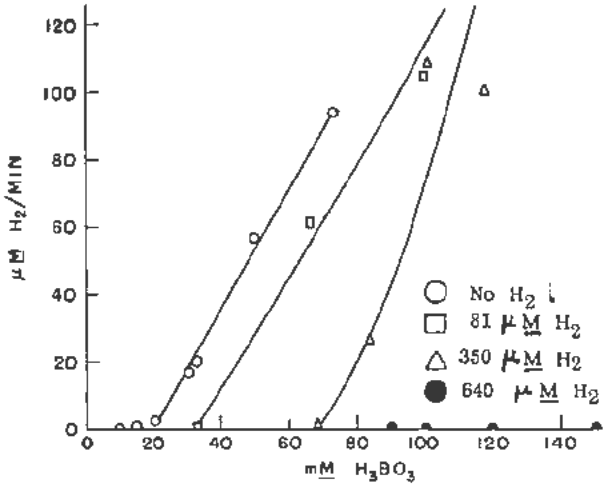

Figure 4. Effect of initial dissolved hydrogen on hydrogen production in boric acid solution irradiated in CP-3'

tration and from the data of Table II may be expressed in the form:

$$B_r/2 = 1.94C \text{ in units of } mM/\text{min}$$

$$B_d = 0.20C \text{ in units of } mM/\text{min}$$

where C = concentration of boric acid in moles/liter. Inserting these constants in Equation 8 one obtains:

$$\frac{d\mathrm{H}_2}{dt} = 0.007 + 1.94C - \frac{k_3(0.054 + 0.20C)(\mathrm{H}_2)}{k_5(\mathrm{H}_2\mathrm{O}_2)} \tag{9}$$

To a first approximation the ratio hydrogen/hydrogen peroxide is unity since these products are formed in equimolar quantities. The constant k_3/k_5 is found to be 0.80 and has been evaluated from the experimental result that the rate of hydrogen evolution is zero at 0.02 molar boric acid. This value is in substantial agreement with 0.94 obtained by Hochanadel.[4] Equation 9 then becomes Equation 10

$$\frac{d\mathrm{H}_2}{dt} = 1.76C - 0.036 \tag{10}$$

where the rate is expressed in terms of millimolar

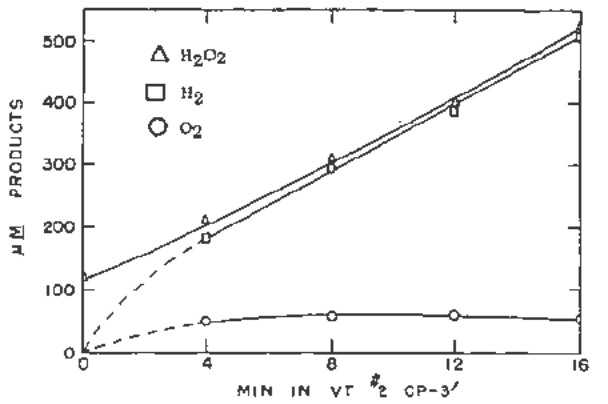

Figure 5. Effect of hydrogen peroxide on the decomposition of water irradiated in CP-3' at 0.03 M boric acid concentration

hydrogen per minute and C = molar concentration of boric acid. The solid curve in Fig. 2 for light water is obtained from Equation 10. This equation holds only for irradiations where the hydrogen peroxide and hydrogen concentrations are equal.

According to Equation 9, initially dissolved hydrogen gas should retard the decomposition of water whereas hydrogen peroxide when present initially should accelerate the decomposition of water. These conclusions have been qualitatively verified as is shown in Figs. 4 and 6. Equation 9 fails at very low concentrations of hydrogen peroxide since the following radical-radical reactions become important relative to Equations 4 and 5:

$$\mathrm{OH} + \mathrm{OH} = \mathrm{H}_2\mathrm{O}_2 \tag{11}$$

$$\mathrm{OH} + \mathrm{H} = \mathrm{H}_2\mathrm{O} \tag{12}$$

$$\mathrm{H} + \mathrm{H} = \mathrm{H}_2 \tag{13}$$

$$\mathrm{OH} + \mathrm{HO}_2 = \mathrm{H}_2\mathrm{O} + \mathrm{O}_2 \tag{14}$$

These reactions have not been considered in the above simplified mechanism. The assumptions inherent in the proposed mechanism are that all hydroxyl radicals disappear by reaction with hydrogen peroxide and hydrogen molecules and that hydrogen atoms dis-

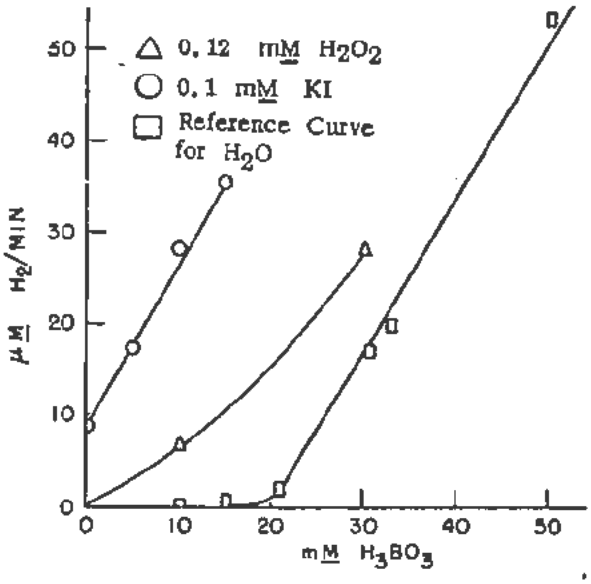

Figure 6. Effect of potassium iodide and hydrogen peroxide on the production of hydrogen in boric acid solutions irradiated in CP-3'

appear only by reaction with hydrogen peroxide and hydroperoxy radicals. Therefore, at sufficiently high boric acid concentrations hydrogen peroxide increases in the solution mainly through reaction (2a), causing a rapid reduction in the ratio $\mathrm{H}_2/\mathrm{H}_2\mathrm{O}_2$. Considering the difficulty in obtaining reproducible results the agreement between experiment and theory is satisfactory.

The extensive work performed by Bonet-Maury and Haissinsky and co-workers[6,7] on the formation of hydrogen peroxide by pile radiations are in qualitative

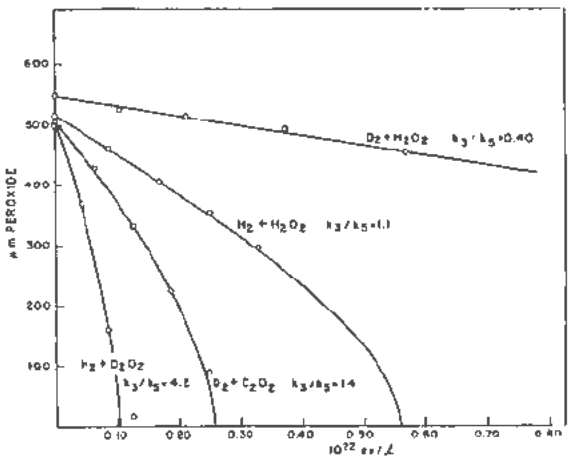

Figure 7. Isotopic effects in the recombination of aqueous hydrogen and hydrogen peroxide induced by Co^{60} gamma radiation

agreement with the present results. It is apparent from their work that the primary decomposition of water by the $B^{10}(n, \alpha)Li^7$ reaction is proportional to the boric acid concentration. This is expected in their case, since they worked in the concentration range from 0.16 to 2.3 molar boron. Under these conditions the gamma-ray energy from the reactor absorbed in the aqueous solution would be a small fraction of the disintegration energy of the boron atoms contained in the solution. Therefore, the delay in the decomposition of water at very low concentrations as observed in our results would not be found.

Table IV. Ratio of Constants (k_3/k_5) for Recombination Reactions

Reactants	k_3/k_5	
	Neutral solution	*0.001 M sulfuric acid solution*
$D_2 + H_2O_2(H_2O)$	–	0.40
$H_2 + H_2O_2(H_2O)$	0.90	1.1
$D_2 + D_2O_2(D_2O)$	1.4	1.4
$H_2 + D_2O_2(D_2O)$	4.2	4.2

Less understandable is the fact that the $G_{H_2O_2}$ for unbuffered boric acid solutions is only 0.35 as reported by the French investigators. We find at lower concentrations of boric acid that the hydrogen peroxide yield is substantially equal to the hydrogen yield. Owing to the thermal and catalyzed decompositions of hydrogen peroxide we prefer to use the hydrogen yield as an index of water decomposition. On this basis, $G_{H_2} = 1.25$.

The data presented for the rates in the recombination reaction between hydrogen and hydrogen peroxide using different permutations of the hydrogen isotope (reactions *A* through C) fit the kinetic Equation 15 based on the chain mechanism postulated above.

$$\frac{-d(H_2O_2)}{dt} = \gamma_d \frac{k_3(H_2)}{k_5(H_2O_2)} - \gamma_r \qquad (15)$$

In Fig. 7, the solid lines represent the integrated form of Equation 15 made to fit the experimental points (circles) by a proper choice of constants. For the light water solutions, values of $\gamma_d = G_1$(molecules/100 ev) = 2.74 and $\gamma_r = G_2/2 = 0.46$ have been taken from Hochanadel's data.[4] For heavy water solutions we have used a value of $\gamma_d = G_1 = 3.4$ and $\gamma_r = G_2/2 = 0.3$ derived from unpublished work on the decomposition of formic acid-oxygen solutions in light and heavy water. The k_3/k_5 ratios, determined by fitting the integrated rate expression to the experimental data, are given in Table IV.

ACKNOWLEDGEMENTS

The authors gratefully acknowledge the help provided by Dr. W. H. McCorkle and the operating crew of the Argonne reactor in carrying out the irradiations and to Miss P. Walsh for assistance in the preparation and analysis of the solutions.

REFERENCES

1. Allen, A. O., *Radiation Chemistry of Aqueous Solutions*, J. Phys. Colloid Chem. 52: 479, (1948).
2. Hart, E. J., *Radiation Chemistry of Ferrous Sulfate Solutions*, J. Am. Chem. Soc. 73: 1891, (1951).
3. Allen, A. O., Hochanadel, C. J., Ghormley, J. A. and Davis, T. W., *Decomposition of Water and Aqueous Solutions under Mixed Fast Neutrons and Gamma Radiation*, J. Phys. Chem. 56: 575, (1952).
4. Hochanadel, C. J., *Effect of Cobalt Gamma Radiation on Water and Aqueous Solutions*, ibid. 56: 587, (1952).
5. Hart, E. J., *The Radical Pair Yield of Ionizing Radiation in Aqueous Solutions of Formic Acid*, ibid, 56: 594, (1952).
6. Bonet-Maury, P. and Deysine, A., *Effects of Atomic Pile Radiation on Water and Solutions of Boron*, Compt. rend. 232: 1101, (1951).
7. Pucheault, J., Lefort, M. and Haissinsky, M., *Radiochemical Reactions in Nuclear Reactors. I. Formation of Water, Oxygenated by Irradiation of Boric Acid Solutions*, J. chimie Phys. 49: 286, (1952).
8. Hart, E. J., *Mechanism of the Gamma Ray Induced Oxidation of Formic Acid in Aqueous Solutions*, J. Am. Chem. Soc. 73: 68, (1951).
9. Peters, J. P. and Van Slyke, D. D., *Quantitative Clinical Chemistry*, Williams and Wilkins Co., Baltimore (1946).
10. Saunders, K. W. and Taylor, H. A., *The Photolysis of Acetone in Presence of Mercury*, J. Chem. Phys. 9: 616, (1941).
11. Scott, W. W., *Standard Methods of Chemical Analysis*, D. Van Nostrand and Co., Inc., New York (1939), Vol. I.
12. Hanna, G. C., *Disintegration of Boron by Slow Neutrons*, Phys. Rev. 80: 530, (1950).
13. McCorkle, W. H., private communication.
14. Hart, E. J. and Gordon, S., *Gas Evolution for Dosimetry of High Gamma, Neutron Fluxes*, Nucleonics 12: No. 4, 40, (1954).
15. Kaplan, L., Ringo, G. R. and Wilzbach, K. E., *Thermal Neutron Absorption Cross Section of Deuterium*, Phys. Rev. 87: 785, (1952).

Radiation-Chemical Processes in Inorganic Systems

(Electrochemical Action of Radiations. Sensitization of Radiation-Chemical Reactions)

By V. I. Veselovsky, USSR

The yield of products of a chemical process caused by the action of radiation on a chemical system is determined by:

1. The elementary processes brought about by the absorbed radiation and the primary chemical products (ions, atoms, radicals and excited molecules) formed.

2. The secondary processes (recombinations, reverse reactions, chemical reaction with solutions, chains, etc.), leading to a major change in initial yield of the chemical reactions engendered by radiation.

A rational approach to radiation-chemical processes is based on thorough investigations into the mechanism of the processes of absorption and transformation of high energy radiation in a chemical system, on a knowledge of the factors determining primary chemical effects of radiation, and an understanding of the kinetics of the complicated secondary reactions produced by active chemical intermediates as the result of radiation.

Two ways for utilizing the energy of nuclear radiations most effectively are:

1. Intensification of the primary radiation-chemical reaction through the methods of homogeneous and heterogeneous sensitization, and,

2. Suppression of reverse reactions by means of chemical or electrochemical fixation of primary radiolysis products.

This paper surveys some experiments aimed at finding the basic laws of the chemical action of radiations in some simple chemical systems.

1. ELECTROCHEMICAL REACTIONS CAUSED BY THE EFFECT OF RADIOACTIVE IRRADIATION OF AQUEOUS SOLUTIONS OF ELECTROLYTES. HYDROGEN POTENTIAL

An electrochemical process might be induced by the direct action of radiation upon an electrode or upon the potential governing surface compounds at the electrode-solution interface or indirectly by the effect of radiation-chemical changes in the solution. In the last case, the primary radiolysis products, oxidizing or reducing in character, might act upon the electrode, stimulating an electrochemical process determined by the electrochemical parameters (thermodynamic and kinetic) of the radiolysis products and of the system as a whole.

Original language: Russian.

The radiolysis of water, attended by the formation of hydrogen, oxygen and hydrogen peroxide as final products is the most thoroughly investigated radiation-chemical process. Data on this process available in the literature may be interpreted on the assumption that hydrogen atoms and hydroxyl radicals (and perhaps also excited water molecules) are the primary chemically active products.[1]

It is known that the final products of radiolysis (hydrogen, oxygen and hydrogen peroxide) are only a part of the primary yield of hydrogen atoms and hydroxyl radicals caused by irradiation.

The yield of the most important primary reaction of the radiolysis of water

$$H_2O \longrightarrow H + OH$$

is 3–4 molecules per 100 electron-volts of radiation energy. The ratio of the yields of the final radiolysis products to the products of the primary reaction depends upon various conditions: the oxidizing and reducing properties of the solute, and the type of radiation used. The relative yields of final products may vary greatly from the order of unity to 0.01 or less. Thus, the effect of an elementary radiation chemical reaction (radiolysis of water) depends on how the primary products (hydrogen atoms, hydroxyl radicals and perhaps also the excited water molecules) are involved in the complete chemical process.

The appearance of oxidizing and reducing compounds in the solution as the result of irradiation will obviously lead to changes in the electrochemical parameters of the system, and in the electrode potential in particular; moreover, the latter may serve as an index of the thermodynamic changes of the system (its redox potential) and of the kinetics of the electrochemical reactions (adsorption and ionization) of the radiolysis products at the electrode.

This conclusion is suggested also by modern concepts of the mechanism and kinetics of electrode processes, and especially by Frumkin's theses concerning the interdependence of the structure of the electrode-solution surface and the kinetics of the electrode reactions.[2]

Thus, the study of electrochemical effects of radiation in aqueous solutions affords an effective method for investigating the mechanism of radiation-chemical reactions in these systems.

At the same time, the stimulation of an electrochemical process through the selective use at the electrode boundary of the oxidizing radiolysis product (hydroxyl radical) or reducing product (hydrogen atom) is a very simple illustration of the fixation and energochemical utilization of the primary products of water radiolysis.

Theoretically, the potential of such a radiation-galvanic element should correspond to the free energy of the reverse electrochemical syntheses of the primary products of the radiolysis of water:

$$(E_{OH} - E_H)F = \Delta F$$

where E_{OH} and E_H are equilibrium electrode potentials of the corresponding radiolysis product, F is the value of the Faraday number and ΔF is the free energy of formation of water from the radicals

$$H + OH \rightarrow H_2O$$

In practice in aqueous solutions the potentials of the electrodes E_{OH} and E_H cannot exceed the potentials of molecular oxygen and hydrogen evolution on the corresponding electrodes at the given current density (rate of ionization of the radicals).

Assumptions found in the literature[3] concerning the probable average potentials of irradiated aqueous solutions ranging up to: $E_{H,OH} = 0.9$ volt are wrong, since they disregard the special kinetic features of the electrochemical process which determine the stationary (non-equilibrium) electrode potential in the given electrochemical system.

Experiments carried out by V. Veselovsky and his collaborators led to the discovery of a number of laws governing the electrochemical action of radioactive radiation.[4]

Of great scientific value is the observation of the hydrogen potential resulting from the reducing component of water radiolysis. A platinum electrode in an aqueous solution of sulphuric acid exposed to gamma rays from a 100-curie source of radioactive cobalt (at a rate of energy absorption equal to 2.0×10^{15} ev/cm^3-sec.) acquires a stable potential equal to the reversible hydrogen potential (somewhat negative). The electrode (practically reversible) can endure anodic polarization currents up to 20–30 micro-ampere/cm^2, which is a measure of the diffusion rate of the reducing radiolysis product under the experimental conditions.

The curves in Fig. 1 illustrate the kinetics of the establishment of the potential, i.e., the dependence of the platinum electrode potential on the duration of the irradiation (curves I and II).

Curve I is obtained when the electrode before the experiment was in contact with air; curve II when the electrode is reduced before the experiment.

From these results, it appears that during irradiation the electrode potential approaches more negative values, and 15-20 minutes after the beginning of irradiation attains the hydrogen electrode potential. The curves resemble those found on simple cathode charg-

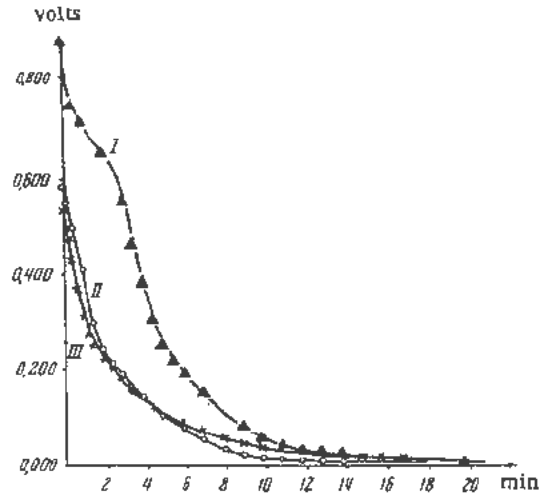

Figure 1. Dependence of Pt electrode potential on the time of gamma radiation action (curves I and II) and on the time of charging the electrode with 10 μa current (curve III)

ing of a platinum electrode (curve III), characteristic of the reduction of oxygen and adsorption of hydrogen on the electrode.

In view of the fact that molecular hydrogen, in the presence of equivalent quantities of oxidizing radiolysis products (hydroxyl radicals, hydrogen peroxide and oxygen), cannot produce the observed effect of the hydrogen potential, the compound which must be responsible for the observed values of the potential is the hydrogen atom formed as the result of the primary process of water radiolysis and selectively adsorbed by the platinum electrode.

$$Pt + H \rightarrow PtH_{ads}; \qquad PtH_{ads} \rightarrow Pt + H^+$$

The establishment of the hydrogen potential in the conditions described above is an independent experimental confirmation of the fact that enduring hydrogen atoms with a high electrochemical activity (reducing power) appear in the process of water radiolysis.

The following equation should hold for the electrochemical oxidation of hydrogen provided no processes occur which complicate the electrode reaction:

$$i = k\,[H]\,e^{\frac{a \cdot F\phi}{RT}}$$

According to this formula, the polarization current (velocity of the ionization of hydrogen atoms) is proportional to the surface concentration of the hydrogen atoms [H] and depends exponentionally on the deviation of the electrode potential (ϕ) from the equilibrium value. Consequently, assuming the adsorption of H atoms on the electrode requires little activation energy, the magnitude of the polarization current on the electrode at low overvoltage will be determined by the quantity of atomic hydrogen diffusing towards the electrode.

Experimental investigations of the kinetics of the process confirmed the fact that the rate of the process was really limited by the diffusion of the reducing component (atomic hydrogen) towards the operating electrode (see Fig. 2).

Figure 2 shows the dependence of the strength of the polarization current on the potential of the electrode. The general character of this dependence shows the low activation energy of the process (steep initial rise) and the diffusion-controlled type of kinetics (the value of the current is independent of the potential of the electrode).

Figure 3 gives the results of a quantitative study of the hydrogen ionization kinetics on a platinum electrode of area = 0.37 cm², obtained by the method of anodic polarography.

The constancy of the diffusion current is established under the experimental conditions in 2½–3 minutes after irradiation of the system begins. (Fig. 4).

The bottom curve of Fig. 3 corresponds to the stationary electrode and the upper one to the rotating electrode.

From the comparison of these curves it is seen that, as the solution is mixed by the rotation of the electrode, the strength of the polarization current increases 6- to 9-fold; an added proof of the fact that alterations of the electrochemical parameters of the system by irradiation are connected with changes in the solution. The curves in Fig. 3 show an increase in the value of the limiting diffusion currents when the electrode potential equals 0.2–0.3 volts. This increase may probably be explained by the differing electrochemical action of two substances diffusing from the solution: H atoms and H_2 molecules.

A comparison of these diffusion currents (velocity of H atom ionization) with currents for the same concentrations of molecular hydrogen furnishes the basis for estimating the concentration of H atoms formed by irradiation during the first 3 minutes, as $[H]_{volume} = 3 \times 10^{-5} N$. (Since there are no data on the H atom diffusion coefficient in water, the assumption is made that the diffusion coefficients of atomic and molecular hydrogen are equal.)

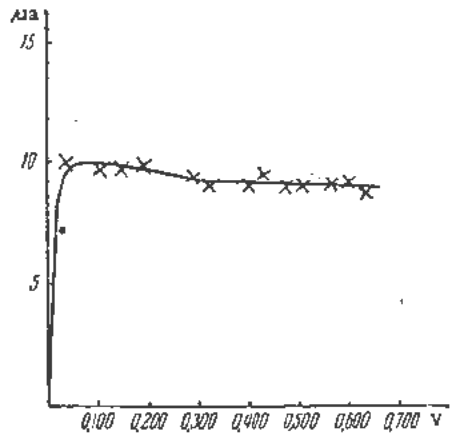

Figure 2. Dependence of the strength of the polarizing current during the action of gamma radiations

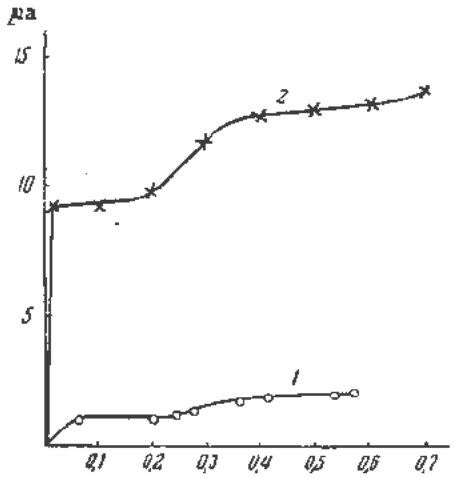

Figure 3. Dependence of the strength of the polarizing current on the potential during the action of gamma radiations: (1) stationary electrode; (2) rotating electrode

The yield of the reducing compound from radiolysis, according to the above data, approximates four equivalents per 100 ev of absorbed energy. Thus the reducing substance must be H atoms, since hydrogen molecules are not formed in such a yield under gamma-irradiation. The difference in the velocities of diffusion of H atoms and OH radicals towards the electrodes may also account for the observed effect.

The following observation is very important: the addition of oxalic acid to an aqueous solution of sulphuric acid leads to a drastic increase of the anodic currents to the Pt-electrode, raising their value (for a rotating electrode) from 20–30 microamperes/cm² up to 150–200 microamperes/cm², while the electrode potential remains close to the equilibrium hydrogen potential.

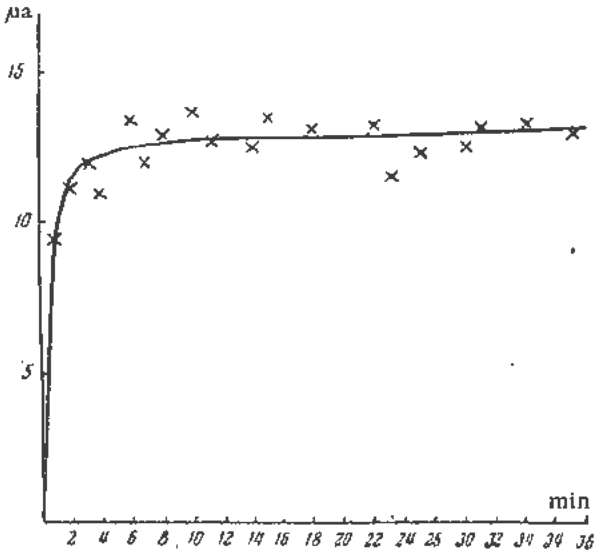

Figure 4. Dependence of the strength of the polarizing current on the time of gamma radiation action, when the constant potential of the electrode is V = 0.4 v

The factor stimulating the "capacity" of the H-electrode system may be the fixation of OH-radicals by the oxalic acid, which prevents the recombination of H atoms with hydroxyl radicals. However, a study of the electrochemical and chemical effects of irradiation in these conditions suggests that the main factor in the increase of the electrochemical capacity of the H-electrode (under radiation) may be the involvement of excited H_2O molecules in the reaction. The amount of atomic hydrogen in the system could increase according to the reaction $H_2O^* + M \rightarrow M{\cdot}OH + H$, where M is a molecule of reducing agent; this would account for the observed effects.

It may be expected that a high radiation intensity should increase the amount of H atom recombination, which should reduce the electrochemical effect of H atoms on the electrode. At the same time, the high reducing activity of H atoms suggests the possibility of inducing powerful reductions in irradiated aqueous solutions (up to the potentials of molecular and atomic hydrogen) with the aid of H atoms.

Of interest in this respect are the observations made by Proskurnin *et al.*[7] By investigation of aqueous solutions of nitrate and nitrite salts, the authors showed that, since there is no equilibrium between water and the two main products of its radiolysis: H and OH, the radiation chemical interaction of nitrate and nitrite with the H and OH-radicals respectively, is irreversible. That is not consistent with the belief that this radiation chemical reaction is reversible.[8]

The most favourable conditions for the radiation chemical reduction of nitrate to nitrite by the reducing compound from water radiolysis (i.e., H atoms), are in alkaline solution at nitrite concentrations $\gg 10^{-3}$ N; the yield of the process is then close to two molecules per 100 ev of absorbed energy.

When 10^{-2} mole of glucose is introduced into an aqueous solution (1 normal potassium nitrate and 1 normal potassium hydroxide) the yield of the radiation chemical reduction of nitrate to nitrite rises to 6 molecules per 100 ev of absorbed energy. The enhanced yield is due not only to the action of water radiolysis products formed by ionization of the water molecules. The authors assume that the enhancement is caused by excited states of water. An essential condition for the involvement of the latter in the chemical process is the presence of acceptors which would serve as an effective binding agent for H atoms and hydroxyl radicals.

Experiments carried out by Veselovsky and his collaborators[9] on the effect of gamma rays on systems of high oxidation potential (ceric sulphate and perchlorate, potassium bichromate and potassium permanganate) have demonstrated that the action of gamma-radiation on these systems shifts the redox equilibrium towards the reduced forms.

Continued irradiation leads to complete reduction, i.e., no equilibrium is established between the given redox system and the initial products of water radiolysis.

Data on the dependence of the yield of the reduction reaction upon the nature of gases which saturate the solution lead to the conclusion that, in all the systems investigated, the reduction is effected by means of H atoms formed in water radiolysis.

In the presence of molecular oxygen, H atoms produce the radical HO_2, which acts as a reducing agent in the above systems.

These results confirm the idea of the high reducing ability of H atoms, and disprove the belief that the processes of radiation chemical reduction are due to OH radicals.[7]

Table I below gives the yields, for all the systems studied, in solutions saturated with air. (Systems marked by an asterisk are oxygen-free.)

Table I

System, aqueous solution	*Normal oxidation reduction potential*	*Yield per 100 electron volts*	*Note*
$Ce(ClO_4)_4/Ce(ClO_4)_3$	1.70	3.3	Ozone is formed
$Ce(ClO_4)_4/Ce(ClO_4)_3$	1.70	4.0*	
$Ce(SO_4)_2/Ce_2(SO_4)_3$	1.44	3.6	
$K_2Cr_2O_7/Cr_2(SO_4)_3$	1.36	2.5	Ozone is formed
$KMnO_4/MnSO_4$	1.51	5.0	

The formation of ozone indicates that radiation may produce non-equilibrium compounds of high oxidizing potential and peroxide compounds, along with the selective reduction process.

II. ELECTROCHEMICAL AND CHEMICAL REACTIONS OF THE OXIDIZING PRODUCTS OF WATER RADIOLYSIS

The electrochemical method of investigation proved of value also for the purpose of studying the basic mechanism of reactions involving the oxidizing components of the radiolysis products of water.

Of great interest was the demonstration of an electrode potential due to the selective ionization of the oxidizing component of the water radiolysis products (hydroxyl radicals and hydrogen peroxide).

According to the reaction:

$$ME + OH \rightarrow MeOH_{ads}, Me{\cdot}OH_{ads} \rightarrow Me^{+} + OH^{-}$$

Silver may be used for the selective electrochemical ionization of the oxidizing product of radiolysis. A good adsorbant for oxygen, silver catalyses the ionization of oxygen, but it adsorbs hydrogen to a very small degree. Experiments have shown that in oxygen-free alkaline or weakly acidic solutions at the Ag electrode there is an unstable reversible potential of 0.5–0.6 volt anodic to that of a hydrogen electrode in the same solution. Moreover, the cathodic polarization currents corresponding to the ionization of the oxidizing component of radiolysis at this electrode (3–5 $\mu a/cm^2$) are smaller than the H-electrode currents described above and far smaller than the diffusion currents of the oxidizing component, under the same conditions of irradiation.

The difficulty of attaining the "oxygen" electrode in the above conditions, through the selective consumption of the oxidizing component of radiolysis, is explained apparently by the great electrochemical and chemical activity of H atoms, leading to the catalytic reaction:

$$Ag \cdot OH + H \rightarrow Ag + H_2O$$

which supersedes the electrochemical ionization reaction of hydroxyl that leads to the high anodic electrode potential.

Other chemical regularities are observed in the case of irradiation of aqueous solutions saturated with oxygen.

A platinum electrode in an alkaline or acid solution saturated with oxygen, under gamma irradiation by a 100 curie source of radioactive cobalt (at an intensity of $\sim 2.0 \times 10^{15}$ ev/cm³-sec) acquires a stable potential more positive by 1 volt than a hydrogen electrode in the same solution. And the polarization current (10 μa/cm²) corresponds to the diffusion rate of the oxidizing compounds formed in water radiolysis.

In this case (the presence of molecular oxygen in the system) the electrochemically active products of water radiolysis, responsible for the oxygen potential, will be not only hydroxyl radicals and hydrogen peroxide but also perhydroxyl radicals resulting from the capture of atomic hydrogen by molecular oxygen

$$H + O_2 \rightarrow HO_2$$

The anodic polarization of the Pt electrode in these conditions gives the characteristic curves shown on Fig. 7. They correspond to the electrochemical kinetics of hydrogen peroxide oxidation according to the equation: $H_2O_2 - 2e \xrightarrow{H_2O_2} O_2 + 2H^+$. This process is analyzed below in greater detail.

The above electrochemical observations are consistent with observations of chemical reactions in irradiated aqueous solutions.

The initial yield of hydrogen peroxide under the action of gamma radiation on water is known to increase many fold if the solution is saturated with oxygen.[1,8]

In that case hydrogen peroxide is formed not only through the recombination of primary hydroxyl radicals but also as the result of the reduction of molecular oxygen by H atoms formed in the process of water radiolysis. This reaction is the simplest example of useful radiation chemical synthesis brought about by the reaction of components introduced into the system with the primary radiolysis products.

However, when a certain concentration limit is reached, the increase in hydrogen peroxide concentration (for a given initial composition and radiation intensity) is stopped due to destructive reactions of hydrogen peroxide with the primary products of water radiolysis, as demonstrated in Hochanadel's work.[8]

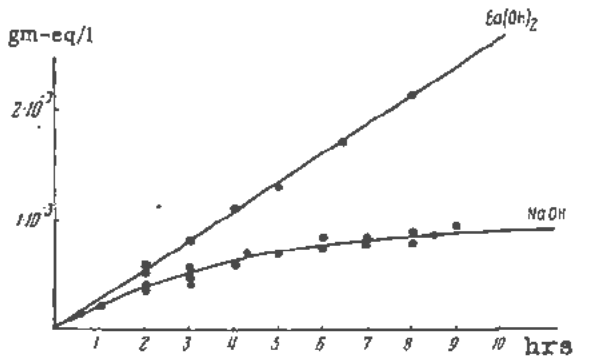

Figure 5. The kinetics of the formation of $BaO_2 \cdot 2H_2O_2$ in $Ba(OH)_2$ solution and of hydrogen peroxide in the 0.3N NaOH solution by gamma irradiation

A continuous process of chemical fixation of the water radiolysis products by molecular oxygen can be realized in various ways. As established by experiment, the action of Co^{60} gamma-radiation or of an electron beam of 300 kilovolts energy (simulating beta radiation) on a saturated aqueous solution of barium hydroxide saturated with oxygen and cooled to 0°C, the precipitation of $BaO_2 \cdot 2H_2O_2$ (removing hydrogen peroxide from the reaction zone) occurs continuously and leads to a linear dependence of the amount of product synthesized upon the duration of irradiation.[12]

The experimental data on the kinetics of hydrogen peroxide formation in a saturated solution of barium hydroxide in the presence of oxygen $P=1$ atmosphere) under the action of cobalt gamma radiation are given in Fig. 5. For comparison, Fig. 5 contains another curve illustrating the process of hydrogen peroxide formation in a solution of 0.3 N NaOH. The time of irradiation of the system is shown as the abscissa, the dose of irradiation absorbed in 1 cm³ of the solution being 2×10^{15} ev/sec. The concentration (in gram-equivalents per liter of the solution) of hydrogen peroxide formed as a result of the radiation-chemical process is given as the ordinates.

From the curves of Fig. 5 it follows that in a barium hydroxide solution there is a definite proportionality between the time of irradiation (the amount of energy absorbed by the system) and the amount of hydrogen peroxide formed. This shows the continuous formation of peroxide which gives a precipitate of $BaO_2 \cdot 2H_2O_2$. In a NaOH solution the limiting concentration of hydrogen peroxide is rapidly established. Under experimental conditions, the yield of hydrogen peroxide approximates 1.5 equivalents per 100 ev.

Figure 6 shows similar curves obtained by irradiating a solution with an electron beam of energy approximating 300 kilovolts. Another curve in the same figure shows the rate of reduction of cerium sulphate under identical conditions. The general regularities characteristic of the kinetics of the precipitation of barium hydroxide and hydrogen peroxide are

the same as for the action of gamma radiation. The yield of the process is also very close to 1.5 equivalents per 10 ev of absorbed energy.

The oxidation of ferrous to ferric ions is a thoroughly explored reaction involving the fixation of the oxidizing product of water radiolysis. It is used as a dosimetric reaction; the yield is about 15.5 equivalents per 100 ev of absorbed energy.[8] This yield corresponds to the utilization in the oxidation process of hydroxyl and perhydroxyl radicals formed as the result of reduction of molecular oxygen by the atoms of hydrogen.

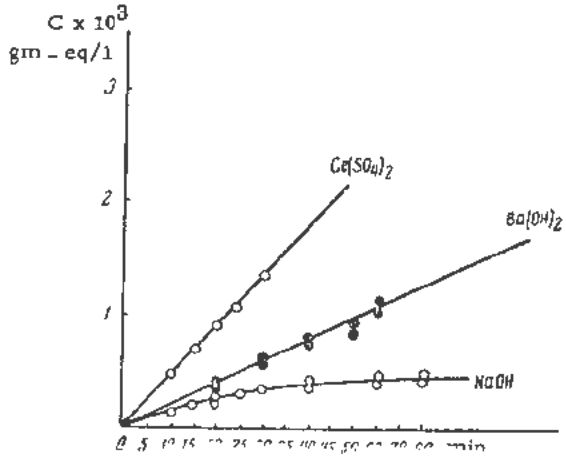

Figure 6. The kinetics of the precipitation of $BaO \cdot 2H_2O_2$ in $Ba(OH)_2$ solution of hydrogen peroxide formation in 0.3N NaOH solution and of $Ce(SO_4)_2$ reduction by an electron beam

However, Proskurnin and his collaborators[9] here found that the yield of radiation-caused oxidation of ferrous ions at a high acid concentration (3-4 N) increases up to 60 equivalents per 100 ev of absorbed radiation energy. That corresponds to the utilization in the oxidizing process of 15 molecules of water (together with molecular oxygen) by way of OH and HO_2 radicals. An important point is that the yield remains constant when acidity is increased above 3 N and also when the kind of acid is changed (H_2SO_4, H_3PO_4 and HCl).

The established facts lead us to assume that in reactions of this type not only ions and radicals are involved in the chemical process but also the excited H_2O-molecules formed as the result of irradiation. The whole process develops in conformity with concepts of Weiss.[1]

III. HETEROGENEOUS SENSITIZATION BY SEMICONDUCTORS OF RADIATION-CHEMICAL FORMATION AND DECOMPOSITION OF HYDROGEN PEROXIDE

On the basis of photochemical investigations carried out by Terenin and his collaborators[10] and photoelectrochemical works of Veselovsky and his collaborators,[11] which established the main laws governing the induction of the chemical processes on the interface between a semiconductor-sensitizer and the reaction medium, it may be assumed that, under the action of intense irradiation, semiconductors of the type of metallic oxides (ZnO, CuO, Fe_2O_3, Al_2O_3) will effectively transform the energy of radiation into a form of electronic energy which can induce chemical processes.

Among other things it was established earlier[11] that the action of ultraviolet light on a water suspension of ZnO in the presence of oxygen causes formation of hydrogen peroxide (quantum yield ~0.5) at the expense of water oxidation and oxygen reduction. The mechanism of the given process of heterogeneous sensitization consists of the following photoelectrochemical acts.

1. Absorption of active radiation ($\lambda < 385$ mμ) by the photosensitizer (microcrystal of zinc oxide).
2. Migration of the electron in the conduction band towards the semiconductor-solution interface.
3. Capture of the photoelectron by an oxygen molecule adsorbed on the microcrystal surface.
4. Electrochemical discharge of OH^- ion on the microcrystal of ZnO charged positively due to the loss of electrons.

The static potential of the process is determined by the relation between the rate of photoelectric ionization: $O_2 \rightarrow O_2^-$ and the rate of electrochemical discharge $OH_{ads}^- \rightarrow OH_{ads}$.

Both reactions lead to the formation of hydrogen peroxide in the aqueous medium.

It can be shown that the static potential of the system V_c which determines the effectiveness of the process, follows the equation:

$$V_c = K \ln \frac{[A]}{[D]} J + k_2$$

where A and D are the surface concentrations of acceptors and donors, J the intensity of the acting irradiation, K and k_2 are constants, involving the electrochemical and optical characteristics of the system.

The specific effect of intense radiation (alpha-, heta-, gamma-radiation) in the process of heterogeneous sensitization consists first of all in the stimulation by a gamma-quantum or an alpha or beta particle of a great number of the semiconductor electrons; thus a new type of elementary act appears, characterized by a constant, the "coefficient of multiplication" of excited electrons. This constant is a very important factor in determining the efficiency of a radiation-chemical process heterogeneously sensitized by a semiconductor.

The similarity of the processes of photoconductivity and fluorescence under the action of optical and ionizing radiations on semiconductors of the ZnO type, led us to assume similarity of mechanism for the different types of radiation also in the process of heterogeneous sensitization of chemical reactions by these semiconductors.

Veselovsky and his collaborators[12,13] have made a study of the heterogeneous sensitization of hydrogen peroxide formation by zinc oxide under the action of Co^{60} gamma rays on aqueous solutions saturated with oxygen, and of the heterogeneous decomposition of concentrated H_2O_2, in the presence of Fe oxides under the action of gamma radiation.

Experiments show that the energy yield of the radiolytic formation of hydrogen peroxide, in aqueous alkaline solutions saturated with oxygen in the presence of zinc oxide, increases four or five-fold (15-12 electron volts per equivalent of H_2O_2 produced instead of 60 electron volts found in the absence of a sensitizer).

The method of anodic polarography at a Pt electrode, described in the above quoted work,[11] was employed for the investigation of the kinetics of the process. The limit currents of the anodic oxidation of hydrogen peroxide give a quantitative determination of the concentration of hydrogen peroxide formed in the radiation chemical process.

Figure 7 gives the results of a series of such measurements. Curve I shows the polarogram of the oxidation of hydrogen peroxide after 30 minutes irradiation of NaOH solution saturated with oxygen; curve II gives the polarogram for the same solution after the addition of ZnO following 15 min irradiation. Curve III is the same with ZnO after 30 min irradiation. The values of limiting currents and consequently the H_2O_2 concentration equal respectively:

$$I_I = 6;\ I_{II} = 18;\ I_{III} = 28\ \mu a$$

The curve marked O shows the background currents in a solution of NaOH or NaOH + ZnO before irradiation.

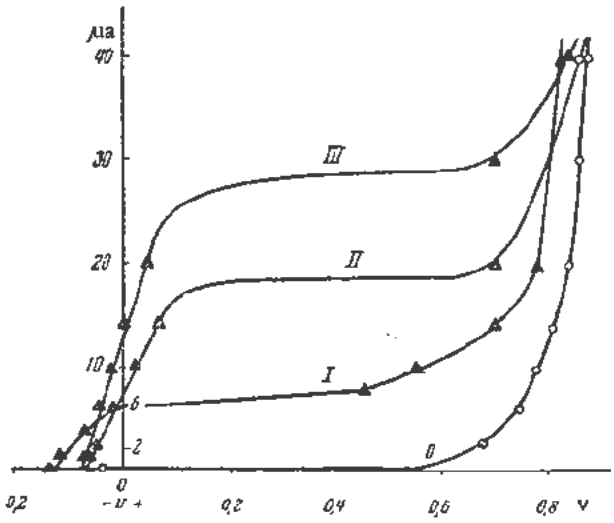

Figure 7. The dependence of the strength of the anodic polarization current on the potential under the action of gamma radiation. Curve I, aqueous solution of NaOH saturated with oxygen; Curve II-III, aqueous solutions of NaOH saturated with oxygen + suspension of ZnO. The background curve (without the action of irradiation) is designated O

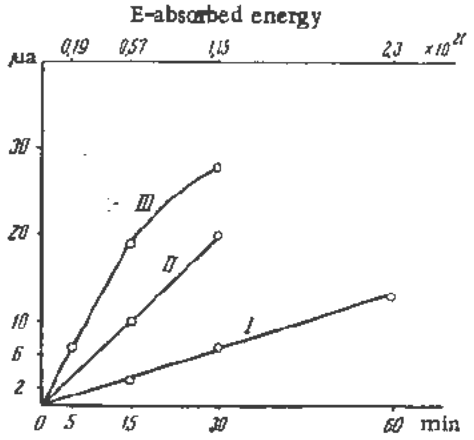

Figure 8. The kinetics of hydrogen peroxide formation by irradiation of aqueous solutions. (The dependence of the strength of the limiting currents of polarization (when V = 0.4 v) on the time of gamma irradiation). Curve I, aqueous solution of NaOH saturated with oxygen; Curves II and III, aqueous solutions of NaOH saturated with oxygen + suspensions of ZnO (of different activity)

Figure 8 illustrates results obtained by the second method of anodic polarography. The duration of irradiation (below) and absorption of energy by the above system are indicated on the axis of abscissas. And the limiting currents of hydrogen peroxide oxidation (characterizing the concentration of hydrogen peroxide formed at the given moment)—on the axis of ordinates. Consequently, the slopes of the curves give a quantitative measure of the rate of accumulation of hydrogen peroxide as the result of irradiation. Curve I illustrates the increase in hydrogen peroxide in irradiated 0.01 *N* NaOH solution. Curves II and III are the same for the NaOH solution with the additon of zinc oxide of different activities. The acceleration of reverse processes limits the increase of hydrogen peroxide concentration for more active zinc oxides.

By analogy with the above-described mechanism of the photoelectrochemical process of the heterogeneous formation of H_2O_2 under optical irradiation it is assumed that the principal feature of the radiochemical process that leads to a drastic intensification of the chemical action of the radiation is the more effective transformation of the gamma-radiation energy absorbed by the semiconductor into the electronic energy of the semiconductor, with the consequent induction of a chemical process on the interface between the sensitizer and the chemical medium.

Taking into consideration the fact that the energy of excitation of an electron in a ZnO semiconductor brought into the conductivity band approximates 3 ev, and taking the efficiency of the transformation of an absorbed gamma-quantum of the radiation energy of Co^{60} (approx. 1.25 Mev) as one unit, we get the maximum value of the "multiplication coefficient"—the number of semiconductor electrons excited by one gamma-quantum—as about 4×10^5.

The experimental value of the "multiplication coefficient" of the electrons in ZnO may easily he com-

puted from the data obtained (assuming the above described mechanism of the process) from the quantity of gamma energy absorbed by the added ZnO (2 gm of ZnO to 100 cm³ of the solution) which equals approximately 9×10^{15} ev per second, and from the increase of the peroxide yield: one gm-equivalent of H_2O_2 per 60 ev to 1 gm-eqnivalent of H_2O_2 per 12–15 ev, which adds the H_2O_2 disintegration of 6×10^{15} equivalent per second. And so the yield of the sensitized reaction equals 1 eq (H_2O_2) per 1.5 ev, and, therefore, the value of "multiplication coefficient" equals 8×10^6, i.e., approximately twice the theoretical value.

The high experimental value of the "multiplication coefficient" is caused by the H_2O_2 formation by excited electrons of the ZnO semiconductor which have an energy below 3 ev, assumed in the calculation of the maximum theoretical value of the "multiplication coefficient", corresponding to an excitation energy of approximately 1.5 ev expended in the elementary act.

The latter assumption is probable, especially if we consider that the electron affinity of the oxygen molecule—approximately 1 ev—facilitates the primary act: the transfer of an electron from the semiconductor to the adsorbed molecule of oxygen. It is also possible that one excited electron of the semiconductor may cause more than one elementary act.

The exact evaluation of the "multiplication coefficient" of electrons in the ZnO sensitized formation of H_2O_2 under the action of high-energy radiation defines the problem of studying the mechanism of the process more closely than is possible in the study of the corresponding photochemical process.

The elementary act of a heterogeneous radiochemical reaction in an aqueous solution just as in the case of optical radiation, is the transfer of an excited electron (with an energy of 3 ev for ZnO) from the semiconductor to a molecule of adsorbed oxygen, and the discharge of the hydroxyl ions which compensate the positive change of the semiconductor.

$$ZnO\begin{vmatrix} O_2 \\ OH^- \end{vmatrix} \xrightarrow{\gamma} \xrightarrow{H_2O} ZnO_+\begin{vmatrix} O_2^- \\ OH^- \end{vmatrix} \xrightarrow{H_2O} ZnO_+\begin{vmatrix} O_2^- \\ OH^- \end{vmatrix} \xrightarrow{H_2O} ZnO\begin{vmatrix} O_2^- \\ OH \end{vmatrix} \xrightarrow{H_2O} H_2O_2$$

The result of the two elementary acts in an aqueous medium is the formation of hydrogen peroxide.

The over-all efficiency of the chemical action of a single gamma-quantum of absorbed radiation will be determined by multiplying the "multiplication coefficient" of the electrons by the efficiency of the elementary act of the heterogeneous process.

The second heterogeneous radiochemical reaction studied was the decomposition of 83% hydrogen peroxide in the presence of a surface of oxidized iron taken as a sensitizer.[13]

From the available data on the accelerating effect of oxidized iron on the disintegration of hydrogen peroxide under the action of optical radiation[14] we could expect a similar effect in the case of gamma-radiation.

The experiments were conducted by use of the manometrical method for measuring the volume of evolved oxygen. The applied intensity of Co^{60} gamma-radiation was varied from 3.2×10^{15} to 7.3×10^{13} ev/cm²-sec. The ratio between the solution and the surface area of the iron (Hilger spectroscopically analyzed iron) was 20 cm² to 40 cm²; the iron was rolled into rings, 3 gm in weight.

The results are given in Table II and in Fig. 9.

The intensity of absorbed energy was 3.2×10^{15} ev/cm³ per sec.

Figure 9 gives the data in graphical form. On the ordinate is the rate of the radiochemical decomposition of hydrogen peroxide expressed in the number of cm³ of gas produced per second, the abscissa is the time in minutes.

Figure 10 shows the dependence of the heterogeneous H_2O_2 decomposition on the time; region I represents the rate of catalytic decomposition before irradiation; region II—the rate of decomposition under irradiation, and III—after it. The equality of the speed of decomposition before and after irradiation shows the unimportance of distorting phenomena (the appearance of iron ions, etc.).

It has been established by experiment that the rate of decomposition varies linearly with the square root of the intensity over the range of dose rates from 7.3×10^{13} to 3.2×10^{15} ev/cm³ per sec.

The yield of the reaction (which evidently is of chain nature) is determined both by the number of elementary chemical acts which produce the initiation centres, and by the length of the developing chain.

The most important problem in the light of the theses developed in this paper, is the nature of the mechanism of excitation at the solid-solution interface (between oxidized iron and hydrogen peroxide), which increases the chemical effect of gamma-radiation in the present process.

Table II. Yields of Homogeneous and Heterogeneous Decomposition of H_2O_2 at Various Temperatures

Temp of solution °C	Rate of H_2O_2 decomposition (vol. of gas evolved from 1 cm³ H_2O_2 per sec)	Yield of homogeneous H_2O_2 decomposition per 100 ev of absorbed energy, mol	Rate of H_2O_2 decomposition in presence of oxid. iron (vol. of gas evolved from 1 cm H_2O_2 per sec)	Yield of reaction of heterogeneous H_2O_2 decomposition per 100 ev of absorbed energy, mol
10	1.1×10^{-4}	185	1.6×10^{-4}	275
25	2×10^{-4}	335	5×10^{-4}	840
40	2.2×10^{-4}	370	5×10^{-4}	840

On the basis of the idea accepted by a number of authors that the chain mechanism of hydrogen peroxide decomposition under the action of radiations follows the scheme

$$H_2O_2 \rightarrow 2OH \qquad \text{Initiation of chain}$$

$$\left.\begin{aligned} OH + H_2O_2 &\rightarrow HO_2 + H_2O \\ HO_2 + H_2O_2 &\rightarrow OH + H_2O + O_2 \end{aligned}\right\} \text{Propagation of chain}$$

$$HO_2 + HO_2 \rightarrow H_2O_2 + O_2 \qquad \text{Termination of chain}$$

the observed effect of an oxidized iron surface on the yield of the radiochemical disintegration of hydrogen peroxide may be due to the appearance of additional initiation centres at the interface.

As in the above examined reaction of heterogeneous ZnO sensitization, the primary act of the process on an oxidized iron surface is the transformation of the energy of an absorbed gamma-quantum into electronic energy, with a definite "multiplication coefficient" for excitation of the electrons of the semiconductor—iron oxide.

The elementary act of direct radiochemical sensitization may be represented as an initiation of the chain decomposition of hydrogen peroxide by superficially adsorbed oxygen or by the peroxide itself, which receives the excitation energy of the semiconductor's electrons.

$$\left.\begin{aligned} Fe{\cdot}Fe_2O_3\,|^{*} \;\; H_2O_2 &\rightarrow Fe{\cdot}Fe_2O_3\,| \\ H_2O_2{}^{*} &\rightarrow Fe{\cdot}Fe_2O_3\,| \;\; + 2OH \end{aligned}\right.$$

$$\left.\begin{aligned} Fe{\cdot}Fe_2O_3\,|^{*} \;\; O \xrightarrow{H_2O_2} Fe{\cdot}Fe_2O_3\,|^{*} \\ O \xrightarrow{H_2O_2} Fe{\cdot}Fe_2O_3\,| \;\; + OH + HO_2 \end{aligned}\right.$$

It would be useless to try to describe the mechanism of the process more definitely, as in the case of sensitization on zinc oxide, because of the lack of the required data.

The fundamental scientific value of the said processes of heterogeneous sensitization lies in that they obviate the necessity of direct ionization and dissociation of molecules, which require energies of the order of tens of electron volts for the excitation of chemical reactions, needing instead only the excitation of semiconductor electrons, which require only a few electronvolts.

Consequently, the processes of heterogeneous radiochemical sensitization open new ways for increasing the effective chemical action of nuclear radiations.

IV. RADIATION CHEMICAL FORMATION OF OZONE AND NITROGEN OXIDES IN LIQUID OXYGEN AND NITROGEN-OXYGEN MIXTURES

Of great interest are the reactions caused by the action of nuclear radiations in air, which lead to the oxidation of nitrogen and formation of ozone. The appearance of powerful sources of nuclear radiation offers new possibilities of radiochemical nitrogen fixation.

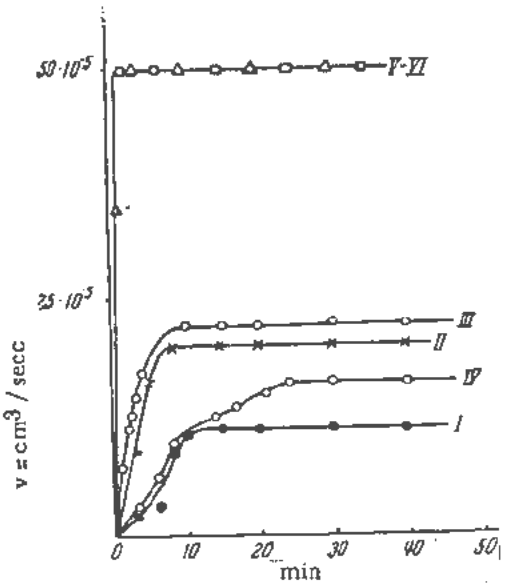

Figure 9. Dependence of the speed of decomposition of H_2O_2 on the time of gamma irradiation under different conditions; Curve I, homogeneous decomposition, t — 10°C; Curve II, homogeneous decomposition, t = 25°C; Curve III, homogeneous decomposition, t = 40°C; Curve IV, heterogeneous decomposition, t = 10°C (in the presence of $Fe \cdot Fe_2O_3$), Curves V and VI, heterogeneous decomposition, t = 25°C and 40°C respectively (in the presence of $Fe \cdot Fe_2O_3$)

The comparative simplicity of these reactions makes it possible to find out their mechanism and specific features and to connect them with the structure of the reacting molecules.

The investigations of ozone formation and nitrogen oxidation in the condensed phase are interesting in the light of the possibilities of increasing the effect of radiant energy absorption, and, perhaps, also of increasing the effective chemical action of irradiation by the specific transfer of electronic excitation energy in the condensation phase.

The effect of electronic action on the above-mentioned substances in the gaseous phase is treated in a number of papers. In addition to the well-known works of Lind[15] and other scientists, the question of

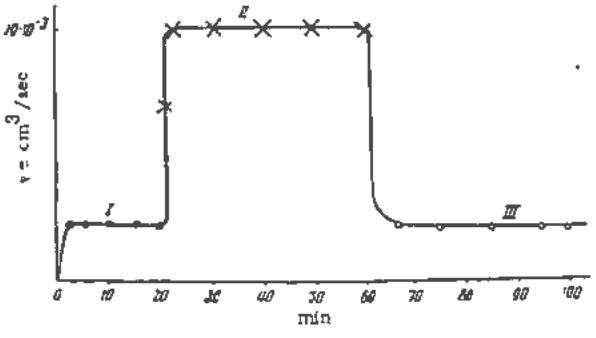

Figure 10. The reversibility of the catalytic and radiation-chemical heterogeneous decomposition of hydrogen peroxide (in the presence of $Fe \cdot Fe_2O_3$). Curve I, decomposition before irradiation; Curve II, decomposition during gamma radiation; Curve III, decomposition after irradiation

radiochemical ozone formation is treated in the latest work of Magee and Barton.[16]

Pshezhetsky and his collaborators have made a study of the effect of gamma irradiation from Co^{60} and an electronic beam (imitating beta-irradiation) on oxygen and nitrogen-oxygen mixtures in the condensed state.

Experiments have established that the yield of nitrogen oxides as the result of irradiation of liquid nitrogen-oxygen mixtures with electrons of 200–300 kilovolts energy amounts to 1–2 molecules per 100 ev of the absorbed energy. The simultaneous formation of ozone gives a yield approximating 15 molecules per 100 ev. The same yield of ozone is produced by irradiation of pure liquid oxygen with gamma rays of Co^{60}.

These high yields of ozone can be accounted for only by the assumption that excited molecules of oxygen are involved in the radiochemical reactions, as discussed in the quoted work.[16]

These molecules may result from primary excitation and from recombination of the ions O_2^+ and O_2^- formed by irradiation.

The reaction of ozone formation from excited oxygen proceeds according to the following scheme:

$$O_2^* + O_2 \rightarrow O_3 + O$$

$$O + O_2 + M \rightarrow O_3 + M$$

where M is a third body to take up excess energy. The state of $^3\Sigma_u^+$ with energy 4.9 ev can be the excited state involved.

Possibly, it is in the liquid phase that the most favorable conditions occur for the transformation, transference and utilization of absorbed energy of radiation in the form of energy of excited molecules effectively usable in the chemical process.

In this sense the radiochemical processes occurring in condensed systems resemble the processes of radiochemical sensitization discussed above.

A study of the kinetics of this reaction has shown that, given a steady state, the rate constant of ozone decomposition exceeds the rate constant of ozone formation by approximately one order of magnitude. This may be explained by a low resistance of ozone to electronic action. It could also probably be explained by the greater ability of ozone molecules to form negative ions, since their electron affinity is approximately three times larger.

The relatively small nitrogen oxide yields may evidently be explained by assuming that the excitation of oxygen and its ionization do not play an important part in this reaction, which is probably caused by the ionization of nitrogen.

The use of electrons of controlled energy has enabled us to find the laws governing the reaction of nitrogen oxidation.

In addition to the previously known facts of nitrogen oxide formation, the data on the kinetics of the oxidation of nitrogen at different pressures, mixture compositions and energies of the bombarding electrons indicate that the formation of NO and NO_2 result from the interaction of N_2^+ and N^+ ions with oxygen molecules. There can also be reactions of N-atoms with oxygen.

The velocity constant of nitrogen oxide formation depends on the energy of the electrons in a similar manner to the total ionization of nitrogen.

Since chemical reactions under ionization are produced by secondary electrons greatly differing in energy, the dependence of the velocity of radiation chemical reactions on the energy of the electrons acting on the molecules is very important.

Evidently the speed of the reaction will depend to a great degree upon the character of the energy spectrum of the electrons produced.

As indicated by the authors of the quoted work[18] the radiation chemical reaction rate constant should be proportional to the product of the distribution function describing the energy of the electrons and the ionization function of the molecules, the positive ions of which produce the chemical reaction.

The author's purpose was to demonstrate in this paper, on the basis of experimental material, the possibility of bringing about a substantial change in the effect of nuclear radiation, i.e., the possibility of changing the portion of the radiation energy absorbed by the system which assists in the production of chemical processes.

The results of experiments such as those mentioned in this paper, establish that (1) the energochemical yield of the radiochemical process may be greatly increased by using the methods of chemical and electrochemical fixation (involvement in the chemical process) of the primary chemically active components of radiolysis (ions, radicals, excited molecules); and (2) the method of sensitization and especially of heterogeneous sensitization by semiconductors, offers new ways of increasing the effect of the radiation, because of the more advantageous transformation of the energy of nuclear radiation absorbed by a sensitizer into a form which effectively stimulates chemical processes in the given medium.

Methods of increasing the efficiency of the chemical action of radiation and establishing the mechanism of radiation chemical transformations, indicated as a result of systematic experiments, have opened up new possibilities in the use of nuclear radiations for the producing of chemical processes.

REFERENCES

1. Discussion of the Faraday Soc., *12*, Rad. Chem. (1952).
2. Frumkin, A. N., *et al.*, Kinetics of electrode processes, Moscow University Press (1952).
3. Dainton, F. S., Ann. Rev. Phys. Chem., *2*, 99 (1951).
4. Zalkind, T. I. and Veselovsky, V. I., Collection of papers on radiation chemistry, Publ. Ac. Sci. USSR (1955).
5. Orekhov, V. D., Chyornova, A. I. and Proskurnin, M. A., Collection of papers on radiation chemistry, Publ. Ac. Sci. USSR (1955).

6. Veselovsky, V. I., Zalkind, T. I., Miller, N. B. and Aladzhalova, N. A., Collection of papers on radiation chemistry, Publ. Ac. Sci. USSR (1955).
7. Haissinsky, M., Lefort, M. and de Bail, H., J. Chem. Phys., *48*, 208 (1951).
8. Hochanadel, C. J., J. Phys. Chem., *56*, 587 (1952).
9. Proskurnin, M. A., Orekhov, V. D. and Chyornova, A. I., Collection of papers on radiation chemistry, Publ. Ac. Sci. USSR (1955).
10. Terenin, A. N., Photochemistry of pigments, Publ. Ac. Sci. USSR (1947).
11. Veselovsky, V. I. and Shub, D. M., J. Phys. Chem., *26*, 509 (1952).
12. Veselovsky, V. I., Miller, N. B. and Shub, D. M., Collection of papers on radiation chemistry, Publ. Ac. Sci. USSR (1955).
13. Veselovsky, V. I. and Tynrikov, G. S., *ibid.*
14. Veselovsky, V. I., J. Phys. Chem, *23*, 1095 (1949).
15. Lind, S. C., The chemical effects of alpha particles and electrons, New York (1929).
16. Magee, J. L. and Barton, M., Journ. Amer. Chem. Soc., *72*, 1965, (1950); *73*, 523 (1951).
17. Pshezhetsky, S. Y., Myasnikov, I. A. and Buneev, N. A., Collection of papers on radiation chemistry, Publ. Ac. Sci. USSR (1955).
18. Pshezhetsky, S. Y. and Dmitriev, M. G., *ibid.*

Record of Proceedings of Session 12B

SATURDAY AFTERNOON, 13 AUGUST 1955

Chairman: Mr. I. Dostrovsky (Israel)

Vice-Chairman: Mr. G. A. Bazargan (Iran)

Scientific Secretaries: Messrs. J. Gaunt and A. Finkelstein

PROGRAMME

P/738 A survey of recent American research in the radiation chemistry of aqueous solutions. . . . . A. O. Allen

P/739 The radiation induced reaction of hydrogen and oxygen in water at 25°C to 250°C . . . . C. J. Hochanadel

Discussion

P/363 Chemical reactions induced by ionizing radiations in various organic substances . . . . . L. Bouby *et al.*

P/683 Radiolytic oxidation of organic compounds. . . . . N. Bach

Discussion

P/7 Experience with heavy water in the NRX reactor. . . . R. F. S. Robertson

P/445 Effect of radiation on heterogeneous systems of air or nitrogen and water. . . . . J. Wright *et al.*

P/679 Radiolysis of water in the presence of H_2 and O_2 due to reactor radiation, fission fragments and X-radiation . . . . . P. I. Dolin and B. V. Ershler

Discussion

The Chairman: This session is devoted to a discussion of the effects of radiation on liquids. This subject, as you know, is of interest to a number of different groups of scientists and for differing reasons. There is the fundamental interest in the mechanism of the primary and secondary effects of reactions induced by absorption of radiations on the one hand and their relationship to other known mechanisms of reaction on the other. There is the practical interest of nuclear engineers and reactor designers in the decomposition of the moderator and cooling medium. The biological effects of absorption of radiation are also a consequence of reactions occurring in the liquid phase. The future use of radiation, either from reactors or from fission waste products, to induce normal chemical reactions of technological importance, will be possible only when a clear understanding of the nature of the interaction of radiation with liquids is achieved. Whilst most of the studies to date have dealt with aqueous media, increasing attention is now being given to partly or wholly organic systems. Here again the interest is both theoretical and practical, to understand the reactions, to make new compounds or known compounds by new methods, and to develop new materials for reactor cooling.

Mr. A. O. Allen (USA) presented paper P/738.

Mr. C. J. Hochanadel (USA), presented paper P/739.

DISCUSSION ON PAPERS P/738 AND P/739

Mr. E. Saeland (Norway): I would like to present in a few words the results obtained by Mr. Ehrenberg and myself concerning the oxidation of the ferrous system and referred to by Mr. Allen in his excellent survey paper. The oxidation efficiency of a number of particle radiations resulting from the reactions of pile neutrons with different elements added to the ferrous solution was examined and the G value plotted against the ion density of the radiation.

In Slide 1 we have plotted the G values against the ion density expressed as ion pairs per micron. If we start at the extreme right, point No. 10 represents the action of fission fragments; No. 9 is our result for alpha particles from the slow neutron reaction with boron; No. 8 is the data of Miller for polonium-alpha rays; No. 7 is our result for protons from the (n,p) reaction on nitrogen; No. 6 is our result for tritons from the (n,α) reaction on lithium; No. 5 represents two data for the beta radiation from tritium, the higher value by Hardwick, the lower by Hart; No. 4 is our result for 180 kv X-rays; No. 3 is an old value from Hardwick's investigation of the beta rays from sulphur-35; No. 2 is the result obtained with the synchrocyclotron at Uppsala giving 160-million volt protons; No. 1 is some of the gamma G values for the ferrous system.

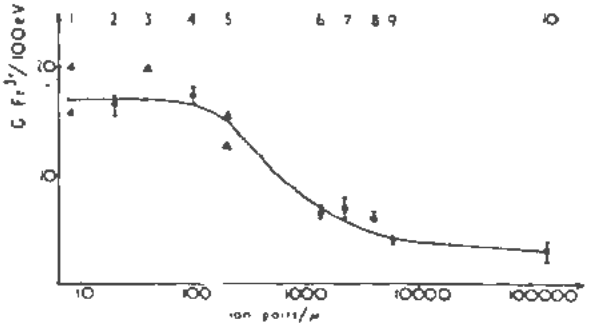

Slide 1

I think the higher values of numbers 1 and 3 should now be disregarded so that the curve might have a maximum and then decrease somewhat in the way indicated.

It might be added that a different dependence of the G values on ion density was found for the reduction of cerium ions.

A confirmation of our tentative curve might be important not only for dosimetry but also for theories of the action of radiations on solutions.

Mr. M. HAISSINSKY (France): I should like to ask Mr. Allen two questions. The first is: would he kindly explain what he means by the negative value of the E yield? Is not that just another way of saying that, not only is the value of E not constant, but even the value of F may vary?

My second question is this. I recently had the opportunity of a long discussion with Mr. Hugo Fricke, the father of activated water, during which he laid great stress on the following question: did I believe that in 1955 a correct explanation of at least the broad outlines of the radiation chemistry of aqueous solutions could be given by assuming that the water is decomposed into H and OH radicals? I venture to ask Mr. Allen the same question.

Mr. ALLEN (USA): In answer to the first question, Mr. Haissinsky is quite correct. I think, as indeed I stated during my talk, that as one changes the concentration in the solution of oxidizing and reducing agents the values of the molecular yield of hydrogen as well as hydrogen peroxide may change, that is to say the values of F and E may change, and the value of E may become in some cases negative.

As to your second question, I think it probable that nearly all the observations of importance in radiation chemistry of dilute aqueous solutions can be explained by radicals H and OH. There are still some anomalies which will require some modification in the present form of theory. Also, I am sure that you must eventually take into consideration exactly how the H and the OH are formed, that is, what are the processes leading up to the formation of H and OH. It may become necessary to investigate these preliminary processes in more detail, in order to have a better understanding of the whole picture, but I think we can say we have done very well so far with this theory of H and OH.

Mr. R. P. HAMMOND (USA): I would like to ask Mr. Hochanadel whether his experiments showing liquid phase recombination eliminate the possibility of wall catalysis.

Mr. HOCHANADEL (USA): While there is a slight decrease in pressure on heating the ampoules after radiation, this was a low rate relative to the induced rate. The higher the temperature the less accurate the results become.

Mr. H. de BRUYN (The Netherlands): I would like to ask this question of Mr. Allen. With regard to the reaction No. 5 which he mentioned in the theory of the decomposition of water by irradiation, I am informed that this reaction can be promoted by hydrogen ions. Does this mean that the decomposition rate of water is a function of the pH value?

Mr. ALLEN (USA): If you refer to the reaction we write as $H + O_2 = HO_2$, I do not think this does depend upon the hydrogen ions. I think it is probably very fast whether the hydrogen ions are there or not.

Mr. de BRUYN (The Netherlands): I believe it is in a publication of Prushkivin of the USSR who has worked in this field, and that it has to do with the following reaction: H ions produce H_2 positive ions. These H_2 ions react with oxygen forming HO_2 radicals plus H ions, and in that case you have an interaction of the hydrogen ions in this mechanism in the formation of HO_2 radicals.

Mr. ALLEN (USA): I do not think we agree with Mr. Prushkivin as to either the facts or the interpretations of them. I think this will require a little more work both in America and Russia in order to clear the question up.

Mr. V. N. KONDRATYEV (USSR): I should like to ask Mr. Hochanadel a question. You postulate one mechanism at low temperatures at 25°C, and another at 250°C. In one mechanism a constant concentration of hydrogen peroxide is maintained by the interaction of hydrogen and hydroxyl radicals with molecules of H_2O_2. At high temperatures, the HO_2 reaction plays the fundamental part in the decomposition of the hydrogen peroxide. What grounds are there for thinking that hydrogen and hydroxyl radicals do not play a part in the decomposition of hydrogen peroxide at high temperatures? Are there any data over and above the kinetic formula which you adduced?

Mr. HOCHANADEL (USA): There is really no reason other than kinetic results to postulate the mechanism as it is, except that the concentration of peroxide is certainly less than 1 micromolar, especially as the interaction of these radicals is believed to be small. Also, if some of those reactions of H and OH and peroxide were to occur, this would lead to a chain reaction. The observed results certainly indicate that there is no chain reaction, and for those reasons I

eliminate the reactions of the oxide and peroxide at high temperatures.

Mr. M. MAGAT (France) presented paper P/363.

Mr. V. N. KONDRATYEV (USSR) presented paper P/683.

DISCUSSION ON PAPERS P/363 AND P/683

Mr. J. W. T. SPINKS (Canada): I would like to make a comment on some of the radiochemical work on solutions, particularly aqueous solutions. Some speakers mentioned that chain reactions can occur, and one quantity of importance when chain reactions occur is the mean lifetime of the free radical chain. I would like to mention that we have recently determined the mean lifetime of some of these free radical chains by using the old photo-chemical method of intermittent irradiation. In the case of intermittent irradiation from, say, gamma rays, instead of using a thin sector we must use a steel sector, for example, fourteen inches or so long, with slots in it. By using this method one may determine, for example, the mean lifetime of free radicals produced in chloroform oxidation to be about one second, and in the case of chloral-hydrate reaction in solution about one-tenth second.

I would like to ask Mr. Kondratyev whether experiments of this kind have been under way in the Soviet Union.

Mr. KONDRATYEV (USSR): Such experiments have not been carried out yet, but they are planned and will be carried out.

Mr. R. F. S. ROBERTSON (Canada) presented paper P/7.

Mr. J. WRIGHT (UK) presented paper P/445.

Mr. L. Y. SUVOROV (USSR) presented paper P/679.

DISCUSSION ON PAPERS P/7, P/445 AND P/679

Mr. E. ROTH (France): I should like to ask Mr. Robertson for a few more details on the phenomenon of mass transfer. At what temperature does it begin to be important, and does Mr. Robertson think that it would occur in aluminium also?

A second question: in the experiments you mention, the recombination of hydrogen and oxygen takes place by catalysis on the walls, which, however, are of stainless steel. You have already made it clear that this phenomenon occurs by catalysis when the walls have been previously reduced. Do you think that aluminium could have a similar action in hydrogen/oxygen recombination catalysis?

Mr. ROBERTSON (Canada): In answer to the first question, I do not know of any lower limit of the temperature at which this fast transfer effect takes place. Our work has been done at about 250–260°C and higher. As far as the effect occurring on aluminium is concerned, I do not think you would find it nearly to the extent that you find it in stainless steels, for instance.

As to your second question—and in it I assume you are speaking of thermal recombination—there again I think the difference in rates found depends on the nature of the oxide. In one case it is Fe_3O_4, in another case Fe_2O_3, and I think it is due to adsorption of hydrogen on the surface that causes the catalytic effect, and again I do not think one finds this effect on aluminium.

Mr. ALLEN (USA): With respect to the work of Dolin and Ershler, Mr. Hochanadel and I are pleased to find confirmation of many of our results in the work of these authors. The very interesting new result which they announce, the eventual decrease of the hydrogen pressure as the oxidation concentration is increased, can perhaps be explained by the decrease in the rate of primary formation of molecular hydrogen as the oxygen is increased, which has already been shown by Hochanadel and Ghormley with oxygen at pressures below 1 atmosphere, and one might expect this effect to continue as the oxygen concentration is further raised until very little hydrogen is produced at all. I think this is probably the explanation of this very interesting observation.

Session 13B

EFFECTS OF RADIATION ON SOLIDS

LIST OF PAPERS

The Theory of Lattice Displacements Produced during Irradiation

By Frederick Seitz and J. S. Koehler,* USA

The study of the changes produced in solids during irradiations has two broad aspects. One is concerned with the qualitative classification of the types of damage, whereas the other is concerned with the quantitative evaluation of effects under the most simple and fundamental conditions attainable in order to obtain as good an understanding as possible of the underlying mechanisms. Both aspects of the subject are essential parts of it, the first not only because of the interest to engineering and general chemistry, but because it serves to delineate the boundaries of the field and provide one with a qualitative feeling for its domains. On the other hand the second part serves to provide the link with other areas of atomic physics and form the basis of understanding from first principles.

In the present article we shall attempt to restrict attention to the fundamental and quantitative aspects of the subject. This procedure obviously requires no apology; however, it is hoped that the process of sifting the rather vast literature in the entire field in such a way as to focus attention on that part of the work which can be discussed in quantitative terms will serve to stimulate more research of this kind. It appears that the field will strengthen our understanding of the imperfections in solids[2] only if this part of the study of radiation effects continues to receive serious attention from the leading investigators.

As a second restriction, we shall focus primary attention on the changes induced by light charged particles such as electrons, protons, deuterons and alpha particles.† Studies with particles of this type seem subject to somewhat more control than those centering about use of neutrons and fission fragments and are on the whole as representative as the latter. It is probable that research in reactors can be made almost as quantitative as that with accelerators; however, it is necessary to emplny cryogenics and careful calibration of neutron fluxes to achieve comparable results and this is not done broadly at the present time. A reactor is relatively easy to use for qualitative, general studies and most of the work has been of this nature. In any event, sufficient attention will be devoted to the behavior of atoms which are knocked on by fast neutrons to make the theory useful to anyone desiring to employ it.

BEHAVIOR OF THE SOLID TYPES

The four basic solid types, namely molecular, ionic, metallic and valence crystals behave in rather different ways under radiation bombardment and it is worth bearing the differences in mind. During bombardment with energetic charged particles, Fig. 1,

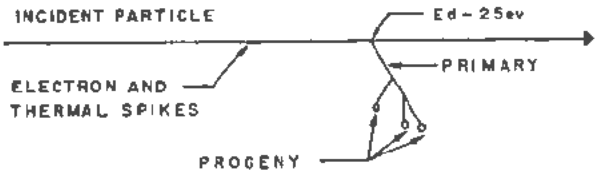

Figure 1. Schematic representation of the effects produced by an incident charged particle. Most of the energy is dissipated in the excitation of the orbital electrons, producing electron spikes. Small fraction, of the order of 0.1 per cent, is expended in stimulating lattice vibrations as a result of coulomb encounters between the incident particle and the nuclei of the solid. Occasionally one of the coulomb encounters is sufficiently close that an energy in excess of the threshold E_d, near 25 ev, is transmitted and an atom is displaced. The displaced atom may produce secondary displaced atoms if it receives enough kinetic energy

most of the energy of the particles is dissipated by electron excitation, the residual amount being only of the order of 0.1 per cent. This part of the energy transferred appears to have the predominant effect in molecular crystals and the simpler ionic solids, such as the alkali halides.

In organic, or molecular crystals, the individual molecules are relatively isolated from one another so that the atoms within the molecules relax rapidly when the electronic state is changed. For example, there is ample evidence that free radicals are introduced and bonds rearranged principally as a result of electron excitation. Such excitation can also be induced by photons and cathode rays so that the importance of massive fast particles becomes secondary.

The experimental studies using the alkali halides[3] particularly the chlorides, bromides and iodides demonstrate that the energy of electron excitation may be converted into atomic displacement with fairly high

* University of Illinois.

† The advantages of studies made with particles of this type were first appreciated by the group working at North American Aviation, Inc., in particular W. E. Parkins, H. Yockey and M. M. Mills. Prior to this interest centered on the changes induced by neutrons and fission fragments.

efficiency near dislocations and possibly other imperfections. Harten,[4] for example, has found that it is possible to produce an F-center near room temperature in KCl with an average expenditure of 60 ev with X-ray irradiation, whereas values near 1000 ev are adequate even at helium temperature. Thus the energy transferred to the electronic system by the incident particles and then transmitted through the crystal to the dislocations in the form of electrons, holes and excitons probably induces the dominant changes in crystals of this type at least at low temperatures. Nuclear reactions can play an important role, of course. It is essential that the recombination energy of electrons and holes be substantially larger than the energy required to form lattice defects such as vacancies and interstitial atoms if electron excitation is to have this effect. It is possible that this is not the case in other ionic solids which contain ions with charges larger than unity and electronic absorption spectra nearer the visible than those of the alkali halides.

Although electrons, holes and excitons probably have long ranges in valence crystals such as diamond, silicon and germanium, one might not expect the conversion of electronic energy into displacement near dislocations in these materials because the energy of recombination of electrons and holes is not large compared with the heat of formation. Actually, significant displacement effects have been observed in these solids only when radiations which actually can knock atoms out of position are employed.

The conduction electrons in most good metals are so loosely coupled to the lattice that one may expect poor conversion of excitation energy from them to the lattice. Electrons of the d and f type form a possible exception and merit special theoretical and experimental study. In any event there seem to be no known cases in which damage related to lattice displacement has been observed to occur in metals purely as a result of electron excitation.

It is useful to note that fission neutrons, which have energies near 1 Mev on the average, do not impart sufficient kinetic energy to atoms of atomic number larger than about 10 to cause them to lose energy by electron excitation. Instead such atoms lose practically all of their energy by colliding with other atoms. Thus selected precise studies in reactors under carefully controlled conditions may have value unattainable by other means.

The energy of sublimation E_s of a typical atom or ion in a tightly bound solid is in the neighborhood of 5 ev. Since atoms sublime from the surface, where approximately half of the binding forces active in the interior are operative, it can be concluded that the energy required to remove the typical atom or ion from an interior site in an adiabatic or reversible manner should be nearer $2E_s$. If, however, the atom is removed and forced into the lattice in a highly irreversible way, as when it is struck by a fast incident particle, an energy at least of the order of $4E_s$ should be required. On the basis of reasoning of this kind, the conclusion was drawn during early research in the field that an energy E_d near 25 ev should be required to displace an atom permanently from a stable site in a well-bound solid (Fig. 1). We shall see later that the existing evidence indicates that this is the proper order of magnitude.

THE SIMPLE THEORY OF DISPLACEMENT

Number of Primary Atoms Displaced

Non-Relativistic Calculation

The number of primary atoms displaced by an incident particle of charge Z_1 and mass M_1, having the energy E, in traversing a distance dR through a solid is

$$dn = n_0 \sigma_d dR \tag{1}$$

Here n_0 is the number of atoms per unit volume and σ_d, which is the cross section for displacement, is given in the form

$$\sigma_d = \frac{\eta}{E} \tag{2}$$

in the non-relativistic case where

$$\eta = 4\pi a_h^2 \frac{M_1}{M_2} \frac{Z_1^2 Z_2^2 R_h^2}{E_d} \tag{3}$$

Here Z_2 and M_2 are the charge and mass of the stationary atom, R_h is the Rydberg energy and a_h is the Bohr radius. Thus the total number of atoms displaced when the incident particle traverses a distance ΔR, so that its total range drops from R_1 to $R_1 - \Delta R$ is

$$n = n_0 \eta \int_{R_1 - \Delta R}^{R_1} \frac{dR}{E} \tag{4}$$

Two interesting cases to consider are that in which $\Delta R = R_1$, so that the lower limit of integration vanishes, and that in which ΔR is small compared with R_1. The two cases evidently correspond to a thick and thin target respectively. If we employ the approximate relation $R(E) = CE^\gamma$ we readily find that in the first case

$$n(\text{thick}) = n_0 R_1 \frac{\eta}{E_1} \frac{\gamma}{\gamma - 1} \tag{5}$$

in which E_1 and R_1 are the initial energy and range. The coefficient $\gamma/(\gamma-1)$ represents, in effect, the amplification of the initial rate of production of displaced atoms resulting from the decrease in velocity. In the thin case we find, to quadratic terms in ΔR,

$$n(\text{thin}) = n_0 \Delta R \frac{\eta}{E_1} \left[1 + \frac{1}{2\gamma} \frac{\Delta R}{R} + \frac{1}{6} \frac{\gamma + 1}{\gamma^2} \left(\frac{\Delta R}{R} \right)^2 \right] \tag{6}$$

Relativistic Case; Fast Electrons

The range of charged particles becomes nearly proportional to the energy in the relativistic region of

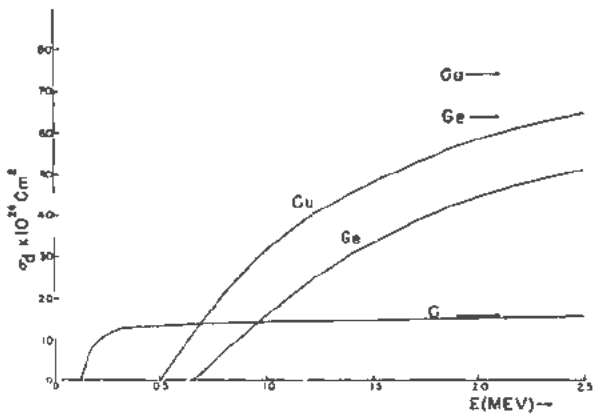

Figure 2. The displacement cross section σ_d for carbon, copper and germanium under electron bombardment evaluated on the assumption that E_d is 25 ev in the first two cases and 31 ev in the third. The horizontal arrows indicate the asymptotes in the three cases

speeds, for v/c approaches unity and the principal source of variation in rate of loss of energy through electron excitation arises from the relativistic deformatinn of the shape of the field of the moving charge. We shall be concerned principally with electrons having energies between 0.1 and about 3.0 Mev.

Katz and Penfold have found that the range of electrons satisfies the relation

$$R(\text{mg/cm}^2) = 412E^{(1.265-0.0954 \ln E)} \quad (E \text{ in Mev}) \quad (7)$$

in the reginn near and below 2.5 Mev. Above 2.5 Mev, Feather's linear rule

$$R(\text{mg/cm}^2) = 530E(\text{Mev}) - 106 \qquad (8)$$

becomes satisfactory. It is to be emphasized that range-eoergy relations do not have as precise a meaning for electrons as for heavier particles because they are scattered strongly, at least in the region of energy interesting to us.

A relatively common situation involving electron bombardment is that in which the thickness of the specimen is sufficiently small that σ_d remains finite throughout the specimen, that is E remains larger than the threshold value E_t (see Fig. 2). This is not true in experiments designed to determine the threshold energy when E actually is close to E_t, but is true when the initial energy is well above E_t. In such cases, it is often satisfactory to replace the actual expression for σ_d over the range of energy of interest by a linear expression of the form

$$\sigma(R) = \sigma(R_1)\frac{R - R'}{R_1 - R'} \qquad (9)$$

in which $\sigma(R)$ is the cross section when the range is R, R_1 is the initial range, $\sigma(R_1)$ is the initial cross section, that is for the entering particles of energy E_1, and R' is to be adjusted to give the best fit of the $\sigma_d(E)$ curve over the range of interest. The parameter R' evidently would be the range associated with the threshold energy E_t if $\sigma(R)$ were accurately linear above the threshold.

Whenever Equation 9 is valid, the number of primary atoms displaced per electron is given by

$$n = n_0\int_{R_0}^{R_1}\sigma(R)dR = n_0\sigma(R_1)(R_1 - R_0) \times\left[\frac{(R_1 + R_0) - 2R'}{2(R_1 - R')}\right] \qquad (10)$$

in which R_0 is the residual range after penetration, so that $R_1 - R_0$ is the thickness.

Number of Secondary Atoms Dislodged per Primary

Let us consider the number of secondary atoms dislodged from the lattice by a primary atom which has in turn been dislodged by the incident particle. The solution of this problem is highly important for the understanding of radiation damage whenever the incident particle possesses sufficient energy to produce primaries with energies well in excess of E_d.

Hard Sphere Collisions

We shall proceed under the assumption that the atoms of the lattice may be treated as though they can be released if and only if they receive a threshold energy E_d, which is independent of the direction in which they are struck. This is equivalent to assuming that each atom is bound in a simple square-well potential trough. We shall also assume, at least initially, that the primary atom is moving sufficiently slowly that it is scattered isotopically in collisions with the stationary atoms. The condition for such scattering is

$$\zeta = 4Z_2^2\frac{R_h}{E'}\frac{a_h}{a'} > 1 \qquad (11)$$

in which E' is the energy of the primary particle, Z_2 is the atomic number and $a' \simeq a_h/2Z_2^{1/2}$. Equation 11 is valid for energies as large as 10^5 ev for values of Z_2 near to or larger than 30.

The problem of determining the number of secondary atoms produced per primary can be solved in several ways when these simplifying conditions are valid. We shall use a method based upon a procedure introduced by Snyder and Neufeld.[5] Let us designate by $g(x)$ the total number of atoms which are displaced when a primary atom is produced with an energy $E = xE_d$ in excess of that required to release it from its bonding forces. The quantity g includes the primary atom as well as the secondaries it produces, so that its least value is 1. As long as the collisions are isotropic, an atom having initial energy E_1 has equal probability of being found in any range of energy dE extending from zero to E_1 after an elastic collision with another atom of the lattice. Thus the probability of being found in the range dE is dE/E_1. The first atom will produce a secondary atom with an energy $E_1 - (E_2 + E_d)$ if the energy of the first is E_2 after the collision. The total number of particles $g(x_1)$ produced by a given atom of energy $E_1 = x_1E_d$ can be expressed in terms of the number

$g(x_2)$ which it will produce after the collision, and the number $g(x_1 - x_2 - 1)$ which the atom it releases in the collision will produce. Here $x_2 = E_2/E_d$ where E_2 is the energy of the first atom after the collision, and $x_1 - x_2 - 1 = y$ is the energy of the displaced atom, also expressed in units of E_d. The relation between $g(x_1)$ and the other quantities is

$$g(x_1) = \int_0^{x_1} g(x_2)\frac{dx_2}{x_1} + \int_0^{x_1-1} g(y)\frac{dy}{x_1} \quad (12)$$

This is the primary equation of Snyder and Neufeld, which they solved by methods of approximation applicable to integral equations.

We shall proceed in an alternative way by differentiating Equation 12 with respect to x_1 to obtain the equation

$$\frac{dg(x_1)}{dx_1} = \frac{g(x_1 - 1)}{x_1} \quad (13)$$

It is clear that

$$g(x_1) = 1 \qquad 0 \leqslant x_1 \leqslant 1$$

for the initial atom is not able to produce a secoudary if its energy is less than E_d. If this solution is inserted into the left hand side of Equation 12, we find

$$g(x_1) = 1 + \log x_1 \qquad 1 \leqslant x_1 \leqslant 2 \quad (14)$$

The solution of Equation 12 may be obtained numerically for values of x_1 greater than 2 and is shown in Fig. 3 for values extending to $x_1 = 5.0$. Beyond this the relation is very accurately linear and may be approximated closely by the relation

$$g(x_1) = 0.561(1 + x_1) \qquad x_1 \geqslant 4.0 \quad (15)$$

The primary displaced atoms are distributed in energy in accordance with a factor $C/(E + E_b)^2$, that is in a manner proportional to $1/(x_1 + 1)^2$ corresponding to Rutherford collisions. The average value of $g(x_1)$, weighted with this factor is found to be

$$\bar{\nu} = 0.885 + 0.561 \log \frac{x_m + 1}{4} \qquad x_m \geqslant 3 \quad (16)$$

in which x_m is the maximum value of x_1, namely

$$x_m = \frac{4M_1M_2}{(M_1 + M_2)^2}\frac{E}{E_d} \quad (17)$$

Here M_1 and E are the mass and energy of the incident particle and M_2 is the mass of the atoms of the lattice. We may note that $\bar{\nu}$ varies slowly with x_m and is relatively insensitive to the quantities which enter into Equation 17. In the case of copper bombarded by 12 Mev deuterons, x_m is 5.64×10^4 if E_d is taken as 25 ev. The corresponding value of $\bar{\nu}$ is 6.23. It is interesting to note that the entire range of x contributes significantly to Equation 16.

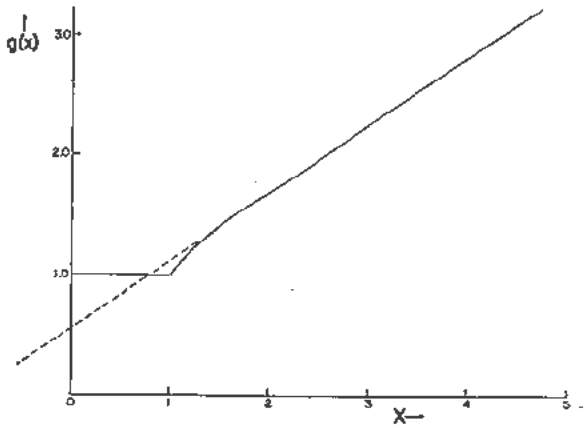

Figure 3. The number of atoms displaced per primary, $g(x)$, as a function of the energy of the primary in units of E_d. The dotted line represents the extrapolation of the essentially linear portion of the curve above $x = 3$ to negative values of x. (See text)

Rutherford Range

The foregoing evaluation of $\bar{\nu}$ rests on the assumption that the collisions are in the hard-sphere or isotropic range. Actually the range of x near x_m may correspond to energies in the Rutherford range. In the case of 12-Mev deuterons in copper just considered, for example, the value of E' for which the left-hand side of Equation 11 is unity is $E_r' = 2.72 \times 10^5$ ev, whereas E_m the maximum energy of the primary knock-ons is 1.41×10^6 ev, which is larger than E_r' by a factor of about 5. Fortunately this fact is not of great consequence in most important cases. This may be shown in the following way in the present instance, in which the scattering is viewed classically.

Since the nuclei are screened by electrons, distant collisions do not produce significant scattering. The critical distance of approach is given by the parameter $a' = a_h/2Z_2^{1/3}$. The energy transferred from the moving atom to the stationary when the collision parameter has this value would be

$$E_{a'} = 4Z_2^4\frac{R_h}{E'}\left(\frac{a_1}{a'}\right)^2 R_h = E_m\frac{(\xi')^2}{4} \quad (18)$$

if the field were perfectly coulombic. The energy is of the same order of magnitude when the field is screened. Thus $E_{a'}$ is far larger than E_d unless ξ' is very small compared with unity. As long as $E_{a'}$ is larger than $4E_d$, the secondaries produced by the primary possess values of $g(x_2)$ which lie in the linear range of Equation 15 and the total number of progeny produced by them will depend only on the total amount of energy transferred to them by the primary. Thus the function $g(x_1)$ for the primary may be extended linearly in the manner of Equation 15 from the value of x_1 for which $\xi' = 1$ to the value for which $E_{a'}$ drops to $4E_d$. The corresponding value of E' is

$$E_0' = Z_2^4\frac{R_h}{E_d}\left(\frac{a_1}{a'}\right)^2 R_h \quad (19)$$

This is of the order of 10^8 ev for copper and hence much larger than the values of E_m to be expected in bombardment with light nucleons having energies in the range of 10 Mev. On the other hand, Equation 19 is about 10^6 for a substance with atomic number 10; hence the coulomb range must be given more explicit attention in materials for which $Z_2 \leqslant 10$. Fortunately, it can be shown that Equation 16 is valid to a fair degree of approximation even in these cases, provided the primary atoms do not enter the ionizing range

Whenever the energy of the primary exceeds that of Equation 19 we may regard the primary as an incident particle and use Equation 16 to determine the average number of progeny derived from each of its secondaries. Now Equation 16 may be placed in the form

$$\begin{aligned} \bar{\nu} &= 0.561\,(\log 4.85 + \log \frac{x_m + 1}{4}) \\ &= 0.107 + 0.561 \log (x_m + 1) \end{aligned} \tag{20}$$

Thus to the extent the first term is negligible, Equation 16 has very nearly the same value it would have if Equation 15 were valid for the range of x_1 extending down to $x_1 = 0$. Hence the secondaries produced by the primary in the coulomb range for which E' exceeds Equation 19 behave closely as if the number of progeny they produced were determined entirely by the net amount of energy they receive, that is by the energy lost by the primary in being slowed to energy E_0'. To summarize, Equation 15 and hence Equation 16 can be used to good approximation even when E' exceeds Equation 19.

Range of Electron Excitation

It is evident that Equation 16 cannot be employed if x_1 attains so large a value that the moving atom is able to excite the electrons of the lattice. This condition is particularly important in light materials. For example a 10^6 ev atom with mass $M_2 = 20$ is equivalent to an electron with an energy of about 25 ev, which can dissipate a major fraction of its energy in exciting electrons in most solids until it is slowed below the critical threshold for the excitation processes. In general such cases may be treated by replacing x_m in Equation 16 by the value of x for which electron excitation ceases.

Estimates of the Number of Displacements and Disordered Atoms

We are now in a position to derive expressions for the total number of displacements N_d produced by a given amount of radiation. The basic equation for the number of displacements is

$$N_d = \bar{\nu} n \phi \tag{21}$$

Here $\bar{\nu}$ is the number of displaced atoms produced for each primary displacement, n is the number of primary displacements per incident particle and ϕ is the total number of incident particles. It will be assumed that ϕ is determinable from knowledge of the experimental arrangements, so that $\bar{\nu}$ and n are the quantities of principal theoretical discussion.

We have derived relations for n earlier on the assumption that there is a well-defined threshold energy E_d for displacing an atom. The cross section σ_d, given by Equation 2 is obtained on this basis and is reasonably precise within the limitations of this assumption.

Presumably the critical energy required to displace an atom from its normal position in the lattice to another metastable position depends both on the direction in which the atom starts to move as a result of the collision with the incident particle and upon chance fluctuations in the vibrations induced during displacement which determine whether it remains in the new position or is drawn back to its original site. The thermal spike associated with the displacement, having energy of the order of E_d, may induce significant diffusion and hence have the effect of guaranteeing that the probability of displacement varies continuously from zero to unity over a range of energy, instead of increasing abruptly.

Similarly, we might expect ambient temperature to play a role in determining the separation at which close Frenkel pairs are stable and hence influence the threshold energy. The influence of ambient temperature presumably could be ascertained by measuring the threshold energy for producing displacements with electrons at liquid helium and nitrogen temperatures; however, it would not be easy to determine the influence of the direction of displacement and thermal spikes on purely experimental grounds. As a result it seems wisest to employ the results of the simple theoretical treatment involving a well defined threshold energy until evidence may arise which indicates that this procedure is significantly in error.

We may expect the parameter $\bar{\nu}$ to be unity (or less) whenever the incident particles are electrons with energies near threshold since the primary displaced atoms then have insufficient energy to displace others. The derivation of $\bar{\nu}$ in other cases involves various assumptions. The problem is simplest if we assume that secondary atoms are freed only by direct impact with the primary atom or one of its progeny and then only when at least the threshold energy E_d is imparted. We saw in the previous section (Equation 16) that this hypothesis leads to a value of ν near 6.0 for a typical incident nucleon. There are good semi-quantitative reasons, based on the theory of thermal spikes, which is not presented here, to suppose that additional disarrangement occurs in the displacement spikes and that the primordial Frenkel pairs are able to migrate to some extent as a result of the thermal pulses. In accordance with the point of view mentioned above, we shall not attempt to make quantitative estimates of the effects originating in the relatively large temperature spikes but shall proceed as if the simple theory were correct and allow the

discrepancies to give us a clue concerning thermal effects. The latter should be relatively small in cases in which displacement is produced by electrons with energies near the threshold value. Thus a comparison of the damage produced by light nucleons and by electrons, using the simple theory as a medium for the comparison, should give some insight into the importance of displacement spikes.

Similarly, we shall ignore possibly significant effects derived from spikes of electron excitation because it is so difficult to estimate the magnitude of such effects. Detailed comparison between experimental results and those derived from the simple theory may make it necessary to revise this procedure. The simple theory seems to give a good account of the behavior of valence crystals, such as germanium; however, there are unresolved discrepancies in the case of metals.

BEHAVIOR OF METALS

Introduction

Much information concerning the behavior of the primary lattice defects which occur in salts can be obtained by investigating electrolytic processes and optical absorption in pure and intentionally contaminated salts.[3] Powerful techniques of this type do not appear to be readily applicable to metals. There remains the hope, however, that similar insight may be obtained in the case of metals by combining studies of diffusion and rapid quenching with those of radiation damage. This hope has not yet been completely achieved even in relatively simple metals, not because of the lack of experimental studies of radiation effects, but because the interpretation of the experimental results has been obscured by complexities. In brief, many of the properties observed in the course of irradiation seem to be coupled with aggregates of imperfections and it has not yet proved possible to disentangle such properties from those associated with isolated interstitial atoms or vacancies. On the whole it would seem that experimental observations must be extended to purer specimens which have been bombarded at lower temperatures and have been subjected to lighter irradiations before the picture can be unravelled. It may also prove necessary to extend the types of observations which are made.

Thus far copper has received the greatest attention among the monatomic metals because it can be obtained in relatively pure form, can be fabricated in various ways, and has been the object of extensive experimental and theoretical research. The investigations carried out with other metals have not indicated in any way that copper is inferior as a reference substance. Gold can be procured in somewhat purer form than copper, which makes it more ideally suited for quenching studies of the type developed by Kauffman and Koehler; however copper is somewhat easier to handle theoretically. In any event, the investigations do seem to show that even under the best circumstances radiation damage becomes comparatively simple only when extreme physical conditions are achieved, for example, when bombardments are made near helium temperatures. Appreciable changes occur during and following radiation at higher temperatures as a result of migration arising from thermal fluctuations. Even liquid nitrogen temperature does not provide complete stability from the influence of ambient fluctuations in the metals which have melting temperatures near 1000°C, although it is possible that such temperatures would be adequate for metals which have much higher melting points.

Unfortunately relatively little is known about the effect of impurities and structural imperfections such as dislocations and grain boundaries upon the course of radiation damage. One would expect such imperfections to play a very minor role in determining the number of atoms which become displaced during bombardment because the incident particle and the primary displaced atoms are sufficiently energetic that they should displace atoms situated at various positions primarily at random. On the other hand, the imperfections could play a very important role at a later period of time when conditions are such that the lattice defects produced by displacement migrate through the crystal. That is, they may play an essential role during a stage in which radiation damage anneals.

The changes induced in alloys by bombardment have received particular attention, especially in cases such as Cu_3Au, Ni_3Mn and CuZn in which the alloy exhibits an order-disorder transition. Experimental evidence shows that such alloys become disordered as a result of bombardment if they are ordered initially, provided the specimen is maintained at sufficiently low temperatures during bombardment. The disordering produced in such alloys is far greater than one should expect from displacement alone and that an explanation must be sought in terms of events which occur in displacement spikes or possibly electron spikes. We shall defer further discussion of this topic until the next section.

Theoretical Treatment of the Scattering of Conduction Electrons

Several general methods have been used to study the damage produced in pure monatomic metals, namely those based on measurement of electrical resistivity, lattice expansion and stored energy during annealing. The first method is by far the most popular because of its inherent simplicity and will be employed here as the basis for most of the discussion. The other procedures provide valuable additional information in special cases and, indeed, may eventually prove to be at least as important.

The greatest drawback to analyses based on resistivity measurement rests upon the fact that there is no independent experimental method of determining the contribution to resistivity arising from a pair of Frenkel defects or from other imperfections induced by irradiation. There have been several at-

Table I. Calculated Values of the Increment of Resistivity Arising from One Per Cent of Vacancies and Interstitial Atoms (After Jongenburger and Blatt. In Units of $\mu\Omega$-cm)

	Vacancies			*Interstitials*	
	Cu	Ag	Au		Cu
$\Delta\rho$	1.3	1.5	1.5	$\Delta\rho$	1.4

tempts to remedy this situation on the basis of theory by calculating the contribution to resistivity arising from vacancies and interstitial atoms. The first calculations of this type were made by Dexter,[6] who considered two contributions to scattering, namely that which arises from the immediate change in lattice potential induced by the withdrawal or insertion of an atom and that which arises from the secondary change associated with readjustment of the positions of the neighboring atoms. He concluded that the second effect was small, although not completely negligible. Jongenburger[7] treated the first contribution to scattering from vacancies in copper, silver and gold using a somewhat more completely self-consistent field and the phase-shift method of Faxen and Holtzmark rather than former approximation. Blatt[8] has extended this work to consider the case of an interstitial atom in copper. The interstitial problem is somewhat more complex because the possibility of resonance arises. All investigators assumed that the conduction electrons possess the true electron mass, at least during the process of scattering in the relatively short-range fields involved. Table I contains values of the contribution to resistivity to be expected from one per cent of vacancies in Cu, Ag and Au and one per cent of interstitial atoms in Cu. It will be noted that the effect of interstitials in Cu is nearly the same as that from vacancies, showing that the scattering from the interstitial atom is not near resonance under the conditions assumed.

The theoretical values at least form a basis for a consistent discussion of the changes in resistivity observed during bombardment. Gross discrepancies between observed values and those calculated with the use of the values of $\Delta\rho$ given in the table, in conjunction with the simple theory of displacements, may provide further insight into the theory.

Huntington's Calculations; Quenching of Defects in Gold

Before turning to the detailed discussion of radiation effects produced in metals, we shall consider two matters of general interest.

Huntington's Calculations

Huntington[9] has employed the best approximational methods available to estimate the energies ϵ_f required to form lattice vacancies and interstitial atoms in copper and the activation energies ϵ_m required to induce the imperfections to move from one equilibrium position to another. The calculations are made on the assumption that the s-p electrons behave essentially as if free, whereas the d-shell cores associated with different atoms interact in accordance with the Born-Mayer approximation commonly employed in ionic crystals. Huntington has found that at equilibrium the vacancy is centered at a normal lattice site and is surrounded symmetrically by the twelve copper atoms which normally surround the site. The vacancy jumps from one such equilibrium position to another during normal migration. In contrast, the calculations do not make it possible to decide whether the interstitial atom normally occupies the typical interstitial site of the face-centered cubic lattice (Fig. 4a) or whether it forces another atom from a normal site in such a way that the pair are symmetrically disposed in the interstitial region (Fig. 4b). In any case, the calculations imply that one of these configurations is the equilibrium one, whereas the other is associated with the saddle point in the process of interstitial migration. It is to be noted that a tagged interstitial atom does not remain interstitial during migration, but ultimately is transferred to a normal position. That is, the configuration, and not a specific atom, wanders during interstitial diffusion. Thus the migration may be termed interstitialcy movement, in analogy with vacancy movement.

Table II. Calculated Values of ϵ_m and ϵ_f for Vacancies and Interstitial Atoms in Copper (After Huntington. In Units of ev)

	Vacancy	*Interstitial*
ϵ_f	1.5–1.8	5.07–6.09
ϵ_m	~0.9	0.07–0.27

Table II contains the best estimates of ϵ_f and ϵ_m for the vacancy and interstitialcy processes. It is to be emphasized that the errors arising from approximations are large and that the numerical values have only semiquantitative value.

It seems reasonable to suppose that the observed

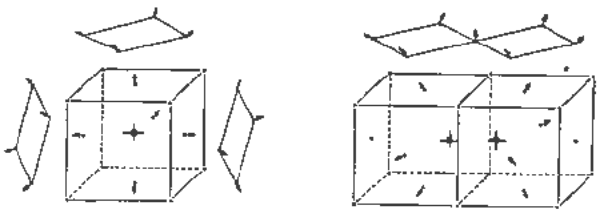

Figure 4. The two interstitial configurations considered by Huntington. The calculations do not permit determination of the more stable member of the pair; however, it is assumed that one represents the stable state of an interstitial atom and the other the saddle point configuration in interstitialcy magration. The cubic cell of the face-centered lattice is shown. The interstitial atom is at the center in (*a*), whereas the interstitial region is shared by two atoms in (*b*), one being a slightly displaced atom of the normal lattice

activation energy for self-diffusion in copper, namely 2.05 ev is the sum $\epsilon_f + \epsilon_m$ for one of the two processes. Huntington's calculations suggest that the vacancy mechanism is to be preferred strongly.

A second indication which ensues from the calculations is that ϵ_m may be very small for the interstitial configuration, that is of the order of 0.1 ev. If this is indeed the case, we should expect an activation energy of this magnitude to enter in the study of bombarded copper in which displacement pairs have been formed.

The Quenching Experiments of Kauffman and Koehler

If lattice defects are formed spontaneously at elevated temperatures, one might hope to preserve the associated disorder by cooling specimens sufficiently rapidly. Kauffman and Koehler[10] have succeeded in cooling coarse-grained wires of gold from temperatures near and below 900°C to room temperature in a time of the order of 0.01 sec. The specimens quenched in this way were quickly immersed in liquid nitrogen and subjected to a sequence of measurements of electrical resistivity. They have found that the residual resistivity of the wires is increased as a result of the quenching. A part of this increase can probably be ascribed to an effect associated with impurities. However, another component, which predominates strongly in wires quenched from above 700°C in the purest specimens (99.999% purity or better), varies in exactly the way one would expect if it were the result of the freezing-in of lattice defects. The corresponding activation energy for formation is found to be

$$\epsilon_f = 1.28 \pm 0.03 \text{ ev}$$

If one assumes that the defects are vacancies and employs Jongenburger's estimate of the resistivity arising from vacancies to determine the density, one finds a mol fraction of about 10^{-5} at 900°C.

The investigators have also studied the annealing of the disorder responsible for the increase in resistivity. They find that the increment in resistivity vanishes if the specimens are warmed from liquid nitrogen to room temperature. Studies of the isothermal annealing rate demonstrate that the activation energy for the process is 0.68 ± 0.03 ev, which one is tempted to identify with ϵ_m for the lattice defects. In this case, we would expect the sum of the two activation energies, namely 1.96 ev, to be identical with the activation energy for self-diffusion in gold. Two measurements give 1.96 ev and 1.74 ev for the activation energy in gold.

Although copper and gold are not identical metals, and in fact are not even ideally soluble in one another, they appear to be moderately homologous and invite comparison. In this connection it may be noted that the melting temperatures of copper, silver and gold are 1084°C, 960.5°C and 1063°C, respectively, whereas the activation energies for self-diffusion[11] are 2.05, 1.92 and 1.97 ev. Thus gold and copper particularly have many properties closely in common. If we combine Huntington's calculations on copper with the quenching experiments on gold, we are tempted to conclude that the prominent lattice defects in both metals at high temperatures are vacancies which have the following energy parameters

$$\epsilon_f \cong 1.3 \text{ ev} \qquad \epsilon_m \cong 0.7 \text{ ev}$$

An Analysis of Observed Radiation Effects in Copper

Threshold Energy

Eggen and Laubenstein[12] have found that the threshold energy of electrons for producing measurable change in the resistivity of copper at liquid nitrogen temperatures is 0.49 ± 0.02 Mev, corresponding to a threshold energy E_d of 25 ± 1 ev. Such measurements are made difficult by the fact that electrons with energies near the threshold are scattered strongly. Moreover electrons with the threshold energy produce displacements only at the surface of the specimen. Thus the damage produced by a given amount of bombarding charge rises rapidly with electron energy making the threshold difficult to determine precisely. Since experiments show that the changes produced by bombardment with 12 Mev deuterons at the same temperature undergo some recovery after bombardment ceases, it would be important to know if the threshold energy for electron bombardment is nearly the same at liquid helium temperatures, where, as we shall see, observable recovery associated with ambient temperature does not occur. It is possible that an atom must be displaced somewhat farther at nitrogen temperatures than at helium temperatures to be placed in a metastable position where thermal fluctuations will not send it back to the vacant lattice site from which it originated. This additional displacement may, in turn, require that the struck atom receive a substantially higher energy. In lieu of evidence to the contrary, we shall assume that the threshold energy for producing a permanent displacement, designated by E_d in previous sections, is 25 ev for copper.

Deuteron Bombardment

Marx, Cooper and Henderson[13] have irradiated 3 mil (0.076 mm) copper foils with 12 Mev deuterons at liquid nitrogen temperatures. Similar measurements have been carried out by Cooper, Koehler and Marx[14] at liquid helium temperatures with 5 mil (0.13 mm) wires. The range of deuterons of the energy employed in copper is 8 mils (0.20 mm), so the particles penetrate through the foils and wires. We shall employ the data obtained at helium temperatures first to calculate the number of atoms displaced per incident deuteron.

A good empirical value[15] for the exponent γ appearing in the range-energy relation is

$$\gamma = 1.63 \qquad (22)$$

so that the quantity in the parenthesis of Equation 6 is

$$1 + \frac{1}{2\gamma}\frac{\Delta R}{R} + \frac{1}{6}\frac{\gamma+1}{\gamma^2}\left(\frac{\Delta R}{R}\right)^2 = 1 + 0.19 + 0.06 = 1.25 \quad (23)$$

for $\Delta R = 5$ mils. The number of atoms displaced by a time-integrated flux ϕ is

$$N_d = 1.25 n_0 \Delta R \frac{\eta}{E_1}\bar{\nu}\phi \quad (24)$$

If ϕ is evaluated for unit area, the fraction of atoms displaced in the volume penetrated by the particles is

$$f = \frac{N_d}{n_0 \Delta R} = 1.25\frac{\eta}{E_1}\bar{\nu}\phi \quad (25)$$

A simple calculation shows that

$$\eta = 0.675 \times 10^{-24}\ \text{cm}^2\text{-Mev} \quad (26)$$

whence

$$f = 4.3 \times 10^{-3} \quad (27)$$

for $\phi = 10^{17}$ particles per cm², if we assume $E_1 = 25$ ev and $\bar{\nu} = 6.2$.

The increment of resistivity to be expected from this fraction of displaced atoms is

$$\Delta\rho = 0.43 \times 2.7 = 1.16\ \mu\Omega\text{-cm} \quad (28)$$

if we employ the data of Table I.

Figure 5 shows the changes of resistivity of copper, silver and gold as function of the time-integrated flux ϕ for specimens irradiated at a temperature near 10°K. It may be seen that the curves start linearly from the origin but have negative curvature. The curvature presumably is to be ascribed to an annealing process associated with bombardment. This process, which we shall discuss later, is generally termed[13] *radiation annealing*. It may be added that

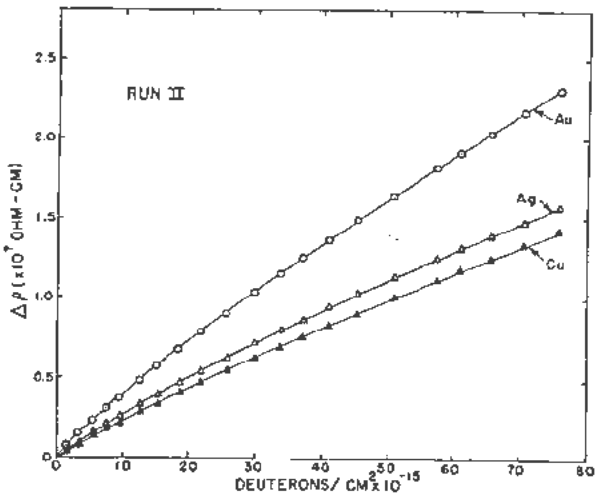

Figure 5. The changes of resistivity $\Delta\rho$ of copper, silver and gold as functions of flux Φ. The curves may be fitted accurately with a function of the form (36). (After Cooper)

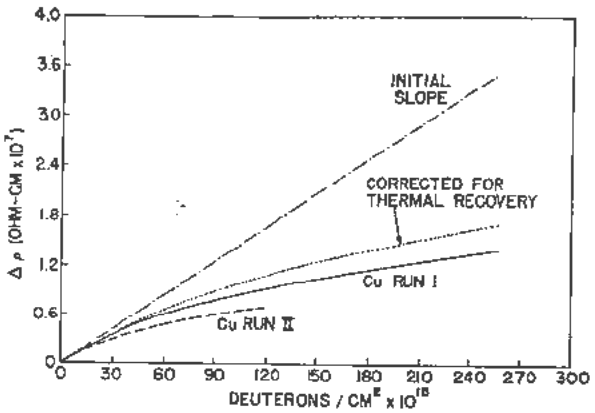

Figure 6. Resistivity versus flux curves for copper bombarded near liquid nitrogen temperatures. The experimental curves for two runs I and II are shown. The temperature was somewhat higher in Run II than in Run I. The dotted curve is calculated from I and II by correcting for the annealing effect of temperature. The straight line represents the extrapolation of the initial slope. (After Marx, Cooper and Henderson)

the resistivity change $\Delta\rho$ obtained after a designated amount of irradiation near 10°K is stable at the bombardment temperature. We shall assume that the initial slope of the $\Delta\rho$ versus ϕ curve is to be used in comparing the results of the experiment with the theoretical value in Equation 28. When the initial slope is extrapolated to $\phi = 10^{17}$ per cm², we find

$$\Delta\rho = 0.23\ \mu\Omega\text{-cm} \quad (29)$$

which is 5.0 times smaller than in Equation 28.

Figure 6 shows similar $\Delta\rho$ versus ϕ curves obtained by Marx, Cooper and Henderson[13] near liquid nitrogen temperatures. The changes in resistivity observed are sensitive to temperature in this region and exhibit annealing after bombardment if held in liquid nitrogen. The isothermal decrease thus obtained is of the order of five per cent and shows that the radiation annealing is interlinked with annealing effects derived from ambient temperature alone, in contrast with the observations near helium temperature. Since the foils employed were only 3 mils thick, the correction factor analogous to Equation 23 is 1.15 and the fraction of displacements for 10^{17} deuterons per cm² is

$$f = 3.9 \times 10^{-3} \quad (30)$$

corresponding to a theoretical increase in resistivity, analogous to Equation 28, of

$$\Delta\rho = 1.06\ \mu\Omega\text{-cm} \quad (31)$$

The extrapolated value of the initial slope of the experimental $\Delta\rho$ versus ϕ curve is more difficult to determine for the data obtained at liquid nitrogen temperature, however a good estimate is

$$\Delta\rho = 0.14\ \mu\Omega\text{-cm} \quad (32)$$

which is about 7.5 times smaller than in Equation 31.

The fact that the measured values obtained at liquid nitrogen temperatures deviate from the theoretical values by a factor nearly twice as great as those obtained at helium temperatures implies than an important annealing process occurs at the higher temperature. In fact we shall see below that the specimens irradiated at 10°K exhibit a large annealing effect at temperatures near 30°K which must be associated with a process that would proceed during irradiation at higher temperatures.

This point of view is supported further by the observation that the change of resistivity of foils prepared from specially purified copper (American Smelting and Refining grade 99.999% purity) and bombarded at 90°K is considerably less than that of the less pure specimens which lead to the value in Equation 32. For example, the actual value of $\Delta\rho$ for 10^{17} deuterons per cm^2 was 3.5×10^{-8} Ω-cm for the purer material in contrast with the value of 6.2×10^{-8} Ω-cm for a typical specimen of the type employed by Marx, Cooper and Henderson. It seems to follow that the impurities entrap a fraction of the imperfections which would anneal at 90°K if no obstacles were present.

Electron Bombardment

It is interesting to compare the preceding analysis with a somewhat preliminary set of conclusions which may be drawn from measurements carried out by Eggen and Laubenstein[12] on the change of resistance of copper foils bombarded with electrons. The foils, which were 0.012 mm thick, were maintained at a temperature between —190° and —150°C and were bombarded with 200 μa-hr/cm^2 of electrons (4.5×10^{18} particles/cm^2) having an energy of 810 kev. The resistivity was measured at —196°C. The change in resistivity appears to vary linearly with integrated flux to within the experimental error. The observed fractional change in resistivity was

$$\frac{\Delta\rho}{\rho} = 0.021 \quad (\phi = 200\ \mu\text{a-hr/cm}^2$$

Since the resistivity at —196°C is 0.21 μΩ-cm, we may conclude that

$$\Delta\rho = 4.4 \times 10^{-9}\ \Omega\text{-cm} \qquad (33)$$

It may be noted that this change is about 100 times smaller than that observed for 10^{17} deuterons. The density of displacements should be correspondingly less.

The cross section for production of a displacement by an 0.81 Mev electron in copper is 21.7×10^{-24} cm^2 if we assume that $E_d = 25$ ev.[16] The range of an electron having an energy of 0.81 Mev is about 316 mg/cm^2, whereas the foils employed by the investigators have a surface density of 10.7 mg/cm^2. Thus the correction for the loss of energy in the foil is of the order of 3 per cent and well within the accuracy of the measurements. We readily find that the fraction of atoms displaced in the foil as a result of bombardment with 200 μa-sec/cm^2 of electrons is about 9.3×10^{-5} if we assume $\bar{\nu} = 1$. This corresponds to a resistivity change

$$\Delta\rho = 2.5 \times 10^{-8}\ \Omega\text{-cm} \qquad (34)$$

analogous to Equations 28 and 31, which is 5.7 times larger than the observed value in Equation 33.

We find again that the calculated value of $\Delta\rho$ is appreciably higher than the observed one. The ratio of the two is somewhat nearer unity than that found for deuteron bombardment at liquid nitrogen temperature (i.e., 5.7 instead of 7.5); however the two ratios are fairly close. The ratio obtained for electron bombardment is also very close to that found with deuteron bombardment at helium temperatures (i.e., 5.0.); however the values do not merit careful comparison since we do not know to what extent thermal annealing affects the results obtained by electron bombardment at liquid nitrogen temperature.

The discrepancy between observed and calculated values could originate in several factors. The most obvious would be an error in the theoretical estimate of the resistivity contributed by a vacancy and an interstitial atom. Evidently it would be necessary to reduce the resistivity for one per cent of displaced atoms from 2.7 μΩ-cm to a value nearer 0.5 μΩ-cm. On the other hand, it is possible that the discrepancy originates in more subtle factors such as the influence of electron excitation. It is interesting to note that the discrepancy is about the same in deuteron bombarded and electron bombarded specimens. There is no ambiguity concerning the value of $\bar{\nu}$, the number of progeny per primary displaced atom, or of the influence of displacement spikes in the latter, so that it does not seem that the discrepancy can be tied in a simple way to errors in these two factors alone.

Expansion Measurements

It is also interesting to consider the experiments of McDonnell and Kierstead[17] on the volume expansion of commercial grade copper held at liquid nitrogen temperature and bombarded with deuterons. We shall devote particular attention to the most recent observations of Kierstead made with use of 19 Mev particles since they are more precise than the initial observations. The copper was employed in the form of a tube bent into the shape of a U and was cooled by flowing liquid nitrogen through the hollow center. The deuterons struck only one side of the U; the volume change of the irradiated section was determined by measuring the amount of bending, as if the system constituted a bimetallic strip. The wall thickness was 0.052 cm, which is about equal to the range of the particles, namely 0.41 gm/cm^2 = 0.046 cm. A total flux of 1.15×10^{17} deuterons per cm^2 was employed, the expansion of the bombarded portion was found to be essentially proportional to the total flux. The fraction of dis-

placed atoms to be expected for the total flux of deuterons involved is found to be

$$f = 6.6 \times 10^{-3} \qquad (35)$$

or 0.66 per cent. The volume change observed corresponds to 0.034 per cent.

We might expect the volume increase per Frenkel pair to be at least as large as the atomic volume because the interstitial exerts a large pressure on the surrounding lattice. In fact a simple calculation based on Huntington's estimates[9] of the amount by which the atoms surrounding an interstitial atom in copper are displaced, leads‡ to a volume expansion of about 2.0 v_a where v_a is the atomic volume. There is no reason to expect a compensating shrinkage about the vacancy if the members of pairs are well separated, so that the gain in volume per pair should be somewhat larger than one atomic volume. We note, however, that the observed expansion of 0.034 per cent is at least 19 times smaller than that to be expected from the fraction of displaced atoms in Equation 35 calculated from the simple theory. This large difference can scarcely be the result of a simple error in the theory leading to Equation 35. Instead it implies that the displaced atoms undergo a major rearrangement as the result of an annealiag process during the bombardment at liquid nitrogen temperatures.

One of the most important conclusions to be drawn from the measurements of volume change is that they suggest that the discrepancies between the measured and calculated values of the electrical resistivity, described above, are not simply a result of a gross error in the assumption that one per cent of displaced atoms contribute 2.7 $\mu\Omega$-cm to the resistivity. The observed density of defects appears to be lower than the calculated one by a factor of at least five when the bombardment is carried on near liquid nitrogen temperature.

Cooper's Analysis of Radiation Annealing

Cooper[14] has found that the resistivity versus flux curves shown in Fig. 5 can be fitted by a function of the form

$$\Delta\rho = A(1\text{-}e^{-\beta\phi}) \qquad (36)$$

to a precision better than one per cent over the entire range. Table III summarizes the situation.

We may note that $\beta\phi$ is of the order of 0.5 for $\phi = 10^{17}$ deuterons per cm² so that the deviation from linearity is significant. On the other hand fluxes at least five times larger would be required to provide an adequate test of the saturation of $\Delta\rho$ implied in Equation 36. In any event, the close obedience to this relation for the limited range of ϕ studied suggests that the variation of the density of displaced atoms N with total flux follows the differential relation

$$dN = \alpha d\phi - \beta N d\phi \qquad (37)$$

in which

$$\alpha = A\beta/r \qquad (38)$$

where r is the contribution to the resistivity per displaced atom. The first term on the right-hand side of Equation 37 describes the production of displaced atoms, whereas the second describes the effects of radiation annealing and is remarkably simple.

The most elementary basis on which to interpret the negative term in Equation 37 would be to postulate that the displaced atoms have an appreciable probability of falling into vacant lattice sites produced as a result of previous displacements. If L is the average range of a displaced atom and σ is the cross section for capture of the displaced atom by a vacancy, this postulate would lead to the relation

$$dN = \sigma_d \bar{\nu} n_o (1 - L\sigma N) d\phi \qquad (39)$$

in which σ_d is the cross section for the primary displacement, $\bar{\nu}$ is the average number of atoms displaced per primary atom and n_o is the density of atoms in the solid. The value of N at saturation evidently is given by the relation

$$N_s = 1/\sigma L \qquad (40)$$

Comparing Equations 37 and 39 we readily find the relations

$$A = N_s r = r/\sigma L \qquad (41)$$

$$\beta = \sigma_d \bar{\nu} n_o L\sigma \qquad (42)$$

We may note that the quantity $L\sigma$ has the connotation of a volume effective for the capture of the displaced atom by a vacancy. Since L should be of the order of $10r_s$ and σ of the order of $\pi(3r_s)^2$, we might expect $\sigma L n_0$ to be of the order of 70 in general magnitude. We shall calculate values of this par-

Table III. Values of the Parameters in Equation 36 Obtained from Experimental Measurements of $\Delta\rho$ versus ϕ (After Cooper)

Run	Sample	A($\mu\Omega$-cm)	β(10^{-17}cm²/D)	Maximum deviation in per cent of $\Delta\rho_{max}$	$A\beta$*
I.	Cu	0.519	0.540	0.3	0.234
I.	Ag	0.396	0.690	0.6	0.273
I.	Au	0.749	0.530	0.7	0.397
II.	Cu	0.513	0.430	0.3	0.221
II.	Ag	0.398	0.660	0.4	0.263
II.	Au	0.612	0.620	0.6	0.379

*The initial slope $A\beta$ is given in units of $\mu\Omega$-cm per $10^{17}D$/cm².

‡The volume by which a sphere under internal pressure expands is given by $\delta V = (3 + 3\mu/k)\epsilon V_c$ in which μ and k are the shear and compressional moduli, V_c is the volume of the interior cavity under pressure, assumed to be spherical, and ϵ is the fraction by which the radius of the cavity is expanded. Huntington's analysis corresponds to conditions in which ϵ is about 0.2 and V_c about $2v_a$,where v_a is the atomic volume. The quantity in parentheses is about 4.5. See F. Seitz, Rev. Mod. Phys. *18*, 384 (1954); J. D. Eshelby, Jour. App. Phys. *25*, 255 (1954).

ameter from Equations 41 and 42 using the experimental data for copper.

In the case of copper we may set

$$r = 270/n_0 \qquad \text{(in units of } \mu\Omega\text{-cm}^4\text{)}$$

Thus we find from Equation 41 and the value of A for copper (Run I) listed in Table III,

$$L\sigma n_0 = \frac{270}{A} = 520 \tag{43}$$

In contrast, we find from Equation 42

$$L\sigma n_0 = \frac{\beta}{\sigma_d \bar{\nu}} = 100 \tag{44}$$

if β is given the value of 0.54×10^{-17} (Table III) and $\sigma_d\bar{\nu}$ is given the theoretical value 4.35×10^{-20} cm^2 employed in connection with Equation 24. The deviation between the values of Equations 43 and 44 reflects the fact that the theory of displacements does not give the proper initial slope of the $\Delta\rho$ versus ϕ curve by a factor of 5. If it were proper to bring the two values into agreement by lowering r by a factor of 5, Equation 44 would be the more nearly correct of the two. Actually, as we have seen above, the studies of expansion imply that the theory does not give the proper density of displacements, at least at liquid nitrogen temperatures. As a result, Equation 43 is probably the more nearly correct. This unfortunately leads to a value of $L\sigma n_0$ about ten times larger than one might expect from elementary reasoning.

Apparently we must hold final conclusions in abeyance until further information is available. However the foregoing reasoning makes it seem unlikely that the applicability of Equation 36 stems from simple origins.

It is perhaps worth noting that a relation of the type in Equation 36 would be expected if some form of thermal agitation produced by the radiation caused interstitial atoms and vacancies produced by a given primary displaced atom to recombine with one another but not with the progeny of other primary atoms. Recombination processes of the second, or bimolecular, type would introduce a term in N^2 in the differential Equation 37 for which there is no evidence. It should be emphasized again that we have at present no good clue of a quantitative nature concerning the source of thermal agitation adequate to promote the recombination. There is the possibility that it is connected with electron spikes.

Relative Damage Observed in Copper, Silver and Gold

Cooper[14] found that the initial slopes of the $\Delta\rho$ versus ϕ curves for copper, silver and gold could be brought almost to coincidence[13] if each is divided by a factor Z_2^2 suggested by Equations 2 and 3 for σ_d. Table IV shows the ratios by which the damage curves for silver and gold differ from those of copper, in comparison with the ratio to be expected if the Z_2^2 dependence were precisely valid.

Table IV. Ratios of the Initial Slopes of the $\Delta\rho$ versus ϕ Curves for Silver and Gold Relative to That of Copper (After Cooper)

	Ratio of observed slopes		
	Run I	*Run II*	*Ratio of Z^2*
Ag/Cu	1.16	1.19	1.07
Au/Cu	1.70	1.71	1.67

The relatively good obedience to the Z_2^2 rule suggests that the three metals form closely homologous systems with respect to displacement as well as in respect to other properties, which is not surprising. Apparently quantities such as E_d and ν are nearly equal for the three metals; moreover the factors which influence radiation annealing and the scattering of conduction electrons are nearly the same.

Annealing Experiments

The experimental observations on the annealing of metals which have been subjected to bombardment are relatively complicated even in the simplest cases and cannot be explained in a simple way at the present time. One or two striking facts emerge, however, and it is worth reviewing the topic to indicate these. The most significant facts appear to be the following:

Annealing Peaks near 30°K

Cooper[14] has found that an important fraction of the increase in resistivity imparted to copper and silver at 10°K by deuteron bombardment anneals over a narrow temperature range near 30°K when the specimens are warmed. Figure 7 shows the resistivities of specimens of copper, silver and gold

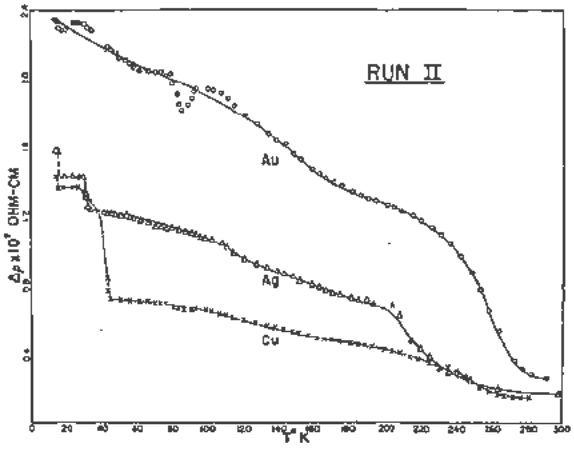

Figure 7. The decrease of bombardment-induced resistivity of copper, silver and gold as the specimens are warmed slowly from liquid helium temperatures (After Cooper). The decrease is irreversible. Sharp drops are found in silver and copper near 30°K and 40°K, respectively. The experiments indicate that no drop occurs in these two materials at lower temperatures. Gold does not appear to show a similar abrupt drop; however, there is reason to believe that the gold specimen was not in as good thermal contact with the cryostat as the other specimens

as functions of temperature during warming. The drops at 40°K in copper and at 30°K in Ag are clearly evident. Detailed investigation shows that the amount of annealing is negligible below the temperature at which the abrupt drop occurs, although there is almost continuous annealing at higher temperatures. A similar sharp drop was not observed in the specimens of gold used in the experiments. About 40 per cent of the radiation-induced increment of copper is recovered in the sharp drop, whereas the corresponding recovery for silver is about 25 per cent.

A simple analysis shows that the activation energy associated with the sharp drop is of the order of 0.1 ev if one assumes that the process is monomolecular and the frequency coefficient is near 10^{13} sec^{-1}. Actually the activation energy is not very critically dependent upon the precise value assumed for the coefficient. This value is just in the range suggested for the migration of interstitial copper atoms by Huntington's calculations for copper (Table II). Unfortunately no knowledge of the order of the reaction is available, so it is not possible to support uniquely the view that the annealing is to be associated with the relatively free migration of interstitial atoms. An alternative possibility is that closely neighboring interstitial atoms and vacancies which have a strong attraction are able to recombine when the critical temperature is reached as a result of the aid of ambient fluctuations. If this is the case, one would expect the reaction to be monomolecular and to have a frequency coefficient near 10^{13} sec^{-1} since the initial state of the close Frenkel pairs could be regarded as a metastable state of a small configuration of atoms which undergoes a relatively simple rearrangement. The reaction should be much less simple if it involves extensive interstitial diffusion.

It is interesting to note that the annealing process continues more or less smoothly at temperatures above the sharp drop, as if a series of recombinations involving a spectrum of activation energies were possible. Gold exhibits the same continuous annealing. There is a smooth, but relatively rapid, decline in $\Delta\rho$ in the range between 220°K and room temperature in all three metals indicative of a rather well-defined activation energy. This activation energy is near 0.7 ev, as if it might be associated with the migration of vacancies. We shall return to this point presently.

We noted in the last section that the value of the increment of resistivity produced in copper near 90°K seems to decrease with increasing purity of the specimen. This result suggests indeed that one of the products of bombardment migrates relatively freely at 90°K and can be trapped by a foreign atom. A migrating interstitialcy should be trapped if it meets a foreign atom which requires less energy to be moved from a substitutional to an interstitial site than an atom of the parent substance. Since the energy for the latter process presumably is near 5 ev in copper, silver and gold it would not be surprising if the value for some solute atoms were substantially less, that is, 1 ev more or less.

Annealing above 90°K

Prior to the foregoing work, based on specimens bombarded at helium temperatures, Marx, Cooper, Henderson[18] and Overhauser[18] carried out a sequence of studies on specimens bombarded at liquid nitrogen temperature. The annealing measurements were made with much greater care than those for any specimens bombarded thus far at temperatures near 10°K. It was found that the annealing takes place almost continuously as the specimens are warmed, indicating a range of activation energies; however, a process with a fairly sharply defined activation energy occurs in the range between 200°K and room temperature. Semi-quantitatively, at least, the specimens bombarded near 80°K behave during subsequent warming much like those bombarded at lower temperatures after they have been warmed to the liquid nitrogen range. The activation energy responsible for the major component of annealing observed at a given temperature was evaluated by studying the rate of change of isothermal annealing when the temperature was varied by a definite amount near the temperature in question. Figure 8 shows the spectrum of activation energies obtained by Overhauser in this manner. It will be observed that a single prominent value close to 0.69 ev is found above —60°C (213°K). About 25 per cent of the damage recovers on warming to —60°C; about 50 per cent more recovers during the stage with a single activation energy extending to room temperature; the remaining 25 per cent can be recovered only by heating to temperatures well in excess of 167°C. Redman, Coltman and Blewitt[19] have shown in fact that temperatures near 400°C are required for complete recovery.

Let us assume that the rate processes responsible for annealing below 220°K are governed by an equation of the form

$$\frac{dr(\epsilon)}{dt} = rfe^{-\epsilon/kT} \tag{45}$$

in which $r(\epsilon)$ is the contribution to resistivity from the imperfection which anneals with the activation energy ϵ, and f is a frequency coefficient. From the slope of the straight line in Fig. 8 and the fact that a time of the order of two hours is required to relax the contribution from one segment of the spectrum which can be annealed at a given temperature, one may readily deduce that f is near 10^{9} sec^{-1}, or is substantially smaller than 10^{13} sec^{-1}. This analysis shows that the process possessing the continuous range of activation energies probably is not simple as would be the case if only the recombination of close Frenkel pairs were involved, for in this event we should expect an equation of the form of Equation 45 with a value of f near 10^{13} sec^{-1}.

Overhauser has studied the annealing process which occurs with an activation energy near 0.69 ev

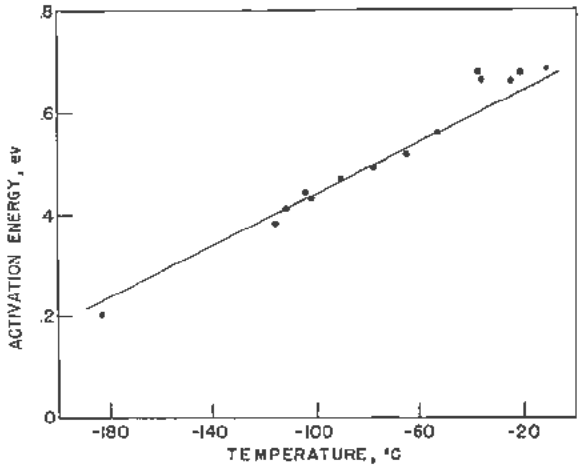

Figure 8. Plot of the principal activation energy effective in the annealing of copper, bombarded at liquid nitrogen temperature, as a function of the annealing temperature (after Overhauser). The value near 0.69 ev appears prominently above −60°C

very carefully and has found that the component of resistivity $\delta\rho$ associated with it anneals in accordance with the equation

$$\frac{d\delta\rho}{dt} = -A(\delta\rho)^n \qquad (46)$$

in which n is close to 2.5 and A is a coefficient depending upon temperatnre primarily through a Boltzmann factor. Figure 9 shows the observed variation of $\delta\rho$ with time at −18.3°C as well as the curve calculated from Equation 46 with $n = 2.5$. The observed behavior is so close to a bimolecular one that it is natural to assume the process involves the formation of bound pairs of undetermined nature which do not contribute to the resistivity from single diffusing imperfections which do contribute. Overhauser has shown in fact that the deviation of n from the value 2 for an ideal

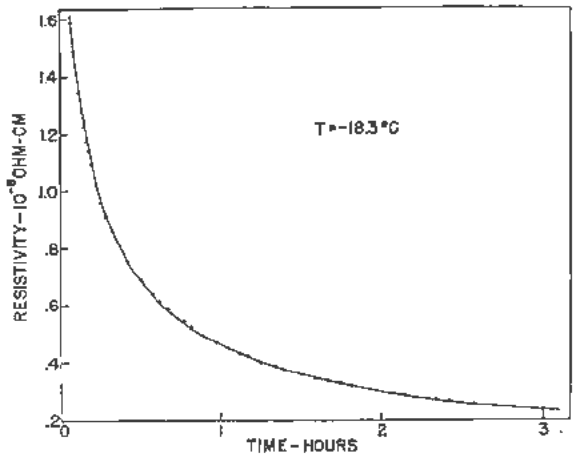

Figure 9. Isothermal annealing curve for a specimen of irradiated copper brought to −18.3°C after an anneal at −90°C. The solid curve is the solution of Eq. (46) of the text for $n = 2.5$. (after Overhauser)

bimolecular reaction can be explained in terms of the variations in lattice strain associated with the effects of irradiation.

Overhauser has also measured the energy released during annealing of specimens of copper during warming from liquid nitrogen temperature. Figure 10 shows the release of energy as a function of temperature for the two specimens studied. He found that the ratio of energy released to the decrease in resistivity is 1.7 cal/gm per $\mu\Omega$-cm. This ratio was obtained by dividing the integrated energy U released by the total change in $\Delta\rho$. However the consistency of the results for the two specimens indicates that the ratio $U/\Delta\rho$ probably is the same for each incremental change over the range of temperature studied. The peak in the curves is clearly associated with the single annealing process having an activation energy of 0.69 ev. Overhauser demonstrated that the contribution from this process enters in the heat curve in exactly the way one would expect from Equation 46 except for a small effect in the tail above 0°C where the experimental curve falls more rapidly than the theoretical one.

If one assumes that the energy is evolved as a result of the recombination of Frenkel pairs and that 5.0 ev are produced for each such recombination,

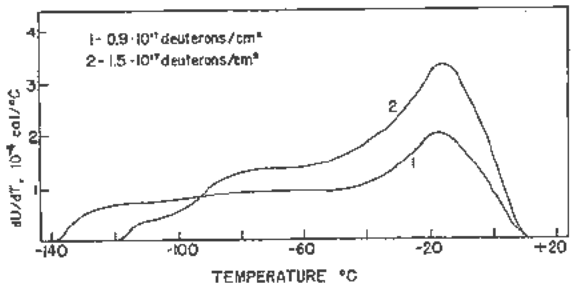

Figure 10. Stored energy release during the annealing of two irradiated specimens of copper. (after Overhauser)

in accordance with the magnitudes derived by Huntington, one finds from the foregoing ratio of $U/\Delta\rho$ that the resistivity associated with one per cent of displaced atoms should be 11 $\mu\Omega$-cm, instead of the value of 2.7 $\mu\Omega$-cm obtained by Jongenburger[7] and Blatt. Overhauser has adopted this viewpoint and has come to the conclusion that the number of displacements produced by deuterons at liquid nitrogen temperature is substantially smaller than the value calculated earlier principally because $\bar{\nu}$ should be taken nearer unity than 6. This pair of revisions would multiply the resistivities calculated from the theory for the case of deuteron bombardment (see Equations 27, 28 and 31 by a factor of about $11/2.7 \times 6 = 0.68$ and would not remove the discrepancies between theory and experiment. It would be necessary to introduce another correction, such as a further decrease in $\bar{\nu}$ to bring about more complete agreement. The increase in resistivity per pair would increase the discrepancy between the calculated and observed resistivities of the specimens

bombarded with electrons (cf. Equations 33 and 34) under the assumption that $\bar{\nu}$ is unity unless it were accompanied by a decrease in ν to a value near 0.05.

A number of alternative possibilities for adjusting the various parameters obviously exist as well. For example, it is possible that the interstitial atoms start diffusing freely at the temperatures near 30°K and that essentially none are present in mobile form after bombardment at liquid nitrogen temperature because they have recombined with impurity atoms, dislocations or vacancies. Under these circumstances the specimens would contain interstitial foreign atoms, vacancies, vacancy clusters and whatever damage is induced by the strain associated with displacement spikes. The annealing which extends to room temperature could then be associated with the aggregation of vacancies. The energy released per vacancy should be near 1.3 ev at maximum. According to this viewpoint, the prominent activation energy of 0.69 ev in copper is to be associated with the migration of vacancies which could coagulate to form pairs that migrate to dislocations very rapidly and disappear. Proposals of this type evidently are not unique and hence not very satisfying.

Annealing of Electron-Bombarded Copper

Eggen and Laubenstein[12] have found that all of the extra resistivity imparted to their specimens of copper by electron bombardment at liquid-nitrogen temperatures anneals when the specimens are warmed to room temperature. It follows that the damage produced by electrons with energies near the threshold value is inherently simpler than that produced by fast nucleons, which is perhaps not surprising in view of the possibilities for irreversible strain which exist in displacement spikes.

Recovery of Expansion of Copper

Kierstead[17] investigated the recovery of the expansion produced in copper by deuteron bombardment at liquid nitrogen temperature (see earlier portions of this section) when the specimens are warmed. One of the most remarkable results is that less than twenty per cent of the volume change appears to anneal below 400°C. Up to this temperature three well-defined annealing stages are found near —130°C, 0°C and 230°C. The percentages of recovery at these stages are 10.8, 2.9 and 3.6 respectively. A fourth stage enters just below 400°C and has produced 2.9 per cent of recovery when the temperature attains 400°C. It is to be noted that there is relatively little annealing between —105°C and —25°C where other investigators have observed a substantial part of the resistivity to anneal with the characteristic activation energy near 0.69 ev. However annealing of the expansion does occur between —140°C and —100°C. Kierstead's material was of commercial grade, so that the differences may be associated with the influence of impurities upon migrating imperfections.

It should be reiterated that the total expansion observed by Kierstead is at least nineteen times smaller than that to be expected from the simple theory of displacements.

We saw earlier that an isolated interstitial atom should cause the specimen of copper to expand by an amount near $2v_a$, where v_a is the atomic volume. This should not be compensated appreciably by the shrinkage around an isolated vacancy so there should be a net expansion near $2v_a$ per displaced pair. The entire amount of this expansion should be retrieved if the interstitial combines with the vacancy and both are annihilated. On the other hand, only about half is retrieved if the interstitial migrates to the surface or joins a jog at a dislocation. Similarly, only about half is recovered if the vacancy goes to the surface or to a jog at a dislocation. The relatively small fraction of recovery observed in Kierstead's experiments imply in turn that the processes of annihilation and migration to the surface or to dislocations play a relatively minor role during the annealing stages observed between the cessation of bombardment and the time the specimens reach 400°C. Instead, it seems almost certain that the major processes are concerned with some form of aggregation of like imperfections. In fact, one is inclined to conclude that only one of the imperfections, such as the vacancies, remains after bombardment and that the annealing procedures center about the coagulation of these into voids. It is unfortunate that the copper employed in this work was not of the same grade as that employed in other experiments since this restrains us from drawing conclusions more freely. It is easy to imagine impurities affecting the migration of vacancies or interstitials in an essential way.

Nature of Activation Energy near 0.69 ev

There is a school of opinion supporting the viewpoint that the prominent activation energy near 0.7 ev is to be associated with interstitial diffusion by the interstitialcy mechanism and that the activation energy for vacancy migration is near 1.2 ev. The basis for this proposal, which was first made by Brinkman, Dixon and Meechan, will be discussed in the section dealing with the properties of ordered alloys. One corollary of this point of view is that the energy of formation of vacancies, ϵ_f, is in the vicinity of 0.9 ev, provided one assumes the vacancy mechanism for normal diffusion, for the sum of ϵ_f and ϵ_m must be near 2.1 ev. The corresponding density of vacancies at the melting point would then be near 1.0 per cent, whereas that at 900°C would be near 0.1 per cent. These estimates presumably would be closely the same for copper and gold.

There is insufficient evidence to dismiss this viewpoint with any degree of finality. On the other hand the evidence against it is quite strong at the present time. In the first place, Kauffman and Koehler have found no evidence to support the existence of a unit for which ϵ_f is below 1.3 ev in the quenched specimens of gold. Moreover, they find that the imperfection possessing this energy of formation migrates

Table V. Physical Properties of Iron, Cobalt and Nickel

Metal	Crystal type	Atomic separation	Atomic number	Atomic weight	Resistivity (20°C)	Melting temperature	Sublimation energy
Iron	bcc	2.48Å	26	56	9.7 μΩ-cm	1540°C	94 kg-cal/mol
Cobalt	hcp	2.50	27	59	6.2	1495	85
Nickel	fcc	2.49	28	59	6.8	1455	85

with a value of ϵ_m near 0.68 ev, all of which supports the view that the activation energy of 0.69 ev in copper is to be associated with the migration of vacancies. Still further, Cooper's experiments on the annealing of specimens of copper irradiated near 10°K indicate the existence of activation energies near 0.1 ev, which may actually be associated with the migration of interstitial atoms, in accordance with Huntington's viewpoint.

Experiments with Other Pure Monotomic Metals

Comparison of Iron, Cobalt and Nickel

Several other experiments merit description in relation to the foregoing work.

Wruck and Wert[20] have bombarded similar specimens of iron, cobalt and nickel with 12 Mev deuterons at —150°C and studied the differences in behavior. The physical properties of the three metals are listed in Table V. It will be seen that the major difference lies in the crystal structures, although the resistivity of iron is larger than that of cobalt or nickel. The specimens were of somewhat better than commercial purity, but probably were not as pure as the specimens of copper, silver and gold employed in most of the work described previously.

The investigators found that the resistivity of iron increased three times more rapidly than that of the other two metals for comparable amounts of bombardment. Or, expressed in terms of the fractional increase in resistivity at the bombardment temperature, $\Delta\rho/\rho$ increases six times more rapidly for iron than for the other metals, which behave very similarly.

The simplest interpretation to place upon the results is either that E_d is smaller for iron than for nickel or cobalt, or that $\overline{\nu}$ is greater. This suggests, in turn, either that atoms are more easily displaced from the more loosely packed body-centered cubic lattice of iron, or that displaced atoms have a smaller probability of returning under the conditions of bombardment. In this connection, it may be mentioned that Denney (private communication) has found that the threshold energy for displacement of iron atoms in precipitates of iron in a 2.4 per cent alloy of iron in copper is 27 ± 1 ev. Values even comparable to this are not available for the other metals.

Wruck and Wert also studied the annealing of the resistivity induced in the specimens and found that the recovery in cobalt and nickel varied almost continuously from the bombardment temperature to room temperature, about forty per cent of the initial value remaining after warm-up. Iron exhibits a more precipitous recovery in the range near —100°C and only about 20 per cent remains at room temperature. It seems unlikely that great significance can be attached to the differences in annealing behavior, for, as we have seen in the case of copper, the purity of specimens is probably an important factor in determining the precise annealing behavior.

Bombardment of Tungsten with High Energy Protons

Pearlstein, Ingham and Smoluchowski[21] have bombarded well annealed tungsten wires with protons in the range between 130 and 410 Mev. The increment in resistivity associated with damage increases over this range for a specified flux. For example the increment is 0.38 per cent for a flux of 10^{16} protons per cm² having an energy of 130 Mev, and is 0.50 per cent for the same flux of 410 Mev protons. One would expect a decrease in increment with increasing energy if the changes were purely a result of the ability of the incident protons to produce primary displaced atoms by coulomb encounters in accordance with the theory of previous sections. It seems almost certain that the observed behavior is to be associated with effects produced by direct nuclear encounters and the consequent production of energetic ionizing particles.

Behavior of Ordered Alloys

Bombardment of Cu_3Au and CuZn with Nucleons

Siegel[22] observed that specimens of ordered Cu_3Au subjected to the neutrons of a reactor become disordered at a rate many fold greater than one would expect if the only atoms which moved to new positions were those displaced as a result of receiving energy greater than 25 ev. The results could be interpreted only by assuming that the temperature spikes produced by the displaced atoms cause disordering. The original experiments were semi-quantitative, however a number of more quantitative results have been obtained in the intervening period. Such experiments make it possible to estimate the number of atoms which are disordered by a primary displaced atom.

Brinkman, Dixon and Meechan[23] have found that the resistivity of a 3 mil (0.0076 cm) foil of Cu_3Au is raised by 4.25×10^{-6} Ω-cm if it is bombarded below —100°C with 5×10^{17} protons having an energy of 9 Mev. The resistivity of a completely disordered specimen is raised by 0.65×10^{-6} Ω-cm, so that the increase in resistivity of the first specimen, arising from the production of disorder is presumed to be 3.60×10^{-6} Ω-cm. Since the change in

resistivity associated with complete disordering is about 10×10^{-6} Ω-cm, it follows that the fraction of the lattice disordered is about 0.36. The range of the 9 Mev protons in Cu_3Au is about 0.215 gm/cm² or about 0.0187 cm. Thus the protons emerge from the foils with most of their energy. The thin target correction factor appearing in the brackets of Equation 6 is 1.15. A straightforward calculation shows that the cross section for the production of a primary displaced atom by the 9 Mev proton is 0.517×10^{-20} cm² if we assume that $E_d = 25$ ev. The relative probability of a copper atom being displaced is 0.56. We readily find that the fraction of atoms displaced *as primaries* by 5×10^{17} protons/cm² is

$$f_p = 2.9 \times 10^{-3} \tag{47}$$

It follows that the number of atoms disordered per primary displaced atom is

$$n_p = \frac{0.36}{f_p} = 124 \tag{48}$$

Dixon[26] has also irradiated Cu_3Au with 33 Mev alpha particles and has found that the resistivity is increased by 0.44×10^{-6} Ω-cm if bombarded with 1.0×10^{-6} amp-hr (1.13×10^{16}) particles per unit area. A simple calculation shows that the number of atoms disordered per primary displaced atom is the same as in Equation 48 to within about twenty per cent.

Eggleston and Bowen[25] have produced disorder in β-brass (CuZn) with alpha particle bombardment. The effect is of the same order of magnitude as that observed in Cu_3Au.

We may note that the number of atoms disordered per primary displaced atom is about ten times smaller than the number of atoms which could be brought to the melting point by dissipation of the energy of the primary. It follows that the spheroidal volume of the displacement spike which actually is raised to the melting temperature cannot come to true thermal equilibrium during the period of time the temperature spike endures, for the disordering temperature is lower than the melting point and we should expect more atoms to be disordered than are raised to the melting temperature if true equilibrium prevailed. At most only the regions near the centers of the hottest spots in the displacement spike become disordered as a result of temperature alone. Actually there seems to be difficulty in accounting for the disorder on the basis of atomic migration produced by temperature alone.

Bombardment with Electrons

Brinkman, Dixon and Meechan[23] have attempted to produce disordering in specimens of Cu_3Au by bombardment with 1 Mev electrons. A 6 mil (0.0152 cm) foil was bombarded with 1500 μa-hr of electrons (3.38×10^{19} particles) per cm² at a temperature below −185°C. The range of such electrons is about 0.412 gm/cm², which is about 0.036 cm. Only the copper atoms can be displaced by electrons of this energy since E_m is less than the threshold, near 25 ev, for gold. The cross section for the displacement of a copper atom by an incident electron is about 34×10^{-24} cm² and the corrective factor for the decrease in energy of the electrons while passing through the foil is 0.66. Thus the fraction of copper atoms displaced is about 7.6×10^{-4} according to the simple theory. In pure copper this would give rise to an increase in resistivity of about 0.2×10^{-6} Ω-cm purely as a result of the scattering by displaced atoms if we assume that one per cent of displaced atoms corresponds to $\Delta\rho = 2.7$ μΩ-cm. Presumably the comparable effect should be almost of the same order in Cu_3Au. The investigators found no significant observable change in the resistivity of the specimens when bombarded at −190°C. Since the experimental error is probably close to 0.1×10^{-6} Ω-cm the absence of an observed component of resistivity arising from displaced atoms is perhaps not surprising, however the question of a component of resistivity from disordering remains.

If each atom displaced by electrons had the same effect as the primary atoms displaced by protons or alpha particles, we should expect a fraction of $124 \times 7.6 \times 10^{-4} = 0.094$ of the atoms to be disordered. This, in turn, would add an increment of about 0.94×10^{-6} Ω-cm to the resistivity. Actually the average atom displaced by a 1 Mev electron is given an energy of about $1.4\ E_d = 35$ ev, which is about one-tenth that given to the average atom displaced by a light charged nucleon. In fact the kinetic energy of motion, available for the production of a thermal spike is proportionately even less in the case of the atom displaced by an electron because a larger fraction is expended in overcoming bonding forces. Thus it appears that the increase in resistivity arising from disordering by electron bombardment may have been within the experimental scatter if an increase of the estimated magnitude exists.

It was noted above that the resistivity of a disordered specimen of Cu_3Au is increased by 0.65×10^{-6} cm as a result of bombardment with 5×10^{17} deuterons per cm². Since the fraction of atoms displaced is about $6f_p$ according to the simple theory (Equation 16), the corresponding increase expected on this basis would be 4.7×10^{-6} Ω-cm if we assumed that one per cent of displaced atoms induced a change of 2.7 μΩ-cm. In this case the calculated increase is about 7.2 times larger than the observed one, which is to be compared with the ratio of 7.5 found for specimens of pure copper bombarded at liquid nitrogen temperature (cf Equation 32). Actually the experiments of Brinkman, Dixon and Meechan were carried out near −100°C where thermal annealing may have been larger. As a result it appears that the atoms displaced in disordered Cu_3Au may produce a somewhat higher change in resistivity than those displaced in pure copper. The conclusion is not reliable because the effects of annealing are uncertain.

Neutron Bombardment of Ni_3Mn

Aronin[26] has studied the disordering produced in Ni_3Mn as a result of irradiation with reactor neutrons and has concluded that about 5000 atoms of the lattice are disordered on the average per collision involving each neutron in the distribution with an energy above 0.5 Mev. If we assume somewhat arbitrarily that the average neutron of this type possesses an energy of 1 Mev and that the average neutron is scattered isotropically by the Ni and Mn atoms of the alloy, the average energy imparted to the primary displaced atoms is about 3.5×10^4 ev. The energy of an electron with the same velocity is about 0.25 ev. Thus the atoms should expend the major fraction of their energy in coulomb and hard-sphere encounters with the other atoms of the lattice, rather than in electron excitation. It may be noted that the typical primary atoms of Ni and Mn can approach the atoms of the lattice to a distance about equal to the screening radius a in head-on collisions. Thus they are scattered more nearly like hard spheres than like weakly screened charged particles.

The average atom displaced by a neutron and possessing 3.5×10^4 ev of energy is equivalent to about 100 primary atoms displaced by light charged nucleons in coulomb encounters. Thus the disorder produced per neutron collision is about the same as if each atom displaced by a charged nucleon disordered 50 atoms of the alloy. This is to be compared with the value of 124 disordered atoms computed for the primaries produced by 9 Mev protons in Cu_3Au. The relatively close agreement between the two numbers shows that the effects produced by atoms knocked on in typical coulomb encounters with charged nucleons are not basically different from those produced by the atoms knocked on by neutrons. Moreover, we note that electron excitation is almost absent in the specimens disordered by neutron bombardment, for even the fastest knock-ons have a velocity equivalent to that of an electron with only 0.5 ev of energy. Thus we may conclude with reasonable certainty that the disordering does not originate primarily in electron spikes. This conclusion is also supported at least qualitatively by Siegel's initial work with Cu_3Au since the knock-ons produced by the neutron flux would not have produced appreciable electron excitation in this case either.

Importance of Displacement Spikes

An analysis concerning events which occur in thermal spikes suggests that the primary cause of disorder in the alloys is the irreversible component of plastic flow which occurs about the displacement spike and which originates in the thermal stresses in the region about the spikes. We would not expect stresses of the same magnitude when the atoms are displaced with electrons having energy just above the threshold value (e.g. 1 Mev electrons). Unfortunately the experiments carried on with electron bombardment and described above are just borderline for testing this point. For example, the increase to be expected in the specimen of ordered Cu_3Au bombarded with 1500 μa-hr of electrons would be near 0.1 $\mu\Omega$-cm if the total energy transferred to primary atoms alone were the important factor. Electron bombardments of five or ten times the duration would be of critical value.

Acceleration of Ordering

A number of experiments on disordered alloys demonstrate that the rate of ordering at a given temperature can be increased[27] if the material is bombarded with particles that produce displaced atoms. It seems safe to conclude that the higher density of lattice defects in the bombarded specimens enhances the rate of self-diffusion and hence the rate of ordering. It seems very difficult to extract satisfactory quantitative information from the existing experiments since the relatively complex process of ordering is involved.

Evidence for Interstitial Migration

Brinkman, Dixon and Meechan[28] have carried out a very interesting study of the annealing of the radiation-induced increment of resistivity in ordered and disordered specimens of Cu_3Au and have used the results to conclude that the prominent annealing process with an activation energy of about 0.7 ev in copper and gold corresponds to interstitial rather than vacancy migration. The ordered and disordered specimens, designated by O and D, were irradiated below $-100°C$ with 5×10^{17} protons per cm^2 having an energy of 9 Mev, and are in fact the specimens for which Equations 47 and 48 were derived. We saw in the previous section that the resistivity of O is raised by 4.25 $\mu\Omega$-cm, whereas that of D is raised by 0.65 $\mu\Omega$-cm. When these specimens were warmed the following sequence of events occurred:

1. In the range between $-60°C$ and $0°C$, specimen D recovered almost all of its original resistivity, the drop being 0.60 $\mu\Omega$-cm. The investigators conclude that no ordering occurs and that most of the additional scattering centers produced by bombardment have been removed. Only a small additional decrease (0.05 $\mu\Omega$-cm) occurs during a further annealing between $0°C$ and $130°C$.

2. The resistivity of specimen O also decreases by 0.60 $\mu\Omega$-cm during the rise from $-60°$ to $0°C$. The investigators conclude that the diffusion process which occurs in this stage removes a major fraction of the displaced atoms, but does not decrease the lattice disorder responsible for most of the rise in resistivity. That is, only the component of the damage which annealed in specimen D is removed during warming to $0°C$. During further warming to $130°C$ the resistivity of O drops still further by 0.45 $\mu\Omega$-cm. It is concluded that the decrease is associated with ordering and that a new migration process which permits ordering has occurred. This process is assumed to occur in specimen D as well, and to be associated with the drop of resistivity by about 0.05

$\mu\Omega$-cm; it is not effective in producing ordering, however, because the appropriate nuclei for the ordered phase are not available.

To summarize, a diffusion process which cannot induce ordering takes place in the lower range of temperature, whereas one which can produce ordering occurs in the higher range. The appropriate activation energies are assumed to be about 0.7 ev and 1.2 ev, respectively.

The investigators associate the lower activation energy with interstitial migration because relatively simple calculations show that only a copper atom should persist as an interstitial. These estimates indicate that the energy required to form an interstitial gold atom in Cu_3Au is about 5 ev greater than the corresponding energy for a copper atom. Hence interstitialcy migration should take place through the copper lattice alone, once the initial interstitial gold atoms have exchanged with copper atoms, and leave the order unaltered. In contrast, the vacancies may presumably jump between both types of site and induce ordering. It follows that the activation energy for vacancy migration is to be associated with the activation energy near 1.2 ev.

Granting both the experimental results and the calculations, a major flaw in the reasoning seems to lie in the exclusive assumption that the activation energy of 0.7 ev in the alloy is to be associated with the closely similar value in monatomic copper and gold. One might equally well argue that the primary result of the analysis is the less quantitative conclusion that interstitialcy migration may involve an appreciably smaller activation energy than vacancy migration (smaller by about 0.5 ev), and hence conclude that the annealing process which occurs near 40°K in copper and possesses an activation energy near 0.1 ev is to be associated with interstitial migration, whereas the higher value near 0.69 ev is to be associated with the migration of vacancies.

It would be interesting to know if specimens of ordered Cu_3Au which are disordered by bombardment near 10°K exhibit annealing near 30°K.

REFERENCES

1. A historical survey of this field to the year 1952, calling attention to the wartime contributions by Wigner, E. P., Burton, M., Franck, T. and others may be found in the paper by one of the writers, Physics Today, *5*, No. 6 (June, 1952), p. 6. See also the following survey papers and articles: Seitz, F., Discussions of the Faraday Society, *5*, 271 (1949); Slater, J.C., Jour. App. Physics, *22*, 237 (1951); Lark-Horovitz, K., Semi-Conducting Materials (Academic Press, New York, 1951), p. 47; Billington, D. S. and Siegel, S., Metals Progress, *58*, 848 (1950); Dienes, J. G., Annual Reviews of Nuclear Science (Annual Reviews, Stanford, California), Vol. II, p. 187; Siegel, S., Modern Research Techniques (American Society for Metals, Cleveland, 1952), p. 312.
2. A survey of the subject may be found in the book edited by Shockley, W., *et al.*, Imperfections in Nearly Perfect Crystals (John Wiley and Sons, New York, 1951).
3. Seitz, F., Rev. Mod. Phys. *26*, 7 (1954).
4. Harten, H. U., Zeits. f. Phys. *126*, 619 (1949); Nachr. Akad. Wiss. Göttingen *1950*, 15 (1950).
5. Snyder, W. S. and Neufeld, J., Bull. Am. Phys. Soc. *29*, 1, p. 23 (1954); Phys. Rev. *97*, 1636 (1955). The treatment in this section is the result of juxtaposition of the method developed by Snyder and Neufeld with a similar method developed independently by Harrison, W. and one of the writers, Bull. American Physical Society meeting, March, 1955.
6. Dexter, D. L., Phys. Rev. *87*, 768 (1952).
7. Jongenburger, P., Phys. Rev. *90*, 710 (1953); App. Sci. Res. Hague, B, *3*, 237 (1953).
8. Blatt, F. J., Bull. Am. Phys. Soc. *29*, 7, p. 30 (1954); Blatt, F. J., Huse, M. C. and Rubenstein, R. A., *ibid*, *30*, 2, p. 30 (1955).
9. Huntington, H. B., Phys. Rev. *91*, 1092 (1953). See also Huntington, H. B. and Seitz, F., *ibid*, *61*, 315 (1942); Huntington, H. B., *ibid*, *61*, 325 (1942).
10. Kauffman, J. W. and Koehler, J. S., Phys. Rev. *88*, 149 (1952); Bull. Am. Phys. Soc. *29*, 7, p. 30 (1954).
11. Sources of diffusion coefficients, Cu: work of Kuper, A., Letaw, H., Jr., Slifkin, L., Sonder, E. and Tomizuka, C. T., Phys. Rev. *96*, 1224 (1954), Ag: Slifkin, L., Lazarus, D. and Tomizuka, C. T., Jour. App. Phys. *23*, 1032 (1952), Au: Gatos, H. D. and Kurtz, A. D., Jour. of Metals *6*, 616 (1954).
12. Eggen, D. T. and Laubenstein, M. J., Phys. Rev. *91*, 238 (1953).
13. Marx, J., Cooper, H. G. and Henderson, J. W., Phys. Rev. *88*, 106 (1952).
14. Cooper, H. G., Koehler, J. S. and Marx, J. W., Phys. Rev. *94*, 496 (1954); Cooper, H. G., Thesis, University of Illinois (1954).
15. Bethe, H. A. and Ashkin, J., Experimental Nuclear Physics, Volume I (John Wiley and Sons, New York, 1953).
16. Since a 0.81 Mev electron is in the relativistic energy range, the cross section is calculated taking into account such effects. See McKinley, W. A. and Feshbach, H., Phys. Rev. *74*, 1759 (1948).
17. McDonnell, W. R. and Kierstead, H. A., Phys. Rev. *93*, 247 (1954); Kierstead, H. A., Bull. Am. Phys. Soc. *29*, 7, p. 30 (1954).
18. Overhauser, A. O., Phys. Rev. *91*, 448 (1953); *94*, 1551 (1954).
19. Redman, J. K., Coltman, R. R. and Blewitt, T. H., Phys. Rev. *91*, 448 (1953); See also Eggleston, R. R., Acta Met. *1*, 679 (1953).
20. Wruck, D. and Wert, C., Bull. Am. Phys. Soc. *29*, 3, p. 19 (1953).
21. Pearlstein, E., Ingham, H. and Smoluchowski, R., Bull. Am. Phys. Soc. *30*, 2, p. 7 (1955); Smoluchowski, R., *ibid*.
22. Siegel, S., Phys. Rev. *75*, 1823 (1949).
23. Brinkman, J. A., Dixon, C. E. and Meechan, C. J., Acta Met. *2*, 38 (1954).
24. Dixon, C. E., see article by Siegel, S. in Modern Research Techniques in Physical Metallurgy (ASM Cleveland, Ohio, 1952), p. 319.
25. Eggleston, R. R. and Bowen, F. E., Jour. App. Phys. *24*, 229 (1953).
26. Aronin, L. R., Jour. App. Phys. *25*, 344 (1954).
27. See for example Blewitt, T. H. and Coltman, R. R., Phys. Rev. *85*, 384 (1952). See also footnote reference 35. Adam, J., Green, A. and Dugdale, R. A., Phil. Mag. *43*, 1216 (1952); Dixon, C. E., Meechan, C. J., Brinkman, J. A., Phil. Mag. *44*, 449 (1953); Unpublished Westinghouse report (1952) by Click, H. L., Brooks, F. C., Witzig, W. F. and Johnson, W. E.
28. See reference 23; See also Meechan, C. J. and Eggleston, R. R., Bull. Am. Phys. Soc. *29*, 8 (1954).

Theoretical Aspects of Radiation Damage in Metals

By G. J. Dienes,* USA

It is well known by now that nuclear radiations may alter drastically the properties of solid materials.[1] Radiation effects are conveniently grouped into two categories, namely, ionization effects and displacement effects. In good conductors, such as metals, ionization effects disappear very quickly and only contribute to the heating of the material. Bombardment with massive fast particles, however, produces atomic displacements in a solid and important changes in physical properties arise from the resultant atomic disorder (crystalline imperfections). This paper is concerned with the theoretical aspects of radiation damage, particularly in metals, caused by the displacement of atoms from their normal lattice sites by high energy particle bombardment. The production of impurity atoms by nuclear transmutations will not be discussed although this effect may be of considerable importance in special cases.

Theoretical work in this field is concerned with three major aspects: (1) theory of the production of displaced atoms by high energy particle irradiation, (2) the nature and mobility of the crystalline defects introduced by irradiation and (3) theories of the relations between physical properties of solids and crystalline imperfections. Each of these topics is discussed in this paper and the current status of theoretical knowledge is summarized.

PRODUCTION OF DISPLACED ATOMS

The production of displaced atoms may be described as follows. Consider first a fast neutron which upon entering a solid produces fast recoil atoms along its path. The recoil atoms in turn produce secondary recoils and so on. The fraction of energy dissipated in ionization decreases rapidly as the particle slows down and a large portion of the displacement damage is done at the end of the range although the integrated damage in the early part of the range cannot be neglected. The picture is essentially the same for fission fragments and for accelerated charged particles except for details of assigning the energy dissipated to ionization and displacement effects.

It is clear that, on an atomic scale, knocked-on atoms will leave vacant lattice sites behind and will finally come to rest in interstitial positions. This is a fundamentally attractive picture according to which many of the experimental results may be correlated. The lattice disturbances may, however, be highly localized and the assumption of a uniform concentration of lattice defects represents a certain degree of idealization. The defects themselves may combine to form pairs and larger clusters. In addition to this, energy may be transmitted to the atoms near the path of the fast particle without displacing them from the lattice. The result is a "thermal spike", i.e., very rapid heating and quenching of a small volume of the material. Such thermal spikes may promote processes associated with high temperatures, such as diffusion or disordering of ordered alloys. Theoretical estimates[2,3] indicate that the high temperature in a thermal spike lasts only for a time of the order of 10^{-11} seconds. In metals, the energy transfer from excited electrons to the atoms of the lattice is inefficient[2] so that the degree of heating depends mainly on direct transfer of energy to lattice vibrations. This is a relatively small fraction of the energy dissipated and consequently rather small additional activation is predicted for rate processes such as self-diffusion.

Brinkman[4] has recently extended these ideas by suggesting that displacement spikes are produced at the end of the range of a fast moving atom. His calculations indicate that, when the energy of the fast moving atom falls below a transition value (which depends on the atomic number) the mean free path between displacement collisions becomes of the order of the atomic spacing. Thus, each collision results in a displaced atom and the end of the trail is believed to be a region containing of the order of one to ten thousand atoms in which local melting and turbulent flow have occurred during a very short interval. Brinkman suggests that vacancies and interstitials will anneal more or less completely in this region and that the damage is left in the form of dislocation loops and small misoriented regions. The calculations indicate that this mechanism, if it exists, is only important in heavy metals.

The thermal spike and displacement spike processes are evidently rather complex and it is difficult to carry out reliable calculations. They have been invoked to explain the unexpectedly efficient disordering of ordered alloys by irradiation. Seitz[5] has indicated recently that the simple picture of heating and quenching is inadequate to explain the disordering. He suggests that the irreversible plastic strain which originates in thermal stresses about displacement spikes is the source of the disorder.

Because of the very speculative nature of thermal

*Brookhaven National Laboratory, Upton, New York, USA.

spike and displacement spike effects the major portion of this paper is devoted to displaced atom production by elastic collision and to the properties of the resultant simple defects (interstitials, vacancies, pairs of defects).

Wigner[6] made the first quantitative estimates of the number of displaced atoms produced by high energy particles. The theory was developed in detail by Seitz,[7] based on earlier work by Bohr and his co-workers.[8] Seitz calculated the fraction of energy lost in elastic collisions using the Born approximation. These are the collisions which are effective in displacing atoms. Recent advances in the theory are due to Snyder and Neufeld[9] and Harrison and Seitz[10] who have pointed out that the problem is better treated on the basis of classical scattering. We shall make use of some of these results at appropriate places but shall not discuss the theory in detail since the material is covered in a paper by Seitz[11] at this conference.

An important parameter which enters the theory is the "displacement energy", E_d, i.e., the energy required to knock an atom out of its position in the lattice. This energy has been measured for germanium[12] (30 ev) and copper[13] (25 ev). Two attempts have been made recently to calculate E_d theoretically. Huntington[14] has considered low energy collisions in copper, a typical close packed metal. He has assumed that the principal interaction between the colliding atoms is the repulsion of closed shells which he approximated by a Born-Mayer type function

$$V(r) = A \exp\left[\frac{-(r - r_0)\rho}{r_0}\right] \qquad (1)$$

Since this force law is short range, a billiard ball model was used for the collision calculations. For copper the value of ρ can be bracketed[23] between 13 and 17. For $\rho = 13$ an energy of 18.5 ev is required to move an atom to an interstitial position in the (111) direction through the triangle formed by its three nearest neighbors. 17.5 ev is required for displacement creation in the (100) direction. In this case the original fast atom moves to another lattice site displacing its nearest neighbor into an interstitial position. For $\rho = 17$ the corresponding energies were found to be 43 and 34 ev. The experimental value lies well inside these rather wide theoretical limits. Because of this rough agreement one is tempted to conclude, at least tentatively, that in a close packed metallic lattice the displacement energy is determined primarily by the closed shell repulsive interactions.

Kohn[15] has carried out similar calculations for germanium and found that some of the nearest interstitial positions can be reached by atoms with substantially smaller energies (of the order of 10 ev) than the experimentally determined value of 30 ev. The main reason for the much lower theoretical value is the open structure of the Ge lattice in contrast to the close packed face-centered cubic structure of Cu. Kohn concludes that in Ge the most easily accessible interstitial positions are either unstable or, if stable, do not give rise to acceptor levels and hence would not have been observed in the threshold energy determination which was based on electrical resistivity measurements.

A test of the general theory of displacement production is difficult mainly because most physical properties depend in a complicated, and theoretically poorly understood, way on the number of vacancies and interstitials. Recent theoretical and experimental work (as yet unpublished) by Antal, Weiss and Dienes[16] using the scattering of long wavelength neutrons led to a significant test of the theory.

It will be shown that neutrons of sufficiently long wavelength are scattered isotropically by isolated point defects and the scattering can be measured when crystalline effects (Bragg scattering) are absent. Babinet's principle may be applied under such conditions and, therefore, vacancies and interstitials scatter in exactly the same manner. The cross section for this nuclear type of scattering is accurately known from other measurements. Thus, if the scattering from the defects is measurable an absolute method is at hand for determining their concentration.

Let long wavelength neutrons be incident on a crystal in the wavelength region of several Angstroms, i.e., the energy region of 0.001 ev. For such extremely low energy neutrons the solution of Schrödinger's equation is the sum of an incident plane wave and a radially scattered wave. The scattered radiation at a large distance is

$$\psi = \Sigma_p\, a e^{i\vec{k}\cdot\vec{r}_p} \qquad (2)$$

where $\vec{k} = \vec{k}' - \vec{k}_0$ = phase difference, and $\vec{r}_p$ = vector distance between origin and pth scatterer in the crystal. Let a monatomic crystal contain m point scatterers per unit volume in the form of interstitial atoms and vacant lattice sites and a total of N atoms per unit volume. The scattering is then described by

$$\psi = \sum_{j=1}^{N} a e^{i\vec{k}\cdot\vec{r}_j} + \sum_{i=1}^{m} a_i e^{i\vec{k}\cdot\vec{\rho}_i} \qquad (3)$$

where the first term is the sum over the perfect crystal and the second one is that over the defects. In the second term $a_i = +a$ for interstitial atoms and $-a$ for vacancies.

For wavelength beyond the Bragg cut-off the first term is zero. The intensity scattered is then the square of the second term and for random location of defects cross terms in this square may be omitted. The resulting total cross section is

$$\sigma = 4\pi m a^2 \qquad (4)$$

The cross section per atom is

$$\sigma_a = \sigma/N = 4\pi a^2 m/N = 4\pi a^2 f \qquad (5)$$

where f is the atomic fraction of scatterers in the

material and σ_d is the cross section for scattering by defects alone. The scattering process is fully described, therefore, by $4\pi a^2$ which is the scattering cross section for vacancies and interstitials, and is the bound atom cross section, σ_d, for the atoms of the crystal.

It is not practical to attempt to measure directly the isotropically scattered neutron intensity. Instead, the attenuation of a long wavelength neutron beam during its passage through the material is measured in a transmission experiment. There are other sources of attenuation which have to be taken into account and whose cross sections should be very small compared to the cross section for defect scattering.

In the absence of defects and past the last Bragg cut-off ($\lambda > 2d_{max}$), the transmitted intensity, I_s, is given by

$$I_s = I_0 \exp\left[- NX\left(\sigma_a + \sigma_i + \sigma_{dis}\right)\right] \quad (6)$$

where I_0 = incident intensity, N = number of nuclei per cm³, X = path length traversed through the sample, σ_a = cross section for absorption, σ_i = cross section for inelastic scattering, σ_{dis} = cross section for disorder scattering other than defects (isotopic spin, etc.).

If m defects are present the transmitted intensity, I_d, is

$$I_d = I_0 \exp[-NX(\sigma_a + \sigma_i + \sigma_{dis} + \sigma_b f)] \quad (7)$$

A direct comparison of a crystal containing a fraction, f, of defects to a control crystal gives

$$\frac{I_d}{I_s} = e^{-NX\sigma_b f} \quad (8)$$

measurement of the ratio I_d/I_s immediately gives then a value for f.

Graphite was chosen for study because of inherent interest in this material and because it fulfilled very well the theoretical and experimental requirements. Samples available to us were expected to contain of the order of a few per cent defects on the basis of Seitz's theory. This concentration should be easily measurable. For graphite $\sigma_b = 4.7$ barns, $\sigma_a + \sigma_i \cong 0.9$ barns at 8 Å, $\sigma_{spin} = 0$; zero spin, $\sigma_{isotope} = 0$. $\sigma_{isotope}$ is negligibly small because of the combination of a low abundance of C^{13}(1.1%) relative to C^{12} and a similarity in cross sections, 4.5 b and 5.5 b. The graphite specimen served also as a neutron filter, which resulted in a most economical use of the very low intensity available in a long wavelength neutron beam.

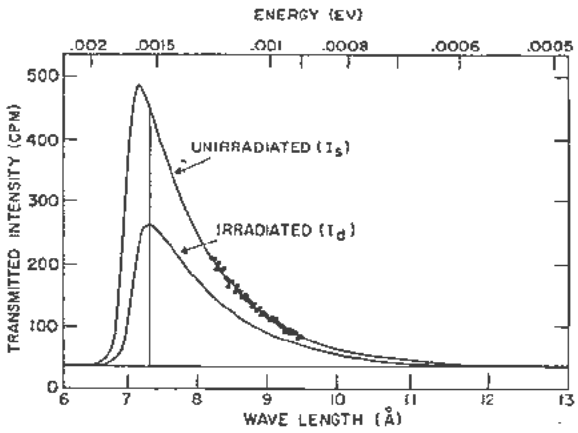

Figure 1. Slow neutron intensity transmitted by an irradiated and unirradiated graphite specimen. For clarity, only a typical group of experimental points had been reproduced along one curve to indicate their number and spread. Only intensities to the right of the vertical line at 7.30 Å were considered in computing I_s and I_d

The slow neutron beam was obtained from the Brookhaven reactor by filtering the thermal neutron spectrum. This spectrum of flux has a Maxwellian energy distribution peaked near 1 Å with a "tail" on the long wavelength side. If a polycrystalline material of sufficient length is placed in such a beam, Bragg scattering removes all neutrons from the incident beam except those having

$$\lambda > 2d_{max} \quad (9)$$

where d_{max} is the largest interplanar spacing for which diffraction is possible. In these experiments the graphite specimens were made long enough (approx. 9 in.) to constitute efficient filters by themselves. A typical spectrum of the neutrons transmitted by a 9 in. graphite specimen is shown in Fig. 1 as the "unirradiated" curve. The "cut-off" wavelength is clearly marked by an abrupt increase in transmitted intensity at $\lambda = 2d_{(002)} = 6.70$ Å.

In order to avoid spurious effects due to the increase in the c-axis of graphite upon pile irradiation a plot of transmitted intensity vs wavelength was obtained using a crystal spectrometer. Any irrelevant change in intensity could then be disregarded and the transmitted intensity obtained by measuring the areas under the curves for $\lambda > 7.30$ Å (see Fig. 1). Onset of second order reflections at about 13.4 Å would place a limit on the usable wavelength region but is of no consequence in these experiments since the beam intensity is too weak to be detected past 12 Å. Care was taken to accept all small angle scattered neutrons, thus eliminating effects of small particle size in the sample.

Several spectra were obtained from the spectrometer for the irradiated and standard (unirradiated) specimen run alternatively and averaged. Figure 1 shows the results. The areas under each curve give

$$\frac{I_d}{I_s} = 0.607$$

The estimated accuracy of this figure is about ± 10%. By Equation 8, $f = 0.0526$. The fraction of displaced atoms is $f/2 = 0.0263$.

The f value obtained by the above method may now be compared to the number of displaced atoms

expected on the basis of Seitz's theory.[7] f was calculated from the equations

$$f/2 = (nvt) \times \sigma_s \sqrt{\frac{\Delta\overline{E}}{E_0}} \qquad (10)$$

$$\Delta\overline{E} = \frac{2mM}{(M+m)^2} E$$

where m = mass of neutron, M = mass of carbon atom, $\Delta\overline{E}$ = average energy loss per collision, E_0 = energy required to displace a carbon atom which will be taken as 25 ev, E = average energy of fast neutron causing displacement, which will be taken as 1 Mev, σ_s = collision cross section for carbon atom = 2.5×10^{-24} cm^2, (nvt) = effective total integrated flux of fast neutrons causing displacement (nv is the flux of neutrons per cm^2 per second and t is the irradiation time).

The number to be used for (nvt) is the most uncertain quantity in these equations since the fast flux and its energy distribution are not known with any accuracy. Our best estimate of the effective (nvt) for the graphite sample used in these experiments is 1.1×10^{20} neutrons/cm^2.

$\Delta\overline{E}$ is 0.142 Mev and with 1.1×10^{20} n/cm^2 for nvt, Equation 10 gives for the number of displaced atoms

$$f/2 = 0.021$$

The uncertainty in this number due to inaccuracy in (nvt) is of the order of 50%. There may be a further error because of possible annealing of the specimen although its temperature during irradiation probably has not been above 50°C. The use of Equation 10 overestimates f since the pile spectrum has been replaced by neutrons of average energy of 1 Mev. On the other hand, recent refinements in the theory[9,10] discussed earlier in this section indicate that the number calculated by Equation 10 should be raised by about a factor of 2. These two effects will largely cancel each other. Because of the uncertainty in (nvt) a more detailed calculation was not carried out.

The experimentally determined value of f is known, therefore, with greater accuracy than any theoretically derived value largely because of uncertainties in the value of (nvt). Consequently, the theory itself cannot be judged too critically. The fraction of displaced atoms determined experimentally by this method is in excellent agreement with the theory within the limitations mentioned above.

The value of f determined in these experiments may be in error. One reason is that if the defects are aggregated into pairs or larger clusters their scattering will not be equivalent to those of isolated interstitials and vacancies. Another reason is that the inelastic cross section may be altered by the irradiation. It has been assumed that this effect is unimportant. It has also been assumed that there is negligible inhomogeneous distortion (i.e., distortion rather than just displacement of the graphite planes) in the neighborhood of the defect. An outward inhomogeneous distortion around the interstitial can be shown to reduce the effective cross section of the interstitial (a similar distortion would increase the cross section of the vacancy). Theoretical estimates of this correction are at present unreliable but it is probably not greater than 20%. In principle the occurence of pairs is detectable by examining the wavelength dependence of the attenuation. These preliminary experiments are not sufficiently accurate past 9 Å to establish the existence of a wavelength dependence. The fact that no wavelength dependence which would be outside experimental error is observable indicates that only a small fraction of the displaced atoms may be present in the form of pairs. More refined experiments will be necessary to establish this point definitely.

The technique described here is applicable, of course, to other materials. The most important limitation is that the absorption cross section has to be small. It appears that with some refinements the number of displaced atoms may be determined in, say, aluminum ($\sigma_a = 0.215$ barns). Experimentation with such a metal calls for low-temperature irradiation and measurement because the defects are known to anneal out well below room temperature. Consequently, the necessary techniques are considerably more involved.

While such experiments have not yet been done on metals the difficulties are experimental rather than theoretical. This work was presented in some detail because the writer feels that it represents a significant test of the basic theory. Tentatively one is led to the conclusion that there is no serious discrepancy between the number of displaced atoms calculated theoretically and determined experimentally.

MOBILITY OF DEFECTS

Radiation effects can be removed (annealed) by appropriate heat treatment. In pure metals annealing has been found at as low a temperature as 40°K.[18,19,20] The current status of this field is that a unique assignment of activation energies and mechanisms to the various annealing states has not yet been achieved. It is clear that the problems are intricate and progress will come from a strong interplay of theory and experiment.

From a theoretical standpoint the important parameters for the various annealing processes are the activation energies for the migration of interstitial atoms, vacancies, pairs of vacancies and larger clusters. These same energies also play an important role in all solid state processes involving diffusion. These activation energies have been estimated theoretically for simple metals. Since the calculations are available in published form only a brief review will be presented in this section.

Huntington and Seitz[21] and Huntington[22] have calculated the energy of formation and the activation

energy of migration for a vacancy in copper. More recently, Huntington[20,24] has presented a detailed calculation on the mobility of interstitial atoms in copper. In these calculations the metal is represented by a lattice of positive point ions immersed in a uniform, compensating distribution of electrons. The repulsion between ions is represented by a Born-Mayer type exponential potential. The calculations are intricate since a number of electrostatic terms must be evaluated, the repulsive energies summed for nearest and next nearest neighbors and the displacement of all these neighbors due to the presence of the defect taken into account. These calculations gave 1 ev as the activation energy for vacancy migration and 0.07 to 0.26 ev for interstitial migration in copper.

Bartlett and Dienes[25] carried out an approximate calculation to estimate the stability and mobility of combined pairs of vacancies in copper. Their estimate of the dissociation energy for a vacancy pair is about 0.6 ev. The activation energies were determined using a Morse potential interaction which resulted in a fairly reliable value for the ratio of the activation energy for a double vacancy to that of a single vacancy. They finally assigned a value of 0.34 ev to the activation energy for bivacancy migration. The important conclusion is that in certain temperature ranges double vacancies are expected to be stable and highly mobile in such metals as copper. Essentially nothing is known theoretically about larger clusters of imperfections. A summary of the theoretical results is given in Table I.

Table I. Theoretical Activation Energy Calculations for Defects in Copper

Mechanism	*Activation energy*	*Reference*
Vacancy migration	1 ev	Huntington and Seitz[21] and Huntington[23]
Bivacancy migration	0.34 ev	Bartlett and Dienes[25]
Interstitial migration	0.07–0.26 ev	Huntington[23]

There are, of course, interactions between point defects and dislocations since the stress fields of these imperfections can act on each other. Interstitials, for example, will tend to migrate to the region of dilation of a dislocation while a vacancy will tend to diffuse to the region of compression. This type of interaction was first suggested by Cottrell[26] and the current status of the field has been fully discussed by Cottrell[27] and Seitz.[28] Recent studies of annealing of electrical resistivity[29] and critical resolved shear stress[30] have shown that an annealing process occurs near 300°C in irradiated copper with an activation energy of about 2 ev. This process is likely to be associated with dislocations since a large portion of the radiation induced increase in critical shear stress anneals in this high temperature range.

Dislocations themselves may facilitate the migration of defects. In combination with the above interactions it is evident that very complex annealing mechanisms may occur. At the present time the interpretation of annealing effects is still at a highly speculative stage.

PHYSICAL PROPERTIES AND IMPERFECTIONS

Many diverse, and often important, changes in physical properties have been observed after high energy particle bombardment.[1] The intricate relations between physical properties and crystalline imperfections are under intensive investigation but theoretical knowledge is still meager. In this connection it is pertinent to mention that radiation effects are not only of interest in themselves but also represent a powerful new tool for studying solid state problems.

The electrical resistivity of metals is increased upon irradiation.[31] This increase is mainly due to an increase in the residual resistivity although some changes in the thermal part of the resistivity have been also observed.[32] Theoretical work has concentrated on the calculation of the cross section for the scattering of conduction electrons by vacancies and interstitials. Dexter[33] extended Mott's calculations on the scattering of electrons from substitutional impurity atoms to include the scattering from interstitial atoms and vacancies. The effects of lattice distortions around the defects were taken into account and were found to represent only a minor correction. Dexter's result for Cu, Au and Ag was that one atomic per cent of vacancies would give an extra resistivity, $\Delta\rho$, of about 0.4 $\mu\Omega$cm. A similar calculation for interstitials gave about 0.6 $\mu\Omega$cm.

Jongenburger[34] suggested that a more reliable calculation is obtained if Born's approximation is not used. He carried out detailed calculations[35] for vacancies based on the free electron approximation and using for the scattering potential the negative of the Hartree potential of a free copper ion. This potential was adjusted to take care of the screening of the conduction electrons which was approximated by creating in the electron gas a spherical hole of unit charge and of radius r_s, where r_s is defined by $4\pi/3r_s^3 = \Omega$ (Ω = atomic volume). On calculating the phase shifts he found that they gave good agreement with the Friedel[36] sum rule. He also confirmed Dexter's conclusion that distortion around the defects can be neglected. For one per cent vacancies in Cu, Ag and Au, Jongenburger obtained the following $\Delta\rho$ values: 1.3, 1.5 and 1.5 $\mu\Omega$cm, respectively.

Blatt[37] has employed recently (work as yet unpublished) a very similar theoretical technique to investigate the extra resistivity due to interstitials in copper. He derived the scattering potentials for the imperfections from the appropriate Hartree self-consistent fields and employed the partial wave method in evaluating the scattering cross sections. The potentials were adjusted until the phase shifts satisfied the Friedel sum rule. The phase shift calculations were carried out on the University of Illinois High Speed Electronic Digital Computer

(ILLIAC). The calculated resistivities do not appear to depend critically on the choice of potentials. Blatt[38] finds, however, that the choice of potential is important for the calculation of thermoelectric power. His calculation of thermoelectric power leads to good agreement with experiment in the case of substitutional arsenic in copper. Blatt's final value for the extra resistivity due to one per cent interstitial atoms in copper is 1.4 $\mu\Omega$cm, which is practically the same as that due to vacancies. For substitutional impurities approximate agreement was obtained with resistivity changes measured by Linde, although the calculated resistivities were consistently too high. In view of this Blatt suggests that his, as well as Jongenburger's, calculations overestimate the resistivity increase due to vacancies and interstitials.

Using the above calculations, Harrison and Seitz[10] compared low temperature irradiation (near 10°K) experiments[26] with the improved theory of displacement production. They found that the experimental increase in resistivity is smaller by a factor of 5 than the theoretical value when a $\Delta\rho$ of 2.17 $\mu\Omega$cm per one per cent Frenkel pairs is used. In view of the essential agreement between experiment and theory obtained by neutron transmission experiments on graphite, the writer is inclined to the view that Jongenburger's and Blatt's calculations for $\Delta\rho$ yield values which are too large by a factor of 3 to 5.

The above theoretical work shows quite clearly that interstitials and vacancies cannot be distinguished by their effect on residual resistivity. Similarly, the neutron transmission technique cannot differentiate between these two defects. It is important, therefore, to find some other physical properties which may be sensitive to one type of defect. With this purpose in mind Dienes[39,40,41] investigated theoretically the effect of vacancies and interstitials on the elastic constants of simple close packed metals. In such substances the elastic constants are determined primarily by the repulsive interactions of the close ion shells. This potential is of an exponential nature and varies extremely rapidly with interatomic distance. As the interaction distance is shortened by creating an interstitial the energy of the system increases sharply on the repulsive side of the potential curve. The creation of vacancies results essentially in the destruction of some normal interactions. Thus, one expects the influence of the interstitials to outweigh heavily the effect of vacancies.

Detailed calculations, in which relaxation of nearest neighbors was taken into account, led to the following conclusions. The presence of a small fraction of interstitials and vacancies results in large increases in the elastic moduli of copper, of the order of 5–7% per 1% interstitial. Lattice vacancies alone were found to decrease the moduli by essentially a bulk effect. Consequently, increases in the elastic moduli are to be attributed primarily to the presence of interstitial atoms. There is a complicating factor arising from modulus changes which may occur by a mechanism of dislocation pinning.[42] A proper experimental test of this theory has not yet been carried out although Dieckamp[43] has reported some preliminary experiments. It is essential to make pre- and post-irradiation measurement at very low temperatures (below 40°K) on low temperature irradiated crystals. In this way annealing effects and interstitial migration to dislocations can be prevented. It should also be mentioned that the theory indicates that the above effect would be absent in a soft body centered cubic crystal such as sodium. In this case the relaxation around the interstitial is large enough, about 30%, to essentially eliminate the crowding upon which the modulus increase depends.

Tucker and Sampson[44] have proposed recently a promising method for distinguishing between interstitials and vacancies, and for measuring the interstitial concentration. They suggest that precision X-ray lattice parameter measurement "see" mainly the interstitial atoms. The basic physical reason is that there is much more distortion[23,39] around an interstitial than around a vacancy. In copper, for example, the nearest neighbors of an interstitial are displaced outward by about 5 to 9% while the nearest neighbors of a vacancy are displaced inward only about 2%. Tucker and Sampson apply the elastic model of Huang[45] and Eshelby[46] to this problem. In this model each interstitial or vacancy is considered a center of pressure (positive or negative) imbedded in an isotropic elastic continuum. For a uniform distribution of such centers of pressure the linear strain and concentration are related by the equation

$$e(p) = \frac{4\pi}{3} \cdot \frac{\gamma C_p}{v} \tag{13}$$

where $e(p)$ is the strain produced by an atomic concentration p of centers of pressure, C is proportional to the strength of each center of pressure, v is the atomic volume, and γ is related to Poisson's ratio, σ, by the expression

$$\gamma = 3\left(\frac{1-\sigma}{1+\sigma}\right)$$

The constant C is then evaluated from the atomic displacements due to the interstitials and vacancies. For a metal such as copper they find that the effect of interstitials is given by

$$e(p) = 1.0\ p \tag{14}$$

i.e., the interstitial concentration in atomic per cent is equal to the linear lattice expansion expressed as a per cent.

The corresponding relation for vacancies is

$$e_v(p_v) = -0.2\ p_v \tag{15}$$

In copper, therefore, an interstitial is five times as effective in expanding the lattice as a vacancy is in contracting the lattice. In a soft body centered cubic

metal, such as sodium, the expansion would be even larger by a factor of 2 to 3, on the basis of Dienes'[37] estimate of the atomic distortion.

On the basis of this work Tucker and Sampson conclude that: (*a*) precision X-ray lattice parameter measurements can detect 0.01 atomic per cent interstitials, (*b*) the X-rays "see" mainly the interstitial atoms, and (*c*) the theory appears sound enough to render the interpretation quantitative. They remark that preliminary experiments have shown lattice expansions in several neutron irradiated metals. This method may become an important tool for observing essentially only the interstitial content of radiation-damaged metals. The interstitial content may be measured as a function of irradiation and of subsequent thermal treatment.

SUMMARY

Three major theoretical aspects of radiation damage in metals have been discussed: (1) theory of displacement production, (2) the mobility of the resultant crystalline point defects, and (3) the relations between physical properties of solids and crystalline imperfections.

The theory of displacement production was treated very briefly since it is discussed elsewhere at this conference. Recent speculations concerning the magnitude of the unit displacement energy were discussed in some detail. The theory of long wavelength neutron transmission of a crystal containing interstitials and vacancies was outlined because it shows that the absolute number of such defects is measurable by such transmission experiments. A significant test of the theory of displacement production has been achieved by such measurements on graphite and the numbers found experimentally fall within the range calculated theoretically. Such measurements have not yet been made on metals because of experimental rather than theoretical difficulties.

It was pointed out that radiation effects can be removed (annealed) by appropriate heat treatment. The obviously important parameters in this process are the activation energies for migration of interstitial atoms, vacancies and their clusters. These activation energies have been estimated theoretically for simple metals. The basic features of these calculations were described and the current status of theoretical knowledge summarized.

Many diverse, and often important, changes in physical properties have been observed after high energy particle bombardment. The intricate relations between physical properties and crystalline imperfections are under intensive investigation but theoretical knowledge is still meager. The cross section for the scattering of conduction electrons by interstitials and vacancies bas been estimated theoretically. Some theoretical speculations have been advanced to relate changes in elastic moduli, density and lattice parameter, to the concentration of simple defects. These theoretical considerations have been outlined.

REFERENCES

1. For reviews see:
   Slater, J. C., *The Effects of Radiation on Materials*, J. Appl. Phys. *22*, 237-256 (1951);
   Dienes, G. J., *Radiation Effects in Solids*, Annual Reviews of Nuclear Science, II, 187-220 (1953);
   Dienes, G. J., *Effects of Nuclear Radiations on the Mechanical Properties of Solids*, J. Appl. Phys. *24*, 666-674 (1953);
   Seitz, F., *Radiation Effects in Solids*, Physics Today *5*, 6, 6-9 (1952);
   Siegel, S., *Radiation Damage as a Metallurgical Research Technique*, Chapter in *Modern Research Techniques in Physical Metallurgy*, American Society for Metals (1953) pp. 312-324;
   Glen, J. W., *A Survey of Radiation Effects in Metals*, AERE M/TN 27 (1954) (Harwell, England).
2. Brooks, H., Unpublished work.
3. James, H. M., Unpublished work.
4. Brinkman, J. A., *On the Nature of Radiation Damage in Metals*, J. Appl. Phys. *25*, 961-970 (1954).
5. Seitz, F., *Source of disordering of alloys during irradiation*, Bull. Am. Phys. Soc. *30*, No. 2, 17 (1955) (A).
6. For a discussion of the early work see: Burton, M., *Radiation Chemistry*, J. Phys. and Colloid Chem. *51*, 611-25 (1947).
7. Seitz, F., *On the Disordering of Solids by Action of Fast Massive Particles*, Disc. Faraday Soc. No. 5, 271-282 (1949).
8. Bohr, N., *The Penetration of Atomic Particles Through Matter*, Kgl. Danske Videnskab. Selskab. Mat. — fys. Medd. *18*, 8 (1948).
9. Snyder, W. S. and Neufeld, J., *Disordering of Solids by Neutron Radiation*, Phys. Rev. *97*, 1636-1646 (1955).
10. Harrison, W. A. and Seitz, F., *On the Theory of Radiation Damage*, Bull. Am. Phys. Soc. *30*, No. 2, 7 (1955) (A).
11. Seitz, F., P/749, *Radiation Effects in Solids*, Vol. 7, Session 13B, these Proceedings.
12. Lark-Horovitz, K., *Nucleon Bombarded Semiconductors*, *Reading Conference on Semiconducting Materials*, Butterworth's Scientific Publications, London, England, 1951, pp. 47-78.
13. Eggen,, D. T. and Laubenstein, M. J., *Displacement Energy of Radiation Damage in Copper*, Phys. Rev. *91*, 238 (1953) (A).
14. Huntington, H. B., *Creation of Displacements in Radiation Damage*, Phys. Rev. *93*, 1414 (1954).
15. Kohn, W., *Bombardment Damage of Ge Crystals by Fast Electrons*, Phys. Rev. *94*, 1409 (1954) (A).
16. Antal, J. J., Weiss, R. J. and Dienes, G. J., *Long Wavelength Neutron Transmission as an Absolute Method for Determining the Concentration of Lattice Defects in Crystals*, to be published in Physical Review.
17. Hughes, D. J., *Pile Neutron Research*, Addison-Wesley Publishing Co., Cambridge, Mass., 1953, pp. 349-366, 250.
18. Overhauser, A. W., *Stored Energy Measurements in Irradiated Copper*, Phys. Rev. *94*, 1551-1557 (1954).
19. Brinkman, J. A., Dixon, C. E. and Meechan, C. J., *Interstitial and Vacancy Migration in Cu, Au and Copper*, Acta Met. *2*, 38-48 (1954).
20. Cooper, H. G., Koehler, J. S. and Marx, J. W., *Irradiation Effects in Cu, Ag and Au Near 10°K*, Phys. Rev. *97*, 599-607 (1955).
21. Huntington, H. B. and Seitz, F., *Mechanism for Self-Diffusion in Metallic Copper*, Phys. Rev. *61*, 315-325 (1942).

22. Huntington, H. B., *Self-Consistent Treatment of the Vacancy Mechanism for Metallic Diffusion*, Phys. Rev. *61*, 325-338 (1942).

23. Huntington, H. B., *Mobility of Interstitial Atoms in a Face-Centered Metal*, Phys. Rev. *91*, 1092-1098 (1953).

24. Huntington, H. B., *Elastic Strains Around an Interstitial Atom*, Acta Met. *2*, 554 (1954).

25. Bartlett, J. H. and Dienes, G. J., *Combined Pairs of Vacancies in Copper*, Phys. Rev. *89*, 848-850 (1953).

26. Cottrell, A. H., *Effect of Solute Atoms on the Behaviour of Dislocations, Report of a Conference on the Strength of Solids*, University of Bristol, Physical Society, London, 1948, pp. 30-38.

27. Cottrell, A. H., *Dislocations and Plastic Flow in Crystals*, Oxford, 1953, pp. 133-147.

28. Seitz, F., *Imperfections in Nearly Perfect Crystals: A Synthesis* (Ed. W. Shockley), John Wiley and Sons, New York, 1952, pp. 3-76.

29. Eggleston, R. R., *The Annealing of Copper After Radiation Damage at Low Temperatures*, Acta Met. *1*, 679-683 (1953).

30. Redman, J. K., Coltman, R. R. and Blewitt, T. H., *The Activation Energy for the Recovery of Reactor Irradiated Copper Crystals*, Phys. Rev. *91*, 448 (1953)(A).

31. For a review see: Broom, T., *Lattice Defects and the Electrical Resistivity of Metals*, Phil. Mag. Supplement *3*, 26-83 (1954).

32. Bowen, D. and Rodeback, G. W., *The Influence of Cold Work and Radiation Damage on the Debye Temperature of Copper*, Acta Met. *1*, 649-654 (1953).

33. Dexter, D. L. *Scattering of Electrons from Point Singularities in Metals*, Phys. Rev. *87*, 768-777 (1952).

34. Jongenburger, P., *The Extra Resistivity Owing to Vacancies in Copper*, Phys. Rev. *90*, 710 (1953).

35. Jongenburger, P., *The Extra Resistivity Due to Vacancies in Copper, Silver and Gold*, Appl. Sci. Res. *B3*, 237-248 (1953).

36. Friedel, J., *The Distribution of Electrons Round Impurities in Monovalent Metals*, Phil. Mag. *43*, 153-189 (1952).

37. Blatt, F. J., *Effect of Point Imperfections on the Electrical Properties of Copper I. Conductivity*. To be published. For abstracts see: Bull. Am. Phys. Soc. *29*, No. 7, 30 (1954); *30*, No. 2, 30 (1955). The writer is indebted to Dr. Blatt for permitting him to see the manuscript prior to publication.

38. Blatt, F. J., to be published.

39. Dienes, G. J., *A Theoretical Estimate of the Effect of Radiation on the Elastic Constants of Simple Metals*, Phys. Rev. *86*, 228-234 (1952).

40. Nabarro, F. R. N., *Effect of Radiation on Elastic Constants*, Phys. Rev. *87*, 665 (1952).

41. Dienes, G. J., *Effect of Radiation on Elastic Constants*, Phys. Rev. *87*, 666 (1952).

42. Friedel, J., *Anomaly in the Rigidity Modulus of Copper Alloys for Small Concentrations*, Phil. Mag. *44*, 444-448 (1953).

43. Dieckamp, H., *Shear Modulus Recovery of Electron Irradiated Copper*, Bull. Am. Phys. Soc. *30*, No. 2, 8 (1955)(A).

44. Tucker, C. W., Jr. and Sampson, J. B., *Interstitial Content of Radiation-Damaged Metals from Precision X-ray Lattice Parameter Measurements. I. Principles of the Measurements*, Acta Met. *2*, 433-438 (1954).

45. Huang, K., *X-ray Reflection from Dilute Solid Solutions*, Proc. Roy. Soc. (London) *A190*, 102-117 (1947).

46. Eshelby, J. D., *Distortion of a Crystal by Point Imperfections*, J. Appl. Phys. *25*, 255-261 (1954).

Radiation Damage in Non-Fissile Materials

By J. H. O. Varley,* UK

In this paper studies of radiation damage in various non-fissile materials carried out by several scientists in the UK A.E.A. are reported. It is hoped that the results obtained from the various classes of materials studied will help to clarify the nature of the mechanisms whereby radiation damage occurs, in addition to leading, along with all other work, to a basic understanding and solution of the materials problems involved in reactor technology. Several excellent reviews of radiation damage studies have already been written by Dienes,[1,2] Dugdale,[3] Kinchin and Pease[4] and by Glen.[5]

RADIATION DAMAGE IN METALS

Kinchin[6] has made a study of the changes in electrical resistivity produced in several high melting point metals by pile irradiation at 50°C. This temperature being relatively low with respect to recrystallisation temperatures for such metals, it may be expected that a larger fraction of the total damage produced is frozen into these materials. The resistivity changes as a function of integrated flux do in fact resemble the curves obtained by workers in the USA[7,8,9] on such metals as copper bombarded at low temperatures. Thus there is an initial somewhat pronounced curvature in the resistivity-integrated flux curves which gives way to an almost linear change with increasing total flux.

Probably the simplest explanation of such a variation of resistivity with total flux is to suppose that at least two classes of defect are contributing to the resistivity increases. One class saturates at relatively low doses whilst there is a steady build-up of the second kind of defect with increasing dose, the latter giving rise to a linear increase of resistivity with dose superposed upon a resistivity change which saturates at low doses. This second class of defect may be due to the clustering of vacancies or interstitials suggested by Seitz[10] whilst the first kind may be isolated vacancies and interstitials.

Kinchin[11] has also studied the release of stored energy from irradiated specimens of molybdenum upon subsequent annealing and has correlated the energy release with corresponding changes in resistivity. He finds that, for a given heating rate, on raising the annealing temperature a small maximum in the energy release is followed at a higher temperature by a larger maximum in the energy released over a given temperature interval. The corresponding changes in resistivity are inverted; thus there is a large resistivity change accompanying the small maximum in the energy release curve and conversely a small resistivity change occurs with a large release of stored energy. This evidence again seems to support the idea that point defects and clusters are both present since point defects are considered to produce a much larger contribution to the resistivity of a metal than are extended discontinuities such as dislocations, grain-boundaries and presumably cluster boundaries.[12,13]

Makin[14] has studied the effect of pile radiation on yield strength, ultimate strength and ductility of several metal wires in both single crystal and polycrystalline form. He finds in the case of copper single crystals a marked increase in critical shear stress as a result of radiation damage, qualitatively confirming the earlier work of Blewitt.[15] However, Makin finds that his results for low doses do not confirm the quantitative relation obtained by Blewitt, viz., that the increase in the critical shear stress is proportional to the cube root of the total flux. There is also some evidence for an incubation period in copper single crystals at small total fluxes which he tentatively ascribes to the accumulation of a critical number of cluster defects. Below this number the separation between these cluster defects is sufficiently great not to interfere with slip originating from the weakest Frank-Read sources within the crystal. Above this critical number of defects the spacing between them becomes less than the length of the weakest dislocation sources, so interfering with the operation of such sources in that they are effectively shortened. The critical shear stress is thus increased only after the accumulation of a sufficient number of cluster defects.

Makin has further shown that there is a marked temperature dependence of critical shear stress at temperatures well below those at which any annealing of radiation damage occurs; this effect is reversible. In keeping with other studies on the effects of radiation damage on physical and mechanical properties it is found that the effects are not completely removed in a given material until annealing is carried out in that temperature range where the rate of creation and movement of vacancies is rapid. Thus in copper the activation energy associated with such a process is about 2.1 ev corresponding to annealing in

*UK A.E.A., Atomic Energy Research Establishment, Harwell, Berkshire.

a temperature range around 300°C. This again suggests that the final defects to be removed may be cluster defects, either of vacancies or interstitials, inasmuch as vacancies will be created at the surfaces of vacancy clusters and diffuse into the crystal so dispersing the clusters, or alternatively vacancies will be produced at dislocations in the crystal and diffuse to interstitial aggregates so annihilating them (cf. ref. 10).

In the case of polycrystalline materials Makin has observed increases in both yield point and ultimate tensile strength and a decrease in ductility. There is a decrease in the breaking strength-yield strength ratio, and this reduction of the ability of the material to work harden coupled with a loss in ductility immediately suggests that the notch sensitivity of a metal under irradiation will be increased. In fact American work[16,17] has already shown this to be the case in that the transition temperature, below which brittle fracture and above which ductile fracture takes place, is raised as a result of radiation damage, and there is in general a decrease in the energy absorbed to fracture a specimen in a ductile manner above the transition temperature. Such a consequence of radiation damage on mechanical properties has an important bearing upon power reactor design.

The creep properties of metals do not appear to be affected significantly by radiation damage.[18,19,20] In this country Jones *et al.*[21] have observed no change in creep rate of polycrystalline aluminium in the secondary creep range under pile irradiation, to within ± 10 per cent. Makin[22] has made an extensive study of the creep of cadmium single crystals under α-particle bombardment from a polonium source giving a flux at the specimen surface of about 5×10^8 particles cm^{-2}-sec^{-1}. He could detect no change in creep rate due to the effects of surface damage by α-particles. Slater[23] has observed that, since radiation damage can produce both a hardening effect, due to the production of point defects and extended defects such as clusters, and a possible softening effect through the thermodynamic instability set up in the system by thermal spikes and increased atomic mobility induced by the bombarding particles, the creep rate may be either reduced or increased under bombardment. Since creep occurs in a temperature range where recovery from any induced thermodynamic instability is relatively rapid the effect of radiation damage on creep rate may in any case be expected to be small, for rapid recovery will never permit a large accumulation of defects.

Charlesby *et al.*[24] have measured the effects of pile irradiation on the Young's Modulus of several polycrystalline metals, including molybdenum, a phosphor bronze and an austenitic stainless steel. No marked change in modulus has been observed for integrated neutron fluxes up to the order of 5×10^{18} neutrons cm^{-2}.

Theoretical considerations of radiation-damage mechanisms have led Kinchin and Pease[25] to the introduction of the concept of replacement collisions. If a collision between a moving interstitial atom and a stationary atom results in ejection of the stationary atom leaving the interstitial with insufficient kinetic energy for it to escape from the vacancy it has been responsible for creating, then this atom will fall into the vacancy dissipating its kinetic energy through lattice vibrations as heat. They assume that for such a process to occur, some threshold energy, which is less than the displacement energy, must be imparted to the stationary atom to eject it into an interstitial position. The energy difference between this threshold energy and the displacement energy necessary to displace the stationary atom is obtained from the potential energy given up by the moving atom as it replaces the stationary atom. Further, for these replacement collisions to occur it is assumed that the moving atom must be left with energy both less than the displacement energy and less than the energy imparted to the stationary atom. Kinchin and Pease then show that for a reasonable choice of energy parameters the number of replacement collisions far exceeds the number of displacement collisions, and they obtain satisfactory agreement with the experimentally determined disordering rate of $MnNi_4$ found by Arowin.[26] The essential importance of this mechanism lies in the concept that by such a process of replacement collisions, more displaced atoms are likely to fall into vacant lattice sites of the wrong kind than would be the case if all the atoms were displaced far from vacancies during bombardment and then migrated at random to vacant lattice sites.

Barnes and Makin[27] have discussed the non-linearity of the resistivity-integrated flux relation obtained by Cooper, Koehler and Marx[28] for copper wires under deuteron bombardment at 12°K. They consider three possible causes for this irradiation annealing, and show that two of these, namely local heating along the deuteron track (the thermal spike) and local melting at the end of the track of a displaced atom (the displacement spike concept of Brinkman[29]) will produce effects too small in magnitude to account for the changes observed. The third possible cause is that during the movement of interstitial atoms with low energy by the interstitialcy mechanism, i.e. by successive interchange of interstitials with atoms on normal sites, an interstitial will pass within some critical distance of a vacant lattice site and will be annihilated. This critical distance they estimate to be three atomic spacings and the distance travelled by an interstitialcy moving with a velocity low enough so that it is in the energy range in which it will be captured by a vacancy is about eight atomic spacings. On this model, Barnes and Makin obtain satisfactory agreement with the results obtained by Cooper *et al.*

Lomer[30] has considered the probable effect of irradiation upon diffusion rates in copper, assuming reasonable values for the activation energies controlling the formation and movement of vacancies. His

calculations are based on the assumption that a high energy particle produces of the order of one effective interstitial-vacancy pair, for he considers that localised damage giving high concentrations of defects will either anneal out very rapidly or take up metastable configurations which will not affect the diffusion rates, i.e., only those interstitials and vacancies which escape from regions of highly localised damage will affect the random distribution of vacancies and interstitial atoms controlling the diffusion process. Lomer's conclusions are that the effect of radiation damage on measurable diffusion rates will be small, for while at low temperatures the equilibrium concentrations of lattice vacancies will be larger under irradiation conditions, the diffusion coefficients are in any case very small. At high temperatures on the other hand the vacancy and interstitial concentration under irradiation is little different from that in an unirradiated crystal since recombination processes are relatively rapid, so that the effect of irradiation on measurable diffusion coefficients is again small. Between these extremes there is some temperature at which the diffusion rate is increased by an optimum amount. In the case of copper, Lomer calculates this temperature to be about 450°K when the diffusion coefficient is increased by about three powers of ten over that of an annealed sample. It is emphasised that the diffusion coefficient is increased by many orders of magnitude at low temperatures, but that such an increase does not bring the diffusion coefficient into the measurable range. Lomer also points out that the saturation numbers of interstitial-vacancy defects produced by irradiation increases only as the square root of the flux; in addition this saturation value is very sensitive to the state of perfection of the crystal, being small in relatively imperfect crystals containing many initial interstitial traps.

NON-METALS

Pease[31] has studied by X-ray examination the effects of radiation-damage on several compounds of boron, including boron nitride. He argues that saturation of the damage will occur when the concentration of vacancies is of the order of the reciprocal of the number of lattice sites surrounding a given interstitial site in the lattice, for then any interstitial will be adjacent to a vacancy and such a vacancy interstitial pair will be unstable. Thus in boron nitride where there are 12 lattice sites surrounding a given interstitial site the concentration of vacancies at which saturation effects should be produced should be of the order of one-twelfth. Pease finds that as a function of dose the c spacing of the hexagonal layer structure of boron nitride and the a dimension obtained from (hkl) reflections $(l \neq 0)$ do in fact saturate at about this value. The a dimension determined from $(hk0)$ reflections does not saturate, however, at this dose, but only shows a change of slope. At greater integrated fluxes a further slight expansion occurs in the c spacing. The a dimension contracts to a saturation value of 0.1% and the c spacing expands by about 1% with a further very small change at larger doses to about 1.05% total expansion.

Pease has developed the simple criterion for saturation given above to allow for the fact that the intensity ratio of certain observed X-ray lines after irradiation is much smaller than is predicted from the saturation concentration of interstitial defects. He concludes that the effective number of atoms displaced into metastable positions for each bombarding particle is an order of magnitude smaller than the total number displaced, due to recombination of close interstitial-vacancy pairs, and that the effective number of lattice sites about any given interstitial site, such that recombination of a vacancy at one of these sites with the interstitial will occur, is an order of magnitude greater than the value 12 quoted above. Moreover, the movement of interstitials is considered to be restricted to sites between layers of the lattice. These refinements lead to a prediction of the correct order of magnitude for the saturation value of the c spacing as a result of radiation damage.

Recovery of damage produced at room temperature occurs by annealing at temperatures above 300°C with an activation energy of about 2 ev.

Pease[32] finds similar effects in other boron compounds. In some cases, including boron nitride, pronounced line broadening is observed. All these effects saturate at, or continue to vary much more slowly after a dose of 2×10^{18} thermal neutrons cm^{-2}.

Turning now to radiation studies in ionic solids typified by the alkali halides, some experiments reported by the author[33] have led to the suggestion of a mechanism whereby ions can be displaced from their normal sites to interstitial sites in a heteropolar lattice by the indirect process of utilising that portion of the energy of a fast charged particle which is given up initially to ionisation losses. Some of the ionisation processes will result in more than one electron being removed from a negative ion in the lattice. If this multiple ionisation leads to the removal of, say, four or five electrons from one negative ion, then, provided the ion does not recover electrons in a time short compared with its vibrational period, this ion may be ejected from its lattice site by the lattice vibrations. Ejection of such a negative ion, stripped of several electrons is probable, because the ion is temporarily a positive ion at a lattice site normally occupied by a negative ion. Thermal activation may then remove the ion from such an unstable position into some interstitial position which to a first approximation is electrically neutral. Alternatively, the multiple-ionised negative ion may displace one of the neighbouring positive ions into an interstitial site, itself temporarily occupying the positive ion lattice site. Considerations of the magnitudes of the ionisation potentials of negative ions such as chlorine, suggest that the anions so displaced into interstitial sites will regain enough electrons to become electrically neutral, the remaining electrons being trapped at

negative ion vacancies. The cations displaced interstitially will probably remain positively charged.

The subsequent fate of these interstitial anions and cations is that they migrate either to normal lattice sites of the right kind so tending to restore the crystal towards equilibrium, or they may be trapped at vacant sites of the wrong kind. Thus a neutral anion may occupy a positive ion vacancy, while an interstitial cation may combine with an electron trapped at a negative ion vacancy, so occupying such a vacancy as a neutral atom. An attempt has been made by the author[31] to interpret radiation induced changes in such physical properties as optical absorption in alkali halides on the basis of these considerations.

This concept of the displacement of ions in solids by the indirect process of multiple ionisation is a logical development of the mechanisms for the production of free radicals already described from studies in radiation chemistry. Furthermore, McLennan's work[35] on bombardment of alkali halide crystals with 50 kev electrons led him to suggest that single ionisation of a halogen ion, leaving it temporarily uncharged, might result in the formation of some interstitial neutral anions. Such a process is, however, unlikely, and it is only if multiple ionisation of a single anion occurs that the displacement probability will be relatively large. Platzman[36] (private communication) has suggested that the multiple ionisation mechanism may arise from Auger cascades following the ejection of a single inner electron.

One important aspect of this multiple-ionisation displacement process is that such relatively low energy radiation as X-rays can give rise to atomic displacements in ionic lattices. Thus X-rays will produce photoelectrons which in turn may multiple-ionise anions and hence indirectly produce displacements. The cross-section, σ, for multiple ionisation is large; thus $\sigma \sim 10^{-16}$ cm^2 for the removal of one electron, decreasing by approximately $(n-1)$ orders of magnitude for the removal of n electrons.

It would appear, then, that the nature of the incident radiation is of significant importance with respect to the type of bonding responsible for the cohesion of the material under bombardment.

To conclude this paper, some work carried out by Levy *et al.*[37] on glasses is reported. Irradiation of fused silica, containing 0.3% boron, 0.04% copper, 0.05% sodium and 0.005% iron impurities by weight, with X-rays, γ-rays or pile radiation produced a patchy coloration of the specimens. The absorption spectrum revealed three bands with maxima at 2.3 ev, 4.1 ev and about 5.6 ev. The coloration could be bleached either optically or thermally, the 2.3 ev and 5.6 ev bands diminishing at about the same rate. By intercomparison of irradiated specimens of sodium tetraborate, sodium silicate and the silica glass, it was concluded that the 2.3 ev and 5.6 ev bands arise from electron traps associated with sodium tetraborate impurities. The inhomogeneous distribution of borate impurity would account for the patchy coloration. The 4.1 ev band was tentatively ascribed to electron traps in the silica network. Strong thermoluminescence was observed in these glasses as also in sodium tetraborate specimens after irradiation. Sodium silicate glasses, however, produced much less intense thermoluminescence. Long pile irradiations resulted in a decrease in intensity of the 2.3 ev and 4.1 ev bands suggesting that increasing radiation damage produces defects which interact with existing electron traps. New centres may be formed with absorption bands lying outside the range in which observations were made (6.2 — 1.2 ev).

CONCLUSIONS

Studies of radiation damage reported in this paper suggest that there is a marked dependency of the intensity and detailed distribution of the damage upon the nature of the incident radiation and the character of the bonding, heteropolar or homopolar, responsible for the cohesion of the material under bombardment. In metals existing evidence points to the formation of isolated point defects and extended defects resulting from non-uniform production of defects within the material and clustering of point defects.

Radiation damage of boron compounds in which pile sources give a high rate of damage through the $B_{10}(n,\alpha)$ reaction, has given evidence of saturation effects in experiments such that each atom in the lattice has been displaced about once.

In ionic crystals it now seems that relatively low-energy radiation such as X-rays can give rise to atomic displacements through the utilisation of incident energy initially given up to ionisation effects.

Finally, in glasses the results of experiments on fused silica containing borate impurities lead to the conclusion that visible coloration is due to these impurities, in keeping with the deductions from other work on fused silica and quartz crystal containing impurities other than boron.

ACKNOWLEDGEMENTS

The author wishes to acknowledge the interest and encouragement given him by Dr. H. M. Finniston and to thank Dr. M. J. Makin for helpful criticism.

REFERENCES

1. Dienes, G. J., *Radiation Effects in Solids,* Ann. Rev. Nuc. Sci., *2*, 187-220, 1953.
2. Dienes, G. J., *Effects of Nuclear Radiations on the Mechanical Properties of Solids,* J. App. Phys., *24*, 666-74, 1953.
3. Dugdale, R. A., *Recent Experiments at Harwell on Irradiation Effects in Crystalline Solids,* Report on Conference on Defects in Crystalline Solids. Phys. Soc. p. 246, 1955.
4. Kinchin, G. H. and Pease, R. S., *The Displacement of Atoms in Solids by Radiation,* Rep. Prog. Phys. 1955.
5. Glen, J. W., *A Survey of Radiation Effects in Metals,* Harwell Report, A.E.R.E. M/TN 27, 1954.
6. Kinchin, G. H., unpublished work. See ref. 4, 261-2.

7. Marx, J. W., Cooper, H. G. and Henderson, J. W., *Radiation Damage and Recovery in Cu, Ag, Au, Ni and Ta*, Phys. Rev. (2) 88; 106-12, 1952.
8. Overhauser, A. W., *Isothermal Annealing Effects in Irradiated Copper*, Phys. Rev. (2) 90; 393–400, 1953.
9. Cooper, H. G., Koehler, J. S. and Marx, J. W., *Irradiation Effects in Cu, Ag, and Au near 10°K*, Phys. Rev. (2) 97; 599-607, 1955.
10. Seitz, F., *On the Generation of Vacancies by Moving Dislocations*, Adv. in Phys. 1; 43, 1952.
11. Kinchin, G. H., unpublished work.
12. Hunter, S. C. and Nabarro, F. R. N., *Propagation of Electrons in a Metallic Lattice*, Proc. Roy. Soc. A 220; 542-61, 1953.
13. van Bueren, H. G. and Jongenburger, P., *Resistivity in Metals*, Nature, 175; 544-6 1955.
14. Makin, M. J., unpublished work.
15. Blewitt, T. H., See Ref. 4, p. 257.
16. Meyer, R. A., *Influence of Deutron Bombardment and Strain Hardening on Mild Steel*, A.E.C. Report, USNRDL-431.
17. Sutton, C. R. and Leeser, D. O., *Radiation Effects on Reactor Materials; Metals*, Nucleonics, 12, No. 9, 1954.
18. Kittel, J. H., Nat. Advis. Cttee. Aero. Res. Memo. (E7E13) 1947.
19. Witzig, W. F., *Creep of Copper under Deuteron Bombardment*, J. App. Phys., 23; 1263-6, 1952.
20. Jeppson, M. R., Mather, R. L. and Yockey, H. P., *Effect of Cyclotron Irradiation on Creep of Aluminium*, A.E.C. Report AECD 3631.
21. Jones, E. R. W., Munro, W. and Hancock, N. H., *The Creep of Aluminium during Neutron Irradiation*, J. Nuclear Energy, 1; 76-86, 1954.
22. Makin, M. J., *The Effect of Alpha-Particle Bombardment on the Creep of Cadmium Single Crystals*, J. Nuc. Energy, *1*, 181-193, 1955.
23. Slater, J. C., *Effects of Radiation on Materials*, J. App. Phys., *22*, 237-56, 1951.
24. Charlesby, A., *Effect of Atomic Pile Radiation on the Elastic Modulus of an Austenitic Steel*, Harwell Report, A.E.R.E. M/R 1434.
25. Kinchin, G. H. and Pease, R. S., *The Mechanism of the Irradiation Disordering of Alloys*, J. Nuc. Energy, 1, 200-2, 1955.
26. Arowin, L. R., *Radiation Damage Effects on Order-Disorder in Nickel-Manganese Alloys*, J. App. Phys., 25; 344-49, 1954.
27. Barnes, R. S. and Makin, M. J., *On the Mechanism of Irradiation Annealing*, Harwell Report, A.E.R.E. M/R 1626, 1955.
28. Cooper, H. G., Koehler, J. S. and Marx, J. W., *Resistivity Changes in Copper, Silver and Gold Produced by Deuteron Irradiation Near 10°K*, Phys. Rev. (2) 94; 496, 1954.
29. Brinkman, J. A., *On the Nature of Radiation Damage in Metals*, J. App. Phys. 25; 961–70, 1954.
30. Lomer, W. M., *Diffusion Coefficients in Copper under Fast Neutron Irradiation*, Harwell Report, A.E.R.E. T/R 1540, 1955.
31. Pease, R. S., unpublished work.
32. Pease, R. S., *X-ray Examination of Irradiation Effects in Boron Compounds*, Acta. Cryst. 7; 633, 1954.
33. Varley, J. H. O., *A Mechanism for the Displacement of Ions in an Ionic Lattice*, Nature, 174; 886-7, 1954.
34. Varley, J. H. O., *A New Interpretation of Irradiation-Induced Phenomena in Alkali Halides*, J. Nuc. Energy, *1*, 130-143, 1954.
35. McLennan, D. E., *Study of Ionic Crystal under Electron Bombardment*, Canadian Journal of Phys. 29; 122-28, 1951.
36. Platzman, R. L., *On the Primary Processes in Radiation Chemistry and Biology*, Symposium on Radiobiology, Wiley and Sons, 1952.
37. Levy, M. and Varley, J. H. O., *Radiation Induced Colour Centres in Fused Quartz*, Proc. Phys. Soc. B, *68*; 223-33, 1955.

Modifications Produced in Non-Metallic Materials by Radiation, and the Thermal Healing of These Effects

By G. Mayer, P. Perio, J. Gigon and M. Tournarie,* France

The problem of the action of radiation on solids makes up a very vast field, the study of which is only just beginning at the Commissariat à l'Energie Atomique. It has been only for a short time, as a matter of fact, that we have had relatively intense fluxes available to us (6×10^{12} thermal neutrons per cm² per sec at the center of the Saclay pile), even though they might be considered very weak compared with those of such reactors as NRX and MTR. In addition, the heavy water reactors offer but limited volumes for a wide variety of experimental needs and studies of the solid state require numerous measurements on numbers of samples.

Thus, we have obtained only the first results in an integrated program of research which is necessary for all the installations concerned with nuclear energy.

In materials subjected to radiation, we can follow the changes in a certain number of physical properties and make a study of the thermal healing of the modifications brought about by irradiation.

The latter is carried out at a moderate temperature, for we still have no space in the high flux areas of our reactors which can be refrigerated or heated. The modifications for which annealing is rapid below approximately 35°C are still completely unknown to us.

According to the needs, we measure one or several of the following properties; optical density, electrical resistance, speed of sound,[1] piezo-electric constant, crystalline parameters, dimensions. We also carry out measurements of the magnetic susceptibility, thermo-electrical power, expansion coefficient, and some calorimetric determinations.

An optical study of glasses and vitreous silica was published earlier.[2] Allain carried out similar research on calcium fluoride which will be published at some later date. Here, we shall merely discuss our experiments on graphite and lithium fluoride.

MEANS USED FOR IRRADIATION

Most irradiations have been carried out in the central part of the core of the Saclay pile, namely in an aluminum tube submerged in heavy water. The temperature there is approximately 35°C; the thermal neutron flux, which varies according to the power of the reactor and the nature and number of irradiated samples, did not exceed 6×10^{12} cm^{-2}-sec^{-1}; the fast neutron flux reached a few hundredths of this value.

At times, we also placed our samples in "converters," namely hollow uranium cylinders, one of which is substituted for a reactor rod (vertical converter, maximum flux of fast neutrons approximately 1.5×10^{12}), and the other in a tangential channel (horizontal converter, maximum flux of fast neutrons, approximately 10^{12}). In view of the difficulty encountered in the dosimetry of neutrons of varying energies, we shall express the various irradiations as total doses of thermal neutrons, by assuming a constant proportionality factor between the efficiency of the converter neutrons and those from the central core area. Since the error on the total doses received by the samples may be considerable (50%) the curves show the variation as a function of the dose and have illustrative value only.

GRAPHITE

The graphite rods used in the construction of piles have properties which vary according to the details of the conditions under which they are fabricated. The systematic study of the relationship between those conditions and the sensitivity of the product to irradiation has barely started. In the samples on which we worked, the apparent density (d), the resistivity at 0°C (ρ_0) and the speed of sound at ordinary temperatures (v), have the following extreme values:

d (gm-cm^{-3}) 1.53 and 1.65

ρ (Ω-cm^{-1}) 9.1×10^{-4} and 9.8×10^{-4}

v (cm-sec^{-1}) 1.9×10^{5} and 2.4×10^{5}

The maximum doses received by our samples were 4×10^{19} thermal neutrons per-cm².

QUALITATIVE RESULTS

1. No sample showed a change in linear dimension reaching to 10^{-4}.

2. The electrical resistance and the speed of sound increased from the very beginning of the irradiation, without any induction period capable of being de-

Original language: French.

* Physical Chemistry Department, Physical Chemistry Division, Commissariat à l'Energie Atomique.

tected by the means at our disposal (we do not make measurements *in situ*). This increase slows down as soon as the total dose reaches 3×10^{19} cm^{-2}, the resistivity at the ordinary temperatures is approximately doubled, while the speed of sound is multiplied by about 1.5.

3. These modifications seem to take place all the sooner if the graphite is more highly crystalline. As an indication of this state of crystallization, we used: (*a*) the appearance of the X-ray diffraction diagrams; (*b*) Young's modulus (which decreases as graphitization improves: (*c*) the magnitude of the temperature coefficient of the resistivity;[3] (*d*) the thermoelectrical power (see below).

4. Different graphites have a thermoelectrical power of such a character that, at the hot junction, the electrons pass from the less well crystallized product to the better graphitized one. For one sample irradiated at 4×10^{18}, the thermoelectrical power with respect to a non-irradiated control was 2.4×10^{-6} v/°C, and the character was such that the irradiated rod behaved as though it had been less graphitized than the control.

5. Magnetic susceptibility decreases due to irradiation.

6. With annealing, the electrical resistivity and the speed of sound tend to go back to their initial values. As regards electrical resistance, this healing can be observed in the vicinity of 100°C. However, we were able to make measurements, beginning at 80°C on some samples, while others showed no changes until a temperature of 120°C was reached.

7. Healing is complete only at a very high temperature, but the main part of it takes place at a relatively low temperature. Electrical resistivity and the speed of sound do not run together, the former goes back at a lower temperature than the other.

QUANTITATIVE RESULTS

When we refer in the following to "centers" created by neutron impact and destroyed by annealing, we mean that a limited number of atoms forms a localised geometric configuration which is different from those they had before the impact. However, while only average *positions* of a limited number of atoms are modified, the thermal *oscillations* (or absolute zero oscillations) of *all* the atoms about their mean positions have been changed in the relevant grain, since the frequencies of the normal modes also were changed.[4] The findings mentioned above, in particular the last, give us reason to believe that a single type of center could not account for the whole of the alterations brought about by irradiation.

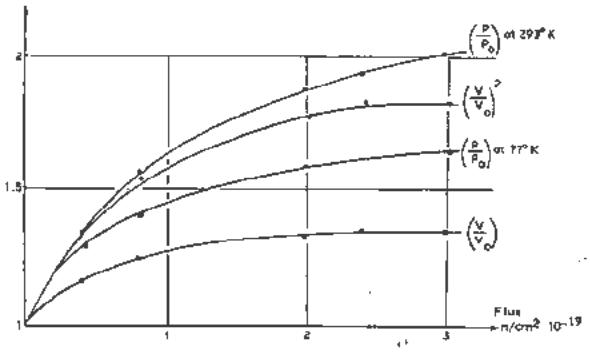

Figure 1

1. Using the measurements of electrical resistance by Kinchin,[3] Johnston[5] evaluates at 10^{20} per cm^3 the number of "voids" which trap the electrons produced by an irradiation of 5×10^{19} thermal neutrons in the BEPO reactor.

The theory of the increase in the speed of sound is not well developed and it seems reasonable that it concerns a variation in Young's modulus E which, for small irradiations, is proportional to the number of centers created.

If d is the density $v = \sqrt{E/d}$. Let us assume that a single type of center strongly affects the speed of sound; let n be the number of centers per cm^3, and N the number of carbon atoms per cm^3 of graphite ($N \simeq 8.10^{22}$)

$$E = E_0 \left(1 + \alpha \frac{n}{N}\right)$$

$$\mathrm{d}\ (v^2 - v_0^2 = \alpha \frac{n}{N} \cdot v^2 d\ \frac{c^2}{c_0^2} = 1 - \alpha \frac{n}{N}$$

It will be seen (Fig. 1) that $\alpha n/N$ reaches a value of 0.1 for a *thermal* neutron dose of 10^{18} cm^{-2}, which would create an enormous number of centers, unless alpha is very large. At first sight one would be tempted to feel that alpha is of the order of magnitude of 0.1 to 10^{-4}. (A "center" may consist of 10^3 or 10^{14} atoms.)

2. Saturation can take place for two distinct reasons: (*a*) by mutual cancelling out between the creation and destruction of the centers by the neutrons: $dn/dt = \alpha\psi - \beta\psi n$ where ψ = flux, n = number of centers, α and β = constants in which the cross section of the carbon atoms comes into play; and (*b*) by mutual cancelling out between the creation of centers by the neutrons and destruction due to thermal agitation: $dn/dt = \alpha\psi - K(T)f(n)$ where T = temperature. These two effects are not absolutely distinct, since it is possible that destruction by neutron effects takes place through a local rise in temperature; the temperature itself is never defined other than by the agitation, regardless of its cause.

Functions $K(T)$ and $f(n)$ are the subject of the "recovery" kinetics studies (below).

3. A graphite plate irradiated by 1×10^{19} neutrons cm^{-2} in the central channel, then by 1.1×10^{19} in a horizontal converter, shows a variation in the parameters determined by X-ray diffraction with respect to a control:

$$\frac{\Delta a}{a_0} = 0 \pm 1 \times 10^{-4} \text{ measured on 1120 reflection}$$

$$\frac{\Delta a}{c_0} = 10 \pm 1 \times 10^{-4} \text{ measured on 0006 reflection}$$

The macroscopic expansion is under 10^{-4}. This is not entirely due to the fact that graphite is not perfectly oriented. Indeed, the *thermal* expansion of industrial graphite is less than that of crystalline graphite. Nelson and Riley[7] give for the latter:

$$\frac{\Delta a}{a} = -0.01 \times 10^{-4}/°C; \quad \frac{\Delta c}{c} = 0.28 \times 10^{-4}/°C$$

thus, in volume

$$\frac{\Delta V}{V} = \frac{\Delta c}{c} + 2\frac{\Delta a}{a} = 0.26 \times 10^{-4}/°C$$

Our sample before irradiation showed linear expansion coefficients which are respectively equal to $0.025 \times 10^{-4}/°C$ in the direction of flow and $0.035 \times 10^{-4}/°C$ at right angles to it and $0.095 \times 10^{-4}/°C$ in volume. Comparison of this value with that of crystalline graphite gave us reason to believe that in the industrial products, part of the expansion of the crystallites is compensated for by a narrowing down of the pores or by compression of the intercrystalline cement.

It would be interesting to follow up the working hypothesis which identifies the grain expansion produced by irradiation with a thermal expansion. The volume expansion of the crystallites is equal to:

$$2\frac{\Delta a}{a_0} + \frac{\Delta c}{c_0} = 10 \times 10^{-4}$$

which would mean a cubic expansion of the whole equal to:

$$10 \times 10^{-4} \times \frac{0.095}{0.26} = 3.7 \times 10^{-4}$$

which would be distributed linearly between the direction of flow and those perpendicular to it in respective ratios of 0.025 and 0.035 to 0.095. Should such a hypothesis apply, one might then expect linear expansion of our irradiated sample of the order of:

$$3.7 \times \frac{25}{95} \times 10^{-4} = 10^{-4}$$

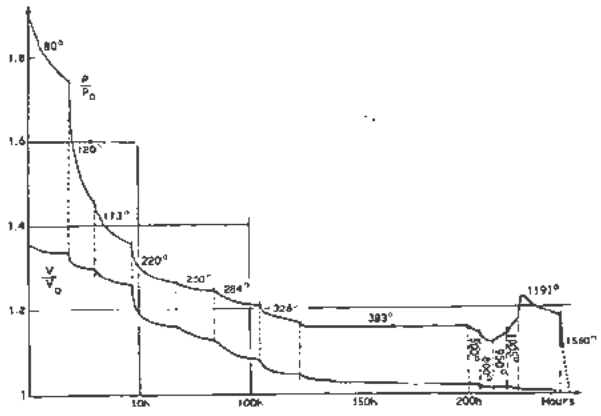

Figure 2

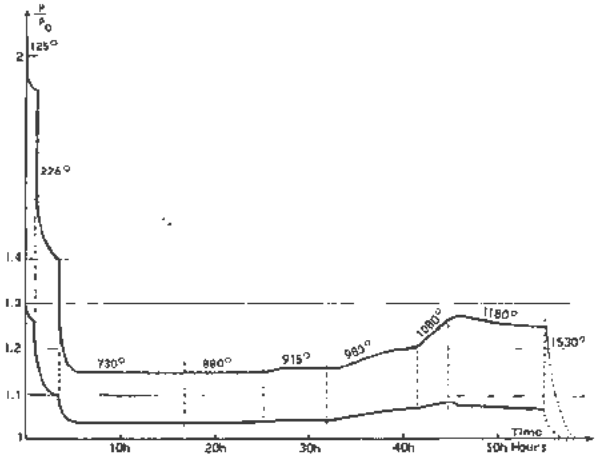

Figure 3. Curve A: sample irradiated with flux of 6×10^{18} n/cm² in central channel. Curve B: sample irradiated with flux of $3–4 \times 10^{18}$ n/cm² in vertical converter

in the direction of flow and

$$3.7 \times \frac{35}{95} \times 10^{-4} = 1.4 \times 10^{-4}$$

at right angles to it.

As we stated above, no expansion reaching 10^{-4} was revealed. Expansions of approximately half that amount were observed by Delcroix on a sample which had been subjected to a slightly higher dose. At the moment of writing, irradiation of this sample is continuing. We have not been able, therefore, to take up a specimen for X-ray examination.

ANNEALING OR RECOVERY EXPERIMENTS

We made a study of the "recovery", following heating up of several rods which had been irradiated to 3.4×10^{19} n-cm^{-2} in a converter, and of a rod irradiated to 6×10^{18} n-cm^{-2} in the central channel.

After each annealing period, we measured the resistivity and speed of sound at 20°C, and in some cases, resistivity at 77°K. In each series of measurements, the irradiated rod was compared with two controls which had not been irradiated and which were taken side by side in the same sample of graphite. One of these remained close to the measuring instruments, and served as a check on them. The other went with the irradiated rod into the annealing oven and was measured at the same time in order to make sure that the changes observed were indeed due to irradiation. Above 350°, the samples were annealed in vacuum.

Treatment at 900°C changes the speed of sound in the control rod which was not irradiated sufficiently to make a quantitative interpretation difficult. However, the variations observed allow us to conclude that v decreases constantly, up to 1500°. In order to complete this type of study numerically, detailed investigation of v in non-irradiated graphite as a function of its earlier thermal history will be necessary.

Figure 2 is the story of the "recovery", at various temperatures, of ρ and v.

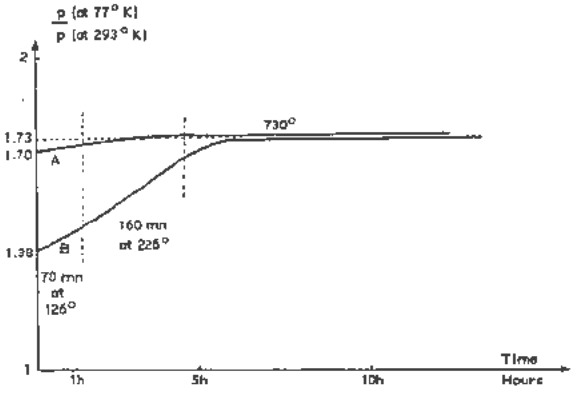

Figure 4. Curve A: sample irradiated with flux of 6 × 10^{18} n/cm² in central channel. Curve B: sample irradiated with flux of 3–4 × 10^{19} n/cm² in vertical converter

Figure 3 shows a comparison of the recovery curves of two unequally irradiated rods undergoing the same annealing process. Figure 4 gives the ratio $\rho_{77°K}/\rho_{293°K}$ for the same samples.

Figure 5 shows the "recovery" of the speed of sound in a sample irradiated at 2.2 × 10^{19}, measurement being made without taking the sample out of the oven, the temperature of which increased as a linear function of time, up to 400° in 55 hours.

INTERPRETATION OF DIFFERENTIAL THERMAL ANALYSIS

Figure 6 shows the differential thermal analysis, namely, the temperature difference between two samples of equal dimensions, one of which is irradiated to 2 × 10^{18} and the other not irradiated, and both annealed at 475°C in the same vessel in a nitrogen atmosphere.

After the solid curve was drawn (annealing at 475°), we allowed the oven to cool off, and then, without altering the experimental set-up, we subjected the whole to the same thermal cycle (dotted line). Comparison of the two curves shows two humps which correspond to a release of heat in the irradiated graphite, one in the vicinity of 125°, the other in the neighborhood of 225°. In the second experiment, the irradiated graphite has recovered in so far as the centers which disappear below 475° are concerned, and the temperature differences between two samples express the imperfections in the set-up.

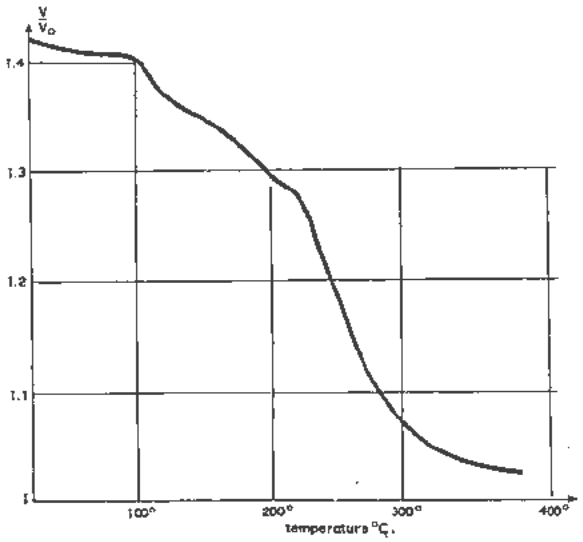

Figure 5

The thermal leak between the graphite and vessel having been approximately determined (time constant τ of the order of 3 minutes), we note in Fig. 6, the average duration t of each exothermal hump and the mean temperature differential ΔT, which expresses it. Replacing the exact integral by the surface of the rectangle, the quantity of heat ΔQ which causes the bump is:

$$\Delta Q \simeq MC_p \times \Delta T \times \frac{t}{\tau}$$

in which M is the mass of the sample.

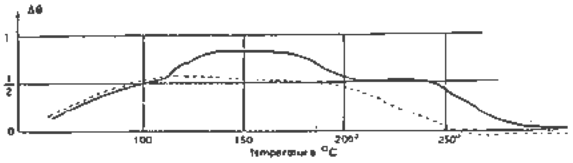

Figure 6

Thus ΔU, the variation of the internal energy per cm³, is approximately $\Delta Q\ d/M$ namely 0.5 cal/cm³ for the phenomena in the vicinity of 125°C and 0.3 cal/cm³ for recovery which takes place around 125°C.

These values give us in principle, the products, n_1W_1 and n_2W_2, of the number of centers and the energy released by their annihilation.

Supposing $W_1 = 3$ ev.† namely 5 × 10^{-12} ergs, one finds that $n_1 \sim 4 \times 10^{18}$ centers/cm³.

Each cc of this sample had received only 3 × 10^{18} thermal neutrons, namely, a maximum of 6 × 10^{17} fast neutrons of which 6 × 10^{16} at most had collided with carbon atoms. After the importance of the alteration of Young's modulus, this is a second indication of the fact that primary impact may modify the mean positions of a number of atoms.

We are currently applying the method in a more precise fashion on more irradiated samples of the same graphite and of natural graphite, and we shall extend the temperature range to 800° at least, a temperature at which the resistivity again starts increasing (Figs. 2 and 3).

ANALYSIS OF THE RECOVERY CURVES

By referring to Figs. 2, 3 and 5, it will be seen that, from 120°, ρ decreases rapidly and v slowly but unmistakably, and that, at 220°, the reverse happens.

† The heat of vaporization of carbon (graphite) is about 6.5 ev.

Continuing our theory of the "centers", we endeavored to cast more light on the kinetics of the disappearance of those two types of centers; one, which disappeared at a measurable speed, around 120° and which affects the resistivity a great deal and the speed of sound but little; and another one which disappears at 220°, reacts strongly on v, and not much on ρ.

If it be assumed that the centers disappear according to the differential law $dn/dt = K(T)f(n)$ t being the time, and T the temperature, with $K(T)$ the product of a function $e^{-W/kT}$ by a function $\psi(T)$ which does not vary much with the temperature as compared with the exponential, the only quantity which could be calculated from (t) and $v(t)$ curves is energy W.

Indeed, the nature of $f(n)$ is not known *a priori* nor is the correlation between n and the measured variable. However, if we start with two equally irradiated samples, it is possible, using the hypotheses suggested for $K(T)$, to obtain W by comparing the times t_1 and t_2, needed to reach at two different temperatures, T_1 and T_2, the same degree of recovery of the same physical variable

$$\frac{W}{k}\left(\frac{1}{T_1} - \frac{1}{T_2}\right) = \log_e \frac{t_1}{t_2}$$

k being Boltzmann's constant.

Another method, less accurate in practice, consists of measuring on a single sample, a variation of the slope α of the recovery curve, when passing from T_1 to T_2:

$$\frac{W}{k}\left(\frac{1}{T_1} - \frac{1}{T_2}\right) = \log_e \frac{\alpha_2}{\alpha_1}$$

None of these methods as applied between 80° and 170°, affords an accurate definition of an activation energy. For W, we find a continuous range of values from 0.75 ev to 1.5 ev, according to the temperature at which one operates.

On the contrary, for the range where recovery takes place at a measurable rate between 210° and 250°, both methods give a value in the vicinity of 2.1 ev.

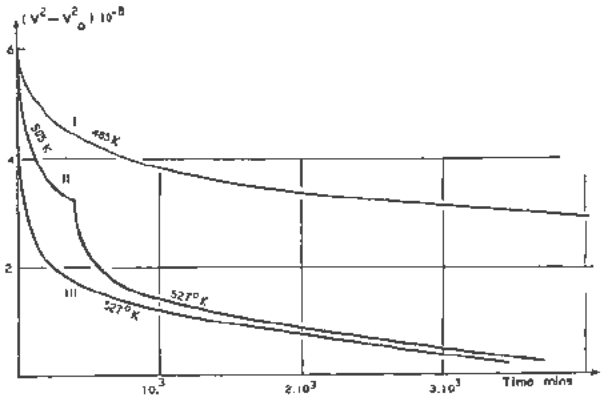

Figure 7

The required experimental values were obtained as follows: a rod irradiated at 1.6×10^{19} n-cm^{-2} was heated for 20 hours at 160° in order to eliminate the centers of the first recovery range. Thereafter, it was cut into three equal length pieces. One of them was heated to 212° for varying lengths of time. The second was annealed at 232° for 400 minutes, then heated to 254°. The third was annealed at 254°.

The speed of sound was measured at 20°C, between heating periods: these experiments are shown by the curves on Fig. 7.

Comparison of the speeds at the beginning of curves II and III gives $W = 2.16$ ev. By comparing curves I and II, it is found that $W = 2.02$ ev. Similarly, the method of slope variation as applied to curve II, gives $W = 2.14$ ev.

We have taken the precaution of using three pieces of the same rod in order to increase our chances of operating on three identical samples before and after the irradiation.

Indeed, some graphite having closely similar physical properties before irradiation, occasionally show deep differences in the kinetics of their recovery.

Function $e^{-W/kT}$, which comes into play in $K(T)$, being thus defined and being approximately 10^{-21} at 232°C, an attempt may be made at determining the order of the reaction.

Let v be the speed of sound obtained by reheating for 50 hours at 260°, we can write:

$$\frac{v^2 - v_0^2}{v_0^2} = \alpha \frac{n}{N}$$

The curves on Fig. 7 are not very different from curves given by this equation

$$\frac{1}{y} = \frac{1}{y_0} + \lambda t \qquad \text{solutions of } \frac{dy}{dt} = -\lambda y^2$$

Independently of all microscopic theories of these effects, the following remarks may be made:

At 232°, on curve II taken at the origin

$$\frac{dn/dt}{n} \simeq 1.5 \times 10^{-5}\ \text{sec}^{-1}$$

(Measurement of the recovery speed is materially feasible only if $(dn/dt)/n$ is somewhere between 10^{-4} and 10^{-6} sec^{-1}.)

(a) Let us assume $dn/dt = -K(T)n$, with $K(T)n^2$, this gives, at 232°

$$\psi(T) \times 10^{-21} \simeq 1.5 \times 10^{-5}$$

$$\psi(T) \simeq 1.5 \times 10^{16}\ \text{sec}^{-1}$$

a value which is a little high for a frequency factor "normally" in the vicinity of 10^{13}.

We must then assume that an elementary event which may be assumed to be exothermal, or else give up the idea of a first order law:

(b) Let us assume that $dn/dt = -K(T)n^2$, and we then have another interpretation of the experimental value:

$$\frac{dn/dt}{n} = -K(T)n$$

By assuming $n \simeq 10^{20}$, we find $\psi(T)\sigma\frac{W}{kT} \simeq 1.5 \times 10^{23}$, and $\psi(T) \simeq 1.5 \times 10^{-4}$.

A second-order law of the disappearance can be interpreted in terms of coincidences of the two types of centers but, there again, one lacks a microscopic theory in order to judge whether this value of $\psi(T)$ is acceptable.

For the problem mentioned above, of knowing whether the saturation effects on the speed of sound observed at ordinary temperatures for doses of 5×10^{16} is due to thermal recovery, we can conclude in the negative.

Lithium Fluoride‡

Some LiF powders and single crystals were exposed to thermal neutrons at doses ranging from 5×10^{16} to 10^{19} n/cm².§

Variation of the Crystalline Parameter

X-ray studies on powder and crystals made it possible to show three stages in the changes which take place during irradiation:

(*a*) Up to approximately 3×10^{17} n/cm² the lattice expands in a manner which is essentially proportional to the dose and without any detectable distortion. The width of the reflecting power (rocking curve) remains under 0.7 (2 θ), a value comparable to the instrumental width of the double crystal spectrometer used. The maximum increase in parameter a_0 reaches:

$$\frac{\Delta a}{a_0} = 1.7 \pm 0.1\ 10^{-3}$$

(*b*) From 3×10^{17} to 2×10^{18} n/cm², the reflecting power is analyzed as a non-broadened line superimposed on a widened base, which is asymmetrical and shifted toward the large angles, with a width which is approximately constant (20') at mid-height. The intensity of the base increases with the dose. In the plates taken on powder, only the centers of gravity of the thin line pair with broadened bases have been shown. They reveal a contraction with respect to the maximum expansion stage reached earlier; and we can write

$$\frac{\Delta a}{a_0} = (6 \pm 1) \times 10^{-4} \text{ for the dose } 1 \times 10^{18} \text{ n/cm}^2$$

(*c*) For the still higher doses, the broadened lines become essentially symmetrical, and the expansion still decreases:

$$\text{for } 7 \times 10^{18} \text{ n/cm}^2\text{: } \frac{\Delta a}{a_0} = (0.5 \pm 2) \times 10^{-4}$$

On this basis, the results of Binder and Sturm[8] would correspond to the first stage of irradiation, and those of Keating[9] for a dose of 7×10^{17}, to the third, with a reserve for the small value of expansion shown by this author.

Thermal Recovery

During thermal recovery, the reflecting power progressively returns to its initial quality: the crystal, completely annealed by treatment between 470 and 500°C is as perfect as it was before irradiation. There is no trace of polygonizing on the samples studied. It should be noted that for doses ranging from 3×10^{17} to 10^{19} n/cm² (range *b* above) annealing to 350° first causes the peak to merge with its base to form a broadened line; before the line gets back to its initial appearance, the powder diagrams reveal two stages of recovery. The first is perceptible from 150°C. Without any change in the color (see below) there is a recovery of the lattice, attended by rapid contraction or shrinkage. For doses above 3×10^{17} n/cm² the parameter becomes smaller than that of the initial product, without any apparent correlation between the rate of irradiation and the shrinkage noted. For a dose of 2×10^{18} n/cm², we noted:

$$\frac{\Delta a}{a_0} = -(2.5 \pm 1)\ 10^{-4}$$

The second stage of the recovery develops only above 350°. The crystalline parameter returns to its initial value to better than 0.5×10^{-4} while the color disappears (see below).

Interpretations

For doses smaller than 2 or 3×10^{17} the main mechanism of recovery seems to be the mutual cancelling out of the voids and interstitials.

At the higher doses, the phenomena appear to be more complex. Contraction or shrinkage of the lattice may be ascribed to a coalescence of interstitials, in which the degree of distortion is related to the concentration gradient of the latter about the centers of coalescence. Recovery below 350° corresponds to total coalescence of this type of point defect and subsequent disappearance of any and all gradients. The contraction of the lattice at this point is attributed to the voids which remain dispersed through the crystals. A certain number of those may already have disappeared due to mutual annihilation with the interstitials during assembly. The last stage of recovery characterized by the return to the initial parameter probably entails more complicated mechanisms which cause certain aggregates and voids to disappear together, and might offer analogies with a regression phenomenon in the alloys which undergo structural hardening.

This interpretation can be reconciled with the results of the study of the central diffusion of RX carried out on our sample by Guinier and Lambert.[10]

‡ In cooperation with Miss M. Gance, Department of Radiation Protection, Commissariat à l'Energie Atomique.

§ Comparison of our results with those of Binder and Sturm, and of Keating, appears to show that our flux estimates are two to three times greater than these authors'. This difference is being studied.

Miscellaneous Effects

Irradiation causes lithium fluoride to become colored. The colors obtained appear to have a relationship with the dimensions of the crystals, particles of over 50μ behave like large single crystals which become increasingly red in color. Above 2×10^{17} n/cm^2, the optical density of single crystals 0.3 mm thick reaches 5 throughout the wavelength range from 0.2 to 30μ, which makes any and all measurements impossible.

For doses equal or greater than 10^{18}, thermal treatment below 350°C no longer has any detectable effect on the color. At higher temperatures, the samples go through a range of hues from violet to greenish yellow, not found during irradiation. Each color appears to belong to a certain temperature range, and total recovery is obtained only above 470° or 480°C.

It should also be noted that the irradiated samples which are not annealed have oxidizing powers as observed by the release of iodine when crystals are mixed in solution with aluminum nitrate. This oxidizing power appears to disappear in the first stage of recovery.

Paramagnetic resonance did not enable us to observe any paramagnetism of $g = 2$, which might have been related to F centers. This is surprising, since the irradiation takes place without cooling off, while the power released under a flux of 10^{12} n/cm^2 is of the order of 2 watts/cm^3.

REFERENCES

1. Mayer, G. and Gigon, J., *J. de Physique et la Radium* (to be published).
2. Mayer, G. and Gueron, J., *J. Chim. Phys. 49*, 204 (1952).
3. Kinchin, G. H., *J. Nuclear Energy, 1*, 124 (1954).
4. Stripp, V. F. and Kirkwood, J. G., *J. Chem. Physics, 22*, 1579 (1954).
5. Johnston, D. F., *J. Nuclear Energy* (to be published).
6. Berman, *Proc. of the Roy. Soc.* London, Series A, vol. 208, p. 30 (1951).
7. Nelson, J. B. and Riley, D. P., *Proc. Phys. Soc.* London, *57*, 477 (1945).
8. Binder, D. and Sturm, W. J., *Phys. Rev. 96*, 1519 (1954).
9. Keating, D. T., *Phys. Rev. 97*, 832 (1955).
10. Guinier and Lambert, personal communication.

A Review of Investigations of Radiation Effects In Covalent and Ionic Crystals

By J. H. Crawford, Jr. and M. C. Wittels,* USA

Perhaps equally important as metals for future use as components in power producing nuclear reactors are the refractory non-metallic solids or ceramics. Consequently, it is important to accumulate a body of knowledge relative to their stability toward reactor radiations. Since this class of materials is generally characterized by varying degrees of ionic and covalent binding, fundamental studies should be directed toward determining the influence of bond type as well as crystal structure on the extent and nature of radiation sensitivity. Therefore, it is appropriate to choose for investigation representative simple materials which cover the complete range of binding type. In addition for interest with regard to future reactor utility, studies of this nature are valuable *per se* since they elucidate the influence of lattice imperfections on the physical properties of non-metallic solids.

Studies of non-metallic crystals exposed to high energy radiations constitute the earliest work in the field of radiation effects and, incidentally, were initiated by European investigatnrs. Although the origin of such effects was not understood until well after the discovery of natural radioactivity, as early as 1815 Wollaston and Berzelius[1] investigated the thermoluminescence of minerals containing radioactive elements. The so-called metamict minerals, i.e., minerals whose structures had been disordered by bombardment over geologic periods with alpha-particles from natural radioactive elements, have been studied for nearly a hundred years. As early as 1860 Des Cloizeaux and Damour[2] observed the optical annealing in such damaged crystals. It is also interesting that the first radiation damage experiment was performed in 1922 when Mügge[3] attempted to disorder minerals by exposure to the radiations of radium. Unfortunately, because of the small exposures, these experiments were unsuccessful. The origin of the lattice disorder, however, was firmly established as early as 1913 when Rutherford and Joly[4] correlated the Pleochroic halo rings in mica containing radioactive inclusions with the known alpha-particle ranges. Besides these early studies involving alpha-particles, studies of radiation effects owe much to the classical investigations initiated by Pohl and coworkers[5] on color centers in X-irradiated alkali halides.

In this paper we wish to survey studies of radiation effects in non-metallic crystals currently being carried out at the Oak Ridge National Laboratory. These investigations may be divided roughly into two categories: (1) the effect of fast neutron bombardment on crystal structure and (2) effects of both corpuscular and electromagnetic radiation on certain properties which are markedly dependent on lattice imperfections. The first category has the greatest practical interest since it is directly related to the dimensional stability and strength of irradiated nonmetals. Consequently, much study has been devoted to this group of effects. The second category includes studies of optical absorption, magnetic susceptibility, paramagnetic resonance and electrical conductivity on various ionic and covalent crystals after exposure to a variety of energetic radiations. Studies of these properties lead to a better understanding of the nature of bombardment induced defects.

Although investigations of the effects of fast neutron bombardment on the electrical properties of diamond-lattice semiconductors falls into the second classificatioa, such studies form a special field of research and, since extensive treatments have been published elsewhere,[6] this topic shall be omitted from this review.

STRUCTURAL EFFECTS

In this section we shall be concerned primarily with the effect of fast neutron bombardment on the structure of non-metallic materials. Structural changes resulting from bombardment were followed by X-ray diffraction studies and density measurements. In addition, the annealing behavior of irradiated specimens was also investigated. In nearly every case, the crystals were exposed to fission-spectrum neutrons at an approximate temperature of 100°C. The integrated fluxes (nvt_f) described here are estimated for neutrons having energies in excess of 50 kev, i.e., neutrons with energies sufficient to displace atoms from their normal lattice sites. In the following discussion we shall consider in turn a number of the materials studied.

* Oak Ridge National Laboratory. Including work by D. Binder, J. H. Crawford, Jr., C. M. Nelson, H. C. Schweinler, F. A. Sherrill, D. K. Stevens, W. J. Sturm, R. A. Weeks, and M. C. Wittels.

Natural Crystals

The natural crystals selected for the investigations described here are in the class of low-density insulators with oxygen atoms forming the structurally dominant component of the lattice. Furthermore, they have relatively high melting temperatures and a considerable percentage of covalent binding. In this regard it is noted that Goldschmidt[7] had observed that little or no ionic binding was found in minerals disordered by natural radioactivity, i.e. metamict minerals. Quartz (SiO_2) and other polymorphs of silica, zircon ($ZrSiO_4$), beryl ($Be_3Al_2Si_6O_{18}$), phenacite (Be_2SiO_4), chrysoberyl ($BeAl_2O_4$), topaz ($Al_2SiO_4(OH)_2$), and garnet ($Ca_3Al_2(SiO_4)_3$) were among the natural crystals selected for this study.

Studies were performed initially on the silica structures[8–11] since it was apparent from early investigations that the silicon-oxygen bond could be readily ruptured upon fast neutron bombardment. Moreover, the lattice disorder is retained at room temperature. Most striking was the effect on their density. Single-crystal quartz specimens suffered a density decrease of 14.7% without the appearance of any macroscopic defects such as cracks or bubbles. Figure 1 shows the change in c/a ratio of a quartz single crystal as a function of exposure, clearly revealing the anisotropic nature of the density change.

Structural effects in these materials are presumably produced by lattice strains associated with displaced atoms. In every material of this group, a decrease in density was observed. However, as will be shown below, the extent and nature of the change is markedly dependent on the structure of and nature of binding in the crystal in question. X-ray diffraction studies indicate that this structure dependence is closely associated with the nature and distribution of interstitial volume or voids in which the displaced atoms, most probably oxygen atoms, may be trapped and hence prevented from returning to their normal lattice sites. In the silica structures the lattice is composed of linked tetrahedra of SiO_4 groups in which each silicon atom is surrounded by four oxygen atoms, and each oxygen, in turn, is shared by adjoining tetrahedra, thereby forming a complete network array. Hence, only two bonds need to be broken to displace an oxygen atom while four bond ruptures would be needed to displace a silicon atom. In addition, many oxygens need be displaced only short distances ($\sim$ 1 Å) to find a relatively large interstitial void. A similar structural condition exists in zircon where the zirconium atom is in tetrahedral coordination with oxygen.

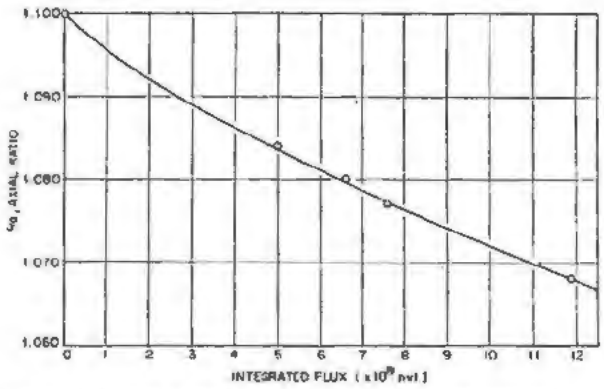

Figure 1. Change in axial ratio of quartz with fast neutron bombardment

In those crystals containing beryllium and aluminum, additional cation-oxygen bonds must be broken in order that oxygen atoms be displaced. As it will be seen, these crystals tend to have a higher radiation stability than the polymorphs of quartz. In addition, it was observed that many irradiation induced defects had a high thermal stability. Temperatures required to anneal the lattice damage appreciably in single crystal specimens were usually in excess of 1500°C. Other noteworthy effects include varying degrees of disorder, mosaic block formation, and large lattice expansion with or without large distortions.

Since Des Cloizeaux and Damour[2] had observed the optical and density annealing of alpha-disordered crystals of zircon, nearly 100 years ago, the effect of fast neutrons on single crystals of this material is of considerable academic interest. In this connection, Vegard[12] in 1916 noted the absence of coherent X-ray reflections in thorite ($ThSiO_4$) a mineral structurally similar to zircon, which had become disordered by natural alpha-emission. In the naturally disordered zircon crystals, impurity atoms from the uranium-actino or thorium series occupy zirconium sites in the crystal lattice and it is these atoms which furnish the high energy alphas that produce the disordering displacements. Some natural crystals have been apparently reduced to the amorphous state following a bombardment with 10^{17} alpha-particles per milligram,[13] these particles having energies close to 6 Mev.

Zircon crystals free of these alpha-emitting impurities were selected for fast neutron irradiation studies. Progressive bombardment with exposures up to 3.6×10^{20} neutrons/cm² produces a highly disordered lattice. Nevertheless, considerable long range order is preserved, as seen in single crystal X-ray studies (Fig. 2). The trapping of displacements in the open portions of the lattice expands the structure anisotropically as shown in Fig. 3 and reduces the crystal density by more than 4%. Mosaic blocks are created, presumably as a result of lattice strain, which may be disoriented by more than 3°, and a large amount of lattice distortion is induced. X-ray transmission photographs of these heavily bombarded crystals show the formation of "extra" reflections at small angles in the forward region visible in Fig. 2. Since these are still visible at liquid nitrogen temperatures, they are not of thermal origin. It is probable that these "extra" reflections (Fig. 2) result from the scattering contributions from interstitials and vacancies residing at preferred positions and which

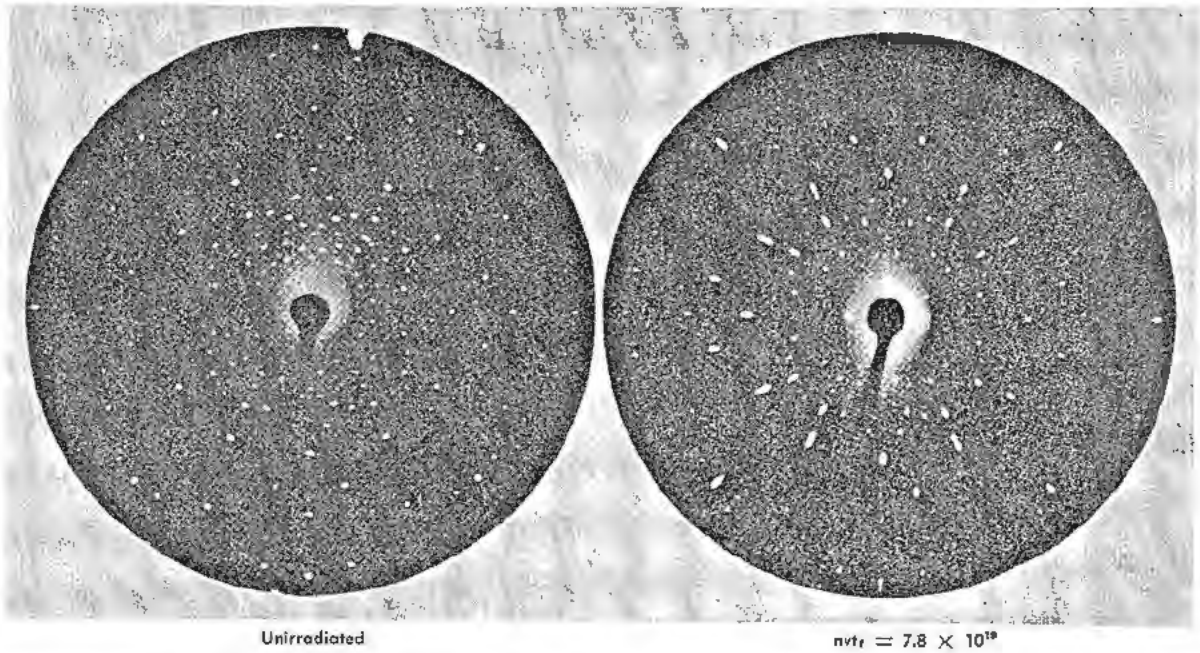

Unirradiated $nvt_f = 7.8 \times 10^{19}$

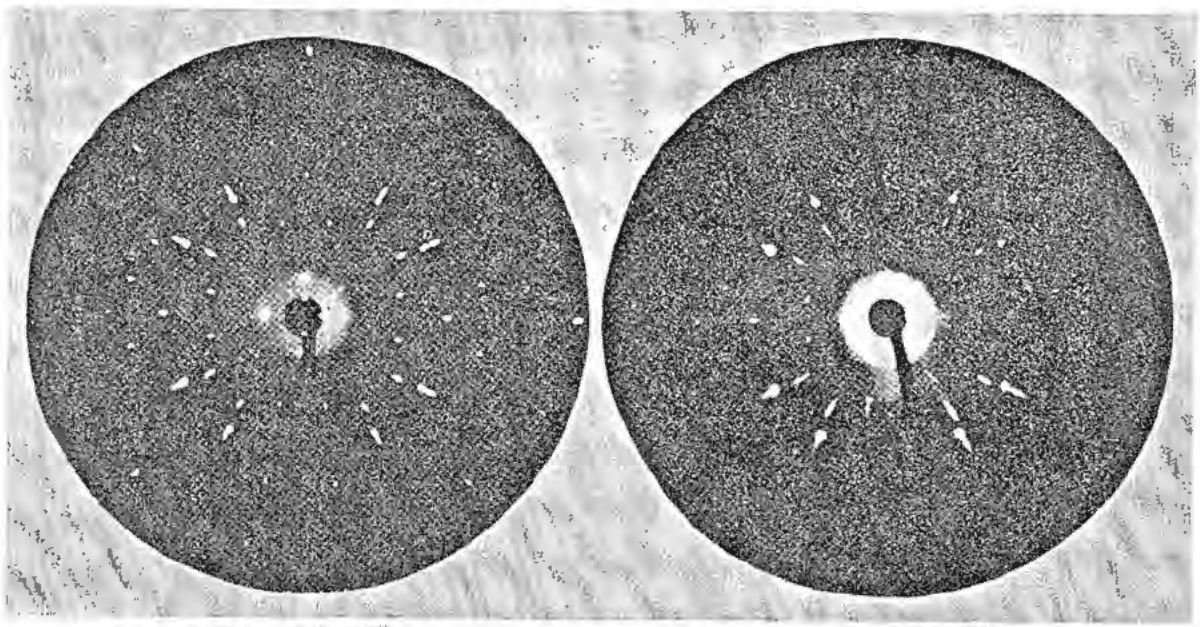

$nvt_f = 1.72 \times 10^{20}$ $nvt_f = 2.8 \times 10^{20}$

Figure 2. Laue transmission patterns of fast neutron bombarded zircon single crystals

give rise to a warped lattice. Another striking feature in these neutron irradiated zircons is their remarkable annealing behavior. Very small amounts of damage are annealed below 1000°C and the annealing is incomplete even up to 1600°C. At these high temperatures, however, the single crystal lattice becomes more perfect as defects tend to diffuse to normal positions. Moreover, the mosaic blocks tend to resume their proper orientation and distortion is considerably reduced.

"Extra" X-ray reflections (Fig. 4) are also observed in single crystals of quartz bombarded in the range of exposures 6 to 9×10^{19} n/cm². Unlike the annealing effects in neutron irradiated zircon, however, quartz single crystals bombarded in this region do not tend to revert to their original condition on annealing. This behavior is not unreasonable since silica has a very complex thermodynamic behavior in the unirradiated state. Attempts to produce single crystal quartz from any of the irradiated phases

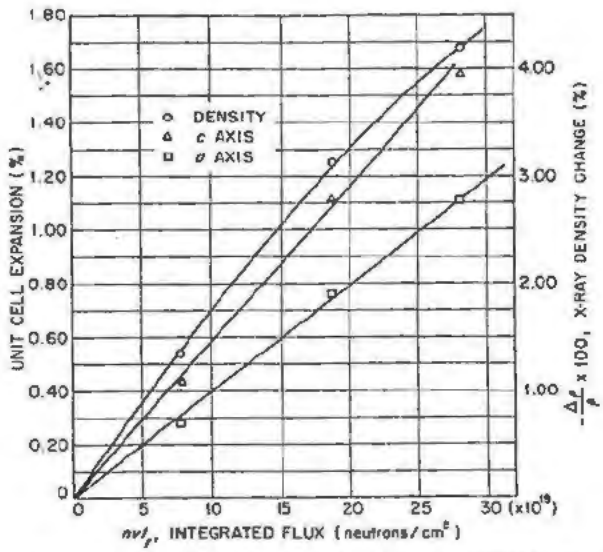

Figure 3. Effect of radiation on density and unit cell expansion for a zircon single crystal

of silica by annealing have proved unsuccessful to date, but the formation of polycrystalline material is readily accomplished.[11] With regard to the annealing behavior of irradiated quartz single crystals, one extremely interesting effect was observed. A Z-cut plate was exposed to 7.6×10^{19} n/cm² and subsequently annealed at 950°C for 30 minutes. Parallel to the c-axis, two rows of macroscopic holes were formed. These were nearly regularly spaced about 0.3 mm apart and were about 0.05 mm in diameter extending entirely through a crystal 5 mm thick. The formation of these holes is expected to bear some kind of relation to the c-axis interstitial channels and the anisotropic expansion of quartz upon neutron bombardment. One possible interpretation of this hole formation is that an a-axis strain is set up in the crystal due to the crowding of oxygen atoms into the interstitial channels, and that the subsequent thermal diffusion of these trapped atoms out of the channels results in a strain release over some small, finite distance perpendicular to the c-axis. This strain relaxation may result in the generation of macroscopic holes parallel to the c-axis.

Beryl, which is structurally and chemically similar to quartz is affected by fast neutron bombardment in much the same manner. Both materials have an open structure with irregular c-axis channels. By analogy from observations on quartz, the effects on beryl are very nearly predictable. With a bombardment of 2.8×10^{20} n/cm² beryl undergoes an anisotropic lattice expansion that exhibits a structure dependence similar to quartz. In addition, at this stage of irradiation, "extra" reflections are again observed in the forward region at small angles (Fig. 5). Bombardment with 3.6×10^{20} n/cm² results in the destruction of all coherent X-ray reflections and the crystal is rendered essentially amorphous. However, as in the case of quartz, large single crystals remain free of macroscopic defects.

Chrysoberyl was selected for irradiation studies of a close-packed system since its oxygen atoms are hexagonally close packed. Bombardment of single crystals with 3.6×10^{20} n/cm² expands the lattice by more than 1% in the c-direction but little or no distortion is observed in single crystal diffraction patterns. A similar lack of distortion is observed in phenacite bombarded with 3.6×10^{20} n/cm². Since phenacite has an open hexagonal structure like quartz, one might expect that it would be affected similarly under neutron bombardment. Indeed, dis-

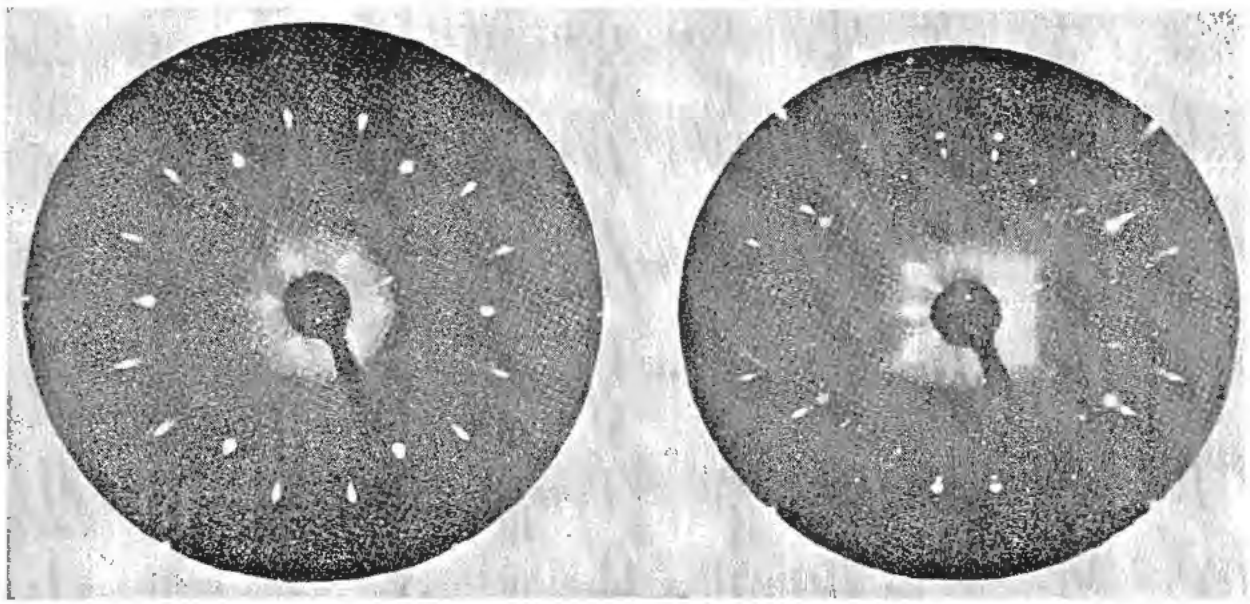

c-axis $nvt_f = 7.8 \times 10^{19}$ a-axis

Figure 4. Irradiated quartz Laue transmission photographs

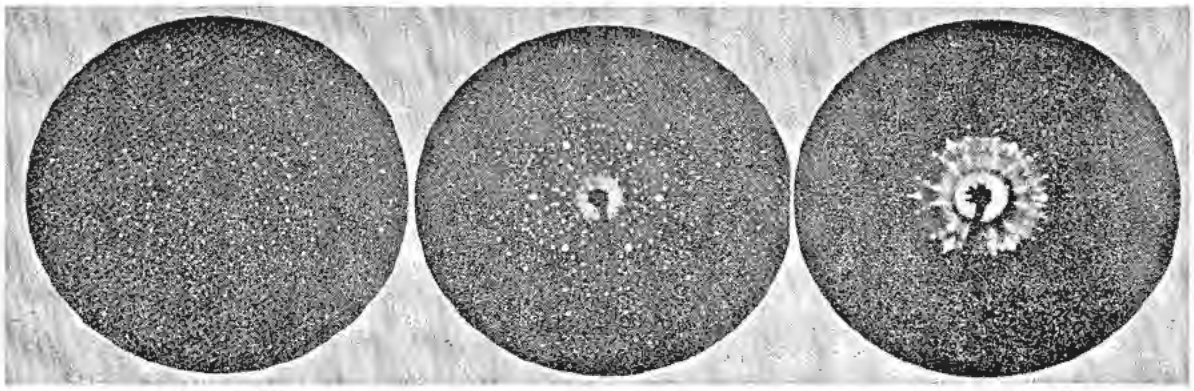

Beryl, c-axis Laue transmission photographs

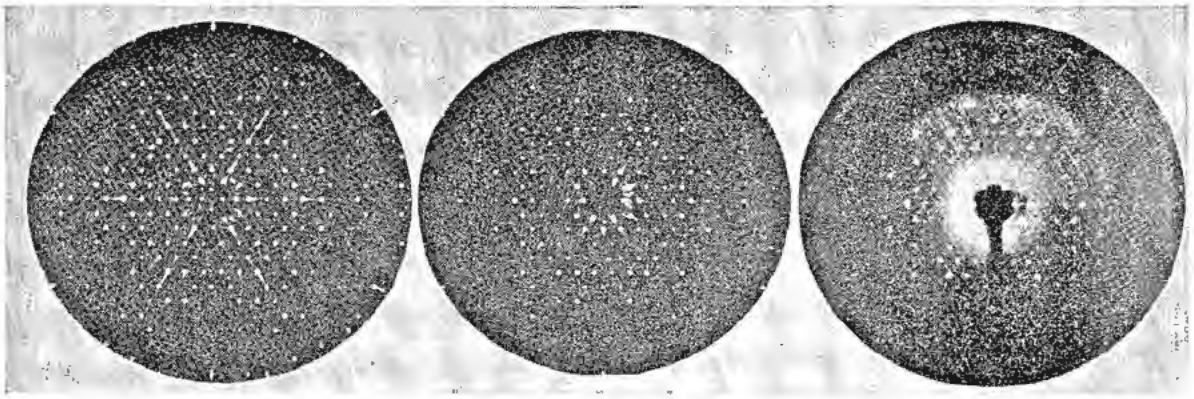

Beryl, (HKD) precession photographs

Figure 5. Transmission patterns of fast neutron bombarded beryl

placed atoms appear to be trapped along the c-axis in phenacite causing an a-axis expansion of about 0.7%.

The effects of fast neutron bombardment on quartz, beryl, phenacite and chrysoberyl, are apparently primarily dependent on crystal structure. In addition, there are indications that wide differences exist in stability of the different cation-oxygen bonds under fast neutron bombardment, or at least that some types which are ruptured by irradiation may be readily reformed at low temperatures. In the order of decreasing stability under irradiation one would place (1) beryllium-oxygen, (2) aluminum-oxygen, (3) zirconium-oxygen, and (4) silicon-oxygen. It is interesting to note that this is also the order of decreasing of ionicity of binding.[7]

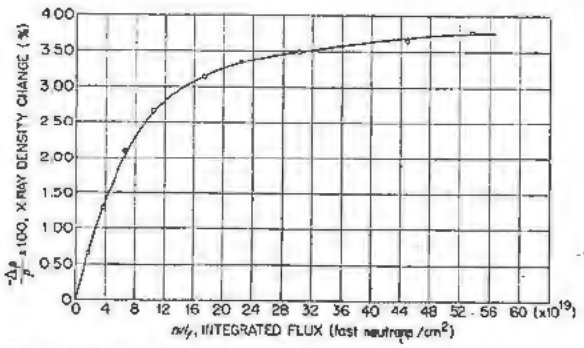

Figure 6. Effect of neutron irradiation on the density of diamond

Knock-on displacements are readily produced in garnet and topaz, and these materials show effects similar to those in zircon. Lattice expansion and distortion of the same order of magnitude is produced, but in topaz the trapping of displacements apparently occurs in layers, thereby producing random stacking along certain lattice planes which is manifested as streaks in Weissenberg patterns.

Diamond and Diamond-Lattice Semiconductors

Lattice expansion of diamond induced by fast neutron bombardment was first observed by Primak and co-workers.[11] Extensive bombardment data have been collected at this laboratory and the following is an account of these studies, as well as some observations on the diamond-lattice semiconductors.

Figure 6 shows the density decrease in diamond as a function of irradiation and indicates this change is approaching saturation near 4%. It is evident that

a large number of atomic displacements are produced in diamond and examination of the diamond lattice reveals the (½ ½ ½) and (¾ ¾ ¾) positions in the unit cell (cubic indexing) to be the most probable trapping sites for interstitial atoms. Random checks on the X-ray density measurements made with conventional density methods were found to agree within experimental error (±0.05%). This is the result to be expected for uniformly distributed Frenkel defects.[15–17]

A high degree of long range order is maintained in heavily irradiated diamonds. This does not lend support to the proposal of unsaturated covalent bonds and weak disordered regions.[18] Single crystal X-ray studies of irradiated crystals reveal no appreciable line broadening and preliminary measurements indicate there is an increase in the integrated intensity of some of the coherent reflections which would follow if Frenkel defects were produced.

Preliminary theoretical calculations by Schweinler have led to the search for the so-called "forbidden" reflections in irradiated diamond and it can be reported that the (200) reflection is observed in neutron irradiated diamond following bombardments as small as 5.0×10^{19} n/cm². At the same time an increase in integrated intensity is observed for the anomalous (222) reflection. In addition to these observations of coherent X-ray scattering in neutron irradiated diamond, the bombardment induced diffuse scattering, which is seen at small angles in the forward region (Fig. 7), is currently being investigated. It is hoped that theoretical and experimental evaluation of these effects will shed light upon the exact atomic configuration of lattice defects induced by fast neutron bombardment.

Annealing phenomena in the damaged diamond structure are indeed complex.[14] It should be mentioned that clear crystals become an opaque black color after an approximate bombardment of 10^{17} n/cm², and remain so upon continued irradiation. One crystal bombarded by 2×10^{20} n/cm² failed to lose this opacity after annealing at 1600°C for two hours. The same crystal recovered approximately 70% of its density change during this anneal. Figure 8 shows the effect of 30-minute isothermal anneals at successively higher temperatures on irradiated diamond powder. The results indicate that approximately 70% of the lattice parameter change is annealed during this process. From Krishnan's work[19] on the thermal expansion of the diamond lattice, the expansion at 2000°C would not even remotely approach the expansion resulting from neutron bombardment. These results indicate that some of the defects in irradiated diamonds have an extremely high thermal stability.

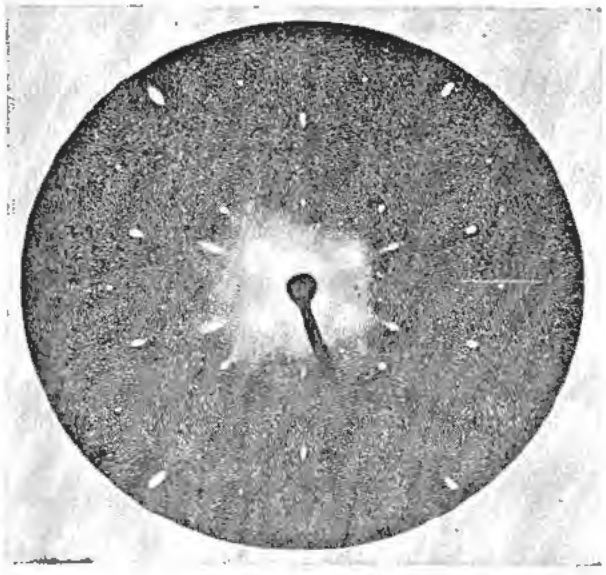

$nvt_f = 4.2 \times 10^{20}$

Figure 7. Diamond (110) Laue transmission photograph

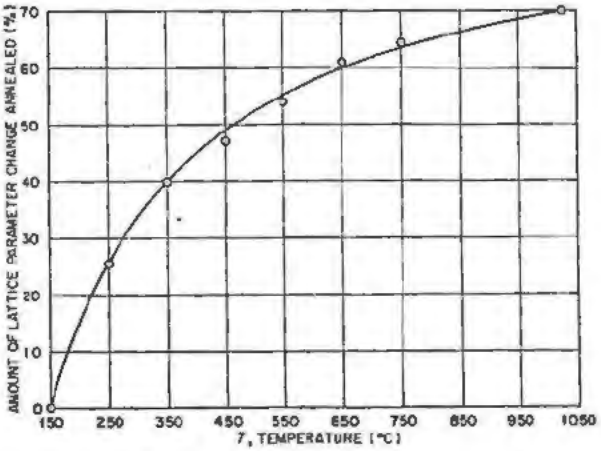

Figure 8. Lattice expansion annealing in diamond

Similar irradiation studies are being carried out on germanium, silicon, indium antimonide, and gallium antimonide. Interesting results have been obtained on single crystals of germanium with X-rays using sensitive Geiger-counter techniques prior to fast neutron bombardment. The following "forbidden" reflections were observed in Sb-doped germanium: (200), (222) and (420). In addition, the (200) reflection was observed in germanium of 99.999999% purity. The existence of these "forbidden" reflections in unirradiated germanium results from the fact that the atoms are not spherical, as is usually assumed, but rather possess a charge density with a lower symmetry. It should be pointed out that these extra reflections are exceedingly weak, being one thousandth as intense as normal reflections.

The fast neutron bombardment of InSb single crystals produces a highly distorted lattice (Fig. 9) but the structural effects of the irradiation are complicated by the very high thermal neutron absorption cross-section of indium. Following bombardment with 1.09×10^{20} n/cm² it is estimated that 1.8% of the indium atoms are transmuted to tin. In addition to the mosaic structure which is induced by bombard-

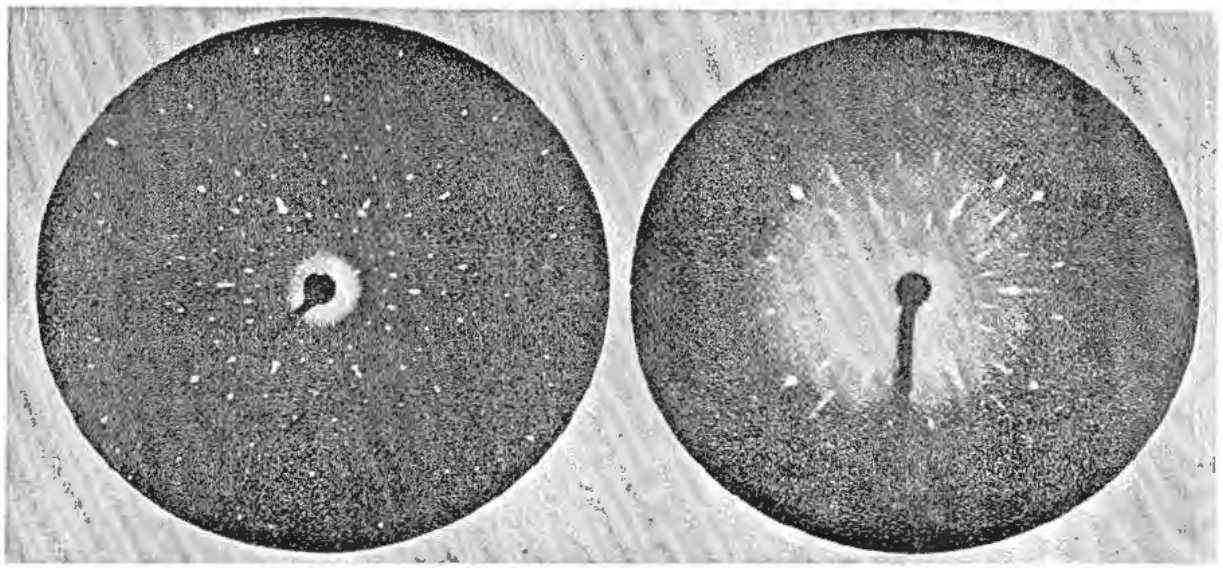

Unirradiated $nvt_f = 1.09 \times 10^{20}$

Figure 9. Indium antimonide (110) Laue transmission photographs

ment, we also observe the irradiation-induced diffuse scattering which is characteristic of the damaged diamond structure previously discussed.

Lithium Fluoride

Structural effects in one ionic crystal, namely lithium fluoride, have been extensively investigated by Binder and Sturm.[20] In this material, by taking advantage of the large cross section for the (n, α) reaction on Li^6, it is possible to introduce throughout the lattice, energetic charged particles, an alpha-particle and a triton, with a total energy of 4.5 Mev. In many respects this process stimulates the fission reaction. Measurements of the density change resulting from reactor exposure were made using both gravimetric and X-ray techniques and both methods gave the same values within experimental error. These results have been interpreted as indicating that the high energy charged particles introduce predominantly Frenkel defects.[15–17] Recent studies of the annealing kinetics indicate that the annealing process is most probably second order and its activation energy is ~1.5 ev. These results are consistent with the assumption that radiation induced lattice damage in this material can be described in terms of Frenkel defects.

OTHER INVESTIGATIONS

Optical and Magnetic Studies of Irradiated Silica

Optical absorption bands introduced into both crystalline quartz and silica glass by energetic radiations have been the subject of numerous investigations. Besides coloration with ionizing radiation,[21–23] recent studies of effects produced[24–27] by reactor exposure have been performed in both France, England and the United States. On irradiation both quartz and glass develop a number of absorption bands in the visible and near ultraviolet. Regardless of the source of material, both forms of silica develop a band in the region of 2100 to 2200 Å, whereas the visible coloration is apparently markedly sensitive to either impurities or lack of stoichiometry. In both materials prolonged exposure to fast neutrons tends to bleach the visible bands while further enhancing the near ultraviolet band.[25]

Work at this laboratory by C. M. Nelson has been confined primarily to silica from three sources: (1) natural quartz crystals, (2) impure fused silica (Vitrosil), and (3) "purified" Corning silica glass. Spectra for quartz and Vitrosil are in agreement with those previously reported. The Corning glass, however, possesses almost no visible absorption, but rather shows a narrow absorption band centered at 2150 Å.[27] In the following we shall consider each of these materials in turn.

For fast neutron exposures up to 10^{18} n/cm^2, studies of optical absorption in natural quartz crystals are in essential agreement with the results reported by Mitchell and Paige.[25] For greater exposures, the visible coloration is rapidly bleached and, after $\sim 2 \times 10^{18}$ *nvt*, the crystals were nearly colorless in the visible, possessing only pink to magenta coloration. Absorption measurements indicate that this is caused predominantly by the long wavelength tail of the intense ultraviolet band at — 2200 Å.

It has been observed that irradiated quartz has a paramagnetic component.[28] If it is assumed that the paramagnetism is associated entirely with unpaired electrons which, in turn, are responsible for the ultraviolet absorption band, the concentration of absorbing centers can be obtained directly from magnetic susceptibility measurements. Stevens has measured the susceptibility of a series of irradiated quartz specimens. The diamagnetic susceptibility vs temperature curves for these specimens are shown

in Fig. 10. The curve for the unirradiated specimen is temperature independent, possessing no paramagnetic component, whereas all irradiated specimens show a decreasing diamagnetism toward low temperature. The paramagnetic component, obtained by subtracting the curves from that of the unirradiated specimen, is plotted against reciprocal temperature in Fig. 11. These curves obey the Curie law and their slope is proportional to the concentration of centers. The dependence of unpaired electron concentration on fast neutron exposure is shown in Fig. 12. It is noted that the concentration is not a monotonic function of exposure but rather reaches a maximum at $\sim 6 \times 10^{19}$ *nvt*. It is interesting that this is the exposure at which the rate of density change of quartz becomes large.[11] The saturation paramagnetic center concentration is estimated from Fig. 12 to be $\sim 2 \times 10^{19}$ for an exposure temperature of 100°C. If these are associated only with the 2200 Å absorption band, it is possible to obtain the oscillator strength of the absorbers directly. Such a determination for Corning fused silica will be discussed below.

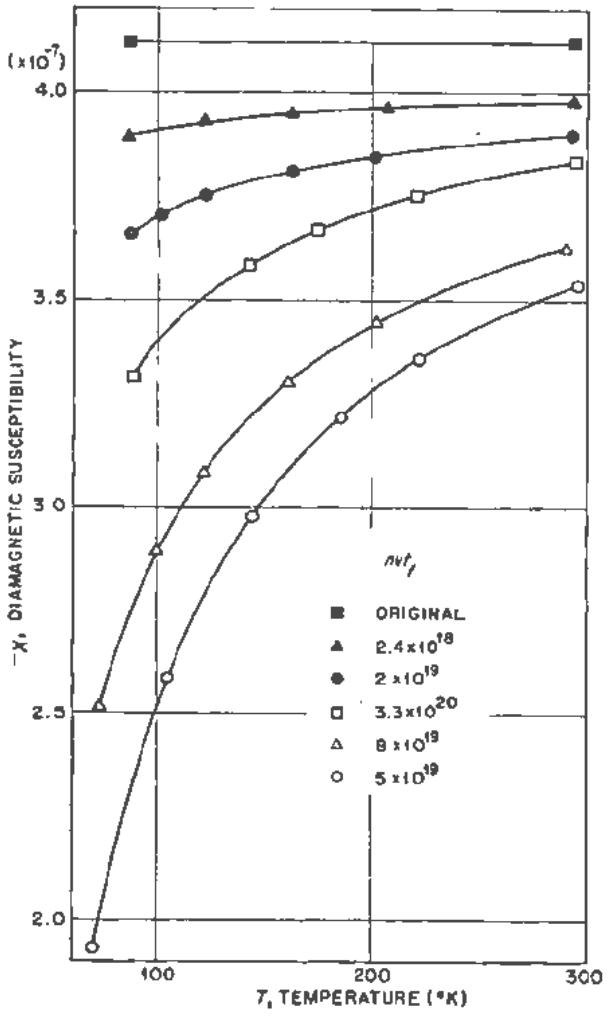

Figure 10. Diamagnetic susceptibility of irradiated quartz

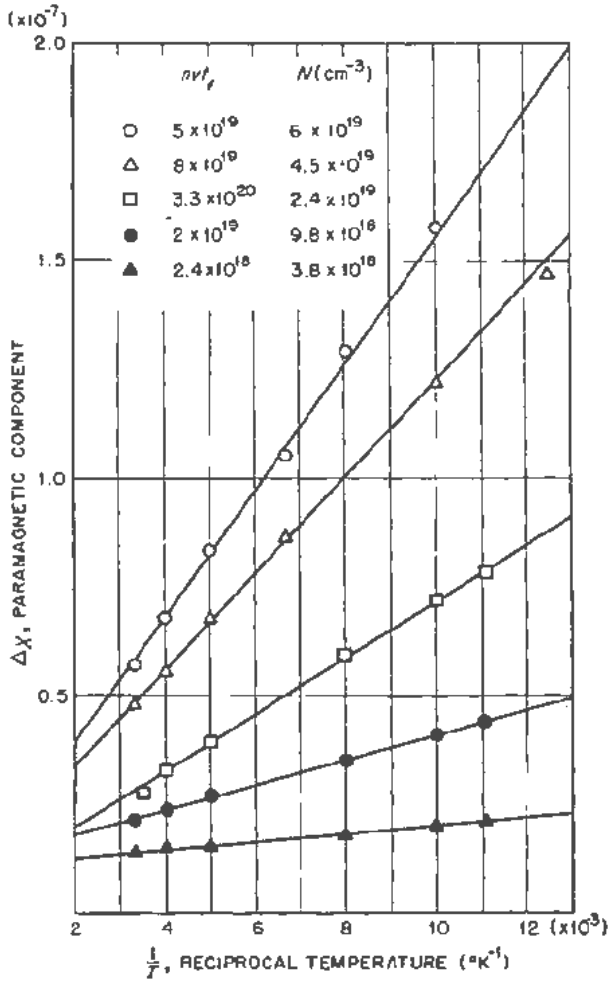

Figure 11. Bombardment-introduced paramagnetic component in quartz

Besides magnetic susceptibility measurements, paramagnetic resonance in neutron irradiated quartz is currently being investigated by Weeks. Preliminary results indicate that for exposures $< 5 \times 10^{19}$ the resonance spectrum is exceedingly complex. A number of lines with spectroscopic splitting factors or g-factors in the vicinity of 2 are observed whose amplitudes and g-factors are orientation dependent. These observations confirm previous results reported by Griffiths *et al.*[10] For exposures of 5×10^{18} n/cm² and greater, the orientation dependence is considerably diminished and, at 3.3×10^{20} n/cm², the resonance lines are isotropic. This behavior is expected from structure studies[11] since, at these high exposures, quartz is converted to an isotropic glass. In addition to becoming isotropic, the spectrum is much simplified. The integrated microwave absorption is plotted against g-factor in Fig. 13 for exposures of 5×10^{19} and 3.3×10^{20} n/cm². After 5×10^{19} n/cm², two overlapping resonance lines are visible, but after the higher exposure, only one line is apparent. However, its asymmetry indicates the presence of a weak unresolved line. These results

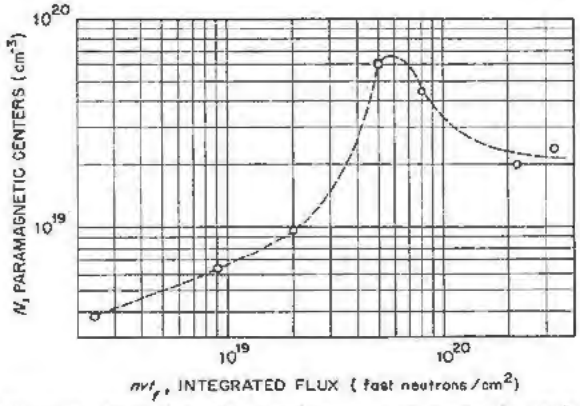

Figure 12. Bombardment introduced paramagnetic centers in quartz vs irradiation

suggest that two fundamental resonance lines are produced by prolonged fast neutron bombardment and that one of these grows more rapidly than the other with exposure. Perhaps the most interesting property of these lines is their narrowness. Even after 3.3×10^{20} n/cm², the half-width is only 3.9 gauss with an exciting frequency of 9121 kilomegacycles.

A number of specimens of Vitrosil glass have been exposed to fast neutrons, high energy electrons (0.2 to 2 Mev), 250 kv X-rays, and gamma-rays from a Co^{60} source. The variety of radiations was used in an attempt to detect possible differences in effects arising from the nature of the radiation. The optical absorption spectra obtained for each type of source were essentially the same. Although not nearly so pronounced as with fast neutrons, prolonged X-ray exposure was also observed to bleach the visible absorption band while further enhancing the ultraviolet band. In agreement with the results of Levy and Varley[26] it was found that the visible bands could be optically bleached to some extent by exposure to light with a range of wave lengths corresponding to that of the band in question. Much more effective bleaching of the entire spectrum could be accomplished by exposing to wave lengths in the ultraviolet band. Studies of magnetic resonance indicate the presence of the same type of resonance lines shown by quartz after prolonged exposure and by Corning silica glass (see below).

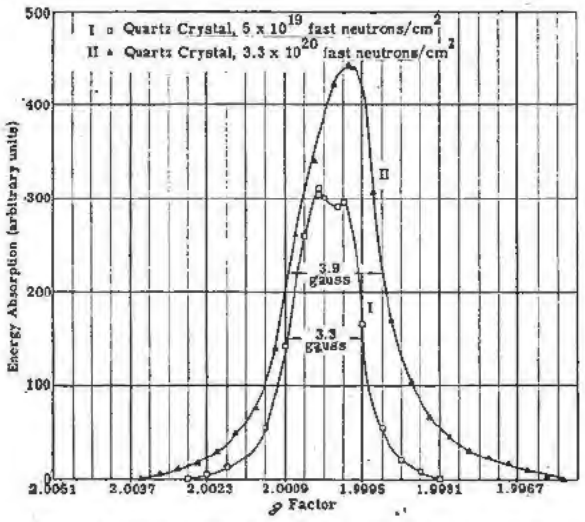

Figure 13. Paramagnetic resonance in irradiated piezo quartz

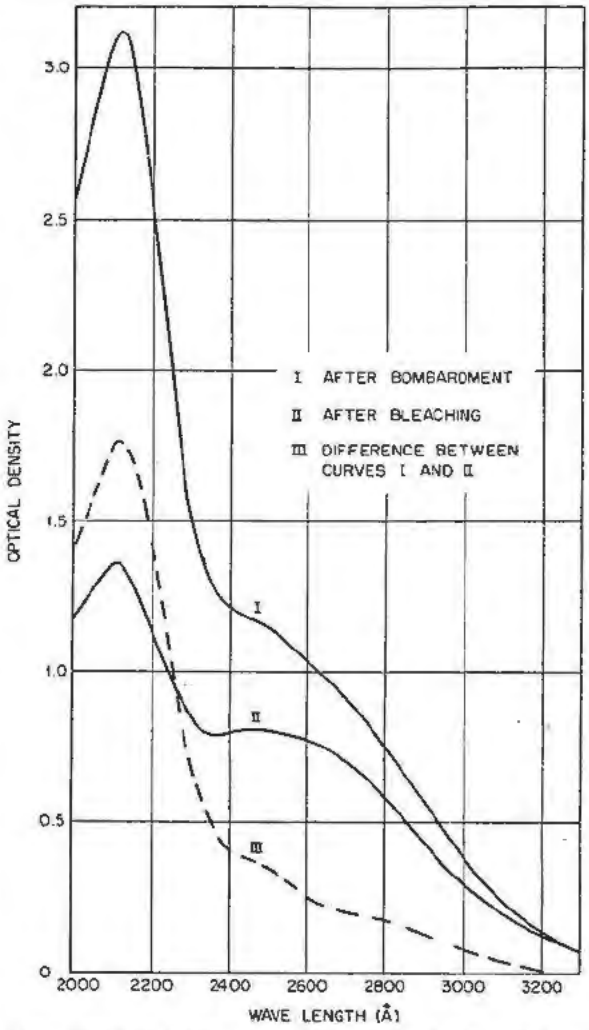

Figure 14. Optical density vs wave length for fast neutron bombarded Corning silica glass

Corning fused silica is extremely resistant to coloration by ionizing radiation.[23,27] Consequently, the material is a valuable one, aside from its practical importance, in which to study the ultraviolet absorption bands without the complication of the visible, impurity-sensitive coloration. Optical studies have been carried out on this material with the same variety of high energy radiations used in studies of Vitrosil. The absorption spectrum was qualitatively the same for each type of radiation, but the efficiency in producing the ultraviolet band differed widely from one type to another. The form of the absorption

band obtained after a fast neutron exposure of 5×10^{17} n/cm² is shown in Curve I of Fig. 14, from which it is evident that the band is a composite of at least two overlapping bands. It was found that the shorter wavelength band, which is apparently the most intense of the two, was bleached much more rapidly with ultraviolet light. Curve II was obtained after prolonged exposure to a mercury-vapor lamp in which most of the emission was concentrated in the 2537 Å line. The difference between Curves I and II, indicated by the dashed line, may be used as a basis for resolving the composite band into two approximately symmetrical bands, one centered at 2120 Å and the other at 2570 Å. The origin of these two absorption bands is not yet understood.

The efficiency of the various radiations in producing the composite ultraviolet band varies widely. Curves of the absorption coefficient at 2150 Å are plotted as a function of exposure in Fig. 15 for both X-rays (Curve I) and gamma-rays (Curve II). It is interesting that the 250 kv X-radiation is four times as effective as the Co^{60} gamma-rays and, in addition, produces a greater saturation absorption. At saturation the absorption coefficient of Curve I is 11.5 cm^{-1} as compared to 8.7 cm^{-1} (not shown in Fig. 15) for gamma-rays. High energy electrons are also effective in producing the ultraviolet bands with both the rate of growth and saturation absorption depending on electron energy. The saturation absorption coefficient for 2 Mev electrons is ~ 20 cm^{-1}.

Of all types of radiation investigated, fast neutrons are the most efficient in developing the ultraviolet band. This presumably results from the fact that fast neutron bombardment introduces additional lattice defects. The growth of the composite band is shown in Fig. 16. Although the absorption at 2150 Å apparently reaches a maximum of 270 cm^{-1} at $\sim 1.5 \times 10^{19}$ n/cm², the point at 2.7×10^{19} n/cm² is somewhat in doubt as indicated by the dashed line. The longest exposure was obtained in a position where the temperature was not controlled and, hence, it is possible that appreciable thermal bleaching could have taken place. Also shown in Fig. 16 is the concentration of paramagnetic centers as determined by magnetic susceptibility measurement. It is interesting to note that the concentration of paramagnetic centers, presumably unpaired electrons, is approximately proportional to the absorption coefficient at the maximum of the composite absorption band.

Using the concentration of unpaired electrons determined magnetically it should be possible to calculate the oscillator strength of the absorbers in Corning silica. Unfortunately, the situation is complicated by the presence of two absorption bands. However, for all exposures used the absorption in the 2570 Å band was less than 20% of that in the 2120 Å band. Hence, if it is assumed that the oscillator strengths are comparable for the two bands, and that there are no absorption bands at shorter wavelengths, it should be possible to obtain an approximate value by means of Smakula's formula. Calculations for three specimens give oscillator strengths of 0.14, 0.18 and 0.22 for exposures of 4×10^{18}, 1×10^{19} and 2.7×10^{19} n/cm². If the assumptions indicated above are valid, it appears that the oscillator strength for the 2120 Å line is ~ 0.2.

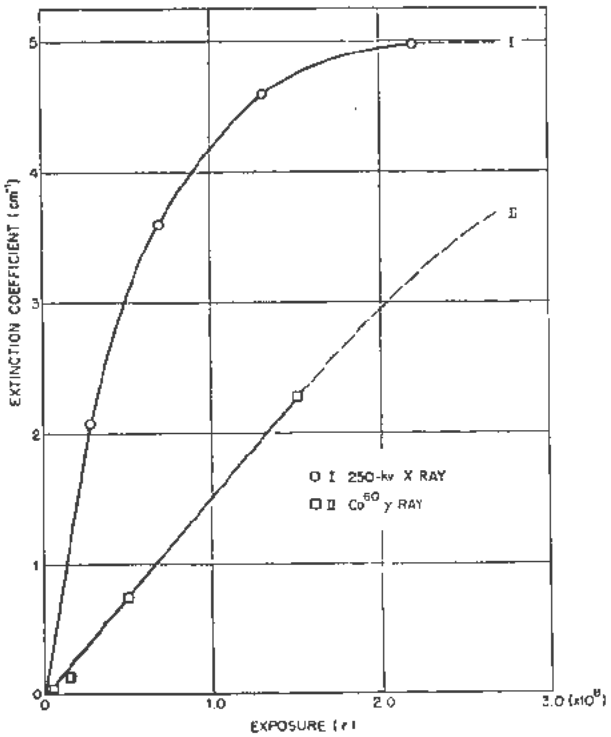

Figure 15. Absorption at 2150 Å in irradiated Corning silica glass

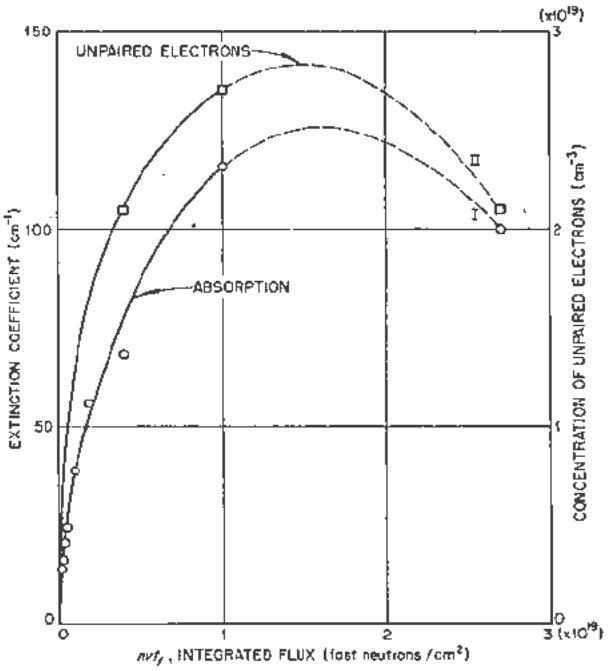

Figure 16. Absorption and unpaired electron concentration in irradiated Corning silica glass

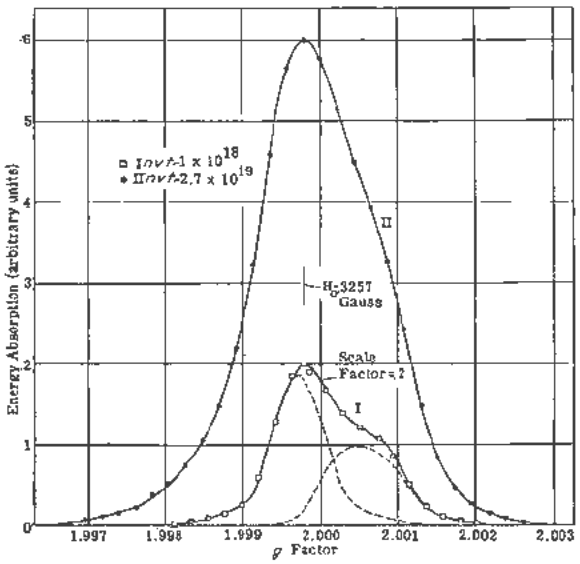

Figure 17. Paramagnetic resonance at 9121 megacycles in Corning silica glass

Paramagnetic resonance absorption was investigated in fast neutron irradiated Corning silica. The results for two exposures, 1×10^{18} and 2.7×10^{19} n/cm², are shown in Fig. 17 where the integrated power absorbed is plotted against g-factor. As in the case of quartz (Fig. 13) two overlapping peaks are observed and again one of these appears to grow more rapidly with exposure than the other. The two resonance lines have been resolved approximately for the short exposure curve.

Preliminary thermal bleaching experiments have been performed for all three forms of silica. The results seem to indicate that the fast neutron induced optical absorption is removed long before any appreciable annealing of structural changes has occurred. It therefore seems reasonable to conclude that the color centers may be identified with trapped electrons.

Radiation Effects in Ionic Crystals

Ionic conductivity and optical absorption are two properties of ionic crystals which are convenient indices of lattice imperfections resulting from high energy irradiation. Ionic conduction is dependent on diffusion rate and hence on the concentration of mobile, charged defects. Optical absorption, on the other hand, is electronic in origin and depends on the concentration of electrons and holes trapped in the vicinity of lattice defects. A number of experiments are currently being performed which are designed to detect any differences which may exist between gamma-ray and fast neutron exposure on these properties in potassium chloride. Potassium chloride was chosen for investigation because it is quite representative of the ionic type crystal and has been extensively studied. Furthermore, it is not rendered excessively radioactive by exposure to neutrons.

The ionic conductivity of a number of specimens were measured as a function of temperature both before and after exposure. A direct current method was used employing a vibrating-reed electrometer for current measurements. Early experiments[30] revealed that exposure to Co^{60} gamma-radiation and short reactor irradiations decreased the ionic conductivity by as much as an order of magnitude, whereas prolonged reactor exposure to both gamma-rays and fast neutrons increased the conductivity by about the same factor. This behavior has been interpreted as follows: the ionizing radiation is expected to produce hole-electron pairs which are trapped at lattice vacancies, thus rendering them electrically neutral. This effect would tend to decrease the concentration of charged positive-ion vacancies (the mobile defect), hence decreasing the conductivity. Fast neutrons, on the other hand, increase appreciably the concentration of both vacancies and interstitial atoms and, even though an appreciable fraction of these defects may be neutralized by trapped charge, the net effect is to increase the conductivity. Similar effects to those of gamma-irradiation have been observed in X-irradiated crystals. Seitz[31] has pointed out that an effect on activation energy for diffusion may be responsible for the conductivity decrease observed here.

Attempts have been made by Nelson to identify the radiation produced defects by studying the annealing kinetics of the property change. Unfortunately, the annealing behavior is exceedingly complex, both increases and decreases of conductivity occurring with time at various annealing temperatures. At certain temperatures a conductivity decrease is successively followed by an increase during a single isothermal anneal. These results indicate that the annealing of the conductivity change produced by both fast neutrons and gamma-rays proceeds by multiple processes. Attempts to separate and to identify the various steps have not thus far been successful.

The results reported here are in qualitative accord with observations on alkali halides bombarded with 400 Mev protons.[32]

Because of the complexity of the annealing of ionic conductivity changes, it is desirable to utilize other structure sensitive properties in order to obtain independent information about some of the processes in question. Consequently, thermal bleaching of the optical absorption of irradiated potassium chloride specimens is now being investigated. Preliminary studies reveal that room temperature irradiation with either gamma-rays or fast neutrons introduces only two bands in the range from 2000 to 10,000 Å: a well developed F-band and a band at 2150 Å which has been attributed to holes trapped at some negatively charged defect[33] (V_3-band). On moderate heating, the F-band apparently reverts to a colloidal band and annealing at ~200°C bleaches the crystal. Attempts will be made to correlate the kinetics of bleaching with those of the ionic conductivity change.

REFERENCES

1. Berzelius, J., *Försök Til Et Rent Kemiskt Mineral System*, Afhandl, Fys. Kem. Min., *4*: 217 (1815).
2. Des Cloizeaux, A. and Damour, A., *Examendes Propriétés Optiques et Pyrogénétiques des Minéreaux Connus Sous les Noms de Gadolinites, Allonites, Orthites, Euxenite, Tyrite, Yttrotantalite et Fergusonite*, Ann. Dhim. Phys. (3) *59*: 357 (1860).
3. Mügge, O., *Über Isotrop Gewordene Krystalle*, Zentralblatt f. Min. u. Geol. (1922) *721*, 753.
4. Joly, J. and Rutherford, E., *Age of Plecchroic Haloes*, Phil. Mag, *25*: 644 (1917).
5. Pohl, R. W., *Electron Conductivity and Photo chemical Processes in Alkali-Halide Crystals*, Proc. Phys. Soc., *49*: 3 (1937).
6. For a review of early work see Lark-Horovitz, K., "Nucleon Bombarded Semiconductors," *Semiconducting Materials*, Academic Press, Inc., New York (1951), p. 47 ff. Other papers include: Cleland, J. W., Crawford, J. H., Lark-Horovitz, K., Pigg, J. C. and Young, F. W., *The Effect of Fast Neutron Bombardment on the Electrical Properties of Germanium*, Phys. Rev., *83*: 312 (1951); Cleland, J. W. and Crawford, J. H., *Neutron Irradiated Indium Antimonide*, Phys. Rev., *95*: 1177 (1954); and Cleland, J. W., Crawford, J. H. and Pigg, J. C., *Fast Neutron Bombardment of n-type Germanium*, Phys. Rev. (in press).
7. Goldschmidt, V. M. and Thomassen, L., *Geochemical Distribution Laws of the Elements III*, Norsk, Ak. Skr., I, 1, No. 5: 58 (1924).
8. Berman, R., *The Thermal Conductivity of Dielectric Solids at Low Temperatures*, Advances in Physics, *2*: 103 (1953).
9. Berman, R., *The Thermal Conductivity of Some Dielectric Solids at Low Temperatures*, Proc. Roy. Soc., A *208*, 90 (1951).
10. Wittels, M., *Lattice Expansion of Quartz Due to Fast Neutron Bombardment*, Phys. Rev., *89*: 650 (1953).
11. Wittels, M. and Sherrill, F. A., *Radiation Damage in SiO_2 Structures*, Phys. Rev., *93*: 1117 (1954).
12. Vegard, L., *Results of Crystal Analysis*, Phil. Mag., *32*: 65 (1916).
13. Hurley, P. M. and Fairbairn, H. W., *Radiation Damage in Zircon*, Bull. Geol. Soc. Amer., *64*: 659 (1953)
14. Primak, W., Fuchs, L. H. and Day, P., *Radiation Damage in Insulators*, Phys. Rev., *92*: 1064 (1953).
15. Miller, P. H. and Russell, B. R., *Effect of Internal Strains on Linear Expansion, X-Ray Lattice Constant, and Density of Crystals*, J. Appl. Phys. *23*: 1163 (1952).
16. Miller, P. H. and Russell, B. R., *Effect of Distribution of Lattice Defects on Linear Expansion and X-Ray Lattice Constant*, J. Appl. Phys. *24*: 1248 (1953).
17. Eshelby, J. D., *Geometrical and Apparent X-Ray Expansions of a Crystal Containing Lattice Defects*, J. Appl. Phys. *24*: 1249 (1953).
18. Dienes, G. J. and Kleinman, D. A., *Nature of Radiation Damage in Diamond*, Phys. Rev. *91*: 238 (1953).
19. Krishnan, R. S., *Thermal Expansion of Diamond*, Proc. Ind. Acad. Sci., A *24*: 33 (1946).
20. Binder, D. and Sturm, W. J., *Equivalence of X-Ray Lattice Parameter and Density Changes in Neutron-Irradiated LiF*., Phys. Rev. *96*: 1519 (1954).
21. Cohen, A. J., *Regularity of the F-Center Maxima in Fused Silica and Quartz*, J. Chem. Phys., *22*: 570 (1954).
22. Arnold, G. W., *Color Centers in Synthetic Quartz*, J. Chem. Phys., *22*: 1259 (1954).
23. Cohen, A. J., *Impurity Induced Color Centers in Fused Silica*, J. Chem. Phys., *23*: 765 (1955).
24. Mayer, G. and Gueron, J., *Centique de la De coloration de Verres Colores par Irradiation dans la Pile de Chatillon*, J. Chim. Phys., *49*: 204 (1952).
25. Mitchell, E. W. J. and Paige, E. G. S., *On the Formation of Color Centers in Quartz*, Proc. Phys. Soc., B *67*: 262 (1954).
26. Levy M. and Varley J. H. O. *Radiation Induced Color Centers in Fused Quartz*, Proc. Phys. Soc., B *68*: 223 (1955).
27. Levy, P. W., *Reactor and Gamma-Ray Induced Coloring in Crystalline Quartz and Corning Fused Silica*, J. Chem. Phys., *23*: 764 (1955).
28. McClelland, J. D and Donoghue, J. J., *The Effect of Neutron Bombardment upon the Magnetic Susceptibility of Several Pure Oxides*, J. Appl. Phys., *24*: 963 (1953).
29. Griffiths, J. H. E., Owen, J. and Ward, I. M., *Paramagnetic Resonance in Neutron-Irradiated Diamond and Smoky Quartz*, Nature. *173*: 439 (1954).
30. Nelson, C. M., Sproull, R. L. and Caswell, R. S., *Conductivity Changes in KCl Produced by Gamma and Neutron Irradiation*, Phys. Rev., *90*: 364 (1953).
31. Seitz, F., *Color Centers in Alkali Halide Crystals. II*, Rev. Mod. Phys., *26*: 7 (1954).
32. Pearlstein, E. A., P/748, *Change of Electrical Conductivity of Sodium Chloride upon Bombardment with High Energy Protons*, Phys. Rev., *92*: 881 (1953). See also paper by R. Smoluchowski, Vol. 7, Session 13B, these Proceedings.

Interpretation of Radiation Damage to Graphite

By G. R. Hennig* and J. E. Hove,† USA

Graphite is used extensively in nuclear reactors both as a moderator and as a structural material. The effects of neutron irradiation on such properties as thermal conductivity, gross dimensions and mechanical strength are therefore important in reactor engineering. Thus the development of a basic understanding of the mechanism of radiation damage in graphite is of great technological significance. It is the purpose of this paper to summarize the present state of our knowledge of the mechanism of the radiation damage. This problem has a great deal of scientific interest, aside from its technological importance, since the thermal and electrical properties of graphite exhibit astonishingly large changes when the material is subjected to particle irradiation. Furthermore, there appears to be good evidence that graphite is one of the few substances in which most of the displacements produced by particle bombardment can be frozen in at bombardment temperatures which are not inconveniently low. Therefore it constitutes a good material on which to test radiation damage theories.

The damage effects anticipated to occur in graphite will be discussed first, together with speculations about annealing processes. The experimentally determined property changes will then be related to these anticipated damage effects. It will be shown that a precise description of the damage centers and the processes by which they anneal cannot be deduced from an analysis of the property changes.

A set of experiments will then be described from which the annealing processes can apparently be deduced.

Structure of Undamaged and Damaged Graphite

Graphite has a hexagonal, planar structure with predominant ABAB stacking of planes and with a very large c/a ratio (6.7/2.46). The in-plane bonding is covalent, made up largely of ($2s$, $2p_x$, $2p_y$) trigonal hybrides, while the bonding between planes is due to van der Waal's forces. The ($2p_z$) orbitals then form the electronic conduction band with extremely anisotropic properties. Thus, the electrical resistivity in a direction perpendicular to the basal plane is greater than that in a direction parallel to the basal plane by a factor of several hundred. The thermal conductivity seems to show about the same anisotropy, and many other properties are considered to be also highly anisotropic.

The structure and properties of graphite are changed considerably by particle bombardment, but ionizing radiation is nearly ineffective. These changes are referred to as radiation damage. The detailed process by which the particles produce this damage has been discussed in a preceding paper.[1] Figure 1 is a schematic representation of this process as it is believed to occur in graphite. A high energy neutron

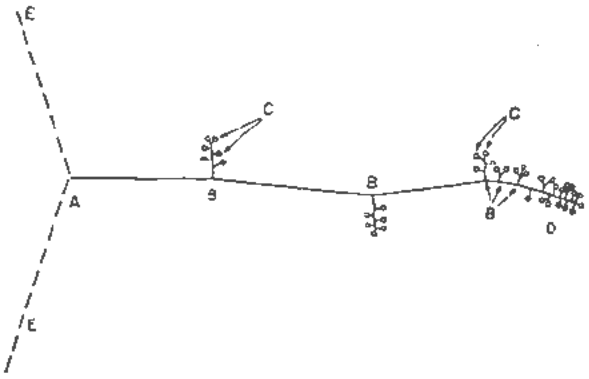

Figure 1. Schematic representation of displacement process

will produce primary displaced atoms at locations relatively far apart: the mean free path of neutrons is about 4 cm, thus the primary deplacements (A, Fig. 1) are spaced about 4 cm apart along the path (E) of the neutron. The vacancies produced in this primary process are very likely single vacancies. The energetic, primary displaced atom loses energy principally by excitation and ionization, with only an occasional elastic collision which produces secondary displacements, until its energy is less than a critical value, assumed to be about 10 kev in graphite. It then loses most or all of its energy by elastic collisions, part of which produce secondary displaced carbon atoms (B, Fig. 1 progressively closer together along the path of the primary. Near the end of its range the primary displaced atom may displace atoms so close together that they remain as C_2 molecular complexes or at least recombine to such molecules immediately. The displaced secondary atom will have enough recoil

*Argonne National Laboratory.

†North American Aviation Incorporated. Including work by A. F. Kurs, G. L. Montet, T. J. Neubert, W. L. Primak, B. Smaller, Argonne National Laboratory; and S. Austerman, R. C. Carter, G. E. Deegan, W. P. Eatherly, J. D. McClelland and A. W. Smith, North American Aviation Incorporated.

energy on the average to displace one more atom, the tertiary (C, Fig. 1). As shown in Fig 1, it appears that the displaced atoms are formed predominantly in clusters, consisting mostly of tertiary atoms near the beginning of the range, and secondary atoms near the end of the range (D).

In order to eject an atom from its lattice position, a collision must transfer to that atom more than the displacement energy, estimated to be 25 ev in graphite,[1] a value which has incidentally been confirmed by electron bombardment experiments.[2] Those collisions which transfer less than the displacement energy will excite lattice vibrational modes; this heating of the lattices becomes progressively more important near the end of the range of the primary.

In many collisions, the displaced atom has little or no excess recoil energy available to move far from the vacancy. These atoms will remain as close vacancy-interstitial pairs and may anneal in a different

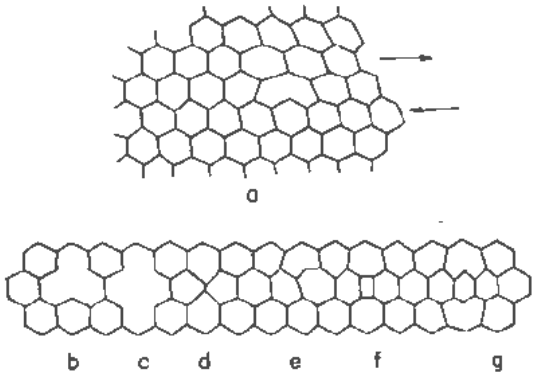

a. Two-dimensional edge-dislocation
b. Single vacancy
c. Double vacancy
d. Double vacancy plus one atom
e. Double vacancy plus three atoms
f. Double vacancy plus four atoms
g. Double vacancy plus six atoms

Figure 2 Probable configurations of 2-dimensional dislocations

way from those atoms which recoiled with sufficient energy to be displaced a relatively large distance. The close pairs are most likely to persist along the early portion of the path of the primary displaced atom, because lattice heating near the end of the range may either anneal these close pairs or cause diffusion and separation of close pairs.

The rate of displacement of atoms can be estimated from the theory of disordering of solids[1] if the energy distribution of the damaging particles is already known.

This leads to an estimate of 0.35 to 0.7 displacement per 10^4 atoms for each Mwd (megawatt day per adjacent ton of uranium) of reactor irradiation in the locations where most of the irradiations have been performed. The bombardment unit, Mwd, has been described in a preceding paper;[3] it is associated approximately with an integrated flux of slow neutrons of 5×10^{17} n/cm^2 for graphite-moderated reactors.

In addition to interstitials and vacancies, it is conceivable that dislocations may also be produced. A plausible type of dislocation which could occur in damaged graphite is the two-dimensional edge-dislocation shown in Fig. 2a. Such dislocations in graphite apparently always constitute regions in which at least one of the rings is no longer six-membered. Such defects are most likely to be formed when displaced atoms try to reintegrate into the lattice and are presumably present only after some annealing has taken place, either thermally, or in the heated region of the track.

In Fig. 2, several possible configurations are drawn which would result from such reintegrations. Type g, for example, represents the same configuration which would be produced by two close edge-dislocations of type a.

Some speculations on the mobility of the damage centers at various temperatures are possible without referring to the actual experimental work to be discussed later. It appears likely that the simple centers of a given kind are always more mobile than the complex ones; single interstitials will move through the lattice at lower temperatures than complexes of several carbon atoms, and single vacancies will move before double vacancies move. This latter assumption is believed to be correct for graphite although it may not apply to metals.[4] It can also be anticipated that the activation energy for motion of single displaced atoms is low. It is likely that they move only against van der Waal's attraction and that their activation energy for motion should be of the order of one electron volt. The activation energy of motion is much more difficult to predict for the single vacancies. Fortunately, the self-diffusion in graphite has recently been measured;[5] the activation energy is 7 ev. If this self-diffusion occurs by a vacancy mechanism, the energy of activation for moving a vacancy is 7 ev minus the energy of formation of a vacancy. The formation energy of a vacancy should be equal to the heat of sublimation of graphite (7.5 ev) minus the relaxation energy associated with formation of an internal vacancy. Therefore, the activation energy of motion of a vacancy is nearly equal to its relaxation energy. If the relaxation is considerable, the activation energy is high and vacancies will be mobile only at high temperatures. If the self-diffusion is not due to a vacancy mechanism, it can be shown that the activation energy for vacancy motion must be even higher than the relaxation energy.

The mobility of damage centers is likely to be sensitive to the amount of damage present. Interstitial atoms will be considerably more mobile in a perfect lattice than in a distorted, strained lattice; thus the interstitial atoms are less mobile in interlayer planes above or below other displaced atoms. Therefore, motion of interstitials in damaged graphite will not be describable by discrete activation energies, one for each size of interstitial complex, but rather by a wide distribution of activation energies.

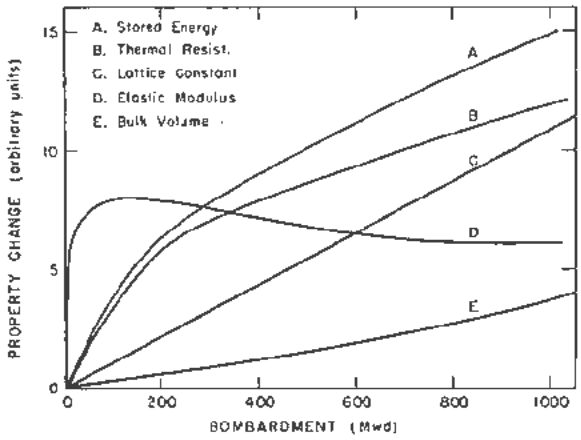

Figure 3. Property changes during bombardment at room temperature

Having described the probable distribution and mobility of damage centers, one is ready to examine whether these are confirmed by experiments.

ROOM TEMPERATURE IRRADIATIONS

Irradiation by pile neutrons produces considerable changes in nearly all the physical properties of graphite, as described in a previous paper.[9] The changes in the mechanical properties are apparently caused by the interstitial atoms which distort the lattice. The production of interstitials immediately increases the c-spacing, as measured by X-ray diffraction (Fig. 3). The bulk expansion is found to be initially much smaller, presumably because the crystallite can expand into voids which are an inevitable consequence of the manufacturing process.[6] This tightening of the structure results in an increase of the elastic modulus. The saturation behavior of this modulus increase (Fig. 3) may be due to progressive loosening of crystallite contacts. Both the c-spacing and elastic modulus increases anneal in approximately the same temperature range, which is higher than for most other properties.

Both the stored energy and change in thermal resistance increase considerably faster for low bombardments than for bombardments in excess of 100 Mwd (Fig. 3). Stored energy is created because bonds are broken in forming interstitials and vacancies. The decrease in accumulation rate with increasing bombardment must therefore be attributed to a decreased rate of formation of interstitial entities. This is most conveniently described as a coagulation during bombardment of single interstitials into larger complexes containing at least two interstitial atoms. This same explanation applies to the changes in the thermal resistance. Both of these properties anneal considerably at about 200°C, presumably because of thermal coagulation of single interstitials. As would be expected, it is observed after heavier bombardments, where coagulation has already occurred to a large extent, that a progressively smaller fraction of the damage anneals near 200°C, and a larger fraction requires much higher temperatures for annealing (Fig. 4).

The changes in the electrical properties (Fig. 5) show conclusively that most of the damage centers are electron traps. Since these damage centers are also very effective electron scatterers, the changes of electrical properties must be separated into contribution from each of these two effects. Electron traps actually increase the number of electrical carriers, by lowering the Fermi energy to a region of higher density of states (see Hall coefficient, Fig. 5). The electrical resistance should, therefore, be decreased by radiation damage were it not for the large increase in scattering probability which overcompensates the first effect at low bombardments and cancels it at high bombardments (Fig. 5). The magnetoresistance, which probably changes as the inverse square of the scattering probability, decreases very rapidly as this quantity is increased by bombardment. The magnetic susceptibility of graphite is highly diamagnetic due to the presence of electrons near the edge of the Brillouin zone. Since the damage centers trap these electrons, the diamagnetism decreases rapidly with bombardment (Fig. 5). This property is nearly independent of the scattering probability.

The concentration of electron traps in irradiated graphite can be determined independently by introducing known amounts of electron traps as chemical impurities into unirradiated graphite. These chemical traps do not materially change the electron scatter-

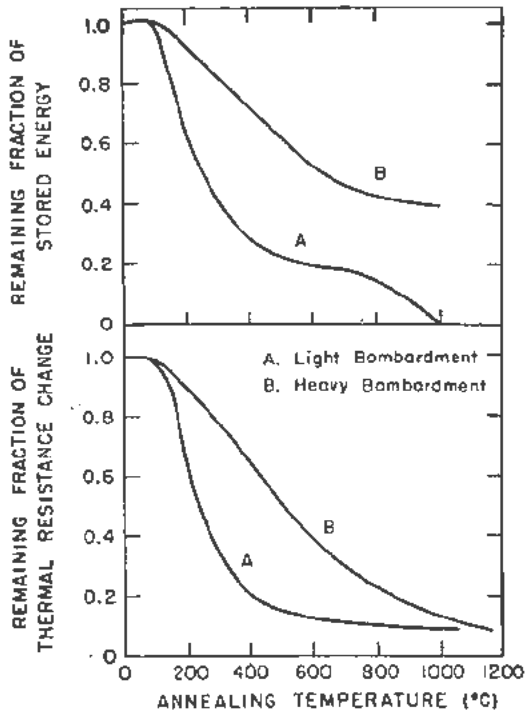

Figure 4. Annealing of damage

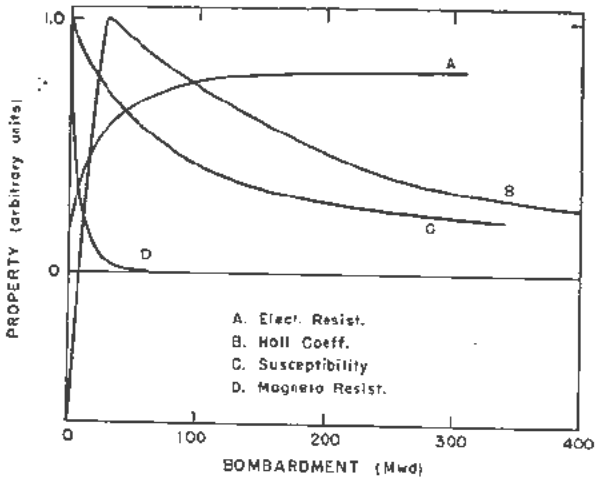

Figure 5. Electrical properties after bombardment

ing. By this method one finds that the electron trap concentration in irradiated graphite is 10^{-4} trap per carbon atom after one Mwd. This value differs by less than a factor of two from the total number of atoms displaced, as calculated by Seitz. The production rate of traps is constant during light bombardments, but appears to decrease by a factor of two after heavy irradiations (100 Mwd).

The annealing of the resistance and susceptibility changes are shown in Fig. 6. These have been converted in Fig. 7 to annealing of electron traps and scattering centers. Both of these anneal predominantly near 200°C, but show a peculiar secondary annealing near 1200°C. Eatherly has shown that all the electrical property changes can be correlated with each other nearly quantitatively. It is, however, not possible to assign the ability to trap electrons to specific types of damage centers or to assess the scattering strength of different centers.

Since different properties anneal predominantly in different temperature regions, it seems reasonable to expect that the quantitative contributions of the various damage centers to the property changes could be obtained from studies of the annealing kinetics. Experience has unfortunately revealed that the annealing kinetics are far from simple. The reasons for this are several. First of all, a given type of damage center will have a broad spectrum of activation energies for annealing because its mobility depends upon the environment. Secondly, the ranges of activation energies for different types of centers seem to overlap for weak bombardments and certainly overlap to a progressively greater extent after heavier bombardments. In addition, the annealing of a given center may affect some properties simultaneously in different ways, as for example by changing both the carrier concentration and the scattering probability in the case of the electrical resistance.

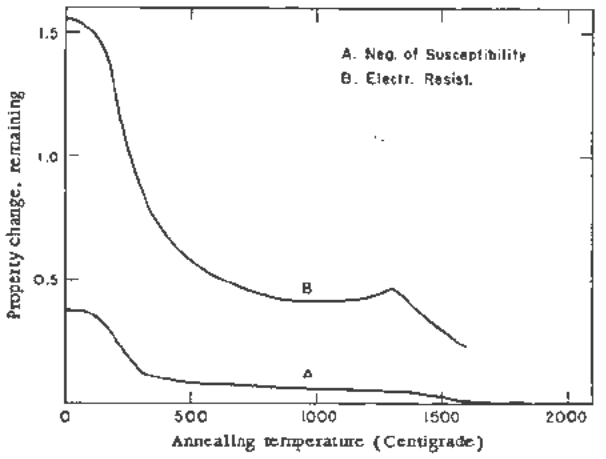

Figure 6. Annealing of electrical properties above room temperature

SPECIAL EXPERIMENTS

It has been shown why a unique damage mechanism and annealing mechanism cannot be deduced from the measurement of property changes described thus far or from annealing kinetics. In order to derive such a damage mechanism one can proceed in one of two ways. One can attempt to control the damaging process in such a way that only one type of center or at least more simple centers are formed, or one can determine changes of such properties which are predominantly affected by one of the many different centers present. Controlling the damaging process is possible in several ways. If graphite is damaged at low temperature, the centers are expected to be simpler and, therefore, to anneal in a more predictable fashion so that conventional kinetics may be applied. It may also be possible to produce only that type of damage center which has the lowest energy of formation, by heating graphite to sufficiently high temperatures so that thermal motion disarranges the lattice. Subsequent rapid cooling may freeze-in the disorder. It can be anticipated that such treatment will produce graphite which contains vacancies only. These experiments have thus far been only partially successful and will therefore not be included in this discussion. The alternative procedure of measuring selectively sensitive properties has been quite successful. Properties which are selectively sen-

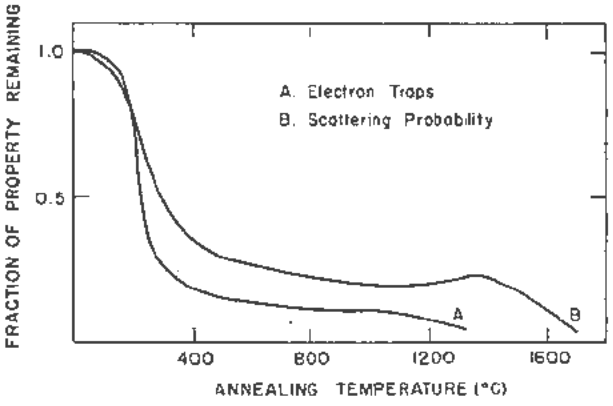

Figure 7. Annealing of electron traps and scattering centers

sitive are lattice expansion (which is sensitive to interstitials), paramagnetic resonance absorption (which is selective to single interstitial carbon ions), radioactivity (by which isolated interstitials can be tagged), and specific heat (which is sensitive to isolated unbonded atoms). As a monitoring property, the neutron scattering can be utilized since it happens to be almost completely non-selective and detects all damage centers.

Irradiations at Liquid Nitrogen Temperature

It was previously mentioned that the damage centers produced at very low temperatures should be of a simpler type than those produced at higher temperatures. Thus, the damage and annealing kinetics should be easier to interpret. Of course, if these centers were immobile below room temperature, no information could be obtained. It was, however, anticipated that they would be mobile because considerable annealing of radiation damage has been observed in metals near liquid helium temperatures.[7]

Radiation damage in graphite has been studied for both proton and neutron bombardments at liquid nitrogen temperatures. The proton irradiations were carried out in the Berkeley 60-inch cyclotron with an energy of about 8 Mev, and the neutron irradiation was done in the low-temperature facility of the Brookhaven reactor. Property measurements were made at —196°C before and after bombardment. In addition, the samples were pulse annealed in 25-degree increments to slightly above room temperature and remeasured after each pulse at a temperature of —196°C. In most cases the annealing time at each temperature was five minutes, which was found to be sufficient to achieve almost all of the property recovery possible at that temperature. The properties measured were the stored energy, the thermal and electrical resistance, the thermoelectrical power, and the magnetic susceptibility. In all cases, thermal annealing to room temperature restored each property to the value it would have had after an equal irradiation at room temperature. The maximum total bombarding flux in the cyclotron caused a damage equivalent to about 50 Mwd neutron exposure and therefore heavy irradiation effects could not be investigated. Only one low-temperature neutron bombardment of 20 Mwd has been studied although heavier irradiations are in progress.

Typical plots of the annealing behavior of the thermal and electrical resistivities and the thermoelectric power are shown in Fig. 8. These data are for a sample which was irradiated with neutrons for 20 Mwd, but proton-irradiated samples show a qualitatively similar behavior. The resistivity ordinate of Fig. 8 gives the fraction of the property change remaining after annealing. The stored energy release rate in this temperature region is shown in Fig. 9, while Fig. 10 shows the change in the fraction of trapped electrons as obtained from the magnetic susceptibility annealing data. Contrary to expectations it is apparent from these curves that there is no sharp annealing, which would be indicative of a single simple process.

It may be noted that all of the properties measured start to change at about —130°C, but that the electrical properties do not begin to recover strongly until about —70°C, while the thermal resistivity does not really begin to recover until —20°C. Furthermore, there is a definite structure to the curves in the low-temperature region, including some apparent reverse annealing. This unusual behavior can be explained and will be discussed more fully later.

X-Ray Diffraction Measurements

The effect of vacancies on the unit cell size in graphite is probably quite small. The only conceivable effect of vacancies might be a slight decrease in the in-plane spacing if the bonds around the vacancies relax considerably. The presence of interstitials would cause an increase of all spacings in isotropic media; in graphite only the c-spacing is appreciably altered.

The observed change in X-ray spacings with room temperature bombardment is shown in Fig. 3. A small contraction of the a-spacing (in-plane spacing) has been reported,[3] which can probably be attributed to buckling of the planes.[8] The c-spacing increases linearly up to very heavy bombardments (greater than about 1300 Mwd), in contrast with the behavior of nearly all other property changes which saturate strongly. The stored energy, for instance, also represented in Fig. 3, increases at more than twice the rate during weak bombardment as during heavy bombardment. This is believed to signify that single carbon atoms, which have a high energy content, are converted during bombardment to complexes of low energy content, or are reintegrated with the lattice at a rate which increases with bombardment. On the other hand, the fact that the c-spacing increases linearly over a wide range of bombardment values shows that the reintegration of displaced atoms with the lattice is independent of bombardment. The linearity of the increases further indicates that single displaced atoms cause nearly the same increase in spacing per atom as complexes of many atoms, because the interstitials formed in weak bombardments are predominantly single, and in heavy bombardments predominantly multiple. Whether these conclusions are valid up to 1300 Mwd is somewhat doubtful, since other compensating effects might occur during heavy bombardments. It is apparent that the X-ray spacing behavior strongly limits the types of damage models which can be postulated.

Attempts have been made to estimate the character and distribution of the interstitial material, but unfortunately only after heavy bombardments. Small angle scattering and the line shape of the 001 lines have been analyzed for this purpose. It appears that after heavy bombardments the interstitial material is

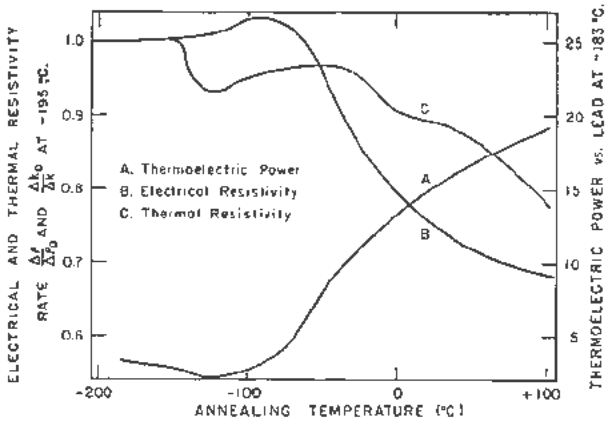

Figure 8. Annealing of electrical properties at low temperatures

present in disk-shaped aggregates, extending several times as far in the *a* direction as in the *c* direction. Furthermore, these complexes tend to position themselves with some degree of regularity so as to avoid being close to one another.[9]

There are also some data on the *c*-spacing behavior of graphite irradiated at liquid nitrogen temperature and subsequently annealed to room temperature.[10] Although these results are rather sparse at present, it may be concluded that the *c*-spacing change is linear with bombardment and that about half of the change is recovered by annealing from −196°C to room temperature. This recovery appears to take place predominantly in the same temperature range as the recovery of the other properties (see Figs. 8, 9, and 10). Further experiments on the low-temperature *c*-spacing annealing, including line shape analyses, are at present underway.

Neutron Transmission and Specific Heat Experiments

The measurement of the transmission of slow neutrons (of wavelengths greater than about 6.7 Å) through the graphic lattice allows an estimate of the total number of defects present if these can be assumed to scatter the neutrons independently. Such measurements, made[11] for a room temperature exposure of about 500 Mwd, indicate a production rate of about 5×10^{-5} displacement per atom per Mwd,

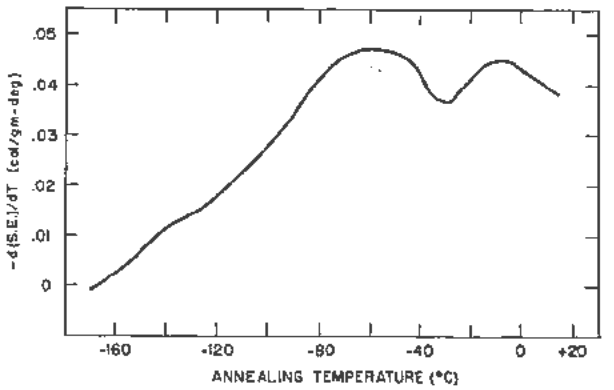

Figure 9. Annealing of stored energy at low temperatures

which is reasonably close to the theoretical value calculated by Seitz and also to the initial electron-trap production rate.

It has been observed that radiation damage has an appreciable effect on the low-temperature specific heat of graphite.[12] The specific heat at −260°C is increased after very heavy irradiations by a factor of about two which is probably to be attributed to the excitation of vibrational modes of single interstitials. Additional modes will be created by the presence of vacancies and interstitial complexes, but these most likely have quite high frequencies which are ineffectual at low temperatures. If specific heat measurements after lower bombardments, and as a function of bombardment, were available, this property would presumably measure the production rate of single interstitial atoms. Such measurements, particularly after bombardment at low temperatures, are at present under way.

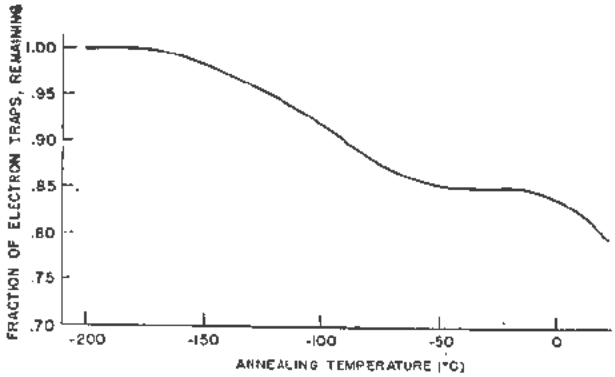

Figure 10. Annealing of electron traps measured by susceptibility

Paramagnetic Resonance Absorption

The intensity of the absorption in graphite irradiated near room temperature is shown in Fig. 11. The intensity of absorption was calibrated against an organic free radical, so that the concentration of centers, which has been plotted as the ordinate in Fig. 11, is known with fair precision. At measuring temperatures below irradiation temperature, the number of paramagnetic centers remains constant. Unfortunately, it is not possible to decide with absolute certainty which of the damage centers are paramagnetic; the assignment can only be made by inference. It is certain that only a small fraction of all the damage centers is paramagnetic, because the rate of electron-trap production is at least twice as large as the rate of Fig. 11. Thus, one concludes that many damage centers are diamagnetic, i.e., they trap two electrons on a center. The saturation at heavy bombardments of the paramagnetic center concentration suggests immediately that the centers are single interstitials or single vacancies, because the heavier bombardments favor formation of more complex centers. It was found in experiments to be described later that the paramagnetic centers produced at −196°C are somewhat mobile at −100°C. It is very unlikely that

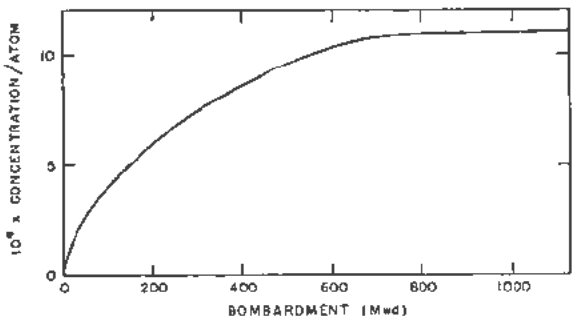

Figure 11. Paramagnetic resonance after bombardment

vacancies are mobile at this low temperature, but quite likely that interstitials are mobile. Thus the paramagnetism is most likely due to single interstitial carbon ions. It is also inferred that all the single interstitials are paramagnetic, because if only a fraction were paramagnetic, this fraction would most likely be temperature dependent, contrary to the observed temperature independence of the paramagnetic center concentration below room temperature.

The annealing of the paramagnetic centers and thus of single interstitials is shown in Fig. 12. It is apparent that the stability of the centers is very sensitive to the total damage; this was anticipated and is attributed to distortion and strain in the lattice which reduces the mobility of interstitials.

If graphite is bombarded at liquid nitrogen temperatures, paramagnetic centers are also produced, but the line width of the paramagnetic resonance absorption is larger than after room temperature bombardment. Line broadening is usually attributed to magnetic interaction of centers with one another, and thus the observation is interpreted to mean that the interstitials produced at low temperature remain in loose clusters. On warming, the line sharpens near —100°C to a minimal width of about one gauss; thus, the interstitials are able to drift apart at this temperature. The contribution to the broadening due to spin-center concentration was determined by line width measurements on material having known concentrations of uniformly dispersed spin-centers (weak pile irradiations). Using this calibration the low-temperature concentration of spin-centers in the clusters was calculated from the resonance line width. An average separation between spin-centers of 10 Å was obtained. Above —100°C, the interstitials drift to an average distance of more than 30 Å, after weak bombardments.

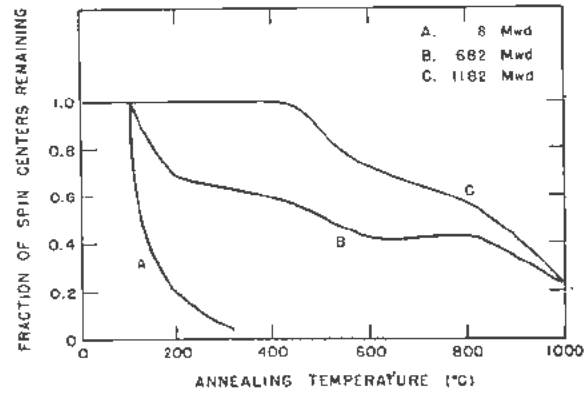

Figure 12. Annealing of paramagnetic resonance

Radiocarbon Tracer Experiments

Another useful procedure to analyze the distribution and mobility of displaced atoms in irradiated graphite is provided by a radiocarbon tracer technique. Whenever radiocarbon C^{11} is produced in graphite by betatron gamma or cyclotron neutron bombardment, the radiocarbon is inevitably displaced from its lattice position by gamma or neutron recoil and becomes a tracer for most of the displaced atoms, but not for all. The recoil energy is so high that the radiocarbon atom travels a considerable distance and ejects many secondary carbon atoms before coming

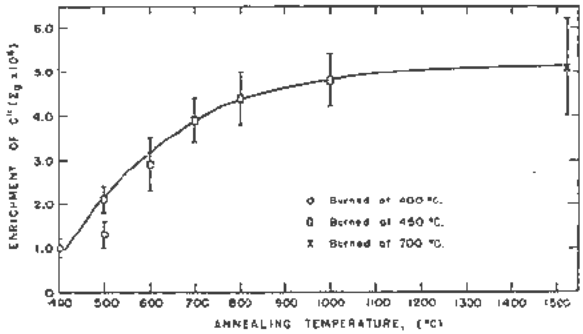

Figure 13. Surface enrichment of radiocarbon during annealing

to rest. It is therefore representative of all of the other displaced atoms which have been displaced far from their original vacancy, but is different and may anneal differently from those displaced atoms which remain close interstitial vacancy pairs. It must, therefore, be remembered that the conclusions which will be drawn from the radiocarbon tracer experiments may not apply to close pairs. The experiments have been carried out on rather well-formed crystallites of natural graphite. The graphite was first bombarded in the pile to produce displaced atoms and then exposed in the accelerator to produce C^{11}.

To study the annealing behavior of the displaced atoms, the distribution of C^{11} throughout the particles was determined. This was accomplished by oxidizing the samples in air at sufficiently low temperatures (400°C) that only outer surfaces of the graphite particles burned. The oxidation products were continually analyzed for radiocarbon. The distribution of radiocarbon was found to be affected by annealing (Fig. 13). The surfaces of the particles contained a higher C^{11} concentration than the interior, and this surface enrichment increased as the annealing temperature was raised. Although the concentrations were affected considerably by annealing, the fraction of all the C^{11} atoms which had migrated

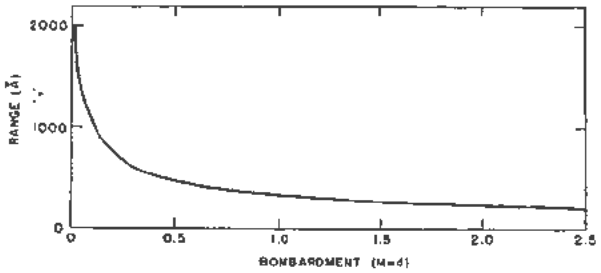

Figure 14. Average range of interstitials after bombardment

to the outer surfaces was, at most, 0.06 per cent. From this surface enrichment and the dimensions of the graphite crystals, the average linear displacement of the displaced atoms during annealing was estimated as 2000 Å (Fig. 12). Obviously, this large scale migration is not due to motion of single displaced atoms, because these are mobile at much lower temperatures. The results seem to indicate that single displaced atoms combine into complexes, probably C_2, without any large-scale migration to surfaces, possibly because they cannot react with surfaces at this low temperature. The complexes are mobile above 400°C and react with surfaces, imperfections, and vacancies between 400°C and 800°C. Obviously, the mean linear displacement of the complex interstitials has to decrease as the vacancy concentration is increased by bombardment. This bombardment dependence (Fig. 14) is very pronounced; thus, the fraction of displaced atoms which does not eventually anneal to vacancies but rather to surfaces and imperfections is quite small. Large-scale motion of interstitial atoms similar to the kind described for graphite was not observed in diamond during annealing of damage. This result may mean that large-scale motion does not occur in diamond or that the displaced atoms lose their identity during migration and thus fail to be detected by radiocarbon tracers.

The reintegration of displaced atoms with the lattice can be detected by the radiocarbon technique if the graphite is oxidized with chromic acid. This agent is able to penetrate the lattice and oxidize loosely bonded atoms preferentially. The results have shown that the displaced atoms become completely indistinguishable from lattice atoms only at annealing temperatures above 1700°C; annealing at all lower temperatures leaves some of the displaced atoms in a more active condition which renders them more susceptible to attack by the oxidizing agent. The experiments have shown also that less than 8% of the radiocarbon has reintegrated with the lattice after room temperature bombardment followed by annealing at 100°C.

DISCUSSION

A unique damage and annealing mechanism can be selected which is consistent with all of the experimental results which have been described. During neutron or proton bombardment at —200°C nearly all the atoms which have been displaced remain displaced. Roughly one-third of the displaced atoms are sufficiently close to vacancies to constitute close pairs; such interstitial atoms are probably not able to trap electrons. The remainder of the displaced atoms are sufficiently far from vacancies that they trap one electron, thus causing paramagnetic resonance absorption. They are, however, still close enough to each other to broaden the paramagnetic resonance line. The vacancies are predominantly single vacancies which trap a pair of electrons and are diamagnetic. On annealing, the process which occurs first is the motion of interstitials. The clustered interstitials will drift apart because of the Coulomb repulsion of their negative charge, and the close interstitial vacancy pairs will reintegrate since they do not repel one another. The separation of interstitials will increase those scattering properties which are associated with wavelengths comparable to the size of the cluster. Therefore, the scattering of electrons will be increased first, and the scattering of thermal waves only later when the separations are larger. The reintegration of close pairs, which occurs simultaneously with this separating process, decreases the scattering property. Thus, the electrical and thermal resistances are affected by opposing processes in this low-temperature region. Initially the separation of close interstitials increases the electrical resistance, while the thermal resistance is decreased by the annihilation of close pairs. Later, the continued annihilation of close pairs decreases the electrical resistance, but now the clustered interstitials have drifted far enough apart to increase the scattering of the relatively long thermal waves so that the thermal resistance increases again and continues to increase until the interstitials are separated by more than the wavelength. This appears to occur near —30°C; above this temperature both the thermal and electrical resistances decrease due to continued reintegration of close pairs. Other properties anneal more simply; the X-ray spacing is affected only by reintegration and therefore decreases uniformly, and the paramagnetic resonance line width is affected only by the separation of clustered interstitials and therefore decreases uniformly. The stored energy is decreased by both processes, reintegration releasing the energy of reformed carbon bonds, and separation of interstitials releasing the stored Coulomb repulsive energy, which is presumably not large.

As the temperature is raised to room temperature, a few close pairs remain to be annealed; their annealing apparently coincides with the next process, recombination of single interstitials into C_2 molecules. This process obviously requires an activation energy sufficiently high to overcome the Coulomb repulsion of the charged interstitials; however, this may not be very large, because of the dielectric constant of graphite (estimated to be about 6) and also because the charge will leak off at least one of the approaching ions as soon as the repulsion exceeds

the effective electron affinity of carbon atoms in a graphite medium. At this critical separation the electron is returned to the graphite conduction band. The considerable annealing of stored energy, resistance, susceptibility, etc., in the range 100°C to 200°C is presumably due to this reaction of single interstitials forming C_2. This reaction will also annihilate the paramagnetic resonance which is associated with C_1. The combination reaction is probably not complete before a third process begins to occur, reintegration of complexes, predominantly C_2, with vacancies. Reintegration decreases the c-spacing because it removes interstitial atoms. This process is practically complete near 600°C, since the c-spacing anneals almost completely at this temperature. Reintegration in this temperature range could conceivably occur either by motion of vacancies or by motion of C_2. The radiocarbon experiments have shown, however, that the complexes are mobile since some of them diffuse to outer surfaces in this temperature range; thus the reaction must be due to motion of the interstitial complexes. Above 600°C, a few damage centers still remain. Some vacancies are left because a few will have reacted with surfaces and imperfections. Dislocations are also probably formed during the reintegration process as was discussed earlier. Furthermore, complete reintegration of interstitials and vacancies may require a higher temperature than trapping of interstitials by vacancies. These residual damage centers are required to explain why some properties show additional annealing at temperatures above 600°C, where no interstitials remain in the lattice. This high temperature annealing appears to affect mainly the electrical resistance. It is quite obviously complex and a detailed explanation has not been attempted here.

Thus far, only the annealing of damage centers produced at low temperature, has been discussed. If graphite is irradiated at room temperature, the damage process will necessarily be different because the C_1 interstitials are relatively mobile at this temperature. Thus, clusters of interstitials will not persist and close interstitial vacancy pairs will immediately recombine. The interstitial atoms may move through considerable distances. Newly formed interstitials may encounter previously formed interstitials and react to form complexes, while the newly formed atoms are still "hot" atoms, i.e., have not dissipated their recoil energy. This reaction may, furthermore, be facilitated because the newly formed interstitial atoms may be temporarily neutral and may thus not have to overcome the Coulomb repulsion. The barrier potential opposing the transfer of an electron to a newly formed carbon atom is probably a considerable fraction of the work function of graphite. Transfer probably occurs by tunnelling but may require sufficient time to permit several encounters of this carbon atom with previously formed interstitial ions. Thus it is possible to explain the strong bombardment dependence of most property changes at room temperature as a progressive conversion of single interstitial carbon ions to complexes of two or more carbon atoms. A corresponding reintegration of interstitials with previously formed vacancies is less likely to occur during room temperature irradiations, because this reaction, which normally occurs above 200°C, requires too high an activation energy. The annealing mechanism discussed here is not expected to apply to heavily irradiated samples, in which more complex damage centers are present.

A curious observation should be mentioned which further confirms the damage mechanism. If two samples are bombarded at different temperatures for exactly the same exposure, and if the sample exposed at the lower temperature is then annealed at the higher temperature for a long time, the properties of the two samples are not always the same, the annealed sample usually showing more damage. This phenomenon seems to occur only in exposures at or above room temperature. It can be explained by the reactions which occur when the displaced atoms are still "hot"; these reactions cannot be duplicated by thermal annealing.

The damage mechanism which has been described here appears at the present time to account best for all the observations. The mechanism is based to some extent on the interpretation of paramagnetic resonance measurements. It was mentioned that the identification of resonance centers as carbon ions was inferential and could not be proved. It can now be shown that any other identification of the resonance centers leads to rather strong contradictions. If the vacancies are supposed to be paramagnetic, they must be assumed to be mobile at —100°C because of the decrease in line width at this temperature. This would imply rather extensive reintegration by vacancy motion below room temperature and could not explain the linear dependence of the c-spacing with bombardment at room temperature.

Other mechanisms which assign the resonance to other interstitial complexes, as well as C_1^-, fail to explain why the resonance anneals at 200°C, where most of the c-spacing has not yet annealed. If one assigns the resonance to C_1^- and C_2^-, and assumes all larger complexes to be neutral, one cannot explain why the annealing of the resonance at 200°C is accompanied by such a large decrease in stored energy.

In view of the ability of the postulated mechanism to explain nearly all property changes and their annealing behavior, it is felt that the mechanism has a good chance of being correct. It is hoped that it can be confirmed by a number of additional experiments. Among these experiments are the introduction of vacancies into graphite by quenching, measurement of their energy and mobility by annealing experiments, completion of the measurements after bombardment at —200°C, and bombardment at liquid helium temperatures and measurement of various properties at this temperature.

REFERENCES

References to papers of authors and contributors of this report have not been included. Decision to list individuals as contributors was based on the extent to which their work was used in the elucidation of the damage mechanism.

1. Seitz, F. and Koehler, J. S., P/749, *Radiation Effects on Solids,* Vol. 7, Session 13B, these Proceedings. Also: Seitz, F., *On the Disordering of Solids by Action of Fast Massive Particles,* Discussions Faraday Soc., *5*: 271 (1949). Snyder, W. S. and Neufeld, J., *Disordering of Solids by Neutron Radiation,* Phys. Rev., *97*: 1636 (1955).
2. Eggen, D. T., unpublished work.
3. Woods, W. K., *Irradiation Damage to Carbon Moderator Materials,* paper of a preceding session of this conference.
4. Bartlett, J. H. and Dienes, G. J., *Combined Pairs of Vacancies in Copper,* Phys. Rev., *89*: 848 (1953).
5. Kanter, M. A., *Diffusion of Carbon Atoms in Natural Graphite Crystals,* PhD. Thesis, Illinois Institute of Technology (1955). Bull. Am. Phys. Soc., *30*: No. 2, 40 (1955).
6. Currie, L. M. *et al.,* P/534, *The Production and Properties of Graphite for Reactors,* Volume 8, Session 16B.2, these Proceedings.
7. Cooper, H. G., Koehler, J. S. and Marx, J. W., *Resistivity Changes in Copper, Silver, and Gold Produced by Deutron Irradiation Near 10°K,* Phys. Rev., *94*: 496 (1954).
8. Zachariasen, W. H., unpublished work.
9. Warren, B. E. and Chipman, D. R., unpublished work.
10. Keating, D. T., *X-ray Measurements on Low Temperature Neutron Irradiated Graphite,* submitted for publication to Phys. Rev.
11. Antal, J. J., Weiss, R. J. and Dienes, G. J., *Long Wavelength Neutron Transmission as an Absolute Method for Determining the Concentration of Lattice Defects in Crystals,* submitted for publication to Phys. Rev.
12. Esterman, I. and Kirkland, G. I., unpublished work. DeSorbo, W. and Tyler, W. W., unpublished work.

Effect of Nuclear Irradiation on Ionic Crystals

By R. Smoluchowski,* USA

The fact that various kinds of low energy ionizing radiations, primarily X-rays, produce well observable effects in ionic crystals has been known for a long time. It is also known that many of the observed effects find an at least qualitative if not quantitative interpretation on the basis of fairly simple models.[1] This is the reason for the hope that the study of effects produced in ionic crystals and in particular in alkali halides by nuclear radiation will lead not only to an understanding of the phenomena in these crystals but that more general conclusions pertaining to other solids may become available.

In this paper some of the results obtained at the Carnegie Institute of Technology together with a brief review of some related results obtained elsewhere will be summarized. Since most of these results have been already reported much experimental detail will be here omitted.

PRIMARY EFFECTS

According to theory[2] a high energy corpuscular particle passing through a solid loses its energy through electronic excitation and by elastic collisions. It can also be captured inelastically. Since the significance of the latter as an important factor in producing radiation effects in solids apart from introducing foreign atoms has not been recognized until quite recently[3] it will be briefly described.

An inelastic collision of an incident particle, proton or deuteron, of an energy say 10–20 Mev with the stationary nuclei of the solid is an occurrence of relatively low probability and its consequences are usually entirely neglected in the theory of radiation effects. On the other hand when high energy protons, in the range 100–400 Mev, are impinging on the solid then the essentially energy independent cross section for an inelastic collision is given by the usual formula

$$\sigma = \pi r_0^2 A^{2/3}$$

where $r_0 = 1.2 \times 10^{-13}$ cm and A is the atomic weight of the nucleus. This leads to about 0.013 proton captures per centimeter path in KCl. Since each capture results in the emission of several secondary nucleons of energy of about 10 Mev, one obtains roughly 0.05 low energy nucleons per centimeter per incident proton. In comparing the effectiveness of the high energy primary protons with the effectiveness of the low energy secondary nucleons as factors in formation of lattice defects by elastic collisions one has to take into account the fact that a typical sample of an alkali halide, say 5 mm thick, can effectively stop the low energy nucleons generated in it while it is an order of magnitude or more smaller than the range of the high energy incident primaries. Thus the number of atoms displaced in a typical sample by elastic collisions of a particle calculated using the formula given by Seitz is at least a factor of one hundred higher for the slower particles than for the fast ones. This result, in conjunction with the number of slow nucleons calculated above, leads to the conclusion that at high energies the radiation effects produced by the secondary nucleons originating in the inelastic collisions are at least as important, if not more, than those produced directly by elastic collisions of the incident primaries.

A plausible evidence that this phenomenon of inelastic collision really plays a significant role is the dependence of the radiation effects on the energy of the incident particles.[4,5] Having at our disposal a 440 Mev synchrocyclotron it was relatively easy to compare the effects obtained at various energies by simply placing the sample between the pole pieces of the magnet at various distances from the center. The measurement of the total flux per sample was obtained by irradiating simultaneously an aluminum foil and measuring its activity. The result was rather unexpected: The influence of radiation, in this case a change of resistivity in a tungsten wire, increased slowly with increasing energy of the primary protons in the range 90 to 410 Mev.

In order to compare this result with theory, one should note first that it is in complete disagreement with the theory of elastic collisions of the primary protons which would lead to a roughly $1/E$ dependence. The theory of the dependence of the effects produced as consequence of inelastic collisions is somewhat more complicated: Using the Monte Carlo calculations of Bernardini[6] *et al.* and of Meadows[7] for 400 and 100 Mev respectively, the

* Carnegie Institute of Technology. Including work by H. Ingham, K. Kobayaski, W. J. Leivo, W. Pearlstein, J. W. Smith and W. H. Vaughan, Carnegie Institute of Technology; C. S. Smith, Case Institute of Technology; P. Day, C. J. Delbecq, L. H. Fuchs, W. Primak and P. Pringsheim, Argonne National Laboratory; G. J. Dienes, D. T. Keating and P. W. Levy, Brookhaven National Laboratory; D. R. Westervelt, North American Aviation Company, Inc.; D. Binder, R. S. Caswell, C. M. Nelson, R. L. Sproull and W. J. Sturm, Oak Ridge National Laboratory.

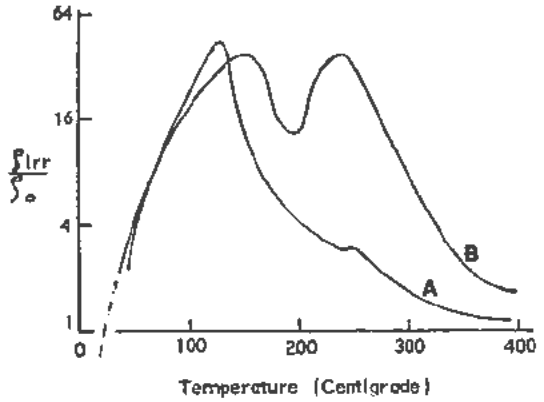

Figure 1. Ratio of electrical resistivities of irradiated and normal NaCl as a function of temperature rising at the rate of 2°C per minute. Total flux of 350 Mev protons 5.3 × 10^{13} (curve A) and 9 × 10^{15} (curve B) per cm^2

spectra of the knock-ons and the thermal evaporation spectra of the secondaries for the two energies were calculated. It appears that the number and the energy of the secondary nucleons per inelastic collision increases slightly with increasing energy of the primaries. This increase is in good agreement with the observed gradual increase of the radiation effects.

The presence of a number of secondary nucleons in a relatively small volume surrounding the site of an inelastic collision may produce a high degree of electronic excitation in this area. As a result the inelastic collision mechanism may be particularly important in producing radiation effects in dielectric materials such as alkali halides in which most effects are caused by electronic excitation rather than by direct displacement of atoms in an elastic collision.

ELECTRICAL CONDUCTIVITY

One of the well-established facts about alkali halides is the mechanism of their electric conduction through the motion of positive ion vacancies. In NaCl and KCl below the so-called "knee" the presence of these vacancies is attributed to a small concentration of divalent impurities. Since irradiation leads, among others, to the formation of lattice vacancies one might expect that electrical conductivity and the closely related self-diffusion would be increased. On the other hand one may also expect the opposite result since as shown by Mapother[8] self-diffusion in NaCl is slowed down during irradiation by X-rays.

First experiments on influence of nuclear irradiation were made by Nelson, Sproull *et al.*[9] They irradiated KCl crystals either in a pile (total fast neutron flux of the order 10^{18}) or with Co γ-rays ($10^6 r$). The electrical resistivities (10^{-9}–10^{-16} ohm) were measured in the range 25–280°C. It appeared that long irradiation with neutrons increased the conductivity while irradiation with γ-rays decreased it. Also some pile annealing was noted. An isothermal annealing at elevated temperatures could not be interpreted for one reaction with a specified order.

In order to throw additional light on these phenomena NaCl and KCl crystals were irradiated[10,11,12] in a 400 Mev proton beam (10^{13}–10^{17} total flux) and by MsTh γ-rays from a 30 mc source. The crystals were previously carefully annealed in helium and the electrical resistivities were measured by means of dc and ac methods while the irradiated crystals and a normal crystal were simultaneously and uniformly heated at the rate of about 1 to 2 degrees per minute from room temperature to over 400°C. Typical curves for NaCl are shown in Fig. 1 for a total flux 5.3 × 10^{13} (curve *A*) and 9 × 10^{15} (curve *B*) protons per cm^2 respectively. In order to avoid an overshadowing of the observed effects by the exponentially decreasing resistivity only the ratio of the resistivity of the irradiated crystal to the control crystal is shown. A similar set of curves for gamma irradiated KCl is shown in Fig. 2. The important characteristic of these results is a striking increase of resistivity during the initial part of the heating curve and a return to normal resistivity at higher temperatures. The first maximum seems to be rather flux independent while the second is increasing rapidly with increasing flux. It is interesting to note that these maxima of the relative increase of resistivity above normal seem to coincide fairly well with minima of dielectric loss tangent (thus of conductivity) and of dielectric constant as measured by Suita[13] at 3 mc/sec while heating an additively colored KCl crystal.

It is thus clear that the simple point of view that additional vacancies produced by irradiation will increase conductivity is not correct in general: Even the positive ion vacancies present in a normal crystal are either eliminated or immobilized. Since conductivity is a product of the number of carriers and of their mobility there are several possible explanations. One of them originally proposed by Mapother[8] is that positive ion vacancies are neutralized by trapping positive holes in the valence band. This explanation may be satisfactory at low temperatures but it is doubtful whether it applies here since the stability of such a configuration is known to be low. On the other hand Seitz[1] suggested that these *F*-centers

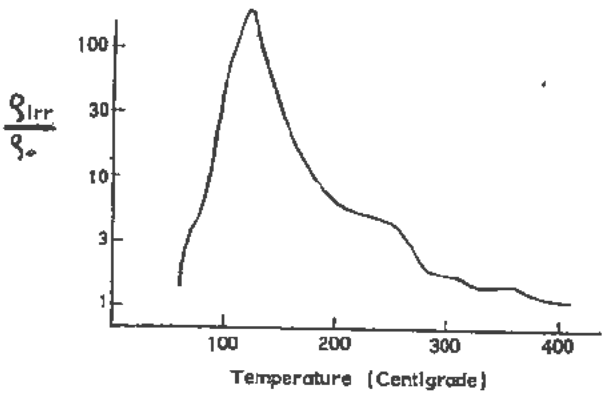

Figure 2. Same as Fig. 1 for KCl irradiated by MsTh gamma rays and temperature rising at the rate of 1¼°C per minute. Total irradiation 1.1 × 10^5 r

may be more stable in the proximity of impurities. This will be discussed further in connection with optical measurements.

A more likely explanation is that the positive ion vacancies form neutral clusters with negative ion vacancies. This possibility is particularly attractive in connection with Varley's suggestion[14] that the primary effect of ionizing radiation on alkali halides is to ionize the halogen ions until they become positive and are easily displaced into interstitial positions. This mechanism provides an overabundance of negative ion vacancies which can be an order of magnitude or so higher than the normal, low temperature concentration of positive ion vacancies. Under such conditions, at temperatures high enough to provide sufficient mobility, neutral clusters of positive and negative ion vacancies will form with the resulting increase of resistivity. Thus the effect is primarily caused by lowering of the number of carriers though mobility may be also affected. At increasingly higher temperatures the clusters of vacancies will dissociate and the defects will anneal out. This will lead to a gradual return to normal conditions.

A partial additional support for this mechanism of clustering can be obtained from isothermal annealing.[11] A KCl crystal irradiated by a total flux of 10^{17} protons per cm^2 was annealed at about 125°C. The decrease of the resistivity difference with time seemed to follow a monomolecular rate equation with a time constant of 37 minutes. Equating the reciprocal of this time to the jump frequency of a positive or a negative vacancy one obtains for the activation energy about 1.5 ev. This is just the activation energy for the motion of the slow negative ion vacancies and it can be interpreted here as the activation energy for the motion of vacancies necessary to form large neutral clusters.

The presence of the second peak in Fig. 1 which is so dependent on the total flux is likely to be associated with capture of vacancies at dislocations, especially at dislocation jogs. Although the crystals have been carefully annealed it is certain that many dislocations are still left and that irradiation, especially the displacement spikes, produce new dislocation. Since dislocations, in contrast to defect pairs, are difficult to anneal, their density and thus the height of the second peak would increase rapidly with the total flux. At still higher temperatures normal equilibrium conditions would be attained. Naturally an interpretation of the observed phenomena on the basis of annihilation of pairs of vacancies and interstitials is not possible since this would not account for immobilizing or annihilating those positive ion vacancies which are present in a normal crystal.

THERMAL EFFECTS

It is clear that in order to interpret satisfactorily the conductivity results additional information is necessary. Important conclusions seem to be obtainable from stored energy measurements.[12] These were performed by measuring very accurately small temperature differences between a normal and an irradiated crystal while both were simultaneously and uniformly heated.

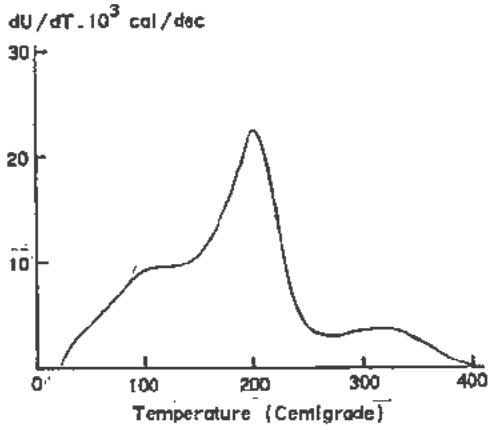

Figure 3. Excess heat evolution by NaCl irradiated with 350 Mev protons as a function of temperature rising at the rate of 2°C per minute. Total flux 9.3 × 10^{15} protons per cm^2. Sample size 1.218 gm

It appears that there is a substantial heat evolved during the process of heating and annealing. The heat emission shown in Fig. 3 reaches a maximum at just about the temperature of the minimum between the two peaks of the resistivity curve shown in Fig. 1. The total heat evolved by a NaCl crystal irradiated to a total flux of 9.1 × 10^{15} protons per cm^2 is 1.43 cal per gm and is very well reproducible. If one assumes that a recombination of a vacancy with an interstitial is associated with the emission of a few ev of energy, one obtains the result that the number of lattice defects produced per incident proton is around 5000. This result will find confirmation in other measurements described below.

OPTICAL ABSORPTION

A very sensitive way to study defects in alkali halides is to measure their absorption spectra. So far this has been done only for crystals right after irradiation that is previous to any special annealing.[12,15] The results for a NaCl crystal irradiated by a flux of the order 10^{14} protons per cm^2 are summarized in Table I.

It should be noted that the positions of the band maxima are slightly displaced from their "normal"

Table I. Concentration of Color Centers in Proton Irradiated NaCl

Band	*Number of centers*	*Centers per proton*
V_3	10^{16}	100
V_2	10^{16}	100
K	5×10^{15}	50
F	3×10^{17}	3000
R_2	7×10^{14}	7
M	7×10^{15}	70

ideal position. This may be due to the high concentration of lattice defects and an associated interaction between them. In connection with the previous discussion of the increase of resistivity it should be pointed out that the concentration of V centers, i.e., of positive ion vacancies with associated holes is rather low and one would expect that with increasing temperature it will still decrease. This makes the interpretation of the high resistivity in terms of the formation of V-centers quite unlikely. The "clustering" bands R and M are still weak but will probably grow with increasing temperature. The F-band is very strong and the production of F-centers per incident proton is about the same as that obtained from stored energy data. The difference can be easily accounted for by the fact that not all negative ion vacancies are converted into F-centers. With increasing temperature one would expect the F-centers to become ionized and clustering of negative and positive ion vacancies to proceed as indicated earlier.

The high concentration of negative ion vacancies in a crystal which has been irradiated by protons shows up clearly in the following experiment.[16] A high intensity proton beam leaves a KCl crystal often in a bleached condition presumably because of general heating. If such a crystal is then irradiated by X-rays it becomes deeply colored throughout its volume while a simultaneously irradiated normal crystal develops the usual thin colored layer on the surface. The difference in coloration at a given depth below the surfaces exposed to X-rays is then a measure of the concentration of negative ion vacancies produced by the proton beam.

A very careful and extensive investigation of the influence of X-ray, electron and neutron irradiation on the absorption spectrum of LiF has been made by Delbecq and Pringsheim.[17] Although most of their results pertain to X-rays certain observations concerning the effect of nuclear irradiation can be made. As an example Fig. 4 illustrates the quite sharp absorption line produced at 5230 Å by a ten minute exposure to neutrons followed by a nine hour irradiation by a Mineralight which gives essentially the 2537 Å resonance line of mercury. The sharpness and intensity of the absorption bands drops rapidly with increasing temperature. It is quite likely that this line is associated with displaced atoms produced during the disintegration reaction of the lithium atoms. The line has been also observed after a strong X-ray irradiation from which one might conclude that this particular color center also may be formed by a Varley[14] mechanism. According to authors the color center is probably an electron ejected from an F (or neighboring) center which has been captured by a lattice defect.

An interesting observation of the effect of irradiation on the absorption of Al_2O_3 was made by Dienes.[18] He found that neutron irradiation produces a pronounced absorption band with a maximum at 2040 Å. Its intensity increases with the total flux, gradually approaching saturation caused by the simultaneously occurring annealing. What is important is that this peak is not formed by huge doses of gamma irradiation and thus seems to provide a direct measure of the intensity of the particle irradiation. Gamma irradiation alone produces a different absorption spectrum with a strong peak near 2300 Å. Irradiation with 400 Mev protons produces both the "particle" peak at 2040 Å and several "ionization" peaks at longer wavelengths.[19] The 2040 Å band may be thus associated with a displaced positive ion. Similar effects are apparently observed in fused pure silica and in crystalline quartz.[20,21]

DENSITY AND X-RAY MEASUREMENTS

An interesting effect of irradiation of crystals is the change of their density. These changes are on the whole small and thus very precise methods have to be used. One of the best is the method of floatation of KCl crystals in di-bromopropane.[22,23] This liquid has a high thermal expansion coefficient and a density similar to that of KCl. The measurement consists of comparing the temperatures of sinking of an irradiated crystal and of a normal crystal. Under well controlled conditions, differences in density as small as 1×10^{-5} can be measured.

A crystal of KCl irradiated by 10^{15} protons per cm^2 showed a change of density of about 5×10^{-4} which if interpreted in terms of vacancies alone would give about 5000 vacancies per incident proton. One should, however, take into account the additional lattice expansion due to interstitial atoms. This would lower the number of vacancies per proton by about 10 to 15%. In any case this number of vacancies formed by an incident high energy proton is in good

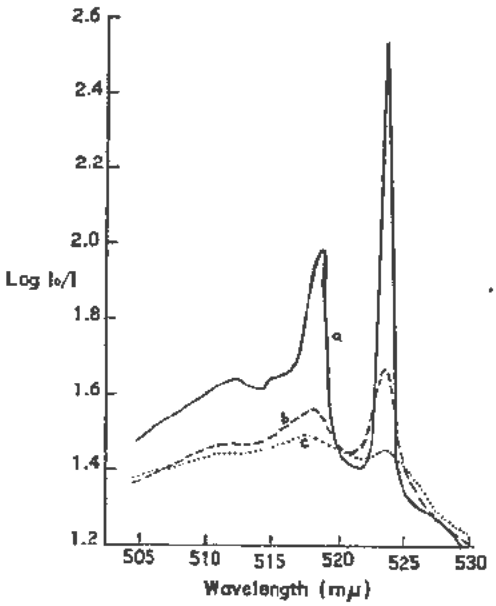

Figure 4. Absorption bands of LiF after ten minute neutron irradiation and nine hours Mineralight at room temperature. Measured at (a) — 190°C, (b) — 120°C and (c) — 75°C

agreement with the value obtained from measurements of stored energy and of optical absorption.

Very important results on neutron irradiated LiF crystals were obtained by Keating[24] and by Binder and Sturm.[25] LiF is particularly suitable for neutron irradiation because lithium absorbs neutrons and disintegrates into helium plus tritium. These have energies over 2 Mev and are very effective in producing lattice defects in the usual way. Keating measured carefully the line broadening caused by neutron irradiation and analyzed it in terms of $<L^2>^{1/2}$, i.e., root mean square distortion in length of a column of length L. He found no particle size broadening but substantial strain broadening from which, following the Warren and Averbach[26] analysis, he concluded that there are large regions of uniform strain which however become gradually non-uniform with increasing L. The suggested atomic model was flat clusters of defects separated by uniformly stressed or uniformly extended material. Recently Bowman, Krumhansl and Stock[27] have shown that actually line shape analysis cannot give uniform strain and that all the published data, including Keating's, give linear dependence of $<\Delta L^2>$ on L in accord with a random distribution of defects. This picture seems to be much more satisfactory.

Binder and Sturm have compared the change of lattice constant and of density of neutron irradiated LiF. For a total flux of 6×10^{16} they obtain a lattice increase of about 0.13 per cent which within a few per cent is in accord with the directly measured change of density. This indicates, using Eshelby's[28] theoretical result, that the defects are of the Frenkel type and not Schottky defects.

In connection with density measurements it may be pointed out that according to Smith[29] total proton flux of the order 10^{16} protons per cm^2 produces no visible surface changes of a KCl crystal but at much higher fluxes appreciable blistering of the surface can be noted.

Primak *et al.*[21] in their extensive studies of the influence of neutron irradiation on quartz and on vitreous silica observed significant changes in the X-ray diffraction spectrum and in density. The density of quartz decreased on irradiation while the density of silica increased. The difference may be associated with the availability of large interstitial spaces in the latter and with the breaking of ordered bands in the former. In vitreous silica, on annealing, the displaced atoms seem to migrate back to their proper places or they join the local configuration. In quartz, neutron irradiation produces a decrease of the refractive index, rotating power and birefringence.

MECHANICAL PROPERTIES

Whether irradiation produces primarily vacancy-interstitial pairs or clusters of defects or dislocations one would expect it to have a pronounced influence on the mechanical properties of alkali halides. So far very few data are available primarily because of the inherent lack of reproducibility of measurements. This is presumably caused by the strong influence of impurities which are difficult to control.

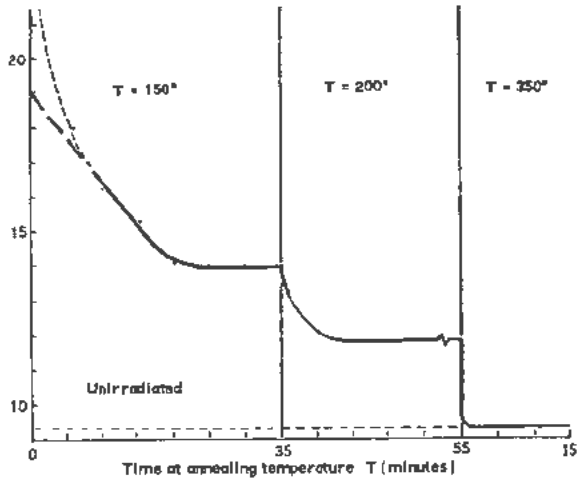

Figure 5. Diamond point hardness as a function of annealing time of KCl irradiated with 2 μa-hr of 1 Mev electrons at 20°C

Westervelt[30] has observed the annealing out of changes in hardness of KCl and NaCl crystals irradiated with electrons and X-rays. To begin with the hardness of crystals more than doubled after irradiation by 2 μa-hr of 1 Mev electron or 16 hours of X-ray irradiatinn from a Cu tube operated at 50 kv and 20 ma. This factor of two in hardness seems to be a saturation value since neither it nor the intensity of simultaneously measured absorption bands did increase with further irradiation. As shown in Fig. 5 the hardness annealed out gradually reaching a constant value at each temperature. An exposure to light, which induces the formation of M, R, N and K centers did not affect the hardness. A decrease of hardness on annealing was accompanied by a gradual disappearance of the F-band aod a growth of the "colloidal" Z-band. A substantial increase of hardness of KCl crystals exposed to high energy protons has also been reported.[31]

A very striking effect of irradiation has been recently observed[32] in a study of elastic constants of KCl. These crystals were irradiated by 400 Mev protons of a total flux of the order 10^{15} and the elastic constants measured before and after irradiation hy means of an ultrasonic method. The results though still incomplete indicate a lowering of the longitudinal and of the transverse sound velocities and thus also of the corresponding elastic constants by amounts varying from one to two per cent. The magnitude of this effect is interesting because it indicates that the vibration frequencies of as many as 10–15 atoms may be affected by one vacancy-interstitial pair. This is based on the assumption, described in previous sections, that one high energy proton produces of the order 10^3 defect pairs per cm^3.

From the above summary of radiation effects produced in alkali halides by nuclear radiation it is clear that certain basic aspects of the effects begin to be understood but that many details of the observable changes require further quantitative analysis.

REFERENCES

1. Seitz, F., Rev. Mod. Phys., *18*: 384 (1946); *26*: 7 (1954).
2. Seitz, F., Disc. Farad. Soc., No. 5, p. 271 (1949).
3. Smoluchowski, R., Phys. Rev., *94*: 1409 (1954).
4. Smoluchowski, R., Pearlstein, E. and Ingham, H., Bull. Am. Phys. Soc., Baltimore Meeting (March 1955).
5. Pearlstein, E., Ingham, H. and Smoluchowski, R., Bull. Am. Phys. Soc., Baltimore Meeting (March 1955); Pearlstein, E., Proc. Naval Res. Lab. Conference on Radiation Effects in Dielectrics (Nov. 1954).
6. Bernardini, G., Booth, E. T. and Lindenbaum, S., Phys. Rev., *85*: 826 (1952); *88*: 1017 (1952).
7. Meadows, J. W., Phys. Rev., *88*: 143 (1952) and private communication.
8. Mapother, D. E., Phys. Rev., *89*: 1231 (1953).
9. Nelson, C. M., Sproull, R. L. and Caswell, R. S., Phys. Rev., *90*: 364 (1953).
10. Smoluchowski, R., Proc. Phys. Soc. (London) (April 1955).
11. Pearlstein, E., Phys. Rev., *92*: 881 (1953); *94*: 1409 (1954).
12. Kobayashi, K. (to be published).
13. Suita, T., Phys. Rev., *94*: 1497 (1954).
14. Varley, J. H. O., Nature, *174*: 886 (1954).
15. Leivo, W. J. and Smoluchowski, R., Phys. Rev., *94*: 771 (1954).
16. Leivo, W. J. and Smoluchowski, R., Phys. Rev., *93*: 1415 (1954).
17. Delbecq, C. J. and Pringsheim, P., J. Ch. Phys., *21*: 794 (1953).
18. Dienes, G. J., Proc. Phys. Soc. (London) (April 1955).
19. Leivo, W. J. (unpublished results).
20. Levy, P. W., J. Ch. Phys., *23*: 764 (1955).
21. Primak, W., Fuchs, L. H. and Day, J., J. Cer. Soc., *38*: 135 (1955).
22. Estermann, I., Leivo, W. J. and Stern, O., Phys. Rev., *75*: 627 (1949).
23. Leivo, W. J., Phys. Rev., *91*: 245 (1953).
24. Keating, D. T., Phys. Rev., *97*: 832 (1955).
25. Binder, D. and Sturm, W. J., Phys. Rev., *96*: 1519 (1954).
26. Warren, B. E. and Averbach, B. L., J. Appl. Phys., *21*: 595 (1950); *23*: 497 (1952).
27. Bowman, J. C., Krumhansl, J. A. and Stock, J. R. J. Appl. Phys. (in press).
28. Eshelby, J. D., J. Appl. Phys., *24*: 1249 (1953); *25*: 1255 (1954).
29. Smith, J. W., Leivo, W. J. and Smoluchowski, R., Phys. Rev., *94*: 1435 (1954).
30. Westervelt, D. R., Acta Metall., *1*: 755 (1953).
31. Vaughan, W. H., Leivo, W. J. and Smoluchowski, R., Phys. Rev., *91*: 245 (1953).
32. Smith, C. S., Leivo, W. J. and Smoluchowski, R. (to be published).

Record of Proceedings of Session 13B

MONDAY MORNING, 15 AUGUST 1955

Chairman: Mr. V. N. Kondratyev (USSR)

Vice-Chairman: Mr. M. Magat (France)

Scientific Secretaries: Messrs. A. Finkelstein and A. Salam

PROGRAMME

P/749	The theory of lattice displacements produced during irradiation	F. Seitz and J. S. Koehler
	Discussion	
P/750	Theoretical aspects of radiation damage in metals	G. J. Dienes
P/444	Radiation damage in non-fissile material	J. H. O. Varley
	Discussion	
P/362	Modification produced in non-metallic materials by radiation and the thermal healing of these effects	G. Mayer *et al.*
	Discussion	
P/753	A review of investigations of radiation effects in covalent and ionic crystals	J. H. Crawford, Jr. and M. C. Wittels
	Discussion	
P/751	Interpretation of radiation damage to graphite	G. R. Hennig and J. G. Hove
	Discussion	

The CHAIRMAN: This session will be devoted to a discussion of the effect of radiation on solids and will in a sense be a continuation of Session 11B.

We know from experiment that irradiation of solids by ionizing radiation and neutrons produces structural changes, namely distortions and defects in the crystal lattice, resulting in alterations of the properties of the irradiated substance: specific weight, elasticity, sound propagation characteristics, electric resistivity, magnetic susceptibility, optical density and other properties. We have seen examples of the effect of radiation on the more readily apparent properties of solids, in particular in the exhibits displayed by the United States of America. Many other cases of the effect of radiation on various substances were brought to our attention in Session 11B.

While the question of the effect of radiation on solids is of great practical significance, it also presents considerable theoretical interest. From the point of view of both practice and theory, investigation of the mechanism of radiation effects in solids is highly important. The papers to be presented at this session are devoted primarily to the study of this mechanism.

The effect of radiation on solids and the mechanism of this effect have been relatively little explored. We know that elastic scattering of fast particles produces displacements of individual atoms and ions in a crystal, displacements resulting in distortion of the crystal structure and the appearance of alien intrusions and vacant sites in the crystal lattice. Under the influence of ionizing radiation and also of nuclei dislodged as a result of elastic scattering of fast particles, ionization of the atoms and ions comprising the structure of a solid occurs, and this leads also to various changes of certain properties of the solid. Furthermore, we know that in a number of cases saturation occurs; this is indicative of the operation of processes the reverse of those giving rise to structural defects in the solid. There is reason to assume that the saturation effect is to an appreciable extent caused by particles formed during the course of the radiation process.

The papers which are to be discussed at this session contain data confirming and refining our understanding of the mechanism of radiation effects in solids. The experimental data cited in the papers prove, in conformity with theory, that the nature of the radiation effects depends both on the type of radiation and on whether the bonds in the irradiated material are metallic, covalent or ionic. In particular, there is reason to think that in the last case multiple ionization of negative ions plays an important part. We shall see that impurities also play a significant role in the changes produced by radiation as well as in the process of recovery of the original properties

of the material. The papers presented for discussion bear convincing evidence of the great value of kinetic measurements, investigation of paramagnetic resonance and the use of tagged carbon atoms for studying the mechanism of radiation effects and establishing the character of defects arising in graphite exposed to irradiation. The importance of theoretical calculations is also brought out; the fact that the values of the calculated parameters are in quantitative agreements with experimental data proves that we are on the right track.

Nevertheless, it should be emphasized that our notions regarding the mechanism of the effect of radiation on solids are still rudimentary and relate mainly to the case of small radiation doses, i.e., to the case presenting the least practical interest. We still know very little regarding the nature of the secondary processes taking place in irradiated substances and the part played in these processes by "hot" atoms. We do not know exactly how far the conventional concept of temperature can be applied to the irradiated substance. Nor do we know exactly which radiation effects lead to reversible changes, i.e., to changes completely healed by heating, and which result in non-reversible changes. We are still in the dark regarding the essential difference between reversible and non-reversible changes where the structure of the solid is concerned.

Answers to these questions can be found only through further detailed investigation in this field. As is rightly emphasized in one of the papers, in such investigations a closer connexion should be maintained between theory and experiment than has hitherto been the case.

Mr. F. Seitz (USA) presented paper P/749.

DISCUSSION OF P/749

Mr. P. Perio (France): The questions I ask Mr. Seitz bear mainly on his written paper.

The first concerns the change in resistivity observed after copper has been bombarded with deuterons at 10°K and 90°K; the theoretical values calculated from the data of Jongenburger and Blatt being respectively 5 and 7.5, the authors conclude that this difference is due to thermal recovery during irradiation in the second experiment. But when bombarding with electrons at between 80°K and 120°K, the theoretical value is again 5. Do the authors think that this shows that the defects caused by the electrons are thermally more stable than those caused by deuterons? As this seems rather improbable, what explanation do the authors suggest?

My second question: There are two theories giving the increment of resistivity in terms either of the number of interstitials or that of the point lattice defects, the first being by Dexter and the second by Jongenburger and Blatt.

What are Mr. Seitz's grounds for preferring the second theory to the first? The first, I believe, is based on Born's approximation, but it seems to me that the same is true for the calculations of threshold energy of displacement and of the number of permanent defects created. That is my second question.

My third question concerns the disordering of Cu_3Au alloy. I should like to know what Mr. Seitz means by the number of atoms disordered. Would it not be better to use the Bragg-James long-distance order parameter, S, which takes account of the co-operative nature of ordering phenomena? In that case, we know that, resistivity being related to the square of the order parameter, Brinkman's results correspond to a reduction of 0.8 of the long-distance order coefficient. Bearing in mind the considerations put forward by Brinkman on the differences in free energy of the gold interstitial and the copper interstitial and taking equal account of the differences in the effective displacement section for the two types of atom, one can show that it would be enough for 10 per cent of the atoms to be displaced at a given moment to enable the change in resistivity observed to be attributed to a disorder effect.

My fourth question bears on Mr. Seitz's treatment of the phenomenon of interstitial migration as presented by Brinkman. Mr. Seitz would attribute recovery in the low temperature range to interstitial migration, and recovery in the intermediate range to vacancy migration. In that case, I should like to know whether Mr. Seitz has any views regarding the third phenomenon that occurs at a temperature higher than the general ambient temperature, and at an activation energy of about 1.2 ev, and which, in the case of the gold-copper alloy, is accompanied by a partial ordering of the alloy.

My last question refers to structurally hardened alloys. The authors do not mention the results obtained by Murray and Taylor, and supplemented by Bilington and Crawford, which seem to show clearly that some phenomena hitherto attributed to "thermal" or "displacement spikes" are due rather to thermal scattering and to selective displacement of the various types of atom. I think that the same type of mechanism might apply to the transformation of heterogeneous alloys into homogeneous alloys during irradiation, reported in Session 11B by Mr. Zhdanov. What is Mr. Seitz's opinion on this point?

Mr. Seitz (USA): It is clear that the results obtained at the temperature of liquid nitrogen include annealing of the step which takes place at 30°K, so that we have more scattering centers. You were emphasizing the difference in specimens bombarded with deuterons and electrons. I am afraid that the experimental accuracy is not high enough to enable us to be certain about this difference, which is in the region of 30 per cent. It could easily be an experimental matter. The analysis of the experiments with electron bombardment, or rather their interpretation, was made by guessing what the resistivity was at the temperature of measurement. Mr. Perio had a number of other questions, but I suspect that

we shall do better if we get together and discuss these as individuals.

Mr. T. HOFFMANN (Hungary): I am studying the theory of melting, and a few days ago a short conversation with Mr. Dienes drew my attention to some problems in Mr. Seitz's paper which perhaps may be cleared up with the aid of the slide which I propose to show. The basis of my work on the theoretical calculation of the melting point and melting entropy of metals was that I have considered the metal as an alloy of the metal itself and of vacancies. Thus it was possible for me to calculate the energy of the metal as a function of the concentration of the vacancies. This has been done up to now for the alkaline metals only, but I think that the qualitative features of this work can be applied to other metals also.

The entropy of the metal, arising from the mixing up of the vacancies, can be calculated in a similar way, so that we can draw the free energy-vacancy concentration curve for different temperature (Slide 1).

This means that in an ideal metal-vacancy alloy there exists an equilibrium concentration of vacancies for all temperatures sufficiently below the melting point. This equilibrium concentration increases with the increase of temperature.

In connection with Professor Seitz's paper, if we irradiate the metal, considering the effect of producing vacancies only, we expect the concentration of the vacancies to become larger than the equilibrium concentration at the temperature of the irradiation. This means that, for instance, on the curve corresponding to the smallest temperature on the slide we are climbing up to the point shown, which corresponds to the natural vacancy concentration plus that resulting by irradiation. Now, if we do not raise the temperature, then this state developed by irradiation will not be stable. The result will be the recombination and wandering of the vacancies to the surface of the elementary crystallites until the equilibrium concentration at this temperature is reached. I wish to emphasize that this does not mean that the starting state was rearranged, because this recovery is probably connected with the breaking up of larger crystallites to smaller ones, which have relatively larger surface, from the sublimation of the vacancies.

On the other hand, if we raise the temperature we can arrive, for instance, at a temperature where the natural concentration of vacancies is the same as the natural plus irradiated one was at the temperature of irradiation. This means that at about this temperature the effect of irradiation due to vacancies ceases. I suppose that this is the annealing point in Mr. Seitz's diagrams; but, if this is true, the following situation must be clear. If the irradiation flux gets larger, the shifting of the concentration increases, and so the temperature of the sudden annealing will be shifted to higher temperatures. I should therefore like to put this question to Mr. Seitz. His Fig. 7 shows the jumps in the annealing at 30°K and 40°K for silver and copper respectively. My question is, will these temperatures remain the same if the intensity of the irradiation is raised?

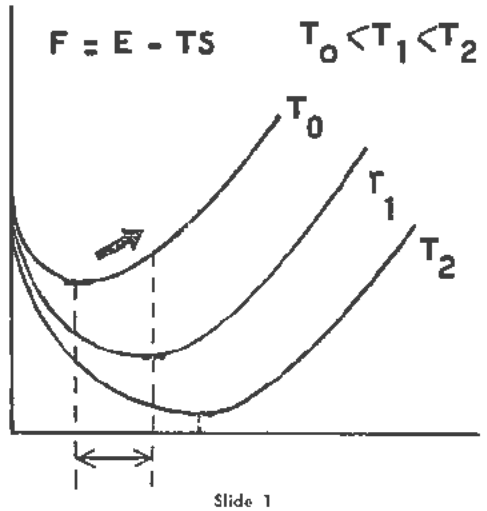

Slide 1

I suppose that with higher flux the annealing temperature would also be higher, if it is caused by the vacancies only.

Mr. SEITZ (USA): I doubt whether there is any influence of flux intensity on the temperature of annealing. Our measurements were made with a cyclotron, and the specimens were bombarded for five days. Similar work is in progress at Oak Ridge. The results are not yet completed, but the workers there are observing the same annealing temperatures in pile irradiation. The equivalent flux density is much lower in the reactor experiment, yet the annealing temperatures are the same. This is what I should expect if the process has to do with the way in which the particles—that is, the defects—are behaving.

Mr. G. J. DIENES (USA) presented paper P/750.

Mr. H. M. FINNISTON (UK) presented paper P/444.

DISCUSSION OF P/750 AND P/444

Mr. LINTNER (Austria): I should like to refer to Mr. Varley's paper. He quoted the experiments by Makin, who studied the influence of alpha particles on the creep of cadmium single crystals and could not detect any change in creep rate. As already mentioned by the speakers, similar experiments have been made in Vienna by Schmid and myself* using single crystals of zinc, and polonium alpha particles. We found with thin crystals of a thickness of only 0.3–0.4 mm an appreciable increase in the creep rate. I should like to illustrate our results by a slide. The

* Schmid E. u. Lintner K.: Sitzungsberichte d. Österr. Akademie, 163, 109, 1954; Z. Metallkunde, 46, 71, 1955; Lintner K. u Schmid E.: Ergebnisse der exakten Naturwissenschaften, 28, 302, 1955.

experiments were carried out in the following way. First a creep curve was taken without irradiating the crystal, then the crystal was allowed to recover without stress for three minutes. Subsequently the stress was applied again under irradiation, and another recovery period of three minutes followed. This was repeated a number of times. In Slide 2 the upper curves represent the creep without irradiation. The lower curves are those with irradiation which followed in the experiment in the way indicated. We believe that we can conclude from our experiments that alpha particles produce a hardening of crystals whereas corresponding experiments with beta particles carried out by us seem to indicate a softening of the crystals.

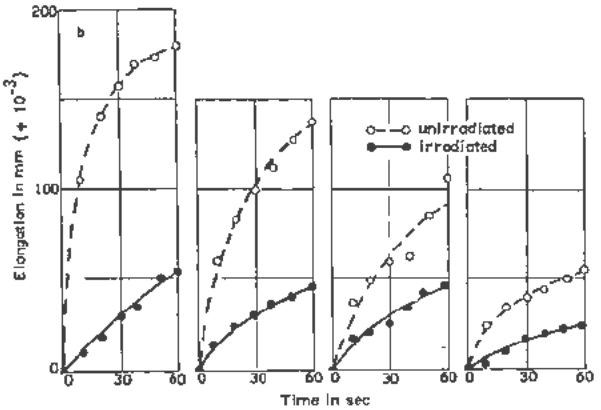

Slide 2. Creep curves

Mr. G. V. KURDIUMOV (USSR): In Session 11B, the question of the influence of neutron bombardment on the transformation of austenite was raised. In that connexion, and also in connexion with the papers presented, I should like to inform the Conference regarding the results of experiments of Zakharov and Maksimova on the influence of radiation on the austenite-martensite transformation. In these experiments, steel containing 0.5 per cent carbon, 7.9 per cent manganese and 2 per cent copper, and also iron-nickel-manganese alloy containing 21.5 per cent nickel and 3.4 per cent manganese, were bombarded. The martensite transition point for both materials was below room temperature.

After irradiation with a flux of about 4×10^{16} neutrons per cm^2, there was a marked change in the shape of the martensite transformation curve incident to cooling to the temperature of liquid nitrogen. In the case of the steel, the martensite point went up by about 20 degrees, while the total amount of martensite forming increased by 50–60 per cent. In the case of the iron-nickel-manganese alloy, the opposite effect was observed; the martensite point was lowered and the total amount of martensite forming was reduced. In this alloy, the austenite can easily be super-cooled, and the amount of martensite forming will vary depending on the rate of cooling. Hence in this alloy, transformation of austenite into martensite occurs even during the subsequent heating of the alloy to room temperature. Thus we see that the effect of radiation is the same in heating as in cooling.

It should be noted that a similar difference in effects stems from the low plastic deformation of austenite: in the steel, it raises the martensite curve and in the alloy it lowers the curve.

I should like to note here that the question of the reasons for the limited nature of the isothermal phase transitions occurring in martensite transformations is one of the most important questions in the field of solid state phase transitions and it arises, in particular, in connexion with the tempering of steel. At temperatures below the martensite point, the number of martensite centres forming in each unit of time rapidly decreases with the temperature and the process soon comes to a stop. Further formation of martensite centres in the remaining austenite occurs only when the temperature is lowered. No satisfactory explanation for this phenomenon has been found so far.

Before we can clarify the nature of martensite centre formation, we must have more experimental data regarding the effect of various factors on their creation. Such factors include plastic deformation and bombardment by neutrons or other particles. It is to be hoped that when we know more about the effect of these factors on phase transitions and the character of the damage to crystal structure produced by these factors, we shall have a clearer understanding of this aspect of martensite transformation phenomena.

Mr. S. F. PUGH (UK): I just wanted to make a short comment on the experiment which Mr. Dienes has described on neutron scattering as a means of determining defects in graphite and metals. We had considered this method at Harwell and came to the conclusion that with metals it would be a very inaccurate way of determining displacements because the neutron scattering from other sources in metals would be so great. Even in favourable cases like lead and bismuth the accuracy would still be quite low, but it may be possible, when we have separated isotopes of low scattering cross section, to obtain something worth while.

Mr. DIENES (USA): In answer to Mr. Pugh's question I am not sure that what he says is true for aluminum. I think experiment should be possible in aluminum.

I have a comment on Varley's proposed mechanism for displacement production. In connection with this proposal I would like to call attention to some experiments with alpha aluminum oxide which we reported on at the Bristol Conference. In this crystal an absorption band has been observed in the ultraviolet which is produced by reactor irradiation but is not produced by heavy gamma radiation. We feel that this crystal is a most important material for testing Varley's proposal on displacement production. If his mechanism operates we would expect the

band to be produced by electron irradiation even when the electron energy is kept well below the threshold energy, say somewhere round about one-tenth Mev.

Mr. FINNISTON (UK): I would like to come back on Mr. Dienes' paper. As he suggested an experiment for us, may I suggest an experiment for him? There is this problem of trying to distinguish between effects due to interstitials and vacancies. I do not think one can do this by simple irradiation experiments; I think one has to do non-irradiation experiments to discriminate. One method of getting extra vacancies into materials without getting extra interstitials is to quench the material at a high temperature, and I think that by comparative experiments with quenched and with irradiated materials we ought to be able to discriminate between effects due to interstitials and those due to vacancies.

Mr. BROOKS (USA): This question is directed to Mr. Finniston. With reference to Mr. Lomer's estimate of effect of radiation on diffusion, this is of course a quantitative question depending on the neutron flux. I would like to ask at what flux will an effect on diffusion first be observed, the other conditions being the same as assumed in the calculation?

Mr. FINNISTON (UK): I am afraid that I cannot in fact answer that off-hand. Perhaps the speaker and I could get together and I will look this up.

Mr. PERIO (France): My question relates to the document submitted by Mr. Dienes. He has told us that experiments on the transmission of long-wave neutrons failed to show the collections of pin-point defects. Now from Mr. Kinchin's paper of last Saturday, it appears that similar collections of defects occur in graphite, even at a low temperature. Does it not therefore seem that comparison between the results of neutron transmission experiments and any theoretical calculation of the number of atoms displaced may not be of much value?

Mr. DIENES (USA): The question is whether there is clustering of defects during even room temperature or low temperature and therefore the concentration of displaced atoms may be quite different from what we measure. The only answer I can give to this is that you do not expect large clusters at low temperatures; you do expect pairs, perhaps. If pairs are present we should see a wavelength dependence in the transmission, and perhaps more accurate experiment will show there is such a wavelength dependence; but with the accuracy we have, if you take the ratio of the transmitted intensity of unirradiated and irradiated material, you find this ratio does not depend on the wavelength of the neutrons over the region we have been able to cover. Therefore my conclusion would be that we are seeing single defect, and the concentration of clusters can only be a relatively small fraction of the total number of displaced atoms.

Mr. G. H. KINCHIN (UK): I would just like to ask Mr. Dienes whether he considers that the relaxation of the atoms near an interstitial would give rise to any contribution to the neutron scattering over and above the direct cross section for the interstitial.

Mr. DIENES (USA): Yes, it actually would. This is not very easy to estimate. This will happen if the displacement of the graphite planes is not just a simple displacement. When there is unhomogeneous distortion on top and over that displacement of the planes, then this distortion will change the cross section somewhat. We tried to make a rough estimate of this, and estimated the effect could not be over about 15 per cent, and again it would introduce a wavelength dependence. Further work, however, is required to really answer this point.

Mr. MAYER (France) presented paper P/362 as follows: The investigations of the effect of fast neutrons on the properties of solids being carried out at the Commissariat à l'Énergie Atomique (Atomic Energy Commission) are principally concerned with the damage to graphite, lithium fluoride and quartz.

The test materials were irradiated in the pile at Saclay. Samples were placed in an aluminium tube (the central channel) immersed in heavy water in the centre of the tank. When the pile is operating at 1000 kw, which is its normal rate, the thermal flux is 4×10^{12} and the temperature is 35°C. Heavy water being an excellent moderator, the energy spectrum of the neutrons lies in a region of lower energies than in the case of a graphite pile. To accelerate our irradiation studies, we irradiated graphite in a tube of cooled uranium placed in the tank, which we call a converter. Under these conditions, the irradiation effects are produced five times faster and have always proved to be of the same nature as in the thermal recovery experiments. Along the abscissa of our curves, therefore, we plotted the values of the total thermal flux which would have been necessary in the central channel, without the uranium tube, to produce the state of irradiation in question. Our curves do not extend beyond 4×10^{19} n per cm^2. Being anxious to study these heavy flux phenomena before the opening of this Conference, we resorted to mixing a lithium salt and graphite in very finely powdered form. In these tests, the function of fast neutrons was performed by atoms of helium and tritium. Internal energy measurements, about which I will say more later, have shown that by this procedure the rate of obtaining radiation effects in the central channel was speeded up by a factor of nearly one hundred.

The quantitative results which I shall give all relate to a polycrystalline graphite obtained from petroleum coke by heating at a temperature at 2500° for several days. Its properties are shown in Table I.

We observed that the effect of fast neutrons on the electric resistivity and on the velocity of sound was more pronounced and more rapid for higher degrees of graphitization. In comparing the degrees of

Table I. Graphite from the Reflector of the Saclay Pile

Density, gm-cm^{-3}		1.59 ± 0.05
Electrical resistivity, ω gm-cm^{-1}		$9.5 \times 10^{-4} \pm 0.3$ ‖
Ratio $\frac{\rho\ 100°C}{\rho\ \ 0°C}$		= 0.822
Velocity of sound	‖	2.1×10^5 cm/sec ± 0.1
Velocity of sound	⊥1	1.6×10^5
Velocity of sound	⊥2	1.4×10^5
Poisson modulus		‖ 0.13

graphitization of the two graphites, we went by the following: comparison of the heating temperatures when the initial material was the same; Young's modulus, which is lower for more fully graphitized specimens; X-ray diffraction; the ratio of the electric resistivities at 100° and 0° (suggested by Kinchin) and the resistivity; and thermoelectric power at 0°.

These parameters are still too few to truly characterize a material but already too many for an investigator to be able to obtain a number of specimens having the same value of all these parameters. Hence, whenever we could, we measured several physical constants on the same specimen, first as affected by irradiation and then during the thermal recovery process.

Slide 3 (Fig. 1 of P/362) shows the beginning of the curves which you already know in their entirety from the reports of Mr. Woods and Mr. Kinchin and the article by Mr. Klimenkov and Mr. Alekseenko.

The resistivity and the velocity of sound, obtained by measuring the resonance frequencies, are for the same rod, in which the axis of the graphite grain runs parallel to the length of the rod. Poisson's ratio does not change, which shows that the modulus of rigidity changes at the same rate as Young's modulus. Internal friction, which is very great before irradiation, decreases by a factor of 10 at the point where Young's modulus appears to reach a saturation value.

Where the increase in the velocity of sound is concerned, theory has not advanced to the same point as in the case of electric properties. There is reason to assume, however, that Young's modulus, rather than velocity itself, varies in proportion to the number of centres created, at least in the case of weak irradiation.

In speaking of centres created by the impact of neutrons and destroyed by annealing, we mean that limited numbers of atoms form local geometric configurations which differ on the average in time from those that they formed before the impact. But while only the mean positions of a limited number of atoms are changed, the thermal oscillations of all the atoms of the grain about their mean position are altered because their normal frequencies are disturbed.

Let us assume that the velocity of sound is influenced primarily by one type of centres; let n be the number of these centres per cm^2 and N be the number of carbon atoms per cm^3 of graphite ($N = 8 \times 10^{22}$); we have

$$\frac{V^2}{V_0^2} = 1 + \alpha \frac{n}{N}$$

where V/V_0 is the ratio of the velocities of sound after and before irradiation. If both of these are squared, V^2/V_0^2 may well be proportional to the number of centres formed, at least at the beginning of the curve.

We saw from Slide 3 that the product $\alpha n/N$ attains a value of 0.1 for a thermal dose of the order of 10^{18} per cm^2, which gives an enormous number of centres, except in the case when α is very large. One might be tempted to assume *a priori*, from an examination of other curves, that α should lie between 1 and 10. Moreover, calculations based on the theory of Seitz show that with the above dose not more than one atom in 10^4 is displaced. The slope at the origin of Young's modulus for graphite has a surprisingly high value as compared with that of curves for other irradiated substances. It is probable that the macroscopic effect observed is only indirectly related to the changes in the elastic parameters of the graphite microcrystals. It will be recalled that non-irradiated polycrystalline graphite has three distinctive properties: as a result of compression, Young's modulus increases, whereas under tension it decreases, which makes static measurements difficult; graphites expand two to four times less than might be predicted from the thermal expansion of single crystals of natural graphite; Young's modulus increases with the temperature, which is an anomaly. Furthermore, our determinations show that when the expansion of the crystal parameter c measured by X-rays has attained a relative value of 2×10^{-3}, the macroscopic expansion is still less than 10^{-4}.

We advance the hypothesis—and hope to be able to prove it quantitatively in the future—that the increase in Young's modulus with the temperature on the one hand and owing to irradiation on the other, have a common cause: the state of compression of the grains, which results from the fact that the microscopic parameter c increases more rapidly than the macroscopic dimensions.

Slide 4 (Fig. 2 of P/362) illustrates the thermal recovery of a graphite specimen irradiated with 2×10^{19} neutrons per cm^2. What you see are successive isotherms; each change of temperature has been indicated by dotted lines. The entire experiment covered a period of about 250 hours. As will be seen from the curve, the decrease in resistivity is very pronounced and starts before the decrease in the velocity of sound. All these measurements were made at room temperature, between periods of heating.

This figure suggest that there may be two types of centres: the first rapidly disappearing at about 150° or under and having a strong effect on the resistivity and little effect on the velocity of sound; the second disappearing at 220° or above and strongly affecting the velocity of sound. We have not succeeded in de-

termining an activation energy for the disappearance of the first type of centres on the basis of the recovery isotherms for either of the properties. Thus, while a value of 1.4 ev would seem to be obtained in the neighbourhood of 160°, we found only 1 ev at 100°. In contrast, one can find a value of 2.1 ev for the energy w from a study of the recovery curve above 220°; this can readily be done with reference to the velocity of sound, because it drops off markedly.

Slide 5 (Fig. 7 of P/362) gives the recovery isotherms we used to obtain the activation energy of 2.1 ev. The activation energy is the only quantity which one can calculate from these curves without knowing the relationship between the physical property being determined and the number of centres which seem to vanish. We can arrive at the energy either by comparing curve 1 with curve 3, i.e., comparing the times required to reach the same degree of recovery, or from the change of slope of curves for the same specimen first heated to 505°K and then to 527°K. Once we have the activation energy, the question arises whether the variation conforms to a law of the first order or of the second order.

$$E = E_0 \left(1 + a \frac{n}{N}\right) \tag{1}$$

$$E = \rho v^2 \tag{2}$$

$$\left(\frac{v}{v_3}\right)^2 = 1 + a \frac{n}{N} \tag{3}$$

where n = number of defects/cm³ and N = number of atoms/cm³.

$$\frac{dn}{dt} = -K(T)n \qquad K(T) = \phi(T)e^{-\frac{w}{kT}} \tag{4}$$

$$\frac{dn}{dt} = -K'(T)n^2 \qquad K'(T) = \Psi(T)e^{-\frac{w}{kT}} \tag{5}$$

If we assume the law to be of the first order, Equation 4 applies. Now that we have w, we can compute $\phi(T)$. We find $\phi(T) = 1.5 \times 10^{-11}$ sec⁻¹. Assuming that the law is of the second order (which is more in keeping with the shape of the curve) and that $n = 10^{19}$, we have

$$\frac{dn/dt}{n} = \phi(T)e^{-\frac{w}{kt}} \text{ and } \quad \phi(T) = 1.5 \times 10^{-3} \text{ sec}^{-1}$$

With these values, we find that the first order law hypothesis leads to an excessively high value for a frequency factor, while the second order law hypothesis gives us a frequency factor of 10^{-3}. We have no macroscopic theory of the phenomena to tell us whether this is reasonable or not.

Slide 6 shows the decrease in the velocity of sound in the case of heating when the temperature increases linearly at the rate of 3.5 degrees per minute. Our procedure allows us to make measurements without removing the specimen from the furnace. The variation of Young's modulus alters the deductions we can draw from this curve, but only very slightly, in view of the very appreciable drop in the velocity of sound. The slope of curve AN does not become clearly apparent until after 200°.

The other curve shows the release of internal energy stored by a specimen similarly irradiated, the rate of heating being exactly the same. We carried out many other tests involving differential heat analyses, since it is surprising to find that the recovery of mechanical properties is accompanied by the liberation of relatively low amounts of heat.

It will be noted that this curve has a first hump. The maximum rate of liberation of heat occurs at about 180°, that is to say, before the large drop in the value of Young's modulus. It is true that there is a small isothermal effect at the point where the velocity of sound falls off markedly, but the amount of heat associated with this effect is only about one-third or one-fourth (of the amount associated with the first hump). Varying the rate of heating changes the appearance of the humps corresponding to the exothermic phenomena, but we feel certain that at about 220° there is a slight but sharp rise in the rate of heat liberation which implies a jump in the activation energy associated with the phenomenon in question.

Tests show that the less the graphite is irradiated, the clearer the separation of the two peaks. Assuming that the heat liberated by the recovery of an individual centre is equivalent to 12 ev, we find that for the given curve the total number of centres is about 6×10^{18}.

The investigation of lithium fluoride was carried out by Mr. Perio and Mr. Tournarie. LiF in the form of powders and single crystals was exposed to thermal neutrons in doses of from 5×10^{16} to 10^{19} neutrons per cm². X-ray diffraction studies on powders and single crystals furnish evidence of three stages in the modifications incident to irradiation:

(*a*) Up to about 3×10^{17} n per cm², the lattice expands proportionally to the dose, without noticeable distortion. The width of the reflecting power

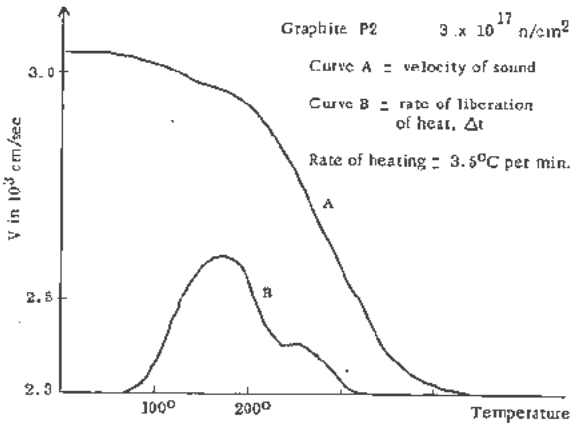

Slide 6

the "rocking curve," as we say even in Paris—remains less than 0.7′ (2θ), a value comparable to the instrumental angle of the twin crystal spectrometer used. The maximum increment of the parameter a_0 reaches

$$\frac{\Delta a}{a_0} = 1.7 \pm 0.1 \qquad 10^{-3}$$

(*b*) From 3×10^{17} to 2×10^{19} n per cm², the "rocking curve" may be characterized in terms of a narrow line which stands out against a broadened base that is asymmetric and displaced to the side of large angles; the width to half weight is approximately constant (20′). The intensity of this base increases with the radiation dose. In the powder diffraction photographs we have marked only the centres of gravity of the fine-line-plus-broadened-base groups. They indicate a certain contraction as compared with the previous state of maximum expansion. Here $\Delta a/a_0 = (6 \pm 1) \times 10^{-4}$ for a dose of 1×10^{18} n per cm².

(*c*) For still higher doses, the broadened lines become fairly symmetrical and the expansion is further reduced. Here $\Delta a/a_0 = 0.5 \pm 2) \times 10^{-4}$ for a dose of 7×10^{18} n per cm².

In the light of the above, the results obtained by Binder and Sturm correspond to the first stage of irradiation and those reported by Keating for a dose of 7×10^{17} correspond to the third, with due allowance for the weak expansion by the last author.

During the thermal recovery, the rocking curve gradually returns to its initial condition; after annealing between 475° and 500°, the crystal becomes as perfect as it was before irradiation. We note that for doses from 3×10^{17} to 10^{18} n per cm² (zone *b*), heating at 350° first leads to fusion of the peak and base into a broadened line. Before the line returns to its original form, the material goes through two stages of recovery, as indicated by the powder diagrams. The first stage becomes apparent at 150°. There is a restoration of the lattice accompanied by rapid contraction, but without any change in colour. For doses above 3×10^{17} n per cm², the constant becomes even smaller than that of the initial material, without any apparent relation between the contraction observed and the rate of irradiation. For a dose of 2×10^{18} n per cm², we found $\Delta a/a_0 = -(2.5 \pm 1) \times 10^{-4}$. The second recovery stage becomes manifest only above 350°. The crystal parameter then returns to its initial value of better than 0.5×10^{-4}, with complete bleaching.

Our suggested interpretation is that, for doses inferior to 3×10^{17}, the recovery mechanism may be mutual annihilation of vacancies and interstitials. At higher doses, the phenomena appear to be more complex. The contraction of the lattice may be attributed to a coalescence of interstitials, the distortions being connected with the concentration gradient of the interstitials about the clustering centres. Recovery below 350° is connected with the total coalescence of this type of point defects and the progressive disappearance of the gradients. Contraction of the lattice at this stage may be attributed to the vacancies still scattered through the crystal, after a certain number of them have disappeared through encounters with interstitials. The final stage of recovery, characterized by a return to the initial parameter, apparently comprises a more complex mechanism by which clusters and vacancies disappear simultaneously. The process may have analogies with the phenomenon of regression in alloys characterized by structural hardening. This interpretation is not in conflict with the results of the X-ray central diffusion study carried out on our specimens by Guinier and Lambert.

Slide 7 (Fig. 8 of P/302) shows the curve for a differential thermal analysis on a specimen irradiated with a dose of 4×10^{17}. We were able to calibrate our differential analysis measurements with reference to measurements of the heat of solution which gives the total internal energy imparted by the radiation, it being assumed that the specific heat is not appreciably affected by irradiation. During the first stage, LiF stores one calorie per 10^{18} n/cm².

According to Voigt's classical theory, quartz has six independent elastic coefficients, two piezoelectric constants and two expansion coefficients (Slide 8, Fig. 9 of P/362). We know from the studies by Wittels, Lukesh and Primak that after radiation doses on the order of 5×10^{20} fast neutrons per cm², crystalline quartz becomes an almost amorphous substance similar to glass and probably isotropic. At this stage presumably only two of the independent elastic coefficients remain, the two piezoelectric constants vanish and the two expansion coefficients become equal. We have begun to follow the evolution of these parameters in quartz crystal specimens of different cut, irradiated in the Saclay pile. The rate of change is very slow. So far we have only the slope at the beginning of the curves for the coefficients S_{11} and S_{33}. S_{11} decreases and S_{33} *increases*. At the bottom of the diagram, we show the two elastic coefficients of non-irradiated vitreous silica. It is probable that the final stage of crystalline quartz after irradiation is not appreciably different from the vitreous stage. This seems to be confirmed by our first measurements. At the dose of 1×10^{19} thermal neutrons per cm², which we have now reached, the piezoelectric constant d_{11} is reduced by about 5 per cent. At the present stage in our experiments, the electric conductivity of quartz had increased to such an extent that static measurements are no longer feasible; we have consequently developed another method for measuring the piezoelectric constants.

At Harwell, Johnson investigated the variation of resonance frequency of a quartz plate of the type employed in electronics. This frequency, which depends on four of the elastic coefficients mentioned above and on the thickness of the plate, was reduced by about 1 per cent after a dose of approximately 10^{19} fast neutrons. At this point it becomes difficult to produce vibration of the plate piezoelectrically, which indicates a considerable reduction of the coefficient d_{11}.

We are diligently continuing these studies.

DISCUSSION OF P/362

Mr. J. H. CRAWFORD (USA): I should like to inquire about the temperature scale on the stored energy release figure that you showed.

Mr. MAYER (France): The ordinates are proportional to the rate of the release of heat, which is a very clear-cut process. We can calibrate our differential thermal analysis tests simply in terms of the heat of solution. The variation of the heats of solution gives the sum total of the internal energy stored up by irradiation. This permits us to calibrate our curves. Thus in Perio's first stage of irradiation, lithium fluoride stores approximately one calorie per 10^{16} thermal neutrons received, which corresponds to about one one-thousandth of the total fission energy of the lithium atoms.

Mr. J. H. CRAWFORD (USA) presented paper P/753.

DISCUSSION OF P/753

Mr. M. MAGAT (France): The luminescence and colouration of vitreous silica produced by irradiation with gamma-rays from cobalt and 30 kev X-rays have recently been investigated by Miss Lautout. I will not speak here of the investigations relating to luminescence, phophorescence and thermo-luminescence; I merely want to mention a few points connected with the questions discussed by Mr. Crawford.

Miss Lautout found five bands situated at 2.3 ev, 3.1 ev, 3.8 ev, 4.8 ev and 5.6 ev in commercial grade quartz. The second and fourth bands are weak and do not become clearly visible until the neighbouring bands (3.8 ev and 5.6 ev) are weakened by irradiation with ultraviolet radiation.

The behaviour of the bands varies greatly. Thus, the 3.8 ev band is readily bleached by heating for one and a half hours at 300°C, as well as by radiation with the near ultraviolet. At the same time, phosphorence ceases.

Then, if we let the quartz specimen rest for several days, the 3.8 ev band comes back; at the same time, it once again becomes possible to excite phosphorescence by irradiation with the near ultraviolet.

The 2.3 ev band, that is to say, the green band, is bleached more slowly by heat than the first one: in about ten hours at 300°C. It does not weaken if the quartz plate is kept several months in daylight. Hence there is disagreement here with the results reported by Mr. Crawford. This band weakens slightly if the specimen is irradiated by ultraviolet of the frequency which produces fading of the 3.8 ev band, but it weakens greatly and rapidly if the specimen is irradiated by the far ultraviolet which causes fading of the 5.6 ev band. This last-named band is not bleached thermally until the heating temperature is raised above 500°C.

The 4.8 ev band observed by Mr. Crawford in Corning quartz was also observed by Miss Lantout; it is first strengthened and then weakened when the specimen is irradiated with the far ultraviolet. This band may therefore be the F' band of the 5.6 ev band which is presumably the F band.

The origin of the 2.3 ev band is probably connected either with the vitreous structure or with the stoichiometric structure. A quartz crystal which was not coloured, or at least not visibly coloured, by irradiation with 500,000 r and which was not phosphorescent, was pulverized and melted in the furnace, with due precautions to prevent the introduction of impurities. The glass so obtained coloured very rapidly and readily became phosphorescent. We therefore think that the only changes that can be involved are either a change in structure transition from crystal to glass—or a change in stoichiometry.

Mr. CRAWFORD (USA): I would like to reply very briefly to the comment. This work is most interesting. We have made observations extending considerably with regard to optical bleaching of the 5500Å peak, and from some of the observations made by us we found—and I think the people in England concur in this—that this can be done optically provided the temperature is elevated slightly.

Mr. G. R. HENNIG (USA) presented paper P/751.

DISCUSSION OF P/751

Mr. KINCHIN (UK): I should like to refer to Fig. 12 of Mr. Hennig's paper. It shows that some paramagnetic resonance effect remains after annealing up to temperatures of about 1000°C, and this should be high enough to remove all the single interstitials. Would it not be better, therefore, to associate the paramagnetic resonance effect with vacancies?

The other point relevant to this is that the dose at which the saturation occurs in the paramagnetic resonance does not seem to fit very well with the dose at which one gets saturation in stored energy and thermal resistivity.

Mr. HENNIG (USA): In answer to the first question, we find actually that our paramagnetic resonance disappears completely at about 250°C after moderate bombardment, and the curve to which reference has been made shows that only after heavy bombardment exceeding 1000 megawatt days will there be some paramagnetic resonance left after 1000 degrees annealing. We think that this residual paramagnetic resonance could be attributed to the breaking up of very large complexes in this temperature range during annealing, producing some paramagnetic ions in the process which are frozen in on cooling. All the explanations, which I have tried to enumerate, do apply and do fit at lower radiation values, where resonance completely disappears. I feel that to attribute resonance to vacancies is not possible, for quite a few reasons as I have already mentioned, one being that the paramagnetic reson-

ance certainly is associated with centers which move below room temperature, and we cannot visualize vacancies moving in graphite near room temperature.

The second question dealt with the region in which the paramagnetic resonance saturates compared with the saturation of the stored energy. I do not feel that there is very much of a difference in the bombardment regions; we found that agreement was fairly good, and that resonance seemed to level off after 200 or 300 megawatt days, while the stored energy certainly had a kink in it after 200 megawatt days. Any disagreement may be due to different bombardment temperatures of the two sets of examples.

Mr. H. F. Morán (Venezuela): In connection with the papers presented in this session, I should like to make a brief comment on a method of examination which is very likely to prove of great value in studies on the structure of normal solids and the effects of radiation. I refere specifically to the electron-microscope and other electron studies of hard solids, like metals and crystalliae substances. Most of the studies which have been carried out up to now have dealt with the surface structure of metals and crystals. Study by means of replica techniques has hitherto not been possible to apply to sections of the order of 200Å or less, especially to the study of metals and crystals. In a series of studies carried out during the past three years in Stockholm, and later in Caracas, we have developed a diamond knife, together with an ultra-microtome, which makes it possible to produce a series of thin sections of metals, including germanium.

Using these instruments, we have been able to carry out a number of studies, particularly in relation to X-ray diffraction patterns which show the degree of orientation of the crystalline and permit other studies of the structure of these materials.

(Mr. Morán demonstrated the application of these instruments with the aid of photographs.)

Mr. G. V. Kurdiumov (USSR): The influence of irradiation on the moduli of elasticity of crystals has been discussed in a number of papers. We know that plastic deformation and irradiation often have the same effect on a number of physical properties, for example, on the strength of metals and on the disordering in solid solutions. For practical purposes, the change of properties by means of irradiation may sometimes be more advantageous than by plastic deformation, since the former does not involve the changes in shape always accompanying the latter.

In this connection it seems to me that parallel investigation of the effects of radiation and plastic deformation should be of great interest.

I should like to take advantage of the fact that we have present here many famous investigators in solid-state physics and the physics of metals, and draw attention to the problem of the influence of radiation on the binding forces in crystals. It has long been known that plastic deformation has the effect of reducing the intensity of X-ray interference. This was commonly ascribed to the displacement of atoms from their normal position in the lattice as the result of plastic deformation. However, the same effect would be obtained if the moduli of elasticity were changed or the thermal factor in the scattering of X-rays modified.

We have carried out plastic deformation of iron and measured the total intensity of X-ray interference at room temperature and at the temperature of liquid nitrogen. These experiments showed that the principal decrease in intensity is due to the static displacement of atoms rather than to changes in the dynamics of the atomic oscillations. However, in the case of solid solutions the situation is entirely different. For example, in the case of an iron alloy, such as iron-chromium, iron-tungsten or iron-nickel, we find that the introduction of a relatively small amount of the alloying element into the solid solution leads to an appreciable change in the thermal factor of X-ray scattering. This occurs only when and if the alloy is annealed at a temperature of 600° to 800°. If after this heat treatment the specimen undergoes plastic deformation, the strengthening of the lattice bonds produced by annealing disappears. In my opinion, it would be desirable to carry out experiments of this kind after irradiation. I believe that this effect is connected with the fact that the short-range order is disturbed as a result of plastic deformation and that the strengthening of the bonds occurs only in the case when a certain short-range order is established in the solid solution.

Mr. Hering (France): I should like to ask Mr. Hennig what chemical reagent did he use to detect the interstitials in his labelling experiments with C^{14}.

Mr. Hennig (USA): We use nearly exclusively chromic sulfuric acid which forms a lamellar compound in which one layer of carbon alternates with a layer of sulfuric acid, and that is propagated throughout the crystal. During the formation of this, anything which has lodged between the planes gets thrown out and converted into carbon dioxide. That is the best penetrating agent we have found. Potassium may also do it, but chromic-sulfuric acid is the best.

PEACEFUL USES OF ATOMIC ENERGY:

Proceedings of the International Conference in Geneva, August 1955.

The following is a complete listing of the sixteen volumes which comprise this publication, together with the main subjects covered by each volume.

VOLUME 1

The World's Requirements for Energy: The Role of Nuclear Power

World Energy Needs
Capital Investment Required for Nuclear Energy
The Role of Thorium
The Role of Nuclear Power in the Next 50 Years
Education and Training of Personnel in Nuclear Energy
Economics of Nuclear Power

VOLUME 2

Physics, Research Reactors

Special Topics in Nuclear Physics
Fission Physics
Research Reactors
Research Reactors and Descriptions

VOLUME 3

Power Reactors

Experience with Nuclear Power Plants
Fuel Cycles
Design of Reactors for Power Production
Power Reactors, Prototypes

VOLUME 4

Cross-Sections Important to Reactor Design

Equipment and Techniques Used in Measuring Cross Sections Important to Reactor Design
Cross Sections of Non-Fissionable Materials: Delayed Neutrons
Cross Sections of Fissionable Materials
Properties of Fissionable Materials

VOLUME 5

Physics of Reactor Design

Integral Measurements
Resonance Integrals
Fission Product Poisoning
Criticality in Solutions
Zero Energy and Exponential Experiments
Zero Energy Experiments on Fast Reactors and Reactor Kinetics
Reactor Theory

VOLUME 6

Geology of Uranium and Thorium

Occurrence of Uranium and Thorium
Prospecting for Uranium and Thorium

VOLUME 7

Nuclear Chemistry and the Effects of Irradiation

The Fission Process
Facilities for Handling Highly Radioactive Materials
Chemistry of Fission Products
Heavy Element Chemistry
Effects of Radiation on Reactor Materials
Effects of Radiation on Liquids
Effects of Radiation on Solids

VOLUME 8

Production Technology of the Materials Used for Nuclear Energy

Treatment of Uranium and Thorium Ores and Ore Concentrates
Production of Metallic Uranium and Thorium
Analytical Methods in Raw Material Production
Production Technology of Special Materials

VOLUME 9

Reactor Technology and Chemical Processing

Waste Disposal Problems
Metallurgy of Thorium, Uranium and their Alloys
Fabrication of Fuel Elements
Liquid Metal Technology
Chemical Aspects of Nuclear Reactors
Chemical Processing of Irradiated Fuel Elements
Waste Treatment and Disposal
Separation and Storage of Fission Products

VOLUME 10

Radioactive Isotopes and Nuclear Radiations in Medicine

Isotopes in Medicine and Biology
Therapy
Diagnosis and Studies of Disease

VOLUME 11

Biological Effects of Radiation

Modes of Radiation Injury and Radiation Hazards
Mechanisms of Radiation Injury
Protection and Recovery
Genetic Effects
Human Implications

VOLUME 12

Radioactive Isotopes and Ionizing Radiations in Agriculture, Physiology, and Biochemistry

Isotopes in Agriculture
Radiation-induced Genetic Changes and Crop Improvement
Tracer Studies in Agriculture
Animal Physiology
Plant Biochemistry
General Biochemistry

VOLUME 13

Legal, Administrative, Health and Safety Aspects of Large Scale Use of Nuclear Energy

Legal and Administrative Problems
Reactor Safety and Location of Power Reactors
Safety Standards and Health Aspects of Large Scale Use of Atomic Energy

VOLUME 14

General Aspects of the Use of Radioactive Isotopes: Dosimetry

Isotopes in Technology and Industry
General Uses, Production and Handling of Radioactive Isotopes
Dosimetry

VOLUME 15

Applications of Radioactive Isotopes and Fission Products in Research and Industry

Radioactive Isotopes in Research
Radioactive Isotopes in Control and Technology
Fission Products and their Applications

VOLUME 16

Record of the Conference

Opening of the Conference and the Presidential Address
International Co-operation in the Peaceful Uses of Atomic Energy
Closing Presidential Address
Evening Lectures
Author Index and Paper Index

SALES AGENTS FOR UNITED NATIONS PUBLICATIONS

ARGENTINA
Editorial Sudamericana S.A., Alsina 500, Buenos Aires.

AUSTRALIA
H. A. Goddard, 255a George St., Sydney; 90 Queen St., Melbourne.
Melbourne University Press, Carlton N.3, Victoria.

AUSTRIA
B. Wüllerstorff, Markus Sittikusstrasse 10, Salzburg.
Gerold & Co., Graben 31, Wien.

BELGIUM
Agence et Messageries de la Presse S.A., 14-22 rue du Persil, Bruxelles.
W. H. Smith & Son, 71-75, boulevard Adolphe-Max, Bruxelles.

BOLIVIA
Librería Selecciones, Casilla 972, La Paz.

BRAZIL
Livraria Agir, Rio de Janeiro, Sao Paulo and Belo Horizonte.

CAMBODIA
Papeterie-Librairie Nouvelle, Albert Portail, 14 Avenue Boulloche, Pnom-Penh.

CANADA
Ryerson Press, 299 Queen St. West, Toronto.
Periodica, Inc., 5112 Ave. Papineau, Montreal.

CEYLON
Lake House Bookshop, The Associated Newspapers of Ceylon, Ltd., P. O. Box 244, Colombo.

CHILE
Librería Ivens, Casilla 205, Santiago.
Editorial del Pacífico, Ahumada 57, Santiago.

CHINA
The World Book Co., Ltd., 99 Chungking Road, 1st Section, Taipeh, Taiwan.
Commercial Press, 211 Honan Rd., Shanghai.

COLOMBIA
Librería América, Medellín.
Librería Nacional Ltda., Barranquilla.
Librería Buchholz Galería, Bogotá.

COSTA RICA
Trejos Hermanos, Apartado 1313, San José.

CUBA
La Casa Belga, O'Reilly 455, La Habana.

CZECHOSLOVAKIA
Ceskoslovensky Spisovatel, Národní Trída 9, Praha 1.

DENMARK
Einar Munksgaard, Ltd., Norregade 6, Kobenhavn, K.

DOMINICAN REPUBLIC
Librería Dominicana, Mercedes 49, Ciudad Trujillo.

ECUADOR
Librería Científica, Guayaquil and Quito.

EGYPT
Librarie "La Renaissance d'Egypte," 9 Sh. Adly Pasha, Cairo.

EL SALVADOR
Manuel Navas y Cía., 1a. Avenida sur 37, San Salvador.

FINLAND
Akateeminen Kirjakauppa, 2 Keskuskatu, Helsinki.

FRANCE
Editions A. Pedone, 13, rue Soufflot, Paris V.

GERMANY
Elwert & Meurer, Hauptstrasse 101, Berlin-Schoneberg.
W. E. Saarbach, Gereonstrasse 25-29, Köln (22c).
Alexander Horn, Spiegelgasse 9, Wiesbaden.

GREECE
Kauffmann Bookshop, 28 Stadion Street, Athens.

HAITI
Librairie "A la Caravelle," Boîte postale 111-B, Port-au-Prince.

HONDURAS
Librería Panamericana, Tegucigalpa.

HONG KONG
The Swindon Book Co., 25 Nathan Road, Kowloon.

ICELAND
Bokaverzlun Sigfusar Eymundssonar H. F., Austurstraeti 18, Reykjavik.

INDIA
Orient Longmans, Calcutta, Bombay, and Madras.
Oxford Book & Stationery Co., New Delhi and Calcutta.
P. Varadachary & Co., Madras.

INDONESIA
Pembangunan, Ltd., Gunung Sahari 84, Djakarta.

IRAN
"Guity", 482 Avenue Ferdowsi, Teheran.

IRAQ
Mackenzie's Bookshop, Baghdad.

ISRAEL
Blumstein's Bookstores Ltd., 35 Allenby Road, Tel-Aviv.

ITALY
Librería Commissionaria Sansoni, Via Gina Capponi 26, Firenze.

JAPAN
Maruzen Company, Ltd., 6 Tori-Nichome, Nihonbashi, Tokyo.

LEBANON
Librairie Universelle, Beyrouth.

LIBERIA
J. Momolu Kamara, Monrovia.

LUXEMBOURG
Librairie J. Schummer, Luxembourg.

MEXICO
Editorial Hermes S.A., Ignacio Mariscal 41, México, D.F.

NETHERLANDS
N.V. Martinus Nijhoff, Lange Voorhout 9, 's-Gravenhage.

NEW ZEALAND
United Nations Association of New Zealand, C.P.O. 1011, Wellington.

NORWAY
Johan Grundt Tanum Forlag, Kr. Augustsgt. 7A, Oslo.

PAKISTAN
Thomas & Thomas, Karachi.
Publishers United Ltd., Lahore.
The Pakistan Cooperative Book Society, Dacca and Chittagong (East Pak.).

PANAMA
José Menéndez, Plaza de Arango, Panamá.

PARAGUAY
Agencia de Librerías de Salvador Nizza, Calle Pte. Franco No. 39-43, Asunción.

PERU
Librería Internacional del Perú, S. A., Lima and Arequipa.

PHILIPPINES
Alemar's Book Store, 749 Rizal Avenue, Manila.

PORTUGAL
Livraria Rodrigues, 186 Rua Aurea, Lisboa.

SINGAPORE
The City Book Store, Ltd., Winchester House, Collyer Quay.

SPAIN
Librería Bosch, 11 Ronda Universidad, Barcelona.
Librería Mundi-Prensa, Lagasca 38, Madrid.

SWEDEN
C. E. Fritze's Kungl. Hovbokhandel A-B, Fredsgatan 2, Stockholm.

SWITZERLAND
Librairie Payot S.A., Lausanne, Genève.
Hans Raunhardt, Kirchgasse 17, Zurich 1.

SYRIA
Librairie Universelle, Damas.

THAILAND
Pramuan Mit Ltd., 55 Chakrawat Road, Wat Tuk, Bangkok.

TURKEY
Librairie Hachette, 469 Istiklal Caddesi, Beyoglu, Istanbul.

UNION OF SOUTH AFRICA
Van Schaik's Bookstore (Pty.), Ltd., Box 724, Pretoria.

UNITED KINGDOM
H.M. Stationery Office, P. O. Box 569, London, S.E. 1 (and at H.M.S.O. Shops).

UNITED STATES OF AMERICA
International Documents Service, Columbia University Press, 2960 Broadway, New York 27, N. Y.

URUGUAY
Representación de Editoriales, Prof. H. D'Elía, Av. 18 de Julio 1333, Montevideo.

VENEZUELA
Librería del Este, Av. Miranda No. 52, Edf. Galipan, Caracas.

VIET-NAM
Papeterie-Librairie Nouvelle, Albert Portail, Boîte Postale 283, Saigon.

YUGOSLAVIA
Drzavno Preduzece, Jugoslovenska Knjiga, Terazije 27/II, Beograd.
Cankarjeva Zalozba, Ljubljana, Slovenia.

Orders and inquiries from countries where sales agents have not yet been appointed may be sent to: Sales and Circulation Section, United Nations, New York, U.S.A.; or Sales Section, United Nations, Palais des Nations, Geneva, Switzerland.